FOR REFERENCE PURPOSES ONLY

AIR POLLUTION

Measurement, Modelling and Mitigation

Fourth Edition

Abhishek Tiwary, Ian Williams and Jeremy Colls

CRC Press
Taylor & Francis Group

FOR REFERENCE PURPOSES ONLY

Air Pollution

FOR REFERENCE PURPOSES ONLY

Air Pollution

Measurement, Modelling and Mitigation

Fourth Edition

Abhishek Tiwary
Ian Williams

CRC Press
Taylor & Francis Group
Boca Raton London New York

CRC Press is an imprint of the
Taylor & Francis Group, an **informa** business

FOR REFERENCE PURPOSES ONLY

CRC Press
Taylor & Francis Group
6000 Broken Sound Parkway NW, Suite 300
Boca Raton, FL 33487-2742

© 2019 by Taylor & Francis Group, LLC
CRC Press is an imprint of Taylor & Francis Group, an Informa business

No claim to original U.S. Government works

Printed on acid-free paper

International Standard Book Number-13: 978-1-138-50366-3 (Hardback)
International Standard Book Number-13: 978-1-4987-1945-2 (Paperback)

This book contains information obtained from authentic and highly regarded sources. Reasonable efforts have been made to publish reliable data and information, but the author and publisher cannot assume responsibility for the validity of all materials or the consequences of their use. The authors and publishers have attempted to trace the copyright holders of all material reproduced in this publication and apologize to copyright holders if permission to publish in this form has not been obtained. If any copyright material has not been acknowledged please write and let us know so we may rectify in any future reprint.

Except as permitted under U.S. Copyright Law, no part of this book may be reprinted, reproduced, transmitted, or utilized in any form by any electronic, mechanical, or other means, now known or hereafter invented, including photocopying, microfilming, and recording, or in any information storage or retrieval system, without written permission from the publishers.

For permission to photocopy or use material electronically from this work, please access www.copyright.com (http://www.copyright.com/) or contact the Copyright Clearance Center, Inc. (CCC), 222 Rosewood Drive, Danvers, MA 01923, 978-750-8400. CCC is a not-for-profit organization that provides licenses and registration for a variety of users. For organizations that have been granted a photocopy license by the CCC, a separate system of payment has been arranged.

Trademark Notice: Product or corporate names may be trademarks or registered trademarks, and are used only for identification and explanation without intent to infringe.

Library of Congress Cataloging-in-Publication Data

Names: Tiwary, Abhishek, author. | Williams, Ian, author. | Air pollution.
Title: Air pollution : measurement, modelling and mitigation / Abhishek Tiwary and Ian Williams.
Description: Fourth edition. | Boca Raton : CRC Press, 2018. | Earlier editions written by Jeremy Colls. | Includes bibliographical references and index.
Identifiers: LCCN 2017060045 (print) | LCCN 2018000769 (ebook) | ISBN 9781498719469 (Adobe PDF) | 9781498719483 (ePub) | ISBN 9781138503663 (hardback : acid-free paper) | ISBN 9781498719452 (paperback : acid-free paper)
Subjects: LCSH: Air--Pollution.
Classification: LCC TD883 (ebook) | LCC TD883 .C573 2018 (print) | DDC 363.739/2--dc23
LC record available at https://lccn.loc.gov/2017060045

Visit the Taylor & Francis Web site at
http://www.taylorandfrancis.com

and the CRC Press Web site at
http://www.crcpress.com

FOR REFERENCE PURPOSES ONLY

Contents

Preface
Authors

1 Overview of air pollution

1.1 What is air pollution?
1.2 Historical perspectives
1.3 Classification of air pollutants
1.3.1 Types of air pollutants
1.3.2 Sources of air pollutants
1.3.3 Source emission data
1.3.3.1 Emission units
1.3.4 What is smog?
1.4 Why does air pollution need attention?
1.5 The basic atmosphere
1.5.1 The origins of our atmosphere
1.5.2 Natural constituents of air
1.5.3 Water in the atmosphere
1.5.4 The vertical structure of the atmosphere
1.5.4.1 Pressure
1.5.4.2 Temperature
1.5.5 Photochemical reactions in the atmosphere
1.5.5.1 Light absorption and emission processes
1.5.5.2 Examples of photochemical reactions
1.6 Methods of describing pollutant concentration
1.7 Units for expressing atmospheric concentrations
1.7.1 Concentration units
1.7.1.1 Conversion between gravimetric and volumetric units
1.7.1.2 Correction for non-standard temperature and pressure
1.7.2 Averaging time
1.8 Unconventional air pollutants

FOR REFERENCE PURPOSES ONLY

1.8.1 Incineration as a source of air pollutants
1.9 Case study – Historical perspective: The Great London Smog
1.9.1 Chronology
1.9.2 Health effects
1.9.3 Environmental effects
1.9.4 Socio-economic impacts
References and further reading resources

2 Gaseous air pollutants

2.1 Primary gaseous emissions
2.2 Anthropogenic emissions
2.2.1 Energy-related emissions
2.2.2 Sulphur oxide emissions
2.2.2.1 Sulphur dioxide
2.2.2.2 Sulphur trioxide
2.2.3 Nitrogen oxide emissions
2.2.3.1 Nitric oxide
2.2.3.2 Nitrogen dioxide formation
2.2.4 Ammonia
2.2.5 Non-methane volatile organic compounds
2.2.6 Carbon monoxide
2.2.7 Hydrogen chloride
2.2.8 Persistent organic pollutants
2.2.8.1 Dioxins and furans
2.2.8.2 Polychlorinated biphenyls
2.2.8.3 Polybrominated diphenyl ethers
2.2.8.4 Polycyclic aromatic hydrocarbons
2.3 Secondary gaseous pollutants
2.3.1 Tropospheric ozone
2.3.2 Wintertime NO_2 episodes
2.4 Measurement of gases
2.4.1 Sampling requirements
2.4.2 Gas sampling
2.4.2.1 Pumped systems
2.4.2.2 Preconcentration
2.4.2.3 Absorption
2.4.2.4 Adsorption
2.4.2.5 Condensation trapping
2.4.2.6 Grab sampling
2.4.3 Gas concentration measurement

FOR REFERENCE PURPOSES ONLY

2.4.3.1 Wet chemical methods
2.4.3.2 Real-time pumped systems
2.4.3.3 Real-time remote systems
2.4.3.4 Gas chromatography
2.4.3.5 Liquid chromatography
2.4.3.6 Chromatography with mass spectroscopy
2.4.3.7 Inductively coupled plasma spectroscopy
2.4.3.8 Optical spectroscopy
2.4.4 Quality control
2.4.4.1 Blanks
2.4.4.2 Calibration
2.4.4.3 Permeation tubes
2.4.4.4 Gas bottles
2.4.4.5 UV O_3 generator
2.4.4.6 Zero air
2.5 Case study – Bhopal gas leak
References and further reading resources

3 Particulate matter

3.1 Why particulates are a special case?
3.2 Particulate terminology
3.3 Particle size distributions
3.3.1 Relative sizes of particles and gas molecules
3.3.2 Specification of size
3.3.3 Presentation of size distributions
3.3.4 General features of real size distributions
3.4 Aerosol mechanics
3.4.1 Drag force
3.4.2 Sedimentation
3.4.3 Brownian diffusion
3.4.4 Coagulation
3.4.5 The influence of shape and density
3.4.5.1 Shape
3.4.5.2 Aerodynamic diameter
3.4.6 Relaxation time
3.4.6.1 Note on units and dimensions
3.4.7 Stopping distance
3.4.8 Impaction and interception
3.4.9 Stokes number and impactors
3.4.10 Thermophoresis

FOR REFERENCE PURPOSES ONLY

3.4.11 Erosion and resuspension
3.5 Particle sources
3.5.1 Primary particles
3.5.1.1 Wind erosion
3.5.1.2 Sea salt
3.5.1.3 Other natural sources
3.5.1.4 Anthropogenic sources
3.5.2 Secondary particles
3.6 Trends in particle emissions
3.7 Measurement of particles
3.7.1 Particle sampling
3.7.1.1 Isokinetic sampling
3.7.1.2 Calibration
3.7.2 Particle measurement methods
3.7.2.1 Filtration
3.7.2.2 British Standard smoke method
3.7.2.3 High-volume sampler
3.7.2.4 Optical methods
3.7.2.5 Beta-attenuation
3.7.2.6 Resonating microbalance
3.7.2.7 Size fractionation
3.7.2.8 Optical sizers
3.7.2.9 Aerosol spectrometer
3.7.2.10 Inertial impactors
3.7.2.11 Electrical mobility analysers
3.7.2.12 Diffusion batteries
3.7.2.13 Condensation particle counter
3.7.3 Chemical composition of aerosols
3.7.3.1 Particle microstructure
3.7.3.2 Real-time chemical analysis
3.7.4 Measurement of coarse particle deposition
3.8 Case study – Asbestos
References and further reading resources

4 Area sources

4.1 Biogenic area sources
4.1.1 Wildfires
4.1.1.1 Forest management practices
4.1.2 Volcanic emissions
4.1.3 Soil emissions
4.2 Anthropogenic area sources

FOR REFERENCE PURPOSES ONLY

4.2.1 Landfills
4.2.1.1 Landfill directive
4.2.1.2 Emerging trends in landfill of waste electrical components
4.2.2 Farm emissions
4.2.3 Fugitive emissions from industrial processes
4.3 Measurement of area sources
4.3.1 Confined emissions
4.3.1.1 Measurement of volume flow rate
4.3.1.2 Measurement of gas concentrations
4.3.1.3 Measurement of particle concentrations
4.3.2 Unconfined emissions
4.3.3 Pervasive sensors
4.4 Measurement uncertainties
4.5 Modelling of area sources
4.6 Case study: The eruption of Eyjafjallajökull, Iceland
4.6.1 Volcanoes on Iceland
4.6.2 Chronology
4.6.3 Impacts of the eruption
4.6.4 Volcanic eruptions in the future
References and further reading resources

5 Mobile sources

5.1 Road traffic emissions
5.1.1 Traffic congestion
5.1.2 Combustion of fuel
5.1.2.1 Petrol engines
5.1.2.2 Diesel engines
5.1.2.3 Traffic biofuel in developing countries
5.1.3 Combustion emissions
5.1.3.1 Emission concentrations
5.1.4 Specific pollutants
5.1.4.1 NO_x
5.1.4.2 CO
5.1.4.3 Combustion HC
5.1.4.4 Benzene
5.1.4.5 Evaporation HC
5.1.4.6 The importance of air–fuel ratio
5.1.4.7 Exhaust particulate matter
5.1.4.8 Non-exhaust particulate emissions
5.1.4.9 Lead

FOR REFERENCE PURPOSES ONLY

5.1.4.10 Polycyclic aromatic hydrocarbons
5.1.5 Reduction of motor vehicle emissions
5.1.5.1 Burn less fuel!
5.1.5.2 Combustion optimisation
5.1.5.3 Emissions recycle
5.1.5.4 Vent controls
5.1.5.5 Exhaust gas recirculation
5.1.5.6 Three-way catalytic converters
5.1.6 Diesel exhausts
5.1.6.1 Diesel particulate filters
5.1.6.2 DeNO$_x$
5.1.6.3 Diesel oxidation catalyst
5.1.7 Vehicle maintenance
5.1.8 Vehicle emission calculations
5.1.8.1 Diurnal variations
5.1.8.2 Emissions measurement from laboratory and real road tests
5.1.8.3 Effect of engine temperature
5.1.8.4 Effect of operating mode
5.1.8.5 Catalyst degradation
5.1.8.6 National vehicle fleets
5.1.9 Fuel composition
5.1.9.1 Basic specification
5.1.9.2 Fuel sulphur content
5.1.9.3 Fuel reformulation
5.1.10 Diesel versus petrol
5.1.10.1 Gaseous emissions
5.1.10.2 Particulate emissions
5.1.11 Impact of control measures
5.1.12 Cleaner vehicle technologies
5.1.12.1 Electric
5.1.12.2 Hybrid
5.1.12.3 Hydrogen
5.1.12.4 Fuel cell
5.1.13 Alternative fuels
5.2 Non-road mobile machinery emissions
5.3 Rail emissions
5.4 Shipping emissions
5.5 Aircraft emissions
5.5.1 Emission calculations
5.5.2 Aerosol precursors
5.5.3 Contrails

FOR REFERENCE PURPOSES ONLY

5.5.4 Dispersion of aircraft emissions
5.5.5 Future jet fuels
5.5.6 Airport emission standards
5.5.7 Carbon dioxide emissions from civil aviation
5.6 Generating emissions inventory for mobile sources
5.6.1 The Bentley approach
5.6.2 The UK National Atmospheric Emissions Inventory
5.7 Case study – Traffic restriction schemes
5.7.1 London congestion charging
5.7.2 Odd-even driving patterns during the Beijing Olympics
5.7.3 Odd-even car driving in New Delhi
References and further reading resources

6 Ambient air quality

6.1 Gaseous pollutants
6.1.1 Nitrogen oxides
6.1.2 Sulphur dioxide
6.1.3 Carbon monoxide
6.1.4 Ozone
6.1.4.1 The general picture
6.1.5 Volatile organic compounds
6.2 Particulate matter
6.3 Patterns of occurrence
6.3.1 Automatic air quality monitoring networks
6.3.1.1 The UK national survey
6.3.1.2 Secondary networks
6.3.1.3 Data processing
6.3.1.4 Other surveys
6.3.2 Other measurement networks
6.4 Dry deposition of gases
6.4.1 Deposition velocity
6.4.2 Resistance
6.5 Wet deposition
6.5.1 Rainfall
6.5.2 Rainout
6.5.2.1 Washout
6.5.3 Dry reactions
6.5.4 Wet reactions
6.5.5 Cloudwater deposition
6.6 Total deposition and budgets
6.7 Analysis of an air quality data set

FOR REFERENCE PURPOSES ONLY

6.7.1 The raw data set
6.7.2 Time-series plot
6.7.3 Roses
6.7.4 Diurnal variations
6.7.5 Frequency distributions
6.7.6 Further statistical analyses
6.8 Effect of fireworks on ambient air quality
6.8.1 The art and science of fireworks
6.8.2 The physics of fireworks
6.8.3 The chemistry of fireworks
6.8.4 Pollutants associated with fireworks and bonfires
6.8.5 Effects on health
6.8.6 Effects on the local air quality
6.9 Case study: Buncefield Oil Storage Depot disaster
6.9.1 Impact of the event on the local air quality
6.9.2 Other environmental pollution impacts
References and further reading resources

7 Indoor air quality

7.1 Building ventilation
7.2 Combustion
7.2.1 Solid-fuel combustion
7.2.2 Gas combustion
7.2.3 Tobacco combustion
7.3 Indoor organic pollutants
7.3.1 Volatile organic compounds
7.3.2 Bioaerosols
7.3.3 Categories of bioaerosols
7.3.3.1 Bacteria
7.3.3.2 Endotoxins
7.3.3.3 Fungi
7.3.3.4 Viruses
7.3.3.5 Allergens
7.3.3.6 Pollen
7.3.4 Sampling bioaerosols
7.4 Sick building syndrome
7.5 Odours
7.6 Indoor air sampling
7.7 Case study – Cigarette smoke
References and further reading resources

8 Air pollution modelling

8.1 Air pollution meteorology
8.1.1 Atmospheric energy balance
8.1.1.1 Dry adiabatic lapse rate
8.1.1.2 Saturated adiabatic lapse rate
8.1.1.3 Atmospheric stability and temperature profile
8.1.1.4 Potential temperature
8.1.2 Atmospheric dispersion parameters
8.1.2.1 Air pressure and wind fields
8.1.2.2 Atmospheric stability classes
8.1.2.3 Other stability estimators
8.2 Dispersion models
8.3 Gaussian dispersion theory
8.3.1 Coordinate system
8.3.2 Fickian diffusion
8.3.3 The Gaussian plume equation
8.3.4 Assumptions of the Gaussian model
8.3.5 Plume rise
8.3.5.1 Buoyant rise in unstable – Neutral atmospheres
8.3.5.2 Buoyant rise in stable atmospheres
8.3.6 The effect of vertical constraints
8.3.6.1 Reflection at the ground
8.3.6.2 Reflection at an inversion
8.3.7 Estimating stability
8.3.7.1 Estimates of σ_y, σ_z
8.3.8 Versions of the Gaussian equation
8.3.8.1 Ground-level concentration due to an elevated source, bounded by the ground surface
8.3.8.2 Ground-level concentration due to an elevated source, bounded by the ground surface, directly downwind of the source at ground level
8.3.8.3 Ground-level concentration due to a ground-level source, directly downwind of the source (e.g. bonfire)
8.4 Dispersion theory in practice
8.4.1 Worked example of Gaussian dispersion
8.4.2 Predictions for planning purposes
8.4.3 Effects of topography
8.4.4 Effects of buildings
8.4.5 Recent developments
8.4.6 Meteorological data

8.5 Emission inventories
8.5.1 UK emissions inventories
8.5.2 European and global emissions mapping
8.6 Dispersion of vehicle emissions and exposure modelling
8.7 Receptor models
8.7.1 Chemical mass balance models
8.8 Stochastic models
8.9 Box models
8.10 Indoor air pollution modelling
8.11 Regional chemistry models
8.12 Case study – Combining a dispersion model with spatial statistics
8.12.1 Vehicle emissions modelling
8.12.2 Dispersion modelling
8.12.3 Spatial statistics
References and further reading resources

9 Air pollution control and mitigation

9.1 Industrial air pollution control technology
9.1.1 Adsorption and absorption of gases
9.1.1.1 Adsorption
9.1.1.2 Absorption
9.1.2 Abatement of SO_x
9.1.3 Abatement of NO_x
9.1.4 Abatement of particulate matter
9.1.4.1 Sedimentation
9.1.4.2 Centrifugation
9.1.4.3 Filtration
9.1.4.4 Washing
9.1.4.5 Electrostatic precipitation
9.1.4.6 Comparison of efficiencies
9.1.5 Abatement of volatile organic compounds
9.1.5.1 Use of catalysts
9.1.5.2 Incineration
9.1.6 Abatement of CO
9.2 Ambient air pollution control
9.2.1 Role of civic regeneration and retrofitting
9.2.2 Low-emission zones
9.2.3 Removal of precursors
9.2.3.1 Mitigation of tropospheric ozone
9.2.3.2 Mitigation of secondary particles

FOR REFERENCE PURPOSES ONLY

9.3 Indoor air pollution control
9.3.1 Indoor particulate removal
9.3.2 Indoor NO_x removal
9.3.3 Indoor CO removal
9.4 Role of green infrastructure
9.4.1 Multi-functional greening strategy
9.4.1.1 Mitigating air pollutants
9.4.1.2 Carbon sequestration
9.4.1.3 Combat urban heat island effect
9.4.2 Designing vegetation intervention
9.4.2.1 Canopy design
9.4.2.2 Filter strip design
9.4.2.3 Factors influencing particle deposition
9.4.3 Modelling vegetation pollution uptake
9.4.3.1 Vegetation canopy model
9.4.3.2 Modelling collection efficiency of vegetative filter strips
9.4.4 Practical concerns of greening
9.4.4.1 Resuspension of pollutants
9.4.4.2 Emission of volatile organic compounds
9.4.4.3 Pollen production
9.4.4.4 Evaluating pros and cons of urban vegetation intervention
9.5 Case study I – Seveso industrial disaster
9.6 Case study II – Ambient air pollution control
9.6.1 Role of hedgerows in the UK for mitigating ambient aerosols
9.6.2 Role of greenbelts in air quality management for quarries in India
References and further reading resources

10 Air pollution impacts

10.1 Effects on visual range
10.1.1 Regional haze in Asian megacities
10.1.2 Rayleigh scattering
10.1.3 Mie scattering
10.1.4 Contrast reduction
10.1.5 Hygroscopic particles
10.2 Impact on humans
10.2.1 Episodes and epidemiology
10.2.1.1 Severe combustion smog
10.2.1.2 Chronic low concentrations
10.2.1.3 Photochemical smogs
10.2.1.4 Animal models

FOR REFERENCE PURPOSES ONLY

10.2.1.5 Heat waves
10.2.2 The respiratory system
10.2.3 Responses to particles
10.2.3.1 Particle deposition in the lung
10.2.3.2 Standards for particle deposition
10.2.3.3 Particle clearance
10.2.3.4 Heavy metals
10.2.4 Responses to gases
10.2.4.1 Sulphur dioxide
10.2.4.2 Ozone
10.2.4.3 Nitrogen oxides
10.2.4.4 Volatile organic compounds
10.2.4.5 Benzene
10.2.4.6 Toluene
10.2.4.7 1,3-Butadiene
10.2.4.8 Carbon monoxide
10.2.5 Immunosuppression
10.2.6 Passive smoking
10.2.7 Persistent organic pollutants
10.2.8 Quantification of health effects
10.2.8.1 PM_{10} and SO_2
10.2.8.2 Ozone
10.2.8.3 Benefits of achieving NAQS targets
10.2.8.4 WHO methodology
10.2.8.5 Example case study
10.2.9 Odours
10.3 Impacts on other animals
10.3.1 Fish and other aquatic species
10.3.2 Industrial melanism
10.3.3 Aphid stimulation
10.4 Effects on plants
10.4.1 Historical evidence
10.4.2 Experimental methods
10.4.2.1 Laboratory chambers
10.4.2.2 Field release systems
10.4.2.3 Field filtration
10.4.2.4 Open-top chambers
10.4.2.5 Ventilated glasshouses
10.4.2.6 Branch bags
10.4.2.7 Ethylene diurea
10.4.2.8 Bioindicators

FOR REFERENCE PURPOSES ONLY

10.4.2.9 Lichens
10.4.2.10 Diatoms
10.4.3 Plant responses to specific air pollutants
10.4.3.1 Visible injury
10.4.3.2 Long-term response of agricultural yields to single gases
10.4.3.3 Nutrient inputs
10.4.4 Pollutant entry into the plant
10.4.5 Pollutants inside plants
10.4.6 Exposure dynamics
10.4.7 Premature senescence
10.4.8 Resistance
10.4.9 Trees
10.4.10 Critical loads and levels
10.4.10.1 Critical loads
10.4.10.2 Critical levels
10.4.11 Interactions
10.5 Damage to materials
10.5.1 Building materials
10.5.2 Other materials
10.6 Case study: Donora acid rain
10.6.1 Chronology of event
10.6.2 Health effects
10.6.3 Environmental effects
10.6.4 Socio-economic effects
References and further reading resources

11 Air pollution and climate change

11.1 State of climate science
11.1.1 Intergovernmental Panel on Climate Change
11.1.2 Trends in co-managing air pollution and climate change
11.1.3 Earth's radiation environment
11.1.3.1 Variations in solar input
11.2 Greenhouse gases
11.2.1 Carbon dioxide
11.2.2 Methane
11.2.3 Nitrous oxide
11.2.4 Halocarbons
11.3 Radiative forcing
11.3.1 Contributions to radiative forcing
11.3.2 The role of aerosols
11.3.3 Volcanoes and aerosol formation

11.3.4 Modelling the radiative impact of aerosol
11.3.5 Gases and aerosols combined
11.4 The main impacts
11.5 Future scenarios and predictions
11.5.1 Atmospheric temperature
11.5.2 Sea level
11.5.3 Rainfall
11.5.4 Effects in the UK
11.5.5 Effects in developing countries
11.5.6 Biodiversity changes
11.6 Feedbacks
11.7 Global responses
11.7.1 European responses
11.7.2 UK responses
11.8 Case study – Carbon footprinting
References and further reading resources

12 Air pollution impacts on ozone

12.1 Tropospheric ozone
12.1.1 Chemical reactions in the troposphere
12.1.1.1 Allotropy
12.1.1.2 Free radical chain reaction
12.1.1.3 Removal of methane
12.1.1.4 Removal of carbon monoxide
12.1.2 Tropospheric ozone formation
12.1.2.1 Reactions involving methane and/or carbon monoxide
12.1.2.2 Reactions involving the hydroxyl radical
12.1.2.3 Formation of peroxyacetyl nitrates
12.2 Stratospheric ozone
12.2.1 Origins of the ozone layer
12.2.1.1 Stratospheric ozone concentrations
12.2.2 Ozone destructive chemistry
12.2.2.1 The role of chlorofluorocarbons
12.2.2.2 Methyl bromide
12.2.3 Ozone depletion potentials
12.2.3.1 Reactions leading to O_3 depletion in the stratosphere
12.2.4 Current situation
12.2.5 Stratospheric ozone and ultraviolet radiation
12.2.5.1 Penetration of UV through the atmosphere
12.2.5.2 Penetration of UV into water

FOR REFERENCE PURPOSES ONLY

12.2.5.3 Absorption of UVB
12.2.5.4 Effects of UV on people
12.2.5.5 Skin responses
12.2.5.6 Eye responses
12.2.5.7 Immune responses
12.2.5.8 Effects of UV radiation on terrestrial biota
12.2.5.9 Effects on marine organisms
12.2.6 Clothing protection from ultraviolet radiation
12.3 Case study – Discovery of the ozone hole
References and further reading resources

13 Noise and light pollution

13.1 Noise as a pollutant
13.2 Types of noise pollution
13.2.1 Occupational
13.2.2 Environmental
13.3 Measuring sound
13.4 Noise and health
13.5 Reduction of noise pollution
13.5.1 Occupational noise
13.5.2 Household and neighbourhood noise
13.5.3 Environmental noise
13.6 Noise legislation and regulation
13.6.1 Occupational noise
13.6.2 Environmental, neighbour and neighbourhood noise
13.6.3 Building and planning guidelines
13.6.4 Noise abatement zones
13.6.5 Night-time noise
13.6.6 Road traffic
13.6.7 Loudspeakers and burglar alarms
13.6.8 Handling noise nuisance
13.7 Light as a pollutant
13.8 Measuring light pollution
13.9 Light pollution and health
13.10 Case study – Noise pollution in Kolkata
13.10.1 The major sources
13.10.2 Health impacts
13.10.3 Mitigation measures
References and further reading resources

14 Air quality standards and legislations

FOR REFERENCE PURPOSES ONLY

14.1 Why do we need air quality standards?
14.1.1 Estimation of standards
14.2 UK air quality legislation
14.2.1 Background
14.2.2 UK National Air Quality Strategy
14.2.2.1 Additional measures
14.2.3 Local air quality management
14.3 EU air quality legislation
14.4 United Nations Commission for Europe
14.5 World Health Organisation
14.5.1 Exceedances
14.5.2 Uncertainty
14.6 EU industrial emissions legislation
14.7 EU vehicle emissions
14.7.1 Emissions testing cycles
14.7.1.1 The ECE15 + EUDC test cycle
14.7.1.2 Real driving emissions testing
14.7.2 EU emissions legislation
14.8 US legislation
14.8.1 Background
14.8.2 Hazardous air pollutants
14.8.3 US vehicle emissions
14.8.3.1 US drive cycles
14.8.3.2 US cars and light-duty vehicles
14.8.4 Vehicle emissions in California
14.8.5 US locomotives
14.8.6 National parks and wilderness areas
14.9 Legislation in the Asian region
14.9.1 National standards
14.9.2 Vehicle emissions regulations in Asia
14.10 Air pollution information systems
14.10.1 Air quality indices
14.10.1.1 UK Daily Air Quality Index
14.10.1.2 Indian National Air Quality Index
14.10.1.3 Pollutant Standards Index
14.10.2 Headline indicator
14.11 Case study – Local Air Quality Management
14.11.1 Background
14.11.2 Recommended methodology
14.11.3 Limitations of the local Air Quality Management approach
References and further reading resources

FOR REFERENCE PURPOSES ONLY

15 Air quality experiments

15.1 Experiment I: Atomic absorption spectrometry
15.1.1 Introduction to experiment
15.1.2 Experimental procedure
15.1.3 Report generation
15.1.3.1 Issues to consider for your practical report
15.2 Experiment II: Colorimetric analysis for nitrogen dioxide
15.2.1 Introduction to experiment
15.2.2 Experimental procedure
15.2.2.1 Preparation of absorbing reagent
15.2.2.2 Sampling procedure
15.2.2.3 Calibration procedure
15.2.2.4 Calculation
15.2.3 Report generation
15.2.3.1 Issues to consider for your practical report
15.3 Experiment III: Colorimetric analysis for ozone
15.3.1 Introduction to experiment
15.3.2 Experimental procedure
15.3.2.1 Preparation of absorbing reagent (1% KI in 0.1 m phosphate buffer)
15.3.2.2 Preparation of iodine stock solution (0.025 M I_2)
15.3.2.3 Preparation of M I_2 solution for calibration
15.3.2.4 Sampling procedure
15.3.2.5 Calibration procedure
15.3.2.6 Calculation
15.3.3 Report generation
15.3.3.1 Issues to consider for your practical report
15.4 Experiment IV: Spectrophotometric method for sulphur dioxide
15.4.1 Introduction to experiment
15.4.2 Experimental procedure
15.4.2.1 Sampling
15.4.2.2 Calibration procedure
15.4.2.3 Calculations
15.4.3 Report generation
15.4.3.1 Issues to consider for your practical report
15.5 Experiment V: Colorimetric analysis for carbonyls
15.5.1 Introduction to experiment
15.5.2 Experimental procedure
15.5.2.1 Sampling of ambient air
15.5.2.2 Storage of samples

FOR REFERENCE PURPOSES ONLY

15.5.2.3 Elution of samples
15.5.2.4 HPLC configuration and sample analysis
15.5.2.5 Calibration procedure
15.5.2.6 Efficiency and interference studies
15.5.2.7 Calculations
15.5.3 Report generation
15.5.3.1 Issues to consider for your practical report
15.6 Experiment VI: Ambient particulate matter analysis
15.6.1 Introduction to experiment
15.6.2 Experimental procedure
15.6.2.1 Calculations
15.6.3 Report generation
15.6.3.1 Issues to consider for your practical report
15.7 Experiment VII: Purge and trap analysis for VOCs
15.7.1 Introduction to experiment
15.7.2 Experimental procedure
15.7.2.1 Calculation
15.7.3 Report generation
15.7.3.1 Issues to consider for your practical report
References and further reading resources

Review questions
Index

FOR REFERENCE PURPOSES ONLY

Preface

Evidence builds that dirty air causes Alzheimer's and dementia (doi:10.1126/science.aal0656). Many readers may probably wonder why the modern world could not yet grapple with the issue of air pollution in this era of *Internet of Things*. While air pollution has been with us since the first fire was lit, different aspects have been important at different times. Although the natural sources of air pollution, such as volcanoes, dust storms, forest fires, and so on, have reduced in frequency over the last century, these have been replaced by more intense and widespread anthropogenic sources, such as industrial and transport-related combustion, with considerable influence on the global environment. In many countries with ambitious economic growth targets and rapidly expanding surface and air transportation, largely fed on fossil resources, the acceptable levels of air pollution have been transgressed, resulting in an urban skyline characterised by smog and dust clouds. The UK particulate matter air pollution episode of spring 2014 was widely associated in the local media with a Saharan dust plume; in early 2017, Beijing saw the longest air pollution episode of this century so far; New Delhi witnessed its worst air quality in November 2016 triggering emergency measures; the air quality in Sydney hit an all-time low in May 2016; and episodic air quality degradation has been reported in multiple cities in central and southern Chile during the austral winter every year.

According to the 2015 UN World Population Ageing Report, by 2050 over 20% of humans will be aged 80 and above. There is now a growing body of literature linking air pollution with short- and long-term health effects on vulnerable populations, including the elderly and young children. On the small scale, point-source releases of individual pollutants can cause localised responses ranging from annoyance to physical injury. In urban areas, high concentrations of gases and particles from coal combustion and, in more recent decades, motor vehicles have produced severe loss of air quality and significant health effects. On a regional scale, tropospheric ozone formation and acid deposition have been the major threats. Emissions of carbon dioxide and other radiative active gases, together with stratospheric ozone depletion, represent planet-scale assaults on the quality of our atmospheric environment. In the Western world, stringent environmental legislation has enabled us to overcome the erstwhile *conventional* air pollution problems of foul and sooty skylines reminiscent of the Industrial Revolution. In addition, growing awareness of sustainable development has also contributed to reductions in aerial emissions of noxious

FOR REFERENCE PURPOSES ONLY
pollutants. In 2017, the United Kingdom and France declared outright bans on sales of petrol and diesel cars from 2040; several other countries are expected to follow suit. It may be said that the lesson has been learned by a *few*, but in order to restore air quality that we need for our very survival, the extent of the crisis has to be appreciated and addressed by the population at large.

The fourth edition of *Air Pollution: Measurement, Modelling and Mitigation* is designed to cover the whole gamut of air pollution issues from a quantitative standpoint. This revised edition has brought the information up to date with changes in legislation and air pollution science. Chapter 1 provides a holistic overview of air pollution for general reading, followed by more specialised contents on the sources – starting with Chapters 2 and 3 dealing exclusively with gaseous and particulate air pollutants, respectively. Chapter 4 covers larger, stationery area sources; mobile sources, which have been a major threat to local air quality for the past decade, are specifically addressed in Chapter 5. Issues pertaining to emerging issues in ambient air quality and indoor air are presented in Chapters 6 and 7, respectively. The fundamentals of meteorology and air pollution modelling are covered in Chapter 8. This field is rapidly picking up with progress in numerical and computational efficiency, and the chapter mainly introduces more recent advancements, capturing information on some of the established methods. Chapter 9 deals with air pollution control and mitigation, with extensive coverage on the industrial and ambient pollution control measures, both currently practiced and forthcoming. The second part of Chapter 9 is dedicated to a growing body of information on ambient air pollution mitigation approaches, specifically the role of green infrastructure interventions. Chapter 10 presents comprehensive coverage of air pollution impacts on human health, plants, animals, materials and visual range. Chapter 11 deals with emerging issues on air pollution and climate change, which is followed by a discussion of air pollution impacts on ozone in Chapter 12. This chapter now brings together the fundamentals of the origins and transformation of ozone in both the troposphere and stratosphere and its impact on humans. Chapter 13 presents new materials on noise and light pollution, which is an emerging issue in many urban areas around the world. The effects of pollutants on the environment have led to a wide variety of standards and legislation for their control, and these are presented in Chapter 14. Sampling and assessment techniques for some common air pollutants are included in Chapter 15. This is followed by a list of intuitive and more probing Review Questions, which can be used by readers to assess their learning.

In this revised edition, air pollution has been acknowledged as an international issue. We have provided additional material on the emerging trends from the developing and fast-growing economies while retaining the original focus of the previous editions on the issues in Europe and the United States. Each chapter contains a list of Further Reading Resources comprising research articles and reports, encouraging readers to pursue more in-depth coverage on any particular issue of their interest.

This book is written in an easy reading style with a target audience having varied levels of interest in air pollution issues, mainly university students with a wide range of academic

FOR REFERENCE PURPOSES ONLY

backgrounds at both the undergraduate and post-graduate levels. We hope it will be a useful learning resource for our readers!

Abhishek Tiwary
Ian Williams

FOR REFERENCE PURPOSES ONLY

Authors

Abhishek Tiwary is a Senior Lecturer in the Faculty of Engineering and Environment at Northumbria University, United Kingdom, and a former Marie Curie Senior Fellow at the University of Southampton, UK. Within the broad remit of Engineering Sustainability, he specializes in environmental feasibility of Renewable Energy Systems and Nature-Based Engineering for Pollution Control.

Ian Williams is a Professor in Engineering and the Environment at the University of Southampton. He is also Head of the Centre for Environmental Studies and specializes in Environmental Pollution and Resource Management.

Dedicated to our family for all their support and motivation.

FOR REFERENCE PURPOSES ONLY

Chapter 1

Overview of air pollution

1.1 WHAT IS AIR POLLUTION?

Our Earth is uniquely gifted with an envelope of chemicals that enables life-supporting activities – commonly known as *air*. At least 3000 different chemicals have been identified in air samples. However, it can safely be assumed that the sum total of these chemicals is at least equal to those that have been originally produced on the Earth, plus additional ones formed by their subsequent reactions.

Air pollution is defined as 'the presence of substances in the atmosphere that can cause adverse effects to man and the environment'. It is a term used to describe any unwanted chemicals or other materials that contaminate the air we breathe, resulting in the reduction of its life-supporting qualities (commonly referred to as *air quality*). In principle, an air pollutant is any chemical species that exceeds the concentrations or characteristics of the natural constituents of air (discussed in Section 1.5.2). However, strictly speaking, a pollutant is defined as a substance that is potentially harmful to the health or well-being of human, animal or plant life, or to the ecological systems.

Pollution (in the general sense) was defined in the Tenth Report of the Royal Commission on Environmental Pollution as:

> The introduction by man into the environment of substances or energy liable to cause hazard to human health, harm to living resources and ecological systems, damage to structure or amenity or interference with legitimate use of the environment.

This is a very broad definition that includes many types of pollution that we shall not cover in this book, yet it contains some important ideas. Note that by this definition, chemicals such as sulphur dioxide from volcanoes or methane from the decay of natural vegetation are not counted as pollution, but sulphur dioxide from coal-burning or methane from rice-growing *are* pollution. Radon, a radioactive gas that is a significant natural hazard in some granitic areas, is not regarded as pollution as it does not arise from people's activities. The

FOR REFERENCE PURPOSES ONLY

boundaries become fuzzier when we are dealing with natural emissions that are influenced by our actions – for example, there are completely natural biogenic emissions of terpenes from forests, and our activities in changing the local patterns of land use have an indirect effect on these emissions. Air pollution, as discussed in this book, is the solid, liquid or gaseous material emitted into the air from stationary or mobile sources, moving subsequently through an aerial path, and perhaps being involved in chemical or physical transformations before eventually being returned to the surface. The material has to interact with something before it can have any environmental impacts. This interaction may be, for example, with other molecules in the atmosphere (photochemical formation of ozone from hydrocarbons), with electromagnetic radiation (by greenhouse gas molecules), with liquid water (the formation of acid rain from sulphur dioxide), with vegetation (the direct effect of ozone), with mineral surfaces (soiling of buildings by particles) or with animals (respiratory damage by acidified aerosol). Pollution arising from human activities is called *anthropogenic*, while those having other natural origins (animals or plants) is said to be *biogenic*. Air pollution has been identified as a major problem in modern society, although in its conventional form of smoke and fumes, its origins date back to the Middle Ages, being closely associated with the Industrial Revolution and the use of coal. Originally, air pollution included only substances from which environmental damage was anticipated because of their toxicity or their specific capacity to damage organisms or structures. However, in the last decade, the scope has been widened to include substances such as chlorofluorocarbons, ammonia or carbon dioxide that have more general environmental impacts. Table 1.1 provides the most recently updated list of local and transboundary air pollutants along with the details of the international and legislative directives that regulate them in the UK. Most of these standards and the legislation are described in greater detail in Chapter 14.

In recent years there has been huge focus on nitrogen oxides (NO_x) – a combination of two gases, nitrogen dioxide (NO_2) and nitric oxide (NO). In fact, it is the NO_2 that affects human health (hence, subjected to more stringent statutory emission limit guidelines set by the European Union, World Health Organization [WHO], United States Environmental Protection Agency [USEPA], etc., as discussed in Chapter 14). The directly emitted NO_2 (also known as *primary NO_2*) immediately influences the ambient concentration. However, our atmosphere is a dynamic lab and the NO eventually reacts with ozone (O_3) to form additional NO_2 (known as *secondary NO_2*), thereby increasing their effective human health concerns.

Table 1.1 Local and transboundary air pollutants along with their regulatory international and UK legislative directives

Air pollutants	*Directive*
PM – PM_{10}, $PM_{2.5}$, NO_x, O_3, SO_2, PAHs, Benzene, 1,3-butadiene, CO, Pb	Air Quality Strategy
SO_2, NH_3, NO_x, NMVOC	National Emissions Ceilings Directive (NECD)

FOR REFERENCE PURPOSES ONLY

SO_2, NH_3, NO_x, NMVOC, Heavy Metals, POPs	Convention on Long-Range Transboundary Air Pollutants (CLRTAP)
91 compounds including: CH_4, CO, CO_2 HFCs, N_2O, SF_6, NH_3, NMVOC, NO_x, PFCs, SO_x, CFCs, As, Cd, Cr, Cu, Hg, Ni, Pb, Zn, PM_{10}, Benzene, HCl, HF, PAHs, PCBs, PCDD, PCDF, Gamma HCH, PCP, HCB	European Pollutant Release and Transfer Register (E-PRTR), which succeeds the European Pollutant Emission Register (EPER)
SO_2, NO_x, CO, VOCs, metals, dust, asbestos, chlorine and its compounds	Integrated Pollution Prevention and Control (IPPC)
SO_x, NO_x, PM	Large Combustion Plants Directive (LCPD)
Dust (PM), HCl, HF, SO_2, NO_x, Heavy metals, Dioxins and Furans, CO	Waste Incineration Directive (WID)
VOCs	Solvent Emissions Directive
VOC	Paints Directive
SO_2	The Sulphur Contents of Liquid Fuels Directive
VOC	Petrol vapour recovery
SO_2, NO_x, PM, Lead, Benzene, CO, Ozone, PAH, Cadmium, Arsenic, Nickel, Mercury	EU Air Quality Directives

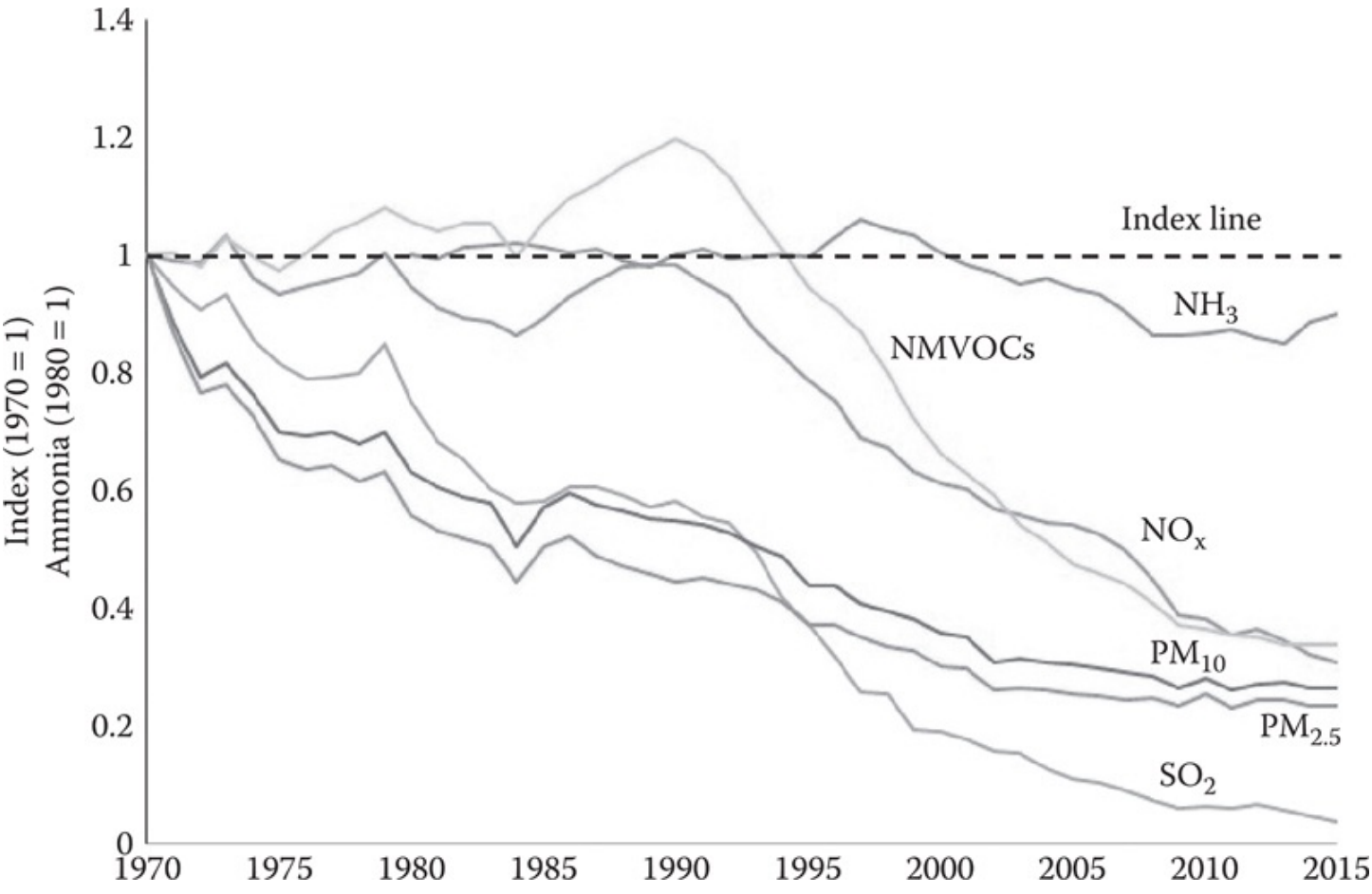

Figure 1.1 Historical trends in UK emissions of key air pollutants between 1970 and 2015. (From NAEI, UK emissions of air pollutants, National Atmospheric Emissions Inventory, http://naei.beis.gov.uk/overview/ap-overview, 2016.)

In the UK, there has been long-term decrease in emissions of all of the air pollutants

FOR REFERENCE PURPOSES ONLY

compared to the historical releases during the second half of the twentieth century. Figure 1.1 presents historical trends in the overall emissions of a number of air pollutants in the UK between 1970 and 2015 in terms of a reference index, which is acquired by normalising the reported annual totals by the UK government with the reference emissions for 1970 (except for NH_3, which uses 1980 as a reference year). More detailed, source-specific emissions for different pollutants are provided later in this chapter, and in Chapters 2 and 3, exclusively covering the gaseous and particulate emissions, respectively. All except NH_3 emissions are currently reducing, with significant reduction achieved for SO_2 in the last two decades. NH_3 seems to be on the rise from 2014 onwards and this is concerning. In Chapter 6, the modelled global nitrogen budget up to 2100 indicates this to be an increasing threat to human health, ecosystems and climate. As nitrogen cycling is highly sensitive to ambient temperature, substantial increase in N-emissions is projected in the coming decades as the climate warms. Consequentially, the relative contribution of nitrogen compounds in ambient aerosols is going to significantly increase, given the lowering of the sulphur emissions otherwise forming an important constituent of inorganic sulphate aerosols.

There are many additional air pollutants that may be important in particular situations. Fluorine is produced as gaseous HF by chemical processes such as fertiliser production and steel manufacture. It accumulates in grass and causes the bone disease fluorosis in herbivores. *Heavy metals* such as arsenic, cadmium, chromium, manganese, mercury, nickel and vanadium are produced from several anthropogenic activities. Airborne heavy metals account for significant fractions of the total heavy metal content of arable soils. The United Nations Economic Commission for Europe (UNECE) Protocol on Heavy Metals targets three particularly harmful substances – lead, cadmium and mercury. The protocol aims to cut emissions from industrial sources (iron and steel industry, non-ferrous metal industry), combustion processes (power generation, road transport) and waste incineration. There are limit values for these heavy metals and the protocol requires employment of the *Best Available Technique (BAT)* for achieving emission reduction via fitting special filters or scrubbers for combustion sources (discussed in Chapter 9). It also requires countries to phase out leaded petrol. Formaldehyde is an irritant chemical released from, for example, urea formaldehyde cavity wall insulation. Asbestos covers a range of mineral fibres released from building thermal insulation and brake linings. Inhalation of the fibres can result in potentially fatal lung disorders.

1.2 HISTORICAL PERSPECTIVES

The composition of the atmosphere has fascinated natural philosophers since the earliest times – the Greeks and the Hindus have regarded air as one of the four elements (fire, earth, water and air). It was not until the late seventeenth century, when Robert Boyle described air as a *confused aggregate of effluviums*, that air was first regarded as a mixture. Even then, whilst oxygen and nitrogen were known to be the principal components of air, the

FOR REFERENCE PURPOSES ONLY

question remained as to whether or not it was a mixture. Sir Humphrey Davy (1778–1829) thought that air was a compound, partly because if it were not a compound, then the heavier gas (oxygen) should sink below the lighter one (nitrogen) and, therefore, oxygen should be found in slightly higher concentrations at the very bottom of the atmosphere. The strength of the mixing process – caused by atmospheric turbulence – was not appreciated.

The development of our understanding that air is a mixture, as opposed to a compound, was based on the following reasons:

- The ratio of oxygen to nitrogen does vary, just slightly, from place to place.
- If air was a compound, the formula would be $N_{15}O_4$, which is very unlikely.
- The physical properties of air are identical to those of the appropriate mixture of nitrogen and oxygen (which make up about 99% of air).
- It is possible to separate the nitrogen and oxygen, which would not be possible if air were a compound.
- There is no volume change or heat release on mixing oxygen and nitrogen, which suggests that a compound is not formed.

Of course, we now know that air is a mixture of many gases, and not just oxygen and nitrogen. Hippocrates, the ancient Greek physician, noticed the harmful effects of breathing polluted air over 2000 years ago. By the thirteenth century, air pollution in London was so bad that a commission was established to address the problem. However, at this time, air pollution was a local issue, being generated by hearths and furnaces. More recent problems caused by air pollution range from the local to the global scale and occur on a variety of time scales. In 1930, over 60 people died in the Meuse Valley, Belgium, due to extremely high levels of industrial air pollution. In 1948, in Donora, Pennsylvania (USA), 20 deaths and nearly 6,000 air pollution-related illnesses were recorded amongst a total population of just 14,000 as a consequence of industrial air pollution. In December 1952, several thousand people died as a result of a *killer fog* that settled over London.

1.3 CLASSIFICATION OF AIR POLLUTANTS

Air pollutants may be classified in many ways but typically take either gaseous or particulate forms (respectively covered in Chapters 2 and 3). Unwanted chemicals or other materials can enter the atmosphere either from natural sources, such as volcanoes, dust storms and forest fires, or be from human-made, known as anthropogenic, sources. The anthropogenic sources can be subdivided into stationary or point sources and area or mobile (linear) sources (respectively covered in Chapters 4 and 5). Point sources include stacks, flues and chimneys. Area sources include groupings of usually small sources spread over an area, such as an industrial complex like a steel works or the combined emissions from domestic heating in a town, landfills, and so on. Mobile sources include cars, aeroplanes, ships and trains. Line sources are pollution that emanate from a linear direction; the most

obvious linear sources are from roads and aircraft.

Naturally occurring pollution includes particulates such as pollen and dust clouds. Volcanic eruptions can produce dust clouds of fine ash, as was recently seen when the Icelandic volcano Eyjafjallajökull erupted on 14 April 2010. Volcanic dust clouds can also contain potentially toxic material, such as crystalline silica. The ash cloud that formed from Eyjafjallajökull drifted across Europe during 2010, causing many countries to close their airspace and prevent aeroplanes from flying. The volcanic cloud posed a significant safety threat to aircraft – if planes flew through the ash cloud, particles in it could damage the engines and even cause them to fail completely.

As most people spend about 90% of their time indoors, many common indoor air pollutants effect our health. These include CO and NO_2 from faulty gas heaters and cookers, CO and benzene (C_6H_6) from cigarette smoke, and volatile organic compounds (VOCs) from synthetic furnishings, vinyl flooring and paints. There are also biological pollutants such as dust mites and mould.

We can also divide air pollutants into regulated and unregulated, based on their treatment by environmental agencies in the United States, the European Union and major Asian countries. The major regulated air pollutants are

- Sulphur dioxide (SO_2).
- Nitrogen oxides (NO_x).
- Carbon monoxide (CO).
- Trace metals such as lead (Pb), cadmium (Cd) and platinum (Pt).
- Organic compounds such as benzene and polycyclic aromatic hydrocarbons (PAHs).
- Photochemical oxidants such as ozone (O_3) and peroxyacetyl nitrates (PANs).
- Particulate matter includes a wide range of sizes (typically between 0.01 and 100 μm) and may be composed of organic or inorganic materials (or mixtures). The types of particulate matter monitored include *total suspended particulates*, smoke and particles of a specific size, such as PM_{10} and $PM_{2.5}$.

The health and environmental consequences of air pollutants arise from the following three processes:

- Emission of pollutants from a source
- Transport of pollutants
- Deposition of pollutants

1.3.1 Types of air pollutants

Here we develop a classification of air pollutants based on general sources and effects. Our first classification is based on the way in which pollutants are formed in the atmosphere. *Primary pollutants* are those which are emitted directly into the atmosphere – for example,

FOR REFERENCE PURPOSES ONLY

CO comes directly from the incomplete combustion of fossil fuels in motor vehicles, and SO_2 is emitted from power stations and industrial plants. *Secondary pollutants* are formed in the air as a result of chemical reactions with other pollutants and atmospheric gases – for example, ozone is generated by photochemical reactions within the atmosphere.

Note that pollutants do not necessarily fall into one or other of these categories – some can be both primary and secondary pollutants. For example, NO_2 is emitted directly into the atmosphere from power stations and vehicle exhaust, and some are also formed from the oxidation of NO in the air.

The distinction between the two types is important for understanding air pollution and devising appropriate control strategies. For primary pollutants, there is likely to be a proportional relationship between emissions and ambient concentrations. However, with a secondary pollutant, reducing emissions of its precursors may not necessarily lead to a proportional reduction in its ambient concentrations – indeed, in some circumstances, it may actually lead to an increase in concentrations.

1.3.2 Sources of air pollutants

Definite sources of air pollutants can be identified and these emission sources may be classified as either

- *Natural* (*biogenic*): Including volcanic eruptions, sand storms, lightning and forest fires, or
- *Human-made* (*anthropogenic*): The major source being the combustion of fossil fuel for energy, particularly in power stations and motor vehicles. There are, though, many non-combustion-related sources, including industrial processes, coal mining, domestic and industrial solvent use, natural gas leakage in the national distribution network, and landfill. Non-combustion sources are particularly important for VOCs and methane.

Anthropogenic pollution sources may be further sub divided according to their geographical distribution. There are three basic types:

- *Point sources*: Large, geographically concentrated emitters whose emission rates are large enough to be significant by themselves, even if no other sources are present, such as (coal-fired) power stations, steel mills, oil refineries, pulp and paper mills, and so on.
- *Area sources*: Collections of small geographically dispersed emitters that are not significant individually but are important collectively, such as residential and commercial areas, and also including agricultural emissions.
- *Line sources*: A collection of relatively small sources that are distributed roughly uniformly along a line, such as a motorway or industries along a major river, a main road or railway line.

FOR REFERENCE PURPOSES ONLY

The distinction between line and area sources is somewhat vague, with a busy city street, for example, being classified as either an area or a line source.

1.3.3 Source emission data

In addition to expressing them as concentrations, pollution levels can be grouped according to their emission from the various different sources. Emission data may be used in two ways:

- To identify the main sources of individual pollutants
- To estimate levels of pollutants where such levels cannot easily be measured on their own – in which case mathematical models based on emission data are employed

The variety of air pollution sources makes estimating the emissions of specific atmospheric pollutants a demanding and time-consuming process. The basis of the process is the systematic compilation of detailed information on pollutant emissions in a given area in the form of an *emissions inventory*. An air pollutant emissions inventory is a schedule of the sources of an air pollutant or pollutants within a particular geographical area (see Chapter 8 for more details). The inventory usually includes information on the amount of the pollutant released from major industrial sources, as well as average figures for the emissions from smaller sources and from transport throughout the area. By identifying the sources of air pollutants, an atmospheric emissions inventory can be used as an aid in interpreting air quality measurements.

In an emissions inventory, data are collected for the three types of sources (line, area and point) within the selected geographical area. Clearly, it is impractical to measure every emission source in a large area. The majority of emissions are therefore estimated from other local information such as fuel consumption figures, vehicle kilometres travelled or some other activity relating to pollutant emissions. *Emission factors* are then applied to the activity data in order to estimate the likely emissions.

An emission factor is a number that represents the relationship between the mass of a given pollutant emitted from a particular source and the given amount of raw material processed. This may be expressed as:

$$\textbf{Activity rate} \times \textbf{Emission factor} = \textbf{Emission rate}$$

Example 1.1

Particulate elemental carbon (PEC) is an important urban pollutant generated by diesel vehicles. In order to estimate the mass of PEC emitted from diesel vehicles in London in a given year (Q), the following equation may be used:

FOR REFERENCE PURPOSES ONLY

Amount of fuel consumed in London for Year Q × PEC emission factor (% by mass) = Amount of PEC emitted

50 kT × 0.2% = 1000 T of PEC emitted

1.3.3.1 Emission units

Pollutant emissions are presented using a number of different mass and/or toxicity units, according to convenience, with specific reporting protocols, including the following:

- NO_x emissions are quoted in terms of NO_x as NO_2.
- SO_x emissions are quoted in terms of SO_x as SO_2.
- PCDD and PCDF are quoted in terms of mass, but account for toxicity (the I-TEQ scale).
- Pollutant emissions are quoted as mass of the full pollutant, unless otherwise stated; for example, NH_3 emissions are mass of NH_3 and not mass of the N content of the NH_3.

1.3.4 What is smog?

Smog can be formed during either summer or winter months respectively arising due to oxidising and reducing chemistry of airborne pollutants under adverse weather and seasonal conditions.

Winter smog is formed by mixing of fog with pollutant smoke during cold periods. It forms when the ground cools rapidly, often on clear calm winter nights. It is composed of NO_x, SO_x, O_3, smoke and other particulates trapped at ground level when a thin layer of the atmosphere near the Earth's surface becomes cooler than the air above it (meteorologically termed as a *temperature inversion*). The atmospheric pollution levels of Los Angeles, Beijing, Delhi, Mexico City, Tehran and other cities have been found to be significantly increased by such inversion that traps pollution close to the ground. In cities like Delhi, smog severity is often aggravated by stubble burning in neighbouring agricultural areas. The smoke is mainly formed from the combustion of fuels. Normally, a hydrocarbon is burnt to produce carbon dioxide and water:

$$C_mH_n + O_{2(g)} \rightarrow CO_{2(g)} + H_2O_{(g)}$$

Smoke is also composed of unoxidised/reduced fuel particles and carbon monoxide and oxidised impurities, such as sulphur dioxide. The sulphur dioxide is soluble in water and so it dissolves in the water droplets of the fog (Andrews et al., 2004). Other contaminants in

the smoke, for example, iron (Fe) or manganese (Mn), then catalyse the reaction of dissolved sulphur dioxide to sulphuric acid:

$$SO_{2(g)} + H_2O_{(l)} \leftrightarrow H^+_{(aq)} + HSO_{3^-(aq)}$$

$$2HSO_{3^-(aq)} + O_{2(aq)} \rightarrow 2H^+_{(aq)} + 2SO_{4^{2-}(aq)}$$

The sulphuric acid makes the smoke a very low pH, which has many effects. One of these is to increase the size of the water droplets as it has a great affinity for water; this creates a thicker fog. The addition of smoke to the fog to make *smog* can increase the thickness of the fog in two additional ways. First, the addition of material (the smoke) can increase thickness. Second, the more pollution in the fog, the more nuclei for the water droplets to condense around. This increases the number of small fog droplets. All these factors, the collecting caused by light winds and valleys, the presence of sulphuric acid, the addition of material and the creation of more nuclei, help to make the fog thicker, which helps the smog to persist through the daylight when normally the sun would cause the water droplets to evaporate.

Photochemical smog (also known as *summer smog*) is another form of secondary pollution caused by chemical reactions in the exhaust fumes of cars in the presence of sunlight on warmer days. Summer smog was first identified as an air pollution problem in the 1950s in the Los Angeles area of California – high concentrations of ozone (several hundred parts per billion [ppb]) were formed in the air, causing breathing and eye irritation and visible damage to vegetation. However, similar episodes of summer smog have now become a dominant phenomenon in a large number of Asian megacities, including Beijing and New Delhi. The exact formation mechanisms turned out to be very complex, involving reactions between hundreds of different hydrocarbons, radicals, NO and NO_2. Hence, a typical summer smog is a mixture of NO, NO_2 and O_3 in concentrations and proportions that depend not only on the source strengths of the precursors but also on the availability of the reactive components, mixing conditions, life histories and weather conditions. The NO_2 concentration peaks in mid-morning, followed by build-up of ozone in the early afternoon, resulting in patterns of the summer smog formation. The main requirements for the formation of photochemical smog are strong sunlight, stable meteorological conditions and the presence of the chemicals listed earlier. Photochemical smog is characterised by brownish, hazy fumes in the atmosphere. It can cause eye and nose irritation as it dries out the protective membranes of the nose and throat and interferes with the body's ability to fight infection, increasing susceptibility to illness.

The smog that occurred in London (discussed in Section 1.9) should not be confused with photochemical smog. Photochemical smog occurs in warm weather and peaks around midday, whereas the winter smog occurs during early winter mornings. Photochemical smog is oxidising whereas London smog is reducing. Most important, photochemical smog does not occur in the presence of fog.

FOR REFERENCE PURPOSES ONLY

1.4 WHY DOES AIR POLLUTION NEED ATTENTION?

Air pollution has implications for both human and plant well-being and climate change (respectively discussed in Chapters 10 and 11). However, totally unpolluted air is probably impossible to obtain anywhere habitable on the Earth in a modern industrial society. The range of health effects is broad, but they are predominantly associated with respiratory and cardiovascular systems. On the other hand, collateral impacts of managing air pollution on climate change, specifically the complex interactions between emissions from initiatives for reducing tropospheric ozone and particulate matter, resulting in mixed cooling and warming effects, and vice versa, have been observed (they are described in more detail in Chapter 11).

Air pollution can cause both immediate (known as *acute*) symptoms and long-term (known as *chronic*) effects (see Figure 1.2 and more details in Chapter 10). The entire population is affected, but differences in health and age may make some people more susceptible. The risk has been shown to increase with exposure, and even relatively low concentrations of air pollutants have been related to a range of adverse health effects. The low end of the range of concentrations at which adverse health effects have been demonstrated is not much above the background concentration. Acute symptoms include eye, nose and throat irritation; aching lungs; bronchitis and pneumonia; wheezing; coughing; nausea and headaches. Chronic effects include heart disease; chronic obstructive pulmonary disease; genotoxic effects such as leukaemia, lymphomas and lung cancer; and airway sensitivity disorders such as asthma. There is growing evidence on the health risks from exposure to fine and ultrafine particles that accelerate cognitive aging and increase the risk of Alzheimer disease and other forms of dementia. According to a WHO assessment, an estimated 6.5 million deaths (11.6% of all global deaths) are associated with indoor and outdoor air pollution together (WHO, 2016). By reducing air pollution levels, the global burden of these diseases, as well as reproductive and neurodevelopmental disorders, can be reduced. Serious respiratory disease-related problems have been identified for both indoor and outdoor pollution in major cities of several countries. It has been estimated that in India alone, about 500,000 premature deaths are caused each year by indoor air pollution for mothers and their children who are under 5 years of age. The terrorist attack on New York in 2001 had significant impacts on air quality, most visibly in the form of a huge dust cloud that spread rapidly after the Twin Towers of the World Trade Centre collapsed. Thousands of tonnes of debris resulting from the collapse of the Twin Towers contained more than 2500 contaminants, including known carcinogens. Subsequent debilitating illnesses among rescue and recovery workers are said to be linked to exposure to these carcinogens. The USEPA estimated that the return to status quo air quality in the affected parts of New York City before 11 September 2000, levels took until June 2002.

FOR REFERENCE PURPOSES ONLY

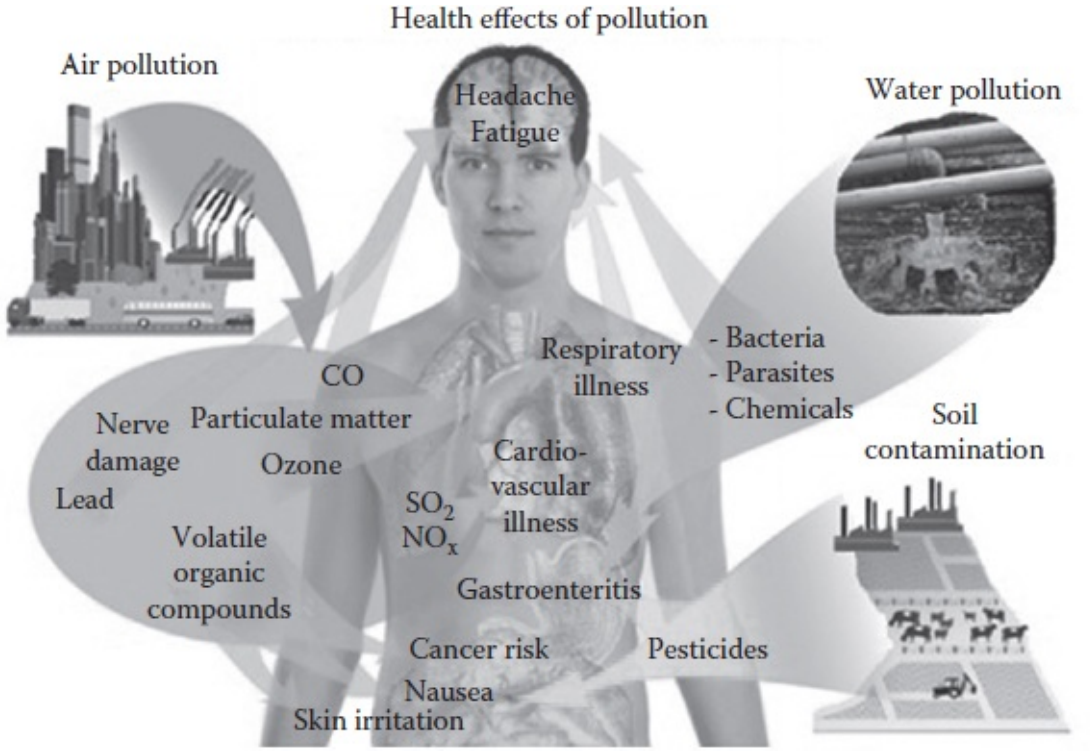

Figure 1.2 Summary of health effects of pollution. (From www.commons.wikimedia.org.)

Fine particulate matter, nitrogen dioxide and ground-level ozone are the main threats to human health from air pollution in Europe. Fine particulate matter includes dust and soot that are suspended in, and move with, the air. Particle pollution can cause eye, nose and throat irritation and can also be carried deep into the lungs, where they can cause inflammation and a worsening of heart and lung diseases. The EU's Clean Air for Europe (CAFE) programme estimated that a total of 348,000 premature deaths per year in Europe are due to exposure to fine particles.

Ozone is formed in the atmosphere by photochemical reactions in the presence of sunlight and precursor pollutants, such as the oxides of nitrogen (NO_x) and VOCs. Ozone occurs in two layers of the atmosphere. When ozone forms in the stratosphere (between 6 and 30 miles above the surface of the Earth) it protects life from the sun's harmful ultraviolet (UV) rays. However, when it is in the troposphere (from ground level extending to about 6 miles up), it is a very harmful air pollutant (discussed in Chapter 12). It is the main ingredient of urban smog.

Breathing ozone can trigger a variety of health problems including chest pain; coughing and wheezing; eye, nose and throat irritation and congestion. It can worsen bronchitis, emphysema and asthma. It can also reduce lung function and inflame the linings of the lungs. Repeated exposure may cause permanent lung tissue scarring. Difficulty in breathing is also experienced by healthy people when exposed to ozone pollution. Because ozone forms in hot weather, anyone who spends time outdoors in the summer may be affected, particularly children, workers and people exercising.

The ozone in the stratosphere is depleted by reactions with human-made chemicals

FOR REFERENCE PURPOSES ONLY

referred to as ozone-depleting substances (ODSs), including chlorofluorocarbons (CFCs), hydrochlorofluorocarbons (HCFCs), halons, methyl bromide, carbon tetrachloride and methyl chloroform. A reduction in the stratospheric ozone layer can cause increased amounts of UV radiation to reach the Earth. This can lead to more cases of skin cancer, cataracts and impaired immune systems.

If occupants of a building experience various ailments and illnesses characterised by headaches, respiratory problems and skin irritations, although no specific illness or cause can be identified, the building is described as having *sick building syndrome*. This is thought to be caused by indoor pollutants, micro-organisms or inadequate ventilation (discussed in Chapter 7). The *syndrome* tends to be associated more with office blocks than factories and is a temporary phenomenon that is relieved when the affected person is no longer inside the building. There is a particularly high incidence in certain types of buildings, especially offices which are sealed and mechanically ventilated or air-conditioned. Building-related illness describes symptoms of a diagnosable disease that can be linked to air pollution, such as Legionnaires disease. Possible causes are inadequate building ventilation, chemical contaminants and/or biological contaminants.

The effect of air pollution on plants can be seen in a variety of ways – from visible markings on the foliage to reduced growth and yield, or even to premature death of the plant. The level of injury depends on the concentration of the particular pollutant and other factors, such as the length of exposure, the plant species and its stage of development and the preconditioning of the plant, which make it either susceptible or resistant to injury. Some plants are more tolerant to air pollution than others. The London plane tree, for example, sheds its bark and therefore stops air pollution reaching the inner trunk of the tree. However, the short, stiff hairs shed by the young leaves and the dispersing seeds of the London plane are an irritant and can exacerbate breathing difficulties for people with asthma.

Certain pollutants, both from natural and anthropogenic sources, accumulate in the atmosphere and are known as greenhouse gases. These include water vapour, carbon dioxide, atmospheric methane, nitrous oxide, ozone and CFCs. Every day, sunlight strikes the Earth's surface and warms the Earth. Some of this heat is then radiated back towards space as infrared radiation. Greenhouse gases absorb some of this infrared radiation which get trapped into the atmosphere, causing the Earth to heat up. If it were not for naturally occurring greenhouse gases, the Earth would be a lot colder than it is now. However, extreme concentrations of greenhouse gases in the atmosphere will cause the Earth's temperature to rise, which is termed as *global warming* (discussed later in Chapter 11). The concentrations of these gases have increased dramatically since the Industrial Revolution. Estimates suggest that greenhouse gases may cause a gradual increase in the global surface temperature by 1.5°C–4°C by the middle of the twenty-first century, although the amount and timing of any temperature increases are speculative.

Certain types of air pollution, such as sulphur dioxide and nitrogen oxides, react with water, oxygen and other components in the air. The resulting precipitation is commonly

FOR REFERENCE PURPOSES ONLY

called *acid rain*. It can fall as rain, snow, fog and also as particles of dry material that settle to Earth. The precipitation is a mild solution of sulphuric and nitric acid. The wind can spread the acidic solution hundreds of miles; for example, much of the acid rain that falls in Scandinavia is caused by air pollution generated in the UK. Acid rain enters water systems and sinks into the soil. It makes lakes and streams acidic and causes them to absorb aluminium. This combination then makes waters toxic to crayfish, clams, fish and other aquatic animals. Acid rain robs the soil of essential nutrients and releases aluminium, which makes it hard for trees to take up water. Leaves and needles are also harmed by acids, which can also cause damage to buildings and structures. The only way to control acid rain is by reducing the release of the pollutants that cause it.

Air pollution can directly and indirectly affect animals. Direct methods include breathing in gases or small particles; eating particles in food, water or from grooming themselves; or absorbing gases through the skin. Earthworms and other soft-bodied invertebrates, or animals with thin, moist skin, are the ones mainly affected by absorbing pollution. Particulates can be especially dangerous when they contain certain metals (e.g. heavy metals), as they can build up to high concentrations in the body tissues of animals.

Indirect effects of air pollution include acid rain and global warming. Acid rain changes the acidity of the water that animals live in and drink from and can decrease the amount of trees that provide shelter, which both create serious problems for wildlife. Global warming, on the other hand, can potentially destroy habitats, cause birds to lay their eggs earlier than usual and force mammals to break their hibernation sooner.

In our complex and rapidly changing modern society, we have to decide what level of pollution is acceptable to us. There is a global debate on the levels of industrial compromise or cost we are prepared to accept to achieve an acceptable environmental quality, especially in our towns and cities where the majority of the world's population is now concentrated. In this book, we will focus mainly on regulated air pollutants, but clearly society has to consider all types of pollution simultaneously.

1.5 THE BASIC ATMOSPHERE

1.5.1 The origins of our atmosphere

What we experience today as our atmosphere is a transient snapshot of its evolutionary history. The planet Earth was formed around 4600 million years ago by the gravitational accumulation of relatively small rocks and dust, called planetesimals, within the solar nebula. There was probably an initial primordial atmosphere consisting of nebula remnants, but this was lost to space because the molecular speeds exceeded the Earth's escape velocity of 11.2 km s^{-1}. A combination of impact energy and the radioactive decay of elements with short half-lives raised the temperature of the new body sufficiently to separate heavier elements such as iron, which moved to the centre. The atmosphere of Earth derived primarily by thermal outgassing of volatile substances from virgin planetary

FOR REFERENCE PURPOSES ONLY

material during and subsequent to the formation of the planet. The volatile substances included water present in the ocean, nitrogen in the atmosphere, and carbon dioxide, now largely residing in the sediments as carbonate deposits. The same heating caused dissociation of hydrated and carbonate minerals with consequent outgassing of H_2O and CO_2. As the Earth cooled, most of the H_2O condensed to form the oceans, and most of the CO_2 dissolved and precipitated to form carbonate rocks. About one hundred times more gas has been evolved into the atmosphere during its lifetime than remains in it today. The majority of the remaining gases was nitrogen. Some free oxygen formed (without photosynthesis) by the photolysis of water molecules. Recombination of these dissociated molecules was inhibited by the subsequent loss of the hydrogen atoms to space (hydrogen is the only abundant atom to have a high enough mean speed to escape the gravitational attraction of the Earth). The effect of atomic mass makes a huge difference to the likelihood of molecules escaping from the Earth. The Maxwell distribution means that there is a most likely velocity, which is relatively low, and a long tail of reducing probabilities of finding higher speeds. For example, a hydrogen atom at 600 K (typical temperature at the top of the atmosphere) has a 10^{-6} chance of exceeding escape speed, while the corresponding value for an oxygen atom is only 10^{-84}. This process results in a steady attrition of lighter atoms. The first evidence of single-celled life, for which this tiny oxygen concentration was an essential prerequisite, is shown in the fossil record from around 3000 million years ago. Subsequently, the process of respiration led to a gradual increase in the atmospheric oxygen concentration. This in turn allowed the development of O_3 which is thought to have been a necessary shield against solar UV. Subsequent evolution of the atmosphere has been dominated by the balance between production and consumption of both CO_2 and O_2.

1.5.2 Natural constituents of air

There is a general misconception that air consists of *air molecules*, which is evidence of the spatial and temporal constancy of its properties that we take for granted. In fact, air consists of a number of constituent gases that have fairly constant average proportions, both at different horizontal and vertical positions and at different times. The typical composition of unpolluted, dry air at sea level is shown in Table 1.2. Note that the values given are for so-called *clean, dry air*, which is a hypothetical construct and excludes the small but exceptionally important amounts of particulate matter and water vapour. This composition has not changed much over time except for methane, nitrous oxide and carbon dioxide, which have increased significantly since the Industrial Revolution, and are still rising.

Nitrogen (N_2) is the most dominant gas in air. It is a primary outgassing product, which enters the biosphere (defined by Eduard Suess as ‘the place on Earth’s surface where life dwells’) by bacterial nitrogen fixation – a process that reduces N_2 to amino compounds and incorporates it directly into the living cell. The biosphere eventually

FOR REFERENCE PURPOSES ONLY

releases nitrogen to the atmosphere by anaerobic bacterial denitrification.

Oxygen (O_2), which is the second most abundant gas in air, is not a planetary outgassing product but a by-product of the assimilation of carbon dioxide (CO_2) by phytoplankton (photosynthesising microscopic organisms that inhabit the upper sunlit layer of almost all oceans and bodies of fresh water) and green plants. Oxygen gas has evolved over time in conjunction with the development of the biosphere. On a geological short time scale, the production and consumption of O_2 are nearly balanced; a small fraction of organic material escapes re-oxidation by incorporation in marine sediments. The present amount of atmospheric oxygen is understood to represent an excess over that used up in the oxidation of organic carbon and other reduced chemical compounds.

Table 1.2 The composition of dry, unpolluted air at sea level

Gas	*Volume (%)*	*Concentration (ppm or μL dm^{-3})*
Nitrogen	78.08	780,800
Oxygen	20.95	209,500
Argon	0.93	9,300
Carbon dioxide	0.038	385
Neon	0.0018	18.0
Helium	0.0005	5.2
Methane	0.00017	1.7
Krypton	0.00011	1.1
Nitrous oxide	0.00003	0.3
Hydrogen	0.00005	0.5
Ozone	0.000004	0.04

Carbon dioxide (CO_2) is readily absorbed by seawater. On a time scale of approximately 1000 years, atmospheric CO_2 is in equilibrium with that residing in the ocean. The majority of CO_2 released by thermal outgassing has entered sediments in the form of limestone deposits. The exchange of CO_2 with the biosphere via photosynthesis and re-oxidation of organic material occur on a time scale of 10–100 years. The increase of CO_2 in the atmosphere since the Industrial Revolution is caused by the combustion of fossil fuels that are taken from deposits of sedimentary organic carbon.

The *rare gases* in the atmosphere have resulted from planetary outgassing. The dominant isotope of *argon*, ^{40}Ar, is a product of the radioactive decay of potassium-40. *Trace gases* include all those gaseous components in the atmosphere that – by virtue of their low concentrations – do not affect the bulk composition of air. This makes it convenient to quantify the local abundance of a trace gas by its molar mixing ratio (the chemical amount fraction). If reference is made to dry air, the influence of the variability of water vapour on the bulk composition of air is eliminated, and the molar mixing ratio becomes independent

FOR REFERENCE PURPOSES ONLY

of changes in pressure and temperature. On the other hand, the presence of *radicals*, such as the *hydroxyl radical* (OH•), are customarily reported in terms of number concentration, although radicals undoubtedly also represent trace gases. Because *the major components of air are chemically rather inert, atmospheric chemistry is for the most part driven by trace gases*.

The concentrations of atmospheric *trace gases* can be shown to adjust to a steady state (a situation in which all state variables are constant in spite of ongoing processes that strive to change them) between the sources and sinks and their global distributions. For trace gases that are long-lived, with residence times of 2 years or longer, the general circulation of the atmosphere guarantees a fairly uniform mixing ratio. For trace gases that are short-lived, the mixing ratio is determined by the local sources and sinks, and it may undergo substantial variations. In this case, the global distribution of sources and sinks as well as advection (a transport mechanism of a substance or conserved property due to the atmosphere's bulk motion) with the winds becomes important.

The average molar mass of dry air can be found by summing the products of the proportions by volume and molar masses of its major components; that is,

$$\begin{aligned} M_a &= (0.781 \times 28.01) + (0.209 \times 32.00) + (0.0093 \times 39.95) \\ &\quad + (0.00037 \times 44.01) \\ &= 28.95 \text{ g mol}^{-1} \end{aligned}$$

Mixed into the quite uniform population of atmospheric molecules is a large range of additional materials that vary greatly in concentration both in space and time:

- *Sulphur dioxide* may be released directly into the atmosphere by volcanoes or formed as the oxidation product of the dimethyl sulphide released by oceanic phytoplankton.
- *Oxides of nitrogen* are created when anything burns.
- *Nitrous oxide* is emitted from the soil surface by bacterial denitrification.
- *Hydrogen sulphide* is produced by anaerobic decay.
- *Ammonia* is released from animal waste products.
- *Ozone* is formed in the stratosphere by the action of UV radiation on oxygen.
- *Ozone* is also found in the troposphere, via both diffusion down from the stratosphere and local natural photochemistry.
- *Volatile organic compounds* (VOCs) are emitted from many different species of vegetation, especially coniferous and eucalyptus forests.
- *Persistent organic pollutants* (POPs) are organic compounds of anthropogenic origin that do not readily break down in the environment. As a consequence of their long lifetime they are transported over long distances, can accumulate in the food chain and can cause chronic human health impacts.

FOR REFERENCE PURPOSES ONLY

- *Non-biogenic particles* are generated by volcanoes or entrainment from the soil.
- *Biogenic particles* include pollen, spores and sea salt.

We shall come back to these materials, and others, throughout this book when we consider them as pollutants rather than as naturally occurring substances.

1.5.3 Water in the atmosphere

The proportions given in Table 1.2 are for dry air, that is, air without water vapour molecules. The gases listed have long residence times in the atmosphere and are well mixed, and their concentrations are broadly the same everywhere in the atmosphere. Water is very different, due to its unusual properties at normal Earth temperatures and pressures. It is the only material that is present in all three phases – solid (ice), liquid and gas (water vapour). There is continuous transfer between the three phases depending on the conditions. We take this situation very much for granted, but it is nevertheless remarkable. Certainly, if we found pools of liquid nitrogen or oxygen on the surface of the Earth, or drops of these materials were to fall out of the sky, these substances would get more attention.

The proportion of water vapour in the atmosphere at any one place and time depends both on the local conditions and on the history of the air. First, the temperature of the air determines the maximum amount of water vapour that can be present. The water vapour pressure at this point is called the *saturated vapour pressure* (SVP), and it varies roughly exponentially with temperature (Table 1.3).

Various mathematical expressions have been used to describe the relationship; an adequate one for our purposes is:

$$e_s(T) = 611 \exp\left(\frac{19.65T}{273+T}\right) \text{Pa}$$

where:

$e_s(T)$ is the saturated vapour pressure in Pa

T is the air temperature in degrees Celsius

Table 1.3 Variation of saturated water vapour pressure with temperature

	Temperature (°C)				
Units	*−10*	*0*	*10*	*20*	*30*
Pa	289	611	1223	2336	4275
mbar	3	6	12	23	43

Second, the ambient (meaning local actual) vapour pressure e_a may be any value between zero and e_s. The ratio of actual to saturated vapour pressure is called the *relative humidity*

h_r, often expressed as a percentage. If water vapour is evaporated into dry air (e.g. as the air blows over the sea surface or above a grassy plain), then the vapour pressure increases towards e_s but cannot exceed it. If air is cooled, for example, by being lifted in the atmosphere, then a temperature will be reached at which the air is saturated due to its original water content. Any further cooling results in the *excess* water being condensed out as cloud droplets. If the cooling occurs because the air is close to a cold ground surface, then dew results. The complexity of this sequence for any air mass is responsible for the variability of water vapour concentration in space and time. For comparison with the proportions given in Table 1.3 for the well-mixed gases, we can say that the highest vapour concentrations occur in the humid tropics, with temperatures of 30°C and relative humidity of near 100%. The vapour pressure will then be 4300 Pa, corresponding to a mixing ratio of 4.3/101 = 4.3%. At the low end, an h_r of 50% at a temperature of –20°C would correspond to a mixing ratio of around 0.1%. The global average mixing ratio is around 1%, so the abundance of water vapour is similar to that of argon.

1.5.4 The vertical structure of the atmosphere

1.5.4.1 Pressure

The pressure of a gas is due to the momentum exchange of individual molecules when they collide with the walls of their container. In the atmosphere, only the molecules at the surface have a container – the remainder simply collides with other gas molecules. At any height in the atmosphere, the upward force due to this momentum exchange must equal the downward force due to gravity acting on all the molecules above that height. As this force decreases with height, pressure decreases with height.

Considering the force dF acting on a small vertical column of height dz, area A and density ρ, with the acceleration due to gravity of g, we have $dF = -g\rho A\, dz$ (the minus sign is because the force acts downwards, but z is usually taken to be positive upwards). Hence

$$dp = df/A \;=\; -g\rho\, dz$$

But for an ideal gas at temperature T

$$\rho = mp/kT$$

where:

m is the molecular mass

k is the Boltzmann constant

Hence

$$\frac{1}{p}\,dp \;=\; -\frac{mg}{kT}\,dz$$

which integrates to give the *hydrostatic equation*

$$p \;=\; p_0 \exp\left\{-\int_0^z \frac{mg}{kT}\,dz\right\}$$

where p_0 is the surface pressure. The average *atmospheric pressure at sea level* over the surface of the Earth is 101.325 kPa = 1013.25 mbar (or hPa).

The equation in this form allows for the variation of m, g and T with height z. In practice, the atmosphere is remarkably shallow, having a thickness of only 0.2% of the Earth's radius up to the tropopause and 1.4% even at the mesopause. Hence for practical purposes g can be taken as constant and equal to its value at the surface, g_0. Also, the major components – nitrogen, oxygen and argon – are well mixed by turbulent diffusion, so m is nearly constant at 28.95. If T were constant as well, the integration would give

$$p \;=\; p_0 \exp\left(-\frac{mg_0}{kT}\,z\right)$$

The exponent in brackets in this equation must be dimensionless, so that kT/mg must have the same dimensions as z, which is length. Hence we can write

$$p(z) \;=\; p_0 \mathrm{e}^{-\frac{z}{H}}$$

where $H = kT/mg$ is the scale height of the atmosphere. H corresponds to the height over which the pressure decreases to 1/e = 0.37. At the surface, where the temperatures are around 20°C or 290 K, the scale height is 8.5 km. At the tropopause, where T is approximately 220 K, the scale height has fallen to 6 km.

The total atmospheric pressure is the sum of the partial pressures from each of the gases present according to its proportion by volume or mixing ratio (e.g. as % or ppm). Hence, the great majority of the pressure is due to nitrogen, oxygen and argon. Superimposed on this long-term average situation are short-term variations due to weather. These may cause the sea level pressure to decrease to 95 kPa in the centre of a severe depression or increase to 106 kPa in an anticyclone.

Looked at the other way round, pressure = force per unit area, so that the surface atmospheric pressure is just the total force (= mass of the atmosphere × acceleration due to gravity) divided by the total surface area of the Earth ($4\pi R^2$):

$$P_{\text{sea level}} = \frac{M_{\text{atm}}\,g}{4\pi R^2}$$

FOR REFERENCE PURPOSES ONLY

By rearranging and substituting the known value of average sea level pressure (101.325 kPa), g = 9.81 m s^{-2} and R = 6.37 × 10^6 m, we can calculate the total mass of the atmosphere to be around 5.3 × 10^{18} kg. This is useful for understanding the significance of differing rates of input of atmospheric pollutants.

1.5.4.2 Temperature

The temperature structure of the atmosphere, which is shown in Figure 1.3, is more complex than the pressure structure, because it is the result of several competing processes. First, the Earth's surface is emitting longwave thermal radiation, some of which is absorbed and re-radiated by the atmosphere. Because the atmospheric pressure and density decrease exponentially with height, the absorption and emission decrease as well, which establishes a non-linear decrease in the equilibrium radiative temperature with height. Second, convective forces come into play. Below an altitude of 10–15 km, the lapse rate of radiative temperature exceeds the adiabatic lapse rate. This promotes overturning and defines the well-mixed region known as the troposphere. The mixing process establishes the *adiabatic lapse rate* (discussed in Chapter 8) of around 6.5°C km^{-1} within this region. Above that altitude, the lapse rate of radiative temperature has dropped to a value well below the adiabatic lapse rate, resulting in the stable, poorly mixed conditions characteristic of the stratosphere. Third, warming due to solar energy absorption by the layer of ozone between 20 and 50 km reverses the temperature decline, so that air temperature increases up to the stratopause at 50 km, further increasing the atmospheric stability. The stratosphere is dry throughout because the main source of moisture is the troposphere, and any air moving into the stratosphere from the troposphere must have passed through the tropopause, where the very low temperatures act as a cold trap. Some additional water molecules are created by the oxidation of CH_4. Above the stratopause, in the mesosphere, the warming effect is offset by decreasing air density, and the temperature falls again. Although the temperature is falling, the rate of decrease is small, at around 4 K km^{-1}, and the mesosphere is also stable, but only just. Finally, above the mesopause at 90 km, the air becomes so thin, and collisions so infrequent, that unequal energy partition between vibrational and translational modes results in very high temperatures. It is these high translational energies that allow light particles such as hydrogen atoms to escape from the Earth altogether.

FOR REFERENCE PURPOSES ONLY

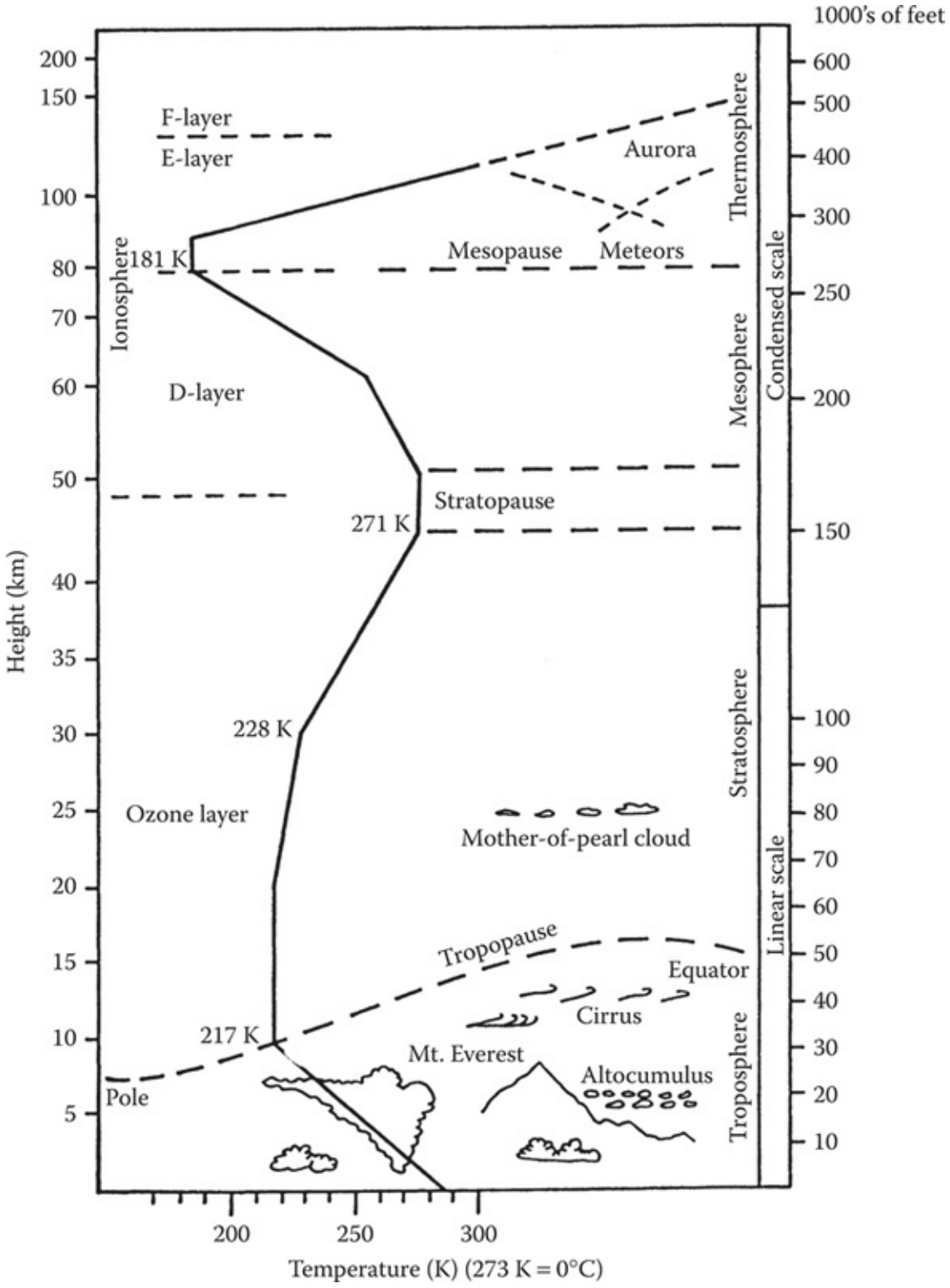

Figure 1.3 The average vertical profile of temperature in the atmosphere, related to other atmospheric features. Note that the vertical scale is linear up to 40 km, and logarithmic above. (From Lawes, H. D., *Weather*, 48, 339–344, 1993.)

1.5.5 Photochemical reactions in the atmosphere

Photochemistry is the branch of science that deals with chemical reactions that occur as a direct or indirect result of the absorption of light. Photochemical reactions are very familiar in everyday life – they include the bleaching of dyes or yellowing of paper by sunlight, and the whole process of photography. We shall be concerned here with the different types of photochemical reactions, which can occur in the atmosphere, as well as clarifying the basic principles and terminology of these types of reactions.

1.5.5.1 Light absorption and emission processes

Light can initiate reactions by exciting atoms or molecules, thereby making them more reactive. In a photochemical reaction, light energy is converted into chemical energy. Many photochemical reactions set up a chain reaction and produce free radicals (see Section 1.5.5.2).

You are probably familiar with the electromagnetic spectrum, which covers the range of radiation from *gamma rays* (very short wave radiation) to *radio waves* (very long wave radiation). For the purposes of photochemistry, we are concerned with region of the electromagnetic spectrum that extends from the far UV (200 nm) to the near IR (800 nm). This is because *light absorption* and other processes of interest occur predominantly in this region.

The absorption process is defined by two basic laws:

- The *first law of photochemistry*, devised by Grotthaus, states that only light absorbed by a molecule can produce a photochemical change in that molecule. This may seem obvious until one realises that it is possible for radiation (light) to pass *through* a molecule without initiating a photochemical change.
- The *second law of photochemistry*, devised by Einstein, states that only one quantum of light is absorbed per molecule, which may then emit luminescence, or be chemically altered following light absorption. Put another way, the law states that photons are absorbed in whole units, and it is one photon only that is responsible for the primary photochemical process.

Photon is the unit of radiation, and can be expressed as the *packet* (or *quantum*) of energy in which light, and other forms of electromagnetic radiation, are emitted. The photon has the following characteristics:

- Has both particle and wave properties
- Has no charge
- Has no mass
- Possesses both energy and momentum

Quantum theory states that light can only be absorbed or emitted in discrete packets of

energy (quanta). The energy changes, E (measured in Joule seconds photon^{-1}, or J s photon^{-1}), associated with the absorption of one mole of photons at various wavelengths can be calculated by the use of *Planck's equation* as follows:

$$E = h\nu = \frac{hc}{\lambda} = hc\sqrt{}$$

where:

h is the Planck's constant (6.6256×10^{-34} J s photon^{-1})
c is the speed of light (2.9979×10^{8} m s^{-1})
ν is the frequency of radiation (s^{-1})
λ is the wavelength of radiation (m)
$\sqrt{}$ is the wavenumber (m^{-1})

In addition, for one mole of photons, we need to take into account the *Avagadro number* (N) – the number of atoms in one mole (6.022×10^{23}).

From Planck's equation, we can see that the energy of a photon is proportional to the frequency of the radiation, which is proportional to the wavenumber. Consequently, we can calculate the energy of a particular wavelength of light and therefore of a particular transition. For example, for λ = 200 nm (far UV):

$$E = \frac{Nhc}{\lambda} = 598\ \text{kJ mol}^{-1}$$

We can extend this calculation to show the energy associated with transitions at further wavelengths up to the near IR:

$$\text{For } \lambda = 400\ \text{nm}: \quad E = 300\ \text{kJ mol}^{-1}$$
$$\text{For } \lambda = 600\ \text{nm}: \quad E = 200\ \text{kJ mol}^{-1}$$
$$\text{For } \lambda = 800\ \text{nm}: \quad E = 150\ \text{kJ mol}^{-1}$$

We can compare these transition energies with the bond energies of certain common atmospheric molecules, for example:

H_2	436 kJ mol^{-1}	O_3	101 kJ mol^{-1}
N_2	946 kJ mol^{-1}	CO	1070 kJ mol^{-1}
O_2	493 kJ mol^{-1}	NO_2	305 kJ mol^{-1}

It is clear then that most of these are in the sort of range, which will allow them to be dissociated by light in the far UV to near IR.

1.5.5.1.1 Quantum yield

The quantum yield in photochemical reactions is defined as:

$$\frac{\text{The number of molecules reacting}}{\text{The number of photons absorbed}}$$

For example, the following reaction illustrates a quantum yield of 2, that is, two molecules decompose when one photon is absorbed.

$$\mathrm{HI} \xrightarrow{h\nu} \mathrm{H^{\bullet}} + \mathrm{I^{\bullet}}$$
$$\text{then } \mathrm{HI} + \mathrm{H^{\bullet}} \rightarrow \mathrm{H_2} + \mathrm{I^{\bullet}}$$
$$2\mathrm{I^{\bullet}} \rightarrow \mathrm{I_2}$$

1.5.5.2 Examples of photochemical reactions

We shall now examine some of the reactions that occur as a result of the process of light absorption.

1.5.5.2.1 Photosynthesis

Photosynthesis is the process by which green plants trap light energy and use it to drive a series of chemical reactions that lead to the formation of carbohydrates. The overall reaction for photosynthesis may be summarised as:

$$6\mathrm{CO_2} + 6\mathrm{H_2O} \rightarrow \mathrm{C_6H_{12}O_6} + 6\mathrm{O_2}$$

However, it is a more complicated process than this reaction mechanism might suggest – it may, in fact, be divided into *light* and *dark* reactions.

During the light reaction, sunlight is used to split water into oxygen, hydrogen ions (photons) and electrons:

$$\textbf{Light reaction} \qquad 12\mathrm{H_2O} \xrightarrow{h\nu} 6\mathrm{O_2} + 24\mathrm{H^+} + 24\mathrm{e^-}$$

Sunlight is not required for the dark reaction, in which the photons and electrons are used to convert carbon dioxide into carbohydrates:

$$\textbf{Dark reaction} \qquad 6\mathrm{CO_2} + 24\mathrm{H^+} + 24\mathrm{e^-} \rightarrow \mathrm{C_6H_{12}O_6} + 6\mathrm{H_2O}$$

1.5.5.2.2 Photosensitisation

Sometimes, chemical reactions occur indirectly due to photosensitisation. For example, the

following series of reactions produce formaldehyde (HCHO), although Hg initiates the process:

$$\mathrm{Hg} \xrightarrow{h\nu} \mathrm{Hg}^{\bullet}$$

$$\text{then} \quad \mathrm{Hg}^{\bullet} \rightarrow \mathrm{Hg} + 2\mathrm{H}^{\bullet}$$

$$\mathrm{H}^{\bullet} + \mathrm{CO} \rightarrow \mathrm{HCO}^{\bullet}$$

$$\mathrm{HCO}^{\bullet} + \mathrm{H} \rightarrow \mathrm{HCHO}^{\bullet}$$

$$2\mathrm{HCHO}^{\bullet} \rightarrow \mathrm{HCHO} + \mathrm{CO} + 2\mathrm{HO}^{\bullet}$$

The $^{\bullet}$ superscript next to the particular atoms indicates the presence of an unpaired electron, that is, a *free radical*. This is described in more detail later and in Chapter 12.

1.6 METHODS OF DESCRIBING POLLUTANT CONCENTRATION

As with many variable quantities, a wide variety of methods are used for describing the amount of material present. Suppose that we have a continuous record of concentration measurements of one pollutant at a given location, taken every minute for a year; this would give us 525,600 individual values. Although this is a comprehensive data set, it is not a lot of use in this form. We must process the data and present it so that the information we want is made clear without having to wade through the half-million values each time. We might wish to decide, for example, on the effects that might result from the pollutant, or compare the concentration record with previous records from the same location or with records from other locations. In the remainder of this section, a brief description is given of the common methods in use for describing pollutant occurrence. The most straightforward measure of such a signal is the time-weighted average – the arithmetic mean of all the original 1-min values. This gives us a single value with which to represent the concentration record. It does not tell us anything about changes during the course of the year, or about the magnitude or duration of either high or low episodes. The next stage of processing might be to average the 60 values from each hour, and to plot these as a complete sequence for the year. A 1-h average is usually regarded as being free from atypically short-term spikes. Such a record would also help to clarify any annual cycles due to changes in source strength or dispersion meteorology, although it is likely that many such annual cycles would need to be averaged to smooth out random variations. If a systematic daily variation is suspected, as with ambient ozone concentrations or pollutants due to vehicle movements, then this can be clarified by calculating the average concentration during each of the 24 h of the day from all 365 available values. Progressively this process can be refined to give weekly, monthly or seasonal means.

Many air pollutant concentrations are highly variable, with a low average and a large

range between near-zero minimum values and maxima during episodes. Furthermore, effects on organisms such as people and plants often depend on short episodes of high concentration. How can we summarise this breadth? The standard method is to examine the frequency distribution of the data, by making a tally of the numbers of hourly or daily means that fall in the ranges 0–4, 5–9, 10–14, and so on; ppb, for example. The number in each range is then converted to a proportion or percentage of the total number of readings – this is the frequency. A common result of such an analysis of air pollutant concentrations is that the data approximate to a *log-normal frequency distribution* – the log of the frequency is normally distributed with concentration. This fact has certain implications for the way in which the data are summarised, and a new set of statistical values must be used. The geometric mean replaces the arithmetic mean, and the geometric standard deviation replaces the standard deviation.

If all the proportions within each concentration range are summed and plotted against concentration, we have the cumulative frequency distribution. This is *sigmoidal* (i.e. an S-shaped curve) on linear scales, but it can be transformed to a straight line on log-probability axes. The gradient of this line then gives the value of σ (standard deviation). From the line itself we can derive the proportions of the time for which any particular concentration is exceeded, or the concentration exceeded for certain proportions of the time (e.g. 50%, 10% and 2%). The latter values are often used in pollution control legislation. The various parameters that can be identified from a given distribution are strongly correlated. For example, the 98th percentile hourly mean NO_2 concentrations measured by UK urban monitors have been consistently around 2.3 times the corresponding annual means. If the record is averaged over different periods, it is often found that $c_{\max,t}$, the maximum average concentration over any period t, is related to the 1-h maximum by an equation of the form:

$$c_{\max,t} = c_{\max,\,1\,\mathrm{h}}\, t^{q}$$

where q is an exponent with a typical value of –0.3.

For example, if $c_{\max,\,1\mathrm{h}}$ (the maximum 1-h average) = 100 ppb, then $c_{\max,\,1\ \mathrm{day}}$ (the maximum 24-h average) = $100 \times (24)^{-0.3}$ = 39 ppb and $c_{\max,\,1\ \mathrm{month}} = 100 \times (720)^{-0.3}$ = 9 ppb.

1.7 UNITS FOR EXPRESSING ATMOSPHERIC CONCENTRATIONS

Before we go any further, we must make a short detour to explain the units in which pollutant concentrations will be discussed throughout this book. The international system of units (Système International d'unités [SI]) has now largely replaced all earlier systems of units used to describe physical quantities. SI is built on seven base quantities, each having

FOR REFERENCE PURPOSES ONLY

its own dimension: length, mass, time, thermodynamic temperature, amount of substance (chemical amount), electric current, and luminous intensity. All other quantities are derived quantities that acquire dimensions derived.

Although SI units are recommended for use in atmospheric chemistry, some non-SI units are still required, for example, time periods such as minutes, hours, days and years, which can be expressed in terms of the second but which defy decimalisation. Where non-SI units are preferred, the appropriate conversion rule to SI units is typically indicated, for example, 1 atm = 101,325 Pa.

It is important to be aware of the way in which the composition of air is measured in the atmosphere. There are two key aspects:

- *The concentration* of particular elements in the air.
- *The averaging time*, that is, the time over which the presence of an element is measured.

1.7.1 Concentration units

The concentration of gaseous pollutants may be expressed in a number of different ways:

- *Gravimetric*: The mass of gaseous pollutant per unit volume of air (usually measured in μg m^{-3}).
- *Volumetric*: The volume of gaseous pollutant per unit volume of air (usually measured in μL L^{-1}). However, litre is not a recognised unit within the SI. The SI unit for amount of substance (meaning number of molecules, not weight) is the mol, so that μmol mol^{-1} is the equivalent SI unit of volumetric concentration.
  OR

Table 1.4 Abbreviations for volumetric and gravimetric units

Volumetric					*Gravimetric*
Parts per million (micro)	10^{-6}	ppm	μL L^{-1}	μmol mol^{-1}	mg m^{-3}
Parts per billion (nano)	10^{-9}	ppb	nL L^{-1}	nmol mol^{-1}	μg m^{-3}
Parts per trillion (pico)	10^{-12}	ppt	pL L^{-1}	pmol mol^{-1}	ng m^{-3}

- *The volume mixing ratio*: The latter represents the ratio of the pollutant volume and the original air volume – this is equivalent to the ratio of the number of pollutant gas molecules to the total number of air molecules (usually measured in parts per million [ppm], i.e. per 10^6; parts per billion (ppb), i.e. per 10^9; parts per trillion [ppt], i.e. per 10^{12}). One ppm is equivalent to a cubic centimetre of gaseous pollutant in a cubic metre of air. These relationships are summarised in Table 1.4 for the typical

FOR REFERENCE PURPOSES ONLY

concentration ranges of ambient gaseous pollutants. For particulate pollutants, the mass or number of particles per unit volume of air is applicable (respectively termed as *mass* or *number* concentrations, as described in Chapter 3).

Both gravimetric and volumetric systems have their uses and their advocates. The volumetric concentration is invariant with temperature and pressure and therefore remains the same, for example, while warm flue gas is cooling in transit through exhaust ductwork. When gas enters a leaf, the effects may depend primarily on the number of molecular sites occupied by the pollutant gas molecules – this is better indicated by the volumetric concentration than by the gravimetric concentration. However, if concentration is being determined by extracting the gas onto a treated filter for subsequent chemical analysis, or health effects are being related to the mass of pollutant inhaled, the result would normally be calculated as a gravimetric concentration.

1.7.1.1 Conversion between gravimetric and volumetric units

As both gravimetric and volumetric systems are widely used in expressing pollutant concentrations, we need to be able to convert between the two. The basic facts to remember are that 1 mol of a pure gas (an Avogadro number of molecules, 6.02×10^{23}) weighs M kg, where M is the relative molar mass, and takes up a volume of 0.0224 m^3 at standard temperature and pressure (STP – 0°C, 1 atmosphere). Here, air denotes gaseous substances, including water vapour, but not condensed phase water or particulate matter.

For gaseous pollutants, the inter-conversion between volume mixing ratios (ppm, ppb, etc.) and mass per unit volume needs some explanation. The atmospheric volume occupied by gaseous air pollutants is tiny; consequently, we can assume that air pollutants behave like a *perfect* or *ideal* gas. The molecules of an ideal gas occupy negligible volume and exert no forces upon one another. The *volume mixing ratio* is independent of temperature and pressure for an ideal gas (and hence for a gaseous air pollutant) because it is a ratio. However, volume is affected by temperature and pressure and so the mass per unit volume depends on temperature and pressure. Therefore, the inter-conversion between the two must incorporate these factors.

The *relationship between the volume mixing ratio and mass per unit volume* is given by the following equation:

$$\mu g\,m^{-3} = \text{ppb} \times \frac{\text{molecular weight}}{\text{molar volume (litres)}} \tag{1.1}$$

---

where:

$$\text{molar volume} = 22.4 \times \frac{T}{273} \times \frac{1013}{P}$$

in which:

22.4 is the volume (in litres) occupied by one mole of gas at one atmosphere of pressure (1013 mb) and at 273 K (0°C)

T is the absolute temperature (K)

P is the atmospheric pressure (mb or Torr)

Similarly, by cross multiplying, we can express the volume mixing ratio as:

$$\text{ppb} = \mu\text{g m}^{-3} \times \frac{\text{molar volume (litres)}}{\text{molecular weight}} \tag{1.2}$$

Example 1.2

To convert 100 ppb of NO_2 at 293 K and 1000 mb into μg m^{-3}:

NO_2 has a molecular weight (from the atomic weights of nitrogen, 14, and oxygen, 16) of 14 + 16 + 16 = 46.

Using Equation 1.1, we get the following:

$$\begin{aligned} \mu\text{g m}^{-3} &= 100 \times \frac{46}{22.4 \times 293/273 \times 1013/1000} \\ &= 189 \end{aligned}$$

Therefore, 100 ppb of NO_2 at 293 K and 1000 mb = 189 μg m^{-3}.

Example 1.3

$$\begin{aligned} \text{Sulphur dioxide } (SO_2) \text{ has } M &= 32 \times 10^{-3} + (2 \times 16 \times 10^{-3}) \\ &= 64 \times 10^{-3} \text{ kg} \end{aligned}$$

So *pure* SO_2 has a density (= mass/volume) of $64 \times 10^{-3}/0.0224 = 2.86$ kg m^{-3} at STP. But pure SO_2 is 10^6 ppm, by definition. Therefore,

$$\begin{aligned} 10^6 \text{ ppm} &\equiv 2.86 \text{ kg m}^{-3} \\ 1 \text{ ppm} &\equiv 2.86 \times 10^{-6} \text{ kg m}^{-3} \\ &= 2.86 \text{ mg m}^{-3} \end{aligned}$$

and

$$1 \text{ ppb} \equiv 2.86\ \mu\text{g m}^{-3}$$

FOR REFERENCE PURPOSES ONLY

For the pollutant gases discussed most frequently in this book, Table 1.5 gives the conversion factors from ppb to μg m^{-3}, and *vice versa*, at 0°C and 20°C.

Table 1.5 Conversion factors between volumetric and gravimetric units

		To convert			
		ppb to μg m^{-3}		μg m^{-3} to ppb	
Pollutant	Molecular weight M/g	0°C	20°C	0°C	20°C
NH_3	17	0.76	0.71	1.32	1.43
CO	28	1.25	1.16	0.80	0.86
NO	30	1.34	1.25	0.75	0.80
NO_2	46	2.05	1.91	0.49	0.52
O_3	48	2.14	2.00	0.47	0.50
SO_2	64	2.86	2.66	0.35	0.38
C_6H_6	78	3.48	3.24	0.29	0.31

The mixing ratio is frequently employed to quantify the abundance of a trace gas in air. The specific advantage of mixing ratio over concentration in this context is that the mixing ratio is unchanged by differences in pressure or temperature associated with altitude or with meteorological variability, whereas concentration depends on pressure and temperature in accordance with the equation of state. As the mixing ratio refers to the total gas mixture, the presence of water causes the mixing ratio to vary somewhat with humidity. For this reason, it is preferable to refer to dry air when reporting mixing ratios of trace gases in the atmosphere whenever possible.

1.7.1.2 Correction for non-standard temperature and pressure

The temperature and pressure are unlikely to be standard, so we also need to be able to convert gravimetric units at STP to other temperatures and pressures. At STP, we have 1 m^3 containing a certain mass of material. When the temperature and pressure change, the volume of the gas changes but it still contains the same mass of material. Hence, we need only to find the new volume from the ideal gas equation:

$$\frac{P_1 V_1}{T_1} = \frac{P_2 V_2}{T_2} \tag{1.3}$$

where:

P_1, V_1 and T_1 are the initial pressure, volume and absolute temperature

P_2, V_2 and T_2 are the final pressure, volume and absolute temperature

In our case:

P_1 = 1 atmosphere

V_1 = 1 m^3

T_1 = 273 K

and we need to find V_2. Therefore, rearranging Equation 1.3, we get:

$$V_2 = \frac{T_2}{P_2} \times \frac{P_1 V_1}{T_1} = \frac{T_2}{273 P_2}$$

For example, the highest ambient temperature that we might find in practice is 50°C, and the lowest ambient pressure at ground level might be 950 mbar. Hence:

$$T_2 = 273 + 50 = 323 \text{ K}$$

and

$$P_2 = 950/1013 = 0.938 \text{ atmosphere (because standard atmospheric pressure} = 1013 \text{ mbar)}$$

Therefore

$$V_2 = \frac{323}{273 \times 0.938} = 1.26 \text{ m}^3$$

The original volume of 1 m^3 has expanded to 1.26 m^3. This is physically reasonable because we have raised the temperature and reduced the pressure – both changes increase the volume. The increased volume will still contain the same number of molecules, which will have the same mass. Hence the concentration must decrease by the same factor, and 1 ppm of SO_2, for example, would now be equal to 2.86/1.26 mg m^{-3} or 2.27 mg m^{-3}. The volumetric concentration, of course, would remain at 1 ppm.

1.7.2 Averaging time

The second key aspect of measuring the atmospheric pollution concentrations is the time over which the measurement is carried out. This is the *averaging time*. Thus, hourly, daily and weekly concentrations are often calculated and used when defining air quality standards.

The averaging time selected for use depends upon the physico-chemical characteristics and health/environmental impacts of the pollutant under consideration. For example, a pollutant such as ozone, which can rise to a high concentration over a short period of time and can cause severe damage to crops, will often have a short averaging time. Seasonal

FOR REFERENCE PURPOSES ONLY

averaging periods are also used. Typically, in the northern hemisphere *winter* refers to the October–March period, whilst *summer* refers to April–September.

1.8 UNCONVENTIONAL AIR POLLUTANTS

At least 3000 different chemicals have been identified in air samples. However, it can safely be assumed that the number of chemicals actually in the Earth's atmosphere is at least equal to the number that has ever been produced on the Earth, plus additional ones formed by subsequent reactions. There are many air pollutants that may be important in particular situations. Additional information is also provided in Chapters 2, 6 and 10. *Fluorine* is produced as gaseous HF by chemical processes such as fertiliser production and steel manufacture. It accumulates in grass and causes the bone disease fluorosis in herbivores. *Heavy metals* such as arsenic, cadmium, chromium, manganese, mercury, nickel and vanadium are produced from several anthropogenic activities. Airborne heavy metals account for significant fractions of the total heavy metal content of arable soils. The UNECE Protocol on Heavy Metals targets three particularly harmful substances – lead, cadmium and mercury. The protocol aims to cut emissions from industrial sources (iron and steel industry, non-ferrous metal industry), combustion processes (power generation, road transport) and waste incineration. There are limit values for these heavy metals, and the protocol requires employment of the best available technique (BAT) for achieving emission reduction via fitting special filters or scrubbers for combustion sources. It also requires countries to phase out leaded petrol. *Formaldehyde* is an irritant chemical released from, for example, urea formaldehyde cavity wall insulation. *Asbestos* covers a range of mineral fibres released from building thermal insulation and brake linings. Inhalation of the fibres can result in potentially fatal lung disorders.

Short-lived climate forcers (SLCFs), also known as *short-lived air pollutants* (SLCAPs), are substances like black carbon, troposheric ozone and methane that have relatively short lifetimes in the atmosphere, ranging between days and weeks (black carbon and ozone) and up to several years (methane) and which contribute to global warming by negatively influencing Earth's radiative budget through absorption of solar radiation. Moreover, black carbon, when deposited on ice and snow fields, reduces surface albedo and thus increases absorption of solar radiation by the surface.

Persistent organic pollutants (POPs) is a common label for a group of organic compounds that are persistent in the environment. It covers a list of 16 substances (or group of substances), which has been classified in three source sectors as follows (discussed in Chapter 2):

- *Pesticides*: Aldrin, chlordane, chlordecone, dichlorodiphenyl trichloroethane (DDT), dieldrin, endrin, heptachlor, hexachlorobenzene (HCB), mirex, toxaphene,

hexachlorocyclohexane (HCH, which includes lindane)

- *Industrial chemicals*: Hexabromobiphenyl, polychlorinated biphenyls (PCBs)
- *By-products* (*or contaminants*): Dioxins, furans, PAHs

1.8.1 Incineration as a source of air pollutants

Incineration is potentially attractive because it can recover thermal energy for electricity generation or district heating schemes. Incineration can generate about three times the energy per kg waste compared to the energy recovered from the decomposition of landfill. However, incineration is a key source of dioxins, including 210 organic compounds, comprising 75 polychlorinated dibenzo-*p*-dioxins (PCDDs) and 135 polychlorinated dibenzofurans (PCDFs). Additional emissions include PCBs and PAHs (discussed in Chapter 2).

There are the following competing technologies:

- The simplest form is *mass burn*, in which the mixed wastes are combusted on a moving grate and energy is recovered from the hot combustion gases. Around 7 MW can be generated for an annual throughput of 100,000 tonnes.
- In *fluidised bed combustion*, the fuel is cleaned of non-combustible material and shredded before being combusted in an updraft of air through a bed of sand and dolomite.
- *Pyrolysis* involves heating the waste to 400°C–800°C in the absence of oxygen; this breaks down complex molecules which can then be burned.
- *Gasification* is similar, but the low-grade gaseous fuel is burned in a turbine.
- More recently, techniques such as *torrefaction* and *microwave pyrolysis* are being utilised for optimal energy recovery and for obtaining acceptable biofuel from waste.

Through the Landfill Directive, the EU intends to divert municipal solid waste (MSW) from landfill to recycling and incineration, and this process will require the commissioning of up to 50 new incinerators in the UK by 2015. But incineration produces emissions other than CO_2 and H_2O, such as acid gases (HCl, HF, SO_2), NO_x, heavy metals (cadmium, mercury, arsenic, vanadium, chromium, cobalt, copper, lead, manganese, nickel, thallium and tin), dioxins, PCBs, PAHs and other particles. Also there is residual solids' ash (typically 10%–20% of mixed urban waste), which is usually very enriched in aluminium, calcium, silicates, iron, sodium, magnesium and potassium, and which may contain 1%–10% lead and zinc. Some of the volatile metals such as cadmium and lead are vaporised and emitted. Polyvinylchloride (PVC) combines with lead to make lead chloride, which is volatile and emitted. If the combustion conditions for MSW are wrong, emissions of dioxins and furans can be increased significantly. The tight control required is shown by the EU emission limit for dioxins, which is 0.1 ng TEQ m^{-3}. Municipal solid waste incinerators are currently

FOR REFERENCE PURPOSES ONLY

responsible for only 3% of UK dioxin emissions, but since the total fell from 1078 to 325 kg year^{-1} between 1990 and 1998, any increase due to incineration will be unwelcome. Production of these toxics can be minimised by keeping the combustion temperature above 1100°C, with a gas residence time in the combustion chamber of at least 1 s and a surplus of oxygen. The UK Hazardous Waste Incineration Directive, which came into force in 2000, brings operating conditions and emissions within a stricter regime. Best available technology must be used for controlling stack emissions and the incineration temperature must exceed 850°C.

Pyrolysis and gasification are competing with incineration for market share. These processes rely on heating the wastes in the absence of oxygen (like producing charcoal from wood or coke and coke-oven gas from coal), so that they are decomposed into energy-rich gas, oil and char. The gas *syngas* can be used as a fuel or as a petrochemical feedstock.

1.9 CASE STUDY – HISTORICAL PERSPECTIVE: THE GREAT LONDON SMOG

In 1952 London was hit by a smog event that lasted five days and killed thousands of people. It was caused by a combination of the burning of coal and anomalous weather conditions. Although seen as a tragedy due to the increased death rate, it led to an increased awareness about air pollution. Smog and air pollution in cities is a long-established problem. Imperial Rome had problems due to wood smoke but in London the problem had a historical bearing of an epic proportion (Table 1.6). In 1852, a century before the Great Smog, Charles Dickens famously described London in his novel *Bleak House*: 'Fog everywhere. Fog up the river, where it flows among green aits and meadows; fog down the river, where it rolls defiled among the tiers of shipping, and the waterside pollution of a great (and dirty) city'.

The Great London Smog of 1952, also known as the *Big Smoke*, was a severe air pollution event that affected London in December 1952. A period of cold weather, combined with an anticyclone[1] and windless conditions, collected airborne pollutants mostly from the use of coal to form a thick layer of smog over the city. Smog, a term coined by Des Voeux in 1905, is a mixture of smoke and fog (*sm*[oke and f]*og*) (Green and Lane, 1964). The smog lasted from Friday to Tuesday, 5–9 December 1952, and then quickly dispersed after a change in the weather. Although it caused major disruption due to the effect on visibility and even penetrated indoor areas, it was not thought to be a significant event at the time as London's infamous *pea soupers* were regular occurrences. In the following weeks, however, medical reports estimated that 4,000 had died prematurely and 100,000 more were made ill because of the smog's effects on the human respiratory system. More recent research suggests that the number of fatalities was considerably higher, at around 12,000. The chronology of the incident and the socio-economic, health and environmental impacts are

FOR REFERENCE PURPOSES ONLY

keys to understanding why this event has been called the 'most disastrous event of its kind anywhere in the world' (Wilkins, 2006, p. 267).

Table 1.6 The number of deaths above the average rate for major smog episodes in London

Date	*Excess deaths*
December 1873	270–700
January 1880	700–1100
December 1892	1000
November 1948	300
December 1952	4000
January 1956	480
December 1957	300–800
December 1962	340–700

Source: Jacobson, M. Z., *Atmospheric Pollution: History, Science, and Regulation*, Cambridge University Press, Cambridge, UK, 2002.

1.9.1 Chronology

From Table 1.6, it is clear that the Great Smog of London was not the first or the last smog episode in London. In December 1892, the death toll was 1000 above average. Other major pollution events of this type also occurred in other cities. In December 1930, a 5-day fog killed 63 people in the Meuse Valley, Belgium, and in 1948 twenty residents of the town Donora in Pennsylvania were killed in similar circumstances (Bell and Davis, 2001). Figure 1.4 shows a timeline of events around the smog.

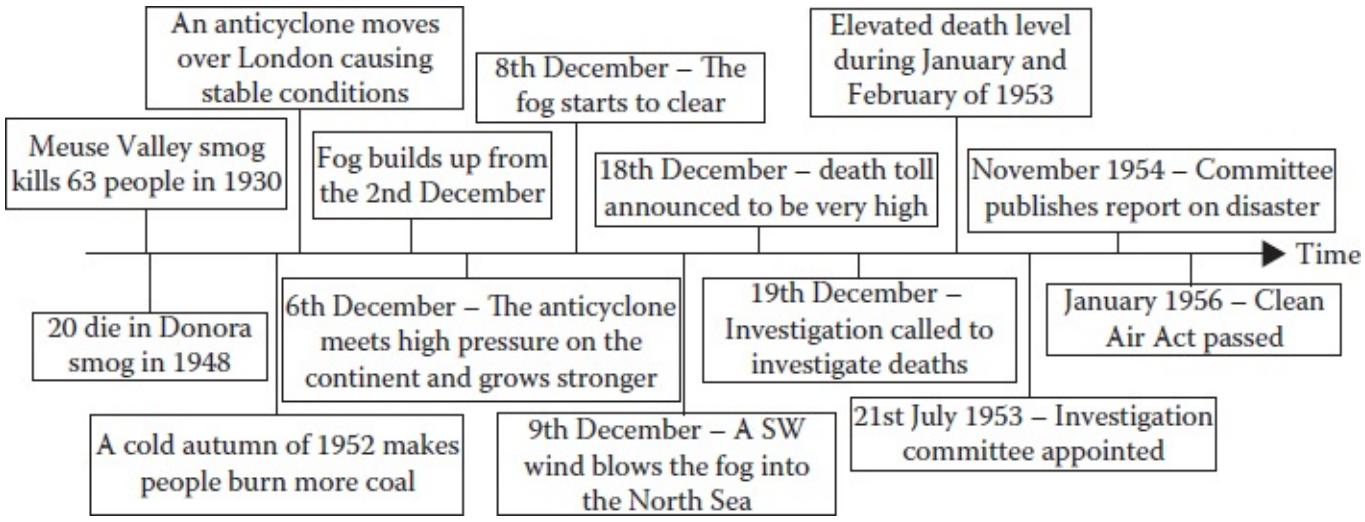

Figure 1.4 Timeline of events surrounding and during the London Smog (not to scale).

FOR REFERENCE PURPOSES ONLY

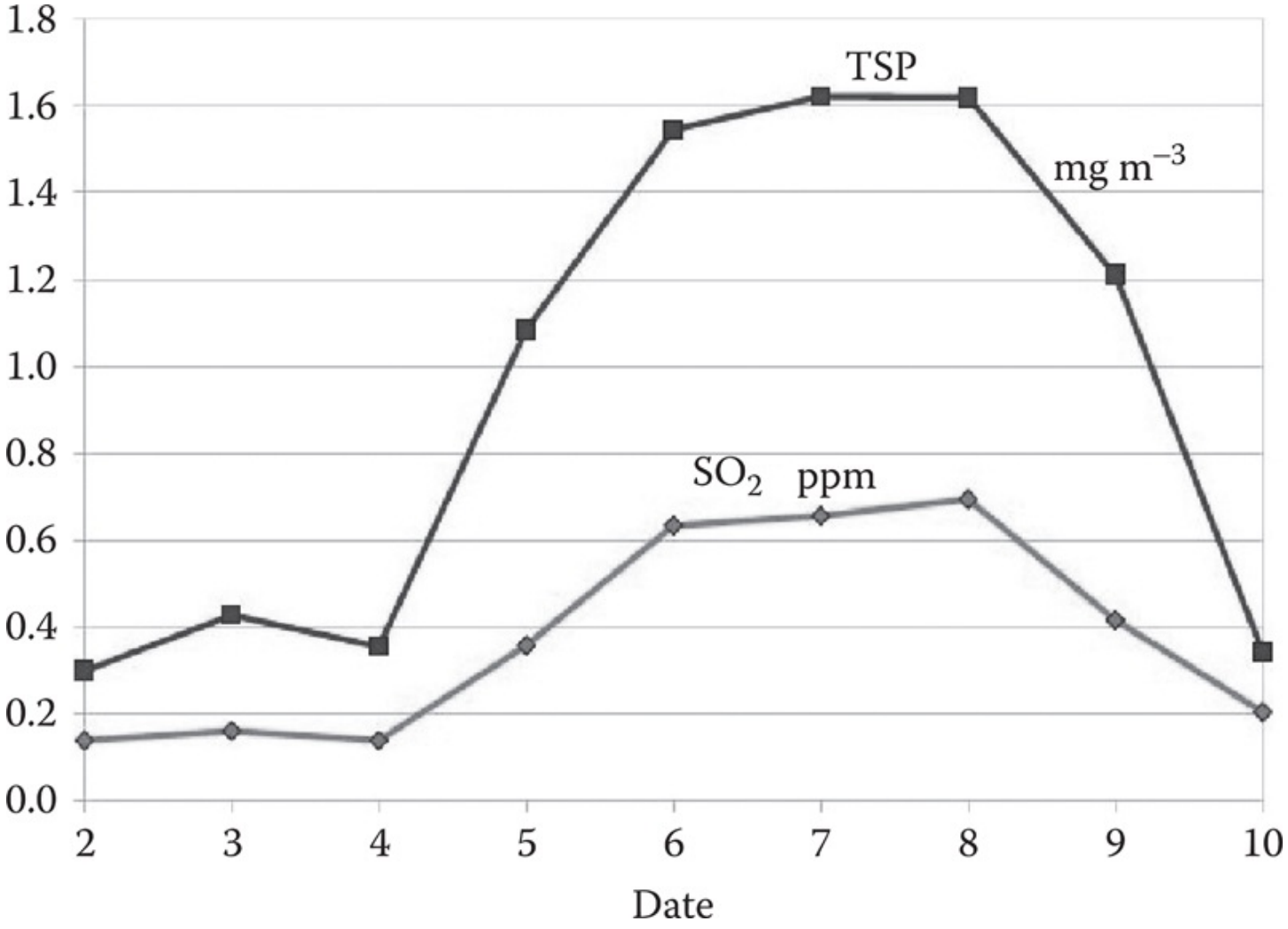

Figure 1.5 The daily air pollution readings during the London Smog, 2–10 December 1952 (Upper line: SO_2 in ppm; lower line: total suspended particulate [TSP] in mg m^{-3}). (Adapted from Absalom, H. W. L., *Q. J. Royal Meteorol. Soc.*, 80, 261–266, 1954.)

September 1952 was colder than average and had above average precipitation. This led to an increase in the coal burnt and a resulting increase in air pollution (Absalom, 1954). November and December were also cold and snowy (Absalom, 1954; Met Office, 2010). An anticyclone moved southeast from Iceland and a temperature inversion was created (Absalom, 1954). On 2 December, fog was present in the early morning but cleared during the day; however, on 5 December, light winds helped to build the fog into a layer approximately 200 m thick, which caused it to last until 6 December, when the anticyclone met with another high-pressure system on the continent, forming extremely stable conditions (Absalom, 1954; Met Office, 2010).

Figure 1.5 shows the patterns of air pollutant recordings between 2 and 10 December 1952; the upper line is the measurement of SO_2 in ppm, and the lower line is the measurement of total suspended particulate (TSP) matter in mg m^{-3}. Although the fog was

FOR REFERENCE PURPOSES ONLY
the most dense on 7 December, the average peak in sulphur dioxide occurred on 8 December.

During January and February following the smog episode, there were elevated mortality rates. This was attributed to influenza; however, more recent analysis has suggested that this could have also been caused by the smog (Bell and Davis, 2001). A committee was appointed on 21 July 1953 to investigate the problem of air pollution with reference to the London fog in December 1952. The final report was published in November 1954, and this report proposed the idea of a *clean air act* as well as a *clean air council* to research and implement the legislation (Committee on Air Pollution, 1954). In January 1956, the *Clean Air Act* was passed (Jacobson, 2002).

1.9.2 Health effects

At the time, eyewitnesses said that, although the *fog* was bad, it did not seem extraordinary (Ministry of Health, 1954). Many of the older population could remember similar *fogs* 40–50 years before. There were, however, unprecedented physiological effects (Wilkins, 1954). Recent analysis has put the number of deaths at 4700, although some research suggests three times that amount (Alloway and Ayres, 1997; Bell and Davis, 2001). Most of the deaths occurred in people of ill health and the elderly. The most common causes of deaths were from bronchitis and associated heart conditions, emphysema and pneumonia. Some of these cases were also associated with common *colds*. Even though these were the causes of death, the increase suggests that they were severely aggravated by the smog (Ministry of Health, 1954).

The following January and February (1953) also had high mortality rates, and these are thought to be caused by an influenza epidemic (Ministry of Health, 1954). However, many sources have shown that it would have to have been an extremely severe outbreak to cause the elevated levels of mortality. Therefore, the high mortality rates have been attributed to the smog, making the population susceptible to the influenza by lowering the immune defences of the lungs (Bell and Davis, 2001; Bell et al., 2004). This raises the death toll of the smog to more than 12,000 (Bell and Davis, 2001).

The extreme levels of fatalities and health effects during the London Smog incident could have resulted from a cocktail of harmful pollutants generated over that period, mainly SO_2, CO and acid particulates and fumes. SO_2 has been associated with aggravated respiratory symptoms, particularly asthma (Chen et al., 2007). The highest concentration recorded was 1.42 ppmv, which could have triggered respiratory infections (Jacobson, 2002). Excessive formation of CO from incomplete combustion would have resulted in a wide range of adverse cardiopulmonary effects (Andrews et al., 2004; Chen et al., 2007). It is known that CO bonds to haemoglobin in place of oxygen to form a compound called carboxyhaemoglobin and stops the haemoglobin adsorbing enough oxygen. This could have resulted in suffocation (Jacobson, 2002). In addition, acidic particulates (such as the soot

FOR REFERENCE PURPOSES ONLY

particles with sulphuric acid) at levels found during that period could have caused bronchitis and emphysema.

1.9.3 Environmental effects

Although many reports and articles, including the report published by the Committee on Air Pollution (1954) about the Great London Smog of 1952 focus on the health effects, there must have been a great effect on the environment from this event. This is because sulphuric acid and soot can be damaging to the environment, and they were at very high concentrations for five days (Committee on Air Pollution, 1953). One of the largest constituents of smoke is sulphur dioxide, which can react to produce sulphuric acid. Sulphuric acid can cause acid deposition. 'Acid deposition is the deposition of acid-containing gases, aerosol particles, fog droplets, or raindrops to the ground, lakes, plant leaves, tree leaves, or buildings' (Jacobson, 2002, p. 260).

Sulphuric acid (and other acids that may be caused by smoke) damages the surface of buildings. It predominantly affects limestone, although some sandstones, mortar and roof slate may also be damaged (Committee on Air Pollution, 1953).

$$H_2SO_{4(aq)} + CaCO_{3(s)} + H_2O_{(l)} \rightarrow CO_{2(g)} + CaSO_{4(s)}.2H_2O_{(l)}$$

This has resulted in blistering, scaling and pocking, affecting the appearance of buildings (Committee on Air Pollution, 1953).

1.9.4 Socio-economic impacts

There are a multitude of economic and social impacts from the Great London Smog of 1952. Some of them are strange and rather sad; for instance, there was a shortage of caskets and flowers due to the number of dead (Davis et al., 2002). The smog produced economic loss through many different means and, although considered less important than the loss of life, was also great. Economic costs came from the repair of damaged buildings, structures and art works and the loss of productivity in agriculture, either through crop damage or livestock illness (Committee on Air Pollution, 1953). As already mentioned, there were a large number of health insurance claims and human illness also caused lack of productivity (Committee on Air Pollution, 1953; Bell and Davis, 2001). There was significant economic loss from the lack of transport (Davis et al., 2002). At the time, the most significant events that were covered in the newspapers were the cancelled sports and the cancellation of the opera, *La Traviata*, by Verdi. This had to be cancelled due to the fog getting into the theatre and so the stage was no longer visible (Hernan, 2010)!

A direct social impact came in the form of the Clean Air Act of 1956 (Jacobson, 2002). This act was firmly recommended by the Beaver Report (Committee on Air Pollution, 1954). The act controlled the emissions of both households and industry. Dark and black

FOR REFERENCE PURPOSES ONLY

smoke were tightly regulated which would in turn reduce the sulphur emissions from coal, even though the law did not regulate sulphur emissions. Power stations were relocated outside cities, and smokeless zones were created inside London (Jacobson, 2002). The effect of the legislation is that between 1950 and 1999, the death rate of both men and women from chronic bronchitis with emphysema was reduced drastically (Hansell et al., 2003).

REFERENCES AND FURTHER READING RESOURCES

Absalom, H. W. L. (1954) Meteorological aspects of smog. *Quarterly Journal of Royal Meteorological Society*, 80: 261–266.

Ahrens, C. D. (2007) *Meteorology Today: An Introduction to Weather Climate, and the Environment*, 8th ed. Thompson Higher Education, Belmont, CA.

Alloway, B. J. and Ayres, D. C. (1997) *Chemical Principles of Environmental Pollution*, 2nd ed. Blackie Academic & Professional, London, UK.

Andrews, J. E., Brimblecombe, P., Jickells, T. D., Liss, P. S., and Reid, B. J. (2004) *An Introduction to Environmental Chemistry*, 2nd ed. Blackwell Science Ltd., Oxford, UK.

Bell, M. L. and Davis, D. L. (2001) Reassessment of the lethal London fog of 1952: Novel indicators of acute and chronic consequences of acute exposure to air pollution. *Environmental Health Perspectives*, 109: 389–394.

Bell, M. L., Davis, D. L., and Fletcher, T. (2004) A retrospective assessment of mortality from the London Smog episode of 1952: The role of influenza and pollution. *Environmental Health Perspectives*, 112: 6–8.

Brimblecombe, P. (1987) *The Big Smoke: A History of Air Pollution in London Since Medieval Times*. Methuen & Co. Ltd., London, UK.

Chen, T. M., Gokhale, J., Shafer, S., and Kuschner, W. G. (2007) Outdoor air pollution: Nitrogen dioxide, sulphur dioxide, and carbon monoxide health effects. *The American Journal of the Medical Sciences*, 333: 249–256.

Committee on Air Pollution (1954) *Report*. Her Majesty's Stationary Office, London, UK.

Davis, D. L., Bell, D. L., and Fletcher, T. (2002) A look back at the London Smog of 1952 and the half century since. *Environmental Health Perspectives*, 110: 734–735.

Green, H. L. and Lane, W. R. (1964) *Particulate Clouds, Dusts, Smokes and Mists*, 2nd ed. E. & F. N. SPON Ltd., London, UK.

Hansell, A., Knorr-Held, L., Best, N., Schmid, V., and Aylin, P. (2003) COPD mortality trends 1950-1999 in England & Wales – Did the 1956 Clean Air Act make a detectable difference? *Epidemiology*, 14: S55.

Hernan, R. E. (2010) *This Borrowed Earth: Lessons from the Fifteen Worst Environmental Disasters around the World*. Palgrave MacMillan, New York.

Jacobson, M. Z. (2002) *Atmospheric Pollution: History, Science, and Regulation*. Cambridge University Press, Cambridge, UK.

Lawes, H. D. (1993) Back to basics. *Weather*, 48(10): 339–344.

Manahan, S. E. (2007) *Environmental Science and Technology: A Sustainable Approach to Green Science and Technology*. Taylor & Francis Group, Boca Raton, FL.

Marshak, S. (2005) *Earth: Portrait of a Planet*. W. W. Norton & Company, New York.

Met Office (2010) The great smog. http://www.metoffice.gov.uk/education/teens/casestudy_great_smog.html (accessed 25 June 2010).

Ministry of Health (1954) Mortality and morbidity during the London fog of December 1952. *Reports on Public Health and Medical Subjects No. 95*. Ministry of Health, London, UK.

NAEI (2016) UK emissions of air pollutants, National Atmospheric Emissions Inventory. http://naei.beis.gov.uk/overview/ap-overview.

Sheppard, F. (1998) *London: A History*. Oxford University Press, Oxford, UK.

Swanepoel, J. W., Krüger, G. H. J., and van Heerden, P. D. R. (2007) Effects of sulphur dioxide on photosynthesis in the succulent *Aguea capensis* Thunb. *Journal of Arid Environments*, 70(2): 208–221.

FOR REFERENCE PURPOSES ONLY

Whittaker, A., BéruBé, K., Jones, T., Maynard, R., and Richards, R. (2004) Killer smog of London, 50 years on: Particle properties and oxidative capacity. *Science of the Total Environment*, 334–335: 435–445.

Williams, I. (2003) *Environmental Chemistry*. John Wiley & Sons, Chichester, UK.

---

[1] An anticyclone is a weather phenomenon that may be defined as a large-scale circulation of winds around a central region of high atmospheric pressure, clockwise in the northern hemisphere, counterclockwise in the southern hemisphere. The effects of surface-based anticyclones include clearing skies as well as cooler, drier air.

FOR REFERENCE PURPOSES ONLY

Chapter 2

Gaseous air pollutants

As discussed briefly in Chapter 1, gaseous air pollutants have either biogenic or anthropogenic origins. The major sources over the last century have been dominated by anthropogenic fossil fuel combustion for energy and transportation applications. However, non-combustion sources are particularly important for volatile organic compounds and methane. Whilst we tend to be familiar with anthropogenic air pollutants, we largely overlook the natural sources of airborne volatile organic compounds (VOCs), such as terpenes and isoprenes from trees, and noxious gases from wildfires. The Great Smoky Mountains in the United States are so-called because of chemical emissions from trees.

Recent years have seen more distinct air pollution emissions characteristics for developed and developing countries, especially the variations in the origins and fate of emissions from their urban and rural activities. This is mainly attributed to the differences in the technologies in processing of fuels and/or the subsequent abatement technologies for the resulting gaseous emissions. According to the World Energy Outlook Special Report on Energy and Air Pollution, the transport sector contributes to over 50% of the global nitrogen oxides (NO_x), power and industry sectors together contribute to over 75% of the global sulphur dioxide (SO_2), buildings contribute to over 40% of the carbon monoxide (CO) and transport and buildings contribute to about 30% each for VOCs (IEA, 2016).

This chapter mainly focuses on regulated gaseous air pollutants, introducing the concepts for their formation and measurements. Presented alongside, where applicable, are the recent trends showing contribution from different natural and anthropogenic sources. The corresponding discussions pertaining to their control and mitigation techniques, impacts to humans and plants, standards and legislations are presented in Chapters 9, 10 and 14, respectively.

2.1 PRIMARY GASEOUS EMISSIONS

Approximate overall global totals for emissions of the different gases are presented in

FOR REFERENCE PURPOSES ONLY

Table 2.1, with corresponding values for Europe in Table 2.2. Table 2.3 summarises the sources of the different gases shown in Table 2.2. The range of different sources, and of the balances between them, for the different pollutants means that the spatial variation of emissions can also be very high.

Table 2.1 Global natural and anthropogenic emissions of different gaseous species

Species	*Natural (Mt yr^{-1})*	*Anthropogenic (Mt yr^{-1})*	*Total (Mt yr^{-1})*
CO_2	7×10^5	0.23×10^5	7.2×10^5
CH_4	160	375	535
CO	430	1815	2245
SO_2	15	146	161
N_2O	26	16	42
NO_x	24	85	109
NH_3	15	30	45
H_2S	1-2	4	5

Table 2.2 EU total air emissions of different gaseous species

Gas	*Emission (Mt yr^{-1})*
CO_2	3250
CH_4	27.2
CO	46.1
SO_2	14.4
N_2O	1.4
NO_x	12.9
NH_3	3.7
NMVOC	17.4

Table 2.3 Percentage contributions of different processes to the totals in Table 2.2

FOR REFERENCE PURPOSES ONLY

Source	CO	NMVOC	CO_2	SO_2	NO_x	NH_3	CH_4	N_2O
Public power	1.23	0.86	32.32	50.88	18.93	0.09	0.18	4.57
Combustion plants	12.9	3.27	19.40	7.18	4.44	0.04	1.53	2.12
Industrial combustion	5.76	0.36	18.29	16.41	9.45	0.05	0.19	2.29
Production processes	5.39	5.87	4.71	3.99	1.75	2.83	0.17	22.12
Fuel extraction and distribution	0.23	6.00	0.08	0.22	0.88	–	13.82	–
Solvent use	–	23.56	0.13	–	–	0.06	–	0.68
Traffic	61.4	27.97	20.74	3.34	47.37	0.96	0.62	3.96
Other mobile sources	7.55	5.03	3.95	1.89	15.87	–	0.07	1.09
Waste treatment and disposal	4.66	1.28	2.09	0.58	0.84	1.09	30.44	1.65
Agriculture	0.74	17.17	−1.80	–	0.29	94.65	39.52	34.45
Nature	0.21	8.64	0.09	15.50	0.17	0.23	13.47	27.06

2.2 ANTHROPOGENIC EMISSIONS

The three major groups of gaseous air pollutants by historical importance, concentration, and overall effects on plants and animals (including people), are sulphur dioxide (SO_2), oxides of nitrogen ($NO_x = NO + NO_2$) and ozone (O_3).

Sulphur dioxide and nitric oxide (NO) are primary pollutants – they are emitted directly from sources. We shall start by looking at the main sources of these and other primary gases, and also consider some of the methods of control that can be used to reduce emissions and concentrations when required. Then we will move on to ozone, which is referred to as a secondary pollutant because it is mainly formed in the atmosphere from primary precursors, and emissions of the gas itself are negligible. Nitrogen dioxide (NO_2) is both primary and secondary – some is emitted by combustion processes, while some is formed in the atmosphere during chemical reactions. Production of SO_2 is commonly associated with that of black smoke, because it was the co-production of these two materials during fossil fuel combustion that was responsible for severe pollution episodes such as the London smog events of the 1950s, discussed earlier in Chapter 1.

2.2.1 Energy-related emissions

During most of recorded history, the population of the world has grown slowly, reaching 200 million in AD 1, 250 million in AD 1000 and 450 million in 1600. During the seventeenth century, we started to learn how to keep people alive before we realised the consequences, and the rate of growth increased explosively. The population reached 6 billion in 2000, and is now forecast to cross the 9 billion mark before 2050 (Figure 2.1). Ninety-eight percent of the future population growth is predicted in developing countries, and most of that will be in urban areas. This rapidly increasing population has also been increasing its standard of living, underpinned by energy obtained from fossil fuels –

FOR REFERENCE PURPOSES ONLY

initially from coal burning but more recently by oil and gas. Although increased energy efficiency in the developed nations stabilised the use per person after 1970, the continuing increase in total population is still driving up the total energy use. We each use about 2 kW on average – equivalent to one fan heater – although this single average conceals a wide range between intensive users such as the United States (10 kW) or Western Europe (5 kW), and less developed countries having very small energy inputs. The combustion of fossil fuels to generate this energy converts carbon into carbon dioxide and releases it into the atmosphere. Guideline energy contents of fossil fuels, and of their alternatives, are shown in Table 2.4.

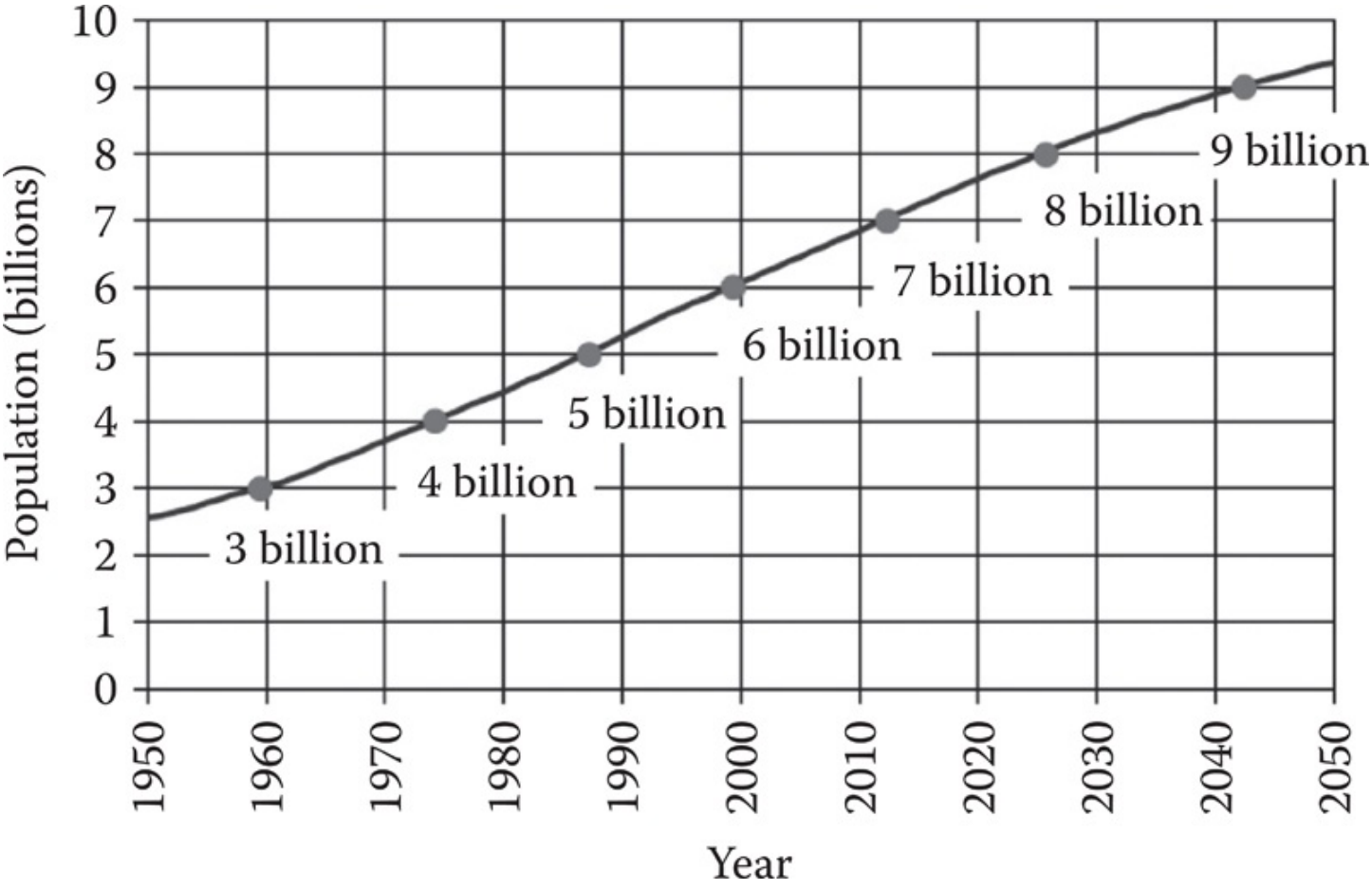

Figure 2.1 The growth of world population between 1950 and 2050. (From US Census Bureau, International database update, August 2016.)

Table 2.4 Typical energy contents of widely used fuels

Energy source	*Energy density (MJ kg^{-1})*
Natural gas	51
Petroleum	37
Coal	30
Anthracite	30
Bituminous	20

FOR REFERENCE PURPOSES ONLY

Sub-bituminous (brown)	10–15
Lignite	
Animal dung (dry weight)	17
Wood (dry weight)	15

Figure 2.2 shows the parallel growth in carbon release (as CO_2) in the nineteenth and twentieth centuries. Coal was the original fossil fuel used, then oil from 1900 and gas from 1930. Also visible are major disturbances to the drive for growth – the recession in the 1930s, World War II and the oil price crisis of 1974.

Coal is the fuel that underpinned successive Industrial Revolutions from the Bronze Age through the eighteenth century. It is the most abundant fossil fuel, with huge reserves of some 1000 billion tonnes that are expected to last another 300 years at present rates of use. What were originally peat deposits became buried and compressed under accumulating sediments. The increased pressure and temperature caused the peat to pass through a series of stages called the coal series, characterised by decreasing moisture content and volatiles and a higher carbon content. The members of this series are called lignite, sub-bituminous brown coal, bituminous coal and anthracite. The earlier members of the coal series (from younger deposits, Cretaceous rather than Carboniferous) are poor quality, low-calorific value fuels which need to be burnt in large tonnages. However, coal use as a proportion of total use is declining, because of the handling advantages of fluid fuels such as oil and gas.

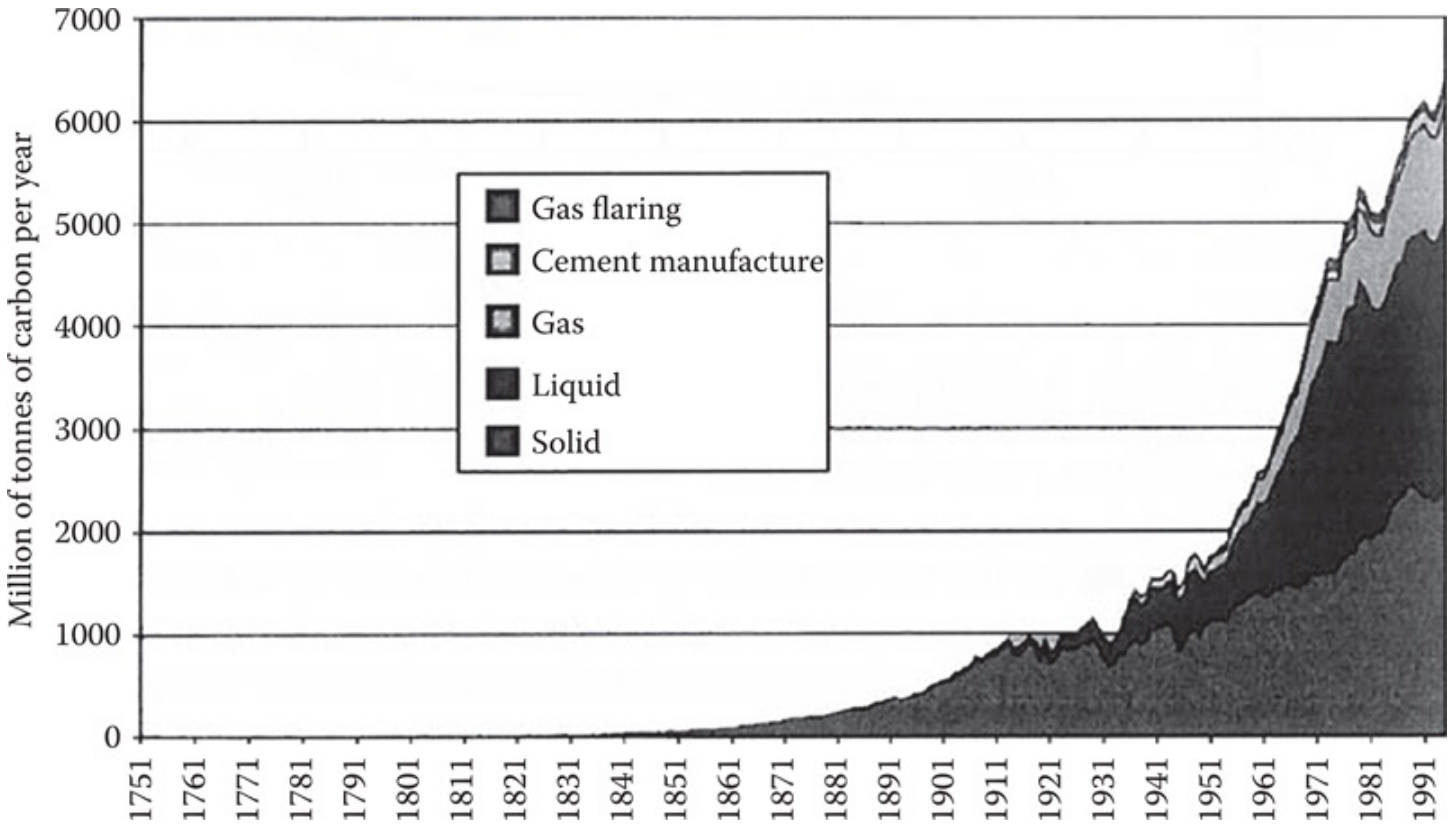

Figure 2.2 Global carbon release 1750–1995. (From Wuebbles, D. J. et al., *Environ.*

FOR REFERENCE PURPOSES ONLY

Pollut., 100, 57–86, 1999.)

The origin of the world's oil deposits is far less well understood than is coal's. Oil itself consists of thousands of different organic molecules, mainly hydrocarbons. Whereas coal formed from the action of sediments on accumulating vegetable matter in a terrestrial environment, it is thought that oil formed in a parallel process acting on accumulating microscopic animal remains in a marine environment. Although fluid, the oil could sometimes be trapped below a domed cap of impermeable rock. As well as these deposits of pure liquid oil, there are extensive deposits of oil shales and sands, in which the oil soaks through a permeable rock much like water through a sponge. More recent excavations in the United States and Europe are focusing on utilising these untapped reserves, albeit with resistance from residents and local communities towards ensuring sustainable consumption. Crude oil as extracted is not useable as a fuel but has to be refined by the process of fractional distillation. This process yields not only fuels such as heavy fuel oil, diesel, petrol and paraffin, but a wide range of chemicals which can be used to make plastics and other materials.

Natural gas, which is mainly the simplest hydrocarbon methane, is associated with both the formation of coal seams and oil deposits. With coal it is usually just a safety issue, being present in sufficient concentrations to foul the air and cause risk of explosions. With oil it is usually present in large volumes, overlying the oil deposit, that have been exploited as a fuel in their own right.

Table 2.5 provides a breakdown of historical and projected global consumption of energy up to 2030. It includes renewables such as wind turbines or biofuels. The overall energy consumption is projected to rise, with an average annual increase of up to 2.5% between 2003 and 2030 for natural gas, coal and renewables. The per capita energy use varies widely between countries according to their stage of development, from 7 to 8 tonnes oil equivalent (toe) per year in North America (where 5% of the world's population uses 25% of the energy), and 4 toe in Europe, to 0.2 toe in India.

Developing countries also offer very different fuel combustion profiles, especially in the domestic sector. Whereas domestic energy supply in the developed countries is likely to be from burning gas in a centralised boiler for a central heating system, developing countries are much more likely to be using fuels such as kerosene, wood, roots, crop residues, or animal dung. Furthermore, these are likely to be burnt in an indoor stove without a flue and with poor combustion efficiency. Hence, the potential for pollutant emissions and enhanced indoor pollutant concentrations is much greater. Ironically, if the renewable fuels could be combusted without pollutant emissions, they would be superior to fossil fuels, because they have no net impact on CO_2 concentrations. In some countries, for example, China and India, national programmes have increased the availability of higher efficiency flue stoves. While these still generate significant emissions to the atmosphere, they certainly reduce the indoor concentrations and consequent health impacts.

FOR REFERENCE PURPOSES ONLY

Table 2.5 Global consumption of energy by fuel between 1990 and 2030 ($\times 10^{15}$ Btu)

	History		Projection	Average annual percent change
Energy source	*1990*	*2003*	*2030*	*2003–2030*
Oil	136.1	162.1	239.1	1.4
Natural gas	75.2	99.1	189.9	2.4
Coal	89.4	100.4	195.5	2.5
Nuclear	20.4	26.5	34.7	1.0
Others (includes renewables)	26.3	32.7	62.4	2.4
Total	347.3	420.7	721.6	2.0

Source: Energy Information Administration, *Annual Energy Outlook 2006*, US Department of Energy, Washington, DC, DOE/EIA-0383, 2006.

2.2.2 Sulphur oxide emissions

All fossil fuels contain sulphur, most of which is released as sulphur dioxide during combustion. Almost all the anthropogenic sulphur contribution is due to fossil fuel combustion. Different fuels offer a wide range of sulphur contents:

- Oil and its by-products contain between 0.1% sulphur (paraffin) and 3% (heavy fuel oil) in the form of sulphides and thiols. Petrol contains negligible sulphur in the context of overall mass emissions, although there can be an odour problem from conversion to hydrogen sulphide (H_2S) on catalytic converters.
- Coal contains 0.1%–4% sulphur, mainly as flakes of iron pyrites (FeS_2). The average sulphur content of UK coal is 1.7%.
- Natural gas (mainly methane [CH_4]) can be up to 40% H_2S when it is extracted from the well. The sulphur is taken out very efficiently at a chemical processing plant before distribution, so natural gas is effectively sulphur-free – one of the reasons for the so-called *dash for gas*.

Using a combination of bottom-up and available inventory methods, including all anthropogenic sources, a global estimate of sulphur dioxide emissions from different meta-regions between 1850 and 2000 is presented in Figure 2.3. It suggests that global sulphur dioxide emissions peaked about 1980 and since then have been declining in most parts of the world. However, emissions from the developing regions rose again around 1990, largely attributed to coal combustion. Emissions from China are now comparable to those from the US, and in 2000 emissions from Asia, North America and Europe accounted for over half the global total.

FOR REFERENCE PURPOSES ONLY

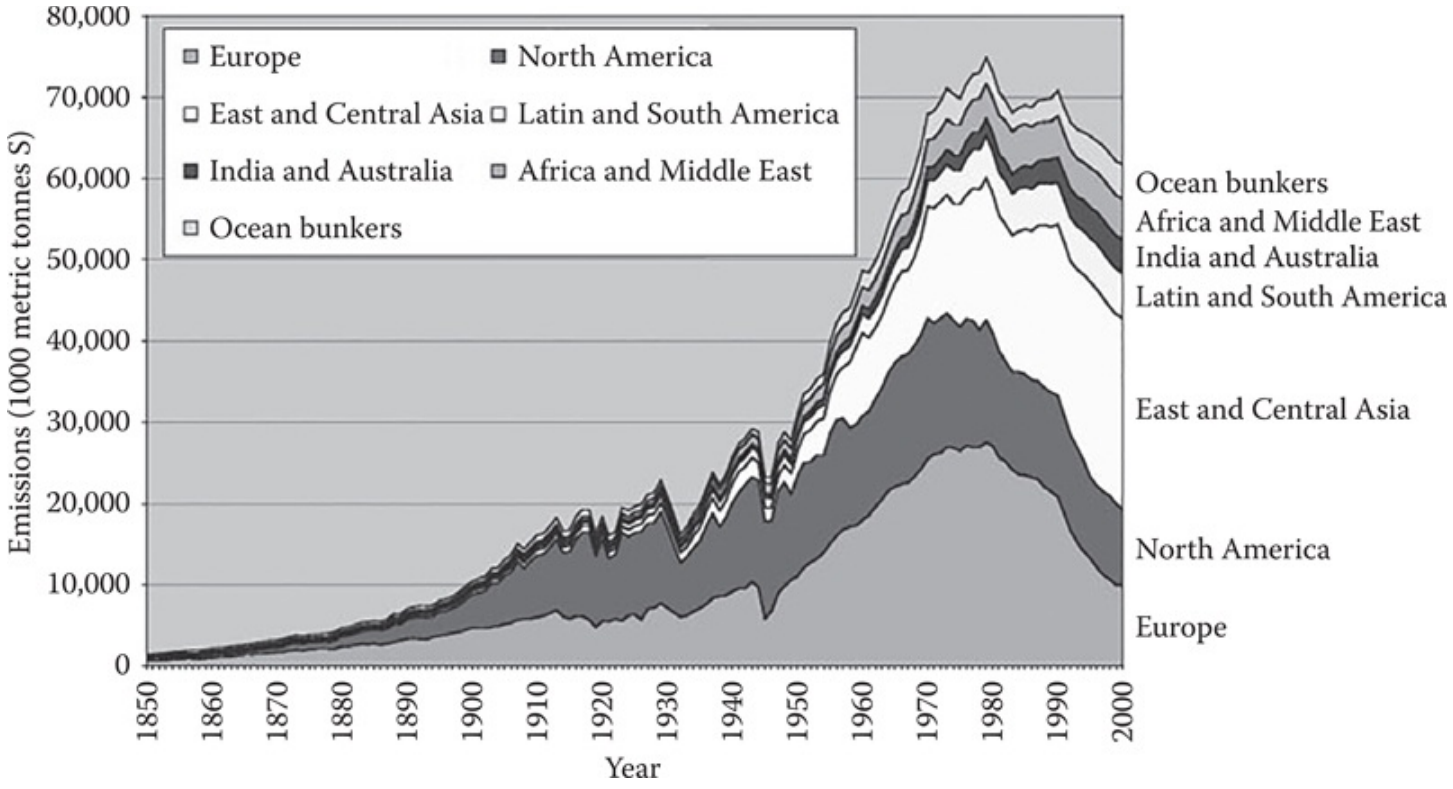

Figure 2.3 Global sulphur dioxide emissions by meta-region between 1850 and 2000. (From Smith, S. J. et al., Historical sulfur dioxide emissions 1850–2000: Methods and results, US Department of Energy, PNNL Report No. 14537, 2004.)

2.2.2.1 Sulphur dioxide

Sulphur dioxide (SO_2) is a colourless gas with a penetrating, choking odour. It dissolves readily in water to form an acidic solution (sulphurous acid). SO_2 (generally expressed as SO_x) has long been recognised as a pollutant because of its role, along with particulate matter, in forming winter-time smog. Sulphur is present in all hydrocarbon fuels to some degree and has especially high concentrations in coal, up to 7% sulphur by weight. SO_2 is formed as a primary pollutant when coal is burnt. The major natural sulphur emissions are in the reduced forms of H_2S (hydrogen sulphide), CS_2 (carbon disulphide) or COS (carbonyl sulphide), and the organic forms CH_3SH (methyl mercaptan), CH_3SCH_3 (dimethyl sulphide [DMS]) and CH_3SSCH_3 (dimethyl disulphide [DMDS]). Dimethyl sulphide is produced by marine phytoplankton and oxidised to SO_2 in the atmosphere, H_2S from decay processes in soil and vegetation and SO_2 from volcanoes. Whatever their original form, much of these sulphur compounds eventually get oxidised to gaseous SO_2 or to sulphate aerosol. Sulphur trioxide (SO_3), another component of the SO_x family, is an intermediate product formed during the manufacture of sulphuric acid (contact process).

SO_2 emissions can be calculated from the knowledge of the sulphur content of the fuel

FOR REFERENCE PURPOSES ONLY

and from the information on the amount of sulphur retained in the ash. The natural sources are now heavily outweighed by human ones, principally fossil fuel combustion, as shown in Figure 2.4. Note that the emission strengths are given as mass of sulphur, not of sulphur dioxide. If these values are compared with others expressed as SO_2, then they must be multiplied by the ratio of the molecular weights, which is 2.0 (64/32) in this case.

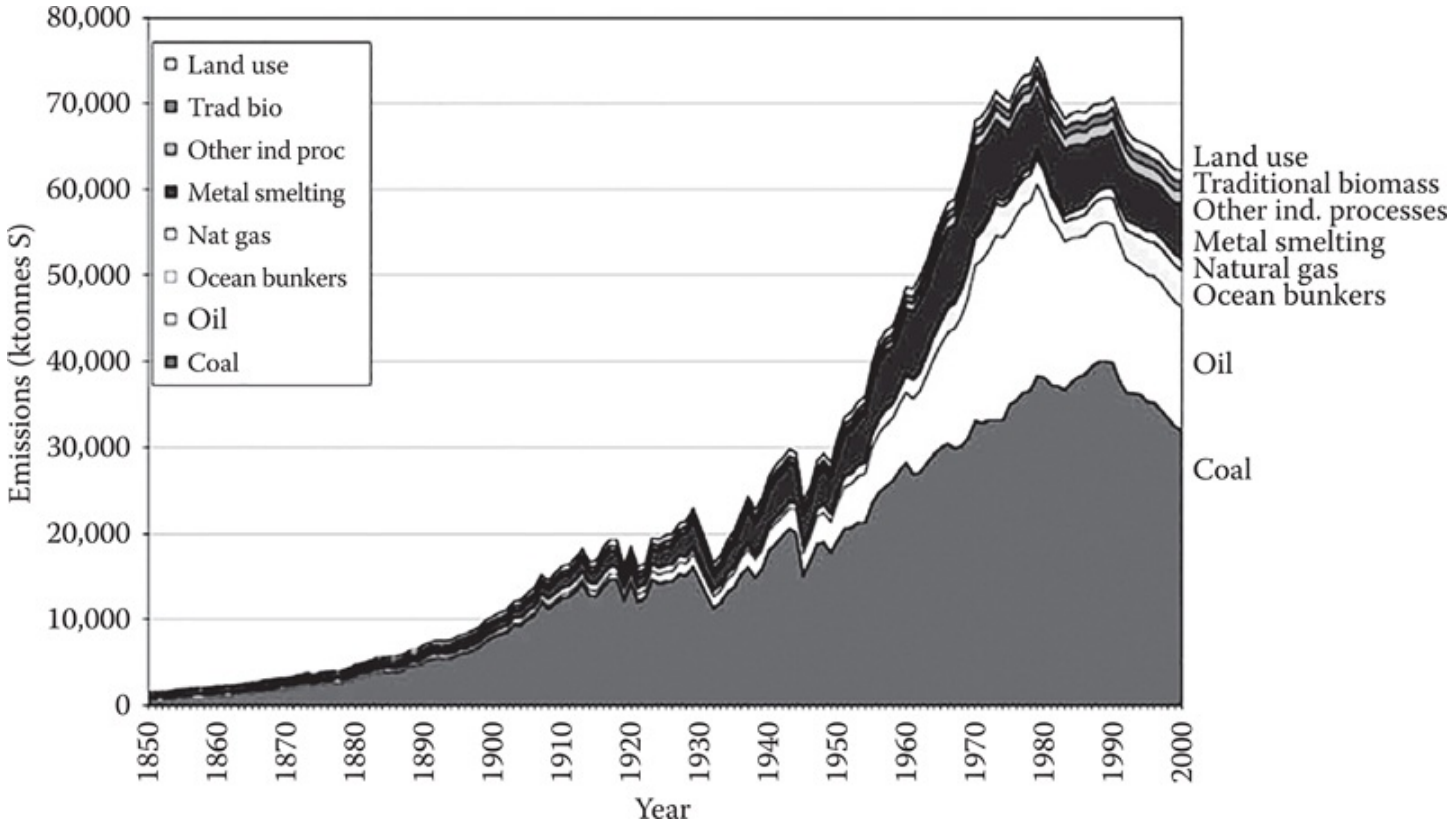

Figure 2.4 Anthropogenic sources of global sulphur dioxide emissions between 1850 and 2000. (From Smith, S. J. et al., Historical sulfur dioxide emissions 1850–2000: Methods and results, US Department of Energy, PNNL Report No. 14537, 2004.)

Table 2.6 Anthropogenic emissions of SO_2 by world regions to 2030 (Tg SO_2 yr^{-1})

FOR REFERENCE PURPOSES ONLY

			Reduction based on current legislation			Maximum feasible reductions		
Region	1990	2000	2010	2020	2030	2010	2020	2030
North America	24	19	11	8	8	3	3	3
Western Europe	18	8	4	3	3	1	1	1
Central and Eastern Europe	11	6	4	2	2	1	0	0
Russia and Newly Independent States (NIS)	19	10	7	6	6	2	2	2
Central Asia	21	21	25	22	22	6	6	6
Other Pacific Asia	5	4	6	7	9	2	2	2
South Asia	5	7	11	17	22	2	3	3
Latin America	7	8	6	5	5	2	2	2
Middle East	3	5	3	3	2	1	1	1
Africa	5	5	5	5	6	1	1	2
World Total	120	96	85	82	87	21	22	22

Source: Cofala, J. et al., *Atmos. Environ.*, 41, 8486–8499, 2007.

Table 2.6 gives the regional split of anthropogenic SO_2 emissions projected up to 2030. Note that the projections are based on two distinct assumptions – (1) where the reductions follow the current legislation and (2) where maximum feasible reductions can be achieved. Both scenarios show marked reductions in SO_2 emissions for 2030 for Western and Eastern Europe, Latin America and Russia but a significant increase in the emissions for Central and South Asian countries.

Information about the budgets of reduced sulphur components is less soundly based than that for oxidised S. Approximate total emissions are given in Table 2.7.

Emissions are not usually spread uniformly across the country. In the UK, the National Atmospheric Emissions Inventory (NAEI) compiles very detailed maps of estimated emissions on a 10 × 10 km grid. These estimates are updated annually. Two factors drive SO_2 emissions – population and power stations. There are clusters of emissions around the large urban centres, because these areas are industrial, as well as population centres. There are also clusters around the group of coal-fired power stations in the English East Midlands. Areas of low population density, such as the Highlands of Scotland and central Wales, have correspondingly low emission densities.

Chapter 6 discusses how such a concentration of emissions also results in a concentration of deposition and the resulting effects on ambient air quality. In industrialised countries, emissions have been falling in recent decades, mainly from application of efficient tail-pipe cleaning technologies and from investment in alternative combustion technologies. Figure 2.3 shows that, even while global emissions continued to rise, European emissions peaked in about 1980 and have been falling since then. This trend is also reflected in the UK emissions (Figure 2.5), which rose fairly consistently until the late 1960s before starting to

FOR REFERENCE PURPOSES ONLY

decline.

Table 2.7 Global emissions of reduced sulphur

Compound	*Emission (Tg yr^{-1})*
Carbonyl sulphide (OCS)	1.3
Carbon disulphide (CS_2)	1.0
Hydrogen sulphide (H_2S)	8.0
Dimethyl sulphide (DMS)	25

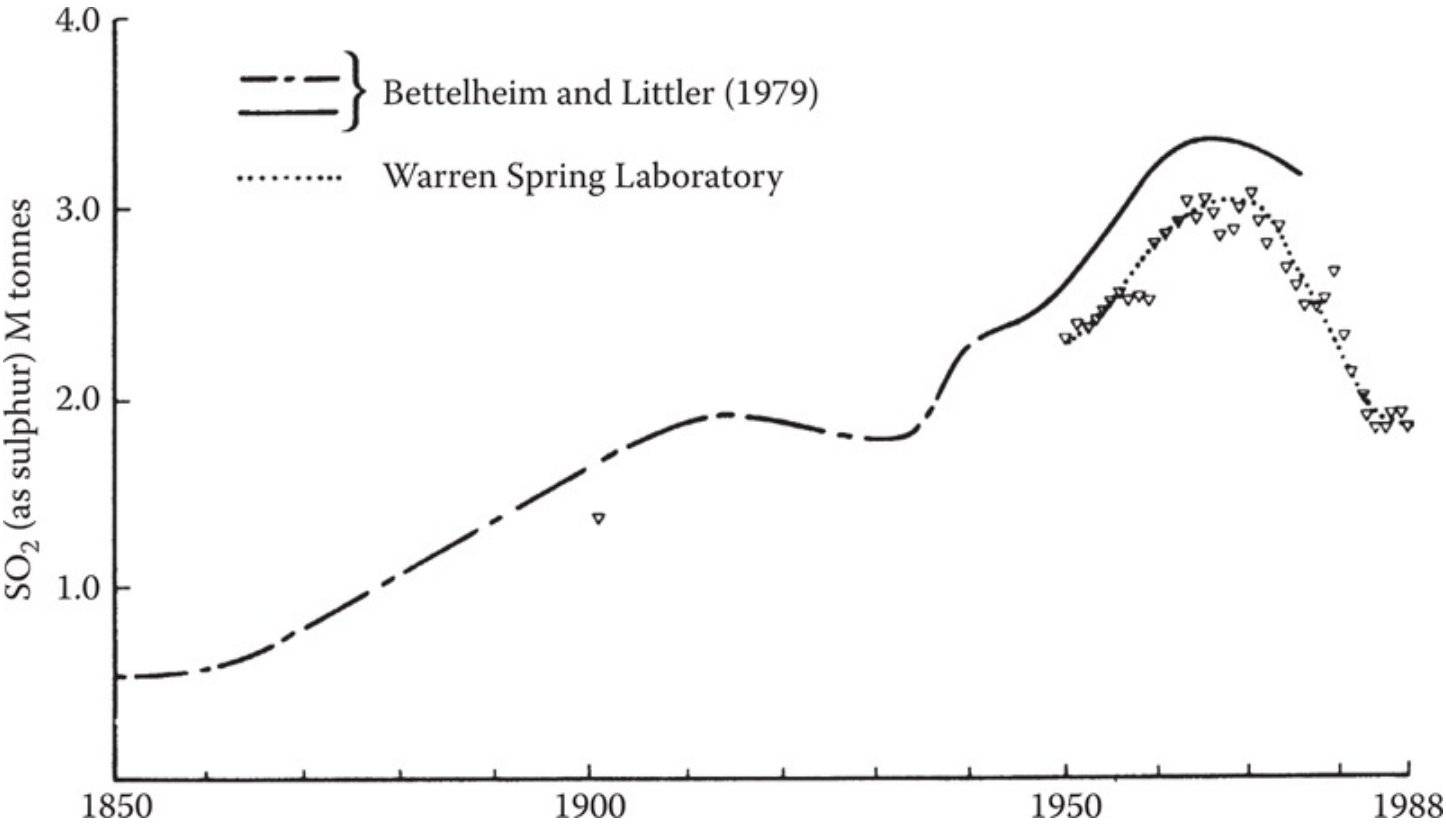

Figure 2.5 UK SO_2 emissions 1850–1988. (From Eggleston, S. et al., *Atmos. Environ.*, 26B, 227–239, 1992.)

Table 2.8 provides the annual UK SO_2 emissions for 1970 and 2015 broken down by United Nations Economic Commission for Europe (UNECE) source categories. Since 1970, SO_2 emissions have declined by 96%, largely due to the combined influence of lower sulphur fuels, the switch from coal to natural gas and increased energy efficiency. A substantial part of the overall emissions is due to public electricity and heat generation, and transport contributes only a negligible proportion (contrast this with NO_x emissions presented in Section 2.2.3). Fuel combustion accounted for 94% of UK SO_2 emissions in 2015 with the main source being the combustion of solid fuel, mainly coal, which has a high sulphur content relative to other fuels. Emissions from the power sector and the

manufacturing industry have seen the largest reductions, mainly from a decrease in coal use (corresponding reduction in CO_2 emissions for the same reason over this period are discussed in Chapter 11). The most important factors associated with the fall in transport emissions from petroleum use are the decline in fuel oil use and the reduction in the sulphur content of gas oil and diesel engine road vehicle (or DERV, diesel fuel specifically used for road vehicles). Between 1994 and 2006 the SO_2 emissions from DERV are estimated to have been reduced by as much as 98%. Emissions in 2015 dropped 19% below the UK's National Emission Ceilings Directive and future emissions targets set by the Gothenburg Protocol targets for 2020 (see Chapter 14).

Table 2.8 UK emissions of SO_2 in 1970 and 2015, by aggregated source category (ktonnes yr^{-1})

	1970 Emissions	*2015 Emissions*	*Percentage reduction*
By source category			
Combustion in energy and transformation industry	3301.36	126.41	96.17
Combustion in manufacturing industry	1748.03	50.16	97.13
Production processes/waste	146.99	13.98	90.49
Residential/commercial/institutional	964.80	40.39	95.81
Transport	162.11	5.18	96.80
Total	6323.28	236.12	96.27

Source: NAEI, *UK Emissions of Air Pollutants 1990 to 2015*, National Atmospheric Emissions Inventory, 2016.

2.2.2.2 Sulphur trioxide

A small proportion of the fuel sulphur (typically up to a few percent) may be further oxidised to sulphur trioxide (SO_3). This has three main consequences: first, a blue mist of sulphuric acid droplets can be emitted from boiler chimneys; second, water vapour and SO_3 combine to condense out sulphuric acid on cool parts of the ductwork, accelerating the corrosion of metal parts; third, smoke particles accumulate on these sticky areas of the ductwork. Small lumps of this acidified deposit, known as *acid smuts*, are entrained into the gas stream, ejected from the chimney and may then fall onto and damage local sensitive surfaces such as car paintwork or clothes. The conversion to SO_3 is catalysed by vanadium, so that some fuel oils that are high in vanadium can convert 20%–30% of the initial sulphur into SO_3. Proprietary chemical oil additives are available that can help to control this problem.

2.2.3 Nitrogen oxide emissions

Nitrogen oxides are acid gases and ozone precursors. As discussed in Chapter 1, in the

FOR REFERENCE PURPOSES ONLY

presence of sunlight, NO_x can react to produce a photochemical smog. Photochemical oxidation in the presence of hydrocarbons can also lead to production of ozone (discussed in Chapter 12), which has a similar health effect to NO_x. The two principal oxides of nitrogen are nitric oxide (NO) and nitrogen dioxide (NO_2). The sum of these two is known as NO_x (pronounced either as 'en-oh-ex' or as 'knocks'). Despite their quite different physical properties, chemical affinities and environmental impacts, they are often lumped together. Combustion always produces a mixture of NO_2 and NO, although typically more than 90% of combustion NO_x production is in the form of NO.

2.2.3.1 Nitric oxide

Nitric oxide is formed in two distinct ways:

Thermal NO is formed from reactions between the nitrogen and oxygen in the air. The reactions can be summarised by the Zeldovitch mechanism:

$$N_2 + O \rightarrow NO + N$$

$$N + O_2 \rightarrow NO + O$$

This is highly endothermic, so that thermal NO production is at a maximum in the highest-temperature regions of a combustion chamber.

Fuel NO is formed from nitrogen in the fuel. Typically, fuel nitrogen contents are 0.5%–1.5% in oil and coal, and rather less in gas.

Total UK NO_x emissions were quite steady until the 1940s, when they started to increase sharply. Emissions from coal combustion fell during the recession in the 1930s before reviving, while those from oil products increased steadily until curtailed in 1974. More recently, the surface transport sector has become the dominant source of NO_x emissions. Figure 2.6 shows the historical UK NO_x emissions from different transport options between 1970 and 2015. The emissions include: combustion of turbine fuel for aviation; utilisation of petrol and diesel oil (DERV), cold start emissions for urban and rural drives for cars; cold start emissions, urban, rural and motorway drives for light goods vehicles (LGVs); urban, rural and motorway drives for heavy goods vehicles (HGVs); urban and rural drives for motorcycles and mopeds; intercity, regional and freight for railways; and, coastal domestic shipping. The figure shows that road vehicle emissions rose steadily between 1970 and 1989; during this period emission from total petrol consumption, mainly by cars, rose by 106% from the 1970 level and emission from diesel consumption rose by 38%. However, since 1989 there has been a steady decline in emissions due to the introduction of three-way catalytic converters on petrol cars and stricter regulations on truck emissions. By 2015, the cumulative emissions from all transport categories reached almost half their

FOR REFERENCE PURPOSES ONLY

corresponding level in 1970.

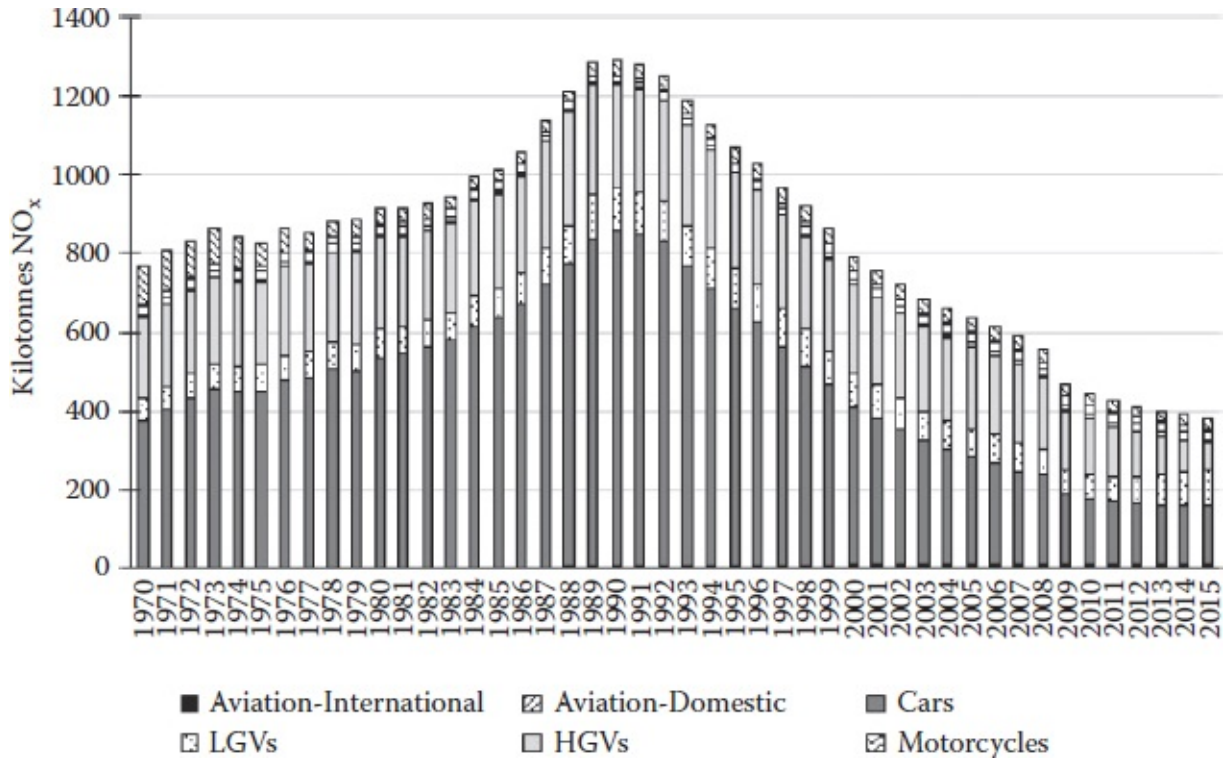

Figure 2.6 Historical UK NO_x emissions from different transport options between 1970 and 2015 (ktonnes). (From NAEI, *UK Emissions of Air Pollutants 1990 to 2015*, National Atmospheric Emissions Inventory, 2016.)

Nitric oxide is also emitted from soils, but it has proved harder to quantify the source strength. Nitrifying bacteria produce both nitric and nitrous oxide – anaerobic production of NO is thought to dominate overall. Guesstimates based on rather sparse data suggest that UK soil production of NO may be equivalent to 2%–5% of the production from fuel combustion.

Table 2.9 gives the UK emissions of nitrogen by aggregated UNECE source categories for 1970 and 2015. The final column in the table indicates the percentage changed (largely reduction) over this period. Since 1970, overall UK NO_x emissions have decreased by 69%. Industrial combustion and road transport are the main contributors to UK NO_x emissions. Although the emission from passenger cars have more than halved over this period, there was a large rise to a peak of 400 kt in 1989 (Figure 2.6) before they were controlled by catalytic converters and stricter EU emissions standards (see Chapter 14). Over the early part of the twenty-first century the power sector emissions have declined due to changes in fuels burnt (more gas and less coal), and the use of control technologies to minimise emissions in response to stringent industrial emissions directives. Around a third of the UK NO_x emissions appear to come from road transport, mostly originating from diesel vehicles. However, the estimation of these emissions is complex since the nitrogen can

FOR REFERENCE PURPOSES ONLY

originate from either the fuel or atmospheric nitrogen. The emission is dependent on the conditions of combustion, in particular temperature and excess air ratio, which can vary considerably. It is important to note that, despite the precision with which the emissions are quoted, the error on these estimates (and on those of corresponding emissions of other gases) has been estimated to be 15%–20%. It should also be anticipated that the emitted nitrogen, once returned to the surface, will have a significant impact on both managed and natural ecosystems.

Table 2.9 UK NO_x emissions in 1970 and 2015, by aggregated source category (ktonnes yr^{-1})

	1970 Emissions	*2015 Emissions*	*Percentage reduction*
By source category			
Combustion in industry	1221.13	292.77	76.02
Heavy-duty vehicles	212.59	70.23	66.96
Other transport	307.56	214.50	30.26
Passenger cars	373.74	147.54	60.52
Production processes/agriculture/waste and other	42.14	5.13	87.82
Public electricity and heat production	814.03	188.16	76.89
Total	2971.18	918.34	69.09

Source: NAEI, *UK Emissions of Air Pollutants 1990 to 2015*, National Atmospheric Emissions Inventory, 2016.

Recent estimates based on Global Ozone Monitoring Experiment (GOME) satellite data attribute over 60% of global NO_x to fuel combustion emissions (fossil + biofuel), 15% to biomass burning and over 20% to soil emissions. Table 2.10 shows the global distribution of anthropogenic NO_x emissions by world regions. Although most of the direct emission is NO, the source strengths are given as NO_2 equivalent as all the NO is potentially available for oxidation to NO_2. Low emissions indicate either an immature economy, which is not energy-intensive, or a mature economy, which is energy-intensive but has extensive pollution controls in place.

Table 2.10 Anthropogenic emissions of NO_x by world regions (Tg NO_2 yr^{-1})

FOR REFERENCE PURPOSES ONLY

			Reduction based on current legislation			Maximum feasible reductions		
Region	1990	2000	2010	2020	2030	2010	2020	2030
North America	24	22	18	12	12	6	6	7
Western Europe	15	11	8	6	6	3	3	3
Central and Eastern Europe	3	2	2	1	1	1	0	1
Russia and NIS	11	7	6	5	6	1	2	2
Central Asia	8	11	14	14	15	4	5	5
Other Pacific Asia	4	6	6	6	7	2	2	3
South Asia	3	6	7	9	10	2	3	3
Latin America	6	7	6	7	8	2	2	2
Middle East	3	4	3	3	4	1	1	1
Africa	3	4	4	5	8	1	1	2
Total	84	83	78	71	80	24	26	30

Source: Cofala, J. et al., *Atmos. Environ.*, 41, 8486–8499, 2007.

2.2.3.2 Nitrogen dioxide formation

Only a small proportion of the NO_2 found in the atmosphere was released in that form from sources. The remainder has been created in the atmosphere as part of the same photochemical activity that is responsible for ozone formation. The nitric oxide from fossil fuel combustion reacts with ozone as follows:

$$NO + O_3 \rightarrow NO_2 + O_2$$

During daylight, the NO_2 absorbs blue and UV radiation <420 nm and decomposes back to NO and O_3, resulting in a photochemical equilibrium between the four gases. In rural areas, away from the NO sources, the NO_2 concentration is usually considerably higher than that of NO. In urban areas, the O_3 becomes depleted and the balance moves in favour of NO. The production of ozone, which requires more complex cycles involving organic compounds and radicals, is discussed in Section 2.3.

On the global scale, the majority of NO_x sources (except aircraft and lightning) are located close to the Earth's surface. As a result of this fact and the relatively short NO_2 chemical lifetime as explained earlier, remote sensing measurements from satellite instruments (GOME and SCanning Imaging Absorption SpectroMeter for Atmospheric CHartographY [SCIAMACHY]) have been utilised recently to estimate the temporal evolution of tropospheric NO_2 columns for several geographic regions (Figure 2.7). This figure shows the mean annual NO_2 column amount normalised to that in 1996. The error bars represent the estimated uncertainty (i.e. the standard deviations [s.d.]) for an individual year. The trend shows substantial reductions in NO_2 concentrations over some areas of

FOR REFERENCE PURPOSES ONLY

Europe and the US, but a significant increase of about 50%, with accentuating annual growth rate post 2000, over the industrialised regions of China.

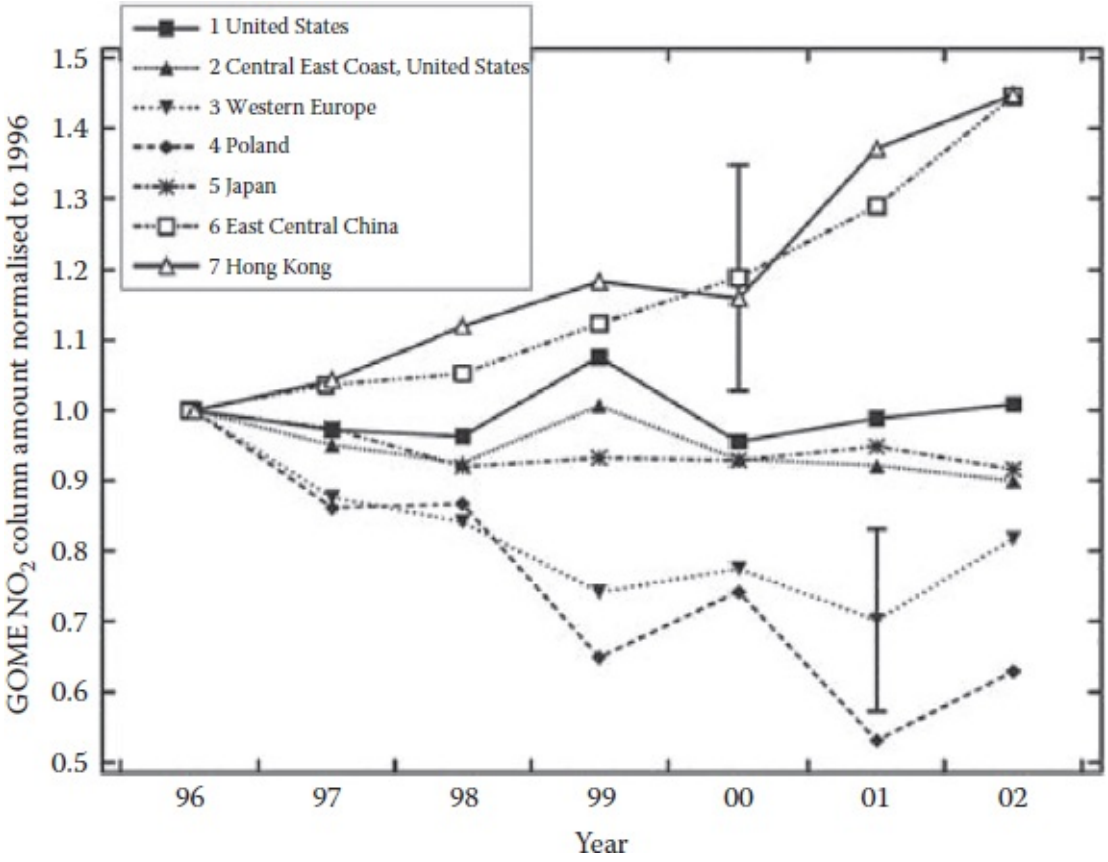

Figure 2.7 The temporal evolution of tropospheric NO_2 columns from GOME for selected areas. (From Richter, A. et al., *Nature*, 437, 129–132, 2005.)

The principal sink for NO_x is oxidation to nitric acid HNO_3. During the daylight hours

$$NO_2 + OH + M \rightarrow HNO_3 + M$$

and at night,

$$NO_2 + O_3 \rightarrow NO_3 + O_2$$

$$NO_3 + NO_2 + M \rightarrow N_2O_5 + M$$

$$N_2O_5 + H_2O \rightarrow 2HNO_3$$

The resulting lifetime of NO_x is only about a day. Furthermore, HNO_3 is highly soluble in water and easily removed by precipitation, so it has not been clear what acts as the effective NO_x reservoir, which is required to explain its occurrence in regions remote from anthropogenic sources. The likely route is thought to be via peroxyacetyl nitrate

($CH_3C(O)OONO_2$, usually referred to as PAN). Peroxyacetyl nitrate is produced in the troposphere by photochemical oxidation of carbonyl compounds in the presence of NO_x. For example, from acetaldehyde CH_3CHO

$$CH_3CHO + OH: \rightarrow CH_3CO + H_2O$$

$$CH_3CO + O_2 + M \rightarrow CH_3C(O)OO + M$$

$$CH_3C(O)OO + NO_2 + M \rightarrow PAN + M$$

As PAN is only slightly soluble in water, it is not removed effectively by precipitation processes. The main loss route is by thermal decomposition which regenerates NO_x:

$$PAN \xrightarrow{heat} CH_3C(O)OO + NO_2$$

This decomposition process has a time constant of 1 h at 295 K but several months at 250 K. Hence, it is thought that PAN generated close to NO_x sources moves into the upper troposphere and lower stratosphere, where the low temperatures allow it to be transported long distances before releasing NO_x. This process maintains NO_x concentrations at 50–100 ppt throughout the remote troposphere.

2.2.4 Ammonia

A further class of emissions is often grouped as NH_y, meaning the sum of ammonia (NH_3) and ammonium (NH_4). The three main sources of atmospheric ammonia are livestock farming and animal wastes, with emissions primarily due to the decomposition of urea from large animal wastes and uric acid from poultry wastes. The overall total emission from these sources has increased with the intensification of agriculture, which has also changed the nature of the emissions from area to point sources. Emissions from housed and field animals are relatively steady in nature, while operations such as slurry and manure spreading result in more intense short-term emissions. Ammonia emissions can be changed by feed N content, the conversion of feed N to meat N (and hence the N content of animal wastes), and the management practices applied to the animals.

Table 2.11 Global ammonia emissions

Source	*Global emission (Mt N yr^{-1})*
Vegetation	5
Oceans	7
Biomass burning	2
Fertiliser application	6
Livestock	25

FOR REFERENCE PURPOSES ONLY

Total	45

Table 2.12 UK emissions of NH_3 in 1980 and 2015, by aggregated source category (ktonnes yr^{-1})

	1980 Emissions	*2015 Emissions*	*Percentage change*
By source category			
Cattle	93.29	73.58	21.13
Combustion and production processes	10.75	13.11	–21.99
Direct soil emissions	150.00	130.17	13.22
Other livestock	35.96	18.75	47.85
Poultry	17.92	15.10	15.76
Waste	17.22	42.13	–144.60
Total	325.13	292.84	9.93

Source: NAEI, *UK Emissions of Air Pollutants 1990 to 2015*, National Atmospheric Emissions Inventory, 2016.

Globally, animal emissions are roughly equal to the combined emissions from other sources (Table 2.11). The largest single source of emissions in the UK is release to the atmosphere for the few days immediately following slurry application to fields. Table 2.12 gives a sectoral breakdown of the principal UK sources of ammonia, aggregated by source categories. Agricultural sources contribute to over 81% of total UK NH_3 emissions in 2015. The pattern is reflected in emission estimates for other countries – the percentages due to cattle, sheep and pigs are around 88% in Germany, 94% in the Netherlands and 83% in Japan. The total European emission is about 7 Mt NH_3 $year^{-1}$, of which some 80% is thought to be due to animal manure from intensive livestock production. This agricultural connection has a sharp influence on the geographical distribution of sources. Unlike emissions of NO_x or SO_2, those of ammonia are at their greatest in rural areas associated with intensive livestock production – the Netherlands, northern parts of Germany and France, southwest and northwest England, Wales and Ireland. The nature of the emission is also different – whereas combustion emissions are produced at very high concentrations from point sources, ammonia emissions are released at very low initial concentrations from large area sources such as pastures and soil. The potential for ammonia release is indicated by the increase in fertiliser use in the second half of the twentieth century – from 200 kt N in 1950 to 1500 kt N in 1990. Much of this fertiliser was used to increase pasture and feed grain production for cattle and sheep. Clover in pasture is used to fix around 200 kg N ha^{-1}, which subsequently increases the amount of N from animal excreta. There is also marked increase in emissions from production processes and combustion (largely from lean burning fuels). But, the most prominent increase is observed from waste emissions, with an increment of over 140%.

Ammonia is also volatilised directly from fertilised crops and grassland. When urea is

FOR REFERENCE PURPOSES ONLY

used, this loss can amount to 5%–20% of the applied N; losses from ammonium nitrate (which makes up around 90% of UK applications) are probably less than 5%. The picture is further complicated by the fact that ammonium is present in plant tissues; when the atmospheric concentration is less than a critical value (known as the compensation point), ammonia can diffuse to the atmosphere from the stomata. Conversely, if the concentration is above the compensation point, then there is deposition. Hence, the emission rate is influenced by plant N status, stomatal aperture and microclimate. There may be both diurnal and annual cycles, with emission being favoured after fertiliser application, during daylight and during leaf senescence, and deposition at night or when the leaf canopy is wet.

Additional sources with small contributions to NH_3 emissions are from the industrial plants where ammonia and fertilisers are produced, human sweat and breath (around 0.2 kg person^{-1} a^{-1}), and wastes from domestic pets such as cats and dogs. However, these emissions are insignificant compared to those of atmospheric ammonia listed in Table 2.12.

2.2.5 Non-methane volatile organic compounds

The general category of non-methane volatile organic compounds (NMVOCs) includes organic compounds, such as hydrocarbons (alkanes, alkenes and aromatics), halocarbons (e.g. trichloroethylene) and oxygenates (alcohols, aldehydes and ketones). Historically, NMVOCs are grouped under one label because the majority of them display similar behaviour in the atmosphere. NMVOCs are mainly emitted as combustion products, as organic vapours from gasoline and solvent use. Within the NMVOCs, hydrocarbons have received the most attention for their role in ozone photochemistry. More recently, the range of molecules of concern has expanded to include other groups such as chlorinated and oxygenated hydrocarbons. NMVOCs can undergo many transformations in the atmosphere, most of which involve reactions with NO_3 or OH radicals, or with O_3. During these reactions, the NMVOC may form more stable or soluble species, or may become converted from gas to particle or *vice versa*.

Table 2.13 provides the source-specific UK NMVOC inventory for 1970 and 2015, followed by estimates of the percentage change over this period. The major emission categories are solvent use and industrial processes (which includes paints, adhesives, aerosols, metal cleaning and printing). Substantial VOC emissions occur during processes such as painting (evaporation of solvents), oil production (flaring and venting of gas), oil refining (flaring and fugitive emissions), distribution of oil or refinery products (evaporation from storage, displacement losses when venting tanks), dry cleaning (final drying of clothes), use of aerosol sprays (both in the product and from the propellant), inefficient combustion of bituminous coal in domestic grates, production of alcoholic drinks (breweries and distilleries) and arable farming (crop growing, silage manufacture, sludge spreading). The two largest sources of UK NMVOC emissions in 2015 are industrial processes and product use, extraction and distribution of fossil fuels (respectively, 56% and 17% of the total).

FOR REFERENCE PURPOSES ONLY

Table 2.13 UK emissions of NMVOC in 1970 and 2015 by aggregated source category (ktonnes yr^{-1})

	1970 Emissions	*2015 Emissions*	*Percentage change*
By source category			
Agriculture/waste/accidental fires	162.03	107.82	33.46
Extraction and distribution of fossil fuels	588.76	145.05	75.36
Production processes	211.58	118.72	43.89
Solvent and other product use	589.00	349.86	40.60
Stationary combustion	336.07	70.63	78.98
Transport	571.72	43.27	92.43
Total	2459.17	835.36	66.03

Source: NAEI, *UK Emissions of Air Pollutants 1990 to 2015*, National Atmospheric Emissions Inventory, 2016.

More detailed surveys have been used to speciate the NMVOC emissions between sectors. The UNECE VOC protocol, for example, identifies three groups of VOC according to their potential for photochemical ozone production. Group I (highest potential) includes alkenes, aromatics, low alkanes and isoprene; Group II includes ethanol and high alkanes and Group III includes methanol, acetone, benzene and acetylene.

Additional natural NMVOC emissions occur from forests; however, we know far less about biogenic VOC (BVOC) emissions than we do about the anthropogenic ones. Plants synthesise many organic molecules as an integral part of their biochemistry – hydrocarbons include hemiterpenes such as *isoprene* (C_5H_8), the *monoterpenes* ($C_{10}H_{16}$) such as α-*pinene* and β-*pinene*, the *sesquiterpenes* ($C_{15}H_{24}$) such as *humulene*. Oxygenated compounds include C_1 such as CH_3OH, HCHO, C_2 such as C_2H_5OH, and C_3 such as acetone (CH_3COCH_3). Some of these VOCs are released to the atmosphere – the turpentine smell characteristic of pine forests, the monoterpenes from mint and the aldehydes from mown grass are well-known examples. Some information is available about emissions of ethylene (ethene) which regulates physiological processes such as fruit ripening and leaf abscission, and isoprene, but less is known about the rest. The release of BVOCs depends on locational and vegetation parameters (discussed in Chapter 9).

Ethylene has been heavily studied, and is known to be associated with plant growth and development, seed germination, flowering, fruit ripening and senescence. There is an interaction with air pollution – damage due to chemicals such as ozone and sulphur dioxide can stimulate the production of stress-ethylene, which is then involved in the production of new atmospheric compounds. Deciduous trees tend to be isoprene emitters, while conifers favour monoterpenes, although the exact role of these substances in plant biochemistry is not clearly understood. The global fluxes are huge – some 400 Mt C in both isoprene and monoterpene.

Hydrocarbons make up the majority, although smaller quantities of partially oxidised compounds such as alcohols, aldehydes, ketones and acids are also emitted. Altogether,

FOR REFERENCE PURPOSES ONLY

around 1000 different compounds (some of which are themselves families with thousands of members) are known to be emitted (Table 2.14).

Table 2.14 Global biogenic VOC emissions

Compound	*Emission rate (Mt C yr^{-1})*
Methane	160
Dimethyl sulphide	15–30
Ethylene (ethene)	8–25
Isoprene	175–503
Terpenes	127–480
Other reactive VOCs	Approximately 260
Other less reactive VOCs	Approximately 260

Indeed, trees and plants may emit as much as two-thirds of the VOCs to the air. In the US, for example, detailed inventories have shown that isoprene emissions exceed anthropogenic hydrocarbon emissions. Hence, O_3 production will not be controlled by reductions in anthropogenic HC emissions alone but will need greater control of NO_x emissions. Once released, the VOCs are involved in a great multiplicity of oxidation reaction pathways, although there is much uncertainty about the details of these at present. In addition, hundreds of photoreactive organic species are present in the polluted atmosphere, each with a different reaction rate coefficient contributing to formation of secondary gaseous and particulate pollutants (described in Sections 2.3 and 3.5.2). As a consequence, the atmospheric chemistry of the troposphere is very complex – a fully explicit chemical mechanism for the tropospheric chemistry could contain millions of reactions!

2.2.6 Carbon monoxide

Complete combustion of any fuel containing carbon would lead to the production of carbon dioxide. There is always an associated production of carbon monoxide (Table 2.15), which is a toxic gas that affects the transport of oxygen in the bloodstream. In the atmosphere at large, the concentrations are negligible. Under the restricted ventilation conditions sometimes found in towns, concentrations can be a significant health hazard. As with NO_x and NMVOC, this source has fallen rapidly since 1990 with the increasing use of catalytic converters on petrol-engine cars.

2.2.7 Hydrogen chloride

Most gaseous hydrogen chloride enters the atmosphere through the dechlorination of airborne sea salt particles by pollutant gaseous nitric acid or sulphuric acid (Table 2.16).

FOR REFERENCE PURPOSES ONLY

$$HCl_{(aq)} + HNO_{3\,(gas)} \rightarrow HCl_{(gas)} + HNO_{3(aq)}$$
$$HCl_{(aq)} + H_2SO_{4\,(gas)} \rightarrow HCl_{(gas)} + H_2SO_{4(aq)}$$

Table 2.15 Global CO budget

	Range of estimates (Tg CO yr^{-1})
Sources	
Fossil fuel combustion/industry	300–550
Biomass burning	300–700
Vegetation	60–160
Oceans	20–200
Methane oxidation	400–1000
Oxidation of other hydrocarbons	200–600
Total sources	1800–2700
Sinks	
Tropospheric oxidation by OH	1400–2600
Stratosphere	Approximately 100
Soil uptake	250–640
Total sinks	2100–3000

Table 2.16 Sources of atmospheric HCl

	Flux (Tg Cl yr^{-1})
Natural	
Volcanoes	2.0
Anthropogenic	
Sea salt dechlorination	50.0
Fossil fuel combustion	4.6
Biomass burning	2.5
Incineration	2.0
Transport from stratosphere	2.0
Total	63.1

As both pollutants and sea salt are needed, the highest HCl fluxes are found around the UK and in Northeast Europe. The other major sources are various types of combustion, except for a small contribution by diffusion down from the stratosphere of HCl that has been formed there from CFCs. HCl dissolves in water to form the chloride ion Cl^-.

There is no upward trend to HCl concentrations, so the deposition must be assumed equal to the emissions. In the UK, HCl is a minority air pollutant, with total emissions of around 90 kt $year^{-1}$, 75% of which is due to coal-burning power stations. There may be localised acidity production in rainfall downwind of such sources.

2.2.8 Persistent organic pollutants

Persistent organic pollutants (POPs) are a common label for a group of organic compounds that are persistent in the environment, with half-lives of years in the soil or sediment and days in the atmosphere. Hence concentrations may still be increasing decades after emissions have started. They favour soil organic matter and fats rather than aqueous media for storage, and hence enter the food chain and can be magnified by bioaccumulation. They readily volatilise into the atmosphere and condense onto particles, so they can be involved in long-range transport. The most common effects reported are of reproductive impairment, short-term memory loss or carcinogenicity; because there are mixtures of POPs and metabolites present, it is often not possible to specify directly the causative agent. The Convention on Long-range Transboundary Air Pollution included POPs in 1998 under the UNECE Persistent Organic Pollutants Protocol. It aims to control human and environmental exposure to substances that are persistent, bio-accumulative and harmful. Table 2.17 provides a list of these POPs pollutants and their total UK emissions in 2015.

Some of the POPs pollutants are described in more detail in the following sections. Their human health impacts are discussed in Chapter 10.

2.2.8.1 Dioxins and furans

The term *dioxins* covers 210 organic compounds, comprising 75 polychlorinated dibenzo-*p*-dioxins (PCDDs) and 135 polychlorinated dibenzofurans (PCDFs). PCDD/F are complex molecules produced by high-temperature combustion processes such as municipal waste incineration. The most common source is the incomplete combustion of plastics such as PVC. The dioxins contain 1–8 chlorine atoms substituted round one of two base structures. The 17 compounds that contain chlorine in all of the 2, 3, 7 and 8 positions are the ones that have toxic effects on humans. They are carcinogenic, though their true health effects are hard to evaluate because of their low concentration.

Table 2.17 Total UK emissions of POPs

Pollutant	*Total 2015 UK emission*
Polycyclic aromatic hydrocarbons (PAHs) (16 compounds identified by USEPA)	1495 tonnes
Dioxins and Furans (PCDD/F)	211 grams I-TEQ[a]
Polychlorinated biphenyls (PCBs)	0.62 tonnes
Pesticides	4.1 tonnes
• Lindane (γ-HCH)	262 tonnes
• Pentachlorophenol (PCP)	27 kg
• Hexachlorobenzene (HCB)	
Short chain chlorinated paraffins (SCCPs)	0.05 kg
Polybrominated diphenyl ethers (PBDEs)	6 tonnes

Source: NAEI, *UK Emissions of Air Pollutants 1990 to 2015*, National Atmospheric Emissions Inventory, 2016.

[a] I-TEQ – International toxic equivalent.

The different compounds have toxicities that vary by 1000:1, and there is an internationally agreed-upon weighting scheme so that the overall toxicity of a mixture can be quantified. The most toxic is 2,3,7,8 tetrachloro dibenzo-*p*-dioxin (2,3,7,8 TCDD). The quantity of 2,3,7,8 TCDD which would have the same toxicity as the mixture is known as the international toxic equivalent (I-TEQ). Dioxins have very limited solubility in water, and low vapour pressures. In the atmosphere they are normally associated with particles, and are extremely persistent. Typical ambient concentrations are in the region of 10–100 fg I-TEQ m^{-3}, where 1 fg (femtogram) = 10^{-15} g. A very wide range of processes contribute to dioxin emissions. Table 2.18 lists the total annual PCDD/F emissions for the UK for 1990 and 2015. As already explained earlier, in the 1990s the largest source was waste incineration. However, between 1990 and 2015 the emissions from this sector have fallen significantly (by over 90%). This significant reduction is associated with the introduction of control measures – improved combustion and flue gas controls and developments in abatement technology in modern municipal solid waste (MSW) incinerator design. The main sources of dioxins in 2015 were domestic and industrial combustion of coal and wood and iron and steel production.

Table 2.18 UK emissions of PCDD/Fs aggregated by source category (grams I-TEQ yr^{-1})

	1990 Emissions	*2015 Emissions*	*Percentage reduction*
By source category			
Combustion residential/commercial/institutional	386.1	115.5	70.10
Iron and steel (combustion)	0.7	0.2	76
Metal production (process emissions)	115.5	28.3	75.5
Other (production processes/agriculture)	132.7	25.8	80.6
Transport[a]	171.5	11.4	93.3
Waste incineration	549.9	29.6	94.6
Total	1356.5	210.6	84.5

Source: NAEI, *UK Emissions of Air Pollutants 1990 to 2015*, National Atmospheric Emissions Inventory, 2016.

[a] Includes railways, shipping, naval vessels, military aircraft, off-road sources and road transport.

2.2.8.2 Polychlorinated biphenyls

Polychlorinated biphenyls (PCBs) are released mainly from production in the electrical industry (especially transformers) as dielectric insulating media. The chemical stability that made them suitable for these applications has also resulted in very long lifetimes in the environment. PCBs occur in sewage sludge due to their persistent nature, and they may occur in significant quantities. PCBs can be formed in trace amounts from chlorinated precursors in thermal processes such as scrap metal recycling. Although most of the

pollution has probably involved direct transfer to water or landfill sites, PCBs can only be destroyed by high-temperature incineration, so that there is a risk of release to the atmosphere if incineration conditions are inadequate. The relative occurrence of different PCB isomers has been found to be consistent with their relative volatilities. There is an elevation of the concentration in the summer, associated with evaporation of the PCB from in-service electrical appliances – primarily capacitors and transformers.

2.2.8.3 Polybrominated diphenyl ethers

There are 209 possible congeners of polybrominated diphenyl ethers (PBDEs), which are mainly found in foams and plastics as flame retardants. They are used in a variety of fireproof materials, including thermoplastics which are used in electrical equipment, computer circuit boards, casings, furnishing, upholstery, rugs, building materials and interiors of vehicles. Production of the brominated mixtures of PBDEs themselves (penta-, octa- and deca-) has virtually ceased in the EU. However, possible release of these compounds is still associated with the production and disposal of the aforementioned materials.

2.2.8.4 Polycyclic aromatic hydrocarbons

Polycyclic aromatic hydrocarbons (PAHs) are formed by incomplete combustion of fossil fuels, such as occurs in vehicle engines (especially diesel), furnaces, coke ovens, bonfires and barbecues. In the UK, until 1996, aluminium production and anode baking (process used in aluminium industry) have been the largest source of PAH emissions. However, in 2006, road transport has been the largest source of PAH emissions in the UK, contributing about 61% of the total emissions. There are also natural sources such as volcanoes and forest fires. There are many PAH pollutants, of which 16 have been designated by the US Environmental Protection Agency (USEPA) as compounds of interest. Of these 16 PAHs, 6 have been considered carcinogenic to humans by the International Agency for Research on Cancer (IARC). Because of their semivolatile status, PAHs are highly mobile throughout the environment through deposition and re-volatilisation between air, soil and water bodies. This tends to accentuate their long-range environmental dispersion through deposition in the oceans. Historically, aluminium production was considered the largest source of PAH emissions in the UK until 1996, but since then there has been drastic reduction in the emissions from this sector. Residential combustion is identified as the largest source of UK PAH emissions, contributing to over three quarters of the emissions of the 16 PAH species. The second largest source is the road transport sector.

2.3 SECONDARY GASEOUS POLLUTANTS

FOR REFERENCE PURPOSES ONLY

2.3.1 Tropospheric ozone

Ozone occurs as a secondary pollutant in the troposphere (commonly known as the *tropospheric ozone*), formed from photochemical disintegration of nitrogen oxides and VOCs. On the other hand, natural ozone mainly occurs in the stratosphere (hence, also called *stratospheric ozone*), formed from dissociation of the oxygen molecules with UV light (more details in Chapter 12). However, some of the stratospheric ozone also diffuses down to the troposphere. Current estimates suggest that this stratosphere–troposphere exchange amounts to between 400 and 500 $\times 10^9$ kg a^{-1}, and can constitute 30%–40% of the total tropospheric ozone burden, although it is uncertain how much actually penetrates down to the surface.

Even at low concentrations, tropospheric ozone is considered to impair the ability of plants to produce and store food, and is harmful for the human respiratory tract and the lungs (discussed in detail in Chapter 10). It is the main component of photochemical smog (commonly known as *summer smog*, described in Chapter 1) and has a *background* concentration of 10–20 ppb. Hospital admissions and respiratory deaths often increase during periods when ozone levels are high.

The following photochemical disintegration of natural NO_x in the presence of UV photons forms the major pathway for yielding tropospheric ozone:

$$NO_2 + h\nu(\lambda < 400\,\text{nm}) \rightarrow NO + O \tag{1.1}$$

This is referred to as NO_2 photolysis (more details in Chapter 12). Photons with a wavelength greater than 400 nm do not have enough energy to break up the NO_2 molecule, while those having a wavelength shorter than 280 nm have been absorbed so effectively in the stratosphere that their tropospheric flux is negligible.

$$O + O_2 + M \rightarrow O_3 + M$$

(M is any *third body* molecule, also known as a *chaperone*, such as N_2 or O_2, which is required for energy absorption but which does not take part in the reaction as such). Under ambient conditions, the generated O_3 reacts readily with NO, which oxidises to form NO_2:

$$NO + O_3 \rightarrow NO_2 + O_2 \quad (NO_2\ \text{production}) \tag{1.2}$$

This cycle of reactions generates a small contribution (a few ppb) to the background ozone concentration.

In the unpolluted atmosphere, equilibrium between the above-mentioned three reactions gives low and stable O_3 concentrations. The O_3 concentration never gets very high because

FOR REFERENCE PURPOSES ONLY

it is consumed immediately by the NO. Additional ozone can be formed in the troposphere as a secondary pollutant when there are increased concentrations of NO_2 for any reason.

Two main routes for the production of additional NO_2 are the reactions of NO with either the hydroperoxy radical HO_2:

$$HO_2 + NO \rightarrow NO_2 + OH$$

or with an organic peroxy radical RO_2.

$$RO_2 + NO \rightarrow NO_2 + RO$$

where R is an organic radical – any atomic group consisting only of C and H (e.g. C_2H_5). For example, in the case of methane (CH_4), R = CH_3. Hence

$$OH + CH_4 \rightarrow CH_3 + H_2O$$

and

$$CH_3 + O_2 + M \rightarrow CH_3O_2 + M$$

Then photolysis releases oxygen atoms, which combine with oxygen molecules to generate elevated ozone concentrations. The sequence of reactions for methane would be:

$$OH + CH_4 \rightarrow CH_3 + H_2O$$

$$CH_3 + O_2 + M \rightarrow CH_3O_2 + M$$

$$CH_3O_2 + NO \rightarrow CH_3O + NO_2$$

$$NO_2 + h\nu(280\text{–}430\,\text{nm}) \rightarrow NO + O$$

$$O + O_2 + M \rightarrow O_3 + M$$

$$CH_3O + O_2 \rightarrow HO_2 + HCHO$$

$$HO_2 + NO \rightarrow OH + NO_2$$

$$NO_2 + h\nu(280\text{–}430\,\text{nm}) \rightarrow NO + O$$

$$O + O_2 + M \rightarrow O_3 + M$$

$$CH_4 + O_2 + O_2 \rightarrow HCHO + O_3 + O_3$$

with a corresponding sequence for other organic compounds.

Note that the OH radical is regenerated during the sequence; as it effectively acts as a

FOR REFERENCE PURPOSES ONLY

catalyst, tiny concentrations (ppt) can play a major role in atmospheric chemistry. Essentially, any hydrocarbons present can be broken down by the hydroxyl radical (OH) to form organic peroxy radicals (RO_2), which react easily with NO to form NO_2, depleting NO from Equation 1.2 and shifting the equilibrium in favour of O_3 production.

First, the OH hydroxyl radical reacts with an organic molecule, which then reacts with molecular oxygen to form an organic peroxy radical RO_2:

$$\mathbf{OH + RH \rightarrow R + H_2O}$$

Then:

$$\mathbf{RO_2 + NO \rightarrow RO + NO_2}$$

RO is an organic alkoxy radical.

$$\mathbf{NO_2 + h\nu \rightarrow NO + O}$$

$$\mathbf{O + O_2 + M \rightarrow O_3 + M}$$

During the daytime, this reaction scheme is the source of NO_2 for NO_2 photolysis, giving O_3 as the by-product. Figure 2.8 shows the results of a laboratory experiment in which initial concentrations of 500 ppb of propene, 400 ppb of NO and 100 ppb of NO_2 were irradiated in a chamber for 7 h. The propene and NO concentrations declined steadily as they were consumed by the photochemical reactions. The NO_2 concentration climbed to a peak after 90 min before declining again. Ozone formation increased steadily during the period of the experiment, reaching nearly 600 ppb by the end. There were also significant concentrations of two further secondary pollutants, formaldehyde (HCHO) and peroxyacyl nitrate (PAN), which are both toxic and irritating. Analysis in terms of reaction rates and sources of OH has shown that around two days of strong sunshine would be sufficient to generate the elevations of around 60 ppb O_3 that are experienced in regional photochemical pollution episodes.

At night, and in the winter in temperate latitudes, there are fewer UV photons, so that NO can no longer be formed by photolysis, and continues to be used up by reaction with O_3. The concentrations of NO and O_3 therefore decline. The excess NO_2 reacts with organic molecules and, through various intermediates, generates nitric acid (HNO_3). These nitric acid molecules can be transferred to water droplets and contribute significantly to the acidification of rain.

The requirement for UV photons and the short lifetime of O_3 molecules in the atmosphere combine to create a characteristic diurnal cycle of ozone concentrations in the lower troposphere. In Figure 2.9, a diurnal cycle of ozone production is shown in Los Angeles air. The morning rush hour is marked by an increase in the primary emissions of NO and CO (and hydrocarbons, which are not shown). With increasing solar radiation, the

FOR REFERENCE PURPOSES ONLY

photochemical reactions accelerate.

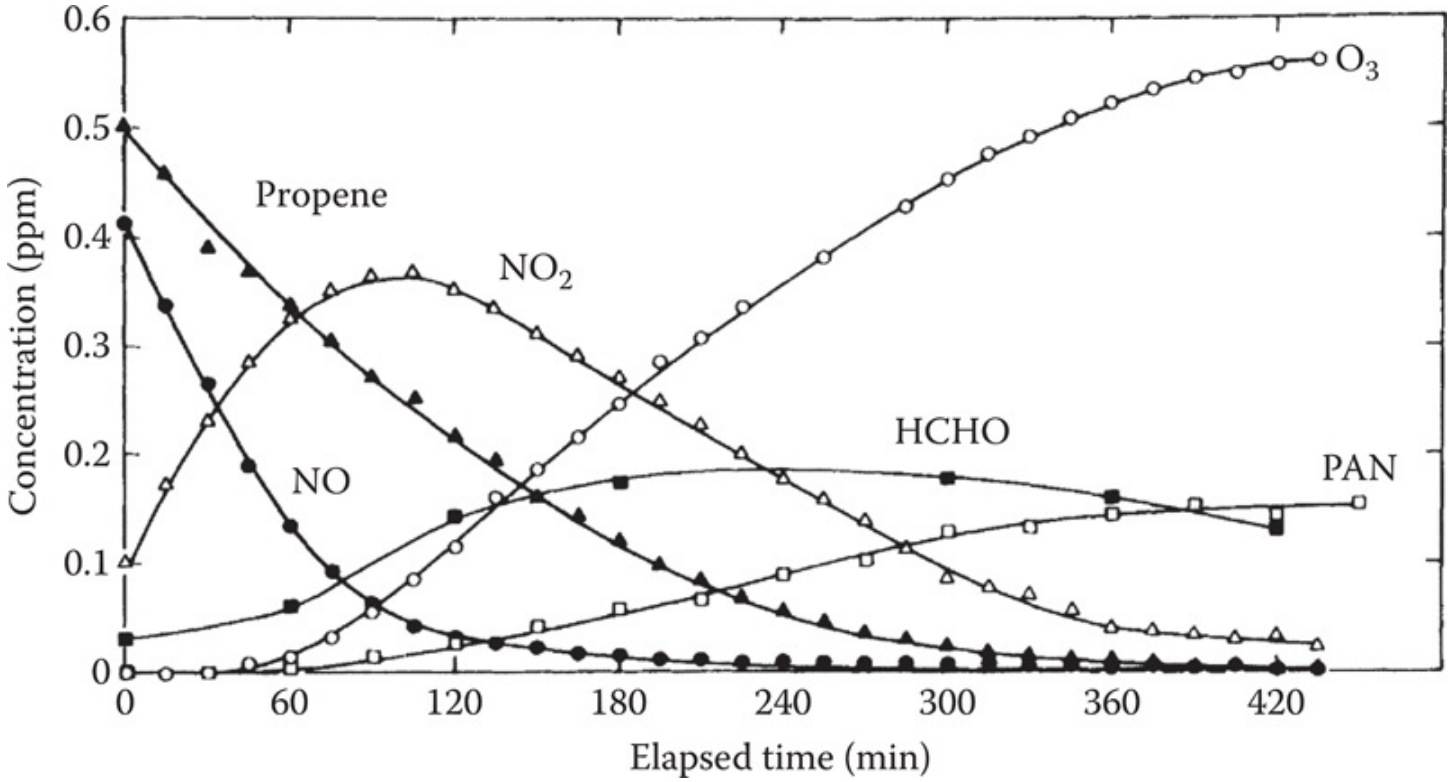

Figure 2.8 Laboratory reaction of NO_x and propene to produce O_3. (From Winer, A. M., Air pollution chemistry, in R. M. Harrison and R. Perry (Eds.), *Handbook of Air Pollution Analysis*, Kluwer Academic Publishers, Dordrecht, the Netherlands, 1986.)

FOR REFERENCE PURPOSES ONLY

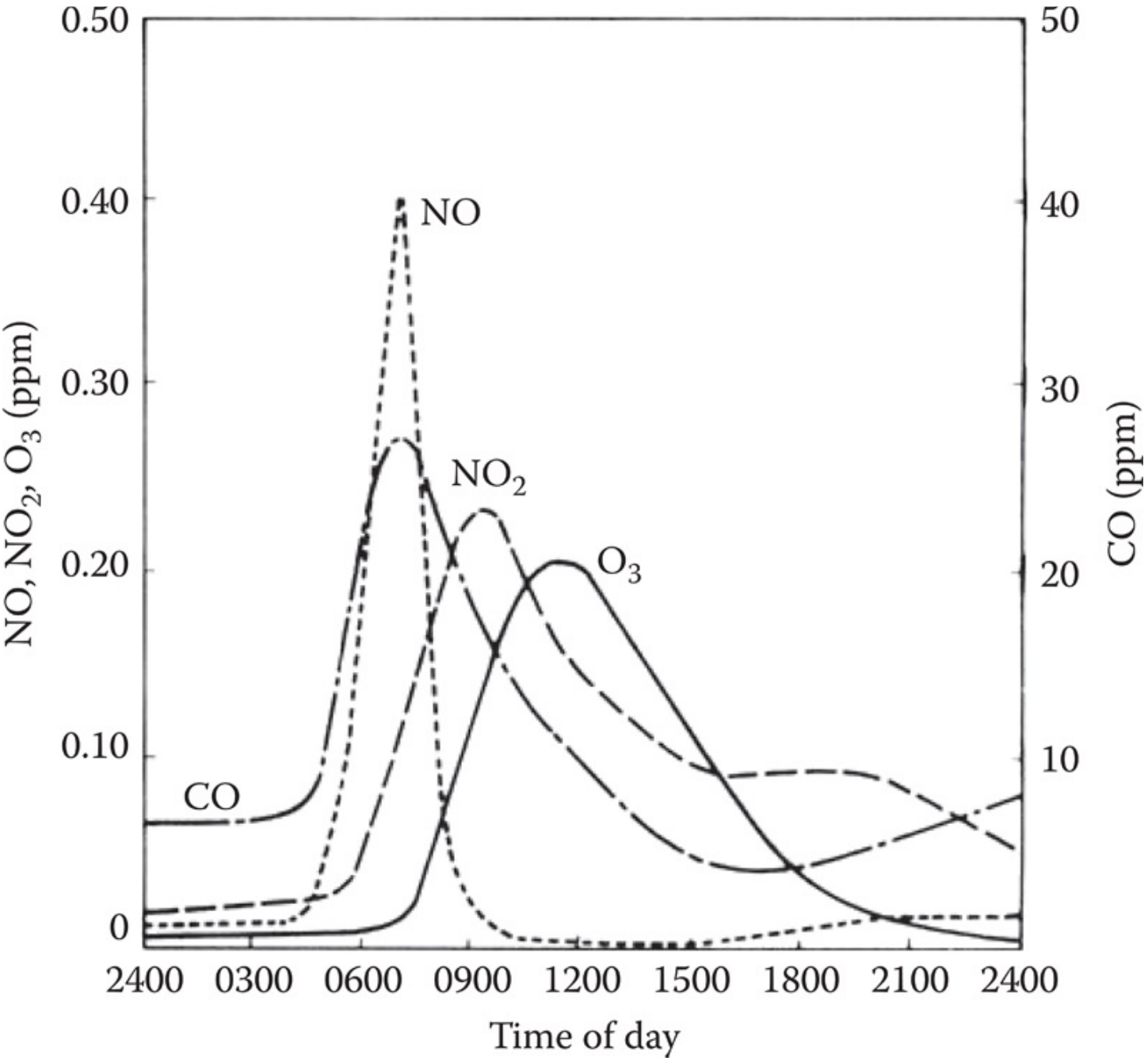

Figure 2.9 Diurnal cycles of ozone production and precursor concentrations in Los Angeles. (From Strauss, W., and Mainwaring, S. J., *Air Pollution*, Edward Arnold, London, UK, Report, European Communities, Luxembourg, 1984.)

NO_2 may be removed from the atmosphere by other mechanisms. In bright light, nitric acid (HNO_3) may be formed by reaction with $^{\bullet}OH$ or O_3. The HNO_3 can be deposited back to Earth by precipitation (wet deposition):

FOR REFERENCE PURPOSES ONLY

$$\text{Example 1} \quad {}^{\bullet}OH + NO_2 + {}^{1}M \rightarrow HNO_3 + M$$

$$\text{Example 2} \quad NO_2 + O_3 \rightarrow NO_3 + O_2$$

$$\text{then} NO_3 + NO_2 + {}^{1}M \rightarrow N_2O_5 + M$$

$$N_2O_5 + H_2O \leftrightarrow 2HNO_3$$

Nitric acid may also react photochemically:

$$HNO_3 \xrightarrow{h\nu} {}^{\bullet}OH + NO_2$$

Additional mechanisms of ozone formation are described in greater detail in Chapter 12. Overall, Table 2.19 provides an estimate of the global tropospheric O_3 budget from different sources. It should be noted that many of these values have been arrived at by complex 3D models of atmospheric photochemistry, and the resulting uncertainty is indicated by the ranges of the values quoted.

2.3.2 Wintertime NO_2 episodes

In London, in December 1991 there was a serious air pollution episode involving elevated concentrations of NO_2. Although the prevailing meteorological conditions restricted dispersion (as they had in the coal smog episodes in 1952 and 1962), the air pollution community was surprised by the concentration increase at the time, because the winter conditions did not favour photochemical generation of NO_2. It was subsequently realised that the NO_2 was due to the direct combination of NO with molecular oxygen:

Table 2.19 Tropospheric ozone budgets

	Tg O_3 yr^{-1}
Sources	
Chemical production (total)	3000–4600
of which HO_2 + NO	70%
CH_3O_2 + NO	20%
RO_2 + NO	10%
Transport from the stratosphere	400–1100
Total sources	3400–5700
Sinks	
Chemical loss (total)	3000–4200
of which $O(^1D) + H_2O$	40%
$HO_2 + O_3$	40%
$OH + O_3$	10%
Other reactions	10%

FOR REFERENCE PURPOSES ONLY

Dry deposition	500–1500
Total sinks	3400–5700

$$NO + NO + O_2 \rightarrow 2NO_2$$

This is a second-order reaction for which the rate increases as the square of the NO concentration. Hence, although the NO_2 production rate is negligible at low NO concentrations, it dominates at high NO concentrations. Figure 2.10 shows the relationship between hourly mean NO_x and NO_2 concentrations at a roadside site in London for 12 months that included the December episode. The NO_2 concentration can be seen ramping up when the NO_x concentration rises above 200 ppb.

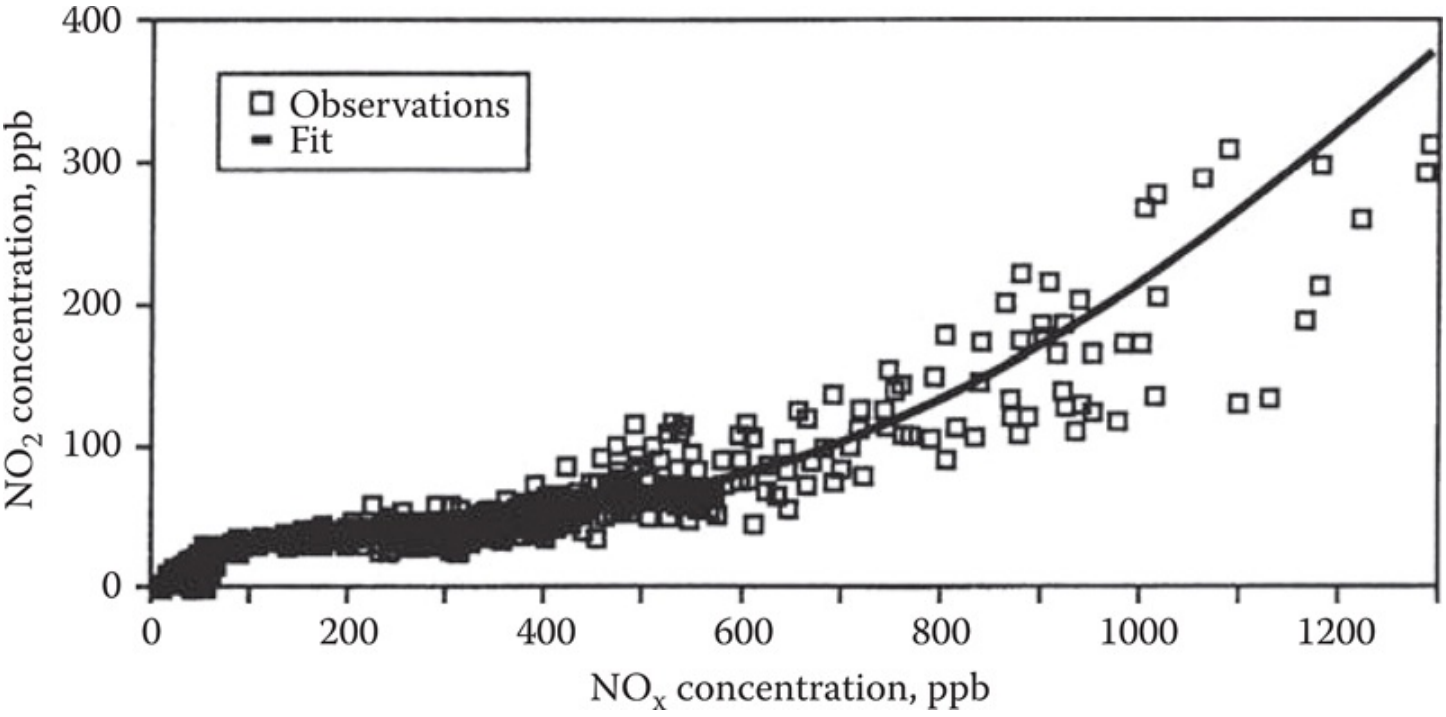

Figure 2.10 Interdependence of NO_x and NO_2 concentrations. (From Williams, M. L., Patterns of air pollution in developed countries, in S. T. Holgate, J. M. Samet, H. S. Koren and R. L. Maynard (Eds.), *Air Pollution and Health*, Academic Press, London, UK, 1999.)

In many parts of the world with significant NO_2 and particulate pollution, smog is a visible air pollution problem even during winter; hence it is called *winter smog* (also known as *pea-soupers*). More details about smog are provided in Chapter 1.

2.4 MEASUREMENT OF GASES

FOR REFERENCE PURPOSES ONLY

Thus far we have discussed the emission and control of trace gases. Now we will look more closely both at how to sample them correctly and how to measure their concentrations (additional details are presented in Chapter 15 for specific pollutant sampling). *Trace gases*, by definition, normally have concentrations in the ppb and ppt ranges, and therefore require more specialist techniques and sensitive methods than those in general use for gases, such as water vapour or carbon dioxide that occur at percentage or ppm concentrations. Correct sampling is important to avoid corruption of the ambient concentration.

2.4.1 Sampling requirements

There are many different reasons why air samples might be needed:

- Determination of community air quality as related to local health, social and environmental effects – for example, NO_x measurements in an urban area.
- Investigation of the influence of specific emission sources or groups of sources on local air quality – for example, CO near a motorway interchange.
- Research into dispersion, deposition or atmospheric reaction processes – for example, measurements to validate dispersion software using the Gaussian dispersion equation.

Before any sampling and measurement programme, the objectives must be defined clearly. These will lead in turn to specifications of sample point locations, frequency of measurement, and other factors. There are no fixed rules on any of these aspects – it is down to experience and common sense. Sample inlets will normally be away from surfaces such as walls and hedges that might affect the concentration. For human relevance, they will usually be about 2 m above the ground; however, lower heights will be appropriate for babies or children, and for growing vegetation the inlet may need to be adjusted periodically to remain close to, but not within, the growing canopy. There should be no major obstructions, or interfering local sources, close upwind. The site must be both accessible and secure from large animals or vandalism.

2.4.2 Gas sampling

Most measurement methods require the pollutant, or the air containing the pollutant, to be sampled. The purpose of sampling is to get some air to the analyser without changing the concentration of the gas to be measured, and in a condition that the analyser can accept. We can divide the available methods into three categories: pumped systems, pre-concentration and grab samplers. There are also combinations of these.

2.4.2.1 Pumped systems

FOR REFERENCE PURPOSES ONLY

A sample is drawn continuously from the ambient air and delivered directly to the analyser (Figure 2.11). Sampling the gas will involve the inlet itself (normally shrouded to prevent the ingress of rain), tubing, the analyser, flow measurement and a pump.

There are many potential sources of error in this combination:

- There are always particles in the air. If we draw these particles in, they may be deposited to the sample tube walls and to the internal parts of the analyser, they may produce a spurious signal from the analyser equivalent to a gas concentration (e.g. a flame photometric sulphur analyser will respond equally whether the sulphur is in sulphate particles or in sulphur dioxide) or they may decompose to release a measurable gas concentration. The particles are therefore usually trapped on a filter close to the sample inlet, but this may introduce errors. For example, if ammonium nitrate particles are trapped on a filter, they can decompose and increase the measured concentration of ammonia gas. When sampling ozone, the buildup of particles on the filter can absorb ozone before it even enters the sample tube.
- As the air sample is drawn through tubing to the analyser, it can be adsorbed in transit on the walls or on connecting fittings. The severity of this effect varies with the gas and the tubing material – ozone must be sampled through glass, stainless steel or *polytetrafluoroethylene* (PTFE, an inert plastic), SO_2 is less reactive and CO_2 is quite inert. The contact time is important here – samples taken down long lengths of tube must have high flow rates to minimise the residence time, which should be kept below 10 s.
- There may be reactions between the gas of interest and other species while the gas is flowing along the tube. For example, O_3 and NO and NO_2 are in a dynamic photochemical equilibrium in the atmosphere. As soon as they are sampled, the conditions are changed and the concentrations will start to change in consequence. The magnitude of this effect varies from system to system. When performing multi-point samples with one analyser, the analyser must be time-shared between the different locations. It is then usual to draw air rapidly and continuously through main sample lines, past a point that is physically close to the analyser. At this point, solenoid valves are used to extract samples cyclically to the analyser from each of the tubes in turn. In this way the dead time spent by air in tubes is minimised, as are the opportunities for adsorption and chemical reactions.

FOR REFERENCE PURPOSES ONLY

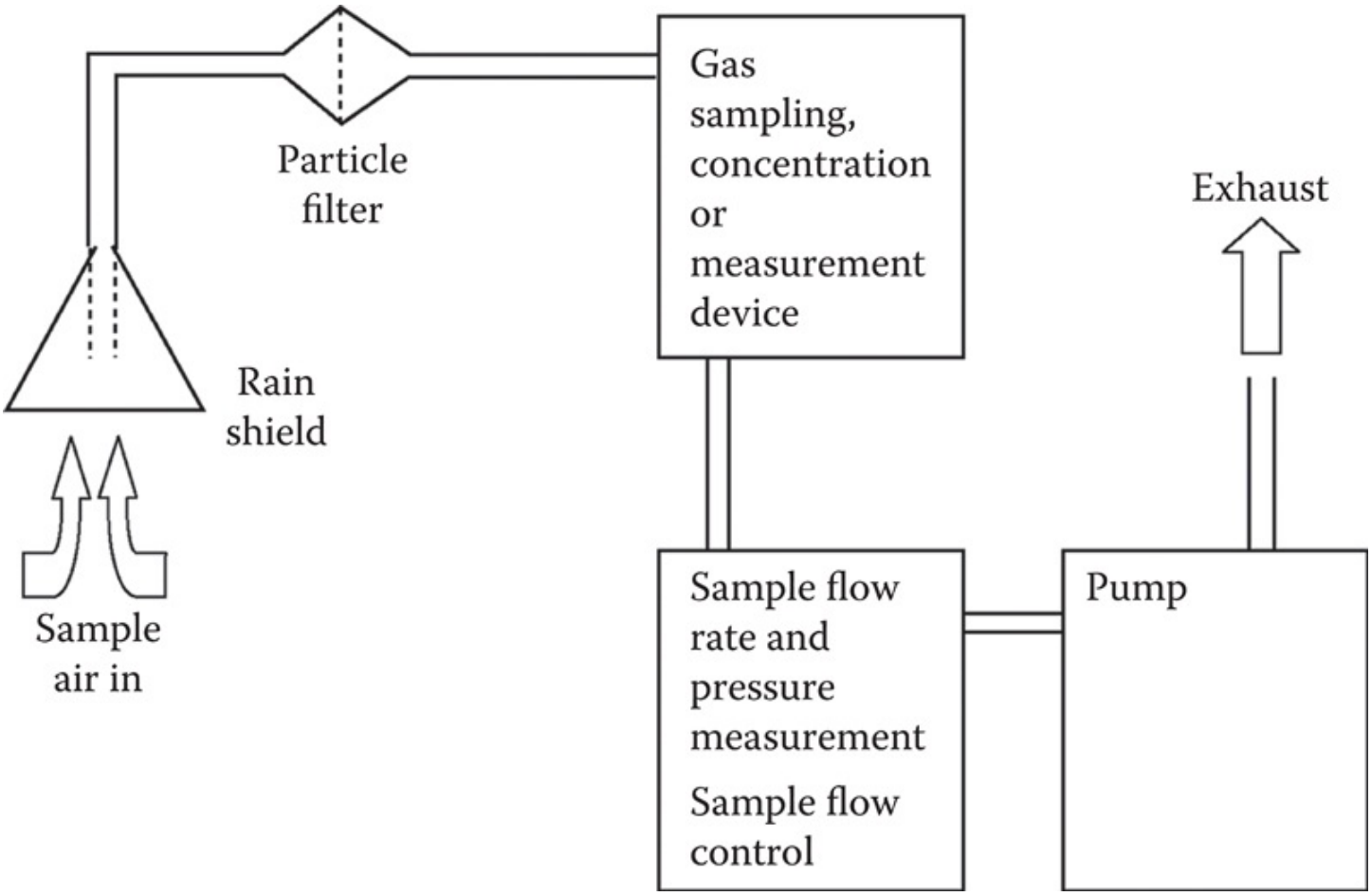

Figure 2.11 Component parts of a gas sampling system.

- The pump will usually come last in the flow path to avoid interfering with the air sample before measurement. The gas sampling system will then be below atmospheric pressure. Hence there is a risk of leaks occurring, in which air from other locations, having a different gas concentration to that of the original sample, is drawn into the sample line and delivered to the analyser. Such leaks can occur at any of the connection fittings required for items such as particle filters, solenoid valves or flow meters, and can be very hard to detect in a complex sampling system which may involve dozens of such connections. Air can only flow down a pressure differential, and the pressure in such a system therefore becomes steadily more negative from the sample inlet towards the pump. Fittings near the pump are thus at the greatest risk from leaks, but the concentration has usually been measured by then.
- As well as particles, ambient air always contains water vapour. Provided that the water remains in the vapour state, no problems should result. If the sampling system allows the air to cool below the dewpoint temperature, then the vapour will eventually become saturated and the excess water will condense out in the sample lines. This can cause problems. First, there is clearly a risk of liquid water being drawn right through the sample system – this is not good news for a £10,000 gas analyser. Second, any drops of liquid water lining the sample tubes will be sites for rapid absorption of some

gases such as ozone and sulphur dioxide, possibly nullifying a major investment in PTFE tubing. One possible solution is to remove some of the water vapour by passing the air sample through an adsorbent such as silica gel. Although this works well for relatively unreactive gases present at ppm concentrations, such as carbon dioxide, it is likely to cause unacceptable loss or corruption of ambient trace gases. The preferred solution is to heat the sample lines so that the air is about 10°C above ambient temperature. Proprietary sample tube is available that has concentric heating elements and insulation built into the tube itself, although it is expensive. An effective alternative can be constructed by wrapping heating tape around the tube before placing it inside plastic drainpipe for physical protection and insulation. The temperature should be regulated thermostatically to maintain its constant elevation above ambient.

2.4.2.2 Preconcentration

Gas analysers have sufficient sensitivity and speed of response to give a continuous measurement of the pollutant concentration as the sample is delivered to them. Many other techniques simply capture the pollutant, or a chemical derived from it, from the sample for later quantitative analysis in the laboratory by standard methods such as titration and spectrophotometry.

2.4.2.3 Absorption

The common theme is that a specific chemical reaction between the gas and captive absorbing molecules retains all the gas from the sample air. There are many different practical arrangements.

2.4.2.3.1 Bubblers

The sample is bubbled through an absorbing chemical solution; the gas is absorbed (a process which is controlled by the equilibrium partial pressure of the dissolved gas over the liquid surface), and preferably then also undergoes an irreversible chemical reaction which prevents it from being subsequently desorbed. If the collection efficiency is too low, then a fritted glass diffuser can be used which reduces the bubble size and hence increases the interfacial contact area and effective contact time, at the expense of higher pressure drop and lower flow rate.

Ideally, 100% of the pollutant molecules will be absorbed while passing through the solution. Absorbers such as bubblers can still be used at lower efficiencies provided that the efficiency is known and constant. Alternatively, the concentration can sometimes be measured by using two bubblers in series. For example, a volume of air V containing a concentration C of the pollutant is sampled. The total mass of pollutant in the sample is then $M = VC$. As the sample passes through the first absorber, a mass M_1 of pollutant is

FOR REFERENCE PURPOSES ONLY

retained, at an efficiency $E = M_1/VC$. The mass of pollutant passed through the second absorber is reduced to $VC - M_1$, of which M_2 is retained.

$$E = \frac{M_1}{VC} = \frac{M_2}{VC - M_1} \text{ and hence } C = \frac{M_1^2}{V(M_1 - M_2)}$$

The method assumes that the efficiency is the same in both absorbers. In practice, the efficiency is itself often a function of the concentration and is lower at lower concentrations.

2.4.2.3.2 Impregnated filters

The sample is drawn through a filter paper that has been impregnated with a chemical that reacts with the gas. Often several different filters are used. The first is a high-efficiency untreated particle prefilter, which prevents particles from interfering with the gas measurements on subsequent filters. It is important that this prefilter does not absorb a significant proportion of the gases of interest – for example, glass fibre filters collect low concentrations of both SO_2 and HNO_3 rather efficiently, while nylon filters absorb HNO_3 and HCl. The second and third filters might be impregnated with two different chemicals to absorb two different gases – for example, KOH for SO_2, NaCl for HNO_3, or H_2SO_4 for NH_3. The collection efficiency of impregnated filters is usually less than 100% and can vary with atmospheric humidity.

2.4.2.3.3 Passive samplers

This category covers any preconcentration technique which relies on the gas diffusing to an absorber without pumping (Table 2.20). Passive samplers rely on diffusion of the sample rather than pumped flow. They are cheap to purchase and do not require electrical power, so they are useful for large-area surveys. On the down side, they are labour- and laboratory-intensive and provide average concentrations over days to weeks, so the results are not directly comparable with standards. They were originally developed so that workers could carry out a full day's work with an unobtrusive sampling device clipped to their clothing. The sample would then be analysed to give the average concentration during the period. The principle has been adapted to give measurements of several ambient gases – NO_2, VOCs, SO_2 and NH_3.

Table 2.20 Examples of passive sampler combinations

Gas	*Absorbent*	*Analytical method*
Ammonia	Oxalic acid	Colorimeter or Spectrophotometer
Hydrogen sulphide	Silver nitrate	Fluorimeter

FOR REFERENCE PURPOSES ONLY

Nitrogen dioxide	Triethanolamine (TEA)	Colorimeter or Spectrophotometer
Ozone	Sodium nitrite	Colorimeter, Spectrophotometer or Ion chromatograph
Sulphur dioxide	Sodium hydroxide	Colorimeter
VOCs	Activated charcoal or Tenax	Gas chromatograph or GC-MS

In the simplest type of diffusion tube, a linear molecular diffusion gradient is set up between the atmospheric concentration at the lower end of an inert plastic tube (7 cm long and 1 cm diameter) and zero concentration at an absorbent-coated substrate at the upper end (Figure 2.12). The gas molecules diffuse down the gradient through the air molecules down the gradient and are absorbed on the substrate. The rate of diffusion depends only on the near-constant molecular diffusivity of the gas, as the long thin tube inhibits turbulent transport on to the substrate. However, high wind speeds can cause turbulent transport up the tube to be a significant source of error. The tube is left in position for a period of days to weeks, capped to prevent further absorption, and returned to the laboratory for analysis. A quantity Q mol of the gas is transferred onto the substrate in time t, where Q is given by:

$$Q = D_{12} A t (C_a - C_0)/z$$

FOR REFERENCE PURPOSES ONLY

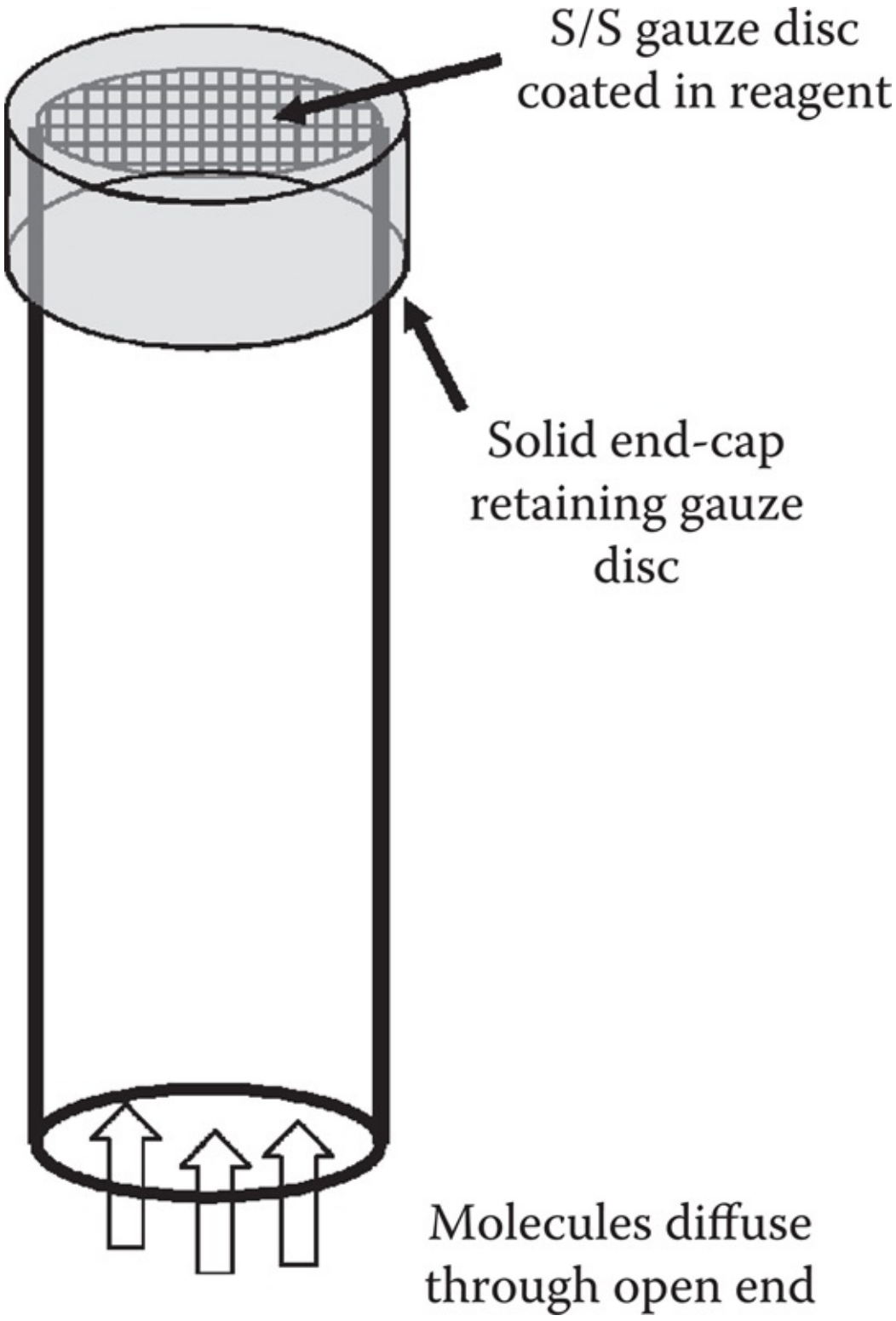

Figure 2.12 A diffusion tube.

D_{12} is the diffusion coefficient of gas 1 (the pollutant) in gas 2 (air), A is the cross-sectional area of the plastic tube, C_a and C_0 are the ambient (at the open end of the tube) and substrate concentrations of the pollutant, respectively. C_0 is usually assumed to be zero, z is the length of the tube, or the diffusion path length.

FOR REFERENCE PURPOSES ONLY

Hence Q is proportional to the average concentration of the pollutant at the mouth of the tube over the exposure period. The same issues arise as for other sampling methods – particularly linearity, specificity, and the effects of temperature, wind speed and humidity. Some of the absorbers used, such as triethanolamine (TEA), absorb more than one gas. This does not matter provided that the detection method is specific to the gas of interest. More complex designs involving diffusion screens have been used in order to compress the tube into a badge geometry, and tubes packed with solid adsorbent have been used for sampling organics.

2.4.2.3.4 Denuder tubes

Denuder tubes are a cunning method of avoiding the potential interference between the particle and gas phases of a pollutant – for example, with nitric acid vapour and particulate nitrates.

The air sample is drawn through a hollow tube, the inside of which is coated with an absorbent for the gas. The flow rate and tube diameter are selected so that the flow is laminar. Under these conditions, the molecular diffusivity of the gas is thousands of times greater than the Brownian diffusivity of the particles, so that the gas moves to the walls much more quickly. The length of the tube is selected so that, by the time the air leaves the tube, most of the gas has been absorbed and most of the particles remain suspended. The particles can then be filtered separately. In a more sophisticated arrangement called an annular denuder, the air sample flows between two concentric tubes. The outer surface of the inner tube and the inner surface of the outer tube are both coated with the absorbent, which gives higher sampling efficiencies, shorter tubes, higher flow rates or shorter sampling times.

2.4.2.4 Adsorption

The gas molecules are bound to the surfaces of a solid collecting substrate by intermolecular forces. Subsequently they are stripped off by heating the substrate to 300°C, or by solvent extraction, and delivered into a gas chromatograph or equivalent analysis system. The most common adsorbent substrates are activated charcoal, organic polymers and silica gel. The most widely used commercial product is Tenax, which has been used to sample a large range of organic compounds such as PAHs, vinyl chloride, and hydrocarbons including benzene.

2.4.2.5 Condensation trapping

The air sample is passed through a chamber cooled almost to the temperature of liquid oxygen (–183°C) so that volatiles condense out but the air itself passes through unchanged. Cooling is normally arranged in a sequence of stages of reducing temperature, so that the

majority of the water vapour is collected first.

2.4.2.6 Grab sampling

For various reasons, it may be impracticable to either measure the concentration continuously or extract the pollutant gas from an air sample for subsequent analysis. In these cases, the fall-back technique is to capture a sample of the air itself and take it back to the laboratory. There are several different ways in which this is put into practice.

Evacuated bottles: A stainless steel, glass or inert plastic bottle is evacuated in the laboratory and sealed securely. The bottle is opened in the ambient air and fills with the sample.

Syringes: The plunger on an empty syringe is pulled out, drawing in a sample of ambient air.

Bellows: A collapsed cylindrical bellows is expanded, creating a volume at low pressure and drawing in the ambient air sample.

Bags: A bag made of an inert material is filled by pumping the air sample into it. The major disadvantage of this method is that the air must pass through the pump before entering the bag, so that reactive gases may be corrupted. In order to avoid this limitation, the bag can be held inside a bottle. The space *outside* the collapsed bag can then be evacuated by pumping out the air. This draws an air sample into the bag. The sample cycle can be repeated many times.

All of these techniques need very careful assessment and management to be successful. The bags and bottles need to be made of inert material and scrupulously clean and leak-free. For some applications, preconditioning of the sample holder with high concentrations of the pollutant gas may be necessary to reduce uptake of the gas from subsequent samples. The samples must be returned to the laboratory as rapidly as possible for analysis, before they degrade. By their nature, grab samples tend to be used at remote sites to which a sampling expedition is a major undertaking. If any of these quality assurance aspects is insecure, it may only be discovered that the samples are worthless after returning home. The risks can be minimised by a careful validation programme – comparison of concurrent real-time and grab samples, and sequential analysis of stored samples over a period of time.

2.4.3 Gas concentration measurement

There are seven factors that need to be balanced when choosing how a particular trace gas is to be measured:

Specificity: Does the method measure only the gas of interest, or does it have a response to some other gas or gases. If so, is this interference or cross-sensitivity likely to be

FOR REFERENCE PURPOSES ONLY

significant at the likely concentrations of all the gases involved?

When the peroxide bubbler technique first became used for SO_2 determination, it was known that it would also respond to alkaline gases such as ammonia, and to other acid gases such as nitrogen dioxide, but there was no problem because the SO_2 concentrations far outweighed the others. When SO_2 concentrations decreased, this imbalance became less certain and a more SO_2-specific analysis was introduced.

Sensitivity: Will the method measure the highest and lowest concentrations expected? If it measures the highest, then the lowest may have a large error due to instrument noise. If it measures the lowest with sufficient sensitivity for the noise not to be a problem, then there might be a risk of it going off-scale during a pollution episode. This is a very frustrating event, as it is always the episode that creates the greatest interest.

Reliability: Is the instrument to be used continuously or intermittently? If continuously, will it be visited daily, weekly or less frequently? Is it important to obtain a complete record, or will it be acceptable to have the analyser out of action for maintenance periods?

Stability: This is an important issue for continuous analysers that are unattended for long periods. They will be calibrated (zero and span values confirmed by measuring the output from standard gas sources) and then left to operate unattended. During the following measurement period, the zero and span outputs will both drift away from their settings, so that an error is introduced into the measurement. The speed of this drift, and the relative magnitude of the resulting errors, will determine the frequency of the calibrations.

Response time: For grab sampling or preconcentration, the response time is the time over which the sample is taken. An almost instantaneous sample can be obtained by opening a valve on an evacuated container, or sample entry can be extended over any longer period. No information is available on concentration variations that are shorter than the sample period. In the same way, pre-concentration methods such as bubblers give an average value over the length of the sample period. In principle, continuous analysers are capable of tracking the actual concentration of the gas. How closely this ideal is met in practice depends on how rapidly the concentration changes and the response time of the analyser. Response times are quoted by manufacturers in terms of the time to reach 90% or 95% of a step change in the input – times for modern analysers are typically 1 or 2 min.

Precision and accuracy: These words are sometimes used interchangeably, but they have fundamentally different meanings, as shown on the three archery targets of Figure 2.13. In Figure 2.13a, the arrows have high precision (they have all landed within a small area of the board) but low accuracy (they are all well away from the centre, which is equivalent to the 'correct' value). In Figure 2.13b, the arrows have high accuracy (the average is close to the centre), but low precision (they are scattered all over the board). Figure 2.13c shows the ideal, with both precision and accuracy being

high. Analyser manufacturers quote overall bands within which the errors due to all sources are expected to lie.

Cost: Although last on this list, cost is bound to weigh heavily in the selection process. The range of possible costs is enormous. Pre-concentration methods such as bubblers and diffusion tubes cost only a few pounds to obtain the sample itself, but have substantial operational costs due to labour and laboratory facilities. Continuous analysers cost c. £10,000, and substantial additional investment is also needed – in data logging and computing equipment, servicing and spares, air-conditioned cabin and calibration facilities.

It is not possible to give here a comprehensive review of all the different measurement methods available for specific gases. We will simply give a few examples of the key techniques in common use.

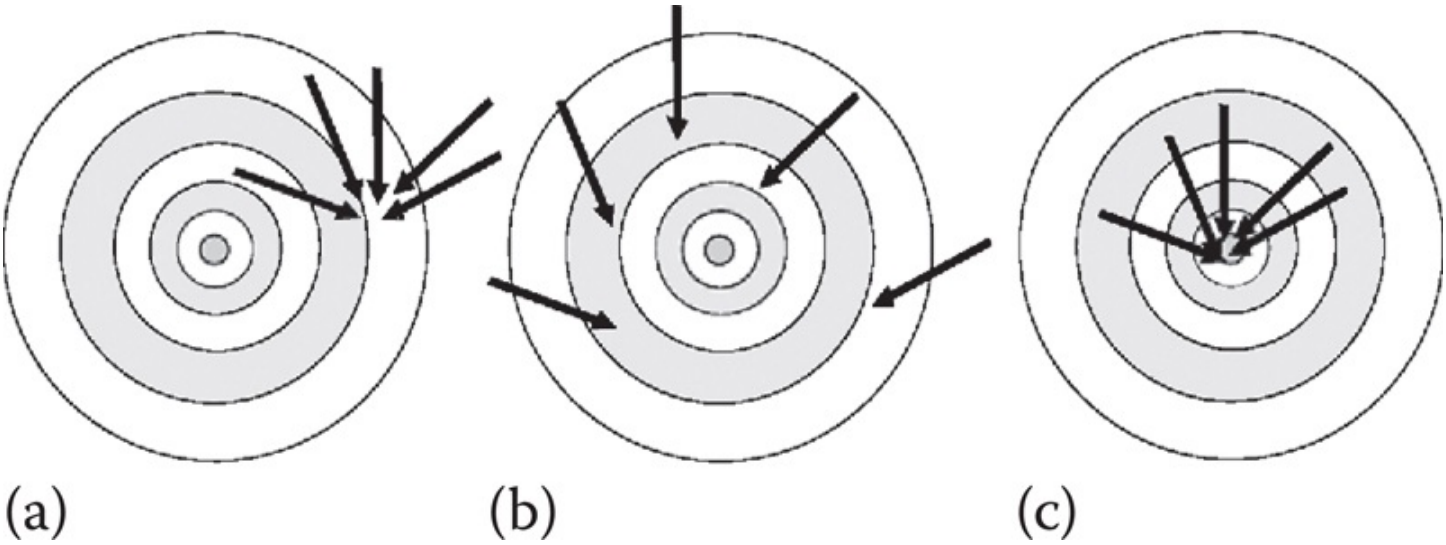

Figure 2.13 The difference between precision and accuracy: (a) precision without accuracy, (b) accuracy without precision and (c) precision and accuracy.

2.4.3.1 Wet chemical methods

The air sample is bubbled at a low rate (typically a few litres min^{-1}) through a solution that absorbs the required gas. At the end of the sample period, which is typically hours or days, the solution is returned to the laboratory for analysis by one of a wide range of standard techniques.

2.4.3.1.1 Example – SO_2

Air is bubbled through dilute hydrogen peroxide (H_2O_2). Any SO_2 is converted to sulphuric acid (H_2SO_4). The amount of acid created can be measured by titration or by pH change. In

this form the method is not specific to SO_2, as other acid-forming gases give an increase in apparent concentration, while alkaline gases such as ammonia give a decrease. Specificity can be improved by analysing colourimetrically for the sulphate ion. The method was adopted for the original UK National Survey monitoring sites – although it was adequate at the high concentrations of the 1960s, the errors are too great at the lower concentrations now prevailing. The standard wet chemical method for low concentrations is known as West-Gaeke and involves more complex chemistry to form red-purple pararosaniline methyl sulphonic acid, which is determined colourimetrically.

2.4.3.2 Real-time pumped systems

Any physical or chemical effect of which the magnitude can be related reliably and repeatedly to the gas concentration can in principle be used. In this section we describe techniques in which an air sample is pumped continuously through the instrument.

2.4.3.2.1 Example 1 – Pulsed fluorescence for sulphur dioxide

The sample air is irradiated with intense UV (wavelength 214 nm) to stimulate fluorescence in a waveband centred on 340 nm (Figure 2.14). The flux density of the emission is measured by a photomultiplier. The sample air must normally be conditioned before the measurement to prevent spurious responses from obscuring the true signal. First, water vapour (which quenches the fluorescence) must be reduced by a diffusion drier; second, hydrocarbons (which augment the fluorescence) must be reduced by passing the air through a scrubber. The main initial drawback of this method was the slow response time, but engineered improvements have made pulsed fluorescence the current method of choice for SO_2.

FOR REFERENCE PURPOSES ONLY

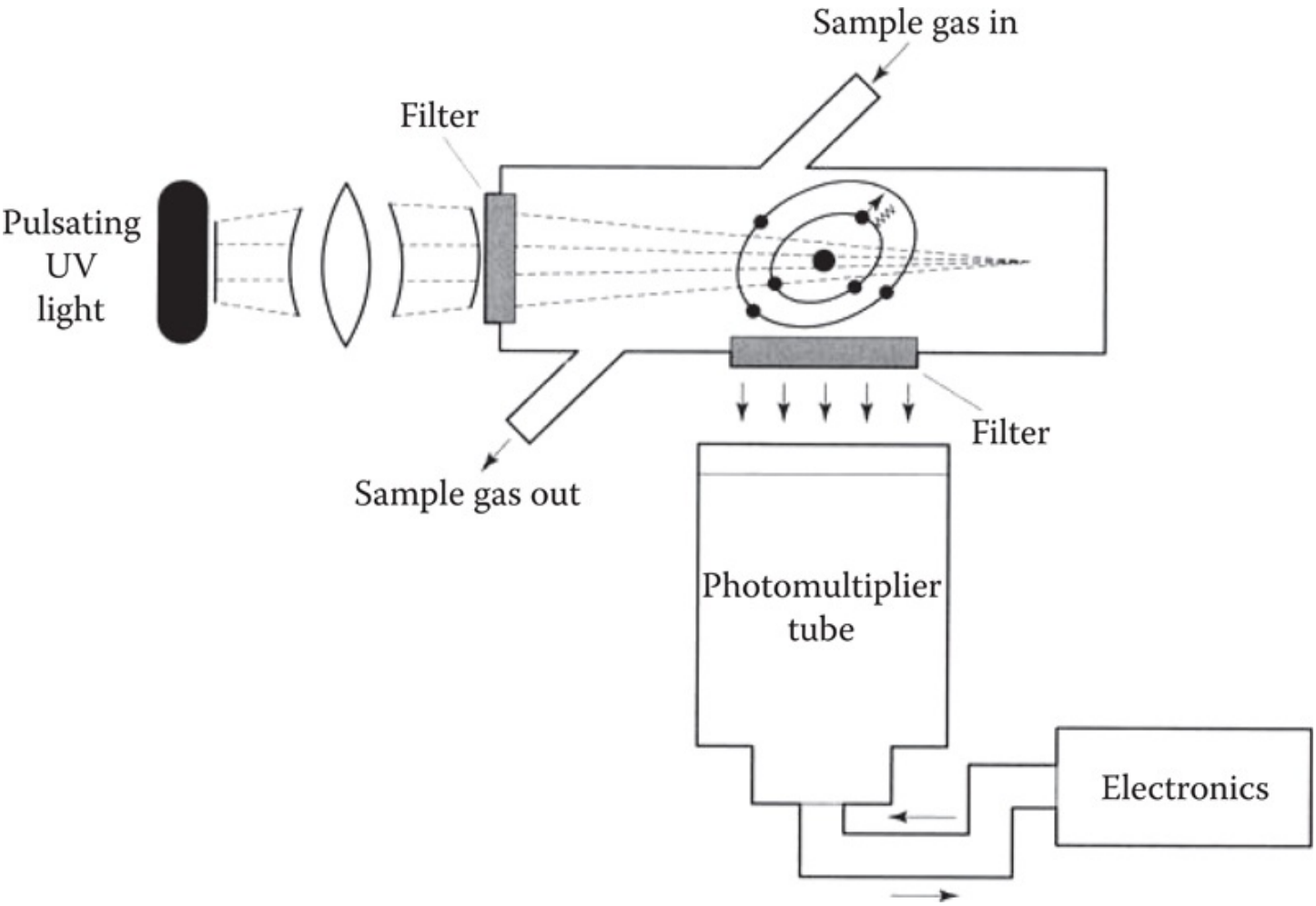

Figure 2.14 Pulsed fluorescence SO_2 analyser. (From Harrison, R. M., Measurements of the concentrations of air pollutants, in S. T. Holgate, J. M. Samet, H. S. Koren and R. L. Maynard (Eds.), *Air Pollution and Health*, Academic Press, London, UK, 1999.)

2.4.3.2.2 Example 2 – UV absorption for O_3

Ultraviolet radiation at 254 nm from a low-pressure mercury vapour lamp traverses the length of a tube through which the sample air is pumped continuously (Figure 2.15). The attenuation of UV flux density at the far end of the tube depends on the O_3 concentration. The attenuation is compared with that due to air from which the ozone has been scrubbed by activated charcoal. The Beer–Lambert law ($I = I_0 e^{-ax}$, where I_0 and I are respectively the intensity of the incident and the attenuated light; a is the extinction coefficient and x is the path length) is then used to relate the attenuation to ozone concentration using the known extinction coefficient for ozone. This is a simple and reliable method for ozone determination.

FOR REFERENCE PURPOSES ONLY

2.4.3.2.3 Example 3 – Chemiluminescence for NO

A supply of ozone is generated within the analyser and reacted with the NO in a sample cell (Figure 2.16). Nitrogen dioxide is generated in an excited state, and decays to the ground state with photon emission. The flux density is measured with a photomultiplier. In most commercial analysers, the NO measurement described earlier is alternated with a measurement on air that has been passed through a molybdenum catalyst to convert any NO_2 into NO. Hence the uncatalysed measurement gives NO directly, while the difference between that and the catalysed measurement gives NO_2. It is not only NO_2 that is reduced to NO, and a variable proportion of other N-containing gases such as HNO_3 will be detected as well. By using a higher temperature catalyst, ammonia can be oxidised to NO to give the NH_3 concentration by difference. As typical ambient NH_3 concentrations are only a few percentage points of NO_x, the errors on the NH_3 value are unavoidably large.

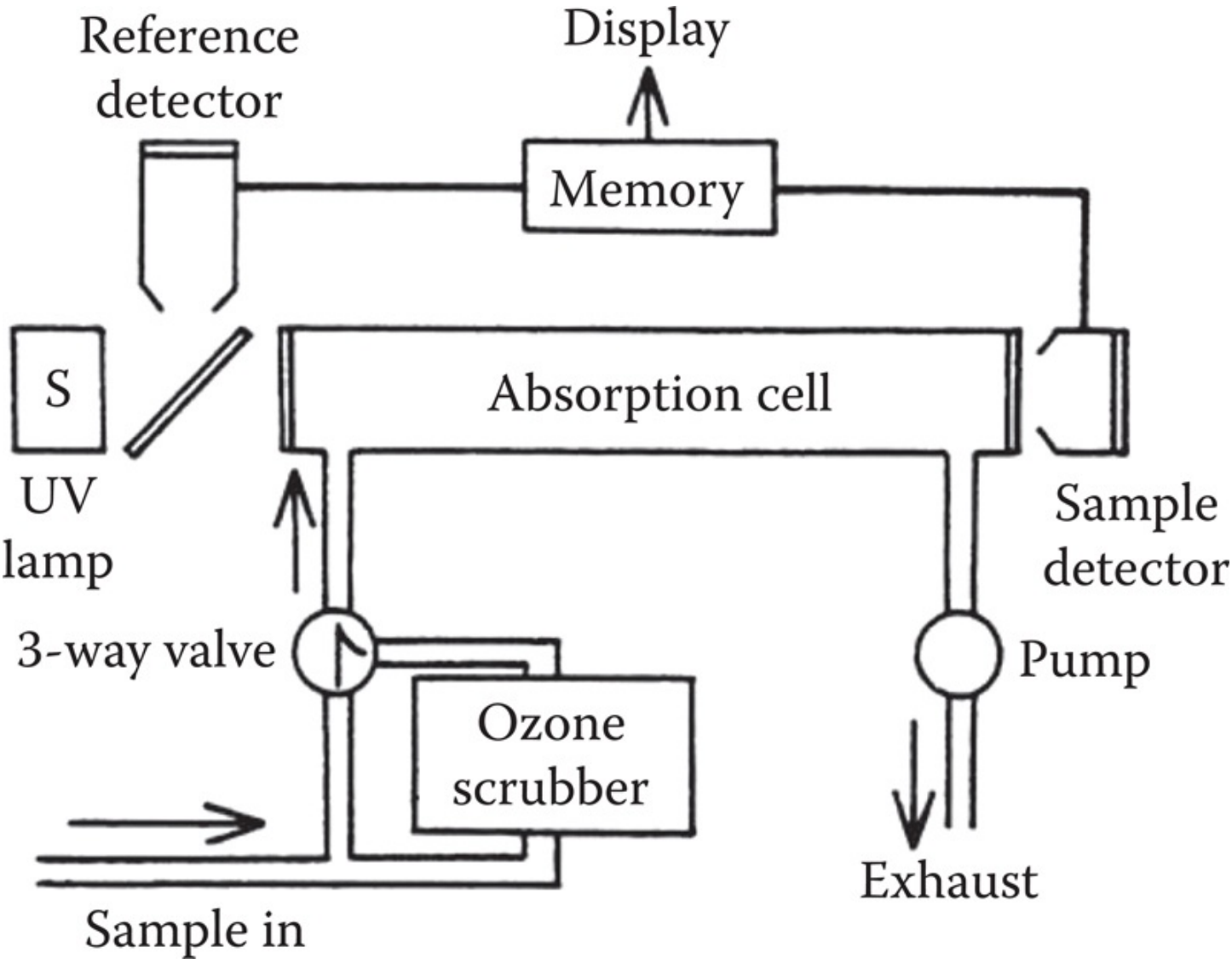

Figure 2.15 UV absorption O_3 analyser. (From Harrison, R. M., Measurements of the

FOR REFERENCE PURPOSES ONLY

concentrations of air pollutants, in S. T. Holgate, J. M. Samet, H. S. Koren and R. L. Maynard (Eds.), *Air Pollution and Health*, Academic Press, London, UK, 1999.)

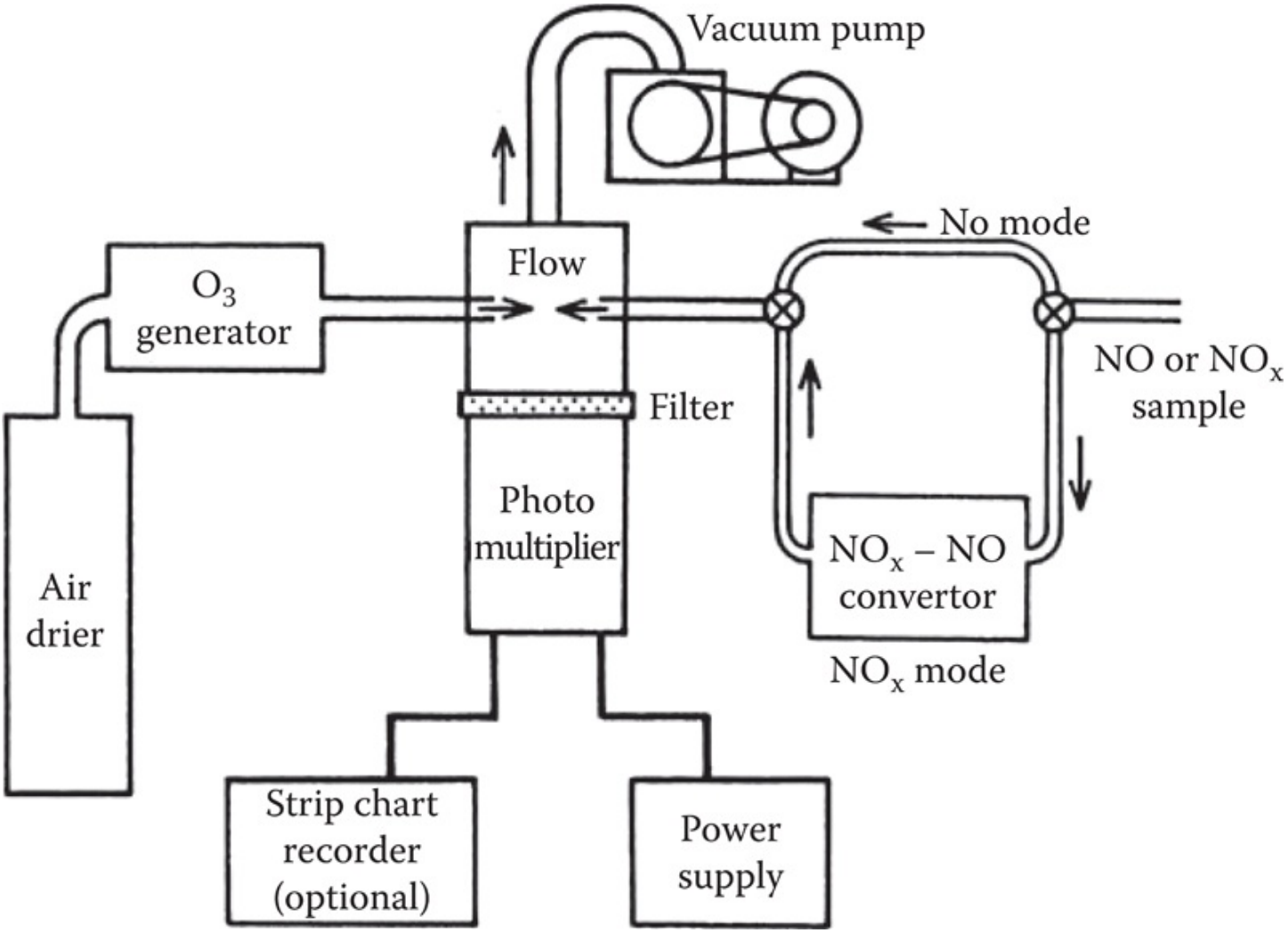

Figure 2.16 Chemiluminescent NO_x analyser. (From Harrison, R. M., Measurements of the concentrations of air pollutants, in S. T. Holgate, J. M. Samet, H. S. Koren and R. L. Maynard (Eds.), *Air Pollution and Health*, Academic Press, London, UK, 1999.)

2.4.3.2.4 Example 4 – Infrared absorption for CO_2 (and many other gases)

Infrared (IR) radiation is attenuated while passing along a tube filled with the sample. By selecting specific wavebands to coincide with the absorption bands of different gases, several hundred different gases can be measured – but the species of gas must be known first. Portable infrared gas analysers are available that can determine the concentration of many gases in air. They employ a continuous IR source, a variable frequency interference filter to select a narrow frequency range at which the absorptivity of a particular gas is

known, and a long optical path folded by means of mirrors into a compact case. The lower detection limit is typically around 1 ppm, so these analysers are mainly of use in the workplace environment.

2.4.3.3 Real-time remote systems

Some detectors measure the optical properties of the gas and have been designed so that the reflected or transmitted signal is received after an extended path length through the air. This arrangement offers the advantages of eliminating the possibility of sample degradation during passage to and through an instrument, and of integrating the concentration over a region of space rather than sampling at one point.

Light detection and ranging (LIDAR) describes a family of active remote sensing methods. The most basic technique is long-path absorption, in which a beam of laser light is reflected from a distant retroreflector and returned to a detector which is co-located with the source. A retroreflector is a corner cube which works in the same way as a *cat's eye* road marker as used in the UK, and returns the incident beam in exactly the opposite direction that it came from, no matter what that direction. The wavelength of the radiation is chosen so that it coincides with an absorption line of the gas of interest. The concentration of that gas is found by applying the Beer–Lambert law to the reduction in beam flux density over the path length. No information is obtained on the variation in density of the gas along the path length; if the gas is present at twice the average concentration along half the path, and zero along the other half, then the same signal will be received as for uniform distribution at the average concentration.

2.4.3.3.1 *Example 1 – Differential absorption light detection and ranging*

Pulses from a tuneable laser are directed into the air at two wavelengths, and the backscattered signals from the air molecules, gas molecules and particles are measured by a cooled detector. One laser wavelength (λ_{min}) is just to one side of an absorption band for the gas of interest, and calibrates the backscatter of the LIDAR system for molecular (Rayleigh) and aerosol (Mie) scattering that occurs whether the gas of interest is present or not. The second laser wavelength (λ_{max}) is tuned to an absorption band, so that the difference between the two can be used to derive absorption due to the gas alone. The ratio of the scattered flux density at the two wavelengths is given by:

$$I(\lambda_{max})/I(\lambda_{min}) = \exp(-2RN\sigma)$$

where:

σ is the absorption cross-section of the target species at wavelength λ_{max}

R is the range

N is the number concentration of the gas

FOR REFERENCE PURPOSES ONLY

By measuring the time for the backscattered signal to return, the range can also be determined to within a few metres over a distance of 2000 m. The technique has been used for studying plume dispersion and vertical concentration profiles, as well as spatial distribution in the horizontal plane. The most widely used sources are CO_2 lasers emitting in the 9.2–12.6 μm band, within which they can be tuned to emit about 80 spectral lines. For example, O_3 absorbs strongly at 9.505 μm, and NH_3 at 10.333 μm. In the UV to visible spectrum, dye lasers pumped by flash lamps or by laser diodes are used. By using different dyes, they are tuneable over the whole visible band. Some examples of the wavelengths used are given in Table 2.21.

2.4.3.3.2 Example 2 – Differential optical absorption spectroscopy

A detector at one end of an atmospheric path (typically 200–10,000 m in length) scans across the waveband of a UV to visible source, such as a high-pressure xenon arc lamp that has a known broad spectrum, at the other end. The physical arrangement can be bistatic (with the receiver at one end and the transmitter at the other) or monostatic (a retroreflector returns the beam to the receiver, which is co-located with the transmitter). Gases that are present on the optical path absorb radiation according to the Beer–Lambert Law, and the absorption varies differently with wavelength for each gas. Variations across the spectrum are compared to stored reference spectra for different gases, and the equivalent amounts and proportions of the gases adjusted in software until the best match is achieved. The main wavelength range used is 250–290 nm (in the UV range), with typical spectral resolution of 0.04 nm. Several different gases can be measured simultaneously. Sensitivity is high, and 0.01% absorption can be detected, equivalent to sub-ppb concentrations of many gases over a path length of 1 km. Detectable gases include SO_2, NO, NO_2, O_3, CO_2, HCl, HF, NH_3, CS_2, Cl_2 and HNO_2 and many organic compounds (aldehydes, phenol, benzene, toluene, xylenes, styrene and cresol). The method is appropriate for obtaining the average concentrations of a pollutant across an urban area or along the length of an industrial plant boundary.

Table 2.21 Absorption wavelengths and cross-sections for dye lasers

Molecule	*Peak absorption wavelength/nm*	*Absorption cross section/ 10^{-22} m^2*
Nitric oxide	226.8, 253.6, 289.4	4.6, 11.3, 1.5
Benzene	250.0	1.3
Mercury	253.7	56000
Sulphur dioxide	300.0	1.3
Chlorine	330.0	0.26
Nitrogen dioxide	448.1	0.69

Scattering LIDAR: The light detection and ranging and differential absorption LIDAR

systems described previously measure the backscattered radiation at the wavelength at which it was emitted. The radiation is scattered elastically, and changes in flux density are not necessarily due to the target species alone. By using other techniques such as Raman scattering, a signal is obtained at different wavelengths which is more directly attributable to the target species.

2.4.3.3.3 Example 3 – Fourier transform infrared absorption spectroscopy

This is the most optically sophisticated remote sensing technique, using a scanning Michelson interferometer to detect the entire spectral region at once, and is therefore capable of measuring many gases simultaneously. The wavebands used are within the atmospheric absorption windows of 8.3–13.3 or 3.3–4.2 μm. However, sensitivity is generally limited to a few tens or hundreds of ppb (depending on the gas) over a 200 m path length; the technique is therefore more appropriate to perimeter monitoring for gas escapes from an industrial site than to general ambient monitoring.

2.4.3.4 Gas chromatography

Chromatography involves the passage of chemical species in a liquid or gaseous mobile phase through a liquid or solid stationary phase. In gas chromatography (GC), the mobile or carrier phase is a gas (commonly nitrogen, helium or argon). In gas–solid chromatography, the stationary phase is a porous polymer. In gas–liquid chromatography, the stationary phase is a liquid (such as methyl gum or an ethylene glycol ester). The liquid coats a solid supporting substrate such as silica or alumina which is packed inside a long thin coiled glass or stainless steel column. The sample is either dissolved into a volatile solvent such as acetone which is injected into the carrier gas or injected directly in the gaseous phase after thermal desorption (Figure 2.17).

As the carrier gas flows along the column, different volatilised pollutant compounds in the gas have different affinities for the stationary phase, and they migrate along the column at different rates so that they separate. With capillary columns, the stationary phase substrate is bonded to the inside surface of a column that might be only 0.1 mm internal diameter and over 100 m long. The exit gas is passed to a detector. The time of passage of the component through the system identifies the material, and the time-integral of the output signal gives the amount and hence the concentration. The most commonly used detectors are the flame ionisation detector (FID) and the electron capture detector (ECD). Both of these detectors have a detection limit of about 1 pg (picogram = 10^{-12} g).

FOR REFERENCE PURPOSES ONLY

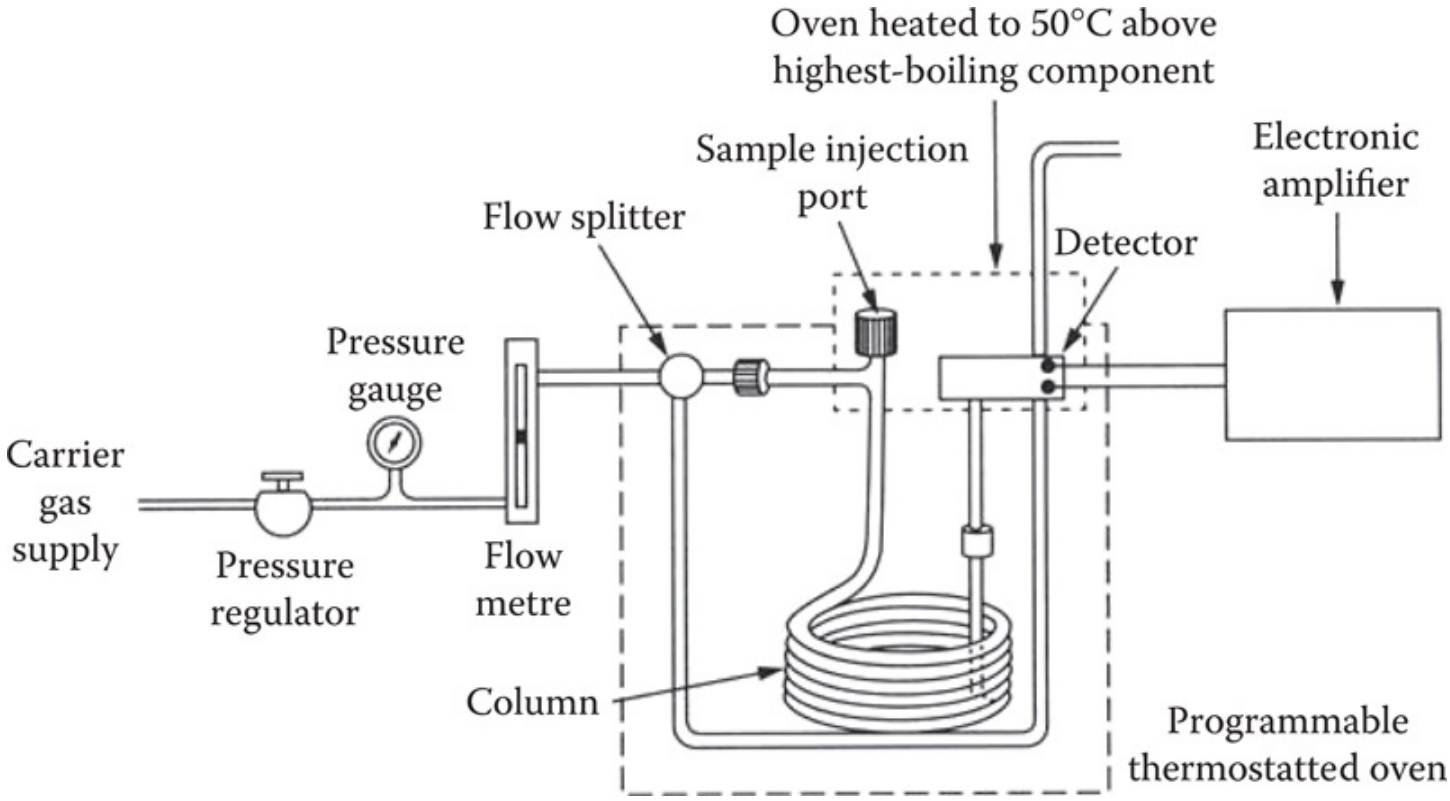

Figure 2.17 Gas chromatograph.

- In the FID, organic compounds, when injected into H_2-in-air flames, are pyrolysed to produce ionic intermediates and electrons. The current generated when an electric field is applied is a measure of the initial concentration.
- In the ECD, the eluent is passed over a radioactive electron source such as ^{63}Ni, which ionises the carrier gas.
- $N_2 + \beta^- \Leftrightarrow N_2^+ + 2e^-$
- This generates a steady current between two electrodes. When molecules that capture electrons are present in the carrier gas, the current decreases. Hence ECD is particularly sensitive for compounds with electronegative functional groups, such as halogens, nitro groups and carbonyls, chlorinated pesticides and polychlorinated biphenyls.
- Flame photometers can be used for S- and P-containing compounds. When these are combusted in a hydrogen-rich flame, they emit at 394 and 526 nm, respectively.
- Katharometers, which respond to the thermal conductivity of the gas stream, can be used for detection of very low concentrations of H_2, He, H_2O, N_2 and CO_2.

2.4.3.5 Liquid chromatography

The principles of high-pressure liquid chromatography (HPLC) are just the same as those of GC, except that the mobile phase is a liquid solvent such as ethanol, methanol or hexane that is forced at pressures of around 40 MPa through a 30 cm long, 5–10 mm diameter

stainless steel column packed with 1–10 μm particles. The stationary phase may be in several forms – a liquid which may be retained on the column either by physical absorption or by the formation of covalent bonds with the support, or a finely divided polar solid such as alumina or silica. This technique is used for the determination of high-molecular-weight insoluble organic compounds. With ion exchange chromatography, the stationary phase is 5 μm beads of an ion exchange resin formed from high-molecular-weight copolymers of styrene and vinyl benzene with functional groups attached to the aromatic ring. As with other chromatography, the polarity of the solvent and substrate may affect the performance of the system dramatically. The most common detectors use UV absorption, fluorescence (especially for organic molecules with organic rings), or electrical conductivity, depending on the molecule concerned. There may be difficulties due to the overlap of the solvent carrier absorbance with that of the analyte. If the analyte does not fluoresce, it may be induced to do so by reaction with a reagent after it has been through the column.

2.4.3.6 Chromatography with mass spectroscopy

A powerful combination of instruments is increasingly being used to discriminate and quantify environmental pollutants. First, either a gas or liquid chromatograph is used to separate a mixture of compounds. The eluate is then delivered to a mass spectrometer for quantitative determination of each component. The mass spectrometer ionises the constituent atoms and measures their mass by firing them into a magnetic and/or electrostatic field and observing the deviation, which depends on their speed, time of flight and charge-to-mass ratio. As well as the chemical determinations, it is an important technique for distinguishing stable isotopes such as ^{15}N and ^{18}O, which are not radioactive but which are chemically identical.

2.4.3.7 Inductively coupled plasma spectroscopy

The inductively coupled plasma (ICP) is a very high-temperature radiation source, created by passing an electric current through an inert gas such as argon. This generates an ionised region, known as a plasma, which radiates strongly due mainly to collisions between the carrier gas ions. Solid particles or liquid droplets of sample are vaporised and ionised in the ICP. When used in conjunction with atomic absorption spectroscopy (AAS), light from a normal source is passed through the plasma and the absorption lines are determined. There is also some radiation from the analyte which is present at low concentration in the carrier gas, and this emission can be analysed by conventional AAS. Alternatively, the ionised material from the ICP can be passed to a mass spectrometer (ICP-MS).

2.4.3.8 Optical spectroscopy

Spectroscopy uses the different energy levels of electronic or vibrational states in atoms

FOR REFERENCE PURPOSES ONLY

and molecules to identify the presence of one of those atoms or molecules. In general, the energy needed to move between levels is lowest for vibrations, higher for the outer electrons and highest for the inner electrons. As photon energy increases as frequency increases, the vibrational states can be excited by IR, whereas outer electrons need visible or UV light and the inner electrons need UV light or even X-ray.

A spectrometer needs a stable and tuneable source of radiation, a transparent sample container, a wavelength selector and a photodetector. The radiation source may be a tuneable laser, which replaces the combination of thermal radiation source, collimation optics, wavelength selector and focussing optics. However, the tuneable range of many lasers, especially in the UV-visible range, is small. In the IR the CO_2 laser, tuneable over 80 lines in the range 9–11 μm, is used. Commercial instruments still largely depend on a range of tried and tested thermal sources such as the Nernst Glower (rare earth oxide), Globar (silicon carbide), incandescent wire (Nichrome), tungsten filament and high-pressure mercury arc. An interference filter can be used to select one line (1–5 nm wide) from a broadband source, or a scanning monochromator with holographic gratings will do the same job over a continuous wavelength range. Photon detection is by photosensitive detector (e.g. mercury cadmium telluride) in the IR or photomultiplier tube in the UV-visible.

Molecular spectroscopy includes absorption, emission, fluorescence and scattering processes. In the UV-visible wavelengths, the transitions are between electronic energy levels, whereas IR radiation causes changes in the vibrational energy.

2.4.3.8.1 Absorption

When the electrons that are bound to atoms change their energy level, the difference in energy is emitted or absorbed at wavelengths determined by the energy change and given by Planck's formula ($E = hv$). The wavelengths are related to the atomic configuration and are therefore specific to the element concerned. For molecules, as well as the energy levels of the constituent atoms, there is a whole new set of energy levels for molecular orbitals of electrons shared by the atoms plus vibrational states.

Absorbance is defined by $A = \log_{10}(1/T)$ where $T = I/I_0 = \exp(-\mu L)$, I, I_0 are the transmitted and incident flux density, respectively; μ is the attenuation coefficient of the medium; L is the path length through the medium. If the molecules of interest are the only significant absorber, then we can write the following:

$$T = \exp(-\alpha CL)$$

where α is the absorption cross-section (usually expressed as cm^2 when the concentration C is in molecules cm^{-3} and L is in cm), or the absorptivity (1 g^{-1} cm^{-1}) when C is in g 1^{-1}, or the molar absorptivity (1 mol^{-1} cm^{-1}) when C is in mol 1^{-1}.

Hence absorbance $A = 0.434\ \alpha CL$, so that if the output from the spectrometer is presented

FOR REFERENCE PURPOSES ONLY

in terms of *A*, it is directly proportional to the concentration provided that the concentration is sufficiently dilute (typically <0.01 M). Ultraviolet-visible molecular absorption mainly involves unsaturated double bonds at wavelengths between 200 and 700 nm. Infrared molecular absorption mainly involves transitions between successive levels of the fundamental stretching vibrational modes, stimulated by radiation in the 2.5–15 μm spectral region. If the excited molecule decays back to an intermediate excited state, rather than to the ground state, then the emitted photon will have less energy (i.e. longer wavelength) than the incident photon. This is called Raman scattering, and each molecular species generates a set of narrow Raman absorption lines in the UV-visible range that correspond to the various vibrational modes observed in infrared absorption spectroscopy.

If the molecule is raised to the lowest vibrational state of the excited electronic level, then radiative transitions to the various vibrational states of the ground electronic state will occur after a relatively long period (10^{-8} s instead of 10^{-12} s). This is called fluorescence and is characterised by having an emitted wavelength longer than the exciting wavelength. The concepts in atomic spectroscopy are very similar to those in molecular spectroscopy. The material is reduced to its atomic components if it is not already, then the absorption, emission and fluorescence of radiation are studied. Instead of dealing with the molecular excited states, we are now involving the electron energy levels of multi-electron atoms. The atomisation is achieved either with a simple flame (temperatures of around 2000°C for natural gas in air, 3000°C for acetylene in oxygen), or with ICP or electric arc–spark (temperatures of 4°C–6000°C).

FOR REFERENCE PURPOSES ONLY

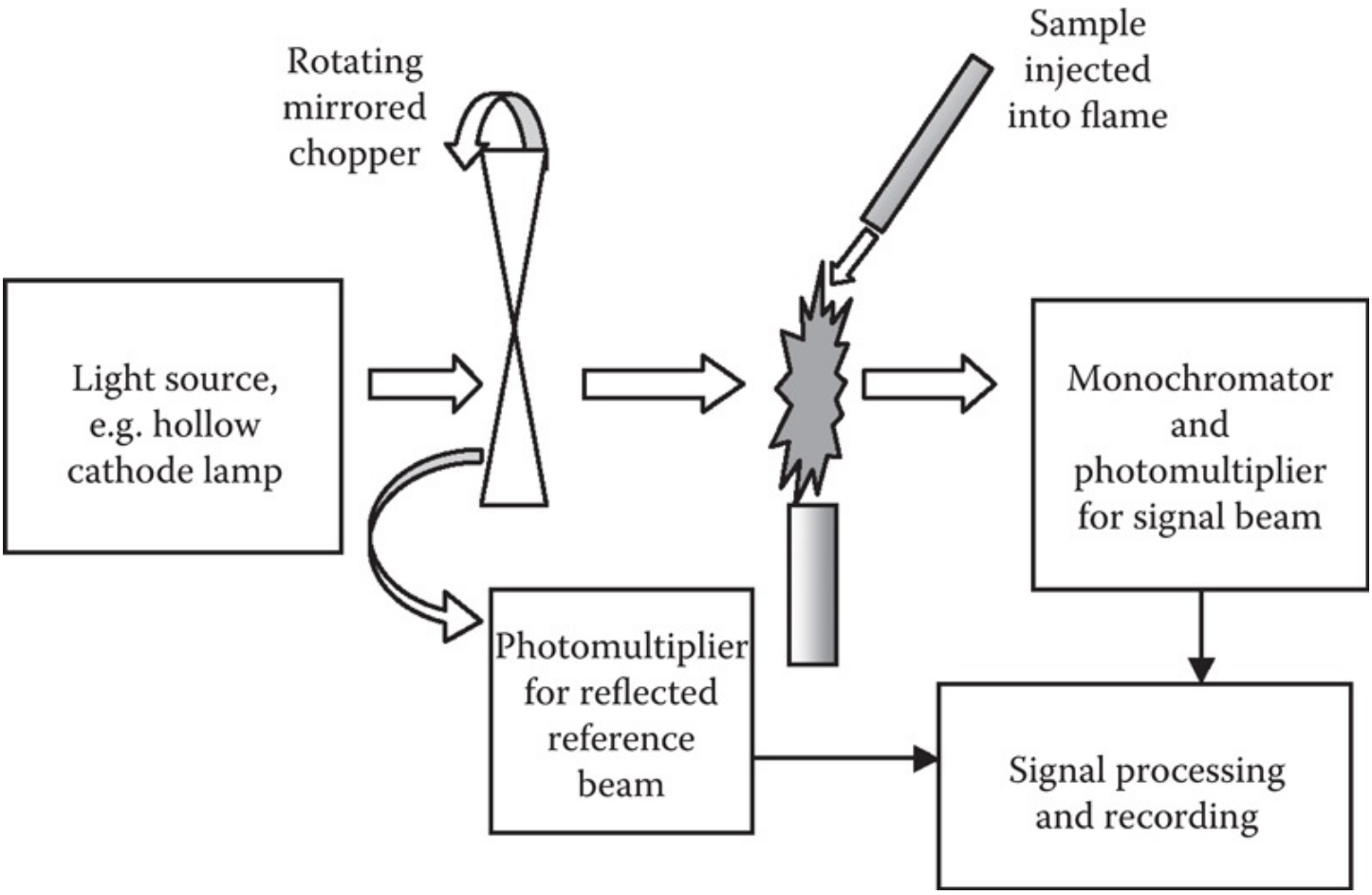

Figure 2.18 Atomic absorption spectrophotometer.

In AAS (Figure 2.18), the material for analysis is atomised at high temperature (either injected into an air–acetylene flame at 3000°C, or vaporised in a graphite furnace). A beam of radiation is passed through the vapour, so that photons knock electrons from a low (usually ground) energy state up to a higher state; hence photons are absorbed and the radiation flux is depleted. The radiation source is a hollow cathode lamp constructed from the element to be analysed, so that it emits narrow spectral lines appropriate to that element rather than a continuous spectrum. This greatly reduces the stray light transmission and increases the sensitivity. The total amount transmitted at different wavelengths is measured photoelectrically, and the absorbance is determined. From the Beer–Lambert law, $I_t = I_0 \exp(-kL)$, where I_t, I_0 are the transmitted and incident flux densities, k is the extinction coefficient and L is the optical path length. Also $k = \varepsilon C$, where ε is a constant for the substance and wavelength, and C is the vapour concentration. Hence, C can be calculated. Atomic absorption spectroscopy is used almost exclusively for determinations of metallic elements.

In atomic emission spectroscopy (AES), atomic collisions due to the high temperature of the sample knock electrons into higher energy states from which they subsequently decay with the emission of a photon (Figure 2.19). The excitation energy is provided by a flame or

FOR REFERENCE PURPOSES ONLY

spark, which also vaporises the sample from solution. The range of elements that can be excited (and therefore detected and measured) depends on the temperature of the source. Low-temperature propane flames have been used for the alkali metals that have emission lines near the low-energy red end of the spectrum (Table 2.22). The typical solution concentration range that can be used is 0–20 ppm. At higher concentrations the response is non-linear.

Nitrous oxide–acetylene flames enable the detection of a similar range of metals to AAS. Inductively coupled plasma sources achieve temperatures of c. 6000 K and make it possible to analyse elements such as Ce, U and Zr that form very stable refractory oxides. If higher excitation energy is provided by a spark rather than a flame, every element above helium can be detected, and the sample can be solid as well as liquid.

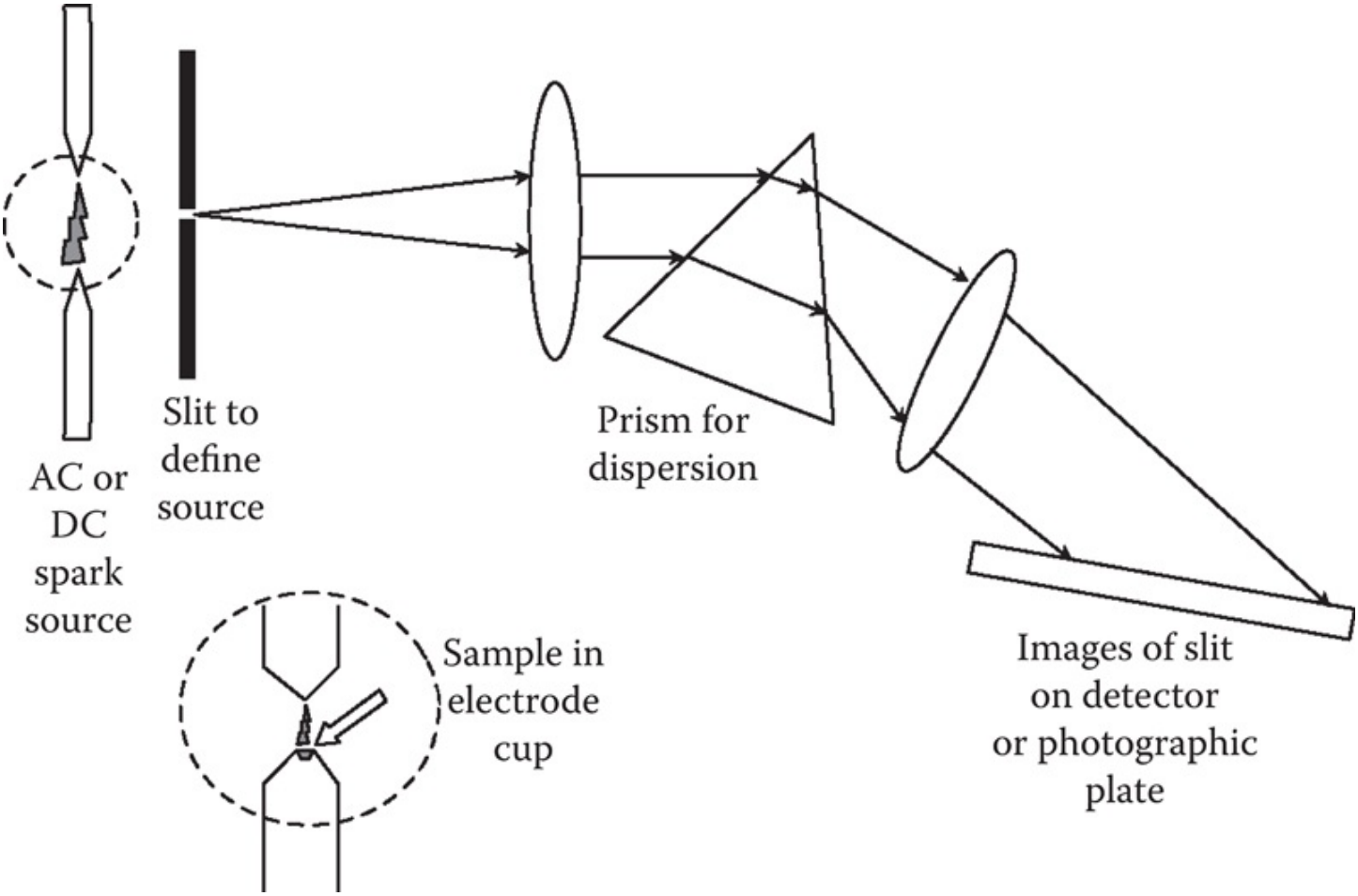

Figure 2.19 Atomic emission spectrometer.

Table 2.22 Elements determined by low-temperature AES

Element	*Wavelength/nm*	*Detection limit/ppm*
Li	671	0.005
Na	589	0.0003
K	766	0.003

FOR REFERENCE PURPOSES ONLY

Rb	780	0.004
Cs	852	0.004
Mg	285	0.008
Ca	423	0.005
Sr	461	0.001
Ba	422	0.004

2.4.4 Quality control

All measurement devices eventually produce an output (voltage, weight, absorbance etc.) that has to be translated into a gas concentration. An effective quality assurance and quality control (QA/QC) programme is an important part of gaining confidence in the truth of the output value and in the errors associated with it. A minimum QA/QC programme includes blanks, duplicates and calibration standards; for more demanding assessments, it may be necessary, for example, to have independent laboratories carry out duplicate analyses.

2.4.4.1 Blanks

If a measurement method such as a bubbler or diffusion tube is being used, then contamination of the absorbent is possible. To evaluate this effect, sample units are prepared and analysed following exactly the same procedure as those used for the measurements themselves, but they are kept sealed. The concentration measured is then a baseline value which should be subtracted from all actual measurements. In an extended sampling programme, it would be normal to retain at least 10% of sampling units for construction of this baseline.

2.4.4.2 Calibration

Even the highest specification gas analysers are not yet as stable or repeatable as other, more common electronic devices such as computers and radios. Over a period of time that may be as short as days, the output signal due to a constant input gas concentration can vary significantly. Such variations might be due to drift in the value of electronic components, dirt penetrating through to the optics, or temperature changes. Large sudden changes can be caused by replacement of failed components. For these reasons it is essential to have good calibration facilities available. Calibration involves supplying the analyser with a known concentration or range of concentrations of the gas to be measured, together with a zero air sample containing none of the gas. Several methods can be used to obtain these supplies.

2.4.4.3 Permeation tubes

Small stainless steel tubes are sealed at one end and capped at the other by a membrane that

is permeable to the gas. The tube is filled under pressure with the liquid phase of the calibration gas. If the tube is kept in a constant-temperature oven (typically 50°C ± 0.1°C), then gas leaks out through the membrane at a very stable rate. The gas is added to a known volume flow rate of clean air to produce a known gas concentration. Tubes are available for hundreds of gases including SO_2 and NO_2 (but not O_3). The release rate from the tube is individually certified by the manufacturer and can be confirmed by the user by weighing the tube at intervals during use. These sources can be incorporated into a self-contained calibrator or built into an analyser to provide a calibration signal on demand.

2.4.4.4 Gas bottles

Specialist gas suppliers can provide pressurised bottles of calibration gases – a known concentration of the gas in an inert carrier. If the concentration is too low, the concentration may change in the bottle because of reactions with the surfaces or with other gas molecules, and also the bottle will be used up very quickly. If it is too high, then an impractical dilution factor will be needed to bring the concentration down within the analyser range. Hence it is normal to store, say, 50 ppm of NO in nitrogen, and to use a precision dilution system to generate concentrations of between 50 and 200 ppb when calibrating an NO analyser that has a 200 ppb range.

2.4.4.5 UV O_3 generator

Ozone cannot be stored, so that any calibration method must create it on the spot. In this method, a proportion of oxygen molecules irradiated with UV light is converted to O_3; by arranging for clean air to be so irradiated by a very stable UV lamp, stable O_3 concentrations can be generated. By mixing NO with O_3, known concentrations of NO_2 can also be made (gas phase titration).

2.4.4.6 Zero air

All of these calibration methods rely on the availability of a clean air supply, known as zero air. It is not a trivial task to generate such a supply, particularly if calibrations in the low- or sub-ppb range are required. In order to make zero air on site, the basic principle is to pass ambient air through activated charcoal to adsorb pollutant molecules, but there are some difficulties. First, the air must be passed through cooling coils to condense out excess water vapour. Second, NO is present at significant concentrations but is not adsorbed by charcoal. Hence the air is first irradiated with UV, to generate O_3 that reacts with the NO, converting it to NO_2 (which *is* efficiently adsorbed by the charcoal). Provided that the charcoal is renewed frequently, very low trace gas concentrations can be achieved. Alternatively, compressed bottles of zero air can be purchased from specialist suppliers.

FOR REFERENCE PURPOSES ONLY

The weakest link in the calibration chain is frequently the measurement of volume flow rate. On a calibrator, for example, the volume flow rate of the clean air used to dilute the output from the permeation tube is often measured with rotameters that are only accurate to 5%. This determines the best overall accuracy of calibration, no matter how accurately the permeation rate is known. The precision can be increased – at a price – by substituting electronic mass flow meters for the rotameters.

A comprehensive QA/QC programme for a network of continuous analysers might involve:

- Daily automatic calibration checks of the analysers.
- Site checks every one or two months.
- Regular analyser servicing by trained instrument engineers.
- Regular intercalibrations (either taking several analysers to the same calibrator or taking one calibrator around all the analysers in succession).
- Periodic checking of the calibrator against primary standards.
- Detailed manual and automatic scrutiny of the data to eliminate false values caused by instrument malfunction or transmission faults. It is much better to have holes in the data set than to have spurious values.
- Comprehensive review of period data sets.
- Telemetry of the data to the processing centre, so that faults can be spotted as soon as they occur.

The automatic urban and rural monitoring networks operated in the UK by Department for Environment, Food & Rural Affairs (DEFRA) and described in Chapter 5 aim to achieve overall error bands of ±5 ppb on SO_2, NO_x and O^3, ±0.5 ppm on CO_2, and ±5 μg m^{-3} on PM_{10}. The actual time for which the network generates valid data, expressed as a percentage of the possible time, is called the data capture. The EU Directive on monitoring ambient NO_2 specifies 75%, the USEPA requires 80%, and the UK Department of Energy (DoE) network achieves 95%.

2.5 CASE STUDY – BHOPAL GAS LEAK

The 1984 methyl isocyanate gas leak from the Union Carbide pesticide plant in Bhopal, India, was the worlds' worst industrial disaster (Boughton, 2005; Weick, 2010), killing an estimated 16,000–30,000 people and injuring around 500,000, with severe birth defects still witnessed in the offspring from the exposed residents.

Bhopal is a large industrial town in the Madhya Pradesh region of central India. In 1969, the US-based Union Carbide chemical company, a large multinational organisation, began building a plant that developed into a full-scale manufacturing unit for pesticides. Bhopal was selected because of its central location; a developed railway system; and reliable

FOR REFERENCE PURPOSES ONLY

sources of water, electricity and labour. The plant's main product was Carbaryl, a carbamate pesticide usually sold under the trade name Sevin.

The infamous incident at the Union Carbide plant started in an underground chemical storage tank on the night of 2–3 December 1984. The tank contained methyl isocyanate (H_3C-N=C=O), also known as MIC, a common industrial chemical used in the manufacture of carbamate pesticides. MIC is clear, colourless, extremely volatile (boiling point 38°C), chemically active (it reacts violently with water, acids and some metals), heavier than air and very toxic. Consequently, MIC is stored very carefully in refrigerated, pressurised tanks containing safety equipment such as rupture discs and temperature and pressure gauges.

On the night of the accident, 450–900 kg of water escaped into the MIC storage tank E610, producing a chemical reaction followed by a rise in temperature, gas pressure and a subsequent leak. The exact composition of the gas is not known, but it is likely to have contained MIC, phosgene and hydrogen cyanide. Subsequent investigations have reported different reasons for the accident. Union Carbide claims that the chemical reaction was deliberately started by an employee. Other reports suggested that the accident was due to multiple errors – technical, procedural and human. The safety devices (refrigeration system, fire hoses, toxic gas alarm) failed through a combination of faulty engineering and inadequate maintenance. Proper procedures were not followed and staff were poorly motivated and were suffering from low morale. It is also clear that the Bhopal plant lacked the computerised warning and fail-safe systems used by Union Carbide in the United States.

The dense cloud of gas drifted over an area with a radius of some 7 km. Low-lying areas close to the factory were the worst affected, including many poor neighbourhoods and shanty-towns. It is believed that 6000–8000 people were killed that night by the gas, many in their sleep, with a further 200,000 injured. Many more died in the weeks after the accident; indeed over 15,000 death claims and 600,000 injury claims were filed with the Indian government. The actual numbers of dead and injured vary according to source and will probably never be known. Thomas Gassert from the Harvard School of Public Health reported in 2013 his estimate that over 558,000 people were exposed to the toxic gas. Reports suggest that up to 20,000 have died prematurely as a direct result (more than 3000 acutely).

The main human health effects included body weight loss, eye and respiratory tract irritation, blindness, cataracts, damage to the intestines and bladder, fatigue, breathlessness, loss of appetite, recurrent fever, neurological problems (loss of memory, damage to motor skills), skeletal problems, persistent cough and vulnerability to secondary infection. Psychological effects included anxiety, depression, post-traumatic stress disorder and fear. Little data is available on the prevalence of cancers. Studies have shown that many pregnancies of women residing close to the Union Carbide plant resulted in spontaneous abortion, stillbirth or the birth of a deformed child. In addition, many women suffered menstrual irregularities and bleeding, infertility, pelvic inflammatory disease, cervical erosion and suppression of lactation. Many became social outcasts, suffering desertion by their husbands and discrimination. Children whose mothers were exposed to the gas during

FOR REFERENCE PURPOSES ONLY

pregnancy have shown delayed gross motor and language development as well as chromosomal aberrations.

The environmental effects of the incident are not well understood as, understandably, most available resources were used for human health treatment and research. However, widespread defoliation of trees was reported. Most vegetables and plants suffered symptoms such as dryness, scorching and bleaching. Fruits and other agricultural plants (alfalfa, banana, mint, mango, date palm) appeared undamaged. Damage to soil and water is largely unrecorded, although a dramatic increase in free CO_2 and ammoniacal nitrogen was detected in water shortly afterwards. The number of animal deaths, including dogs, cats, birds and cattle, probably exceeded 4000.

The disaster had a marked effect upon the social and economic well-being of the area and led to a huge lawsuit. The Union Carbide company denied liability for the incident but paid $470 million to the Indian government, although not all of this was distributed to the relief effort. In general, compensation for personal injuries has been very small and some victims have not yet been compensated. An International Campaign for Justice in Bhopal (www.bhopal.net) continues to fight for justice and compensation for those affected by the disaster.

REFERENCES AND FURTHER READING RESOURCES

Boughton, E. (2005) The Bhopal disaster and its aftermath: A review. *Environmental Health*, 4(1): 6.

Cofala, J., Amann, M., Klimont, Z., Kupiainen, K., and Höglund-Isaksson, L. (2007) Scenarios of global anthropogenic emissions of air pollutants and methane until 2030. *Atmospheric Environment*, 41: 8486–8499.

Commission of the European Communities (2001) *The Clean Air for Europe (CAFÉ) Programme: Towards a Thematic Strategy for Air Quality*. CEC, Brussels, Belgium.

DEFRA (2016) *Emissions of Air Quality Pollutants 1990–2014*. Ricardo Energy & Environment, London, UK.

Eggleston, S., Hackman, M. P., Heyes, C. A., Irwin, J. G., Timmis, R. J., and Williams, M. L. (1992) Trends in urban air pollution in the United Kingdom during recent decades. *Atmospheric Environment*, 26B: 227–239.

Energy Information Administration (2006) *Annual Energy Outlook 2006*. US Department of Energy, Washington, DC, DOE/EIA-0383.

Finlayson-Pitts, B. J. and Pitts, J. N. (2009) *Chemistry of Our Natural and Polluted Atmosphere*. Wiley, New York, NY.

Griffin, R. D. (2006) *Principles of Air Quality Management*. CRC Press, Boca Raton, FL.

Harrison, R. M. (1999) Measurements of the concentrations of air pollutants. In: S. T. Holgate, J. M. Samet, H. S. Koren and R. L. Maynard (Eds.), *Air Pollution and Health*. Academic Press, London, UK.

Heck, R. M., Farrauto, R. J., and Gulati, S. T. (2009) *Catalytic Air Pollution Control: Commercial Technology*. Wiley-Blackwell, Hoboken, NJ.

IEA (2016) *World Energy Outlook Special Report on Energy and Air Pollution*. International Energy Agency. OECD/IEA, Paris, France.

Jacobson, M. Z. (2002) *Atmospheric Pollution: History, Science and Regulation*. Cambridge University Press, Cambridge, UK.

Li, A., Tanabe, S., Jiang, G., and Giesy, J. P. (2007) *Persistent Organic Pollutants in Asia: Sources, Distributions, Transport and Fate*. Elsevier Science, Amsterdam, the Netherlands.

Maas, R. and Grennfelt, P. (2016) *Towards Cleaner Air. Scientific Assessment Report 2016. EMEP Steering Body and Working Group on Effects of the Convention on Long-Range Transboundary Air Pollution*. United Nations Economic Commission for Europe (UNECE). Oslo, Norway.

FOR REFERENCE PURPOSES ONLY

Mehmetli, E. and Koumanova, B. (Eds.) (2007) *The Fate of Persistent Organic Pollutants in the Environment*. Springer, Dordrecht, the Netherlands.

Misselbrook, T. H., Gilhespy, S. L., Cardenas, L. M., Williams, J., and Dragosits, U. (2016) *Inventory of Ammonia Emissions from UK Agriculture 2015*. UK National Atmospheric Emissions Inventory, London, UK.

Monteith, J., and Unsworth, M. (2007) *Principles of Environmental Physics*. Academic Press, Oxford, UK.

NAEI (2016) *UK Emissions of Air Pollutants 1990 to 2015*. National Atmospheric Emissions Inventory, London, UK.

National Academy of Engineering (2008) *Energy Futures and Urban Air Pollution: Challenges for China and the United States*. National Academy Press, Washington, DC.

Richter, A., Burrows, J. P., Nüβ, H., Granier, C., and Niemeier, U. (2005) Increase in tropospheric nitrogen dioxide over China observed from space. *Nature*, 437: 129–132.

Smith, S. J., Andres, R., Conception, E., and Lurz, J. (2004) *Historical sulfur dioxide emissions 1850-2000: Methods and results*. US Department of Energy, PNNL Report No. 14537, Richland, WA.

Strauss, W., and Mainwaring, S. J. (1984) *Air Pollution*. Edward Arnold, London, UK. Report, European Communities, Luxembourg.

Tsagatakis, I., Brace, S., Passant, N., Pearson, B., Kiff, B., Richardson, J., and Ruddy, M. (2015) *NAEI UK Emission Mapping Methodology 2015*. Ricardo Energy & Environment, London, UK.

UNEP (2017) *Global Energy Outlook*. United Nations Environmental Programme, Nairobi, Kenya.

US Census Bureau (2016) International database update, August 2016.

van Loon, G. W., and Duffy, S. J. (2000) *Environmental Chemistry: A Global Perspective*. Oxford University Press, Oxford, UK.

Weick, K. E. (2010) Reflections on enacted sense making in the Bhopal disaster. *Journal of Management Studies*, 47: 537–550.

Williams, M. L. (1999) Patterns of air pollution in developed countries. In: S. T. Holgate, J. M. Samet, H. S. Koren and R. L. Maynard (Eds.), *Air Pollution and Health*. Academic Press, London, UK.

Winer, A. M. (1986) Air pollution chemistry. In: R. M. Harrison and R. Perry (Eds.), *Handbook of Air Pollution Analysis*. Kluwer Academic Publishers, Dordrecht, the Netherlands.

Wuebbles, D. J., Jain, A., Edmonds, J., Harvey, D., and Hayhoe, K. (1999) Global change: State of the science. *Environmental Pollution*, 100: 57–86.

FOR REFERENCE PURPOSES ONLY

Chapter 3

Particulate matter

This chapter focuses on particulate air pollutants, specifically introducing the concepts for their formation, propagation and measurements. Presented alongside, where applicable, are the trends showing contribution from different natural and anthropogenic sources to the ambient air concentrations. The corresponding discussions pertaining to their Control and mitigation techniques, Impacts to humans and plants, Standards and legislations are respectively presented in Chapters 9, 10 and 14.

3.1 WHY PARTICULATES ARE A SPECIAL CASE?

Airborne particulates, also commonly known as *aerosols*, are an important environmental pollutant, being responsible for loss of visual range, soiling of surfaces and health effects on people. As described in later sections, particles in the atmosphere can be *primary* or *secondary*, solid or liquid. They come into the atmosphere, and leave it again, by a wide variety of routes. Particles less than 10 μm in diameter have very low sedimentation speeds under gravity, and may remain in the air for days before eventually being washed out by rain or impacted out onto vegetation or buildings. Knowledge of their concentrations, size distributions and chemical composition is therefore needed, but for various reasons these are quite hard to obtain correctly. There is an important historical difference in the way that gases and particles have been treated as pollutants. Measurement methods for gases rapidly became specific to the gas, so that concentrations of SO_2, NO_2, and so on, have been quantified. In contrast, the predominant inexpensive method for particle concentration measurement has been filtration, from which mass loading is identified regardless of chemical composition. However, last decade has seen significant progress in particulate monitoring techniques, albeit cost-intensive, through *in situ* chemical speciation and characterisation using state-of-the-art ion mass spectrometry (described in Section 3.7).

The following sections of this chapter will first discuss the general aspects of particles, such as definition of size and the way they behave in the atmosphere, and then we will

FOR REFERENCE PURPOSES ONLY

describe the sources of particles and their measurement methods.

3.2 PARTICULATE TERMINOLOGY

Many different terms are used to describe the origins and characteristics of particles. They tend to be used somewhat casually, and to have different meanings in popular and scientific contexts. Here are some of them:

- *Suspended particulate matter* (SPM), and *total suspended particulate* (TSP), both mean total airborne particles; often as measured by a high-volume sampler without a size-selective inlet.
- *Particulate matter* (PM): Sometimes used in this form as an abbreviation, but more commonly as PM_{10} or $PM_{2.5}$. PM_{10} is the mass concentration of particulate matter (PM) from those particles that can pass through a size-selective inlet with 50% efficiency at an aerodynamic diameter of 10 μm. $PM_{2.5}$ is the corresponding concentration for a cut diameter of 2.5 μm.
- *Fine particles*: In general, those smaller than a few μm. Often used synonymously with $PM_{2.5}$.
- *Ultrafine particles* or *nanoparticles*: Those smaller than about 0.2 μm, for which the size is normally expressed in nm.
- *Aerosol*: Any solid or liquid particles of aerodynamic diameter ranging from sub-micron to several microns that remain suspended in the air. Common usage refers to the aerosols as the particulate component only and throughout this book the terms *aerosols* and *particles* have been used interchangeably to refer to airborne particulates.
- *Grit*: The coarsest fraction of material usually formed by a mechanical process, such as crushing or grinding. Size range is sometimes defined.
- *Dust*: As for grit but smaller, typically greater than 1 μm.
- *Smoke:* Particles formed by incomplete combustion, as a mixture of carbon and condensed volatiles. Usually less than 1 μm.
- *Black smoke*: Suspended particulate as determined by the reflective stain method. Size range not specified, but later measurements have shown no particles sampled above 10 μm aerodynamic diameter, and a 50% cut at about 4 μm, so the measurement would correspond to the respirable fraction.
- *ACGIH and ISO conventions*: The human breathing system has evolved to filter out large particles at an early stage, and the proportion of particles reaching the lungs depends strongly on particle size. The American Conference of Government Industrial Hygienists (ACGIH) and the International Standards Organisation (ISO) have defined particle fractions on this basis. They are discussed in more detail in Chapter 14.

3.3 PARTICLE SIZE DISTRIBUTIONS

3.3.1 Relative sizes of particles and gas molecules

Figure 3.1 shows the relative scale of air molecules (typically 0.3 nm diameter), the average separation between them (typically 3 nm, or 0.003 μm) and the average distance they move between collisions (a statistical value called the mean free path, which is about 70 nm). Figure 3.2 shows the relative scale of air molecules (now represented by dots); the space between them, and the edges of spherical particles having diameters of 100 nm (0.1 μm, typical of the peak of the number concentration in vehicle exhaust), 500 nm (0.5 μm, typical of the accumulation mode), and 5 μm. Note that single molecules are always referred to as molecules, and that the term ‘particles’ does not normally include molecules, unless they are in clusters. In between single molecules and *particles* we have an interesting no-man’s-land.

FOR REFERENCE PURPOSES ONLY

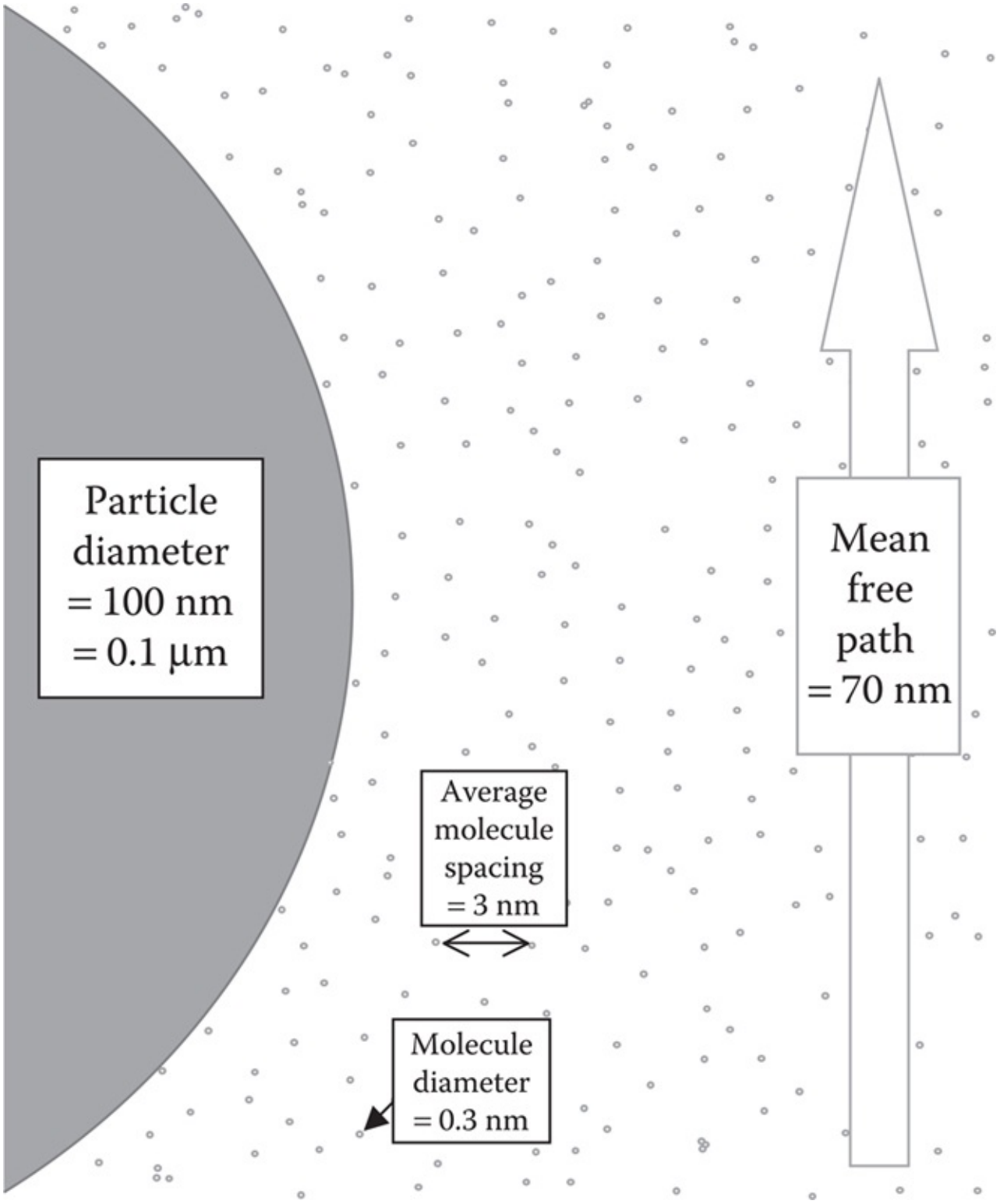

Figure 3.1 The scale of *air* molecules relative to the separation between them and the mean free path.

FOR REFERENCE PURPOSES ONLY

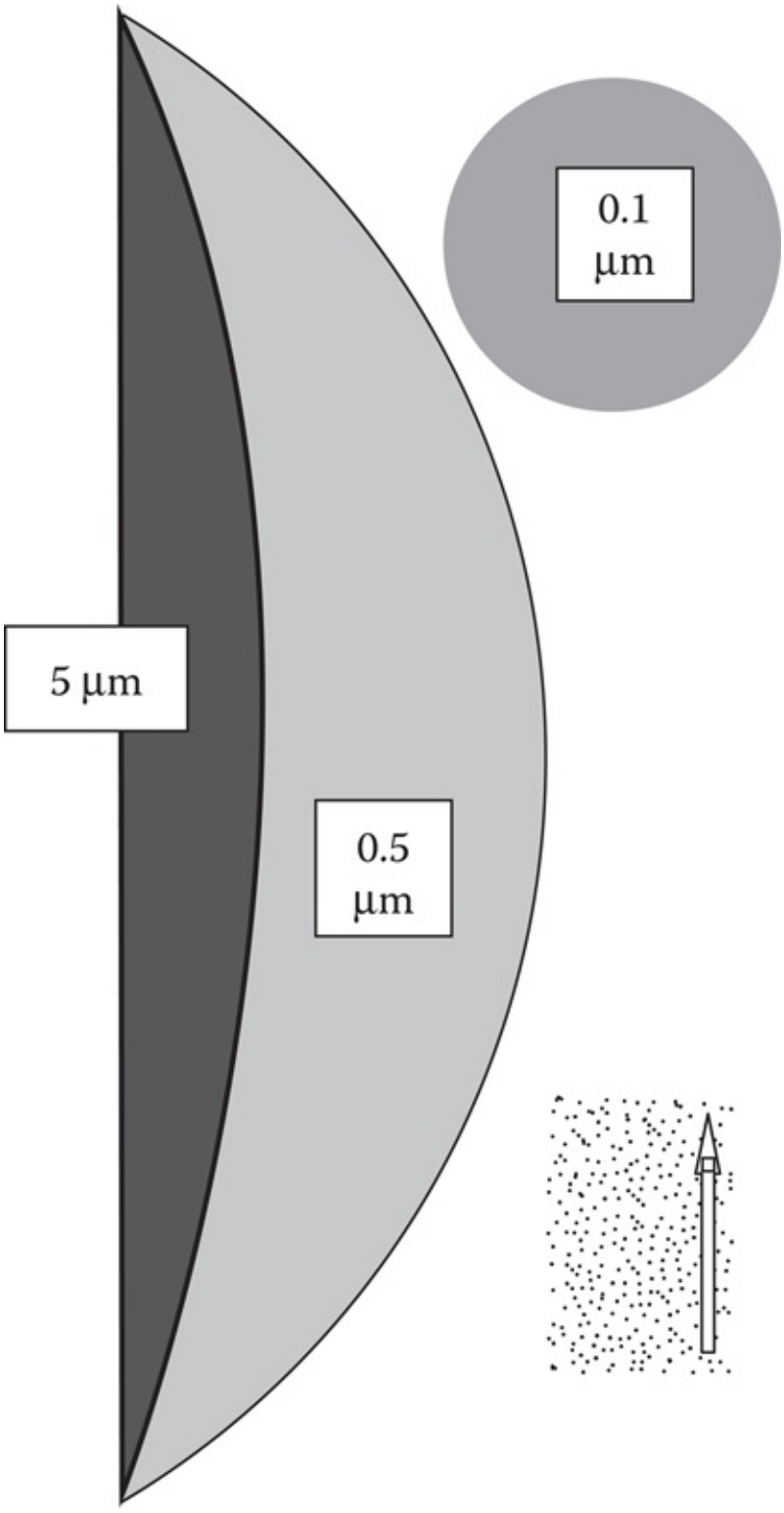

Figure 3.2 The scale of *air* molecules and the mean free path relative to particles of different sizes.

Below sizes of about 20 nm we lose the continuum that we take for granted, the surface of the particle starts to become associated with the surface of individual atoms and molecules, and most of the molecules that make up the particle are on its surface. At 5 nm, the particle may contain only a few hundred molecules. Such *quasi*-particles have

FOR REFERENCE PURPOSES ONLY
extremely high Brownian diffusion velocities and aggregate extremely fast with other small particles. Hence their short lifetimes.

Accumulation mode particles are mainly the secondary particles generated in the atmosphere as the result of photochemical reactions between primary gases. These primary gases may themselves be anthropogenic (sulphur dioxide and ammonia, for example) or natural (conversion of low-volatility hydrocarbons). Sea salt is the evaporated residue of innumerable droplets, injected into the atmosphere whenever a wave breaks at sea. The salt particles remain in the atmosphere until they eventually serve as the nuclei on which cloud droplets form.

The size ranges of some other families of atmospheric particles are shown in Figure 3.3. The finest metallurgical fumes are condensed volatiles that are so small that they overlap with the molecular size range, although these are often quickly aggregated into longer chains.

FOR REFERENCE PURPOSES ONLY

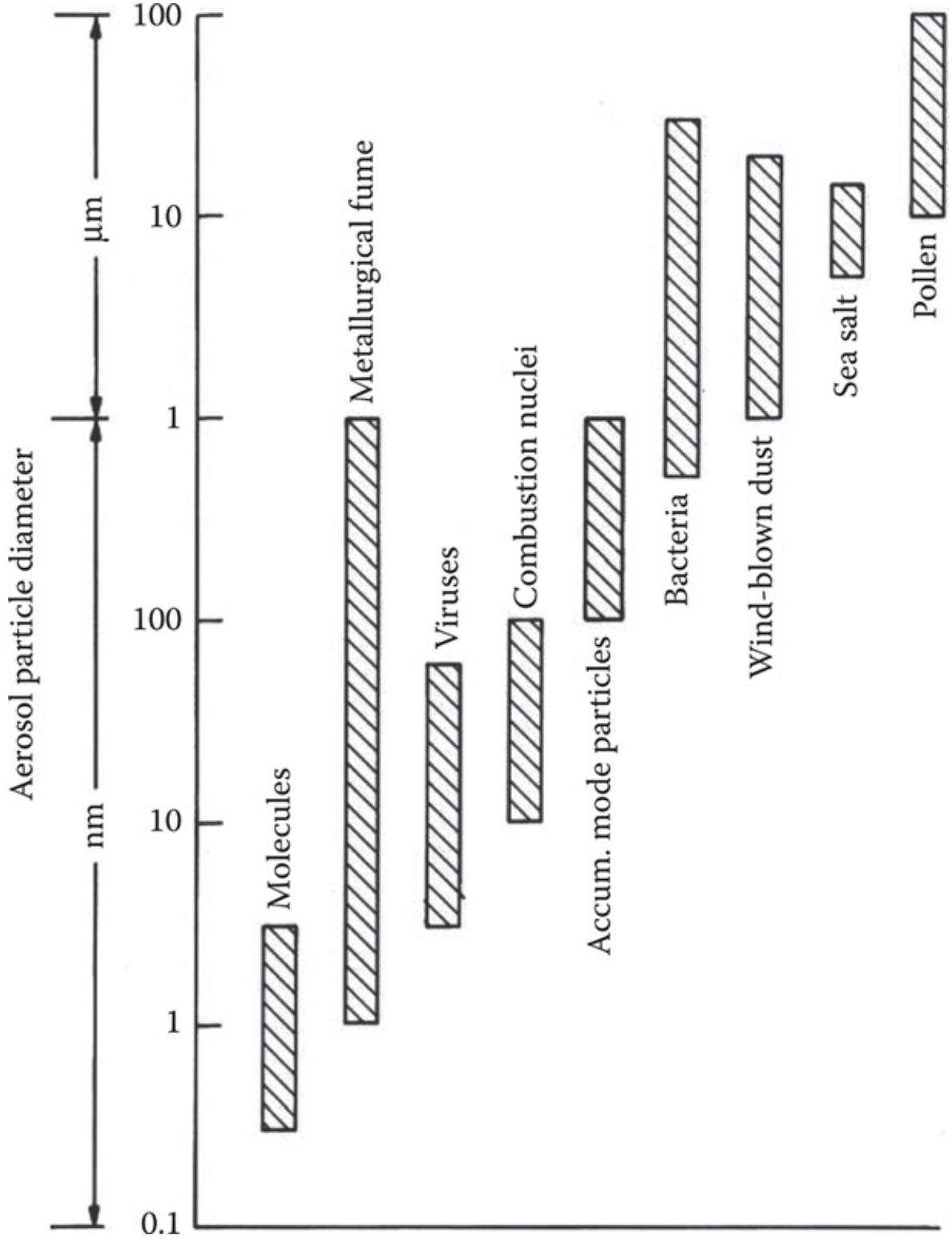

Figure 3.3 Characteristic size ranges of particles from different sources, with molecular sizes shown for comparison. (From Leygraf, C. and Graedel, T., *Atmospheric Corrosion*, John Wiley & Sons, New York, 2000.)

If all the particles in a volume of gas are of the same diameter, the size distribution is said to be monodispersed. *Monodisperse aerosols* are only found when they have been

FOR REFERENCE PURPOSES ONLY

made artificially for calibrating sampling equipment; even then they soon start to become *polydisperse*, due to collisions and agglomeration between the original particles. Atmospheric aerosol distributions are always polydisperse. Imagine that we have *frozen* a cubic metre of air in space and time, and that we can move around within it to examine each particle in turn. At the smallest scale would be the molecules of nitrogen, oxygen, water vapour and argon, all rather less than 0.001 μm (1 nm) in diameter, that make up about 99.999% of the total 1.3 kg mass in that cubic metre. Then there would be a lower concentration of larger molecules such as organics, blending into a rapidly increasing concentration of particles not much larger than the molecules – around 0.01 μm (10 nm) in diameter – formed by the condensation of volatilised material – for examples, iron vapour released during steel manufacture or volcanic eruptions, or VOCs from trees. These are clusters of molecules, and mark the start of the nucleation range, which extends from molecular diameters up to about 0.1 μm (Figure 3.4).

These very tiny particles have high thermal energies and coagulate rapidly with others, so that this size range has a high number density and short residence time. The main bulk of atmospheric aerosol mass lies between 0.1 and 1 μm. There are many different types of aerosols: aggregated chains of smaller particles, salt crystals (from the evaporation of ocean spray) that will go on to become condensation nuclei for cloud droplets, fly ash from power station chimneys, black carbon from inefficient fuel combustion, and photochemical ammonium salts. This is the so-called accumulation diameter mode, where particle concentrations tend to increase because deposition is inefficient. Finally, there will be a smaller number of larger particles (bigger than a few μm) which will be lost soon after we unfreeze our sample because they will impact easily or sediment fast. They might include some giant sea-salt particles, mineral dust eroded from bare soil surfaces, volcanic emissions or biological material such as spores, pollen or bacteria. These three mechanisms – *nucleation*, *accumulation* and *mechanical production* – generate the classical *tri-modal size distribution*.

FOR REFERENCE PURPOSES ONLY

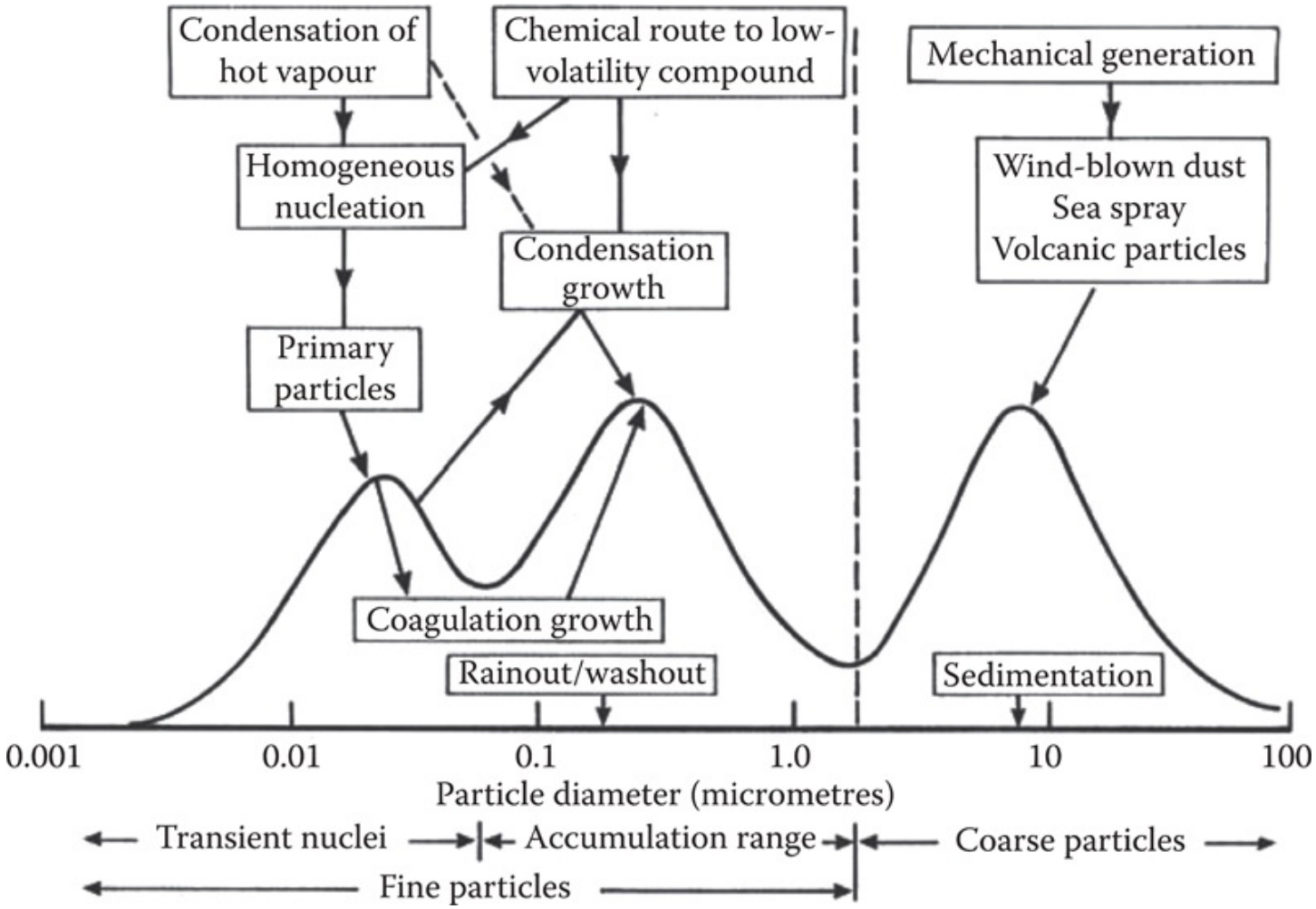

Figure 3.4 The trimodal size distribution, showing general relationships between the three common size ranges and the particle sources. (From Harrison, R. M., Measurements of concentrations of air pollutants, in S. T. Holgate, J. M. Samet, H. S. Koren and R. L. Maynard (Eds.), *Air Pollution and Health*, Academic Press, London, UK, 1999.)

3.3.2 Specification of size

Now imagine that we are going to measure each particle in the cubic metre, and build up a size distribution. In some cases, we will be able to trap the particles in a filter, put the filter under an optical or electron microscope, and compare the observed dimensions with a graticule or scale calibrated in μm or nm. Even if this is possible, the particle is unlikely to be spherical, and we will have to decide on a convention, such as the average of the smallest and the largest dimensions. In the great majority of cases, direct measurement will not be possible, and we will have to use some other property of the particle to characterise its size in terms of an equivalent diameter. The two most common such properties are the equivalent aerodynamic diameter and the equivalent light scattering diameter. The *aerodynamic diameter* is the diameter of a spherical particle of density 1000 kg m^{-3} (the

FOR REFERENCE PURPOSES ONLY

same as water) which is equivalent in following airflow streamlines. The *light scattering diameter* is the diameter of a spherical particle of specified refractive index, which scatters the equivalent amount of light. These definitions work reasonably well for some particles that are *almost* spherical, but very poorly for others such as asbestos fibres that are very long and thin, or flat crystalline platelets. A further complication is that it is often not in fact the distribution of number with diameter that is needed. For light scattering effects, we need to know the distribution of surface area with diameter, while for inhalation studies we need the distribution of mass with diameter. This is where life really gets complicated! Particles may have very different densities and shapes (from a density of about 7000 kg m^{-3} for a long-chain iron aggregate, down to a density of 800 kg m^{-3} for spherical organic condensates), so it may not be meaningful to average any properties over the size distribution as a whole.

3.3.3 Presentation of size distributions

Figure 3.5 gives a stylised example of one common way of presenting size distributions in graphical form. The vertical axis is scaled in $dN/d\log D$, $dA/d\log D$ or $dV/d\log D$, and the horizontal axis in $\log D$. The range of sizes from a given sample is expressed as the normalised number distribution – the number of particles per unit size interval. Note that there has to be an interval – if we only give a single value of diameter, there will be a vanishingly small number of particles that have exactly that diameter. Hence, the concentration is always expressed as μg m^{-3} μm^{-1} or equivalent. Both the number concentration and the size scales are logarithmic because of the wide ranges of the values involved – there are hundreds or thousands of particles per cm^3 in polluted tropospheric air, compared with around ten in the stratosphere. The number distribution – which we obtain simply by counting the number of particles within each diameter range as described earlier – is the left-most peak in Figure 3.5, showing that the number population peaks at 0.01 μm. As a 10 μm particle has 10^6 times the surface area of a 0.01 μm particle, and 10^9 times the volume, the area and volume dependencies can give very different significance to different diameters.

These curves, for the same number distribution, are also shown in Figure 3.5. Note that 0.2 μm particles now dominate the area distribution, and for the volume distribution there is an additional peak at 8 μm that was not even visible on the number distribution because it is due to a very small number of these larger particles. This has implications for particle sampling, because if we really want to know the rate of inhalation of particle mass (for health effects studies, for example), then we must be sure to sample this tiny proportion with sufficient accuracy.

FOR REFERENCE PURPOSES ONLY

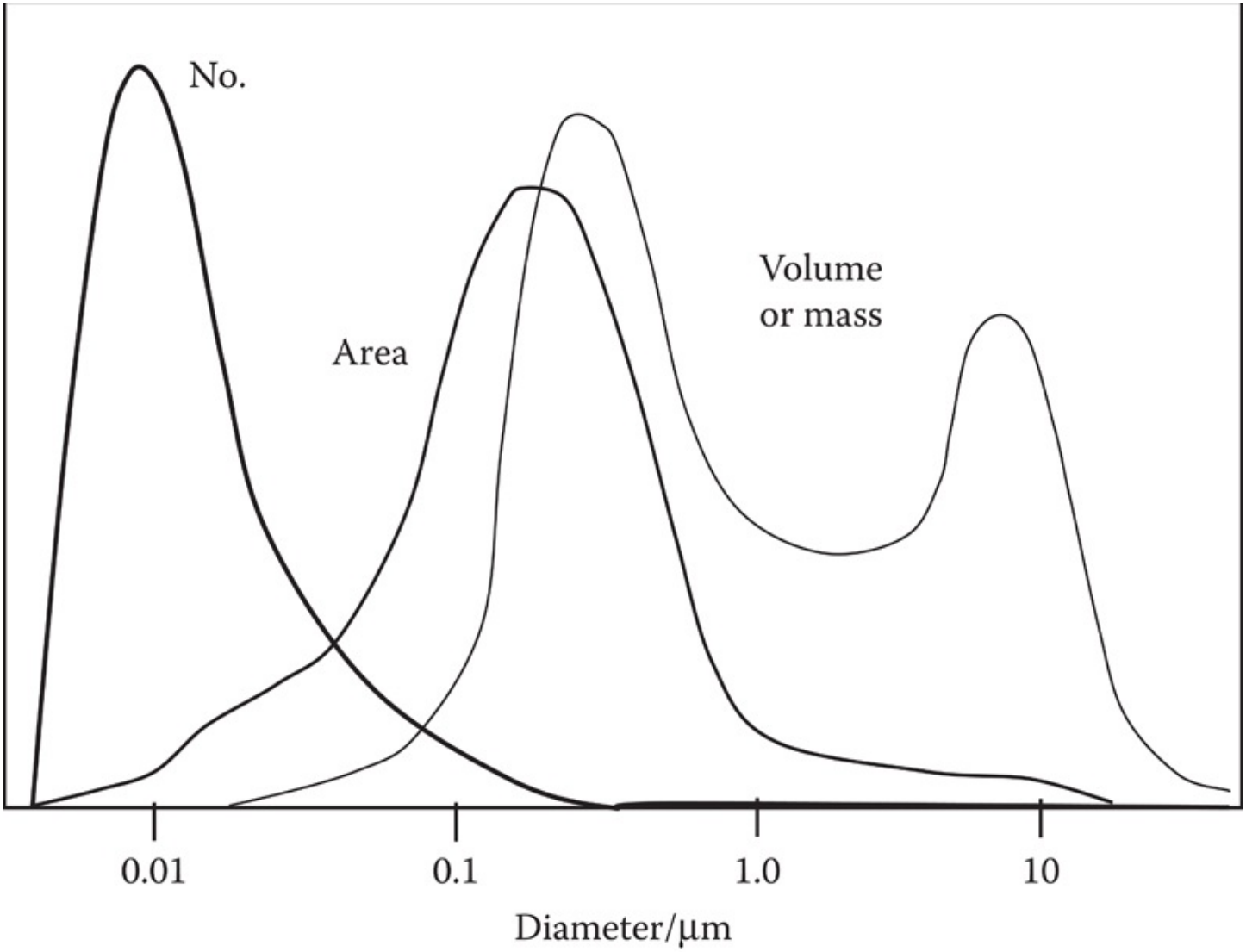

Figure 3.5 A simple distribution of particle number with diameter, and its transformation into surface and volume (or mass) distributions.

The size distributions discussed earlier were in the differential form, for which the concentration refers to the actual concentration at that size or within that size range. An alternative widely used presentation is the cumulative distribution. All the concentration values are accumulated, starting at the smallest particles, so that the concentration refers to particles larger than a given diameter, rather than at that diameter. In this formulation, it is easy to calculate, for example, the mass loading of particles smaller than 2.5 μm.

Even nominally monodisperse populations, such as are found for latex calibration aerosols, will always have a range of diameters smaller and larger than the mean. These very tight distributions can often be represented by normal, or Gaussian distributions, characterised by an arithmetic mean diameter d_{mean} and a standard deviation σ, such that

$$d_{\text{mean}} = \frac{\sum n_i d_i}{\sum n_i}, \text{ and } \sigma = \left[\frac{\sum n_i (d_{\text{mean}} - d_i)^2}{(\sum n_i - 1)}\right]^{0.5}$$

FOR REFERENCE PURPOSES ONLY

where n_i is the number of particles of diameter d_i, usually approximated by the number in a size class with mean diameter d_i. This curve is symmetrical about the mean diameter. However, ambient particle distributions usually have a long tail out to larger sizes (Figure 3.6a), which can often be approximated by the lognormal distribution, in which it is the logs of the diameters that are normally distributed rather than the diameters themselves (Figure 3.6b).

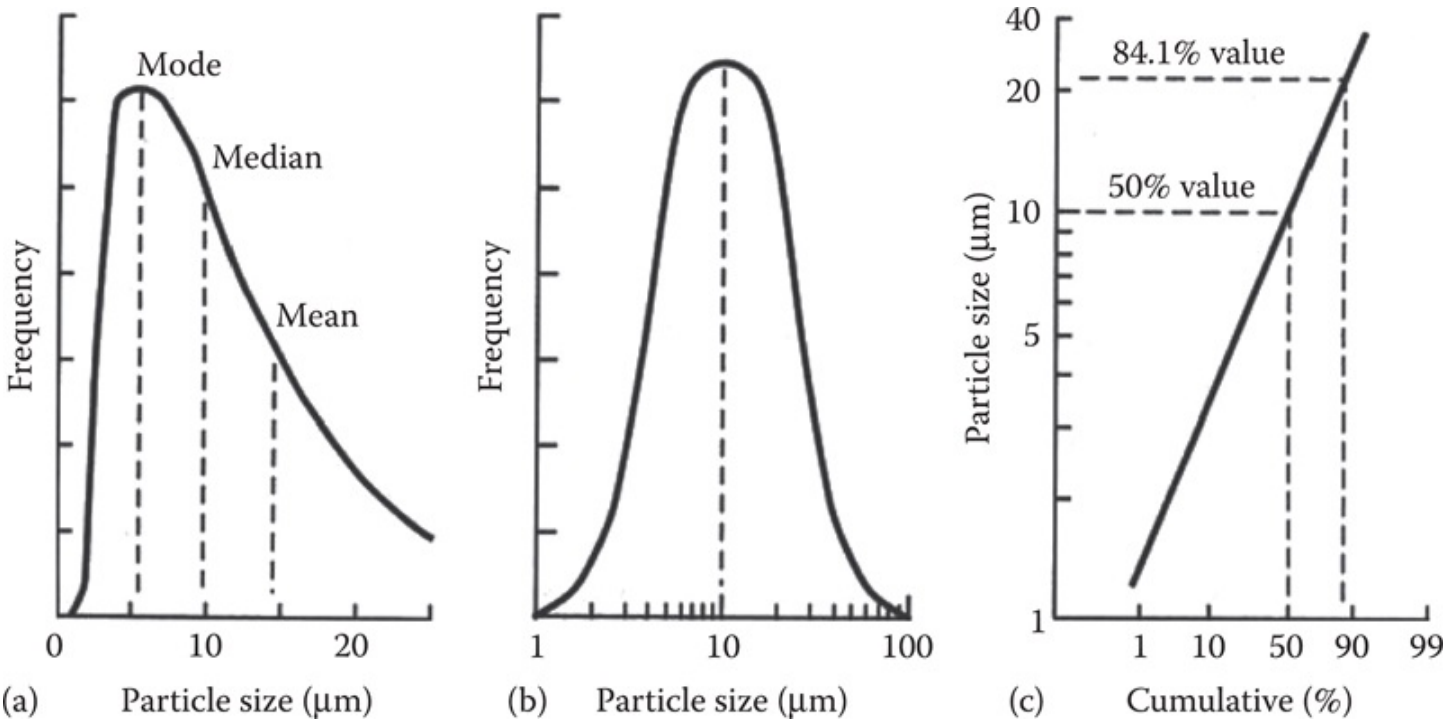

Figure 3.6 Differential and cumulative particle size distributions, (a) linear size increment; (b) geometric size increment; (c) cumulative log-normal plot. (From Lippmann, M., Introduction and background, in M. Lippmann (Ed.), *Environmental Toxicants*, Wiley, New York, 2000.)

In that case we have

$$\log d_{geo} = \frac{\sum n_i \log d_i}{\sum n_i} \text{ and } \log \sigma_{geo} = \left[\frac{\sum n_i (\log d_{geo} - \log d_i)^2}{(\sum n_i - 1)} \right]^{0.5}$$

where d_{geo} is the geometric mean diameter. The actual distribution is then given by

$$n(\log d) = \frac{N}{(2\pi)^{1/2} \log \sigma_{geo}} \exp \left[- \frac{(\log d - \log d_{geo})^2}{2 \log^2 \sigma_{geo}} \right]$$

Log-normal distributions have the convenient feature that if they are plotted in the cumulative form on log-probability axes (Figure 3.6c), they are transformed into straight

FOR REFERENCE PURPOSES ONLY

lines from which σ_{geo} can be estimated:

$$\sigma_{geo} = \frac{d_{84.13}}{d_{50}} = \frac{d_{50}}{d_{15.87}}$$

where d_n is the diameter exceeded by n% of the sample.

3.3.4 General features of real size distributions

Real atmospheric particle size distributions are the outcome of many competing processes – *condensation*, *sedimentation*, *evaporation*, *agglomeration*, *impaction*, *gas-to-particle conversion*. We can therefore expect the distributions to be very variable, and background aerosol has a wide range of characteristics, depending on the history of the airmass. There are often only two modes in the mass distribution. The *nucleation mode* will still be present in these distributions, but as they are given by mass not number, the peak is often not significant. The *coarse mode* corresponds to particles larger than about 2–3 μm in diameter, and the accumulation mode to those between 0.1 and 2.5 μm.

The coarse mode is composed mainly of primary particles generated by mechanical processes such as crushing and grinding, or by entrainment of soil particles from fields or roads. Sedimentation velocities are significant at these larger diameters, so settling occurs with a time constant of a few hours within the atmospheric boundary layer unless strong winds stir the air effectively. The *accumulation mode* particles, in contrast, are mainly from gas-to-particle conversion and agglomeration of ultrafine particles. Deposition velocities are low and residence times long. The ultrafine range ($d_p < 0.1$ μm) may stem from local combustion sources or photochemical homogeneous nucleation. The flux through the population is rapid, and mainly due to Brownian diffusion towards, and attachment to, larger particles in the accumulation mode. The timescale for this process would range from a few minutes to a few hours, depending on the diameter of the ultrafine particles and the concentration of the accumulation particles.

In situations for which a single log-normal distribution cannot represent the real data, several log-normal distributions may be combined (Figure 3.7). The distributions shown here were used to model biomass aerosol in a calculation of radiative forcing. Three log-normal distributions, with mode radii of 0.08, 0.33 and 0.96 μm respectively and standard deviations of around 1.4 were used. As discussed in Section 3.3, the number distribution (top graph) is dominated by the smallest mode, and the volume (or mass) distribution by the largest.

FOR REFERENCE PURPOSES ONLY

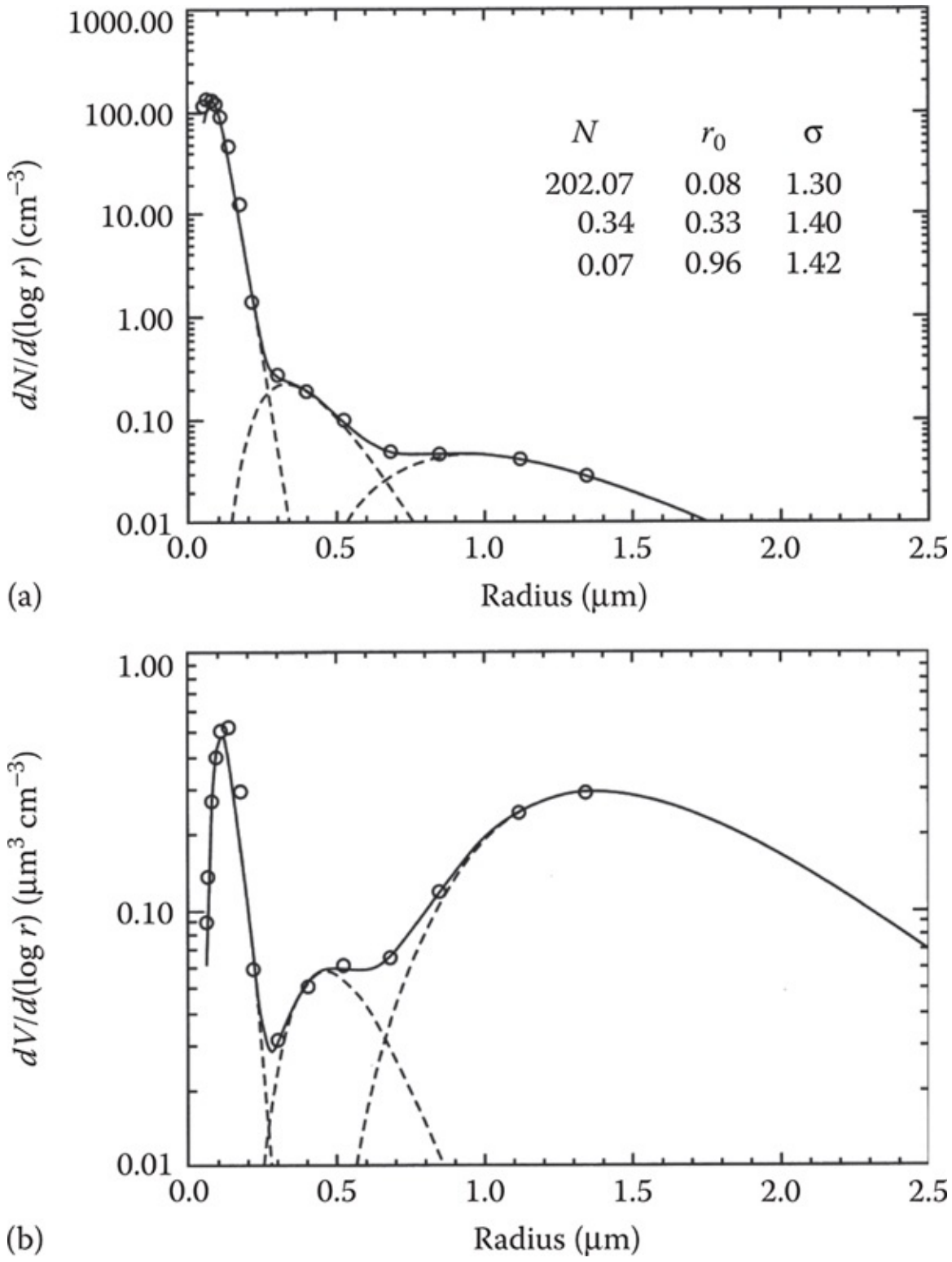

Figure 3.7 Combination of three log-normal distributions, (a) Number concentration; (b) Volume concentration. (From Grant, K. E. et al., *Atmos. Environ.*, 33, 2603–2620, 1999.)

With increasing sophistication of imaging techniques combined with chemical analysis, we are now getting a better idea about what all these particles actually look like. Figure 3.8 shows images of various particle types collected in a sampling campaign on the North Sea

FOR REFERENCE PURPOSES ONLY

coast of Germany.

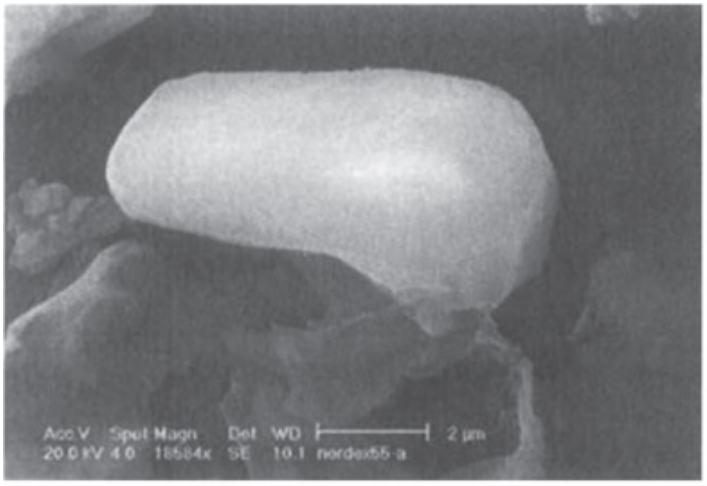

(a)

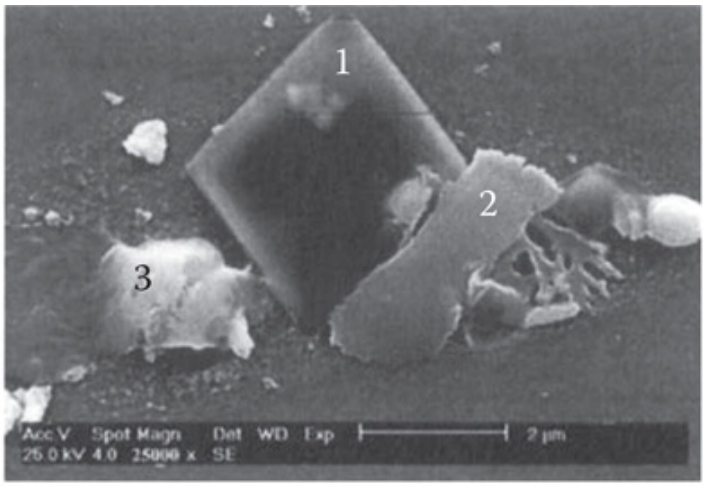

(b)

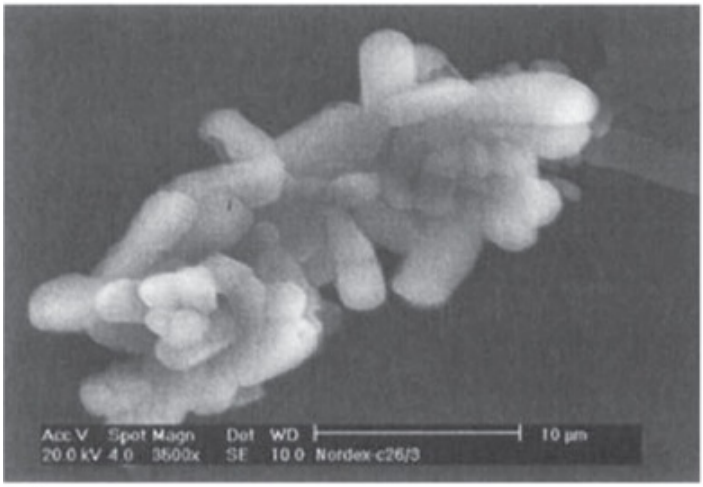

(c)

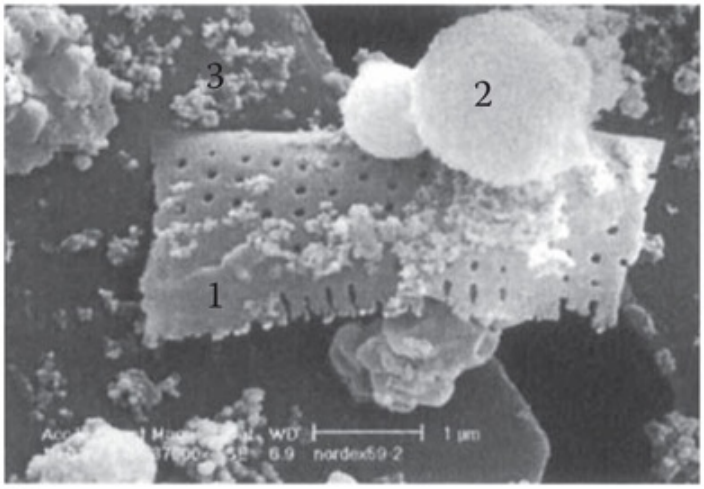

(d)

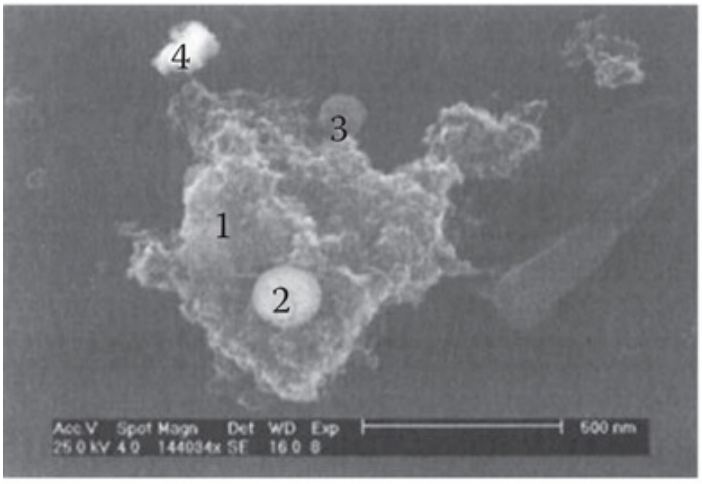

(e)

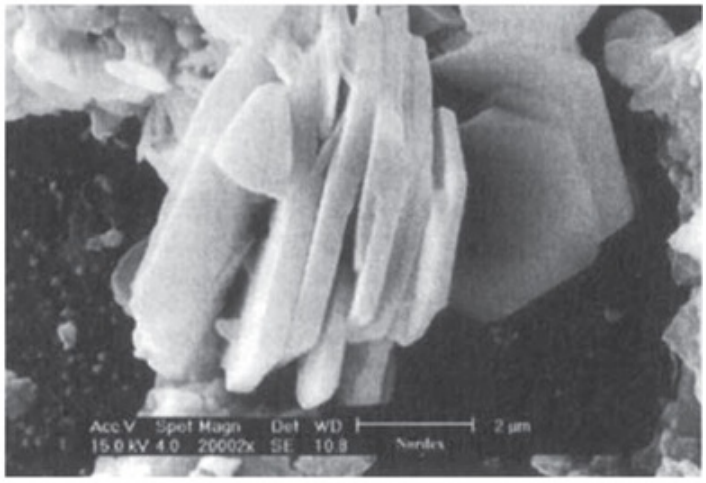

(f)

FOR REFERENCE PURPOSES ONLY

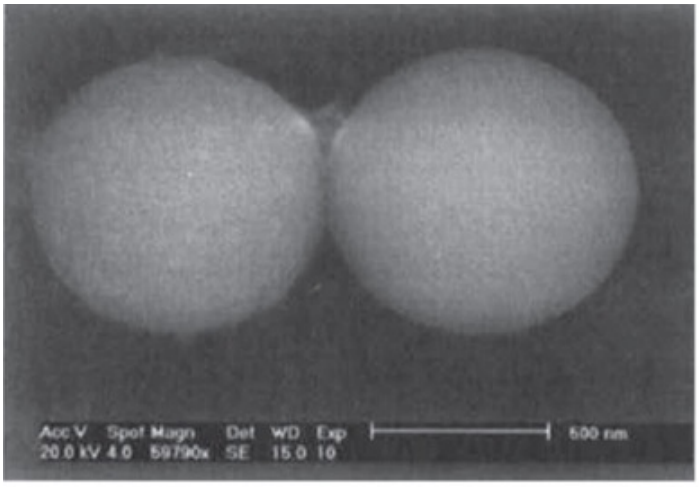

(g)

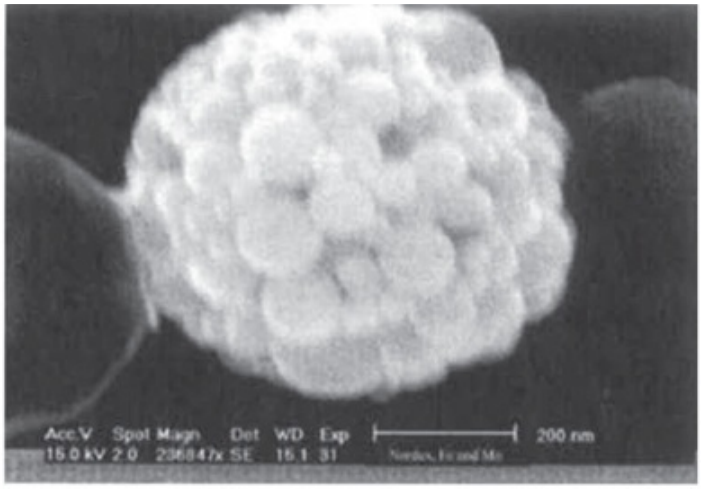

(h)

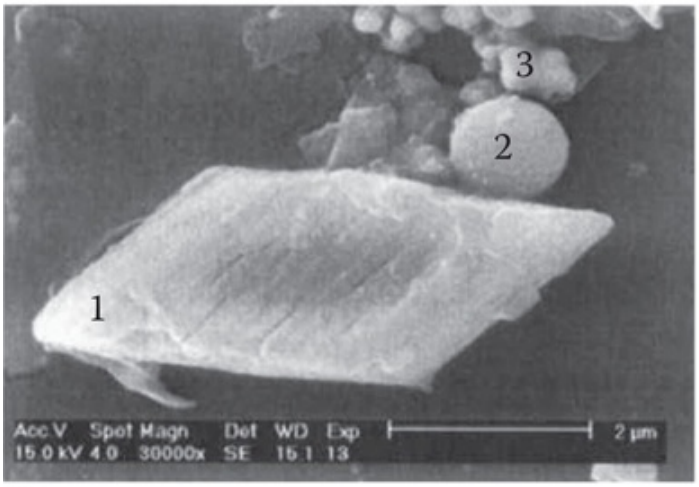

(i)

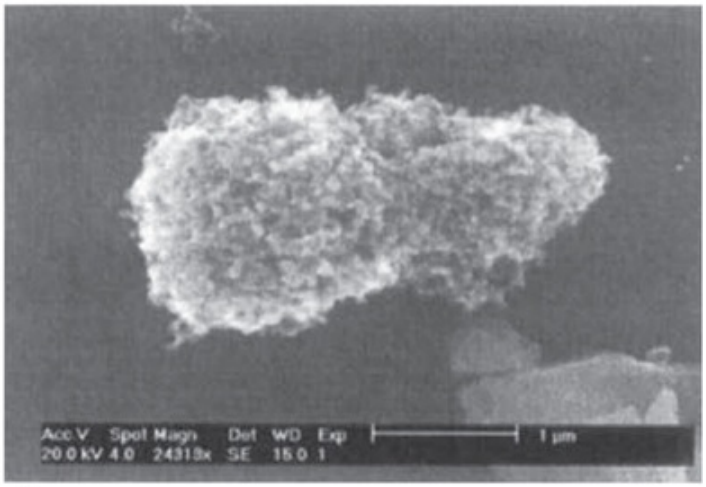

(j)

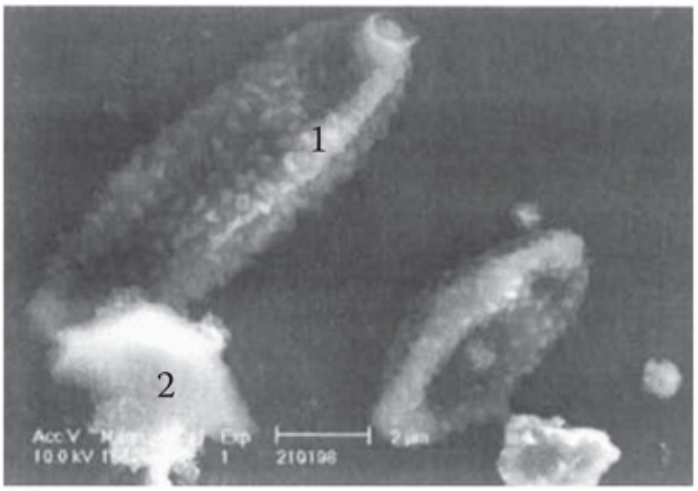

(k)

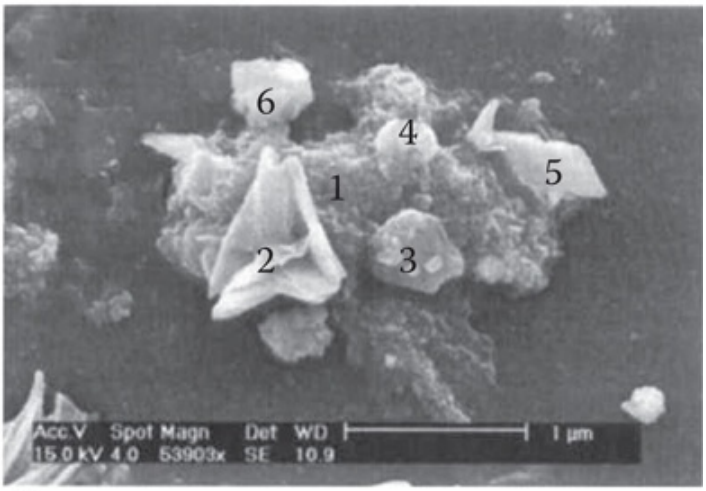

(l)

Figure 3.8 Scanning electron microscope images of particles: (a) Irregularly shaped sea-salt particle; (b) sea-salt particle with typical cubic morphology (1), irregularly shaped sea-salt particle (2), and alumosilicate particle (3); (c) aged sea-salt particle; (d) biological particle (1), Si-rich fly ash particle (2), and

various soot particle (diameter of primary particles below 100 nm); (e) soot agglomerate (1) with alumosilicate particles (2, 4), and carbonaceous material (3); (f) alumosilicate particle (clay material). (g) two alumosilicate fly ash particles; (h) agglomeration of iron oxide spheres; (i) calcium sulphate (presumably gypsum) particle (1), spherical iron oxide particle (2), and titanium oxide particle (3); (j) typical soot agglomerate; (k) biological particle (1) and sea-salt (2); (l) agglomerate of carbonaceous material (1, 2), alumosilicates (3), Si-rich fly ash (4), and calcium sulphate (5, 6). (From Ebert, M. et al., *J. Aerosol Sci.*, 31, 613–632, 2000.)

3.4 AEROSOL MECHANICS

As we discussed earlier, primary particles get emitted into the air directly, whereas secondary particles get formed from chemical processed in the air. They spend some time in the air, commonly known as *residence time* before being deposited from the air either naturally or artificially. In this section we shall look at some of the fundamental principles that control how particles behave under various conditions. Particles are deposited to surfaces by three main mechanisms: *Sedimentation*, *Brownian diffusion* and *Impaction/Interception*. Each of the three processes operates most effectively in a different particle size range.

3.4.1 Drag force

If a particle is moving through air, or the air is moving past a particle, then a viscous drag force acts on the particle. Provided that the flow past the particle is smooth (laminar) and not turbulent, then this drag force F_D is given by

$$F_D = 3\pi\eta V d$$

where η is the gas viscosity. For air at tropospheric temperatures and pressures, η is around 1.8×10^{-5} Pa s, V is the relative speed between the gas and the particle, d is the particle diameter. We can determine whether the flow is smooth by calculating the Reynolds number $\mathrm{Re} = \rho_g V d/\eta$, where ρ_g is the gas density. Flow starts to become turbulent for Re > 1.

The drag equation assumes that the particle is large compared to the spaces between the molecules in the gas. This latter distance, known as the mean free path λ, is about 0.07 μm for standard atmospheric temperature and pressure. As particle diameter decreases, there becomes an increased probability that the particle will move a distance without experiencing a collision, effectively slipping through the gaps between the molecules. Then we must add the Cunningham slip correction factor C_C where

FOR REFERENCE PURPOSES ONLY

$$C_C = 1 + \frac{2.52\lambda}{d}$$

for

$$d > 0.1\ \mu\text{m}$$

and

$$C_C = 1 + \left[2.34 + 1.05\exp\left(-0.39\ \frac{d}{\lambda}\right)\right] \text{ otherwise.}$$

Table 3.1 shows that this slip correction is worth 2% for a 10 μm particle and 20% for a 1 μm particle, so it is an important factor in the design of cascade impactors that typically have several stages operating within that size range.

Table 3.1 Properties of airborne particles[a]

Diameter (mm)	*Slip correction (C_C)*	*Terminal speed, V_{term} ($m\ s^{-1}$)*	*Relaxation time ($t\ s^{-1}$)*	*Mobility, B ($m\ N^{-1}\ s^{-1}$)*	*Diffusion coefficient, D ($m^2\ s^{-1}$)*	*Coagulation coefficient, K ($m^3\ s$)*
0.001	224	6.75E-9	6.89E-10	1.32E+15	5.32E-6	3.11E-16
0.01	23	6.92E-8	7.05E-9	1.35E+13	5.45E-08	9.48E-16
0.1	3	8.82E-7	8.99E-8	1.72E+11	6.94E-10	7.17E-16
1.0	1.2	3.48E-5	3.54E-6	6.77E+09	2.74E-11	3.35E-16
10.0	1.02	3.06E-3	3.12E-4	5.95E+08	2.41E-12	3.00E-16
100.0	1.002	2.49E-1	3.07E-2	5.87E+07	2.37E-13	2.98E-16

[a] At 20°C and 1 atm, for particle density 1000 kg m^{-3} (e.g. water).

3.4.2 Sedimentation

Every particle in the Earth's gravitational field experiences a force due to gravity towards the centre of mass of the Earth. If, for example, a stationary particle is released into the atmosphere, the gravitational force will accelerate it downwards. As its speed increases, the drag force described earlier will also increase. The gravitational force acts downward, but the drag force acts upward. The net force, which is the difference between the two, therefore decreases as the particle accelerates. As the gravitational force remains constant, a speed will eventually be reached at which the two forces are equal and opposite and no more acceleration can take place. This is called the *terminal* or *sedimentation* velocity. Particles that fall out of the air under the action of gravity do so at their terminal velocity.

$$F_{\text{grav}} = mg = \rho_{\text{part}}\ \frac{\pi d^3}{6}\ g \text{ (for a spherical particle)}$$

FOR REFERENCE PURPOSES ONLY

When $F_{drag} = F_{grav}$, we have

$$3C_C \pi \eta V_{term} D_{part} = \rho_{part} \frac{\pi d^3}{6} g$$

Hence

$$V_{term} = \frac{\rho_{part} d^2 g C_C}{18\eta}, \text{ which is Stokes law}$$

Values of V_{term} are given in Table 3.1. The other columns in Table 3.1 refer to particle properties that are discussed in Section 3.3.

Figure 3.9 shows the dependence of this terminal speed on particle radius, not only for the particles discussed earlier ($r < 30$ μm) but also for larger particles, such as cloud droplets and raindrops. The curve is linear up to a particle diameter of 50 μm and a Reynolds number (the ratio of inertial to viscous forces) of 1 (this is the region in which Stokes' law is valid). For larger particles, the curve starts to depart from linearity, as the Stokes' law starts to fail. Large raindrops become nonspherical due to the gravitational and fluid forces acting on them, and depart a little from this curve (dashed line). If the particle is non-spherical and of a density different from water, a Stokes diameter can be assigned to it which is the diameter of a sphere having the same density and sedimentation velocity.

3.4.3 Brownian diffusion

All the particles discussed here are very much larger than atmospheric molecules such as nitrogen and oxygen, and are continually bombarded all over their surfaces by such molecules. For very small particles, two effects become important. First, the rate of collisions with molecules becomes small enough so that there is a reasonable probability of the collisions from one direction not being instantaneously balanced by collisions from the opposite direction. Second, the particle mass becomes small enough so that the resultant momentum of these colliding molecules can exert a significant impulse in the unbalanced direction.

FOR REFERENCE PURPOSES ONLY

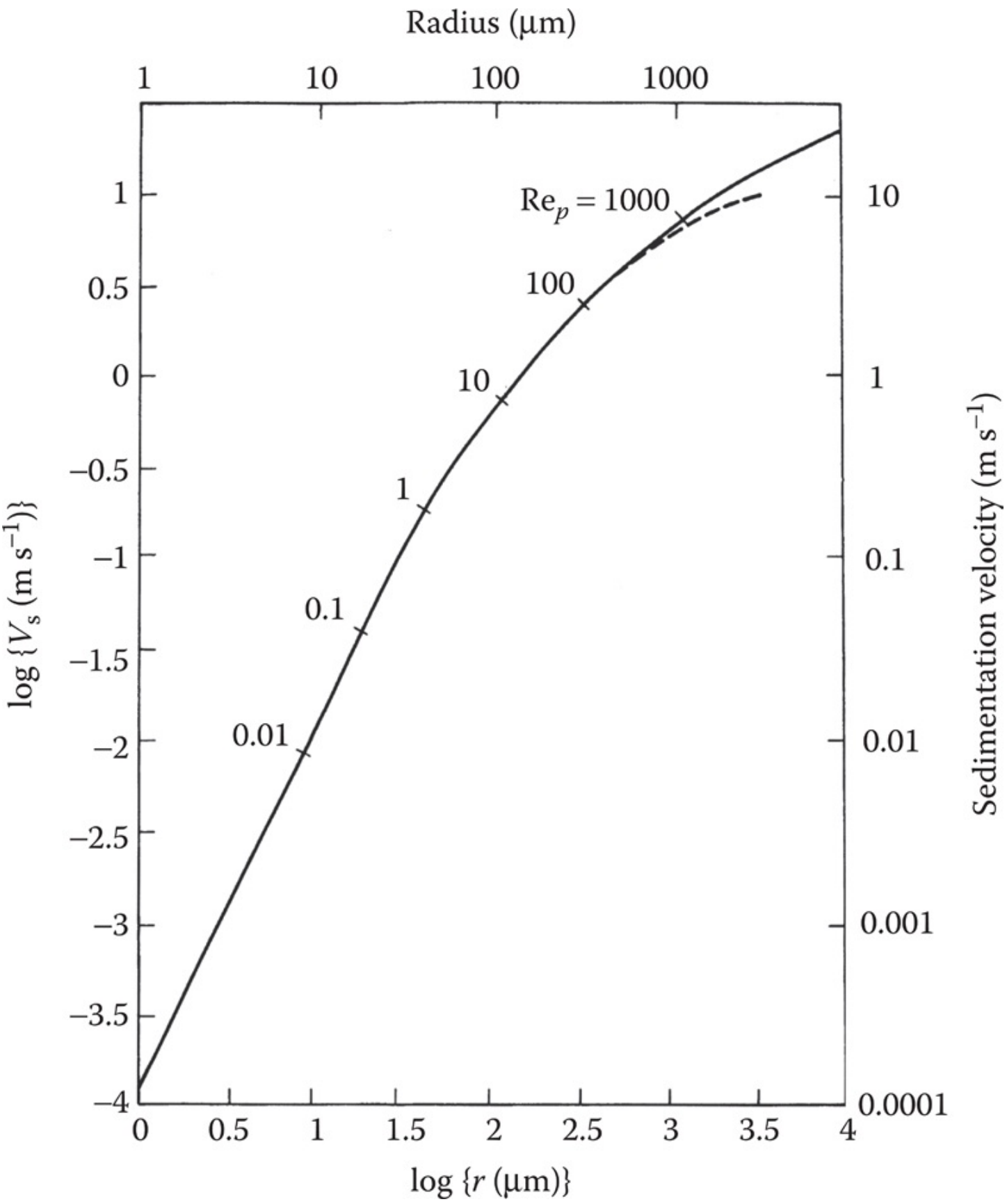

Figure 3.9 The variation of terminal speed with radius for spherical particles with density 1 g cm^{-1} falling in air. (From Monteith, J. L. and Unsworth, M. H., *Principles*

FOR REFERENCE PURPOSES ONLY

of Environmental Physics, Edward Arnold, London, UK, 1990.)

The resultant erratic motion of the particle gives it a mean square displacement

$$\overline{x^2} = 2Dt$$

where D is the Brownian diffusion coefficient for the particle ($m^2\ s^{-1}$) given by

$$D = \frac{kT}{6\pi\mu r}$$

where:

k is the Boltzmann's constant

T is the absolute temperature

μ is the dynamic viscosity of air

Furthermore, the effective value of μ itself falls when the particle diameter is significantly less than the mean free path of the air molecules (about 70 nm at sea level temperature and pressure). As a result, $D \propto r^{-1}$ when $r >> 70$ nm, and $D \propto r^{-2}$ for $r << 70$ nm.

Table 3.2 Ratio of Brownian and gravitational displacements in 1 s

Particle diameter (mm)	*Displacement ratio*
0.01	4800
0.1	42
1.0	0.21
10	7×10^{-4}

Hence, although the individual steps in Brownian displacement involve an erratic random walk, the statistical average is a well-behaved function of time and particle radius. We can see from Table 3.2 that Brownian motion is really important compared to gravity for particles of 0.01 μm or even 0.1 μm, but trivial for 10 μm particles. This aspect of particle behaviour is also significant when particles have to be sampled through pipes before measurement. Even if the designer takes meticulous care to avoid impaction of large particles by bends and fittings, small particles will diffuse to the walls of the pipes and distort the size distribution.

3.4.4 Coagulation

When there is relative movement of particles within a cluster by Brownian or turbulent diffusion, there will be collisions between particles and this will sometimes result in their combination to form a single new larger particle. This process is called coagulation. The new particle may be spherical if the original particles were liquid, as with sulphuric acid

FOR REFERENCE PURPOSES ONLY

aerosol, but it is more likely to be an untidy asymmetric clump of discrete parts, held together by electrostatic and molecular forces. As we would expect, coagulation is fastest for smaller particles, and the denser the particle cloud, the more collisions and coagulation there will be.

The basic rate equation is

$$\frac{dN}{dt} = -K_0 N^2$$

where:

$$K_0 = 4\pi d_{\text{part}} D = \frac{4kTC_C}{3\eta}$$

and N is the number concentration of particles. For air at ambient temperatures, $K_0 \approx 3 \times 10^{-16}\ C_C\ \text{m}^3\ \text{s}^{-1}$.

For a monodisperse particle cloud with initial concentration N_0, the number concentration decreases with time according to

$$N(t) = \frac{N_0}{1 + N_0 K_0 t}$$

The particle diameter increases correspondingly, although at a slower rate because it takes eight original particles to produce one new particle of double the diameter (Table 3.3).

$$d(t) = d_0 (1 + N_0 K_0 t)^{1/3}$$

Table 3.3 Concentration halving times and diameter doubling times for various initial concentrations, $K_0 = 5 \times 10^{-16}\ \text{m}^3\ \text{s}^{-1}$

Initial concentration (N_0 cm^{-3})	*Time to reach 0.5 N_0*	*Time for particle diameter to double*
10^{14}	20 ms	140 ms
10^{12}	2 ms	14 ms
10^{10}	0.2 s	1.4 s
10^{8}	20 s	140 s
10^{6}	33 min	4 h
10^{4}	55 h	16 days
10^{2}	231 days	4 years

3.4.5 The influence of shape and density

The earlier discussion refers to spherical particles having the same density as water (1000 kg m^{-3}). Although a significant proportion of particles in the atmosphere have these

FOR REFERENCE PURPOSES ONLY

characteristics, many do not, and this will affect their behaviour in the air.

3.4.5.1 Shape

Any non-spherical particle can be given an equivalent diameter d_{equ}, which is simply the diameter of a sphere that has the same volume and density as the particle. It can then be assigned a dynamic shape factor F (Table 3.4), which corrects for the influence of shape on viscous drag.

$$F_D = F.3\pi\eta V d_{\text{equ}}$$

so that

$$V_{\text{term}} = \frac{\rho_{\text{part}} d^2 g C_C}{18\eta F}$$

3.4.5.2 Aerodynamic diameter

The aerodynamic diameter d_a is an equivalent diameter which is used to compare the dynamic properties of particles of different shapes and/or densities. It is the diameter of the spherical particle of density 1000 kg m^{-3} that has the same terminal speed as the particle in question.

Table 3.4 Dynamic shape factors

Shape	*Dynamic shape factor, F*	*Ratio of length to diameter*		
Sphere	1.00			
Cube	1.08	2	5	10
Cylinder				
Axis vertical		1.01	1.06	1.20
Axis horizontal		1.14	1.34	1.58
Cluster of three spheres	1.15			
Dusts	1.05–1.88			

That is,

$$V_{\text{term}} = \frac{\rho_0 {d_a}^2 g}{18\eta}$$

If the particle is spherical, and neglecting slip, then

$$d_a = \sqrt{\frac{\rho_{\text{part}}}{1000}} d_{\text{part}}$$

For example, a spherical particle of density 4000 kg m^{-3} and diameter 2 μm would have an aerodynamic diameter of 4 μm. For a non-spherical particle of actual diameter d_{part}, density ρ_{part}, dynamic shape factor F, Cunningham slip factor C_{part} and flow Reynolds number Re_{part}, the aerodynamic diameter is calculated as:

$$d_a = \left[\frac{\rho_{part} C_{part} Re_{water}}{\rho_{water} C_{water} Re_{part} F}\right] d_{part}$$

3.4.6 Relaxation time

When a particle experiences a change in the forces acting on it, it does not instantaneously switch to the new equilibrium condition but approaches it exponentially, because the force causing the acceleration gradually decreases to zero as the equilibrium is approached. In general, the speed $V(t)$ at any time t is given by

$$CO(NH_2)_2 + H_2O \rightarrow CO_2 + 2NH_3$$

where:

V_{final} and $V_{initial}$ are the final and initial speeds, respectively
τ is the time constant of the process, also called the relaxation time

τ can be thought of as the characteristic timescale on which the particle adjusts to the new conditions, and is given by

$$\tau = \frac{\rho_{part} d^2_{part} C_C}{18\eta}$$

3.4.6.1 Note on units and dimensions

It is worth checking that an expression like the one above really does give a time in units that everyone can understand. The symbols on the righthand side of the equation have the following units

ρ_{part} – density – kg m^{-3}
d_{part} – diameter – m
C_C – dimensionless factor
η – viscosity – N s m^{-2} = kg m^{-1} s^{-1}

Table 3.5 Diameter dependence of particles to reach 95% of their terminal velocity

Particle diameter (μm)	*Time to achieve 0.95 V_{term} (ms)*

FOR REFERENCE PURPOSES ONLY

0.01	0.00002
0.1	0.00027
1.0	0.011
10.0	0.94
100.0	92

If we combine these we get

$$\frac{\left(kg\,m^{-3}\right)m^2}{kg\,m^{-1}\,s^{-1}}$$

which yields *seconds* after cancellation.

For the situation described earlier, when a particle is accelerating from rest to its terminal speed under gravity, we have

$$V(t) = V_{\text{term}} - (V_{\text{term}} - 0)e^{\frac{-t}{\tau}} = V_{\text{term}}\left(1 - e^{\frac{-t}{\tau}}\right)$$

At $t = 1\tau$, the particle will have achieved $1 - (1/e) = 0.63$ of V_{term}, and at $t = 3\tau$, $V(t) = 0.95\ V_{\text{term}}$. Hence after a time longer than 3τ has elapsed, the particle will effectively have reached its terminal speed. This happens extremely quickly for all the particles that we shall be dealing with in this book, as shown in Table 3.5. Even a 100 μm particle achieves its terminal speed in less than 100 ms.

3.4.7 Stopping distance

Whereas the relaxation time can be thought of as the characteristic timescale over which changes in particle motion occur, the stopping distance S corresponds to the characteristic length scale over which the particle decelerates to rest after it has been projected into still air at an initial speed V_0 (Table 3.6). It is related to relaxation time very simply:

$$S = V_0\tau$$

Table 3.6 Stopping distances for spherical particles

Particle diameter (μm)	*Stopping distance (mm) from an initial speed V_0=10 m s^{-1}*	*Time to travel 0.95 of stopping distance (s)*
0.01	7.0×10^{-5}	2.0×10^{-8}
0.1	9.0×10^{-4}	2.7×10^{-7}
1.0	0.035	1.1×10^{-5}
10.0	2.3	8.5×10^{-4}
100.0	127	0.065

FOR REFERENCE PURPOSES ONLY

As with relaxation time, the concept can be useful to gain a qualitative feel for a particle's behaviour under different conditions. For example, the smallest scale of atmospheric turbulence is around 10 mm. As most airborne particles are <10 μm, and the stopping distance for 10 μm particles is only a few mm, they will normally follow the flow fluctuations very closely.

3.4.8 Impaction and interception

When air blows round an obstacle, the streamlines curve (Figure 3.10). The trajectory of each particle is then determined by the balance between inertial forces (which tend to keep the particle on a straight line path), pressure gradient forces (which tend to keep it following the stream lines) and viscous forces (which act to slow down movements across the stream lines). The smallest particles have negligible inertia, and will follow the streamlines as well as the gas molecules themselves do.

FOR REFERENCE PURPOSES ONLY

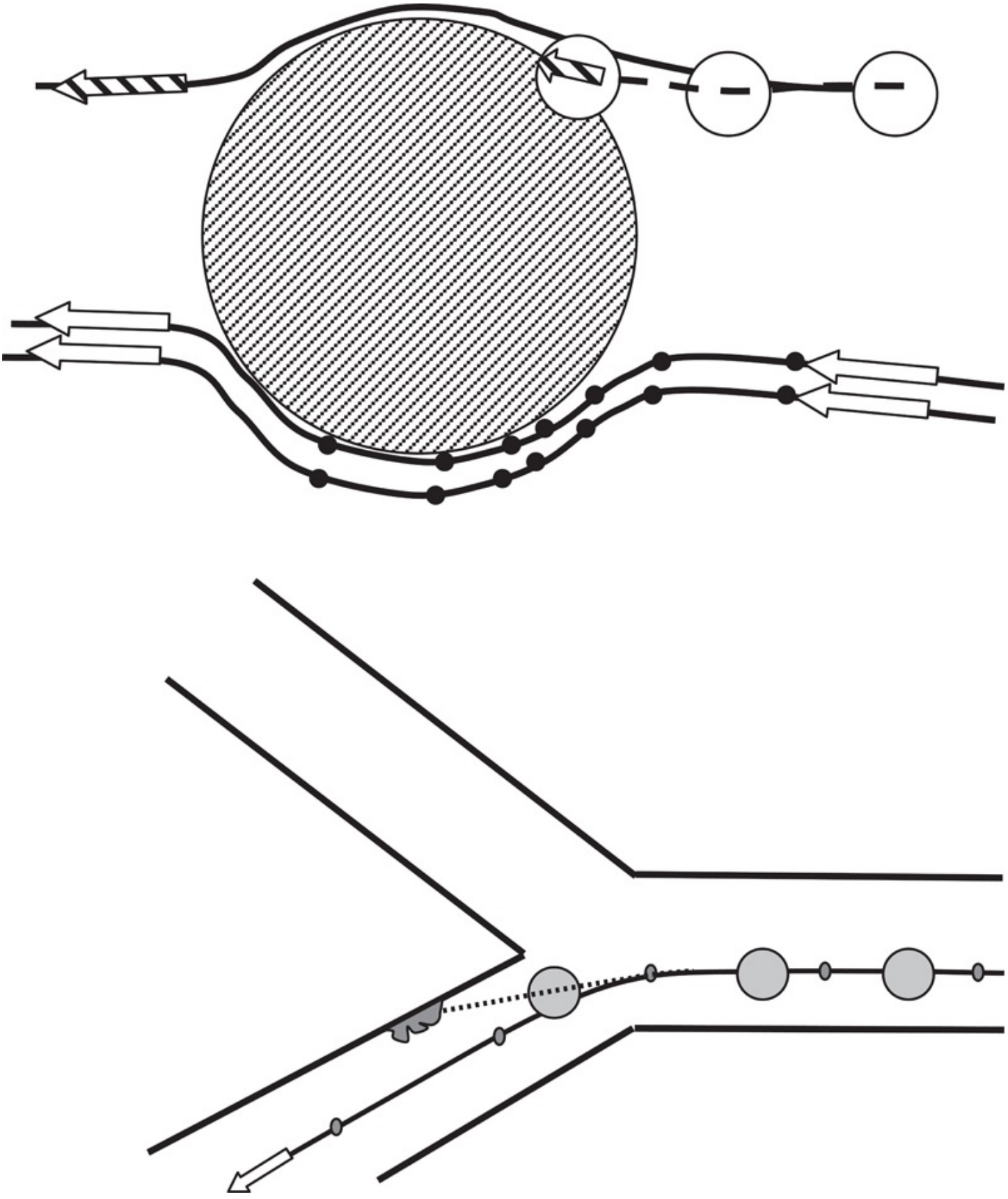

Figure 3.10 Streamlines of air flowing round a cylinder and a bend, showing how particles are deposited from streamlines onto the surface.

FOR REFERENCE PURPOSES ONLY

The larger a particle is, the more its inertia will tend to take it across the streamlines to be deposited on the object. This is called *impaction*, and is shown happening to the particle on the upper streamline of Figure 3.10. The same phenomenon applies when particles are deviated by bends in pipes – in the respiratory system, for example – as is shown in the lower diagram of Figure 3.10. For any given combination of obstruction, particle population and airspeed we can expect some of the particles to impact and some to flow round. Hence we can define the efficiency of impaction, c_p, by

$$c_p = \frac{\text{number of collisions on the obstacle}}{\text{no. of particles that would have passed through the space occupied by the obstacle if it hadn been there}}$$

Hence for a cylinder of length L and diameter D, oriented normal to an airflow of speed U and particle concentration C

$$c_p = \frac{\text{no. of collisions}}{ULDC}$$

The probability of a particle impacting onto an obstruction is indicated by the ratio of its stopping distance to the radius R of the obstruction. This special parameter is called the *Stokes number*. The curves in Figure 3.11a,b show the theoretical variation of impaction efficiency with Stokes number (Stk) for Re > 100 and Re = 10, respectively.

The dashed curve C is from experimental results with droplets, while the individual points are from measurements with spores. One visible example of these relationships is the collection of snowflakes on different parts of trees. The airflow around the trunks and large branches has low curvature, so that snowflake accelerations are small and they remain on the streamlines – deposition to the tree is small. For small branches and twigs, however, the local curvature is high, accelerations are large and deposition to the tree much greater. We can gain a semi-quantitative feel for the likelihood that impaction will occur from the Stokes number of the particle/obstacle combination. For example, a 1 μm particle in a 2 m s^{-1} wind has a *stopping distance* of 25 μm. Hence, impaction will only occur on obstacles smaller than about 80 μm across. If the main obstacle is a leaf, the particle will avoid it. However, some leaves are covered in thin hairs, and the particle can be impacted on these. As the wind speed increases, particles may tend to bounce off even after they have been impacted.

FOR REFERENCE PURPOSES ONLY

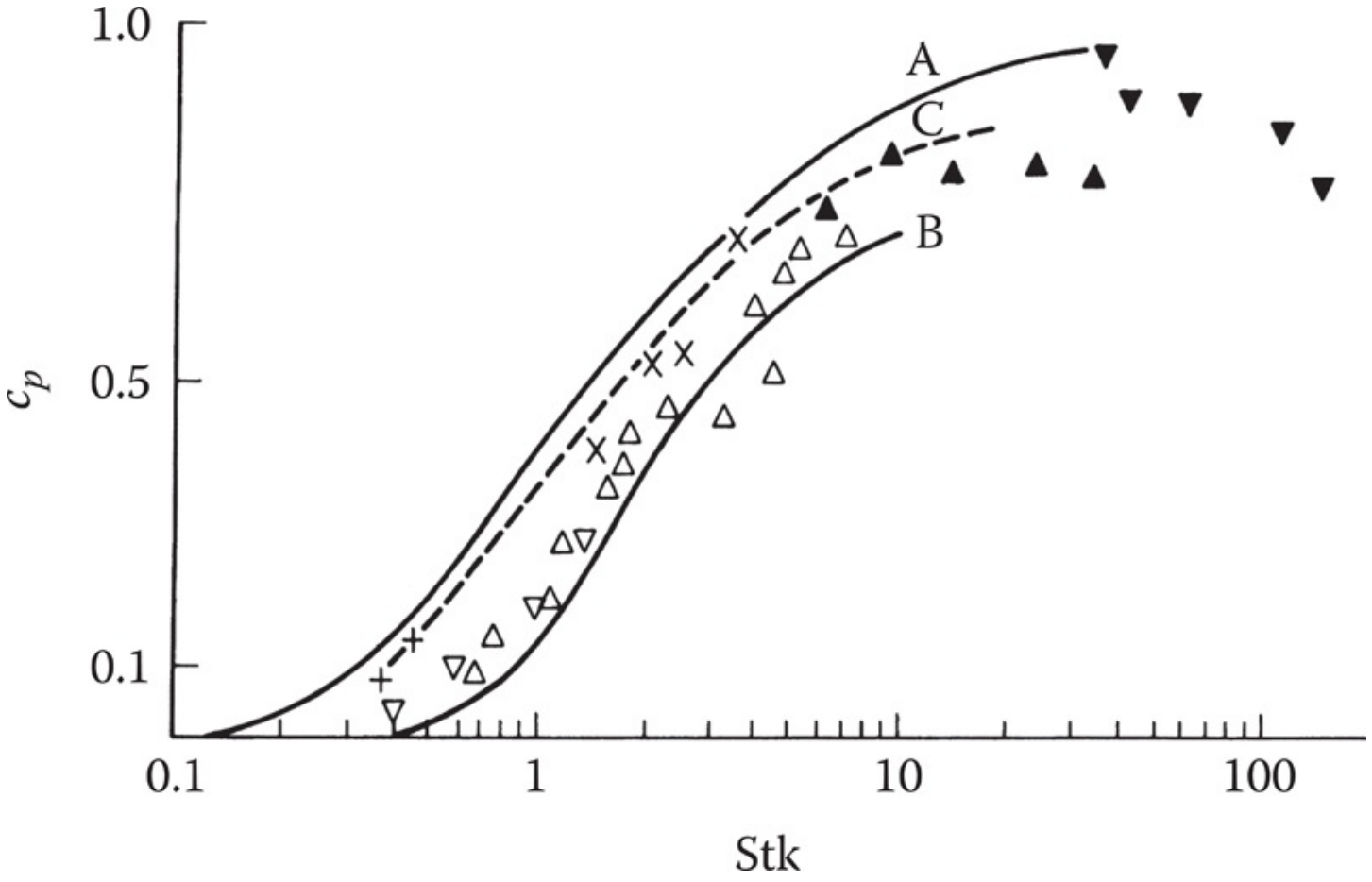

Figure 3.11 Variation of collection efficiency with Stokes' number. (From Monteith, J. L. and Unsworth, M. H., *Principles of Environmental Physics*, Edward Arnold, London, UK, 1990.)

FOR REFERENCE PURPOSES ONLY

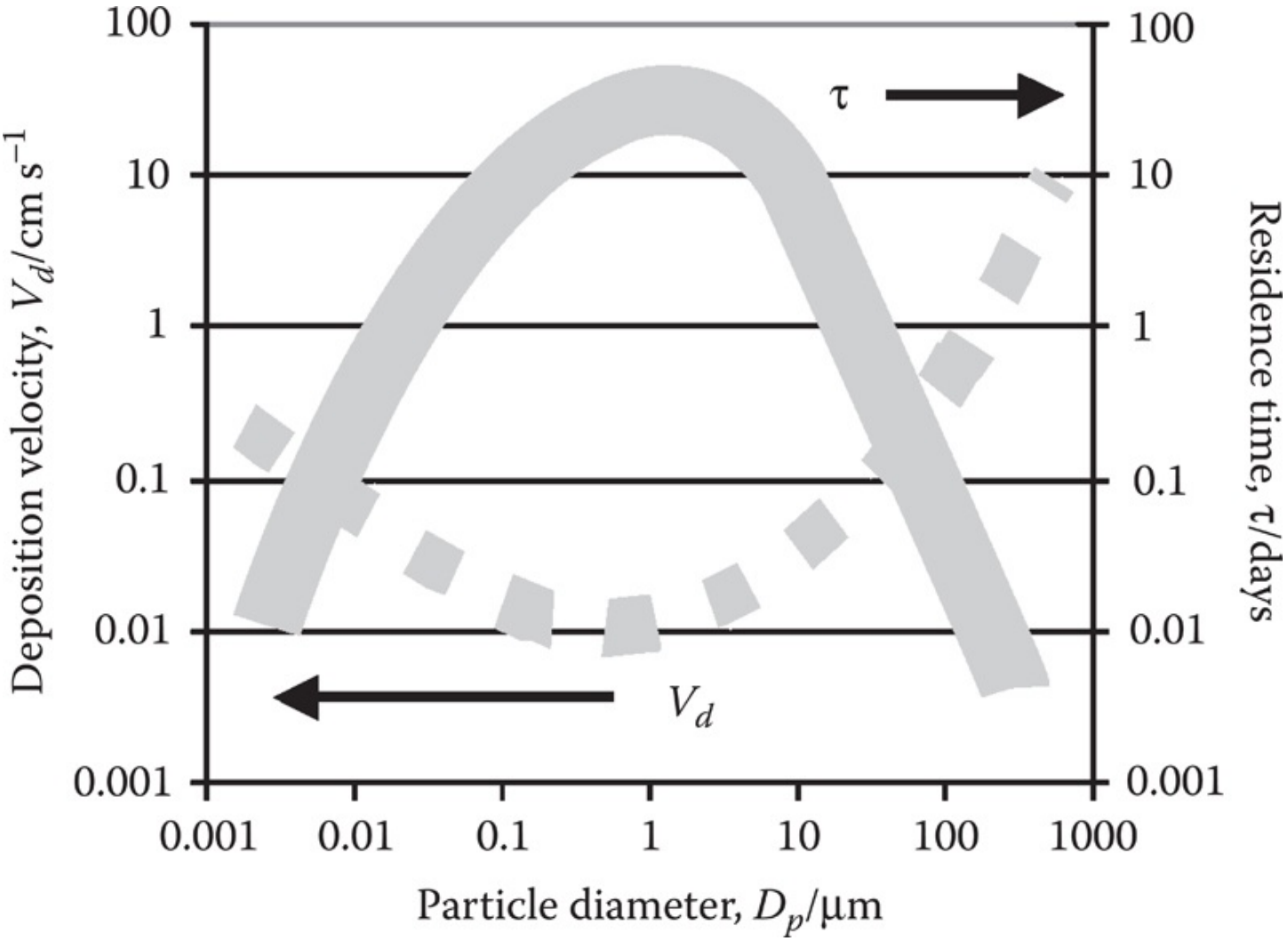

Figure 3.12 Variation of deposition velocity and residence time with particle diameter.

Interception is a special case of impaction which applies when a particle remains on its streamline but nevertheless collides with the obstruction because it passes so close that physical contact is unavoidable. Interception efficiency increases with r/R, and this relationship has been used very effectively to sample small fog droplets with very fine threads such as spiders' webs, for which R << r.

In natural situations, all of the deposition processes can operate simultaneously; the importance of each one is determined by the relationship of factors such as particle size, object size and wind speed. Figure 3.12 shows schematically the variation of particle deposition velocity and residence time with diameter. For particles less than about 0.01 μm, Brownian diffusion is dominant. For particles larger than about 1 μm, sedimentation becomes important. In the range 0.01–1 μm, neither of those processes is important, and experimental results confirm that deposition is slow. This is just the size range of pollutant aerosol, such as ammonium sulphate and ammonium nitrate, and accounts for the long residence times that allow them to build up significant haze until washed out by rainfall. The concentration of particles in the atmosphere at any place and time is the net result of

FOR REFERENCE PURPOSES ONLY

production and deposition; as discussed earlier, these processes often lead to a *tri-modal size distribution*.

3.4.9 Stokes number and impactors

The Stokes number Stk is also useful when considering the effect of a jet, for example, on particles passing through it. Stk is simply the ratio of the particle stopping distance S (at the jet throat speed, in this case) to the characteristic diameter of the jet.

$$\mathrm{Stk} = S/d_c = \tau U_0/d_c$$

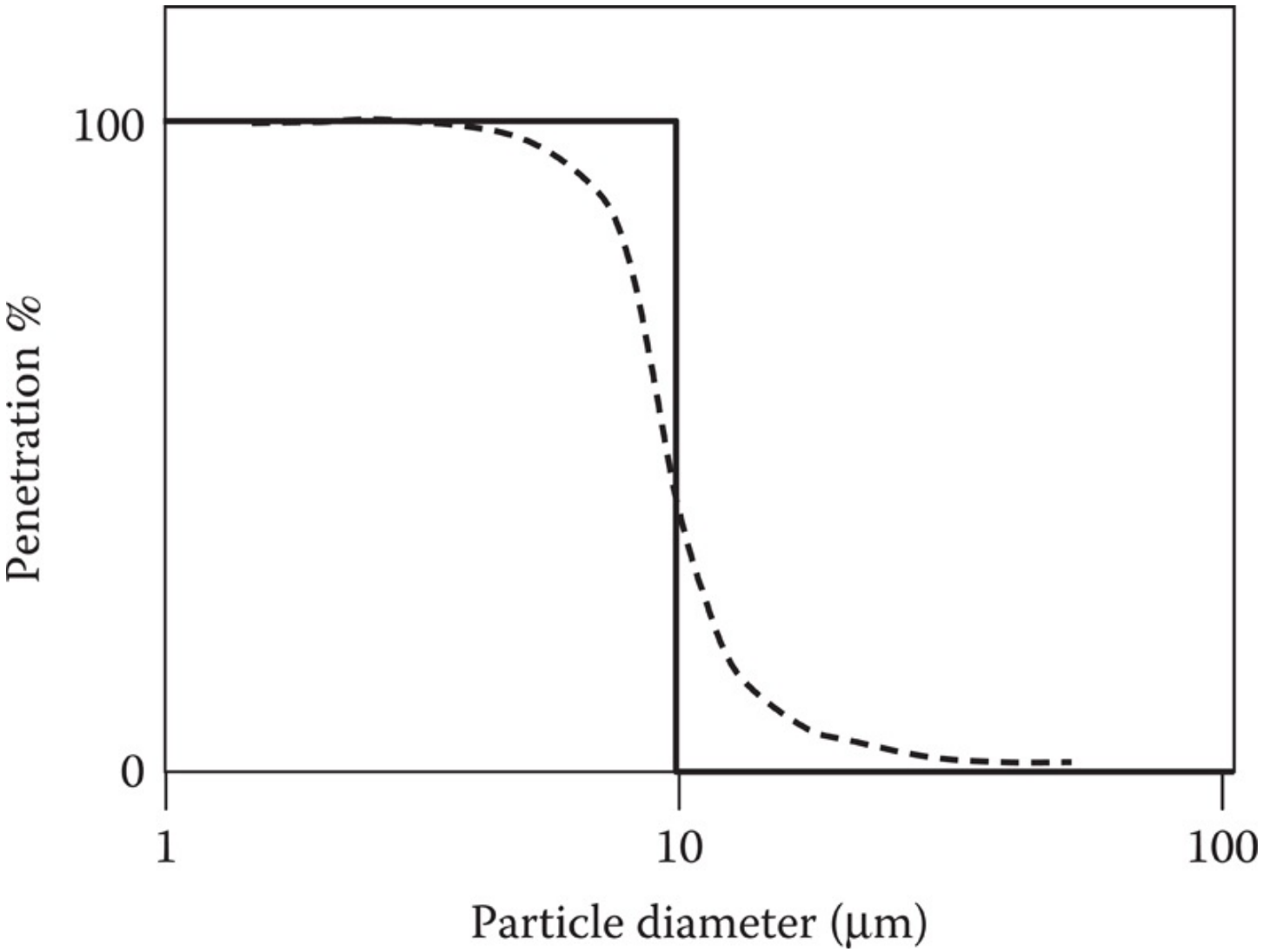

Figure 3.13 Ideal variation of collection efficiency with particle diameter.

All combinations of jet diameter, air speed and particle aerodynamic diameter can then be summarised by one graph of collection efficiency against Stk.

An ideal impactor would have the step-function variation of collection efficiency shown

by the solid line in Figure 3.13. For values of Stk less than some critical value, all particles would follow the streamlines through the impactor without being collected. For greater Stk values, all particles would be collected. Life is never this neat, and in practice there is always a smoothing of the step function as indicated by the dashed line, so that some *undersized* particles get collected and some *oversize* ones get through. It turns out that for round jets, this critical value of Stk is 0.5. At this value of Stk, 50% of the particles are collected and 50% go through, so it is called Stk_{50}. The particle diameter corresponding to this value of Stk is called d_{50}, and is the *cut diameter* of the jet under those conditions. Note that the cut diameter is only fixed if the density, pressure and flow rate of the air are fixed, and will have to be recalculated if there are changes in these parameters.

$$\mathrm{Stk} = \frac{\tau U}{d_{\mathrm{jet}}/2} = \frac{\rho_{\mathrm{part}} d_{\mathrm{part}}^2 U C_C}{9\eta d_{\mathrm{jet}}}$$

At the cut diameter, $\mathrm{Stk} = \mathrm{Stk}_{50}$ and $d_{\mathrm{part}} = d_{50}$ then

$$d_{50} C_C^{1/2} = \left(\frac{9\eta d_{\mathrm{jet}} Stk_{50}}{\rho_{\mathrm{part}} U} \right)^{1/2}$$

or, As the volume flow rate Q through the jet = $\pi {d_{\mathrm{jet}}}^2 U/4$

$$d_{50} C_C^{1/2} = \left(\frac{9\pi\eta d_{\mathrm{jet}}^3 \mathrm{Stk}_{50}}{4\rho_{\mathrm{part}} Q} \right)^{1/2}$$

3.4.10 Thermophoresis

When particles are in a temperature gradient in a gas, there will be more energetic collisions from gas molecules on the high temperature side of the particle than there are from molecules on the low temperature side. The result is a net force acting on the particle in the direction in which temperature is falling. For most natural particles in naturally occurring temperature gradients, the effect is insignificant. In some situations, however, it can be very important. When particles are being formed in vehicle exhaust gases, high temperature gradients exist between the hot gas and the cool walls. The particles are also very small – typically a few nm. Thermophoretic deposition may then be a significant factor.

3.4.11 Erosion and resuspension

The blowing wind moves soil and other surface deposits around and can lift them into the atmosphere and transport them great distances. The process is known as *deflation* and can contribute to:

FOR REFERENCE PURPOSES ONLY

- Sandstorms, desert and dune formation
- Erosion of agricultural soils
- Geomorphology of wind-blown deposits such as *loess*
- Atmospheric particle burden
- Loss of visibility
- Ocean sediments
- *Red rain* events

Three stages are involved – suspension from the surface into the air, transport and deposition. If the particle happens to protrude above the general ground level, then it will be subject to a drag force from the wind and can be lifted off if the instantaneous shear stress is greater than the gravitational force. If the particle is too small (<100 μm) then it remains within the viscous sub-layer where the flow is aerodynamically smooth. Also, adhesive forces start to add significantly to the gravitational forces.

It may not be obvious how a wind flowing parallel to the surface can generate a lifting force. One common mechanism is *saltation* (from the Latin for jump or leap). Once particles such as sand grains have been set in motion, they strike other grains on the surface. Sometimes they bounce up into the airflow after such a collision. The particles' relaxation time is comparable to the time they take to return to the surface at their sedimentation speed, so that they accelerate to the wind speed at that height (which might be several m s^{-1} only a few cm above the surface). This gives them momentum for the next collision, and so on. Theory and experiment show that the rate of saltation depends on the cube of the wind speed.

Saltating grains will usually be in the 50–300 μm diameter range, moving amongst larger grains, which either remain stationary or roll along, and amongst smaller ones. When the smaller ones are ejected by the saltating grains, they become airborne and leave the area, possibly to form loess soils or red rain or ocean sediment thousands of km downwind. In addition, the sand blasting effect of the windborne grains on larger rocks can create a new supply of smaller grains for removal. Although the saltation process is most easily visualised for a dry sand region such as a desert or beach, it will contribute to soil erosion for all soils, depending on the fetch upwind, the size distribution of the soil particles, the moisture content and the extent of vegetation.

3.5 PARTICLE SOURCES

3.5.1 Primary particles

The primary sources of direct particle injection into air are natural withering, sandstorms, smoke and soot from combustion sources. However, the residence time of these particles can vary, largely depending on the particle size characteristics, compositions and the

microenvironment where they are airborne.

3.5.1.1 Wind erosion

Much of the primary natural aerosol is generated from the erosion of soil by the wind. These processes are intermittent and can generate highly episodic erosion fluxes, concentrated into short periods when strong winds over bare soil follow extended dry periods. It will be seen from Figure 3.9 that typical sedimentation speeds are about 0.3 cm s^{-1} for a 10 μm particle and 30 cm s^{-1} for a 100 μm particle (the size of the smallest drizzle droplets). Typical updraft speeds in stormy conditions can be metres s^{-1}, so that particles can remain suspended for significant periods and travel long distances before deposition. The principal sources are in the northern hemisphere, where the Saudi Arabian peninsula, the US south west, the Gobi and the Sahara are the major contributors to a total entrainment of 1500 Mt each year. This process is going on all over the world all the time, but is not noticed until revealed by a particular event. About 100 Mt of dust is blown off the Sahara each year, and a significant proportion of the rain events in southern Europe involve *red rain*. General wind-entrained soil particles tend to fall into two distinct size ranges. The coarser fraction is mainly quartz grains of 10–200 μm, which tend to sediment out close to the source, while clay particles are in the range <10 μm and can get transported further. Airborne measurements in a plume from the Sahara have shown that the mass median diameter was over 50 μm close to the source, and that this fell steadily with distance until it was only 2–3 μm after 5000 km. These particles tend to be the most common crustal oxides of iron, aluminium, silicon and titanium. The chemical composition can be significant – it has been estimated that the 1.4 Mt of calcium contained in the 24 Mt of dust eroded from European soils each year would be sufficient to neutralise 10% of the annual SO_2 emission. The flux can be huge – measurements have shown source strengths of up to 10^{-6} cm^3 of particles per cm^2 of soil per second, equivalent to around 1 mm soil depth day^{-1}. On a larger scale and longer term, a belt of loess (wind-blown deposits from adjacent areas) up to a hundred metres deep runs from France to China.

3.5.1.2 Sea salt

Another major natural source of airborne particles is the evaporation of droplets of sea water. Every time that a wave breaks or a bubble bursts in the oceans, many droplets are flung into the air. For those that remain suspended, the water will evaporate away and leave a salt crystal. Table 3.7 shows that around 3 billion tonnes of sea salt particles are generated in this way each year. The mass median diameter of these salt particles near the sea surface is around 8 μm. Their chemical composition closely tracks that of the dissolved species in the surface seawater, that is 55% Cl^-, 31% Na^+, 7.7% SO_4^{2-}, 3.7% Mg^{2+}, 1.2% Ca^{2+} and 1.1% K^+. These ions exist mainly as the salts NaCl, KCl, $CaSO_4$ and Na_2SO_4.

FOR REFERENCE PURPOSES ONLY

Table 3.7 Global particle production trends

Source	*Production rate (10^6 t yr^{-1})*
Natural	
Primary	3000
Sea salt	1500
Mineral dust	300
Volcanic dust	100
Forest fires	
Total natural primary	4900
Secondary	40
Sulphates	30
Nitrates	20
Hydrocarbons	
Total natural secondary	90
Total natural	5000
Anthropogenic	
Primary	200
Secondary	300
Total man-made	500
Grand total	5500

3.5.1.3 Other natural sources

Further primary natural sources include volcanoes, forest fires, spores and pollen. Natural processes also operate to convert gases into particles. The conversion may be physical – for example, the condensation of terpenes and pinenes in forested areas, or chemical – the production of sulphuric acid aerosol from sulphur dioxide, dimethylsulphide (CH_3SCH_3) and hydrogen sulphide. Even in the stratosphere, sulphuric acid aerosol is formed via the photodissociation of carbonyl sulphide (COS) into CO and S.

3.5.1.4 Anthropogenic sources

Human sources of particles are also legion. All activities such as combustion, melting, grinding, crushing, ploughing or spraying produce particles; a variable proportion of these will be fine enough to remain suspended in the air, depending on the initial size distribution. Human biomass burning has made up 95% of all biomass combustion over the most recent several decades, and generates a variable mixture of soot, sulphates, nitrates and hydrocarbons. Small diesel engines (cars and vans) emit around 5 g particles per litre of fuel, while this figure rises to around 12 g for heavier duty vehicles.

In contrast, petrol-engined vehicles without catalysts emit only around 0.5 g. The effects of these emissions, of course, depend also on the size distribution. Secondary human sources include sulphate and nitrate particles converted from the primary gas emissions,

FOR REFERENCE PURPOSES ONLY

and organics from VOC emissions. Hence, of the total 5.5×10^9 *t* produced, 90% is of natural origin. Nevertheless, anthropogenic particles have had a profound effect on the atmosphere, both because their production is concentrated in urban and heavily inhabited areas, and because they are mostly formed as small secondary particles with long atmospheric residence times.

Table 3.8 lists the ten largest UK industrial sources of particle emissions (past records from 1998). This is a subset of the Chemical Release Inventory generated by the UK Environment Agency (now relaunched as the Pollution Inventory) for major processes that come within Part A of the Environmental Protection Act (1990). These figures do not include some thousands of much smaller Part B processes which are controlled by Local Authorities (LAs).

The particle form that has received the most attention from the public and legislators is *black smoke* – the *soot* associated with incomplete combustion of fossil fuels. Figure 3.14 graphs the decline in black smoke emissions in the UK between 1970 and 1999. The dominant source had been domestic coal combustion, which decreased steadily as gas-fired central heating replaced the domestic hearth and smoke-control regions were established in urban areas. In 1989 the new smoke source – diesel road vehicles – equalled domestic emissions in magnitude for the first time, and is now the main source of black smoke, although that is in decline.

Table 3.8 UK particle emissions from different processes

Process	*Particle emission (tonnes yr^{-1})*
Acids	8473
Cement and lime	4456
Incineration	2031
Petroleum processing	1614
Ceramics	723
Carbonisation	626
Mineral fibres	536
Organic chemicals	511
Inorganic chemicals	347
Fertiliser	132

FOR REFERENCE PURPOSES ONLY

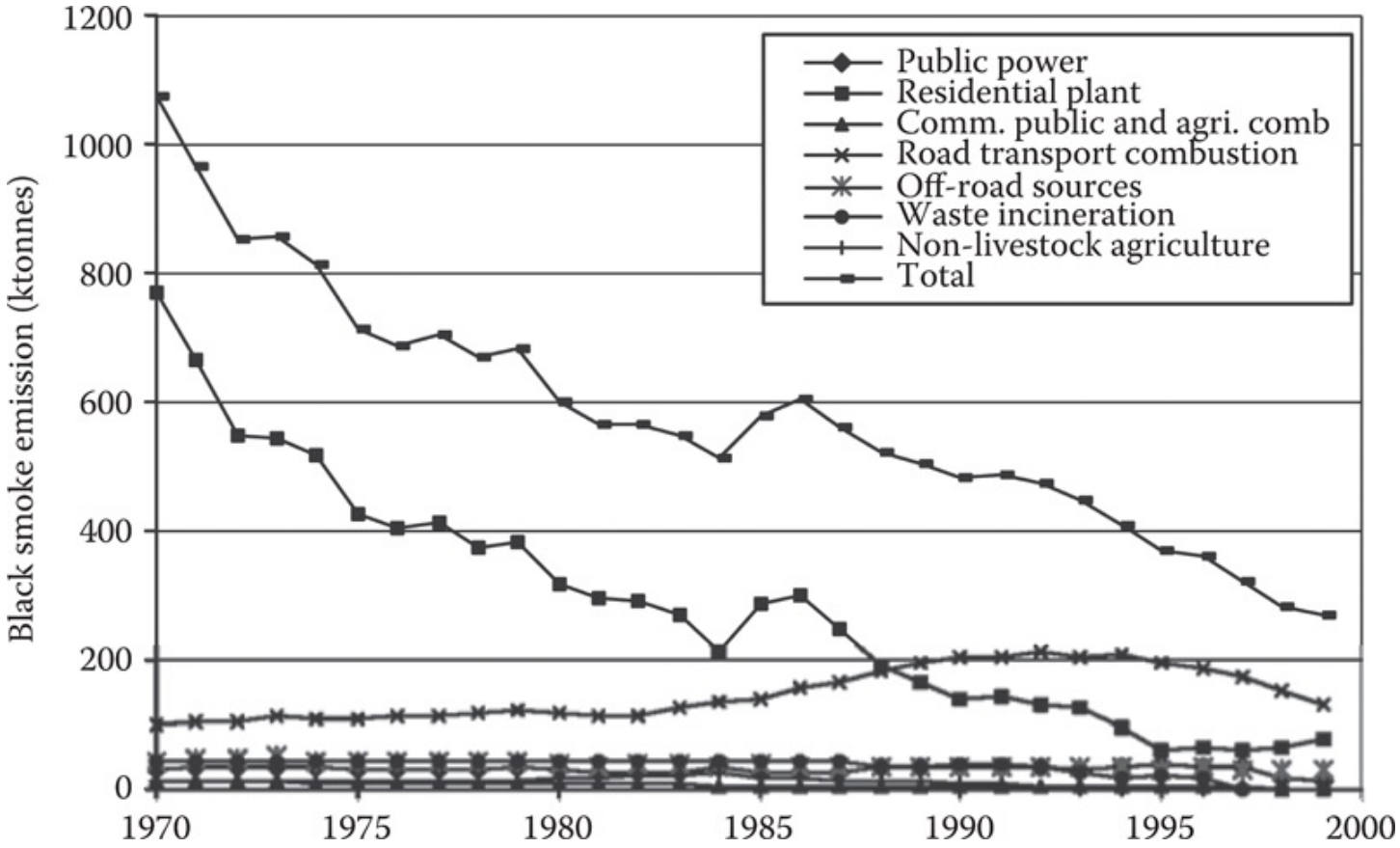

Figure 3.14 UK black smoke emissions by type 1970–1999.

3.5.2 Secondary particles

Reducing ambient PM levels is difficult due to the large contribution of secondary particles formed in the atmosphere from a range of gaseous pollutants. The same summertime photochemical conditions that can generate ozone in the troposphere from pollutant precursors (Chapter 2) can also generate particles. Chemical analysis of collected material has shown that the principle species found are:

- Ammonium sulphate
- Ammonium bisulphate
- Ammonium nitrate
- Ammonium chloride
- Sulphuric acid
- Sodium nitrate
- Elemental carbon

The main source of secondary particles is the atmospheric oxidation of SO_2 by the hydroxyl radical to form sulphur trioxide (SO_3). The latter reacts with water vapour to form sulphuric acid (H_2SO_4) vapour, which in turn nucleates to form a sulphuric acid mist. As with gas-

phase photochemistry, the OH radical is recycled and small concentrations can exert a powerful influence. The other major player in secondary particle formation is ammonia (NH_3). This alkaline gas is released at low concentrations over large land areas from animal wastes that have been spread on fields, or from animal urine which contains urea, or from nitrogenous fertilisers such as ammonium nitrate (NH_4NO_3) or urea itself ($CO(NH_2)_2$). Urea hydrolyses to generate carbon dioxide and ammonia.

$$CO(NH_2)_2 + H_2O \rightarrow CO_2 + 2NH_3$$

The ammonia is readily taken up on the surfaces of both sulphuric acid droplets and of acidified particles, where it forms ammonium sulphate or ammonium bisulphate. The formation of particles from vapour naturally generates extremely small particles (well below 1 μm) and does so rather fast because of their high surface area to volume ratio. These small particles coagulate rapidly to move into the accumulation size mode, with sizes that give them long residence times in the atmosphere and high efficiency at scattering light and reducing visibility.

The ammonium nitrate and ammonium chloride particles are generated by corresponding reactions between gaseous ammonia and nitric acid vapour or hydrogen chloride, respectively. Long-term records of suspended particulate show that European sulphate concentrations rose slowly but steadily from the 1950s, peaked in the late 1970s and have since declined. This pattern reflects the improved control of SO_2 emissions over the same period. Particulate nitrate, on the other hand, has continued to increase, although concentrations are expected to fall again as vehicle NO_x emissions decline. On a larger scale, measurements from the European Monitoring and Evaluation Programme (EMEP) network have shown a gradient of particulate sulphate concentration from peak values in south-east Europe of around 3 μg S m^{-3}, through about 1.5 μg S m^{-3} down to around 0.5 μg S m^{-3} in Scotland. This sulphate probably contributes about 6 μg m^{-3} to the background PM_{10} concentration in both rural and urban areas of southern Britain, and about one-third of that in the north. The corresponding values for nitrate PM_{10} would be about two-thirds of these figures. Hence, in industrial countries that also have intensive animal husbandry and/or crop production, a characteristic haze of fine particles is produced. The long range *import* of secondary particles can also make it hard to achieve standards for PM_{10} concentration.

3.6 TRENDS IN PARTICLE EMISSIONS

While emissions in the UK and its immediate European neighbours is expected to decrease over the longer time scale, the relative (and in some cases the absolute) contributions from emissions in the rest of the northern hemisphere are likely to increase. There are considerable differences in the per capita emissions from different countries, with the EU

FOR REFERENCE PURPOSES ONLY

figure typically 5–10 kg per head, and former Eastern bloc countries typically 10–30 kg per head. Note, however, that the $PM_{0.1}$ emissions are an order of magnitude less than those of PM_{10}. Specifically, the anthropogenic aerosols released from the Asian region (mainly China and India) are projected to dominate the anthropogenic aerosols component worldwide, attributed largely to the transboundary movements at hemispheric scale from the earth's rotation. The Indian Ocean Experiment (INDOEX), an international study conducted between 1995 and 1999, revealed complex environmental interactions beyond the confines of local scale of several issues – including air pollution, haze, smog, ozone and global warming. A phenomenon, termed the *Asian Brown Cloud* by the INDOEX team, involves formation of a sooty brown haze particularly during December to April over the South Asia region and the tropical Indian Ocean, Arabian Sea and Bay of Bengal. It is found to occur in the season following the southwest monsoon and northeast monsoon seasons and is considered to be transported far beyond the source region. The first comprehensive study of this South Asian haze published by the United Nations Environment Programme (UNEP) in 2002 suggested that as much as 75% of the observed haze results from anthropogenic sources. However, the emission sources of the aerosol components such as organics, black carbon, fly ash and dust are very poorly characterised. For black carbon, available estimates suggest that the Asian region may contribute about 30%–50% of the total world emissions.

Size-specific emission inventories have been constructed for particles by using information on measured size distributions from different sources such as transport, industrial combustion processes and other production processes.

Tables 3.9 and 3.10, respectively, present the source-specific trends in UK PM_{10} and finer particulate (PM_1, $PM_{0.1}$) emissions between 1970 and 2015; the final column gives the percentage change for each category and the overall trends.

Overall, the UK PM_{10} emissions decreased by over 70% between 1970 and 2015, mainly due to the reduction in coal use. There is significant reduction in emissions from industrial and residential combustions, largely due to switch from solid fuels to gas and electricity. However, in recent years road transport has become the largest single contributor with a negative trend of increase in emissions. All road transport modes emit PM_{10}, but diesel vehicles emit a greater mass of particulates per vehicle kilometre. Further, there has been a significant increase in the resuspension of dust from road transport. Estimates of resuspension are based on the deposition of primary particles from all UK road sources, which include vehicle tailpipes, brake and tyre wear.

Table 3.9 UK emissions of PM_{10} in 1970 and 2015 by aggregated source category (ktonnes yr^{-1})

	1970 Emission	*2015 Emission*	*Percentage change*
By source category			
Agriculture/waste	27.31	19.10	30.07
Combustion in industry/commercial/residential	342.54	66.02	80.73

FOR REFERENCE PURPOSES ONLY

Other transport	21.09	5.62	73.38
Production processes	65.99	29.43	55.40
Public electricity and heat production	67.10	4.76	92.90
Road transport	19.05	20.55	–7.88
Total	543.09	145.48	73.21

Source: NAEI, *UK Emissions of Air Pollutants 1990 to 2015*, National Atmospheric Emissions Inventory, 2016.

Table 3.10 UK emissions of finer particulates (PM_1, $PM_{0.1}$) in 1970 and 2015 by aggregated source category (ktonnes yr^{-1})

	1970 Emission	*2015 Emission*	*Percentage change*
PM1 – by source category			
Agriculture/waste	8.61	2.47	71.29
Combustion in industry/commercial/residential	226.95	31.99	85.90
Other transport	16.46	4.48	72.78
Production processes	22.93	6.24	72.77
Public electricity and heat production	13.81	1.76	87.23
Road transport	11.21	6.79	39.44
Total	299.97	53.74	82.08
PM0.1 – by source category			
Agriculture/waste	1.52	0.46	69.39
Combustion in industry/commercial/residential	34.51	7.89	77.15
Other transport	3.17	1.00	68.40
Production processes	10.65	2.54	76.17
Public electricity and heat production	5.51	0.78	85.89
Road transport	6.71	4.29	36.06
Total	62.07	16.96	72.68

Source: NAEI, *UK Emissions of Air Pollutants 1990 to 2015*, National Atmospheric Emissions Inventory, 2016.

Stationery combustion, mainly residential wood burning, is the single largest source of $PM_{1.0}$ (Table 3.10). On the other hand, road transport has been the single largest source of $PM_{0.1}$ emissions. However, with tighter regulations on PM emissions from new vehicles this trend has seen steep decline.

3.7 MEASUREMENT OF PARTICLES

Although filtration provides the simplest method of measuring particles, other techniques enable real-time measurements, or size distributions, or chemical analyses to be made. The following sections cover the state of the art in this field.

FOR REFERENCE PURPOSES ONLY

3.7.1 Particle sampling

The task of sampling is to get a representative sample of particles from the air into the measuring device without changing the concentration or the characteristics on the way. Thus, we must make sure that we capture all the particles from a known volume of air in the first place, and then that we do not lose any to tubing walls, and so on, or break up large particles and aggregates into small particles, or lose particles by the evaporation of volatile materials, or gain them by condensation.

3.7.1.1 Isokinetic sampling

As soon as we extract an air sample into the inlet of a measuring device, we start to corrupt the sample. We can think of the air as moving along streamlines that are parallel if the air is not flowing around an obstacle. If the air deviates round an obstacle, the streamlines bend. For each particle, there is then an imbalance between the inertial forces that tend to keep its movement in a straight line, and pressure gradient forces that tend to make it follow the streamlines. The heavier the particle, the more it will tend to come off the streamlines. When we sample air through an inlet, the streamlines will almost always be deviated to some degree. In the ideal case, the inlet is faced directly into the prevailing wind, and the sampling flow-rate is chosen so that the inlet speed is the same as the wind speed. This condition is said to be isokinetic (Figure 3.15a) and results in the least possible distortion of the particle sample.

FOR REFERENCE PURPOSES ONLY

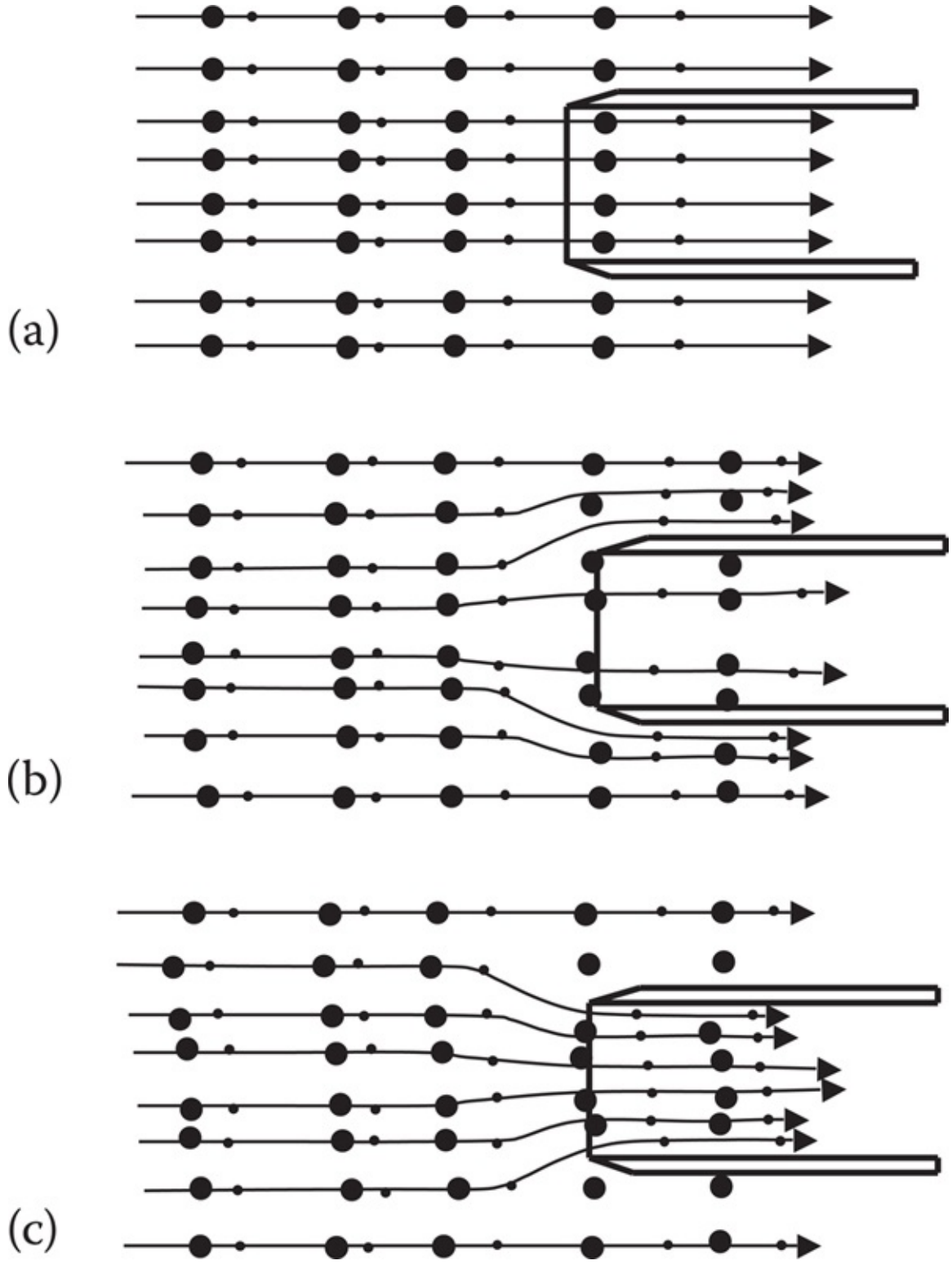

Figure 3.15 Flow streamlines of air into a sampling inlet: (a) isokinetic flow; (b) inlet speed less than the free stream speed; (c) inlet speed greater than the free stream speed.

FOR REFERENCE PURPOSES ONLY

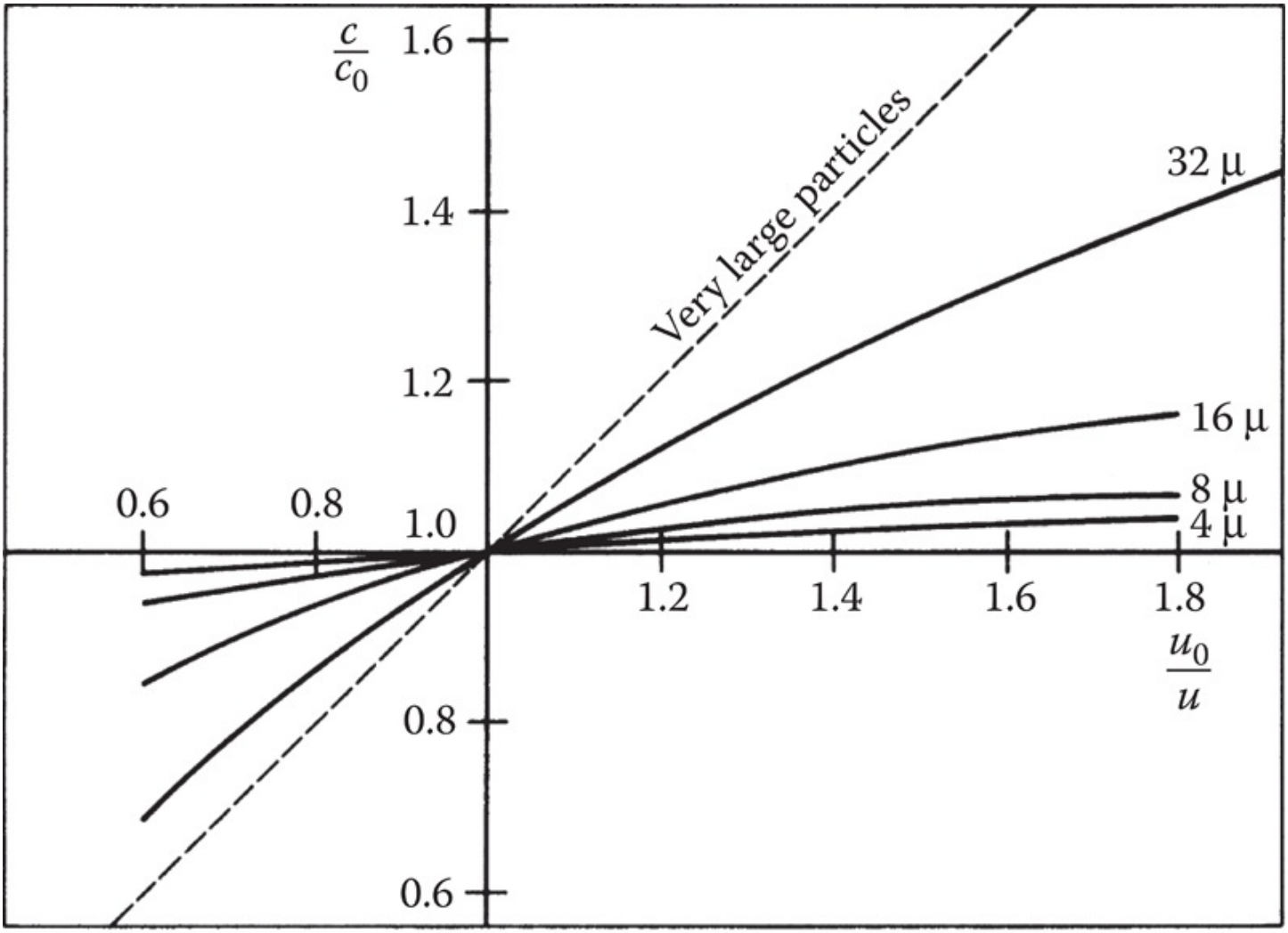

Figure 3.16 Variation of sampling efficiency (c/c_0) with degree of isokineticity (u_0/u) for particles of different sizes. (From Pio, C. A., in R. M. Harrison and R. Perry (Eds.), *Handbook of Air Pollution Analysis*, Kluwer Academic Publishers, Dordrecht, the Netherlands, 1986.)

Even when this condition is achieved on average, however, the turbulence that is always present in wind outdoors means that the instantaneous speed and direction at the inlet will usually differ from isokinetic. When the average inlet speed is too low (Figure 3.15b), the streamlines diverge around the inlet. Some particles enter the inlet from air that has not been sampled; the larger the particle, the less likely it is to follow the streamlines, so that the sampled air becomes enriched with larger particles. Conversely, when the average inlet speed is too high (Figure 3.15c), the streamlines converge on the inlet so that the sampled air is depleted of larger particles.

FOR REFERENCE PURPOSES ONLY

In Figure 3.16, the ratio of wind speed u_0 to the inlet speed u is plotted against the ratio of sampled concentration c to true concentration c_0 for different diameters of particles having unit specific gravity. For the smallest particles (the fine particle fraction <2.5 μm, for example), the concentration ratio is within a few percent at all speed ratios. As the diameter increases, so does the distortion of the sample, up to the limit for very large particles at which the ratios are equal (that is, a 20% error in the sampling speed gives a 20% error in the concentration). This description holds for an inlet that is oriented directly into the wind.

If the inlet is at an angle to the wind, then even if the speed is correct, the whole set of streamlines will have to bend on their way into the inlet, so that the sample will always be depleted of heavier particles. Figure 3.17 shows that this depletion could be 5%, 10% and 15% for 4, 12 and 37 μm particles (respectively) entering an inlet aligned at 30° away from the mean wind direction.

These issues are especially severe when the sampling is to be undertaken from an aircraft. The aircraft will be flying at typical speeds of 40–200 m s^{-1}, which requires a very small inlet diameter if a reasonable volume flow rate is used. There may be very high wall deposition losses just inside the inlet due to severe turbulence. Furthermore, the air must then be rapidly decelerated before the particles are filtered out. This raises the air temperature by 5°C–20°C, evaporating water and volatile species and changing the size distribution.

FOR REFERENCE PURPOSES ONLY

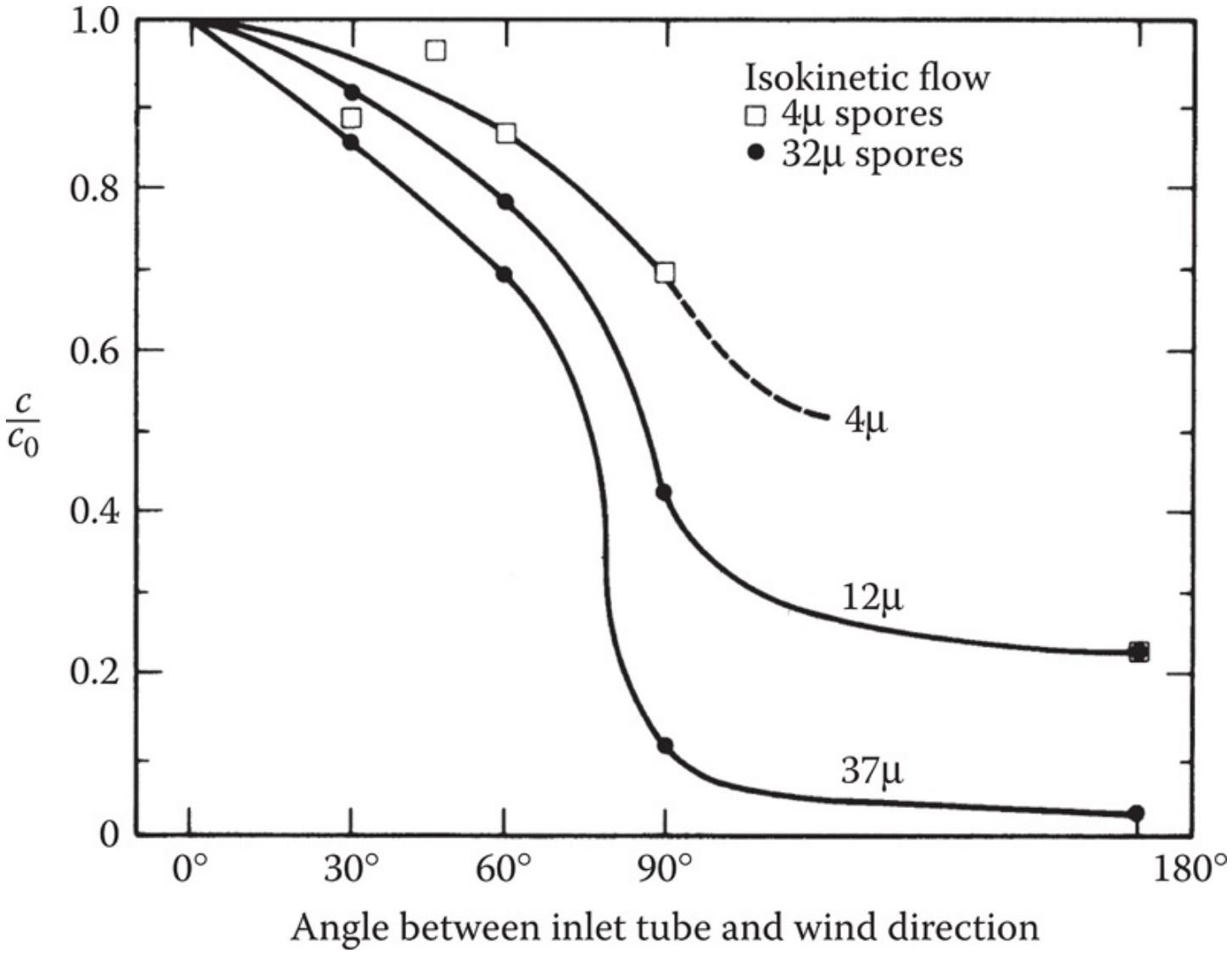

Figure 3.17 Variation of sampling efficiency (c/c_0) with the angle of the inlet to the wind direction, when sampling isokinetically. (From Pio, C. A., in R. M. Harrison and R. Perry (Eds.), *Handbook of Air Pollution Analysis*, Kluwer Academic Publishers, Dordrecht, the Netherlands, 1986.)

A different set of problems arises if the sampling is to be undertaken from still air. Now there is no wind direction to be oriented into, and no wind speed to be matched isokinetically. The errors are due both to the particles' settling velocities and to their inertia. For example, suppose the inlet tube is facing vertically upward. Then particles that were not originally present in the sampled air volume will fall into the inlet, so increasing the apparent concentration. The situation is reversed for an inlet that points downward. In principle there should be no error from this cause if the inlet is horizontal. Provided that the inlet velocity is sufficiently high (>25 V_s, where V_s is the terminal velocity of the largest particle of interest) then settling errors should be negligible.

It is not so easy to eliminate inertial errors. If the air is still then the flowlines in the sampled air must converge into the inlet, so that particles will have to follow them. The

larger the particles, the faster the flow or the smaller the inlet, the more will be lost. Inertial errors always result in an underestimate of the concentration. The general criterion for negligible errors is for $D_s > 4\,(Q\tau)^{1/3}$, where D_s is the diameter of the sample tube inlet, Q is the volume flow rate and τ the relaxation time of the largest particles. Taking the relaxation times given in Table 3.1 for particles of 0.1, 1, 10 and 100 μm, sampled at a flow rate of 20 L per minute, we would need inlet diameters of 2, 6, 28 and 129 mm respectively. Thus, the inertial and settling criteria set upper and lower bounds for the inlet diameter at a specified volume flow rate. Once particles have been coaxed into the inlet in the correct proportions, it follows that they should be measured as soon as possible to reduce risks of corruption. This involves the shortest physical path lengths, least severe bends, shortest practical residence time and closest approach to ambient temperature, pressure and humidity.

3.7.1.2 Calibration

Whatever size classification method is used, it will need calibrating during and after the design stage, as well as by the user to confirm correct operation. It is not possible to generate a polydiperse aerosol with known standard deviation and median diameters. Instead, calibration is achieved with the use of a series of quasi-monodisperse aerosols with very narrow size distributions. A range of methods exists for generating these.

The process of condensing a vapour on to a nucleus, which is used to count aerosol particles in the condensation nucleus counters (CNC), can also be used to create almost monodisperse aerosol. The aerosol material, which is typically a high-boiling substance such as dioctyl phthalate or oleic/steric esters, is atomised and evaporated in an electrically heated glass tube. Residual non-volatile impurities provide the condensation nuclei for droplet formation. Although the nuclei may vary in size initially, the rate of condensation growth slows as the droplet diameter increases, so that after a suitable time all the droplets have achieved almost the same diameter. The original solution is diluted with alcohol, which evaporates to produce smaller droplets. By controlling system parameters such as dilution, temperature and residence time, particles in the size range 0.04–1.0 μm can be produced at number concentrations of around 10^7 particles cm^{-3}.

Bottles of spherical polystyrene latex beads in aqueous suspension are available, with diameters in the range 0.02–100 μm. Aerosols can be generated by nebulising a diluted suspension and mixing the droplet suspension with dry air to evaporate the liquid component. The distribution is extremely monodisperse, and the particles are almost the same density as water so that the aerodynamic diameters are nearly the same as the physical diameters. Hence, these particles are favoured for instrument calibration. There may be problems with chain formation if multiple particles are present in one drying droplet, and with formation of nanoparticles from stabilisers if there are no particles present in a drying droplet.

With a spinning disc generator, a small (3 cm diameter) conical disc with a flat top is suspended on the airflow leaving a vertical pipe. Fluting on the underside of the disc forces

FOR REFERENCE PURPOSES ONLY

it to rotate in the airstream, achieving up to 60,000 rpm. Liquid is fed onto the top centre of the disc, and moves radially across the surface under centripetal force before being projected from the edge in a thin sheet. Hydrodynamic forces break the liquid sheet into droplets. Most of the droplets are in one larger size class, while about 10% of the liquid forms satellite droplets which are about ¼ of that diameter.

$$d = \frac{0.47}{\omega}\left(\frac{\gamma}{\rho_l R}\right)^{1/2}$$

where:

ω is the speed of rotation (revs s^{-1})

γ and ρ_l are the surface tension and density, respectively, of the liquid

R is the disc radius

The two size groups separate because of their different stopping distances and both groups can be used. The droplet diameter is changed by adjusting the rotation speed of the disc. Further control can be achieved by air-drying solutions of different concentrations to leave a solid residue. By using both of these techniques, aerosol particles in the range 0.6–3000 μm can be generated.

Highly monodisperse droplets can be produced from a vibrating orifice. For example, a liquid is forced under pressure through a 5–50 μm orifice, which is vibrated in the direction of the jet by the application of a sinusoidal force from a piezoelectric crystal. The Rayleigh instability which breaks up the jet into droplets occurs at the imposed frequency, and the droplet diameter can be calculated directly from

$$d = \left[\frac{6}{\pi}\frac{Q}{f}\right]^{1/3}$$

where:

Q is the liquid flow rate

f is the applied frequency

The initial droplet diameters are 15–100 μm. As with other liquid-based particle generators, solvent dilution and evaporation can be used to create solid particles and to further extend the diameter range. Rapid dilution with clean air is essential to prevent the droplets from coagulating.

In a fluidised-bed aerosol generator, a chamber is filled with bronze beads about 200 μm diameter, to a depth of 15 mm. An upward air current suspends the beads above the floor of the container. Dust from a reservoir is fed into the chamber, ground up by the bronze beads, and entrained into the updraft leaving the chamber. This technique is used to disperse powders such as ground Arizona road dust. It generates a broad but quasi-reproducible size distribution rather than a monodisperse aerosol.

3.7.2 Particle measurement methods

There are many particle measurement methods, each with its own merits and disadvantages. Selection of a particular method will depend on the objectives of the measurement and the resources available.

3.7.2.1 Filtration

Probably the oldest method of extracting particles from the air in which they are suspended is to pass them through a filter. Yet even this primitive technology is full of subtleties that have to be appreciated if we are to understand how the collected sample differs from the original population of particles in the air. A particle sampling filter consists either of a mat of tightly-packed, randomly oriented fibres, or a membrane with a network of randomly arranged air passages through it, or a membrane punctured by microscopic cylindrical pores. Particle collection mechanisms are complex, and vary with filter type. For fibrous filters, the particles are collected by a mixture of impaction, interception, Brownian diffusion and electrostatic attraction, with the relative significance of each depending on the flow rate, face velocity, porosity, fibre and particle composition. Filtration is not at all like sieving, because although a nominal pore size is quoted for a filter material, particles much smaller than that will be retained. Also, *collection of particles will itself change the airflow through the filter and the collection efficiency*. There are many different filter types, and selection will depend on the properties of both the particles and gases in the air and the ultimate purpose of the sample collection.

Among the critical factors are:

Particle collection efficiency and pressure drop: For normal applications, filters should remove >99% of the particles presented to them. However, the efficiency is increased by reducing the pore size, which also increases the pressure drop; this in turn reduces the flow rate or increases the pump size required. The pressure drop across the filter must not clog the filter, even when the highest expected particle loading is sampled, otherwise the flow rate will fall and the measurement of the once-in-20-years pollution episode will be corrupted. Glass fibre filters have been the mainstay of particle sampling for decades. They are cheap and rugged and offer high collection efficiencies at low pressure drops. Particles are trapped on fibres through the depth of the filter rather than on the surface alone. Hence, the rate of increase of pressure drop as the sample collects is low. Membrane filters made from cellulose nitrate or cellulose triacetate are suitable if the sample needs to be recovered for chemical analysis, because the substrates dissolve easily. Polyvinylchloride (PVC), which is widely used for quartz particles, suffers less from weight change due to water absorption. Membrane filters typically have higher flow resistances than fibrous ones, so are used for low flow rate applications. Increasing the face velocity can increase the collection

FOR REFERENCE PURPOSES ONLY

efficiency, because more of the particles will be collected by impaction on fibres. On the other hand, the smallest particles will be less likely to be collected by diffusion. On a more exotic level, nuclepore filters are made by piercing holes through a membrane with sub-atomic particles, then etching the holes to enlarge them to repeatable and known diameters. Particles are deposited on the flat smooth surface of the membrane. Costs and pressure drops are both high.

Figure 3.18 shows how the different particle collection mechanisms contribute to the overall filter efficiency of a fibre filter, with different mechanisms having quite different effectiveness in different size ranges, based on the aerosol mechanics that were discussed in Section 3.4.

Chemical stability and purity: Filters must be inert to gases present in the air sample, and not react with the deposited particles even in the presence of extraction solvents. Glass fibres absorb sulphur dioxide, quartz fibres absorb organic vapours, and cellulose fibres absorb water. If chemical analysis of the deposits is needed, then the filter must not contain significant and/or variable levels of the elements of interest. These properties must be determined *before* the sampling programme. For a basic determination of particle mass concentration, the filter will need to be conditioned by being kept at 50% ± 3% relative humidity and 20°C ± 0.5°C until constant weight is achieved before weighing clean; this conditioning is repeated after use to minimise errors due to water vapour uptake or loss by the filter. It is also done at a fairly low temperature to reduce any effect of volatilisation of ammonium nitrate and other salts. The microbalance used for the weighing should be kept in a cabinet at the same controlled conditions.

FOR REFERENCE PURPOSES ONLY

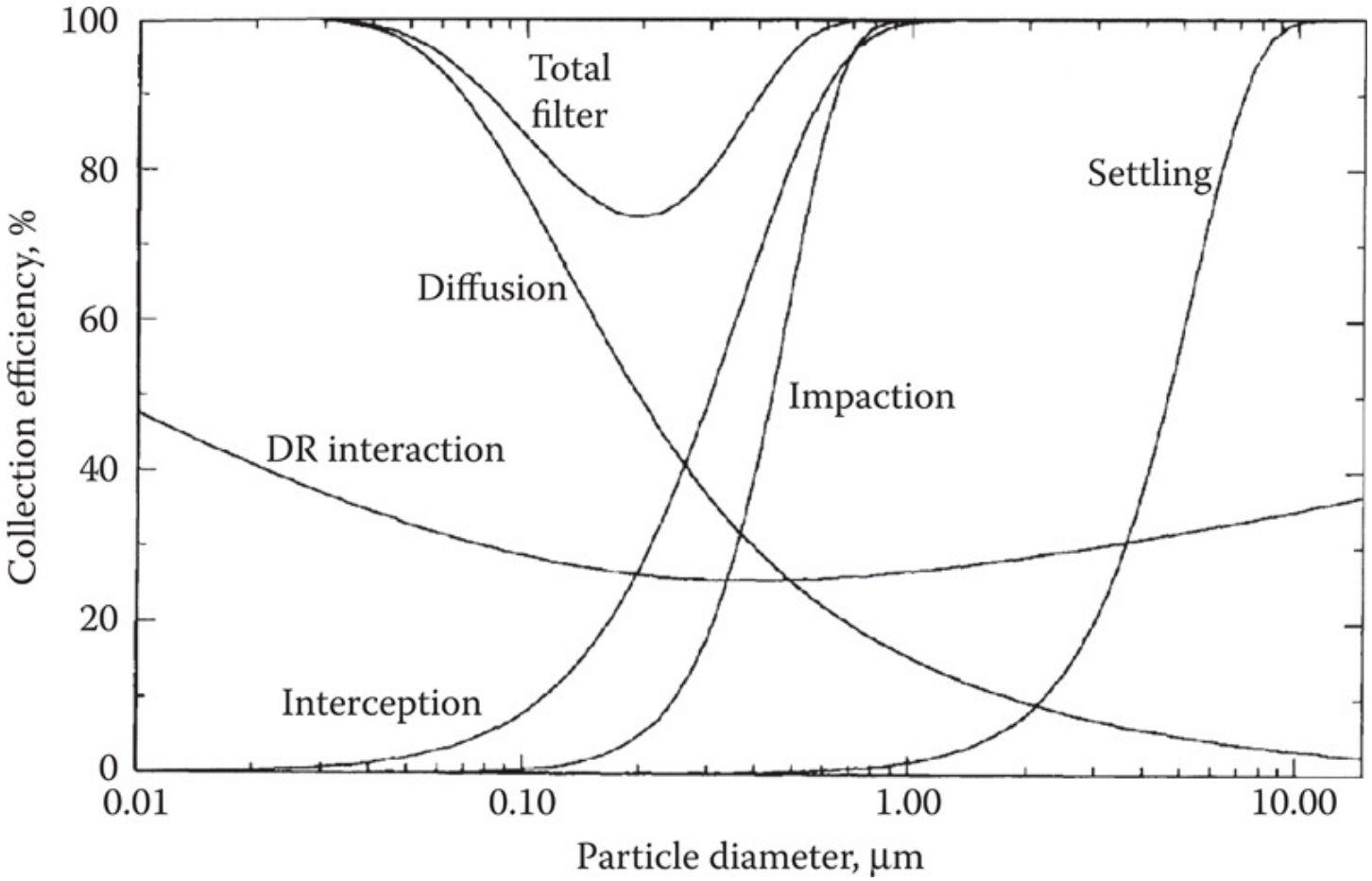

Figure 3.18 Filter efficiency due to different mechanisms. (From Hinds, W. C., *Aerosol Technology: Properties, Behaviour and Measurement of Airborne Particles*, Wiley, New York, 1999.)

3.7.2.2 British Standard smoke method

This technique was devised in the 1920s to measure rather high urban concentrations that were known to be made up mainly of black carbonaceous smoke particles; the method was widely adopted, both for the British National Survey and elsewhere. Ambient air is drawn through a Whatman No. 1 (cellulose) filter paper at around 1.5 1 min^{-1} for 24 h. The standard inlet arrangements involve passing the air down small-bore tubing, giving a size cut of around 5 µm. There is no attempt to sample isokinetically or even to point the sample inlet into the wind. The volume of air sampled is measured by gas meter. The method was originally devised to assess the *blackness* due to smoking chimneys, and the amount of material collected is impracticably small for routine mass determination by weighing (e.g. a concentration of 50 µg m^{-3} would give a deposit of about 100 µg after 24 h). Hence the standard method of analysis is based on reflectometry, which is much more sensitive at low particle loadings. As urban particle concentrations have declined from the hundreds of µg m^{-3} that were common in the 1960s to the tens that are more typical today, and the

FOR REFERENCE PURPOSES ONLY
components have become less influenced by black smoke and more by other materials, such as ammonium sulphate, the reliability of this method has decreased. Although results are issued in gravimetric units, conversion factors must be used to compare these with other, truly gravimetric methods.

3.7.2.3 High-volume sampler

The *Hi-Vol* (Figure 3.19) was developed in North America, where it has been widely used. This device produces the equivalent result over the same time period as the filter above, but gravimetrically. Air is drawn in below the eaves of a protective roof, then vertically down through a rectangular 254 × 203 mm (10″ × 8″) glass-fibre filter paper. A separator may be included before the filter, as in Figure 3.19, to confine the measurement to PM_{10}, for example. The airflow rate is about 1 m^3 min^{-1}, so that over a 24-h period about 1400 m^3 of air are sampled, which would contain 70 mg of particles, if the mass loading was 50 μg m^{-3}. The filter papers themselves weigh around 2.7 g, and with careful procedures such as the equilibration described earlier, the mass can be determined within a few percent.

FOR REFERENCE PURPOSES ONLY

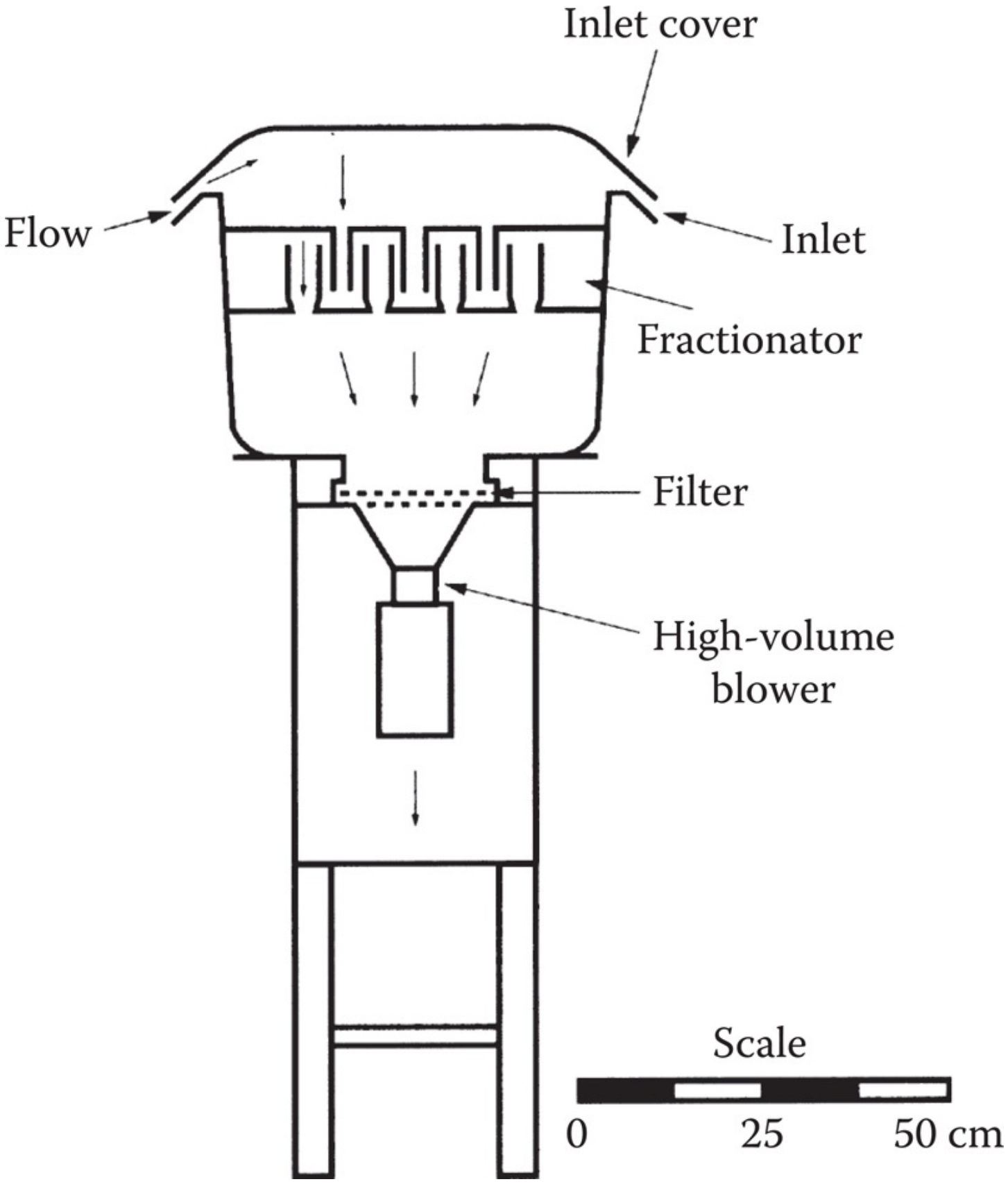

Figure 3.19 Schematic of the high-volume sampler, including PM_{10} head. (From Quality of Urban Air Review Group, *Airborne Particulate Matter in the United Kingdom*, Third Report of the UKQUARG, Department of the Environment, London, UK,

1996.)

The filter material must collect >99% of 0.3 μm particles. If the filters are to be analysed for chemical composition, then various grades of filter that have reduced or more stable background concentrations of certain elements are available. Glass or quartz-fibre filters can also be treated by high-temperature soaking, or by washing with distilled water to remove volatile organics or ionic species. Although glass-fibre filters are widely used, care must be taken because conversion of gaseous SO_2 to particulate sulphate on the filter surface itself can artificially elevate apparent particle loadings. The USEPA specifies an alkalinity of less than 25 microequivalents per gram, and that the filter itself should not gain or lose more weight during a 24-h sample than is equivalent to 5 μg m^{-3}. Additional errors are possible due to reactions of gases with particles on the filter surface, or volatilisation of particles after they have been collected. The supporting measurement needed in order to calculate particle concentration is the volume of air sampled. This is obtained by measuring the pressure drop across orifice plates in the flow path. For basic models the flow rate is measured before use, and again at the end because the build-up of particles reduces the flow; more sophisticated (and therefore more expensive) models have electronic flow controllers to keep the sample rate within ±5% throughout the 24 h.

3.7.2.4 Optical methods

Some of the electromagnetic radiation shining on a particle is scattered away from its original direction. The amount scattered depends on various parameters including the particle's size, and several instruments use this fact to measure properties of the particle population without collecting the particles (which means, of course, that they are not available for chemical analysis either). First, we describe methods for the overall mass loading. Methods which are mainly used to give information on the size distribution are described in Section 3.7.2.7 onwards.

Nephelometers: This family of instruments employs a large view volume to measure scattering from many particles simultaneously. The air sample is passed through a cylinder (typically 2 m long and 15 cm diameter) that is illuminated from one side, and light scattered between 5° (almost forward) and 175° (almost backward) is detected by photomultiplier at one end of the cylinder. Single-wavelength instruments are principally used for measurement of atmospheric optical properties such as extinction coefficient or visibility. Multiple wavelength nephelometers can provide additional information on aerosol size distributions.

Aethalometer: The *aethalometer* is used to measure real-time total concentrations of black carbon (BC) particles. The particles are sampled at around 10 L min^{-1} onto a quartz fibre filter, through which a broad-spectrum light source is shone. The beam is attenuated, and the attenuation converted into a mass concentration of BC on the filter

via a calibration factor (expressed in $m^2\ g^{-1}$). The calibration factor itself varies from site to site, as it will depend on the detailed properties of the BC particles; different workers have found values ranging from 20 in urban areas down to five in remote regions. These values compare with a figure of around 0.05 for mineral dusts such as Saharan sand or road quartz. There is a problem with converting the measurements directly into the equivalent scattering of those particles in the atmosphere, because the close packing of the particles on the filter results in multiple scattering. The same principle has been used in the US to measure coefficient of haze (COH).

A related handheld device known as the direct-reading aerosol monitor (DRAM) is used to measure ambient and workplace particle concentrations. The PM_{10} fraction is selected from an inlet stream that has a flowrate of 2 L min^{-1} and is passed to an optical cell. Near-infrared light is forward scattered from the sample, then the scattered signal is converted to mass concentration via a calibration factor. No information is given on the size distribution. The device is useful for fast semi-quantitative determinations or assessment of changes, but the calibration factor varies with aerosol characteristics.

3.7.2.5 Beta-attenuation

The air sample (possibly after being drawn through a size-selective inlet for PM_{10} or $PM_{2.5}$) is pulled through a filter to deposit particles. A beam of ~0.1 MeV electrons from a radioactive source (a few MBq of krypton 85 or carbon 14) is directed through the filter paper and the flux measured by a Geiger–Müller counter or silicon semi-conductor on the other side. There is an initial attenuation of the beam due to the filter itself, and an increasing attenuation, described by the Beer–Lambert law, as particles accumulate on the filter. The method is most commonly employed as an automated sampler, with separate samples taken on a continuous reel of filter tape. The mass loading is measured intermittently, with a typical minimum time resolution of 30 min, and a detection limit of 5 μg m^{-3} for a 1-h average. System calibration can be automated by inserting a membrane of known mass density into the beam, although this does not allow for the effects of different sample properties. One attraction is that the attenuation is quasi-gravimetric – it should only be affected by the mass of material collected, and not by the size distribution, particle shape or chemical composition. In fact attenuation is due to scattering of the beta particles by atomic electrons in the filter media and deposited particles, and therefore depends on the areal density of these electrons.

Different elements have different ratios of atomic number (i.e. number of electrons) to mass. The ratio varies between 0.4 and 0.5, except for hydrogen for which it is one. In practice, for the mixtures of elements found in particle samples, the ratio is in the range 0.47–0.50, and the error is acceptable. Ammonium compounds such as ammonium nitrate and ammonium sulphate, which contain a high proportion of hydrogen atoms, may require local calibration.

FOR REFERENCE PURPOSES ONLY

3.7.2.6 Resonating microbalance

There are two main variants of this principle. In the first, particles are impacted inertially or electrostatically onto a piezoelectric quartz crystal that oscillates at its natural resonant frequency of around 10 MHz. As the weight of deposited material accumulates, the resonant frequency decreases according to

$$\Delta m = K\left(\frac{1}{f^2} - \frac{1}{f_0^2}\right), \text{ or } \Delta m \cong \frac{2}{f_0^3}\Delta f$$

FOR REFERENCE PURPOSES ONLY

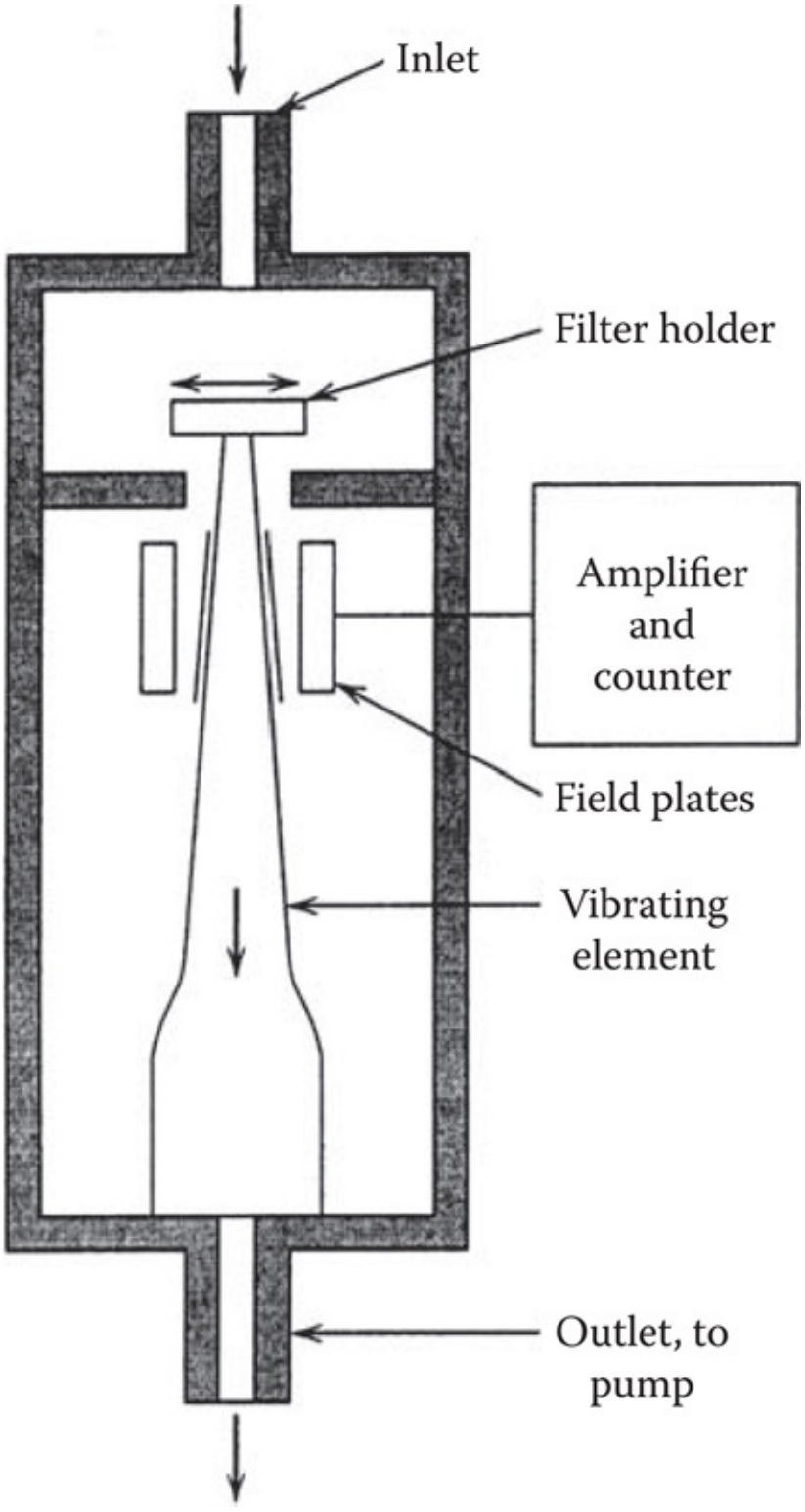

Figure 3.20 The tapered element oscillating microbalance (TEOM). (From Hinds, W. C., *Aerosol Technology: Properties, Behaviour and Measurement of Airborne Particles*, Wiley, New York, 1999.)

so that the change in frequency Δf is directly proportional to the change in mass Δm, provided that Δf is small compared to f_0. The frequency is continuously compared to that of

a reference crystal placed out of the particle flow, and the frequency difference is directly proportional to the collected mass. The device is sensitive, with a minimum time resolution of one minute, but requires the crystal to be manually cleaned periodically.

The other variant of this principle is known as the tapered element oscillating microbalance (TEOM, commonly pronounced tee-om, Figure 3.20). The particles are collected continuously on a filter mounted on the tip of a glass element that oscillates in an applied electric field. Again the natural frequency falls as mass accumulates on the filter. This device has been chosen for PM_{10} measurements in the UK Automated Urban Network, largely because it was the only gravimetric method capable of the required 1-h time resolution when the network was set up in the early 1990s. Although the method is specific to mass loading, there has been a significant systematic error. In order to maintain the constancy of the base resonant frequency while humidity is fluctuating, the oscillating element was maintained at a temperature of 50°C. This temperature is high enough to evaporate volatiles from some particles, resulting in a long-term gradual loss of mass. In specific experiments in which pure ammonium nitrate aerosol was sampled, serious volatilisation losses were experienced which were greatly reduced when the substrate was maintained at 30°C rather than 50°C.

In field trials where the TEOM was compared with co-located high- or low-volume gravimetric samplers, it was found that the TEOM underestimates daily mean PM_{10} concentrations by about 30%, and that this proportion varied with particle composition. As attainment of concentration limits is framed in terms of the number of days on which the limit is exceeded, significant errors in attainment may be generated by this under-reading. For the UK network, it was initially recommended that the indicated mass loadings be increased by 30% to correct for this effect. More recently, the manufacturers have developed a sample pretreatment based on a diffusion drier, which enables the substrate temperature to be reduced to 30°C and effectively eliminates the volatilisation error. Despite this imperfection, the TEOMs in the Automatic Urban and Rural Networks (AURN) have certainly shown the power of rapid-response continuous monitors for understanding the behaviour of urban particulates.

3.7.2.7 Size fractionation

The aforementioned methods give only the total mass loading of particles after arbitrary changes to the ambient distribution have occurred in the sampling system. The methods were widely used in the first generation particle networks – high volume samplers in the US, smoke shade in the UK. Subsequently, it has been realised that we need more specific information about the mass loading in specific size fractions in order to assess potential health effects: the very minimum information required is the mass concentration of particles less than 10 μm (PM_{10}); we are now moving towards a need to know the mass of particles less than 2.5 μm, and for some research activities a complete breakdown of mass loadings in each of five or ten diameter sub-ranges below 10 μm. The range of sizes that we

might be interested in stretches for five decades – from 0.001 μm up to 100 μm. No available particle sizer will cover that range, and at least three quite different techniques would be needed. Each technique will be based on a different particle property such as inertia or mobility, each of them will have been calibrated using a precisely controlled laboratory aerosol quite unlike that being measured, and the results from the different methods may not be directly comparable. Laboratories need to use a bank of different instruments to build up an overall particle size distribution. This requirement has become more pressing as it has become recognised that vehicle exhausts generate significant particles below 1 μm, which are not measurable by the most common (and cheapest) methods.

3.7.2.8 Optical sizers

Single particle counter: A small view volume (a few mm^3) is illuminated by a laser, and the light scattered from it, at an angle to the beam direction, is measured by photomultiplier. When there is no particle in the volume, no light is scattered towards the photomultiplier and no signal results. A pump draws an air sample through the view volume at such a rate that there is usually only one particle in view at a time. Each particle traversing the volume scatters a pulse of light which is recorded, and the larger the particle, the larger the scattered light signal. When enough particles have been sampled to give statistically meaningful results (a minute or two at typical ambient air particle concentrations) the pulse heights are analysed in terms of the number of particles within different diameter ranges. The minimum particle diameter that is measurable with commercial instruments is around 300 nm. Although more powerful lasers can in principle detect smaller particles, there may be a problem with particle heating. The technique has a very large dynamic range, so that one device can be used for a wide range of concentrations, from clean-room conditions with 10 particles m^{-3} up to polluted ambient air with millions of particles m^{-3}. The lower limit is set by the length of time it takes to build up a statistical description of the concentration distribution, and the upper limit by the increasing probability of having more than one particle in the view volume at a time. The manufacturer's calibration is usually achieved by using homogeneous spherical particles of latex or similar material. Natural particle populations are neither spherical nor chemically homogeneous, and it will often be necessary to recalibrate the device gravimetrically against a sample of the aerosol of interest.

3.7.2.9 Aerosol spectrometer

With this technique, light is used to detect the particles but not to size them. The sample air stream in which the particles are suspended is accelerated rapidly. The acceleration of the particles lags behind that of the air because of their inertia, and the lag is larger for aerodynamically larger particles. The lag is measured by the transit time between parallel

laser beams. Hence the true aerodynamic diameter (rather than the mass or physical diameter), which is the parameter that defines particle inhalation and deposition, is determined directly.

3.7.2.10 Inertial impactors

Ironically, this technique relies on exactly the inertial properties of particles that make them so difficult to sample accurately. Air is drawn through an orifice (or jet) towards an obstruction (or particle sampling substrate). The orifice diameter, jet speed and separation of the jet tip from the substrate combine to determine the cut diameter of the stage – that is, the particle diameter above which 50% of particles will be deposited on to the substrate, and below which 50% will remain airborne. The efficiency of each stage depends on the Stokes number, which in this instance is the ratio of the particle stop distance to the half-width of the nozzle aperture.

$$\mathrm{Stk} = \frac{C\rho_p U d_p^2}{18\mu d}$$

The cut diameter is then given by

$$d_p^* = \left[\frac{18\mu d \mathrm{Stk}_{50\%}}{C\rho_p U}\right]^{1/2}$$

$\mathrm{Stk}_{50\%}$ is around 0.25 for round jets, 0.5 for rectangular jets. In practice the impaction stage will be designed approximately using these criteria, then calibrated using monodisperse aerosols. This principle is used in a variety of devices. First, there are size-selective PM_{10} inlets that fit above the filter of the standard high-volume sampler in place of the gabled roof (Figure 3.19). Air is drawn in along a curved path which, at the normal sampler flow rate, leaves most particles of less than 10 μm diameter still in the airstream *en route* to the filter but separates out the larger particles. Although a cut diameter of 10 ± 0.5 μm is specified, it is very hard to achieve this level of precision in practice, because the cut diameter is affected by the flow rate and inlet cleanliness. When properly carried out, the method should yield a precision within ±5 μg m^{-3} for PM_{10} concentrations less than 80 μg m^{-3} or ±7% for higher concentrations. This is one of the reference methods used in the United States for measuring compliance with the National Ambient Air Quality Standards (NAAQS).

FOR REFERENCE PURPOSES ONLY

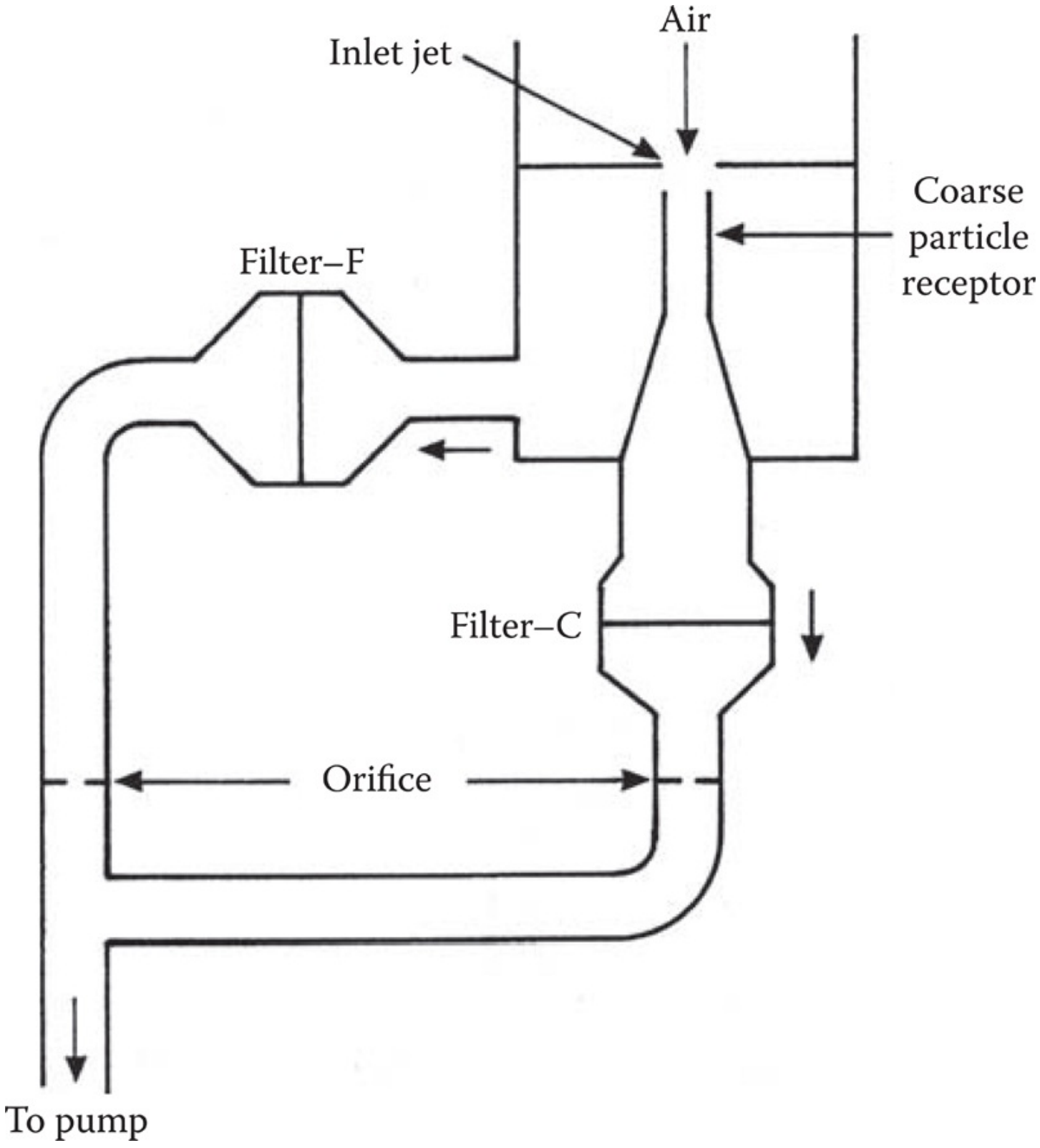

Figure 3.21 Dichotomous sampler. (From Harrison, R. M., Measurements of the concentrations of air pollutants, in S. T. Holgate, J. M. Samet, H. S. Koren and R. L. Maynard (Eds.), *Air Pollution and Health*, Academic Press, London, UK, 1999.)

FOR REFERENCE PURPOSES ONLY

Second, with the so-called dichotomous sampler (Figure 3.21), air from a PM_{10} pre-separator is passed to a virtual impactor. The latter involves a very slow flow rate through filter *C*, so that particles greater than 2.5 μm are *impacted*, whereas those less than 2.5 μm follow the flow to filter *F*. This provides both respirable and fine-particle fractions, usually averaged over a 24-h period. The sample rate is much lower than that of the high volume sampler, at around 17 L min^{-1}. This volume flow rate is not arbitrary – it is designed to simulate the typical adult average breathing rate.

Finally, various specialised size discriminators, called cascade impactors, are available both as inlets for high-volume samplers and as stand-alone devices. Figure 3.22 shows the basic principle. The sample air is passed first through Jet 1, which has the largest diameter and greatest separation from the substrate below it. Hence, the larger particles are deposited on substrate 1 but smaller particles follow the streamlines around it. Jet 2 is smaller in diameter (higher air speed) and closer to substrate 2, so that the smaller particles are retained. By correct arrangement of a sequence of stages having smaller jets, higher speeds and closer substrates, up to ten different cut diameters can be accommodated. The performance of each stage is determined by the Stokes number, and characterised by the cut diameter for which the collection efficiency is 50%. The smallest particles which escape deposition on the final stage may be collected on a back-up filter.

Each substrate can be weighed individually if the variation of mass loading with diameter is required, and the collected material is available for analysis to show the variation of chemical properties with particle size. Of course, as with most things in life, there are trade-offs. The large number of stages gives a high pressure drop and uses more power. High jet speeds in the final stages mean a greater risk of breaking up large particles into smaller ones, and also of re-entraining deposited particles back into the air stream. The very small amounts collected on some stages may make it difficult to weigh or analyse them with the required accuracy.

FOR REFERENCE PURPOSES ONLY

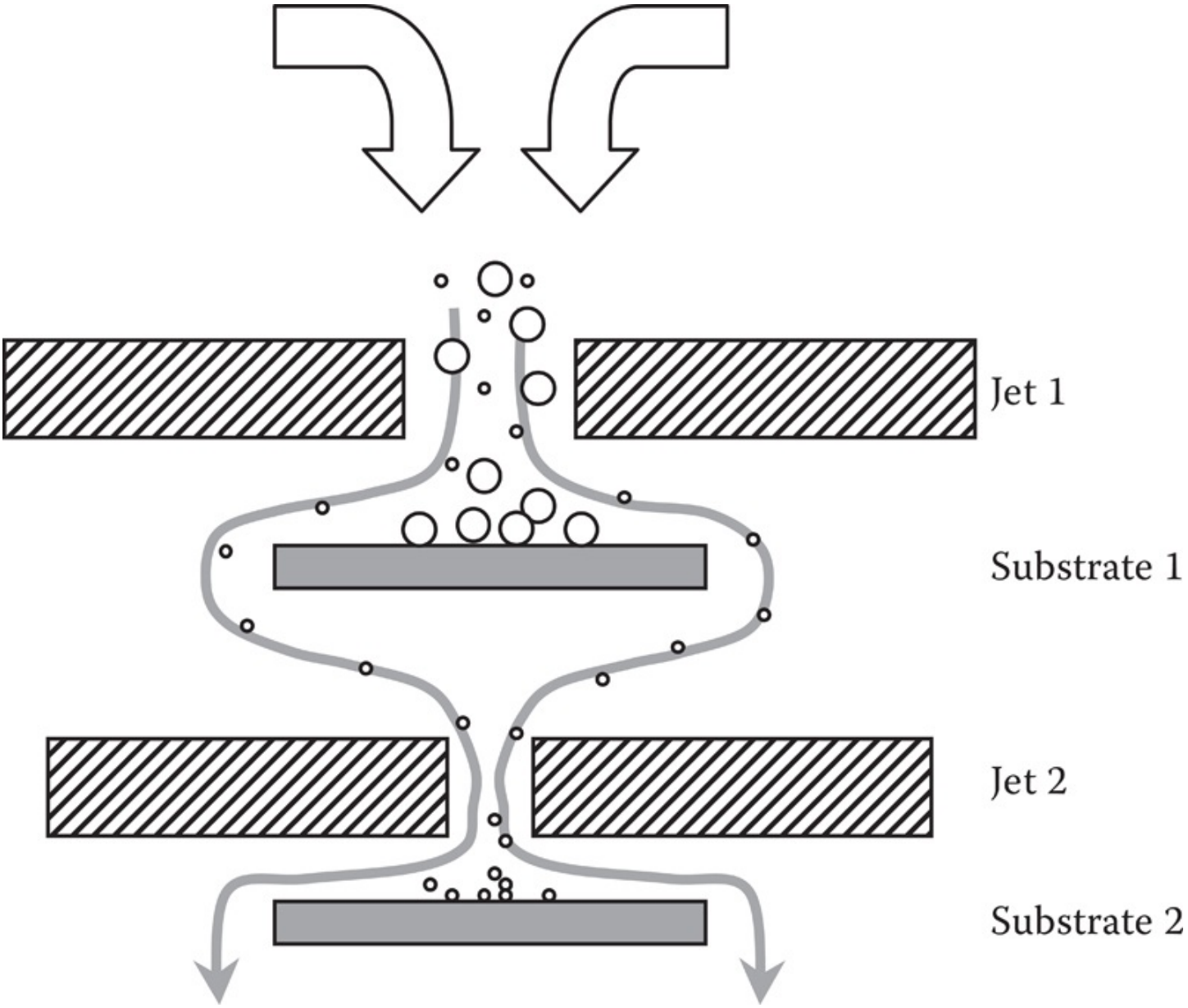

Figure 3.22 The principle of a two-stage cascade impactor.

The standard cascade impactor cannot normally be used to measure particles smaller than about 0.3 μm because the high air speeds needed for deposition cause unacceptable pressure drops and impact forces. The size range has been extended with the *electrostatic low pressure impactor* (ELPI), in which reduced air pressure (and hence a larger value for C) enables deposition of particles down to around 30 nm. Even this is not small enough to include the mode of the number distribution produced by engines running on low-sulphur fuel. One disadvantage is that the low air pressure (about 8 kPa at the final stage) increases the evaporation from semi-volatile particles. The ELPI also charges the particles electrostatically and measures the rate of particle deposition from the current flow to each stage. Hence it can be used in real time rather than having to wait for a weighable deposit to accumulate on each stage. However, these image and space charges themselves generate a

FOR REFERENCE PURPOSES ONLY

new force on the particles which may change their deposition characteristics. In the *micro-orifice uniform deposit impactor* (MOUDI), which is another equipment using the same principle, the particles are deposited on rotating substrates to avoid re-entrainment, and the mass is determined gravimetrically.

3.7.2.11 Electrical mobility analysers

In the differential mobility analyser (DMA)/spectrometer, electric fields are used to separate particles according to their mobility (which is a function of diameter). The transfer function is the particle penetration as a function of the electrical mobility for a given voltage and flow setting. The DMA has also been used to measure both cloud droplets and the aerosols that accompany them. If an individual droplet is first charged and then evaporated to dryness, the electric charge on the residue is a function of the original droplet diameter. Detection is via either condensation of water vapour on each particle and subsequent light scattering, or deposition of electric charge to an electrometer. In instruments such as the scanning mobility particle sizer (SMPS) and electrical aerosol analyser (EAA), the aerosol is first passed through a charger (e.g. Krypton 85) that applies a bipolar electrostatic charge to the particles (Figure 3.23). The mean particle charge is close to zero, but a fraction of the particles carry charges of ±1, ±2, and so on.

FOR REFERENCE PURPOSES ONLY

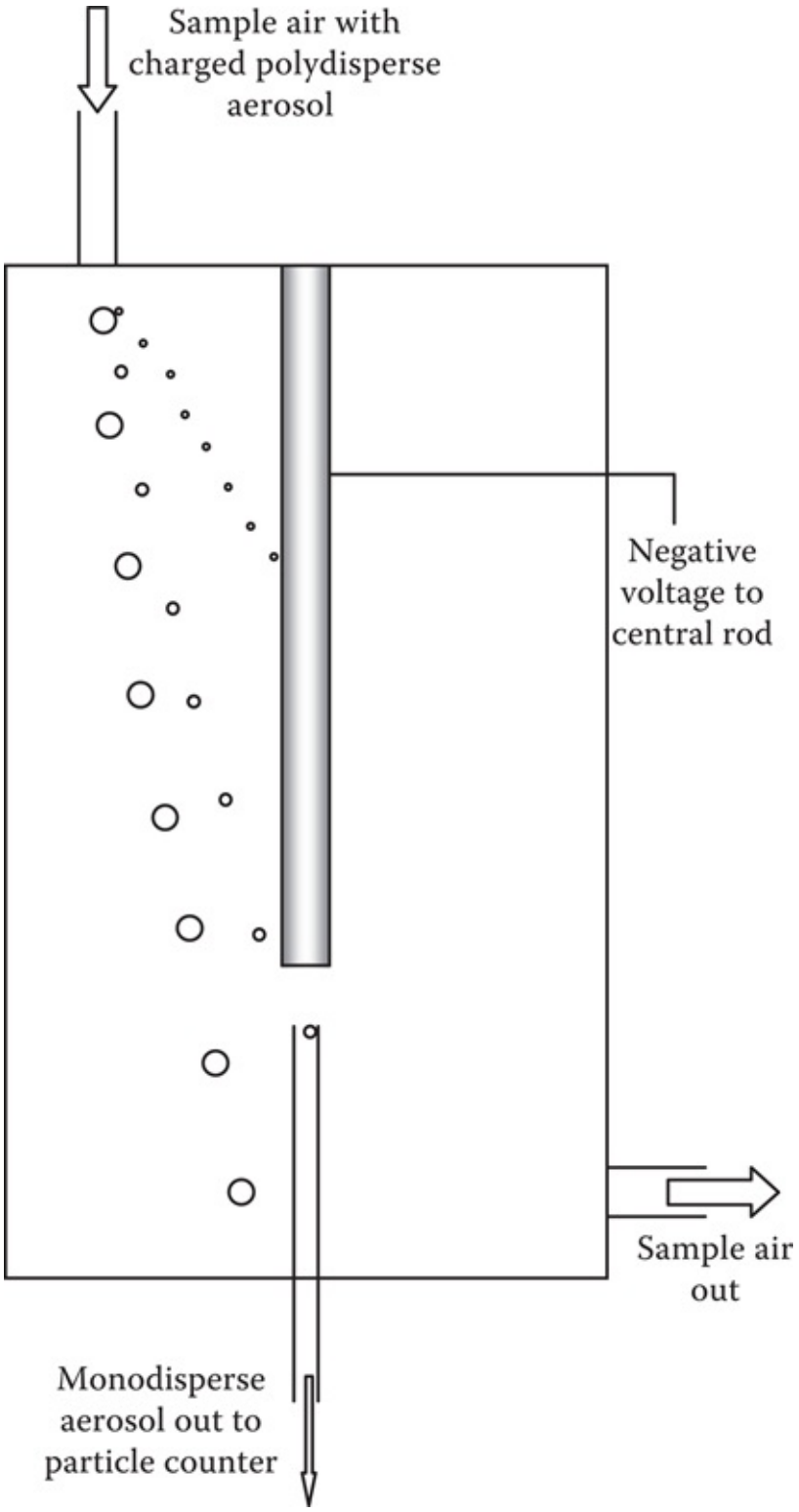

Figure 3.23 Electrostatic classifier.

The system is designed so that the charge distribution is independent of the chemical composition and morphology of the particles. Then the aerosol flows through the annular region between a cylindrical steel housing and a coaxial central rod. A variable voltage difference is applied between the two. Positively charged particles are attracted towards the negative central rod, while negatively charged particles are attracted towards the outer

cylinder. Each particle takes up an equilibrium radial drift velocity v_{drift} towards the appropriate plate such that

$$v_{\text{drift}} = \frac{EeC}{3\pi\mu d_p}$$

where:

E is the electric field strength
e is the electron charge
C is the Cunningham slip correction factor
μ is the air viscosity
d_p is the particle diameter

The particles will have a residence time in the cylinder which is determined by the axial velocity v_{axial} and the length. At any given voltage setting, the smallest particles with the highest mobilities will be deposited on the rod. The largest will leave without attaining significant radial velocities. Hence a small diameter range will be selected by the outlet, where they can be counted by a condensation particle counter (or the current measured). By varying the field strength and residence time, particles of different sizes may be allowed to pass through. The measured size range is typically 10 nm–0.5 μm, and 2–3 min are needed to accumulate the measurements across the sequence of cut diameters. This makes the technique too slow, for example, to determine variations in particle emissions from engines operating in a transient mode.

3.7.2.12 Diffusion batteries

The sample air passes in laminar flow between closely spaced parallel plates or along cylindrical pipes. Particles of different sizes diffuse with different speeds to the walls, with the smaller particles more likely to be retained. By varying the flow parameters, particles above a cut diameter will penetrate and be counted (by a CNC). Size ranges of 5–500 nm have been determined.

3.7.2.13 Condensation particle counter

The *condensation particle counter* (CPC, also known as the *condensation nucleus counter* (CNC) or *Aitken nucleus counter*) is used to measure the total number concentration of particles in the diameter range from a few nanometres to 1 μm. The particles are introduced into a chamber where they are exposed to a water- or alcohol-based supersaturated vapour. The particles act as condensation nuclei for droplets that grow to around 10 μm diameter, when they are large enough to be detected and counted, usually by optical methods. As the growth is diffusion-limited, all the droplets are of similar diameter even if the original

particles were highly polydisperse. Because the supersaturation is very high, it makes no difference what the original particle was made of – it simply serves as a condensation centre. In some designs the supersaturation is created cyclically by adiabatic expansion, and in some it is created continuously by conduction cooling. Individual particles can be counted if the concentration is low enough. At higher concentrations an optical method based on attenuation of a beam by the droplet cloud is used. Problems may be caused by excessive concentrations of nanoparticles (<20 nm), which are undercounted because the vapour has been depleted. An adaptation of this technique is used to count cloud condensation nuclei (CCN) particles. These are activated by the low supersaturations (0.01%–1%) found in updrafts and clouds. The controlled supersaturation is achieved by maintaining two wetted surfaces at different temperatures.

3.7.3 Chemical composition of aerosols

The primary component of the accumulation and ultrafine aerosol includes elemental carbon and high-molecular weight organic compounds from fossil fuel combustion and biomass burning. The secondary component includes photochemical reaction products and organic condensates. Some of the particles include significant water if they are hygroscopic and the relative humidity is high (over about 60%). Other substances include short-lived intermediates, such as peroxides and free radicals, of gas- and aerosol-phase chemical reactions. Many of the measurements made of airborne particles have focussed on the mass loading and size distribution regardless of the chemical composition, and this has been reflected in legislation and air quality guidelines concerning particles. We are just beginning to address this lack of understanding, and it is possible that in the future it will be seen just as naive to discuss total particle concentration as it is to discuss total gas concentration today. A range of techniques has been used to achieve our current understanding:

- *Wet chemistry of bulk samples*: Particles are accumulated on a filter, typically over a period of at least a few hours, and analysed by the full range of chemical laboratory techniques for the materials of interest. This method has been used to investigate the photochemical formation of ammonium sulphate and nitrate, the production of sea salt particles from ocean droplets, fluoride pollution from point sources. Increased sophistication is available from other devices. Atomic absorption is routinely used for metal analysis; ion chromatography for ions such as sodium and calcium; inductively coupled plasma (ICP) spectroscopy can give 20 metals simultaneously, neutron activation analysis (NAA) can give up to 35 elements. Carbon content (by solvent extraction or thermal decomposition) can also be determined. For semi-volatile compounds such as ammonium nitrate, volatilisation of the collected particles in the presence of variable concentrations of gaseous component before analysis is a serious source of error. In this case the diffusion denuder can be used to separate the gas from

FOR REFERENCE PURPOSES ONLY

the particles.

- *Optical microscopy*: Studies of individual particles on a substrate can be useful for source attribution. Collections of photographs of known materials are available for comparison. Standard microscopy can be enhanced with techniques such as polarising filters.
- *Scanning electron microscopy* (*SEM*): Not only does this give 3-D images of particles, which makes visual identification more straightforward, but the instrument can be used with a number of bolt-on analytical devices, such as energy-dispersive analysis of X-rays (EDAX), which give a powerful method of performing chemical analyses on individual particles once they have been collected on a substrate.
- *Transmission electron microscopy* (*TEM*): Again, collections of micrographs are available for comparison.
- *X-ray fluorescence* (*XRF*): It allows for multi-element bulk aerosol sample analysis. Particles are first collected on a membrane filter (so that they remain on the surface rather than getting buried within the filter as they would with glass fibre). Photons (X-rays) are used to knock an inner orbital electron out of an atom. The vacancy is filled by an outer electron, and the excess binding energy released as an X-ray. The energy of the X-ray is determined by the difference between the energies of the two orbits, and hence spectroscopic analysis gives the element involved, with determination of all elements simultaneously. Elements with atomic numbers less than 12 cannot be determined by this method, which rules out many environmentally important elements such as sodium and magnesium. The methods for determining the energy of the emitted X-ray are either *wavelength dispersive* or *energy dispersive* (EDXRF), with the latter being more common because it is cheaper. Detection limits for both methods are in the 1–10 μg g^{-1} range. However, the vacuum environment of the electron microscope, together with local heating from the electron beam, tend to give problems with volatile components.
- *Proton-induced X-ray emission* (*PIXE*): In this method heavy charged particles, such as 1–4 MeV protons, are used to generate the X-ray fluorescence instead of photons. The X-ray spectrum is measured with an energy-dispersive detector. The minimum sample mass is lower, and the detection limit an order of magnitude smaller, than for EDXRF (down to pg g^{-1}), although the inability to sample light elements remains.
- *Neutron activation analysis* (*NAA*): The sample is irradiated with thermal neutrons from a nuclear reactor, which makes a small proportion of the stable atomic nuclei radioactive. The original elements present can be determined by measuring the radioactivity. Normally, the emitted γ-rays are measured with a spectrometer and the elements identified from the occurrence and strength of the lines in the γ-ray spectrum.
- *Laser microprobe mass spectrometry*: Particles collected on a substrate are irradiated with a high power laser. The ejected ion fragments are then analysed by a mass spectrometer. Trace levels of metals can be detected at the ppm level in individual

particles, inorganic compounds such as nitrates and sulphates can be speciated, and surface species can be differentiated from those in the body of the particle.

These methods only give the composition in terms of elements rather than compounds, although much can be inferred from the ratios of components. A further limitation is that examination of a statistically significant number of individual particles can be both laborious and time-consuming. Clearly, there is no simple single method that will give the information needed for a complete characterisation of particle chemistry. Use of complementary methods is needed in order to build up as full a picture as possible. Even when that has been done, it must be remembered that repeat sampling at a different time of year or in a different location will probably give different results.

3.7.3.1 Particle microstructure

With advances in instrumental analysis techniques it has become feasible, although not yet routine, to investigate the microstructure of individual particles on spatial scales of ~0.01 μm. Very few particles are physically or chemically homogeneous. It is more normal for any particle to have, for example, a core of one material such as carbon, with a surface shell of another material such as condensed volatiles. Elements of anthropogenic origin such as tin, titanium, chromium and lead are mainly released into the atmosphere in gaseous form during fossil fuel combustion. They eventually form a thin surface film on large mineral particles. Fly-ash particles from coal burning can also have very non-uniform element distributions, with surface concentrations of toxic elements such as lead which can be thousands of times the average concentration in the particle. These particles have been much studied due to their large emissions and widespread prevalence in the troposphere. Studies downwind of smoke plumes from oil well fires have shown that particle surface sulphate deposits increase with distance, indicating a gas-to-particle conversion process. Urban aerosol particles have been found to have a shell structure, with an inner core of soil-based material, a layer of carbonate and organic carbon compounds, and a surface layer only 60 nm thick of nitrate and ammonium sulphate.

3.7.3.2 Real-time chemical analysis

Some of the methods normally used for laboratory analysis have been automated to give *in situ* measurements in near-real time, usually on a cycle that integrates over about 1 h. Methods are currently being developed to give true real-time chemical properties of individual particles, although the smallest particle size for which they have been used thus far is around 1 μm. The most developed technique is *particle analysis by mass spectrometry* (PAMS). Typically, a few hundred particles per minute are first sized by a time-of-flight method. The particles are then individually volatilised and ionised by a high-energy (e.g. excimer) laser, which is itself triggered by the passage of the particle through the sizing

FOR REFERENCE PURPOSES ONLY

laser. The ionised fractions then enter a *time-of-flight mass spectrometer* (TOFMS).

3.7.4 Measurement of coarse particle deposition

Large particles (having aerodynamic diameters greater than about 20 μm) have sedimentation speeds that are significant compared to vertical turbulent speeds in the atmosphere and therefore settle out onto surfaces. When industrial processes such as crushing, grinding, ploughing, quarrying or mining generate significant emissions of these large particles, there can be a local nuisance problem with deposition to the surrounding area, making cars, paintwork and laundry dirty. There is unlikely to be a health issue, as the particles are too large to be inhaled. Standards have been difficult to lay down, as what is clean to one person may be dirty to another, and the effect will vary depending on the combination of surface colour and dust colour – coal dust will be noticed much more quickly on white windowsills than would limestone quarry dust. A guide value of 200 mg m^{-2} day^{-1} has been suggested, but is certainly not accepted universally. These particles are not in suspension in the air and cannot be measured by the active sampling/filtration methods discussed earlier for aerosol. Particle deposition has instead been measured for many years by a variety of deposit gauges. Their common feature is a collector which presents a horizontal circular area into which the particles fall.

For the BS deposit gauge (see Section 3.7.2), the circular area is the upper rim of a glass or plastic funnel, as in Figure 3.24. Particles that fall into the funnel are washed by rain into a collecting bottle during a period of one month, after which they are filtered from the liquid, dried and weighed. The mass of particles is then divided by the funnel area and the collection period to calculate the deposition rate in mg m^{-2} day^{-1}. The sample can also be analysed for soluble and insoluble fractions or other chemical components which might give additional information on the source of the dust. The collection process sounds straightforward but is far from it. First, although the particles are sedimenting, their terminal speeds are much lower, typically by factors of 10 or 100, than typical horizontal wind speeds in the lower atmosphere. Hence they are *falling* almost horizontally, and the deposit gauge will present a very thin ellipse rather than an open circle. Edge effects caused by turbulence as the wind blows over the rim of the gauge also interfere with the smooth deposition process. Wind-tunnel tests have shown the collection efficiency to be very low at normal combinations of particle diameter and wind speed. Second, rainfall is an intermittent process – it only rains for 7% of the time in the UK. Hence dust will be deposited into a dry container most of the time, and can get blown out again, or re-entrained, by atmospheric turbulence. As the gauges are usually left out for many days or weeks, significant losses can occur during long dry spells.

FOR REFERENCE PURPOSES ONLY

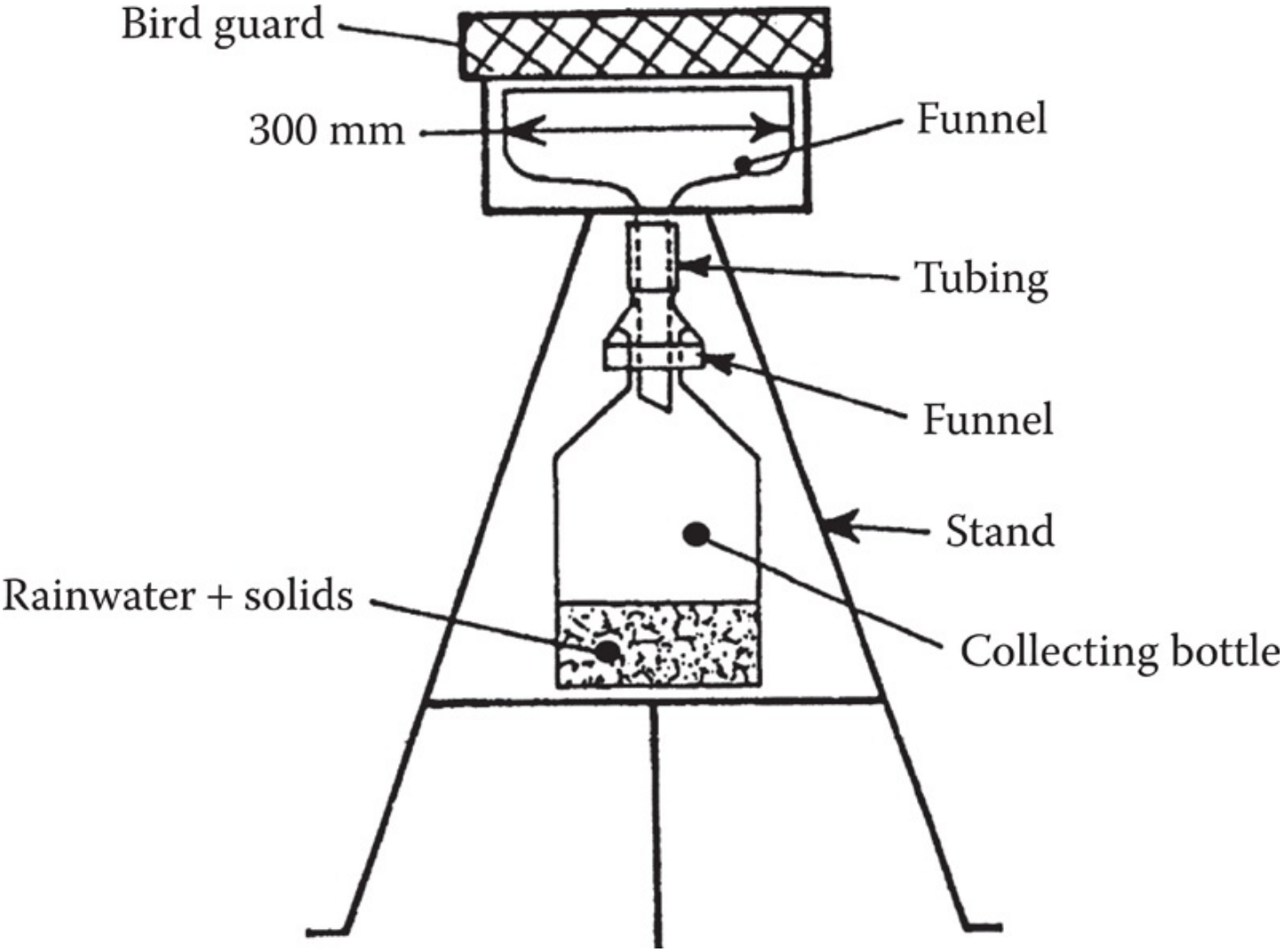

Figure 3.24 BS deposit gauge.

Other deposit gauges have been designed on the same basic principles. The International Standards Organisation (ISO) gauge is simply an upright vertical cylinder, designed to allow particles to fall into stagnant air well below the rim and reduce particle re-entrainment. The flow disturbance and re-entrainment problems of deep gauges have prompted the development of very shallow dish collectors with a low rim, often referred to as frisbee gauges (Figure 3.25). They are cheaper and lighter, which also makes them attractive for short-term surveys where vandalism might be a problem. Their low profile reduces both the disturbance to the flow and the development of the internal vortex that causes re-entrainment, and their collection efficiency is less sensitive to wind speed. Various modifications have been tested to improve their performance, such as fitting a nylon mesh across the top and a foam liner to the inside to reduce splash. These changes will all affect performance by uncertain amounts. Petri dishes have also been used for measurements taken over short periods (a day or two) under calm conditions.

FOR REFERENCE PURPOSES ONLY

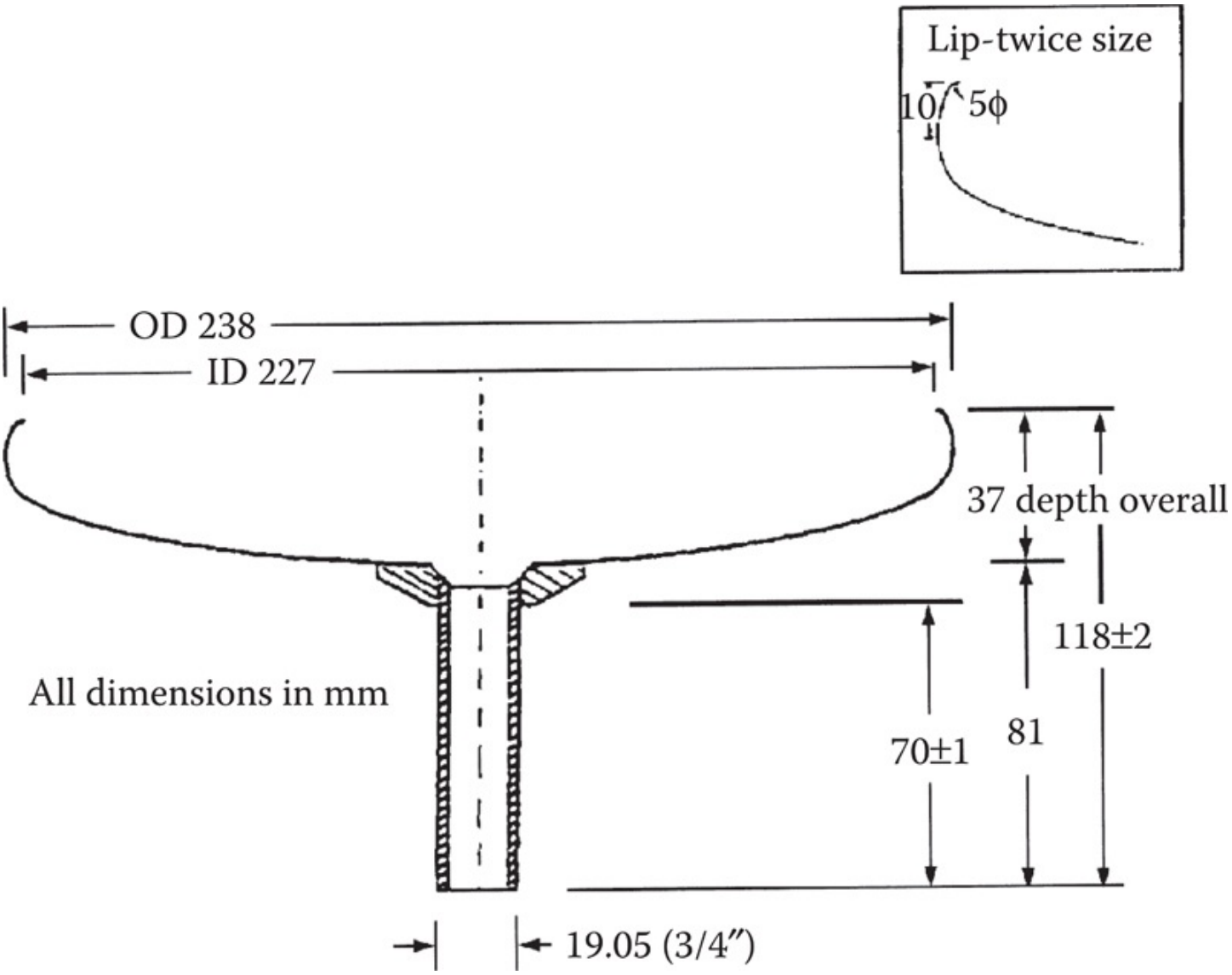

Figure 3.25 Frisbee deposit gauge. (From Mark, D., in R. M. Harrison and R. van Grieken (Eds.), *Atmospheric Particles*, Wiley, Chichester, UK, 1998.)

In the middle part of the twentieth century these deposit gauges were the main method of measuring atmospheric particulate pollution in urban areas, and formed a part of the UK National Survey. As coarse dust emissions have been reduced, urban deposition values have fallen from around 500 mg m^{-2} day^{-1} to below 100. Attention has switched to smaller suspended particles, and deposit gauges have fallen into disuse for general air pollution measurements, although they are still appropriate for specific source investigations.

The fact that most particles are falling with almost horizontal trajectories has been used to advantage with the directional dust gauge. In this design (Figure 3.26), there are four cylindrical collectors, each of which has a vertical slit facing outward. When the wind is blowing towards a particular slit, the streamlines diverge around the cylinder and the particles are deposited inertially into the slit, after which they settle into removable bottles below. The directional gauge can be placed, for example, on the perimeter of a source such

FOR REFERENCE PURPOSES ONLY

as an open-cast coal mine or quarry. After exposure for a few days or weeks, examination of the relative amounts collected in the four bottles, after correction for the proportion of time for which the wind has been blowing from those directions, will give an indication of the source direction. This might be confirmed by microscopic or chemical analysis of the samples. There are uncertainties connected with swirl around the cluster of cylinders causing deposition in the *wrong* collector, and the variability of collection efficiency with wind speed.

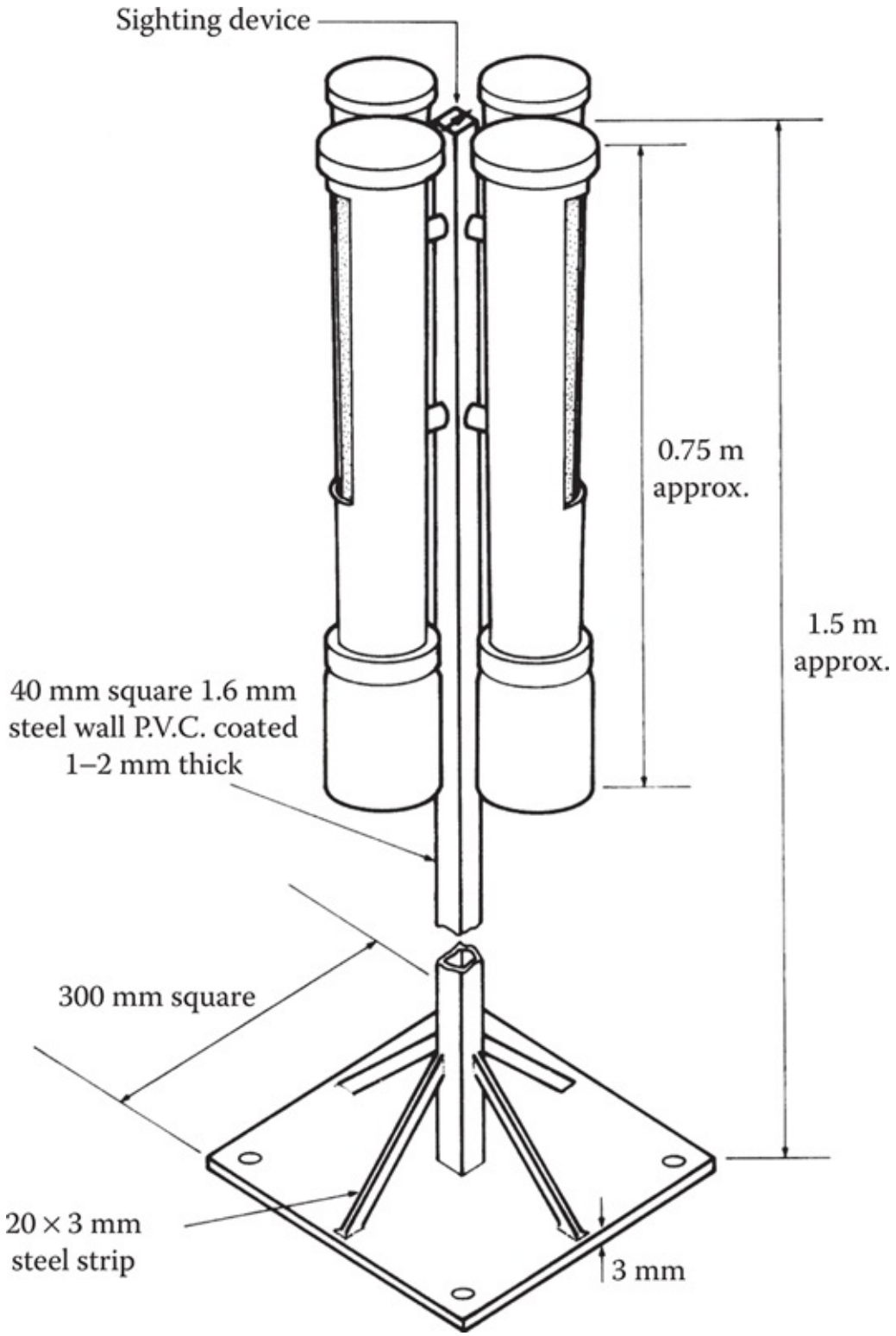

FOR REFERENCE PURPOSES ONLY

Figure 3.26 BS directional deposit gauge. (From Pio, C. A., in R. M. Harrison and R. Perry (Eds.), *Handbook of Air Pollution Analysis*, Kluwer Academic Publishers, Dordrecht, the Netherlands, 1986.)

It is possible to determine the size distribution of coarse particles, but much care is needed with sampling conditions in order retain the larger particles. Size fractions can be separated by means of an elutriator, in which a vertical updraft of air carries away particles having less than the designed sedimentation speed while retaining the remainder. Centrifugal forces generated by relatively gentle bends can be used to discriminate particles in the 10–100 μm diameter range. Other simpler semi-quantitative methods are also in use to assess nuisance from deposited dust. First, white sticky tape can be exposed and the results expressed as percent area coverage by measuring the percent reduction in reflectance (per day). Second, glass microscope slides can be exposed horizontally, and the resulting reduction in reflectance expressed in soiling units, where one soiling unit is a 1% reflectance reduction.

3.8 CASE STUDY – ASBESTOS

The term asbestos includes several naturally occurring fibrous inorganic minerals with remarkable thermal and structural properties, which have been widely used as a thermal insulating material in lagging, pipe insulation, fire doors and partitions, as an additive in the manufacture of roofing sheets, cement and gypsum, and in the manufacture of brake linings. The asbestos minerals fall into two groups: (1) chrysotile, and (2) the amphiboles. They are characterised by their crystallographic properties, which result in the formation of weakly bound *fibrils* with an initial length of around 1 mm. The fibrils of all forms of asbestos, and especially of the amphiboles such as crocidolite (blue asbestos) break down lengthways so that the width of the fibre may be only 0.05–0.5 μm. Identification of a particle as asbestos requires that it be asbestiform (Figure 3.27). This width gives them an aerodynamic diameter range of around 0.1–1 μm (the aerodynamic diameter of a long thin cylinder is around three times the cylinder diameter), so that they can easily penetrate into the alveolar regions of the lung.

The fibres are deposited by the usual mechanisms of sedimentation, impaction, interception, electrostatic precipitation and diffusion. They are not cleared efficiently by the usual processes of dissolution and phagocytosis, especially if they are longer than about 10 μm, because the macrophages are 10–15 μm in diameter and cannot ingest long fibres. The attempts by alveolar macrophages to remove the fibres generates reactive oxygen species such as hydrogen peroxide which damage the alveolar epithelial lining and mesothelial lining. The regeneration of mesothelial cells in this environment can result in uncontrolled proliferation, which is the cancer known as malignant mesothelioma. Asbestosis, which is a fibrosis of the lung, may also result. Although asbestos has been

FOR REFERENCE PURPOSES ONLY

replaced for most of its former uses, it can be released at any time – if old insulation is removed, for example. Asbestos health issues originally focused on the acute exposures (~1 fibre cm^{-3}) experienced by miners and factory workers, but it has since been realised that the chronic exposures of those living in asbestos-clad homes and other high ambient concentrations (~0.001 fibre cm^{-3}) pose a serious threat to population health. The mortality rate associated with asbestos exposure in industrialised countries is believed to total tens of thousands of people per year. However, there is not thought to be a significant risk from outdoor ambient concentrations.

FOR REFERENCE PURPOSES ONLY

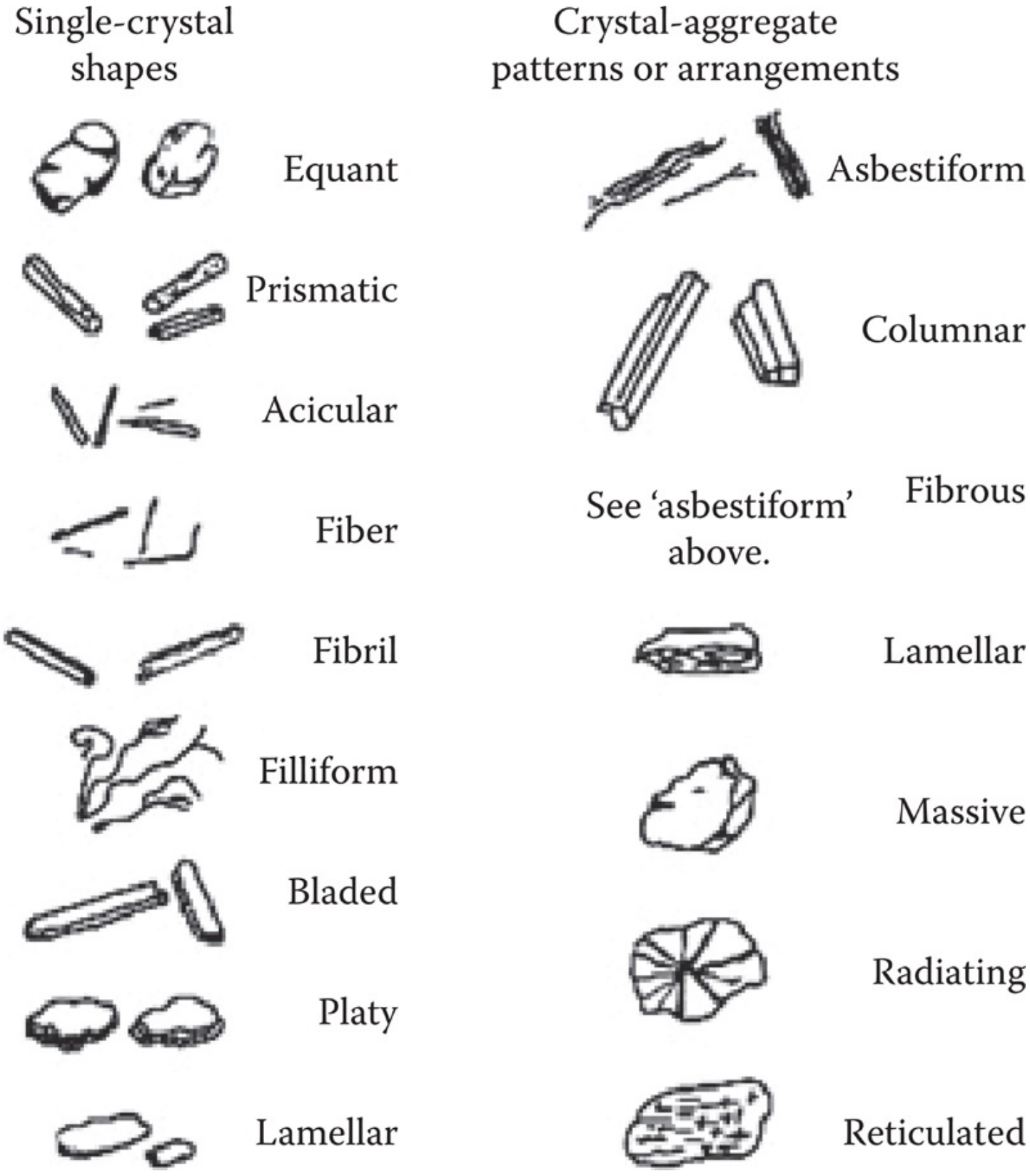

Figure 3.27 Patterns of particle arrangements in asbestiform relative to other single- and aggregate-crystal particle shapes. (From Department of Industrial Relations, US Bureau of Mines, www.dir.ca.gov.)

Because the risk is associated with the presence of a fibre rather than with the mass

FOR REFERENCE PURPOSES ONLY

loading, the health guidelines are framed in terms of a number density at 0.1–0.2 fibres mL^{-1}. Average concentrations in rural air have been found to be around 0.00001 fibres mL^{-1}, rising by a factor of ten in urban air. There are also man-made vitreous fibres such as glass fibre. These materials are around 10 μm diameter and do not split lengthways, so that they do not penetrate beyond the thorax, if inhaled, and do not cause cancers.

REFERENCES AND FURTHER READING RESOURCES

Baron, P. A. and Willeke, K. (2005) *Aerosol Measurement: Principles, Techniques and Applications*. Wiley, New York.

Carmichael, G. R., Adhikary, B., Kulkarni, S., D'Allura, A., Tang, Y., Streets, D., Zhang, Q. et al. (2009) Asian aerosols: Current and year 2030 distributions and implications to human health and regional climate change. *Environmental Science & Technology*, 43(15): 5811–5817.

Colbeck, I. (Ed.) (1998) *Physical and Chemical Properties of Aerosols*. Blackie, London, UK.

Conti, M. E. and Cecchetti, G. (2001) Biological monitoring: Lichens as bio indicators of air pollution assessment – A review. *Environmental Pollution*, 114: 471–492.

Department of Industrial Relations, U.S. Bureau of Mines. www.dir.ca.gov.

Ebert, M., Weinbruch, S., Hoffmann, P., and Ortner, H. M. (2000) Chemical characterization of North Sea aerosol particles. *Journal of Aerosol Science*, 31(5): 613–632.

Friedlander, S. K. (2000) *Smoke Dust and Haze: fundamentals of Aerosol Dynamics*. Oxford University Press, New York.

Grant, K. E., Chuang, C. C., Grossman, A. S., and Penner, J. E. (1999) Modelling the spectral optical properties of ammonium sulfate and biomass burning aerosols: Parameterization of relative humidity effects and model results. *Atmospheric Environment*, 33: 2603–2620.

Harrison, R. M. (1999) Measurements of concentrations of air pollutants. In: S. T. Holgate, J. M. Samet, H. S. Koren and R. L. Maynard (Eds.), *Air Pollution and Health*. Academic Press, London, UK.

Harrison, R. M. and van Grieken, R. (Eds.) (1998) *Atmospheric Particles*. Wiley, Chichester, UK.

Hinds, W. C. (1999) *Aerosol Technology: Properties, Behaviour and Measurement of Airborne Particles*. Wiley, New York.

Lacey, M. E. and West, J. S. (2006) *The Air Spora: A Manual for Catching and Identifying Airborne Biological Particles*. Springer, Dordrecht, the Netherlands.

Leygraf, C. and Graedel, T. (2000) *Atmospheric Corrosion*. John Wiley & Sons, New York.

Lippmann, M. (2000) Introduction and background. In: M. Lippmann (Ed.), *Environmental Toxicants*. Wiley, New York.

Mark, D. (1998) Transport and sampling of aerosols. In: I. Colbeck (Ed.), *Physical & Chemical Properties of Aerosols*, pp. 80–152. Blackie Academic & Professional, London, UK.

Mark, D. (1998) In: R. M. Harrison and R. van Grieken (Eds.), *Atmospheric Particles*. Wiley, Chichester, UK.

McMurry, P. H. (2000) A review of atmospheric aerosol measurements. *Atmospheric Environment*, 34: 1959–1999.

Monteith, J. L. and Unsworth, M. H. (1990) *Principles of Environmental Physics*. Edward Arnold, London, UK.

NAEI. (2016) *UK Emissions of Air Pollutants 1990 to 2015*. National Atmospheric Emissions Inventory, London, UK.

Pio, C. A. (1986) In: R. M. Harrison and R. Perry (Eds.), *Handbook of Air Pollution Analysis*. Kluwer Academic Publishers, Dordrecht, the Netherlands.

Quality of Urban Air Review Group (1996) *Airborne Particulate Matter in the United Kingdom*. Third Report of the UKQUARG, Department of the Environment, London, UK.

Raes, F., Van Dingenen, R., Vignati, E., Wilson, J., Putaud, J.-P., Seinfeld, J. H., and Adams, P. (2000) Formation and cycling of aerosols in the global troposphere. *Atmospheric Environment*, 34: 4215–4240.

Ruzer, L. S. and Harley, N. H. (Eds.) (2004) *Aerosol Handbook: Measurement, Dosimetry and Health Effects*. CRC Press, Boca Raton, FL.

Spurny, K. R. (2000) *Aerosol Chemical Processes in the Environment*. CRC Press, Boca Raton, FL.

FOR REFERENCE PURPOSES ONLY

Vincent, J. H. (2007) *Aerosol Sampling: Science, Standards, Instrumentation and Applications*. Wiley-Blackwell, Chichester, UK.

FOR REFERENCE PURPOSES ONLY

Chapter 4

Area sources

Area sources of air pollution are relatively dispersed emissions over large areas with relatively constant source strength over space but can have very large temporal changes in their emissions. Common area sources of gaseous and particulate air pollution in the past have mainly geological origins, such as volcanoes, dust storms and wildfires. However, with the growing human influence on the earth's system processes there have been additional anthropogenic area emission sources, such as landfills, farm emissions, slurry lagoons, and so on. In this chapter we will discuss some of the common area sources and the emerging trends in their management practice, with specific focus on anthropogenic emissions.

4.1 BIOGENIC AREA SOURCES

4.1.1 Wildfires

Wildfires (also known as forest fires) can be as potent source of air pollution as conventional traffic, despite having natural origins. For example, the wildfires blazing across Northern California in autumn 2017 produced more than 10,000 tonnes of $PM_{2.5}$, which is approximately the $PM_{2.5}$ amount released by on-road vehicular sources in the state in the entire 2014. Wildfires can have a significant impact on local air quality, visibility, and human health. Emissions from forest fires can travel large distances and produce harmful effects far away from the fire location. Typical forest fire emissions include: particulate matter, carbon monoxide, atmospheric mercury, ozone-forming chemicals and volatile organic compounds. This exacerbates the air pollution levels in developed countries to comparable levels in other more pollution parts of the world. Especially, high increase in fine particulate matter due to wildfire smoke is associated with increased risks on acute respiratory admissions.

According to the US National Oceanic and Atmospheric Administration, a warmer and

FOR REFERENCE PURPOSES ONLY

drier climate is expected to lead to more frequent and more intense wildfires near or within populated areas in the US West and Canada. Widespread burning in summertime (and even spring) is rapidly becoming the *new normal* in the American West. Wildfires also emit substantial amounts of volatile and semi-volatile organic materials and nitrogen oxides that form ozone and organic particulate matter. Direct emissions of toxic pollutants can affect the local residents. In addition, the formation of other pollutants as the air is transported can lead to harmful exposures for populations in regions far away from the wildfires (Figure 4.1). Therefore, several studies have focused on improving the understanding of fire emissions and chemistry as well as conducting quantitative assessments through both lab-based simulations and field measurements of fire pollutants that could affect human health.

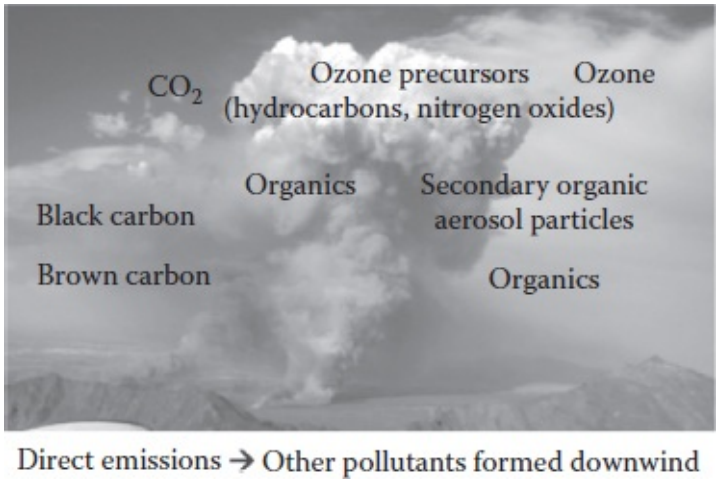

Figure 4.1 Air pollutant generation from wild fires. (From NOAA, *Wildfires*, National Oceanic and Atmospheric Administration, www.noaa.gov/topic-tags/wildfires, 2017.)

According to an international study conducted by the European Commission Joint Research Centre (JRC), Lund University in Sweden and the US National Centre for Atmospheric Research (NCAR), global wildfire trends could have significant health implications due to rising harmful emissions (Knorr et al., 2017). The JRC also projects longer and more intense fire seasons in Europe and its neighbouring regions. Regions that are growing towards a medium population density (South America, Central America, sub-Saharan Africa, eastern and southern Europe, central Asia, South East Asia and southern China) are likely to become more prone to air pollution from fires (Figure 4.2). This figure clearly shows that regions likely to become prone to wildfires, air pollution could reach dangerous levels during the fire season.

4.1.1.1 Forest management practices

Air quality policies currently do not target wildfires. Thus far, there is no widely accepted

FOR REFERENCE PURPOSES ONLY
method for wildfire management that has been shown to lead to lasting reductions in fire activity or emissions. Improved forest management practice has been considered a key factor in controlling wild fires. A variety of methods can be used to change vegetation composition, structure, and ladder fuels, which will help reduce fire hazards. For example, fire suppression practices in the United States have led to a buildup of fuels in forests, a breakdown in natural forest ecology, and increased wildfire risk at urban-wildland boundaries (Figure 4.3). The Cohesive Wildland Fire Management Strategy in the United States is informed by regional and national analyses, including in-depth risk-based analysis that delves into the specifics of national challenges, underlying causes, and the management opportunities available to address them. The strategy recommends mechanical thinning, clearing debris in forests or mowing in rangelands, and so on. As a result, new policies now allow burning where possible. It is understood that climate change will further aggravate the problem (according to NOAA, the area burned is projected to at least double for every degree of climate warming).

FOR REFERENCE PURPOSES ONLY

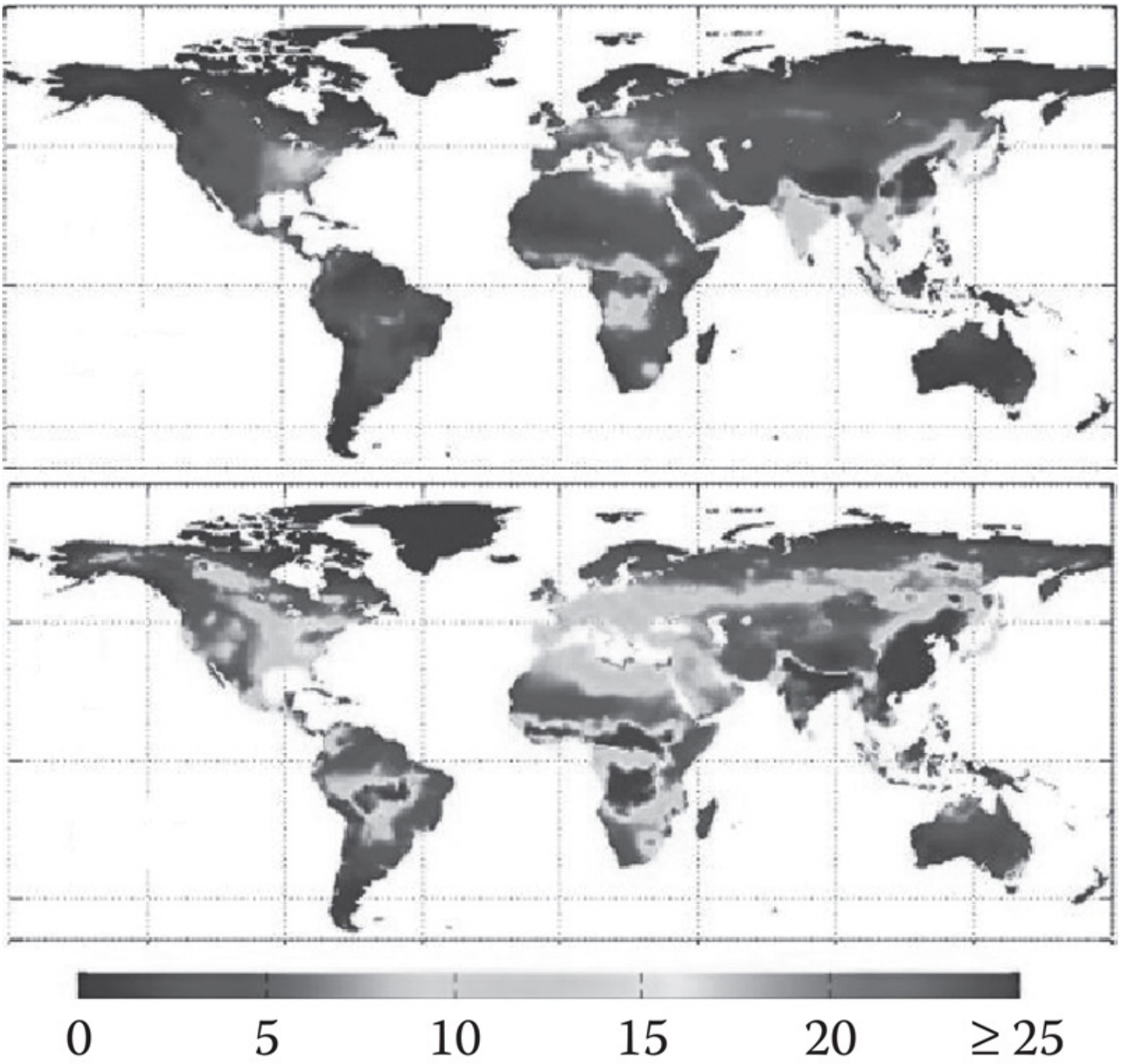

Figure 4.2 Global current-day average $PM_{2.5}$ concentration (μg m^{-3}), upper panel – annual average; lower panel – peak monthly average, accounting for highest concentration at each grid point. (From Knorr, W. et al., *Atmos. Chem. Phys.*, 17, 9223–9236, 2017.)

FOR REFERENCE PURPOSES ONLY

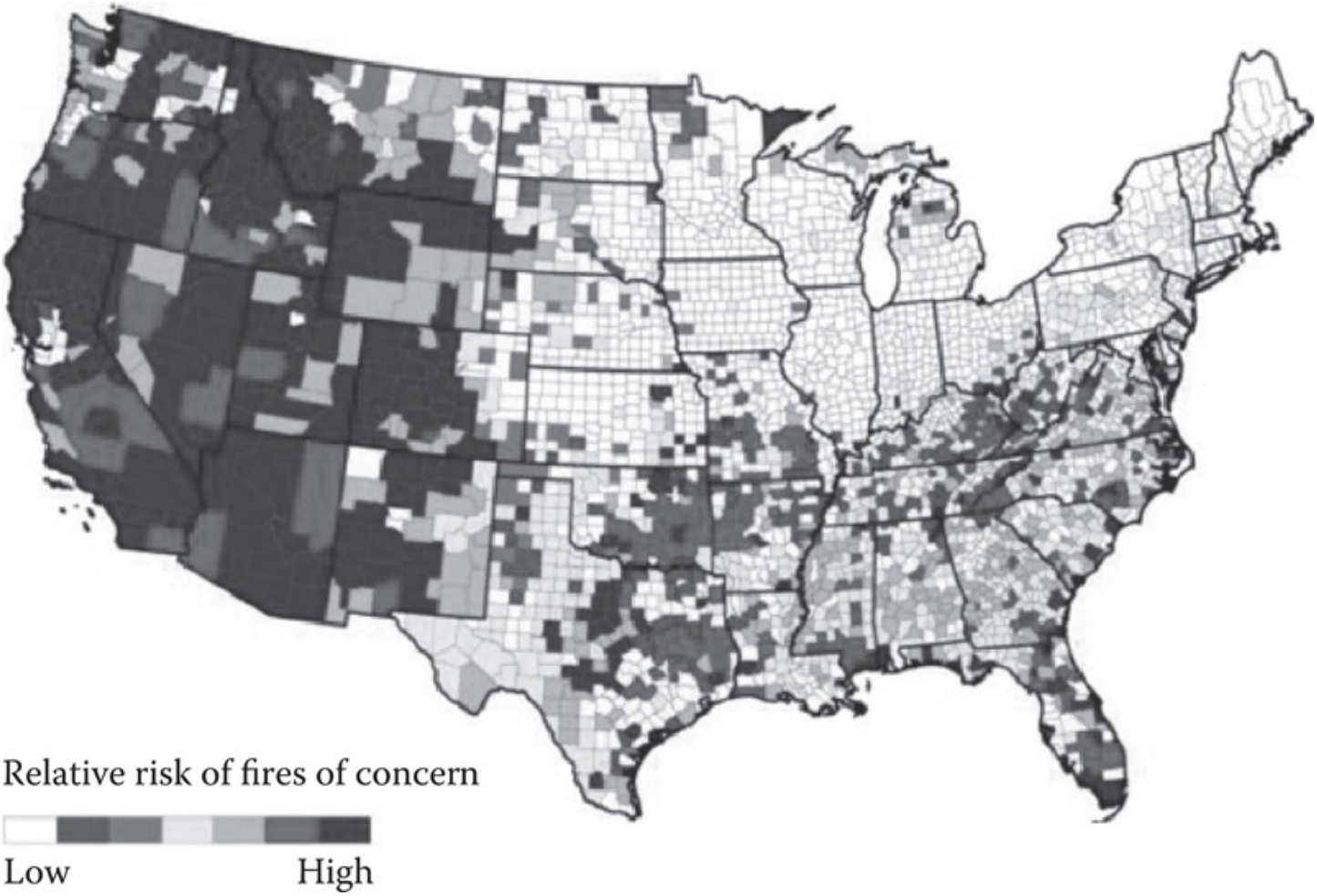

Figure 4.3 Wildfire risk-prone zones in the United States. A fire of concern is greater than 1 square mile in extent and requires 2 weeks or more to contain. (From USDA, A national cohesive wildland fire management strategy, 2014.)

4.1.2 Volcanic emissions

Large volcanic eruptions can release enormous amounts of toxic gas, including sulphur dioxide, hydrogen sulphide and hydrogen halides, into the atmosphere in a short time. The 1991 eruption of Mt. Pinatubo in the Philippines is thought to have injected more than 250 megatons of gas into the upper atmosphere on a single day. SO_2 emissions can cause acid rain and air pollution downwind of a volcano. Typically, high SO_2 concentrations can produce *volcanic smog* (called VOG), which is a hazy mixture of SO_2 gas and aerosols, which are primarily composed of sulphuric acid droplets and other sulphate (SO_4) compounds. Aerosols are created when SO_2 and other volcanic gases combine in the atmosphere and interact chemically with oxygen, moisture, dust, and sunlight over periods of minutes to days. VOG can cause persistent health problems for downwind populations. During very large eruptions, SO_2 can be injected to altitudes of greater than 10 km into the stratosphere and is readily converted into sulphate aerosols, which reflect sunlight and

affect the Earth's radiation budget (see Section 11.1.3). They also have a role in ozone depletion, as many of the reactions that destroy ozone occur on the surface of such aerosols. Volcanoes can also emit the halogens fluorine, chlorine and bromine in the form of hydrogen halides (HF, HCl and HBr). These species are all strong acids and have high solubility; therefore they rapidly dissolve in water droplets within volcanic plumes or the atmosphere where they can potentially cause acid rain. In an ash-producing eruption, ash particles are also often coated with hydrogen halides. Further information on volcanic emissions is presented later in Section 4.6 with a case study on air pollution from Icelandic volcanic eruption in the recent past.

4.1.3 Soil emissions

In some parts of the world soil emissions, especially of nitrogen oxides, are a bigger component of air pollution (estimated to be approximately 22% of the total global NO_x emissions, which is about 70% greater than the scientists previously thought) (Jaeglé et al., 2005). From satellite observations these excessive soil NO_x emissions are seen primarily in equatorial Africa at the beginning of the rainy season, especially in a region called the Sahel, and in the agricultural regions in the Western United States (Great Plains), Southern Europe (Spain, Greece, Turkey), and Asia (North China Plain and North India). When the rains come to the Sahel after a 6-month dry season, dormant soil bacteria reawaken and begin processing nitrogen. Similarly, the NO_x emissions in the mid-latitudes of the northern hemisphere spike during the growing season, spurred by warmer temperatures after a cold winter, and also magnified by intense fertiliser use (see Section 4.2). Regional air chemistry models often underestimate soil NOx emissions and their contribution to the NOx budget at the surface and in the troposphere (Oikawa et al., 2015).

The effect of climate change on mercury cycling between soil and atmosphere compartments is also an important source of air pollution. Increased volatilisation of soil mercury under a warming climate could potentially be of considerable importance, especially in the boreal latitudes this could release large amounts of soil mercury to the atmosphere, through both increased respiration and wild (Section 4.1.1). Boreal peatland fires may have very high mercury emissions from burning of the peat.

4.2 ANTHROPOGENIC AREA SOURCES

4.2.1 Landfills

Landfills are waste disposal sites. They are often man-made depressions in the ground, or mounds above the ground, with a lining designed to prevent any leakage of waste materials. According to the U.K. Environmental Agency, about two-thirds of landfill waste are biodegradable organic matter from households, business and industry. The more organic

waste and moisture present in a landfill, the more landfill gas is produced by the bacteria during decomposition. The more chemicals disposed in a landfill, the more likely volatile organic compounds and other gasses will be produced. As a consequence, the emissions from landfills (terms as *Landfill gas*) is composed of mainly methane and CO_2 but also contains trace amounts of hundreds of other gaseous compounds. Municipal solid waste (MSW) landfills emit a large amount of volatile organic compounds, collectively known as non-methane organic compounds, mainly aromatic compounds (such as Toluene). At a local scale these contribute to typical noxious smell emanating from landfills. At a much larger scale, these emissions lead to formation of ozone and secondary organic aerosols.

In addition, landfills also generate large volumes of inorganic compounds, such as SO_2 and hydrogen sulphide. Landfills are also a significant source of Polychlorinated Napthalenes (PCN) emissions.

4.2.1.1 Landfill directive

The Landfill Directive is a Europe wide initiative, which defines the different categories of waste (municipal waste, hazardous waste, non-hazardous waste and inert waste) and applies to all landfills. Directive 1999/31/EC sets stringent technical requirements for waste and landfills in order to prevent (or reduce as far as possible) the negative effects on the environment, in particular on surface water, groundwater, soil, air, and human health from the landfilling of waste.

From this Directive landfills are divided into three classes:

- Landfills for hazardous waste
- Landfills for non-hazardous waste
- Landfills for inert waste

The Directive does not apply to

- The spreading on the soil of sludges (including sewage sludges and sludges resulting from dredging operations).
- The use in landfills of inert waste for redevelopment or restoration work.
- The deposit of unpolluted soil or of non-hazardous inert waste resulting from prospecting and extraction, treatment and storage of mineral resources as well as from the operation of quarries.
- The deposit of non-hazardous dredging sludges alongside small waterways from which they have been dredged and of non-hazardous sludges in surface water, including the bed and its subsoil.

A standard procedure for the acceptance of waste in a landfill is laid down, so as to avoid any risks, including:

- Waste must be treated before being landfilled.
- Hazardous waste within the meaning of the Directive must be assigned to a hazardous waste landfill.
- Landfills for non-hazardous waste must be used for municipal waste and for other non-hazardous waste.
- Landfill sites for inert waste must be used only for inert waste.
- Criteria for the acceptance of waste at each landfill class must be adopted by the Commission in accordance with the general principles of Annex II.

The following wastes may not be accepted in a landfill:

- Liquid waste
- Flammable waste
- Explosive or oxidising waste
- Hospital and other clinical waste which is infectious
- Used tyres, with certain exceptions
- Any other type of waste that does not meet the acceptance criteria is laid down in Annex II.

The Directive sets up a system of operating permits for landfill sites. Applications for permits must contain the following information:

- The identity of the applicant and, in some cases, of the operator
- A description of the types and total quantity of waste to be deposited
- The capacity of the disposal site
- A description of the site
- The proposed methods for pollution prevention and abatement
- The proposed operation, monitoring and control plan
- The plan for closure and aftercare procedures
- The applicant's financial security
- An impact assessment study, where required under Council Directive 85/337/EEC on the assessment of the effects of certain public and private projects on the environment.

Member states must ensure that existing landfill sites may not continue to operate unless they comply with the provisions of the directive.

4.2.1.2 Emerging trends in landfill of waste electrical components

In many parts of the developing world emissions of polychlorinated biphenyls (PCBs) during disposal of waste electronic components and old equipment containing dielectric fluids are considered to be significant. In the UK sale of products containing PCBs has not been legal since 1986, however, large quantities of PCBs are thought to have been disposed

FOR REFERENCE PURPOSES ONLY

of to landfill in the past, mainly in the form of electrical components or fragmentiser residues, but now such equipment containing PCBs are disposed of by chemical incineration. This process ensures significant reduction in the amount of PCBs being released into the environment. PCBs are also emitted from the soil having previously been deposited there from the air.

4.2.2 Farm emissions

Soil nitrogen oxide ($NO_x \rightarrow NO + NO_2$) is one important form of N trace gas that can be released from fertilised soils and plays an important role in the formation of tropospheric ozone, a toxic air pollutant. Nitrogen (N) losses to the atmosphere from high-temperature agroecosystems are not well characterised and are estimated to be higher due to the combination of N fertilisation, nonlinear temperature dependence of biological processes and pulsed fluxes in response to irrigation – drying cycles (Oikawa et al., 2015). These emissions are found to vary nonlinearly with environmental and land management factors, including fertilisation, temperature and soil moisture (Figure 4.4). Considering the factors that regulate soil NO_x emissions in a high-temperature agricultural region, farming management has shown potential for reducing soil NO_x emissions, thereby improving air quality.

As discussed in Chapter 6, livestock farming is the other major source of anthropogenic area source emissions, especially in Europe and North America. The US Department of Agriculture (USDA) estimates that more than 335 million tons of manure is produced annually on US farms, which typically stored in lagoons can pollute the air with hundreds of different gases. Hydrogen sulphide, methane, ammonia, and carbon dioxide are the major hazardous gases produced by decomposing manure. Additional air pollution is caused when huge amounts of stored manure are sprayed onto fields. Atmospheric ammonia and nitric oxide – both produced on farms – contribute to what is known as the *nitrogen cascade*, in which each ammonia molecule can potentially impact atmospheric visibility, soil acidity, forest productivity, terrestrial ecosystem biodiversity, stream acidity and coastal productivity. Primary particulates, and/or aerosolisation of precursors, emitted from factory farms can also contribute to regional haze.

FOR REFERENCE PURPOSES ONLY

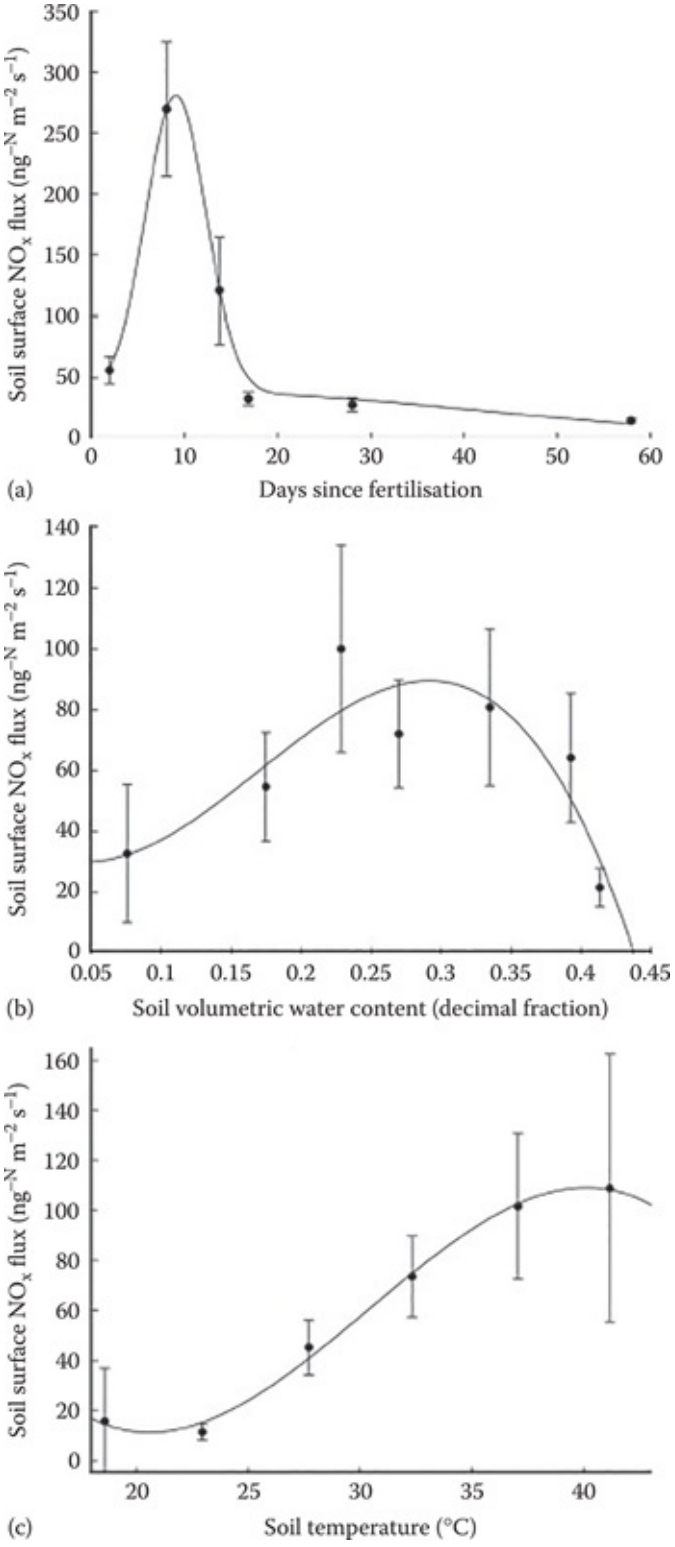

Figure 4.4 Relationship between soil surface NOx flux ($ng^{-N}\ m^{-2}\ s^{-1}$) and (a) days since fertilisation, (b) soil volumetric water content (0–10 cm) and (c) soil temperature (average 2 and 10 cm; °C). (From Oikawa, P. Y. et al., *Nat. Commun.*, 6, 8753, 2015.)

Improved farming practices, including better storage of manure, air-breaks positioned

near farms, and increased attention to the nutritional needs of specific types of livestock, can reduce these harmful emissions. The most efficient way to reduce air pollution from farms is to reduce the size and increase the number of farms. Many small farms scattered throughout the country will create less air pollution than huge, centralised factory farms. Sustainable livestock farms are pasture-based systems that rely on the animals to harvest feed and spread manure. This is the way livestock has been raised for thousands of years, right up until the twentieth Century, and it remains the model for sustainable farming and reducing farm-related air pollution.

4.2.3 Fugitive emissions from industrial processes

The US Environmental Protection Agency (USEPA) defines *fugitive emissions* as unintended emissions from facilities or activities (e.g. construction) that 'could not reasonably pass through a stack, chimney, vent, or other functionally equivalent opening'. Some of the common examples of fugitive emissions and fugitive emissions sources are: dust, fine particles, aerosols, quarries, storage piles, leaks or releases from valves, pumps, compressors, flanges. When natural gas escapes via fugitive emissions from pipelines, methane as well as VOCs and any other contaminants in the gas (e.g. H_2S) are released to the atmosphere.

Sampling fugitive emission is a difficult task as not all possible emissions sources are visibly quantifiable. Common methods of controlling fugitive particulate emissions include: enclosures, water spray, chemical dust suppressants, windscreens, vegetative barriers, sweeping paved roads, reducing speed on unpaved roads, paving roads, covering open trucks.

4.3 MEASUREMENT OF AREA SOURCES

Emissions from stationary sources may be divided initially into confined and unconfined. Confined emissions are those from chimneys and other organised release arrangements, usually as a result of a specific ventilation process and driven by a fan or other prime mover. Unconfined emissions are those from roof vents and other gaps, often driven by natural convection due to buoyancy. Confined emissions are much easier to quantify. For both types of emission, two measurements are often of interest – the concentration of the pollutant and its mass flow rate. Calculation of the latter requires knowledge of the gas flow rate. Both the temperatures and pressures of process gas emissions are likely to be different to ambient values. Gravimetric concentrations are therefore converted to mass per normal m^3 (Nm^3, at 20°C and 1 atmosphere), by the method given in Chapter 1, before reporting.

4.3.1 Confined emissions

FOR REFERENCE PURPOSES ONLY

These are usually chimney stacks from continuous or intermittent sources such as power stations, chemical works and many other processes.

4.3.1.1 Measurement of volume flow rate

For various reasons it may be useful to measure either the distribution of gas velocities across the cross-section of a duct or stack, or the gas volume flow rate. First, correct particle sampling involves establishing isokinetic flow through the sample inlet – that is, an inlet speed equal to the local gas speed. Second, process emission limits may be expressed in mass of pollutant per day, for example, as well as or instead of pollutant concentration.

The classical method for measuring the local value of gas speed is by the velocity head. In a single-point fixed installation, a small-bore tube points upstream (there is no flow through it) and measures the total head, which is the combined static and dynamic pressure. A second tube just penetrates the duct wall and measures the static pressure alone. The difference between them, which can be measured on one manometer, is the velocity head. This is equal to $\frac{1}{2}\rho v^2$, where ρ is the gas density at the flow conditions (composition, temperature and pressure) and v is the fluid velocity. If the gas speed has to be measured at different points across a section of the duct, then a pitot-static probe is used, in which the total and static heads are combined at the end of a stainless steel probe which may be several metres long. For low particulate loadings, the standard type is preferred as its calibration is within 1% of the theoretical value. For high particulate loadings the small upstream hole of the standard type tends to get blocked, and the *S*-type should be used, although the calibration of this may be as much as 15% away from theoretical and corrections must be applied. The pressure differential is measured by a slant oil-filled manometer or magnehelic gauge. There are also available electronic digital instruments which measure the differential pressure, temperature and static pressure, take averages and compute the flow.

Volume flow rate is determined as the average gas speed over a cross-section of the chimney or a duct leading to it, multiplied by the cross-sectional area. The volume flow rate may then be multiplied by the gas concentration (which is usually assumed uniform) to obtain the mass emission rate. It is important to take the measurement in a section of the duct where the flow is as uniform as possible – guidelines are at least five duct diameters downstream and two diameters upstream, of any disturbance or obstruction such as a damper or elbow. Many flows are rather non-uniform across the width of the duct, especially if the measurement has to be taken close to a bend, and the average value will need to be constructed from many point measurements. These are taken according to a standard protocol (Figure 4.5), with the pitot probe marked up beforehand so that it is inserted to the correct depth. In a rectangular duct, sample points should be chosen to sample equal areas, while in circular ducts they should sample equal annular areas. For example, in the configuration shown, the radii of the two annuli will be 0.58 and 0.82 of the duct radius.

FOR REFERENCE PURPOSES ONLY

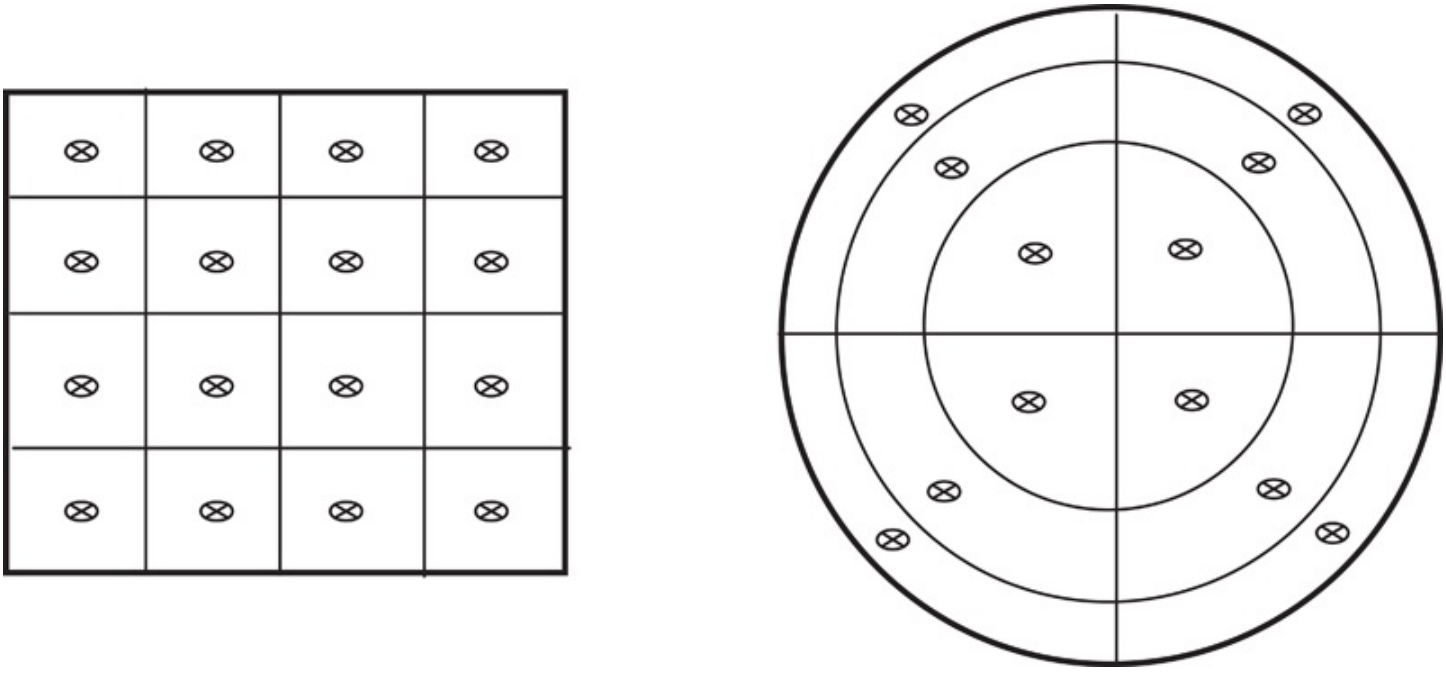

Figure 4.5 Measurement locations in rectangular and circular ducts.

The dry bulb temperature, wet bulb temperature and static pressure will all be needed as well in order to convert the flow rate to standard conditions. Basic methods for these have been the mercury in glass thermometer and water U-tube manometer respectively, although these are being replaced by thermocouple probes and electronic pressure sensors. The internal cross-sectional area of the duct or stack can often be obtained from drawings without needing direct measurement. If the duct is under significant suction (if the main extraction fan is downstream) then the sample access hole will need to be sealed to prevent the inward flow of air from affecting the readings.

Gas volume flow rate from combustion processes can also be calculated from a knowledge of fuel combustion rate and composition, together with either oxygen or carbon dioxide content of the flue gases. This is more likely to be done for efficiency optimisation than for pollutant emission calculations.

4.3.1.2 Measurement of gas concentrations

A wide range of methods is in use, corresponding to those described for ambient air. The measurements may be either extractive, in which a sample is drawn from the flue gases and presented to the analyser, or *in situ*, in which the measurement is made directly in the flue gases. The standard manual extractive method (e.g. US EPA Method 6 for sulphur dioxide) is to reduce the particle interference problem by plugging the sample inlet with a quartz wool filter before drawing the sample gas at a flow rate of about 1 L min^{-1} through a heated probe into an appropriate absorber for the gas of interest. The absorbant is taken back to the laboratory for analysis. A wide range of absorbers and systems has been developed to cope

FOR REFERENCE PURPOSES ONLY

with the wide range of gases. For SO_2, for example, it is hydrogen peroxide in midget impingers, whereas for NO_x it is sulphuric acid and hydrogen peroxide in evacuated flasks. The flue gases are often hot, acidic, saturated with moisture and laden with particles, so getting the sample to the analyser can be difficult. A variety of solutions to this problem are commercially available.

First, hot/wet systems keep the flue gas sample at source conditions by heating the sample line and pump to a higher temperature than the dew point and delivering the gas to an analyser with a heated sample cell. This method is appropriate for water-soluble gases such as SO_2, NH_3 and NO_2 which would be lost or reduced in condensate.

Second, cool/dry systems cool the sample under controlled conditions to remove moisture while minimising absorption of the gas of interest. The sample is then measured by an analyser at ambient conditions. The sample stream is extracted through a sintered stainless steel or ceramic filter to remove most of the particles. The filter will often be blown back intermittently with pressurised air or gas to clear blockages. The sample is then drawn down a 6 mm internal diameter heated line made of Polytetrafluoroethylene (PTFE) or stainless steel, at a flow rate of a few 1 min^{-1}, to the moisture removal system. This sample line may be 100 m long, and there must be no condensation anywhere along its length. In a properly engineered system designed for long life with minimum maintenance, the sample line may be integrated into an *umbilical* assembly which also carries power cables, an air line for cleaning the filter and a calibration gas line, all mounted inside the heating elements (Figure 4.6). Moisture is then removed by passing the sample stream through either a condensation drier in which the gas is cooled below the water dew point, or a permeation drier in which the gas flows through ion exchange membranes which only allow the passage of water vapour.

Both the hot/wet and cool/dry extractive systems can be close-coupled to the extraction point by removing the sample line and putting the pump and analyser close to the extraction point. This eliminates sample absorption in the cooler and elsewhere, which may improve the accuracy of VOC measurements. It also eliminates a long length of expensive sampling line, although the downside is that the analyser may be at an inaccessible location halfway up a tall stack.

FOR REFERENCE PURPOSES ONLY

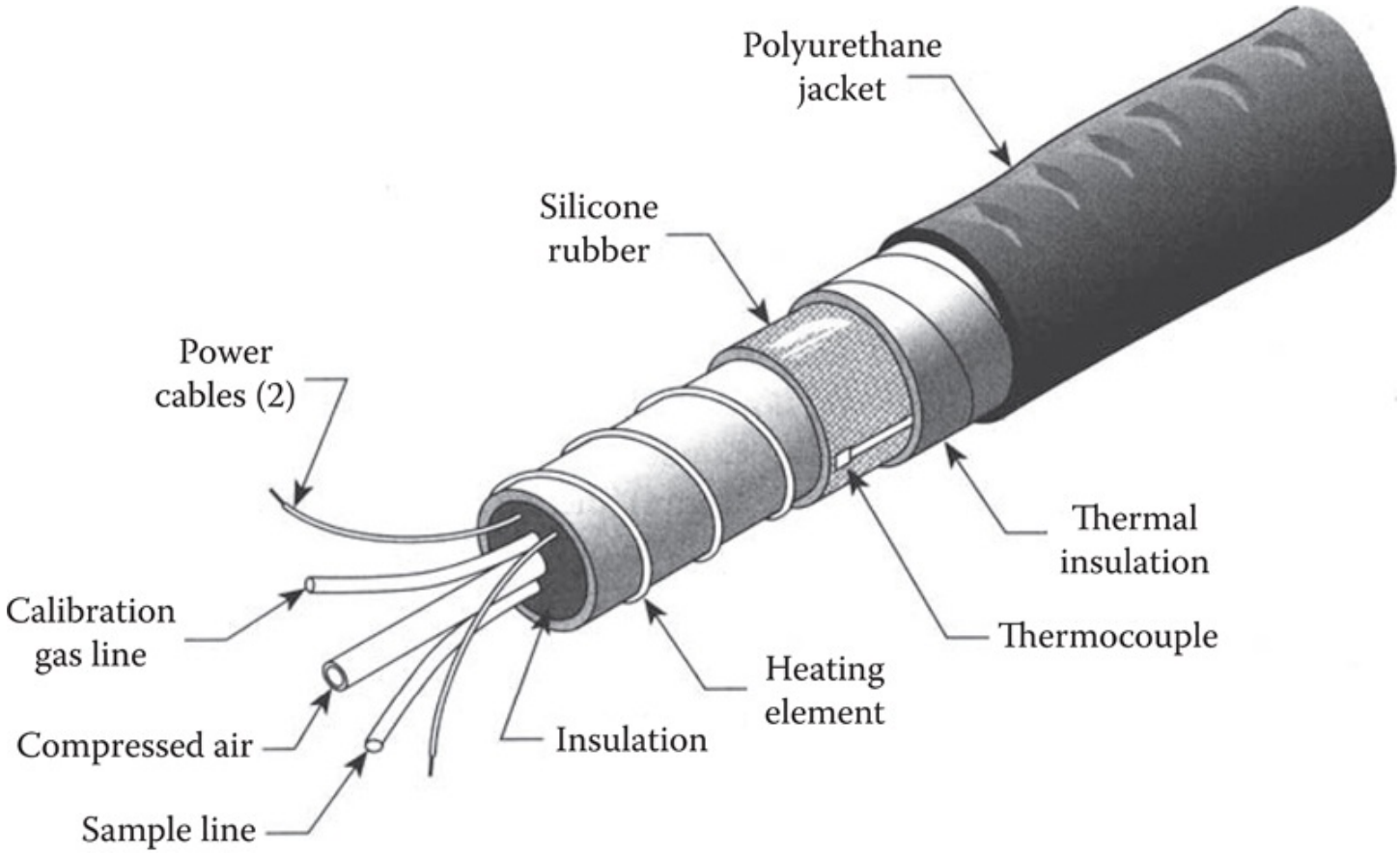

Figure 4.6 Integrated heated sample, power and calibration line. (From Jahnke, J. A., *Continuous Emissions Monitoring*, Wiley, New York, 2000.)

With a dilution system, a much lower sample flow rate (20–500 mL min^{-1}) is extracted, which reduces the particle and moisture contamination problems. The sample gas is immediately diluted with a known flow rate of clean dry air (a few 1 min^{-1}, giving dilution ratios between 50 and 300:1). The dew point is thus lowered to below ambient temperatures, and the sample can be brought to the pump and analyser (which can be an ordinary ambient model) in an unheated sample line. In one common design of dilution probe (Figure 4.7) the dilution air supply drives an ejector pump which draws the sample from the flue gases. The quartz wool filters out particles, and the enclosed design means that calibration air and zero air can be injected to displace the sample when required. Dilution systems automatically give a concentration in terms of the volume including moisture, which may be a benefit if an emission limit is expressed that way.

The extractive methods described earlier deliver a sample of the gas through a pipe to an analyser, and the analysis method can be any of those described earlier for the component of interest. A further range of techniques is available by which the gas concentration is measured *in situ*, by optical techniques based on some form of the Beer–Lambert law. The Beer–Lambert law is the simplest description of the change in flux density of a light beam as it passes through a medium.

$$\tau = \frac{F}{F_0} = e^{-\alpha(\lambda)CL}$$

where:

τ is the transmittance (dimensionless)

F (W m^{-2}) is the flux density after distance L (m)

F_0 is the initial flux density (W m^{-2})

α (λ) is the molecular absorption coefficient (m^2 kg^{-1}) as a function of wavelength

C is the concentration of the gas (kg m^{-3})

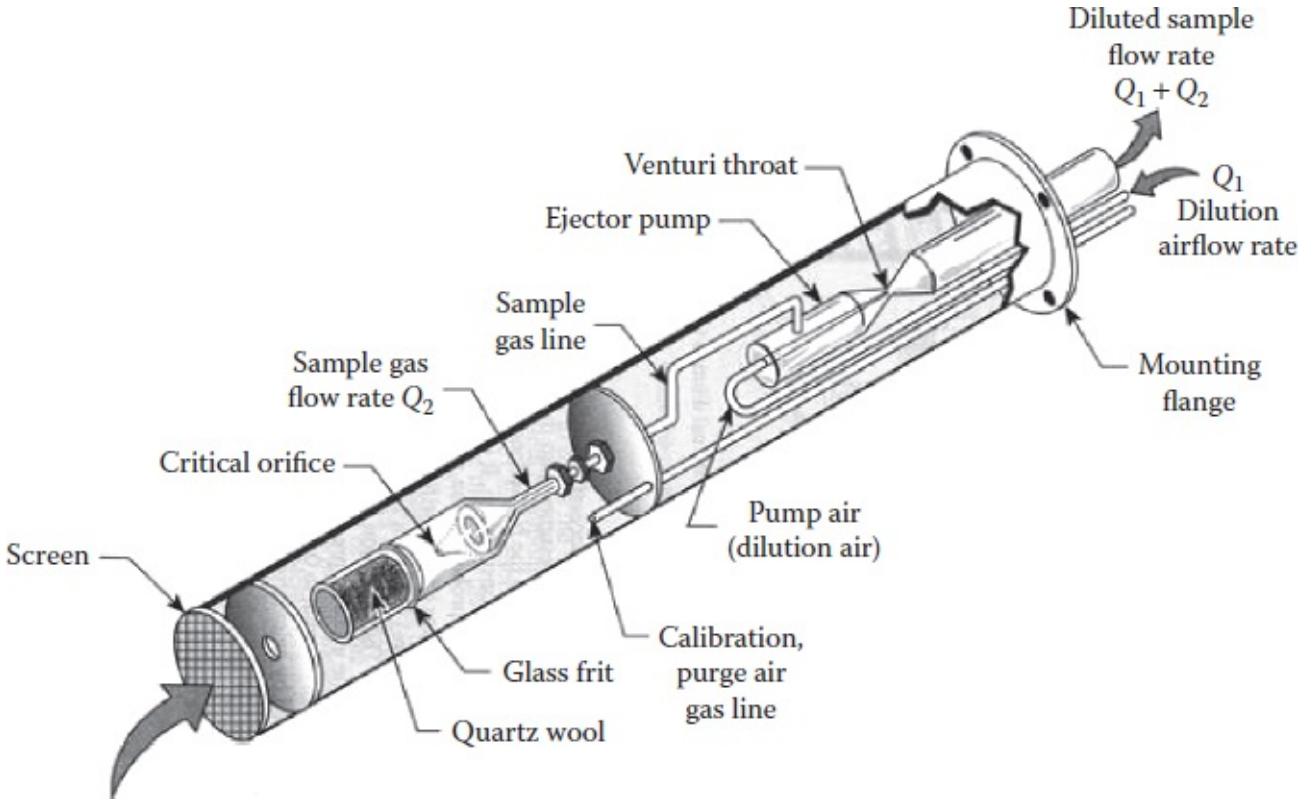

Figure 4.7 Dilution probe for stack gas sampling. (From Jahnke, J. A., *Continuous Emissions Monitoring*, Wiley, New York, 2000.)

Optical measurements may be made in the IR, visible or UV regions of the spectrum. Infrared sources are either Globars (rods of zirconium and yttrium oxides, or of silicon carbide, heated to around 1500°C) or solid-state lasers. Visible sources include conventional tungsten and quartz-halogen lamps, light-emitting diodes and lasers. Ultraviolet sources include hollow-cathode gas discharge tubes, xenon arc lamps and mercury discharge lamps. A narrow region of the emission spectrum, within which the gas of interest absorbs strongly, is selected by an interference filter or diffraction grating. The transmitted flux density is detected by solid-state quantum detectors, photomultiplier tubes or photodiode arrays. The optical arrangement can be single pass, with the transmitter and receiver on opposite sides of the stack, or double pass (Figure 4.8), with the transmitter and

FOR REFERENCE PURPOSES ONLY

receiver co-located. Some instruments, known as *point in situ*, have the optical path (i.e. the source and detector) fixed on a probe in the gas stream, with a shorter path length of 1–100 cm.

One important issue is calibration. It will often be a requirement to automatically zero and calibrate the system every 24 h by inserting either clean air or air containing a known concentration of the gas of interest (from a certified cylinder) into the optical path. This is not usually possible with single-pass systems, possible with difficulty with double-pass systems, and more straightforward with *point in situ* arrangements. The latter have a compact sample measurement volume which is often protected from particle deposition by enclosure in a sintered filter which allows penetration of the flue gases but keeps the particles out. The filter will retain zero or span gas when it is injected into the view volume, driving out the flue gas.

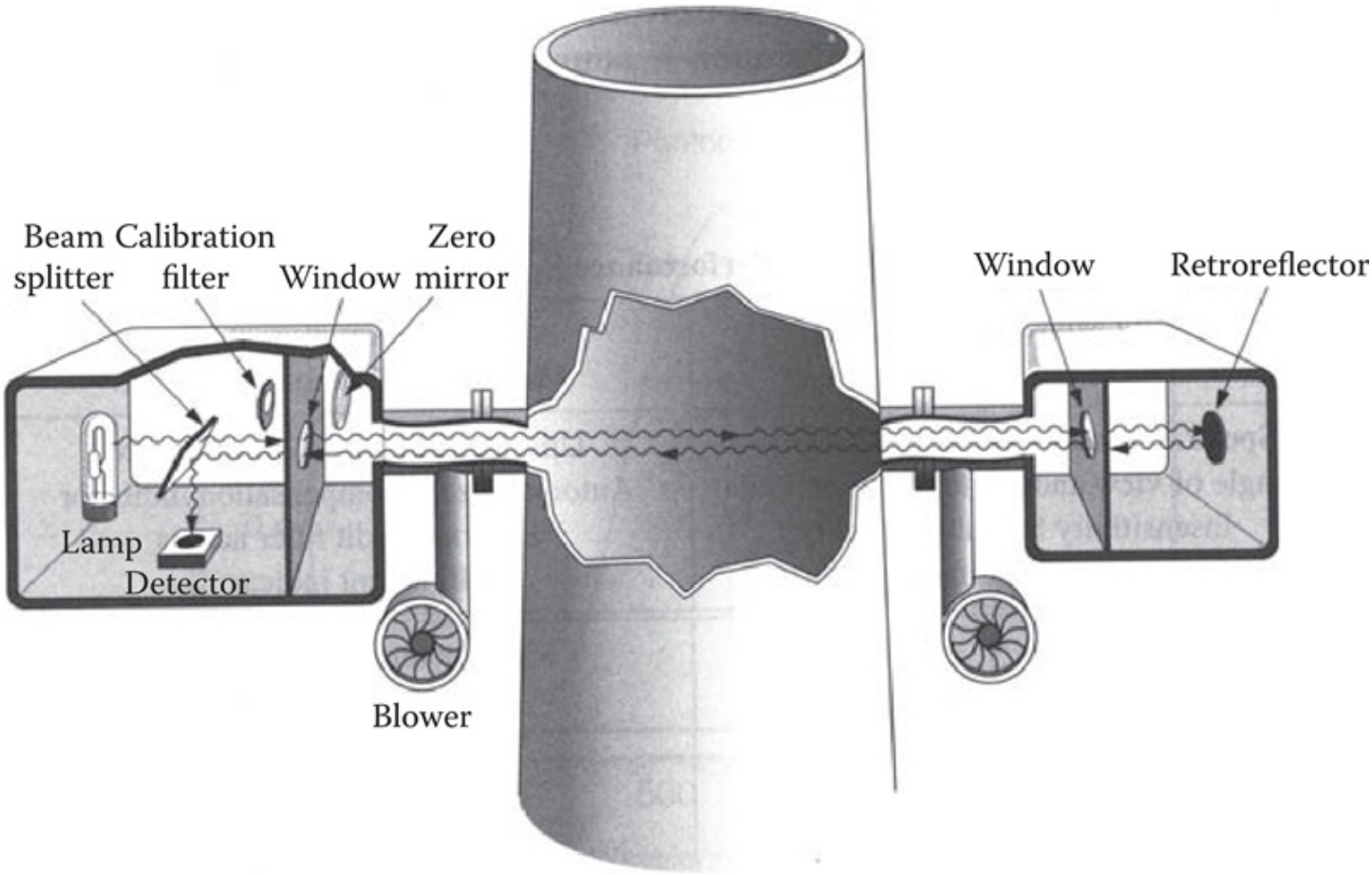

Figure 4.8 A double-pass transmissometer. (From Jahnke, J. A., *Continuous Emissions Monitoring*, Wiley, New York, 2000.)

Two main measurement methods are in use:

Differential optical absorption spectroscopy has been described previously for the long path measurement of ambient concentrations, and the same technique is applied for

stack gas concentrations. Commercial DOAS systems can measure NO, NO_2, SO_2, CO, CO_2, NH_3, VOCs, HCl and HF.

Derivative spectroscopy involves scanning a spectral absorption peak to obtain its second derivative at the maximum. This is accomplished in practice by modulating the output from a tunable diode laser so that it sweeps sinusoidally through a range of wavelengths. Stack concentrations of HF, NH_3, HCl, O_2, CO, H_2S and NO have been measured with such systems.

4.3.1.3 Measurement of particle concentrations

4.3.1.3.1 Standard gravimetric sampling

Standard methods have been developed to sample particles from ducts and stacks. The gases are often hot and humid, which poses problems for repeatable measurement. The US EPA has developed Method 5 for out-of-stack measurements of low particulate loadings, and Method 17 for in-stack measurements of high loadings, which might block the sample probe used for Method 5. The requirements are simple in principle – to separate the particles from a known volume of gas. The essential features are a stainless steel sample probe, a heated filter for coarse particles, a set of impingers in iced water to trap fine particles and condensates, a vacuum pump and a dry gas meter. In addition to the particles trapped in the filter and impingers, the sample probe will be washed out with acetone and the deposited particles collected. Although particle size analysis can be done on all the collected material, it will not usually be known how that compares with the *in situ* size distribution.

4.3.1.3.2 Opacity

The most obvious sign of high particle emissions from a chimney is thick black smoke, and this has been the basis of pollutant observations for many years. It is no longer acceptable for a chimney to discharge such emissions continuously, although there may be circumstances when it is allowed for a short period for a specific purpose, such as lighting up or soot blowing in a large boiler. The severity of such emissions has been measured by trained observers, and put onto a semi-quantitative basis by comparing the appearance of the smoke with a standard series of increasing shades of grey (the Ringelmann chart).

The instrumental equivalent of the trained observer is the opacity monitor. A light is shone single- or dual-pass across the stack and the transmittance measured. Then opacity (%) = 100 – transmittance (%). The spectrum of the lamp must peak between 500 and 600 nm, and not extend into the UV or IR, so that the results can be compared with those of the human eye. A zero value is created by inserting a mirror into the optical path close to the transmitter. A span value is created by inserting a filter of known attenuation in front of the zero mirror. The optical density of the particles depends on factors such as particle size

distribution as well as number concentration, so this method is strictly for opacity only.

Accurate measurement of process particle emissions is much more difficult than for gas concentrations. The types of technique used include:

- *Manual in-stack*: Isokinetic sampling procedures must be followed strictly if a representative sample is to be obtained. Large particles cannot be extracted as they do not remain suspended in the gas sample, so the particle capture must occur right at the inlet of a probe inserted into the flow. As the gas flow speed varies across the duct, multiple samples need to be taken at different points, with the sample gas flow rate (and hence the sample inlet speed) adjusted to maintain isokinetic sampling at each location. Bends and other flow disruptions produce turbulence and inhomogeneous particle distributions; hence particle emission measurements are often made halfway up the chimney. Commercial devices are available either to give total particulate matter or a size distribution from a cascade impactor.
- *Manual extractive*: If the particle emission is downstream of an efficient control device such as a fabric filter or an electrostatic precipitator, the particle diameters will usually be small enough to extract without serious losses. Isokinetic samples can then be extracted through a heated pipe to a filter for determination by weighing.
- *Instrumented in-stack*: Most commonly, optical transmissometry is used to determine total concentration from the reduction in flux density of a beam passing across the width of the duct. This is similar to the opacity technique discussed earlier but requires a calibration of the transmittance against gravimetric concentration determined by a manual isokinetic method. The transmittance τ is related to particle properties by Bouguer's Law, which is a re-phrased version of the Lambert-Beer law discussed previously for gases.

$$\tau = e^{-Na\kappa L}$$

where:

N is the particle number concentration
a is the particle projected area
κ is the particle extinction coefficient
L is the path length of the light beam

In practice it is more likely that optical density will be used. Optical density is defined by

$$D = \log 10 \frac{1}{1-\text{opacity}} = \log_{10} \frac{1}{\tau}$$

Also since ln τ = –$Na\kappa L$, then ln (1/τ) = $Na\kappa L$ = 2.303 D, since ln 10 = 2.303. Hence D = $Na\kappa L$/2.303. This is framed in terms of the particle number concentration N, whereas it is usually the mass concentration C which is measured, and in terms of which the regulations

are framed.

We write κ_S = specific mass extinction coefficient = $\pi r^2\kappa$/m. This is a property of the given particle composition and size distribution, and will be effectively constant for an individual source. Then $D = \kappa_S CL/2.303$, so that the optical density is directly proportional to the mass concentration and path length.

An electrodynamic method is available in which an electrical current, which is measured directly by an electrometer, is generated by charge induction on a probe inserted into the gas stream. Although the technique is useful for detecting gross changes such as bag failure in a baghouse, the many factors such as particle charges and resistivity, probe surface condition and humidity which affect the results render it only semi-quantitative. A more quantitative version of the method relies on AC detection of the variable voltage induced by particles as they move past the probe.

4.3.2 Unconfined emissions

Intermittent industrial processes such as steel manufacture, when hundreds of tonnes of molten metal are poured from one container to another, can generate heavy particulate and gaseous emissions. Most of these may be collected by an extraction system for subsequent cleaning and discharge from a chimney. Part of the emissions, however, is often not collected and leaves the building by whatever routes are available. These are referred to as fugitive emissions, because they have escaped the control system. Measurement of fugitive emissions follows the same principles of concentration and volume flow measurement as described earlier for confined emissions. Obtaining representative values is harder, however, because the releases are often sporadic, and both the source strength and the ventilation are variable. Quantitative manual assessment involves multiple repeat sampling at many locations. Long-path optical transmissometry may be able to provide an average concentration along the length of a vent.

4.3.3 Pervasive sensors

Application of *diffused automated pervasive sensors* is getting more common for continuous online *passive monitoring* of area sources. Generally, portable systems based on low-cost solid-state chemical sensor arrays have been applied for air quality measurements in a distributed deployment of networked sensors in large urban areas and industrial zones. This serves a good compromise between accuracy of expensive and bulky chemical analyses and the lower cost of distributed gas sensors, avoiding the need for qualified operators and maintenance. The main advantage of deploying a distributed sensor network is that it allows the users to identify the nature and location of the source material, take appropriate actions to protect human life, and monitor trace concentrations of air pollutants of interest from industrial processes, waste treatment activities, and so on. It enables the measurement of air-pollutant concentrations and odour concentrations at higher spatial and

temporal resolution with a good precision for real-time applications.

Highly sensitive and selective detection of hazardous gases at ppb levels using miniaturised-sensing devices are an open challenge in chemical-sensing applications, including environmental air-pollutant monitoring and odour control in factories. Many sensor enhancements are demanded for small size, high sensitivity, fast response, fast recovery, reliability, accuracy, minimal power consumption, high reproducibility, selectivity, long-term stability and wireless communication. Consequently, there are industrial interests in online sensor-based instrumentation capable of detecting odours and air-pollutants. Portable commercial sensor systems for real-time monitoring are emerging proof-of-concepts for rapidly progressing citizen-based scientific research.

4.4 MEASUREMENT UNCERTAINTIES

Uncertainty can be treated as an inherent part of measurement errors, arising from a combination of the systematic and the random components. The systematic error is a measure of the accuracy whereas the random error can be considered as a measure of the precision of the measurements. Uncertainty is usually expressed in terms of standard deviation about a mean (also called *deterministic*) value. In standard terms uncertainty can be expressed as one standard deviation, however, the 95% confidence interval covers approximately two standard deviations of the measurement on either side of the mean value. This is known as *expanded uncertainty*. In simple terms, the estimated uncertainty – for both continuous and periodic measurements – characterises the performance of a monitoring instrument by accounting for its abnormal operation. The overall uncertainty of a monitoring instrument has been found to be a function of number of performance characteristics – drift, linearity, sensitivity/cross-sensitivity to environmental conditions and other determinants, and so on. Several reports in the field of risk assessment and impact pathway analysis suggest that the variability in fate and effect factors is better characterised by lognormal than normal distributions. An added feature is that lognormal distributions always yield non-negative values, better suited to characterise emission measurements which are always positive. Uncertainty estimation techniques are numerous, and have been covered in detail in dedicated texts (some listed in the ‘Further Reading’ section). Therefore, in this section we have only provided limited information on some of the relevant aspects of uncertainty consideration while estimating air pollutant concentrations. In the UK, BS EN ISO 14956 – Air Quality describes a procedure for determining uncertainty of monitoring through evaluation of the suitability of a measurement procedure by comparison with a required measurement uncertainty. For sensitive issues, such as waste incineration, EN14181 – Quality Assurance of Automated Measuring Systems, describes a procedure for ensuring that monitoring systems are suitable at the outset and perform sufficiently to continue meeting the uncertainty requirements of the EU Waste Incineration Directive.

FOR REFERENCE PURPOSES ONLY

Table 4.1 Uncertainty of the emission inventories for air quality pollutants

Pollutant	*Estimated uncertainty (%)*
Carbon monoxide	–20 to +30
Benzene	–30 to +50
1,3-butadiene	–20 to +40
PM_{10}	–20 to +30
$PM_{2.5}$	–20 to +30
$PM_{1.0}$	–20 to +30
$PM_{0.1}$	–20 to +30
Black smoke	–30 to +50
Sulphur dioxide	±4
Nitrogen oxides	±10
NMVOCs	–9 to +10
Ammonia	±20
Hydrogen chloride	±20
Hydrogen fluoride	±20

Source: NAEI, *UK Emissions of Air Pollutants 1970 to 2006*, National Atmospheric Emissions Inventory, 2008.

Table 4.1 shows the uncertainty in the UK emission inventories for air quality pollutants, expressed as a percentage relative to the mean values for 2006 total emissions. The estimation of these uncertainties is based on a combination of two methodologies – first, the simulation technique corresponding to the IPCC Tier 2 approach recommended for greenhouse gases, (discussed in the Good Practice Guidance, IPCC 2000); second, the proposed method in the draft guidance of the United Nations Economic Commission for Europe (UNECE) Taskforce on Emission Inventories.

As can be seen from Table 4.1, SO_2 emissions have the lowest uncertainty of all the pollutants, because they can be estimated directly from fuel sulphur level. NO_x emission estimates are less accurate than SO_2 because their emissions vary widely depending on combustion conditions. Also, NO_x emissions from road transport are heavily dependent on speed and vehicle type. Non-methane volatile organic compounds (NMVOCs) have higher uncertainty because of the difficulty in obtaining good emission estimates for some sectors, such as fugitive NMVOC emissions from industrial processes and natural sources. Emission estimates for ammonia are more uncertain relative to SO_2, NO_x and NMVOCs. This is mainly linked to the fact that ammonia sources are more spatially distributed and their emissions, mostly agricultural, depend on a large number of factors – animal species, age, weight, diet, waste management, and so on. The higher level of uncertainties for benzene, CO, and 1,3-butadiene are mainly associated with the limited number of emission measurements from road transport, which themselves show highly variable results. It has been generally agreed that CO_2 emissions show much lower uncertainty as compared to CO emissions because the former is usually calculated from fuel input while the latter depends

on variable parameters such as boiler characteristics, engine maintenance and load factors. The high levels of uncertainty in particulate matter estimates are associated with uncertainties in their emission factors and their size distributions emitted from different sources (emission estimates from fuel combustion are generally considered more reliable than from industrial processes, quarrying and construction activities). In addition, the method for estimating emissions of smaller particles is subjected to a number of assumptions, which further contributes to their overall uncertainties. Black smoke has a high uncertainty because the methodology used for its estimation from road transport and industrial sources is considered to be obsolete and therefore inadequate.

4.5 MODELLING OF AREA SOURCES

Modelling area sources is relatively more complex than modelling point sources due to the sheer volume of activities that needs to be accounted for in the first instance, as well as, the challenge encountered in assigning representative source strengths to each activity within an area of interest. For example, modelling landfill emissions to the atmosphere is a complex task as their very nature means that they contain a variety of different chemicals. Furthermore, landfill gas (LFG) is not produced immediately after waste disposal but is the result of its degradation by both aerobic and anaerobic processes occurring for up to 40 or more years afterwards. Typical area source models need to incorporate terrain effects explicitly alongside spatial description of the source configurations; complex area sources can be modelled using several circular sources of various diameters in the model set up, packed to provide a good representation of the actual source area (Mohan et al., 2009). However, recent advances in online regional chemistry model and availability of monitored emission databases now allow more sophisticated simulation of *anthropogenic-biogenic interactions* at regional, national and continental scales (Tiwary et al., 2013) (there will be more of a description in Chapter 8).

4.6 CASE STUDY: THE ERUPTION OF EYJAFJALLAJÖKULL, ICELAND

On the 20 March 2010, a volcano in Iceland called Eyjafjallajökull began erupting. Eyjafjallajökull (pronounced: AY-uh-fyat-luh-YOE-kuutl-uh) means *island mountain glacier*. This case study will explain why one relatively small volcano brought the aviation industry in Europe to a standstill with considerable air pollution emissions.

4.6.1 Volcanoes on Iceland

Volcanoes are caused by certain activities of plate tectonics: hotspots, spreading ridges, and

FOR REFERENCE PURPOSES ONLY
subduction zones all produce volcanic activity. Iceland lies over an area mid-ocean ridge, which has a hotspot beneath it, which is why it is part of the mid-ocean ridge but is above sea level. Ten percent of Iceland is covered by ice and 60% of that ice covers active volcanoes. This produces sub-glacial eruptions which characteristically produce a lot of ash (Björnsson, 2002).

Sub-glacial eruptions are a type of *phreatomagmatic*[1] *eruption* caused when seawater, meltwater or meteoritic water enters a lava chamber. The result is an explosive reaction; as the water hits the magma it boils and expands which increases the pressure in the magma chamber. In this instance, the water was produced by melting of ice from the heat of the volcano. The water vapour interacted with the lava creating ash which was especially fine (50%–70% of the ash was smaller than 100 micrometres). The finer the ash, the longer it can remain airborne. Eventually the heat melted though the 200 m thick glacier. Some of the ash had escaped with the glacial outburst floods in flows known as Jökulhlaups; however, most was pumped into the sky with the water vapour. On 18 April, the University of Iceland estimated that 100 million m^3 of ash had been released. At the peak of the eruption it was estimated that 750 tonnes of magma were being ejected every second (Sigmundsson et al., 2010).

4.6.2 Chronology

Eyjafjallajökull last erupted from 1821 to 1823 and this was immediately followed by a larger eruption from the volcano Katla that lies only 25 km away. However, since 1994 the volcano has had minor earthquakes and crustal deformation (Sturkell et al., 2003). Figure 4.9 shows a timeline of events around the eruption of Eyjafjallajökull. During May and December 2009, several global positioning system (GPS) points on the surface of Eyjafjallajökull moved a few centimetres; this movement was a sign of rising magma. Seismic tremors also occurred at a depth of 5 km (Laursen, 2010).

During March 2010, flood warnings were issued in Iceland. However, there was a lack of low seismic frequency signal from the volcano and so people were only evacuated from the flood plain after there was a glow seen on the summit in the evening of 20 March (Laursen, 2010).

The initial eruption (the effusive phase) occurred on the 20 March from Fimmvörðuháls just past the east edge of the glacier. The eruption was from a 500 m fissure and was initially treated as a tourist attraction by the Icelandic population; the British television programme *Top Gear* even visited the volcano! This phase of eruption produced lava in a Hawaii style and this phase of the eruption continued from the 20 March to the 12 April, followed by a short hiatus.

The second (explosive) phase started on 14 April when meltwater managed to penetrate into the crater of the volcano (Sigmundsson et al., 2010). This meant the magma type shifted from basaltic magma to more silica rich magma and the eruption site moved to under the glacier. This was when the tephra (ash) started to be extruded into the atmosphere

FOR REFERENCE PURPOSES ONLY

and that evening, the ash began to fall in the southeast of Iceland. As a consequence, video conferences were organised to discuss options for air traffic control and that evening the first regulations closing airspace were applied.

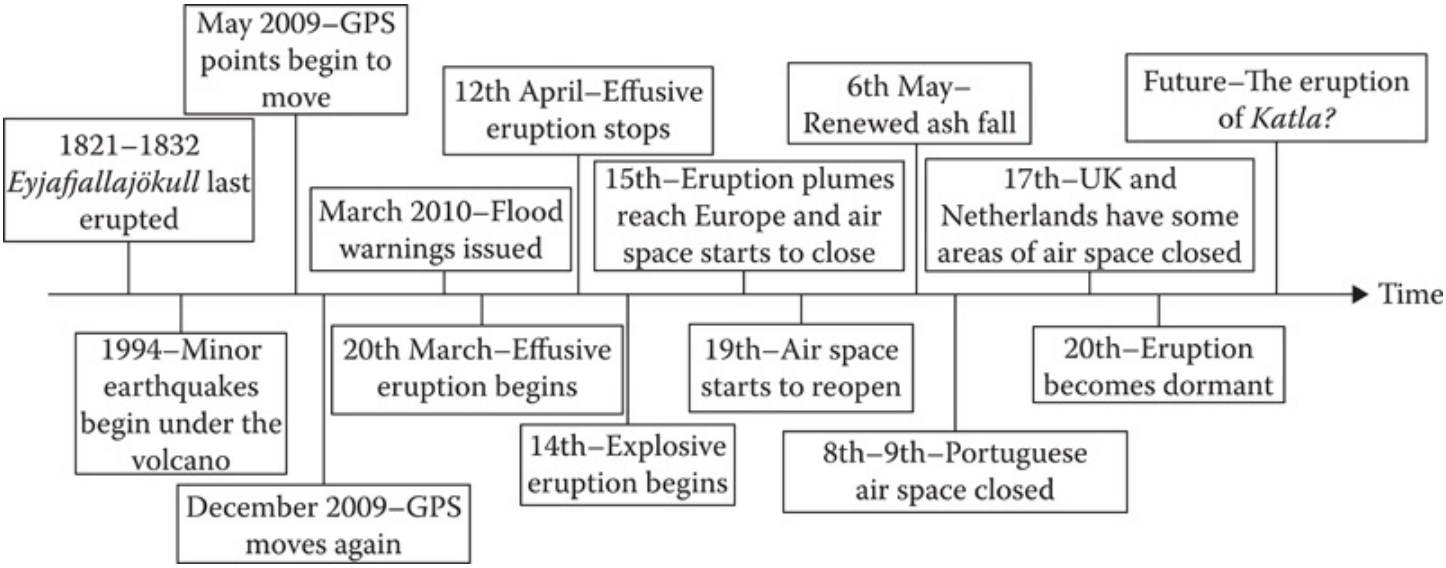

Figure 4.9 Timeline of events around the eruption of Eyjafjallajökull in 2010.

The eruption plume reached Northern European Airspace on the 15 April and throughout the 15 and 16 the eruption column remained stable with an average height of 5 km (Sigmundsson et al., 2010). This caused airports all over Europe to close one at a time. From the 16 to the 21 the rate of eruption declined to 75 tonnes s^{-1}. The deposits of tephra around the volcano were then estimated to be up to 30 m thick (Sigmundsson et al., 2010). The complete closure of airspace was regarded by many as an overreaction and on 20 April, in response to rising criticism, the European Union's transport ministers declared that a volcanic ash concentration of up to 2 mg/m^3 was deemed *safe* for flight operations, provided that certain risk mitigation measures were applied. The *safe* concentration was determined arbitrarily during the course of the emergency and faced criticism for having no basis in science (Alexander, 2013).

From 21 April until 1 May, the eruption continued and tephra continued to pore out at a reduced rate. However, by the 21st, most of the airspace has reopened except in Northern Scotland, Sweden, Helsinki, Finland and an area of North Western Brest. On 2 May, the explosive phase was producing 10 tonnes s^{-1} and there were also extensive lava flows (Sigmundsson, 2010). On 4 May, more tephra was produced and on the 5th seismologists found indicators that new material was rising to the surface. The new material brought high amounts of tephra and renewed ash fallout on the 6th.

From 7 to 20 May, the explosive reaction decreased overall, although there were some fluctuations. For example on the 13th and 18th of May, the output seemed to increase (Sigmundsson, 2010). Airports in Ireland and Scotland were often closed and on 8 and 9

FOR REFERENCE PURPOSES ONLY

May, airspace in parts of Portugal was closed. On 17 May, the airspace around south-east UK and Netherlands was closed. On 20 May the eruption decreased and became dormant with only steam coming from it and from then continued to cool (Sigmundsson, 2010). The eruption was declared officially over in October 2010, when snow on the glacier did not melt.

4.6.3 Impacts of the eruption

The major impact of the Eyjafjallajökull eruption was on the aviation industry as a result of its ash. Over the past 20–30 years there have been a number of incidents when jet engine power has been lost in a flight due to ash. The ingested ash melts and builds up in the hot sections of the engine. The molten glass coats the fuel nozzles, the combustion and the turbine. This reduces fuel mixing and restricts the movement of air, causing the engine to flame out. In past cases, the engine restarts when cooled in the oxygen rich air that the plane has glided down to. The molten ash can also accumulate in the cooling passages, blocking airflow and reducing engine life.

Volcanic ash can abrade plastic, glass and metal and so windshields on planes can become so abraded that there is a serious loss of visibility. There is also a loss of efficiency when engine parts are eroded (Grindle and Burcham, 2003). If ash is ingested into the engines, it can pass into the ventilation system and travel through the entire plane. Electronic systems that are vital such as navigation may be damaged. The ash can also set off the fire detectors. Ash in the ventilation system can clog the air filters (Grindle and Burcham, 2003). Charged ash particles can cause radio interference; this again may interfere with aircraft systems (Harrison et al., 2010). Heavy ash fall can also damage grounded planes by weighing them down and the ground support systems for aircraft can also become damaged.

The effect was that during April 2010, 104,000 flights were cancelled and during May 7000 flights were cancelled (Eurocontrol, 2010b). The effect on UK tourism was a potential total of £741 million; however, this includes the loss from having to make alternative travel arrangements and deferred travel. Due to alternative arrangements, the transport sector in general only lost £258 million (Oxford Economics, 2010). Mazzocchi et al. (2010) studied the effect of the aviation ban on nine airlines and found that they had total losses of Euro 3.3 billion. The net loss to UK GDP including direct and indirect effects is estimated as a loss of £466 million (Oxford Economics, 2010).

This eruption also showed the lack of monitoring for volcanic ash. Many scientists hope that this event will encourage the aviation industry to fund the development of on board ash sensors and live satellite observations (Sigmundsson and Höskuldson, 2010). Unfortunately, this incident also raised questions about the reliability of the predictions, with many media commentators saying the predictions were *overwrought*. However, before the incident there was a lack of information and so the regulations were over-protective to reduce the risk of a plane full of passengers plummeting to their deaths (Brooker, 2010). It must be noted that

FOR REFERENCE PURPOSES ONLY
the weather was important because, usually when eruptions occur in Iceland, Europe does not get any ash. This is because over the North Atlantic is usually cyclonic weather system. During the first week of the eruption however, there was an anti-cyclone south of Iceland which pushed the ash south-east onto Europe (Petersen, 2010).

More local effects are the effects from heavy ash fall. The heaviest ash fall occurred on the 17 April (Petersen, 2010). The area of Iceland affected was actually relatively small. The area contained 200 farms and a town called Vik with a population of 400 (Jenkins, 2010). Ash fall can reduce visibility, making driving dangerous. Vehicle traction can be lost as ash can become slippery and ash on the road can cover vehicle markings. Driving also causes ash on the roads to fly into the air and this can be a health hazard. Ash can damage signal equipment on railways, making train journeys dangerous. Ash can damage the vehicles in a similar way to how it damages aeroplanes; getting into the filter systems, damaging brakes, alternators and abrading the engine.

Farmers in southern Iceland had problems harvesting their crops, as the very fine ash of the volcano became clay when wetted and suffocated the crops, although rain is needed to wash the ash away from grazing areas. During summer, livestock is usually grazed on the highlands; however, due to the ash this was not possible and so the livestock was kept inside which is rather crowded. Usually the stock is relocated to another area of Iceland but due to a disease in sheep, this could not happen and so it is likely that some stock died from overcrowding. When the livestock was allowed out there was concerns as the pasture, and water, could have been contaminated with ash which abrades their skin and eyes. Fluoride ingestion may also have been a problem (Jenkins, 2010).

There was an increase in tourism in Iceland during and after the eruption. This interest also manifested itself in the science community. For example, there were no low frequency seismic signals coming from the volcano just before it started erupting. This meant that the flood plain for Jökulhlaups was not evacuated. The eruption of Jökulhlaups could also have destroyed civic infrastructure, although there were already mitigation plans in place in case of an eruption from Katla and so machines from a nearby quarry were used to prepare for flooding. Levees were built to protect valuable farmland and roads were bulldozed to protect adjacent expensive bridges. This meant that the impact was limited (Jenkins, 2010).

Whilst ash is bad for human health, there were no reported human fatalities from the 2010 Eyjafjallajökull eruption. Ash inhalation as a health problem became of interest after Mt St. Helens erupted ash into a populated area on 18 May 1980. Although eruptions are often short lived, ash can remain in the environment for a considerable period of time. Volcanic ash is defined as a pyroclast of 2 mm or less in diameter. When ash is freshly erupted it is not weathered like other dust particles on the earth's surface and so may contain acids or trace metals. Acute problems include asthma attacks and bronchitis which can sometimes be fatal in older people. Chronic problems include silicosis and nodular fibrosis. Chronic obstructive pulmonary disease (COPD) also occurs in people who have been exposed to ash for a considerable period of time. The population who lived near the volcano had high levels of irritation symptoms, and 6 months later, this population had

FOR REFERENCE PURPOSES ONLY

more respiratory symptoms than a control group from North Iceland, where there was no ashfall. In the United Kingdom, the Heath Protection Agency issued a paper that said that health effects were unlikely to occur and if they did it would be slight irritation to the eyes or the lungs of asthmatics (Maynard et al., 2010). The World Health Organisation also concluded that there was no health risk from the ash (WHO, 2010).

In Iceland, facemasks had been stockpiled in preparation for swine flu and so these were distributed to the affected areas. The general advice was to wear a mouth mask of a recommended type and to stay inside with the heat turned up to keep the ash out. Homes in Iceland are well sealed against the cold and so not much ash can get in. In Vik, the roads were wetted and there was a speed limit in order to limit re-suspension of ash. People were concerned for children and outdoor workers as exposure could lead to long-term respiratory effects. Nevertheless, as Iceland is a very volcanic country, there was no particular worry about this volcano as long as everyone followed the government advice.

A dangerous side effect of the ash fall is that when wetted it can cause dangerous mud flows called lahars. Lahars are caused by the wetting of unstable ash and other debris. Once the mixture is saturated with water, it flows very fast down the flanks of the volcanoes. Lahars can be very destructive and on 19 May there was a lahar in the Svaðbælisheiði river (Jenkins, 2010). In fact, the main environmental effect of the ash cloud may end up being some cooling of the northern hemisphere. This effect is due to the sunlight being blocked out, not by the ash, but by the sulphur aerosols. This may have a knock-on effect of less biomass growth for a few years.

4.6.4 Volcanic eruptions in the future

Just four years after Eyjafjallajökull eruption in September 2014, a huge volcanic eruption in Holuhraun, Iceland emitted up to nine times as much sulphur dioxide per day as all European industry combined. The eruption of Eyjafjallajökull highlighted the society's demand for unaffected mobility, as well as aviation's vulnerability to natural hazards. It was especially disruptive to air travel for a number of reasons: (1) the volcano was directly under the jet stream, which was abnormally stable at the time of the eruption, continuously south-east; (2) the second eruptive phase happened under glacial ice and the resulting meltwater flowed back into the erupting volcano, increasing its explosive power and creating a cloud of highly abrasive glass-rich ash; and (3) the power was sufficient to introduce ash directly into the jet stream. As a consequence, the eruption of Eyjafjallajökull caused significant financial losses to the aviation industry in Europe by pouring ash into the atmosphere which was then carried over European airspace by weather conditions.

The eruption also impacted farming in the area around Vik and caused respiratory problems to local populations. The eruption may have a longer term effect of blocking out the sun and therefore reducing global temperatures for a few years. A larger volcano (Katla) lies only 25 km and the eruption of Eyjafjallajökull could trigger a much larger one from its neighbour in future. The response to the crisis was widely considered a policy fiasco, in

FOR REFERENCE PURPOSES ONLY

need of significant improvement in the event of further eruptions. Subsequently, a conference was held in Reykjavik, outlining the future dangers posed by Iceland's vigorous volcanic activity and the need for better preparation.

REFERENCES AND FURTHER READING RESOURCES

Alexander, D. (2013) Volcanic ash in the atmosphere and risks for civil aviation: A study in European crisis management. *International Journal of Disaster Risk Science*, 4(1): 9–19.

Björnsson, H. (2002) Subglacial lakes and jökulhlaups in Iceland. *Glacial and Planetary Change*, 35: 255–271.

Brooker, P. (2010) Fear in a handful of dust: aviation and the Icelandic volcano. *Significance*, 7(3): 112–115.

European Commission (1999) *Directive 1999/31/EC on the Landfill of Waste*. European Commission, Brussels, Belgium.

Eurocontrol (2010a) *Volcanic Ash Cloud Timeline – April Events*.http://www.eurocontrol.int/corporate/public/standard_page/volcanic_ash_cloud_chronology.html.

Eurocontrol (2010b) *Ash-cloud of April and May 2010: Impact on Air Traffic*. Eurocontrol Statistics and Forecast Service, Brussels, Belgium.

European Commission Joint Research Centre (2017) Danger to air quality from forest fires. *ScienceDaily*, 19 October.

Grindle, T. J. and Burcham, F. W. (2003) *Engine Damage to a NASA DC-8-72 Airplane from a High-Altitude Encounter with a Diffuse Volcanic Ash Cloud*. National Aeronautics and Space Administration, Dryden Flight Research Center, Edwards, CA.

Harrison, R. G., Nicoll, K. A., Ulanowski, Z., and Mather, T. A. (2010) Self-charging of the Eyjafjallajökull volcanic ash plume. *Environmental Research Letters*, 5: 1–4.

Jaeglé, L., Steinberger, L., Martin, R. V., and Chance, K. (2005) Global partitioning of NOx sources using satellite observations: Relative roles of fossil fuel combustion, biomass burning and soil emissions. *Faraday Discussions*, 130: 407–423.

Jahnke, J. A. (2000) *Continuous Emissions Monitoring*. Wiley, New York.

Jenkins, S. (2010) *Observations of the Eyjafjallajökull Eruption*. Cambridge Architectural Research Ltd., Cambridge, UK.

Knorr, W., Dentener, F., Lamarque, J. F., Jiang, L., and Arneth, A. (2017) Wildfire air pollution hazard during the 21st century. *Atmospheric Chemistry and Physics*, 17(14): 9223–9236.

Laursen, L. (2010) Iceland eruptions fuel interest in volcanic gas monitoring. *Science*, 328(5977): 410–411.

Maynard, B., Mills, I., and Exley, K. (2010) *Paper on the Possible Effects on Health of Exposure to Volcanic Ash and Associated Gases*. Health Protection Agency, London, UK.

Mazzocchi, M., Hansstein, F., and Ragona, M. (2010) The 2010 volcanic ash cloud and its financial impact on the European airline industry. *CESifo Forum*, 11(2): 92–100.

Mohan, R., Leonardi, G. S., Robins, A., Jefferis, S., Coy, J., Wight, J., and Murray, V. (2009) Evaluation of methodologies for exposure assessment to atmospheric pollutants from a landfill site. *Journal of the Air & Waste Management Association*, 59(4): 490–501.

NAEI (2008) *UK Emissions of Air Pollutants 1970 to 2006*. National Atmospheric Emissions Inventory.

NOAA (2017) *Wildfires*, National Oceanic and Atmospheric Administration. www.noaa.gov/topic-tags/wildfires.

Oikawa, P. Y., Ge, C., Wang, J., Eberwein, J. R., Liang, L. L., Allsman, L. A., and Jenerette, G. D. (2015) Unusually high soil nitrogen oxide emissions influence air quality in a high-temperature agricultural region. *Nature Communications*, 6: 8753.

Oxford Economics (2010) *UK Economic Loss Due to Volcanic Ash Air Travel Restrictions*. Oxford Economics, Oxford, UK.

Petersen, G. N. (2010) A short meteorological overview of the Eyjafjallajökull eruption 14 April–23 May 2010. *Weather*, 65(8): 203–207.

Sigmundsson, F. (2010) Eruption in Eyjafjallajökull 20 March to present. http://www2.hi.is/page/ies_EYJO_compiled.

Sigmundsson, F., Gudmundsson, M. T., Larsen, G. et al. (2010) Eruption in

FOR REFERENCE PURPOSES ONLY

Eyjafjallajökull.http://www.earthice.hi.is/page/ies_Eyjafjallajokull_eruption.

Sigmundsson, F. and Höskuldsson, A. (2010) Develop instruments to monitor volcanic ash fallout. *Nature*, 466: 28.

Sturkell, E., Sigmundsson, F., and Einarsson, P. (2003) Recent unrest and magma movements in *Eyjafjallajökull* and *Katla* volcanoes, Iceland. *Journal of Geophysical Research*, 108(B8): 2369.

Tiwary, A., Namdeo, A., Fuentes, J., Dore, A., Hu, X. M., and Bell, M. (2013) Systems scale assessment of the sustainability implications of emerging green initiatives. *Environmental Pollution*, 183: 213–223.

USDA (2014) A national cohesive wildland fire management strategy. doi:10.1234/12345678.

World Health Organization (WHO) (2010) WHO/Europe expert group concludes Icelandic volcanic ash currently poses no threat. http://www.euro.who.int/en/what-we-do/health-topics/environmental-health/air-quality/sections/news/2010/04/whoeurope-expert-group-concludes-icelandic-volcanic-ash-currently-poses-no-threat-to-public-health.

---

[1] Phreatomagmatic eruptions are juvenile forming eruptions that result from interaction between water and magma.

FOR REFERENCE PURPOSES ONLY

Chapter 5

Mobile sources

Mobile sources of air pollutants largely comprise of *technology emissions* from modern means of transport. Some may consider this as the insoluble dilemma of human progress at its own peril. Comparisons between the air pollution implications of different transport modes are also of interest. Which comparisons are relevant depends partly on the route length and terrain. Long-distance passenger travel is dominated by aircraft, but most freight is carried on the surface by ships. Trains compete with aircraft on land-based trips of up to several hundred kilometres. Roads and railways compete over shorter distances. Ships are involved at all distances, but need water. Ships also have specialist niches such as ferries and long distance movement of freight and raw materials. The air pollution impact can be quantified in various ways. In order to compare emissions per passenger km (or per tonne km for freight) we also need to know the capacity and the load factor (proportion occupied). The majority of this chapter provides a broader understanding of the road traffic emissions of air pollutants. This is followed by a relatively brief description of other non-road mobile machinery sources, rail transport, shipping and aircraft emissions. There is also a section describing the development of emissions inventory specifically for mobile sources.

Typical rail journeys work out at about 40% of the emissions of the various regulated pollutants per passenger km, compared to those from a petrol engine car conforming with EURO-I. The methodologies for estimating air pollutant emissions from transport (MEET) project report considered the CO_2 and NO_x emissions created by two typical trips in Europe. First, a passenger travelled from Vienna to Rome by air, rail or road (Table 5.1). Trains were the clear winner. Second, a freight cargo was moved from Rotterdam to Zurich by water (mainly), train or road. Again, the train is the winner (Table 5.2), especially for NO_x emissions. The inland water transport carries far more than a goods vehicle, and is more fuel efficient. However, the emission per tonne of fuel from the ship engine is also much higher. In practice, the decisions on what transport mode to employ are rarely made on pollution grounds, but on speed, cost or convenience.

In terms of the CO_2 emitted per passenger km, long-haul aircraft are similar to passenger cars at 30–40 g C per passenger km. However, one long-haul flight can cover as many km in

FOR REFERENCE PURPOSES ONLY

a day as the average car covers in a year, so the total emissions must be considered. For freight, aircraft cannot compete. Air freight transport generates 100–1000 g C per tonne km, as against 1–10 for ships, 1–20 for trains and 10–100 for heavy goods vehicles (HGVs).

Although much attention has been paid to vehicular emissions because of their impact on the urban environment, there are substantial emissions from other types of transport. In general, they have less impact on people, and people are less aware of them, than for vehicle emissions simply because they occur in more remote locations. Nevertheless, they make a significant contribution to some aspects of chemical budgets in the atmosphere. The first part of this chapter covers road transport; emissions from planes, boats and trains will be discussed following this.

Table 5.1 Emissions due to different passenger transport modes

Mode	CO_2/g (passenger km)$^{-1}$	NOx/g (passenger km)$^{-1}$
Air	125	0.4
Rail	20	0.05
Road	70	0.23

Table 5.2 Emissions due to different cargo transport modes

Mode	CO_2/g (tonne km)$^{-1}$	NO_x/g (tonne km) $^{-1}$
Water	65	0.83
Train	42	0.08
Road	92	0.81

5.1 ROAD TRAFFIC EMISSIONS

Pollution from motor vehicles has become an issue simply because of the steady increase, both in the number of vehicles in use and the distance travelled per vehicle each year. Road transport has been identified as the main low-level source of NO_2 and fine particulate matter pollution for a long time; the Quality of Urban Air Review Group (QUARG) in 1993 had concluded that halving of NO_x emissions from motor vehicles in the UK is required to achieve the elimination of episodes of severe NO_2 pollution. In 1950 there were 50 million cars for 3.5 billion people. Since the 1960s, the number of motor vehicles in the world has been growing faster than its population. There are now over 600 m cars for 6.7 billion people, with a global production of 45 million cars per year. The net growth rate for all motor vehicles is now around 5%, compared to a population growth rate of 1%–2%, with a billion cars on the roads in 2020 (Figure 5.1). The population is set to stabilise at 9–10 billion between 2030 and 2050, but the vehicle fleet will continue to grow. Vehicle production in India is increasing at 15%–25% per year (depending on category) and the

FOR REFERENCE PURPOSES ONLY

vehicle population of China is growing at an average annual rate of 13% (approximately 270 million vehicles by 2020).

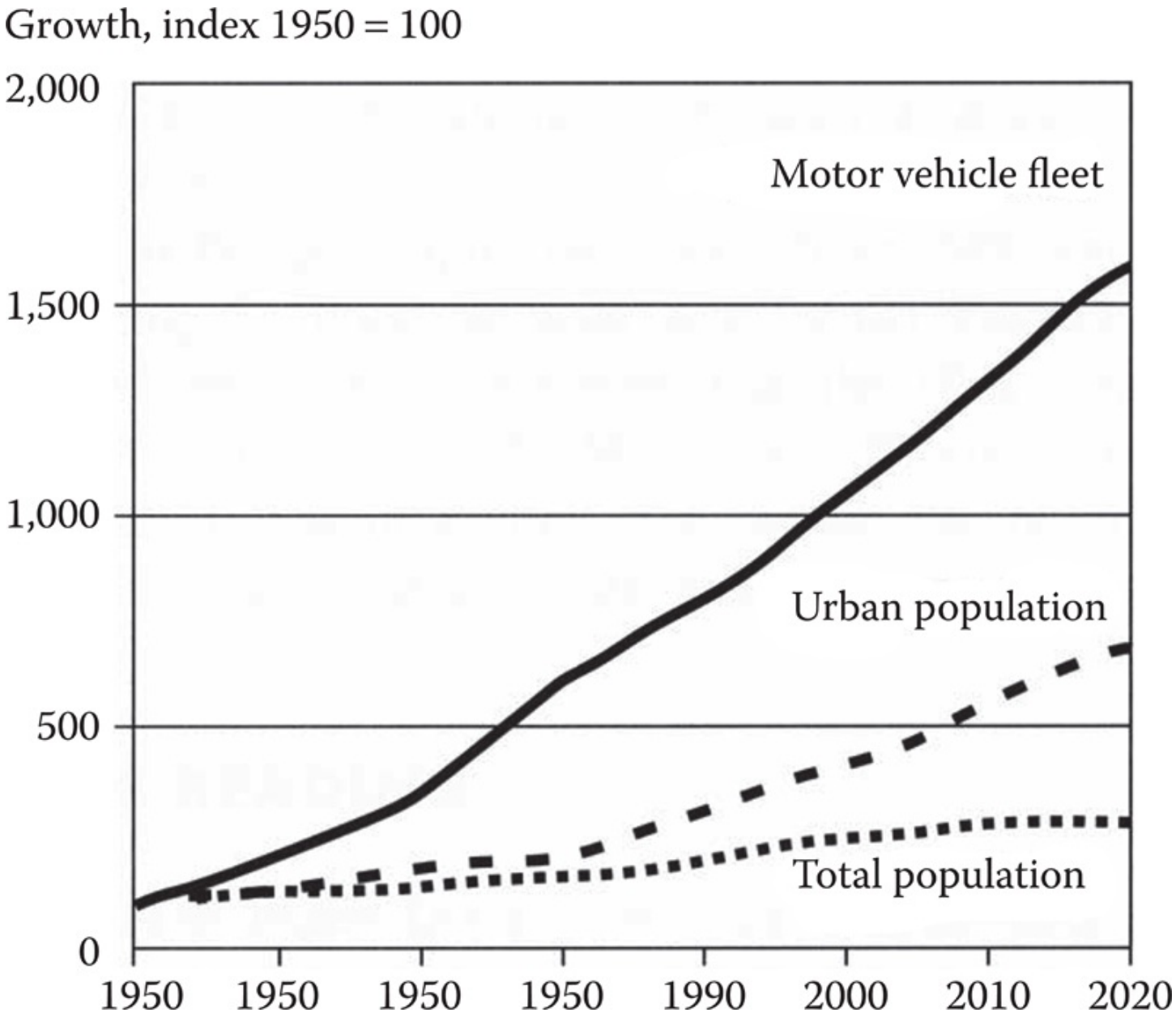

Figure 5.1 Relative growth of vehicles and global population, 1950–2020. (From Fenger, J., Atmos. Environ., 33, 4877–4900, 1999.)

Around 2005 two-thirds of the global share of passenger cars were used in Europe and North America (Figure 5.2, upper panel). However, it is noteworthy that although the European trend seems to be declining beyond 2004, the Asia-Pacific region is witnessing a steep increase in car use. In some part of Asia, this is associated with increased use of two- and three-wheelers powered by small engines. On a per vehicle basis these are considered to be contributing disproportionately to particulate, hydrocarbon and carbon monoxide emissions. Overall, in the Asia-Pacific region, the use of passenger cars increased by a

FOR REFERENCE PURPOSES ONLY

factor of about 2.5 between 1987 and 2003, with the highest increase seen in the North East Asia region (Figure 5.2, lower panel). During the past 50 years, mobile sources have taken over from static combustion of fossil fuel as *the* major threat to air quality. There are four main polluting emissions from motor vehicles: carbon monoxide (CO), NO_x, hydrocarbons (HC) and particles. In this chapter we will discuss the sources of motor vehicle emissions as a group, because the pollutants are emitted together. It must also be borne in mind that the emissions from the vehicles themselves are not the end of the story. Any full estimation of emission potential should be made on a life-cycle basis – including the emissions that are created before and after use by processes such as mining and steel manufacture, making the plastics, spraying the paint, making and distributing the fuel, and disposing of the vehicle at the end of its useful life. For petrol vehicles, for example, fuel production might account for up to 70% of the total lifetime HC emissions, whereas fuel use will make up a similar proportion of lifetime CO_2 emissions.

FOR REFERENCE PURPOSES ONLY

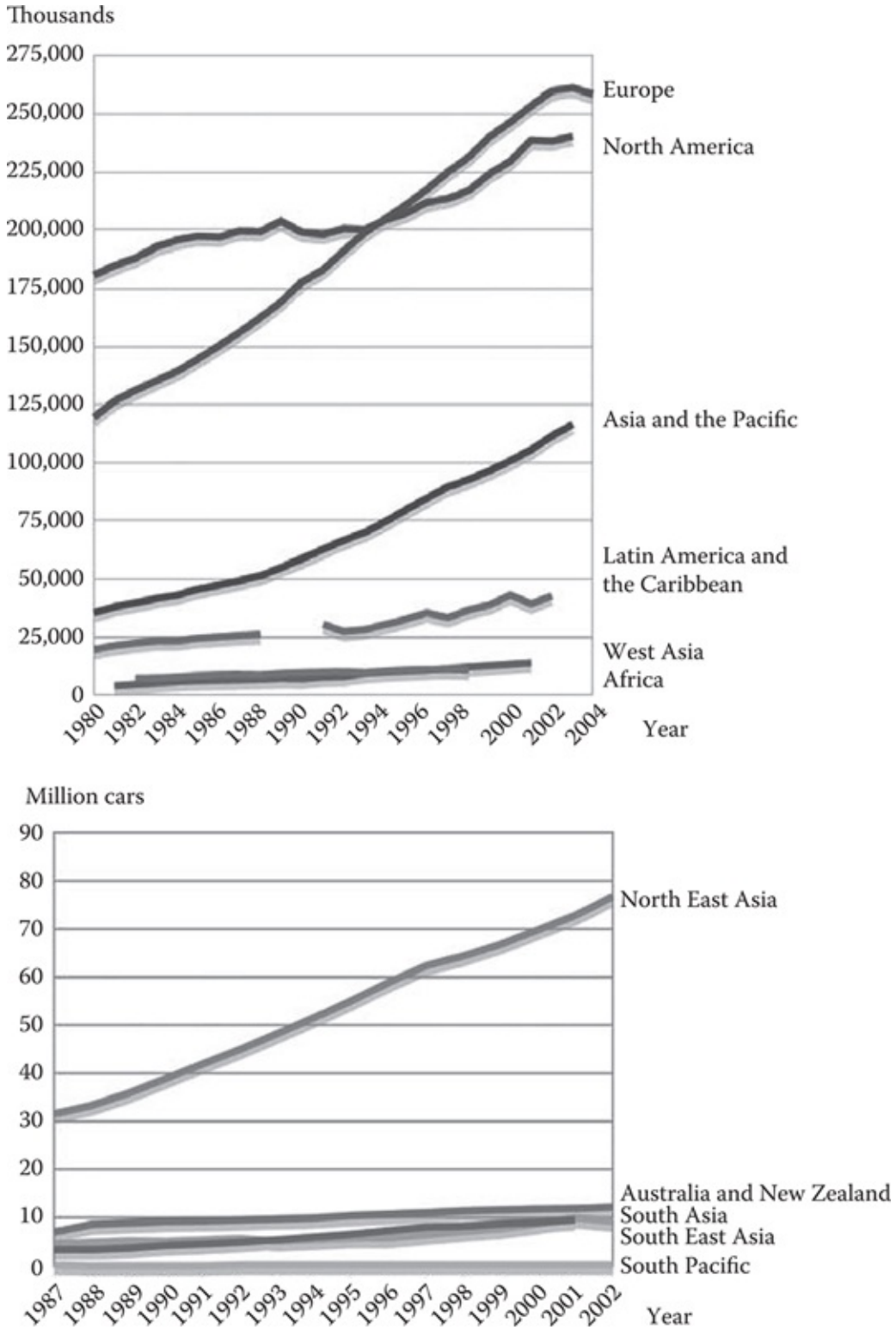

Figure 5.2 Trend in the use of passenger cars globally, by region (upper panel) and in the Asia-Pacific region (lower panel). (From UNEP, *Global Environment Outlook* [*The Fourth Assessment, GEO-4*], Progress Press Company Limited, Valletta, Malta, 2007.)

In the UK, motorists drove an average of 7900 miles each in 2015. As a consequence, the

FOR REFERENCE PURPOSES ONLY

use of motor vehicles now generates more air pollution than any other single human activity. It is the fastest-growing source of CO_2, and in urban areas accounts for the bulk of emissions of CO, HC and NO_x. Both people and vehicles are concentrated in urban areas, where the emission densities per unit area are the highest and the dispersion conditions the worst. Vehicles are now recognised as having the major environmental impact on our towns and cities. Table 5.3 shows recent historical trends in the contribution of road transport to urban pollution in selected cities of the world.

Table 5.3 Relative contribution of road transport to pollution in different cities

		Relative contribution of road transport to urban pollution in the year given/%					
City	*Population (2005) thousands*	*CO*	*HC*	*NO_x*	*SO_2*	*SPM*	*Year*
Beijing	10,717	84	NA	73	NA	NA	2000
Budapest	1,693	81	75	57	12	NA	1987
Buenos Aires	12,721	99	98	48[a]	38	69	1989
Cochin		70	95	77	NA	NA	1993
Delhi	15,048	90	85	59	13	37	1987
Lagos	13,857	91	20	62	27	69	1988
London	8,505	95	NA	75[a]	1	76	1988
Los Angeles	12,298	90	NA	70[a]	60	89	1987
Manila	10,686	97	NA	91[a]	23	82	1990
Mexico City	19,411	99	33	77	21	26	1996
Moscow	10,654	80	NA	20[a]	1	1	1990
Mumbai	18,196	NA	NA	57	5	24	1992
Santiago	5,683	92	46	71	15	86	1997
São Paulo	18,333	94	89	92	64	39	1990
Seoul	9,645	56	17	78[a]	12	30	1990

[a] NO_2.

5.1.1 Traffic congestion

More than 50% of the global population lives in urban areas and by 2030, the number of urbanites is expected to reach almost 5 billion (UNFPA 2007). High urban population density presents myriad challenges that include servicing requirements for transportation, both of passengers and freight. This focused travel requirement can often overwhelm a transport system leading to congestion on urban road networks during peak periods.

Congestion may be defined as the deterioration of smooth, free-flowing traffic conditions due to increased travel demand and/or reduced traffic movement capacity (Smit et al., 2008), that is travel demand exceeding the supply of road capacity. Traffic movement capacity is dictated by factors such as network characteristics (e.g. link length, number of

FOR REFERENCE PURPOSES ONLY

lanes, intersection types and layouts, number of intersections per kilometre, pedestrian crossing types, speed limits etc.), traffic management strategies (e.g. traffic signal control, rerouting, dynamic speed limit systems), or adverse weather (e.g. heavy rain, fog, snow). Congestion can be considered at multiple scales, for example around a single intersection, along a certain corridor (series of links and intersections), or for a network as a whole. It is generally accepted that under the stop-and-go traffic conditions associated with congestion there is an increase in the number of acceleration and deceleration events experienced by vehicles, which results in increased emissions (Madireddy et al., 2011). Congestion has been repeatedly identified as a major factor when estimating road traffic emissions and ranks alongside vehicle kilometres, vehicle speed and vehicle category as one of the most important influences (Smit et al., 2008).

As an example of the situation in a typical developed nation, according to the United Kingdom national government Department for Transport (DfT) (2017), the national total of 521 bn vehicle-kilometres[1] (VKMs) travelled in Great Britain in 2016 was split approximately evenly between those driven in urban areas (341 bn VKMs = 65%) and those driven outside urban areas (180 bn VKMs = 35%). However, congestion is a much bigger problem in urban areas, with 14% (29.2 bn) of VKMs being driven in very congested conditions, compared to just 2% (4.1 bn) outside urban areas.

The large number of vehicles using urban road networks has damaging environmental impacts, including emissions from vehicle tailpipes, including both greenhouse gases and pollutants detrimental to ambient air quality (discussed in Chapter 6). Road traffic is often the dominant anthropogenic source of air quality emissions in urban areas, and poor local air quality in the vicinity of busy roads is of particular concern, especially as emissions occur in close proximity to people. Consequently, urban areas produce a disproportionate amount of road traffic emissions compared to their geographic size, and should be a focus for efforts to mitigate such emissions as part of overall strategies to reduce anthropogenic GHG emissions and improve air quality. Indeed, some Local Authorities (LAs) provide a forecasting service for poor air quality to individuals with respiratory disease to reduce preventable admissions to hospital (McLaren and Williams, 2015).

One way to combat urban congestion due to road traffic is to introduce a so-called *congestion charge scheme* (CCS). This is a daily levy imposed on vehicle drivers that drive within a specific urban area in specific time periods. London is the largest city to have adopted a central area CCS. It was introduced by the (then) Mayor of London Ken Livingstone in February 2003. The original central London congestion charging zone (CCZ) covered 22 km^2 in the heart of London. In February 2007, the zone was expanded by about 50% to include parts of west central London and included a free route through the centre of the enlarged zone. The features of the London CCS include:

- Fixed cameras placed at the entrance points of the CCZ automatically capture vehicle number plates. A financial penalty is applied to the registered keepers of vehicles recorded within the CCZ that have not paid the charge.

FOR REFERENCE PURPOSES ONLY

- Drivers pay the charge via the Internet, by text message, at outlets equipped with a specified electronic payment system, or via telephone. There are no toll booths.
- Selected vehicle types are exempt, including taxis, buses, private hire vehicles and motorcycles. Some other types of vehicle can register for a discount, including vehicles used by those with a disabled persons badge and used by residents of the CCZ.

Ten years after its introduction, TfL (2014) reported that the London CCS had resulted in a 10% reduction in traffic volumes from baseline conditions, and an overall reduction of 11% in VKM between 2000 and 2012. Nevertheless, traffic speeds also got gradually slower, probably due to interventions that have reduced the operational capacity of the road network to increase road safety, improve the urban environment and prioritise public transport, pedestrian and cycle traffic, as well as an increase in road works by utilities and general development activity. TfL (2014) concluded that although levels of congestion in central London were close to pre-charging levels a decade later, the success of the scheme in reducing traffic volumes means that the situation would have been worse without the CCS.

In terms of other impacts, Tonne et al. (2008) modelled the impact of the CCS on concentrations of traffic pollutants, levels of life expectancy and socio-economic inequalities. Their results showed that absolute and relative reductions in NO_2 and PM_{10} concentrations following the introduction of the CCS were greater among charging zone wards compared to remaining wards. They also predicted life expectancy benefits in the charging zone wards as 183 years of life per 100,000 population compared to 18 years among the remaining wards. In addition, more deprived areas had higher air pollution concentrations and these areas experienced greater air pollution reductions and mortality benefits compared to the least deprived areas.

In summary, the London CCS appears to have resulted in significant reductions in traffic volumes and distances travelled, alongside modest benefits to air pollution concentrations and associated life expectancy, and a small contribution to reducing socio-economic inequalities.

5.1.2 Combustion of fuel

Most of the world's vehicles use internal combustion engines, which burn petrol or diesel or gas hydrocarbon fuels for their energy supply. If a pure hydrocarbon fuel was burned under ideal conditions, then the simple reaction taking place would be similar to:

$$\mathrm{C}_x\mathrm{H}_y + \left(x + \frac{y}{4}\right)\mathrm{O}_2 = x\mathrm{CO}_2 + \frac{y}{2}\,\mathrm{H}_2\mathrm{O}$$

so that carbon dioxide and water would be the only combustion products. For example, pure octane (C_8H_{18}) would react as follows:

$$C_8H_{18} + 12.5O_2 \rightarrow 8CO_2 + 9H_2O$$

Also, the masses of the reactants and products are related exactly by their molar masses. Hence the masses of CO_2 and H_2O are specified by the mass of fuel burned. For example, the mass of carbon in the fuel is given by

$$[C] = [C_xH_y] \times \frac{12}{(12x+1y)}$$

because the molar masses of carbon and hydrogen are 12 and 1, respectively. This mass of carbon would combine with the corresponding mass of oxygen (molar mass = 32) as follows:

$$[C] + \left([C] \times \frac{32}{12}\right)O_2 = [CO_2]$$

Taking octane as an example again, a molecule with a mass of 114 combines with 12.5 molecules of oxygen having a mass of 400, a ratio of 3.5:1 by mass. As oxygen makes up about 23% of air by mass, this represents around 15:1 of air to fuel. This proportion is known as the *stoichiometric ratio*; although it varies depending on the proportions of different hydrocarbons, a global value of 14.7:1 is accepted for the general mixtures used in petrol and diesel engines.

In practice, this perfect combustion never occurs. First, the oxygen does not come alone, but mixed with nitrogen and a variety of other components of the atmosphere. Second, the fuel is not a single pure hydrocarbon, nor even a blend of pure hydrocarbons, but a rather impure mixture of hydrocarbons and other compounds that contain sulphur, nitrogen, lead and other minor constituents. Third, perfect combustion implies perfect mixing – that is the availability of the correct ratios of reacting molecules in the same place at the same time – and internal combustion engines cannot achieve this. As a result of these factors, some atmospheric and fuel nitrogen is oxidised to NO_x, some fuel is imperfectly combusted to form new HC or CO or carbon particles instead of CO_2, some fuel is not combusted at all and is emitted as VOC, and the minor contaminants are emitted in various forms. A carbon balance can still be made, providing that all the carbon-containing components are included:

$$[\text{Fuel}] = (12 + r_1) \times \left\{ \frac{[CO_2]}{44} + \frac{[CO]}{28} + \frac{[HC]}{(12+r_2)} + \frac{\alpha[PM]}{12} \right\}$$

where square brackets indicate masses. r_1 and r_2 are the hydrogen to carbon ratios of the fuel and HC emissions, respectively. These may be taken as equal to a first approximation, though they vary between fuel types, being typically 1.8 for petrol and 2.0 for diesel. α is the proportion of carbon in the PM emissions. It will usually be acceptable to assume that α = 1, because PM makes up such a small proportion of total carbon emissions. The typical

FOR REFERENCE PURPOSES ONLY

PM emission for a diesel is only a small fraction of 1% of its CO_2 emission factor. No such mass balance can be made with certainty for the other components. A variable proportion of the nitrogen in the air will be oxidised, depending on exact combustion conditions such as peak temperature reached during the combustion cycle. It is usually assumed that all the sulphur in the fuel will be emitted, although some may be as SO_2 and some adsorbed to carbon particles. It is also presumed that 75% of the lead in the fuel will be emitted, with the remainder being retained in the exhaust system, engine parts and lubricating oil.

Table 5.4 Typical petrol composition

Component	*Percent by volume*
n-hexane	31.5
n-octane	21.2
2-methylpentane	10.5
methylcyclopentane	7.2
toluene	6.0
m-xylene	5.2
benzene	4.4
styrene	3.9
ethylbenzene	3.5
3-ethylpentane	3.4
o-xylene	2.2
n-nonane	1.0

5.1.2.1 Petrol engines

The majority of petrol or spark-ignition engines operate on a four-stroke cycle of *suck* (draw in petrol and air mixture), *squeeze* (compress the mixture), *bang* (ignite the mixture with a spark) and *blow* (exhaust the waste gases). Petrol is a complex and variable mixture of many different hydrocarbons ranging from C_7 to C_{35}. A typical composition is shown in Table 5.4.

In addition to four-stroke petrol engines, there are two-stroke engines, which are widely used for engines up to 0.5 L capacity and are more efficient because they fire every cycle rather than on alternate cycles. However, there are two disadvantages for air quality. First, the air–fuel mixture is introduced to the cylinder on the same piston movement that exhaust gases are discharged, so that unburned hydrocarbons can be lost. Second, the engine is often lubricated by means of oil mixed with the petrol, which leads to a serious emissions problem, often characterised by visible blue smoke from the exhaust. Two-stroke engines on motorcycles and small three-wheeler vehicles such as Tuk-Tuks have become very popular in developing countries, especially India, Indonesia and Malaysia where 60%–70% of the vehicles on the roads are two- or three-wheelers. Measurements in Bangkok have

shown that total suspended particle emissions from two-stroke motor-cycles are similar to those from HGVs and buses. Emissions from motorcycles, lawnmowers, chainsaws, strimmers, jet skis, outboards and other small petrol-engined devices are becoming proportionally more significant as their number increases and emissions from large vehicles decrease.

5.1.2.2 Diesel engines

Diesel engines also operate on a four-stroke cycle in which the fuel is injected into the compressed air. The air–fuel mixture is leaner (more air per unit fuel), the compression ratio is higher (typically 15:1 instead of 9:1) and the ignition is spontaneous due to the high temperature achieved by the compression. Although diesel engines are more efficient than petrol ones, they are both still enormously wasteful. Of the initial energy content of the fuel, only about 30% is converted into useful mechanical energy, with about 35% each going into heating the exhaust gases and the cooling water. A further 5% is spent on flexing the tyres and on friction in the drive train, leaving just 25% for propelling the vehicle.

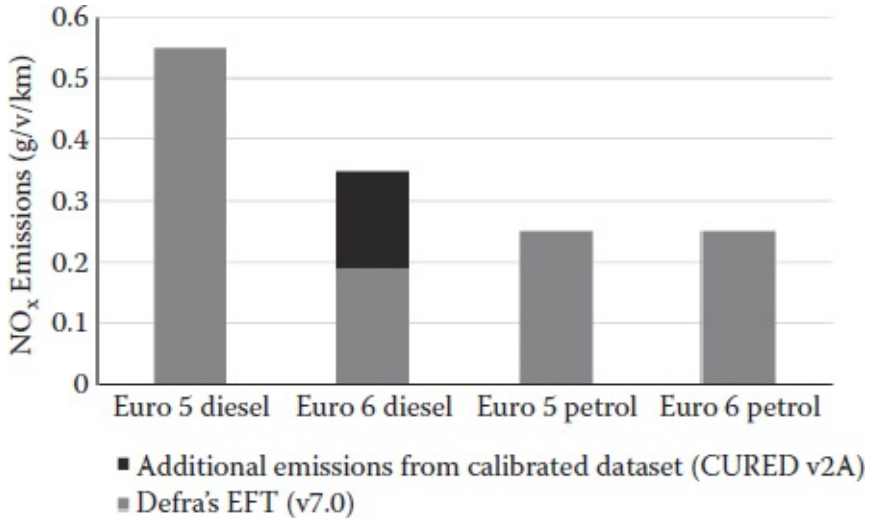

Figure 5.3 Comparative NO_x emissions from Euro 5 and 6 diesel cars (at 50 kmph).

It is important to note that despite emitting more than the originally prescribed emission standard, on average, Euro 6 diesel cars produce significantly less NO_x than Euro 5 and 4 diesel cars (Figure 5.3).

5.1.2.3 Traffic biofuel in developing countries

Where vehicles are important contributors to poor urban air quality, biofuels may be environmentally preferable to petroleum-based fuels. Ethanol has the greatest air quality benefits where vehicle fleets are old, as is often the case in developing countries. It helps to reduce the exhaust emissions of carbon monoxide and hydrocarbons, especially in cold

climates. Ethanol can replace harmful lead additives for raising the octane of gasoline, and all biofuels are sulphur-free. Biodiesel reduces emissions of carbon monoxide, hydrocarbons, and particulate matter, but can slightly increase emissions of nitrogen oxides. More information on these biofuels is provided in Section 5.1.13 while discussing alternative fuels.

During the 2nd World conference for Biomass and Climate Change in Rome (May 2004), developing countries were considered large potential suppliers of biomass. In the developing world Brazil has the largest commercial programme to utilise sugarcane-based ethanol in passenger cars and light vehicles. More recently India, Thailand, China, Peru and several other Latin American countries have joined in this effort to exploit the benefits of low-polluting traffic biofuels. The National Renewable Energy Laboratory of the US Department of Energy has been involved in some of the pioneering research in this field. However, terrestrial biofuels have come under heavy criticism for accelerating the race for cultivating fuel crops in lieu of essential food crops, leading to an inadvertent surge in global food prices in the last decade.

5.1.3 Combustion emissions

For both petrol and diesel engines, complete and incomplete combustion of the fuel generates a complex mixture of gaseous and particulate pollutants, many of which are harmful to human health.

5.1.3.1 Emission concentrations

The order-of-magnitude emission concentrations generated by the above-mentioned processes in the exhaust gases of a non-catalysed petrol engine and a diesel engine are indicated in Table 5.5. The concentrations are very sensitive to the engine operating mode. With the emission concentrations being some 10^4–10^5 times typical ambient backgrounds, and released only a few tens of centimetres above ground level, excellent dispersion is essential.

5.1.4 Specific pollutants

5.1.4.1 NO_x

Worldwide emissions of NO_x have not declined for two decades; the on-road NO_x emissions from Euro 5 being similar to those from Euro 1 diesel cars. The transport sector has been considered the largest contributor to NO_x emissions, accounting for 46% of total emissions in 2013 in the European Union. Petrol is a low-*N* fuel, so there is little fuel NO. Thermal NO is created in high temperature regions via the Zeldovitch mechanism discussed in Chapter 2. The ratio of NO to NO_2 is typically >0.95 for petrol engines, >0.8 for diesel.

FOR REFERENCE PURPOSES ONLY

Travelling at speeds between 30 and 60 miles per hour emit less harmful pollutants than vehicles travelling at speeds below 30 miles per hour or greater than 60 miles per hour (Figure 5.4). Diurnal variations in NO_x concentration are also to be expected because of variations in traffic flow and atmospheric dispersion. Data for London (Figure 5.5) show a minimum at about 4 am, a strong peak between 8 and 10 am during the weekday morning rush-hour when atmospheric stability is high, and a gradual decline during the remainder of the day. Although there must be an equivalent peak in emissions during the evening rush-hour, increased advective and convective dilution, together with reactions with the O_3 created during the afternoon, prevent a recurrence of the concentration peak. On Sundays the variation is quite different – the average concentration is lower because of the general reduction in traffic, and the peak occurs in the early morning as people return home from Saturday night activities.

Table 5.5 Exhaust gas emission concentrations

Fuel and pollutant	*Emissions (ppm by volume in the exhaust)*			
	Idling	*Accelerating*	*Cruising*	*Decelerating*
Petrol				
CO	69,000	29,000	27,000	39,000
HC	5,300	1,600	1,000	10,000
NO_x	30	1,020	650	20
Diesel				
CO	Trace	1000	Trace	Trace
HC	400	200	100	300
NO_x	60	350	240	30

FOR REFERENCE PURPOSES ONLY

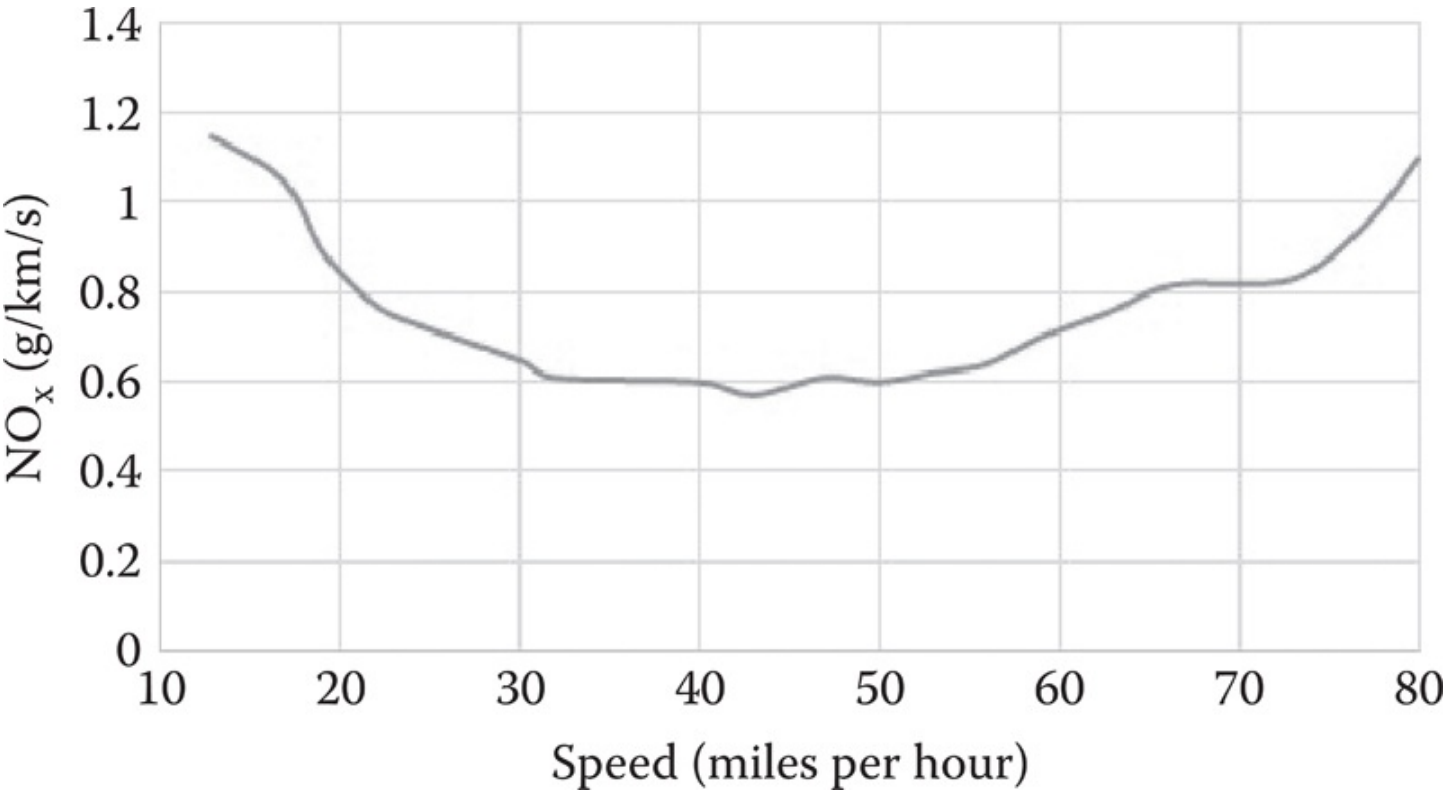

Figure 5.4 Speed dependent variation in NO_x emissions. (From DEFRA, *Emission Factor Toolkit*.)

FOR REFERENCE PURPOSES ONLY

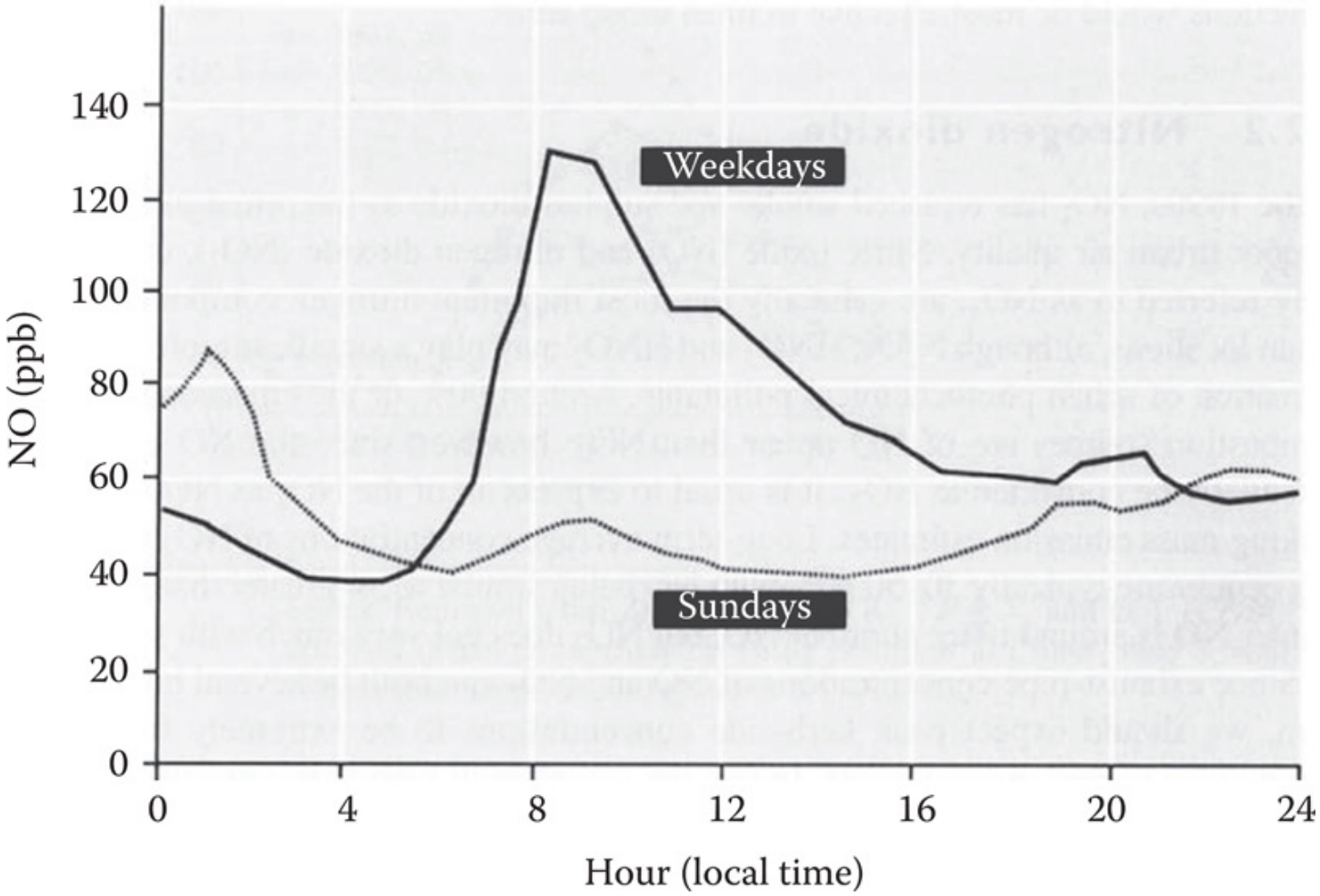

Figure 5.5 Diurnal variation of NO concentration on weekdays and Sundays at Earls Court in London, 1987. (From United Kingdom Quality of Urban Air Review Group, *Urban Air Quality in the United Kingdom*, DoE/HMSO, London, UK, 1993.)

Short-term episodes of high NO_2, lasting from a few hours to a few days, can occur in either summer or winter via different mechanisms. In the summer, high NO_2 levels are brought about by rapid photochemistry, and are therefore associated with low NO levels. In the winter, trapping of emissions beneath temperature inversions is responsible, so that NO concentrations are also high. A particularly severe NO_x smog occurred in London between 12 and 15 December 1991. Figure 5.6 displays the NO_2 record for the whole of 1991 from one London monitoring site, and shows how strongly the episode, with a peak concentration over 400 ppb, stood out from the typical NO_2 concentrations that year of 30–50 ppb. The episode extended over 4 days, with average NO_2 concentrations of around 150 ppb and the peak concentration rising to 423 ppb; this was associated with NO concentrations (not shown) of around 1200 ppb. Comparison of mortality data for the period indicated that about 160 deaths could be attributed to the incident.

Direct NO_2 emissions, which have been shown from measurements in road tunnels to make up only 5%–7% of the NO_x in exhaust gases, cannot have been responsible because

FOR REFERENCE PURPOSES ONLY

the NO_2/NO_x ratio in the smog was 20%–30%. Furthermore, NO_2 concentrations at three different sites in London were much more similar than the NO concentrations at those sites, indicating that the NO_2 had been formed in the atmosphere. It has been proposed that certain very specific hydrocarbons might enhance the production of NO_2 from NO. If this is the case, then the reduction of NO_x emissions by three-way catalyst (TWC) (see description later in this chapter), may have unpredictable effects on NO_2 concentrations. It is also ironic that, despite this being the worst pollution episode in London As the combustion smogs 30 years previously, the EC limit value for NO_2 was not broken. The limit is framed in terms of a 98th percentile exceedance, so the concentration would have had to remain high for 7 days. In future years, as more petrol cars become fitted with TWCs, these pollution episodes should be controlled.

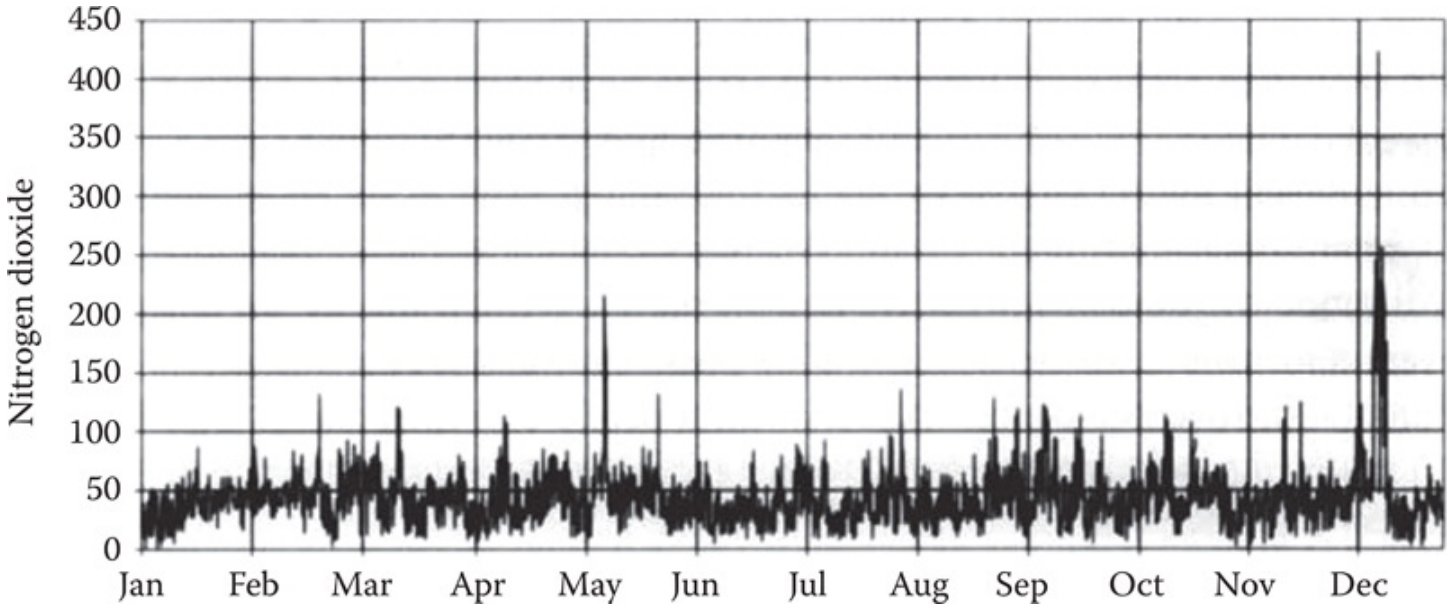

Figure 5.6 The annual record of NO_2 concentrations at Bridge Place in London during 1991. (From United Kingdom Quality of Urban Air Review Group, *Urban Air Quality in the United Kingdom*, DoE/HMSO, London, UK, 1993.)

5.1.4.2 CO

Imperfect combustion in fuel-rich regions of the combustion chamber means that some carbon is only partially oxidised to CO. The emitted concentration may be several percent. As shown in Table 5.3, motor vehicles emit a substantial quantity of CO in most of the cities. The amount of CO produced by a vehicle increases when the engine is idling or is not working efficiently, so congested and stop-start traffic produces much more CO than on motorways. Engines also produce much more CO when they are running cold (approximately for the first 2–3 km of a trip).

5.1.4.3 Combustion HC

Hydrocarbon emissions arise both as unaltered components of the original fuel and through partial oxidation of the fuel molecules. Benzene, for example, may arise via both routes. The main families of molecules are alkynes, alkenes, alkanes and aromatics. Alkanes contain single hydrogen–carbon bonds and are referred to as saturated. Alkenes contain both single and double bonds, and alkynes, single, double and triple bonds. Molecules containing double or triple bonds are referred to as unsaturated. Several hundred different hydrocarbons have been distinguished, with detailed proportions depending on combustion conditions. Diesel engines emit HCs of higher molecular weight (typically C_8 to C_{28}) than do petrol engines (typically C_5 to C_{12}). There are also non-hydrocarbon VOC emissions, which are also referred to as oxygenates. The two largest HC groups are ketones and aldehydes (including formaldehyde HCHO, acrolein CH_2CHCHO and acetaldehyde CH_3CHO). The oxygenates are a small proportion of total VOC for conventionally fuelled engines, but the proportion is larger if the fuel is methanol or natural gas. All these VOCs are ozone precursors to varying degrees, and a small number are toxic in their own right (benzene, toluene, xylene and 1,3-butadiene in particular). Reasons for the HC emissions are complex, but have been grouped into the following categories:

5.1.4.3.1 Imperfect combustion

Wall cooling: The thin boundary *quench* layer in close proximity to the water cooled combustion chamber wall fails to reach optimum combustion temperature.

Crevice trapping: Dead spaces in parts of the combustion chamber where the flame front does not penetrate, such as between the sides of the piston and the cylinder wall, or the threads of the spark plugs. Any porous deposits on the combustion chamber walls can have a similar effect by protecting the absorbed mixture from getting burned.

Poor mixing: Any region of the mixture which is oxygen-deficient. This situation is most likely to occur under transient engine operating conditions.

5.1.4.3.2 Leakage

Piston blow-by: Leakage of air–fuel mixture past the piston rings and into the sump.

Oil seep: Leakage of lubricating oil in the reverse direction.

5.1.4.4 Benzene

Two-thirds of atmospheric benzene in the UK is derived from extraction and distribution of fossil fuels for road vehicles (see Section 2.2.5). In large urban areas, this may rise to over 90%. Furthermore, 90% of the exhaust emissions, and almost all the evaporative emissions, are from petrol engines. The rural benzene concentration is around 0.5 ppb, while the

FOR REFERENCE PURPOSES ONLY

normal range of urban concentrations is 2–10 ppb. This means that the range of daily benzene intake varies by at least a factor of ten, from a few tens to a few hundreds of μg. At the low end of this range the atmospheric intake would be dominated by that from food, while at the high end it would exceed that due to food, and be similar to that due to smoking 20 cigarettes per day.

5.1.4.5 Evaporation HC

In addition to the combustion HC that are emitted from the exhaust pipe, HC may evaporate directly into the air from various sources on the vehicle. The latter include:

Evaporation of fuel directly from the carburettor (becoming less important due to fuel injection).

Fuel tank displacement: Every time an empty tank is filled, the corresponding volume of air saturated with petrol vapour is displaced into the atmosphere. This only occurs when the vehicle is refuelled. In addition, every time that a fuel tank warms up during the day after cooling down at night, a further, though smaller, volume of saturated vapour is expelled. These are known as diurnal, or breathing, losses.

Table 5.6 Typical petrol vapour composition

Component	*Vapour composition (% by volume)*
n-hexane	49.6
2-methylpentane	19.0
Methylcyclopentane	10.9
n-octane	6.0
Benzene	5.4
3-ethylpentane	3.4
Toluene	3.2
m-xylene	0.9
Ethylbenzene	0.7
Styrene	0.5
o-xylene	0.3
n-nonane	0.1

Hot soak losses: Evaporation that continues from the engine or its fuel supply system after the engine is switched off.

Running losses: Evaporation of fuel while the engine is running. The composition of the vapour is determined by the vapour pressure of the components as well as by the composition of the liquid fuel. For the petrol composition given in Table 5.4, for example, the vapour composition at 20°C would be as given in Table 5.6. Clearly, the

FOR REFERENCE PURPOSES ONLY

processes in which the hydrocarbons are exposed to the high temperatures of the combustion zone may lead to the generation of new molecules, whereas evaporation will simply release original fuel molecules. Evaporative emissions can be estimated from the following equation:

$$E_{\text{evap},j} = 365 \times a_j \times (e_d + S_c + S_{fi}) + R$$

where:

$E_{\text{evap},j}$ are the annual emissions due to vehicles in category j

a_j is the number of vehicles in category j

e_d is the mean emission factor for diurnal losses

S_c and S_{fi} are hot soak emission factors for vehicles fitted with carburettors and fuel injection, respectively

R is an emission factor for running losses

The functions given in Table 5.7 have been used to calculate evaporative losses, where RVP is the Reid Vapour Pressure of the fuel in kPa, T_a is the average monthly ambient temperature, in °C, $T_{a,\text{min}}$ is the monthly average of the daily minimum temperature, ΔT is the monthly average of the daily increase in temperature.

To get a rough idea of the significance of these evaporative emissions compared to exhaust emissions, suppose a car uses fuel with an RVP of 70 kPa. The monthly average ambient, minimum and daily increases in temperature are 15°C, 10°C, and 10°C, respectively. The car is driven to work and back every weekday, each of which ends in a warm soak (engine not fully warmed up). On the weekends there are four further short trips which end in warm soaks and two longer ones that end in hot soaks. The total mileage during the year is 16,000 km, of which 60% is warm and 40% hot. This driving profile would result in the evaporative emissions given in Table 5.8.

Table 5.7 Functions for calculating evaporative losses

Emission factor and units	*Function*
Diurnal (g day^{-1})	9.1 exp (0.0158 (RVP-61.2) + 0.0574 ($T_{a,\text{min}}$-22.5) + 0.06l4(Δ–11.7)
Warm soak (g per soak)	exp(– 1.644 + 0.01993 RVP + 0.07521 T_a)
Hot soak (g per soak)	3.0041 exp(0.02 RVP)
Warm running losses (g km^{-1})	0.1 exp(–5.967 + 0.04259 RVP + 0.1773T_a)
Hot running losses (g km^{-1})	0.136 exp(–5.967 + 0.04259 RVP + 0.1773T_a)

Table 5.8 Example of annual evaporative emissions

Source	*Emission/g a^{-1}*

FOR REFERENCE PURPOSES ONLY

Diurnal breathing	3100
Warm soak	2168
Hot soak	2436
Warm running	693
Hot running	628
Total	9025

Table 5.9 Vehicle exhaust emissions

Pollutant	*Per litre of fuel/g*	*Single car/kg per year*	*UK fleet/Mt per year*	*Global fleet/Mt per year*
CO	100	100	2.5	60
VOC	20	20	0.5	12
NO_x	30	30	0.8	18
CO_2	2500	2500	50	1500

The total is a little less than half the corresponding rough estimate of exhaust hydrocarbon emissions (shown Table 5.9). Although this type of calculation is very crude, it does show that evaporative hydrocarbon emissions must be addressed just as seriously as exhaust emissions if the total atmospheric concentration is to be controlled. The functions also show the sensitivity of the emissions to RVP. Indeed, in some countries limits are being set on petrol RVP to control emissions.

5.1.4.6 The importance of air–fuel ratio

All the gaseous emissions vary systematically with air–fuel ratio, as shown in Figure 5.7. This variation is central to understanding recent developments in engine management and emission reduction.

The chemically optimum air–fuel ratio, regardless of air pollution production, is called *stoichiometric* (just the right weight of oxygen to exactly combine with the available fuel on a molecule-for-molecule basis), and is indicated by the vertical dashed line. As mentioned in Section 5.1.2, this ratio is typically about 14.7 kg air per kg fuel, although it varies with fuel composition. At this ratio, NO production is close to a peak, while CO and HC are both low. With richer mixtures (lower air–fuel ratio), there is not enough oxygen to fully combust the available fuel, so CO and HC increase. Less energy is released, so less NO is created in the cooler conditions. When the air–fuel ratio is increased above 16 (leaner combustion), there is excess oxygen so that CO and HC stay low.

FOR REFERENCE PURPOSES ONLY

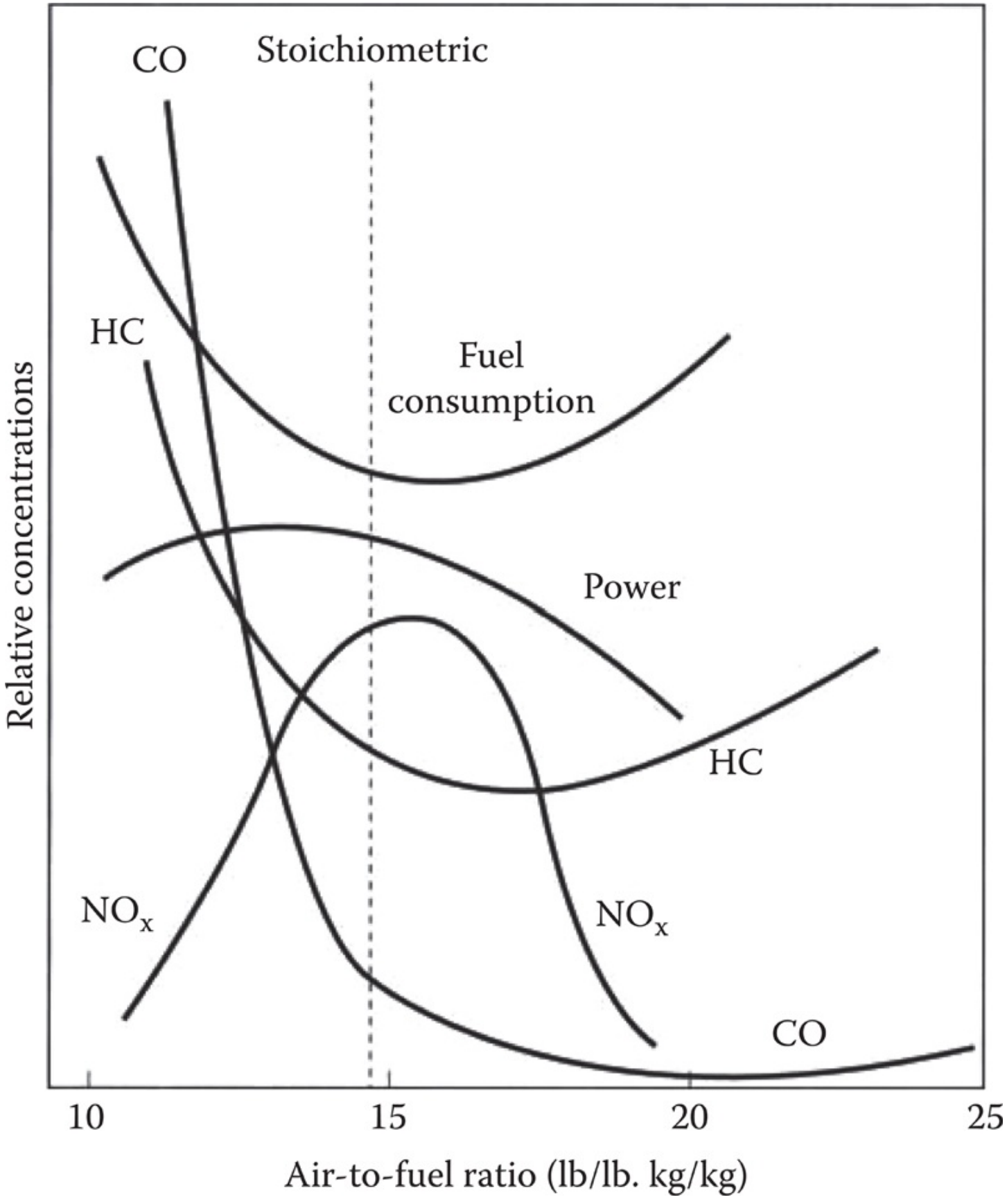

Figure 5.7 The variation of NO, CO and HC emissions with air–fuel ratio. (From Masters, G. M., Environmental Engineering and Science, Prentice Hall, Upper Saddle River, NJ, 1998.)

FOR REFERENCE PURPOSES ONLY

However, excess air is also being imported into the combustion chamber, warmed up and exhausted. This reduces the temperature and again lowers NO production. Running the engine at non-stoichiometric conditions also reduces thermal efficiency, so that more fuel is burned to offset any reductions in emission concentration. The variation of stoichiometric ratio with fuel composition has led to the development of the lambda scale. Lambda (λ) is just the air–fuel ratio divided by the stoichiometric value for that particular fuel. Hence λ is unity for a stoichiometric mixture of air with any fuel (regardless of composition), less than one for a rich mixture and greater than one for a lean mixture.

5.1.4.7 Exhaust particulate matter

Smoke (mainly particles of condensed carbonaceous material, typically 1 μm or less in diameter) is now the major toxic particle emission from vehicles. Well maintained petrol engines have a low emission rate, although the predominance of petrol engines means that their total contribution is still important. Diesel vehicles are the largest source, accounting for about 40% of total UK smoke emissions. Diesel aerosol consists mainly of highly agglomerated solid carbonaceous material and ash, together with volatile organic and sulphur compounds. Solid carbon is formed during combustion in locally fuel-rich regions because there is not enough oxygen to form CO_2. Metal compounds in the fuel generate a small amount of inorganic ash. Figure 5.8 shows a typical composition for diesel exhaust for particulates.

For many years, it was assumed that the relevant metric for particles was the mass concentration. In the recent past attention has focussed on the number concentration of very tiny particles, called nanoparticles, typically having aerodynamic sizes below 0.1 μm. These nanoparticles constitute an insignificant proportion of the mass in the ambient aerosol, although they may dominate the particle population before it leaves the exhaust pipe. They are mostly volatile, except those formed from metallic fuel additives such as lead. They are formed very rapidly as the exhaust is diluted into the ambient air, and the number formed is strongly dependent on details of the dilution process. They may be important for health effects if, for example, an alveolar cell is neutralised by any particle, whatever its size. Measurements of particles made before this was realised generally paid no attention to particle number, and most of the measurement techniques were insensitive to particles as small as nanoparticles.

There is a complex set of processes that go on within the exhaust gases as they leave the exhaust pipe. Almost all the original particles are present as solid carbonaceous agglomerates. There are also volatile organics and sulphur compounds in the gas phase. As the exhaust gases dilute and cool, these may be transformed into particles by nucleation, adsorption and condensation. New particles are formed either by homogeneous nucleation (direct gas-to-particle conversion at high supersaturations to form new particles), or by heterogeneous nucleation (deposition of vapour molecules onto a starter particle at lower saturation ratios).

FOR REFERENCE PURPOSES ONLY

The volatiles are also adsorbed onto existing carbonaceous particles. Initially, a single layer of HC molecules will become attached to the surface of a carbon particle. Then additional layers may attach if the saturation ratio (the ratio of actual vapour pressure to saturated vapour pressure) for that component is high enough. These are physical processes, not chemical binding, so the organic molecules may desorb later. The particles may be thought of as sponges that soak up gaseous volatile organic particle precursors. Hence, if the concentration of these substrate particles is reduced by, for example, a filter in the exhaust pipe, then the concentration of homogeneous nanoparticles may be increased. Laboratory experiments have shown that nanoparticle concentrations may be changed by three or four orders of magnitude (1000–10,000 times) by manipulating the dilution conditions. It is important to note that natural dilution into the ambient air is only one aspect. When measurements of exhaust gas particle concentrations are taken, the exhaust is usually diluted before measurement to bring the concentrations within the operating range of the analyser. Typically, the exhaust gases are diluted by 30–50 times within five seconds. For vehicles on the road, the exhaust gases are diluted by around 1000 times in 1 s. Hence, laboratory measurements may generate size distributions that are an artefact of the measurement process. Furthermore, petrol (spark-ignition) engines have been shown to emit as many nanoparticles, around 10^{14} km^{-1}, as diesel engines under high speed cruising conditions. This understanding may change the common perception, that it is diesel engines that are mainly responsible for particle pollution from vehicles.

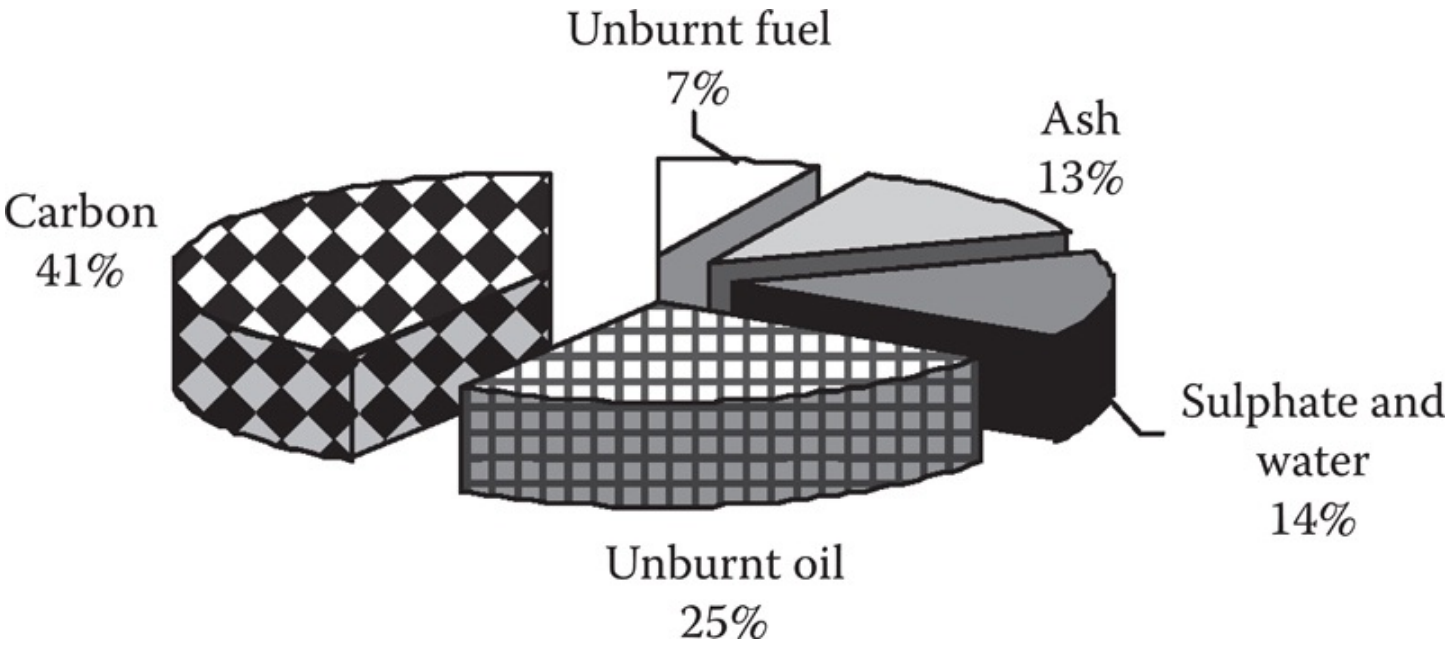

Figure 5.8 Composition of diesel exhaust emissions. (From Kittelson, D. B., *J. Aerosol Sci*., 29, 575–588, 1998.)

The analytical techniques used for particulate determination have contributed to the nomenclature for these particle emissions. The insoluble fraction is in the solid phase and

FOR REFERENCE PURPOSES ONLY

consists mainly of carbon, plus some incombustible ash from the engine oil and fuel additives. Fuel sulphur compounds are emitted as sulphur dioxide or sulphur trioxide gases, which then form sulphate particles. Most of the sulphur in the fuel is oxidised to SO_2, but a small proportion is oxidised to SO_3 and leads to the formation of sulphate and sulphuric acid aerosol. The sulphuric acid/sulphate fraction depends on the sulphur content of the fuel – hence the importance of clean diesel. A small fraction of the fuel, together with atomised and evaporated engine oil, escape oxidation and appear as volatile or soluble organic compounds. This soluble organic fraction (SOF) is a complex mixture of high molecular weight organic compounds, HCs, oxygenates, polycyclic aromatic compounds containing oxygen, nitrogen and sulphur, and can vary widely, between 10% and 90%, both from one engine and between one engine and another. It is called SOF because it is the material that will be dissolved in methylene chloride after all particles have been collected on a filter. The SOF depends a lot on maintenance and load, and is often identified as a *smokey* exhaust. Both the sulphates and SOF are collectively referred to as the volatile component, because the proportion of them that resides in the particulate form depends strongly on the thermodynamic history of the emissions. Conversely, the SOF/sulphate fraction can be identified by strong heating of the sample.

The ambient concentration of particles from diesel exhausts is a few μg m^{-3}. In confined environments, such as underground mines, this can rise by three orders of magnitude. Idealised particle size distributions (weighted by number and mass) from a diesel exhaust are shown in Figure 5.9. There are three modes. The nuclei mode, between 5 and 50 nm, consists mainly of the volatile organic and sulphur compounds that form during exhaust dilution and cooling, together with solid carbon and metallic compounds from the combustion process. This mode dominates the number distribution, but contributes only a few percent to the mass. The accumulation mode, between 50 nm and 1 μm, contains carbonaceous agglomerates and their adsorbed materials and makes up most of the mass. The coarse mode contains around 10% of the mass, made up of a small number of larger particles which have been re-entrained from deposits on the walls of the exhaust system.

The compounds responsible for the mutagenicity, and possibly carcinogenicity, of diesel soot extract once the particles have been deposited in the lungs have been the subject of intensive research in Europe and the US. Polycyclic aromatic hydrocarbons, especially benzo[a]pyrene, have been prime suspects. More recently many nitrated polycyclics, such as the nitropyrenes, have also been invoked.

FOR REFERENCE PURPOSES ONLY

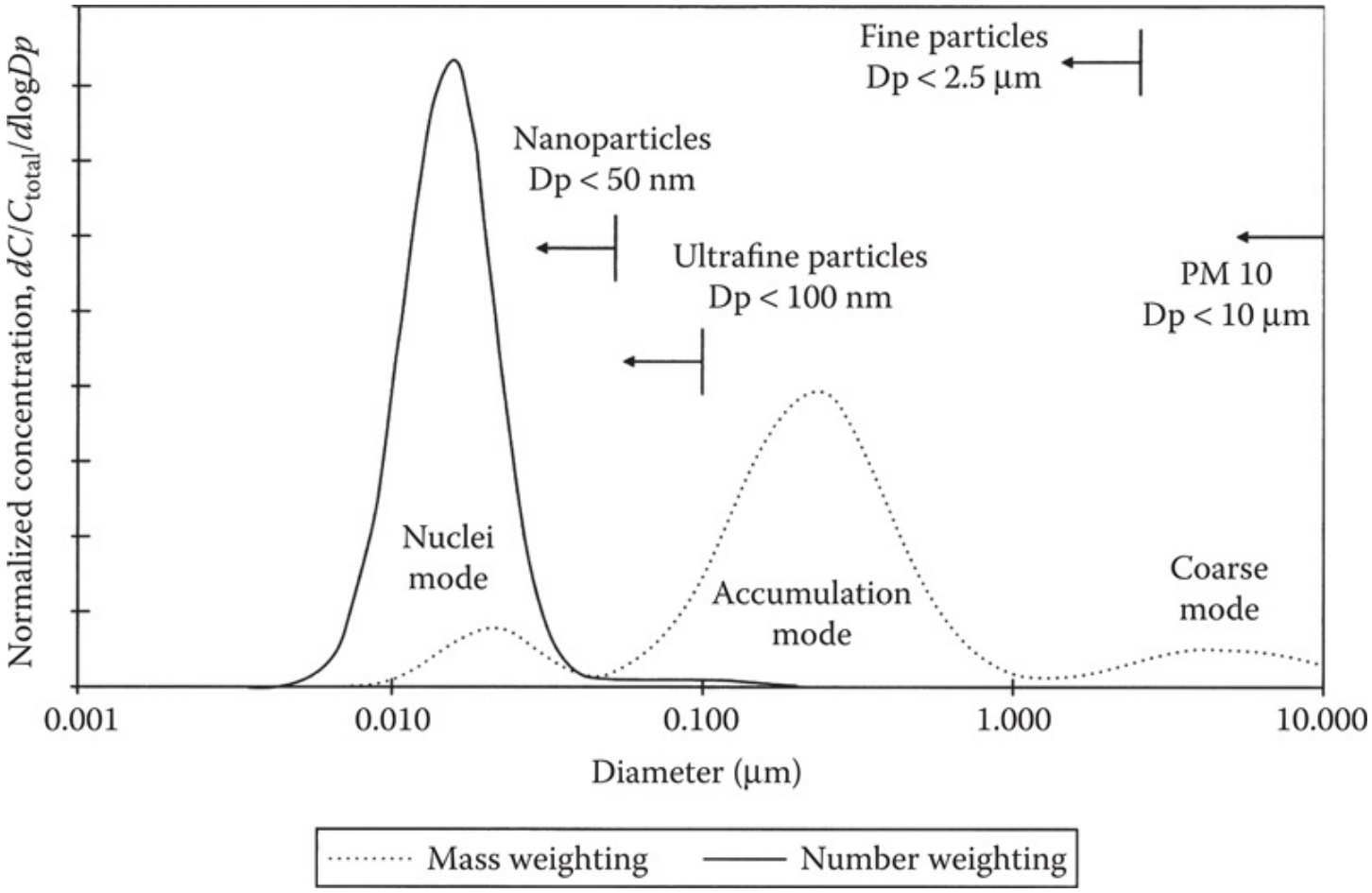

Figure 5.9 Particle size distribution in diesel exhaust. (From Kittelson, D. B., *J. Aerosol Sci.*, 29, 575–588, 1998.)

5.1.4.8 Non-exhaust particulate emissions

Non-exhaust particles from abrasion of tyres and brakes and the wearing of road surfaces is a growing proportion of road transport emissions, which is still not adequately attributed to mobile sources. Casual observation tells us that unpaved roads can be major sources of dust and fine particles. More surprisingly, perhaps, some measurements have shown that, even on paved surfaces, roads themselves can be significant sources of PM_{10}. The source is loose material, called silt, lying in the irregularities in the road surface. The passage of a vehicle, with the associated turbulent air movement due to the car itself and its tyres, entrains some of this silt into the air. It has been estimated that around 30% of the PM_{10} emissions in California are due to this process. A simple model has been derived by the US Environmental Protection Agency (USEPA) to predict road surface emissions. The model states:

$$E = k(sL)^{0.65} W^{1.5}$$

where:

E is the emission factor (g per vehicle kilometre)

k is an empirical constant

s is the fraction of the total surface silt loading that passes through a 75 μm sieve

L is the total surface silt load (g m^{-2})

W is the vehicle weight

The model is intuitively and empirically rather than mechanistically based. The empirical constants were derived by fitting the model to limited specialised data sets, and the model makes poor predictions if used in new situations without optimisation.

5.1.4.9 Lead

For a long time, lead was added to petrol to improve its combustion properties. In a petrol engine, the ratio of the maximum cylinder volume when the piston is at the bottom of its stroke to the minimum volume at the top is called the compression ratio. Thermodynamically, there is an efficiency advantage in raising the compression ratio. The efficiency of a four-stroke internal combustion engine (commonly known as the Otto cycle consisting of adiabatic compression, heat addition at constant volume, adiabatic expansion and rejection of heat at constant volume) is given by:

$$\frac{\text{Work out}}{\text{Energy in}} = 1 - \left(\frac{1}{\text{compression ratio}}\right)^{\frac{R}{c_V}}$$

where:

R is the gas constant

c_V the specific heat at constant volume

However, if the compression ratio is raised too far, the engine acts similar to a diesel, heating the petrol/air mixture enough to detonate it before the spark does. This condition is called knocking or pinking and damages the engine. It has been found that different blends of petrol, namely those with a higher proportion of certain hydrocarbons such as branched-chain alkanes, are much less susceptible to knocking. One particular fuel, called 2,2,4-trimethylpentane or isooctane, was found to be the most knock-resistant and hence other fuels have been given an octane number to compare with it. A high octane number means that the engine can be designed for a high compression ratio and hence extract more power from the fuel. It has also been found that the octane rating of otherwise low-octane petrol can be increased by adding certain organic lead compounds, especially tetraalkyl leads (PbR_4, where R is either CH_3 or CH_2CH_3). These compounds have been added to petrol since the 1920s at the rate of around 1 g L^{-1}. After combustion, lead particles are emitted in the exhaust gases. Some of them are emitted directly in the 0.1–1.0 μm diameter size range and a proportion is deposited in the exhaust pipe and emitted later as coarser flakes >10 μm.

FOR REFERENCE PURPOSES ONLY

Unfortunately, lead is a toxic heavy metal to which the nervous systems of babies and children are particularly sensitive. Adults absorb 0%–15% of ingested lead from the gastrointestinal tract, children up to 40%. The unexcreted fraction is distributed between blood, soft tissue and mineralised tissue (bones and teeth). About 95% of the body burden of lead in adults, and about 70% in children, is located in the bones. Tetraalkyl lead is absorbed through the respiratory tract and through the skin, then metabolised in the liver to trialkyl lead, the most toxic metabolite. It has effects on neurological development, particularly in children. Lead is also transported across the placental barrier into the foetus, and there may be release of maternal lead stored in bones during pregnancy. Lead uptake may also be affected by nutritional status – deficiencies in Ca, Fe or Zn have been associated with high blood lead concentrations.

Although there have been many routes by which significant lead intakes to the body could be made, such as lead-based paint and lead water pipes, airborne particles became significant due to the growth of motor vehicle use. By the mid-1970s, 160,000 tonnes of lead were being used each year in American petrol alone. Although fatalities and illness due to lead poisoning were common in the plants at which the tetraethyl lead was manufactured, the benefits were sufficient that it took 50 years of scientific debate, research and campaigning to get lead banned in America, and subsequently in Europe. By the 1970s, the use of motor cars had grown to the extent that there was serious concern about the lead exposure of people living near main roads, busy intersections or other areas with high traffic densities. As a consequence, legislation was introduced both to cut the lead content of petrol, and to limit the concentration of lead in the air. In the UK, the maximum allowable lead content of leaded petrol was reduced from 0.45 to 0.40 g L^{-1} in 1980, and to 0.15 g L^{-1} in 1986. The WHO guideline for maximum lead content of petrol is 0.15 g L^{-1}, however, in some developing countries average lead concentrations ranging between 0.10 and 2.0 g L^{-1} have been reported. Though several developed countries have achieved much lower concentrations than the WHO limit value through economic incentive, such as waiving of excise duty on unleaded petrol, and through increased use of catalysts, which cannot be used with leaded petrol because the lead poisons the precious metals. The combined effect of all these measures caused a rapid increase in the use of unleaded petrol between 1989 and 1999, to take over 90% of the petrol market (Figure 5.10). Total road vehicle fuel use remained fairly constant over the same period, although diesel fuel use increased by 50%. Consequently, although total petrol consumption was flat, emissions of lead and airborne lead concentrations in urban areas both fell by over 95% (Figure 5.11).

In the UK, typical urban lead concentrations are 0.1–0.2 μg m^{-3}, while typical rural ones are 0.01–0.05 μg m^{-3}. Total inhaled mass loadings of lead are trivial compared with the amounts ingested via food and drinking water, although there may be some concern that nano particulate lead can penetrate very effectively into the blood directly through the alveoles. Although blood lead levels in developed industrial countries have declined steadily in recent years, this reflects the combination of many independent controls on

FOR REFERENCE PURPOSES ONLY

sources such as lead water pipes, leaded paint and leaded solder on tin cans, as well as leaded petrol. Effects of elevated blood lead have only been shown conclusively at concentrations above around 10 μg dL^{-1}, and as the transfer rate by inhalation is believed to be around 4 μg dL^{-1} per μg m^{-3} of atmospheric concentration, the range of urban concentrations given earlier is unlikely to result in detectable effects. An increase in blood lead from 10 to 20 μg dL^{-1} has possibly been shown in epidemiological studies to result in a decrease of IQ by two points, although this remains contentious. The issue is now more urgent in developing countries, where low-lead petrol has taken longer to be accepted. Average blood lead levels up to 20–30 μg dL^{-1} have been measured in urban/industrial populations in Peru, India, China and Mexico.

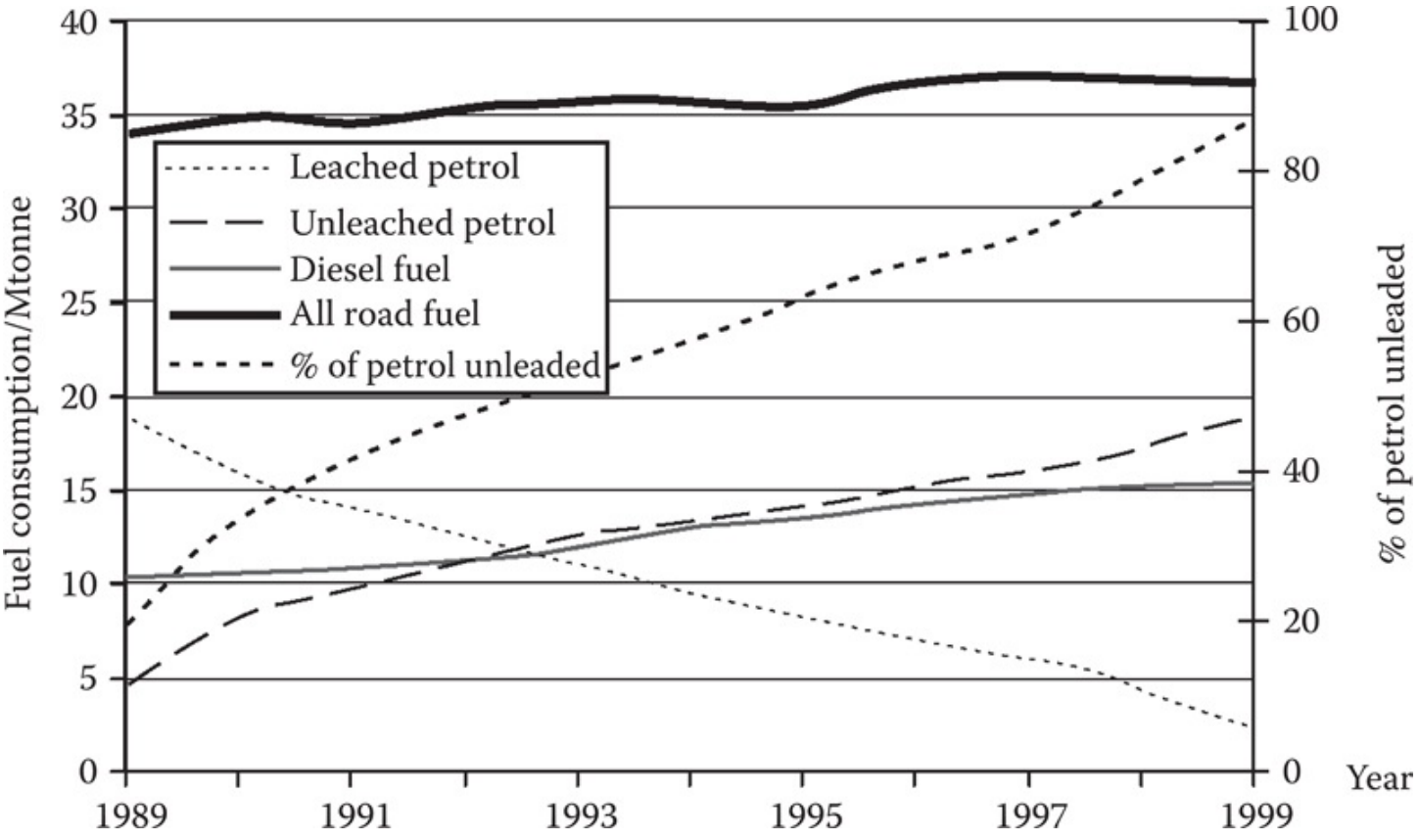

Figure 5.10 Changes in fuel use and proportion of unleaded petrol used in the UK, 1989–1999.

FOR REFERENCE PURPOSES ONLY

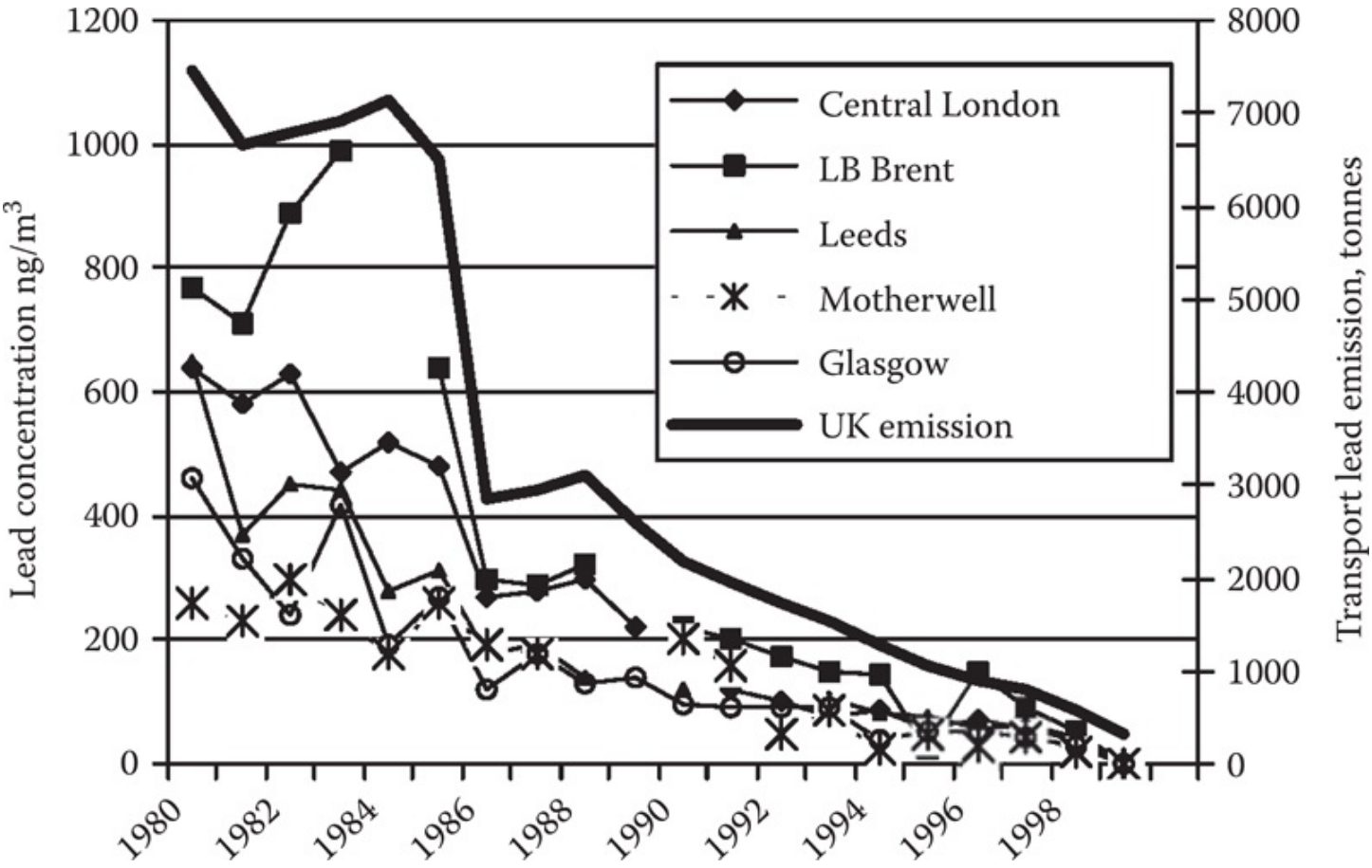

Figure 5.11 Changes in the amounts of lead emitted by vehicles in the UK, and in the airborne lead concentrations at urban sites, 1980–1999.

5.1.4.10 Polycyclic aromatic hydrocarbons

Another class of materials emitted from vehicle exhausts that has caused concern due to their carcinogenicity is the polycyclic aromatic hydrocarbons (PAHs) such as benzo-*a*-pyrene (BaP) and benzo-*e*-pyrene (BeP) (described in Chapter 2). Measurements in Copenhagen have shown peak concentrations of around 4 ng m^{-3}, a winter contribution by traffic to PAH of around 90% for street air on a weekday, falling to 60% on the weekend. Diesel buses in Denmark now have to use a fuel having a low distillation end-point, which gives reduced particle and PAH emissions. The USEPA evaluation is that 0.3 ng BaP-equivalent m^{-3} will cause one additional lung cancer per 10^6 individuals, while the corresponding WHO guideline is that a lifetime exposure to 1 ng m^{-3} will cause 90 additional respiratory cancers per 10^6 individuals. High exposures to PAH can be tested by sampling the urine for PAH metabolites such as 1-hydroxypyrene and β-napthylamine.

5.1.5 Reduction of motor vehicle emissions

5.1.5.1 Burn less fuel!

Fewer vehicles, smaller lighter cars with smaller more efficient engines, more public transport, shorter journeys, park and ride, bicycle lanes, pedestrianisation schemes – these are all common-sense ways to reduce emissions, but we have been slow to adopt them because we are still hooked both on the freedom of movement and flexibility of access that the motor vehicle provides, and on the power and speed of unnecessarily large cars.

5.1.5.2 Combustion optimisation

Detail design improvements to the cylinder head can give better mixing, less dead space and more optimum air–fuel ratio throughout the volume of the chamber. *Lean-burn* engines have been designed that operate at a high air–fuel ratio of 18 or more (Figure 5.7) to give the best compromise of low NO, CO and HC. These conditions lead to combustion instability (e.g. stalling) and need advanced fuel and air management. Although large research programmes have been carried out by individual manufacturers, lean-burn lost out to catalytic converters for reliable emission reduction, and it is clear from Figure 5.7 that it cannot compete with the potential reductions of 90+% achieved by catalytic converters. Lean-burn engines still generate unacceptable NO emissions, and there has been considerable research into a catalyst which will clean up this NO efficiently even under the oxygen-rich conditions. Some manufacturers are experimenting with direct injection, in which petrol is injected into the cylinders instead of being mixed into the inlet air.

5.1.5.3 Emissions recycle

The sump (or crankcase) is sealed and combustion gases that have leaked past the pistons (blow-by) are piped back to the inlet manifold so that the fuel and oil vapours are burnt instead of being vented to atmosphere.

5.1.5.4 Vent controls

Several measures have been adopted or are being considered in different countries:

- Small canisters (typical volume 1 L) of a vapour adsorbent such as activated charcoal are fitted to fuel tank inlets to control breathing emissions. These are standard in the United States. The canister is purged to recover the fuel when the vehicle is running. The canister may overload if the vehicle is standing for many days.
- The fuel filling system is redesigned so that the pump nozzle seals the tank inlet to prevent direct emission of vapour. The displaced gases are either routed through an absorbent or pumped back into the underground storage tank.
- The petrol composition is changed to reduce fuel volatility (often reported as RVP, which is the vapour pressure of the fuel at a standard temperature of 34.4°C). Butane is

FOR REFERENCE PURPOSES ONLY

usually the first component to be reduced.

5.1.5.5 Exhaust gas recirculation

A small fraction of the exhaust gases is directed back into the air inlet. This dilutes the air–fuel mixture and reduces combustion temperature, thereby reducing thermal NO_x production.

5.1.5.6 Three-way catalytic converters

When the mixture of HCs and air in the combustion zone is burned, reactions proceed at different rates for the different components. All the reactions are ended (quenched) at the same moment when the combustion stroke ends and the exhaust stroke starts. Hence the exhaust gas contains a partly combusted mixture, at a temperature too low for normal combustion to continue. It is the purpose of catalytic converters to complete the combustion at a lower temperature. As this type of catalyst converts all three gases at once, it is known as a *three-way catalyst* (TWC). Catalytic conversion of the main pollutant gases in the exhaust has been used in America and Japan for many years and as the arrival of Euro 1 standards has been mandatory in the countries of the European Union (see Chapter 14 for more details). Currently about 98% of the UK petrol-engined car fleet is equipped with catalysts. Other countries are gradually following suit – for example, India legislated for compulsory use of catalytic converters in its four largest cities from April 1995.

5.1.5.6.1 Construction

The catalytic converter typically consists of a ceramic support matrix (cordierite $Mg_2Al_4Si_5O_{18}$ is commonly used) and alumina washcoat to provide a very large surface area, on which the precious metal catalysts are deposited. The catalyst is presented to the exhaust gases either as a packed bed of beads of catalysed washcoat, or as coated honeycomb. There is a power reduction of up to 10% (and hence associated increase in fuel consumption) from engines fitted with converters, due to the higher pressure drop across the exhaust system and consequent reduction in gas throughput. The catalysts are usually platinum, palladium and rhodium; endless combinations and physical arrangements of these have been tried in order to increase the conversion efficiency and reduce the cost. The first catalyst contacted as the exhaust gas flows through is rhodium, which promotes the reduction of NO, using one of the incompletely oxidised components such as CO, H_2 or HCs. For example,

$$NO + CO \rightarrow \tfrac{1}{2}N_2 + CO_2$$

or

FOR REFERENCE PURPOSES ONLY

$$NO + H_2 \rightarrow \tfrac{1}{2} N_2 + H_2O$$

or

$$(2 + n/2)\, NO + C_yH_n \rightarrow (1 + n/4)\, N_2 + yCO_2 + (n/2)\, H_2O$$

Reduced components such as HCs and CO are then oxidised by passing them over a second catalyst such as palladium or platinum. There must be excess oxygen in the exhaust gases for this to occur. For example

$$C_yH_n + (1 + n/4)O_2 \rightarrow yCO_2 + (n/2)H_2O$$

or

$$CO + \tfrac{1}{2} O_2 \rightarrow CO_2$$

or

$$CO + H_2O \rightarrow CO_2 + H_2$$

Hence all the oxidising agents in the exhaust gas are caused to react with all the reducing agents, which is a clever trick. Other materials, such as ceria (CeO_2) or zirconia are added to increase oxygen storage capacity or to promote HC conversion in rich exhaust conditions.

5.1.5.6.2 The lambda window

To make TWC work, the O_2 content of the exhaust gases must be maintained within narrow limits; this is achieved by measuring the equilibrium O_2 partial pressure with a zirconia/platinum electrolytic sensor (the lambda sensor) and feeding a control signal back to the fuel injector. The air–fuel mixture must be kept very close to, and slightly on the rich side of, stoichiometric at all times. Figure 5.12 shows that a catalytic converter can only achieve a conversion efficiency above 90% for *all three* gases if the air–fuel ratio is always within a very narrow range close to stoichiometric.

On the one hand, this means that precise mixture control is essential; on the other, the potential emission reductions associated with lean burn are not available. Overall, provided that the exact combustion conditions are maintained, the benefits of 90% reduction of toxic emissions will be combined with those of minimum fuel consumption due to the engine operating at its maximum thermal efficiency. If the combustion conditions are not so tightly controlled, the emission reduction can easily fall away to between 50% and 70%, and European standards cannot then be met.

The nature of a feedback similar to this is to develop a small oscillation in the output,

FOR REFERENCE PURPOSES ONLY

such that even when the engine is operating under constant load (cruising) the exhaust gas composition will oscillate between slightly excess oxygen and slightly deficient. To handle this, an oxygen-labile material such as cerium oxide (CeO_2) is added to the washcoat mixture. Excess oxygen is stored in the CeO_2 by conversion to CeO_3 when there is some spare, and released when it is deficient. Oxygen storage materials can make up 10%–20% of the washcoat, as compared to only 0.1%–0.2% precious metals.

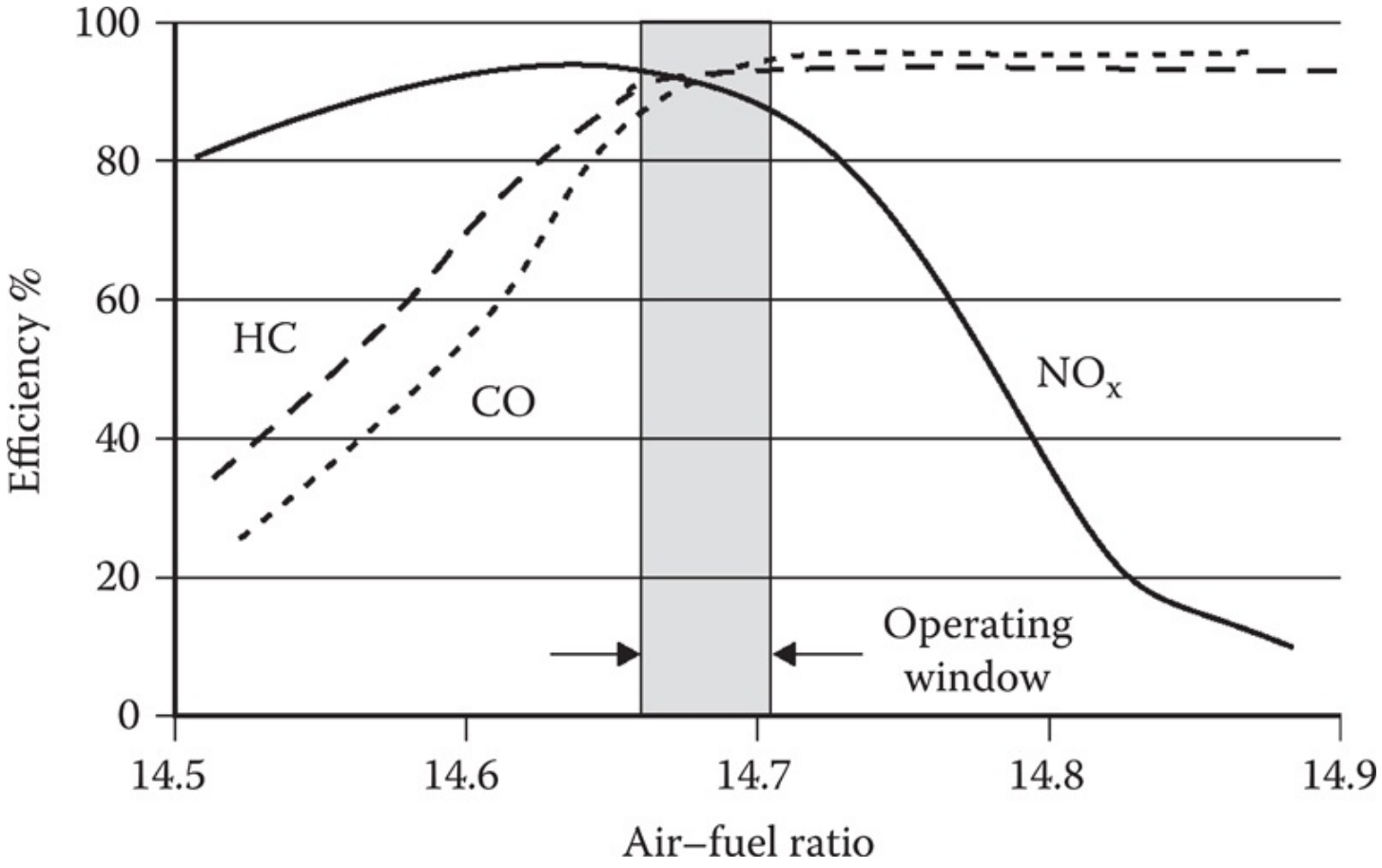

Figure 5.12 The variation of catalytic conversion efficiency with air–fuel ratio.

5.1.5.6.3 Other catalyst issues

The chemical reactions occurring on the catalyst surfaces are combustion, and the temperature has to be high enough for these to occur. Conversion efficiency is zero if the engine exhaust system temperature has not reached its *light-off* value of around 300°C. As this may take several minutes, and around 20% of journeys are of less than 1 km, there are important consequences for emissions. Likely solutions will be either to electrically preheat the TWC or to adsorb the HCs in a charcoal trap before desorbing them into the TWC when it has warmed up. This poor conversion by the cold catalyst is compounded by poor fuel vaporisation in the cold engine, so that some fuel remains in droplet form and HC emissions are increased.

Hydrogen sulphide formation in catalytic converters has been an issue since the 1980s. Although the concentrations are small and probably no threat to health, the low odour threshold and unpleasant smell of H_2S has made the emissions noticeable. Emissions often occur as a spike when rapid deceleration to idle follows a period of cruise at high speed. Sulphur is stored in the TWC matrix during lean or stoichiometric operation, and released during rich transients. The exact chemistry is not yet clear, but minor washcoat components such as ceria are also believed to be involved. As shown later in Section 5.1.9.2, sulphur is higher in diesel fuel than it is in petrol, and this again increases particle emissions. Hence, particle traps will be more practicable where lower sulphur fuel is available.

5.1.6 Diesel exhausts

More recently, emissions from diesel vehicles have been identified as the main cause of NO_2 exceedance in several countries. Although widespread adoption of three-way catalyst technology (as discussed earlier) is meant to get this into acceptable limits, the sheer pace of market penetration of diesel vehicles as cost-efficient and carbon-restrained motorised transport globally from 2005 onwards has dwarfed their effectiveness. For example, according to the UK Department for Transport Vehicle Licensing Statistics (2016), between 1990 and 2015 the share of diesels in UK car fleet have risen from mere 7% to nearly 40%, and is still rapidly growing. In California in 2000, diesel engines made up around 3% of the vehicle population and travelled 5% of the miles, yet 35% of the vehicle NO_x and 56% of the vehicle exhaust PM were attributed to these vehicles.

The big issue with diesel emission control is how to reduce the concentration of NO without increasing that of particles, and *vice versa*. For example, retarding the fuel injection reduces the peak flame temperature and hence NO_x formation. However, it also lowers fuel efficiency, giving higher overall PM emissions. Emission controls can be acceptably cost-effective. For example, the successive legislation enacted in the United States to control mobile source emissions, including diesel, cost typically US$1500 per tonne of ozone precursors.

5.1.6.1 Diesel particulate filters

The simplest approach to reducing diesel particulate emissions is the diesel particulate filter (DPF), or trap. These devices take many forms, such as ceramic or metal foams, wire mesh or ceramic wool; they all trap particles by the normal range of filtration processes. As the particles accumulate, they create a pressure drop which reduces engine efficiency, so they must be burned off before the pressure drop becomes excessive. The burning off may occur spontaneously if the exhaust gases ever attain a high enough temperature, but usually some form of assistance is needed. This may take the form of electrical or combustion heating, or the engine may be run temporarily in an inefficient mode to artificially raise the exhaust gas temperature, or a catalyst may be included in the filter to promote combustion

at lower temperatures. The holy grail of the catalyst method is the *continuously regenerating trap* (CRT), which filters and burns particles continuously. Ideally, NO is oxidised to NO_2, which then supplies the oxygen to burn the carbon, thus solving both of the most serious diesel emission problems at a stroke. These devices cannot work with high sulphur fuels, which promote the formation of sulphate particulate and block the filter. Even at 50 ppm S in the fuel, the catalyst can increase the exhaust gas sulphate loading by a factor of ten.

However, despite the positive influence on reducing PM from vehicle transport, the vehicle and engine manufacturers have not been fitting DPF to diesel vehicles even until 2000s, mainly due to the added complexity and costs to vehicles.

5.1.6.2 DeNO$_x$

There are technologies to deal with the NO_x emissions from lean combustion systems independently of the particles. These are known as $DeNO_x$ methods. With storage $DeNO_x$, NO_x is scavenged from the exhaust gas by an adsorber and stored as nitrates. The adsorber is regenerated by operating the engine rich for a short time. In passive lean $DeNO_x$, existing HCs in the exhaust gas are used to reduce the NO_x, while in active lean $DeNO_x$, HCs or ammonia are injected to achieve the same end.

5.1.6.3 Diesel oxidation catalyst

The lowering of the sulphur content of diesel fuel has opened up the possibility of treating at least some of the particulate emissions catalytically. The DOC reduces HC, CO and PM, but needs a low-sulphur fuel (below 50 ppm S by weight). However, the same oxidising conditions limit the potential for reducing the NO to N_2. DOC can also reduce particle emissions by removing SOF, although creation of sulphate particles from SO_2 can more than offset this improvement. Turbocharging reduces both NO_x and PM emissions by around 30%, more if combined with after cooling. The more active the catalyst, the greater the reduction in gas-phase emission, but the greater the sulphation of sulphur to produce particulate. Diesel oxidation catalysts has been used on off-road vehicles in the US since the 1960s, and fitted to over 1.5 million trucks and buses since 1990. Efficiency can be further increased by 10%–15% by the use of a fuel-borne catalyst. Various combinations of washcoat and catalyst have been tried. Such catalysts are not prone to thermal deactivation because they operate at lower temperatures than TWCs – typically 650°C rather than 950°C. They can be poisoned more easily by P and Zn from the engine oil, more of which is burned in diesel than in petrol engines. Test programmes in the United States have shown that various combinations of these technologies can be used to reduce the emissions from modern HGV engines below proposed standards, and that doing so will often improve fuel economy and reduce noise as well. It is not cheap, typically costing a few thousand dollars

per tonne of particulate matter reduction.

5.1.7 Vehicle maintenance

Vehicle maintenance is another major factor in emission control. Roadside measurements have been made in several countries with the Fuel Efficiency Automobile Test (FEAT), which is a non-dispersive infrared transmissometer-based instrument that can be used to determine the concentrations of CO, HC, NO_x and particles in the air above the road surface. As it has a response time of only 1 s, the measurements can be related to the passage of individual vehicles. By making certain assumptions about dilution, the emission concentration can also be derived. Such measurements consistently show that 1% of vehicles is responsible for 5%–10% of the total CO emissions, and 10% of vehicles for 50% of the emissions. Contrary to expectation, this *dirty 10%* is not just older or high-mileage vehicles, but is evenly distributed across model years. Although some countries such as the United States have a long history of vehicle emission legislation (catalysts were first introduced there in 1971), and strict enforcement policies (biannual smog checks), the dirty 10% continues to evade control.

5.1.8 Vehicle emission calculations

There are many practical issues that need to be considered when calculating potential emissions from a given length of road. The overall rate of emission will vary not only with obvious factors such as traffic density (flow rate in vehicles per hour), vehicle speed, driving mode (accelerating, decelerating, cruising or idling), mix of vehicle types (cars, buses, goods etc.), and engine types (petrol or diesel or other), but also with less obvious ones such as engine maintenance, meteorology (air temperature and humidity), and engine operating temperature.

We can make order-of-magnitude calculations of quantities such as vehicle emissions to get a general idea of how significant they are compared to other factors. In broad terms, combustion of 1 L of fuel generates 100 g CO, 20 g VOC, 30 g NO_x and 2.5 kg CO_2, together with smaller quantities of other materials such as sulphur oxides, lead and fine particles. Consider the example of a single car which is driven an average 16,000 km per year with a fuel economy of 16 km L^{-1}, hence using 1000 L of fuel. This single car will generate the emissions shown in Table 5.9 (assuming no emission controls). Also shown in Table 5.9 are the corresponding emissions from the UK fleet of 25 million vehicles and the global fleet of 600 million vehicles. Although this back-of-the-envelope calculation ignores factors such as different vehicle types and different driving patterns in different countries, it does show how serious vehicle emissions are on a global scale, not merely as a local pollution problem in urban environments.

FOR REFERENCE PURPOSES ONLY

5.1.8.1 Diurnal variations

The primary factor controlling vehicle emissions from a length of road is the number of vehicles passing along the road per unit time. This variation follows a characteristic cycle related to human social patterns – most people are at home in the early hours of the day, go to work by car or public transport sometime between 6 and 9 am, go about their business during the day, and go home again in the evening. Some of those people will go out again in the evening. Of course, there are many exceptions to these patterns, such as for shift workers. Nevertheless, the resulting pattern of vehicle movements is quite reliable (Figure 5.13).

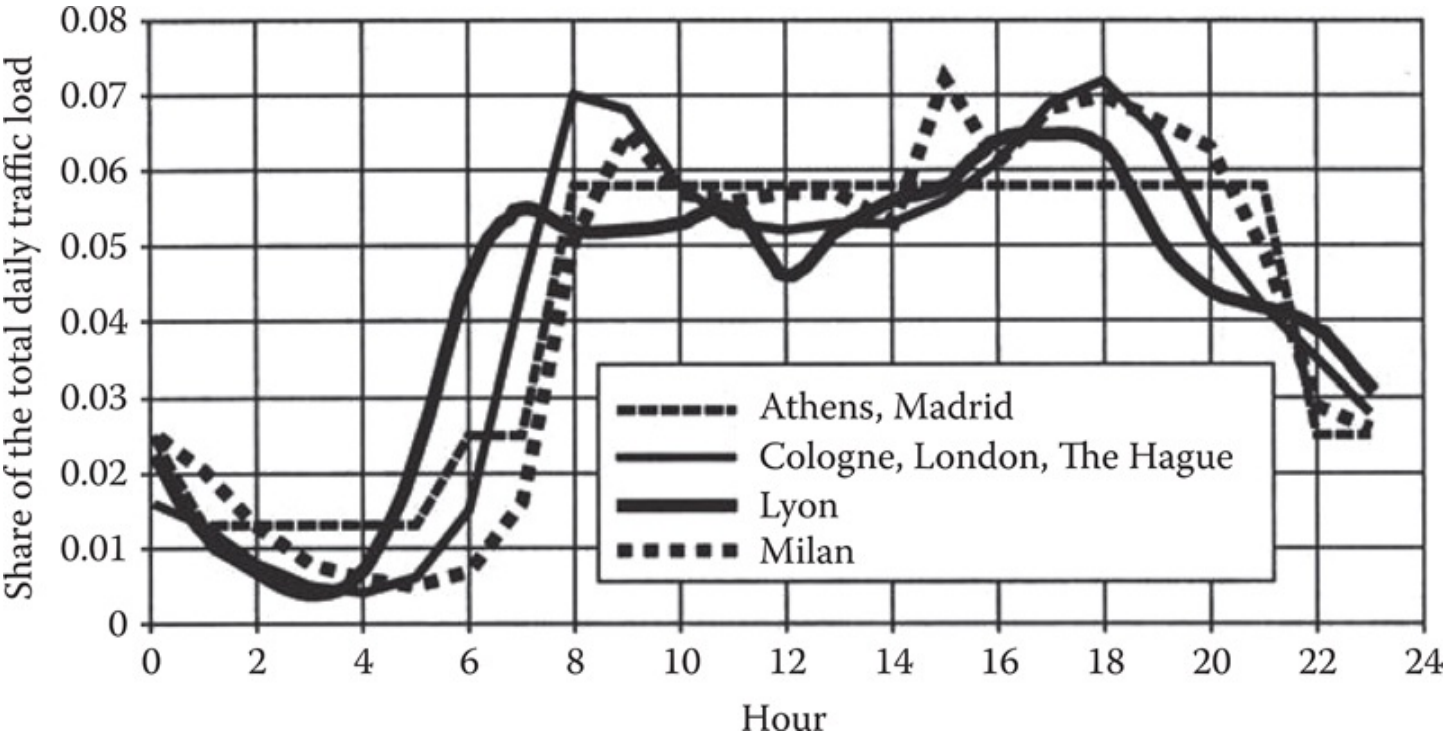

Figure 5.13 Typical patterns of traffic movements in European cities. (From Samaras, Z. and Sorensen, S. C., Mobile sources, in J. Fenger, O. Hertel and F. Palmgren (Eds.), *Urban Air Pollution: European Aspects*, Kluwer Academic Publishers, Dordrecht, the Netherlands, 1998.)

5.1.8.2 Emissions measurement from laboratory and real road tests

5.1.8.2.1 Cars and light-duty vehicles

Recent developments in NO_2 emissions exceedances from on-road diesel vehicles have opened a new realm on emissions testing protocols. It has been acknowledged that despite newer vehicles emitting less than earlier models within the laboratory emissions tests, they often emit equivalent, or even more, than earlier models under *real-road* conditions. By the

FOR REFERENCE PURPOSES ONLY

early 2010s improved methods for measuring real-world driving emissions enabled vehicle emissions to be quantified when driven on the roads. More recently, there is a considerable database of direct measurements of emission rates from cars and their variation with speed. This data shows that whilst the engine and vehicle manufacturers successfully passed the laboratory-based test, once on the road, the pollution abatement technology gets less effective. Between 2017 and 2021, the UK introduced a mandatory test for all new cars and vans, which will include more detailed laboratory test cycles, alongside Real Driving Emissions (RDE) that is testing conducted during the driving of the vehicle on real roads using portable measuring equipment (Table 5.10). Results show RDEs estimating between 50% and 100% surplus emissions compared to the corresponding lab tests.

Table 5.10 Real Driving Emissions (RDE) NO_2 emissions (RDE) requirements for diesel cars in the UK

			Limit value (Mg km^{-1})	
Deployment date	*Model*	*Conformity factor (engine size, L)*	*Laboratory test*	*Real driving emissions*
September 2017	New models	2.1	80	168
September 2019	All new cars	2.1	80	168
January 2020	New models	1.5	80	120
January 2021	All new cars	1.5	80	120

However, much of the earlier work has been performed on chassis dynamometers, in which the vehicle is run on a rolling road for cars and light-duty vehicles. The range of driving conditions simulated in this way was relatively small and was well known to the vehicle manufacturers. As a result, there has been little change in roadside NO_2 levels for many years. The European research programme CORe INventory AIR emissions (CORINAIR) had published a series of technical guidance to prepare national emission inventories with equations relating emissions to vehicle type and speed. In 1999 a major programme of work resulted in the Methodology for Calculating Transport Emissions and Energy Consumption (MEET). Two kinds of analysis are made. In the first, the straightforward variation of emissions with speed is measured under constant conditions. In the second, average emissions are determined while the vehicle performs a standard cycle of acceleration, cruise and deceleration in a pattern that is intended to simulate urban, motorway or cross-country driving or a combination of these. Although the cycles look quite complicated, and some have been derived from direct measurements of driving patterns in the appropriate environment, they usually remain less transient and complex than real driving patterns. Clearly, a wide range of speed cycles may all generate the same average speed, so that comparison between vehicles depends on standardisation of the test cycle. Naturally, different organisations and countries have tended to develop their own standards, and it has taken some years for any uniformity to be achieved. This averaging process facilitates comparisons between different vehicles. There may also be variations

due to the condition of the specific vehicle tested (whether it is representative of those on the road), and the analysis itself. For example, gas analysers with response times of 1 min would be quite adequate to measure steady-state emissions but would not track the transient changes during rapid acceleration/deceleration cycles. The analysis becomes even more difficult when dealing with particles, where it has been shown that the details of exhaust gas dilution may affect the production of the smallest particles by orders of magnitude.

The outcome of many such tests is a set of algebraic relationships that enables the emissions to be predicted if the speed is known. Quadratic equations of the general form, emission (g km^{-1}) = $a + bV + cV^2$, are fitted to the data. For CO_2 the equations are more complex, with combinations of logarithmic and inverse functions being used. The fit is often not good because of the large variability from test to test on the same vehicle and from vehicle to vehicle in the same category.

Note that the emissions are expressed in g km^{-1}. In real life, an idling engine will emit an infinite mass per km when the vehicle is stationary, and this situation is not handled by the equations. Indeed, some of them give zero, some of them give a constant, and some of them give infinity when $V = 0$ is substituted into them. This is why all the speed ranges start at a non-zero speed, either 5 or 10 km h^{-1}. Very low speeds (traffic creep) or idling are best handled by assuming that the mass emission per unit time at the lowest speed considered in the equation is also correct for a stationary vehicle. A stationary queue of traffic is then treated as a line source at the appropriate total emission rate per unit length and time (g m^{-1} s^{-1}). For example, a single petrol car with the smallest size of engine, fitted with emission control to EURO I requirements, had a mass emission rate for CO given by

$$9.846 - 0.2867V + 0.0022V^2$$

This equation is valid down to 10 km h^{-1}, at which speed the mass emission rate is

$$9.846 - (0.2867 \times 10) + (0.0022 \times 10^2) = 7.2 \text{ g km}^{-1}$$

At 10 km h^{-1} this corresponds to $7.2 \times 10 = 72$ g h^{-1}. Hence a stationary car of this type will emit 72 g h^{-1} = 0.2 g s^{-1} and can be treated as a point source of this strength. A queue of 100 such cars over a 1 km length of road would be treated as a uniform line source of strength $100 \times 0.2 = 20$ g km^{-1} s^{-1}. At the next level of sophistication, the instantaneous emissions are related both to the speed and to the product of speed and acceleration (with units of m^2 s^{-3}), as the latter gives a better indication of the power supplied. A matrix is created which specifies an emission factor for each combination of these two factors. This type of model is useful not only for estimating normal road emissions, but for estimating the impact of measures such as traffic calming, when repeated acceleration/deceleration cycles may increase emissions compared to the baseline case.

5.1.8.2.2 Heavy-duty vehicles

The term heavy-duty vehicles (HDVs) covers HGVs, buses and coaches. They are almost entirely diesel-fuelled. Far fewer emission data are available for heavy-duty vehicles, and they are mostly from engine test beds, in which the engine alone, rather than the complete vehicle, is studied. The MEET Report recommended that emissions from HGVs be described by polynomial functions of the general form

$$E = K + aV + bV^2 + cV^3 + \frac{d}{V} + \frac{e}{V^2} + \frac{f}{V^3}$$

where:

E is the emission rate in g km^{-1}

K is a constant

a–f are coefficients

V is the mean speed of the vehicle in km h^{-1}

Figure 5.14 shows examples of the relationships discussed earlier, taken from the UK National Atmospheric Emissions Inventory (NAEI) database of emission factor estimates for 1999. As speed increases, emissions per km generally decrease, except for NO_x from petrol engines which is low anyway. The decrease in emissions of PM_{10} and VOC is very marked. Conversely, there is a sharp increase in these emissions when traffic slows down, in urban rush-hours for example. A car might emit ten times the weight of CO, and seven times the weight of VOC, in crawling 1 km at 10 km h^{-1} as it would covering the same distance at a cruising speed of 60 km h^{-1}. For vehicle speeds above 60–80 km h^{-1}, emissions start to rise again. Note that in the graphs described here, the motorbike emissions are constant. This is only because there is no data available from NAEI on the variation of motorbike emissions with speed. A new real-driving emissions test for HGVs has been introduced in the UK in 2014.

5.1.8.3 Effect of engine temperature

Recent work from the European group Transport & Environment (2016) has shown that devices that work during the laboratory test are often switched off in *cold* weather (meant to be around 17°C). However, in places with lower average ambient temperature (e.g. UK), the NO_x control does not work for the majority of the time, of the key reasons for the prevalent exceedances of the NO_2 emissions from diesel vehicles in the UK. For all new cars this issue should be addressed by the introduction of real driving tests to supplement the laboratory tests.

FOR REFERENCE PURPOSES ONLY

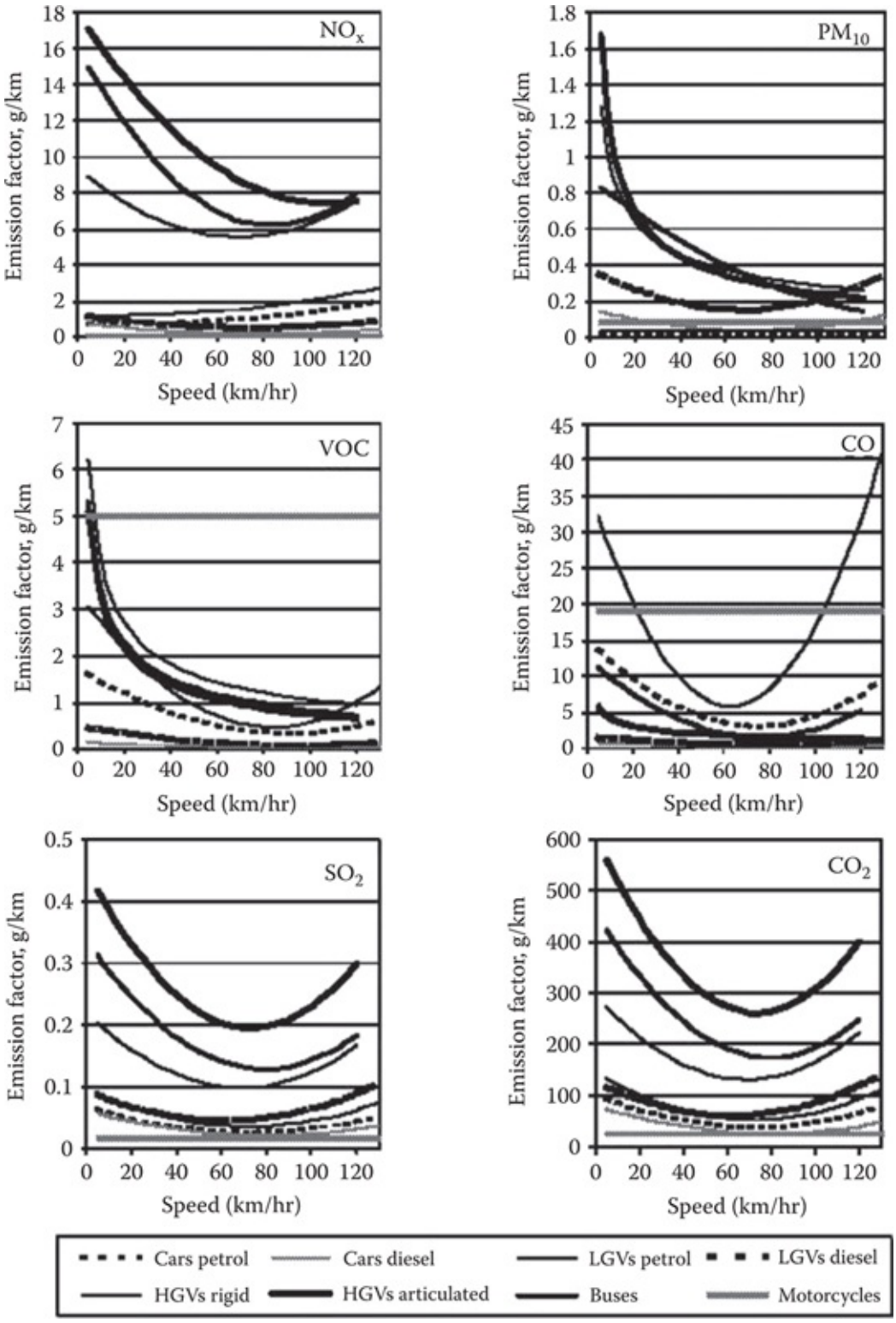

Figure 5.14 Variations of exhaust emission factors with vehicle speed for NO_x, PM_{10}, VOC, CO, SO_2 and CO_2.

Figure 5.14 ignores one major source of error in estimating vehicle emissions, which is lack of knowledge of the engine operating temperature. Many urban engines operate at reduced efficiency (i.e. higher fuel consumption and less complete combustion) because they are not yet warmed up, and catalytic converters do not achieve their potential 90%

FOR REFERENCE PURPOSES ONLY

efficiency until they reach an operating temperature of about 300°C.

The range of average journey lengths in different European countries is only 6–15 km; of the average UK trip length of 10 km, 3.4 km is *cold* and 6.4 km *hot*. Typically, 80% of car journeys are under 8 km, 33% are under 2 km, and it has been estimated that 75% of total CO is emitted from the first 1 km of a 10 km journey. The excess emissions are highest when the engine is started, and gradually decrease as the operating temperature approaches its stable value at the fully warmed-up condition. Hence the vehicle does a *cold* distance, the length of which also depends on the average speed, because the faster it is driven, the greater distance it will go before it is warmed up. Thus if a car travels slowly over the cold distance, it will be warmed up in 5–10 km. Alternatively, if it drives at the UK motorway speed limit of 70 mph (=112 km h^{-1}), then it can take over 30 km to warm up.

In covering this cold distance, the vehicle will emit *excess* of each of the pollutants compared to the amounts that it would have emitted covering the same distance in the warmed-up condition. If the vehicle trip length exceeds the cold distance, then the excess emissions due to the cold start are maximum and are fixed. If the trip length is less than the cold distance, which is quite likely given the short average trip lengths described earlier, then the excess emissions are expressed as a function of the ratio of the trip length to the cold distance

$$\text{Distance correction} = \frac{1-e^{-a\delta}}{1-e^{-a}}$$

where δ is the ratio of the trip distance to the cold distance, and a is a constant that varies with pollutant and vehicle type. Surveys have shown that on average, 60%–70% of total annual mileage is driven without the engine having achieved its warmed-up operating conditions.

Air temperature, whether high or low, also affects emissions. This is allowed for by a correction factor that multiplies with the emission factor. The correction factor takes the form $AT + B$, where A and B are constants that depend on the operational state of the engine and the pollutant concerned, and T is the ambient temperature in °C.

As TWC efficiencies increase and legislated emissions fall, cold emissions make up an increasing proportion of total trip emissions and increasing effort is being spent to control them. In the US FTP-75 test cycle, for example, which lasts 1900 s, around 80% of the total HC has been emitted after typically 300 s. Various improvements to engine management are being made or discussed. These involve pre-heating the engine block to improve initial efficiency, improving the evaporation of fuel droplets in the inlet manifold, or boosting the oxygen content of the mixture. Possible improvements to TWCs include adjusting the catalyst mix to reduce light-off temperature, placing the catalyst closer to the engine to increase warm-up rate, insulating it to retain heat while not in use, and storing the cold-start emissions for later treatment.

FOR REFERENCE PURPOSES ONLY

5.1.8.4 *Effect of operating mode*

A further source of error, as we have seen in Table 5.5, is the operating mode of the engine – whether it is idling, accelerating, cruising or decelerating. Idling and cruising are steady-state operations that can be reproduced fairly precisely and for which the air/fuel supply and exhaust controls can be properly engineered. In urban areas, driving is likely to involve repeated acceleration/braking cycles associated with intersections, roundabouts, traffic lights, queues or car parks. Under acceleration, the engine enters a transient regime during which current management practices are unlikely to be able to maintain stoichiometric combustion, or to deliver exhaust gases to the catalyst within the narrow tolerances needed for efficient operation. A summary of modal effects is seen in Table 5.11, in which the emissions during each mode are expressed as a fraction of those at idle. During acceleration, and to a lesser extent during cruising, the combustion is efficient and there is excess air, so HC and CO are low.

Table 5.11 Relative emissions under different operating modes

Mode	*Gas*		
	CO	HC	NO_x
Idle	1	1	1
Acceleration	0.6	0.4	100
Cruising	0.6	0.3	60
Deceleration	0.6	10	1

However, combustion chamber temperatures are high so NO_x is also high. During deceleration, there is some excess fuel so HC emissions are increased. Even when driving conditions are relatively steady, emissions are likely to vary very abruptly, as shown in Figure 5.15. The upper graph shows CO and NO_x emissions from a vehicle driving the speed profile shown in the lower graph. Although some emission peaks are associated with obvious events such as changing gear, others have no such clear relationship.

FOR REFERENCE PURPOSES ONLY

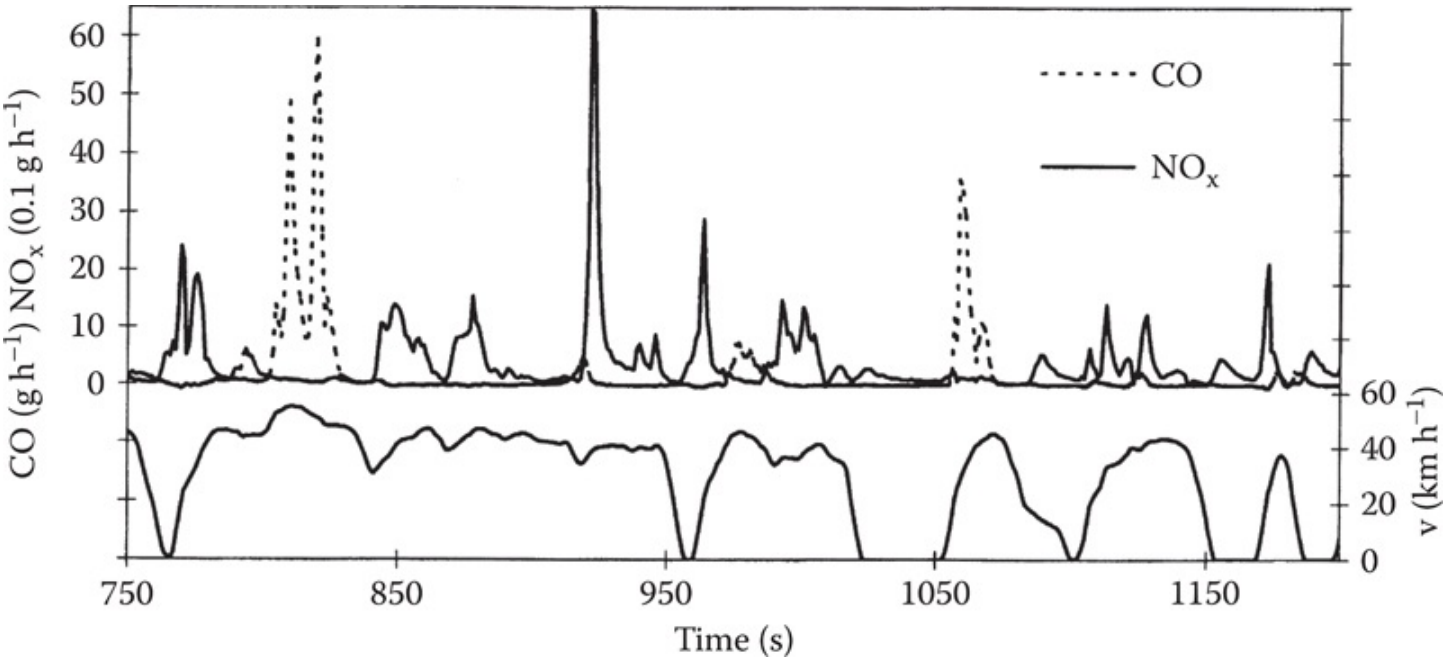

Figure 5.15 Short-term emission changes from a petrol-engined car fitted with a catalytic converter. (From de Haan, P. and Keller, M., Atmos. Environ., 34, 4629–4638, 2002.)

5.1.8.5 Catalyst degradation

In extreme cases, contamination of the catalyst by lead can render the converter useless very quickly. For all catalyst-equipped cars, thermal ageing and contamination will result in a gradual decrease in conversion performance. This is internal and irresolvable by maintenance. European and American legislation allows for this deterioration by specifying that the emission limits are not exceeded within a distance of 80,000 or 100,000 km. The test for this performance is undertaken on a continuously operating engine, whereas an engine in actual use will undergo many stop/start, hot/cold cycles that normally act to reduce lifetime. The MEET Report gives equations to describe the deterioration, which occurs rather uniformly up to around 100,000 km before levelling off.

5.1.8.6 National vehicle fleets

It is clear from the previous discussion that accurate prediction of the emissions from a fleet of vehicles in an urban area requires a very high level of detailed information. Not only must we know the flow rate and mix of vehicles (the engine type and size, and years of legislation in which they were manufactured), but also their engine operating temperatures, speeds and acceleration modes. If these parameters are not known for a particular situation, then we can use default values from national average statistics. It can be clearly seen from Figure 5.16 (and Table 14.8 in Chapter 14), how successive waves of legislation impact the car fleet, rising to a peak usage and then declining as the stock is replaced, until eventually

FOR REFERENCE PURPOSES ONLY

the whole fleet conforms with EURO 6 standards of emission control. Also, as we note that the total number of cars continues to rise, so that emissions per car have to reduce just to stand still. As these successive improvements are made to control emissions from both light-duty and heavy-duty vehicles, emissions per vehicle are expected to come down.

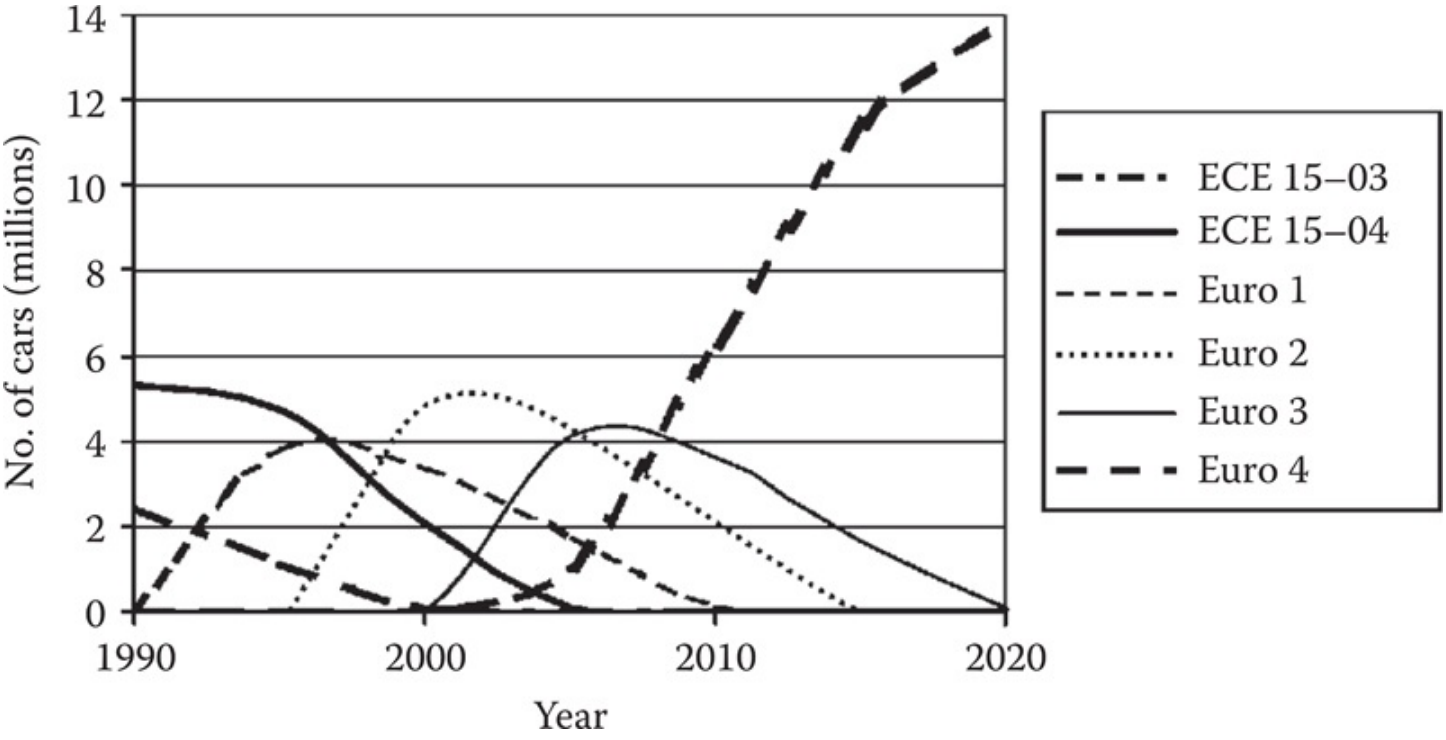

Figure 5.16 Historical trends in composition of petrol cars (<1.4 L) in the UK by class of emission legislation, 1990–2020.

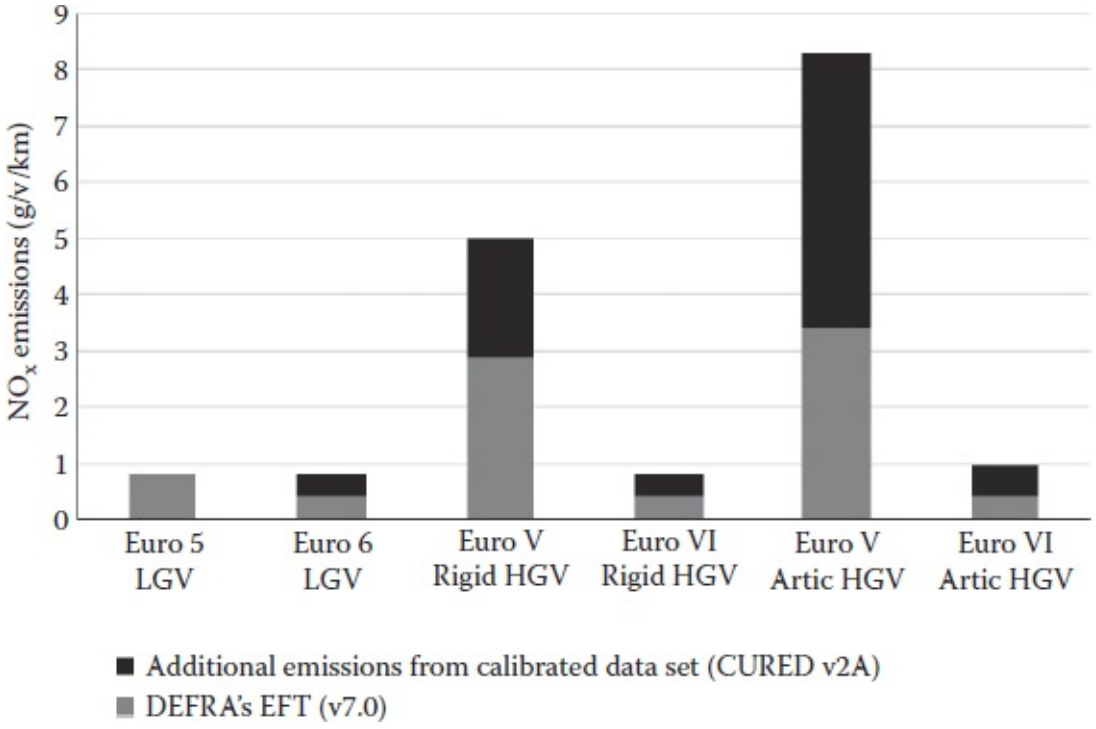

FOR REFERENCE PURPOSES ONLY

Figure 5.17 Comparative NO_x emission from Euro 5 and 6 HGVs (at a speed of 50 kmph in an urban area outside London).

In the United States, there are around 230 million road vehicles, of which 68% are passenger cars and 26% light goods vehicles (LGVs). Thirteen percent of the cars and 19% of the LGVs, are more than 15 years old. As legislated and actual emissions have decreased significantly over that period, overall emissions will again decrease as these older vehicles are replaced. The NO_x emission tests for HGVs in the UK already include real-drive emissions (RDE) since 2014, which is showing evidence of the benefits over earlier emission standards (Figure 5.17).

5.1.9 Fuel composition

5.1.9.1 Basic specification

The phasing out of lead additives has created another conflict. Engines have been designed around the fuel octane rating, which was lowered by the reduction in lead content (Table 5.12). The octane ratings of unleaded petrol were maintained by an increase in the proportion of aromatics – as lead content fell from 0.7 to 0.15 g L^{-1}, average aromatic content rose from 28% to 42%, but is currently back down to 35%. Under the EU Fuel Quality Directive 98/70/EC, tight and very detailed environmental specifications were introduced for both petrol and diesel which cover various aspects of combustion and evaporation emissions (Table 5.13). These were amended further by Directive 2003/17/EC. In January 2007, the European Commission proposed revising the standards in order to permit higher volumes of biofuel use. The commission also implemented mandatory monitoring and reporting of *life cycle greenhouse emissions* from fuels as of 2009, and an obligation for fuel suppliers to ensure that greenhouse gases produced by their fuels throughout their life-cycle (i.e. production, transport and use) are cut by 1% per year between 2011 and 2020 (Article 7a). These amendments led to a maximum limit of 10 mg kg^{-1} of sulphur in all diesel fuels, from 2009 for road transport and from 2011 for non-road vehicles and inland waterway vessels, and further cutting the permitted content of PAHs in diesel from 11% to 8%.

Table 5.12 EU environmental specifications for petrol

		Limits	
Parameter	*Unit*	*Minimum*	*Maximum*
Research octane number		95	–
Motor octane number		85	–
Reid vapour pressure (summer period)	kPa	–	60.0
Distillation:	% v/v	46.0	–
• Percentage evaporated at 100°C	% v/v	75.0	–

FOR REFERENCE PURPOSES ONLY

• Percentage evaporated at 150°C			
Hydrocarbon analysis:	% v/v	–	18.0
• Olefins	% v/v	–	35.0
• Aromatics	% v/v	–	1.0
• Benzene			
Oxygen content	% m/m	–	2.7
Oxygenates	% v/v	–	3
	% v/v	–	5
• Methanol (stabilising agents must be added)	% v/v	–	10
• Ethanol (stabilising agents may be needed)	% v/v	–	7
• Iso-propyl alcohol	% v/v	–	10
• Tert-butyl alcohol	% v/v	–	15
• Iso-butyl alcohol	% v/v	–	10
• Ethers with five or more carbon atoms			
• Other oxygenates (other mono-alcohols and ethers)			
Sulphur content	mg kg^{-1}	–	50
	mg kg^{-1}	–	10[a]
Lead content	g L^{-1}	–	0.005

[a] 1 January 2009 onwards.

Table 5.13 EU environmental specifications for diesel

		Limits	
Parameter	*Unit*	*Minimum*	*Maximum*
Cetane number		51.0	–
Density at 15°C	kg m^{-3}	–	845
Distillation:	°C	–	360
• 95% (v/v) recovered at			
Polycyclic aromatic hydrocarbons	% m/m	–	11
Sulphur content	mg kg^{-1}	–	50
	mg kg^{-1}	–	10[a]

[a] 1 January 2009 onwards.

In North and South America the oil industry has taken a different route to maintain the combustion properties of petrol. The organometallic manganese compound MMT (methylcyclopentadienyl manganese tricarbonyl) has been added at much lower concentrations than for lead – typically 18 mg L^{-1}. This material is emitted as Mn_3O_4 particles, and about 300 tonnes per year are currently being used in Canadian petrol. Manganese is both an essential trace element and a toxic metal, which is known to impair neuromotor performance. Although there is some public concern, it is not thought to be a health hazard, as airborne particle monitoring has shown that a guide value of 0.1 mg m^{-3} is not exceeded, and only 2% of Mn intake is from the air.

5.1.9.2 Fuel sulphur content

FOR REFERENCE PURPOSES ONLY

The average sulphur content of diesel fuel in the UK, which was 0.2% in 1994, was reduced to 0.05% (50 ppm) in 1996. This was expected to reduce particle emissions overall by about 15%. Although the sulphur content of petrol is only 10%–20% of that of diesel, the greater proportion of petrol cars means that total sulphur emissions (as particles or as SO_2) are similar. A refined and desulphurised diesel fuel, sometimes known as City Diesel, which had been used in Scandinavia for some years, was introduced to the UK in 1996. City diesel is claimed to reduce sulphur and particle emissions by 99% and 40%, respectively. The maximum permitted sulphur content of diesel (for road vehicles) in the EU fell rapidly from 3000 ppm in 1989 to 350 ppm in 2000, and further to 50 ppm in 2005. Correspondingly, petrol sulphur was limited to 500 ppm in 1993, 150 ppm in 2001, and 50 ppm in 2005. Actual levels in fuel are already below these limits, and there are emission-control incentives for decreasing the sulphur content of both petrol and diesel still further – to below 10 ppm. Currently (2009), ultra-low sulphur diesel fuel having a sulphur concentration of 10–15 ppm is widely available in the US and Europe.

Low-sulphur petrol is also necessary to reduce NO_x emissions through the use of storage catalytic converters, which employ a base coat of barium or potassium oxides. Nitrogen oxides are converted to nitrates and stored temporarily in the base coat. Intermittently the engine fuel mixture is turned from slightly lean to slightly rich, which converts the nitrates to N_2. The storage capacity is greatly reduced by the presence of S, which forms sulphates in the base coat irreversibly. The current trends with catalyst development are to fit the catalyst closer to the manifold so that it warms up faster and runs hotter, tighten up the feedback so that the engine spends more of its time close to the optimum, and replace rhodium and/or platinum with palladium because it is cheaper. NO_x emissions from catalyst-equipped vehicles may be reduced by around 40% when the petrol sulphur content is reduced from 130 to 30 ppm. Also, low-sulphur fuels enable the use of new generation catalysts which in turn enables more fuel-efficient engine technology. Low sulphur emissions reduce the formation of sulphate nanoparticles (<50 nm) (see Section 5.1.10.2), which may have the most important health effects. The reduction of S from 50 to 10 ppm reduces particle emission factors by 35% and 20% for petrol and diesel, respectively. While all this is going on, of course, it has to be remembered that the extra refining involves the release of additional CO_2, which will offset the efficiency gains at the point of use.

Ultra Low Sulphur Petrol (ULSP) is currently available at UK petrol stations. Although it will reduce tailpipe NO_x emissions by 5%, this will have negligible impact on UK air quality. The long-term benefit is that ULSP will enable the introduction of more fuel-efficient petrol direct-injection engines. The sulphur content of fuel used in other applications can be far higher than the figures given earlier. For diesel used elsewhere (known as gas oil), including marine diesel used in EU waters, the maximum sulphur content in the EU has been reduced from 0.2% by mass (2000 ppm) to 0.1% (1000 ppm) in 2008. For fuel oil used in combustion plants the limit is 1% (10,000 ppm) from 2003.

FOR REFERENCE PURPOSES ONLY

5.1.9.3 *Fuel reformulation*

For both petrol and diesel fuel, there has been considerable interest in whether toxic emissions can be reduced by processing the fuel at the refinery. In some cases the effect is obvious – reducing the benzene content of petrol, for example, decreases benzene emissions. Addition of an oxygenate decreases CO emissions. Particle emissions from diesel decrease with sulphur content. Understanding of both these relationships is already being used to reduce emissions. California has required the use of a low sulphur (31 ppm), low Reid vapour pressure (51 kPa), narrow distillation range fuel with reduced aromatics, olefins and benzene and enhanced methyl tertiary butyl ether (MTBE). In other cases, the effects are less clear-cut. For example, increasing the cetane number (an equivalent ignition value) of diesel fuel can reduce CO and VOC emissions, but increase particle emissions. Overall, it seems unlikely that fuel reformulation as currently practiced will significantly reduce emissions.

5.1.10 Diesel versus petrol

Diesel engines operate under different combustion conditions to those of petrol engines. The leaner mixture and higher thermal efficiency lead to lower exhaust gas temperatures (200°C–500°C), with highly oxidising conditions which make for low HC/CO emissions. Therefore, while three-way catalyst has proved to be very effective at controlling emissions from conventional petrol cars (both during the regulatory laboratory tests and real-world measurements), the picture for diesel cars has been very different (Figure 5.18). In the Euro standards, the diesel engines always have higher permitted limits for NO_x emissions than petrol cars.

Table 5.14 compares emissions from cars with warmed-up petrol engines (with and without catalysts) and diesels. One disadvantage of diesel engines is that they tend to have high emissions from a cold start. The cold/hot ratios for the usual pollutants are 1–2, similar to those for non-TWC petrol engines and much lower than those for TWC engines. On the other hand, diesel engines achieve operating temperature in half the distance of petrol engines.

In recent years, public awareness of environmental issues, the introduction of lead-free petrol and the good fuel economy of diesel engines have combined to give diesel a rather green image. The popularity of diesel cars varies greatly from country to country, being influenced by public perception, the price of fuel and the price differential between diesel and petrol (both fuel and cars). In the US, fuel is cheap and the fuel-economy advantage of diesel is not sufficient to outweigh the higher first cost and reduced smoothness of diesel engines. In France, the tax regime results in generally higher fuel costs and in diesel fuel costing around 65% that of petrol. Potential purchasers of new cars regularly use their annual mileage to calculate the pay-back period for recovering the higher initial cost of a diesel car. As a consequence of these financial incentives, diesel sales in Europe have been

FOR REFERENCE PURPOSES ONLY
around 40% of new car registrations. However, the fuel economy of diesel cars for owners has backfired on the environmental challenge of controlling the escalation in NO_x emissions, largely as a result of the poor performance of the catalytic reduction processes under urban drive and/or lower ambient temperature. The latter attributed mainly to hybrid vehicles with low combustion fuel temperature to activate catalytic converters.

FOR REFERENCE PURPOSES ONLY

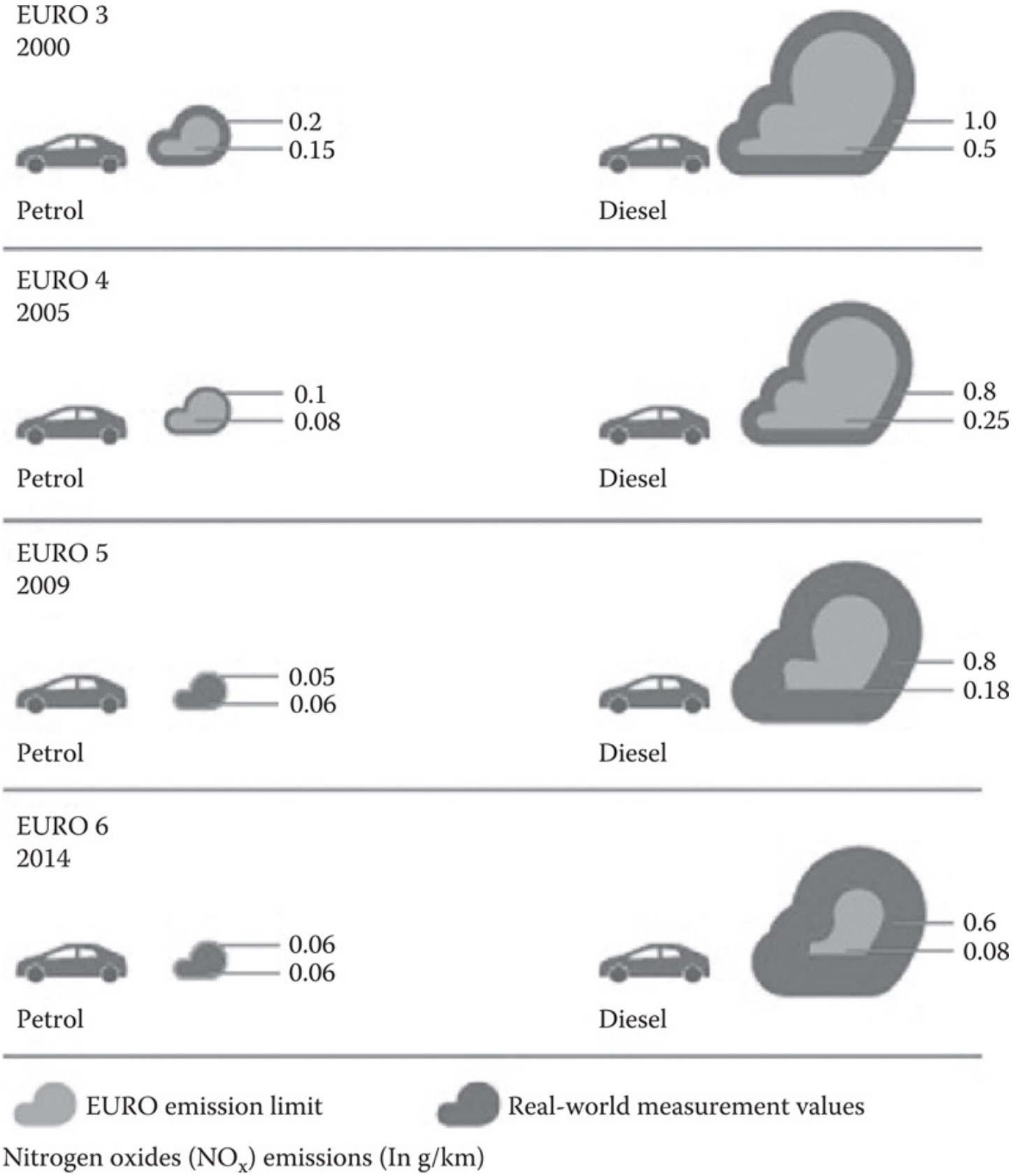

Figure 5.18 Comparison of NO_x emissions and standards for different Euro classes. (From European Environment Agency, *Explaining Road Transport Emissions*, 2016.)

FOR REFERENCE PURPOSES ONLY

Table 5.14 Emission factors for petrol and diesel cars

Vehicle type	*Average on-road emissions/g* km^{-1}			
	CO	HC	NO_x	Particles
Petrol, unleaded	27.0	2.8	1.7	0.02
Petrol, TWC	2.0	0.2	0.4	0.01
Diesel	0.9	0.3	0.8	0.15

5.1.10.1 Gaseous emissions

Due to the excess oxygen in the air–fuel mixture, carbon monoxide emissions from diesel vehicles are lower even than those from petrol vehicles fitted with TWC. Hydrocarbon emissions are similar, although there is evidence that those from diesel engines have higher proportions of the light hydrocarbons such as ethylene and propylene that are important precursors of ozone (Table 5.15). Diesel engines operate on very lean mixtures (up to 20:1), and with present technology diesel emissions can only be treated with an oxidation catalyst (which will convert HC to H_2O and CO_2, and CO to CO_2) but not with the full TWC (which requires the air/fuel ratio to be very close to stoichiometric). Hence, NO_x emissions are higher than from a TWC, although there is an improvement by a factor of two over the non-TWC exhaust. Nevertheless, the increasing proportion of diesel cars will eventually offset the reduction in NO_x concentrations being made by mandatory fitting of TWCs to petrol cars. The required breakthrough in this area is the development of a $DeNO_x$ catalyst that will convert NO efficiently at the high oxygen concentrations found in diesel exhaust.

Prototype versions of such catalysts are being trialled currently, but do not have acceptable lifetimes or conversion efficiencies (especially when high-sulphur fuel is used). Diesel cars are very low emitters of carcinogenic aromatics such as benzene and toluene, but high emitters of high molecular weight hydrocarbons such as the PAH (e.g. benzo(a)pyrene). Evaporative emissions are inherently very low from diesel vehicles as a result of the low vapour pressure of the fuel.

Table 5.15 Concentrations of untreated emissions from diesel and petrol engines

Gas	*Petrol/ppm*	*Diesel/ppm*
CO	20,000 – 50,000	200 – 4000
HC	10,000	300
NO_x	600 – 4000	200 – 2000
Aldehydes	40	20

5.1.10.2 Particulate emissions

Petrol-engine cars are usually thought of as negligible particle emitters (except in the case

FOR REFERENCE PURPOSES ONLY

of leaded petrol), although this is not necessarily the case. The carbon particles from leaded petrol are mainly organic rather than elemental, whereas those in diesel exhaust gases are two-thirds elemental. In the UK, a *blackness factor* has traditionally been used to quantify the different effectiveness of particles from different sources in reducing the reflectivity when sampled on to a filter paper. This factor cannot be related to health effects, but bears some relationship to soiling of surfaces. The scale is based on a factor of one for coal smoke; particles from petrol combustion have a factor of 0.43, and those from diesel have a factor of 3 – a ratio of 7. Experimental determinations from an urban mix of vehicles in Leeds have given an overall factor of 0.92.

Figure 5.19 shows typical particle size distributions (by number) for different engine types. The old petrol engine peaked at around 30 nm, while the line for the new petrol engine is hardly visible along the diameter axis. The indirect injection (IDI) diesel engine gets significantly worse with age, but can be improved greatly by the use of a particle trap. In terms of blackness, typical emission factors of 1.5 and 6 mg (kg fuel)$^{-1}$ for petrol and diesel respectively become transformed to 0.7 and 18 mg (kg fuel)$^{-1}$ – a ratio of 26.

5.1.11 Impact of control measures

In the UK, catalytic converters (CATs) have been fitted in the exhaust of the majority of petrol cars manufactured since 1992, and diesel cars since 2001. This change will significantly reduce emissions of CO, NO_x and HC. On the other hand, the proportion of the fleet that uses diesel engines will continue to increase. First, these vehicles cannot at present be fitted with three-way catalysts, so their emissions will be uncontrolled. Second, they will have much higher particle emissions than their petrol counterparts. During the past quarter century, the impact of emission controls (amongst other changes) has gradually been bringing down the concentrations of SO_2, CO and NO_2 in urban areas. Figures 5.20 and 5.21 show predictions of the overdue but nevertheless dramatic effects of catalytic converters, cleaner fuels and other measures on vehicular emissions of NO_x and PM_{10}, respectively. At present, just over halfway through the time period shown, emissions of these two key pollutants are less than they were in 1970. By 2025 they will be typically 25%–35% of their values in 1970. The pattern and scale of reduction will be echoed for other vehicular pollutants such as CO and HCs.

FOR REFERENCE PURPOSES ONLY

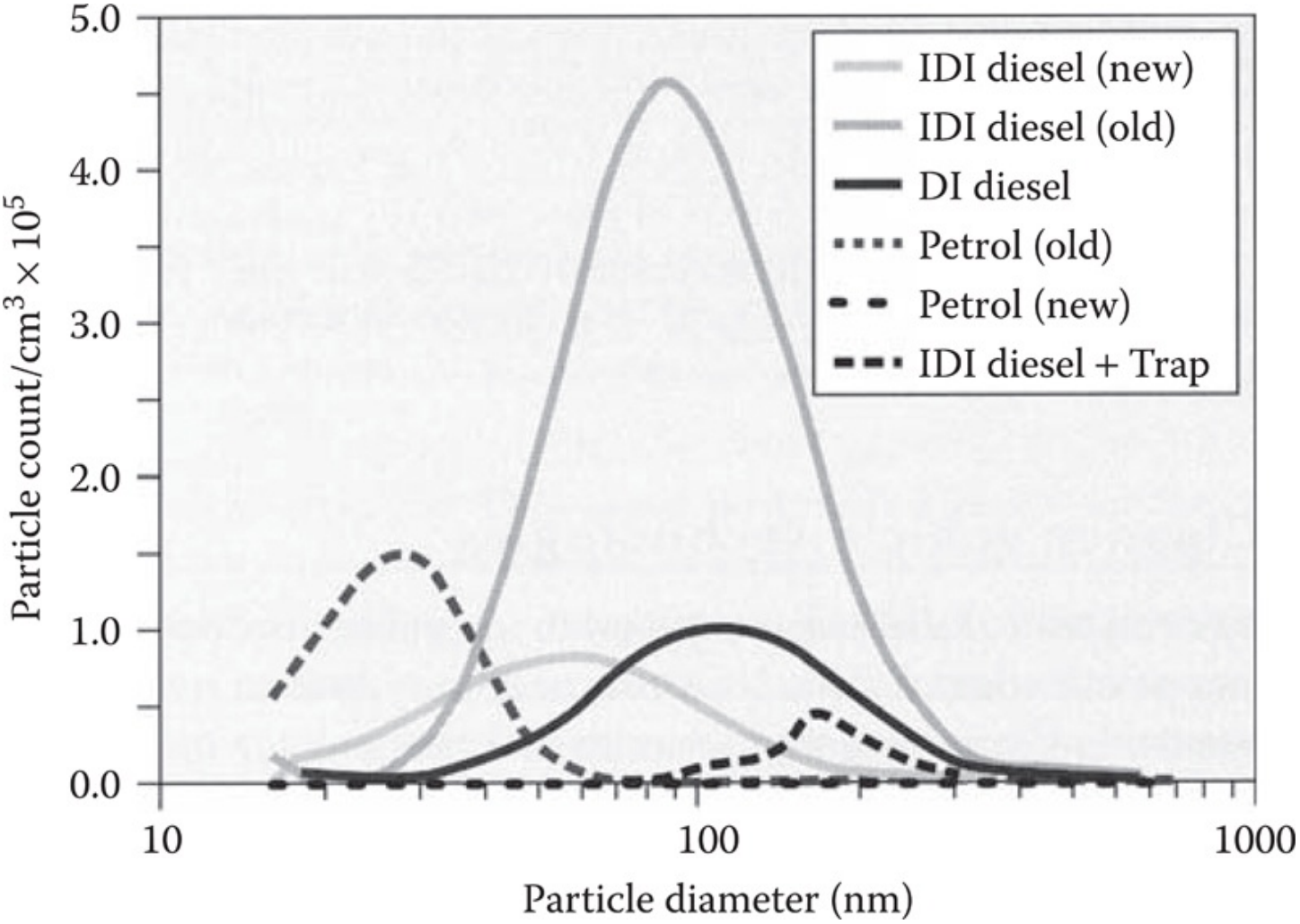

Figure 5.19 Particle emissions from petrol and diesel engines. (From Airborne Particles Expert Group, *Source Apportionment of Airborne Particulate Matter in the United Kingdom*, Department of the Environment, London, UK, 1999.)

FOR REFERENCE PURPOSES ONLY

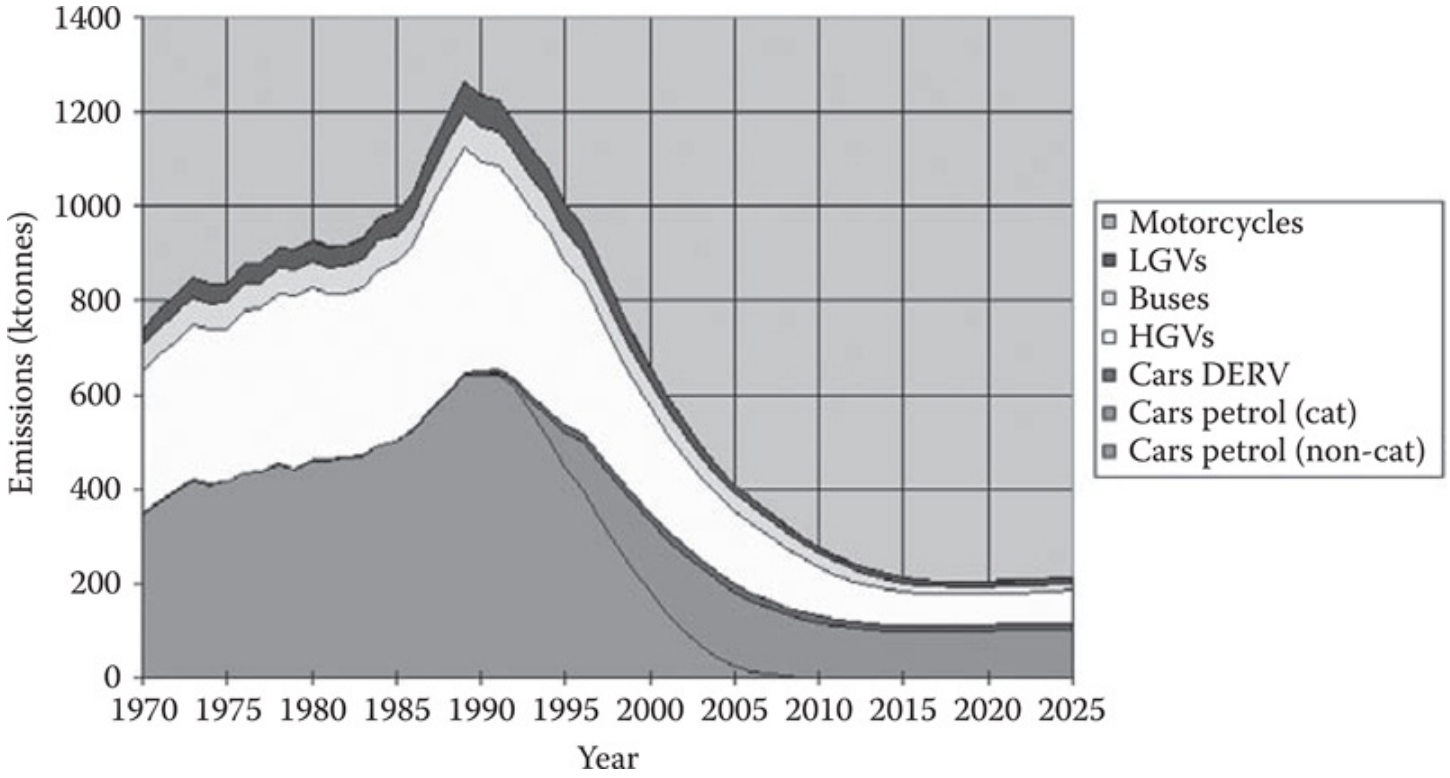

Figure 5.20 UK urban road transport NO_x emissions, 1970–2025. 20% diesel car sales; Central 1997 NRTF; Euro III, Euro IV reduction in emission from new vehicles; 2000 and 2005 fuel standards.

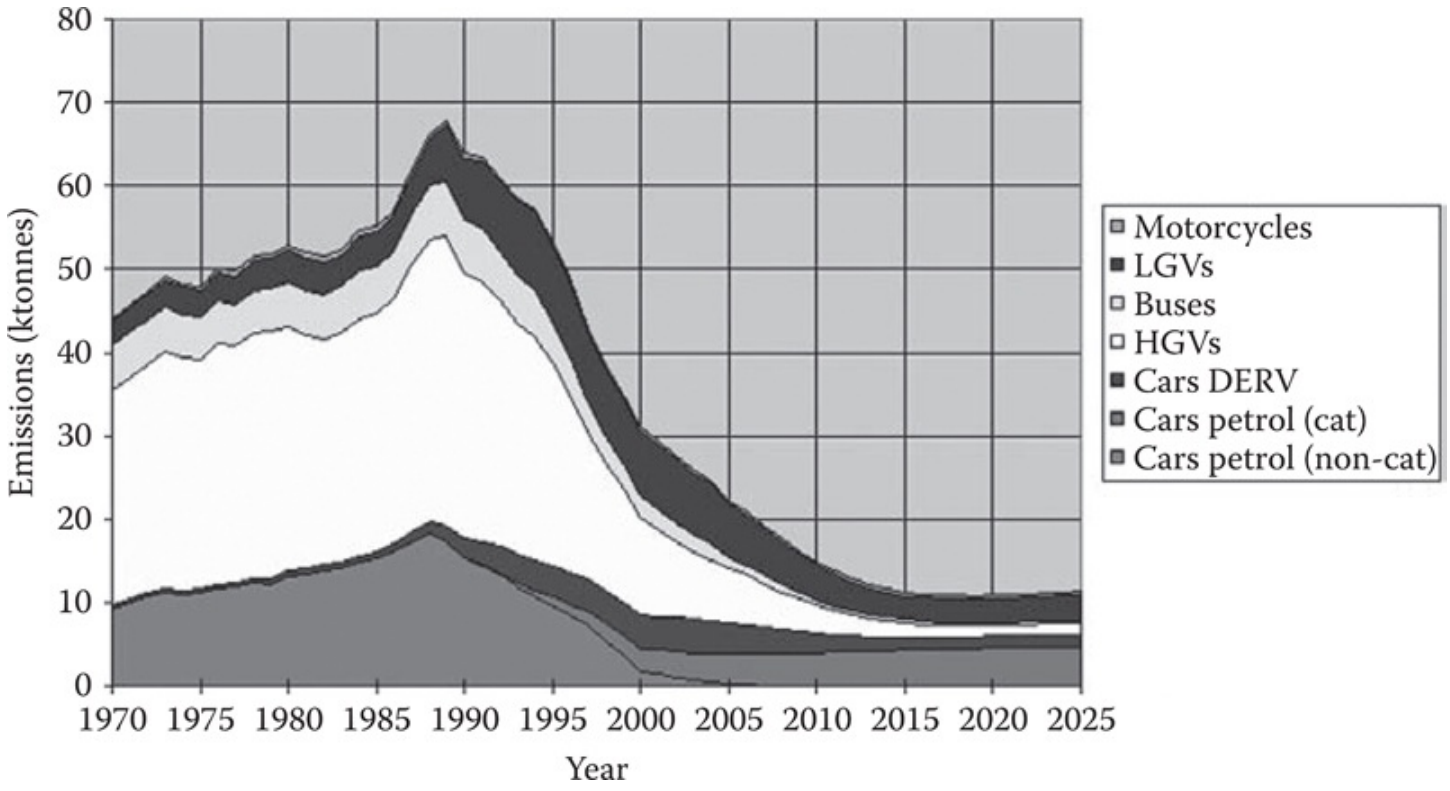

Figure 5.21 UK urban road transport PM_{10} emissions, 1970–2025. 20% diesel car sales;

FOR REFERENCE PURPOSES ONLY

Central 1997 NRTF; Euro III, Euro IV reduction in emission from new vehicles; 2000 and 2005 fuel standards.

5.1.12 Cleaner vehicle technologies

There is a major ongoing global research effort to try and replace petrol and diesel fuels with other power sources. This is seen as necessary both to reduce pollutant emissions and also to keep cars going when the oil runs out.

5.1.12.1 Electric

Electric vehicles were serious contenders with the internal combustion engine in the early development of the motor car. Their clear attractions of quiet operation and no emissions at the point of use have been offset by one main drawback – the low energy density compared to petroleum-based fuels has meant that vehicles have had to be rather heavy, and this has made them uncompetitive on range and performance. There has been a long period of research into better batteries – sodium/sulphur and nickel/metal hydride, for example, instead of lead/acid – but progress has been slow. In California, where there is still a serious problem with photochemical pollutants despite over 20 years of catalyst use, an increasing proportion of vehicles sold will have to be *zero emission vehicles* (ZEVs, assumed to be electric). There are still emissions associated with electric vehicles, but they occur at the power station rather than at the vehicle itself. Emission factors, which are now expressed as gram of pollutant emitted per GigaJoule of electricity generated, therefore vary greatly from country to country, depending on the way the electricity is produced. Examples of the extreme cases, together with the European average emission factors, are given in Table 5.16.

These generation emission factors are divided up amongst the vehicle fleet, with a proportion being allocated to each vehicle according to its use. The effective emission factor F for each vehicle type can then be written in the form:

$$F = aV^2 + bV + c$$

where:

a, b and c are coefficients

V is the average vehicle speed in km h^{-1}

Table 5.16 Emission factors from electricity generation

FOR REFERENCE PURPOSES ONLY

Country	Emission factor/g GJ^{-1}						
	CO_2	CO	NO_x	NMHC	SO_2	CH_4	PM
Norway (mainly hydro)	1700	0.6	2.8	0.2	3.7	6	0.2
France (mainly nuclear)	17600	3.2	61	3.2	184	36.1	7.9
UK (mainly coal and gas)	167800	27.4	632	20.2	1446	459	70
European average	127400	21.3	326	22.6	745	283	39

Table 5.17 Electric vehicle emission coefficients

Pollutant	Passenger cars			Light-duty vehicles		
	a	*b*	*c*	*a*	*b*	*c*
CO_2	0.0233	−3.249	198	0.419	−5.848	356
CO	0.0000	−0.001	0.03	0.0000	−0.001	0.06
NO_x	0.0001	−0.008	0.51	0.0001	−0.015	0.91
VOC	0.0000	−0.001	0.04	0.0000	−0.001	0.06
SO_2	0.0001	−0.019	1.16	0.0002	−0.034	2.09
CH_4	0.0001	−0.007	0.44	0.0001	−0.013	0.79
PM	0.0000	−0.001	0.06	0.0000	−0.002	0.11

Table 5.18 Example of emission factor calculation

Pollutant	*Electric passenger car emission factor/g km^{-1}*	*Petrol passenger car (EURO 1) emission factor/g km^{-1}*
CO_2	87.2	141
NO_x	0.51	0.39
SO_2	0.28	–

Table 5.17 gives the coefficients for the European average emission factors from electricity generation. For example, a passenger car travelling at an average speed of 50 km h^{-1} would have the emission factors given in Table 5.18.

In urban areas, there would clearly be a huge reduction in local pollutant burdens if a substantial proportion of the vehicles was electric, because the power stations are in the country. The arguments are less clear-cut in other ways. Electricity generation by fossil fuel combustion is only 40% efficient, at best.

While this may be slightly more efficient than individual internal combustion engines, it will not result in significant reduction of CO_2 emissions. Unless $DeNo_x$ and flue-gas desulphurisation (FGD) equipment is fitted to all fossil fuel stations, there may well be an increase in overall NO_x and SO_2 emissions, although these will be released from tall stacks in rural areas rather than from ground-level exhaust pipes in towns.

5.1.12.2 Hybrid

The need for a combination of low emissions in congested urban areas and extended range out of town has prompted the development of hybrid vehicles, in which electric and conventional power work together. The electric motor can also act as a generator, so that when the vehicle is braking some energy is recovered and stored in the battery.

5.1.12.3 Hydrogen

There is increasingly vocal lobby to make hydrogen the fuel of the future. Burning hydrogen creates water as the major waste product. There is no HC, CO, CO_2 or particle production, although there is some thermal NO_x if air is used to supply the oxygen. If the hydrogen is made from petrol, gas or biomass, then there are substantial emission possibilities at the point of manufacture. If it is made by the electrolysis of water, then energy of some type will have to be used. Although the use of hydrogen in the internal combustion engine would reduce emissions, the engine itself is only 20%–25% efficient and even greater emission reductions would be obtained by the use of fuel cells and electric motors.

5.1.12.4 Fuel cell

Electricity is generated directly from the low-temperature chemical reaction of hydrogen and oxygen. In the front-runner proton exchange membrane (PEM) cell, a thin polytetrafluorethylene (PTFE) membrane is sandwiched between an anode, where the fuel enters, and a cathode to which oxygen (from air) is supplied. The membrane has been treated to make it permeable to protons but not electrons. The hydrogen atoms split into their constituent protons and electrons, and because the former are separated by the membrane, the latter are driven round the external circuit to power a motor or other device. Current fuel cells obtain power densities of 1.5 kW L^{-1}, which is marginal if enough power output is to be fitted within a car engine compartment. However, this power density is increasing, and the fuel cells already operate at twice the efficiency of the internal combustion engine. A variety of fuels can be used to supply the hydrogen, with the leading contender being liquid organic fuels such as methanol and liquefied natural gas (LNG), from which the hydrogen is recovered in situ using a reformer. Ideally, a hydrocarbon should be used that produces maximum hydrogen for minimum carbon dioxide, and methane has the highest H/C ratio of all the hydrocarbons. Potentially, pure hydrogen could be stored and used, but this would demand an even bigger change in society infrastructure for the generation, delivery and storage of the gas. Hydrogen does not liquefy until the temperature is below –253°C, so could only be stored on board as a highly compressed gas. The state-of-the-art vehicle at present stores about 80 L of hydrogen on board at pressures up to 355 bar, giving the car acceptable but not startling performance and a range of up to

250 km. If the hydrogen is obtained from hydropower this would sever the link with fossil fuels and greatly reduce emissions of both CO_2 and air pollutants. Estimates have shown that gasoline CO_2 emissions could be reduced by 70% overall by the use of hydrogen produced from the large-scale reforming of natural gas. Larger reductions would require the energy for the hydrogen production to be generated by greener means such as solar, wind or hydropower. Eventually, we can imagine a hydrogen-based economy with the fuel being generated from the water and electricity at hydroelectric power stations. Dream on!

5.1.13 Alternative fuels

Whereas the cleaner technologies described in the previous section all require a radically different engine, there is a parallel development of alternative (non-petroleum) fuels that are intended to be used in a conventional engine but to have particular advantages over conventional fuels.

Natural gas: Predominantly methane (75%–95%) plus ethane (5%–20%), propane (3%–20%) and butane (1%–7%). Used either in single or dual-fuel spark-ignition engines, when they can be swapped with diesel. CO, NO_x and particle emissions are reduced, HC are increased, and fuel consumption is about the same. The λ window is smaller than for petrol engines, so that it is harder to maintain TWC efficiency.

Methanol: Methanol (CH_3OH) is a good fuel for lean-burn *petrol* engines. It has a high octane number and low vapour pressure (hence low evaporative emissions). It can be manufactured from a range of feedstocks – natural gas, crude oil, biomass and urban refuse. However, it has thus far failed to live up to its promise. The high heat of vaporisation makes it difficult to vaporise fully in the combustion chamber, so that 10%–15% petrol has to be added to ensure reliable cold starting. This offsets the emission advantages of pure methanol, which emits less CO, HC, NO_x and CO_2 than petrol. However, the ability to make methanol from non-fossil resources is a major advantage. Emission problems with formaldehyde and unburned methanol have been found.

Ethanol: Major programmes have developed ethanol (CH_2OH) as a vehicle fuel in some countries – notably in Brazil, where it is made from sugarcane wastes. It can be used alone or blended with petrol. In fact, it was the fuel recommended by Henry Ford for the Model T. Today, around 4 million cars (one-third of the fleet) run on ethanol in Brazil. It has similar operational advantages and disadvantages to methanol.

Biodiesel: Biodiesels are fuels derived from renewable lipid feedstocks, such as vegetable oils and animal fats, or from the fermentation of vegetable matter. In a process called esterification, the large branched triglyceride lipid molecules in oils and fats are broken down into smaller chain molecules (esters and glycerol). The glycerol is removed, and the remaining esters are similar to those in petroleum diesel. They are

FOR REFERENCE PURPOSES ONLY

not a new idea – Rudolf Diesel demonstrated in 1900 that his engine would run on groundnut oil.

They have received much press and research attention because of the perceived advantages of growing fuel sustainably rather than using up fossil supplies, especially if this could be combined with lower emissions (Table 5.19). Again they have not yet fulfilled their promise. It is more difficult to make a biofuel diesel engine run smoothly and start reliably, and emission performance is not startling. In general, emissions of regulated air pollutants are reduced. Whether these alternative fuels become widely adopted depends on the economics of production and distribution, as well as on air quality. There are major side issues, such as the fertiliser use which is necessary to achieve high plant productivity, and the loss of food crop area.

Dimethyl ether (DME) is a liquefied gas with handling characteristics similar to propane and butane, but with a much lower auto ignition temperature. Hence, it is suitable as an alternative fuel for diesel engines. The DME molecule consists of two methyl groups separated by an oxygen atom ($H_3C\text{-}O\text{-}CH_3$). On a large scale, DME can be produced in a similar manner to methanol via synthesis gas (a mixture of CO, CO_2 and H_2) from a variety of feedstock including (remote) natural gas, coal, heavy residual oil, waste and biomass. Particulate emission is very low, because of the absence of carbon–carbon bonds and the significant oxygen content. Formation of components such as PAH and Benzene, Toluene, Xylene (BTX) is reduced. Low NO_x emission is possible through fuel injection *rate shaping* and exhaust gas recirculation.

Table 5.19 Emissions due to alternative fuels

If you replace	CO	HC	NO_x	PM
Petrol by natural gas in an	Decreases	Increases	Decreases	N/A
LDV with catalyst	(0.4–0.5)	(1.5–2.0)	(0.4–0.6)	
Petrol by methanol in an	No change	Decreases	Decreases	N/A
LDV with catalyst	(0.7–1.1)	(0.5–0.8)	(0.8–0.9)	
Diesel by methanol in	Decreases	Decreases	Decreases	Decreases
HDV	(0.5–0.8)	(0.4–0.6)	(0.4–0.75)	(0.1–0.2)
Diesel by biodiesel in	Decreases	Decreases	Increases	No change
HDV	(0.75–0.8)	(0.2–0.8)	(1.1–1.2)	(0.6–1.2)

5.2 NON-ROAD MOBILE MACHINERY EMISSIONS

Non-road mobile machinery (NRMM) is defined as any mobile machine, item of transportable industrial equipment, or vehicle (with or without bodywork) that is not intended for carrying passengers or goods on the road. It is installed with a combustion engine, either an internal spark ignition petrol engine or a compression ignition diesel

engine. Examples of NRMM include heavy plant equipment used on construction sites or agricultural sites. Typical examples of NRMM on construction sites are excavators, dumpers, telehandlers, cranes, piling rigs, generators, compressors and pumps. Other machines such as truck-mounted cranes having multiple engines are also counted as NRMM, where the primary truck engine is affected by on-road regulations, but any secondary engine installed to power the crane is covered by the NRMM regulations.

Across the EU, emissions from NRMM, specifically those used in construction industry, are coming under closer scrutiny. The London Atmospheric Emissions inventory (LAEI) currently (2017) attributes 7% of the NO_2, 8% of PM_{10} and 14.5% of the $PM_{2.5}$ emissions in London air as originating from the NRMM diesel engines used in the construction industry. The air pollutant emissions from construction-related NRMM are thus far regulated through the Control of Dust and Emissions during Construction and Demolition best practice guidance, issued by the Mayor of London (2014). This guidance mainly aims to reduce NO_x, PM_{10}. The European Union have brought out a set of new Emission Standards for engines used in NRMM (January 2017), which have significantly reduced gaseous emissions. The standards are split into categories for spark ignition (petrol) and compression ignition (diesel) engines, and then further classified according to the engine power rating. The new EU NRMM regulation legislation sets out the Stage V limits, mainly limiting the particulate matter and gaseous emissions from compression ignition that is diesel engines.

5.3 RAIL EMISSIONS

Rail engines, also known as *locomotive*, may be powered by either electric (so that the emissions are from power station point sources) or diesel (emissions from the train itself). Rail emissions comprise of both stationary emissions from idling locomotives in stations and depots, as well as mobile emissions on busy lines. Globally, there is a great range of train types and operating regimes. The powers, weights and duty cycles of the trains and engines all vary greatly. As a consequence, the emission factors vary by an order of magnitude, and the calculation of total emissions needs detailed knowledge of train operating parameters, including factors such as mean distance between stops. Such calculations usually start with an estimate of energy consumption in kJ per tonne km, which is independent of the motive power. This is then multiplied by the appropriate emission factor. The diesel engines used on diesel-electric trains are quite similar to those used on HGVs, with emissions based on the gas-oil consumption rates for moving locomotives. Whist emissions of air pollution from road traffic sources have been widely studied, there is relatively less information on air pollution from trains. The majority of available studies have focused on either in-train exposure or PM in underground environments. Recent modelling based on the London Atmospheric Emissions Inventory (LAEI) suggests that diesel trains may be responsible for breaches of the NO_2 annual air quality objective up to

FOR REFERENCE PURPOSES ONLY

200 m on either side of the railway lines. LAEI 2010 suggest that the total emissions of NO_x for the railway in London area (passenger and freight) are about 62 t/km/yr. The LAEI also provides estimates of CO_2 emissions that allows ratios of NO_x/CO_2 to be calculated. On average, the rail source NO_x/CO_2 ratio is 0.013, which is consistent with expectations based on emissions from large diesel engines. However, current limited ambient measurements of rail emissions suggest that the modelled predictions often exceed ambient concentrations. Therefore, our understanding based solely on modelling approach may provide a skewed impression of the severity of the issue.

Table 5.20 EU train emission factors

Pollutant	*Electrical power generation g(kWh)$^{-1}$*		*Diesel locomotive emissions g (kW h)$^{-1}$*	
	1998	2020	1998	2020
SO_2	2.7	0.8	1.0	0.03
NO_x	1.2	0.35	12	3.5
HC	1.1	0.55	1.0	0.50
CO	0.08	0.04	4.0	0.50
PM	0.14	0.07	0.25	0.08

The MEET Report calculated the emission factors for all EU trains in 1998 and 2020 (Table 5.20). It was expected that the share of traffic powered by electricity would increase from 65% to 80% over this period, although a much lower proportion of the rail network would be electrified. It can be seen that electrical power generation leads to higher SO_2 emissions than diesel because of the higher sulphur content of the fuel; that other emissions are generally lower from power stations, and that both sources will be reduced by new fuel standards and emission controls.

In the UK, the Department for Transport specifies locomotive emission factors so that Local Authorities can compute emissions in their regions. Published emission factors for diesel trains in the UK suggest a mean NO_x/CO_2 ratio of 0.0094. A ratio of around 0.01 is very similar to that for large vehicles (HGVs and buses) based on the vehicle emission remote sensing analysis, suggesting that large diesel engines tend to emit very similar amounts of NO_x for a given amount of fuel burned. In the United States, where locomotive diesel engines are unregulated and have very high NO_x emissions, they account for about 10% of mobile source emissions of this gas. Test-bed measurements from US diesel locomotives have explored NO_x emissions, reporting greatest NO_x emissions at low engine loads, decreasing as load increased, but were constant for all settings above ¼ throttle. Emission factors are in the range 80–110 g (kg fuel)$^{-1}$, which is about three and ten times the corresponding values for the HGV and LGV fleets, respectively. PM emissions showed a similar pattern with respect to engine throttle settings, however, emissions at idle were dominated by organic particles with elemental carbon being dominant as the engine throttle was increased. In some part of the world where coal-fired locomotives are still in operation,

either for common transportation or vintage usage, there are also additional SO_2 emissions, depending on the sulphur content of the coal used.

In addition to the direct emissions from the operation of the locomotive engine, there are also evidence of particle emissions from operation of a train. For example, a series of experiments in Switzerland have measured the particle emissions from electric trains. PM concentrations were mainly dominated by Fe particles, which added around 1 μg m^{-3} to the local PM concentrations at 10 m from the railway line. Lesser concentrations of Cr, Cu and Mn have also been found; consistent with track and conductor wear. At 120 m from the tracks, the concentration PM from the railway was around 25% of that measured at 10 m distance. These studies found that around 60%–70% of the metal particles from the railway were in the $PM_{2.5–10}$ size range. Other studies in Switzerland have also found Ca and Al particles close to electric railways consistent with track bed wear.

5.4 SHIPPING EMISSIONS

A large ship on average emits NO_x, CO_2 and carcinogenic particles respectively equivalent to 70,000, 2 million and 2.5 million cars. There are around 86,000 ships in the world fleet, of which about half are cargo vessels, a quarter fishing vessels and 10% tugs. As shipping is an international industry, environmental, security and safety standards are developed by the International Maritime Organization (IMO), a United Nation specialised agency. MARPOL 73/78 is the International Convention for the Prevention of Pollution from Ships (Annex VI covers air pollution prevention). Ships must be issued with an International Air Pollution Prevention (IAPP) Certificate, specifically stating that the ship uses fuel oil with a sulphur content that does not exceed the applicable limit value. The interpretation of *fuel oil used on board* includes use in main and auxiliary engines and boilers. Shipping generally uses rather poor-quality diesel-type fuels variously termed bunker fuel oil (BFO, a heavy residue from petroleum refinery processing), marine gas oil and marine diesel oil (MDO). Large ships such as container ships, passenger ships and ferries typically use 60–80 tonnes of fuel each day, while at the other end of the size spectrum a fishing vessel would use less than one tonne per day. The calculation of emission factors involves a comprehensive accounting for shipping fleets in terms of fuel use and duty cycle (Table 5.21). There are good data available on tonnage and fuel use from organisations such as Lloyd's Register. The most sophisticated models allow for the different phases of a vessel's trip, such as berthing, cruising and manoeuvring, with specific emission factors for each. Hence, a medium-sized ferry, powered by medium speed diesel engines, burning 20 tonnes of 1% S fuel each day, and having a 50% duty cycle, will emit annually around 200 tonnes NO_x, 25 tonnes CO, 11,000 tonnes CO_2, 8 tonnes VOCs, 4 tonnes PM and 70 tonnes SO_2. Although BFO may be up to 3% S, the sulphur contents of marine fuels are being reduced by legislation. Directive 93/12/EEC set a limit of 0.2% for the sulphur content of gas oils and 1% for fuel oils. The International Maritime Organisation (IMO) has introduced measures

FOR REFERENCE PURPOSES ONLY

for substantial reductions in the sulphur content of marine fuel from 2020.

Table 5.21 Shipping emission factors (kg (tonne fuel)$^{-1}$) for different engine types

Engine type	NO_x	CO	CO_2	VOC	PM	SO_x
Steam turbines (BFO)	6.98	0.431	3200	0.085	2.50	20S[a]
Steam turbines (MDO)	6.25	0.6	3200	0.5	2.08	20S
High-speed diesel engines	70	9	3200	3	1.5	20S
Medium-speed diesel engines	57	7.4	3200	2.4	1.2	20S
Low-speed diesel engines	87	7.4	3200	2.4	1.2	20S
Gas turbines	16	0.5	3200	0.2	1.1	20S

[a] S is the sulphur content of the fuel expressed as percent by mass. Hence there would be S kg sulphur per 100 kg fuel, and 10S kg per tonne fuel. If all the S were emitted as SO_2, there would be 20S kg SO_2 per tonne fuel, because the molar mass of SO_2 is twice that of S.

With the ongoing reduction in land-based emissions, the maritime S emissions have now taken on a more significant aspect. For example, North Sea shipping emissions alone in 1990 were similar in magnitude to the entire UK emission ceiling for 2010 set in the Gothenburg Protocol. Cost-effective measures to reduce acid deposition in continental Europe will include reductions to the S-content of bunkering fuels. In this context the IMO has agreed that all ships use marine fuels with a maximum sulphur content of 0.5% by 2020. An increasing number of ships are also now using gas as a fuel as when ignited it leads to negligible SO_2 emissions (the International Code for Ships using Gases and other Low Flashpoint Fuels, 2015). Another alternative fuel is methanol which is being used on some short sea services. In addition, from 2015, member countries have established more stringent local Emission Control Areas with 0.1% limit for sulphur emissions.

5.5 AIRCRAFT EMISSIONS

There has been sustained growth in civil aviation for the last 50 years, and it now plays a major role in global freight and personal transport. Demand has grown at around 5% each year during the last 20 years from rapid globalisation, especially in the developing economies, and is expected to grow at a similar rate over the next 15 years. Predictions even further ahead are less certain, but estimates of around 25,000 billion revenue passenger kilometres (RPK) by 2050 have been made (corresponding fuel demand estimated to range between 426 and 766 Tg). The RPK is a measure of volume of traffic, which is calculated by multiplying the number of revenue-paying passengers aboard an aircraft by the distance travelled. Because passenger and freight transport is concentrated over a relatively small number of high-density routes in and between Asia, Europe and North America (often called as air transport hubs), the fuel burned and resulting emissions are unevenly distributed as well. There is also a clear association between deterioration of

FOR REFERENCE PURPOSES ONLY
local air quality and the level of ground operations as such excessively busy airport hubs.

Engines for civil and general aviation are generally classified as gas turbine engines (turbofan and turboprop) fuelled with aviation kerosene (also named jet fuel) and internal combustion piston engines fuelled with aviation gasoline, often referred as avgas. The propeller-based fleet of the 1950s and 1960s was superseded by jets and then by turbofans. Cruise speeds have increased from 100 to 500 knots, and cruise altitudes for long-haul flights from 3 km for propeller-powered aircraft to 10–13 km today. The height increase has been designed mainly to reduce drag forces (and hence fuel consumption) and is environmentally significant because it means that a substantial proportion of the emissions is released into the stratosphere, where the increased atmospheric stability and reduced role of washout and rainout give the emissions a much longer residence time.

The International Civil Aviation Organisation (ICAO) through the Committee on Aircraft Engine Emissions (CAEE) and the subsequent Committee on Aviation Environmental Protection (CAEP) have set up protocols for the measurement of carbon monoxide (CO), NO_x, unburned hydrocarbons (UHC) and smoke number (SN) for aircraft engines. Figure 5.22 shows the improvement in efficiency that has occurred over the last 50 years. During the period 1950–1997, average fuel efficiency (as measured by aircraft seat km per kg fuel) increased by 70%, and this is expected to be followed by a further 45% improvement by 2050. Aircraft fuel burned per seat has also decreased by about 70% during the period of jet passenger flight. However, these efficiency gains may be dwarfed by the forecast growth in aviation traffic and the additional emissions from associated ground-level operational activities, including ground-service equipment and vehicular transport.

In addition to the commercial flights discussed earlier, flights are made by some 55,000 military aircraft (combat, trainer, tanker, transport), although the proportion of military flights has been falling and will continue to do so. Aviation fuel currently makes up 2%–3% of total fossil fuel consumption, which corresponds to 20% of all transportation fuel, with 80% of this used by civil aircraft. All these aircraft emit the usual range of combustion gases and particles into the atmosphere either at the airports, in the troposphere or stratosphere, and the pollutant burden has therefore been increasing too.

FOR REFERENCE PURPOSES ONLY

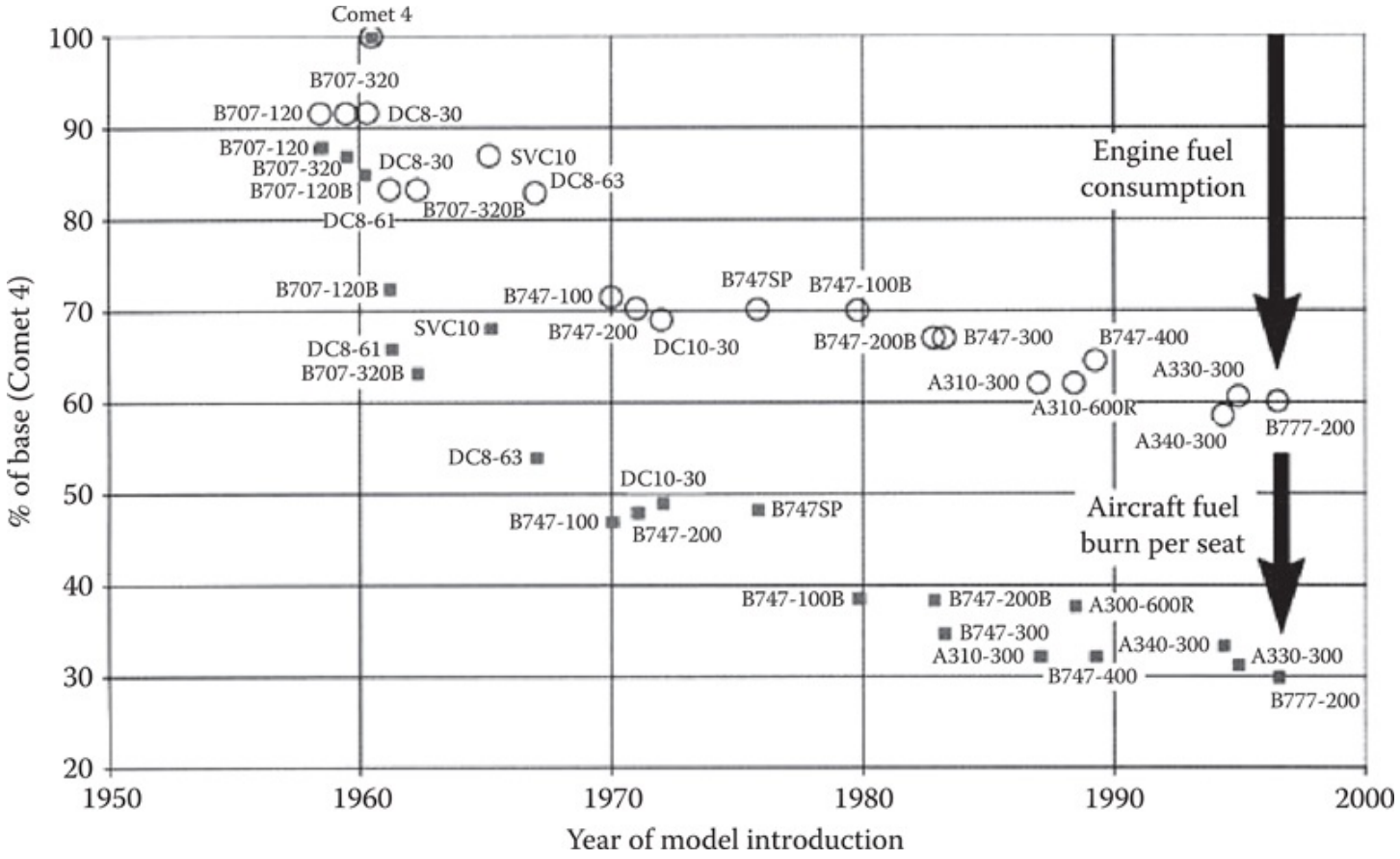

Figure 5.22 Reductions in engine fuel consumption and aircraft fuel burn per seat, 1950–1997. (From Intergovernmental Panel on Climate Change, *Aviation and the Global Atmosphere*, Cambridge University Press, Cambridge, UK, 1999.)

5.5.1 Emission calculations

Calculation of overall emissions, as with other sources, requires a detailed inventory of aircraft in use, flight patterns and emission factors. Operations such as taxiing should be included. Taking off (and, to a lesser extent, landing) may be especially important because the engines are operated at high power and the emissions are released close to the ground.

Aircraft emission factors for different operational modes are given in Table 5.22. The emission indices for CO_2 and H_2O are simply those for stoichiometric combustion of kerosene (paraffin), which is the universal aviation fuel and of fairly uniform composition. All jet fuels are composed primarily of hydrocarbons as a blend of saturates, with no more than 25% aromatics. A fuel may contain up to 0.3% S by weight, although the general level is less than 0.1% and falling, with average reported values in the range 0.04%–0.06%.

A more realistic, but simplified, combustion scheme in aircraft engines can be summarised as Lee et al. (2009) (Figure 5.23):

$$C_nH_m + N_2 + O_2 + S \rightarrow CO_2 + N_2 + H_2O + O_2$$

FOR REFERENCE PURPOSES ONLY

$+ CO + SO_x + NO_x + HC + soot$

Table 5.22 Typical emission indices (g kg^{-1}) in different operational modes

Species	*Operating mode*		
	Idle	*Take-off*	*Cruise*
CO_2	3160	3160	3160
H_2O	1230	1230	1230
CO	25 (10–65)	<1	1–3.5
HC (as CH_4)	4 (0–12)	<0.5	0.2–1.3
NO_x (as NO_2)			
Short haul	4.5 (3–6)	32 (20–65)	7.9–1 1.9
Long haul	4.5 (3–6)	27 (10–53)	1 1.1–15.4
SO_x	1.0	1.0	1.0

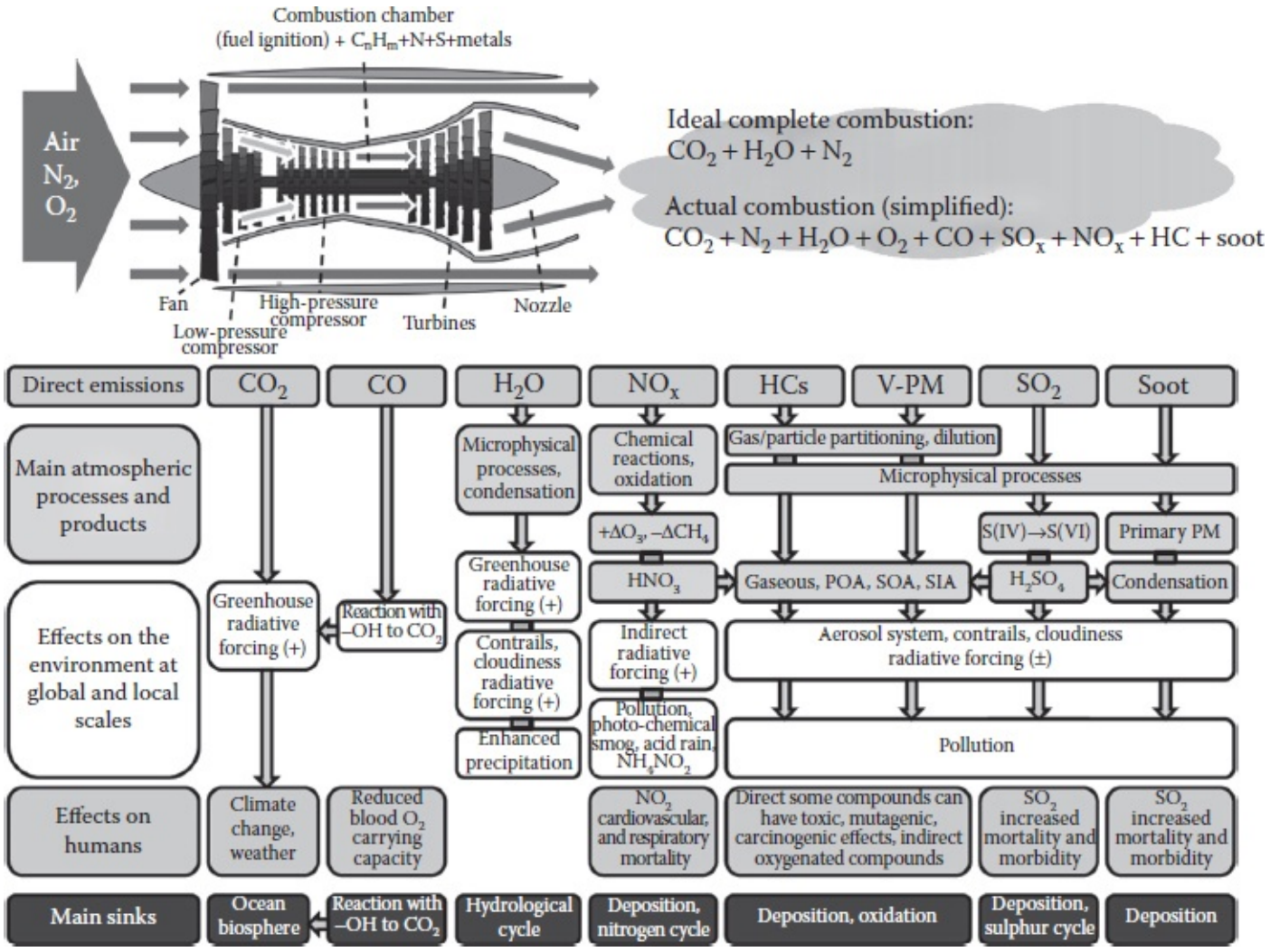

Figure 5.23 Simplified diagram of a turbofan engine (upper left); products of ideal and actual combustion in an aircraft engine (upper right); and related atmospheric

FOR REFERENCE PURPOSES ONLY

processes, products, environmental effects, human health effects and sinks of emitted compounds (bottom). (From Masiol, M., and Harrison, R. M., Atmos. Environ., 95, 409–455, 2014.)

Intergovernmental Panel on Climate Change (IPCC) reported that approximately 99.5%–99.9% of the molar content of typical commercial engine exhaust consists of N_2, O_2, CO_2 and H_2O.

Emissions of NO_x, CO, HC and soot, as with other fuel-burning devices, are strongly influenced by operational factors such as power setting and the inlet air-conditions. At low power, the engine is running cool, air–fuel mixing is least effective and CO/HC emissions highest. At full power, combustion temperatures are higher and the endothermic NO_x production greater. In principle there is scope for reducing emissions by varying fuel composition. For example, a fuel with higher H:C ratio will produce less CO_2. In practice, aviation kerosene is such a uniform composition around the world that there is little room for manoeuvre. Over recent decades, jet engine technology development has involved a trade-off between fuel efficiency and production of NO_x. Increases in fuel efficiency tend to result in higher temperatures and pressures at the combustor inlet, thus increasing NO_x formation. Therefore, the challenge is to reduce fuel-consumption whilst also guarding against a tendency for increased NO_x production. For example, combustor designs that keep NO_x emissions down through incorporating additional cooling.

Emission data for each engine type are available from the International Civil Aviation Organisation (ICAO) Engine Exhaust Emission Databank. European emissions have been computed in a standard format from:

$$\mathbf{TE}_p = \sum_r \sum_p \mathbf{SE}_{j,p,r} \times N_{j,r}$$

where

$$\mathbf{SE}_{j,p,r} = \int_{D_1(A)}^{D_2(A)} \mathbf{FC}_j(D_r) \times \mathbf{EI}_{j,p}(D_r) dD_r$$

TE_p is the total emission of pollutant p (kg per period)

$\mathrm{SE}_{j,p,r}$ is the specific emission of pollutant p from aircraft/engine combination j on route r (kg per aircraft)

$N_{j,r}$ is the number of aircraft of category j on route r during the period

$\mathrm{FC}_j(D_r)$ is the fuel consumption of aircraft in category j (kg km^{-1})

$\mathrm{EI}_{j,p}(D_r)$ is the emission index for pollutant p from category j (kg of pollutant per kg fuel)

D_r is the distance between airports on route r

$D_2(A) - D_1(A)$ is the distance flown within area A

Table 5.23 shows the total emissions of CO_2 and NO_x from aircraft (depending on the growth scenario) predicted by 2050.

5.5.2 Aerosol precursors

The exhaust plume of a jet aircraft contains around 10^{17} particles per kg of fuel burned, plus gaseous combustion products. These together constitute the precursors from which the particulate aerosol is constructed. Three distinct families of particle are formed: volatiles, non-volatiles (soot/metal) and ice/water (contrails). The volatile particles, which are only 1–10 nm in diameter, form initially from sulphuric acid, ions such as NO_3, and water vapour. Due to their small diameters they grow rapidly by coagulation and uptake of water vapour. Figure 5.24 shows particle size distributions in jet aircraft exhausts.

Table 5.23 Annual total fuel consumption and pollutant emissions in 2050

Approx traffic/10^9 RPK	*Fuel burned/Tg*	CO_2/Tg C	NO_x/Tg NO_2
20,000	800	800	11
40,000	2000	1700	14

FOR REFERENCE PURPOSES ONLY

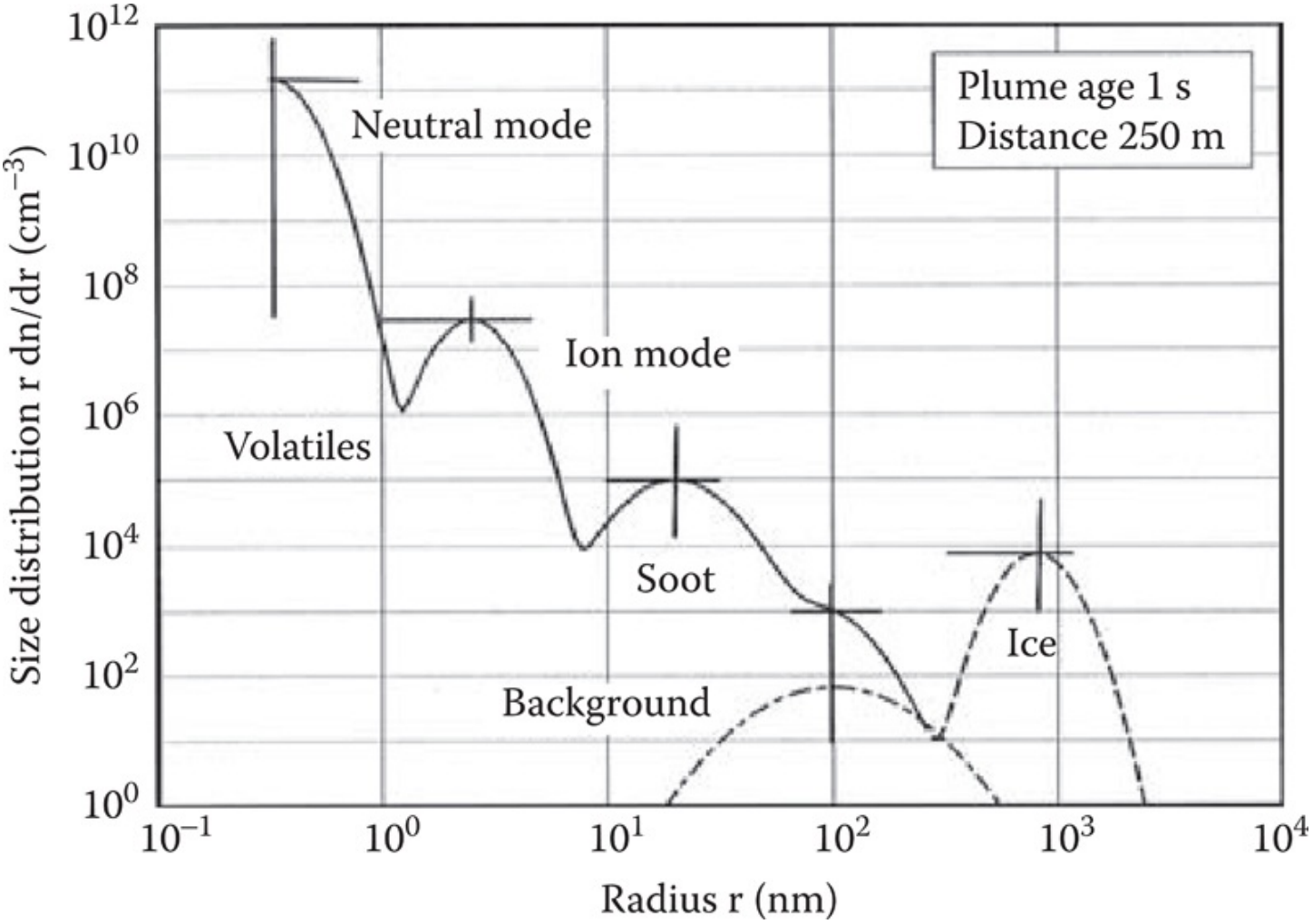

Figure 5.24 Particle size distributions in jet aircraft exhaust. (From Intergovernmental Panel on Climate Change, *Aviation and the Global Atmosphere*, Cambridge University Press, Cambridge, UK, 1999.)

The smallest diameters (neutral mode) are formed by homogeneous nucleation of hydrated sulphuric acid molecules, and the next larger mode (ion mode) by rapid scavenging of charged molecular clusters by chemi-ions. These particles are not constant once they have been formed, but interact with others from the three families by coagulation, freezing, condensation and evaporation. Although the total aerosol emission is small in comparison to ground-level sources, the effects may be disproportionate due to the high release altitude.

Soot includes all primary, carbon-containing particles generated from incomplete combustion in the engine. Soot formation in gas turbines is complex and not yet fully understood. A simplified scheme is believed to involve the formation of nucleation liquid droplets with high carbon: hydrogen ratios, which then undergo rapid surface growth to form small soot particles. Some of the latter are charged and grow by aggregation to form soot. Soot emissions are specified on a mass basis (typically 0.04 g/kg fuel), and measured as smoke number, but neither of these measures involves the size distribution, which is

critical for environmental impact. Recent measurements have shown that the size distribution is log-normal and peaks at 20–30 nm, with concentrations of order 10^6–10^7 cm^{-3}, representing 10^{14}–10^{15} particles per kg fuel burned. The particles are nearly spherical and have diameters of 20–60 nm. Although initially separate, they soon aggregate into chains.

The sulphur content of aviation fuel is typically 400 ppm (i.e. 0.4 g S/kg fuel). Most fuel sulphur is expected to be emitted as SO_2, with 2%–10% in the higher oxidised forms of H_2SO_4 and SO_3. The turbofan uses the hot exhaust gas flow to drive a fan which draws a *bypass* flow through the engine and contributes to the thrust. The bypass ratio has been raised to increase engine efficiency, and along with this trend the combustion temperatures and pressures have also been increased. These high-bypass, more fuel efficient engines reduce CO_2 and H_2O emissions (due to greater fuel efficiency), and also HC and CO emissions. However, NO_x emissions are increased, and there is an inevitable trade-off. One of the burning issues associated with aircraft emissions is the increased levels of ozone in the upper troposphere and lower stratosphere resulting from the atmospheric chemistry of emitted NO_x. More recent detailed investigations using Chemical Transport Model (CTM), including detailed tropospheric and stratospheric chemistry have estimated the short-lived radiative forcing (RF) from O_3 to range between 16.4 and 23.5 mW m^{-2}. Generally, NO_x contributes to production of O_3 in the troposphere and to destruction of O_3 in the stratosphere. Cruising at 2000 ft higher altitude increases the total RF due to aircraft NO_x emissions by 2 ± 1 mW m^{-2}, while cruising at 2000 ft lower altitude reduces RF by 2 ± 1 mW m^{-2}, which is mainly controlled by short-lived O_3 chemistry.

5.5.3 Contrails

If the thermodynamic conditions are right, some of the water vapour forms condensation trails (contrails) of liquid/ice condensate. The relative humidity is elevated in the plume anyway because of the high water vapour content of the exhaust gases. As the plume cools it mixes with the ambient air. If cooling predominates, the temperature falls below the local dewpoint and condensation occurs. If mixing predominates, the dewpoint falls faster than the temperature and no condensation occurs. The activation temperature for contrail formation from exhausts of current engines is about 220 K (–53°C). As engines are made more efficient, more of the fuel energy is used to propel the aircraft, and less to heat the exhaust gases. Hence the exhaust gas temperatures are closer to their dewpoint, and contrails are formed at higher ambient temperatures and over a larger range of altitudes. As efficiency has been increasing and specific fuel consumption decreasing, the critical altitude at which contrails will form in saturated air has decreased from around 8.5 to 7.7 km.

The ice particles nucleate on exhaust soot and volatile particles. These will usually evaporate rapidly (seconds to minutes) into air of low relative humidity; while they do so

FOR REFERENCE PURPOSES ONLY

they change the size and composition of the remaining liquid aerosol particles. If the relative humidity is above the ice saturation, the contrails can persist and grow by further deposition of ambient water vapour onto the crystals. Eventually the ice water content of the cirrus crystals is around 100 times the original exhaust water mass. In this sense the exhaust particles are *seeding* the process. The cirrus can then have a significant impact on atmospheric transparency, which affects visibility, amenity and global heat budget.

Contrails are not visible until the exhaust is about 50 m behind the aircraft. This takes around 250 ms, during which the ice crystals grow large enough to give the plume a visible opacity. Persistent contrails have similar properties to cirrus clouds, which are characterised by large ice crystals that have significant terminal velocities and fall out of the cloud to give it a feathery edged appearance. As aged contrails are indistinguishable from cirrus, it is hard to quantify their occurrence after they have lost their original linear structure. Correlations with fuel use have indicated that cirrus cover is increased by around 4% on average for the highest rates of fuel use above an altitude of 8 km. Although the modelled global mean cover is only 0.1%, the occurrence is naturally concentrated on the high density airline routes in and between North America and Europe (93% of aviation fuel is used in the northern hemisphere), where the local cirrus coverage can rise to 10%.

The increase in high-altitude cloud cover may contribute to the recorded decrease in diurnal surface temperature range that has been seen on all continents, although changes in other parameters such as aerosol loading and cloud height would also be implicated. High-flying aircraft can also disturb existing natural cirrus cloud, to which the exhaust adds additional freezing nuclei to enhance crystal production. Contrails in general cause both a negative shortwave flux change (due to reflection of solar radiation) and a positive longwave flux change (due to absorption of up going terrestrial radiation). The net change due to 100% cirrus cover is estimated to be +50 W m^{-2} at the top of the atmosphere.

For an estimated mean global linear-contrail cover of 0.1% of the Earth's surface and contrail optical depth of 0.3, radiative forcing is computed to be 0.02 W m^{-2}, with a maximum value of 0.7 W m^{-2} over parts of Europe and the US. This is similar in magnitude to other terms due to greenhouse gases and aerosol (see Chapter 11). The IPCC has calculated the likely changes in both the contrail cover and the resulting radiative forcing by 2050; the significant increases are shown in Figure 5.25.

FOR REFERENCE PURPOSES ONLY

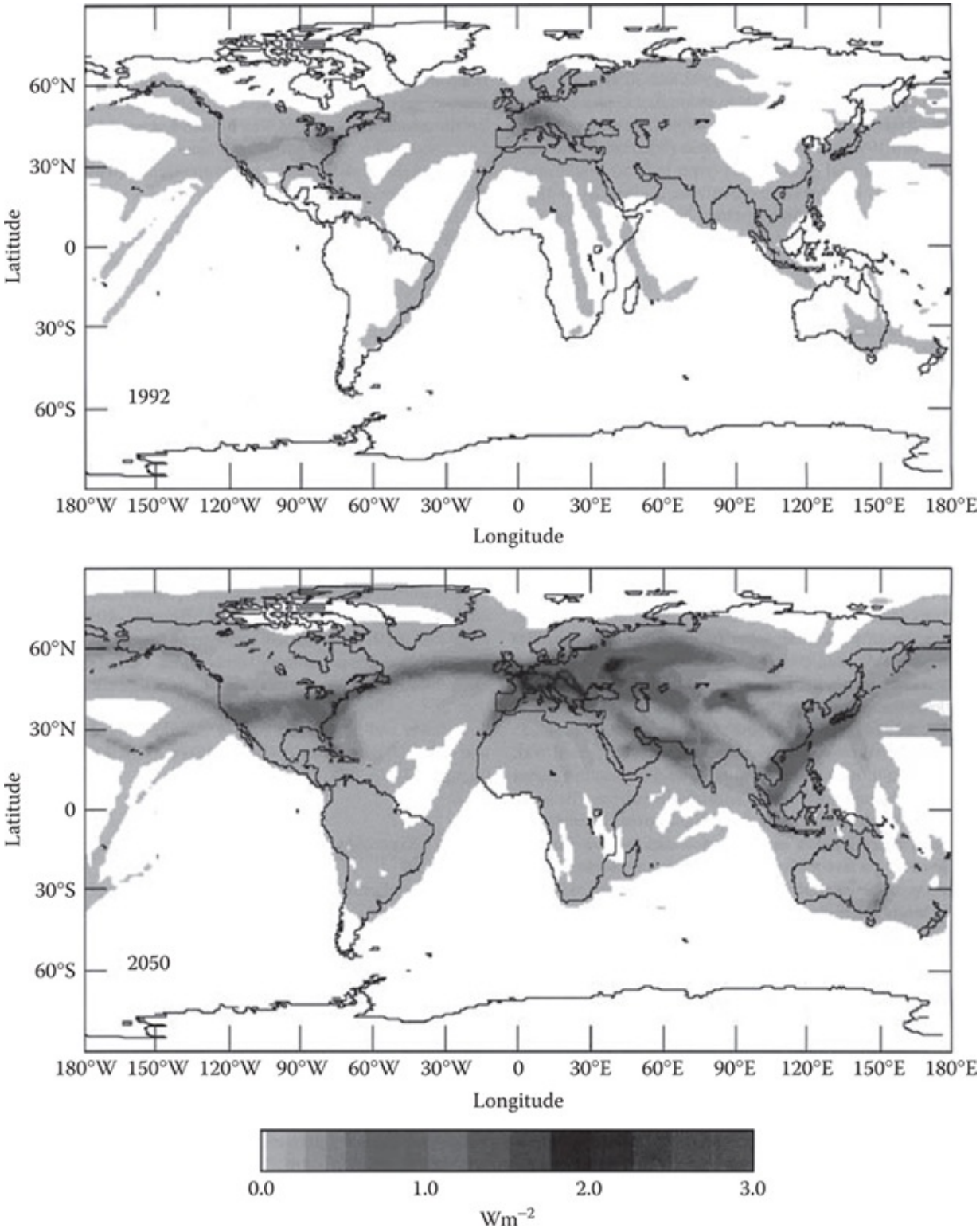

Figure 5.25 Predicted contrail radiative forcing in 1992 and 2050. (From Intergovernmental Panel on Climate Change, *Aviation and the Global Atmosphere*, Cambridge University Press, Cambridge, UK, 1999.)

5.5.4 Dispersion of aircraft emissions

The normal cruise heights of medium and long-haul aircraft are between just-below and just-above the tropopause, and the height of the latter changes with latitude and season. As the troposphere and stratosphere have very different mixing environments, predictions about plume dispersion vary from case to case. The majority of exhaust from aircraft is emitted at high altitudes (between 8 and 12 km). Aircraft cruise emissions have been found to impact surface air quality through the mean meridional streamlines due to the polar, Ferrel, and Hadley cells. After release from the engine, the jet aircraft exhaust wake passes through three distinct regions in which mixing affects the potential impact of the constituents on the atmosphere. In the jet and wake vortex regions, which take up to 10 s and 10–100 s, respectively, mixing is suppressed and only a small amount of ambient air is entrained. Hence high concentrations of emitted species react with small proportions of ambient air at rather elevated temperatures. When the wake vortex disintegrates, the plume region extends over a timescale between minutes and tens of hours and a distance scale up to thousands of km. Here, the plume mixes into the ambient air in a Gaussian manner. During this process it may grow to 50–100 km in width and 0.3–1.0 km in height, with an eventual dilution of 10^8. Throughout this dilution process, photochemical reactions and particle condensation and coagulation further change the pollutants that had been emitted initially. NO_x, sulphur oxides, soot and water all have the potential to affect the concentration of atmospheric ozone. The effects do not necessarily act in the same direction. For example, increases in NO_x in the upper troposphere and lower stratosphere are expected to increase ozone concentrations, whereas sulphur and water increases are expected to decrease ozone. Higher in the stratosphere, NO_x increases will *decrease* ozone. Thus far, however, there is no direct observational evidence that aircraft movements have affected ozone. Aircraft emissions are calculated to have increased NO_x at cruise altitudes by some 20%, although this change is substantially smaller than the observed natural variability. The effect is mainly a contribution to global warming; it is estimated that the small amount of NO_x emitted into the free troposphere by aircraft (only about 3% of total emissions) generates global warming equal to that of the surface emissions.

5.5.5 Future jet fuels

Interestingly, aviation traffic growth and jet fuel demand have been shown not to be strictly correlated, as the efficiencies of aircraft engines and air traffic management are improving and modern airliners are 75% quieter with consequent fuel consumption reduced by 70% with respect to the 1960s. The AERO2k global aviation emissions inventories reported a total of 176 Tg of kerosene used in 2002 for both civil (156 Tg) and military (19.5 Tg) aviation. The world jet fuel demand is projected to grow by 38% between 2008 and 2025 with some forecasts estimating aviation fuel demand for 2025 as 327 Tg y^{-1}. Other estimates of future global aviation emissions, based on four of the (Intergovernmental Panel on Climate Change/Special Report on Emissions Scenarios) marker scenarios varying

from 426 to 766 Tg for 2050. However, a reduced emission estimate of 325 Tg is predicted for 2050, if the ambitious technology targets of the Advisory Council for Aeronautical Research in Europe (ACARE, 2002) were to be achieved. Examples of the alternatives to conventional jet-fuel (mineral kerosene) that have been investigated include: liquefied hydrogen (LH2), methane, methanol, ethanol, biodiesel (methyl esters) from processing plant-oils and animal-fats, nuclear power, synthetic paraffinic kerosene (SPK, created either by the Fischere Tropsch (FeT) process from feedstocks such as biomass, natural gas, or coal; or hydroprocessing of plant-oils and animal-fats to hydroprocessed renewable jet (HRJ), also called bio-SPK or hydroprocessed esters and fatty acids (HEFA). Drop-in fuels are alternative fuels that meet existing jet-fuel specifications, and hence are interchangeable with mineral-kerosene. Up to 50% SPK blended with mineral-kerosene is being considered the easiest alternative fuel for aviation-use in the short and medium-term.

5.5.6 Airport emission standards

Aircraft movements are concentrated at airports, where the emissions are closest to the surface and most likely to be noticed and to have effects on people and the local environment. The ICAO has drawn up measurement procedures and compliance standards to control pollutant emissions from aircraft in the vicinity of airports. These cover soot (measured as smoke number), HC, CO and NO_x. The basis of measurement is the landing and take-off (LTO) cycle, which is illustrated in Figure 5.26. SN was defined as a ‘dimensionless term quantifying smoke emission level based upon the staining of a filter by the reference mass of exhaust gas sample and rated on a scale of 0–100”. However, SN gives only a qualitative estimate of particle emission and was recognised to be dependent on sampling conditions, soot characteristics and morphology, and therefore was assumed to have little value for estimating atmospheric impacts. Also, only particles with a diameter less than 300 nm pass through the filter and therefore only the larger particles are collected resulting in a relative weak accuracy of measurement using this technique.

Emissions are measured for appropriate power settings (approach 30%, taxing 7%, take-off 100% and climb-out 85%) then summed over the cycle, weighted by the time spent in each mode. Finally, the mass of pollutant released is normalised by dividing by the engine thrust in kN for comparison with the ICAO standards. As with motor vehicle emissions, the standards are being gradually tightened to improve emission performance. However, while aircraft exhaust comprise the majority of emissions, there are additional sources directly associated with aircraft operation which contribute to local air pollution, such as tyre, brake and asphalt ware as well as resuspension of particles due to the turbulence created by the aircraft movements.

FOR REFERENCE PURPOSES ONLY

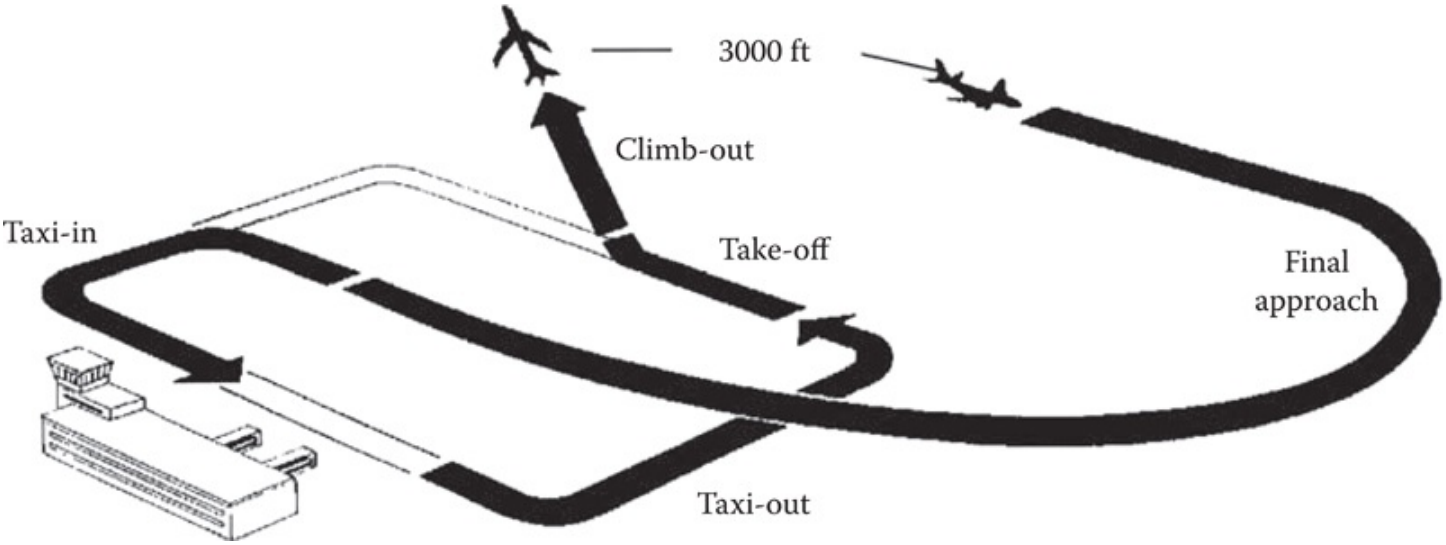

Figure 5.26 ICAO landing and take-off cycle. (From Intergovernmental Panel on Climate Change, *Aviation and the Global Atmosphere*, Cambridge University Press, Cambridge, UK, 1999.)

5.5.7 Carbon dioxide emissions from civil aviation

Emissions of CO_2 from aircraft engines are proportional to fuel used by a factor of approximately 3.15. With oil consumption in excess of 5 million barrels of oil per day, civil aviation is one of the key contributors of global CO_2 emissions, which approximates to 3160 ± 60 g kg^{-1} of fuel for complete combustion from modern aircraft engines. Improved fuel efficiency is a key method for reducing CO_2 emissions. Since 1960, aircraft fuel efficiency has improved by approximately 70%–80%, and some estimates suggest a further 40%–50% improvement is achievable by 2050. A global emission of 44 Tg CO_2 is produced by aircrafts below 1000 m, of which approximately 9.8 Tg are emitted annually within Europe.

5.6 GENERATING EMISSIONS INVENTORY FOR MOBILE SOURCES

Although concentration models are routinely *validated* by comparison to measured concentrations, this is normally undertaken for typical roadside and background concentrations without focus on specific emission sources. The amendment or introduction of emission sources needs to be verified against real-world measurements before being used in air quality and policy assessments. The following are some common approaches applied to modelling mobile emissions, specifically from mobile, line sources.

5.6.1 The Bentley approach

This approach uses simultaneous measurements of NO_x and CO_2 to better understand the contribution of NO_x from combustion sources. Specifically, if plumes of NO_x and CO_2 can be detected then it should be possible to quantify a NO_x/CO_2 ratio, which can then be related to fuel use. In particular a NO_x/CO_2 ratio can be compared directly with emission inventory estimates to determine their accuracy and also be used as the basis of correcting emission inventories.

5.6.2 The UK National Atmospheric Emissions Inventory

Hot exhaust emissions from road vehicles and the related fuel consumption estimates are calculated within the NAEI using fuel consumption and emission factors for each vehicle type. These emission factors are calculated on the basis of the composition of the vehicle fleet (age profile and fuel mix). Fuel consumption factors and emission factors combined with traffic data for six major classes of vehicles are used to estimate national fuel consumption and emissions estimates from passenger cars, light goods vehicles (LGVs), rigid and articulated HGVs, buses/coaches and mopeds/motorcycles. The vehicle classifications are further sub divided by fuel type (petrol or diesel) and the regulatory emission standard the vehicle or engine had to comply. The source of fuel consumption factors changed in the 2014 inventory and factors for all vehicle types are now derived from the fuel consumption-speed relationships given in the COPERT 4v11 source. COPERT 4 'Computer Programme to Calculate Emissions from Road Transport' is a model and database of vehicle emission factors developed on behalf of the European Environment Agency and is used widely by other member states to calculate emissions from road transport.

The UK total diesel rail emissions are compiled for three journey types: freight, intercity and regional. The rail mapping methodology was updated for the 2011 emission maps. The emissions were spatially disaggregated using data from the Department for Transport's Rail Emissions Model (REM). Additional coal based rail emissions have been accounted for by extracting station, line and operating information from the latest version of the *UK Heritage Railways* resource.

The shipping emissions in the NAEI account for coastal shipping, naval shipping, and international marine. Typical emissions calculation from a vessel uses a bottom-up procedure based on detailed shipping movement data for different vessel types, fuels and journeys, including:

- Installed engine power
- Type of fuel consumed
- Vessel speed and the distance travelled (or the time spent travelling at sea)
- Time spent in port

- Installed emission abatement technologies

Aircraft emissions in the NAEI are estimated using the national total emissions from aircraft operating on the ground and in the air over the UK, up to an altitude of 1000 m (capturing mainly the take-off and landing emissions). Emissions estimates are calculated from the number of movements of aircraft by type at UK airports (data provided by the Civil Aviation Authority) and from estimates of fuel consumption for component phases of the take-off and landing cycle. In addition, at larger airports emissions from aircraft on the ground (e.g. whilst taxiing or on hold etc.) have been separated from emissions whilst in the air (e.g. climb and approach phases below 1000 m) as such activities tend to be more prevalent at larger airports, where greater movement by aircraft on the ground is often required.

5.7 CASE STUDY – TRAFFIC RESTRICTION SCHEMES

5.7.1 London congestion charging

The Congestion Charge Scheme (CCS) was introduced by Transport for London (TfL) in February 2003 to tackle the traffic problems in London, hoping to reduce the high traffic flow and increase the use of the city's public transport. The congestion zone covers zones 1 on the Transport for London tube map. The charge is imposed for driving a vehicle within the restricted congestion charging zone (CCZ) between 07:00 and 18:00, Monday to Friday, with the payment only required once a day, no matter how many times you drive in and out of the zones. There is no charge on weekends, public holidays, between Christmas Day and New Year's Day inclusive, or between 18:00 and 07:00 on weekdays.

Studies have compared modelled and measured air quality data from roadside and background monitoring stations to understand the periods before (2001–2002) and after (2003–2004), mainly on concentrations of NO_x, NO_2 and PM_{10} in the CCZ. Comparing model results within and outside the zone suggested that introducing the CCS and has measurably reduced traffic flows in central London. It has been associated with a net 0.8 μg m^{-3} decrease in the mean concentration of PM_{10} and a net 1.7-ppb decrease in the mean concentration of NO_x within the CCZ. In contrast, a net 0.3-ppb increase in the mean concentration of NO_2 was predicted within the zone; this was partly explained by an expected increase in primary NO_2 emissions due to the introduction of particle traps on diesel buses (one part of the improvements in public transport associated with the CCS) (Kelly et al., 2011). A plot of percentage change in NO_x and PM_{10} emissions, (on each road in central and inner London), due only to changes in average link speed produces a scatter of points with an increasing range at the lowest speed (approx. 15 km h^{-1}) (Figure 5.27).

FOR REFERENCE PURPOSES ONLY

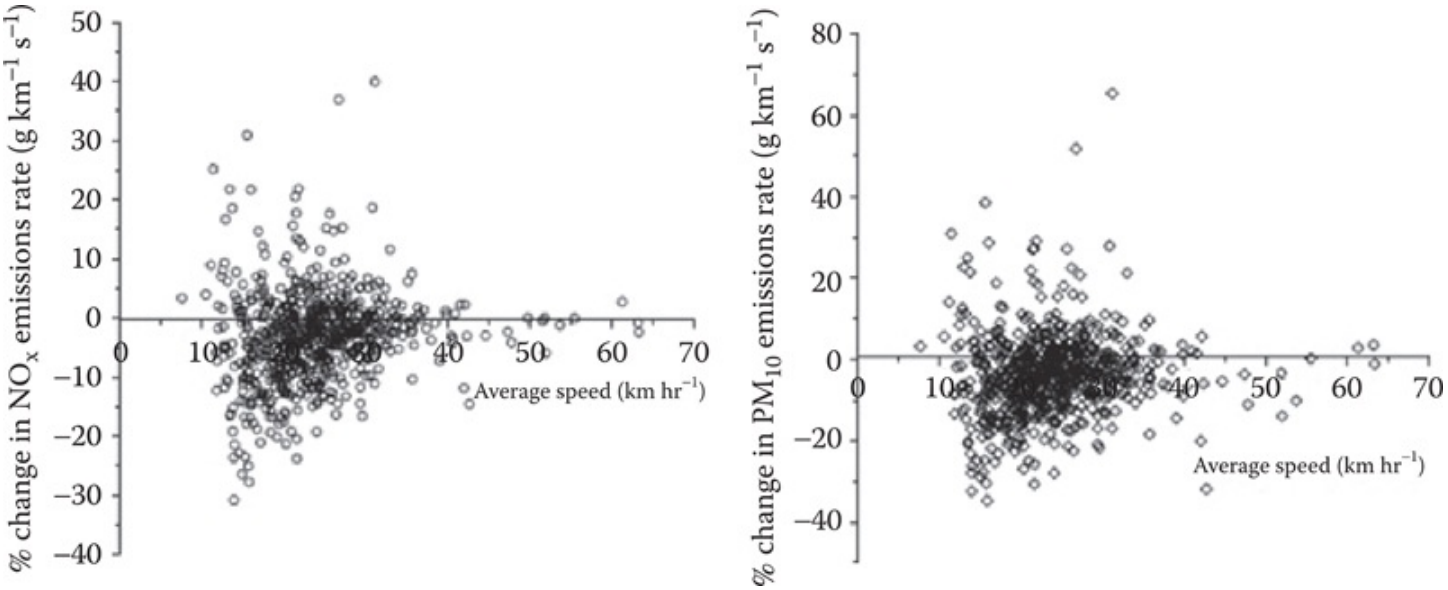

Figure 5.27 The percentage change in air pollution emissions (post CCS – pre CCS) due only to changes in average link speed. (Left panel – NO_x; Right panel – PM_{10}). (From Beevers, S. D. and Carslaw, D. C., *Atmos. Environ.*, 39, 1–5, 2005.)

In October 2017, London introduced a new additional T-Charge (toxicity) requiring drivers of older cars, vans, minibuses, buses, coaches and HGVs in central London needing to meet minimum exhaust emission standards, or else to face extra charges if they enter the Congestion Zone.

5.7.2 Odd-even driving patterns during the Beijing Olympics

On-road vehicular emission is one of the major anthropogenic sources of atmospheric particulate matters in several mega cities in China (e.g. Beijing, Chongqing, Shanghai, Guangzhou). In order to improve short-term air quality in Beijing during the 2008 Olympic Games to fulfil World Health Organisation Air Quality Guidelines, the following five particular control schemes were placed to reduce traffic-related air pollution: (1) issuance of new automobile emissions standards; (2) decommissioning of high emissions vehicles, buses and taxis; (3) recovery of fuel vapours at gas stations and from tankers; (4) banning of non-local heavy-duty diesel trucks within the Beijing Administrative area; and (5) control of emissions from small stationary diesel generators

Particularly, an odd-even day traffic restriction scheme (TRS) based on vehicle registration plates was enforced for 2 months from 20 July to 20 September 2008, to help ease congestion and improve air quality during the Olympics and Paralympics games. A study has compared the ambient concentrations of CO, PM_{10}, NO_2 and O_3 at a height of 1.5 m for the periods of *pre-TRS* (10–19 July 2008), *during TRS* (20 July–20 September 2008) and *post-TRS* (21–30 September 2008), respectively, based on traffic flows on the dense network of the 2nd, 3rd and 4th Ring Roads (RR) and Linkage Roads (LRs, including major

FOR REFERENCE PURPOSES ONLY

intercity expressways and intercity roads between RRs). With the reduction of traffic flows, the traffic conditions were improved and the traffic running speeds on hourly average increased by about 15% over the TRS period; with the reductions of traffic flows and emission factors (Figure 5.28), the emissions on daily average decreased by about 26.1%, 25.4% and 25.2% for CO, PM10 and NO_x, respectively (Figure 5.29) (Cai and Xie, 2011).

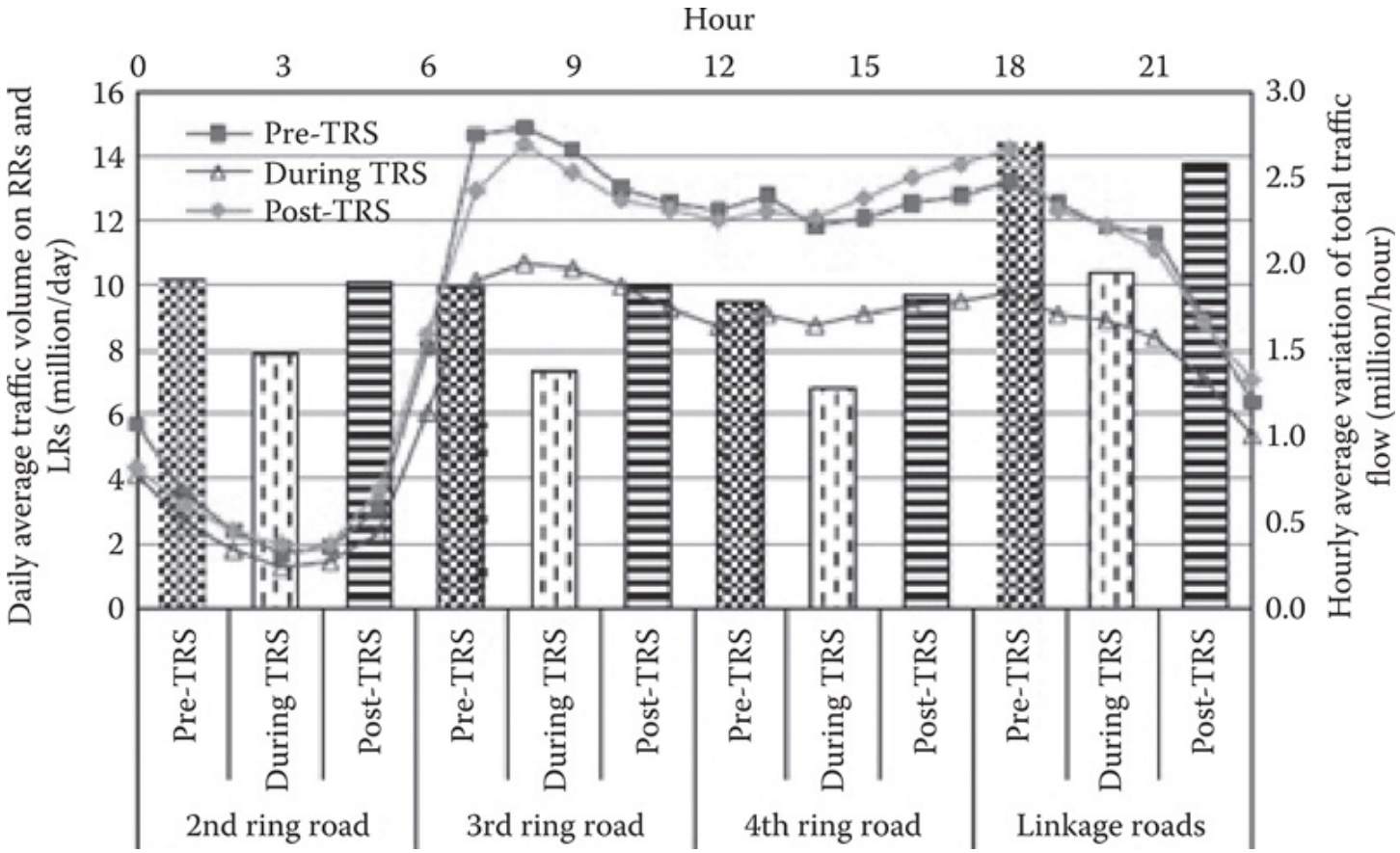

Figure 5.28 Comparison of traffic flows on 2nd RR, 3rd RR, 4th RR and the LRs on daily average (histograms), and diurnal variation of total traffic flow on hourly average (scatter plots) for the pre-TRS, during TRS and post-TRS periods, respectively. (From Cai, H. and Xie, S., *Sci. Total Environ.*, 409, 1935–1948, 2011.)

FOR REFERENCE PURPOSES ONLY

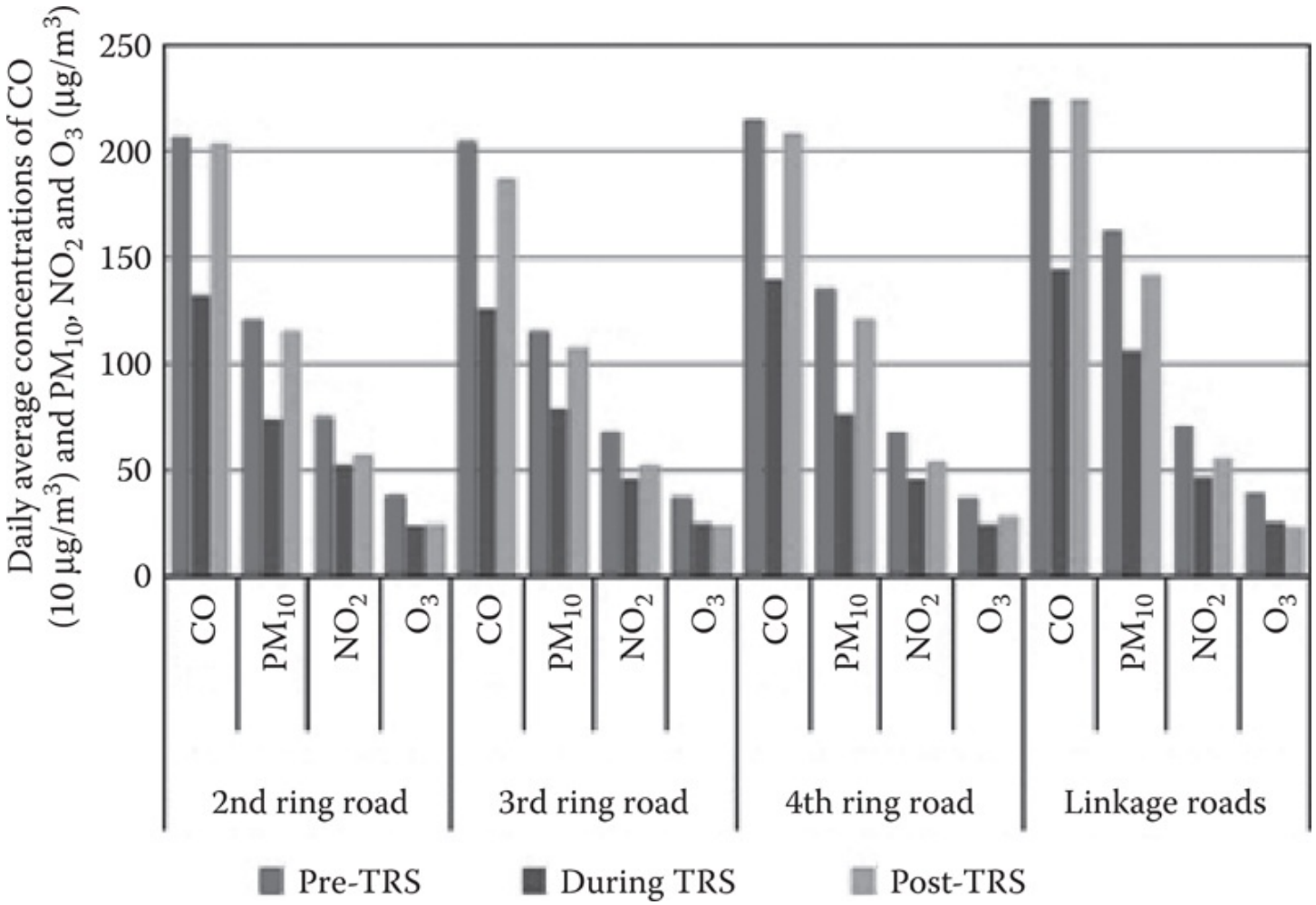

Figure 5.29 Comparison of daily average predicted concentrations of CO, PM_{10}, NO_2 and O_3 on different road types for the pre-TRS, during TRS and post-TRS periods. (From Cai, H. and Xie, S., *Sci. Total Environ.*, 409, 1935–1948, 2011.)

5.7.3 Odd-even car driving in New Delhi

In an attempt to reduce the number of vehicles using the roads of Delhi and the associated problem of air pollution, Delhi Administration implemented the *odd-even* car scheme from 1 January 2016 to 15 January 2016. The scheme restricted the use of privately owned petrol and diesel cars on alternate days based on the last digit of the car registration number (odd or even number). Several steps were taken by the Delhi Administration to make the intervention feasible. For example, schools were shut during this period to execute this intervention in full mode. Women drivers and cars under certain categories (similar to security vehicles or those carrying important persons) were exempt from the restrictions. While a number of studies are exploring the viability of this scheme in reduction in air pollution in Delhi area (mainly NO_x, PM_{10}) and its effect on winter-time visibility, this initiative saw significant reduction in traffic and consequently fewer traffic jams and a shorter driving duration. A study by The Energy and Resources Institute (TERI) reported a

FOR REFERENCE PURPOSES ONLY

15%–20% increase in the average car speed on national highway 24, resulting in better driving conditions, such as less exposure to the ambient air pollution, lower noise and more *stress free driving*.

Alongside the odd-even vehicle movements, the Delhi government is considering the following additional measures to control vehicle-related air pollution emissions, specifically in the peak winter months with adverse metrological conditions restricting the dispersion of the pollutants, thereby effecting visibility in Delhi area: (1) increasing the penalty on the burning of waste and use of furnaces in the open air; (2) controlling the movement of heavy-duty trucks in Delhi, and so on; (3) flexible and staggered work hours, flexible work place, enhanced carpooling using mobile apps, and so on; (4) enhanced use of metro and public buses, reserved seating in public transport at higher rates; (5) restriction of freight vehicles in Delhi; (6) alternatives to agriculture residue burning; (7) improved network of highways and road infrastructure; and (8) expediting the implementation of EURO VI.

REFERENCES AND FURTHER READING RESOURCES

ACARE (2002) *Strategic Research Agenda, Vol. 2. Advisory Council for Aeronautics*. Research in Europe. Brussels, Belgium.

Air Quality Consultants (2016) *Emissions of Nitrogen Oxides from Modern Diesel Vehicles*. London, UK.

Airborne Particles Expert Group (1999) *Source Apportionment of Airborne Particulate Matter in the United Kingdom*. Department of the Environment, London, UK.

Auto Oil II Programme (2000) *A Report of the Services of the European Commission*. Directorate General for Economic and Financial Affairs, Enterprise, Transport and Energy, Environment, Research and Taxation and Customs Union.

Beevers, S. D. and Carslaw, D. C. (2005) The impact of congestion charging on vehicle emissions in London. *Atmospheric Environment*, 39: 1–5.

Bukowiecki, N., Gehrig, R., Hill, M., Lienemann, B., Zwicky, C. N., Buchmann, B., Weingartner, E., and Baltensperger, U. (2007) Iron, manganese and copper emitted by cargo and passenger trains in Zürich (Switzerland): Size-segregated mass concentrations in ambient air. *Atmospheric Environment*, 41(4): 878–889.

Burchill, M. J., Gramotnev, D. K., Gramotnev, G., Davison, B. M., and Flegg, M. B. (2011) Monitoring and analysis of combustion aerosol emissions from fast moving diesel trains. *Science of the Total Environment*, 409(5): 985–993.

Cai, H. and Xie, S. (2011) Traffic-related air pollution modeling during the 2008 Beijing Olympic Games: The effects of an odd-even day traffic restriction scheme. *Science of the Total Environment*, 409: 1935–1948.

Carslaw, D. C., Beevers, S. D., Tate, J. E., Westmoreland, E. J., and Williams, M. L. (2011) Recent evidence concerning higher NOx emissions from passenger cars and light duty vehicles. *Atmospheric Environment*, 45(39): 7053–7063.

Carslaw, D. C. and Rhys-Tyler, G. (2013) New insights from comprehensive on-road measurements of NOx, NO2 and NH3 from vehicle emission remote sensing in London, UK. *Atmospheric Environment*, 81: 339–347.

DEFRA. *Emission Factor Toolkit* (v8.0 User Guide). UK Department of Environment Food & Rural Affairs, November 2017, London.

de Haan, P. and Keller, M. (2002) Emission factors for passenger cars: Application of instantaneous emission modelling. *Atmospheric Environment*, 34: 4629–4638.

Department for Environment, Food and Rural Affairs (2016) *Local Air Quality Management Technical Guidance (TG16)*. DEFRA, London, UK.

Department for Transport (2017) *Road Traffic (vehicle kilometres) by Vehicle Type and Road Class. Table TRA0204. Great Britain, annually to 2016*. Department for Transport, London.

Eastwood, P. (2000) *Critical Topics in Exhaust Gas after Treatment*. Research Studies Press, Baldock, UK.

FOR REFERENCE PURPOSES ONLY

Eastwood, P. (2008) *Particulate Emissions from Vehicles*. Wiley-Blackwell, Chichester, UK.

European Commission (2017) FAQ – type approval of vehicles: What is the conformity factor in the real driving emissions (RDE) test procedure? www.ec.europa.eu./growth/sectors/automotive/technical-harmonisation/faq-auto_en.

European Environment Agency (2016) *Explaining Road Transport Emissions*. doi:10/2800/71804.

Fenger, J. (1999) Urban air quality. *Atmospheric Environment*, 33: 4877–4900.

Freight Electric Vehicles in Urban Europe (FREVUE). www.frevue.eu.

Gehrig, R., Hill, M., Lienemann, P., Zwicky, C. N., Bukowiecki, N., Weingartner, E., Baltensperger, U., and Buchmann, B. (2007) Contribution of railway traffic to local PM10 concentrations in Switzerland. *Atmospheric Environment*, 41(5): 923–933.

Grote, M., Williams, I., Preston, J., and Kemp, S. (2016) Including congestion effects in urban road traffic CO_2 emissions modelling: Do Local Government Authorities have the right options? *Transportation Research Part D: Transport and Environment*, 43: 95–106.

Han, X. and Naeher, L. P. (2006) A review of traffic-related air pollution exposure assessment studies in the developing world. *Environment International*, 32: 106–120.

Heck, R. M., Farrauto, R. J., and Gulati, S. T. (2009) *Catalytic Air Pollution Control: Commercial Technology*, 3rd ed. Wiley-Blackwell, Hoboken, NJ.

Hobson, M. and Smith, A. (2001). *Rail Emission Model*. AEA Technology, Culham, UK.

Intergovernmental Panel on Climate Change (1999) *Aviation and the Global Atmosphere*. Cambridge University Press, Cambridge, UK.

Kim, D. (2007) *The Challenges of Consensus Building in a Consolidating Democracy: Diesel Vehicles and Urban Pollution in Korea*. VDM Verlag, Saarbrücken, Germany.

Kittelson, D. B. (1998) Engines and nanoparticles: A review. *Journal of Aerosol Science*, 29(5/6): 575–588.

Kelly, F. Anderson, H.R., Armstrong, B., Atkinson, R., Barratt, B., Beevers, S., Derwent, D., Green, D., Mudway, I., and Wilkinson, P. (2011) The impact of the congestion charging scheme on air quality in London. Part 1. Emissions modeling and analysis of air pollution measurements. *Research Report Health Effects Institute*, 155: 5–71.

Lee, D. S., Fahey, D. W., Forster, P. M., Newton, P. J., Wit, R. C. N., Lim, L. L., Owen, B., and Sausen, R. (2009) Aviation and global climate change in the 21st century. *Atmospheric Environment*, 43: 3520–3537.

Madireddy, M., De Coensel, B., Can, A., Degraeuwe, B., Beusen, B., De Vlieger, I., and Botteldooren, D. (2011) Assessment of the impact of speed limit reduction and traffic signal coordination on vehicle emissions using an integrated approach. *Transportation Research Part D: Transport and Environment*, 16(7): 504–508.

Masiol, M., and Harrison, R. M. (2014). Aircraft engine exhaust emissions and other airport-related contributions to ambient air pollution: A review. *Atmospheric Environment*, 95: 409–455.

Masters, G. M. (1998) *Environmental Engineering and Science*. Prentice Hall, Upper Saddle River, NJ.

McLaren, J. and Williams, I. D. (2015). The impact of communicating information about air pollution events on public health. *Science of the Total Environment*, 538: 478–491.

Samaras, Z. and Sorensen, S. C. (1998) Mobile sources. In: J. Fenger, O. Hertel, and F. Palmgren (Eds.), *Urban Air Pollution: European Aspects*. Kluwer Academic Publishers, Dordrecht, the Netherlands.

Schwela, D., Haq, G., Huizenga, C., Han, W., Fabian, H., and Ajero, M. (2006) *Urban Air Pollution in Asian Cities: Status, Challenges and Management*. Earthscan, London, UK.

Smit, R., Brown, A. L., and Chan, Y. C. (2008) Do air pollution emissions and fuel consumption models for roadways include the effects of congestion in the roadway traffic flow? *Environmental Modelling & Software*, 23(10–11): 1262–1270.

Tonne, C., Beevers, S., Armstrong, B., Kelly, F., and Wilkinson, P. (2008) Air pollution and mortality benefits of the London Congestion Charge: Spatial and socioeconomic inequalities. *Occupational and Environmental Medicine*, 65: 620–627.

Transport for London (TfL) (2014) Public and stakeholder consultation on a variation order to modify the Congestion Charging scheme: Impact assessment. https://consultations.tfl.gov.uk/roads/cc-changes-march-2014/user_uploads/cc-impact-assessment.pdf (Accessed 25 July 2017).

UNEP (2007) *Global Environment Outlook (The Fourth Assessment, GEO-4)*. Progress Press Company Limited, Valletta, Malta.

United Kingdom Quality of Urban Air Review Group (1993) *Urban Air Quality in the United Kingdom*. DoE/HMSO, London, UK.

FOR REFERENCE PURPOSES ONLY

United Nations Population Fund (UNFPA) (2007) *State of World Population 2007 – Unleashing the Potential of Urban Growth*. United Nations Population Fund, New York.

---

[1] One VKM is achieved when one vehicle travels 1 km.

FOR REFERENCE PURPOSES ONLY

Chapter 6

Ambient air quality

Air quality is an abstract term referring to the air pollution levels in the context of exposure to humans. However, a more generalised scope of air quality also includes the levels of air pollutant exposure to buildings, crops, vegetation, and so on. *Ambient* refers to a criterion (or standard) relating to the immediate outdoor (or indoor) surroundings. *Ambient air quality* varies greatly from place to place at any one time, and with the time of day and from year to year at any one place. This is the result of the rapid variations in the pollutant concentrations in response to these changes. Improving air quality undoubtedly is a difficult undertaking as both understanding the causes and the potential solutions to the problem are complex. Before we can understand where and when the concentrations of hazardous air pollutants rise to unacceptable levels, we need to have an extended period of data available from a network of pollution monitors having appropriate spatial distribution and response time. The UK Air Information Resource (UK-AIR) releases live air pollution data from continuous monitoring stations, reported on the National Air Quality website at www.airquality.co.uk. However, given the nature of diffused air pollutant contributions from varied sources, recent calls have emphasised adopting a twin approach where local air quality strategies and initiatives are combined with initiatives at a national level (Tiwary et al., 2014). This is further augmented by involving *citizen-based initiatives* in deploying diffused miniature sensors for enhanced online monitoring of air quality at human exposure scales.

In this chapter we will look at measurement networks in the UK and elsewhere that have given us our current understanding of the occurrence of air pollutants, and present some results that demonstrate key aspects of the prevalent conditions, both in the developed and the developing worlds. We will also look in some detail at the factors that determine both the short- and long-term airborne concentrations and the rates of dry and wet deposition of gaseous pollutants. We will relate much of the discussion of gases to sulphur and nitrogen oxides and to ozone, as they have been the subjects of the longest-established and most systematic measurement programmes. We will also highlight the difference between

FOR REFERENCE PURPOSES ONLY

regional-scale measurements of concentrations and deposition across a country at large, and local-scale measurements that are more appropriate to quantify urban air quality. The discussions on ambient air quality strategy and the corresponding standards and legislations are provided in Chapter 14.

For several hundred years, air pollution in towns was dominated by domestic emissions from wood and coal combustion, so that sulphur dioxide and smoke were the key issues. During the last 50 years these pollutants have declined, to be replaced by new ones such as PM_{10}, NO_2 and volatile organic compounds (VOCs), largely due to *people-related* activities. According to the United Nations World Urbanization Prospects report, world urban population will rise to over 66% by 2050. The largest urban growth will take place in India, China and Nigeria, accounting for over 37% of the projected growth of the world's urban population between 2014 and 2050. With rapid urbanisation and industrial activities, severe PM_{10} pollution has mainly become a daunting issue in megacities of the growing economies (Figure 6.1).

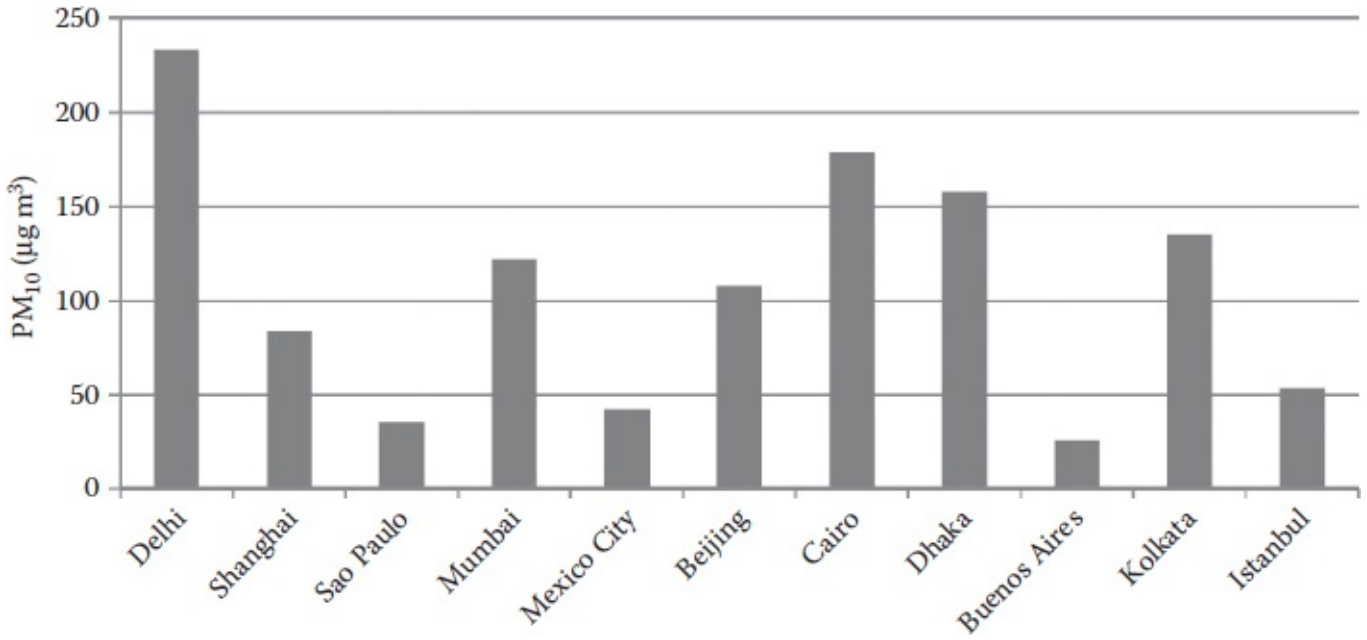

Figure 6.1 Trends in PM_{10} pollution in mega-cities of more than 14 million habitants for the last available year in the period 2011–2015. (From World Health Organization, *WHO's Urban Ambient Air Pollution Database – Update 2016, Version 0.2*, WHO, Geneva, Switzerland, 2016.)

Concerns have shifted away from acute health problems due to specific episodes and towards the more insidious threat posed by low levels of pollutants that may have a significant impact yet be hard to detect. For example, there has been a steady increase in the number of asthma cases reported in England and Wales. This increase is certainly one health impact that has become associated in the public's mind with motor vehicle pollution, and the two may well be related, yet there is no scientific proof of causality. For example,

according to an extensive 2-year survey conducted by the International Study of Asthma and Allergies in Childhood (ISSAC), the highest prevalence (>20%) of asthma is observed in Latin America and in the English-speaking countries of Australasia, Europe and North America as well as South Africa.

As a next step towards improving air quality, the European Commission adopted in 2013 a Clean Air Policy Package, including a Clean Air Programme for Europe setting objectives for 2020 and 2030, and accompanying legislative measures. The EU Clean Air Forum provides an occasion for decision makers and stakeholders to share knowledge and assist in the implementation of European, national and local air policies. The Forum focused on three areas: air quality in cities; agriculture and air quality; and clean air business opportunities (EC, 2017).

6.1 GASEOUS POLLUTANTS

The majority of pollutants emitted to air are gaseous, composed predominantly of nitrogen, sulphur or carbon sources. They have lifetimes in the atmosphere of days, and they return to the surface either as gases (dry deposition), as acidified rain (wet deposition) or as acidified cloud droplets (droplet deposition). All of these processes have different characteristics and different implications for different organisms. Many of the implications are not yet fully understood. As ozone is formed in the atmosphere from precursors rather than being emitted directly, its occurrence is quite different in character. The following sections describe these core constituents of ambient air quality in more detail.

6.1.1 Nitrogen oxides

In the 1990s, nitrogen oxides (NO_x) replaced smoke and sulphur dioxide as the prime indicator of poor urban air quality. Nitric oxide (NO) and nitrogen dioxide (NO_2), collectively referred to as NO_x, are generally the most important nitrogen compounds in urban locations, although N_2O_5, HNO_3 and HNO_2 may play significant roles in the formation of urban photochemical pollutants. Around 90% of the emissions from combustion sources are of NO rather than NO_2; however, as the NO can all potentially be converted to NO_2, it is usual to express all of the NO_x as NO_2 when making mass emission estimates. Long-term average concentrations of NO_2 in UK city centres are typically 30–50 ppb, with NO being similar to, or greater than, NO_2. Winter NO is around twice summer NO, but NO_2 does not vary much with the season. As exhaust-pipe concentrations of NO and NO_2 can both be several hundred ppm, we should expect peak kerb-side concentrations to be extremely high in comparison to background levels. In fact the record-high kerb-side concentrations of these gases in London are around 2000 ppb. Annual mean concentrations of NO are around 4.5 times those of NO_2, reflecting their higher concentrations in the exhaust gases. Concentrations should also be expected to fall off fairly rapidly with

distance from the road – measurements of NO_2 in London, for example, have shown 80–90 ppb at the centre of a road; 50–60 ppb on the kerb; 40–50 ppb at the back of the pavement, decreasing to background within about 20 m of the kerb. More details on NO_x emissions from mobile transport sources are provided in Chapter 5.

As mentioned in Chapter 14, the EU Air Quality Directive requires the short-term NO_2 threshold of 200 μg m^3, measured over 1 h, not to be exceeded for more than 18 h in a year (often assessed as the 99.78th percentile of 1-h means, that is, the 18 highest hours out of 8760 h in a year). Air quality managers and the wider public are now concerned with the issues surrounding increased NO_2 emissions from diesel road vehicles, but there is still some concern about the air quality impact from diesel generators. As of 2017, there have been no regulations on emissions from stationary diesel generators in the UK, also known as Short-Term Operation Reserve (STOR) facilities. While assessing the NO_2 emissions from STOR there are two elements to consider: (1) the impact on the long-term concentration, that is, the annual mean, and (2) the impact on short-term concentrations, for example, the 1-h NO_2 objective. Typically, operating a large diesel generator plant for a small number of hours can have significant adverse impacts on annual mean concentrations (amounting to several μg m^3) at nearby sensitive receptors, such as residential properties. This is noteworthy, given the Environmental Protection UK (EPUK) planning guidance considers a small impact to be associated with additional 0.2–0.6 μg m^3 of NO_x concentration.

As part of the UK Department of Environment, Food and Rural Affairs consultation on Medium Combustion Plant Directive (MCPD), the Environment Agency has conducted a dispersion modelling and air quality impact analysis for diesel generators (Table 6.1). It compared the NO_x emissions from a typical diesel plant with an output of $8MW_{elec}$ to a vehicle driving on a 30–50 km stretch of the M25 motorway (as per the assumptions shown in this table). The new EU MCPD was incorporated into UK law in December 2017, limiting the emissions from existing off-road diesel engines to 190 mg/nm^3 (normalised to 0°C, 101.325 kPa, 15% O_2, dry).

6.1.2 Sulphur dioxide

The diurnal and annual cycles of SO_2 used to be clear when ground-level concentration was dominated by low-level sources. Both coal burning and the likelihood of stable atmospheric conditions increased in the winter, and concentrations rose. However, with the decrease in importance of domestic emissions in Western nations, temporal cycles have become of less significance. In China, in contrast, 75% of the energy consumption, 93% of the SO_2 emissions and 62% of the particle emissions are from coal, and the majority of that is domestic. There is a strong annual cycle in the concentrations of these pollutants, and a strong diurnal cycle with peaks at 8:00 am and 8:00 pm associated with domestic cooking.

FOR REFERENCE PURPOSES ONLY

Table 6.1 Typical diesel generator NO_x emissions and equivalent lengths of the vehicular emissions from the M25 motorway around London

	Megawatt thermal input (MW_{th})				
	1.25	*2.5*	*5.5*	*16.25*	*20*
Megawatt electrical output (MW_e)	0.5	1	2.2	6.5	8
NO_x emission rate (g/s)	1.7–2.6	3.3–5.3	7.2–11.4	21.6–34.2	26.7–42.2
M25 equivalent emissions (km) [including 157,498 vehicles, with around 10% heavy duty vehicles (HDVs) travelling at 100 kmph]	2–3	3.8–6.1	8.3–13.1	24.9–39.4	30.8–48.6

Source: Environment Agency, UK.

Note: Heavy-duty vehicles = heavy goods vehicles (HGVs)+ coaches and buses.

The situation for urban SO_2 is quite different to that for NO_x. The sulphur content of petrol is low (150 ppm) and falling, though it is still rather higher for diesel; hence vehicle emissions are quite small. Domestic and commercial (non-industrial) emissions from coal and oil combustion have now been replaced by those from natural gas, which are essentially free of sulphur at the point of use. The consequence has been the steady decline in urban SO_2 concentrations described earlier. Even in towns that have never been heavily industrialised, such as Lincoln, the concentration in the centre has fallen since the early 1960s and by 1990, at around 10 ppb, was below that in the surrounding countryside.

6.1.3 Carbon monoxide

About 90% of the UK emission of CO is from road vehicles, having increased from 61% in 1970. The rural ambient background of less than 50 ppb may be increased to several 10 s of ppm in urban conditions in the short term, although annual mean urban concentrations are likely to be below 1 ppm. Maximum hourly mean concentrations during the London smog episode in December 1991 were 13–18 ppm, indicating that concentrations in urban areas can certainly come close to those having recognised health effects (World Health Organisation [WHO] guideline for CO is an 8-h average of 10 ppm).

6.1.4 Ozone

The instantaneous concentration of tropospheric ozone is influenced by five main factors:

- Photochemical production (which depends in turn on the supply of precursor materials and the availability of sunlight)
- Chemical destruction (largely by reaction with NO)
- Atmospheric transport (which may generate a net increase or reduction)

FOR REFERENCE PURPOSES ONLY

- Surface dry deposition to vegetation, water or other materials
- Folding down of stratospheric ozone

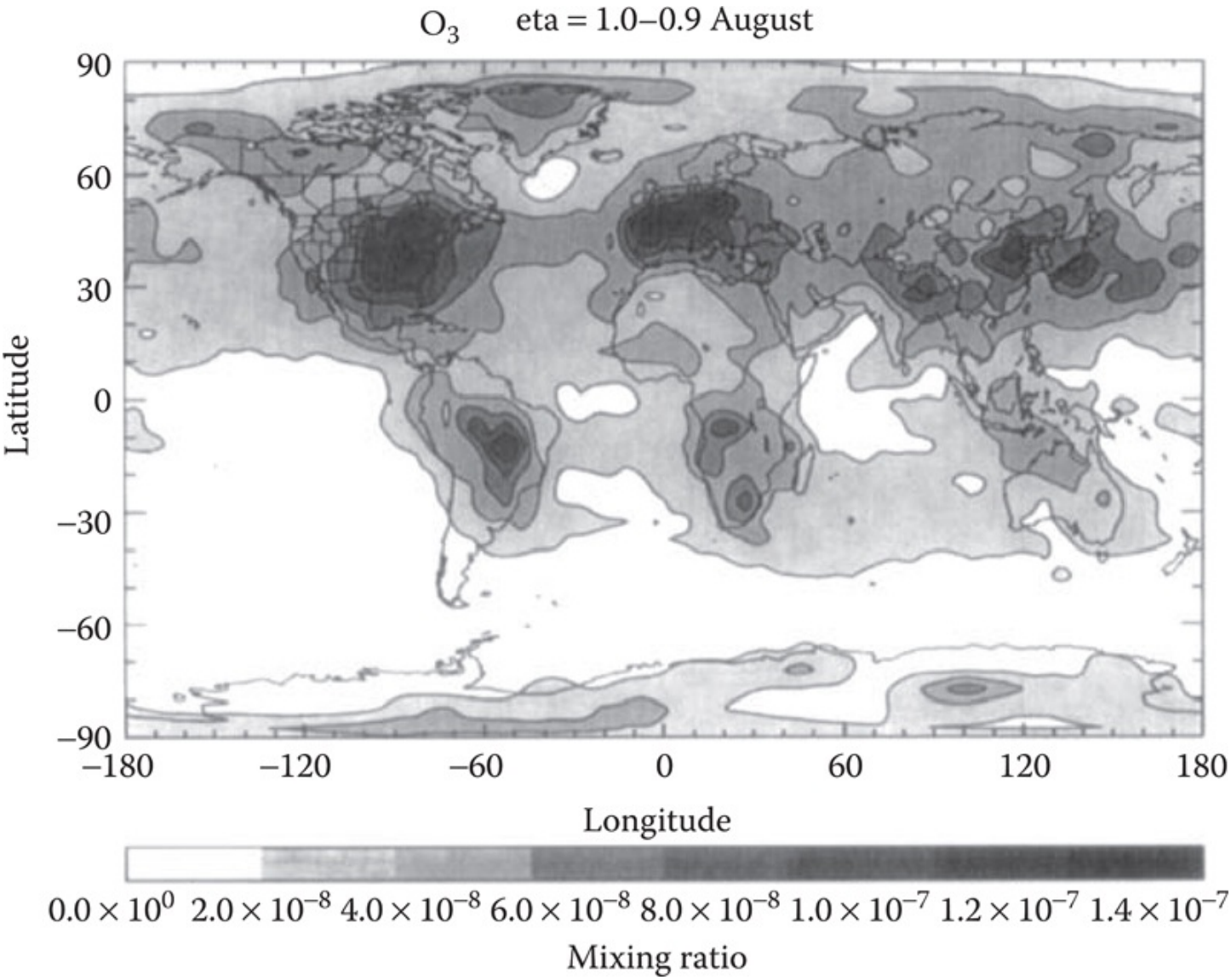

Figure 6.2 Modelled global ozone concentrations in August. (From Collins, W. J. et al., *J. Atmos. Chem.*, 26, 223–274, 1997.)

In Europe, the resulting average concentrations show a broad pattern of increase from north-west to south-east, although this masks substantial annual variability. In the summer months, there is a general gradient from lower concentrations in the north-west to higher in the south-east. This is effectively the outer limb of a pan-European gradient which generates the highest concentrations in Italy and Greece due to the combination of solar radiation and precursors. In the winter the relative situation is reversed, because without the solar radiation the NO emissions (which continue all year-round) remove the ozone most effectively over mainland Europe, leaving the concentrations higher in the north-west.

Globally, summer ozone peaks are created over five large areas of the world, as seen in

FOR REFERENCE PURPOSES ONLY

Figure 6.2. Fossil fuels and solvents are largely responsible for the northern hemisphere production over North America, Europe and Asia, biomass combustion in the southern hemisphere. These results were generated by the UK Meteorological Office model, which is a Lagrangian 3D model incorporating 50 chemical species and 90 reactions within 50,000 cells that represent the Earth's atmosphere up to the tropopause. Surface emissions are added at a spatial resolution of 5° × 5°, and stratospheric exchange is included. Some coarse approximations currently have to made in such models, either to reduce computing time or simply because our understanding of processes is incomplete.

Nevertheless, many useful results can be generated, and *what if* experiments enable the consequences of changes to be predicted. For example, when the model was run with European NO emissions reduced to half their current value, ozone concentrations fell by 17% at the most (Figure 6.3).

The same factors that influence the north-south ozone gradient also influence the diurnal variation. Typically, ground-level ozone concentration decreases at night, because there is no UV to photolyse NO_2, and the stable atmospheric temperature profile allows ozone to deposit to the surface without replenishment from the atmosphere earlier. In the morning, emissions from motor vehicles and other sources into the stable atmosphere increase concentrations of precursors; the increasing flux density of UV radiation produces more ozone, so that the concentration peaks in the middle of the afternoon. As the sun sets, concentration decreases once again. Figure 6.4 shows diurnal profiles taken in the same month of the same year at different sites in Europe. All the profiles show a night-time minimum and a peak at about 3 pm solar time, but there are differences between sites due to their local conditions. The French site (FR) has very low wind speeds and high solar radiation, so that concentrations go very low at night and high during the day. The Nottingham site (GBN) has higher wind speeds that keep the night-time concentration up, and lower average solar radiation that suppresses the afternoon peak.

FOR REFERENCE PURPOSES ONLY

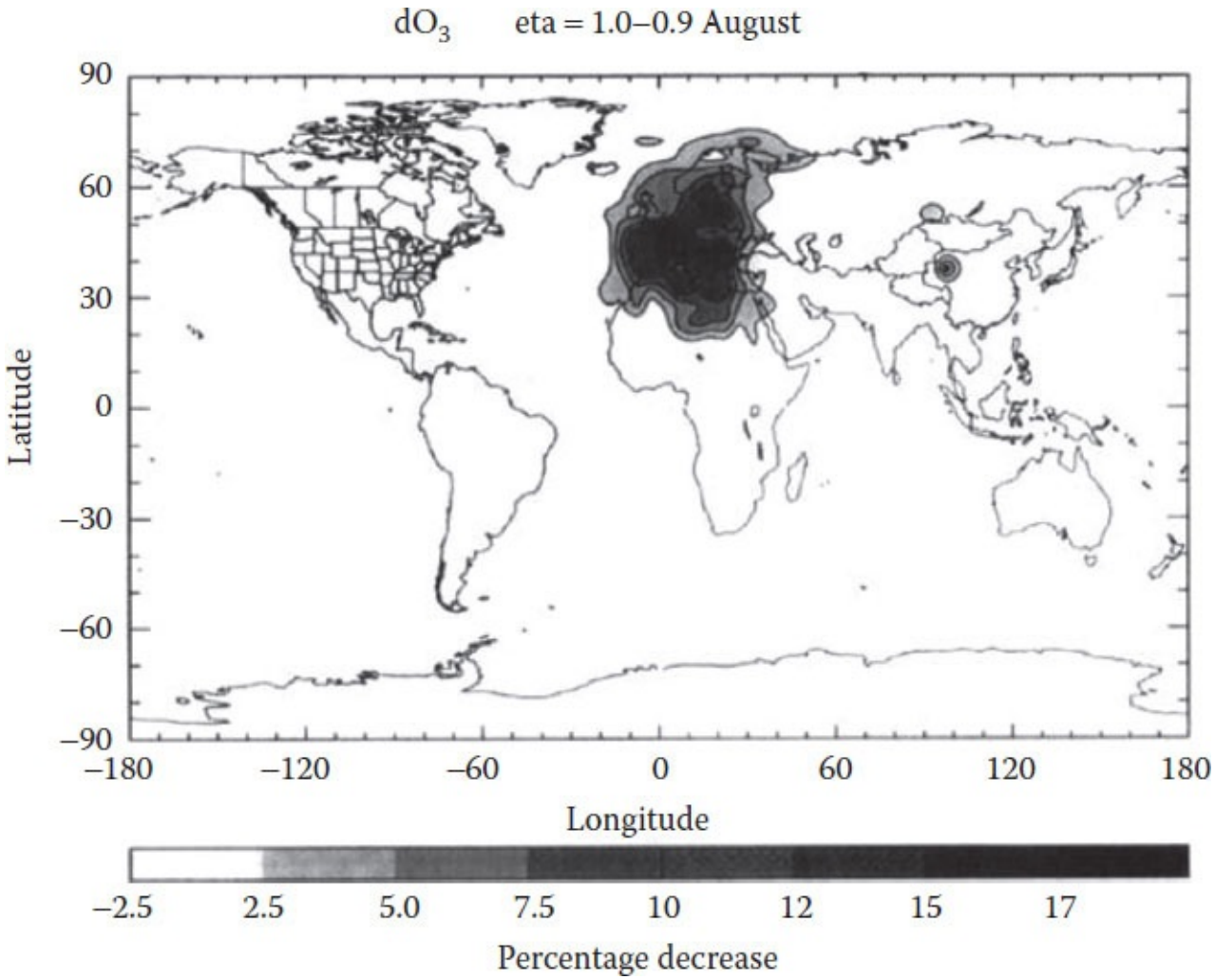

Figure 6.3 The response of global ozone concentrations to a 50% reduction in NO emissions from Europe. (From Collins, W. J. et al., *J. Atmos. Chem.*, 26, 223–274, 1997.)

FOR REFERENCE PURPOSES ONLY

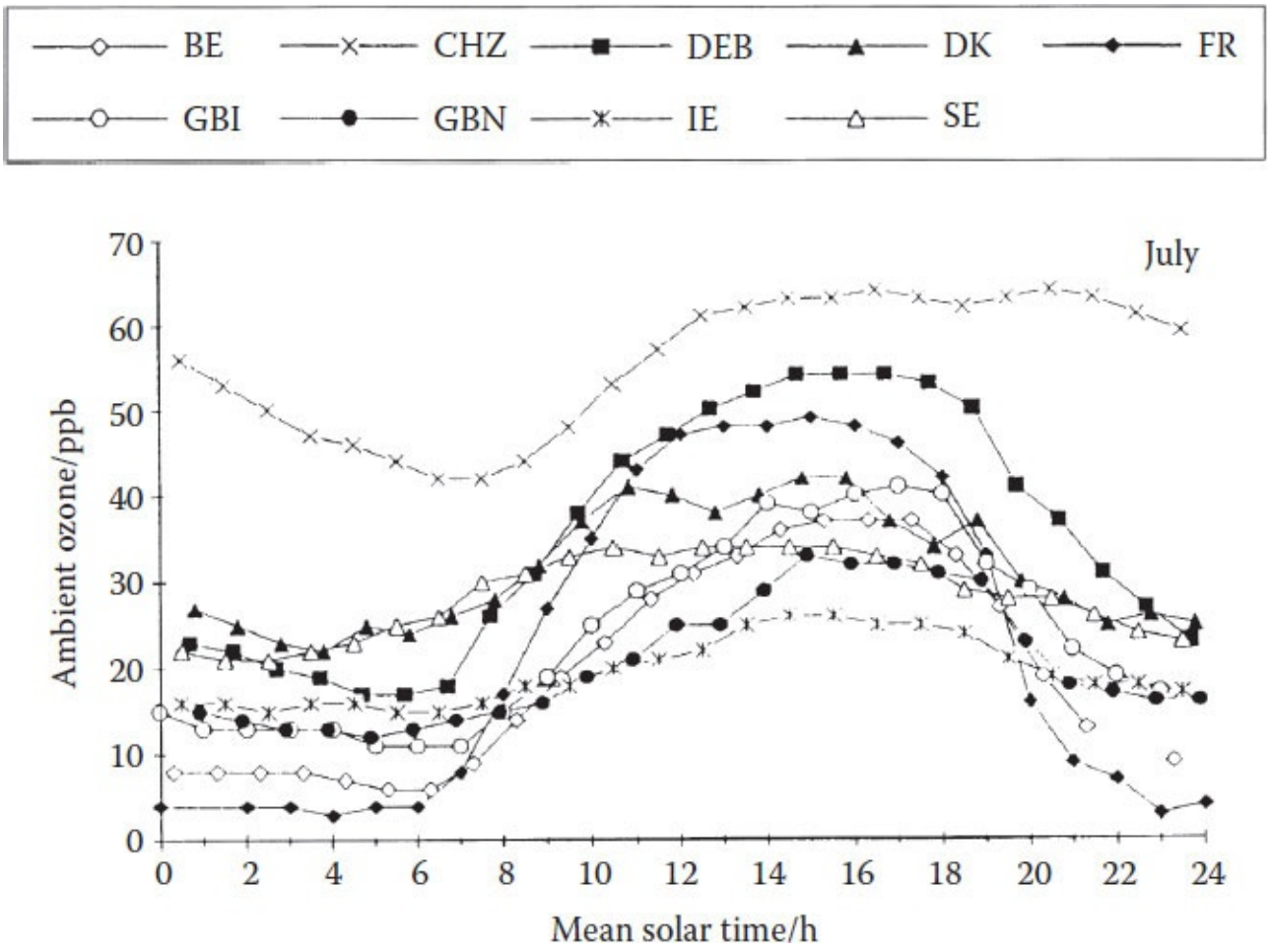

Figure 6.4 Diurnal ozone profiles from different sites in Europe. BE = Belgium, CHZ = Switzerland, DEB = Germany, DK = Denmark, FR = France, GBI = London, GBN = Nottingham, IE = Ireland, SE = Sweden.

There are also higher concentrations of NO in the English Midlands that sweep up the O_3. The Swiss profile (CHZ) is characteristic of a high-altitude (900 m) site, above the stable inversion so that night-time ozone deposition can be replaced from the upper troposphere and maintain the concentration. Although this can result in high 24-h average concentrations, it is not necessarily damaging to plants because their gas exchange is minimised at night. On an annual basis, tropospheric ozone production depends on the availability of precursors and solar UV, and on atmospheric conditions that suppress mixing. The optimum period tends to be April–June. During the remainder of the year, production is driven mainly by the level of UV flux. Occasionally, ozone from the stratospheric ozone layer can be injected into the troposphere by a weather system, resulting in a short-lived spike at any time of the year.

Studies of ozone episodes in middle Europe have shown that exceedances are characterised by certain meteorological situations, namely:

- Anticyclonic conditions

FOR REFERENCE PURPOSES ONLY

- A ridge of high pressure across middle Europe
- A wind direction that brought air from regions expected to have high concentrations of ozone precursors
- High daily maximum surface temperatures
- Low surface wind speeds

Although measures are in place in Europe and North America to reduce emissions of ozone precursors and hence reduce ozone concentrations, the same is not true in developing countries. Figure 6.5 shows diurnal average ozone concentrations during April or June from an analyser in Beijing, China. The peak concentration in the early afternoon has increased by a factor of 3, from 40 ppb in 1982 to 120 ppb in 1997. As will be discussed in Chapters 10 and 11 in this book, the latter concentration is high enough to damage both people and plants.

It has been quite a challenge to work out long-term trends of global average ozone concentrations because of the high variability of the concentrations at any one location. Concentrations at remote sites appeared to increase through the 1970s and 1980s, both on the surface and higher in the troposphere. Since 1990, concentrations at some of those background sites have levelled off.

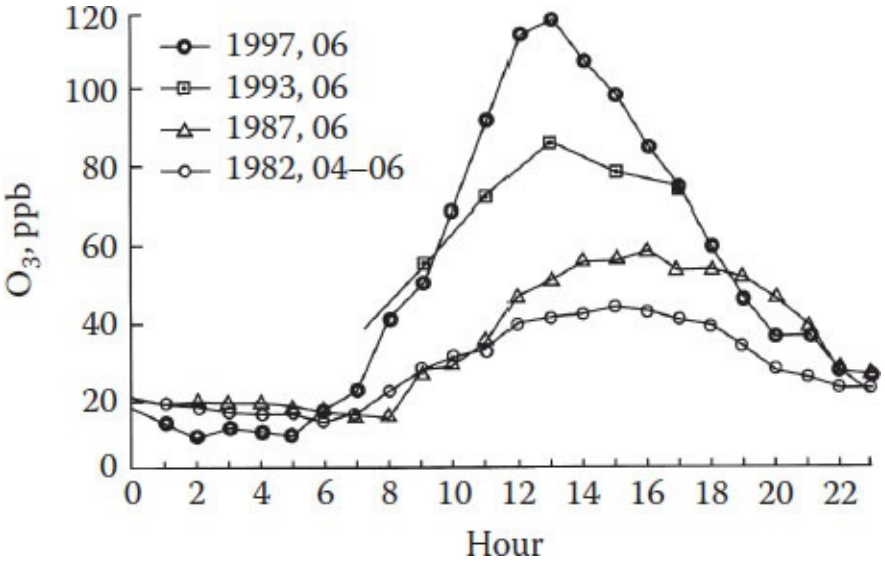

Figure 6.5 Spring ozone concentrations in Beijing, China. (Redrawn from Zhang, Y. et al., *Acta Sci. Natur. Univ. Pekinensis*, 34, 392–400, 1998.)

6.1.4.1 The general picture

In the decade 1990–2000, it has been estimated that at least $600 million were spent in Europe and North America to conduct over 30 major field studies on the precursor emissions, chemistry and meteorology of ozone. These studies have confirmed the general role of anthropogenic emissions in ozone formation, with biogenic emissions such as

isoprene also being important in some areas such as the south-eastern United States. Methane and CO may also be important, despite their lower reactivities, because of their widespread abundance in the troposphere. Meteorological processes drive the patterns of ozone occurrence, generating the substantial variations that are found on daily, seasonal and annual timescales. High concentrations of ozone are most likely to be observed during an episode of air stagnation lasting a few days, when there are high temperatures, low wind speeds, strong sunlight and an ample supply of either natural or anthropogenic precursors. Local recirculation due to temperature differentials caused by mountain–valley or water–land opposition may also be important. In contrast to short-lived pollutants such as SO_2, O_3 pollution is a regional-scale phenomenon, with areas of elevated concentration extending over many hundreds of km, and atmospheric transport moving ozone over similar scales. Most rural areas have been found to be VOC-rich, so that O_3 concentrations could be most effectively reduced by reducing NO_x emissions. Conversely, VOC reductions would be most effective in most urban areas.

6.1.5 Volatile organic compounds

As we have seen in Chapters 1 and 2, VOCs include a wide range of chemical compounds, largely associated with vehicles. Effects are covered elsewhere, and here we will look at particular features of the urban environment. Urban VOC levels can be expected to be high because of the concentration of traffic; although the VOCs may take part in photochemical ozone production in the downwind urban plume, their toxicity *per se* is what makes them important within the city limits. A comprehensive UK non-methane volatile organic compounds (NMVOCs) emission inventory has been published by the National Atmospheric Emissions Inventory (NAEI). It shows that some 40% of emissions from stationary sources are solvents (mainly alcohols, acetates, and chlorinated compounds), whereas, overall, transport emissions (mainly alkanes, alkenes, aromatics and aldehydes), contribute 33% of the total. These percentages will be higher in urban areas because of the absence of other sources such as vegetation.

Concentrations of VOCs in urban air have annual averages of a few ppb and show the expected diurnal variation due to human activity. VOCs are unlikely to represent a health hazard from their immediate toxicity, since the WHO guidelines, even allowing for large and arbitrary safety margins, are a few ppm. However, there is also the much more difficult aspect of carcinogenicity, particularly of aromatics, to consider. It is generally not possible to specify a safe concentration of a carcinogen, as any exposure, however small, increases the risk of cancer by a finite amount.

6.2 PARTICULATE MATTER

Black smoke from coal combustion was the first form of suspended particulate matter

FOR REFERENCE PURPOSES ONLY

recognised as being a hazard in the urban environment. As with SO_2, the combination of regulations such as those for smokeless zones, together with social/energy changes such as the move from open coal fires to gas-fired central heating, led to a steady decline in particle emissions and concentrations. Later measurements of black smoke from the much wider range of instruments in the National Survey confirmed the influence of the UK Clean Air Act (CAA) in reducing concentrations. As discussed in Chapter 1, the Great London Smog of 1952 led to the development of the 1956 CAA. However, the CAA was primarily designed for Local Authorities (LAs) to control emissions from domestic and commercial coal burning; it was never meant to control the new regime of air pollution arising from modern road vehicles. By the end of the twentieth century concentrations had come down to only a few percentage points of those at the start. As with gaseous pollutants, Britain was not alone in improving the atmospheric environment, and similar trends were apparent in other countries. Measurements from the UK Automated Network show that typical urban PM_{10} concentrations now lie in the range 10–50 μg m^{-3}, and cumulative frequency distributions show 1% exceedances of around 100 μg m^{-3}. Four issues remain of concern: (1) the long-term chronic effects on health of very low concentrations of very small particles (<2.5 μm in diameter), whatever their chemical composition; (2) the presence among these small particles of especially toxic materials such as heavy metals and polychlorinated biphenyls (PCBs); (3) the soiling properties of smoke particles on buildings and other surfaces and (4) the loss of amenity caused by light attenuation and reduction in visual range.

Determination of the chemical composition of particles, and of its variation with particle size, is a challenge. Many research programmes have concentrated on one aspect such as nitrogen or sulphate partitioning without any sizing. Many other programmes have concentrated on measuring size distributions, for example, with a cascade impactor, with little or no chemical analysis. Identification of the components of an aerosol requires use of several complementary techniques such as wet chemistry, atomic absorption, electron microscopy with energy dispersive X-ray analysis (EDXA), mass spectrometry. It is rarely possible to conduct an investigation with this full suite of analytical methods. For example, cascade impactor samples at low flow rates may not yield enough sample on each substrate to permit chemical analysis at all. Other effects may also interfere, such as the change in diameter of hygroscopic particles when the humidity changes.

FOR REFERENCE PURPOSES ONLY

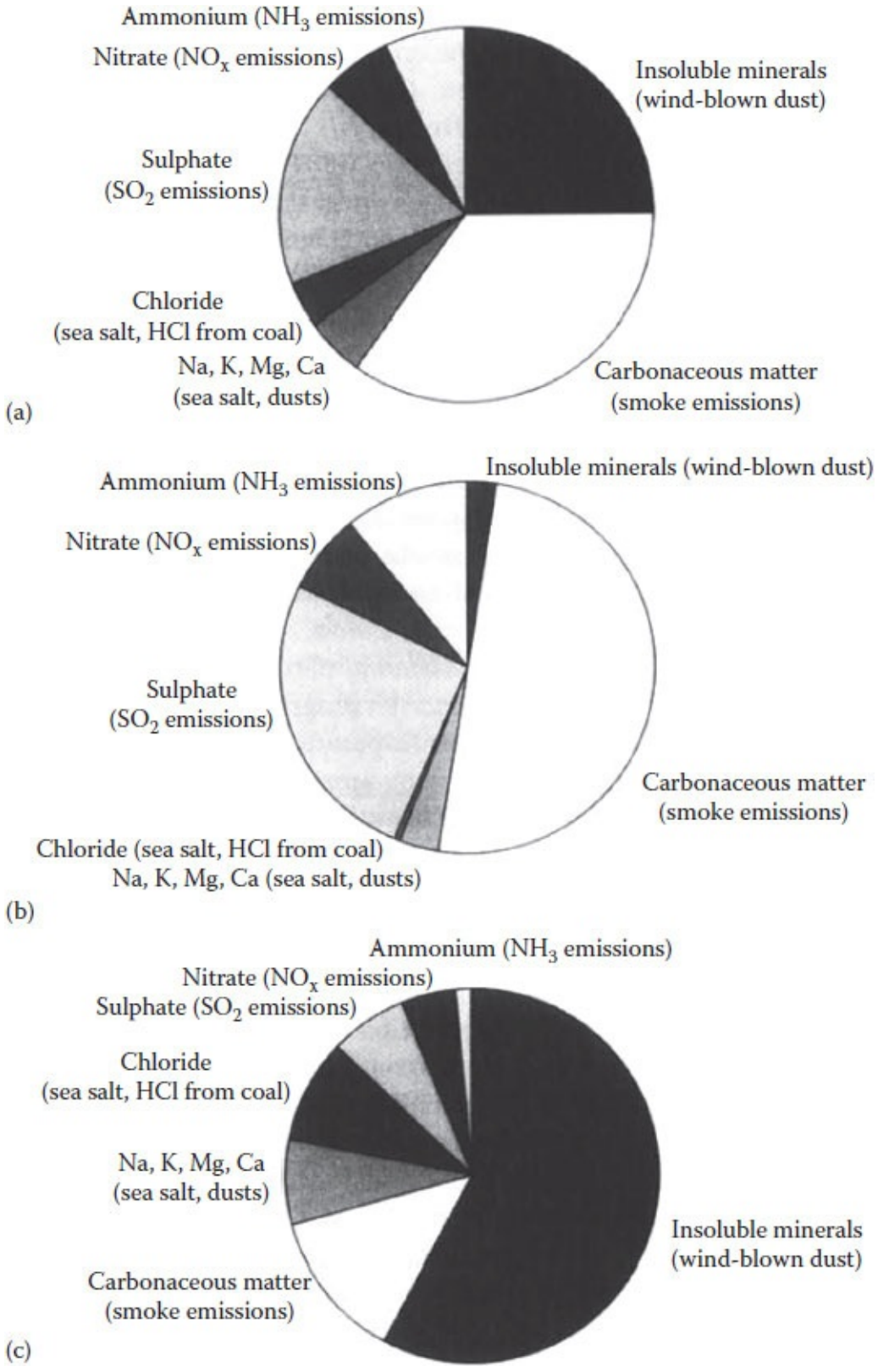

Figure 6.6 Particle chemical composition in different size fractions: (a) total, (b) fine fraction and (c) coarse fraction. (From United Kingdom Quality of Urban Air Review Group, *Urban Air Quality in the United Kingdom*, DoE/HMSO, London, UK, 1993.)

FOR REFERENCE PURPOSES ONLY

Many sources contribute to the particles found in urban air. A generic description of the chemical composition in different size fractions, formed by compounding the results from different sampling campaigns, is shown in Figure 6.6. The proportion (by mass) of the fine fraction is most heavily influenced by smoke emissions, whereas that of the coarse fraction is largely due to wind-blown dust and other insoluble minerals. The carbonaceous fraction is made up mainly of organic carbon, plus typically 20%–40% of particulate elemental carbon (PEC). PEC is effective at both scattering and absorbing light, being responsible for 25%–45% of visual range reduction, and at soiling surfaces.

Diesel engines are major and increasing sources of PEC; even in 1986 they were thought to be responsible for 91% of total PEC emissions in the UK, and diesel use has increased greatly since then. The preponderance of diesel is due to its high emission factor – 0.2% of diesel fuel burned is emitted as PEC, compared to 0.002% for petrol.

Anthropogenic particulate metals are derived from activities such as fossil fuel combustion (including vehicles), metal processing industries and waste incineration. They may occur as elemental metals, as inorganic oxides or chlorides, or as organic compounds. Reactivity, absorptivity and toxicity all vary from compound to compound, and there are no European Commission (EC) standards for metals other than lead. Both the emission and airborne concentrations of lead have fallen steadily since the mid-1980s due to the introduction of unleaded petrol. Unsystematic *ad hoc* measurements of the concentration of other heavy metals in UK suspended particulate over the last 10 years have indicated that WHO guideline values are not generally approached, let alone exceeded. The concentrations lie in the range 10–30 ng m^{-3} and do not present an environmental hazard.

Finally, we should expect correlations between gaseous and particulate pollution, since to some extent they derive from the same sources and activities. Figure 6.7 gives an example of such a relationship, between NO_x and $PM_{2.5}$.

FOR REFERENCE PURPOSES ONLY

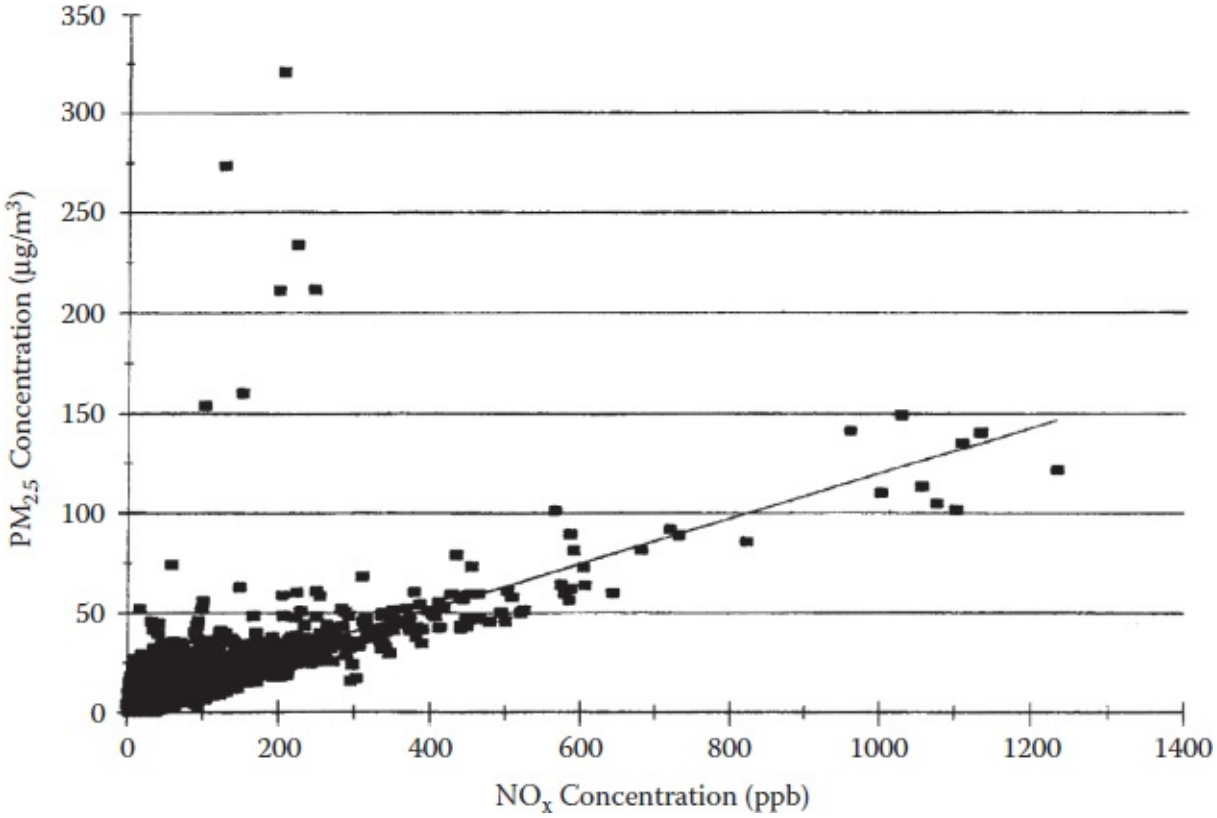

Figure 6.7 Co-occurrence of NO_x and $PM_{2.5}$. (From Williams, M. L., Patterns of air pollution in developed countries, in S. T. Holgate et al. (Eds.), *Air Pollution and Health*, Academic Press, London, UK, 1999.)

6.3 PATTERNS OF OCCURRENCE

6.3.1 Automatic air quality monitoring networks

Air pollution does not recognise boundaries, and transboundary sources (often considered as background) play an important role in local air pollution. Measurements of airborne concentrations are derived from one of several extensive networks of sampling and measurement stations that have been established to achieve various objectives:

- Assessing population exposure and health impact
- Identifying threats to natural ecosystems
- Determining compliance with national or international standards
- Informing or alerting the public
- Providing input to air quality management schemes
- Identifying and apportioning sources

Assessment of health effects is usually the first reason for air pollution monitoring. There are then choices that are related mainly to the budget available. A single advanced

FOR REFERENCE PURPOSES ONLY

monitoring station to measure the pollutants for which there are agreed health guidelines might cost £100,000. Although concentrations might vary widely across a city, there would not normally be such a monitoring station in a large town or small city, but there might be one in a city of a few hundred thousand population, and 2–4 in large metropolitans. These will be used as representative of the concentrations in that urban area. It may also be useful to divide the population into groups according to the amounts of time spent on different activities such as home, commuting and city work. There might be one group that lives and works in the suburbs, one that lives in the suburbs but commutes into the city, one that lives and works in the city. Then contributions could be calculated for each group provided that modelled or measured concentrations were available from each of the area types.

Another issue is exposure dynamics. The health impact of some pollutants, such as carcinogens, depends on the integrated lifetime exposure. For these pollutants, there is no safe lower limit, simply a reduction in the statistical probability of an adverse health outcome. Other pollutants, such as photochemical smog, have health effects that depend on the concentration and duration. The body can accommodate steady low levels but some people, especially those who are predisposed to react for any reason, may have acute responses if the concentration exceeds a threshold value. Concentration limits are usually written in terms that recognise this relationship, so that both short-term (1 h or 1 day) and long-term (1 year) targets have to be met. Also, the response may be acute or chronic. Cancer may take years to develop, continues to develop once the exposure has stopped, and is then irreversible without treatment, whereas carbon monoxide poisoning may have acute effects which reverse completely once the exposure stops.

6.3.1.1 The UK national survey

Following the severe smog events and loss of life in London in 1952, the National Survey of smoke and SO_2 concentrations was set up in 1961 to monitor progress following the implementation of pollution control measures. All the stations used identical standard equipment, known as an 8-port sampler, to take 24-h average samples of black smoke and SO_2. Smoke is captured on a filter paper and measured by the reflectance method described in Chapter 4. SO_2 is absorbed in hydrogen peroxide and the concentration calculated by acid titration. In the 8-port sampler, 8 pairs of smoke filter/wash bottle combinations are connected to a common pump and air volume flow recorder. An automatic timer switches the sample flow to a new pair at midnight, so that the system accumulates daily averages while being left unattended for a week. The National Survey started with 500 sites, grew to a peak of 1200 stations in 1966 and clearly revealed the marked decline in annual average urban smoke and sulphur dioxide (Figure 6.8). The pattern of concentration decline has not been only a British phenomenon. Figure 6.9 shows that SO_2 concentrations in five US cities increased steadily from 1880 to 1930, and after falling since 1950, by 1980 were lower than they had been 100 years previously.

FOR REFERENCE PURPOSES ONLY

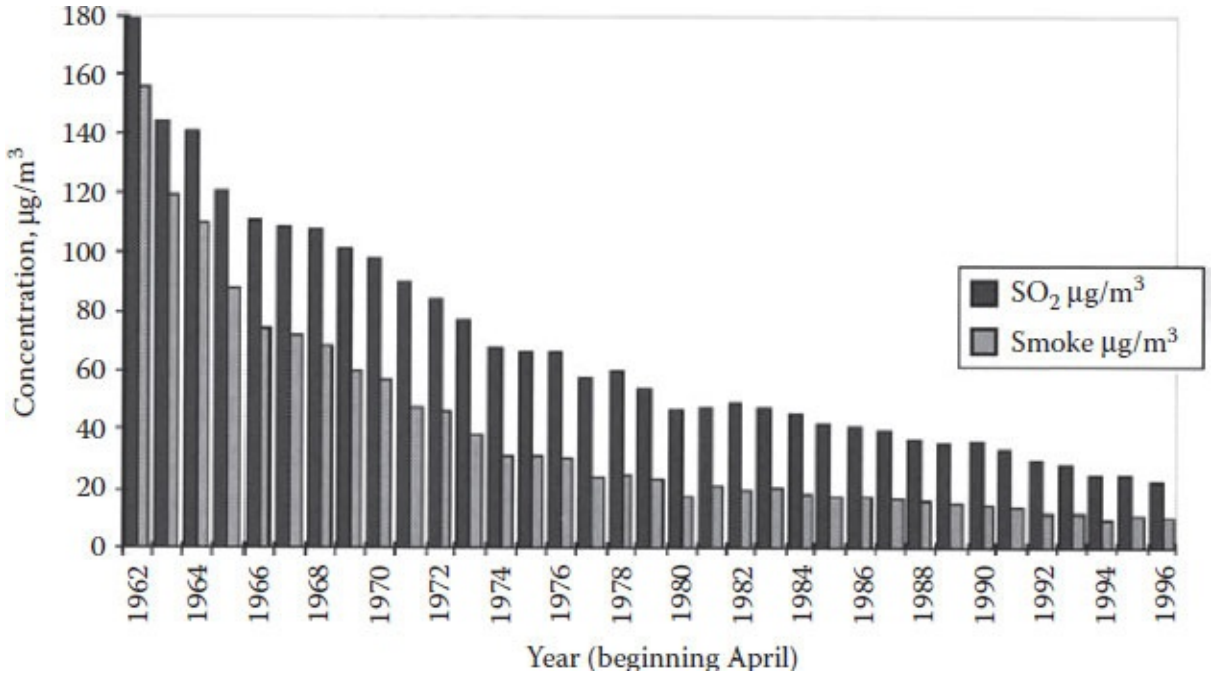

Figure 6.8 The decline in UK SO_2 and smoke concentrations between 1962 and 1996.

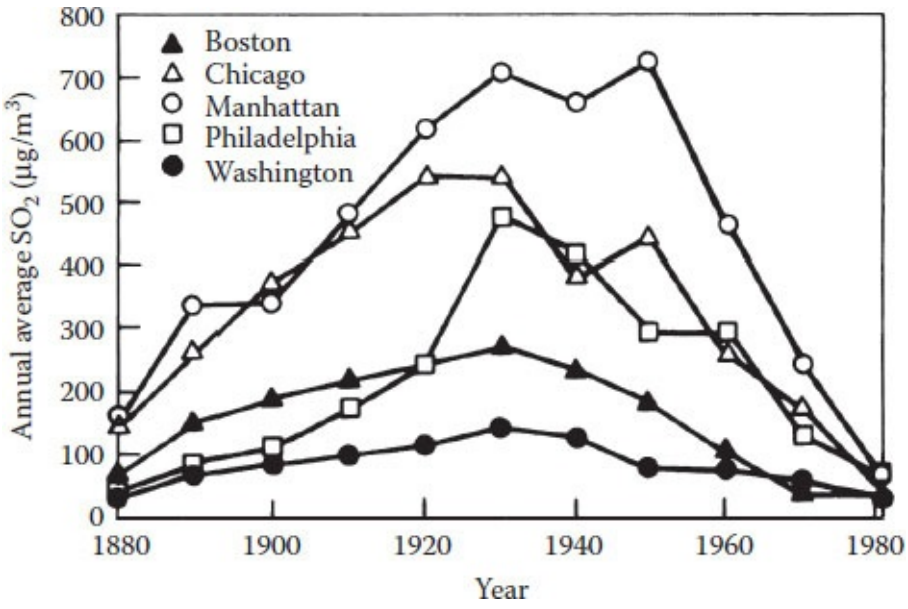

Figure 6.9 Historical rise and fall of SO_2 concentrations in five US cities, 1880–1980. (From NAPAP, *Integrated Assessment Report*, National Acid Precipitation Assessment Program, Washington, DC, 1990.)

In 1981 the National Survey was reorganised in response to these falling urban concentrations. The basic urban network (BUN) involved 154 sites selected to provide information on long-term changes across the whole of the UK.

The EC Directive Network involves sites in areas of relatively high concentration, monitoring compliance with EC Directive 80/779/EEC on smoke and SO_2. There were

initially 370 sites in the network, but a number were withdrawn as the concentrations declined. This network is by no means representative of the country as a whole, with pollutant information being confined to areas of high population density such as London and/or industrial activity such as the north-west of England. If the concentrations at an individual site do not exceed the directive limit values for three consecutive years, the site can be taken out of service, so the numbers of operational sites should continue to decline. There is some overlap between the basic urban and EC directive networks, giving a current total of about 225 sites.

6.3.1.2 Secondary networks

Although the National Survey had measured high urban concentrations successfully, some major defects became apparent in the 1980s:

- Urban smoke and SO_2 concentrations had declined to such low levels that the relatively crude methods of the National Survey no longer offered adequate sensitivity.
- The network had naturally been concentrated in urban areas so that there were relatively few rural measurements.
- There was no capability at all to measure ozone or its precursors, which had by that time been identified as major factors in poor air quality.
- There was no capability to measure the most toxic organic compounds, which were by then known to be carcinogenic at very low concentrations.
- Although the existing National Survey results were appropriate to show compliance with the Commission of the European Communities (CEC) directive on SO_2 and TSP, there was no corresponding capability for the directive on NO_2 (see Chapter 14).

To meet these needs, new networks of monitoring sites based on high-sensitivity continuous analysers were established by the UK Department of Energy (DoE) from the mid-1980s to measure O_3 and other pollutants in rural areas and a wider range of pollutants in urban areas. Air quality is monitored across the UK through a variety of automatic urban and rural network (AURN) sites. The government uses this information to comply with European Air Quality Directives as well as to monitor progress in the Air Quality Management Areas. As of 2017, there are 146 sites across the UK providing data from 1973 onwards. The following pollutants (at least) are measured at each site:

O_3 – by ultraviolet absorption
NO_x – by chemiluminescence
SO_2 – by pulsed fluorescence
CO – by infrared (IR) absorption
PM_{10} – by tapered element oscillating microbalance (TEOM)

FOR REFERENCE PURPOSES ONLY

The NO_2D network has been incorporated into the AURN, and hydrocarbons and toxic organic micro-pollutants (TOMPS) are measured continuously at a small number of sites. Hourly measurements of 27 species of hydrocarbons, including two known carcinogens – benzene and 1,3 butadiene – are taken by automatic gas chromatographs.

Between 1992 and 2003, NO_2 concentrations at most monitoring sites in the UK reduced significantly, but then, around 2003, levels plateaued.

6.3.1.3 Data processing

The information is collected, quality checked, ratified and provided to the public through DEFRA's National Air Quality Archive. For all the continuous data, average concentration values over periods of 15 and 60 min are compiled from instantaneous readings taken every 10 s, and telemetered to a central data processing station. The measurements from these networks are compared with a broad range of international criteria, including EU directives, WHO guidelines and United Nations Economic Commission for Europe (UNECE) critical levels. As the data are available almost in real time, it has been possible since 1990 to make daily summaries of the data available to the public on television information systems and by telephone. The full data set of hourly observations from all the stations is available on the web. The objectives of these networks have been summarised as follows:

- To provide a broad picture of the spatial and temporal distribution of photochemical pollutants throughout the country
- To aid the assessment of the impact of these pollutants on sensitive areas, particularly in relation to the exposure of crops and the natural environment
- To permit trend analysis as the data accumulate over a period of years
- To improve understanding of the sources, sinks and national-scale transport of these pollutants
- To allow validation and evaluation of the performance of computer-based models

6.3.1.4 Other surveys

These continuous sites have been supported by intermittent surveys of NO_2 taken with diffusion tubes. Although diffusion tubes have rather poor time resolution – typically 1 month – their low cost means that spatial variations of average concentration can be investigated. Figure 6.10, for example, shows the results of a NO_2 survey of Madrid.

Diffusion tubes were placed at the locations marked by crosses. Contour calculation and plotting software was then used to generate the spatial concentration distribution. These results could not have been obtained with a small number of continuous analysers at fixed sites, or with a mobile instrumented vehicle. National UK diffusion tube surveys in 1986 and 1991 showed that NO_2 concentrations were increasing in urban areas, primarily due to increased densities of motor vehicles. In response to this finding, an enlarged long-term

FOR REFERENCE PURPOSES ONLY

diffusion tube survey was started in 1993. Three hundred Local Authorities are now operating diffusion tubes at over 1200 sites. The tubes are placed at three different types of site by each local authority – one kerbside, two background and one in between.

Rural sulphur dioxide samples are taken at 38 sites in the UK. The sample is captured in a peroxide bubbler as with the urban surveys; the low rural concentrations and risk of interference from ammonia require sulphate analysis by ion chromatography in place of acid titration. The measurements of national SO_2 levels are subsequently input to a dry deposition model in order to calculate sulphur inputs to sensitive ecosystems.

Wet deposition of rain and snow is sampled at 32 sites in order to assess pollutant inputs by this route. The samples are analysed for conductivity, pH, five cations (NH_4^+, Na^+, K^+, $Ca^{2+}$and Mg^{2+}) and four anions (NO_3^-, Cl^-, SO_4^{2-} and PO_4^{3-}). The total deposition (whether it is raining or not) is measured at all the sites, and at five of the sites there are wet-only collectors that are covered when it is not actually raining.

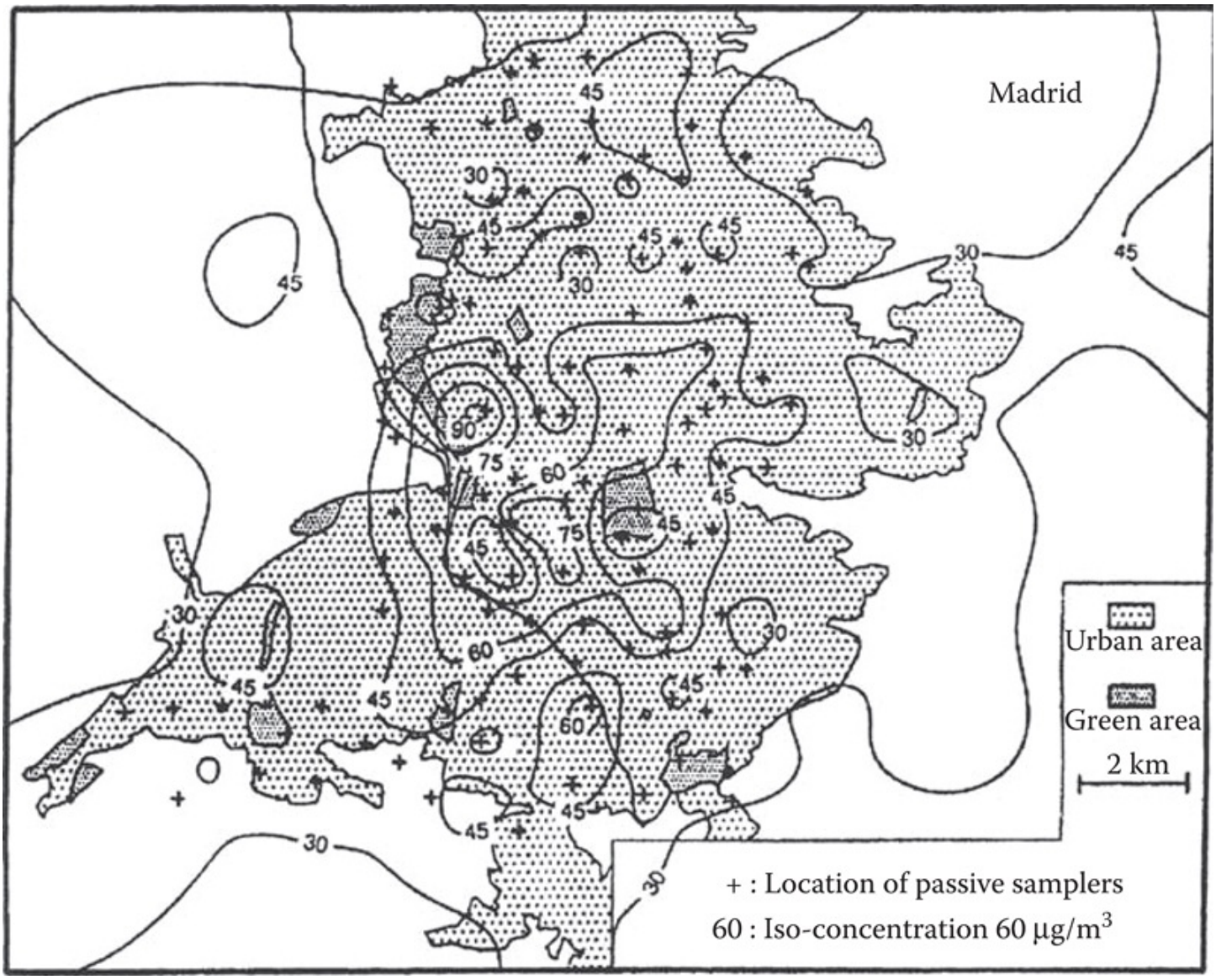

FOR REFERENCE PURPOSES ONLY

Figure 6.10 Results of a diffusion tube survey of NO_2 taken in Madrid. (From http://europa.eu.int/comm/environment/air.)

6.3.2 Other measurement networks

There are extensive air quality monitoring networks in all the developed nations. In the EU the Air Quality Monitoring and Information Network (EUROAIRNET) has been developed in close cooperation with the European Environment Agency (EEA). These monitors have generally been put in place during rather haphazard and uncoordinated monitoring campaigns by the constituent countries of the EU rather than by planned EU monitoring programme; hence they are by no means uniformly distributed. For example, Figure 6.11 shows the ozone monitors that were known to be operating in Europe in 1999.

The network has been analysed in terms of spatial representation and found to cover only 20%–40% of forests and 30%–50% of crops. Only 25% of EU city dwellers, and 12% of total EU residents, were within the area that was covered effectively by the monitors. EEA coordinates Europe-wide monitoring through its European Topic Centre on Air Emission (ETC/AE) and European Topic Centre on Air Quality (ETC/AQ). Both of these topic centres are part of the European Environmental Information and Observation network (EIONET), although this organisation has a much broader remit than air quality.

FOR REFERENCE PURPOSES ONLY

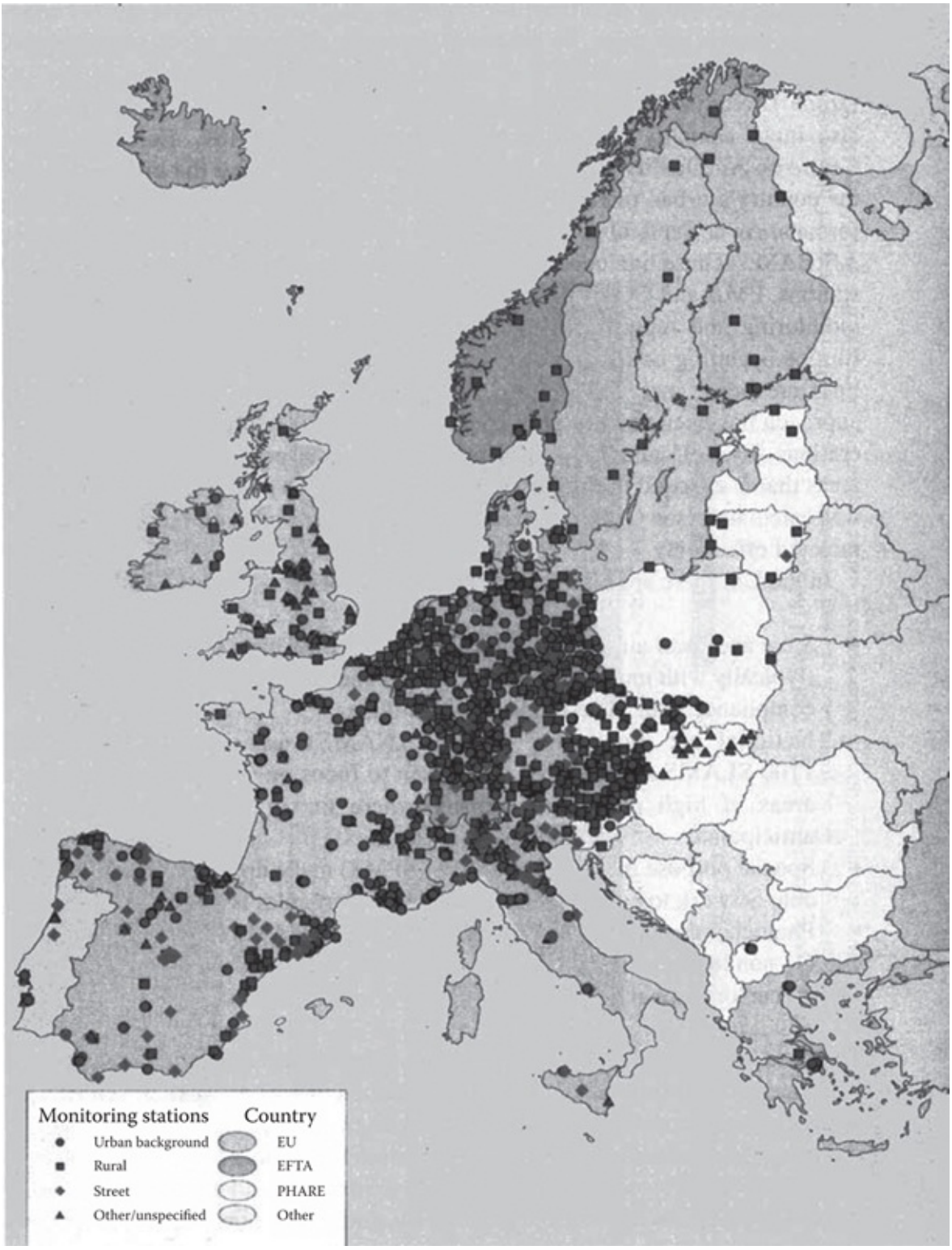

Figure 6.11 EU ozone analyser network. (From de Leeuw, F. et al., *Air Pollution by Ozone in Europe in 1998 and Summer 1999*, European Environment Agency, Copenhagen, UK, 2000.)

Data from selected stations of EUROAIRNET is also input annually to the air quality database, AIRBASE. One of the major purposes of all this monitoring and reporting of data is to work out whether air quality across Europe is getting better or worse, and whether the

FOR REFERENCE PURPOSES ONLY
air quality limits and guidelines are being met. For example, a rather broad-brush empirical modelling approach has been used to evaluate air quality in 200 European urban agglomerations for 1995 and 2010. The proportion of the population of these urban areas that is exposed to background concentrations in excess of the limit values was calculated (see Chapter 14). Hence, appropriate emission reductions can be targeted effectively. In the United States, there are four major network categories:

- State and local air monitoring stations (SLAMSs) number around 4000 (typically with multiple monitors at each one) which are designed to confirm compliance with state implementation plans.
- National air monitoring stations (NAMSs) are a subset of around 1100 SLAMS stations that are chosen to focus on urban and multi-source areas of high population density where maximum concentrations are anticipated.
- Special-purpose monitoring stations (SPMSs) make up a flexible and relocatable network to conduct special studies of particular issues.
- Photochemical assessment monitoring stations (PAMSs) are required in each O_3 non-attainment area that is designated serious, severe or extreme. O_3 precursors (about 60 VOCs and carbonyl) are measured.

There are hundreds more sites in North America within national air pollution surveillance (NAPS) in Canada, and metropolitan networks in Mexico. The stations at these sites generally measure O_3, NO, NO_x, CO, SO_2, TSP, PM_{10} and $PM_{2.5}$. The focus of these networks is to measure air quality in or near large urban centres. In addition, there are many other smaller networks set up to monitor air quality for more specific purposes – for example, in national parks. On the other hand, the picture for Asia is still quite grim with an estimate of less than 20% of its cities having some form of air quality monitoring. However, more recently, combined efforts from several countries in the Asia-Pacific, South and Central Asia region under the Clean Air Initiatives for Asian Cities (CAI-Asia) have resulted in some progress in development of integrated monitoring networks.

Even when spatial variations in concentration appear to be smooth, they may conceal large variations with time from hour to hour and day to day depending on wind direction and other variables. Nevertheless, when averages are taken over a sufficient number of individual days, patterns can often be seen. While assessing air quality in the UK, say, for a 2050 scenario, adequate consideration is needed for hemispheric, if not global, emissions (Tiwary et al., 2013). For example, increases in anthropogenic emissions from China and India have been shown to enhance urban air quality issues in the United States (Zhang et al., 2010). This is also evidenced by a recent Review of Transboundary Air Pollution (RoTAP, 2012), which found background ozone concentrations to have grown by about 15% despite decline in peak ground-level ozone concentrations by about 30% in the UK and continental Europe. This is primarily explained through increases in precursor emissions elsewhere in the northern hemisphere.

FOR REFERENCE PURPOSES ONLY

6.4 DRY DEPOSITION OF GASES

The main factor that determines deposition of a particular gas species to a surface is the concentration gradient between the atmosphere and the surface. Three processes contribute to the movement of gases down the gradient. First, turbulent diffusion brings the gas close to the surface (within a few mm); second, molecular diffusion takes the gas across the laminar boundary layer adjacent to the surface; third, the gas molecules must adhere to, dissolve in or react with the surface itself. If any of these three processes is absent or inhibited, then the surface concentration tends towards the atmospheric concentration, and both the gradient and the flux is reduced.

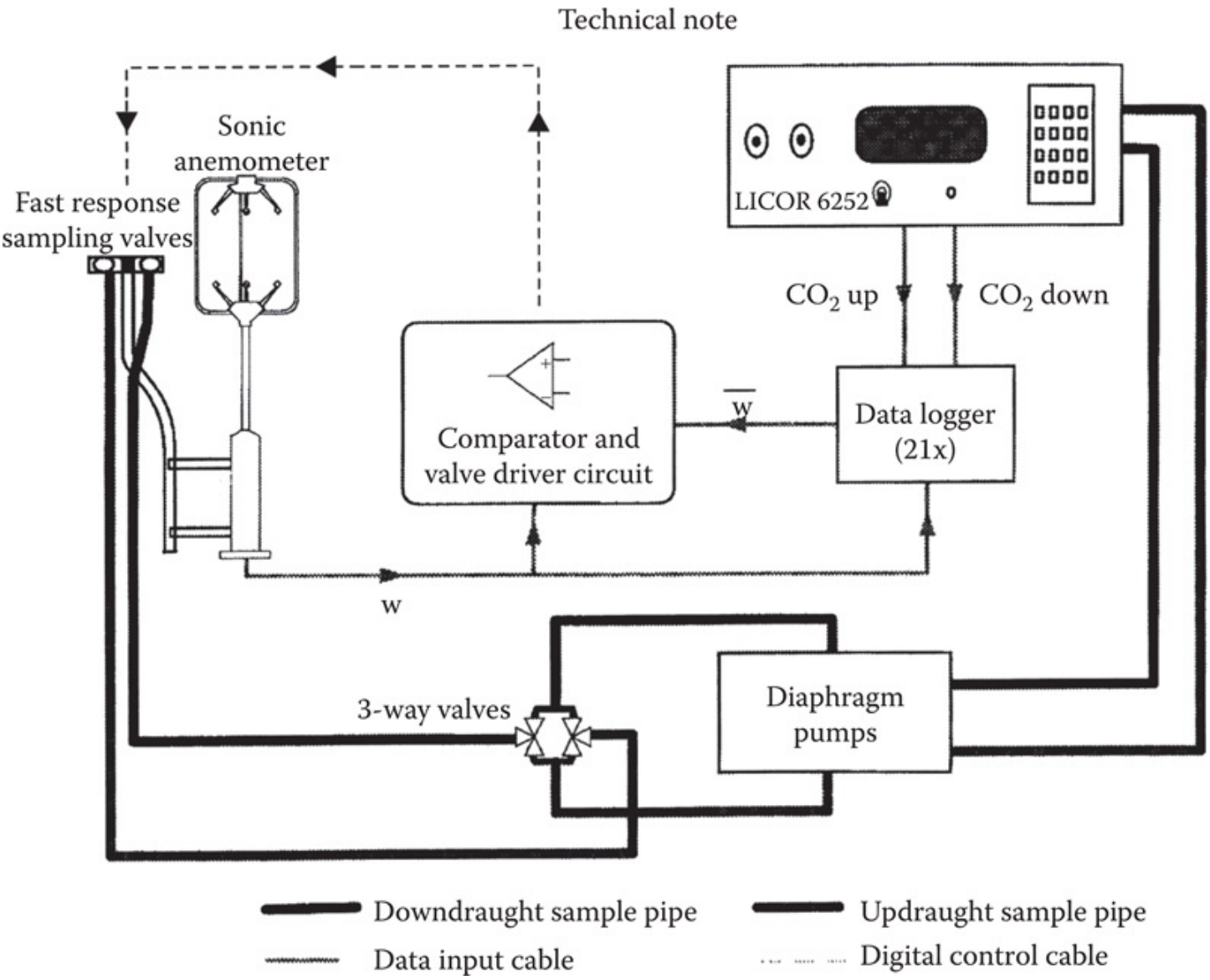

Figure 6.12 Conditional sampling system for flux measurement. (From Beverland, I. J. et al., *Atmos. Environ.*, 31, 277–281, 1997.)

The gas flux can be measured by a variety of methods. The most straightforward is to

FOR REFERENCE PURPOSES ONLY

measure the concentration gradient between one point close to the surface and another point at a reference height such as 2 m. Then by using Fick's law and a measured value for the turbulent diffusivity, the flux can be calculated. Usually the measurement is averaged over a 30-min period to smooth out short-term fluctuations. A more sophisticated technique, known as conditional sampling, is shown in Figure 6.12. The principle of the device is to measure directly the upward-going and downward-going fluxes, and subtract them to give the net flux. An ultrasonic anemometer measures the wind speed and direction with very high time resolution.

When the vertical component of the wind vector is upward, the air is switched by high-speed solenoid valve into one sample line. When the wind is downward, the sample air is switched into a second line. Either the samples can be accumulated in bags for later analysis or the difference measured in real time by an in-line gas analyser (for CO_2 in this example, but in principle any gas can be measured this way). A sample of the results from this system is shown in Figure 6.13. The CO_2 flux is small and upwards (respiration) during the night, large and downwards (photosynthesis) by day.

Two concepts are commonly used to parameterise gas deposition: the deposition velocity and the transfer resistance.

FOR REFERENCE PURPOSES ONLY

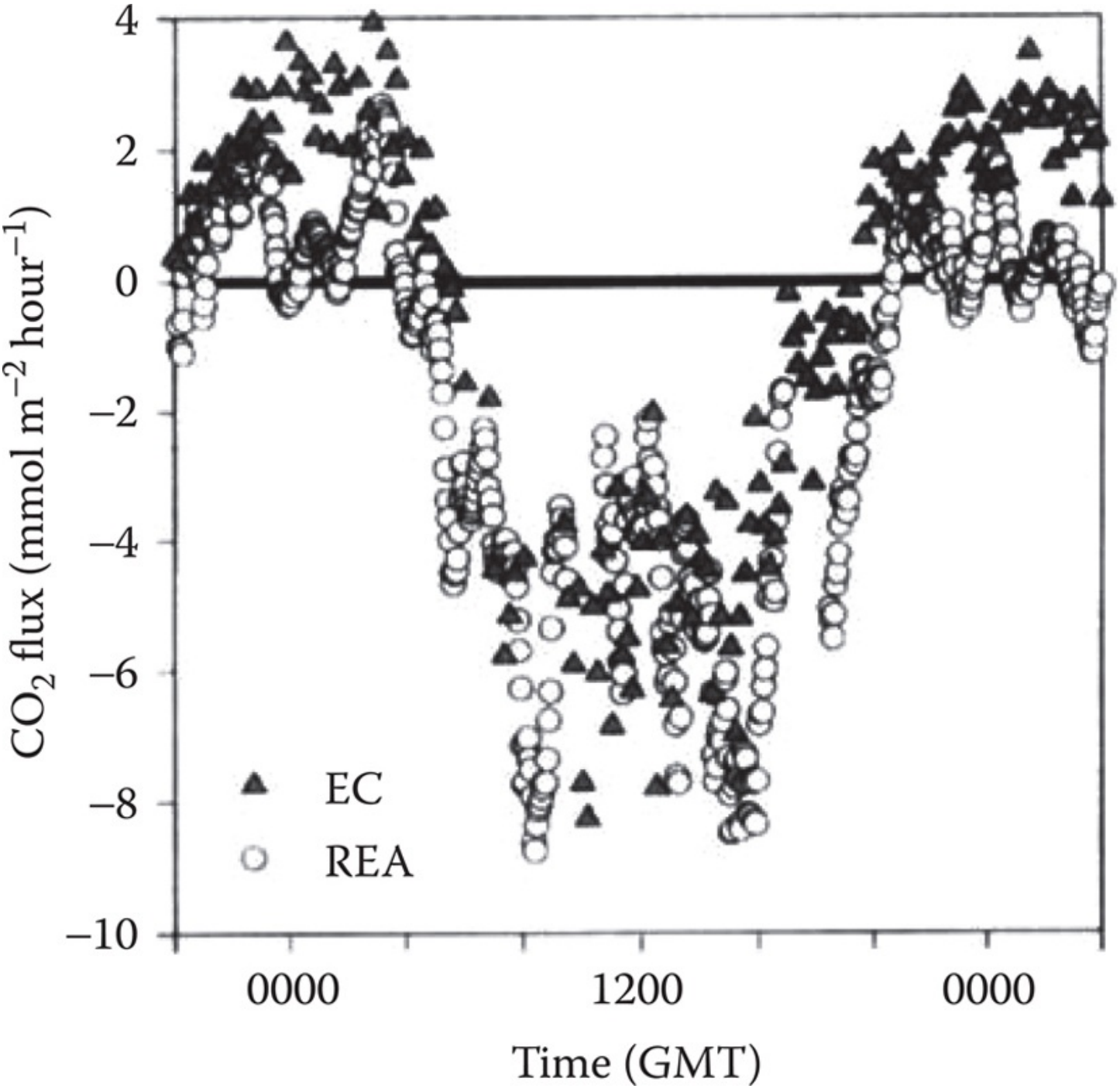

Figure 6.13 CO_2 flux measured by the conditional sampler. (From Beverland, I. J. et al., *Atmos. Environ.*, 31, 277–281, 1997.)

6.4.1 Deposition velocity

Estimation of deposition velocity assumes that the flux is due to a gradient between atmospheric concentration measured at a reference height (usually 1 or 2 m) and zero concentration at the surface (because of absorption by the surface). This variation of any parameter above the surface is called the profile. The basic relationship is the wind speed

profile, which often follows a logarithmic variation with height which is due to the loss of air momentum by turbulent interaction with roughness elements at the surface. This is expressed by the standard wind profile equation, which in differential form becomes:

$$\frac{\partial u}{\partial z} = \frac{u_*}{k(z-d)}$$

where:

u_* is the friction velocity (the larger the value of u_*, the larger the turbulent velocity variations)

k is the von Karman's constant = 0.41

d is the zero plane displacement

Under neutral atmospheric stability conditions the turbulent *eddies* can be thought of as circular, with equal components from horizontal and vertical velocity fluctuations. When there is surface heating with associated instability, the vertical variations are enhanced, and the wind speed increases rapidly going away from the surface. Conversely, in stable conditions the vertical eddy component is suppressed, and the wind speed increases more slowly going away from the surface. Then:

$$\frac{\partial u}{\partial z} = \frac{u_*}{k(z-d)} \Phi_M$$

where Φ_M is a dimensionless stability function which has a value larger than unity in stable conditions and less than unity in unstable conditions.

The flux of momentum τ from the atmosphere to the surface is given by:

$$\tau = \rho u_*^2 = K_M \frac{\partial(\rho u)}{\partial z}$$

where K_M is the turbulent diffusivity for momentum, and by:

$$K_M = k u_* (z - d) / \Phi_M$$

Essentially the same process drives the fluxes of molecules such as water vapour and carbon dioxide, and these can be written generally as:

$$K_S = -\frac{F}{\partial S / \partial z}, \text{and } K_S = \frac{k u_* (z-d)}{\Phi_S}$$

where:

F is the flux of material

S is its concentration at height z

Corresponding stability functions Φ_S are used, and there has been much discussion in the

FOR REFERENCE PURPOSES ONLY

literature about whether the values of K and Φ are really the same for heat, water and other molecules when the conditions are non-neutral. The relationships should also apply to particles if they are small enough for their sedimentation speeds to be insignificant. Then:

$$v_g = \frac{F_g}{C(z_r)}$$

where:

F_g is the flux to surface (kg m^{-2} s^{-1})

$C(z_r)$ is the atmospheric concentration (kg m^{-3}) at reference height z_r

Hence the SI units of v_g are m s^{-1}, as we would expect for a velocity (Table 6.2). The area that is measured in m^2 is normally the land or sea surface, although in some cases it can be the leaf area (one side or two, or projected). It should be remembered that this single parameter of deposition velocity, while being convenient to use, does combine the overall effects of three processes – the turbulent diffusion that brings molecules and particles close to a surface, the molecular or Brownian diffusion that takes them across the final few millimetres to the surface itself, and the absorption/dissolution/adhesion which results.

Note that the roughness lengths are not simply the physical height of the surface roughness elements but have been determined experimentally as the effective length of the surface elements for turbulence generation (Table 6.3). The roughness length of some surfaces varies with wind speed – water develops ripples and waves, long grass blows flat, trees bend over.

Table 6.2 Typical values of v_g (mm s^{-1})

Gas	*Surface*		
	Soil	*Grass*	*Sea*
SO_2	2 for acid soil 10 for basic soil	8	10
O_3	5 to wet soil 15 to dry soil	6	0.4
PAN	2.5	2.5	<0.2
NO_2	5	5	
CO_2	–	0–0.2	0.1
NH_3	–	–	–

Table 6.3 Values of roughness length for different surfaces

Surface	*Roughness length/m*
Still water or smooth ice	0.00001
Smooth snow or smooth sand	0.0003

Soil	0.003
Short grass	0.005
Long grass	0.05
Uniform crops	0.1
Open countryside	0.4
Suburbs	1.0
Forests or urban areas	2.0

6.4.2 Resistance

Another way of looking at the idea of v_g is as a measure of the conductance of the atmosphere – surface combination for the gas. Resistance is the inverse of conductance, and R_t (= $1/v_g$, with units of s m^{-1}) is then the total transfer resistance for the pollutant between the reference height and the surface. Now, since

$$R = \frac{1}{v_g} = \frac{C(z_r)}{F_g}$$

we can add and subtract the surface concentration C_s. Hence:

$$R = \frac{C(z_r) - C_s}{F_g} + \frac{C_s}{F_g} = R_{\text{atm}} + R_{\text{surface}}$$

The resistance R_{atm} can further be separated into two resistances in series, R_a to describe turbulent transport by eddies to within a few mm of the surface, and R_b to describe molecular diffusion of the gas through the laminar boundary layer to the surface itself. When the surface roughness is high (as in a forest or an urban area), or the wind speed is strong, R_a will be low, and *vice versa*. Typically, R_a is around 200 s m^{-1} for wind speeds <1 m s^{-1} over vegetation 10 cm tall; 20 s m^{-1} for wind speeds >4 m s^{-1} over 1 m vegetation; <10 s m^{-1} over a forest canopy. These atmospheric resistances are then subtracted from the total resistance R to give the surface resistance R_{surface}.

FOR REFERENCE PURPOSES ONLY

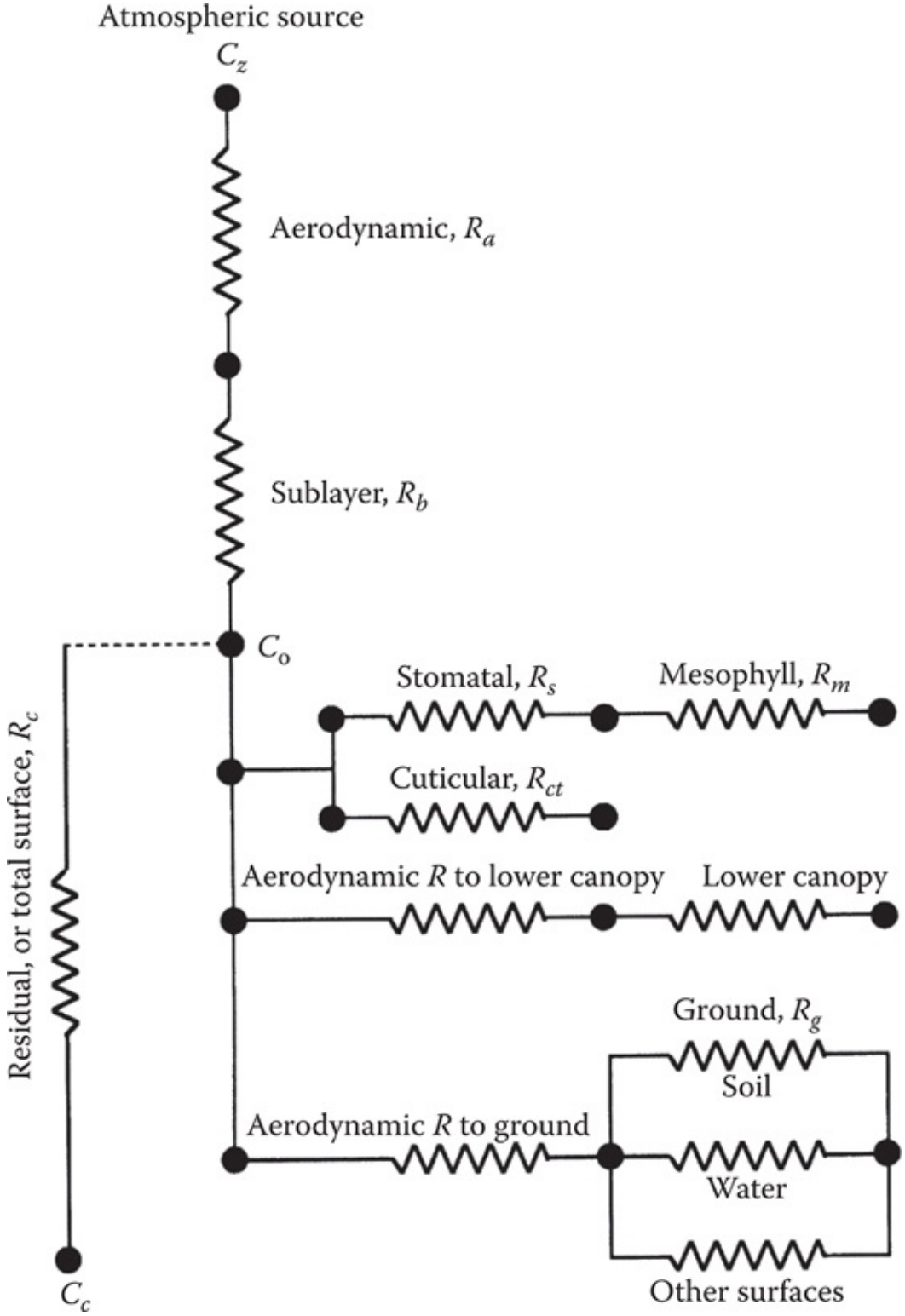

Figure 6.14 A schematic diagram of the series and parallel resistances that control the flux of pollutant to a vegetated surface. (From Wesely, M. L., and Hicks, B. B., *Atmos. Environ.*, 34, 2261–2282, 2000.)

Figure 6.14 shows the application of this concept to the complex surface of a vegetation canopy. After a gas molecule has penetrated close to the surface, there are several possible paths by which it can be taken up. In the figure, the paths involve entry through the stomata,

deposition to leaf surfaces, transport and deposition to the lower canopy, and deposition to the soil. Each of these paths involves its own resistance and flux. In this case we have:

$$\frac{1}{R_d} = \frac{1}{R_a} + \frac{1}{R_b} + \frac{1}{R_c}$$

where:

R_d is the dry deposition resistance

R_a is the aerodynamic resistance of the atmospheric surface layer (above the canopy)

R_b is the resistance due to molecular diffusion across the quasi-laminar boundary layer

R_c is the canopy resistance

Also:

$$\frac{1}{R_c} = \left[\frac{1}{R_{\text{stom}}+R_{\text{meso}}} + \frac{1}{R_{\text{cut}}} + \frac{1}{R_{\text{lowercanopy}}} + \frac{1}{R_{\text{soil}}}\right]$$

where:

R_{stom} is the resistance to pollutant flux through the stomata

R_{meso} is the resistance of the internal organs of the plant

R_{cut} is the resistance of the leaf cuticle

R_{soil} is the soil resistance

As mentioned earlier, the behaviour of gases is also influenced by factors such as their reactivity (very high for HF, moderate for SO_2, O_3, NO_2, PAN), or their biological activity (high for CO_2), or solubility (high for SO_2).

This scheme is highly simplified compared to the real world. A real vegetated surface has components of resistance due to atmospheric transport to the soil (depends on canopy structure, density and turbulence); across the soil boundary layer and into the soil (depends on roughness, wetness, organic matter content); and to the plant, into the non-leaf plant parts, into the leaves through cuticles and stomata, and eventually into the intercellular spaces. Equivalent models can be constructed for other surfaces such as water bodies, buildings and animals. In practice, canopy resistance typically makes up around 70% of the total, so that deposition rate is controlled by changes in r_c rather than in roughness or wind speed, even over forests.

6.5 WET DEPOSITION

6.5.1 Rainfall

As well as being deposited in the gaseous form, S and N are eventually incorporated into cloud droplets, raindrops and snowflakes, and deposited back to land and water bodies via

cloud droplet deposition, rainfall and snowfall. If the gas molecules or particles are incorporated into cloud droplets which then turn into raindrops, it is called rainout. If they are collected by the raindrops as the latter fall through the atmosphere, it is called washout. It may be hard to distinguish the two routes in practice. A particle may form the cloud condensation nuclei on which a cloud droplet first condenses, or it may be collected by a raindrop as it is falling to the surface. Equally, gases may dissolve into cloud droplets or into the falling raindrops. Droplets may have lifetimes of a few minutes in convective shower clouds or a few hours in frontal rain systems. Also, the raindrops themselves do not have a simple history. They may start as frozen hail or snow but melt in the warmer air they fall through. They may undergo several lifting and falling cycles in convective motions in the cloud, and they may evaporate substantially in the drier air below the cloud. Many clouds generate rain which falls out of the cloudbase but never reaches the ground. During this process all the particles and gases that were taken up into the raindrops are converted into quite different forms.

6.5.2 Rainout

Cloud droplet formation involves the generation of air supersaturated with water vapour during convective or orographic uplift. Droplet formation is a complex process involving competition between several different mechanisms. As the air rises and cools, the saturated vapour pressure decreases towards the actual vapour pressure. Eventually the vapour becomes supersaturated, and condensation is possible. When an air mass that is completely free of particles is cooled, no condensation occurs until extremely high supersaturations are reached, several times the saturated vapour pressure. This is because saturated vapour pressure over a curved water surface follows the Kelvin relationship:

$$\ln \frac{e_d}{e_\infty} = \frac{4\sigma v_B}{RT} \cdot \frac{1}{d}$$

where:

e_d, e_∞, are the SVPs above a surface of diameter d and a flat surface, respectively

σ and v_B are the surface tension and molar volume, respectively, of the liquid

R is the gas constant

T is the absolute temperature

When $d = 0$, the required supersaturation is infinite. When there are no particle surfaces present, condensation can only occur onto chance clusters of a few molecules. The latter have values of d of a few $\times 10^{-10}$ m, so the supersaturation needed is extremely high. This Kelvin effect also controls natural aerosol production from vapours and the manufacture of aerosol particles for instrument calibration. When very high values of supersaturation occur, it is possible to get homogeneous nucleation – the formation of droplets from

FOR REFERENCE PURPOSES ONLY

combining clusters of molecules.

Although supersaturations in the real atmosphere rarely exceed 1%, cloud droplets do form and grow, due to the presence of CCN. When CCN are present, they will usually be either hydrophobic, insoluble materials such as silica or carbonates from soil particles, or hygroscopic soluble salts such as chloride. In maritime air, oceanic sources of secondary sulphate particulate from planktonic differential mobility spectrometer (DMS), and primary sea salt particles, contribute to the CCN. When the air is of continental origin, the CCN are from anthropogenic combustion and soil entrainment.

The hydrophobic nuclei simply present surfaces onto which condensation can begin when the supersaturation is sufficiently elevated, although this represents an order of magnitude increase on the activation supersaturation for hygroscopic CCN. The latter are often salts such as sulphates, nitrates or chlorides, and can be of natural or human origin. One of the main natural production routes is sea spray. On average, a low percentage of the surface area of the world's oceans is covered by breaking wave crests. Each of these crests generates millions of breaking bubbles, and each of the breaking bubbles typically generates a few larger droplets (up to a few hundred μm in diameter) and many smaller droplets (5–20 μm in diameter). Some of these droplets fall back into the sea, but many remain airborne long enough for their water to evaporate and leave behind a residual salt particle. For example, sea water contains about 3.5% salts, of which 2.9% or 29 g L^{-1} is NaCl. If a sea water droplet of 50 μm diameter is ejected from spray and evaporates, it will leave a salt CCN having a mass of 2.2 ng and a diameter of 15 μm. In addition, the droplets and particles are formed from sea water in the very near surface layer, where there are enriched concentrations of many materials. These CCN then remain unchanged in the air mass until the latter is involved in convective uplift. As the relative humidity increases in the uplifted air, the hygroscopic CCN absorb water vapour. Eventually they deliquesce, or dissolve into their own water content, to form a small liquid droplet of highly concentrated salt solution. There is a hysteresis effect here – if the relative humidity is then decreased, the droplet evaporates water but does not recrystallise until a relative humidity of 40% (in the case of sodium chloride) is reached. Low-solubility salts such as NaCl absorb a lot of water before they dissolve and hence make large droplets. High-solubility salts, such as those in the ammonium family, form smaller initial droplets of more concentrated solutions. If the relative humidity were constant, the droplet could exist at a stable radius depending on the mass of the initial CCN. As uplift continues and reduces the saturated vapour pressure, the droplet grows, the salt concentration declines but so does the curvature, and growth can continue. Hence the supersaturation within the cloud is kept below about 0.5%.

A hygroscopic CCN promotes the formation of a cloud droplet in two ways. First, it provides a surface with a larger radius of curvature onto which new water vapour molecules can condense at lower supersaturations. Second, the presence of the dissolved salt reduces the surface vapour pressure below that of pure water, and hence reduces the supersaturation needed for the uptake of new water molecules from the vapour. The Kelvin equation

FOR REFERENCE PURPOSES ONLY

becomes:

$$\ln \frac{e_d}{e_\infty} = \frac{a}{d} - \frac{b}{d^3}$$

where a and b are constants.

For droplets that have just dissolved and for which the solution is very concentrated, the reduction in vapour pressure due to this effect (the second term on the right-hand side) outweighs the increase due to curvature, and condensation can be initiated even while the relative humidity is as low as 70% or 80%. The new cloud droplet can grow at low supersaturations, with the two effects competing: as the radius increases, the salt concentration decreases with the droplet volume (cube of radius) while the curvature of the surface decreases with the radius. The result of these opposing tendencies is the set of Köhler curves shown in Figure 6.15.

First, note that the supersaturation scale is expanded by a factor of 100 compared to the relative humidity scale. This accounts for the strange discontinuity at the boundary. It further emphasises the very small supersaturations that are present in clouds. Second, the supersaturation over a pure water surface (the outer curve) is almost zero for very large droplets, which have almost flat surfaces. As the droplet diameter falls, the surface curvature increases, and the supersaturation goes off to infinity. Third, note that each of the curves is for a different initial CCN mass. The smallest CCN at the left gives the least benefit from solute reduction of vapour pressure, and the saturated vapour pressure needed for growth becomes very high while the droplet is still very small. Fourth, on the left sides of the curves, the droplets are in equilibrium – if the humidity increases, the droplet will grow, but if it decreases, then the droplet will shrink again.

An NaCl CCN that grows from activation at 75% relative humidity to equilibrium at 90% will take on about six times its initial mass of water vapour molecules, by which point its diameter will have increased by a factor of 1.8. This is a confusing situation for aerosol sampling, because if the sample is based on the aerodynamic diameter at ambient humidity, the adsorbed water will determine the cut diameter, whereas when the water evaporates, the smaller CCN will remain. Hence a sampling protocol should involve bringing the particles to equilibrium at an agreed low relative humidity (RH) – the World Meteorological Organisation (WMO) suggestion is an RH of 40%.

However, if the droplet radius exceeds the value corresponding to the peak of the curve, then the *activated* droplet will grow continuously even if the humidity falls (provided it remains above saturation). The rate of growth decreases as the diameter increases and is extremely slow for droplets above about 40 μm diameter. The increase in diameter necessary to reach even drizzle-drop size of about 100–200 μm is achieved by collision and coalescence with other droplets. Hence in an air mass that contains a size distribution of CCN, together with turbulence which causes variations in humidity, a complex selection process operates that determines which nuclei get activated (scavenged) and eventually contribute to the growing droplet population. CCN may participate in 10–20

FOR REFERENCE PURPOSES ONLY

condensation/evaporation cycles before eventually becoming incorporated in a raindrop which reaches the ground. CCN concentrations are rather low (tens to hundreds cm^{-3}) in maritime air, and higher (hundreds to thousands cm^{-3}) in continental air. Of these, 20%–30% become activated in an updraught. The concentration of activated CCN depends on the supersaturation, going as cS^k where c is the total CCN concentration, S is the supersaturation and k is a constant. The supersaturation achieved is a function both of the number of CCN (the more there are to be activated, the faster they will sweep up the excess water vapour generated by the updraught) and of the updraught (the faster the air rises, the faster it will cool and release water vapour). Hence, activated CCN concentration N is directly proportional to $c^{2/(k+2)}U^{3k/(2k+4)}$.

FOR REFERENCE PURPOSES ONLY

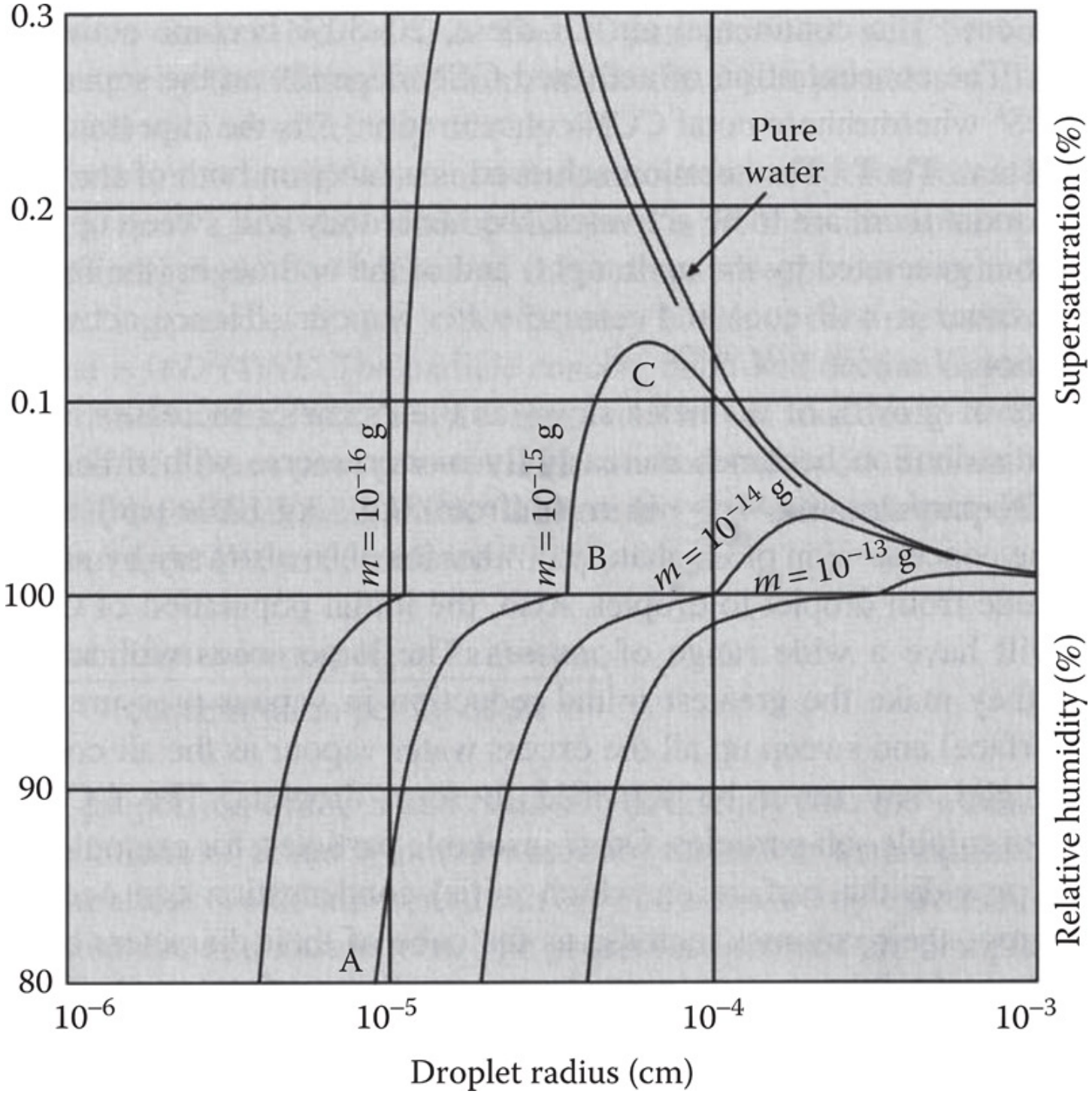

Figure 6.15 Köhler curves to show the variation of equilibrium water vapour concentration with droplet radius and mass of CCN. (From Wells, N., *The Atmosphere and Ocean*, Wiley, Chichester, UK 1997.)

The rate of growth of diameter slows as the diameter increases, so that the smaller particles catch up and the diameter distribution becomes increasingly monodisperse with time. As the initial CCN particles may vary in mass from 10^{-21} kg (0.01 μm) to 10^{-5} kg (1 μm), the concentration of sulphate and other ions can also vary by many orders of

magnitude from droplet to droplet. Also, the initial population of CCN in the updraft will have a wide range of masses. The larger ones will activate first (because they make the greatest initial reduction in vapour pressure above the droplet surface) and sweep up all the excess water vapour as the air cools. Hence smaller nuclei may never be activated to form droplets. The CCN are not restricted to soluble salt particles. Other insoluble particles, for example, entrained dust, can provide the surface on which initial condensation can occur. As the droplets grow, their volumes increase as the cube of their diameters, but the rate of vapour uptake increases only as the square (i.e. surface area). The rate of diameter growth declines. Eventually collision processes between drops, which are unimportant for small drops because of low impaction efficiency, become the dominant way in which droplet diameter increases. All this depends on the droplet remaining suspended in the updraft. As the diameters are increasing, the sedimentation speeds increase, and eventually the old cloud droplet or new raindrop acquires a fall speed greater than the updraft and fall out of the cloud.

Growth by condensation can be dramatically accelerated by the presence of ice crystals. When the air temperature is less than 0°C, some of the condensation occurs as ice-onto-ice CCN. At temperatures between –40°C and 0°C, there is a mixture of ice crystals and water droplets. However, the SVP over ice is lower than the saturated vapor pressure (SVP) over water at the same temperature, so the supersaturation with respect to ice may be 10% while that with respect to water is zero. The ice crystals then grow extremely rapidly. When the large ice crystal falls out of the cloud, it will probably melt back to water on its way down to the ground.

6.5.2.1 Washout

As a raindrop is falling out of the cloud, it has an opportunity to collect raindrops, particles and gases within the cloud, and particles and gases below. We can use the Stokes number to get an idea about the efficiency of particle collection. For example, a raindrop of 1 mm diameter has a fall speed of around 4 m s^{-1}. At that speed a 10 μm diameter particle has a stopping distance of 1 mm and a Stokes number of 2, while a 3 μm particle has a stopping distance of 0.1 μm and a Stokes number of 0.2. The 10 μm particles will be collected at 55% efficiency by the falling raindrop, while the 3 μm particles will hardly be collected at all, with an efficiency of only 4%.

We can also define a time constant λ for particle concentration decay. If the rainfall rate is R m s^{-1}, and the raindrop diameter is D, then the raindrop rate N is $R/(\pi D^3/6)$ raindrops m^{-2} s^{-1}. Each of these drops sweeps out a cylinder of area $\pi D^2/4$, collecting particles from it with efficiency E. Hence the time constant for particle removal is $(\pi D^2/4)NE$. The particle concentration declines exponentially in continuing rain according to $\exp(-\lambda t)$. For 1 mm h^{-1} of rain due to drops 1 mm in diameter, half of 10 μm particles would be washed out in 50 min, whereas it would take 10 h for the 3 μm particles to be reduced by the same

proportion.

A washout ratio W can be defined as:

$$W = \frac{\text{concentration per kg of rainwater}}{\text{concentration per kg of air}}$$

A small proportion of the S and N dissolves directly into the water. However, the concentrations of S and N in rainwater are far higher than equilibrium solution concentrations would allow and can only be achieved by oxidation processes that form sulphate and nitrate ions. The processes involved are complex, involving not only the S and N species themselves but also other gaseous compounds such as O_3 and H_2O_2 and reactions with catalysts such as manganese and iron that take place on the surface of aerosol particles. The timescale of these reactions is typically days, so that the S and N from emitted gases may be deposited thousands of km from their source.

6.5.3 Dry reactions

An important requirement is the availability of the OH radical through the decomposition of O_3 and the subsequent reaction of the free excited oxygen atom with water vapour:

$$O_3 + h\nu \rightarrow O^* + O_2$$

$$O^* + H_2O \rightarrow 2OH$$

and hence:

$$SO_2 + OH + M \rightarrow HSO_3 + M$$

$$HSO_3 + O_2 \rightarrow HO_2 + SO_3$$

$$SO_3 + H_2O \rightarrow H_2SO_4$$

where M is a passive reaction site such as a nitrogen molecule. Measurements in dispersing plumes indicate that the conversion rate can rise as high as 4% per hour on a sunny summer afternoon, with a typical overall rate of about 1% per hour.

The OH radical is also involved in the dry production of nitrate:

$$NO + O_3 \rightarrow NO_2 + O_2$$

$$NO_2 + OH + M \rightarrow HNO_3 + M$$

This conversion occurs an order of magnitude faster than for sulphate.

At night, a second route is available which involves the nitrate radical NO_3:

$$NO_2 + O_3 \rightarrow NO_3 + O_2$$

$$NO_2 + NO_3 \rightarrow N_2O_5$$

$$N_2O_5 + H_2O \rightarrow 2HNO_3$$

This process is unimportant in the daytime because the radical is photolytically unstable.

After 24 h, a dispersing plume with an average wind speed of 10 m s^{-1} would travel about 1000 km (up to the highlands of Scotland from Northern Europe, or across the North Sea to Sweden from the UK). In this time around 30% of the sulphur dioxide would be dry-converted to sulphuric acid, and all of the nitric oxide to nitric acid. These acid molecules may condense onto existing particles, or they may self-nucleate to form pure acid droplets. Such droplets absorb ammonia rapidly to form hygroscopic ammonium sulphate or ammonium nitrate aerosol particles, which eventually acts as CCN and is returned to the surface in precipitation.

6.5.4 Wet reactions

Within cloud droplets the production of sulphuric acid is much faster. Sulphur dioxide dissolves in water to form mainly the bisulphite ion:

$$2SO_2 + 2H_2O \rightarrow SO_3^- + HSO_3^- + 3H^+$$

There are then two main routes for oxidation to sulphuric acid, depending on the SO_2 concentration. At the low SO_2 concentrations found in remote areas, the bisulphite is oxidised by hydrogen peroxide, that is:

$$HSO_3^- + H_2O_2 \rightarrow HSO_4^- + H_2O$$

A key role is played by the hydrogen peroxide, which is regenerated slowly from reactions involving HO_2 and carbonyl compounds such as CO and HCO. The availability of H_2O_2, and of other pollutants and their by-products, can therefore control the rate of sulphuric acid production. In more polluted regions, where the SO_2 concentration is higher, the peroxide supply is inadequate. Then oxidation by ozone, which is highly non-linear with SO_2 concentration, becomes significant. Hence turbulent entrainment of new supplies of oxidants may play an important part in determining the overall rate of sulphate or nitrate production. Carbon monoxide, which is usually thought of for its toxicity at high concentrations in urban areas, is also important in atmospheric photochemistry at low concentrations. Both nitric oxide and nitrogen dioxide have low solubilities in water, and the rate of wet oxidation is less significant.

These conversion processes have several impacts on the quality of precipitation. First, they change the acidity. The acidity is indicated by the pH, which is the negative logarithm

FOR REFERENCE PURPOSES ONLY

of the hydrogen ion concentration:

$$\mathrm{p[H]} = -\log_{10}[\mathrm{H^+}]$$

For pure water, $[H^+] = 10^{-7}$ M, giving a p[H] of 7.0. A reduction of one p[H] unit, from 7.0 to 6.0, for example, indicates that the H^+ ion concentration has increased by a factor of 10. In the clean atmosphere, water is in equilibrium with 360 ppm CO_2, giving a p[H] of 5.6. In remote temperate areas of the world, average rain p[H] is about 5.0. In the UK, precipitation quantity and quality are measured at 68 sites in two precipitation composition monitoring networks. In the secondary network, precipitation is sampled every week or fortnight at 59 sites by bulk collectors that remain open to the atmosphere all the time and hence collect dry deposition from gases and particles as well as rain, snow or hail. In lowland areas, it only rains for 7% of the time, so that dry deposition of sulphate and nitrate can make a significant contribution (perhaps as much as one-third) to the total. The secondary network is therefore supplemented by a primary network of nine wet-only collectors. These are uncovered automatically when rain is actually falling and store the rainfall in a different container for each 24-h period. There are several penalties for this improvement. First, the first part of each precipitation event, which is the period when solute concentrations are often the highest, is lost because the collector is still covered. Second, the rainfall measurement itself is affected by the aerodynamics of the collector. As wet-only collectors are a different shape than their less sophisticated counterparts, the results are not automatically comparable. Third, the wet-only collectors normally need an electricity supply and cannot necessarily be sited in the optimum position. Across Europe, a further 90 sites in the European Monitoring and Evaluation Programme (EMEP) also record precipitation quality. Standard analyses include H^+, SO_4^{2-}, NO_3^-, NH_4^+ and a range of other ions. The results have shown that the annual average pH of European precipitation ranges between 4.1 and 4.9. The record low pH from a single rain event in the UK is 2.4, which occurred at Pitlochry in 1974. This amounts to a hydrogen ion concentration which is over 1500 times that found in clean rain, and represents a similar acidity to that of lemon juice. In fact there are naturally acidified lakes around the globe that sustain ecosystems at similar pH values – it is the short-term shock of relatively sudden changes in pH that causes stress.

The second impact of the acidity lies in the quantities of sulphur and nitrogen that are returned to the terrestrial environment by precipitation. Two factors determine the total amounts of S and N that are deposited – the concentration of the ions in the rain, and the total amount of rain. It is thought that some biological processes may be sensitive to the former, and others to the latter. The spatial distributions of the two factors are normally quite different. For example, the annual mean nitrate *concentration* in UK rainfall falls strongly from east to west, because it is influenced by European sources to the east of the UK. On the other hand, total nitrate *deposition* is influenced heavily by topography, with the total deposition being increased by the high amounts of rainfall over the uplands of

Wales, north-west England and Scotland. The maximum annual values of wet deposition in the UK are over 6 kg N ha^{-1} and over 14 kg S ha^{-1}. The effects of this deposition on terrestrial environments vary greatly with the mode of deposition and the chemical properties of the particular ecosystem. For example, although the precipitation in the English Midlands has low pH, it falls mostly as rain, is evenly distributed during the year and falls on to alkaline soils. In contrast, in Scandinavia, the winter precipitation falls as snow onto acid soils. During the spring thaw, all the stored winter acidity is released over a short period, generating an *acid pulse* with potentially severe consequences for aquatic life.

The networks show that the lowest pH in the UK (<4.1) is found in the East Midlands while the highest total deposits are found in the upland regions where the rainfall is highest. In mainland Europe, the lowest pH values are found within a belt stretching from southern Sweden down into eastern Germany and Poland. The concentrations of ions in precipitation are known from analyses of material collected largely from rain gauges in lowland areas. These concentrations are not necessarily the same as those experienced in the higher rainfall upland areas, because of a process called the seeder–feeder mechanism. An orographic feeder cloud forms when advected air cools as it rises over hills. Droplets are washed out of the cloud by raindrops falling from a seeder cloud above. As the ionic concentrations in the small feeder cloud droplets are several times as high as those in the larger seeder raindrops, this process enhances the ionic concentrations in the rain. The higher the altitude, the greater the orographic cloud cover, and the greater the total wet deposition. Wet deposition values calculated from rain gauge data must be corrected for this altitude effect.

During the period that the old industrialised nations have been controlling emissions, the chemical balance of precipitation has been changing. By 1993, sulphur emissions in Western Europe had decreased by around 50% from their value in 1980, and both the acidity and sulphur content of precipitation had fallen by 35%. Emissions and deposition of nitrogen remained about the same, however, so that N now generates around 60% of the acidity in European precipitation.

6.5.5 Cloudwater deposition

The processes of droplet formation from CCN, together with the deposition mechanisms that are common for all particles, mean that significant fluxes of salts and acidity can occur to vegetation by the deposition of droplets when it is not actually raining. This is most likely to occur from orographic clouds which are formed when air blows up the windward side of a range of hills. Some upland areas can be in cloud for a high proportion of the year. At such sites, the deposition of cloud droplets to vegetation – a process also known as occult precipitation, because it is not detected by a standard rain gauge – can be a significant S and N supply in itself, and the high concentrations (up to 50 times those in raindrops) may have important effects on the affected vegetation. For example, experiments have shown that the freezing resistance of conifers is reduced by acid mists, making the

FOR REFERENCE PURPOSES ONLY

trees more liable to cold damage in the winter. Altitude effects on precipitation chemistry are likely to be significant above 200 m, and above 400 m cloudwater deposition can be more important than the direct input from precipitation. Although direct measurements of droplet deposition are technically difficult and infrequently made, values that have been taken over moorland and forests show that the deposition velocity is similar to that for momentum. This has provided the basis for calculations of deposition across the country from known average wind speeds, land-use data and cloud water ion concentrations. Such calculations have shown that in upland areas of Wales and Scotland, droplet deposition can increase wet nitrate deposition by 30%. The deposition rate is strongly influenced by the aerodynamic roughness of the surface and is therefore higher over forests than over grass or moorland.

6.6 TOTAL DEPOSITION AND BUDGETS

The total deposition at any site is the sum of wet (rain/snow or droplets) and dry deposition. The relative proportions of these three vary greatly with the location. In the south of England, rainfall and altitude are both low, while proximity to urban and industrial sources is high, so that dry deposition is high, rainfall and droplet deposition are both low. In the uplands of Wales and Scotland, on the other hand, dry deposition is low and wet deposition high. As wind speeds also increase with altitude, the efficiency of droplet impaction onto vegetation increases, so that droplet deposition becomes a more significant fraction of the wet proportion. There has been considerable debate on the influence of vegetation type on deposition – for example, when an upland area is forested, the trees act as efficient droplet and gas collectors and can significantly increase the total N and S fluxes. These fluxes are very significant for the nutrient balance of the vegetation – total upland N fluxes can be around 30 kg ha^{-1} a^{-1} for systems that normally receive no fertiliser nitrogen.

Once all the dry and wet emission and deposition fluxes have been estimated for a particular element, they can be combined into a budget for an area, country or region. Table 6.4 shows one such calculation for nitrogen for the UK, for fluxes averaged over the period 1988–1992. The total deposition on any one country or area consists of some material that is emitted from the country itself, and some that is *imported* from other countries. Similarly, some of the total national emissions are exported, and some deposited internally. The balance between these import and export terms can be very different for different countries. The UK is a relatively small, intensively industrialised landmass surrounded by water, so it is bound to be a net exporter. Scandinavian countries recognised in the 1970s that they were importing S, N and acidity on the prevailing winds from the high emitters in the UK, Germany and Central Europe, while their own emissions were low because of their dependence on hydroelectric power. For Europe as a whole, we have the balance given in Table 6.5. Estimates are given in Figures 6.16 and 6.17 of the corresponding global budgets for sulphur and nitrogen, including natural emissions. Both budgets confirm that

FOR REFERENCE PURPOSES ONLY

anthropogenic emissions (Figures 6.16 and 6.17) dominate the totals.

Table 6.4 UK historical nitrogen budget

Source	*Direction*	*Flux/kt N a^{-1}*
Stationary sources of NO_x	Emission	425
Mobile sources of NO_x	Emission	421
Agricultural NO_x	Emission	350
Dry dep of NO_2	Deposition	100
Dry dep of NH_3	Deposition	100
Wet dep of NO_3^-, NH_4^+	Deposition	108, 131
Dry dep of HNO_3	Deposition	15
	Net export of NH_x[a]	119
	Net export of NO_y[a]	623

Notes:

[a] $NH_x = NH_3 + NH_4^+$

$$NO_y = NO + NO_2 + HNO_3 + HONO + NO_3 + N_2O_5 + NO_3^- \text{ aerosol} + PAN.$$

Table 6.5 European emissions and deposition of S and N

Emitted from Europe	*Deposited in Europe*
7 Mt NO_x-N	3.6 Mt NO_3-N
22.3 Mt SO_2-S	13.9 Mt SO_x-S
7.6 Mt NH_3-N	5.9 Mt NH_X-N

FOR REFERENCE PURPOSES ONLY

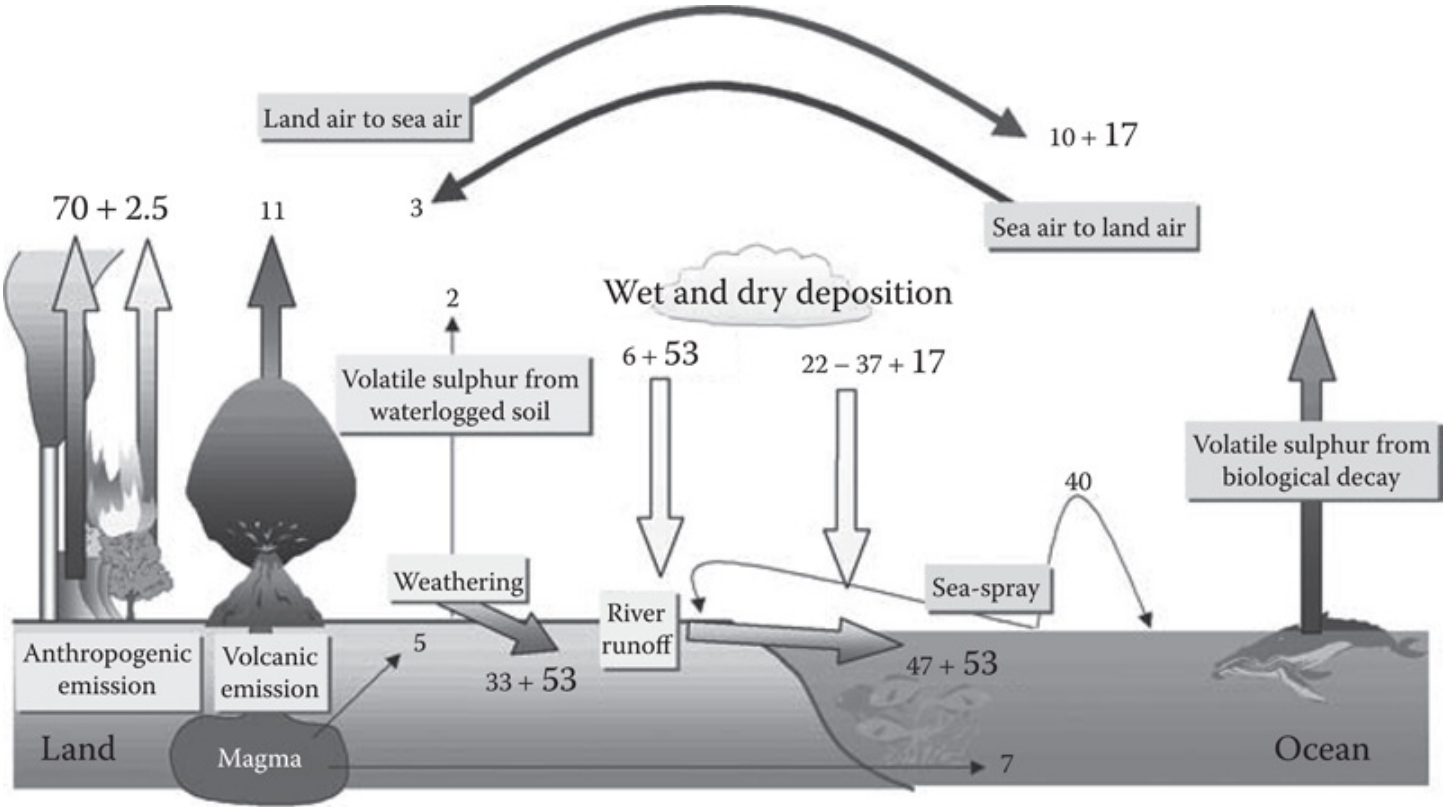

Figure 6.16 Global sulphur budget. (From National Expert Group on Transboundary Air Pollution, Transboundary Air Pollution: *Acidification*, *Eutrophication and Ground-Level Ozone in the UK*, Centre for Ecology and Hydrology, Edinburgh, UK, 2001; Graedel, T. E., and Crutzen, P. J., *Atmospheric Change – An Earth System Perspective*, W. H. Freeman, New York, 1993.)

FOR REFERENCE PURPOSES ONLY

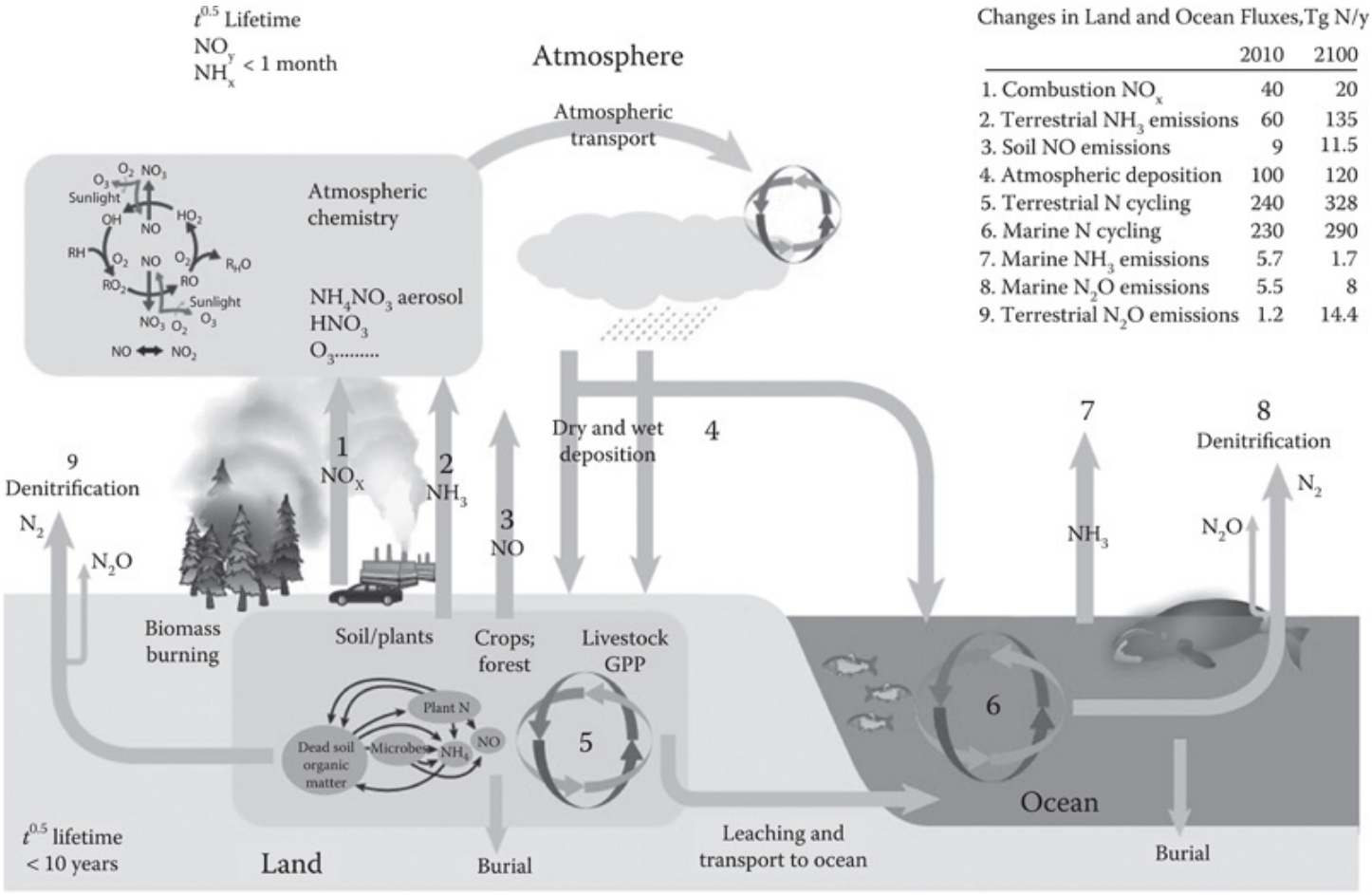

Figure 6.17 Global nitrogen budget. (From Fowler, D. et al., *Atmos. Chem. Phys. Discuss.*, 15, 1747–1868, 2015.)

6.7 ANALYSIS OF AN AIR QUALITY DATA SET

This section demonstrates a detailed analysis of a comprehensive set of air pollution concentrations and their associated meteorological measurements. The measurements were taken over a one-year period for the period 1 January–31 December 2015 at an automatic monitoring station operated in the UK. Three gas analysers provided measurements of O_3, SO_2, NO, and NO_x; estimates for NO_2 were obtained as the difference between NO_x and NO. Wind speed, wind direction, air temperature and solar radiation were measured by a small weather station. The signals from the instruments were sampled every 5 s by a data logger, and hourly average values were calculated and stored (i.e. 8760 data points).

6.7.1 The raw data set

A full year's data set would involve 8760 means of each of the nine quantities, or 78,840 data values in all. An initial inspection of the data set showed that it was incomplete. This is quite normal for air quality data – there are many reasons for loss of data, such as

FOR REFERENCE PURPOSES ONLY

instrument or power failures or planned calibration periods. Any missing values have to be accounted for in subsequent data processing. The data availability for this particular data set is given in Table 6.6.

Many of these lost values were due to random faults and were uniformly distributed throughout the year. The reliability of gas analysers depends largely on the simplicity of their design, and the ranking of the analysers in this example is quite typical. Ozone analysers based on UV absorption are very straightforward instruments that rarely fail provided that regular servicing is carried out. UV fluorescence sulphur dioxide analysers are rather more complicated, and NO_x analysers even more so. The lower availability for the nitrogen oxides in this case was in fact due to an extended period at the start of the year when problems were being experienced with the analyser.

Table 6.6 Data availability from the automatic monitoring station

Measurement	*Number of hours available*	*Percentage of 8760*
Ozone	8569	97.8
Sulphur dioxide	8251	94.2
Nitric oxide	7010	80.2
Nitrogen oxides	7010	80.2
Nitrogen dioxide	7010	80.2
Wind speed	8443	96.4
Wind direction	8459	96.6
Air temperature	8650	98.7
Solar radiation	8642	98.7

The raw data for gas concentrations, wind speed and wind direction are shown as time sequences in Figure 6.18. Plotting the data in this form is an excellent rapid check on whether there are serious outliers (data values lying so far outside the normal range that they are probably spurious). Differences in the general trends of the concentrations through the year are also apparent. The O_3 concentration (Figure 6.18a) rose to a general peak in April–May before declining steadily through to November, and the most common values at any time were around half the maxima of the hourly means. Sulphur dioxide concentrations (Figure 6.18b) were typically much smaller, although the maxima were nearly as great as for ozone. Typical NO concentrations (Figure 6.18c) were low throughout the year, although the intermittent maxima were higher than for the other gases. NO_2 concentrations (Figure 6.18d) were high around May and November, and particularly low in June and July. There were occasions when the concentrations of any of these gases increased and declined very rapidly – they appear as vertical lines of points on the time series. Superficially, there does not appear to be any systematic relationship between the timing of these occasions for the different gases. The wind speed (Figure 6.18e) declined during the first half of the year and then remained low. The wind direction (Figure 6.18f) was very unevenly distributed, being mainly from around either 200° (just west of south), or 0° (north).

FOR REFERENCE PURPOSES ONLY

6.7.2 Time-series plot

Many countries estimate their annual emissions of air pollutants and publish the information in statistical digests and, increasingly, on the Internet. Such data is fundamental to studying patterns of pollutant emissions and informing policy makers. The year-by-year information is often represented graphically as a *time-series* plot. The plots shown in Figure 6.18 give an immediate impression of the variations during the year, but they are not of much use for summarising the values – for comparison with other sites or with legislated standards, for example. We therefore need to undertake further data processing. The most straightforward approach is to explore the time variations by averaging the hourly means over different periods. First, we need to decide how to handle those missing values.

When we plotted the (nominal) 8760 h means, a few missing values did not have a big effect on the appearance. As we average over longer periods, the number of values decreases to 365 daily means, 52 weekly means and only 12 monthly means, so that the effect of missing values becomes proportionately greater. Before we start averaging, we must decide on a protocol that includes as much of the data as possible but does not create an average value when there is simply not enough data to justify it. For example, consider the calculation of a daily average from the 24 individual hourly averages that contribute to it. If one value is missing, and the sequence of values before and after is varying smoothly, then it is legitimate to substitute the missing value with the average of the adjacent values. If the sequence varies erratically, this procedure serves little purpose. Instead, we can ignore the missing value and calculate the daily mean as the average of the remaining 23 h, arguing that the whole day was still well represented. If only 12 or 8 h remain (as might happen if a faulty instrument was reinstated in the early afternoon), then this argument loses credibility and the whole day should be discarded. The same idea can be applied to the calculation of weekly, monthly and annual averages, with a requirement that, say, 75% of the contributing values be present if the average is to be calculated. This philosophy must particularly be adhered to when the data is missing in blocks, so that no measurements have been taken over significant proportions of the averaging period. For example, it is clear from Figure 6.18d that the annual average NO_2 concentration would not include any of January or February, and therefore might not be representative of the year as a whole. In Figure 6.19a, b, c the monitored data for gas concentrations are presented as daily, weekly and monthly averages, respectively. The short-term variations are successively reduced by the longer averaging periods, and the trends that we originally estimated from the raw data become clearer.

FOR REFERENCE PURPOSES ONLY

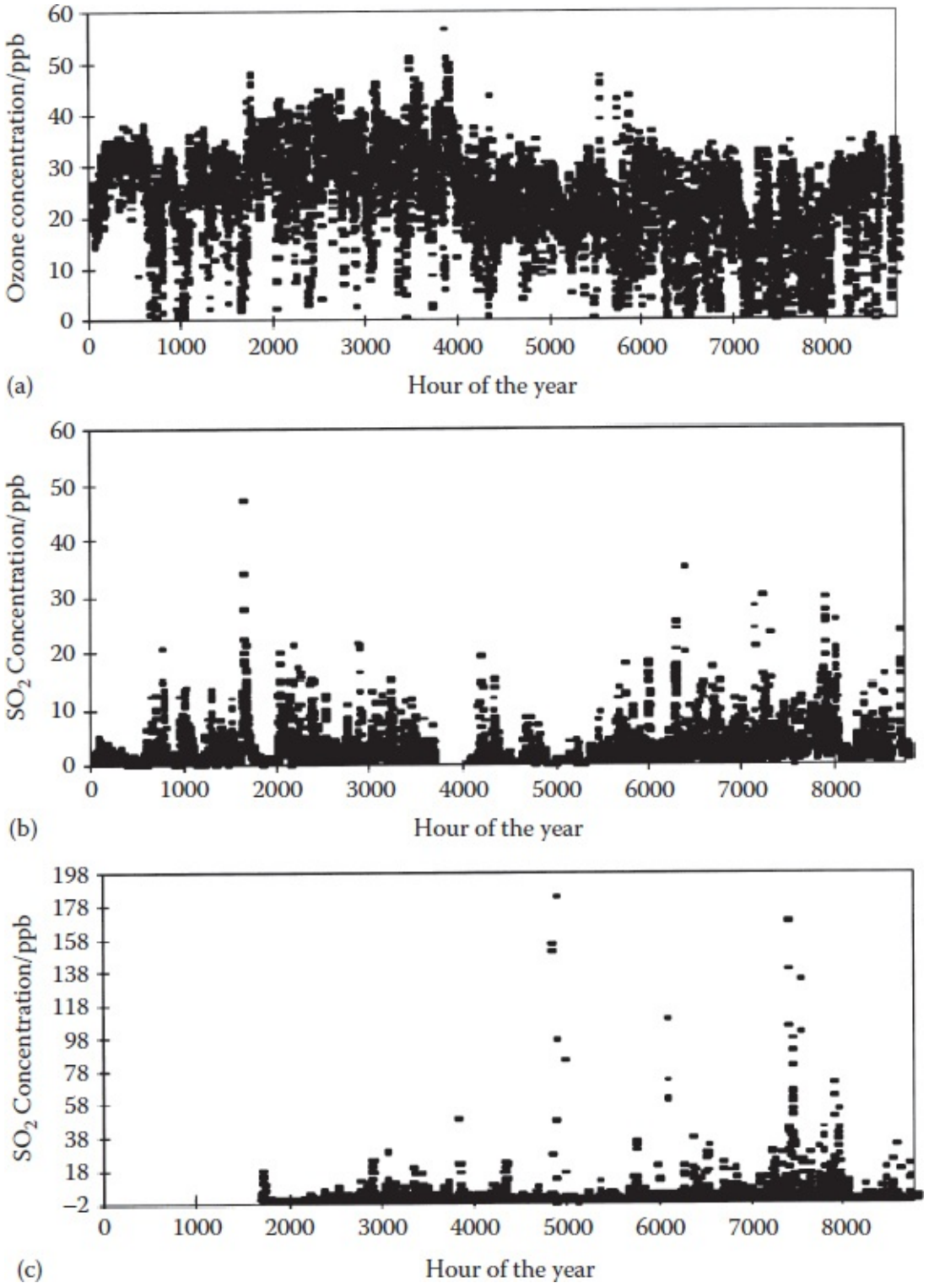

Figure 6.18 Time series of hourly means for the data set from the automatic monitoring station: (a) ozone, (b) sulphur dioxide, (c) nitric oxide. (d) nitrogen oxide, (e) wind speed and (f) wind direction.

FOR REFERENCE PURPOSES ONLY

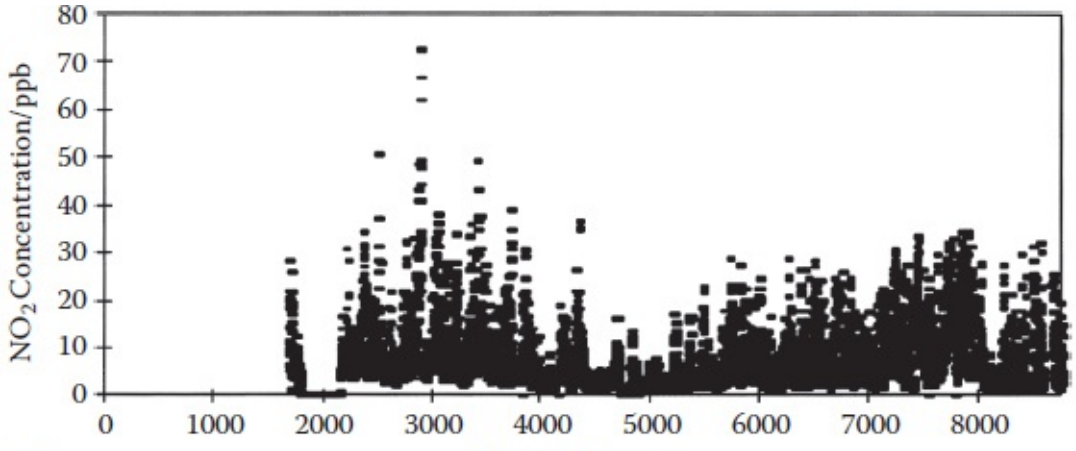

(d)

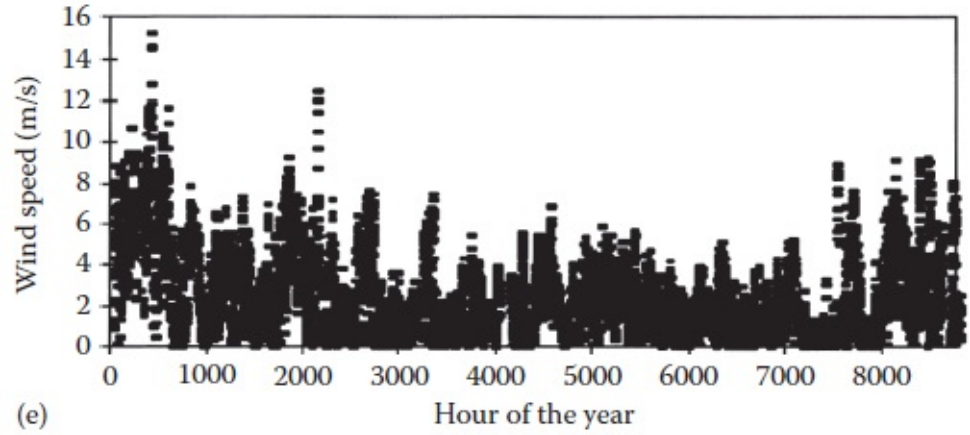

(e)

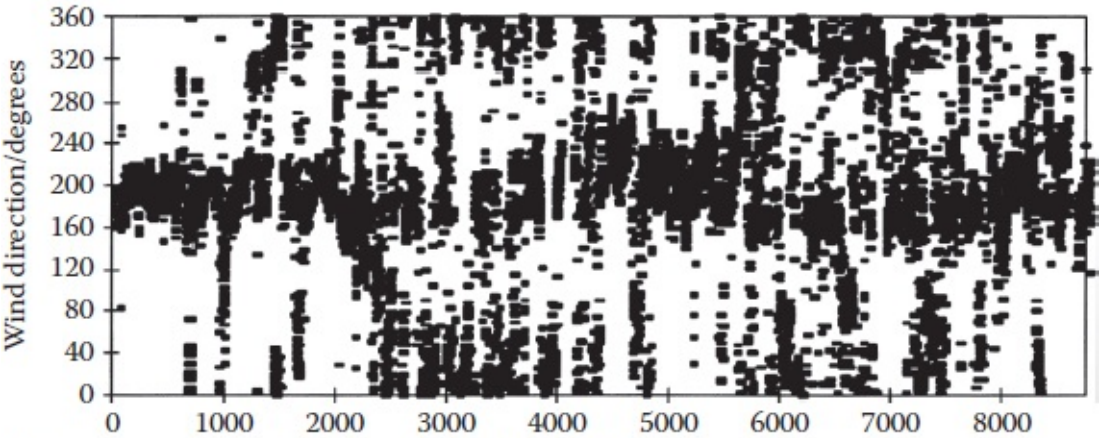

(f)

FOR REFERENCE PURPOSES ONLY

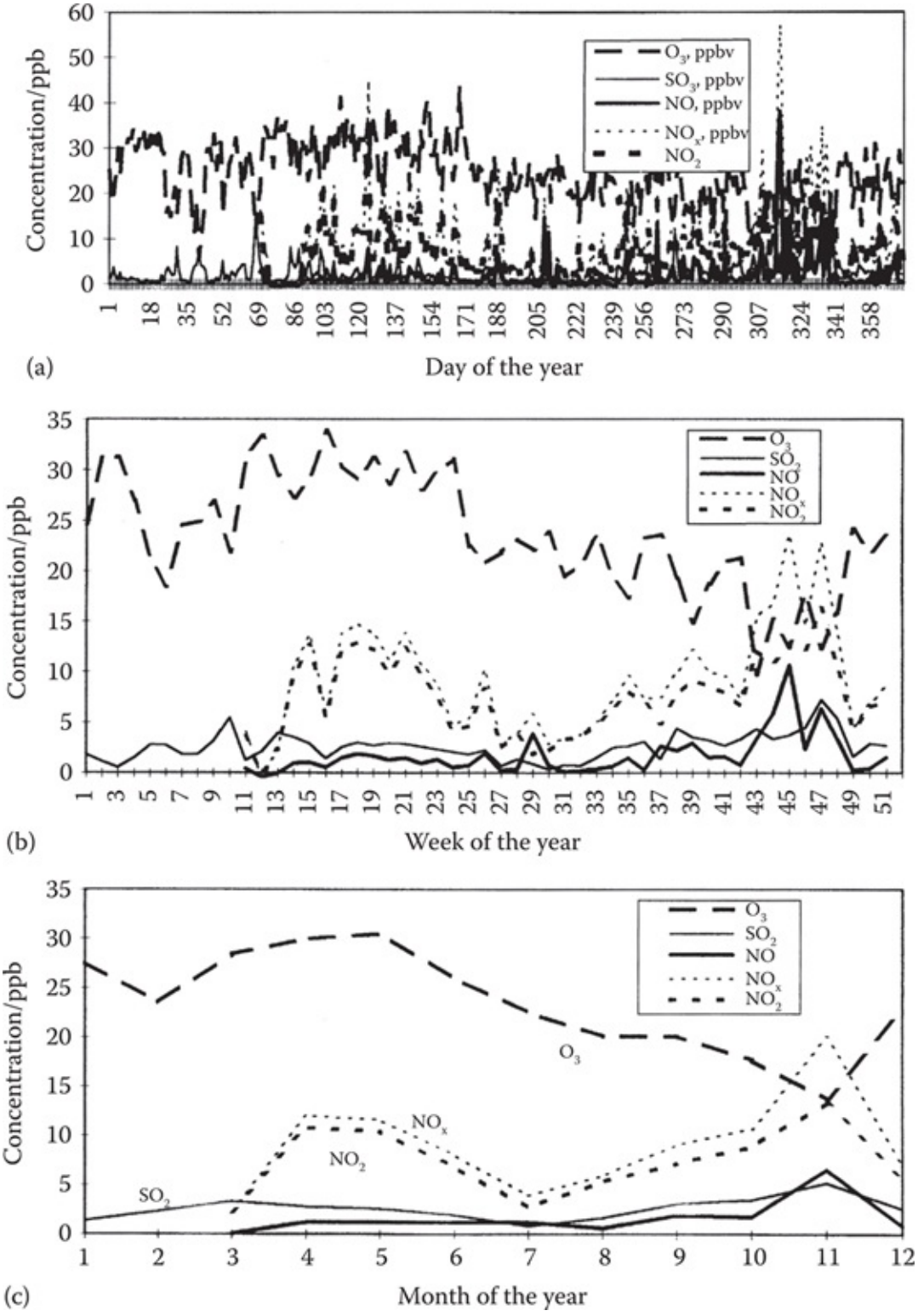

Figure 6.19 Time series of: (a) daily, (b) weekly and (c) monthly means of the monitored data set.

6.7.3 Roses

In Chapter 8 we discuss the influence of wind field, that is, speed and direction (either real data or statistical) on the modelled pollutant concentration at a point. Usually, a wind rose

approach is applied to incorporate this influence. For the monitored wind, the 360° of the compass are divided into 16 sectors of 22.5° each. The hourly means taken when the wind was from each sector were then averaged, and the values plotted in the form shown in Figure 6.20. These diagrams are known as roses or rosettes. Figure 6.20a shows that the wind direction was usually from between south and south-west, and Figure 6.20b that these were also the winds with the highest average speeds. Figure 6.20c gives the ozone rose for the year – the almost circular pattern is expected because ozone is formed in the atmosphere on a geographical scale of tens of km rather than being emitted from local sources. Hence the concentration should be relatively free of directional dependence. Sulphur dioxide, on the other hand, is a primary pollutant which influences concentrations downwind of specific sources. Figure 6.20d indicates possible sources to the north, south-east and west-north-west of the measurement site. Concentrations from the sector between south and south-west – the predominant wind direction – are the lowest. The roses for NO (Figure 6.20e) and NO_2 (Figure 6.20f) are not so well defined. These gases are both primary pollutants (dominated by NO) and secondary pollutants (dominated by NO_2). Hence we can see both patterns of directional dependence, with NO behaving more like SO_2, and NO_2 more like O_3.

6.7.4 Diurnal variations

Another way of gaining insight into pollutant occurrence is to average the concentrations according to the hour of the day. We must be careful, though, to allow for the ways in which the characteristics of the days themselves change during the year. In Figures 6.21 and 6.22, we have carried out diurnal analyses for the months of June and December, respectively. In June, the period of daylight is long and the peak solar radiation high (Figure 6.21a). The air temperature is warm (Figure 6.21b) and shows a pronounced afternoon increase in response to solar radiation. Average wind speeds are low, with convective winds increasing during daylight hours (Figure 6.21c). The ozone concentration (Figure 6.21e) shows a background level of about 23 ppb, with photochemical production increasing this concentration to a peak of 30 ppb at around 1600. The diurnal variation of SO_2 (Figure 6.21f) is quite different – there are sharp peaks centred on 1000 and 1700 which result from local emissions, and no clear dependence on solar radiation. As with the pollutant roses, the diurnal variations of NO and NO_2 are a blend of these two behaviours. Figure 6.22a, b, c, d, e, f, g, h show the corresponding variations during December. Typical of temperate Europe, the days are short and solar energy input is at a minimum during the winter months. Air temperatures are low and barely respond to the sun, wind speeds are higher and almost constant through the day. As a consequence of these changes, ozone shows no photochemical production in the afternoon. Somewhat surprisingly, SO_2 has lost all trace of the 1000 and 1700 spikes, although these remain very clear for NO. The pattern for NO_2 is very similar in December and June.

FOR REFERENCE PURPOSES ONLY

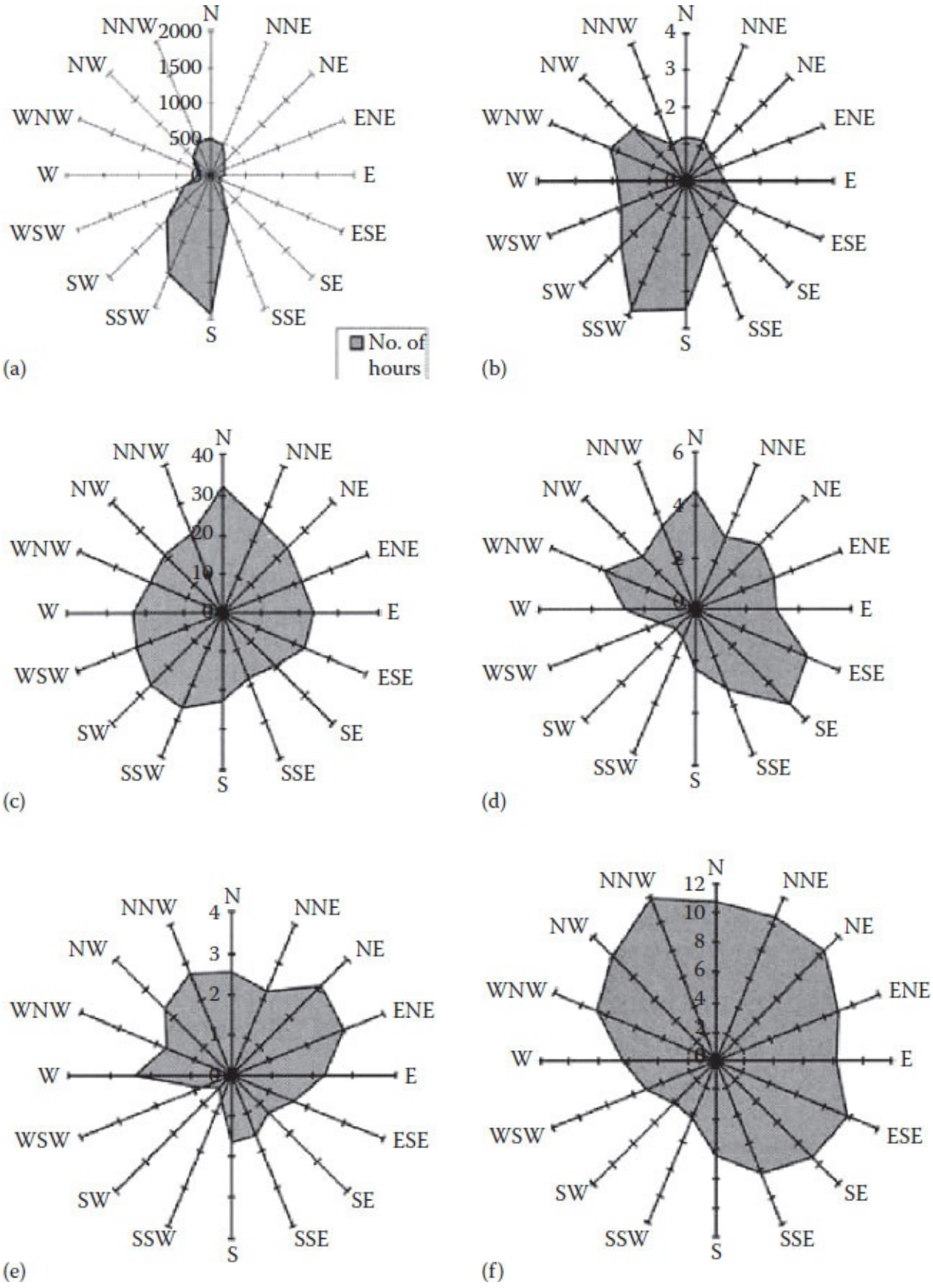

Figure 6.20 Direction roses of wind frequency, wind speed and pollutant gas concentration: (a) wind direction rose, (b) wind speed rose, (c) ozone rose, (d) SO_2 rose, (e)

FOR REFERENCE PURPOSES ONLY

NO rose and (f) NO_2 rose.

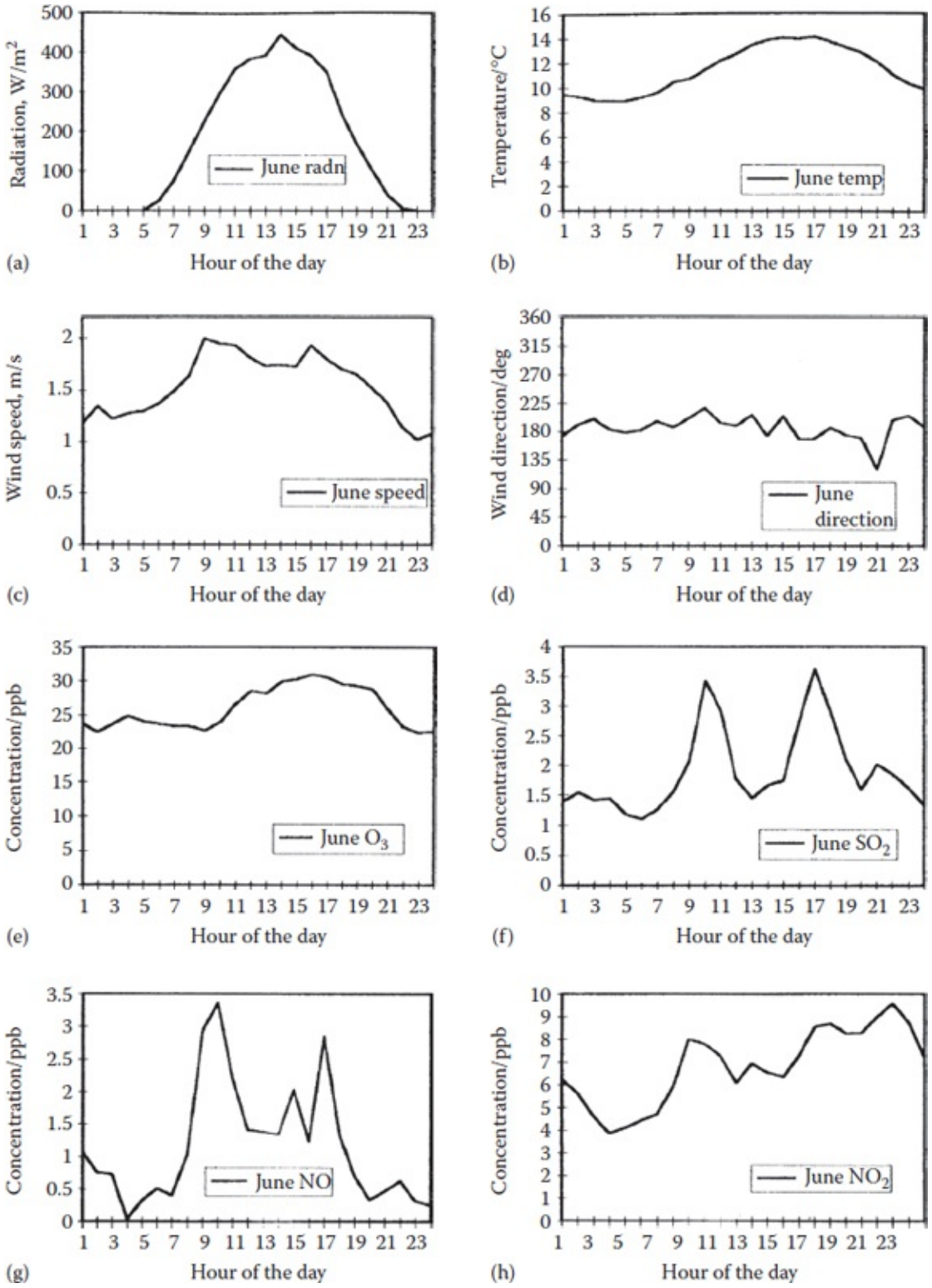

Figure 6.21 Average diurnal concentration variations during summer (June): (a) diurnal radiation, (b) diurnal temperature, (c) diurnal wind speed variation, (d) diurnal wind direction, (e) diurnal ozone variation, (f) diurnal SO_2 variation, (g) diurnal NO variation and (h) diurnal NO_2 variation.

FOR REFERENCE PURPOSES ONLY

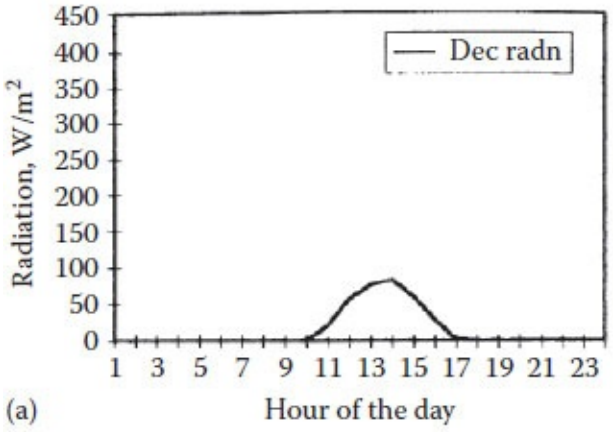

(a)

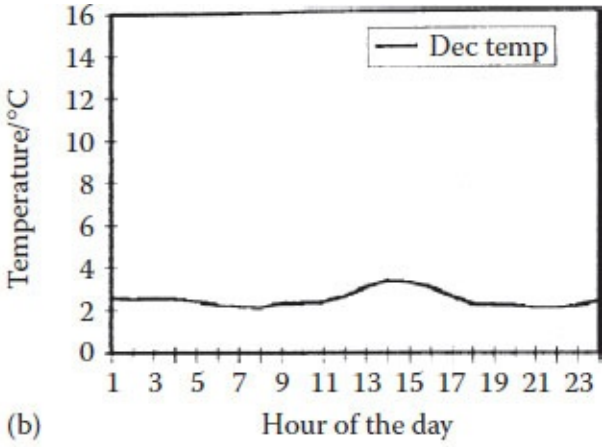

(b)

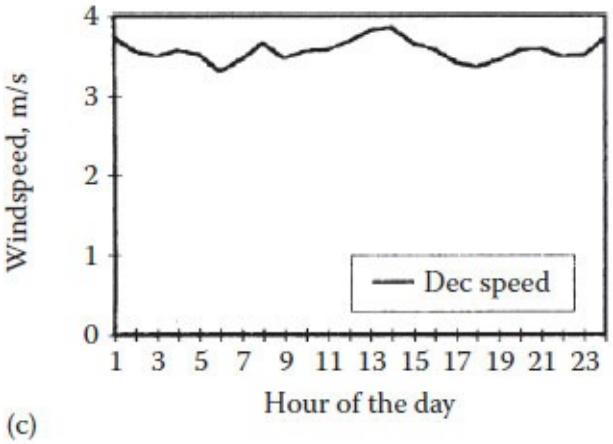

(c)

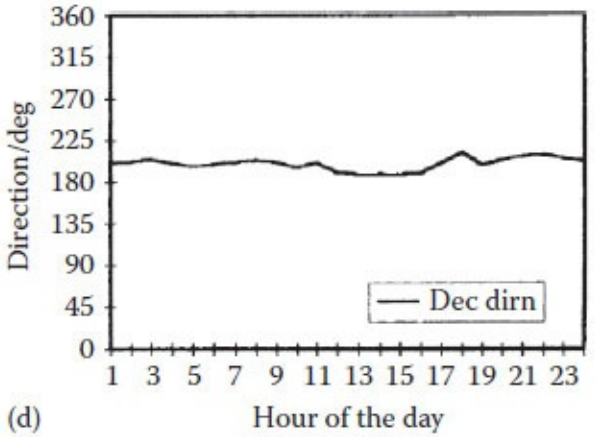

(d)

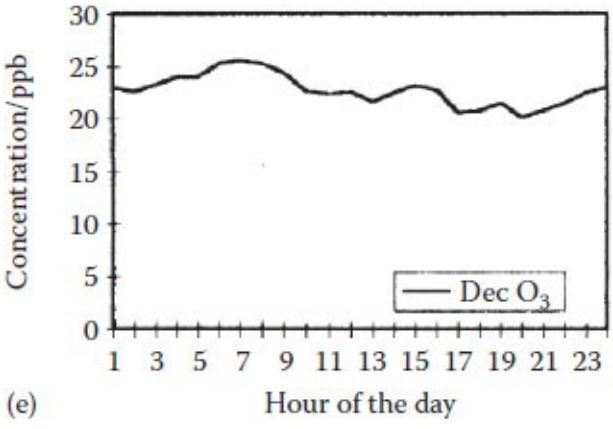

(e)

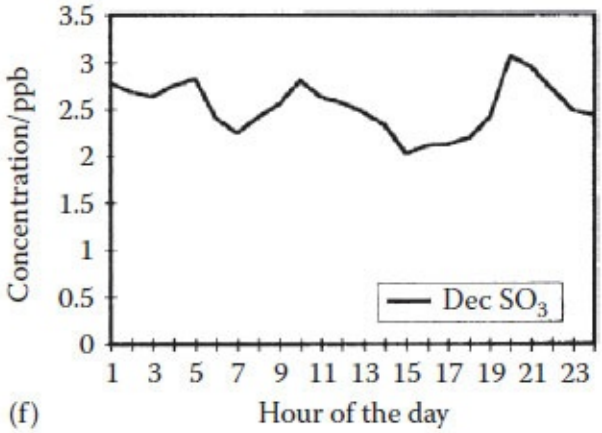

(f)

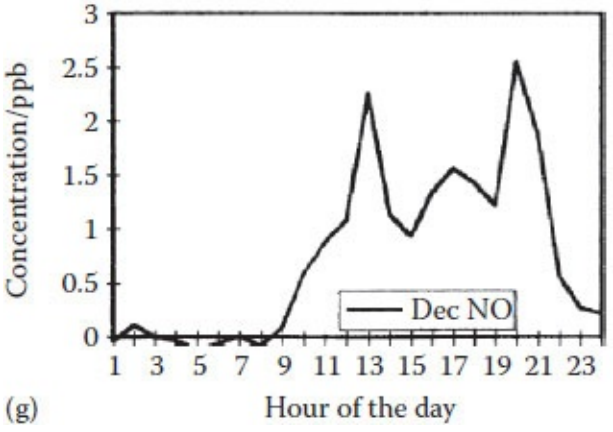

(g)

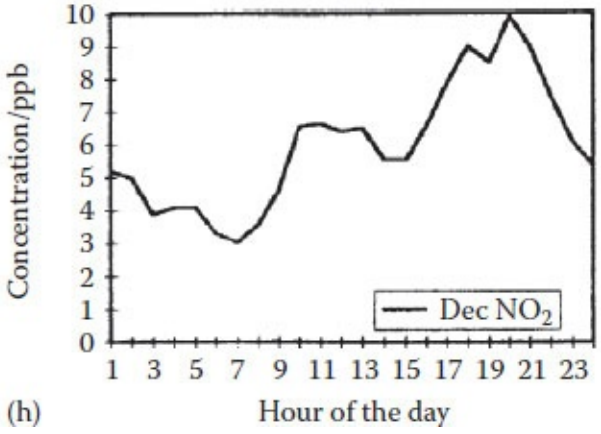

(h)

FOR REFERENCE PURPOSES ONLY

Figure 6.22 Average diurnal concentration variations during winter (December): (a) diurnal radiation, (b) diurnal temperature, (c) diurnal wind speed variation, (d) diurnal wind direction, (e) diurnal variation of ozone, (f) diurnal variation of SO_2, (g) diurnal variation of NO and (h) diurnal variation of NO_2.

6.7.5 Frequency distributions

The concentrations of air pollutants often show a log-normal frequency distribution – that is, the logarithms of the concentrations are distributed normally. We have analysed the hourly and daily means from the Centre for Ecology and Hydrology data set to confirm this. The overall range of the concentrations that occurred over the year was divided into subranges, and the number of values that fell within each subrange was counted. This is the frequency distribution. These counts were then expressed as a percentage of the total number and summed by subrange to give the cumulative frequency distribution. If the frequency distribution is log-normal, then the cumulative distribution plots as a straight line on log-probability axes. In Figures 6.23 and 6.24, the distributions for the hourly and daily means of the five gases are shown. Those for SO_2, NO and NO_x are quite linear, NO_2 less so, and O_3 not at all. The O_3 distribution is characteristic of a variable that has a significant background component – the concentration was not low for as high a proportion of the time as the log-normal form requires. Certain statistical parameters can be derived from the log-probability curves. Commonly quoted are the concentrations below which the value falls for 50% (median), 90%, 98% and 99% of the time.

The 98% value of daily means is used in European Union directives on air quality – it is equivalent to stating that the concentration should not be exceeded for more than 7 days in the year. The values indicated by Figures 6.23 and 6.24 are extracted in Table 6.7. It is clear that one such parameter alone is not sufficient to define the distribution. If the distribution is linear, we can measure the gradient, which is equivalent to the standard geometric deviation of the sample. Then the median and gradient completely define the population distribution. There are more complex formulations of the log-normal distribution that can be used to describe non-linear data sets.

FOR REFERENCE PURPOSES ONLY

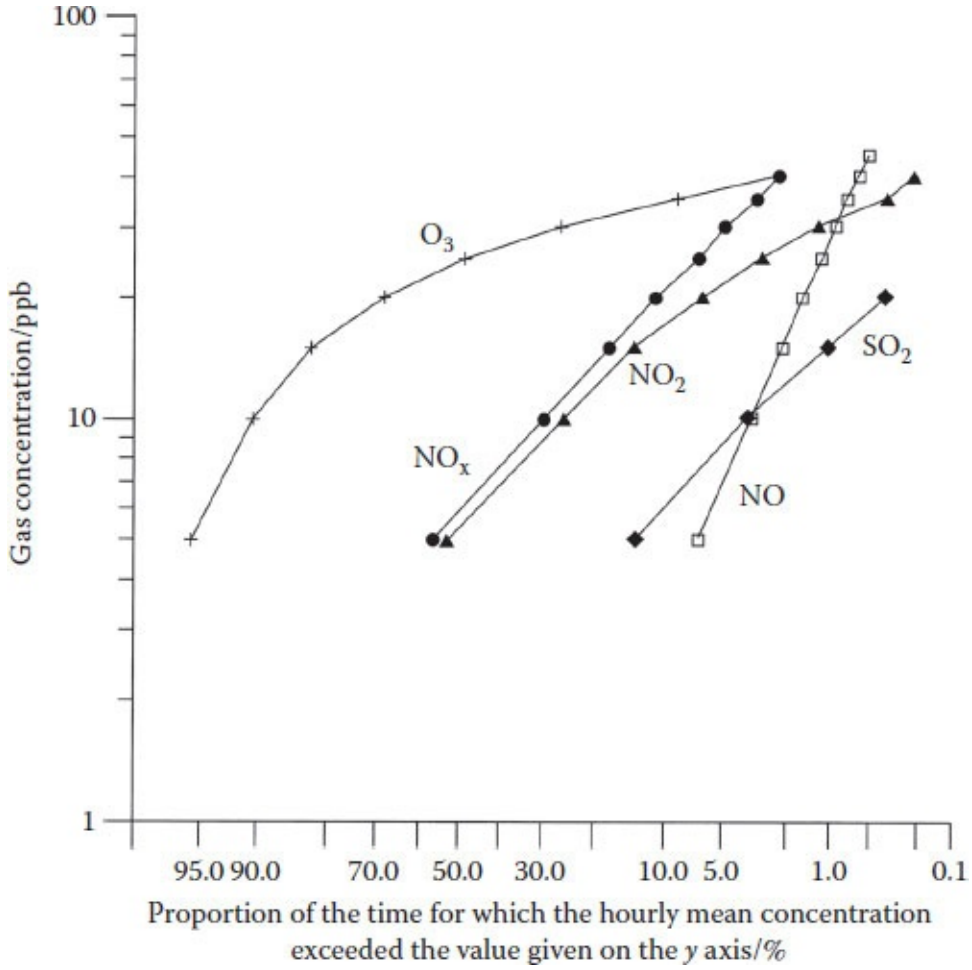

Figure 6.23 Cumulative frequency distributions of hourly mean pollutant concentrations.

FOR REFERENCE PURPOSES ONLY

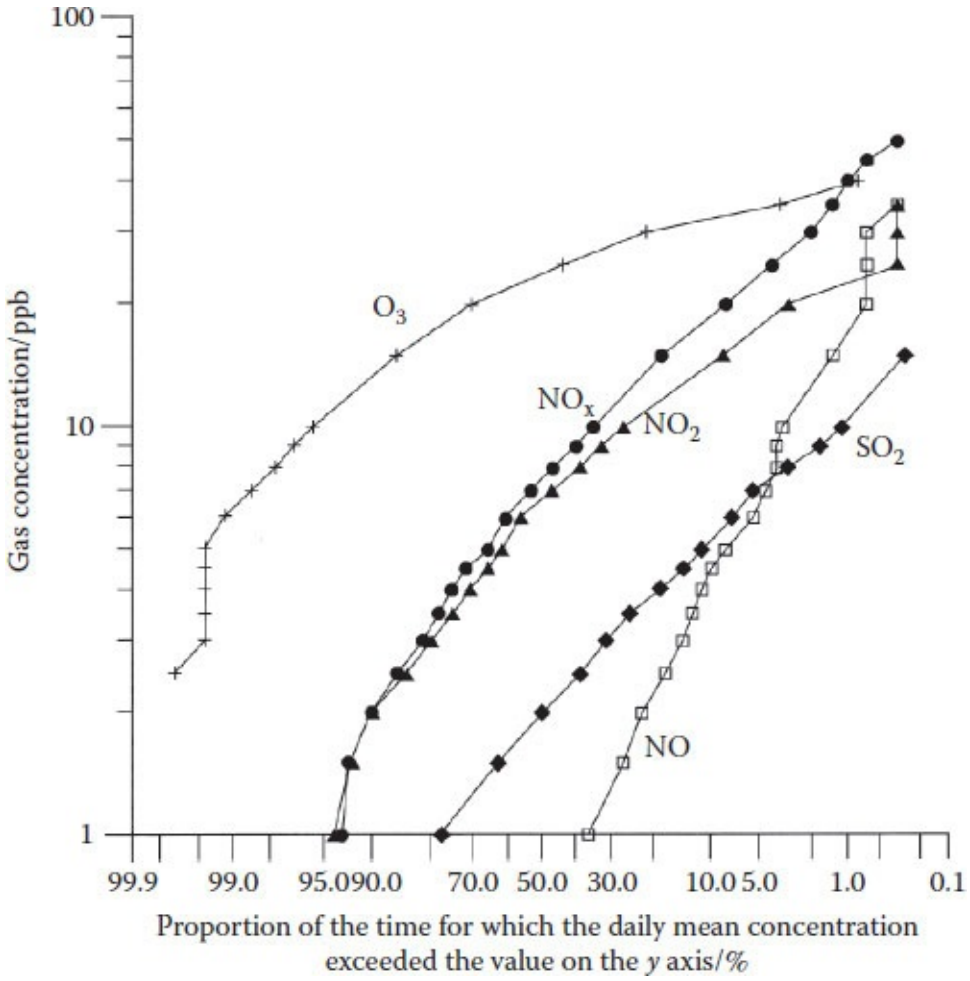

Figure 6.24 Cumulative frequency distributions of daily mean pollutant concentrations.

Table 6.7 Percentiles of hourly and daily means

Pollutant	Hourly means				Daily means			
	50	90	98	99	50	90	98	99
	(%)				(%)			
O_3	24	34	40	42	24	32	36	38
SO_2	1.5	6	13	15	2	5	9	11
NO	<1	3	16	27	<1	4	13	18
NO_x	5	21	41	56	7	18	30	39
NO_2	5	17	27	31	7	14	22	23

6.7.6 Further statistical analyses

Other standard statistical parameters can be used to describe the data. The summary statistics for the monitored data are given in Table 6.8. Finally, we can apply the ideas on the relationships between the period maxima – if the maximum 1-h concentration is $C_{max,\ 1}$

FOR REFERENCE PURPOSES ONLY

$_{h}$, and the maximum over any other period t is $C_{\max,t}$, then we should find that $C_{\max,t} = C_{\max,\ 1\ h}t^{q}$, where q is an exponent for the particular gas. For the monitored data set, the maximum values over the different averaging periods are shown in Table 6.9. Plotting log $C_{\max,t}$ against log t gives the results shown in Figure 6.25, in which the gradients of the lines give the values of q for the different gases.

Table 6.8 Summary statistics for the monitored data set

Gas	Hourly means/ppb			Daily means/ppb		Weekly means/ppb	
	Mean	Median	Standard deviation	Median	Standard deviation	Median	Standard deviation
O_3	23.6	24.7	9.2	23.8	7.4	23.4	5.8
SO_2	2.6	1.6	3.1	2.0	2.2	2.7	1.4
NO	1.7	0.3	7.5	0.7	3.7	1.3	2.0
NO_x	9.2	5.8	11.6	7.5	7.8	8.9	5.3
NO_2	7.5	5.3	6.9	6.7	5.2	7.8	27.2

Table 6.9 Values of $C_{\max,t}$ for the different pollutants

$C_{max,t}$	Pollutant				
	O_3	SO_2	NO	NO_x	NO_2
$C_{max,\ 1\ h}$	57	47	185	186	72
$C_{max,\ 1\ day}$	43	16	38	57	37
$C_{max,\ 1\ week}$	34	7	11	24	16
$C_{max,\ 1\ month}$	31	5	7	20	13
q	−0.095	−0.35	−0.51	−0.35	−0.27

FOR REFERENCE PURPOSES ONLY

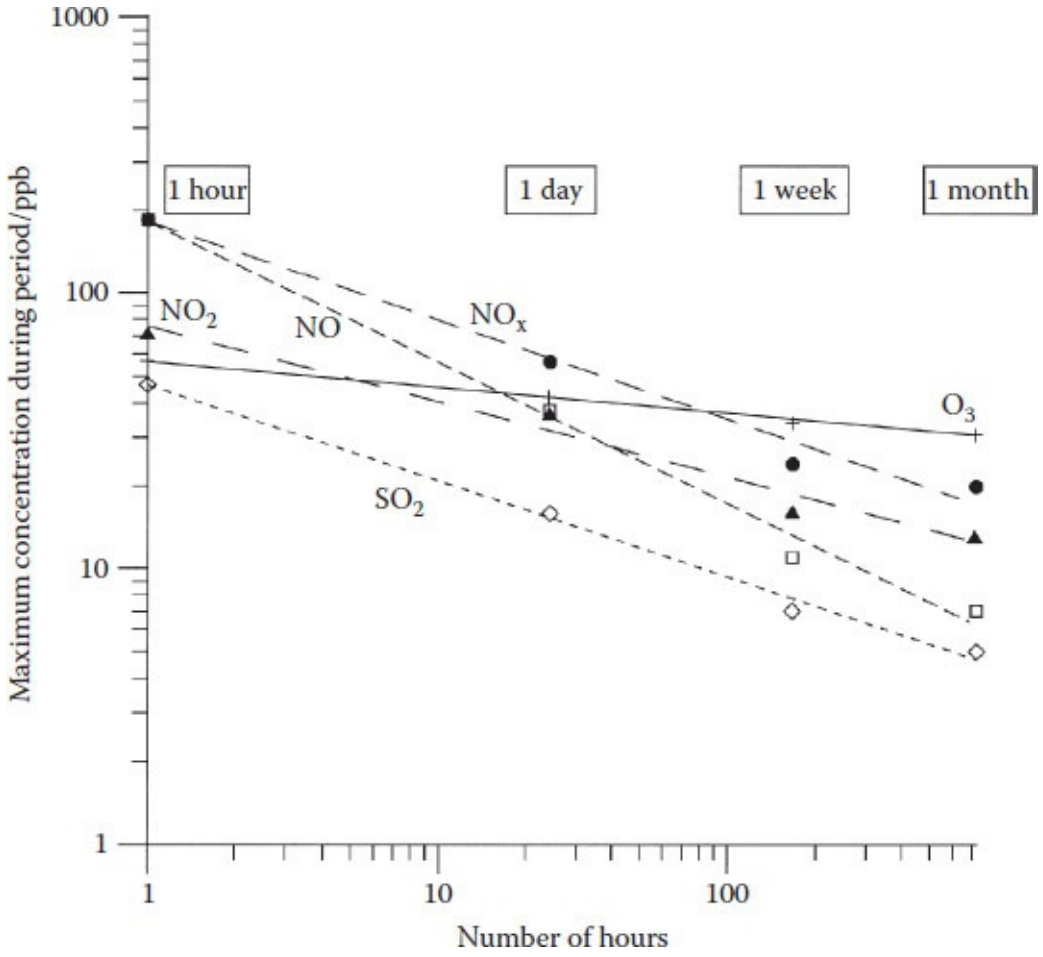

Figure 6.25 Correlations between the maximum period average and the averaging period.

6.8 EFFECT OF FIREWORKS ON AMBIENT AIR QUALITY

Fireworks were first introduced to the UK from China in the 1300s. They are used as a form of entertainment and create noise, heat, light and colour in the night sky when the gunpowder they contain explodes, sending their mixture of different chemicals burning through the air. Fireworks and firecrackers are always associated with positive occasions in life, with joy, victory, happiness and celebrations. Whilst fireworks have been used for many years to delight crowds of people, their effects on air quality, human health and the environment are only recently becoming clear. This is also a major activity observed during the Diwali festival in India and other parts of the world.

6.8.1 The art and science of fireworks

Fireworks are a class of low-explosive pyrotechnic devices used for aesthetic and entertaining purposes as part of a fireworks display. Fireworks can be generally classified

FOR REFERENCE PURPOSES ONLY

as to where they perform (a ground or aerial firework) and according to BS 7114 into four categories:

- *Category 1*: Indoor fireworks for use in small areas.
- *Category 2*: Garden fireworks which must be safely viewable from 5 m without debris scattering beyond 3 m.
- *Category 3*: Display fireworks that should be safely viewable from 25 m and must not scatter debris beyond 50 m.
- *Category 4*: Professional fireworks that may be used by individuals or companies that have a proof of adequate insurance and storage to purchase and use these fireworks.

There are a number of traditional types of fireworks, well known and popular all over the world:

- *Peony*: A spherical break of coloured stars that burn without a tail effect.
- *Chrysanthemum*: A spherical break of coloured stars that leaves a visible trail of sparks.
- *Willow*: Long-burning silver or gold stars that produce weeping willow-like effect.
- *Palm*: A burst of colours producing a palm tree–like effect, sometimes with a different colour inside the tree simulating coconuts.
- *Kamuro*: An intense eruption of silver or gold stars which leave a heavy glitter trail.
- *Spider*: Appears as a series of radial lines creating a spider-like effect.
- *Horsetail*: A heavy long-burning tail that only travels a short distance and falls freely to the ground in the shape of a waterfall.
- *Catherine wheel*: Rotates quickly, producing a display of sparks and coloured flame.
- *Mine*: Bursts near the ground, expelling stars into the sky.
- *Roman candle*: A long tube containing several stars which fire at a regular interval.
- *Fountain*: Cone-shaped firework that shoots coloured sparks into the air.
- *Rocket*: Contains a thunder flash or coloured stars that leave a graceful trail of sparks. There are also screechers, whistlers and maroon–type rockets with exploding heads.

Due to their fantastic explosions and the brilliant light displays, fireworks are enjoyable and welcomed all over the world. However, these spectacles are much more than just a form of entertainment. Each firework launched into the sky is a precisely formed assembly of chemicals and fuel, carefully calibrated to produce a particular effect. Understanding how the contents of a firework produce the impressive variety of colours, forms, and sound intensities requires understanding the science that lies behind fireworks, in other words, physics and chemistry.

FOR REFERENCE PURPOSES ONLY

6.8.2 The physics of fireworks

Fireworks generate three very noticeable forms of energy: an incredible release of sound; bright, intensely coloured light; and heat. The loud bangs heard at ground level are the result of the rapid release of energy into the air, causing the air to expand faster than the speed of sound. This produces a shock wave known as a sonic boom. The colours are produced by heating metal salts, such as sodium nitrate and calcium chloride, which subsequently emit characteristic colours. The atoms of each element absorb energy and release it as light of specific colours. The energy absorbed by an atom rearranges its electrons from their lowest-energy state, called the ground state, up to a higher-energy state, called an excited state. The excess energy of the excited state is emitted as light, as the electrons descend to lower-energy states, and ultimately the ground state. The amount of energy emitted is characteristic of the element; therefore the amount of energy determines the colour of the light emitted. For example, when sodium nitrate is heated, the electrons of the sodium atoms absorb heat energy and become excited. This high-energy excited state does not last for long, and the excited electrons of the sodium atom quickly release their energy (approximately 200 kJ/mol), which is the energy of yellow light.

Table 6.10 The chemicals responsible for the colours generated by fireworks

Colour	*Compound*	*Wavelength (nm)*
Red	Strontium salts, for example, strontium carbonate (bright red) Lithium salts, for example, lithium carbonate (red)	600–700
Orange	Calcium salts, for example, calcium chloride	591–608
Yellow	Sodium salts, for example, sodium chloride	589
Green	Barium compounds + chlorine producer, for example, barium chloride	505–535
Blue	Copper compounds + chlorine producer, for example, copper(I) chloride	435–480
Purple	Mixture of strontium (red) and copper (blue) compounds	380–430
Silver	Burning aluminium, titanium or magnesium	

Source: Conkling, A. J., *Chemistry of Pyrotechnics*, Marcel Dekker, New York, 1985.

The amount of energy released, which varies from element to element, is characterised by a particular wavelength of light. Higher energies correspond to shorter wavelength light, whose characteristic colours are located in the violet/blue region of the visible spectrum. Lower energies correspond to longer wavelength light, at the orange/red end of the spectrum. The colours are produced by elements with the characteristic emissions listed in Table 6.10.

During the manufacture of fireworks, metal salts are put into stars, small clay or dough-like lumps or cubes 3–4 cm in diameter. Stars consist of a blend of oxidising agent, reducing agent, colouring agent (metal salt) and binders. When ignited, the stars produce both sound and light effects.

From lift-off to colour release, a carefully choreographed sequence of events takes place

FOR REFERENCE PURPOSES ONLY

in order to produce the desired effects. The power needed to lift each firework into the air is provided by the highly exothermic combustion of black powder, a slow-burning combination of 75% potassium nitrate, 15% charcoal, and 10% sulphur. Gunpowder or black powder was invented in China by alchemists experimenting with a naturally occurring salt, potassium nitrate, also known as saltpetre. Said to have first been used in China about 1000 years ago, the recipe for black powder has undergone little change since then. This formulation explodes at a rate of about 3 ms^{-1}, classifying it as a low explosive. In fact, when it burns in the open air, black powder's heat and gas dissipate quickly. The key to fireworks' success is to trap the heat and gas in the bottom of the shell, which is positioned in a launch tube or mortar, until the trapped gas pressure builds to such a force that, when it escapes, it hurls the firework high into the air.

A firework is ignited by lighting the main fuse, which simultaneously starts both the fast action fuse, which quickly carries the flame down to the lift charge, and the time delay fuse, which continues to burn upward toward the cardboard compartments containing the stars, even as the firework is hurtling skyward. The black powder lift-charge is calculated to exhaust itself precisely when the slow-burning, time-delay fuse reaches the first compartment packed with light-producing stars and black powder. This happens when the firework is at the very apex of its upward flight. Simultaneously the fuse sets off sound-producing explosives and detonates the stars, initiating colour emission. If the timing of the fuses is off, however, the firework may detonate early, too close to the ground, or late, when the firework is falling back to Earth.

6.8.3 The chemistry of fireworks

The chemistry of fireworks is based on the simple theory of combustion. The composition inside the firework must contain six vital ingredients, as shown in Figure 6.26.

For about 500 years black powder or fuel enjoyed dominance as a propellant, explosive and igniter and, as the major firework ingredient, its use remains unsurpassed. The prime reason for the longevity of black powder is its *quickness*, even at relatively low pressures, and this is brought about by manufacturing techniques and the chemical reactivity of the constituents (Russell, 2000).

Various oxidising agents[1] are used in both the black powder and the stars, including nitrates, chlorates, and perchlorates. The most commonly used oxidising agents are nitrates, the major component of black powder. Nitrates are composed of nitrate ions (NO_3^-) with metal ions. The most common oxidiser is potassium nitrate, which decomposes to potassium oxide, nitrogen gas, and oxygen gas:

$$2KNO_{3\,(s)} \rightarrow K_2O_{(s)} + N_{2\,(g)} + 2.5O_{2\,(g)}$$

When reacting, nitrates release two of their three oxygen atoms. Because the oxidation does not result in the release of all available oxygen, the reaction is not as vigorous as that of

FOR REFERENCE PURPOSES ONLY

other oxidisers and is more controlled. This is why nitrates are used as the major component of black powder. In fireworks their main purpose is to provide the initial thrust to power the package into the sky and to ignite each bundle of stars. Nitrates are usually not used in star explosions because reactions of nitrates do not produce a temperature high enough to energise many of the more colourful metal salts.

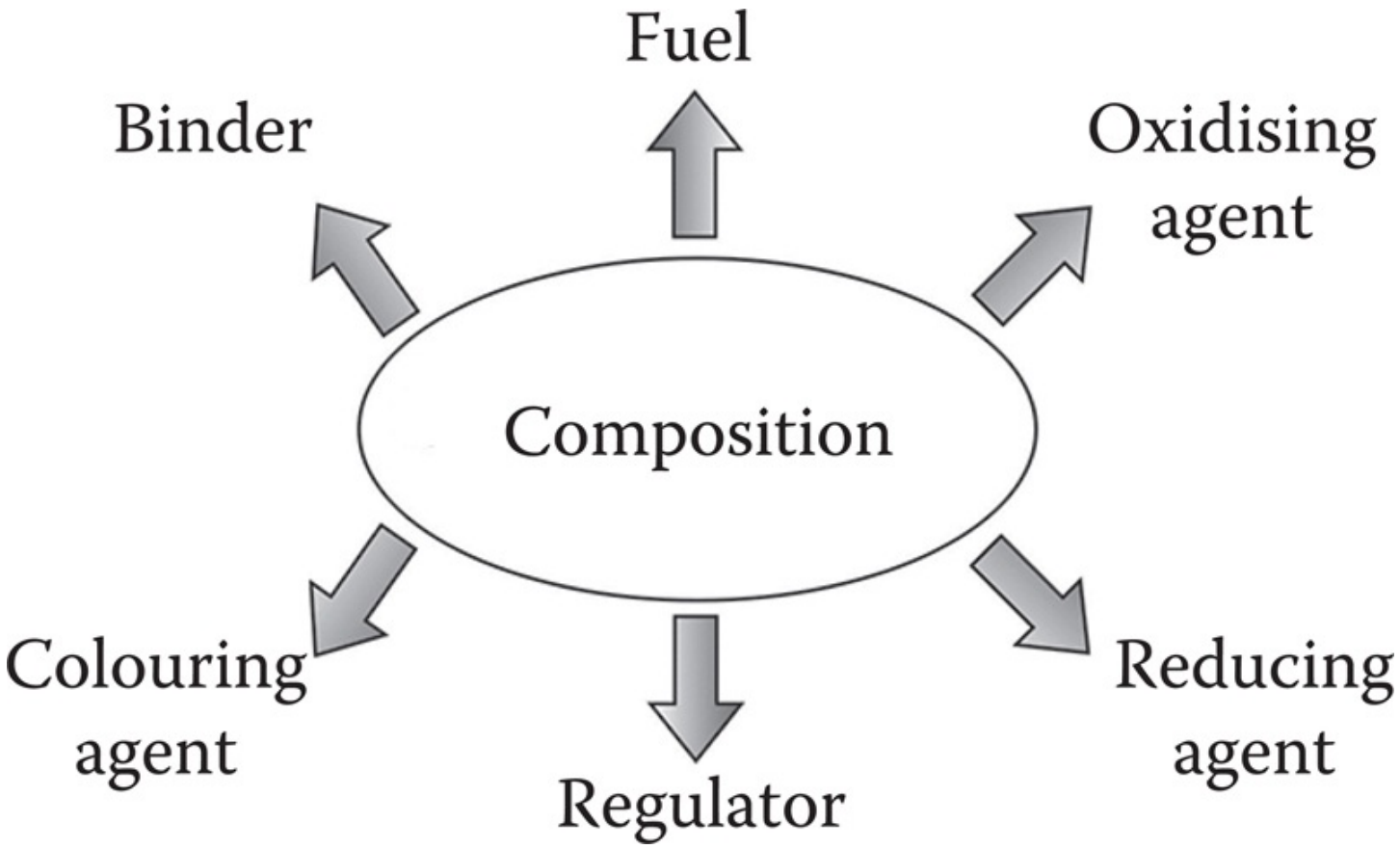

Figure 6.26 Typical composition of fireworks.

In the 1830s, Italian fireworks makers found a group of more explosive oxidisers, which produced temperatures of 1700°C–2000°C and made possible the creation of much more intense colours. These oxidisers are the chlorates, which contain the chlorate ion (ClO_3^-), and they give up all their oxygen upon reaction:

$$2KClO_{3\,(s)} \rightarrow 2KCl_{(s)} + 3O_{2\,(g)}$$

This results in a much more intense and spectacular reaction. These chlorates have the disadvantage of being less stable than nitrates and are therefore more dangerous to handle. Chlorate compounds sometimes can be detonated just by dropping them on the ground. This instability results because, although the chlorine atom has the potential to bond with four oxygen atoms, in chlorates it bonds with only three, leaving the chlorine atom unsaturated and reactive. The complete release of its oxygen atoms makes chlorate a better oxidising

agent than nitrate. Unlike nitrate-containing compounds that produce a relatively slow burning rate, the oxidation by chlorates produces a much faster detonation – an explosion. In recent years, fewer fireworks manufacturers are using chlorates. Instead, perchlorates are now more commonly used because of their increased stability and oxygen release.

Perchlorates contain the perchlorate ion (ClO_4^-), in which each chlorine atom is bonded to four oxygen atoms. The chlorine is bonded to its maximum number of oxygen atoms, and so perchlorates are more stable than chlorates. Yet perchlorate is able to release all four of its oxygen atoms:

$$KClO_{4\,(s)} \rightarrow KCl_{(s)} + 2O_{2\,(s)}$$

Thus perchlorates are not only more stable, they are also more oxygen-rich than chlorates. They, similar to chlorates, produce more vigorous reactions than nitrates. The oxygen released by nitrates, chlorates, and perchlorates in the star compartments immediately combines with the reducing agents to produce hot, rapidly expanding gasses.

The most common reducing agents[2] are sulphur and carbon (charcoal) – standard components of black powder – which react with oxygen to produce sulphur dioxide and carbon dioxide, respectively.

$$O_{2(g)} + S_{(s)} \rightarrow SO_{2(g)}$$

$$O_{2(g)} + C_{(s)} \rightarrow CO_{2(g)}$$

The reactions that produce these gases also release a great deal of heat energy, so not only are the gases produced rapidly, they are hot and rapidly expanding gases. This adds to the explosive force of the reaction.

6.8.4 Pollutants associated with fireworks and bonfires

Fireworks are one of the most unusual sources of pollution in atmosphere; although transient, these pollution episodes are responsible for high concentrations of particles (especially metals and organic compounds) and gases. Burning of fireworks releases pollutants, such as sulphur dioxide (SO_2), nitrogen dioxide (NO_2), carbon dioxide (CO_2), carbon monoxide (CO), suspended particles (including particles below 10 mm in diameter, i.e. PM_{10}) and several metals such as aluminium, manganese and cadmium, which are associated with serious health hazards. In addition, firecrackers often result in serious accidents and lethal injuries. The full composition and the relative concentration of the various gaseous vapours and particulate pollutants emitted is not known. However, SO_2, NO_2 and particulate matter (specially PM_{10}) are of special interest, as they are known to be potentially injurious to the respiratory passages and to have other health effects.

Wang et al. (2007) state that primary components peak on Bonfire Night whilst

FOR REFERENCE PURPOSES ONLY

secondary component concentrations rise later. In terms of aerosols (suspended particles in a gas) produced by fireworks, primary aerosols are usually found in the fine phase, whilst secondary aerosols are coarse particles. High levels of Cu, Sr, Ba, Sb, K and Pb are typical of firework aerosols (Moreno et al., 2007; Vecchi et al., 2007), with Ba becoming 1091 times higher after a firework festival than on the previous day (Parkhi et al., 2016). Such concentrations are higher than those at industrial sites. The pollution episodes associated with firework displays are very concentrated and are large contributions to yearly metal emissions (Moreno et al., 2007). Wang et al. (2007) found that fireworks produced more than 90% of the total yearly mineral aerosol emissions in Beijing on Lantern Night.[3]

During the Bonfire Night period, furan and dioxin concentrations can rise by a factor of 4 (Dyke et al., 1997); these are particularly produced when blue-lightning fountains and rockets are set off (Fleischer et al., 1999). As well as the fireworks themselves, the bonfires can also create dioxins through wood combustion. Dioxins are produced by bonfires, with up to 14% of emissions produced during this period alone. Not only wood is burnt on bonfires. Fuels such as diesel or petrol may be used to start a fire and toxic substances like those found in old tyres or other rubber or plastic materials used to sustain it. Burning such kind of materials in the open can produce large quantities of smoke, toxic compounds and gases. Composition of the waste gases and material carried over depend on the material burnt, combustion conditions and local atmospheric conditions. As the burning on bonfires is not controlled, combustion can be very poor due to low flame temperatures, incomplete mixing of fuel and oxygen or low residence times at high temperatures. Once burnt, the surrounding soil is also contaminated with these pollutants, and water used to control the fire or rainfall causes pollutants to run off into nearby watercourses.

6.8.5 Effects on health

The colours formed, the launch method and type of gunpowder used all influence the toxicity of fallout from the combustion of fireworks. For example, green colours are produced by radioactive barium, and the cadmium that is also used to produce colouring is both toxic and carcinogenic.

The consequences of long-term exposure to low concentrations of toxins are unknown. However, studies have shown that existing health concerns can be aggravated. For example, smog can be produced during a cold bonfire night and this may negatively affect those patients with diseases of the lung, nervous system or heart (Ravindra et al., 2003). At one location in Hawaii, the number of total suspended particles (TSPs) in the lung-penetrating size range rose by 700% after New Year's Eve (Bach et al., 1975).

PM_{10} can easily penetrate the lungs, with higher concentrations in the air resulting in higher quantities being inhaled (Ravindra et al., 2003). Bonfire Night can lead to concentrations of PM_{10} in the moderate band where the UK Air Quality Archive website states, 'mild effects, unlikely to require action, may be noticed amongst sensitive individuals'. Particulate matter is responsible for up to 10,000 deaths each year according

FOR REFERENCE PURPOSES ONLY

to a *New Scientist* article from 1994, where 'every increase of 10 μg of PM_{10} in a cubic meter of city air raises death rates from respiratory diseases such as bronchitis and asthma by more than 3%, and raises deaths from heart diseases by more than 1%' (Table 6.11). An increased PM_{10} concentration is also known to reduce children's peak expiratory flow. In addition to affecting existing cardiovascular and respiratory problems, PM_{10} can contribute to cancer, alter host defence and lead to an early death (Ravindra et al., 2003).

Table 6.11 Combined effect estimates of daily mean particulate pollution

Health impacts	*Change (%) in health indicator per each 10 μg m^{-3} increase in PM_{10}*
Increase in daily mortality	
Total deaths	1.0
Respiratory deaths	3.4
Cardiovascular deaths	1.4
Increase in hospital usage (all respiratory diagnoses)	
Admissions	1.4
Emergency department visits	0.9
Exacerbation of asthma	
Asthmatic attacks	3.0
Bronchodilator use	12.2
Emergency department visit	3.4
Hospital admissions	1.9
Increase in respiratory symptom report	
Lower respiratory	3.0
Upper respiratory	0.7
Cough	2.5
Decrease in lung function	
Forced expiratory	0.15
Peak expiratory flow	0.08

Source: Ravindra, K. et al., *J. Environ. Monit.*, 5, 260–264, 2003.

The combination of high SO_2 and high PM_{10} levels associated with Bonfire Night is unfortunate as the SO_2 can adsorb to the PM_{10} and therefore enter the lungs. This complex is acidic and has a long residence time and so damages the tissues of the lungs. SO_2 alone aggravates emphysema and other respiratory diseases particularly at values above 2.1 mg m^{-3}. However, concentrations at this level are typically not seen after Bonfire Night.

Most health effects of NO_2 are respiratory, with concentrations as low as 376–565 μg m^{-3} causing bronchoconstrictors to become more responsive (Ravindra et al., 2003). It increases flow resistance and may lead to oedema or emphysema and in some cases makes individuals more susceptible to asthma through affecting nasal skin. However, as with SO_2, even after Bonfire Night, NO_2 values typically remain in the low-banding system, being in

index 1 (0 – 96 μg m^{-3}) where according to the UK Air Quality Archive website 'effects are unlikely to be noticed even by individuals who know they are sensitive to air pollutants'. As an indirect effect of Bonfire Night, firework makers can experience increased concentrations of Cr, Mn and Mg and therefore experience headaches and dizziness (Sukumar and Subramanian, 1992). Dioxins are also produced from bonfires and fireworks, and may cause cancer.

As well as the pollutants themselves, fireworks and bonfires can cause physical injuries to people such as burns. During the Bonfire Night period of 2003, 1136 people went to hospital to receive treatment for injuries from fireworks (NSCA). The noise produced is also a problem, particularly for the young and elderly, and the smoke produced can decrease visibility leading to accidents and annoyance. To control noise created by fireworks, the Firework Regulations Act of 2004 states that throughout the year fireworks are permitted only before 11 pm with a number of exceptions, including Bonfire Night when restrictions are extended until midnight.

Firework chemicals, particularly heavy metals, can contaminate water bodies. The fireworks chemicals can also harm buildings and vegetation through the formation of acid rain. Many consumer fireworks also leave behind both degradable and non-degradable items in the form of solid debris. These remains can contain up to 142 ng 1-TEQ/kg of octa-chlorinated dioxins. Dioxins, even at low concentrations, can be toxic to animals and bioaccumulate through the tropic levels. It is not just the pollutants associated with Bonfire Night that can be harmful to animals. Over 25,000 were injured or killed in 2004 because of fireworks. Some of these deaths are the result of physical contact with the bonfire or fireworks (e.g. hedgehogs being burnt in a bonfire in which they have entered to sleep), whilst others are a result of the noise. Loud bangs can startle animals, and aborted young are also known to result from this trauma.

6.8.6 Effects on the local air quality

To illustrate the impact of Bonfire Night and activities leading up to it on local air quality, we shall look at three cities in the south of England. Portsmouth and Southampton are coastal cities that experience similar meteorological conditions, whilst Reading is an inland city just to the north of the south coast. Hourly air quality data for urban sites in each city during 2011 and 2012 was obtained from the UK Automatic Urban Network website. Data was then filtered to display only 1–11 November; larger fireworks displays likely occur at weekends, therefore by choosing these dates, weekends preceding and succeeding Bonfire Night will be captured in the study. Time-series plots for PM_{10} and NO_2 during 1–11 November for 2011 and 2012 are shown in Figures 6.27 and 6.28, respectively. They show noticeable peaks for PM_{10} on days around 5 November, most notably at weekends. All major peaks in PM_{10} concentrations occur in the evening.

FOR REFERENCE PURPOSES ONLY

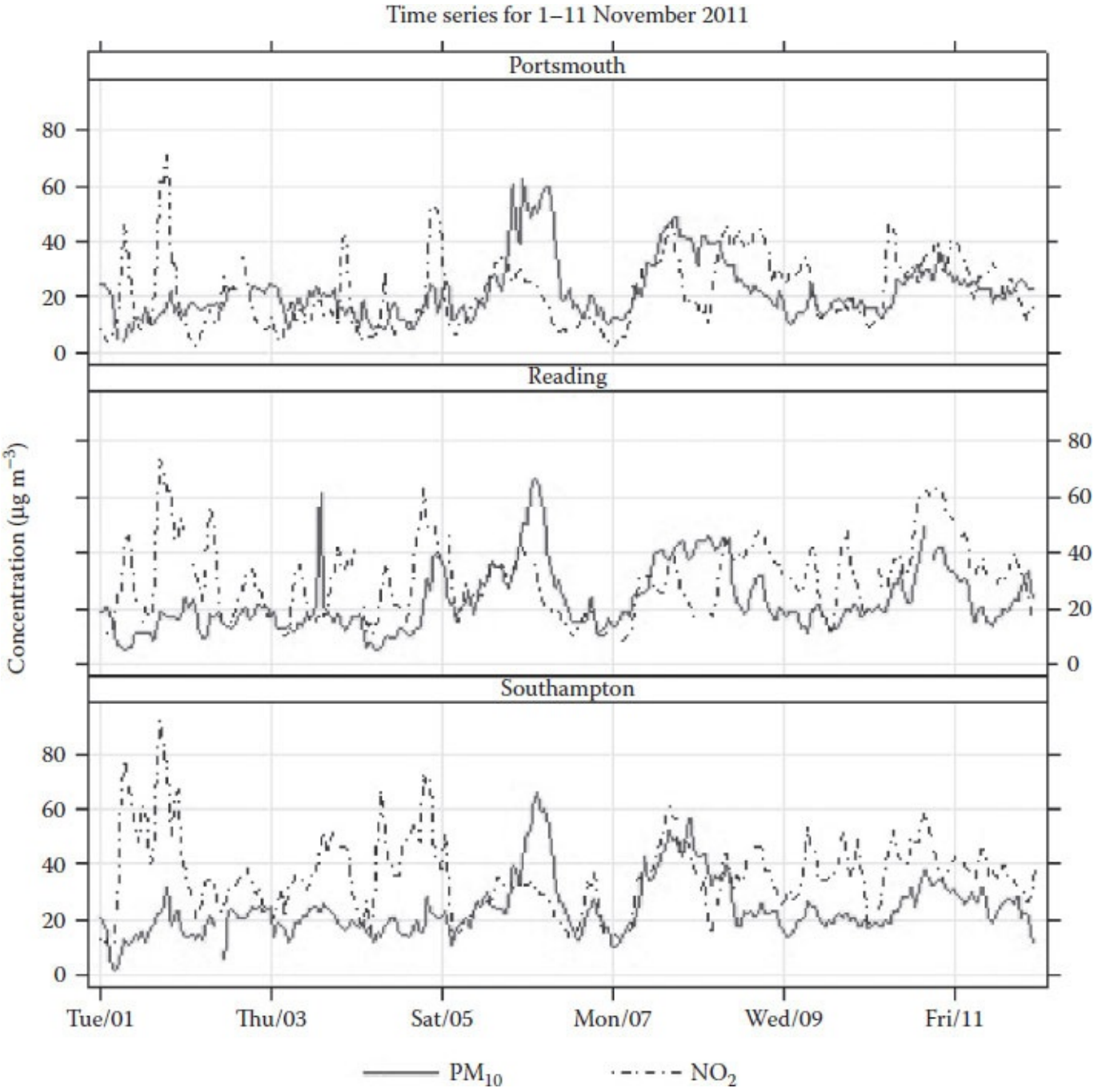

Figure 6.27 Time-series plot showing the hourly concentrations of PM_{10} and NO_2 for the three sites during 1–10 November 2011.

FOR REFERENCE PURPOSES ONLY

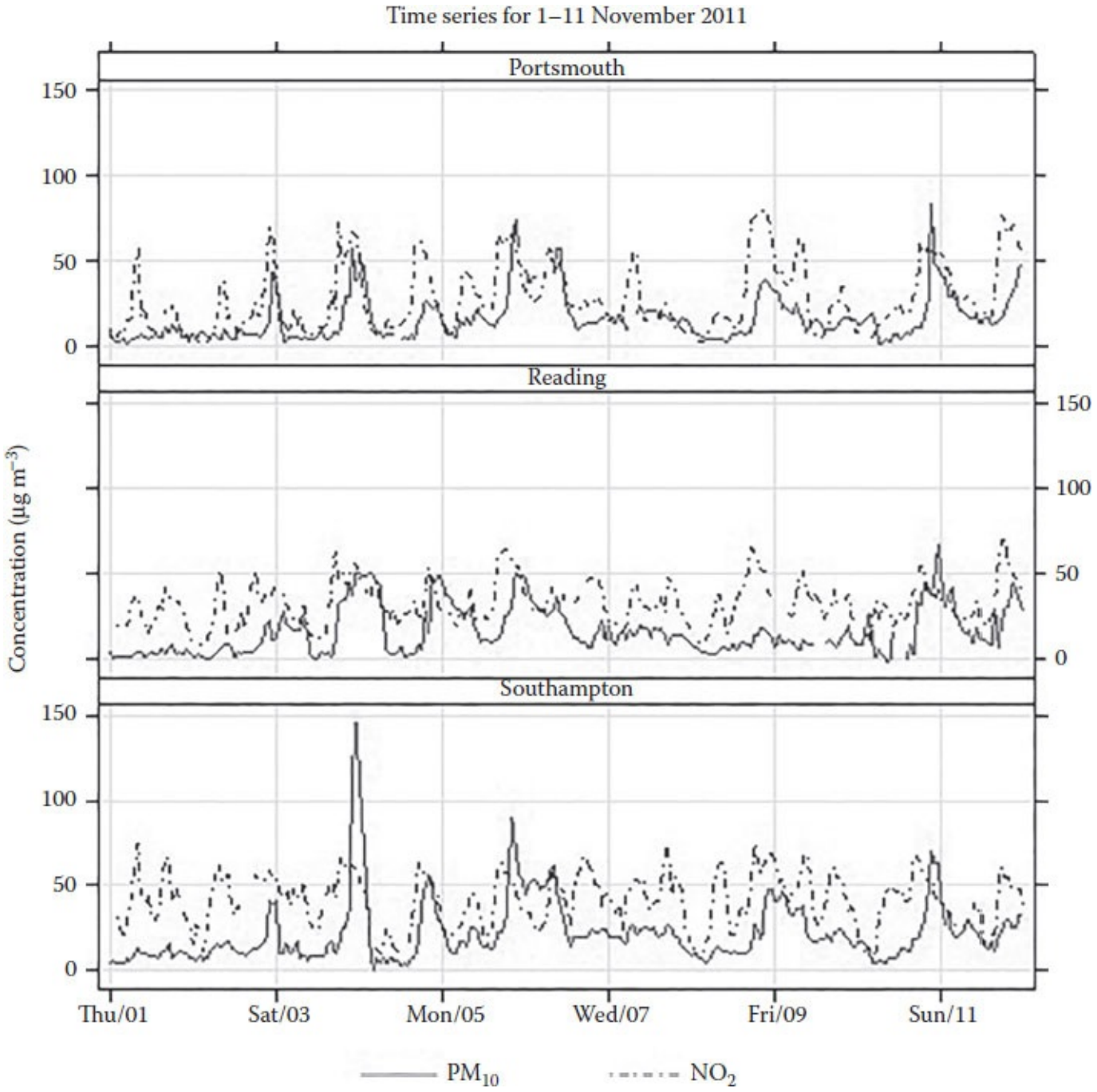

Figure 6.28 Time-series plot showing the hourly concentrations of PM_{10} and NO_2 for the three sites during 1–10 November 2012.

6.9 CASE STUDY: BUNCEFIELD OIL STORAGE DEPOT DISASTER

The Buncefield Oil Storage Depot disaster in Hertfordshire, UK, was considered one of the most catastrophic events in recent European history since World War II because of the sheer scale of the explosive emissions. The majority of the oil depot located close to the M1

motorway leading to London was comprehensively damaged by a series of explosions and fires that started at approximately 6 am on Sunday, 11 December 2005, but by midday on 12 Monday, 10 of the 20 tanks on the site were affected by the blast. According to the UK Health and Safety Laboratory, the primary cause of the incident was found to be the overfilling of a tank containing unleaded petrol causing the malfunction of the tank control and alarm systems, resulting in the escape of 250,000 L of fuel. Eventually, large quantities of petrol overflowed from the top of the tank. A vapour cloud formed which ignited, causing a massive explosion and a fire that lasted 5 days. The pollution episode was aggravated by the adverse meteorology, that is, little or no wind at the time, and a vapour cloud, consisting of air and hydrocarbon vapour, formed. This cloud spread around the site, following the natural topography, until it encountered a source, or sources, of ignition.

6.9.1 Impact of the event on the local air quality

It is estimated that 8000 tonnes of PM_{10} particles may have been released during the fire; this is equivalent to approximately 6% of the total annual emissions of this pollutant in the UK (based on 2003 figures from the UK National Atmospheric Emissions Inventory). However, despite the unprecedented scale of the Buncefield explosion and fire, a wide range of air pollution monitoring undertaken before, during and after the event showed that ground-level concentrations of a range of pollutants remained low to moderate over local, regional and national scales. It appears that the high plume buoyancy and favourable meteorological conditions resulted in the plume being trapped aloft, with minimal mixing to the ground. As a result, there are unlikely to have been widespread air quality impacts at ground level due to the pollutants emitted from the Buncefield fires. Measurements taken from within the plume by the Facility for Airborne Atmospheric Measurements (FAAM) BAe146-301 research aircraft, operated by the UK Met Office and the Natural Environment Research Council (NERC), showed that the plume was mainly black carbon soot.

Table 6.12 shows the amount of pollutants emitted and their percentages in relation to UK 2003 total emissions, as reported in the National Atmospheric Emissions Inventory (NAEI). The quantities of air pollutants emitted were estimated for four possible scenarios for the event: Scenario 1: 90% of fuel from the British Pipeline Agency and 60% of fuel from the Hertfordshire Oil Storage Terminal lost; Scenario 2: LOW estimate (50% loss of fuel on site assumed); Scenario 3: MEDIUM estimate (75% loss of fuel on site assumed); Scenario 4: HIGH estimate (100% loss of fuel on site assumed). The emission estimates indicate that PM_{10}, $PM_{2.5}$ and Benzo[a]pyrene (B[a]P) emissions represented the greatest relative proportion of corresponding national emissions. Estimated PM10 and PM2.5 emissions were between 4% and 8.5% of total UK annual emissions, while B[a]P emissions were between 5% and 10%. The emissions for other pollutants such as NO_2 and dioxins would be around 40 tonnes and 1.5 WHO-TeQ g, (0.003% and 0.6% of total UK annual emissions, respectively).

FOR REFERENCE PURPOSES ONLY

6.9.2 Other environmental pollution impacts

The depot is sited on a variable layer of clay with flints, 2–10 m thick, over the Upper Chalk stratum. The Upper Chalk is classified as a major aquifer that provides drinking water as well as other uses including private abstractors, agriculture and industry. The pollutants from fuel and firefighting liquids flowed from leaking bunds down the drains and *soakaways*, both on- and offsite, and entered the groundwater. These containment systems were inadequately designed and maintained, and the pollutants in this liquid runoff consisted of perfluorooctane sulphonate (PFOS) from the foam, and hydrocarbons such as benzene and xylene.

Table 6.12 Estimates of total air pollutant emissions from the Buncefield Oil Storage Depot fire. Shown in brackets are the indicative percentage share of the total UK annual emissions (estimated for 2003)

Pollutant	*Unit*	*Scenario 1*	*Scenario 2*	*Scenario 3*	*Scenario 4*
NO_x	*Tonnes*	37.2 (0.0024)	27.3 (0.0017)	40.9 (0.0026)	54.6 (0.0035)
PM_{10}	*Tonnes*	8249.5 (5.85)	6054.8 (4.29)	9082.2 (6.44)	12109.6 (8.58)
$PM_{2.5}$	*Tonnes*	4949.7 (5.69)	3632.9 (4.18)	5449.3 (6.27)	7265.7 (8.36)
Dioxins	*g-TeQ g*	1.32 (0.51)	0.97 (0.37)	1.45 (0.56)	1.93 (0.75)
B[a]P	*kg*	285.4 (7.08)	209.5 (5.19)	314.3 (7.79)	419.0 (10.39)
CO	*Tonnes*	1712.7 (0.062)	1257.0 (0.045)	1885.6 (0.068)	2514.1 (0.091)
NMVOC	*Tonnes*	101.0 (0.009)	74.2 (0.007)	111.2 (0.01)	148.3 (0.014)
Benzene	*Tonnes*	58.3 (0.43)	42.8 (0.32)	64.2 (0.47)	85.6 (0.63)
CO_2	*Mtonne*	0.144	0.105	0.158	0.211
C	*kTonne*	39.2 (0.026)	28.7 (0.019)	43.1 (0.028)	57.5 (0.038)

Source: DEFRA, Initial review of air quality aspects of the Buncefield Oil Storage Depot explosion, 2006.

REFERENCES AND FURTHER READING RESOURCES

Bach, W., Daniels, A., Dickinson, L., Hertlein, F., Morrow, J., Margolis, S., and Dinh, V. D. (1975) Fireworks pollution and health. *International Journal of Environmental Studies*, 7(3): 183–192.

Beverland, I. J., Scott, S. L., ÓNéill, D. H., Moncreiff, J. B., and Hargreaves, K. J. (1997) Simple battery powered device for flux measurements by conditional sampling. *Atmospheric Environment*, 31: 277–281.

FOR REFERENCE PURPOSES ONLY

Brunt, H., Barnes, J., Longhurst, J.W.S., Scally, G., and Hayes, E. (2016) Local air quality management policy and practice in the UK: The case for greater Public Health integration and engagement. *Journal of Environmental Science and Policy*, 58: 52–60.

CIE (1932) *Commission internationale de l'Eclairage proceedings*. Cambridge University Press, Cambridge, UK.

Clark, H. (1997) New directions. Light blue touch paper and retire. *Atmospheric Environment*, 31(17): 2893–2895.

Collins, W. J., Stevenson, D. S., Johnson, C. E., and Derwent, R. G. (1997) Tropospheric ozone in a global-scale three-dimensional Lagrangian model and its response to NOx emission controls. *Journal of Atmospheric Chemistry*, 26: 223–274.

Conkling, A. J. (1985) *Chemistry of Pyrotechnics*. Marcel Dekker, New York.

DEFRA (2006) *Initial Review of Air Quality Aspects of the Buncefield Oil Depot Explosion*. Department for Environment, Food and Rural Affairs, London, UK.

DEFRA (2013) *Review of Effectiveness of Local Authority Action Plans and Future Policy Options for LAQM*. Department for Environment, Food and Rural Affairs, London, UK.

DEFRA (2017) *Local Air Quality Management (LAQM) Support*. Department for Environment, Food and Rural Affairs, London, UK.

de Leeuw, F., Sluyter, R., and Camu, A. (2000) *Air Pollution by Ozone in Europe in 1998 and Summer 1999*. European Environment Agency, Copenhagen, UK.

Dye, A., Rhead, M., and Trier, C. (1998) The physical nature of airborne particulate matter PM10 in Plymouth. *International Journal of Vehicle Design*, 20(1–4): 3–9.

Dyke, P., Coleman, P., and James, R. (1997) Dioxins in ambient air, Bonfire Night 1994. *Chemosphere*, 34(5–7): 1191–1201.

EC (2017) EU Clean Air Programme. http://ec.europa.eu/environment/air/.

Fleischer, O., Wichmann, H., and Lorenz, W. (1999) Release of polychlorinated dibenzo-p-dioxins and dibenzofurans by setting off fireworks. *Chemosphere*, 39: 925–932.

Fox, B. (2004) Blast of air sends fireworks sky high. *New Scientist*, 183(2459): 21.

Fowler, D., Steadman, C. E., Stevenson, D., Coyle, M., Rees, R. M., Skiba, U. M., Sutton, M. A. et al. (2015) Effects of global change during the 21st century on the nitrogen cycle. *Atmospheric Chemistry and Physics Discussions*, 15: 1747–1868.

Graedel, T. E., and Crutzen, P. J. (1993) *Atmospheric Change – An Earth System Perspective*. W. H. Freeman, New York.

Griffin, R. D. (2006) *Principles of Air Quality Management*. CRC Press, Boca Raton, FL.

Kent, A. (2002) *Air Pollution Forecasting Ad-hoc Report: Bonfire Night, 2002*. National Environmental Technology Centre, Abingdon, UK.

Moreno, T., Querol, X., Alastuey, A., Minguillon, M. C., Pey, J., Rodriguez, S., Miro, V. J., Felis, C., and Gibbons, W. (2007) Recreational atmospheric pollution episodes: Inhalable metalliferous particles from firework displays. *Atmospheric Environment*, 41(5): 913–922.

NAPAP (1990) *Integrated Assessment Report*. National Acid Precipitation Assessment Program, Washington, DC.

National Expert Group on Transboundary Air Pollution (2001) *Transboundary Air Pollution: Acidification, Eutrophication and Ground-Level Ozone in the UK*. Centre for Ecology and Hydrology, Edinburgh, UK.

Parkhi, N., Chate, D., Ghude, S. D., Peshin, S., Mahajan, A., Srinivas, R., Surendran, D. et al. (2016) Large inter annual variation in air quality during the annual festival 'Diwali' in an Indian megacity. *Journal of Environmental Sciences*, 43: 265–272.

Quality of the Urban Air Review Group (1993) *Diesel Vehicle Emissions and Urban Air Quality*. Prepared for the Department of the Environment, London, UK.

Ravindra, K., Mor, S., and Kaushik, C. P. (2003) Short-term variation in air quality associated with firework events: A case study. *Journal of Environmental Monitoring*, 5(2): 260–264.

RoTAP (2012) *Review of Transboundary Air Pollution: Acidification, Eutrophication, Ground Level Ozone and Heavy Metals in the UK*. Centre for Ecology & Hydrology, Penicuik, UK, p. 292.

Russell, M. (2000) *The Chemistry of Fireworks*. The Royal Society of Chemistry, Cambridge, UK.

Sukumar, A., and Subramanian, R. (1992) Trace-elements in scalp hair of manufacturers of fireworks from Sivakasi, Tamil-Nadu. *Science of the Total Environment*, 114: 161–168.

Tiwary, A., Chatterton, T., and Namdeo, A. (2014) Co-managing carbon and air quality: Pros and cons of local

FOR REFERENCE PURPOSES ONLY

sustainability initiatives. *Journal of Environmental Planning and Management*, 57(8): 1266–1283.

Tiwary, A., Namdeo, A., Fuentes, J., Dore, A., Hu, X.-M., and Bell, M. (2013) Systems scale assessment of the sustainability implications of emerging green initiatives. *Environmental Pollution*, 183: 213–223.

United Kingdom Quality of Urban Air Review Group (1993) *Urban Air Quality in the United Kingdom*. DoE/HMSO, London, UK.

Vecchi, R., Bernardoni, V., Cricchio, D., D'Alessandro, A., Fermo, P., Lucarelli, F., Nava, S., Piazzalunga, A., and Valli, G. (2007) The impact of fireworks on airborne particles. *Atmospheric Environment*, 42(6): 1121–1132.

Wang, Y., Zhang, G. S., Xu, C., and An, Z. S. (2007) The air pollution caused by the burning of fireworks during the Lantern Festival in Beijing. *Atmospheric Environment*, 41(5): 417–431.

Wells, N. (1997) *The Atmosphere and Ocean*. Wiley, Chichester, UK.

Wesely, M. L., and Hicks, B. B. (2000) A review of the current state of knowledge on dry deposition. *Atmospheric Environment*, 34: 2261–2282.

Williams, M. L. (1999) Patterns of air pollution in developed countries. In: S. T. Holgate, J. M. Samet, H. S. Koren and R. L. Maynard (Eds.), *Air Pollution and Health*. Academic Press, London, UK.

World Health Organization (2016) *WHO's Urban Ambient Air Pollution Database – Update 2016, Version 0.2*. WHO, Geneva, Switzerland.

Zhang, Y., Olsen, S. C., and Dubey, M. K. (2010) WRF/Chem simulated springtime impact of rising Asian emissions on air quality over the U.S. *Atmospheric Environment*, 44(24): 2799–2812.

Zhang, Y., Shao, K., Tang, X., and Li, J. (1998) The study of urban photochemical smog pollution in China. *Acta Scientiarum Naturalarum Universitatis Pekinensis*, 34: 392–400.

---

[1] Oxidizing agents produce the oxygen which is required to burn the mixture of reducing agents and to excite the atoms of the light-emitting compounds.

[2] The reducing agents are agents that combine with the oxygen from the oxidizers to produce the energy of the explosion.

[3] Lantern Festival in Beijing presents an important traditional Chinese festival celebrated on the 15th day of the first month of the Chinese lunar calendar (end of February), which is usually viewed as the end of Chinese New Year celebrations. On the night of the festival, parks, streets and the gates of family houses are decorated with lanterns and people go out to watch the lanterns and fireworks.

FOR REFERENCE PURPOSES ONLY

Chapter 7

Indoor air quality

Not only do most people in the most polluted regions of the world live in urban areas, but they also spend nearly 90% of their time inside buildings, a further few percent in vehicles and only around 6% outdoors. Therefore, in this chapter we shall look briefly at special features of indoor air quality. Despite its importance and complexity, the indoor environment has been much less thoroughly studied than has outdoors. The general perception is that one is *safe* from air pollutants indoors, and many who are today aware of high NO_2 concentrations near roads do not worry about cooking with a gas hob that potentially gives them an even higher NO_2 exposure. The sources of air pollution that have been discussed in this book thus far have been characterised by their release into the atmosphere at large. In general, the concentrations of these pollutants inside buildings are lower than the concentration outside, because the pollutants are deposited to internal surfaces during the residence time of air in the building. However, there are many additional sources inside buildings, and the same reduced air turnover that protects from external pollutants may cause the concentrations from internal sources to rise to unacceptable levels. Furthermore, the species involved include not only the same gases and particles that penetrate in from the outside, but a whole range of new pollutants that only increase to significant concentrations in the confines of the indoor environment. Table 7.1 provides a list of major health-damaging pollutants generated from indoor sources. Additional sources include people and domestic animals, micro-organisms, moulds and fungi. The concentration of any particular pollutant at any time is the result of the external and internal source strengths, deposition velocities to different surfaces, air turbulence and building ventilation rate.

Extremely high standards of particle control are required in some activities, for example, electronic chip manufacture, food and pharmaceutical industry, and so on, to reduce the risk of product contamination (Table 7.2). US federal standards are based on particle counts per volume of circulated air, with the performance graded into classes. The class number corresponds to the number of particles larger than 0.5 μm being less than that value per ft^3.

FOR REFERENCE PURPOSES ONLY

Corresponding to these are SI classes, in which the cleanness is indicated by an exponent p, where the number of particles larger than 0.5 μm is less than 10^p m^{-3}. For example, M 6.5 on the SI system can contain no more than $10^{6.5} = 3.53 \times 10^6$ particles per m^3 greater than 0.5 μm, which corresponds to 100,000 ft^{-3} (Table 7.3). The American Society for Testing & Materials (ASTM) have developed 62 standards, covering the latest research on the measurement of critical indoor air quality parameters and on the quantitative characterization of sources of indoor air contamination. A primary objective of these standards is to provide tools for the accurate and reproducible measurement of indoor air contaminants including volatile organic compounds (VOCs), pesticides, particulate matter and radon (ASTM, 2018).

Table 7.1 Major health-damaging pollutants generated from indoor sources

Sources and potential health effects of indoor air pollutants		
Pollutant	*Major indoor sources*	*Potential health effects*[a]
Arsenic and fluorine	Coal combustion	Dermatological, neurological, respiratory, cardiovascular, immunological and endocrine effects
Environmental tobacco smoke	Cigarettes, cigars and pipes	Respiratory irritation, bronchitis and pneumonia in children, emphysema, lung cancer and heart disease
Carbon monoxide	Unvented or malfunctioning gas appliances, wood stoves and tobacco smoke	Headache; nausea; angina; impaired vision and mental functioning; fatal at high concentrations
Nitrogen oxides	Unvented or malfunctioning gas appliances	Eye, nose, and throat irritation; increased respiratory infections in children
Sulphur oxides	Coal combustion	Coughing, wheezing, shortness of breath
Volatile organic compounds (VOCs)	Aerosol sprays, solvents, glues, cleaning agents, pesticides, paints, moth repellents, air fresheners, dry cleaned clothing and treated water	Eye, nose, and throat irritation; headaches; loss of coordination; damage to liver, kidney and brain; various types of cancer
Formaldehyde	Pressed wood products such as plywood and particleboard; furnishings; wallpaper; durable press fabrics	Eye, nose, and throat irritation; headache; allergic reactions; cancer
Respirable particles	Cigarettes, wood stoves, fireplaces, aerosol sprays and house dust	Eye, nose and throat irritation; increased susceptibility to respiratory infections and bronchitis; lung cancer
Biological agents (bacteria, viruses, fungi, animal dander, mites)	House dust; pets; bedding; poorly maintained air conditioners, humidifiers and dehumidifiers; wet or moist structures; furnishings	Allergic reactions; asthma; eye, nose and throat irritation; humidifier fever, influenza, and other infectious diseases
Asbestos	Damaged or deteriorating insulation, fireproofing and acoustical materials	Asbestosis, lung cancer, mesothelioma and other cancers
Lead	Sanding or open-flame burning of lead paint; house dust	Nerve and brain damage, particularly in children; anaemia; kidney damage; growth retardation
Polycyclic aromatic hydrocarbons (PAHs)	Fuel/tobacco combustion, cooking	Short-term symptoms: eye irritation, nausea, vomiting, diarrhoea; Long-term symptoms: cataracts, kidney and liver damage
Radon	Soil under buildings, some earth-derived construction	Lung cancer

FOR REFERENCE PURPOSES ONLY

materials and groundwater

[a] Depends on factors such as the amount of pollutant inhaled, the duration of exposure and susceptibility of the individual exposed.

Table 7.2 Extreme US clean-room standards

Particle concentration ft $^{-3}$ not to be exceeded	
Class 100,000	*Class 1*
100,000 > 0.5 μm	1 > 0.5 μm
700 > 5 μm	3 > 0.3 μm
	7.5 > 0.2 μm
	35 > 0.1 μm

Table 7.3 Equivalence between US and SI clean-room standards

US	*SI*
100,000	M 6.5
10,000	M 5.5
1,000	M 4.5
100	M 3.5
10	M 2.5
1	M 1.5

Obtaining these very low concentrations requires a special branch of control technology. Specialist methods used are called high-efficiency particulate air (HEPA) or ultra-low penetration air (ULPA) filtration which obtain efficiencies of 99.97% for 0.3 μm particles, and 99.999% for 0.2–0.3 μm particles, respectively. Very large airflows may also be needed in order to remove particles emitted from within the controlled volume. An M 6.5 clean room may have 30 air changes per hour (ACH, see description in Section 7.1), which can rise to 600 for an M 2.5 room.

7.1 BUILDING VENTILATION

Ventilation of buildings controls the rate of exchange of inside air with outside air and hence not only the ingress of outside pollutants into the building but the release of indoor pollutants from the building. Controlled ventilation of buildings is a compromise between energy costs, maintenance of comfort and air quality. If a building is well sealed, energy efficiency is high, but emissions from occupants and other sources quickly generate unacceptable concentrations. In many buildings, there are significant routes for air infiltration (i.e. leaks, as distinct from ventilation) other than through doors and windows. This infiltration is either advective or convective. Advective flow is driven by pressure

FOR REFERENCE PURPOSES ONLY

gradients across the building, so that it increases with wind speed. Convective flow is driven by the density difference between the building air and ambient air, so that it increases with temperature difference.

The most basic model of building air exchange involves an enclosure with two vents (Figure 7.1). One vent represents the sum of all the areas (whether specific controlled ventilation devices or simply gaps around doors and windows) through which at any time air is leaking inwards. The other vent is a corresponding one for air leaking outwards. The air venting inwards has the properties of the outdoor ambient air – temperature, humidity, pollutant concentrations, and so on. The air venting outward has the corresponding properties of the room air. The mass and volume flow rates of air through the two vents must be equal, or the room would become pressurised with respect to ambient. During a short time interval dt, the mass of pollutant in the room increases by an amount dm, where dm = inward ventilation mass flow + internal production – outward ventilation mass flow. Hence:

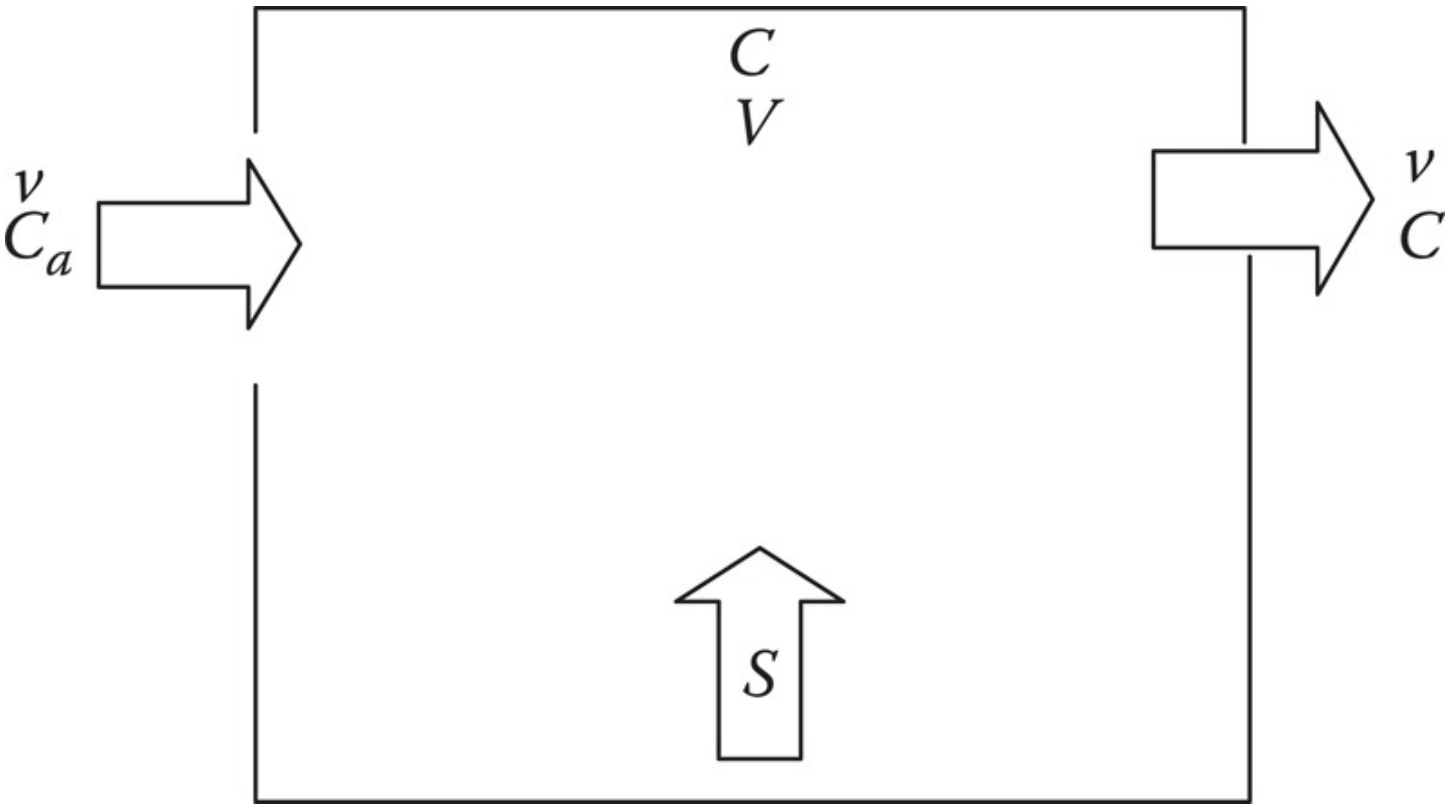

Figure 7.1 Basic building venting.

$$dm = VdC = vC_a dt + Sdt - vCdt$$

where:

V is the room volume

dC is the small change in concentration C during time dt

v is the ventilation rate

C_a is the ambient (outside) concentration

S is the internal source strength of that pollutant

It is assumed here that the compound is stable (does not decay or react) and does not deposit to surfaces, and that the air in the room is well mixed so that the concentration is C everywhere. Hence:

$$\frac{dC}{C_a + \frac{S}{v} - C} = \frac{v}{V}\,dt$$

which integrates to give:

$$C_t = C_a + \frac{S}{v} - \left(C_a + \frac{S}{v} - C_0\right) e^{-\frac{vt}{V}}$$

where:

C_t is the concentration at time t

C_0 is the initial concentration at $t = 0$

Inspect the behaviour of this equation: if $C_a = S = 0$ (outside concentration negligible and no internal sources), then we have:

$$C_t = C_0 e^{-\frac{vt}{V}}$$

and the indoor concentration decays exponentially from its initial value. This equation is used for measuring the ventilation rate of a room, provided the air is well mixed. For example, the concentration of an inert tracer such as CO_2 or N_2O is raised by releasing some from a bottle into the room. When the supply is turned off, the decay in concentration is measured over a period of an hour or so.

As $\log_e C_t = \log_e C_0 - (v/V)t$, a graph of $\log_e C_t$ against time has a gradient of $-v/V$ from which v can be determined. In fact the result is often left as v/V, which has units of s^{-1}. This represents the air turnover rate in the room, and is usually expressed in air changes per hour (ACH).

If $S \neq 0$ in the ventilation equation, an equilibrium concentration C_{equ} is achieved, at which there is as much pollutant leaving in the ventilation air as there is entering and being generated. Then $C_{equ} = C_a + S/v$. Note that this equilibrium concentration is independent of the room volume.

Additional pollutant behaviour can be added to this basic method. If a gas such as ozone, which deposits readily to surfaces, is involved, then a term would be included which specified the rate of loss in terms of appropriate deposition velocities to the carpet,

FOR REFERENCE PURPOSES ONLY

paintwork and other materials. If particles were involved that were large enough to have significant sedimentation velocities, then corresponding loss terms would be used. For example, if a particle of diameter d has a deposition velocity of $v_{d,\ t}$ and a concentration at time t of $C_{d,t}$, then the exponential decay occurs with a time constant of $(v + Av_{d,t})/V$, where A is the surface area to which deposition can occur. Hence we could use the decay rate of gas concentration to measure the ventilation rate v, and the decay rate of $C_{d,t}$ to measure $v_{d,t}$.

Figure 7.2 shows the results of an informal test of these relationships. The particle concentration in a kitchen was artificially increased by burning some toast (deliberately, for once). Then the ventilation rate was set at a high constant value by turning on an extractor fan, and the concentration was measured by an optical particle counter which generates size distributions as 1-minute averages. The three particle size ranges shown in Figure 7.2a are inhalable (all particles less than 50 μm), thoracic (roughly equivalent to PM_{10}) and alveolar (about PM_4). The concentrations increased to a sharp peak at around 78 min, then decayed roughly exponentially between the dashed vertical time limits. The increases in concentration before the peak and after 110 min were due to moving around in the kitchen rather than burning the toast; this mechanical process generated inhalable and thoracic fractions but little alveolar material.

Inhalable includes thoracic and alveolar, while thoracic includes alveolar. Hence the size classes were subtracted to generate three narrower ranges, which are referred to here as coarse (inhalable minus thoracic), medium (thoracic minus alveolar) and fine (alveolar). These three ranges are plotted in Figure 7.2b, which shows much more clearly that the burning toast was generating fine particles. Natural logs of the three size classes were then plotted (Figure 7.2c), for the exponential decay period. The gradients are in the order that we would expect if sedimentation was increasing the loss of larger particles above the rate due to ventilation alone. The gradient of the fine particle regression line (which is assumed to be by ventilation alone) gives a ventilation rate of 0.12 min^{-1}, or 7 ACH. Using a floor area of 16 m^2 and a room volume of 40 m^2 gives deposition velocities for the medium and coarse fractions of 2.7 and 8.9 mm s^{-1}, respectively.

The indoor concentrations of some pollutants are affected mainly by their penetration into the room from outdoors and their subsequent deposition to internal surfaces. For other pollutants there are significant indoor sources, and concentrations are determined by the rate at which emissions from those sources are diluted by the outdoor air that ventilates the room. The most effective ventilation rate for indoor pollution control varies with the circumstances. For example, a high ventilation rate prevents the build-up of volatile organic compound (VOC) concentrations from new paintwork or carpet, but encourages the penetration of particles from outside. Personal exposure of an individual is computed as the sum of the exposures in different microenvironments, each of which has a characteristic concentration of the pollutant or pollutants:

FOR REFERENCE PURPOSES ONLY

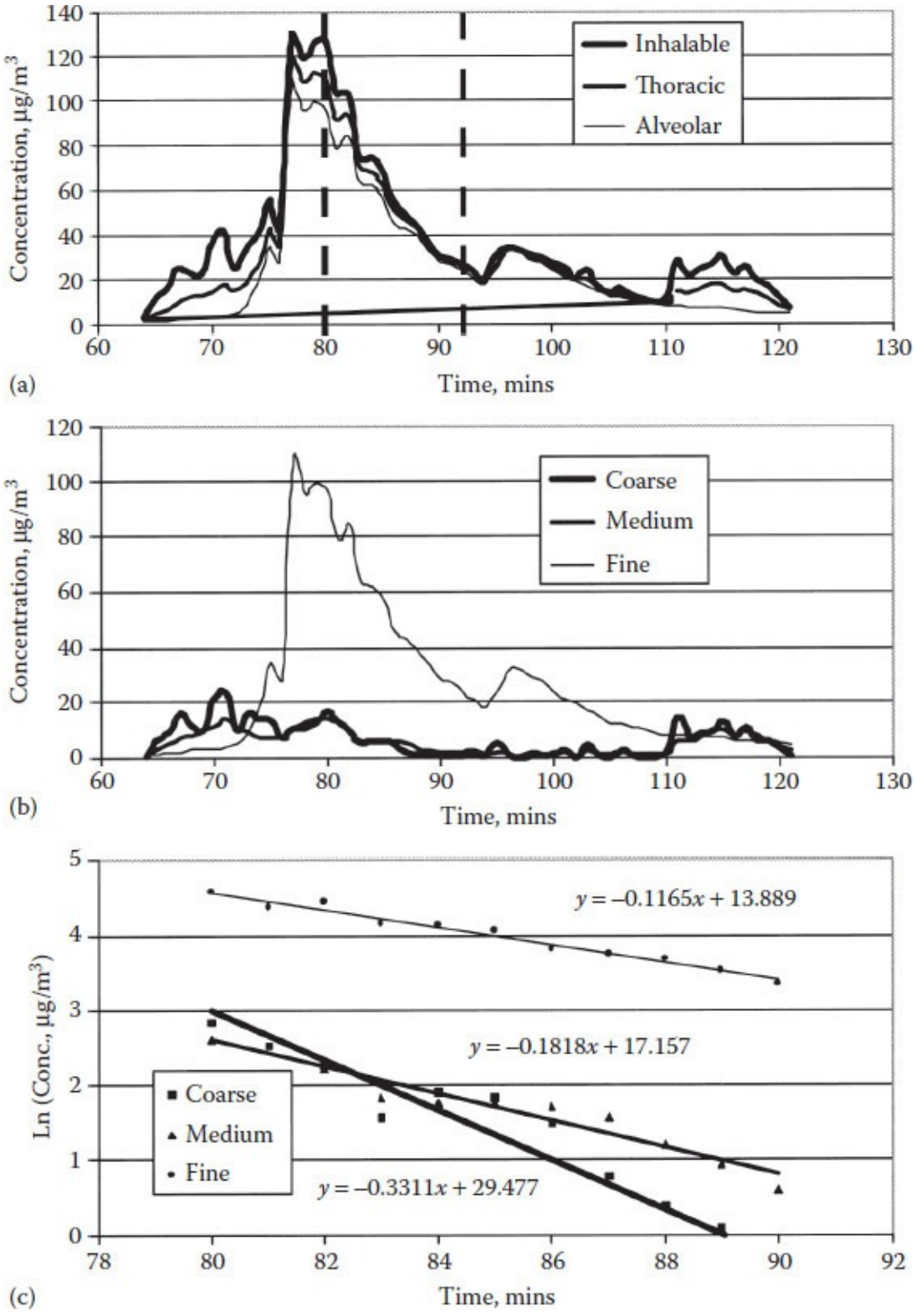

Figure 7.2 Particle concentration decay over time, showing - (a) different respirable size ranges; (b) different size classes; (c) logarithmic profiles.

$$E_i = \sum_{j=i}^{m} E_{ij} = \sum_{j=1}^{m} f_{ij} \times C_{ij}$$

where E_{ij} is the exposure of individual i who spends a fraction of her or his time f_{ij} in

FOR REFERENCE PURPOSES ONLY

microenvironment j, in which the pollutant concentration while she or he is there is C_{ij}.

Certain severe microenvironments contribute disproportionately to the total exposure–for example, if someone in the room is smoking, there is cooking or new paint or other VOC-emitting substances are in the room. The number of microenvironments should be kept to a minimum, subject to adequately representing the exposure of the individual. National studies have shown that in industrialised countries, people average around 87% of their time indoors, 7% in transit and only 6% outdoors. Hence full representation of the indoor environment is vital if the overall exposure estimate is to be meaningful. The particle Total Exposure Assessment Methodology (TEAM) study in the United States calculated the indoor particle concentration as a function of ventilation parameters and contributions from outdoor air, environmental tobacco smoke, cooking and other unaccounted sources:

$$C_{\text{in}} = \frac{P \times a}{a+k} C_{\text{out}} + \frac{N_{\text{cig}} S_{\text{smoke}} + t_{\text{cook}} S_{\text{cook}}}{(a+k) V t_{\text{sample}}} + \frac{S_{\text{other}}}{(a+k) V}$$

where:

C_{in} is the pollutant concentration indoors (μg m^{-3})

C_{out} is the pollutant concentration outdoors (μg m^{-3})

P is the penetration fraction (no units)

A is the air exchange rate (h^{-1})

k is the pollutant decay or deposition rate (h^{-1})

N_{cig} is the number of cigarettes smoked during the period

V is the house volume (m^3)

T_{cook} is the cooking time in hours

T_{sample} is the sampling time in hours

S_{smoke} is the source strength for cigarette smoking (μg/cigarette)

S_{cook} is the source strength for cooking (μg h^{-1})

S_{other} is the source strength for other indoor sources, including resuspension (μg h^{-1})

Note that the units of the three terms on the right-hand side are all μg m^{-3}, as they have to be if we are going to add them together. Factors in the numerator, such as source strengths and penetration, act to increase the concentration. The air exchange rate increases the concentration due to outdoor particles but decreases it if the sources are internal. The higher the deposition rate k, or house volume V, the lower the concentration.

Relationships similar to this have been used to show that indoor/outdoor ratios for PM_{10} are about 0.5, rising to 0.7 for $PM_{2.5}$. The value for $PM_{2.5}$ is higher because the deposition rate is lower (around 0.4 h^{-1} against 0.65 h^{-1} for PM_{10}). Indoor NO_2 concentrations are greatly influenced by whether there is a permanent pilot light on the gas cooker, which can add 5–10 ppb to the average concentration. NO_2 is not a highly reactive gas, and indoor

concentrations are around 0.6 of those outdoors if there are no internal sources. In contrast, O_3 concentrations are greatly reduced when outdoor air comes indoors, because O_3 is deposited rapidly, with a decay rate of around 2.8 h^{-1}, and indoor concentrations in houses with the windows closed might only be 0.1–0.2 of those outdoors. Indoor VOC concentrations, on the other hand, depend on which VOCs are included. For a new building, within which paint solvents, furnishings and carpet glue are strong sources, the concentration may be a hundred times ambient. Many other indoor sources contribute to VOC concentrations, including smoking, dry-cleaned clothes, air fresheners, house cleaning materials, chlorinated water, paints, adhesives and deodorisers.

Building regulations are framed in terms of a target minimum number of ACH – typically 0.35–0.7 – in association with a guide value for volume flow rate per person of around 12 L s^{-1} (when smoking is permitted) down to 2.5 (when it isn't). The values found in practice range from 0.1 ACH (modern well-sealed office building) to 3 ACH (old accommodation with sash windows and open fireplaces). For housing used by people or other animals, the carbon dioxide concentration is the basic measure of ventilation effectiveness. The outdoor concentration is usually between 300 and 600 ppm. A person doing light work exhales 0.5–1 L of air s^{-1}, corresponding to about 25 L h^{-1} of CO_2. This would need a ventilation rate of outside air of 10–30 L s^{-1} $person^{-1}$ to reduce the concentration to 1000–500 ppm. Of course, ventilation may act either as a net importer of an ambient pollutant or as a net exporter of an internal pollutant, depending on the balance between indoor and outdoor concentrations. As energy costs for space heating and air conditioning continue to increase, there is also increasing financial pressure to restrict building ventilation rates.

7.2 COMBUSTION

Any combustion source (e.g. gas, wood or coal fires, gas ovens and hobs) emits a wide range of pollutant gases – NO, NO_2, CO, hydrocarbons – and particles. The particles may comprise mainly soot (if combustion conditions are poor). High-temperature combustion may produce carcinogenic polycyclic aromatic hydrocarbons (PAHs).

7.2.1 Solid-fuel combustion

In developing countries, women who spend long periods in poorly ventilated cooking areas with open stoves without flues are at the greatest risk. The most common traditional fuels are wood, coal, kerosene, agricultural residues and animal wastes. Around 2 billion people rely on these fuels to meet most of their energy needs, amounting to around 25% of the total energy consumption in these countries. Table 7.4 provides a comparison of particulate levels as determined in some recent studies in developing countries. For NO_2, values in

FOR REFERENCE PURPOSES ONLY

homes in developing countries have been reported in the following ranges (μg/m^3) for various fuels measured during cooking or for periods of between 8 and 24 h – wood from <100 to several hundred, coal from several hundred to nearly 1000, kerosene from <30 to nearly 200, and liquefied petroleum gas (LPG) from <10 to nearly 200. For SO_2, the corresponding values are – wood from <30 to nearly 200, coal from <100 to nearly 1000, kerosene from <50 to over 100, and LPG from <25 to several hundred.

In the more developed nations, concentrations have generally decreased with improved ventilation and displacement of solid-fuel stoves by gas-fired central heating, although wood-burning stoves can produce serious emissions during lighting and refuelling. There is some evidence of a higher incidence of respiratory illness and reduction of lung function, especially amongst children, in homes with such stoves. In developed countries, domestic solid-fuel combustion usually takes place in a grate with a chimney and, provided that ventilation is adequate, the increase of indoor pollutant concentrations should be small.

Table 7.4 Comparison of particulate levels from solid-fuel combustion in developing countries

Location	*Averaging time/size fraction*	*Type of fuel*	*Mean levels/range (μg m^{-3})*
Nepal	Cooking period/$PM_{2.5}$	Wood/crop residues	8200 (traditional stove) 3000 (improved stove)
Garhwal, India	Cooking period/TSP 24 h exposure/TSP	Wood/shrubs	4500 (Geometric mean) 700–1690 (winter) 250–1130 (summer)
Pune, India	12–24 h/PM_{10}	Wood	2000 (area) 1100 (personal)
Mozambique	Cooking period/PM_{10}	Wood	1200
Rural Bolivia	6 h/PM_{10}	Dung	1830 (Indoor kitchens) 280 (Outdoor kitchens)
Kenya	Daily average exposure/PM_{10}	Mixed	1000–4800
Tamil Nadu, India	Cooking period/respirable fraction (d_{50} = 4 μm) Daily average exposure/respirable fraction (d_{50} = 4 μm)	Wood/agricultural waste Wood/agricultural waste	1307–1535 (personal) 172–226
Guatemala	24 h/$PM_{3.5}$	Wood	1560 (traditional stove) 250 (improved stove) 850 (LPG/open fire combination)
Andhra Pradesh, India	24 h/respirable fraction (d_{50} = 4 μm) Daily average exposure/respirable fraction (d_{50} = 4 μm)	Wood/dung/agricultural waste Wood/dung/agricultural waste	297–666 (kitchen area) 215–357 (living area) 431–467
Bangladesh	24 h/PM_{10}	Wood/dung/agricultural waste	196–264 (personal) 60–1165 (area)

Source: WHO, *Air Quality Guidelines – Global Update 2005*, World Health Organisation, Copenhagen, Denmark, 2006.

7.2.2 Gas combustion

Combustion of natural gas (CH_4) always produces some CO (from incomplete combustion to CO_2) and NO_x (from fuel and thermal routes). Personal exposure is highly erratic and depends on factors such as room ventilation, time of operation and the movements of a person in the vicinity of the source. For example, people cooking may be exposed to intermittent peaks of several hundred ppb of NO_2 when they bend over a gas hob. If measurements of personal exposure are to be meaningful, they need to be taken with a personal dosimeter worn near the face; otherwise they are likely to be erroneous. Also, we need to measure peak short-term exposures, as personal response is likely to be dominated by the concentration exceeded for 1% or 10% of the time rather than by the long-term arithmetic mean.

7.2.3 Tobacco combustion

A large number of gaseous and particulate air pollutants are produced by tobacco combustion. Of course, the exposure of a smoker is very high compared to a non-smoker, but a smoker's exposure is voluntary, whereas a non-smoker's is not. Of the more than 4500 compounds found in tobacco smoke, 50 are known or suspected to be carcinogenic. Conventionally, the emissions are classified into mainstream (MTS), side-stream (STS) and environmental (ETS) tobacco smoke.

Mainstream emissions, formed during active puffing, are sucked directly from the end of the cigarette into the mouth; burn temperatures are up to 1000°C, so thermal NO_x is formed, as well as hydrogen cyanide (HCN) and *N*-nitrosamines (carcinogenic). Most of the components are generated by a combination of pyrolysis and distillation in an oxygen-deficient atmosphere. Very high concentrations (around 10^{10} per cm^3 of evolved gas) of particles (mode diameter around 0.5 μm) are produced. Although these are serious pollutants, they are only inhaled by the smoker.

Side-stream tobacco smoke refers to emissions from cigarettes that are alight but not being actively puffed; the burn temperature then falls to 400°C. Such a low combustion temperature can lead to the formation of more toxics than in MTS. Concentrations can be extremely high (many ppm of formaldehyde, for example), before they are diluted by air turbulence. Some compounds, such as the carcinogen *N*-nitrosodimethylamine, are emitted much more strongly in STS than in MTS, so that an adjacent non-smoker can have a higher exposure than the smoker. About half of the cigarette tobacco is consumed during the production of MTS, half during STS, but puffing only takes about 4% of the total lifetime of the cigarette. Environmental tobacco smoke is the mixture present in a room, consisting of a variable proportion of MTS (after inhalation and subsequent exhalation) and STS. It is not possible to measure and specify the whole range of possible toxins. Various investigators have identified and measured different fractions, such as carbon monoxide, nicotine, NO_x, hydrocarbons, acrolein, acetone, benzene, benzo-*a*-pyrene (BaP) and

particles.

Concentrations of PM_{10} in ETS can be up to 1000 μg m^{-3} (this compares with 1–5 μg m^{-3} in clean ambient air, 100 μg m^{-3} in polluted ambient air, 1000–3000 μg m^{-3} in the air during the London smog events). At the highest concentrations, such as those found in crowded and poorly ventilated pubs and clubs, the nicotine concentration alone can reach hundreds of μg m^{-3}. About 1 μg m^{-3} of PM_{10} is added to long-term indoor concentrations for each cigarette smoked per day (e.g. two heavy smokers would add several times the ambient background). Homes with smokers have been found to have around three times the mass concentration of suspended particulate as homes without smokers. Inhalation of ETS is colloquially known as passive smoking; it can induce effects ranging from eye watering (tearing), increased coughing and phlegm production and allergic reactions through lung cancer to death. There is also evidence for reduced lung function development in children, increased asthma incidence, increased rates of hospitalisation from bronchitis and pneumonia. One study showed that around 17% of lung cancers among non-smokers may be attributed to ETS exposure during childhood. About 100,000 people die each year in the UK through smoking-related illness, and extrapolation from the mortality statistics of these active smokers indicates that an additional several thousand people die from passive smoking. The general effects of cigarette smoke include:

- Bronchoconstriction
- Depletion of intracellular antioxidants
- Stimulation of excess mucus production
- Increased permeability of airway epithelial linings to macromolecules
- Reduced mucociliary function
- Suppression of immune response (alveolar macrophages have impaired capacity to kill bacteria)
- Inflammation of mucus-secreting glands

7.3 INDOOR ORGANIC POLLUTANTS

7.3.1 Volatile organic compounds

Hundreds of VOCs are emitted by many processes and/or materials in buildings. They are compounds that mainly exist in the vapour phase at the normal range of air temperatures and pressures. There are also semi-volatile VOCs that are present both as liquids and solids but also evaporate. Many compounds are outgassed over a long period of time from the increasing range of synthetic materials, particularly polymeric ones. For example, just one popular polymer, polyvinyl chloride (PVC), can emit a wide range of substances including dibutylphthalate, vinyl chloride, mesethylene, toluene, cyclohexanol and butyl alcohol. A single source may dominate, such as a damp-proof membrane, or many separate sources

FOR REFERENCE PURPOSES ONLY

such as carpet glue, paint, chipboard and plastics may contribute. Flooring materials may involve thermoplastic polymers compounded with process aids such as stabilisers, viscosity modifiers and co-solvents. Some materials are produced from monomers and other low-molecular-weight reactive organic compounds and involve curing processes such as cross-linking, vulcanisation or oxidation. Additives such as plasticisers, antioxidants, surface-treating agents and colourisers may be used. Natural materials such as wood and cork contain many volatile compounds.

The release process is diffusion of the compounds through the body of the material to the surface, followed by evaporation from the surface. Conversely, some flooring materials such as foam-backed carpet can adsorb materials such as tobacco combustion products from the atmosphere and release them later, possibly creating an odour problem. Varnished or lacquered wooden furniture is coated in a material containing binders, solvents, light stabilisers, antioxidants, radical starters and other additives. The binders might be polyurethane, unsaturated polyesters or cellulose nitrate. Acid-curing lacquers are notable for their formaldehyde emissions.

Emissions have been measured from a great range of everyday products found around the home or office – newspapers, books, electronic devices, air freshener, adhesives, cleaning fluids, furniture polish, wax and hair spray. Some of the most commonly found VOCs are toluene, benzene, xylenes, decane and undecane. Many VOCs are bioeffluents – ethanol, acetone, methanol, butyric acid, acetic acid, phenol and toluene are examples. Others are quasi-bioeffluents – components of deodorants or make-up are examples. Exhaled breath contains around 2000 μg m^{-3} acetone and ethanol, several hundred μg m^{-3} isoprene, methanol and 2-propanol. These are endogenous metabolism by-products originating inside the body. Smoking naturally raises the exhaled concentrations of many substances. One smoker, even when not smoking, can significantly raise the room concentration of a compound such as benzene. Microbial VOCs have been used as indicators – 3-ethylfuran, dimethyldisulphide and 1-octen-3-ol in combination have been shown to be strongly correlated with microbial activity.

One survey of 100 homes found that the average total concentration of the 50–300 VOC species that are normally found in indoor air was 553 μg m^{-3}, with 2% (i.e. 2 homes) above 1777 μg m^{-3}. The average ambient concentration during the period of the survey was 32 μg m^{-3}. Another survey showed that total VOC concentrations might be several thousand μg m^{-3} in new homes, but fall to around 1000 μg m^{-3} in homes more than 3-months old. The EU has issued a list of 50 VOCs relevant to indoor air exposure, although the proportional representation of each varies from case to case. In general, as one might expect, the emissions from all building products tend to be greatest when new and to decay fairly rapidly (within days to weeks). Exceptions to this decay are the actions of heat and moisture which can accelerate oxidative reactions.

The measurement of these organic compounds indoors is often a trade-off between time resolution and sensitivity. Real-time methods, such as flame ionisation detectors, do not

FOR REFERENCE PURPOSES ONLY

have the necessary sensitivity in many situations, so the sample has to be pre-concentrated by adsorbing it over a period of time. Active samplers pass the sample air through the adsorbent with a pump. Often 30 min is sufficient to generate a desorbed concentration which is 1000–100,000 times the original ambient value. Passive samplers rely on molecular diffusion over periods of hours to days. This is convenient for low-maintenance integrated measurements, although errors can accumulate if the adsorbed gas self-desorbs during the sampling period. Solid adsorbents (Table 7.5) may be inorganic, porous materials based on carbon and organic polymers. They vary in specific surface area, polarity, thermal stability and affinity for water; hence each tends to have preferred applications.

Carbon-based adsorbents with high specific surface areas can be used to trap very low-boiling compounds, but high-boiling compounds may be difficult to desorb once trapped. If they are reactive, they may even decompose before desorption. Although porous polymers have lower specific surface areas, they can be used effectively for high-boiling compounds such as glycols and phthalates, but not for low-boiling materials such as alkanes. The sample may be removed from the adsorbent by solvent extraction or thermal desorption. In the former method, an organic solvent such as dimethylformamide, carbon disulphide or dichloromethane, having a high affinity for the sample gas and low response on the detector, is flushed through the adsorbent. With thermal desorption, the adsorbent is heated to at least 20°C above the boiling point of the adsorbed sample to drive it out of the adsorbent.

Formaldehyde (HCHO) is used in many products – in urea-formaldehyde resins for making chipboard, as a preservative in medicines and cosmetics, and as a carrier solvent for fabrics and carpets. Emissions from chipboard and similar wood products are aggravated by dampness, which accelerates the reversible polymerising reaction. Formaldehyde is also given off by most combustion sources – solid-fuel, gas, petrol, diesel and cigarettes (up to 40 ppm). But HCHO is a pungent, irritating toxic gas. One key indoor air pollution problem in the 1970s was the release of formaldehyde from urea-formaldehyde foams used for cavity wall insulation. The formaldehyde gas leaked out of cracks in walls and gaps at door and window frames, and accumulated in the indoor air. If the rate of leakage was high, and the ventilation rate low, then sensitive individuals could experience a serious level of skin and respiratory irritation. Substitution by other materials such as rockwool has decreased the significance of this issue. The ambient concentration of formaldehyde is rarely above 10 ppb, but concentrations of several hundred ppb have been reported in buildings that contain formaldehyde-generating materials. Formaldehyde can also be photodissociated by the ultraviolet A (UVA) light emitted from fluorescent sources ($\lambda < 330$ nm) and oxidised to the hydroperoxy radical.

Table 7.5 Solid adsorbents

FOR REFERENCE PURPOSES ONLY

Type	Structure	Specific surface area ($m^2 g^{-1}$)	Tradenames	Water affinity	Application
Inorganic	Silica gel	1–30	Volasphere		PCBs, pesticides
	Molecular sieve				Permanent gases
	aluminium oxide	300	Alumina F1		Hydrocarbons
Carbon-based	Activated charcoal	800–1200		High	Non-polar and slightly polar high-boiling VOCs
	Carbon molecular sieve	400–1000	Carbosieve	Low	Non-polar and slightly polar low-boiling VOCs
	Graphitised carbon blacks	12–100	Carbotrap	Low	Non-polar high-boiling VOCs
Porous polymers	Styrene	300–800	Porapak Chromosorb	Low	Non-polar and moderately polar high-boiling VOCs
	Phenyl-phenylene oxide	12–35	Tenax	Low	Non-polar high-boiling VOCs
	Polyurethane foams			Low	Pesticides

7.3.2 Bioaerosols

Although not conventionally regarded as air pollutants, many biological materials can accumulate in buildings to higher concentrations than are normally found outdoors, and they can be irritating or toxic to occupants. This category includes airborne particles, large molecules or volatile compounds that are either living or were released from a living organism. Some *bioaerosols*, such as bacteria and viruses, may replicate. Others such as pollen and mite faeces may simply be an irritant *per se*. In the limit, a single bacterium or virus can be fatal. The particles can vary in size from 100 nm to 100 μm (Figure 7.3). As with other air pollutants, direct measurement of personal exposure may be very difficult. Measurements of airborne concentration, combined with collection of samples from carpets, mattresses and other surfaces, provided an indication of presence or absence and relative abundance, but not of personal exposure.

FOR REFERENCE PURPOSES ONLY

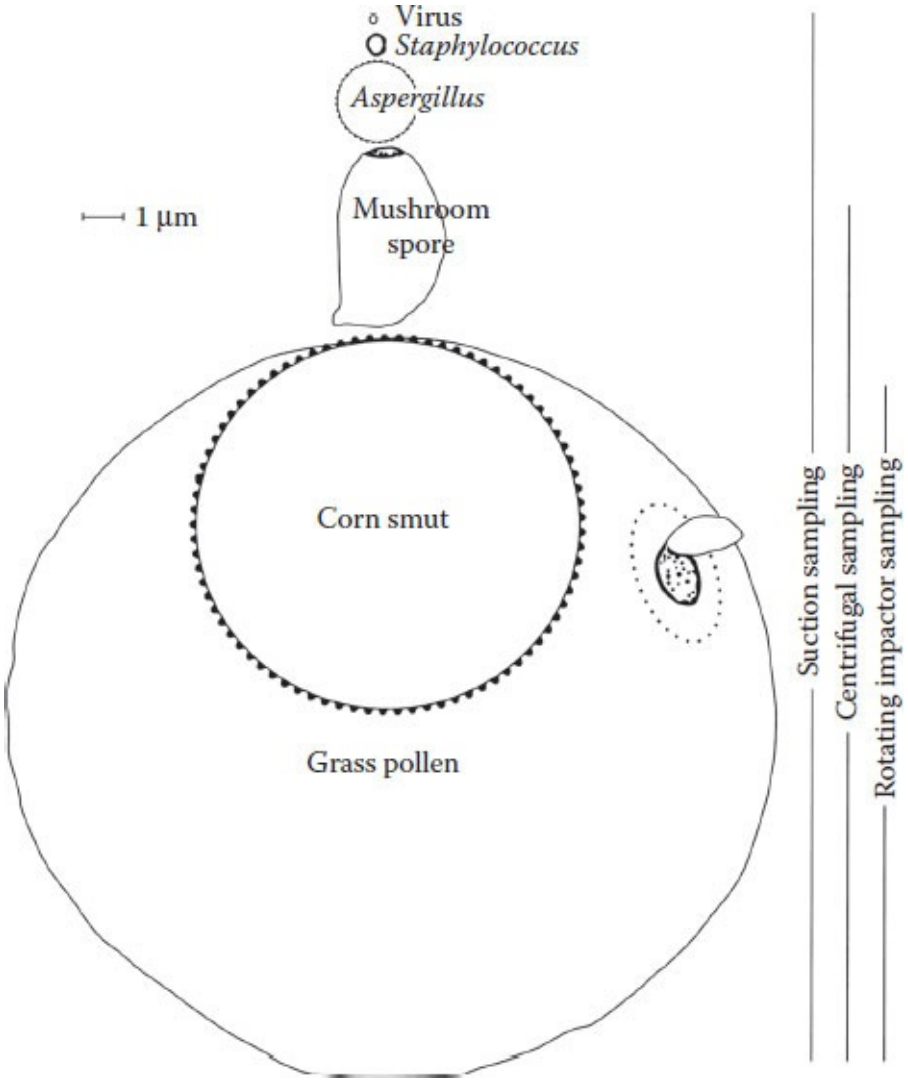

Figure 7.3 Size ranges of bioaerosol. (From Yocom, J. E., and McCarthy, S. M., *Measuring Indoor Air Quality*, Wiley, Chichester, UK, 1991.)

7.3.3 Categories of bioaerosols

The major categories of bioaerosol are bacteria, endotoxins, fungi, viruses, antigens and pollen. Pollen can stimulate allergic reactions. Viruses, bacteria and fungi spread disease. Skin scales (dander) and lice excreta can cause allergic reactions (e.g. allergic rhinitis due to the house dust mite).

7.3.3.1 Bacteria

Bacteria are prokaryotic (no distinct cell nucleus) organisms that have a cell membrane, DNA and some sub-cellular components. Some bacteria such as *Legionella pneumonophila, Streptococcus* and *Meningococcus* are associated with specific diseases; others such as *Thermoactinomyces* and *Enterobacter* are non-infectious (i.e. not pathogenic by inhalation).

Drinking water contaminated with *Legionella* does not cause Legionnaire's disease; the aerosolised water droplets must be inhaled. Other toxic materials such as endotoxins and exotoxins are associated with them. Their rate of multiplication and dissemination can depend strongly on certain aspects of the indoor environment, such as humidity. The size range of bacteria is 0.3–30 μm, while that of bacterial spores is 0.3–10 μm. Microbial growth needs a surface relative humidity above 25%, and then increases with RH up to RH values of 70%.

7.3.3.2 Endotoxins

Endotoxins are highly toxic lipopolysaccharide materials contained in the outer membranes of Gram-negative bacteria. They stimulate the immune systems of a small proportion of sensitive individuals, which may produce fever, malaise, airway obstruction and acute pulmonary infection (humidifier fever). In the airborne environment, they are usually associated with dust particles or liquid aerosol having a wide distribution of sizes.

7.3.3.3 Fungi

Fungi are eukaryotic (having a nucleus). Some such as yeasts are unicellular while others such as moulds are multicellular. Fungal growth usually needs a relative humidity >70%, so bathrooms and kitchens are favoured. Although fungi live on surfaces or in liquids, many produce spores which are often airborne. Apart from the production of infectious diseases such as by *Aspergillus fumigatus*, most fungi generate metabolic products such as proteins that can induce an antibody response and hypersensitivity symptoms. Fungi also achieve reproductive success by releasing mycotoxins to kill off competitor organisms. *Penicillium* is the classic case which has been turned to human advantage, but airborne mycotoxins are not generally good news. Problems are commonly experienced by people handling damp (i.e. mouldy) paper, furniture and textiles. The most publicised mycotoxin is aflatoxin, which is a known human carcinogen, although the predominant uptake route for that is ingestion of mouldy foodstuffs such as groundnut rather than inhalation. The fungal spore size range is 0.5–30 μm.

7.3.3.4 Viruses

These are the smallest life forms, parasitic replicating organisms that are dependent on their host cell for reproduction. Their size range is 0.02–0.3 μm, although most airborne viruses are attached to other particles.

7.3.3.5 Allergens

Allergy, which is any adverse reaction resulting from immunologic sensitisation towards a

specific substance (the allergen), is an increasing problem in society, and airborne uptake of allergens plays a significant part. Allergens are macromolecules, produced by living organisms, that produce a detectable response from the immune system. The symptoms are characteristic, such as allergic rhinitis (runny nose) and allergic aspergillus. Human sensitivity may be three orders of magnitude greater than for the classic air pollutants such as ozone, with serious responses to concentrations in the ng m^{-3} range. The allergens are produced from a wide variety of sources such as fungal and bacterial spores, cat and rodent dander and hairs, house dust mites and cockroach excreta.

Each person can shed as much as 1 g of skin cells each day, and this constitutes the organic matter for the domestic micro-ecology, regardless of the additional supply from pets, foodstuffs, and so on. The skin scales accumulate in furniture, carpets and bedding, where they are colonised by saprophytic fungi, and in turn by mites. The latter 300 μm arthropods (*Dermatophagoides*, which means skin-eater) enjoy conditions of 25°C and 70%–80% relative humidity, and grow from egg to adult in 25 days. Hence their abundance has been favoured over the last 50 years by increased use of central heating (which raises temperatures), combined with reduced ventilation (which increases humidity) and use of fitted deep-pile carpets (which reduces cleanability). Floor or mattress dust samples typically contain 100–1000 mites (dead or alive) g^{-1}. Mite faeces, which are sticky pellets about 20 μm in diameter, constitute a large proportion of the allergen in house dust. The gastric enzymes produced by the mites, which are in their faeces and are strong human allergens, become airborne and are eventually inhaled. The concentrations of the two specific allergenic proteins are in the range 2–10 μg (g settled dust)$^{-1}$ or 5–50 ng m^{-3} air in the houses for which house dust mite allergy has been implicated in triggering an asthma attack. Corresponding allergens are produced by cats (*Fel d*), dogs (*Can f*) and cockroaches (*Bla g*). Again, the concentrations and inhalation rates are increased by the use of tighter buildings with better draught-proofing and reduced ventilation. The allergic response may be a gentle *runny nose* of little concern, but it may also be associated with a violent or even fatal asthma attack. Although specific materials are related to sources – cat allergen concentrations are naturally higher in homes with cats, for example – there may be high enough concentrations in adjacent properties, or in trains and other public places, to cause reactions in sensitive individuals.

7.3.3.6 Pollen

Pollen grains are the largest bioaerosol particles, having diameters from 10 up to 170 μm (predominant range 30–50 μm). They are produced by plants to transport genetic material to the flowers of other plants. Pollen may be either windborne or insect borne. Windborne pollen is produced on the end of protruding anthers: as with many of the bioaerosols, airborne dispersion is an evolutionary tool for reproduction, so we can expect the pollen to become airborne easily and to remain so for long periods. Both number and mass

FOR REFERENCE PURPOSES ONLY
concentrations are generally small; even a high pollen episode involving hundreds of pollen grains per m^3 would correspond to only around 10 μg m^{-3}. However, sensitivity to pollen as allergens can be extremely high for a small proportion of the population. For most people this amounts only to an inconvenience such as allergic rhinitis (hay fever), but at worst it can exacerbate chronic obstructive pulmonary disease and possibly be fatal. Different pollen species are not uniformly irritating – maple, birch and sycamore are generally the worst tree pollens, while bluegrass and Timothy are the worst grasses. Additional information on pollen production from common vegetation species is provided in Chapter 9.

7.3.4 Sampling bioaerosols

Bacteria, fungi and viruses are all *bioaerosols* and, in principle, they can all be sampled by the standard particle sampling methods described in Chapter 3. In practice a specialised subset of equipment has been developed over the years for sampling these organisms. Viruses are in practice not sampled physically but identified by their effects on people. For bacteria and fungi, there are sampling methods based on gravity, inertial impaction, filtration and liquid impingement. Cascade impactors have their cut-diameters optimised for bacteria or fungi, which are relatively coarse compared to suspended particles in general. For organisms of a few μm or smaller, the acceleration and impact forces needed to separate them from the airstream are too violent, and other methods must be used. Filtration and electrostatic precipitation, or impingement in a solution, are the preferred techniques. If the morphology of the organisms is known, direct microscopy on the substrate can be used for identification. More sophisticated laboratory techniques, such as analysis for guanine to identify house dust mite excreta, are also used. Often the collection substrate is coated in a growth medium such as agar (a nutrient jelly prepared from seaweeds, blood, soy and other materials) so that the microorganisms can be identified from the colonies formed, and the areal density quantified. The plated colonies are cultured over periods of a few days to a week at constant temperature, with the media and growth conditions optimised for the species of interest. Often this agar plate is the substrate of an impactor stage so that the bioaerosol is deposited directly onto it. Multi-jet impactors may have up to 500 jets arranged in this way, spreading out the collected particles to avoid overloading. This is quantitatively important because if two bacteria are deposited close to each other, only one colony will develop. The most complex collectors ramp up the volume flow rate and/or decrease the jet-substrate spacing in order to change the cut-off diameter. There are imperfections in this capture and identification process. Some fungi can repress the growth of other organisms, which would lower the predicted count. The sampling process itself is quite violent, with impaction speeds of up to several hundred m s^{-1} needed to separate the smallest microorganisms from their streamlines.

Not all important bioaerosol particles are culturable – indeed, up to 95% of viable bioaerosol particles are not. For such material, other techniques come to the forefront for

identification after capture. A non-specific count of total bacteria can be made by staining them with a fluorescent dye such as a monomeric or dimeric cyanine and identifying them with scanning confocal microscopy. Species can be identified by polymerase chain reaction (PCR) techniques to amplify their DNA. Pollen grains can be impacted onto a rotating, adhesive, square transparent rod for microscopic counting and identification. Liquid impingers trap the micro-organisms by impinging the airstream onto the agitated surface of the collection liquid, which is usually a dilute nutrient solution. Many interactions such as asthma and allergic responses are due to dead material. Techniques such as enzyme-linked immunosorbent assay (ELISA) are used to identify such material, by binding an antibody with specificity for the aeroallergen. This primary antibody is then reacted with an enzyme-linked second antibody. The enzyme in turn reacts with a substrate to produce a spectral shift which can be quantified. These techniques are only semi-quantitative or indicative at present.

7.4 SICK BUILDING SYNDROME

In controlled-environment office buildings, there has sometimes been reported a high incidence of minor but discomforting illnesses such as headache, sore throat, runny nose and coughing. This phenomenon has come to be known as sick (or tight) building syndrome (SBS). It is probably a compound response which is partly due to air quality and also due to factors such as isolation from the natural environment, thermal discomfort, light flicker and other unsettling aspects of working conditions. In early investigations, VOCs were thought to be responsible, but this finding has not been supported by later work. Ventilation rate has been investigated but not conclusively shown to be a cause. Although there have been many investigations of alleged SBS, the complexity of the problem has meant that many of these have only measured a small subset of the possible relevant parameters. Building-related illness is distinguished from SBS because it is a specific response due to a single identifiable factor such as bio-allergens from air conditioning or formaldehyde from insulation.

7.5 ODOURS

Odour is one of the most exacting indoor air quality problems to deal with. Some chemicals such as ammonia (from the body) and mercaptans (from tobacco smoke) have extremely low odour thresholds; a ventilation rate that is entirely adequate for health and thermal comfort may still leave a perceptible smell in the air. For example, in one study, it was found that an air exchange rate of 50 L s^{-1} per smoking occupant was still insufficient to eliminate a smell problem. *Olf* is a unit used to measure the strength of a pollution source; one olf (= olfactory unit) is the emission rate of bioeffluents from a standard sedentary

person in thermal comfort. A smoker has been reported as being about six olf even when not actually smoking, and in practice the carpets and other fittings can contribute at least as much as the occupants. A further complication is caused by acclimation – people who find a smell noticeable or even offensive when they first walk into a room usually adapt after a short time and reduce their sensitivity to that particular compound. Ammonia has a very low odour threshold and is given off by the human body, especially when sweaty. Surveys of ammonia which have been carried out with diffusion tubes in the kitchens, living rooms and bedrooms of a small sample of UK homes have shown average concentrations, in the range 30–40 μg m^{-3}, which were surprisingly similar in the three environments.

7.6 INDOOR AIR SAMPLING

Correct measurement of personal exposure in indoor air is quite complicated. Often the pollutant is very non-uniformly distributed both in space and time. Many of the instruments that are used for outdoor ambient pollutant monitoring are therefore unsuitable for indoor monitoring. The main uptake routes for airborne pollutants are through the nose and mouth, so this is where the concentrations need to be measured. Most real-time analysers are bench-based, mains-powered items which cannot be carried around. Although devices such as diffusion tubes are highly portable and take no power, they offer only time-integrated measurements which give no information about short-term peaks.

Indoor air sampling and analysis therefore have specific protocols which need to be observed to measure realistic indoor air quality. A pre-sampling inspection should be performed prior to each sampling event to identify conditions that may affect or interfere with the proposed testing. The inspection should evaluate the type of structure, floor layout, physical conditions, and airflows of the building(s) being studied. In addition, potential sources of chemicals of concern should be evaluated within the building by conducting a product inventory. The primary objective of the product inventory is to identify potential air sampling interference by characterising the occurrence and use of chemicals and products throughout the building. Air samples are sometimes designed to represent typical exposure in a mechanically ventilated building, and the operation of heating, ventilation, and air conditioning (HVAC) systems during sampling should be noted. Unnecessary building ventilation should be avoided within the 24 h prior to and during testing. During colder months, heating systems should be operating under normal occupied conditions (i.e. 65°F–75°F) for at least 24 h prior to and during the scheduled sampling time.

Air samples should be collected from an adequate number of locations to understand likely sources of volatile chemicals and to assess potential exposure to occupants in various locations. In private residences, air samples should be collected from the basement, first-floor living space, and outdoors. In settings with diurnal occupancy patterns such as schools and office buildings, samples should be collected during normally occupied periods to be representative of typical exposure. Sample collection intakes should be located to

approximate the breathing zone for building occupants (i.e. 3 ft above the floor level where occupants are normally seated or they normally sleep). To ensure that an air sample is representative of the conditions being tested and to avoid undue influence from sampling personnel, samples should be collected for at least a 1-hour period, and personnel should avoid lingering in the immediate area of the sampling device while samples are being collected. If the goal of the sampling is to represent average concentrations over longer time periods, then longer duration sampling periods may be appropriate. Detailed information must be gathered at the time of sampling to document conditions prior to and during sampling to aid in interpretation of the test results.

Sample collection techniques vary depending on the analytical method(s) being used, and sample flow rates must conform to the specifications in the sample collection method. Some methods specify collecting samples in duplicate (e.g. passive sampling devices for tetrachloroethene). There is a major need for real-time, highly portable gas and particle instrumentation which can be used to assess personal exposure. As an added complication, it has also been found that personal exposure to many pollutants can exceed that predicted from the ambient concentration – this has been called the *personal cloud effect*. In the United States, the Relationships of Indoor, Outdoor and Personal Air (RIOPA) project, with major funding from the Health Effects Institute, investigated seasonal concentrations of 16 VOCs, 10 carbonyls and $PM_{2.5}$ in homes in Los Angeles (California), Houston (Texas) and Elizabeth (New Jersey). As an invaluable output, never done before, this study has generated a database on concentrations of air toxins and $PM_{2.5}$ in the personal breathing zone of 100 adults in each city as well as inside and outside their homes. More information on the findings of this project can be found in the report listed in the recommended 'References and Further Reading Resources' section at the end of this chapter.

Appropriate QA/QC measures must be followed for sample collection and laboratory analysis. Items that should be addressed in sampling protocols include sampling techniques, certified-clean sampling apparatus and appropriate sample holding times, temperatures and pressures. In addition, laboratory accession procedures must be followed, including field documentation (sample collection information and locations), chain of custody, field blanks, field sample duplicates and laboratory duplicates, as appropriate.

7.7 CASE STUDY – CIGARETTE SMOKE

Exposure to environmental tobacco smoke (ETS) has long been associated with premature death and morbidity. It is generally agreed that smoking cigarettes is the single biggest avoidable cause of cancer in the world (IARC, 2004). Globally, there are more than 1 billion smokers (WHO, 2017). Exposure to ETS prematurely kills more than 7 million people a year, with more than 6 million of those deaths being the result of direct tobacco use, while almost 900,000 are the result of non-smokers being exposed to secondhand smoke (WHO, 2017). The World Health Organisation (WHO, 2017) has estimated that

FOR REFERENCE PURPOSES ONLY

tobacco was responsible for more than 100 million deaths worldwide in the twentieth century, and if current trends continue, tobacco could cause 1 billion deaths in the twenty-first century. Doll et al. (1994, 2004) estimated that up to two-thirds of all long-term smokers will be killed by their habit. Smoking increases the risk of several types of cancer, including cancer of the lung, larynx, oesophagus, mouth and pharynx, bladder, pancreas, kidney, liver, stomach, bowel, cervix, ovary, nose and sinuses, as well as some types of leukaemia (Cogliano et al., 2011). It is generally agreed that, on average, smokers lose around a decade of life compared with non-smokers.

Studies have shown that there are more than 5300 different chemicals in ETS, including more than 70 chemicals that have been found to cause cancer in studies involving people or in the laboratory (IARC, 2012). There is no safe level for ETS exposure (Atlanta, 2006). In the 1990s, changing social attitudes towards the acceptability of smoking in public places led to a number of studies focusing on ETS (Jenkins et al., 1996; Ott et al., 1996). In addition to the potential carcinogenicity and toxicity of ETS, some studies indicated clear evidence of a relationship between smoking and indoor particulate concentrations (Ott et al., 1996). Simoni et al. (1998) showed that respirable suspended particulate matter (RSPM) was significantly higher in indoor environments where smoking took place, and was significantly related to the number of cigarettes smoked. Hedge et al. (1994) showed that smoking policy in buildings can have an effect on RSPM, ultraviolet particulate matter (UPM) and nicotine (the usual marker for ETS). These studies indicated that there may be implications for the health and safety of people who are regularly exposed to smoky environments.

A case study (Williams and Elam, 2000) illustrates the impact of ETS in workplaces in the 1990s. The atmospheres of two public houses in London, England, were sampled and analysed to determine the degree and nature of atmospheric pollution caused by the activities of tobacco-smoking customers. Pub A was small and family owned, whilst Pub B was quite large and owned by a nationwide chain. Pub A had two bars – a public bar of approximately 85 m^2 and a smaller saloon bar separated by a lobby. As a village pub it had a regular clientele and boasted two domino teams and two dart teams. The pub was directly adjacent to a road but also very close to an area of common land, and air quality in the area is (subjectively) good. Pub B had a public area of 90 m^2, which is divided into a small non-smoking area and a larger, smoking area. The pollutants selected – total suspended particles (TSPs) and nicotine – were chosen because of their potential health and subjective impacts (e.g. visual impairment, smell) and because nicotine is the usual tracer for ETS.

Summaries of the TSP concentrations determined at each location are displayed in Tables 7.6 and 7.7. In both pubs, arithmetic mean and median TSP concentrations recorded during the evening sessions were markedly higher than afternoon values, probably due to increased numbers of tobacco-smoking customers. The TSP values were much higher than those typically found outdoors in the UK at the time, and the topmost values are above the maximum value of 500 μg m^{-3} generally quoted by the US Environmental Protection Agency (EPA) at that time for indoor air quality. Analyses by scanning electron microscopy

FOR REFERENCE PURPOSES ONLY

indicated that a substantial proportion – over 65% – of the atmospheric particles deposited in Pub A were <10 μm in diameter. These respirable or inhalable particles are capable of taking potentially harmful, adsorbed chemical species directly into the lungs of customers and bar staff. Although this was only a *snapshot* study, the results were alarming from a public health point of view as they demonstrated that the air quality inside pubs is potentially extremely poor.

Table 7.6 TSP concentrations recorded in two public houses in London, England, during 1994–1996 (μg m^{-3})

					Percentiles			
Location	*Session*	*N*[a]	*Mean SD*[b]	*Min*[c]	*25*	*50*	*75*	*Max*[d]
Pub A								
Public bar (working hours)	Afternoon	28	419 ± 105	188	352	402	509	648
	Evening	28	575 ± 146	224	498	556	638	939
	All	56	498 ± 148	188	380	503	583	939
Public bar (outside working hours)	[e]N/A	2	145	127	[e]N/A	[e]N/A	[e]N/A	163
Domestic area above pub (non-smoking)	[e]N/A	2	21.5	21	[e]N/A	[e]N/A	[e]N/A	22
Pub B								
Smoking area	Afternoon	8	70 ± 37	25	41	63	96	139
	Evening	9	241 ± 137	143	174	189	262	582
	All	17	160 ± 133	25	63	143	193	582
Non-smoking area	Afternoon	10	103 ± 75	37	48	80	135	276
	Evening	13	162 ± 115	18	46	141	260	380
	All	23	136 ± 102	18	49	116	190	380

[a] N = Number of samples.

[b] Mean ± SD = arithmetic mean ± standard deviation.

[c] Min = minimum value.

[d] Max = maximum value.

[e] N/A = not applicable.

Table 7.7 Diurnal variations in TSP concentrations recorded in a public house (Pub B) in London, England (μg m^{-3})

Day	*Session*	*Arithmetic mean standard deviation*	*Range*
Monday	Afternoon	417±47	357–464
	Evening	456±156	224–548
Tuesday	Afternoon	347±61	258–369
	Evening	632±17	617–655

FOR REFERENCE PURPOSES ONLY

Wednesday	Afternoon	353±12	343–370
	Evening	559±56	515–639
Thursday	Afternoon	328±96	188–400
	Evening	838±77	798–939
Friday	Afternoon	467±70	405–556
	Evening	537±86	471–658
Saturday	Afternoon	436±114	279–524
	Evening	468±106	343–556
Sunday	Afternoon	586±45	540–648
	Evening	536±61	474–588

Concern about the adverse health impacts of ETS continued to rise until, despite protests from the tobacco industry and publicans, the Republic of Ireland became the first country in the world to implement a comprehensive smoking ban in workplaces in March 2004. The Irish initiative spread rapidly and as of September 2010, national smoke-free legislation had been ratified by over 170 countries (Nagelhout et al., 2011). The principal goals of a smoking ban in public places are to protect non-smokers from the perils of ETS and to provide supportive conditions for those who want to quit smoking, although it is argued that they also reduce health-care costs, increase productivity and reduce the risk of fire. The bans have generally been very successful; several studies have documented the significant health and economic benefits attributed to smoking bans (Been et al., 2014).

REFERENCES AND FURTHER READING RESOURCES

ASTM (2018) *ASTM Standards on Indoor Air Quality*. American Society for Testing & Materials Press West Conshohocken, USA.

Atlanta, G. (2006) The health consequences of involuntary exposure to tobacco smoke: A report of the surgeon general.https://stacks.cdc.gov/view/cdc/13252/ (Accessed 24 July 2017).

Been, J. V., Nurmatov, U. B., Cox, B., Nawrot, T. S., van Schayck, C. P., and Sheikh, A. (2014) Effect of smoke-free legislation on perinatal and child health: A systematic review and meta-analysis. *Lancet*, 383(9928): 1549–1560.

Burroughs, B., and Hansen, S. J. (2008) *Managing Indoor Air Quality*. Fairmont Press, Lilburn, GA.

Cogliano, V. J., Baan, R., Straif, K., Grosse, Y., Lauby-Secretan, B., El Ghissassi, F., Bouvard, V. et al. (2011) Preventable exposures associated with human cancers. *Journal of the National Cancer Institute*, 103(24): 1827–1839.

Doll, R., Peto, R., Boreham, J., and Sutherland, I. (2004) Mortality in relation to smoking: 50 years' observations on male British doctors. *British Medical Journal*, 328(7455): 1519.

Doll, R., Peto, R., Wheatley, K., Gray, R., and Sutherland, I. (1994) Mortality in relation to smoking: 40 years' observations on male British doctors. *British Medical Journal*, 309(6959): 901–911.

Eadie, D., Heim, D., Macaskill, S., Ross, A., Hastings, G., and Davies, J. (2008) A qualitative analysis of compliance with smoke-free legislation in community bars in Scotland: Implications for public health. *Addiction*, 103: 1019–1026.

Guerin, M. R., Jenkins, R. A., and Tomkins, B. (2000) *The Chemistry of Environmental Tobacco Smoke: Composition and Measurement (Indoor Air Research)*. CRC Press, Boca Raton, FL.

Hedge, A., Erickson, W. A., and Rubin, G. (1994) The effects of alternative smoking policies on indoor air quality in 27 office buildings. *Annals of Occupational Hygiene*, 38(3): 265–278.

FOR REFERENCE PURPOSES ONLY

Heinsohn, R. J., and Cimbala, J. M. (2003) *Indoor Air Quality Engineering: Environmental Health and Control of Indoor Pollutants*. CRC Press, Boca Raton, FL.

Hocking, M. B., and Hocking, D. (2005) *Air Quality in Airplane Cabins and Similar Enclosed Spaces*. Springer, Berlin, Germany.

IARC (2012) *Personal habits and indoor combustions: A review of human carcinogens*, Vol. 100 E. WHO Press, Lyon, France.

International Agency for Research into Cancer (IARC) (2004) Monographs on the evaluation of carcinogenic risks to humans. *Tobacco Smoke and Involuntary Smoking*, 83: 1–1438.

Jenkins, R. A., Palausky, A., Counts, R. W., Bayne, C. K., Dindal, A. B., and Guerin, M. R. (1996) Exposure to environmental tobacco smoke in sixteen cities in the United States as determined by personal breathing zone air sampling. *Journal of Exposure Analysis and Environmental Epidemiology*, 6(4): 473–502.

Nagelhout, G. E., Mons, U., Allwright, S., Guignard, R., Beck, F., Fong, G. T., de Vries, H., and Willemsen, M. C. (2011) Prevalence and predictors of smoking in 'smoke-free' bars. Findings from the International Tobacco Control (ITC) Europe surveys. *Social Science & Medicine*, 72: 1643–1651.

Ott, W., Switzer, P., and Robinson, J. (1996) Particle concentrations inside a tavern before and after prohibition of smoking: Evaluating the performance of an indoor air quality model. *Journal of the Air & Waste Management Association*, 46(12): 1120–1134.

Pepper, D. W., and Carrington, D. (2009) *Modelling Indoor Air Pollution*. Imperial College Press, London, UK.

Pluschke, P. (2004) *Indoor Air Pollution: Handbook of Environmental Chemistry*. Springer, Berlin, Germany.

Salthammer, T., and Uhde, E. (Eds.) (2009) *Organic Indoor Air Pollutants: Occurrence, Measurement and Evaluation*. Wiley, Weinheim, Germany.

Simoni, M., Biavati, P., Carrozzi, L., Viegi, G., Paoletti, P., Matteucci, G., Ziliani, G. L., Ionnilli, E., and Sapigni, T. (1998) The Po River Delta (North Italy) indoor epidemiological study: Home characteristics, indoor pollutants and subjects' daily activity pattern. *International Journal of Indoor Air Quality and Climate*, 8(2): 70–79.

Spengler, J. D., McCarthy, J. F., and Samet, J. M. (2001) *Indoor Air Quality Handbook*. McGraw-Hill Education, New York.

Tucker, W. (2006) *Sources of Indoor Air Contaminants: Characterizing Emissions and Health Impacts*. New York Academy of Sciences. New York, NY.

Warwick, H. (1999) *Smoke: The Silent Killer – Indoor Air Pollution in Developing Countries*. ITDG Publishing, London, UK.

Watt, J., Tidblad, J., Kucera, V., and Hamilton, R. (Eds.) (2009) *The Effects of Air Pollution on Cultural Heritage*. Springer, New York.

Weisel, C. P., Zhang, J., Turpin B. J., Morandi, M. T., Colome, S., Stock, T. H., Spektor, D. M. et al. (2005) *Relationships of Indoor, Outdoor and Personal Air (RIOPA). Part I, Collection Methods and Descriptive Analyses*. The Health Effects Institute, Boston, MA, Report No. 130-I.

WHO (2006) *Air Quality Guidelines – Global Update 2005*. World Health Organisation, Copenhagen, Denmark.

WHO (2017) *Tobacco*. World Health Organisation. http://www.who.int/mediacentre/factsheets/fs339/en/.

Williams, I. D., and Elam, D. (2000) Indoor air quality in public houses. *Issues in Health & Environment*, 1(2): 3–15.

Yocom, J. E., and McCarthy, S. M. (1991) *Measuring Indoor Air Quality*. Wiley, Chichester, UK.

FOR REFERENCE PURPOSES ONLY

Chapter 8

Air pollution modelling

Air pollution models help us to understand the way air pollutants behave in the environment. In principle, a perfect model would enable the spatial and temporal variations in pollutant concentration to be predicted to sufficient accuracy for all practical purposes, reducing the need for measurements. It is noteworthy, however, that a model is no use unless it has been validated to show that it works. Hence, the process of model development goes hand in hand with developments in measurement. There are many reasons for using models, such as for regulatory purposes in establishing which sources are responsible for what proportion of concentration at any receptor, estimating population exposure on a higher spatial or temporal resolution than is practicable by measurement, targeting emission reductions on the highest contributors, predicting concentration changes over time. There are four main families of models:

- *Dispersion models*, which are based on a detailed understanding of physical, chemical and fluid dynamical processes in the atmosphere. They enable the concentration at any place and time to be predicted if the emissions and other controlling parameters are known.
- *Receptor models*, which are based on the relationships between a data set of measured concentrations at the receptor and a data set of emissions that might affect those concentrations.
- *Stochastic models*, which are based on semi-empirical statistical relationships between the pollutant concentrations and any factors that might affect them, regardless of the atmospheric physical processes.
- *Compartment or box models*, in which inputs to, and outputs from, a defined volume of the atmosphere are used to calculate the mean concentration within that volume.

All air pollution modelling and validation need some understanding of the underlying meteorology, so we will first cover this topic and then discuss the models themselves in this chapter.

8.1 AIR POLLUTION METEOROLOGY

The main meteorological factors that affect the dispersion and transformation of air pollutants are discussed in the following sections.

8.1.1 Atmospheric energy balance

8.1.1.1 Dry adiabatic lapse rate

For a dry atmosphere (containing water vapour, but not liquid water droplets), the rate of decrease of temperature with height caused by this type of displacement is called the *dry adiabatic lapse rate* (Γ, or DALR). *Adiabatic* simply means that the air parcel's total energy content is conserved during the displacement, not exchanged with the surrounding air.

In a *neutral atmosphere*, that is, when the atmosphere is in a state in which adiabatic air parcels are in equilibrium with their surroundings during their vertical movement, the temperature profile $T(z)$ is derived in the following steps. First, for an air parcel of mass m moving infinitesimally in the atmosphere, the change in its internal energy dU can be obtained from the first law of thermodynamics as:

$$dU = dQ + dW \tag{8.1}$$

where:

dQ is the heat transferred to the air parcel from its surroundings

dW is the work done on the system

But

$$dW = -pdV \tag{8.2}$$

where:

p is the system pressure

dV is the change in its volume

For an adiabatic system $dQ = 0$ and dU can be also written as:

$$dU = mc_v dT \tag{8.3}$$

where:

c_v is the specific heat capacity of air at constant volume

dT is the temperature difference

Thus, for the adiabatic air parcel, the first law of thermodynamics gives:

$$mc_v dT = -pdV \tag{8.4}$$

Replacing dV using the ideal gas law ($pV = mRT/M_{air}$) we can re-write Equation 8.4 as:

$$mc_v dT = \frac{mRT}{M_{air}} \frac{dp}{p} - \frac{mR}{M_{air}} dT \tag{8.5}$$

Re-arranging and dividing both sides by dz, we get

$$\left(mc_v + \frac{mR}{M_{air}}\right) \frac{dT}{dz} = \frac{mRT}{pM_{air}} \frac{dp}{dz} \tag{8.6}$$

Substituting $\frac{dp}{dz} = \frac{-M_{air} g p(z)}{RT(z)}$ in Equation 8.6, we finally get:

$$\frac{dT}{dz} = \frac{-g}{c_v + \frac{R}{M_{air}}} \tag{8.7}$$

But $c_v + \frac{R}{M_{air}} = c_p$

Therefore, the value of $\frac{dT}{dz}$ (or Γ) is fixed by physical constants, and can be calculated from:

$$\Gamma = g/c_p \tag{8.8}$$

where:

g is the acceleration due to gravity = 9.81 m s^{-2}

c_p is the specific heat of air at constant pressure = 1010 J kg^{-1} K^{-1}

Hence, Γ = 9.8°C km^{-1}. This value applies, to sufficient accuracy, in the lower 20 km of the atmosphere. Above that height, changes in the molecular composition (which affect the molar mass) and in g (due to increasing distance from the centre of the Earth) start to affect the value. This is the reason for the steady decrease in temperature with height – on mountains, for example.

8.1.1.2 Saturated adiabatic lapse rate

If the air temperature falls below the water vapour dew point while the parcel is being lifted, then the excess water vapour starts to condense. This releases latent heat of vaporisation which reduces the rate of cooling. Conversely, if a descending parcel contains liquid water droplets, then the process is reversed – the droplets evaporate as the parcel warms, extracting sensible heat from the air and reducing the rate of warming. The variation of temperature with height when there is liquid water present is known as the *saturated adiabatic lapse rate* (SALR), or Γ_{sat}, which is calculated as follows. For SALR we can write Equation 8.8 as:

$$\Gamma_{sat} = g/c_{p'}$$

where $c_{p'}$ is the heat capacity of a mixture of air and water vapour. If the ratio of the mass

of water vapour to the mass of dry air in the air parcel (also known as *saturation mixing ratio*) is q_s then:

$$c_{p'} = (1-q_s)c_p + q_s c_{p(\text{watervapour})} \tag{8.9}$$

If m_w is the mass of water vapour in the air parcel and L is the latent heat of evaporation of water per gram, then the heat released for the infinitesimal motion of the air parcel is $-Ldm_w$. Therefore, the air parcel energy balance (Equation 8.4) can be re-written as:

$$mc_v dT = -pdV - Ldm_w \tag{8.10}$$

We can still apply the ideal gas law since, despite the air parcel being saturated, the thermodynamic properties of the gas phase remain the same as for air. This gives:

$$mc_v dT = \frac{mRT}{M_{\text{air}}}\frac{dp}{p} - \frac{mR}{M_{\text{air}}}dT - Ldm_w \tag{8.11}$$

On dividing both sides by air parcel mass and substituting c_v and c_p, we have:

$$c_p dT = \frac{RT}{M_{\text{air}}}\frac{dp}{p} - L\frac{dm_w}{m} \tag{8.12}$$

But m_w/m is same as q_s. So dividing the entire expression by dz and substituting

$$\frac{dp}{dz} = \frac{-M_{\text{air}}gp(z)}{RT(z)}$$

in Equation 8.12 we finally get:

$$\Gamma_{\text{sat}} = \frac{dT}{dz} = \frac{-g}{c_p}\left\{\frac{1}{1+(L/c_p)\,(dq_s/dT)}\right\} \tag{8.13}$$

As the saturated vapour pressure of water depends on both the temperature and pressure, the SALR is also variable (Table 8.1). The minimum values are found for surface pressures and the warmest temperatures. As the air also has to be saturated, this is more likely to be in the tropics than above the Sahara. Maximum values are found where the air is very cold, because then the water vapour content is low. The *average lapse rate* over the Earth is about 6.5°C km^{-1}.

8.1.1.3 Atmospheric stability and temperature profile

The adiabatic lapse rates describe the temperature changes expected in a parcel of air when it is displaced vertically. This is not usually the same as the vertical temperature profile of the air, as would be measured, for example, by recording the temperature transmitted by a sounding balloon as it rose through the atmosphere. This *environmental lapse rate* (ELR) is the vertical variation, or profile, of air temperature with height that exists at any particular time and place. It may be equal to the adiabatic lapse rate over at least part of the height range of interest (up to, say, 1 km for pollutant dispersion), but it may be substantially

FOR REFERENCE PURPOSES ONLY

different. The local balance between the two lapse rates gives an insight into the concept known as *atmospheric stability*, which in essence is a measure of the atmosphere's tendency to encourage or deter vertical movement of air, that is, exchange processes – stable air tends to resist vertical air movement, and vice versa.

First, consider the different physical situations shown in Figure 8.1. In Figure 8.1a, a marble is at rest in a bowl. Any small displacement of the marble results in a restoring force – a force that moves the marble back towards its initial position. Such a system is said to be stable. In Figure 8.1b, the marble is on a flat surface. No force in any direction is generated by a displacement, and the system is described as neutral. Finally, in Figure 8.1c, the marble is poised on the top of the upturned bowl. Now, any displacement results in a force away from the initial position, and the system is unstable.

Table 8.1 Variation of saturated lapse rate (°C km^{-1}) with temperature and pressure

Pressure/mb	Temperature/°C				
	−40	−20	0	20	40
1000	9.5	8.6	6.4	4.3	3.0
800	9.4	8.3	6.0	3.9	
600	9.3	7.9	5.4		
400	9.1	7.3			
200	8.6				

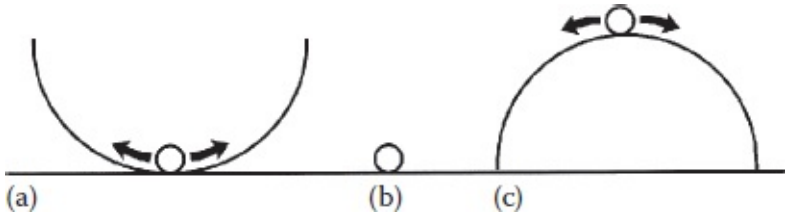

Figure 8.1 Stable (a), neutral (b) and unstable (c) systems.

FOR REFERENCE PURPOSES ONLY

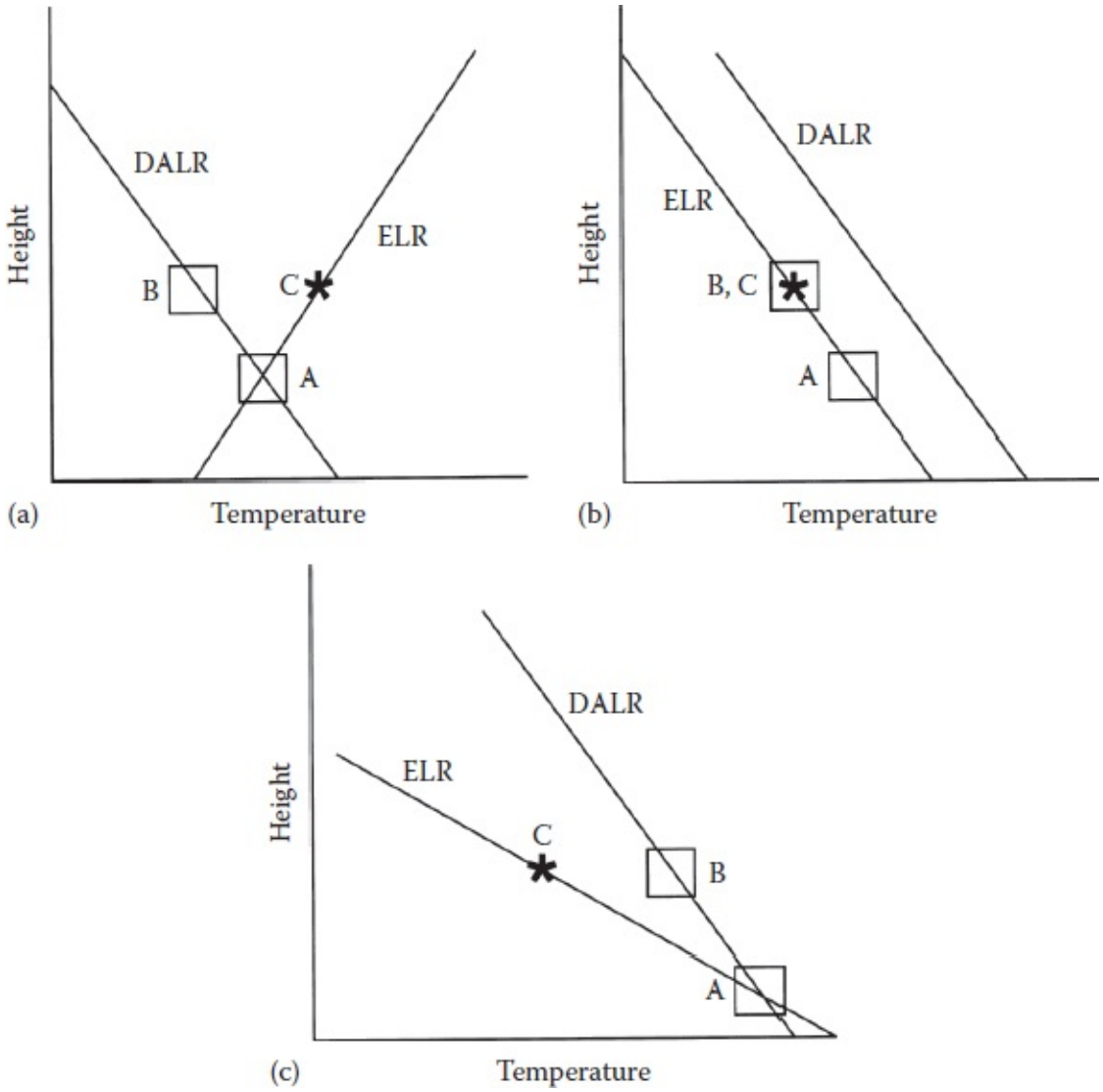

Figure 8.2 Stable (a), neutral (b) and unstable (c) environmental lapse rates.

These ideas can be applied to air parcels in the atmosphere. Consider, for example, the different situations shown in Figure 8.2a, b, c. In each figure, the prevailing ELR is shown, and the DALR is given for comparison. A parcel of air that starts at A in Figure 8.2a and moves upwards cools at the DALR, reaching a lower temperature at B. However, the air around the parcel at the same height is at C on the ELR. The parcel has become cooler and denser than its surroundings and tends to sink back towards its starting height. If its initial displacement is downward, it becomes warmer and less dense than its surroundings and tends to rise back up. The ELR is therefore stable, because small disturbances are damped out. In Figure 8.2b, a rising parcel again cools at the DALR. As this is equal to the ELR, the parcel is in air of the same temperature and density after displacement. The ELR is therefore neutral, because vertical motions are neither accelerated nor damped. Examination of vertical displacements for Figure 8.2c shows that they are accelerated and that such an ELR is unstable.

If we look at the forces acting on a parcel displaced upwards in a stable atmosphere, an

FOR REFERENCE PURPOSES ONLY

equation of motion can be written for which the solution is an oscillation about the starting height. That is, the parcel experiences a restoring force that accelerates it back towards its original position. Since by then it is moving, it overshoots downwards, and a restoring force accelerates it upwards again, and so on. The frequency of this oscillation, which is called the buoyancy frequency, corresponds to a natural period of a few minutes in the lower atmosphere.

In practice, real temperature profiles in the atmosphere often consist of a mixture of different ELRs, so that vertical dispersion is different at different heights. Consider the ELR shown in Figure 8.3. Between A and B, strong solar heating of the ground has warmed the lowest layers of air; the middle layer BC is close to DALR, while the layer CD shows an increase of temperature with height (this is known as an inversion of the temperature profile).

This profile is very unstable (strong dispersion) in AB, close to neutral in BC and very stable (poor dispersion) in CD. When a persistent anti-cyclonic high-pressure region is present, there is often an area in the centre where high-level air is sinking. The sinking raises the pressure and hence the temperature, generating an elevated inversion which may act as a lid to vertical plume dispersion and increase ground-level pollutant concentrations. As the pressure gradients, and hence wind speeds, are low under these meteorological conditions, a serious pollutant episode may result.

8.1.1.4 Potential temperature

A useful additional concept is that of potential temperature, θ. The DALR shows a steady reduction of temperature with height, and it is not obvious at first glance whether a particular rate of reduction is greater than or less than the DALR. This divergence is important for the assessment of atmospheric stability and pollutant dispersion, as we have seen. We can define the potential temperature of an air parcel at any pressure (i.e. height) as the temperature that it would have if the parcel were moved adiabatically to a standard or reference pressure. This reference pressure is normally taken to be 100 kPa, which is very close to the standard global average atmospheric pressure at sea level of 101.325 kPa. The potential temperature, then, is the temperature that the parcel would have if it was moved down to sea level adiabatically.

FOR REFERENCE PURPOSES ONLY

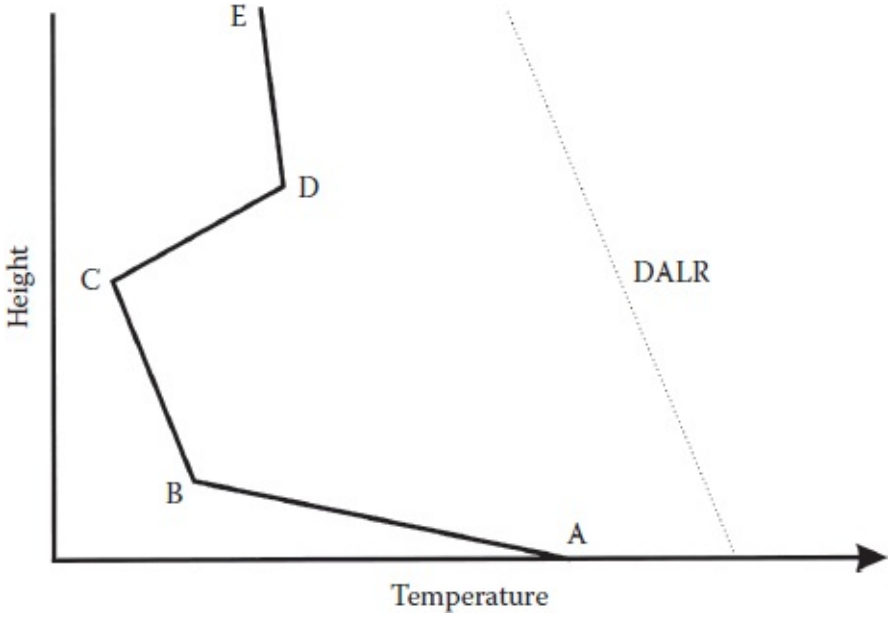

Figure 8.3 An atmospheric temperature profile involving a range of stabilities.

If an air parcel is in equilibrium with its surroundings at temperature T and pressure p, then θ can be calculated by integrating Equation 8.5 from initial conditions (T, p) to the final state (θ, p_0). This yields:

$$\theta = T\left(\frac{p_0}{p}\right)^{\frac{R}{c_p M_{\text{air}}}} \tag{8.14}$$

By definition, θ is constant for an air parcel that is moved upwards adiabatically from sea level. An actual temperature profile such as that in Figure 8.4 is transformed into a potential temperature profile, where layers having neutral stability are vertical; in stable atmospheres θ increases with height, while in unstable atmospheres it decreases with height. This can be explained mathematically by differentiating Equation 8.14 with respect to z, which yields:

$$\frac{1}{\theta}\frac{d\theta}{dz} = \frac{1}{T}\frac{dT}{dz} - \frac{R}{c_p M_{\text{air}} p}\frac{dp}{dz} \tag{8.15}$$

Substituting $\frac{dp}{dz} = \frac{-M_{\text{air}} g p(z)}{RT(z)}$ and then $g/c_p = \Gamma$ we get:

$$\frac{1}{\theta}\frac{d\theta}{dz} = \frac{1}{T}\left(\frac{dT}{dz} + \Gamma\right) \tag{8.16}$$

FOR REFERENCE PURPOSES ONLY

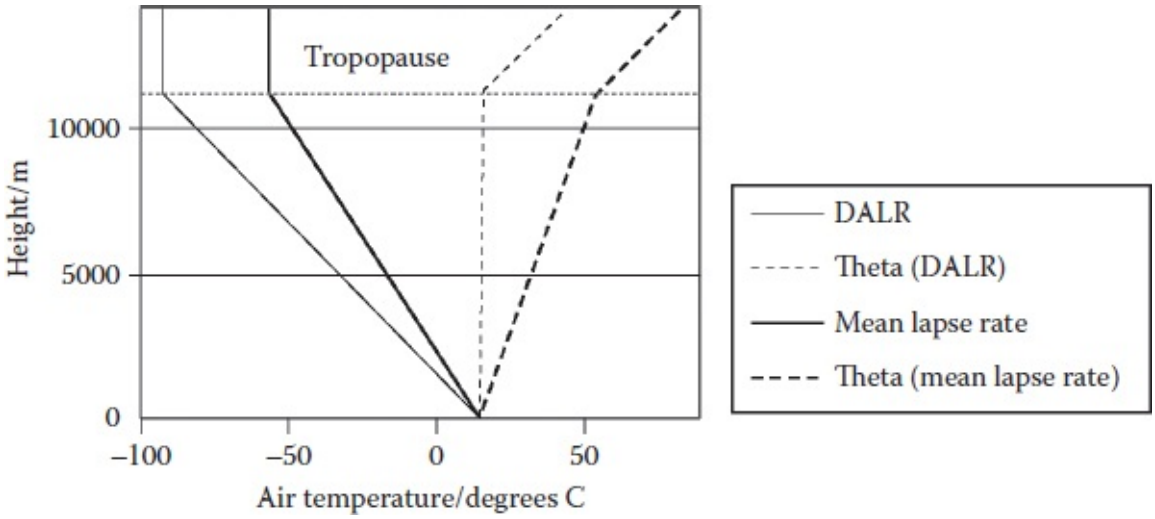

Figure 8.4 Actual and potential temperature profiles.

But in a neutral atmosphere $dT/dz = -\Gamma$ so, $d\theta/dz = 0$ from Equation 8.16. Thus, in a neutral atmosphere $\theta = T_0$ (i.e. it is constant).

8.1.2 Atmospheric dispersion parameters

8.1.2.1 Air pressure and wind fields

Air pressure decreases exponentially with height. Hence, as an air parcel moves up (or down) in the atmosphere, it must expand (or compress) and cool (or warm). In metrological terms *wind is a manifestation of the constantly varying air pressure across the space and time in the Earth's atmosphere*. Therefore, pressure has been key to modelling wind fields and the resulting air pollutant concentrations.

Consideration of wind in air pollution modelling primarily includes wind direction, wind speed and atmospheric turbulence (which is closely linked with the concept of stability). Wind direction is conventionally specified as the direction from which the wind is blowing, because we have been more interested in what the wind has collected before it reaches us than in where it will go afterwards. Wind direction is commonly identified with one of 16 (or sometimes 32) points of the compass (e.g. a south-westerly wind is a wind blowing from the south-west), or more scientifically as an angle in degrees clockwise from north (so the south-west wind will be blowing from between 213.75° and 236.25°). What is spoken of colloquially as the wind direction is rarely constant in either the short or long term. The average value over periods of between one and a few hours is determined by meteorology – the passage of a frontal system, or the diurnal cycle of sea breezes near a coast, for example. This medium-term average value of wind direction is of fundamental importance in determining the area of ground that can be exposed to the emission from a particular source. Short-term variations (between seconds and minutes), due to turbulence, are superimposed on this medium-term average – they can be seen on a flag or wind vane. In

FOR REFERENCE PURPOSES ONLY

addition to these short-term horizontal variations, there are also short-term variations in the vertical component of the wind that affect turbulent dispersion. The magnitudes of both horizontal and vertical variations are influenced by the atmospheric stability, which in turn depends on the balance between the adiabatic lapse rate and the environmental lapse rate. These concepts are described in Section 8.1.1.

Wind speed is measured in m s^{-1} or knots (one knot is one nautical mile per hour; one nautical mile is 6080 ft, or 1.15 statute miles). Although the use of SI units is encouraged in all scientific work, some professions have stuck with earlier systems. Thus mariners, pilots and meteorologists are all comfortable with knots. Mariners also use the Beaufort Scale, which relates wind speed to its effects on the sea.

Wind speed is important for atmospheric dispersion in three distinct ways. First, any emission is diluted by a factor proportional to the wind speed past the source. Second, mechanical turbulence, which increases mixing and dilution, is created by the wind. Third, a buoyant source (hot or cold) is *bent over* more at higher wind speeds, keeping it closer to its release height. Friction with the ground reduces the wind speed near the surface, so that the speed at the top of an industrial chimney (such as that of a power station, which might be 200 m tall) is substantially greater than at the bottom.

The change with height can be approximated by a power law such as:

$$u(z) = u_0(z/z_0)^p \tag{8.17}$$

Table 8.2 Variation of the wind speed exponent p with stability category

Pasquill stability Class	*Exponent p for rough terrain*	*Exponent p for smooth terrain*
A – the most unstable	0.15	0.07
B	0.15	0.07
C	0.20	0.10
D	0.25	0.15
E	0.40	0.35
F – the most stable	0.60	0.55

where:

$u(z)$ is the wind speed at height z

u_0 is the wind speed measured by an anemometer at height z_0

p is an exponent that varies with atmospheric stability

Table 8.2 gives the values of the exponent p appropriate to the *Pasquill stability categories* which are described in the following section. This supports the intuitive idea that the best-mixed air (Class A) has the smallest variation of speed with height.

We saw in Section 8.1.1 that the lapse rate for saturated air is lower than for dry air. Hence the same air mass may be stable or unstable, depending on whether it is saturated or

FOR REFERENCE PURPOSES ONLY

not. As an unsaturated air parcel starts to rise, it cools at the dry lapse rate of 9.8°C km^{-1}. If the ELR is, say, 8°C km^{-1}, then the movement is stable. But if the upwards movement cools the air enough to cause condensation of water vapour, then the lapse rate falls to the saturated value of, say, 7°C km^{-1}, and the displacement is now unstable. This is called conditional instability. The condition is not rare – as the average global lapse rate of 6.5°C falls between the dry adiabatic rate and the average moist lapse rate of 6°C, conditional instability is the norm. Furthermore, a humidity gradient can change the stability. This is most often seen in the warm atmosphere near the surface above the tropical ocean. The sea surface evaporates water into the atmosphere. Hence the density is reduced (because the molar mass of water is 18 compared with an average of 29 for the nitrogen, oxygen and argon), so the air density decreases and instability is promoted.

8.1.2.2 Atmospheric stability classes

The general effect of environmental variables on atmospheric stability can be summarised as follows:

- On cloud-free days, solar radiation warms the ground during the day, making the lowest air layers unstable.
- On cloud-free nights, net upwards longwave thermal radiation cools the ground, making the lowest air layers stable and creating a ground-level inversion.
- As wind speed rises, vigorous vertical exchange tends to generate a neutral ELR equal to the DALR.
- As cloud cover increases, daytime heating and night-time cooling of the ground are both reduced, again making the ELR closer to the DALR.
- A persistent-high pressure region has a downward air movement at the centre, which often creates an elevated inversion and traps pollutants near the ground. This is known as *anti-cyclonic gloom.*

Table 8.3 Dependence of stability on meteorological parameters

Surface wind speed ms^{-1}	*Daytime sun (flux density in* W m^{-2}*)*			*Nighttime (cloud amount in oktas)*		
	Strong (>590)	*Moderate* (300–590)	*Weak* (<290)	8	4–7	0–3
<2	A	A–B	B	D	G	G
2–3	A–B	B	C	D	E	F
3–5	B	B–C	C	D	D	E
5–6	C	C–D	D	D	D	D
>6	C	D	D	D	D	D

FOR REFERENCE PURPOSES ONLY

The influence of solar radiation and wind speed on stability led Pasquill to identify stability classes on a scale from A (very unstable) to G (very stable), and to relate them to meteorology in the simple way shown in Table 8.3. Hence, they are also known as *Pasquill stability classes*.

First, look at the stability classes during the daytime. When the sun is strong and the winds light, we would expect maximum ground heating, raising the temperature of the lowest layers of air and creating unstable conditions. With less sunshine, this effect is reduced and the instability is less marked. As the wind speed increases, vertical mechanical mixing starts to override the buoyancy effects, and frequent exchanges of air parcels at DALR generate a neutral ELR (Class D). At night, net radiation losses and ground cooling are most marked under clear skies. As the ground cools, the lowest air layers become stable (Class G). The cloudier or the windier it becomes, the more probable Class D becomes again.

8.1.2.2.1 Occurrence of Pasquill classes

Table 8.4 shows the average occurrence of different stability classes in the UK. As would be expected, our temperate maritime climate gives us high average wind speeds and cloud cover, so that Classes C and D are the most likely. The very high values for ELR given here, equivalent to up to 40°C km^{-1}, can only be sustained within the lowest few metres of the atmosphere.

Table 8.4 Occurrence of different stability classes in the UK

Stability class	*Occurrence in UK/%*	*ELR °C (100 m)$^{-1}$*	*u at 10 m ms^{-1}*	*Weather*
A: Very unstable	1	<–1.9	1.0 to 2.5	Very sunny
B: Moderately unstable	5	–1.9 to –1.7	1.0 to 5.0	Sunny
C: Slightly unstable	15	–1.7 to –1.5	2.0 to 6.0	Part cloud (day)
D: Neutral	65	–1.5 to –0.5	2.0 to >10.0	Overcast
E: Stable	6	–0.5 to +1.5	2.0 to 5.0	Part cloud (night)
F: Very stable	6	+1.5 to +4.0	2.0 to 3.0	Clear night
G: Even more stable than F	2		Calm	

8.1.2.3 Other stability estimators

The Pasquill scheme described earlier is semi-quantitative, as it ascribes categories to ranges of the driving variables wind speed and solar radiation, but it does not involve a formula with explicit values. There are two more quantitative parameters in common use – the *Richardson number* and the *Monin–Obukhov length*.

8.1.2.3.1 The Richardson number

The Richardson number *Ri* is calculated from gradients of temperature and wind speed:

$$Ri = \frac{\frac{g}{T}\frac{\partial T}{\partial z}}{\left(\frac{\partial u}{\partial z}\right)^2}$$

where *T* is the absolute temperature.

The Richardson number is dimensionless. We can see by inspection that if temperature increases strongly with height, which is the stable condition that we have discussed in Section 8.1.1, then *Ri* tends to be large and positive. If *T* decreases with height at the adiabatic lapse rate, *Ri* is negative. If there is a large gradient of wind speed with height, *Ri* is small.

$Ri < -1$	Free convection
$-1 < Ri <$ –	0.01 unstable mixed convection
$-0.01 < Ri < +0.01$	Forced convection
$+0.01 < Ri < +0.1$	Damped forced convection
$Ri >$	0.1 increasingly stable

The Richardson number is mainly used by meteorologists to describe events in the free atmosphere, rather than by air pollution scientists discussing dispersion closer to the ground.

8.1.2.3.2 The Monin–Obukhov length

The Monin–Obukhov length, *L*, is a function of heat and momentum fluxes:

$$L = -\frac{\rho c_p T u_*^3}{kgC}$$

where:

T is the absolute temperature

C is the vertical sensible heat flux

The formula for *L* recognises the two contrasting processes that drive atmospheric turbulence and dispersion. Mechanical turbulence is generated by wind blowing over surface roughness elements. It is therefore strongest at the surface and reduces upward depending on the stability. Convective turbulence is generated by heat flux from the surface and increases upwards in unstable conditions but is damped out in stable conditions (Table 8.5). The result has units of metres and represents the scale of the turbulence. As *C* may be

positive (up) or negative (down), L may be positive or negative. When conditions are unstable or convective, L is negative, and the magnitude indicates the height above which convective turbulence outweighs mechanical turbulence. When conditions are stable, L is positive, and indicates the height above which vertical turbulence is inhibited by stable stratification. In practice, values range between infinity (in neutral conditions when C is zero) and –100 m. Atmospheric stability is related to the ratio h/L, where h is the depth of the boundary layer. L is increasingly being used in dispersion models as a more sophisticated estimator of turbulence than the Pasquill category.

Table 8.5 Stability as a function of L and h

Stability	*Range of h/L*
Stable	$h/L \geq 1$
Neutral	$-0.3 \leq h/L < 1$
Convective	$h/L < -0.3$

For practical use in the lowest few hundred metres of the atmosphere, we can write:

$$L = \left(\frac{\rho c_p T}{kg}\right)\frac{u_*^3}{C} = \text{const.}\,\frac{u_*^3}{C} \tag{8.18}$$

Note that, although this expression does not look like a length at first sight, the dimensions do confirm that it is, that is, (kg m^{-3})(J kg^{-1} K^{-1})(K)(m s^{-1})^3/(m s^{-2})(W m^{-2}) has dimensions of length and units of metres. The values of ρ, c_p, T, k and g are then taken as constant.

With the following:

ρ = 1.2 kg m^{-3}
c_p = 1010 J kg^{-1} K^{-1}
T = 288 K (15°C)
k = 0.41
g = 9.81 m s^{-2}

We have $L = 8.7 \times 10^4\ u_*^3/C$.

Other stability estimators have been used, such as the standard deviation of the fluctuations in the horizontal wind direction, and the ratio of the wind speeds at two heights. Comparisons of the predictions made by different estimators from the same data set have shown that the Monin–Obukhov length method correlates best with the Pasquill classes.

8.1.2.3.3 Boundary layer height

The Monin–Obukhov formulation can also be used to estimate the height of the boundary layer in stable-to-neutral conditions, from:

$$\frac{h}{L} = \frac{0.3u_*/|f|L}{1+1.9h/L}$$

Table 8.6 Relationships between stability estimators

Wind speed u/ms^{-1}	*Pasquill category*	*Boundar layer height h/m*	*Monin–Obukhov Length/m*	*h/L*
1	A	1300	–2	–650
2	B	900	–10	–90
5	C	850	–100	–8.5
5	D	800	OO	0
3	E	400	100	4
2	F	100	20	5
1	G	100	5	20

The situation in unstable conditions is more complex, because the boundary layer grows from an initial value of zero when the surface heat flux becomes positive, at a rate governed by the surface heat flux, the temperature jump across the top of the layer, and the friction velocity (Table 8.6).

8.2 DISPERSION MODELS

The qualitative aspect of dispersion theory is to describe the fate of an emission to the atmosphere from a point, area or line source. Quantitatively, dispersion theory provides a means of estimating the concentration of a substance in the atmosphere, given specific information about meteorological factors and the geometry and strength of the source. Dispersion models include:

- *Eulerian models*, which numerically solve the atmospheric diffusion equation. Eulerian models work on the measurement of the properties of the atmosphere as it moves past a fixed point. A wind vane or cup anemometer are Eulerian sensors.
- *Gaussian models*, which are built on the Gaussian (normal) probability distribution of wind vector (and hence pollutant concentration) fluctuations. Strictly these are a subset of Eulerian models but are usually treated as a group in their own right.
- *Lagrangian models*, which treat processes in a moving airmass, or represent the processes by the dispersion of fictitious particles. Tracking a neutral-density balloon as it moves downwind is a Lagrangian measurement.

Dispersion is essentially due to turbulence, and turbulence occurs with a great range of

FOR REFERENCE PURPOSES ONLY

length scales in the atmosphere. Hence there are additional families of models depending on the length (or time) scale of interest:

- *Macro scale* (approximately 1000 km, or days). Atmospheric flow is driven by synoptic phenomena such as high-/low-pressure areas, for example, the long-range transport of air pollution from Central Europe to the UK or from the UK to Scandinavia.
- *Meso scale* (10s–100s of km, or hours). Air movement is synoptically driven, but it is modified by local effects such as surface roughness and obstacles, for example, the dispersion of emissions from a power station chimney over the surrounding countryside.
- *Microscale* (<1 km, or minutes). Airflow depends mainly on local features, for example, urban flows in the labyrinth of street canyons formed by urban skyscrapers.

Many examples are available in the literature with information on evaluation of different dispersion modelling approaches and tools. In this chapter we have mainly focused on Gaussian plume models first, because of their wide application in air pollution dispersion modelling. The more recent advances in regional chemistry modelling are then presented towards the end of the chapter.

8.3 GAUSSIAN DISPERSION THEORY

Eulerian models are based on the concept of a fixed reference point, past which the air flows. Lagrangian models, in contrast, are based on the concept of a reference point that travels with the mean flow. In the commonly used Gaussian method, the simplest realisation of this idea is to think of an instantaneous release of a pollutant from a point source. This *puff* moves downwind along the average wind direction. As it does so, it expands in volume, incorporating dilution air from around it and reducing its concentration. The puff also experiences small random movements, caused by turbulence, away from the mean direction. A continuous emission is then described as an infinitely rapid series of small individual puffs. Gaussian dispersion theory enables the concentration due to such a trajectory to be calculated at any location downwind.

We are now going to outline the system of equations that we need in order to predict what concentration of a substance is found at any point in the atmosphere, if that substance is being released at a known rate from a source. We will show how the practical equations are related to physical processes in the atmosphere, but we will not derive the equations from first principles.

8.3.1 Coordinate system

FOR REFERENCE PURPOSES ONLY

First, we have to be able to describe the position of the place at which we wish to estimate concentration, relative to both the source and the ground. A standard Cartesian (x, y, z) coordinate system is used (Figure 8.5). In this coordinate system:
The physical source (e.g. the base of a chimney) is located at the origin (0, 0, 0).

The x axis lies along the mean wind direction.
x is the distance downwind from the source.
y is the lateral distance from the mean wind direction.
z is the height above ground level.
h is the physical height of the chimney.
dh is the additional height by which the plume rises due to its buoyancy and/or momentum.
$H = h + dh$ is the effective height of the release.
$\overline{u}$ is the mean wind speed at plume height.

8.3.2 Fickian diffusion

The starting point for dispersion theory is to consider the diffusion of a cloud of material released into the atmosphere instantaneously from a point source. In one dimension, turbulent transfer in the atmosphere can be described by a Fickian equation of the form:

$$\frac{d\overline{q}}{dt} = K\frac{\partial^2\overline{q}}{\partial x^2}$$

FOR REFERENCE PURPOSES ONLY

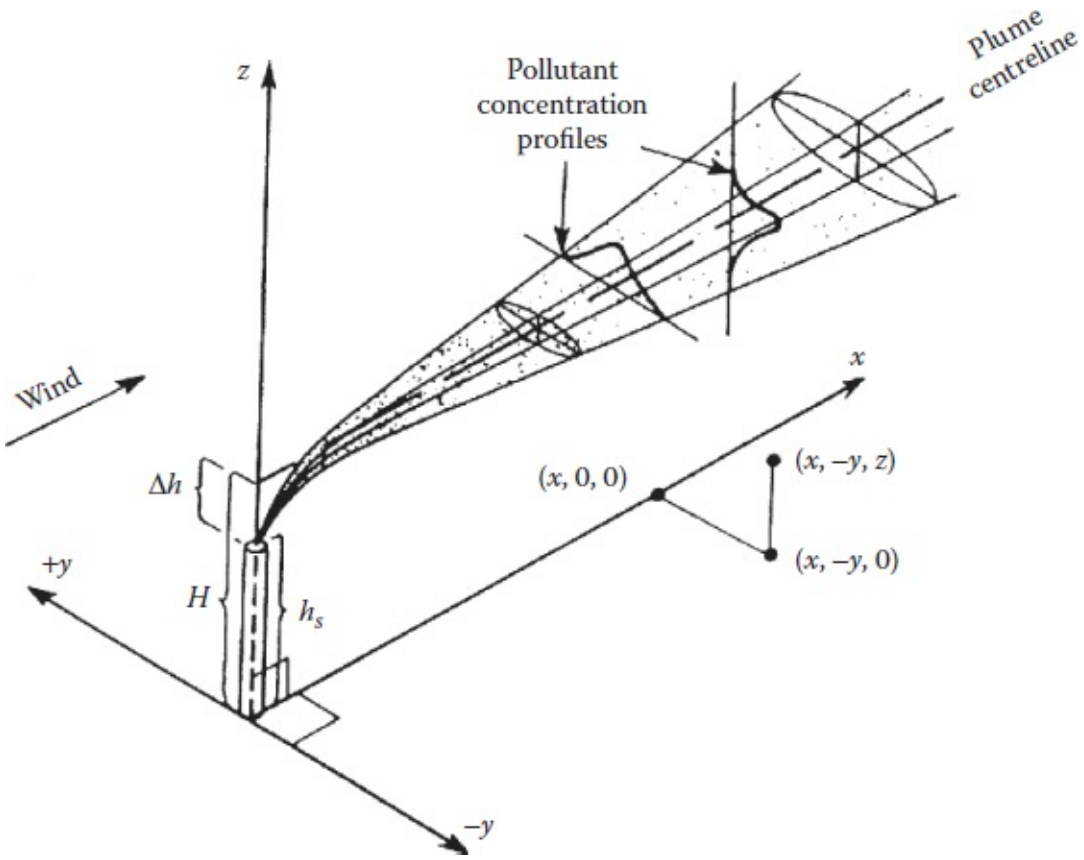

Figure 8.5 The Cartesian coordinate system used to specify dispersion geometry.

where:

q is the concentration of material

K is the turbulent diffusivity

This equation has an analytical solution:

$$\overline{q} = \frac{Q}{(4Kt)^{0.5}} \exp\left(\frac{-x^2}{4Kt}\right)$$

where Q is the source strength (e.g. in kg s^{-1}). The concentration is a maximum at the point of release, and it decays away in both positive and negative directions following the Gaussian bell-shaped distribution (Figure 8.6). Hence the value of σ at any distance from the source is a distance in metres which represents the lateral or vertical half *width* of the plume.

Now imagine that this instantaneous point source of material is diffusing isotropically in three dimensions (puff model) and at the same time drifting away from the point of release at the average wind speed $\overline{u}$. The solution becomes:

$$q(x, y, z, t) = \frac{Q}{(2\pi\sigma^2)^{3/2}} \exp\left(\frac{-r^2}{2\sigma^2}\right)$$

FOR REFERENCE PURPOSES ONLY

where σ is the standard deviation of the puff concentration at any time *t*, and:

$$r^2 = (x - \bar{u}t)^2 + y^2 + z^2$$

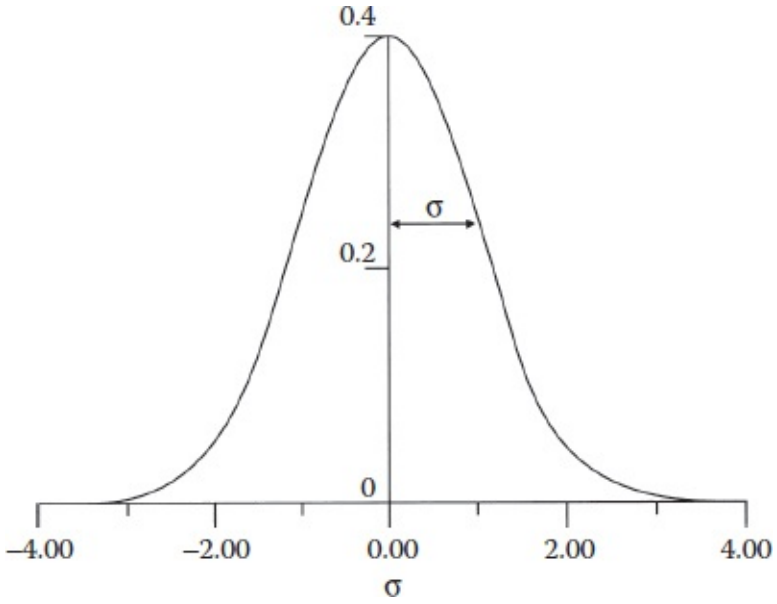

Figure 8.6 The standard Gaussian (normal) distribution, showing the physical significance of sigma.

8.3.3 The Gaussian plume equation

Following the analysis given for puff dispersion, emission from a continuous source can be considered as a continuous series of overlapping puffs, giving:

$$q(x,y,z) = \frac{Q}{2\pi\bar{u}\sigma_y\sigma_z} \exp\frac{-y^2}{2\sigma_y^2}\left\{\exp\frac{-(z-H)^2}{2\sigma_z^2}\right\} \tag{8.19}$$

where:

σ_y and σ_z are the standard deviations in the *y* and *z* directions, respectively

H is the total height of release

The first exponential term describes lateral dispersion, and the second describes vertical dispersion. Equation 8.19 is the basic Gaussian dispersion equation which is at the heart of many air quality prediction models.

It is important to realise that σ_y and σ_z describe the width of the concentration distribution, not of the plume itself. This aspect is clarified in Figure 8.7. The plan view shows a snapshot of the plume at any one time as the plume wanders either side of the mean wind direction. The concentration within the plume itself is approximately uniform, as shown by the *top hat* shape of the distribution.

FOR REFERENCE PURPOSES ONLY

The plume moves across to locations A and C only rarely – although the peak concentration may be high for a short time, the average is low because most of the time the plume is elsewhere. Point B is on the centre line of the plume along the mean wind direction. By definition, the plume spends a higher proportion of the time in this direction than any other, so the average concentration is highest. The frequency distribution of direction variations about the mean is Gaussian – hence the lateral Gaussian profile is built up. Similar variations in the vertical plane also give a Gaussian profile.

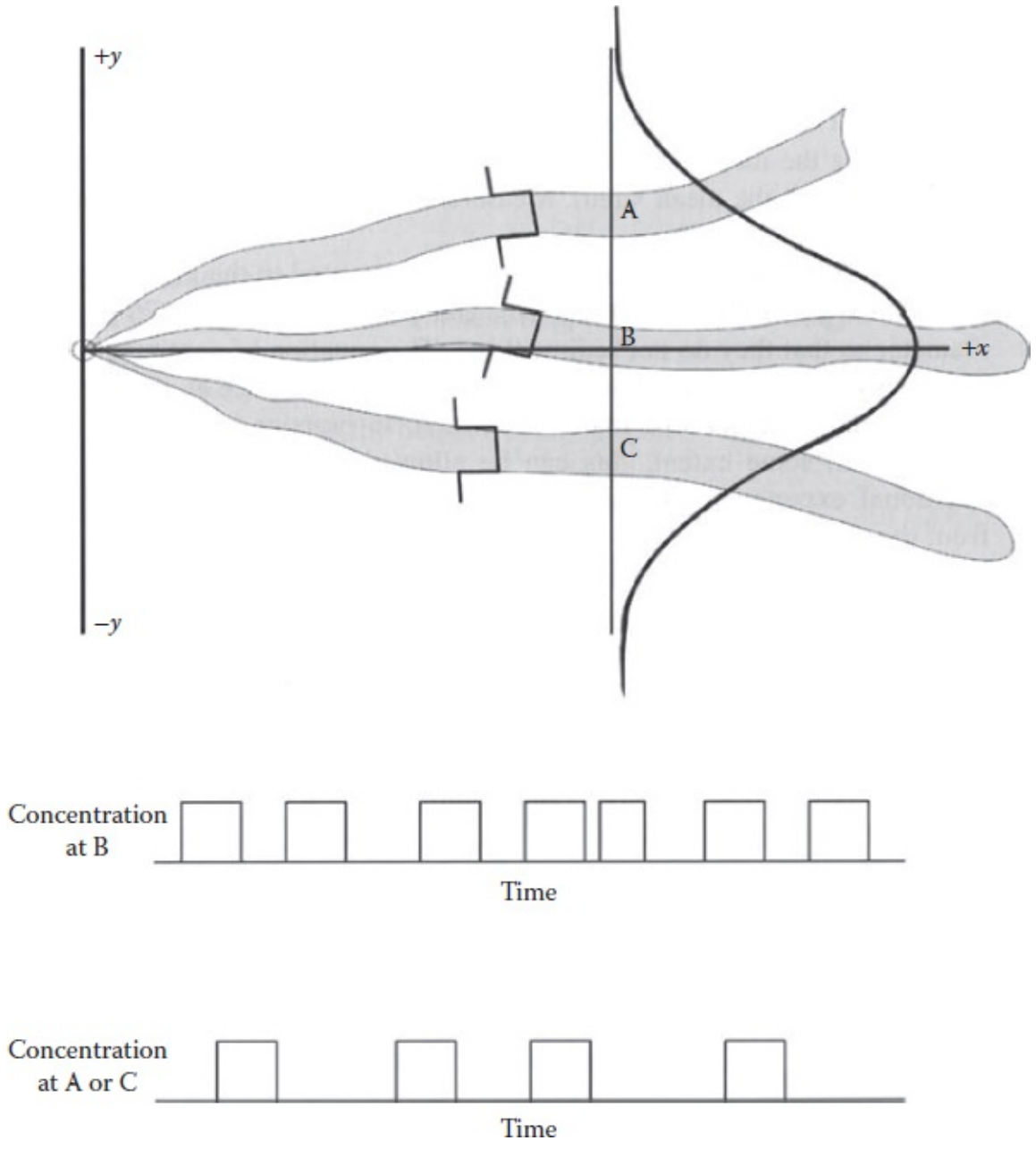

Figure 8.7 A plan view showing how the Gaussian distribution is formed from the differing frequency of exposure to the plume as it wanders about the mean wind direction.

8.3.4 Assumptions of the Gaussian model

The following key assumptions have to be fulfilled for implementation of Gaussian models:

- Release and sampling times are long compared to the travel time from source to receptor. This means that the release is effectively steady state and that diffusion along the mean wind direction is negligible compared to advection (movement with the mean wind). Measurement time scales of hours rather than minutes are implied.
- The material is chemically stable and is not deposited to the ground. This means that gases must be unreactive, and particles must be <20 μm in diameter so that they do not sediment out. The equation of continuity will then apply – the integral of the concentration over all space at any time is equal to the total mass of material emitted. In practice, most gases are deposited to some extent; this can be allowed for by, for example, an additional exponential decay factor in the concentration with distance from the source.
- The lateral and vertical variations of the material concentration can both be described by Gaussian distributions, which are functions of x only.
- The wind speed is constant with height. This is never true in practice, as has already been seen. Wind-speed variation with height can often be described by a logarithmic profile. More advanced versions of the Gaussian formulation divide the atmosphere into layers, each layer having a specified set of characteristics such as wind speed and stability.
- The wind direction is constant with height. Again, this is rarely true. The most common form of the variation is the Ekman spiral, in which the direction tends towards the geostrophic (parallel with the isobars) as height increases, over the first few hundred metres.

8.3.5 Plume rise

Most plumes have either some exit velocity that carries them up into the air or some degree of buoyancy due to temperature or density difference with the surrounding air, or both. Hence the effective plume height is likely to be different (usually, greater) than the physical height of the chimney. The dispersion equation shows that concentration is a function of the square of the release height, and hence much research has been done into the dependence of plume rise on other factors.

In principle it is possible to solve the conservation equations for mass, momentum, enthalpy and amount of emitted material, and hence predict the trajectory of the plume and the rate of entrainment into it of surrounding air. A simplified, more empirical method has often been used which is less mathematically and computationally intensive, although increased computing power is making full solution more practical. The standard theory assumes that a rising buoyant plume entrains ambient air at a rate proportional to both its cross-sectional area and its speed relative to the surrounding air. The driving force is

expressed in terms of an initial buoyancy flux F_b, where:

$$F_b = w_0 R_0^2 \frac{g}{T_{p0}} (T_{p0} - T_{a0})$$

in which:

w_0 is the initial plume speed

R_0 is the inside stack radius

T_{p0} is the initial plume temperature (K)

T_{a0} is the ambient temperature at stack height

Hence the SI units of F_b are $m^4\ s^{-3}$. Briggs solved the equations of motion for a bent-over plume in a neutral atmosphere to show that the height z at any distance x downwind was given by:

$$z = \frac{C_1 \left(\frac{F_b}{\pi}\right)^{\frac{1}{3}} x^{\frac{2}{3}}}{u} \left(1 + \frac{u\tau}{x}\right)^{\frac{1}{3}} = C_1 Br(F_b, x, u)$$

where $Br(F_b, x, u)$ is the *Briggs variable* and

$C_1 = \left(\frac{3}{2\beta^2}\right)^{\frac{1}{3}}$, with plume radius $r = \beta z$.

The most important value for use in dispersion calculations is the final plume rise *dh*. This has usually been found by fitting curves to observed data from a range of sources, and Briggs recommended the following relationships.

8.3.5.1 Buoyant rise in unstable – Neutral atmospheres

In Pasquill categories A–D, different equations are to be used depending on whether F_b is greater or less than 55 $m^4\ s^{-3}$.

$$\text{For } F_b < 55 \text{ use } dh = 21\ F^{0.75}/u_h \tag{8.20}$$

$$\text{For } F_b \geq 55, \text{ use } dh = 39\ F^{0.6}/u_h \tag{8.21}$$

where u_h is the wind speed at height h.

8.3.5.2 Buoyant rise in stable atmospheres

In a stable atmosphere, Briggs found that the most reliable expression for the final plume

rise *dh* was given by:

$$dh = 2.6 \left(\frac{F_b}{uS}\right)^{1/3}$$

Here *S*, the ambient stability factor = $\frac{g}{T}\left(\frac{\partial T}{\partial z} + \Gamma\right)$ and is a function of atmospheric conditions only.

Clearly, these estimates of plume rise need quite detailed information about the properties of the source. If less is known about the source, *dh* can be estimated from:

$$dh = \frac{515\, P_T^{0.25}}{\overline{u}}$$

which gives the plume rise in metres when P_T is the thermal power of the chimney gases in MW – that is, the product of mass flow rate, the specific heat of the flue gases and their temperature difference from that of the ambient air. For example, a large power station has an electrical output at full load of 2000 MW, and a thermal output in the flue gases of about 280 MW. Hence a plume rise of 220 m would be expected in a wind speed of 10 m s^{-1}. The chimney height for such a power station in the UK is around 200 m, so plume rise contributes significantly to dispersion, especially as ground-level concentrations are inversely proportional to the square of the effective source height.

8.3.6 The effect of vertical constraints

The simplest Gaussian solution (Equation 8.19) assumes that the plume is free to expand in all directions without constraint. This may be true in practice during a limited period of time when an emission is moving away from an elevated source and has not yet moved close to the ground. For real sources, the pollutant cannot disperse in all directions without constraint. In the usual situation of an elevated source (chimney + plume) at some height above the ground, downward dispersion is always limited by the presence of the ground, while upward dispersion may be limited by an elevated inversion.

8.3.6.1 Reflection at the ground

Assuming that no pollutant is absorbed by the ground, any pollutant that reaches the ground is available for upward dispersion into the atmosphere again. This is accounted for theoretically by adding an *image source*, equal in magnitude to the actual source but located at (0, 0, –H), that is, a distance 2*H* vertically below the actual source and distance *H beneath* the ground surface (Figure 8.8). Although this is a physically meaningless mathematical contrivance, it does the required job of effectively reflecting the plume away from the ground. The dispersion equation therefore becomes:

FOR REFERENCE PURPOSES ONLY

$$q(x,y,z) = \frac{Q}{2\pi\bar{u}\sigma_y\sigma_z}\exp\frac{-y^2}{2\sigma_y^2}\left\{\exp\frac{-(z-H)^2}{2\sigma_z^2} + \exp\frac{-(z+H)^2}{2\sigma_z^2}\right\} \quad (8.22)$$

where the second exponential term inside the curly brackets represents *additional* material from the image source located at (0, 0, –H). This is shown as Image source A in Figure 8.9.

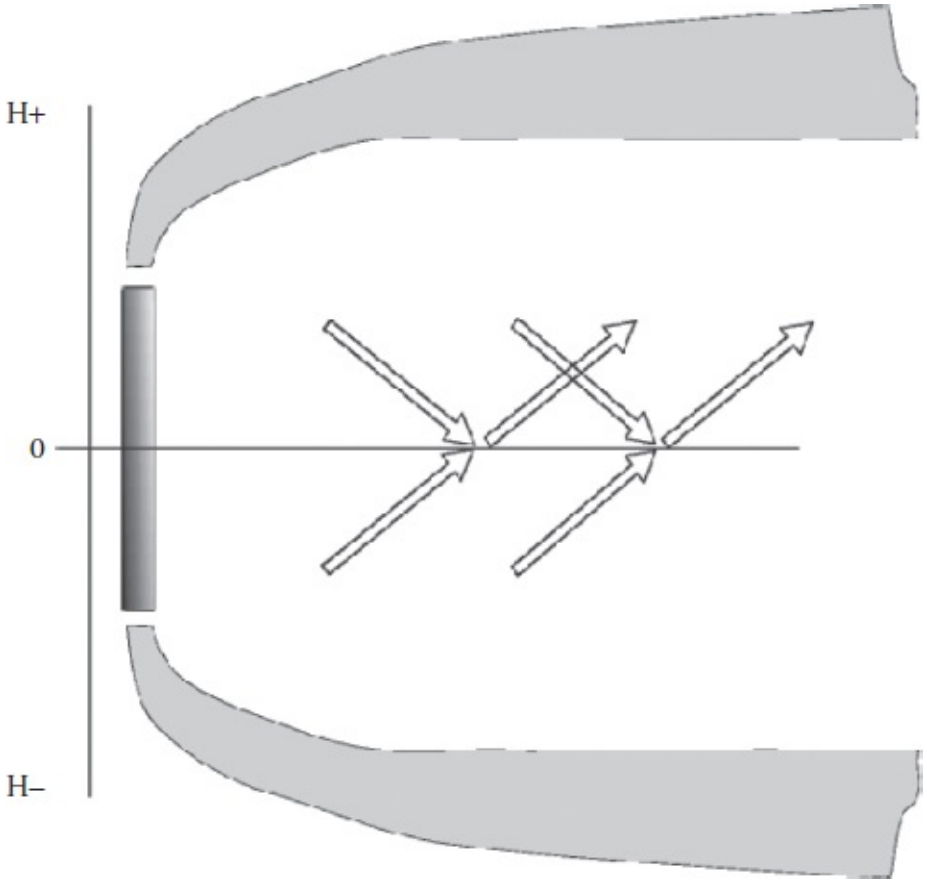

Figure 8.8 Side view to show how the image source allows for reflection of plume material at the ground.

FOR REFERENCE PURPOSES ONLY

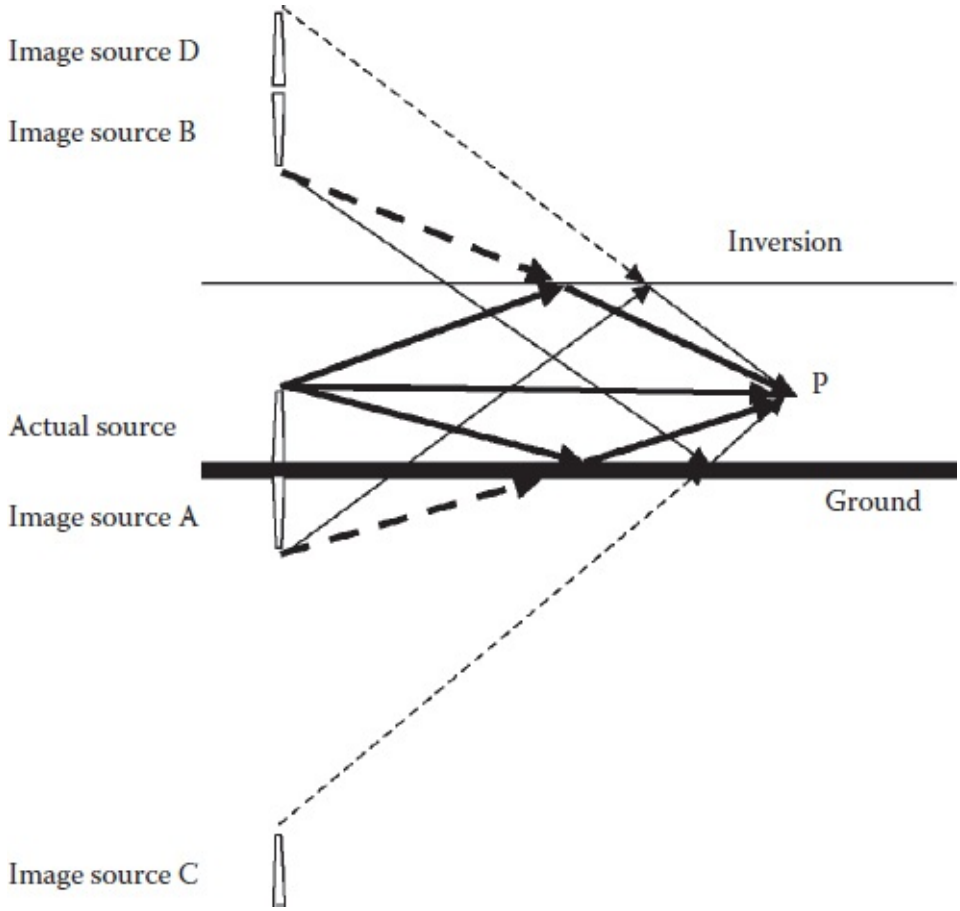

Figure 8.9 Schematic showing reflections of the plume at ground and inversion.

8.3.6.2 Reflection at an inversion

Dispersion downwards is always constrained by a physical surface such as water or vegetation. Dispersion upwards may also be constrained – not by a physical surface but by the temperature structure of the atmosphere itself. If there is an elevated inversion present, as was described in Figure 8.3, then this can act as a barrier to free upward dispersion. Buoyant air parcels penetrating into an elevated inversion from below have buoyancy removed because the temperature of the surrounding air increases with height while that of the parcel decreases. The worst pollution episodes, such as those that occurred in London in 1952 and 1991, are often associated with the presence of ground-level or low-altitude elevated inversions that trap ground-level emissions within a thin layer of the atmosphere.

This is allowed for in the solution to the diffusion equation by the addition of further reflection terms, which are generated by an image source as far above the inversion as the actual source is below it (i.e. at a height of $[2H_{bl} - H]$). Hence:

(8.23)

FOR REFERENCE PURPOSES ONLY

$$q(x,y,z) = \frac{Q}{2\pi\bar{u}\sigma_y\sigma_z}\exp\frac{-y^2}{2\sigma_y^2}\left\{\exp\frac{-(z-H)^2}{2\sigma_z^2} + \exp\frac{-(z+H)^2}{2\sigma_z^2} + \exp\frac{-(z-2H_{bl}+H)^2}{2\sigma_z^2} + \exp\frac{-(z+2H_{bl}-H)^2}{2\sigma_z^2} + \exp\frac{-(z-2H_{bl}-H)^2}{2\sigma_z^2}\right\}$$

where H_{bl} is the height of the inversion or the top of the boundary layer. In this equation, the first term in the curly brackets is the direct component, and the second is due to the image source discussed earlier. Figure 8.9 shows how these and the other components contribute to the concentration at any point P. The third exponential term in the curly brackets represents reflection of the source at the inversion (Image source B in Figure 8.9), the fourth term (Image source C) is a reflection of Image source B at the ground, and the fifth (Image source D) is a reflection of Image source A at the inversion.

Far enough downwind, the plume has expanded thus far vertically that it fills the boundary layer completely. This occurs for $\sigma_z > H_{bl}$. After that, it expands as a horizontal wedge, as though it had been released from a vertical line source above the height of the boundary layer. The plume is well mixed throughout the boundary layer, so there is no z dependence, and the concentration is given by:

$$C(x,y) = \frac{Q}{\sqrt{2\pi}\sigma_y h U_{h/2}}\exp\left(\frac{-y^2}{2\sigma_y^2}\right) \tag{8.24}$$

The Gaussian formulation described earlier applies to stable and neutral boundary layers. There is increasing evidence that the distribution of vertical velocities, and hence of concentrations, is non-Gaussian (skewed) when the boundary layer is convective. The result of this skewness is that for elevated sources, the height within the plume at which the concentration is a maximum descends as the plume moves downwind, while the mean height of the plume rises.

8.3.7 Estimating stability

Figure 8.10 shows the idealised effect of the different ELRs on plume behaviour. Each diagram shows a temperature profile in the atmosphere, together with the expected plume behaviour. The most unstable conditions (a, Pasquill A) can result intermittently in very high concentrations of poorly diluted plume close to the stack. This is called looping. Neutral conditions (b, Pasquill C–D) disperse the plume fairly equally in both the vertical and horizontal planes. This is referred to as coning. A strong inversion of the profile (c, Pasquill E–F) prevents the plume from mixing vertically, although it can still spread horizontally. If the plume is released above a ground-based inversion (d), then it is prevented from mixing down to the ground and ground-level concentrations are kept low. Conversely, if it is released below an elevated inversion (e), then it is prevented from dispersing upwards and ground-level concentrations are enhanced. In practice, complex

ELR structures interact with stack and plume heights to create a much more variable picture.

The effect of stability on dispersion pattern can also be seen in Figure 8.11. Pasquill A generates the highest maximum concentration and does so closest to the stack, although the narrow peak means that the integrated downwind concentration is low. As stability increases, the peak concentration decreases and moves downwind.

8.3.7.1 Estimates of σ_y, σ_z

Expressions for σ_y and σ_z have been derived in terms of the distance travelled by the plume downwind from the source under different Pasquill stability classes. They are available both as graphs and as empirical equations that are valid in the range 100 m < x < 10 km. Figure 8.12a and b show the variations of standard deviation with distance from the source for the different Pasquill stability categories. Note that the x scale runs from 100 m to 100 km – this dispersion methodology is designed for medium physical scales, neither small enough to be influenced by individual topographic features nor large enough to be controlled by synoptic wind flows. Note also that σ_z, the vertical standard deviation, is much more influenced by stability than is σ_y, the horizontal standard deviation, due to the influence of buoyancy forces.

FOR REFERENCE PURPOSES ONLY

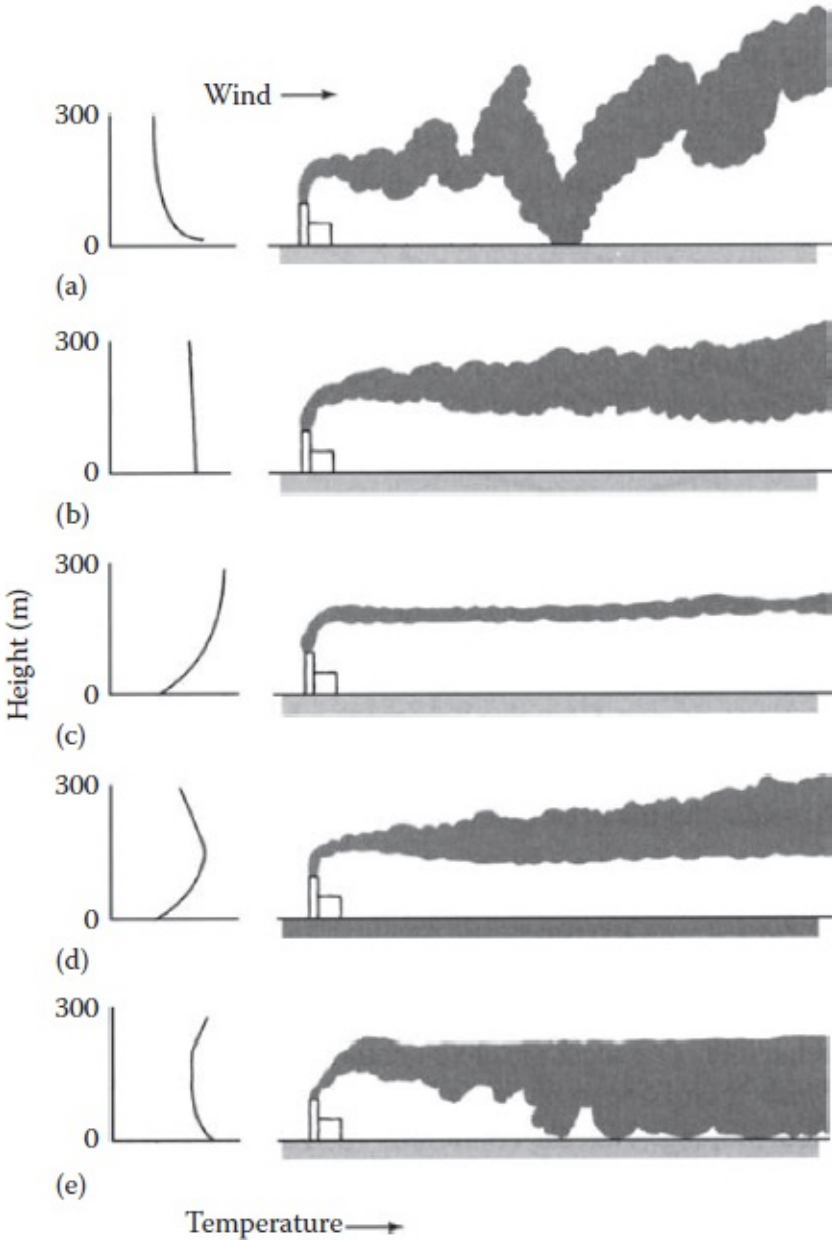

Figure 8.10 Effect of lapse rate on plume dispersion: (a) looping, (b) coning, (c) fanning, (d) lofting and (e) fumigation. (From Oke, T. R., *Boundary Layer Climates*, Methuen, London, UK, 1987.)

FOR REFERENCE PURPOSES ONLY

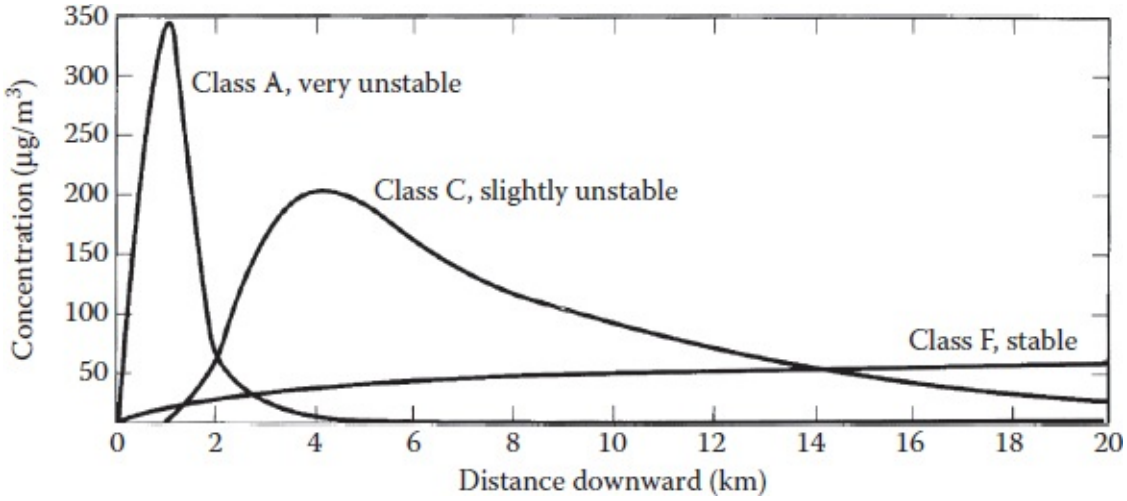

Figure 8.11 Variation of ground-level concentration with distance downwind, under different atmospheric stabilities. (From Masters, G. M., *Environmental Engineering and Science*, Prentice Hall, Upper Saddle River, NJ, 1998.)

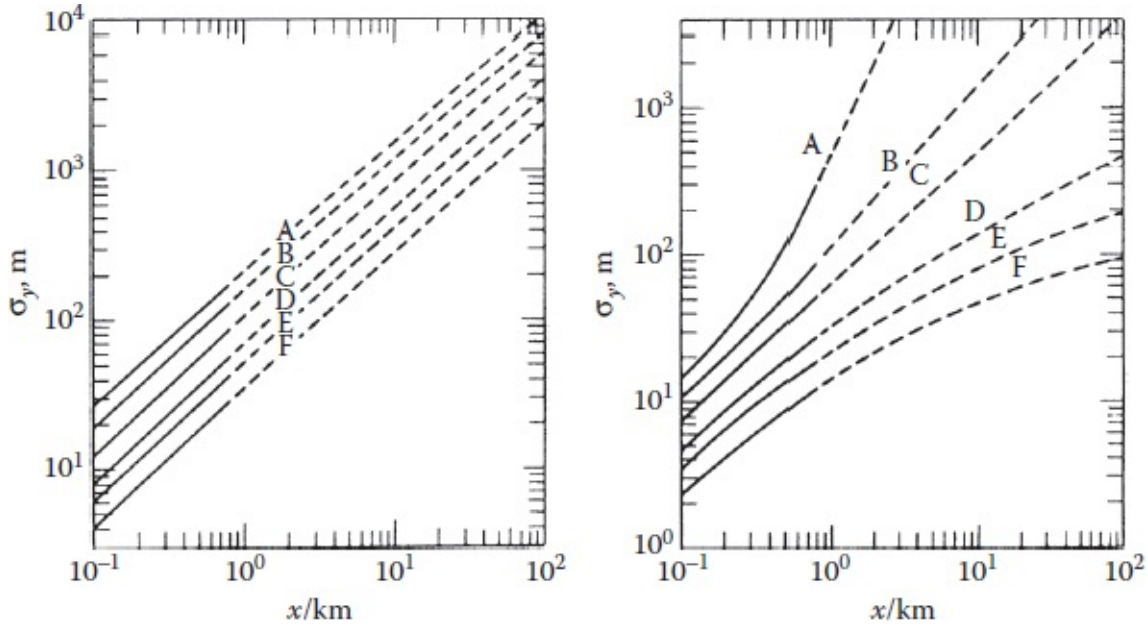

Figure 8.12 Variations of plume standard deviation in the y and z directions with distance x from the source. A, B, C, D, E and F are Pasquill stability categories.

Table 8.7 gives corresponding equations for open-country and urban conditions. The main difference is that the greater surface roughness in built-up areas generates greater turbulence.

Table 8.7 Equations for the variation of σ_y and σ_z with stability class

Pasqu1ll category	*(σ_y/m*	*σ_z/m*
Open-country		

FOR REFERENCE PURPOSES ONLY

A	$0.22x\ (1 + 0.0001x)^{-0.5}$	$0.20x$
B	$0.16x\ (1 + 0.0001x)^{-0.5}$	$0.12x$
C	$0.11x\ (1 + 0.0001x)^{-0.5}$	$0.08x\ (1 + 0.0002x)^{-0.5}$
D	$0.08x\ (1 + 0.0001x)^{-0.5}$	$0.06x\ (1 + 0.0015x)^{-0.5}$
E	$0.06x(1 + 0.0001x)^{-0.5}$	$0.03x\ (1 + 0.0003x)^{-1}$
F	$0.04x\ (1 + 0.0001x)^{-0.5}$	$0.0l6x\ (1 + 0.0003x)^{-1}$
Urban		
A–B	$0.32x\ (1 + 0.0004x)^{-0.5}$	$0.024x\ (1 + 0.001x)^{0.5}$
C	$0.22x\ (1 + 0.0004x)^{-0.5}$	$0.20x$
D	$0.16x\ (1 + 0.0004x)^{-0.5}$	$0.14x\ (1 + 0.0003x)^{-0.5}$
E–F	$0.1\ 1x\ (1 + 0.0004x)^{-0.5}$	$0.08x\ (1 + 0.0015x)^{-0.5}$

8.3.8 Versions of the Gaussian equation

The full Gaussian Equation 8.22 describes the concentration field everywhere in the free atmosphere due to a point source. More typically, we need to know the concentration at ground level, or from a ground-level source or directly downwind of the source. In these cases various simplifying assumptions can be made.

8.3.8.1 Ground-level concentration due to an elevated source, bounded by the ground surface

Set $z = 0$ everywhere in Equation 8.22:

$$q(x, y, 0) = \frac{Q}{\pi \bar{u}\, \sigma_y\, \sigma_z} \exp - \left[\frac{y^2}{2\sigma_y^2} + \frac{H^2}{2\sigma_z^2} \right]$$

8.3.8.2 Ground-level concentration due to an elevated source, bounded by the ground surface, directly downwind of the source at ground level

Set $y = z = 0$ everywhere in Equation 8.22:

$$q(x, 0, 0) = \frac{Q}{\pi \bar{u}\, \sigma_y\, \sigma_z} \exp \left[\frac{-H^2}{2\sigma_z^2} \right] \tag{8.25}$$

It can also be shown that the maximum downwind concentration, $q_{\max}$, is given by:

$$q_{\max} = \frac{2Q}{\pi \bar{u}\, e\, H^2} \frac{\sigma_z}{\sigma_y} \tag{8.26}$$

at the distance $x_{\max}$ for which $\sigma_z = \frac{H}{\sqrt{2}}$.

In Equation 8.26, $e = 2.71828$, the base of natural logarithms. First, use the known value

of H to calculate σ_z, and read off this value on the vertical axis of Figure 8.12b. Now move across to the curve corresponding to the known stability class, and read down to the horizontal axis to find x_{max}. Set this value on the x-axis of Figure 8.12a, and read up to the same stability class and across to the y-axis. This gives the value of σ_y at x_{max}. Finally, use these values of σ_y and σ_z, together with Q, u and H, to find q_{max} from Equation 8.26. Note that the maximum ground-level concentration is inversely proportional to the square of the effective release height H, so that building taller chimneys is a very cost-effective method of reducing ground-level pollution.

8.3.8.3 Ground-level concentration due to a ground-level source, directly downwind of the source (e.g. bonfire)

Set $y = z = H = 0$. Hence:

$$q(x,0,0) = \frac{Q}{\pi \bar{u} \sigma_y \sigma_z} \tag{8.27}$$

8.3.8.3.1 Line source

When a continuous series of point sources moves along a line, as vehicles do along a road, they are equivalent to a continuous line source. If the x-axis is perpendicular to the road, then there is no variation of concentration in the y direction, and we have:

$$q(x,z) = \sqrt{\frac{2}{\pi}} \frac{Q}{\bar{u} \sigma_z} \exp\left[\frac{-z^2}{2\sigma_z^2}\right] \tag{8.28}$$

where Q now has units of kg m^{-1} s^{-1}.

8.4 DISPERSION THEORY IN PRACTICE

Do not be misled into thinking that the neat-looking equations given earlier provide us with an infallible method of predicting dispersion – they fall well short of this ideal. Many field measurement programmes have been undertaken to validate both the plume rise and dispersion equations. A favourite method for evaluating plume dispersion is to release sulphur hexafluoride (SF_6) into the flue gases where they enter the stack.

SF_6 is a passive conservative tracer – it is very stable and there is no ambient background, so one can be sure that the concentration measured in the ambient air was emitted from the source under investigation and not from somewhere else altogether. Alternatively, the sulphur dioxide emissions from major commercial sources such as power stations have been monitored. The underlying problem in validation is the large spatial and temporal variability of the plume concentrations caused by the random nature of

atmospheric turbulence. This is graphically illustrated by Figure 8.13, which is a computer simulation of plume geometry – the wiggly tube represents a snapshot of a surface of constant concentration. Dispersion theory must predict the average concentration at a point in space due to the highly variable exposure of that point to this fluctuating plume.

8.4.1 Worked example of Gaussian dispersion

We will apply the concepts that have been described earlier to predict the downwind ground-level concentration of sulphur dioxide that is produced from a chimney of known height. We are given the following information:

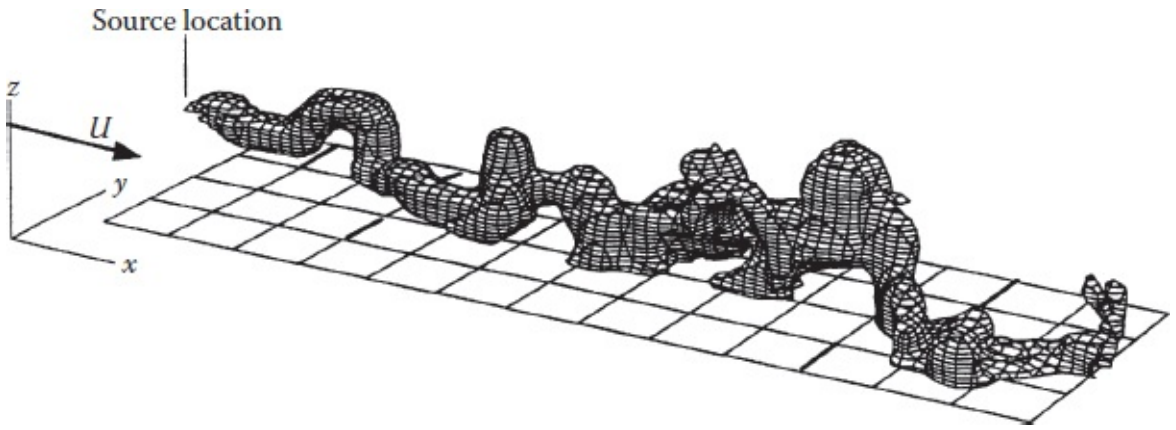

Figure 8.13 A modelled surface of constant concentration downwind of a continuous release. (From Henn, D. S., and Sykes, R. I., *Atmos. Environ.*, 26A, 3145–3159, 1992.)

Source characteristics

Height = 100 m
Internal radius = 5 m
Exit speed = 20 m s^{-1}
Exit temperature 80° = 353 K
Coal burn = 3000 t day^{-1}: S content = 1.4%

Environmental conditions

Wind speed at 10 m = 8 m s^{-1}
Weather – cloudy
Air temperature at stack height = 10°C = 283 K

Receptor location

6000 m downwind of the source, at ground level on flat terrain

The data given earlier have been invented for this example, but they are representative of a

medium-sized coal-fired facility. The same Gaussian equations can be applied to a wide range of possible source configurations and weather conditions.

Step 1: Find the stability category.
Use Table 8.3 to find the stability from the environmental conditions. Because it is windy and cloudy, we have Category D.

Step 2: Calculate σ_y *and* σ_z.
Now go to Table 8.7. In open country, with stability category D and $x = 6000$ m, we have:

$$\sigma_y = 0.08 \times 6000(1 + 0.0001 \times 6000)^{-0.5} = 379 \text{ m}$$

$$\sigma_z = 0.06 \times 6000(1 + 0.0015 \times 6000)^{-0.5} = 113 \text{ m}$$

Step 3: Calculate the wind speed at the release height.
Use Equation 8.17 to find the wind speed at 100 m. From Table 8.2 for Category D, $p = 0.15$. Hence $u(100) = 8(100/10)^{0.15} = 11.3$ m s^{-1}.

Step 4: Calculate the plume rise and effective release height.
From:

$$F_b = w_0 R_0^2 \frac{g}{T_{p0}} (T_{p0} - T_{a0})$$

the buoyancy flux $F_b = 20 \times 5^2 \times 9.81 \times (353 - 283)/353 = 973$ m^4 s^{-3}. Following Section 8.3.3, with Category D and $F_b > 55$, we use Equation 8.21 to find the plume rise dh. Hence $dh = 39 \times 973^{0.6}/11.3 = 214$ m and $H = 100 + 214 = 314$ m.

Step 5: Calculate the SO_2 *release rate.*

$$\text{Coal burn} = 3000 \text{ t day}^{-1}, \text{ S content} = 1.4\%$$

$$\text{Sulphur emission} = 0.014 \times 3000/(24 \times 60 \times 60) \text{t s}^{-1}$$
$$= 4.86 \times 10^{-4} \text{t s}^{-1} = 4.86 \times 10^2 \text{g S s}^{-1}$$

$$\text{Sulphur dioxide emission} = 2 \times \text{S emission (because the molecular weight of } SO_2 \text{ is twice that of S)} = 9.72 \times 10^2 \text{g s}^{-1}$$

Step 6: Solve the dispersion equation.
For ground-level concentration on the plume centreline, use Equation 8.25:

FOR REFERENCE PURPOSES ONLY

$$q(x,0,0) = \frac{Q}{\pi \bar{u} \sigma_y \sigma_z} \exp\left[\frac{-H^2}{2\sigma_z^2}\right]$$

with $Q = 9.72 \times 10^2$ g s^{-1}, $u = 11.3$ m s^{-1}, $\sigma_y = 379$ m, $\sigma_z = 113$ m and $H = 314$ m. Hence:

$$q(6000,0,0) = \frac{9.72\times10^2}{\pi\times 11.3\times 379\times 113} \exp\left[-\frac{314^2}{2\times 113^2}\right]$$

$$= (6.39 \times 10^{-4}) \times 0.021$$

$$= 13.4 \times 10^{-6}\,\text{g m}^{-3} = 13.4\,\mu\text{g m}^{-3} \text{ (about 5 ppb)}$$

8.4.2 Predictions for planning purposes

When a new industrial development involving pollutant emissions is proposed, calculation of pollutant concentrations can become an important component of the environmental impact assessment. Long-term exposures due to a point source are determined by accumulating average values for the 8760 hourly means of wind direction, wind speed, atmospheric stability and other environmental variables, and then running the dispersion model for each hour. The most important factor is the wind rose – the proportion of the time for which the wind blows from each direction (Figure 8.14).

Commonly, the 360° of the compass is divided into 16 sectors of 22.5° or 32 sectors of 11.25°, and the pollutant concentration is determined while the wind is blowing from that sector. The resulting angular distribution is then called the pollutant rose. As the statistical distribution of the concentrations follows a log-normal pattern, the correct description of concentrations is in terms of the median (the value exceeded for half the time, or 4380 h), together with the 10% (876 h) and 1% (88 h) exceedances.

Very often organisms, including people, respond to the highest values that occur for the shortest periods, so that this knowledge of statistical distribution is important for predicting effects. Measurement of the pollutant rose also suggests attribution of the concentrations to a particular source. In many areas of the UK, winds come most often from the south-west to west sector and from the north-east, and this is reflected in the spatial distribution of concentrations around a source.

There may be complications in matching the predicted concentrations to guidelines and limit values. For example, the UK air quality standard for SO_2 specifies a 15-min mean of 266 μg m^{-3} as the 99.9th percentile (equivalent to no more than 35 exceedances per year), whereas the chimney heights memorandum (which must be used by Local Authorities to calculate stack heights for planning purposes) specifies 452 μg m^{-3} as a 3-min average. In such cases, empirical factors derived from more complete data sets can be used to convert. For example, the factor 1.34 is recommended to convert the 99.9th percentile 15-min mean from short stacks to the 99.9th percentile 1-h mean. Unfortunately the factor itself varies with parameters such as stack height, adding another level of uncertainty to the predictions.

FOR REFERENCE PURPOSES ONLY

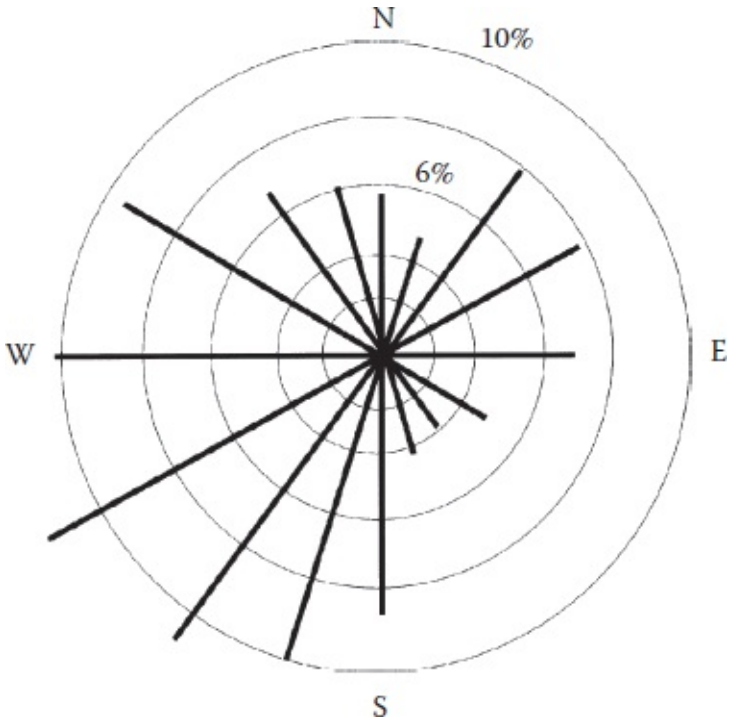

Figure 8.14 A typical wind rose. The length of the bar shows the proportion of the time for which the wind was blowing from the sector centred on that direction.

8.4.3 Effects of topography

The simplest dispersion theory deals with a source situated in the middle of a flat plain. Although such sources do exist, most landscapes involve hills of some sort, and for some landscapes the hills seriously affect dispersion. Valleys tend to deviate and concentrate the wind flow, so that the average wind speed is higher than, and the wind blows along the valley for a higher proportion of the time than, would be expected in the open. There are also thermal effects due to differential heating of the valley sides. For example, the north side of an east-west oriented valley receives stronger solar radiation during the day than the south side. This asymmetry generates a convective circulation which involves air rising up the relatively warm northern slope and descending down the relatively cool southern slope. At night, cool air may accumulate in the valley floor, producing a stable temperature inversion in which pollutants emitted from activities on the valley floor (which is where towns, roads and factories tend to be located) accumulate.

The actual flow pattern of air over non-uniform terrain is not easy to predict or measure. For an isolated obstacle, the upwind streamlines are gradually compressed as the flow approaches the obstacle. At some point near the obstacle, the flow separates, with a turbulent and possibly recirculating region in the downstream wake where the wind direction is opposite to the initial direction. At some further distance downstream, the flows converge again. The wake region must be allowed for in pollutant release calculations; if an emission is released into such a recirculation zone, it can build up to much higher

concentrations than simple dispersion theory would indicate. Airflow over hilly terrain involves a mixture of processes. In smoother areas, the streamlines follow the contours. In rougher areas there may be flow separation and turbulent wake formation under some combinations of wind direction and speed but not under others.

8.4.4 Effects of buildings

It would be unusual for any emission to be released from an isolated chimney, standing alone in the middle of a flat plain. More often, the chimney is part of a complex of other buildings which disturb the flow in the boundary layer and change the dispersion of the chimney gases. The flow patterns are very complex, and only the main features will be indicated here. Furthermore, the predictions are part theoretical, part empirical and part based on wind-tunnel studies which often do not reliably predict full-scale field results. The main features of the disturbed flow for air impinging directly onto the upwind face of a cuboidal building are seen in Figure 8.15 and are listed here:

- A stagnation point (SP) where streamlines impinge on the upwind face.
- A re-circulating flow region, separated from the main flow, immediately downwind of the downstream face. This recirculation may separate from the top edge of the upwind face, or it may attach to the roof and separate from the top edge of the downstream face. Concentrations are assumed to be uniform in this well-mixed region.
- A downstream wake where the turbulence is enhanced and the average flow vector is down towards the ground.
- A long trail of more structured (i.e. less randomised) vortices downwind.

The effects of these disturbances on the dispersion of emissions from the building, or from nearby sources, depend sensitively on the exact position and characteristics of the source. For example, a weak (in the jet sense) source close to the roof may be entrained into the recirculation, and thence into the wake, or it may mix into the wake, or it may avoid both and mix into the undisturbed flow. Variable proportions of the plume may also experience these histories. If a roof-level emission does not escape the recirculation, then its effective emission height is zero. This can clearly have serious consequences for downwind pollution concentrations.

FOR REFERENCE PURPOSES ONLY

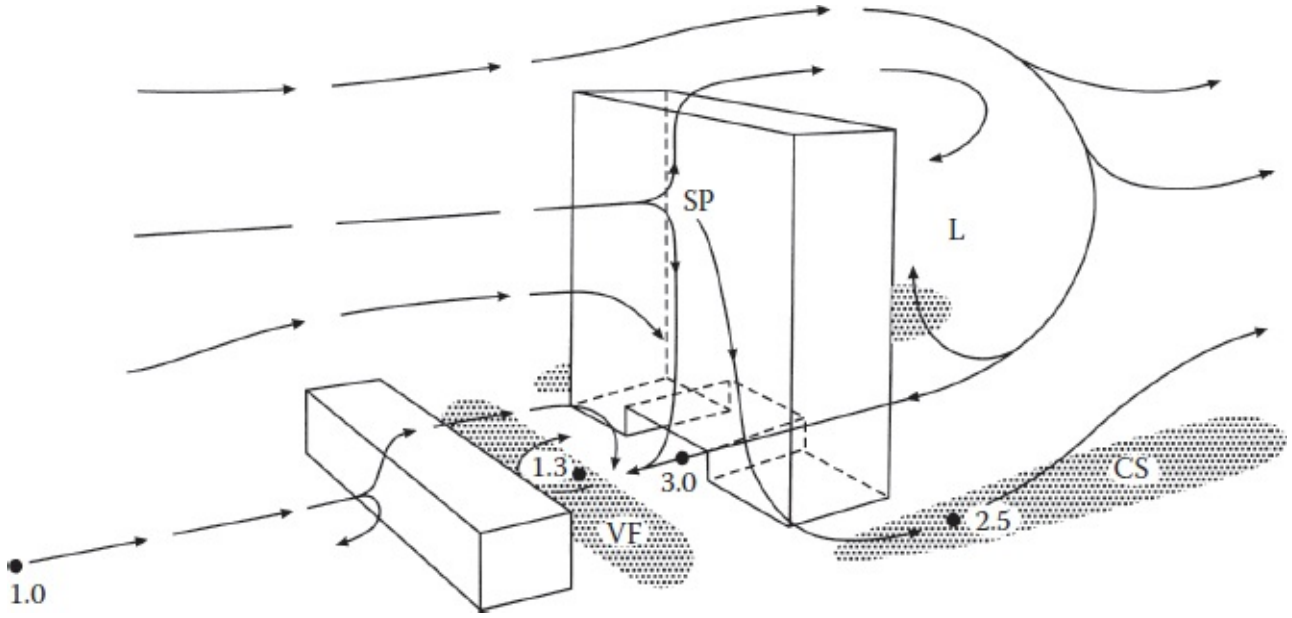

Figure 8.15 Idealised flow pattern round a cuboidal building. Values are relative wind speeds; SP = stagnation point; CS = corner stream; VF = vortex flow; L = lee eddy.

8.4.5 Recent developments

The diesel vehicle emission issue has gripped air pollution modelling from mobile sources in recent years. The current assumptions in many air quality modelling, both for heavy goods vehicles (HGVs) and light goods vehicles (LGVs), have been found to be fallacious, and more rigorous *real-drive emissions* have been introduced for both the vehicle categories to address this alarming issue, especially in European countries, including the UK. These new data are being compiled to develop a new set of strategies on emission standards, with further adjustment in 2020 to the way the standards will be implemented. The following recent developments are attempts to improve air quality modelling and are specifically targeted to handle this issue:

- An alternative emission model, the Calculator Using Realistic Emissions from Diesels (CURED), was published in 2016. It uses calibrated emission functions for Euro 6 diesel cars, along with other types of vehicles.
- The European Environment Agency has updated its published emission functions for Euro 6 diesel cars, and these now predict higher emissions than the data set previously used by air quality modellers.

A European initiative – Harmonisation within Atmospheric Dispersion Modelling for Regulatory Purposes – has been involved in a series of annual workshops to promote the use of new-generation models and to provide a forum for discussing general model updates and improvements. The Pasquill categorisation scheme was the first method to be widely

FOR REFERENCE PURPOSES ONLY

adopted for relating plume standard deviation to atmospheric conditions and has become the most generally used. Although it has proved its worth in many trials, it certainly has important deficiencies. The method works best under stable and neutral conditions but tends to fail under the more fluctuating conditions typical of an unstable atmosphere. In order to improve the predictions, changes have been made to the model. First, the values of σ_y and σ_z can be derived from fundamental characteristics of turbulence. If we measure the lateral and vertical components of wind speed (v and w, respectively), we find that there is a normal distribution of speeds above and below the mean. The widths of these distributions can be characterised by their standard deviations, σ_v and σ_w, which can then be related in turn to the standard deviation of the concentration.

The Gaussian model is in widespread use because of its comparative simplicity, but it should be clear by now that it can only offer rather coarse predictions of dispersion in practice. More powerful models have been developed based on more rigorous turbulence theory. Although a detailed treatment is beyond the scope of this book, we can see the potential improvements. Figure 8.16 gives an example of how an SF_6 release experiment was used to test the differences in prediction performance of two dispersion models used in the United States. In each graph, the measured 1-h average concentration c_o is plotted against the concentration predicted by the particular model, c_p. The *pdf* model (Figure 8.16a) is based on the probability distribution function describing the relative abundance of convective updraughts and downdraughts in the advecting plume, while the CRSTER model (Figure 8.16b) is a conventional Gaussian dispersion model as described earlier. In this instance the pdf model clearly offered improved prediction power over the standard Gaussian. In particular, the concentration c_p predicted by the Gaussian model was zero on a large number of occasions when a concentration was actually observed (the column of points up the y axis of Figure 8.16b). The correlation coefficient of the pdf model was substantially higher than that of the Gaussian ($r^2 = 0.34$, 0.02, respectively).

FOR REFERENCE PURPOSES ONLY

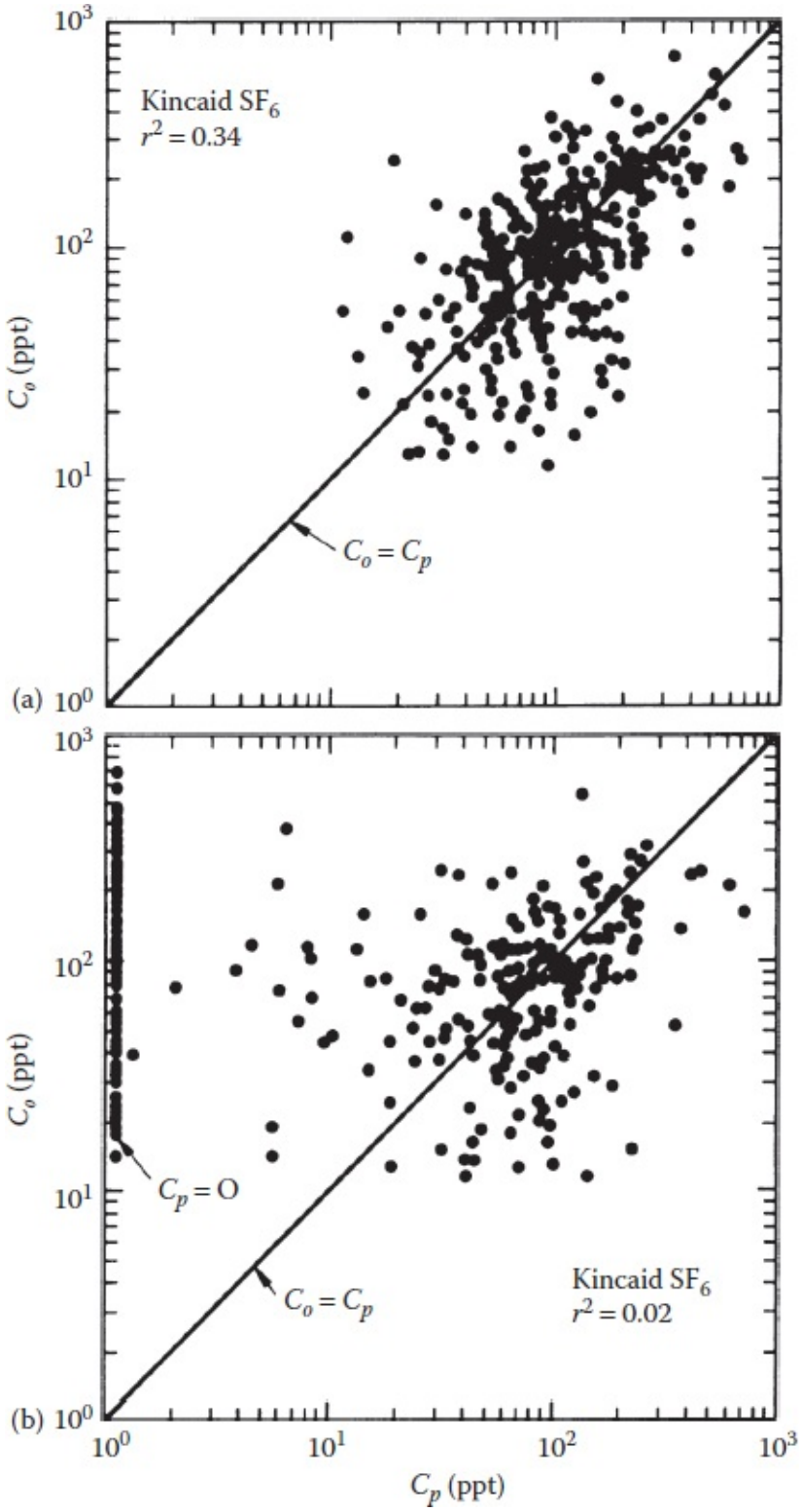

Figure 8.16 Comparisons of measured ground-level concentrations with those predicted by (a) the *pdf* model and (b) a standard Gaussian model. (From Weil, J. C. et al., *J. Appl. Meteorol.*, 31, 1121–1145, 1992.)

Computational fluid dynamics (CFD) is a powerful technique for calculating the movement of fluids. The method involves dividing the whole space of interest into cells,

and then calculating the flow between adjacent cells directly from the fundamental Navier-Stokes equations. It has been restricted in its application to atmospheric dispersion problems by intensive computational requirements, but as computing power increases it will most likely displace Gaussian methods. CFD is better able to handle complex topography, the influence of buildings and transient meteorological or emission variability.

8.4.6 Meteorological data

In the UK, the main provider of meteorological data is the Meteorological Office. Typically a user, such as a local authority, will need to use a commercial dispersion model to calculate ground-level concentrations of a pollutant from a particular source. If this is done hour-by-hour for 1 year, then 8760 sets of meteorological data are needed. Each set includes values of wind speed, wind direction, boundary layer height and an atmospheric stability criterion such as Pasquill class or Monin–Obukhov length scale. Wind speed and direction may be measured locally, but the other parameters are derived from other values, and different methods are in use. Trinity Consultants are the main provider of nationwide data in the US, and this company also supplies compilations of UK data in the UK.

8.5 EMISSION INVENTORIES

Before we can hope to understand the budgets of different materials in the atmosphere, we must be able to quantify the emission of each pollutant into the atmosphere: this leads to a cascade of finer and finer spatial resolution, from global totals through regional and national to local – currently 1° latitude × 1° longitude for global maps, 50 × 50 km (European Monitoring and Evaluation Programme [EMEP]), 20 × 20 km for regional maps and 1 × 1 km for local maps. The general principle of emission inventories is to form the triple sum:

$$\Sigma\Sigma\Sigma\, N_{s,a}\, P_{s,t}\, \Phi_{i,s}$$

where:

$N_{s,a}$ is the number of sources of type s in area a

$P_{s,t}$ is the production from the sources of type s in time period t (e.g. tonnes steel/year)

$\Phi_{i,s}$ is an emission factor for the species i from source s (e.g. kg SO_2/tonne of steel)

There is a wide range of values of Φ, depending on the conditions. For example, the emission factor for black smoke production during coal combustion ranges from 0.25 kg/tonne coal for a power station to 40 kg/tonne coal for an open domestic fire. Furthermore, there is a great range of uncertainty in the values for specific processes. For example, some industrial processes run continuously at a nearly constant rate under tightly

FOR REFERENCE PURPOSES ONLY

controlled conditions, and pollutant emissions are measured and logged continuously. In this way, a substantial and reliable database is accumulated from which an emission factor can be calculated with some confidence. At the other extreme, we may be trying to quantify particle emissions from ploughing, where there is not only great natural variability due to soil type, wind speeds, soil moisture, and so on, but few measured results are also available. Depending on the activity being considered, the emission factor may involve a wide range of statistics, such as process output or sales volume in place of simple consumption. Many processes are far from continuous, and they become increasingly intermittent as the time resolution is increased. For example, a power station might operate at a similar average output from year to year. But from month to month, there are sharp variations in output due to factors such as seasonal load changes and boiler servicing. Hence the concepts of emission factors and budgets are usually applied to time scales of a year or more. Again, it must be emphasised that there is no bank of coal consumption metres that can be read at will. Instead, an exhaustive survey is done by a group of researchers who gather, collate and analyse all the available information on a particular topic, such as sulphur emissions. The published output from that research then becomes the *state of the art* until it is updated in due course. Furthermore, the information about emissions of a particular substance is improved retrospectively, so that, for example, the 1990 estimate of 1970 sulphur emissions might be different to (and hopefully better than) the 1970 or 1980 estimates.

In principle, an emissions inventory attempts to make estimates of all known emissions to air in as high a level of disaggregation as possible. However, by following international guidelines on emissions reporting, there are a number of known sources which are deliberately not included in the inventory:

- Natural sources are not included in the national totals (although estimates of some sources are made).
- The inventory is a primary emissions inventory (as per international guidelines). Consequently resuspension of, for example, particulate material is not included in the national totals (although estimates for some resuspension terms are made).
- Cruise emissions from civil and international aviation are not included in the national totals.
- Natural sources and cruise emissions from civil and international aviation are not included in the national totals (although estimates of some sources are made).
- Estimates of *international* emissions such as shipping are made and reported as memo items (excluded from the UK national totals).
- Greenhouse gas (GHG) emissions associated with short-term changes to the carbon cycle are not included; whilst this is not of particular concern here, the principle is extended to other pollutants.

8.5.1 UK emissions inventories

FOR REFERENCE PURPOSES ONLY

The UK emissions inventory estimates annual pollutant emissions from 1970 to the most current inventory year for the majority of pollutants. A number of pollutants are estimated from 1990 or 2000 to the most current inventory year due to the lack of adequate data prior to the later date. The scope of pollutants and years for which they are compiled varies according to data availability, and inclusion of new pollutants in the inventory is usually driven by legislation. However, the UK government is pro-active in this area, and the inventory includes emissions of pollutants which are not currently required by international or national reporting obligations but which are of use to various areas of the scientific community. For example, reporting emissions of base cations allows the modelling community to better estimate the impacts of acidic gases.

The UK National Atmospheric Emissions Inventory (NAEI) collates emissions of over 30 major pollutants. It applies hundreds of different emission factors to fuel consumption and other national statistics to calculate totals, disaggregated breakdowns, spatial distributions and temporal trends of pollutants. Estimates are made of emissions from seven categories of stationary combustion source; mobile sources including road vehicles, off-road vehicles, aircraft and others such as trains and shipping; seven categories of industrial process; offshore oil and gas; construction and solvent use. The UK Department for Environment, Food and Rural Affairs (DEFRA) publishes an emission factor database, so that, for example, a local authority that has compiled a list of processes and activities within its area that might generate emissions can make a first estimate of the emissions and decide whether a more detailed assessment is required. Urban inventories have also been compiled for 10 of the major urban areas in the UK. These give contributions from line, area and point sources within 1 × 1 km squares, separated according to type of source. One set of emission maps is produced each year for the most recent NAEI year. Improvements to methodologies are logged continually and are reviewed every 6–12 months.

The UK emissions inventory, compiled on behalf of the relevant governmental department, is responsible for reporting the pollutants covered under the EU National Emissions Ceilings Directive (NECD) and the United Nations Economic Commission for Europe (UNECE) Convention on Long-Range Transboundary Air Pollution (CLRTAP) under the Gothenburg Protocol. Directive 2001/81/EC of the European Parliament and the Council on National Emissions Ceilings for NO_x, SO_2, NMVOC and NH_3 sets upper limits for each member state for the total emissions in a given year. Pollutants that have to be reported to CLRTAP include:

- Main pollutants (nitrogen oxides, sulphur dioxide, carbon monoxide, non-methane VOCs, ammonia)
- Particulate matter (PM_{10}, $PM_{2.5}$, total suspended particulates)
- Priority heavy metals (lead, cadmium, mercury)
- Other heavy metals (copper, zinc, nickel, chromium, arsenic, selenium)
- Persistent organic pollutants (benzo[a]pyrene, benzo[b]fluoranthene, benzo[k]fluoranthene, indeno (1,2,3-cd)pyrene, polychlorinated dibenzo-p-dioxins

(PCDDs), polychlorinated dibenzofurans (PCDF), polychlorinated biphenyls, hexachlorocyclohexane (HCH), hexachlorobenzene)

These pollutants are responsible for acidification, eutrophication and ground-level ozone pollution. Member states are required to prepare and annually update national emissions inventories and emissions projections for specified years for these pollutants.

Note that PCDDs are a group of organic polyhalogenated compounds that are significant environmental pollutants. They are commonly but inaccurately referred to as dioxins for simplicity, because every PCDD molecule contains a dioxin skeletal structure as the central ring. PCDFs are a group of halogenated organic compounds which tend to co-occur with PCDDs.

The geographical scope of reporting needs to be defined. The UK has associated overseas territories (OTs), Crown dependencies (CDs) and sovereign bases (SBs). The exact definition of the UK varies under different protocols within the CLRTAP. Emission estimates for the relevant locations and pollutants are made so that the UK emissions accurately reflect those specified in the individual protocols. The only CD, OT or SB which is included in emission estimates is Gibraltar. However, Gibraltar is only included in the definition of the UK for some of the protocols within the CLRTAP. The UK does not yet make emission estimates from inland waterways.

8.5.2 European and global emissions mapping

The European Monitoring and Evaluation Programme (EMEP) administers issues with transboundary air pollution under the CLRTAP. This concerns air emissions from all sources relevant to the environmental problems of climate change, acidification, eutrophication, tropospheric ozone, air quality and dispersion of hazardous substances. The major inventory for Europe is organised by the European Environment Agency under the EMEP/EEA air pollutant emission inventory (formerly known as CORINAIR inventory until 2007). Eight pollutants (SO_2, NO_x, NMVOC, CH_4, N_2O, CO_2, CO and NH_3) are covered, emitted from 30 countries by 250 activities within 11 main source categories. Before 1995 the CORINAIR project was developed under the CORINE (CO-oRdination d'INformation Environnementale, programme of the EU, a programme established by Council Decision 85/338/EEC).

Emission Database for Global Atmospheric Research (EDGAR) provides global past and present-day anthropogenic emissions of air pollutants and greenhouse gases by country and on a 0.1° × 0.1° grid. A further series of global inventories, known as Global Emissions Inventory Activity (GEIA), is being prepared within the framework of the International Global Atmospheric Chemistry project. In the US, the Department of Energy and Environmental Protection Agency compile similar inventories. Within the Reanalysis of the Tropospheric Chemical Composition (RETRO) project, global gridded data sets for anthropogenic and vegetation fire emissions of several trace gases were generated, covering

the period from 1960 to 2000 with monthly time resolution. Anthropogenic emissions in the RETRO inventory are derived from the Netherlands Organization for applied scientific research (TNO) database and the Bureau Veritas (VERITAS) inventory of international ship traffic emissions.

8.6 DISPERSION OF VEHICLE EMISSIONS AND EXPOSURE MODELLING

In Chapter 5, we discussed the complicated set of procedures that has to be undertaken in order to compile an estimate of vehicle emissions. After these source strengths (in g m^{-1} s^{-1}, for example) have been calculated, ambient concentrations can be found from dispersion theory. Away from built-up areas, for motorways, main roads and other roads in the open, the Gaussian method described previously can be used. There are many implementations of the method in common use; a parent model called California Line Source (CALINE) was developed in California, and has evolved into CALINE4. The basic principles are quite straightforward and include vehicle specification and traffic flow for a street network (as a proxy of speed and number) to estimate the corresponding vehicle emissions. An urban network of roads is divided into links, where each link is a straight length of road having known emission characteristics. That link is treated as a line source for the calculation of concentrations at receptors (the points at which a concentration estimate is required). The total concentration is estimated as the sum of the contributions due to all the individual links, plus any background concentration due to the unmapped parts of the area. Certain features of the dispersion are not accounted for in the simple Gaussian method. For example, the effective source is regarded as the roadway itself, after initial dilution of the exhaust gases by mechanical (wake) and thermal (due to waste vehicle heat) turbulence. These effects are used to modify the dispersion parameters such as stability class.

Modelling ambient exposure to pollutant concentrations due to vehicles involves calculation of source strengths for a series of road links, then dispersion in an urban area that usually consists of a mixture of open and canyon environments. In built-up urban areas, simple Gaussian dispersion theory does not apply – the sources are often at the bottom of *street canyons* which reduce wind speeds below the ambient level, especially when the wind direction is almost perpendicular to that of the road. Under those conditions, a re-circulating vortex can keep emissions confined within the canyon, so that road-level concentrations build up to several times the values they would have in the open. Several methods of analysis have been developed for this situation. One example is the Canyon Plume Box (CPB) model, originally developed for the German EPA and subsequently refined by the US Federal Highway Administration. CPB models the vehicle-induced initial turbulence, plume transport and dispersion (Gaussian) on the lee side of the canyon, advective and turbulent exchange at the top of the canyon, pollutant re-circulation, and clean air injection on the downwind side of the canyon. Allowance can also be made for the

FOR REFERENCE PURPOSES ONLY

effects of canyon porosity – that is, gaps in the canyon wall due to intersections, missing buildings or other irregularities.

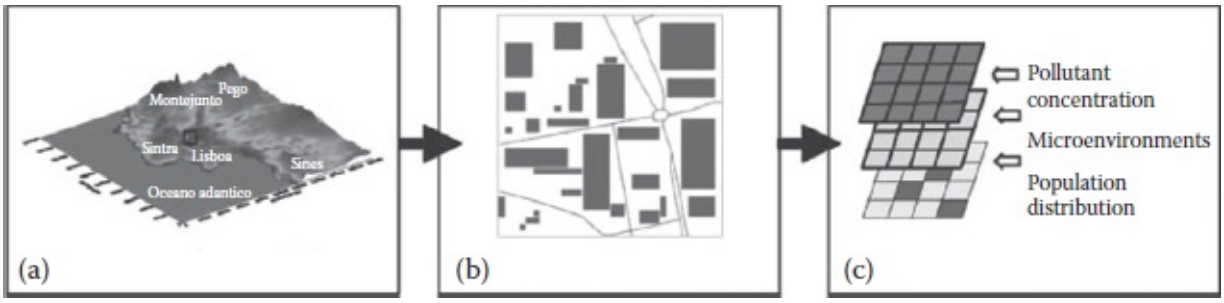

Figure 8.17 Schematic diagram of an integrated methodology for urban population exposure estimation to particulate air pollution: (a) mesoscale modelling, (b) local scale modelling and (c) exposure modelling. (From Borrego, C. et al., Urban population exposure to particulate air pollution induced by road transport, in C. Borrego and A. Norman (Eds.), *Air Pollution Modelling and Its Application XVII*, Springer, New York, 2007.)

To achieve exposure modelling, the pollution concentration can be either directly linked to dose-response functions for known air pollutant effects, or it can be mapped onto socio-demographics and hospital admissions (including both respiratory and circulatory), to derive the human health impacts. A methodology to estimate the population exposure to PM_{10} has been developed, which integrates a mesoscale meteorological model, a CFD model and a population exposure model (Figure 8.17). The mesoscale model, comprising a PM dispersion and deposition module, uses input data for synoptic forcing, topography, land use and emissions to generate 3D meteorological fields (wind, temperature, turbulent kinetic energy etc.) and 3D dispersion fields for the pollutant. The CFD model allows for evaluation of the maximum short-term local concentrations in urban geometries from vehicle emissions. The population exposure module estimates the total human exposure to air pollution as the sum of exposure in different locations and times. This approach is based on modelling the exposure of a population present in different microenvironments to the corresponding modelled air quality concentrations, applying geographic information system (GIS).

8.7 RECEPTOR MODELS

Receptor models are used to estimate the contribution of different sources to the concentration at a location (the receptor) using statistical evaluation of the data collected at that receptor. This process is called source attribution or source apportionment. Receptor models have been used most intensively for the attribution of sources to explain particle

concentrations, because the distinctive chemical fingerprints of particles enable them to be identified with specific emissions. In some ways the process is the reverse of dispersion modelling, because the source is worked out from the concentration rather than *vice versa*. The first step is to collect a large data set of concentration measurements at the receptor, using as comprehensive an analysis as possible. Typically elemental, organic and gaseous concentrations would be measured, as well as particle concentration and possibly size distributions. Intensive and sophisticated analytical methods would often be used, such as X-ray fluorescence, inductively coupled plasma mass spectrometry (ICP-MS), particle-induced X-ray emission (PIXE) and neutron activation analysis. Certain elemental tracers may be used to identify sources, such as lead for petrol, but in that case the link needs to be unambiguous.

Hydrocarbons such as ethane and propane may be used as tracers for exhaust or petrol storage tank emissions, polycyclic aromatic hydrocarbons (PAHs) for wood combustion and diesel smoke, toluene for solvents. In chemical mass balance methods, data on chemical composition of the ambient measurements are related to that of known emissions. It is assumed that the elements or compounds are not reactive in the atmosphere. Clearly, the chemical and physical characteristics of the measured pollutants emitted from different potential sources must be different, and those characteristics must be preserved during transit through the atmosphere to the receptor. By using more powerful statistical methods, such as principal component analysis (PCA) with multiple linear regression, the sample properties alone can be used to work out the number of source categories, the chemical composition of their emissions and their relative contributions to the measured concentrations. This is necessary if some sources have not been identified or if their emissions characteristics are poorly defined – as with roads.

8.7.1 Chemical mass balance models

Chemical mass balance was the first receptor modelling method developed for source attribution. It uses two data sets: (1) the chemical composition of the atmospheric aerosol at a measurement site and (2) the chemical composition of the aerosol emitted from the principal sources in the region. The material collected, for example, on a high-volume filter paper, is composed of contributions from various sources:

$$\rho = \sum_{j}^{p} m_j \quad (j = 1, 2, \ \ldots \ p)$$

where ρ is the local aerosol mass concentration, m_j is the contribution from source j, and there are p sources altogether. In practice, there may be some discrete individual sources if large local ones exist, and other smaller sources are lumped together and treated collectively as domestic, vehicular, and so on. It is also normally assumed that the overall chemical balance of the sources is the same as that at the receptor – that there have been no

changes due to selective deposition or gas/particle conversion. The concentration ρ_i of the ith chemical component in the aerosol sample is related to the source contributions by:

$$\rho_i = \sum_j^p c_{ij} m_j \quad (i = 1, 2, \ \ldots \ n)$$

where c_{ij}, which is the mass fraction of component i in m_j, is the source concentration matrix, and there are n chemical components. The main task is to invert this equation to give the source contributions m_j. This could be done by varying the source contributions to minimise the weighted mean square deviations. The method has been applied to a wide variety of source attribution problems, from single point sources to complex urban and regional airsheds and Arctic air quality.

8.8 STOCHASTIC MODELS

Statistical models do not involve emissions at all. Data on concentrations at a location are collected, together with data on local factors that might affect those concentrations. Such factors might include wind direction and speed, solar radiation, air temperature, time of day, day of the week, season. Statistical correlations are made to suggest what proportion of the variability of the concentration about the mean value is due to each of the factors. Then if a value for each of the factors is known, an estimate can be made of the likely concentration. Because it is based on historical data sets, the prediction assumes that the influence of the factors on concentration will be the same in the future. This is likely to be true on a time scale of a few days; of course, each new day's data set may be input to the model so that any gradual changes in the effects of the different factors are incorporated.

8.9 BOX MODELS

Box models are the simplest ones in use. As the name implies, the principle is to identify an area of the ground, usually rectangular, as the lower face of a cuboid which extends upwards into the atmosphere. A budget is then made on the box over a specified timestep, for the pollutant(s) of interest. This budget involves the initial contents of the box due to the prevailing pollutant concentration, emissions into the box from sources, deposition from the box to surfaces, additions to and losses from the box due to wind and concentration gradients, and gains/losses due to chemical reactions. At the end of the timestep, a new average concentration within the box is calculated, and the process is repeated to track temporal variation of the pollutant concentration. Spatial variability is calculated by having a grid of adjacent boxes of appropriate size, and vertical variations by extending the boxes upwards using the same principles.

8.10 INDOOR AIR POLLUTION MODELLING

As discussed in Chapter 7, indoor air pollution may be either of outdoor or indoor origin. Therefore, modelling indoor air pollution can be more complex as it defies the meteorological principles described earlier in this chapter. Such models are applied for predicting indoor air-pollutant concentrations and dosages as functions of outdoor air-pollutant concentrations, indoor-outdoor air-exchange rates, and indoor air-pollutant sources and sinks. In the past these models have been mainly developed for the purpose of building design, but since have been adopted and adapted for use in various epidemiological and health impact studies. The most widely used are *dilution* (or *ventilation*) *models*. These simulate changes in concentrations of contaminants under the influence of atmospheric mixing within a room, and air exchange with the outdoor environment and/or between rooms. However, for general modelling of exposure to contaminants released into the indoor air, dilution models often lack important terms: decay, for example, absorption to room surfaces and furnishings; removal, for example, filtration by air cleaning devices; medium transfer, for example, sedimentation and absorption from air to dust; and contact rate/time.

Two main approaches to dilution modelling may be identified: *mass balance models* and *computational fluid dynamics* (CFD) models. The simplest (mass balance) models apply to a single compartment (i.e. a room where the source, ventilation and the exposed target occur), steady-state conditions and complete mixing. Multi-zone models are also available to simulate more complex situations, with several interconnected compartments. The most advanced CFD models deal with dynamic conditions, including changing or intermittent release and ventilation, multiple interconnected compartments and displacement ventilation. Indoor air chemistry, sedimentation and absorption (deposition) of pollutants indoors can also be incorporated into the models.

Assuming steady-state conditions and complete mixing, the indoor concentration (C) can be estimated as the product of a constant source term (m) (mass/time) and ventilation rate (Q) (volume/time):

$$C = m/Q$$

In case of incomplete mixing, this is adjusted by introducing a dimensionless empirical correction factor ($0 < c < 1.0$), in which $c = 1.0$ would indicate complete mixing:

$$C = \frac{m}{c} * Q$$

Further, it is assumed a source release with discharge Q, starting at time $t = 0$, leads to an indoor concentration (in room of volume V) and asymptotically changes the concentration C towards the steady state. Conversely, stopping the source release at any point of time leads to a similar concentration decay towards zero. Thus, a generalised form of the single

compartment model as a function of time can be expressed as:

$$C(t) = \frac{m(t)*e^{-\left(V/Q(t)*t\right)}}{c*Q(t)}$$

where both the source term m and its discharge Q are time-dependent.

Instantaneous releases are numerically incompatible with complex mixing: in reality mixing, that is, source decay, is not instantaneous. Indoor concentrations from instantaneous releases can therefore be modelled only from the time required for complete mixing. The contribution of pollution from outdoor air to indoor exposure can be incorporated simply by adding the outdoor air concentration, corrected if necessary by an indoor/outdoor removal term. However, more complicated cases of dynamic releases and ventilation, multiple interconnected compartments, incorporation of decay and removal by indoor air chemistry or pollutant deposition on indoor surfaces require increasingly complicated and often numerical dilution models. Some of the commonly used mass-balance indoor air-pollutant modelling tools include: I-BEAM, CONTAM-W and RISK IAQ models from the USEPA and the Indoor Exposure Model (INDEX).

8.11 REGIONAL CHEMISTRY MODELS

The Fifth-Generation Penn State/NCAR Mesoscale Model (MM5) was the first generation of mesoscale air quality models including advanced chemistry schemes in the late 1990s. The chemistry solver used is CHEMA, with an emission model called EMIMA (emission model for anthropogenic and biogenic sources). There is also a land-use classification module REMO and a deposition parameterisation module called DEPO. The traffic emissions are calculated using the CORINAIR and EPA methodologies. It needs a 24 h emission profile to produce the next 96 h of prognostic outputs.

The Weather Research and Forecasting/Chemistry (WRF/Chem) is a more advanced, fully coupled chemistry and meteorology system model, suitable for simulating the transport and dispersion of pollutants and their impacts. It allows for full weather and chemical transport simulation to be conducted (Zhang et al., 2010). The model consists of the following major programs:

- Pre-processing system (WPS)
- Data assimilation system
- Solver (including chemistry)
- Post-processing and visualisation tools

The following are the main attributes and advantages of WRF/Chem, as identified in the user literature to date (WRF/Chem user manual; Hu, 2008):

FOR REFERENCE PURPOSES ONLY

- A fully coupled online modelling system.
- Several choices for physical parameterisations of meteorology processes, which enable the model to be applicable on different scales ranging from meters to thousands of kilometres.
- Nesting capability for running a combination of grid resolution.
- The air quality component is fully consistent with the meteorology component, both of which use the same transport scheme, same gridding and same physics (Grell et al., 2005).
- The chemistry package consists of modules for dry deposition (*flux resistance* method), biogenic emissions, the reaction scheme for modelling radical chemistry and a photolysis scheme.
- Chemistry is simulated simultaneously with dynamics. The update frequency of input of metrological parameters to chemistry simulation could be as short as minutes.
- As the same coordinate is used for both chemistry and dynamics simulation, no interpolation is needed.
- The chemical-dynamical feedback can be simulated.

The WRF/Chem model simulates biogenic-anthropogenic interaction by using the appropriate input files. It uses the anthropogenic and biogenic emissions data set for gaseous species (CO_2, CO, NO_x, NO, NO_2, SO_2, NH_3, and total VOCs) (Figure 8.18), which needs to be input in a structure prescribed by the EDGAR system (see Section 8.5). The dedicated Model of Emissions of Gases and Aerosols from Nature (MEGAN) allows for introduction of green infrastructure components in the model set through alteration in the albedo of surface (simulating the adjusted temperature profile) and the biogenic sources (bVOCs) and sinks.

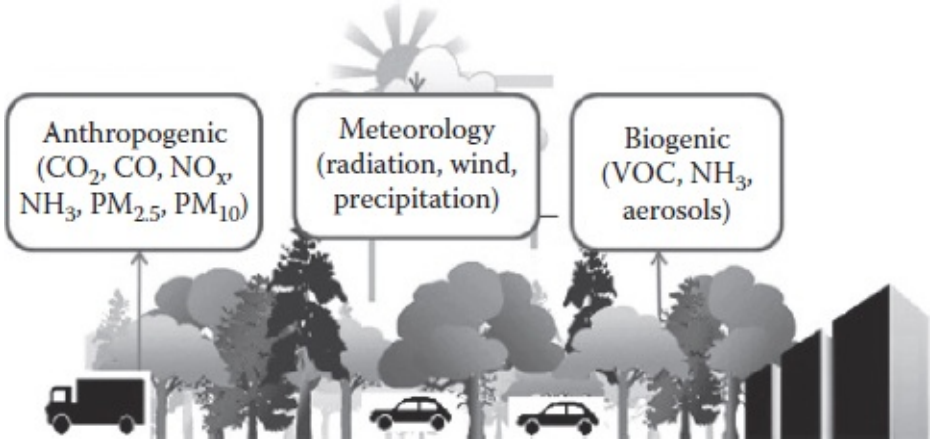

Figure 8.18 Scope of WRF/Chem modeling, including anthropogenic and biogenic emissions and meteorological data inputs.

The air quality component of the model is fully consistent with the meteorological

component; both components use the same transport scheme (mass and scalar preserving), the same grid (horizontal and vertical components) and the same physics schemes for subgrid-scale transport (Grell et al., 2005). The components also use the same time step; hence no temporal interpolation is needed. The chemistry package consists of dry deposition (*flux-resistance* method), biogenic emission using the chemical mechanism from RADM2, a complex photolysis scheme (Madronich scheme coupled with hydrometeors), and a state-of-the-art aerosol module MADE/SORGAM aerosol parameterisation. WRF/Chem outputs have been field validated against detailed photochemical data model forecasting the O_3 precursors (CO and NO_x).

However, such model setups are both data intensive and computationally demanding. For example, WRF/Chem requires two 3D (i.e. *x, y, z* layers) anthropogenic emissions data files, each containing 12 h (1 h update interval) of emissions data (0000 UTC to 1100 UTC and 1200 UTC to 2300 UTC). The data files need to be in the WRF NetCDF format. In the US these data files can be constructed from the emissions data (4-km horizontal spacing) made available from the WRF/Chem download site; outside the US, anthropogenic emissions are available around the globe from RETRO and EDGAR data sets. The installations require a high-performing Unix/Linux cluster facility as typical execution time on a single PC is reported to be longer (e.g. up to 4 days).

8.12 CASE STUDY – COMBINING A DISPERSION MODEL WITH SPATIAL STATISTICS

This case study presents application of a suite of dispersion and statistical techniques to model air pollution exposure and associated health implications, which includes the three steps discussed in the following sections.

8.12.1 Vehicle emissions modelling

Pollutant emissions were calculated using the Platform for Integrated Traffic, Health and Emission Modelling (PITHEM) software (Namdeo and Goodman, 2012). This software, which is proprietary to Newcastle University, UK, allowed the development of bespoke mappings between the user classes defined in a strategic transport network of a UK local authority with the hierarchical vehicle fleet information within the UK National Atmospheric Emissions Inventory (NAEI) (Venfield and Pang, 2012). The vehicle kilometres travelled and the average speed information for each user class were then combined with the NAEI speed-emissions curves (Boulter et al., 2009) to produce period-based emissions totals for regulated air pollutants. These period totals were then scaled by appropriate diurnal and seasonal flow profiles (DfT, 2012) and normalised by link lengths to produce average annual emissions rates for each link, as well as diurnal hourly emissions profiles.

8.12.2 Dispersion modelling

The traffic emissions estimated from PITHEM in the previous step were used as input to set up the air dispersion modelling using ADMS-Roads v3.1 (CERC, 2011). The model inputs comprised of traffic-generated emissions of CO, NO_2, PM_{10}, $PM_{2.5}$ and meteorology. Long-term (annual average) outputs were obtained for a 250 m grid resolution applying an intelligent gridding along the roads. The latter generated additional output points on both sides of the modelled roads where the pollutant concentration gradients are the greatest. This was conducted in two stages – first, in the pre-run stage, up to 5000 extra receptor points were added in and around the roads in sets of 4, with at least one set of points added to each road segment that lies within the output grid; second, at the end of the model run, three sets of additional points were added between the first set of intelligent grid points for generating concentration output by linearly interpolating between the values at the first set of points. The second stage was conducted in ADMS-Roads after the model run by default, to create a regular Cartesian grid within the rectangular region specified (CERC, 2011).

For effective visualisation of the pollutant concentrations, the gridded outputs obtained from the dispersion model were used to generate interpolated surface maps using an inverse distance weighted (IDW) technique (ArcGIS Spatial Analyst) (ESRI, 2012) and overlaid on the existing road network for the study area (Figure 8.19).

8.12.3 Spatial statistics

Two spatial statistics were applied to evaluate the strength of explaining the outcome (dependent variable) through a set of inputs (explanatory variables) – (1) *weighted overlay* and (2) *ordinary least squares regression*. The weighted-overlay technique allows for an integrated analysis to solve multi-criteria problems (such as site selection and suitability models) by applying a common scale of values to diverse and dissimilar inputs. Different rasters with different value scales can be analysed on a common scale. The cell values for each input raster in the analysis are assigned values from the evaluation scale and reclassified to these values. This makes it possible to perform arithmetic operations on the rasters that originally held dissimilar types of values. Each input raster is weighted, or assigned a percentage influence, based on its importance to the model. Any class can also be assigned a restricted value, which means that the corresponding area is unacceptable or cannot be used. Restricted areas are excluded from the analysis. The cumulative influence for all the rasters should sum to 100%. The cell values of each input raster are multiplied by the rasters' weights. The input rasters are weighted by importance and added together to produce an output raster scaled on 1–10 (with 10 being the most favourable). Values at one end of the scale represent one extreme of suitability (or other criterion); values at the other end represent the other extreme. The ordinary least squares (OLS) regression method allows for developing a regression model for quantifying the spatial associations between different attributes with unique identifiers.

FOR REFERENCE PURPOSES ONLY

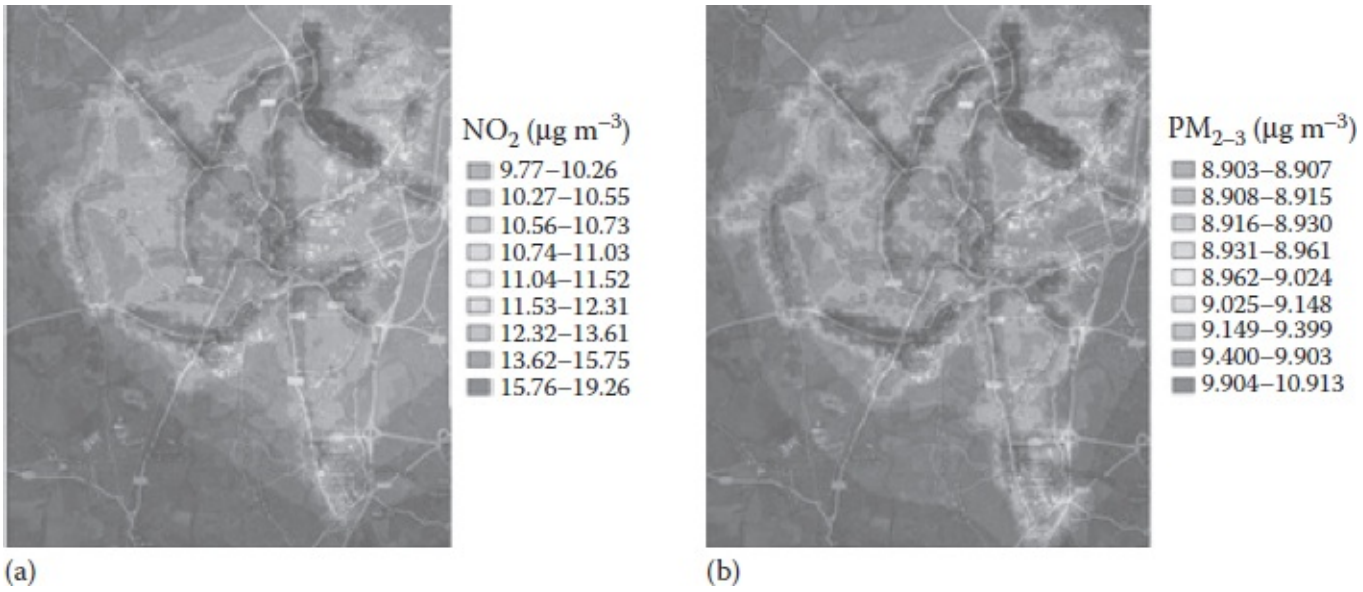

Figure 8.19 Hourly average pollutant concentrations: (a) NO_2 and (b) $PM_{2.5}$. (From Tiwary, A., personal communication.)

FOR REFERENCE PURPOSES ONLY

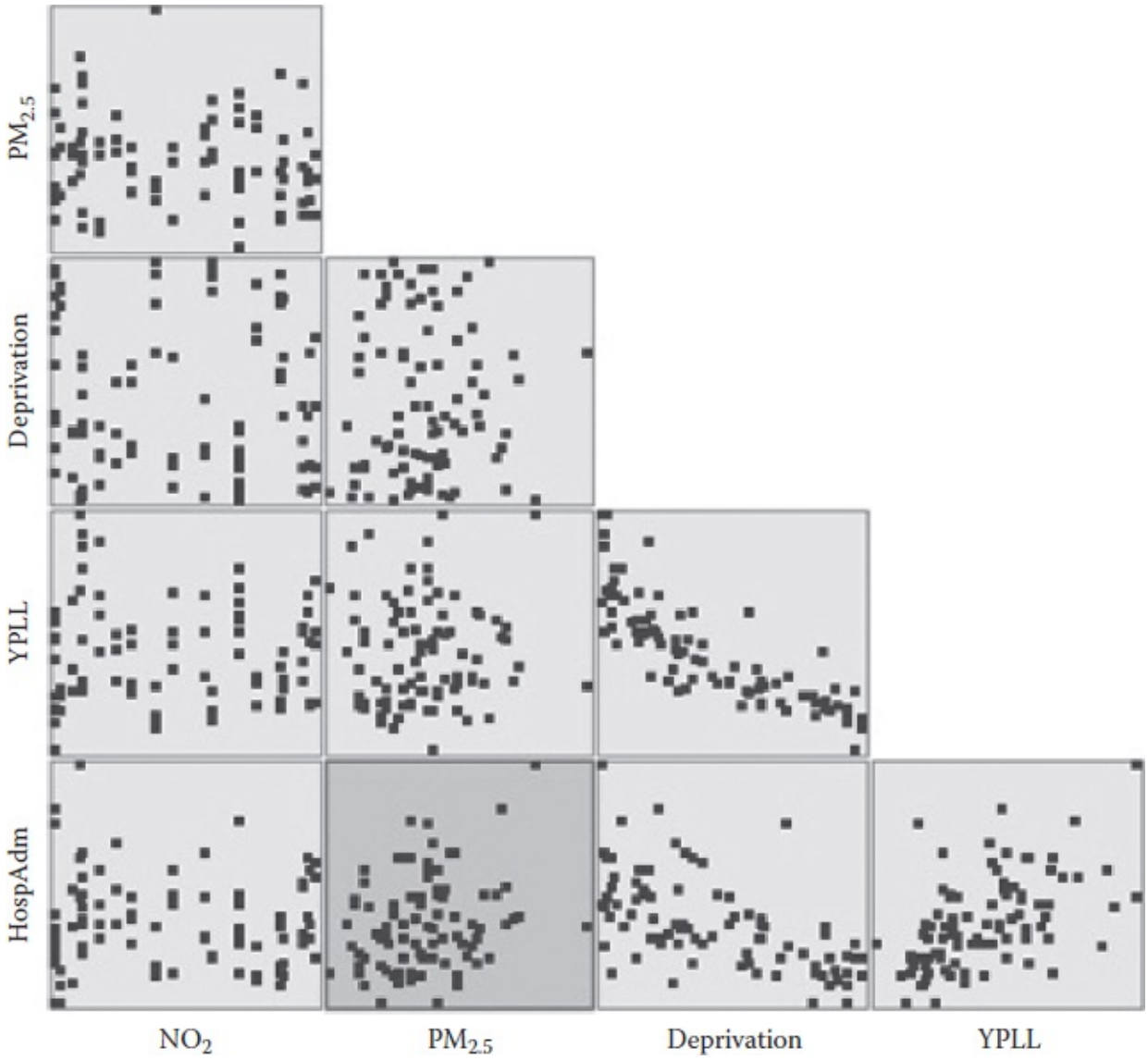

Figure 8.20 Scatter plot of cross-thematic spatially referenced statistical parameters. (From Tiwary, A., et al., *Environ. Pollut.*, 183, 213–223, 2013.)

Figure 8.20 uses the statistical and analytical tools available in ArcGIS v10.1 (ESRI, 2012) to show the associations between pollution concentration, socio-demographics and hospital admissions (including both respiratory and circulatory) into a single layer at the lower super output area (LSOA) unitary authority boundary (comprising minimum population size 1000; mean population size 1500); scatter plots can be generated to assess the cross-thematic correlations.

As can be inferred from the plots, the reported hospital admissions (combined for respiratory and circulatory illnesses) in the study area has stronger correlations with the modelled $PM_{2.5}$ than with NO_2 concentrations. Also, there seems to be a direct association of hospital admissions with the reported Yearly Potential Life Lost Indicator (YPLL). However, a strong negative correlation is observed for both of these variables with the reported deprivation index (RIMD). This is expected and solely an artefact RIMD, which is

FOR REFERENCE PURPOSES ONLY

reported in an inverse order, that is, lower values reflecting high deprivation areas.

In the next step, weighted-overlay analysis was performed, combining the pollutant concentrations from modelled traffic-related emissions with the reported socio-demographics for the site, acquired from publicly available statistics at LSOA level (http://www.neighbourhood.statistics.gov.uk/). The LSOAs in the UK represent the smallest geographic units for disseminating robust census statistics while the confidentiality of individual census returns remains preserved (ONS, 2010). The input layers and their percentage weighting applied to this exercise are shown in Table 8.8. Essentially, this approach allowed for multi-criteria decision making, utilising a ranked score, based on a common scale for traffic emissions, deprivation and reported health implications.

The output from weighted-overlay analysis is shown in Figure 8.21 on a *ranking of preference* from 1 to 10 (in increasing order). Shown alongside on the same map is the traffic intensity, in terms of the annual average daily traffic (AADT), on the road network of the local authority – ranging from blue (low: 2214) to red (high: 57977) vehicles. The weighted-overlay of associated layers provides an LSOA-level spatial map of the spread of potential locations of priority areas to improve the traffic-related air quality. The ranked outputs link the explanatory variables (both pollutants and socio-demographics, including RIMD and YPLL) with the outcome (hospital admissions) to locate the regions requiring better understanding of the pollutant exposure. The lower values (lighter tone) reflect sites requiring least interventions, while the higher values (darker tone) indicate the sites where management interventions have to be implemented.

Table 8.8 Weightings applied to the multi-criteria layers with reference to hospital admissions from the scatter plot

Input layer	*Data source*	*Weighting (%)*
$PM_{2.5}$	Dispersion model	25
NO_2	Dispersion model	20
Deprivation (ranked index of multiples deprivation, RIMD)	ONS (2010)	30
Potential life lost indicator (Yearly Potential Life Loss [YPLL] indicator)	ONS (2010)	25

FOR REFERENCE PURPOSES ONLY

Figure 8.21 Hot spots from weighted overlay analysis (area) superimposed with traffic information (lines). (From Tiwary, A. et al., *Environ. Pollut.*, 183, 213–223, 2013.)

This study demonstrates the application of spatial statistics in refining dispersion model outputs based on a multi-criteria approach using a suite of spatial statistics. The main feature of the methodology is to customise air quality modelling to decision making through an iterative refinement of the input explanatory variables while evaluating their contributions to a preferred outcome, for example, hospital admissions in our case study.

REFERENCES AND FURTHER READING RESOURCES

Air Quality Consultants (2016a) *Emissions of Nitrogen Oxides from Modern Diesel Vehicles*. Bristol, UK.

Air Quality Consultants (2016b) *Overview of Changes Introduced by EFT V7.0 and by CURED V2A*, Bristol, UK.

Borrego, C., Tchepel, O., Costa, A. M., Martins, H., and Ferreira, J. (2007) Urban population exposure to particulate air pollution induced by road transport. In: C. Borrego and A. Norman (Eds.), *Air Pollution Modelling and Its Application XVII*. Springer, New York.

Boulter, P. G., Barlow, T. J., McCrae, I. S., and Latham, S. (2009) Emissions factors 2009, Final summary report. TRL Published Project Report PPR361 for the UK Department for Transport.

CERC (2011) *ADMS-Roads, An Air Quality Management System, User Guide Version 3.1*. Cambridge Environmental Research Consultants Ltd., Cambridge, UK.

DfT (2012) *Traffic Distribution by Time of Day on All Roads in Great Britain*. Table TRA0307(2010). UK Department

FOR REFERENCE PURPOSES ONLY

for Transport, London, UK.

Dieselnet (2016) Emissions standards – EU: Nonroad engines. www.dieselnet.com/standards/eu/nonroad.

ESRI (2012) ArcGIS Software Version 10.1. Environmental Systems Research Institute. http://www.esri.com/software/arcgis.

Grell, G. A., Peckham, S. E., Schmitz, R., McKeen, S. A., Frost, G., Skamarock, W. C., and Eder, B. (2005) Fully coupled online chemistry within the WRF model. *Atmospheric Environment*, 39: 6957–6975.

Henn, D. S., and Sykes, R. I. (1992) Large-eddy simulation of dispersion in the convective boundary layer. *Atmospheric Environment*, 26A(17): 3145–3159.

Hu, X. (2008) Incorporation of the model of aerosol dynamics, reaction, ionization and dissolution (MADRID) into the Weather Research and Forecasting Model with Chemistry (WRF/Chem). PhD thesis, North Carolina University.

Kaimal, J. C., and Finnigan, J. J. (1994) *Atmospheric Boundary Layer Flows: Their Structures and Measurements*, pp. 66–108. Oxford University Press, New York.

Masters, G. M. (1998) *Environmental Engineering and Science*. Prentice Hall, Upper Saddle River, NJ.

Namdeo, A. K., and Goodman, P. S. (2012) Platform for Integrated Traffic, Health and Environmental Modelling (PITHEM). *Better Air Quality 2012 Conference*, Hong Kong, 5–6 December.

Oke, T. R. (1987) *Boundary Layer Climates*. Methuen, London, UK.

ONS (2010) *Neighbourhood Statistics*. UK Office of National Statistics.

Pepper, D. W., and Carrington, D. (2009) *Modelling Indoor Air Pollution*. Imperial College Press, London, UK.

Schlichting, H. and Gersten, K. (2000) *Boundary-Layer Theory*. Springer-Verlag, Berlin, Germany.

Steyn, D., and Mathur, R. (2014) *Air Pollution Modeling and its Application XXIII*. Springer, Cham, Switzerland.

Tiwary, A., Namdeo, A., Fuentes, J., Dore, A., Hu, X. M., and Bell, M. (2013) Systems scale assessment of the sustainability implications of emerging green initiatives. *Environmental Pollution*, 183: 213–223.

Venfield, H., and Pang, Y. (2012) New vehicle fleet composition projections (Base 2011). National Atmospheric Emissions Inventory (NAEI). Department for Environment, Food and Rural Affairs. NAEI Reference: ED57422004.

Versteeg, H. K., and Malalasekera, W. (1995) *An Introduction to Computational Fluid Dynamics: The Finite Volume Method*. Longman Scientific & Technical, Harlow, UK.

Weil, J. C., Sykes, R. I., and Venkatram, A. (1992) Evaluating air-quality models: Review and outlook. *Journal of Applied Meteorology*, 31(10): 1121–1145.

Zannetti, P. (Ed.) (2013) *Air Pollution Modeling: Theories, Computational Methods and Available Software*. Springer Science & Business Media, New York.

Zhang, Y., Olsen, S., and Dubey, M. (2010) WRF/Chem simulated springtime impact of rising Asian emissions on air quality over the U.S. *Atmospheric Environment*, 44(24): 2799–2812.

FOR REFERENCE PURPOSES ONLY

Chapter 9

Air pollution control and mitigation

This chapter provides a comprehensive overview of the techniques for air pollution control and mitigation. The first part covers industrial air pollution, discussing conventional air pollution control using established engineering methods. This is followed by more planning oriented air pollution control and mitigation measures for ambient applications, both in indoor and outdoor environments. It captures some of the recent developments in systems thinking and nature-based solutions, presenting the state of the art and the way forward. A dedicated section on emission control from mobile sources has been provided in Chapter 5.

A typical air pollution problem can be resolved through one of the following three mitigation options:

- *Enhancing dispersion*: Improving the dispersion of an emission lowers the pollutant concentrations to which living beings are exposed within an acceptable threshold. This can be achieved by increasing the stack height or through production curtailment. However, this option simply displaces the problem rather than providing a lasting solution; therefore, it is not considered suitable for industries.
- *Pollution prevention by process change*: It involves modification of the production process in order to reduce the emissions; therefore, it has wide-ranging industrial applications. This is considered to be the most economical option and can be achieved through switching fuels (e.g. replacing coal with natural gas or other renewable), enhancing process efficiency (e.g. using fluorescent lamps instead of incandescent lamps) and/or minimising the production of hazardous wastes.
- *Intervention*: Also known as *downstream pollution control*. Its technical premise is to remove or destroy sufficient contaminants from the gas stream through chemical or mechanical processes using an end-of-pipe control device so that the final discharge into the ambient air is below an acceptable threshold. Most industrial activities tend to adhere to this option for mitigating foul emissions; however, in industrial economics more credit is given for devising a process change (pollution prevention) than for developing end-of-pipe controls.

In order to pinpoint the hot spots of air pollution sources within a system – be it an industrial production process or an urban activity – life cycle assessment (LCA) and/or material flow analysis (MFA) methodologies have proven to be useful diagnostic tools. The main objective of applying LCA/MFA is to assess the critical environmental burdens and impacts contributing to the adverse effects on human and ecological health. These critical air pollutants can then be dealt with and their impacts mitigated through implementation of effective control measures. Detailed texts describing the LCA/MFA methodologies exist in the literature. Interested readers can find some useful sources listed in the 'References and Further Reading' section at the end of this chapter. Air pollution control measures are predominantly industrial in nature.

9.1 INDUSTRIAL AIR POLLUTION CONTROL TECHNOLOGY

This section extends the generic information covered in Chapters 2 and 3 on controlling gaseous and particulate air pollutant release respectively to the ambient environment, including emission-specific abatement and control techniques, such as catalytic control. It describes the industrial air pollution control initiatives that are commonly applied in removal of the main culprits exiting a combustion process via a flue (i.e. a vent, a pipe or channel for conveying exhaust gases) – termed *flue gas*. The composition of the flue gas largely depends on the fuel burned, but it is mainly comprised of nitrogen (nearly 75%), CO_2, water vapours, PM (soot), CO, NO_2, SO_2, SO_x, NO_x and particulate matter (PM). The measures described here present a snapshot of some of the established industry-specific techniques, termed *best available techniques* (BATs), conforming to the European Commission's Industrial Emissions Directive. For example, a typical flue gas treatment system in a pulverized coal combustion power plant consists of a dust collector, a De-NO_x equipment and a desulphurization equipment. These are described in later sections. The Intergovernmental Panel on Climate Change (IPCC) reckons that supporting clean energy in the developing world should help to improve air quality in the region (discussed later in Chapter 11).

9.1.1 Adsorption and absorption of gases

This technique is used for controlling gaseous pollutants, mainly concentration of SO_2 and NO_x from the gas stream before release to the atmosphere. In some cases, these create a useable by-product – for example, nitric acid can be recovered when NO_x is removed.

9.1.1.1 Adsorption

FOR REFERENCE PURPOSES ONLY

Gaseous air pollutants such as organics are captured on the surface of a bed of porous material (the adsorbent) through which the gas flows. The adsorbents used are materials such as activated carbon (charcoal made from wood or coconut shells), silica gel (sodium silicate), alumina, synthetic zeolites and clays such as fullers' earth (magnesium aluminium silicates). Activation refers to the thermal pre-treatment of the adsorbent to maximise its surface area per unit volume. This large specific surface area is an essential requirement for good adsorption systems. Commonly used adsorbers such as silica gel and activated charcoal have surface areas of up to 2 km^2 per kg, and adsorption capacities of up to 0.5 kg kg^{-1}. The adsorption process may be physical (due primarily to Van der Waals short-range forces), or it may be chemical. When it has become saturated, the adsorbent is regenerated by heating (often with steam) with or without a reduction in pressure. Adsorption is most effective at high concentration and low temperature. The relationship between the concentrations in the gas and solid phases at a particular temperature is known as the adsorption isotherm. In general, the concentration in the solid phase increases with molecular weight and pollutant concentration and decreases with increasing temperature. The adsorption is most effective for non-polar (hydrophobic) compounds, such as hydrocarbons, and less so for polar (hydrophilic) compounds, such as organic acids and alcohols.

9.1.1.2 Absorption

The gas stream is given intimate contact with an absorbing solution by means of bubbling or spraying. The absorption may either be chemical (by reaction) or physical (by dissolution). Solvents in common use include water, mineral oils and aqueous solutions. Gases that are commonly controlled by absorption include HCl, H_2SO_4, HCN, H_2S, NH_3, Cl_2 and organic vapours such as formaldehyde, ethylene and benzene. The absorption process depends on the equilibrium curve between the gas and liquid phases and on the mass transfer between the two, which in turn is a function of the driving force divided by the resistance.

In commercial absorbers, the gas and solvent are brought into intimate contact, with equilibrium being achieved if the results are to be predictable, before the cleaned gas and solvent are separated. In stagewise absorption, such as tray scrubbers, the gas is bubbled through the liquid to achieve one absorption step under one set of equilibrium conditions before going on to the next step. A vertical casing contains several trays, one above the other.

Solvent cascades from the top downwards, while gas moves upwards (counter-current absorption). Each tray has many small vents across its surface through which the gas bubbles, into and through the layer of solvent. These bubbles provide the high surface area and thin gas–solvent interface necessary for efficient movement of the gas into the solvent. In continuous differential contact systems, such as packed towers, the interfacial surface is maintained on a subdivided solid packing (Figure 9.1). Very high efficiencies, greater than

99.9%, can be achieved.

A common application of gas scrubbers is for odour control. Some gases have extremely low odour thresholds, which are unrelated to their toxicity, and scrubbers must operate at consistently high efficiencies to avoid odour complaints. Often, the odorous contaminant is absorbed into a solvent, then reacted with an oxidising agent such as potassium permanganate to fix it as a less harmful compound.

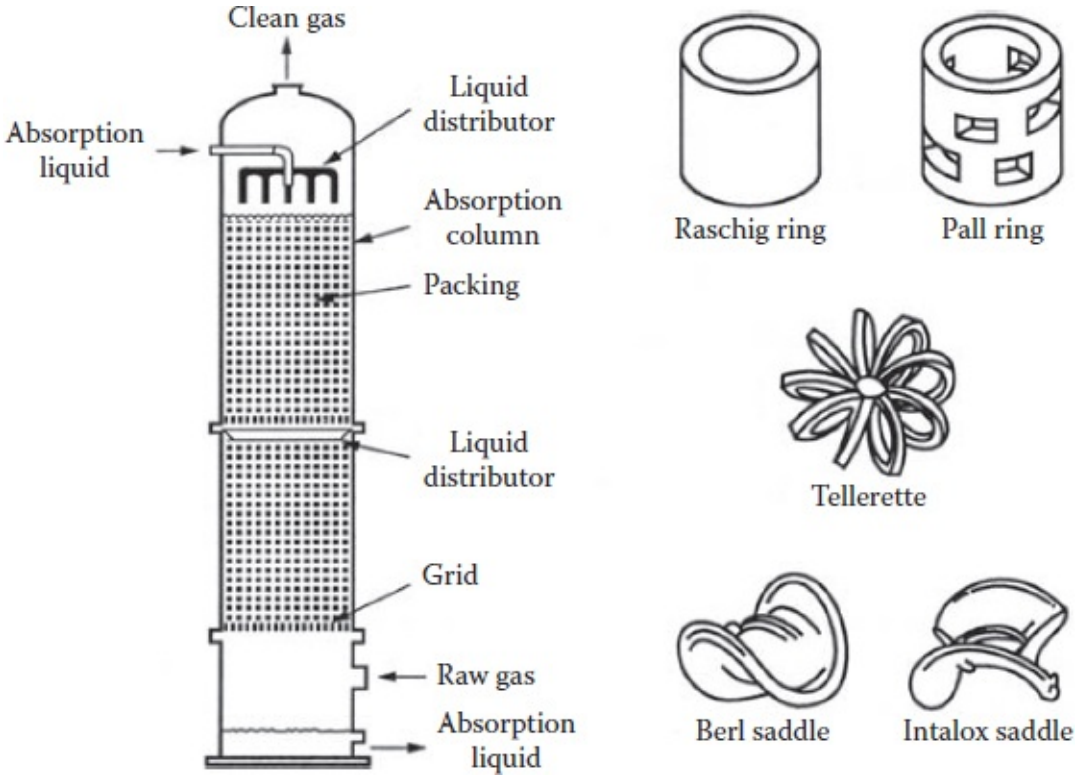

Figure 9.1 A packed absorption tower. (From Johnsson, J.E., Urban sources of air pollution, in Fenger, J., Hertel, O., and Palmgren, F. (Eds.), *Urban Air Pollution: European Aspects*, Kluwer Academic Publishers, Dordrecht, the Netherlands, 1998.)

9.1.2 Abatement of SO_x

The following are some of the recommended means for reducing SO_x emissions:

Burn less fuel!: It is self-evident that, other things being equal, we can always reduce pollutant emissions by burning less fuel. However, for several hundred years, as we have already seen, the rising standards of living of the developed countries have been based fundamentally on production and consumption of energy that has mostly been derived from fossil fuel. We live in an increasingly energy-intensive society, and reductions to our quality of life in order to save energy are not yet politically acceptable. Many measures, such as improved thermal insulation and draught-proofing

FOR REFERENCE PURPOSES ONLY

of buildings, offer enormous potential for improved quality of life and reduction of emissions. Wonderful opportunities for change have been missed. For example, the price of oil was arbitrarily quadrupled by the Gulf States in the 1970s; this incentive could have been used to redirect society quite painlessly, raising the price of energy over a 20-year period and encouraging people to live closer to their work and relatives and travel on public transport. Nevertheless, in 2008 the UK government prioritised long-term initiatives to make homes less energy-wasteful through adequate insulation. In addition, combined heat and power (CHP) generation units, that can potentially raise the overall energy efficiency of fossil fuel combustion from below 40% to above 80%, have been identified as a vital part of the energy mix.

Fuel substitution: Apart from smelting of metal ores, sulphur oxides are mainly formed from combustion of fuels (coal, natural gas, oil, peat, wood), so the most straightforward method for their mitigation would involve minimising the oxidation of sulphur-containing fuels. Fuel sulphur content generally falls in the order coal > oil > wood. In natural gas most of the sulphur is in the form of H_2S, which can be removed through chemical separation from the other constituent gases. This involves the use of a lower-S fuel to reduce emissions and is very logical, but may have other implications. For example, we have seen from the aforementioned data that power stations must be the first target for sulphur control.

In the UK, a large investment in coal-fired stations was made in the 1960s, with coal sourced from the nationalised British coal pits. Most British coal, particularly in the Trent valley where the power stations are concentrated, is not low-sulphur. When acid deposition and the sulphur content of coal became an issue in the 1970s, there was little flexibility for these stations to import low-sulphur coal. In the 1980s and 1990s, the British coal industry collapsed under both economic and political pressures, increasing the freedom of power stations to import low-sulphur coal. In addition, this led to increased reliance on gas-fired power stations that emit much less sulphur dioxide. Coal remained a dominant fuel source until the 1990s. By 1996, however, gas generation had taken 21% of the market and coal had declined to around 45%. The effects of changes in sulphur content can be dramatic. In Hong Kong, the use of fuel oil containing more than 0.5% S by weight was prohibited in July 1990. Ambient SO_2 concentrations in the most polluted areas dropped from around 120 to around 30 μg m^{-3} within weeks.

Fuel cleaning: In recent years there has been more emphasis on lowering the sulphur content of conventional fuels or, if possible, removing sulphur from the fuel altogether. To the latter end techniques such as *coal cleaning* (removing pyritic sulphur) or *solvent refining*(dissolving coal in strong solvents followed by catalytic hydrogenation) have been developed to mitigate SO_2 emissions to the ambient air. The coal used in large-scale generating plants is ground in a ball mill to the texture of a fine powder so that it can be blown down pipes and mixed with air before combustion.

FOR REFERENCE PURPOSES ONLY

As the sulphur-containing pyrites occur as physically distinct particles having a different density to the coal, a process such as froth flotation can be used to separate the relatively dense flakes of pyrites from the powdered coal. Reductions of 80% in S content can be achieved, but 40% is more typical and this process is not widely used.

Chemical reduction: Reduction of sulphur oxides can produce inert products that are harmful to humans. Sulphur in reduced form can be removed from a gas stream through the *absorption and stripping* method. The liquid solvent used is required to have higher affinity for the gaseous component containing reduced sulphur than the rest of the components in the gas stream. This method can be used to mitigate sulphur dioxide emissions from oil refineries and coal gasification.

Concentration: This method is used to mitigate SO_2 concentrations in off-gases from smelting of metal sulphide ores. The general procedure is to convert incoming SO_2 to H_2SO_4 which is then used to produce phosphate fertiliser.

Flue gas desulphurisation (*FGD*): Chemical engineering plants can be built into or added onto power stations to remove most of the sulphur dioxide from the combustion (flue) gases before they are exhausted to the atmosphere. Several different methods are available. The limestone-gypsum process is one of the most popular FGD techniques, where a finely divided limestone slurry is sprayed into the flue gas (Figure 9.2). The calcium carbonate from the limestone reacts with the SO_2 to produce hydrated calcium sulphate (gypsum), which can be used to make plasterboard for the building industry:

$$\mathrm{CaCO_3 + SO_2 \rightarrow CaSO_4 \cdot 2H_2O}$$

In a modification of the above, a lime slurry is atomised by a spinning disc. Although, the reaction between the absorbent and the acid gas takes place mainly in the aqueous phase, the water content and rate of evaporation are controlled to give dry calcium sulphite, which is captured in a conventional dust collector and can be used for landfill or cement manufacture:

$$\mathrm{SO_2 + CaO + \tfrac{1}{2}\,H_2O \rightarrow CaSO_3 \cdot \tfrac{1}{2}\,H_2O}$$

Finally, for plants located near the sea, the natural alkalinity of seawater can be utilised to form sulphuric acid in a packed bed absorber:

$$\mathrm{SO_2 + H_2O + \tfrac{1}{2}\,O_2 \rightarrow H_2SO_4}$$

The acid effluent is normally disposed of at sea, which may or may not be environmentally acceptable. This process is a good example of the need to consider air, water and land pollution as a whole when evaluating different control strategies.

Although the underlying chemistry of this method is quite simple, it has high installation and operational costs. Limestone must be quarried in, and transported from, rural areas, and the gypsum may have to be disposed of in a landfill if a market cannot be found for it.

FOR REFERENCE PURPOSES ONLY

Apart from this, using limestone scrubbers has a number of operational problems – including corrosion, plugging, poor reagent utilisation and poor solid-liquid separation. There is also a consequent risk of leachate creating a water pollution problem. As a consequence, alternative approaches (other wet systems) have been developed to overcome these limitations. In addition, several dry and dry-wet systems have also been in practice to treat SO_2-containing flue gases in order to mitigate their aerial emissions.

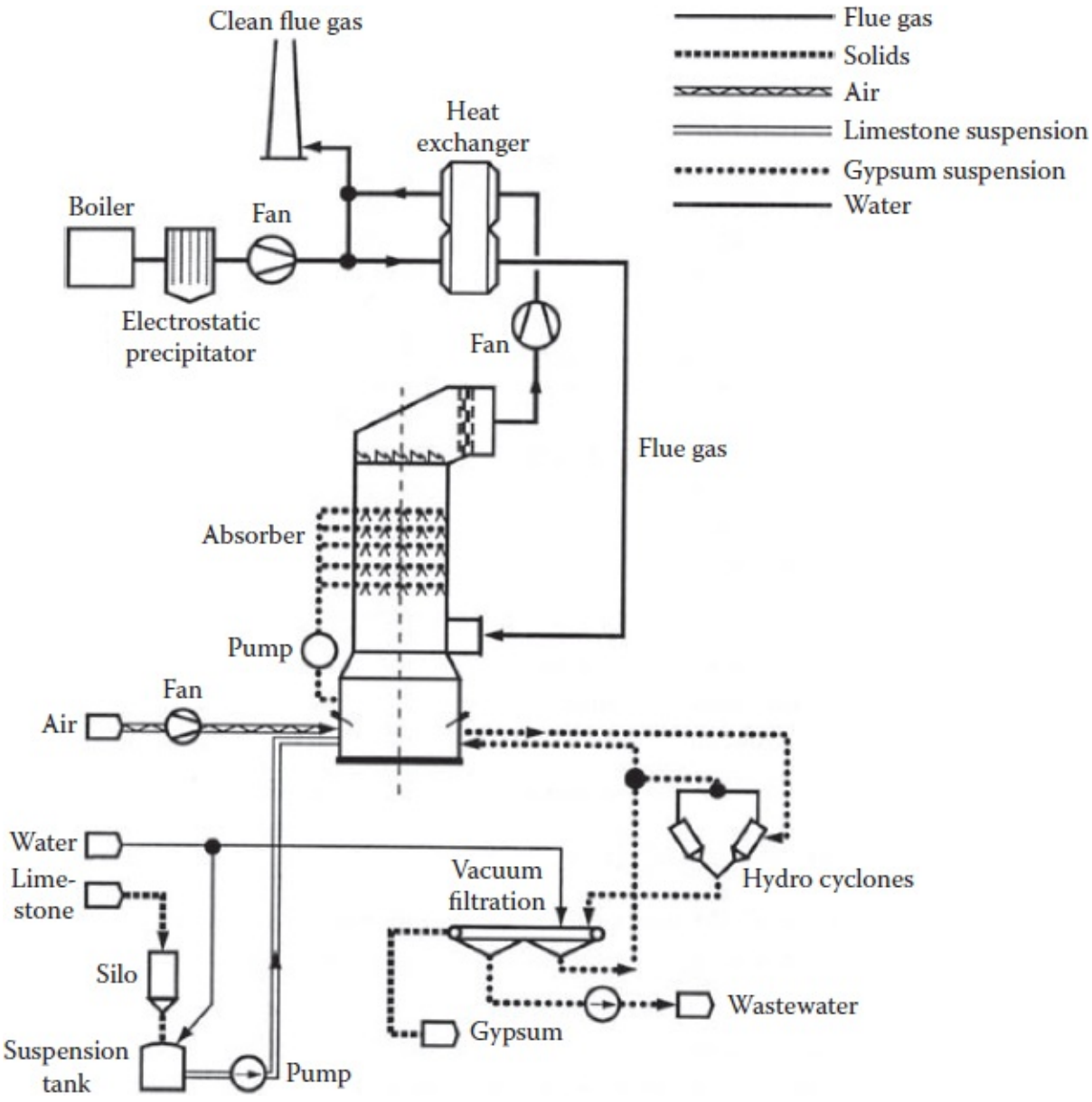

Figure 9.2 Calcium carbonate FGD system. (From Johnsson, J.E., Urban sources of air pollution, in Fenger, J., Hertel, O., and Palmgren, F. (Eds.), *Urban Air Pollution: European Aspects*, Kluwer Academic Publishers, Dordrecht, the Netherlands, 1998.)

Although the old industrialised countries have the wealth and level of technology to

lower SO_2 emissions to whatever value they choose, we cannot be complacent on a global basis. For example, China currently burns around 1400 Mt coal, accounting for 66% of its total primary energy consumption, and emits around 25 Mt SO_2. About half of China's SO_2 emissions are attributed to burning coal. By 2020, around 2000 Mt coal will be burned, emitting up to 55 Mt SO_2 depending on the sulphur content of the coal and the level of sulphur emission control installed on new plants. The 1999 Gothenburg Protocol of the Convention on Long Range Transport of Air Pollution has set a combined EU annual emissions ceiling of 4.044 Mt SO_2 to be achieved by 2010. Remarkably, this is similar to the SO_2 emission from the UK *alone* during the 1980s.

9.1.3 Abatement of NO_x

While there are 8 different oxides of nitrogen, it is mainly nitric oxide (NO) and nitrogen dioxide (NO_2) which are commonly found and thus require air pollution control in most cases. NO_x are mainly produced during combustion in two ways: from interaction of oxygen and nitrogen in the air (termed *thermal* NO_x), with participation of some active carbon species from the fuel. The most straightforward option would be to burn a fuel with no carbon (e.g. H_2). However, it may not be as simple as that as some combustion processes also produce NO_x from conversion of nitrogen originally present in the fuel itself (termed as *fuel* NO_x). Apart from combustion, NO_x is also produced from production and use of nitric acid and from agricultural processes (e.g. silage production). However, the major NO_x problem is considered to be associated with combustion as the total volume of NO_x released from other sources is much smaller.

The following are some of the recommended means for reducing NO_x emissions:

Burn less fuel!: This means fewer motor cars, smaller engines, more public transport, more home insulation and similar measures. As the same combustion processes are involved, all the arguments and methods that applied to SO_2 would reduce NO_x production correspondingly.

Low-nitrogen fuel: There is not much to be gained by using low-N coal or oil, as they tend to have similar N content. Also, a perversity of thermodynamics means that low-N fuels convert their N more efficiently to NO than do high-N fuels, offsetting the expected benefit.

Peak temperature reduction: The endothermic nature of thermal NO generation means that production can be lessened by reducing peak temperatures everywhere within the combustion zone; it is better to have a uniform distribution at the average temperature than to have high-temperature peaks and low-temperature troughs. A technique called flue gas recirculation can also be used, in which a small proportion of the flue gases (which are inert because their oxygen has been used up) are fed back to dilute the air–

FOR REFERENCE PURPOSES ONLY

fuel mixture before combustion and reduce the intensity of the flame.

Air–fuel ratio: Fuel NO can be reduced by making the combustion fuel-rich (i.e. by reducing the air–fuel ratio). However, this also reduces the thermal efficiency, which is of paramount importance to large-scale users such as electricity generators, and means that more fuel has to be burnt. Hence it is not widely used.

Low-NO_x burners: This technique mainly aims to prevent NO_x formation through modification of the combustion process. It is achieved through *two-stage combustion* where part of the combustion air is mixed with the fuel and burnt in the first stage. In the second stage the remaining air is used to complete the combustion. This way, the maximum combustion temperature is lowered as the maximum temperature is reached when all the oxygen is used up in the first stage, thereby alleviating NO formation. This approach is considered cheap and is therefore more commonly used. N is still released from the fuel, but under reducing conditions so that it forms N_2 rather than NO. These burners can be retrofitted to existing plants and have the potential to reduce fuel-NO by 40%. The EC Large Combustion Plants (LCP) Directive (88/609) specifies emission limits for new plants and a revised EC LCP Directive (2001/80) for NO_x emissions came into force in 2008. This is covered in more detail in Chapter 14.

Flue gas denitrification: Conventional coal and oil-fired power stations may be used in areas with tight NO_x emission limits. Also, nitrogen-rich fuels such as sewage, refuse, some heating oils and waste wood can generate high NO_x emissions. For such emissions, two types of flue gas denitrification (De-NO_x) system are in use, both involving reduction of NO_x in the gas phase with ammonia, yielding the natural air gases nitrogen and water vapour:

$$4NH_3 + 4NO + O_2 \rightarrow 4N_2 + 6H_2O$$

The first, used at lower nitrogen loads, operates without a catalyst at temperatures of 850°C–1000°C. Hence, it is called selective non-catalytic reduction (SNCR). Ammonia or urea is injected into the flue gas at the combustion chamber outlet. SNCR involves simple installation and can provide up to 85% NO_x removal. The second, called selective catalytic reduction (SCR), again involves the injection of ammonia or urea, but this time at lower temperatures (250°C–350°C) in the presence of a catalyst such as vanadium pentoxide or titanium dioxide. NO_x removal in this process is higher still, up to 90%, without increased consumption of the reducing agent. However, this process is expensive; there may be up to 5 ppm of ammonia slip, which in turn can be controlled with transition metal ions in the catalyst washcoat. The selective catalytic converter is upstream of any dust removal equipment, so the operating conditions for such a catalyst are poor, with very high dust loadings and acid gas concentrations, and the pore structure can get blocked with sulphates and fly ash. Partial regeneration may be possible by soot blowing.

As previously mentioned, NO_x is the sum of NO and NO_2. The latter, known as *primary*

NO_2, is mainly released from vehicle sources and disproportionately affects ambient NO_2 concentrations near to roads, but thus far these emissions are not regulated as part of lab-based official emission tests. It is noteworthy, systems designed to reduce the emissions of fine particles (e.g. diesel particulate filter [DPF]) and total NO_x (e.g. SNCR) can dramatically increase primary NO_2 emissions. As a consequence, ambient NO_2 concentrations may not be effectively reduced in line with a reduction achieved in NO_x emissions from these control measures.

Non-combustion NO_x released from industrial sources (such as nitric acid plant) can be mitigated through chemical treatment, such as scrubbing with solutions of NaOH and $KMnO_4$. Here $KMnO_4$ is used as an oxidising agent to convert NO to NO_2 which is then captured by alkaline NaOH. This technique is not suitable for large combustion sources as it involves expensive electrochemical regeneration of $KMnO_4$.

9.1.4 Abatement of particulate matter

There are many competing techniques for control of particle emissions. Primary particles (such as asbestos and heavy metals) are generally larger than secondary particles, thereby enabling their effective abatement through mechanical controls. They all have one common principle – the application of a force to cause the deposition of particles to a receiving surface. The techniques can be classified into sedimentation, filtration, centrifugation, washing and electrostatic precipitation. Each of these methods is worth a book in itself, and only the barest details will be given here.

All particle collectors have a collection efficiency $E(D_p)$, for particles of diameter D_p, given by:

$$E(D_p) = 1 - \left[\frac{\text{Concentration of particles of diameter } D_p \text{ in the exhaust gas}}{\text{Concentration of particles of diameter } D_p \text{ in the inlet gas}} \right]$$

The term in square brackets is also known as the particle penetration. For most collectors, the efficiency decreases as the diameter decreases. Hence the particle diameter for which the efficiency is 0.5, called the cut diameter, is often used to parameterise and compare collector efficiencies. Any collector also has an overall efficiency E for a given inlet particle diameter distribution, but if the process that is producing the particles changes, then the diameter distribution and overall efficiency may change too. Schematic diagrams of the different types of collector, except for settling chambers, are given in Figure 9.3. These collecting devices are discussed in more detail in the following sections.

FOR REFERENCE PURPOSES ONLY

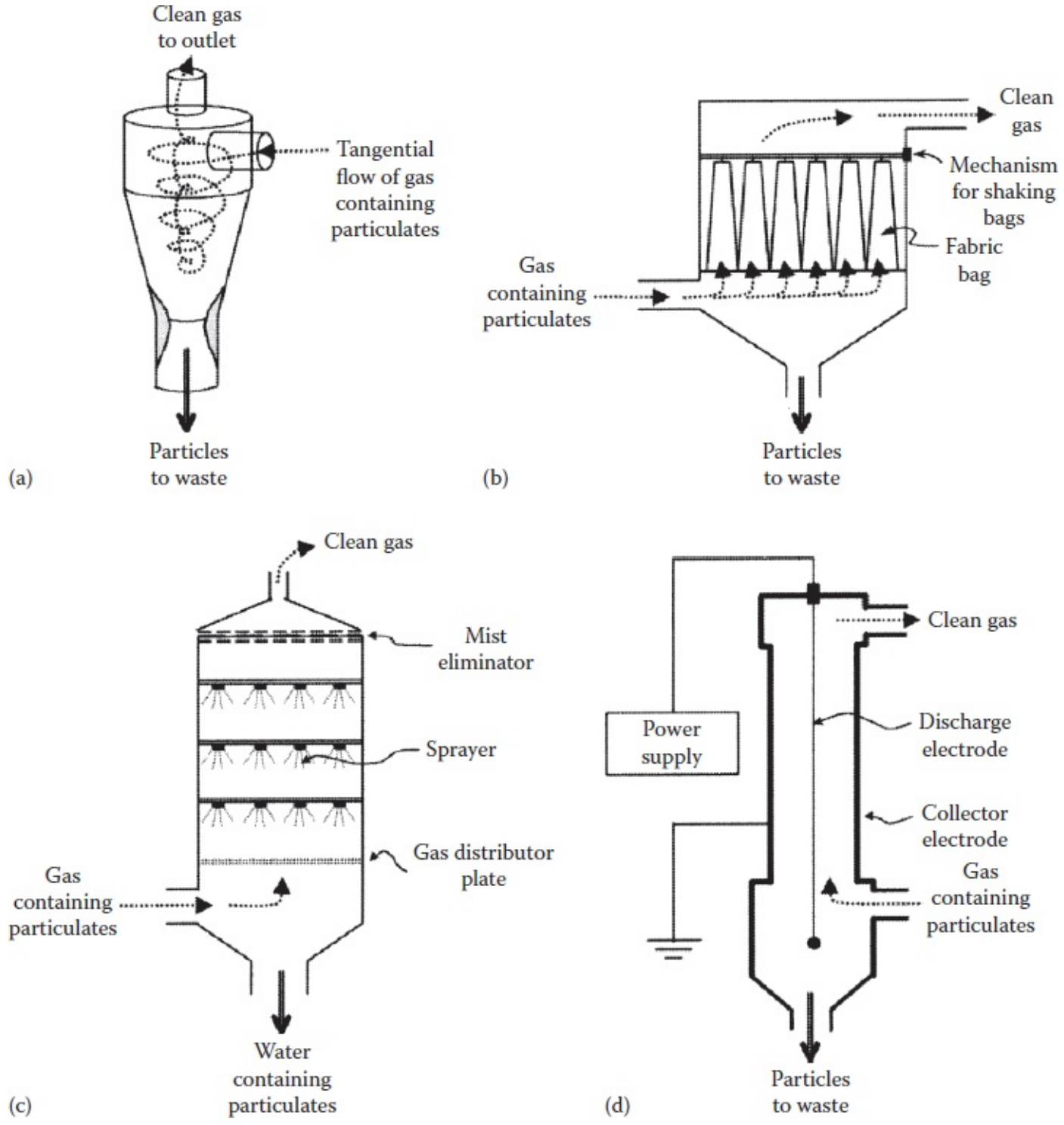

Figure 9.3 Schematic diagrams of different particle collectors: (a) cyclone, (b) filter, (c) spray tower and (d) precipitator. (From van Loon, G.W. and Duffy, S.J., *Environmental Chemistry – A Global Perspective*, Oxford University Press, Oxford, UK, 2000.)

9.1.4.1 Sedimentation

The gas is passed horizontally through a large-volume chamber, so that the average speed is

FOR REFERENCE PURPOSES ONLY

low and the residence time long. Particles which are large enough (typically > 20 μm) to sediment under gravity fall directly into hoppers:

$$E(D_p) = 1 - \exp\left[-\frac{u_t(D_p)\,L}{u\,H}\right]$$

where:

$u_t(D_p)$ is the terminal speed of particles of diameter D_p in still air
u is the horizontal gas speed through the settling chamber
L and H are the length and depth respectively of the chamber

For laminar flow, the terminal speed is given by:

$$u_t = \frac{\rho_p g D_p^2 C_C}{18\eta}$$

where:

ρ_p is the particle density
g is the acceleration due to gravity
μ is the dynamic viscosity of the gas

Hence:

$$E(D_p) = 1 - \exp\left[-\frac{g\rho_p L D_p^2}{18\mu u H}\right]$$

9.1.4.2 Centrifugation

For particles less than 20 μm diameter, gravitational force is not strong enough to deposit them within a practical time. The force can be multiplied by passing the air through a cyclone; a spiral path within a cone generates centripetal force and moves the particles to the wall of the cone, where they slide down to the vertex. The cleaned air leaves the cyclone from the central core to the cone (Figure 9.3a). Cyclones are cheap, reliable and straightforward gas-cleaning devices with a wide range of applications. They are not only used for air pollution control, they are also useful for process control (e.g. capture and return of entrained fluidised-bed materials), as pre-cleaners for other air pollution control equipment, and as separators for liquid droplets after a wet scrubber or similar. High-efficiency cyclones offer an efficiency of over 90% for aerodynamic diameters of larger than 2 μm. The simplest theoretical model, which assumes that the flow within the cyclone is everywhere laminar, gives:

$$D_{50} = \left[\frac{9\mu W}{2\pi N_e \rho_p V_g}\right]^{\frac{1}{2}}$$

where:

W is the width of entry duct

N_e is the effective number of turns of gas on spiral path

V_g is the gas velocity at entry

More sophisticated models allow for turbulent flow within the cyclone and the finite depth of the boundary layer at the walls. Although cyclones could in principle be used for removing particles less than 2 μm, the high velocities required to generate the centripetal forces increase the pressure drop across the cyclone, which in turn increases the energy used and operating cost.

9.1.4.3 Filtration

Based on their operational characteristics particulate filters (both natural and human-made) can be broadly classified into the following three categories – surface, cake or depth (Figure 9.4). The occurrence of these three characteristics, acting either in isolation or in combination, defines the filtration efficiency and the frequency of filter replacements. Fabric filters – known as baghouses in the United States – work just like domestic vacuum cleaners. The particle-laden air is drawn through a permeable, tortuous path through fibres which results in the deposition of the particles. The collection mechanisms for filters include sieving, impaction, interception and diffusion.

As a layer of particles builds up, the collected particles themselves act as the deposition sites for new particles. The accumulating layer also increases the pressure drop required to draw the air through, which reduces the gas flow rate. In the most basic systems, such as those used in heating ventilation and air-conditioning (HVAC), the used filter is disposed of and a new one fitted. On industrial systems (Figure 9.3b), the flow is stopped intermittently and the layer of particles shaken or blown off into hoppers. The three main media types that are used for industrial gas cleaning are needle-punched felt, woven synthetic or cotton, and filter paper. Fabric filters offer the highest efficiency for collection of small particles, and the efficiency increases as diameter decreases. Efficiencies of 99.9% at 0.1 μm are commonly reported.

FOR REFERENCE PURPOSES ONLY

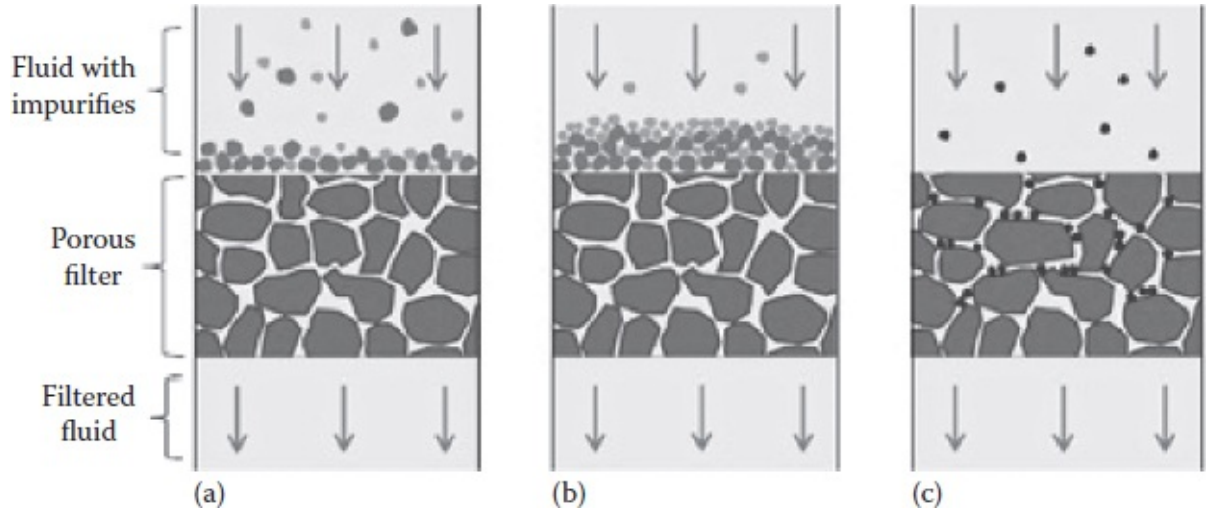

Figure 9.4 Schematic showing the three filtration modes: (a) surface filtration (captures particles at the entrance of the filter due to size exclusion), (b) cake filtration (additional filtration from built-up impurities on the upstream surface) and (c) depth filtration (impurities move into and get deposited on the pore structure). (From Hammel, E.C. et al., *Ceram. Int.*, 40, 15351–15370, 2014.)

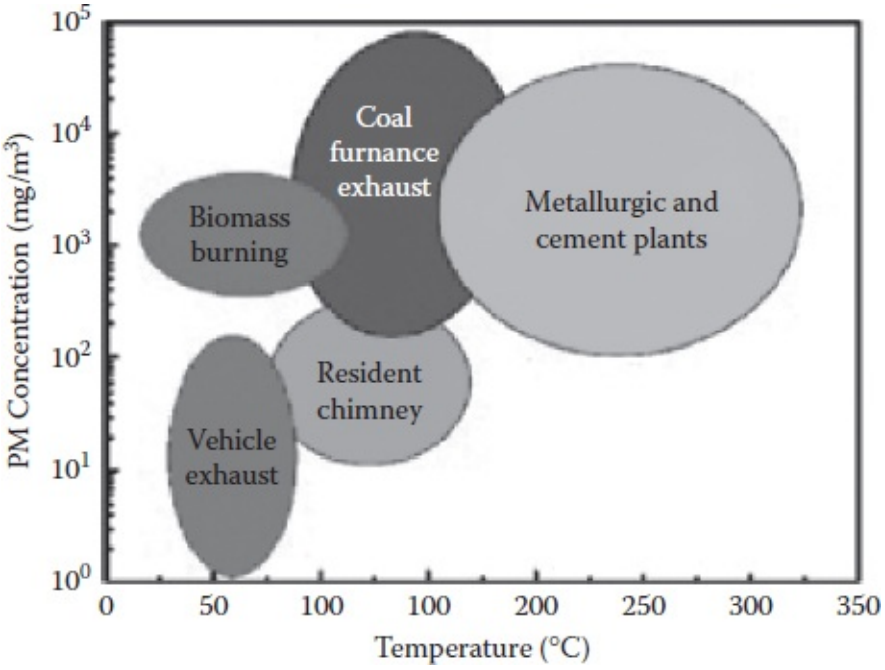

Figure 9.5 Temperature and PM concentration distribution of various high temperature PM sources. (Reprinted with permission from Zhang, R. et al., *Nano Lett.*, 16, 3642–3649, 2016. Copyright 2016 American Chemical Society.)

High-temperature dust removal from exhaust gas has recently attracted more attention. High-performance granular ceramic filters using silicon carbide (SiC) have been extensively used to remove particulate matter from hot flue gas due to its high filtration

FOR REFERENCE PURPOSES ONLY

efficiency and high thermal durability. Under such high-temperature corrosive conditions, the physical properties and filtration performance due to SiC powder size have been evaluated in terms of a filter performance factor, as a product of the conventional filter quality factor (ratio of collection efficiency and pressure drop) and its maximum mechanical strength (Choi et al., 2014). It suggests the choice of proper powder size crucial to its efficiency – intermediate grain sizes outperforming the extremes. This is largely due to their impact on morphology, physical characteristics, and filtration performance in terms of collection efficiency and pressure drop. As shown in Chapter 3, the total collection efficiency, E, of a granular filter is an exponential function of the physical properties, namely, filter thickness (L), powder size (d_c), porosity (s) and total single collector efficiency (η_T) (Kuo et al., 2010). Here, η_T is the sum of collection efficiencies by a combination of individual collections mechanisms, that is, diffusion, inertial impaction, interception and gravitational. Figure 9.5 shows the temperature profile of PM originating from a range of industrial and combustion applications with a clear indication of high-temperature metal and soot arising from large activities, such as metallurgic and cement plants, coal furnace and residential combustion sources.

9.1.4.4 Washing

Water droplets can be used to collect particles. The droplets are sprayed into the gas stream so that there are high relative speeds between the particles and the droplets and the impaction efficiency is high. The droplets themselves are relatively large (e.g. number distribution mode at 50 μm) and are therefore easy to collect.

The smaller the particles, the smaller the droplets and the higher the relative speeds required. In the most common design, the dirty gas, containing water droplets and particles, flows through a contraction or venturi (Figure 9.3c). As the gas flow accelerates, the particles go with it due to their small inertia, but the larger droplets lag behind. Hence the particles collide with the droplets. As with other processes based on impaction, the particle collection efficiency decreases with particle diameter. Downstream of the venturi, the gas and particles slow down faster than the droplets, so the collision process continues. A cyclone separator will usually follow immediately after the venturi. Wet scrubbing is typically used to collect sticky emissions not suitable for dry systems, to recover water-soluble dusts and powders, or to collect both particles and gases simultaneously. The pressure drop through the system, which is an important parameter in the calculation of operating costs, can be derived from formulas. No such simple relationships exist for collection efficiency because of the wide variety of droplet dispersion designs in use. A collection efficiency of 0.99 can be achieved for 1 μm particles through a pressure drop of 20 kPa.

9.1.4.5 Electrostatic precipitation

FOR REFERENCE PURPOSES ONLY

The electrostatic precipitator (ESP) is widely used for collecting emissions from certain process industries – notably coal-fired power plants, cement kilns, pulp and paper mills, steel mills and incinerators. The ESP casing (Figure 9.3d) has a large cross-sectional area to slow the gas down (0.9–1.7 m s^{-1}), establish laminar flow and give a long residence time. Within the casing, the gas flows between vertical parallel plates which are the positive electrodes. Sandwiched in alternate layers between the plates are vertical frames carrying wires, the negative electrodes, which are maintained at 20–100 kV. Uniform distribution of velocities over the cross-section is important, as collection efficiency depends on residence time.

During its passage between the plates, the corona discharge between the electrodes imparts net negative charges to the particles, which then migrate to the positive plates under the influence of the electrostatic field. When a layer of particles has accumulated on the plates, it is knocked off (rapped) into collecting hoppers. The detailed theory of operation is very complex, involving the corona current, attachment of ions to particles of different diameters and electrical properties, and movement of the charged particles at their terminal speeds to the collecting plate. These processes can be summarised in the Deutsch equation, by which:

$$E = 1 - exp(-w_e\ SCA)$$

where w_e is the effective migration speed for the particle population (i.e. the mean terminal speed). This varies from 0.01 to 0.2 m s^{-1} depending on the material and the conditions. The variable w_e is not a measurable speed but a factor used to parameterise an ensemble of particle properties, such as diameter distribution and resistivity, appropriate to a process such as steel-making. *SCA* is the specific collection area (plate area per unit volume flow rate). This is typically in the range 20–200 s m^{-1}.

There are several persistent problems with achieving high collection efficiencies. Dusts with high electrical resistivity ($>2 \times 10^{11}$ ohm-cm) are slow to take on a charge as they pass through the ESP. The ESP therefore has to be longer. Such particles are also slow to discharge when they reach the positive electrode plates, so they adhere under electrostatic forces and build up an insulating layer on the plates, which generates back corona and reduces current flow. Dusts with resistivity $<10^8$ ohm-cm, on the other hand, are not held onto the plates and can be easily re-entrained into the gas stream. Resistivity can vary greatly with operating conditions such as temperature, so stable process control is a major factor in attaining consistent collection efficiency. Physical design constraints mean that some particles can pass through the precipitator without being charged. The rapping process itself ejects particles back into the gas flow, and if this occurs near the discharge, then there is little chance to recapture the particles. Efficiencies of commercial large-scale precipitators tend to be a minimum of about 0.95 at around 0.5 μm, and to increase for both larger and smaller particles.

FOR REFERENCE PURPOSES ONLY

9.1.4.6 Comparison of efficiencies

To some extent, the overall particle collection efficiencies of any of these control devices can be increased to whatever level is required. Nevertheless, the different methods have certain common characteristics – baghouses offer high collection efficiencies but need high pressure drops, electrostatic precipitators have large volumes, cyclones have reasonably low pressure drops but cannot deliver high efficiencies for submicrometre particles. These characteristic collection efficiencies are illustrated in Figure 9.6. Figure 9.7 emphasises in a different way that each of the particle collection devices has a *natural* size range within which it works with the best combination of installation and operational costs.

9.1.5 Abatement of volatile organic compounds

The potential for reduction of volatile organic compound (VOC) emissions falls into two categories – mobile and stationary sources. Mobile sources are discussed in Chapter 5. In the UK, many stationary processes are prescribed under the Environmental Protection Act of 1990, and emissions from these will fall steadily as the legislation comes into effect. Many of the emissions are from small-scale operations that are hard to control – for example, surface cleaning is performed by dipping parts into open tanks of solvent. There are estimated to be 150,000–200,000 sites in the EU at which solvent degreasing is carried out in the metals and electro-technical industrial sectors.

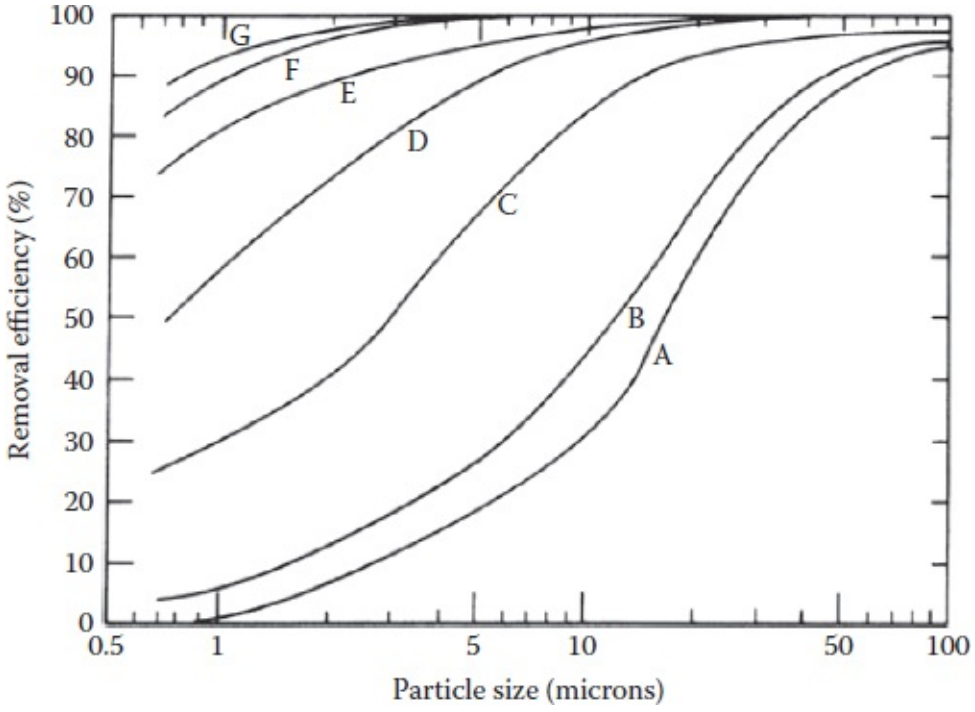

Figure 9.6 Collection efficiencies of different control devices: (a) baffled settling chamber, (b) simple cyclone, (c) high efficiency cyclone, (d) electrostatic precipitator, (e) spray tower, (f) venturi scrubber and (g) fabric filter. (From

FOR REFERENCE PURPOSES ONLY

Peirce, J.J. et al., *Environmental Pollution and Control*, Butterworth-Heinemann, Boston, MA, 1998.)

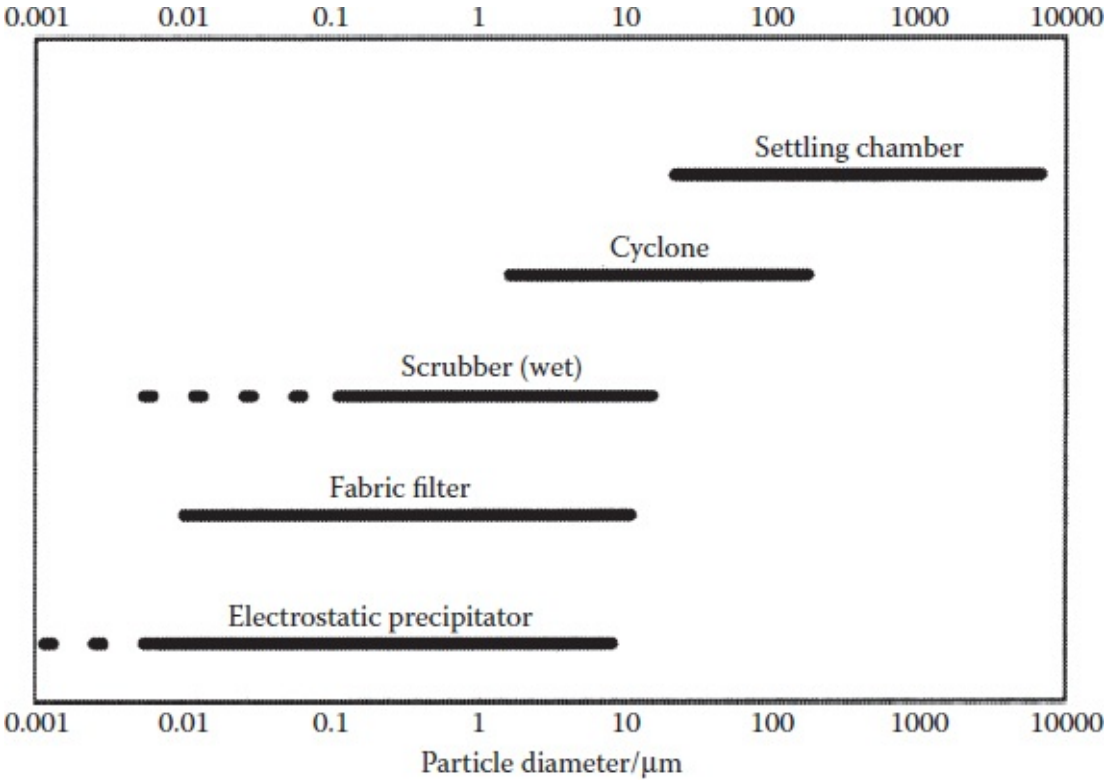

Figure 9.7 Optimum particle size ranges of different collecting devices. (From van Loon, G.W. and Duffy, S.J., *Environmental Chemistry – A Global Perspective*, Oxford University Press, Oxford, UK, 2000.)

These are the methods for industrial VOC control:

Condensation: The gas stream is cooled to a temperature at which the partial pressure of the required VOC component exceeds its dew point, so that it condenses out as a liquid. The procedure is most effective for compounds with high boiling points. If the gas stream also contains compounds that solidify at the reduced temperature, they block the condenser.

Adsorption: The VOC is adsorbed onto a material such as activated carbon which has a large surface area per unit volume. When the adsorber is saturated, the VOCs are stripped off by steam, which is in turn condensed.

Absorption: In absorbers, or scrubbers, the gas stream is put in intimate contact with an absorbing solution by means of spraying the liquid through the gas or bubbling the gas through the liquid. The solution absorbs gas until the concentration is in equilibrium under Henry's law.

Thermal and catalytic incineration: These processes are discussed in detail in the following.

Flaring: The organic stream is burned in an open flame. With proper design the flame stability is insensitive to gas flow rate, so that wide variations (1000:1) can be handled. This makes the method useful in plant start-up or shut-down situations, or in an emergency when a process stream has to be dumped.

Biological treatment: Microorganisms are used to break down the large organic molecules, using some of them as their energy supply. The method can have high efficiency for dilute gas streams and is most effective on alcohols, ethers, aldehydes and ketones.

9.1.5.1 Use of catalysts

A catalyst is a material that increases the rate of a chemical reaction by lowering the activation energy for a particular step in the reaction sequence; the catalyst does not itself get changed in the reaction. The reaction products can be controlled by choice of catalyst – for example, platinum catalyses the full oxidation of ethylene to carbon dioxide and water, whereas vanadium catalyses partial oxidation to aldehyde. Catalytic control of air pollutants has been given a prime role in the reduction of motor vehicle emissions; there are also many industrial process emissions that can be reduced by catalytic conversion. The effectiveness of catalytic reactions partially depends on access by the reactants to the catalytic sites. Hence, catalysts are usually presented as a coating on a porous support matrix having large surface area.

Common matrix materials, such as Al_2O_3, SiO_2 and TiO_2, are applied as a washcoat to an inert mechanical substrate. This washcoat is precipitated from solution and then heat-treated to form a network of 2–5 μm particles interlaced with pores 1–10 μm across. Such a washcoat can have a surface area as high as 200 $m^2\ g^{-1}$. Choice of washcoat may be critical for particular gases – for example, alumina reacts with sulphur dioxide and is unsuitable for catalysing sulphurous exhaust gases. The washcoat is then impregnated with the catalyst by soaking it in a solution containing a salt such as $Pt(NH_3)^{+2}$. The exhaust gases to be treated could be passed directly through the catalysed washcoat. However, at high flow rates this generates high pressure drops and hence energy costs (or equivalently, a loss of power). To reduce the pressure drop, the washcoat is applied to an inert ceramic monolith having a honeycomb structure of 50–60 channels cm^{-2}, each channel being 1–2 mm across and giving a surface area density of 0.3 $m^2\ g^{-1}$. Temperature is another important factor. Catalysis of relatively cold gases is limited by the chemical reaction rates at the catalyst sites, while for hot gases the rate-limiting process is diffusion of reactant and product molecules to and from the sites.

Process VOC emissions can be controlled by commercially available thermal or catalytic oxidisers. With thermal oxidisers, the incoming contaminated air is preheated in a heat exchanger before passage through a burner section. In the burner section, the air is heated to around 800°C in the presence of excess oxygen, oxidising the VOCs to CO_2 and water. The

hot gases leave through a heat exchanger which preheats the inlet gases and increases energy efficiency. The heat exchanger may be either continuous (recuperative) or cyclical (regenerative). With catalytic oxidisers, a thin-walled honeycomb lattice is coated with a washcoat to provide high surface area and then impregnated with a fine dispersion of platinum-group metals. A range of catalysts is available to cover methane, ethane, propane and other VOCs. Inlet concentrations are typically a few hundred ppm.

The catalytic converters operate at lower temperatures of 150°C–350°C, so they have lower energy requirements, although again much of the energy expenditure can be recovered with an efficient heat exchanger. Choice of system is influenced by factors such as expected working life, inlet gas composition and temperature, and process intermittency. With either type of system, VOC destruction efficiencies up to 99% can be achieved.

An interesting application of catalytic control is for ozone in the cabins of high-altitude jets. The current World Health Organisation (WHO) guideline for personal exposure to ozone is 0.1 ppm. During very high pollution episodes in Los Angeles, California, the concentration has risen to 0.6 ppm. Yet long-haul passenger aircraft routinely fly at altitudes at which the ozone concentration is several ppm. Although this air is very thin, if it is compressed for use as the source air for cabin air conditioning, the ozone content could be unacceptably high. Ozone abaters based on a palladium catalyst are carried aboard such aircraft.

9.1.5.2 Incineration

VOCs and many other substances such as halogenated compounds, dioxins and furans, and N- or S-containing materials can also be treated by incineration, which effectively uses the waste gas as the air supply to a high-temperature burner. Temperatures of 700°C–1200°C are reached, with lower temperatures resulting in higher CO emissions and higher temperatures resulting in higher NO_x emissions. In a typical example from the chemical industry, a waste gas stream is treated for the removal of acetone, isopropanol, toluene, cresole, ethanol, acetic acid, dichlorobenzol, methyl bromide, epoxy propane, methanol, acrylonitrile and dimethyl ether. Quite a soup!

For either incinerators or oxidisers, where the process gas stream involves a large flow at a relatively low concentration, a concentrator can be used as a pre-treatment. A concentrator consists of a large wheel coated in an absorbent such as zeolite (e.g. a sodium or potassium aluminosilicate). The wheel rotates slowly. Part of the wheel is immersed in the process gas and absorbs the pollutant. Another part is immersed in a low-volume flow of hot gas which desorbs the pollutant. Then this low-volume flow is treated in the usual way.

9.1.6 Abatement of CO

CO is produced from the partial oxidation of carbon-containing compounds when there is

not enough oxygen to produce carbon dioxide (CO_2). In the presence of oxygen, carbon monoxide burns with a blue flame, producing carbon dioxide. Examples of industrial plants that produce carbon monoxide include metals (iron, steel, non-ferrous) manufacturing, electricity supply, mining (metal ore, coal), food manufacturing, oil and gas extraction, chemical manufacturing, cement lime, plaster and concrete manufacturing and petroleum refining.

Regenerative thermal oxidizers (RTOs) and *catalytic thermal oxidizers* (CTOs) are combustion systems that control CO emissions by combusting them to CO_2 and water. The design of the system depends on the pollutant concentration in the waste gas stream, type of pollutant, presence of other gases, level of oxygen, stability of processes vented to the system, and degree of control required. Important design factors include temperature (a temperature high enough to ignite the organic constituents in the waste gas stream), residence time (sufficient time for the combustion reaction to occur), turbulence or mixing of combustion air with the waste gas. RTOs are capable of combusting up to 98.5% of CO, depending on chamber design. Despite the high destruction efficiency potential within the combustion chamber, any leakage across the inlet or outlet valves may limit the ultimate performance of the systems. Consideration should be given to the required control efficiency and alternate methods of valve arrangement (such as in-series), or with a positive air seal should higher destruction efficiencies be required. Consideration must also be given to performance decline of the valve seal over its lifetime. Systems should be maintained on a semi-annual basis, during which valve seals should be observed for any possible leaks.

9.2 AMBIENT AIR POLLUTION CONTROL

9.2.1 Role of civic regeneration and retrofitting

Adequate air pollution mitigation explores *ideal acceptable alternatives*, largely focusing on human exposure reduction to regulated pollutants. For example, as distance from a pollution source is an important factor in reducing exposure, plausible mitigation measures include reconfiguring the layout of civic infrastructures, such as car parks and access roads; screening of residential areas, schools and playing fields from traffic sources using vegetation filter strips (described in a later section); and so on. With regards to indoor air pollution, alternative ventilation system, which draws less polluted air into the buildings, or use of a filtration system to remove pollutants can be considered. There is a growing awareness about the trade-off from initial investment in improving air quality in terms of the health benefits accrued over a longer term, especially reducing exposure for more vulnerable population, including elderly and children. In the UK, air quality impacts at schools located in pollution hot spots have been specifically raised as a concern in the Environmental Audit Committee Action on Air Quality report (2014).

FOR REFERENCE PURPOSES ONLY

9.2.2 Low-emission zones

In order to reduce exposure to traffic emissions, Low Emission Zone (LEZ) has been in operation in London since 2008, requiring higher European standard engines to run on the roads, or installation of retrofit technology to the existing vehicles to comply with the stringent emissions regime. In 2019, emissions from road vehicles will be further reduced in London through the introduction of the Ultra-Low Emission Zone (ULEZ). A low emission zone for non-road mobile machinery (NRMM) (Chapter 5) was introduced through the introduction of 'Cleaner Machinery for London' in September 2015, making London the first city in the world to introduce a dedicated scheme for regulating off-road vehicle emissions. London has also established a Low Emission Construction Partnership, which is conducting a study to characterize NRMM diesel emissions using a portable emissions measurement system (PEMS), mainly focusing on diesel generators which are commonly used as off-grid power source during construction projects. Unlike other heavy equipment, the generators are often left running overnight, resulting in large emissions of NO_x, PM_{10} and hydrocarbons.

More recently, there is increased emphasis on Clean Air Zones in many UK cities, primarily targeted at reducing the NO_x concentrations. As of 2017, the government has identified five Clean Air Zones (and a ULEZ in London); however, over 60% of the UK Local Authorities have one or more Air Quality Management Areas (AQMAs). Typical urban journeys, marked with stop-start low-average speed trips, are well-suited for the electric vehicles, specifically buses in the city and residential suburbs.

On the other hand, since 2016 UK highway infrastructure has initiated several *smart motorways* which essentially use active traffic management techniques to increase capacity by using variable speed limits and use of hard shoulders at busy times. Such initiatives, while meant to adequately manage traffic congestion on highways during peak hours, can aggravate potential air pollution from increased traffic volumes running at high speeds. For example, a study from the UK Highways Agency (2014) predicts smart motorways operating with a 70-mile-per-hour speed limit generate significant air quality impacts, potentially breaching the EU limit values. Proposed mitigation to address this issue includes reducing the speed limit on such motorways to 60 miles per hour during the normal operating hours (deemed to be considered the first UK pollution-linked speed limit). Mitigation of air quality through control of traffic speed has even been endorsed by the UK's National Institute of Health and Care Excellence (NICE). The NICE draft guidance on outdoor air quality and health (2016), proposes recommendations to avoid acceleration and deceleration on roads, specifically through 'use of variable speed limits and average speed technology on the roadside to promote a smoother driving style'. As shown in Chapter 5, air quality can be significantly improved, mainly for NO_x emissions, if more vehicles are subjected to a cruising speed between 30 and 60 miles per hour for a greater proportion of the time.

Other passive measures for air pollution mitigation from road sources include coating

barriers and pavements with catalytic paints and putting out piles of *mineral polymer* as absorbents. A key report by the UK Department for Environmental Food and Rural Affairs Air Quality Expert Group (2016) concluded that, under laboratory conditions, photolytic surfaces are effective at reducing concentrations of traffic-related NO_2. However, such coatings have not been demonstrated to effectively mitigate large volumes of air pollutants due to the sheer difference in scale between the coated surface area and the ambient nature of air pollution. The laboratory findings identified a risk of these materials to produce other chemical compounds, further aggravating lateral health issues. Therefore, such initiatives require more prudence while being considered part of an air pollutant mitigation strategy, as they are still in their infancy and not fully proven on their foolproof effectiveness.

There is also a lobby group calling for an entirely new approach to controlling air pollution in the UK by introducing a new duty for Local Authorities rather than focusing on pollution hot spots in order to reduce public exposure to air pollution, specifically to the vulnerable groups, such as children and older people. Such initiatives include:

- Introducing fiscal incentives to clean up polluting air, to phase out the most polluting vehicles and other pollution sources
- Incentivising the adoption of sustainable transport infrastructure, such as cycling and walking infrastructure
- Planning framework and guidance to include a duty to reduce pollution
- Promoting public information about pollution by mass communication social media, alerting people to avoid pollution hot spots
- Inculcating a *pollution busting* attitude, through significant public engagement to encourage attitudinal change, behavioural change and adaptation to minimize the health impacts of pollution

9.2.3 Removal of precursors

With deeper understanding of the systems-scale interactions and disintegration of air pollutants over different spatio-temporal scales, more emphasis is now placed on minimising the potential formation of secondary pollutants by alleviating the constituent source emissions. The techniques involved can be quite complex and have co-benefits for controlling more than one secondary pollutant, as shown in the following.

9.2.3.1 Mitigation of tropospheric ozone

As mentioned in Chapters 2 and 12, favourable photochemical conditions with high levels of photosynthetically active radiation (PAR, see description in Section 9.4.4.2) can generate ozone in the troposphere from pollutant precursors. In principle, tropospheric ozone concentrations can be reduced by controlling the concentrations of the precursor hydrocarbons (mainly biogenic volatile organic carbons [BVOCs]) in combination and

FOR REFERENCE PURPOSES ONLY

NO_x:

- Reduce NO/NO_2 emissions from power stations (with low NO_x burners) and vehicle exhausts (with catalysts)
- Reduce VOC emissions from vehicle exhausts (with catalysts), fuel systems, solvent evaporation

However, the detailed effects of any control measure depend on the balance between the precursor gases. This topic has taken a high profile in the United States, where ozone concentrations have been an issue since the 1950s. Laboratory and modelled experiments on irradiated gas mixtures confirm the general form given in Figure 9.8 for the relationship between the VOC and NO_x concentrations that prevail in the morning rush hour and the peak ozone concentration that results in the early afternoon.

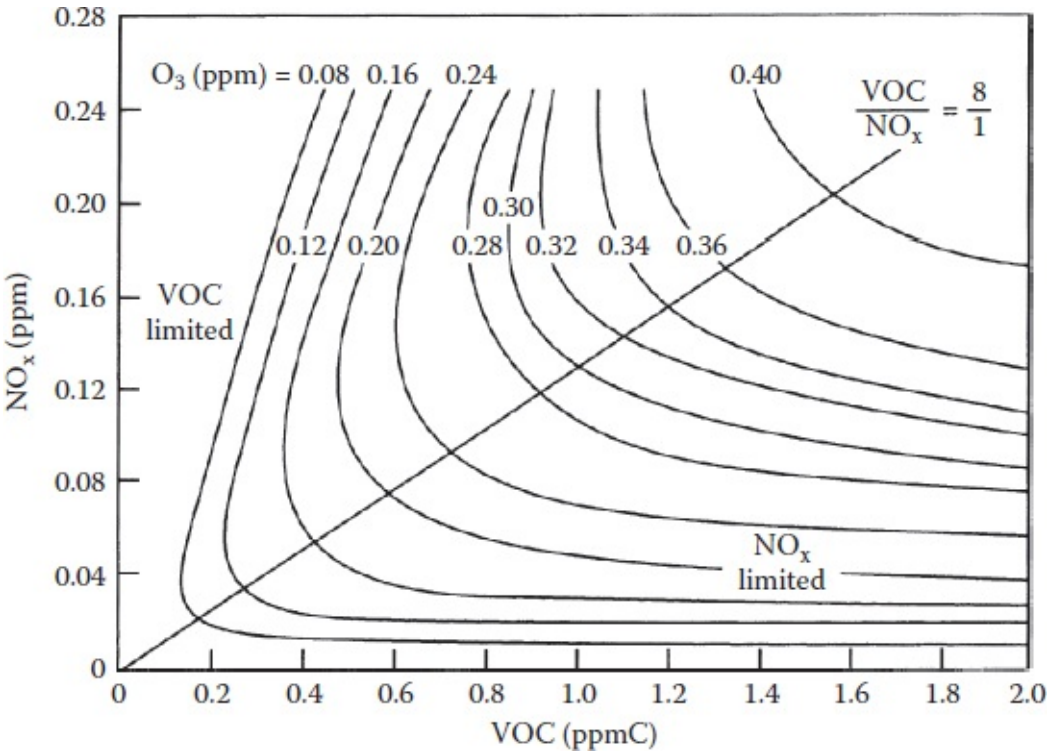

Figure 9.8 Dependence of peak O_3 concentration on the initial concentrations of VOC and NO_x. (From Finlayson-Pitts, B. J. and Pitts, J.N., *J. Air Waste Manag. Assoc.*, 43, 1091–1100, 1993.)

In the top-left part of the diagram, known as the NO_x-inhibition region, reduction of VOCs at constant NO_x reduces peak O_3 effectively. However, reduction of NO_x at constant VOC *increases* O_3. This interaction has been reported in measurements from Belgium, in which it was shown that weekend O_3 concentrations were higher than weekday ones because vehicle NO_x emissions were reduced. In the centre part of the diagram, known as the knee

FOR REFERENCE PURPOSES ONLY

region, reductions in either VOCs or NO_x reduce peak O_3. In the lower right area, known as the VOC-saturation region, O_3 formation is insensitive to VOC concentration. The critical parameter for evaluation of the effectiveness of precursor reductions is therefore the VOC:NO_x ratio, which is about 10:1 (i.e. 10 ppb carbon per 1 ppb NO_x) in the middle of the knee region.

As an air mass moves away from an urban area, photochemical reactions and meteorological processes decrease the NO_x concentration faster than that of VOC, so that the VOC:NO_x ratio increases and the chemistry tends towards the NO_x-limited case. NO_x reduction is probably the most effective precursor control in this situation. Application of these concepts to the European atmosphere gave predictions that UK O_3 concentrations would *increase* by 6 ppb if the NO_x concentration was *reduced* by 60%, while the same level of NO_x reduction in Norway would reduce O_3 by 1 ppb. Although these ideas look quite straightforward on the ozone isopleth diagram, it is a quite different matter to derive sensible control procedures, because of the complexity of the photochemical processes in an urban airmass. There is a further complication due to BVOCs, which can make up a significant proportion of the total. If, for example, the VOC:NO_x ratio falls in the knee region but the VOCs are mainly biogenic, then VOC reduction alone may be insufficient to meet target air quality standards. In California, current knowledge about the reactivity of different VOCs with OH to generate ozone has been incorporated into new legislation on vehicle exhausts (Chapter 14). Another factor which must be taken into account is the accumulation of pollutants in special meteorological circumstances. Whereas the high NO concentrations generated by urban vehicles should reduce O_3 concentrations, some Mediterranean cities such as Barcelona, Marseilles, Rome and Athens experience their highest O_3 concentrations right in the city centre. This is due to the trapping of coastal emissions in a recirculating land–sea breeze system. For example, in Athens during the summer, a special synoptic situation favours northerly winds (from the land to the sea). The weakening of these winds (Etesians) allows the development of the land–sea breeze circulation. The sea breeze stratifies the air above the city, trapping pollutants near the ground. Furthermore, the pollutants are advected out to sea and then back over the city in a daily cycle, with the concentration building up each time.

9.2.3.2 Mitigation of secondary particles

As shown in Chapter 3, the main source of secondary particles is the atmospheric oxidation of industrial emissions of SO_2 and traffic-related NO_2 by the hydroxyl radical. The other major player in secondary particle formation is the agricultural release of ammonia (NH_3). The underlying precursor chemistry for particle formation is similar to that of summertime photochemical conditions that can generate ozone in the troposphere. Therefore, formation of secondary particles under ambient conditions can be controlled by achieving reduction in release of industrial/vehicular SO_2, NO_2 (as discussed in Section 9.1) and/or in the

agricultural release of NH_3 from livestock farming and fertilisation.

9.3 INDOOR AIR POLLUTION CONTROL

As shown in Chapter 7, indoor air pollution control is vital for both residential and industrial applications: the former mainly to alleviate pollution exposure for health reasons and the latter to maintain high standards of precision manufacturing and/or cross-contamination of products with microscopic airborne pollutants. Specifically, clean room standards have been developed as benchmark for controlling indoor air pollution for industrial applications. Pollutant removal efficiency is usually determined in controlled laboratory environments, which may not be realised in practice. However, the existing data make it difficult to extract information such as clean air delivery rate (CADR; defined as the product of the single-pass removal efficiency and volumetric airflow rate through the cleaning device), which represents a common benchmark for comparing the performance of different air-cleaning technologies. To compare and select suitable indoor air-cleaning devices, a labelling system accounting for characteristics such as CADR, energy consumption, volume, harmful by-products, and life span is recommended. The majority of focus in indoor air pollution control is laid on removal of particulates (both inorganic and bioaerosols), NO_x and CO.

9.3.1 Indoor particulate removal

In the case of particulates, obtaining low concentrations requires a special branch of control technology. Specialist methods are called high-efficiency particulate air (HEPA) or ultra-low penetration air (ULPA) filtration which obtain efficiencies of 99.97% for 0.3 μm particles, and 99.999% for 0.2–0.3 μm particles, respectively. Very large airflows may also be needed in order to remove particles emitted from within the controlled volume. An M 6.5 clean room may have 30 air changes per hour (ACH, see description in Chapter 7), which can rise to 600 for an M 2.5 room.

Fan-driven air cleaners are commonly used for indoor particle removal, where the indoor air flows through a device and is returned to the indoor environment. Mechanical air filters (with activated carbon) have been shown to be effective in particle removal (higher removal efficiencies for larger particles) alongside some removal of VOCs (Bekö et al., 2008). However, they act as a pollution source if they are not properly used, and a combination of particulate filter and activated carbon has been recommended to overcome this issue. Fibre arrangement has been shown to be effective in improving HEPA filtration efficiency: the more homogeneous the better; many layers of media can give high efficiency for PM of 0.1–2.5 micron range and nanosize range of 12.6–514 nm. Plasma air cleaners (generated using corona discharge with alternating current, direct current and dielectric barrier discharge) have been reported to remove particles at high efficiency, for example, within

the range of 76%–99% (Park et al., 2008). However, these cleaners can also produce harmful by-products such as ozone and oxidation intermediates, and their energy consumption tends to be high.

Electrospun nanofibres using a range of polymeric materials have been used for removal of aerosols, such as polyamides, polyvinyl acetate, polyacrylonitrile, cellulose acetate, and so on. A recent comparison of filtration efficiency and quality factors using different nanofibrous filters using 100–300 nm particle size showed polyvinyl acetate, polyacrylonitrile filters outperforming others (Matulevicius et al., 2016). Electrospun fibres tend to overcome some of the issues identified with traditional filters as they have unique characteristics such as large surface area-to-volume ratio, low basis weight, small pore size, and relatively uniform fibre size. Specifically, because of the finer fibre size, the pressure drop around the nanofibres is much lower compared to a filter with equivalent surface area composed of micron-size fibres (Sambaer et al., 2011).

Different from the existing filters based on nonpolar polymers, the polar chemical functional groups (i.e. in polyacrylonitrile [PAN] polymer) have been reported as important to have strong binding affinity with $PM_{2.5}$ (Zhang et al., 2016). Some other recent developments on using carbon nanotubes and polymer nanofibers are notable examples toward $PM_{2.5}$ filtration; nanofibre air filter for the high efficiency $PM_{2.5}$ removal which can be used for personal and building protection.

9.3.2 Indoor NO_x removal

NO_x is mainly emitted in indoor air from fuel combustion during cooking and wood burning in winter months. Thermal NO_x is also formed during puffing of cigarettes. Portable equipment for controlling indoor NO_x comprises specially formulated gas filters which are fitted in mechanical ventilation system in homes and commercial buildings, allowing the foul air to pass through activated carbon and chemical mix.

Alternative technology called *heterogeneous photocatalytic oxidation*, which uses energy from light to activate chemical reactions to degrade indoor NO and NO_2, is also becoming common. Such approaches utilize photocatalytic wall-covering with a modified TiO_2 (carbon-doped TiO_2) on materials including paint, concrete and glass under indoor conditions. However, efficient utilization of this technique requires very high surface area-to-volume ratios, which is often not feasible in indoor environments. Overall, this technique is gripped with uncertainty in the composition of the reaction products arising from photocatalytic reactions and its resulting chemistry. Photocatalytic surfaces can reduce concentrations close to the treated surface. However, there is a risk that these materials will produce other undesirable species such as nitrous acid and formaldehyde, which can have adverse health impacts.

9.3.3 Indoor CO removal

FOR REFERENCE PURPOSES ONLY

Indoor CO air pollution is generated by incomplete oxidation of carbon fuels, typically from malfunctioning gas boilers and traditional indoor cooking practices. Because it is impossible to see, taste or smell the toxic fumes, CO can kill before even it can be detected by human senses, and is hence termed an *invisible killer*. The easiest method to control high levels of CO poisoning over a short period of time is through increased ventilation in the indoor environment. Other, more routine measures involve maintenance and regular safety testing of gas appliances and tune-up of the central heating system (furnaces, flues and chimneys), installing an exhaust fan vented to the outdoors, open flues where fireplaces are in use, use of proper fuel in kerosene heaters, and so on.

Common portable CO detectors are widely available, which use sensor technology of following four types: *opto-chemical* (uses a coloured chemical which changes colour upon reaction with CO); *biomimetic* (uses cyclodextrins, a chromophore, and a number of metal salts, which darkens in the presence of CO); *electrochemical* (CO is oxidised at one electrode to carbon dioxide while oxygen is consumed at the other electrode; its advantages over other technologies is that it has a highly accurate and linear output to carbon monoxide concentration, requires minimal power as it is operated at room temperature and has a longer life); *semiconductor* (uses thin wires of the semiconductor tin dioxide on an insulating ceramic base). For greater precision monitoring, relatively high-cost infrared radiation adsorption and electrochemical instruments are also available.

9.4 ROLE OF GREEN INFRASTRUCTURE

Green infrastructure is defined as ‘an interconnected network of natural areas and other open spaces that conserves ecosystem values and functions, sustains clean air and water, and provides a wide array of benefits to people and wildlife’ (Benedict and McMahon, 2006). Examples of types of green infrastructure found in urban areas include parks, gardens, urban forests, green roofs and walls. The concept of green infrastructure has grown in importance in recent years, attracting the attention of both decision makers and academics. For example, Target 2 of the EU biodiversity strategy states: ‘By 2020, ecosystems and their services are maintained and enhanced by establishing *green infrastructure* and restoring at least 15% of degraded ecosystems’ (EC 2001:5). A considerable number of studies have concluded through modelling that green infrastructure is beneficial to urban air quality. Meanwhile, a search of *Science Direct* articles reveals that between 2010 and 1 March 2014, 226 articles were published containing the phrase *green infrastructure* in their title, abstract or keyword list. This is a substantial increase from the 59 articles, which were published between 2000 and 2009, while 18 articles were published between 1990 and 1999. With this increasing focus, it is important to determine the effectiveness of green infrastructure at addressing environmental and social problems associated with twenty-first-century urban living.

FOR REFERENCE PURPOSES ONLY

This section focuses on the role of natural vegetation in mitigating air pollution. It provides insight into some of the fundamental aspects of numerical modelling of pollution uptake by vegetation. Applications of these modelling approaches are then demonstrated through suitable case studies. Practical concerns associated with adopting vegetation intervention for mitigating air pollution are also discussed.

9.4.1 Multi-functional greening strategy

Green infrastructure provides a variety of provisioning, regulating and cultural ecosystem services. As discussed in the following paragraphs, green infrastructure is reported to improve air quality by

- Mitigating concentrations of air pollutants such as NO_2, SO_2 and particulates (PM_{10}).
- Sequestration of carbon, thus acting as a mechanism to mitigate climate change.
- Combating the urban heat island effect resulting in lower temperatures in urban areas.

Table 9.1 provides examples of some services commonly stated in the scientific literature, although this list is by no means exhaustive.

9.4.1.1 Mitigating air pollutants

The literature concerning green infrastructure and air pollution primarily focuses on the effectiveness of vegetation in removing SO_2, NO_2 and particulate matter (PM_{10}) through the processes of dry deposition or gas transfer:

Table 9.1 Common ecosystem services provided by green infrastructure

Type of service	*Service*	*Reference*
Provisioning	Food (urban farming) Water	Escobedo et al., 2010; Natural England, 2010; Benedict and McMahon, 2006; Escobedo et al., 2010; Naumann et al., 2011
Regulating	Carbon sequestration	Escobedo et al., 2010; Naumann et al., 2011; Foster et al., 2011
	Reduce urban heat island effect/lower temperatures	Getter and Rowe, 2006; Natural England, 2010; Foster et al., 2011; Naumann et al., 2011
	Flood prevention and reduction of surface runoff	Getter and Rowe, 2006; Foster et al., 2011; Naumann et al., 2011
	Reduce air pollutants	Benedict and McMahon, 2006; Getter and Rowe, 2006; Escobedo et al., 2010; Foster et al., 2011; Naumann et al., 2011
	Pollination	Niemelä et al., 2010; Naumann et al., 2011
	Biodiversity/habitat provision	Getter and Rowe, 2006; Natural England, 2010; Foster et al., 2011; Naumann et al., 2011
Cultural/social	Recreation	Benedict and McMahon, 2006; Jim and Chen, 2008; Escobedo et al., 2010; Natural England, 2010; Naumann et al., 2011
	Cultural values (sense of place, social cohesion)	Jim and Chen, 2008; Naumann et al., 2011

FOR REFERENCE PURPOSES ONLY

Education	Kambites and Owen, 2006; Jim and Chen, 2008; Naumann et al., 2011
Improved health	Benedict and McMahon, 2006; Qureshi et al., 2010; Foster et al., 2011
Noise reduction	Getter and Rowe, 2006; Foster et al., 2011
Increased house prices	Escobedo et al., 2010; Foster et al., 2011

- During *dry deposition*, pollutants adhere to the surface of plants but they may then become re-suspended in the atmosphere, washed off by rainfall or absorbed into the plant.
- During *gas transfer*, gaseous pollutants are removed from the air permanently by entering plants through leaf stomata and reacting with compounds within the plant, a process which may result in damage to the plant itself.

The effectiveness of vegetation in performing these functions is affected by factors such as plant species, leaf area index, atmospheric conditions and time of day (i.e. levels of incoming solar radiation affecting the rates of plant gas exchanges). An estimated 711,000 tonnes of air pollutants were removed by urban trees annually in the United States, improving air quality by an average of approximately 1% (Nowak et al., 2006). Therefore, the evidence suggests that, although green infrastructure is insufficient in counteracting all urban air pollution, it is still vital in improving urban air quality. Other forms of green infrastructure, in addition to trees, are also important in reducing air pollution. For instance, green walls have been reported to reduce concentrations of NO_2 and PM_{10} by up to 40% and 60%, respectively (Pugh et al., 2012); up to 1675 kg of air pollutants were removed annually by green roofs in Chicago (Yang et al., 2008). Overall, trees are more effective than green walls and roofs in lowering NO_2, SO_2, PM_{10} and O_3 concentrations. Further, large trees have been found to be more effective at air pollutant removal than small trees; where large trees were excluded, shrub air pollutant removal was greater than that of trees (Currie and Bass, 2008).

Subsequently, some studies which investigate the effect of green infrastructure in reducing air pollution using urban data collection imply that the benefit of green infrastructure is overstated. In particular, a study in Finland investigating NO_2, PM_{10} and VOCs in cities found concentrations did not significantly differ between tree canopies and adjacent areas (Setälä et al., 2013). This could partially be due to problems with the study's methodology in that measurements from open areas were too close to the trees, suggesting air quality improvement from trees affects an area larger than the immediate vicinity of vegetation. This outcome could also be due to the country chosen for the study. Finland has relatively high levels of air quality; in 2008, Finland had the tenth lowest annual mean of PM_{10} in the world (WHO, 2011) and therefore levels of air pollutant removal are less likely to yield significant results. This is evident from a study by Escobedo and Nowak (2009) where removal of PM_{10} by trees was most significant in heavily polluted areas of the city, although other factors such as tree cover, leaf area index and proportion of evergreen leaf

area were also important.

Some studies suggest that some tree species are detrimental to air quality. For example, the presence of certain trees in urban canyons can increase levels of NO_2 in highly polluted areas by affecting air circulation, thereby reducing mixing of air between the street canyon and upper boundary layer (Pugh et al., 2012). Meanwhile, some tree species are relatively high emitters of VOCs and O_3 and so contribute to photochemical smog on a regional scale (Jim and Chen, 2008). For example, the weeping willow tree (*Salix babylonica*) can emit 134 g of ozone per tree per day while the olive tree (*Corbresus forbsii*) emits negligible volumes. However, reductions in ozone and other air pollutants facilitated by trees are generally greater than the trees' individual emissions of ozone (Escobedo et al., 2010).

9.4.1.2 Carbon sequestration

Much of the literature regarding the role of green infrastructure in carbon sequestration comprises studies which have calculated the annual carbon sequestration ability of urban trees for a city or region. These studies show that, although green infrastructure is capable of sequestering large volumes of CO_2, it is insufficient in offsetting all of a region's carbon emissions – other forms of management are required. These estimates only provide an indication rather than precise volumes of the carbon-sequestering ability of urban trees in different regions. Further, rates of carbon sequestration are found to decrease as a tree matures so young trees in urban areas could be considered beneficial. Nonetheless, rapidly growing trees tend to die at lower ages and therefore may decompose and release sequestered carbon, negating their benefit. Therefore, for the purpose of carbon storage, it may be more beneficial to protect existing forests rather than carry out tree-planting schemes.

There is a lack of literature concerning the effectiveness of other forms of green infrastructure, such as green roofs and walls, in carbon sequestration. However, a study in Michigan of a green roof system found the roof was able to sequester 375 g C/m^2 (Getter et al., 2009).

The carbon sequestration ability of vegetation varies with species. For example, broad-leaved forests have higher carbon sequestration rates than coniferous forests, while woody trees and shrubs tend to store more carbon than herbaceous plants. Conversely, grass is found to release 1.5 times the volume of carbon it sequesters annually, primarily due to mowing. Similarly, poor management of green infrastructure can result in carbon being released if, for example, a tree dies and decomposes. Nonetheless, this is relatively minor compared to the large volumes of CO_2 that green infrastructure can sequester annually.

9.4.1.3 Combat urban heat island effect

Ambient air temperature plays a key role in exacerbation of air pollution episodes, as well

FOR REFERENCE PURPOSES ONLY

as in secondary pollution formation. Vegetation can influence local air movements, thereby affecting heat exchange, a response which varies according to species. The success of green infrastructure in reducing local air temperatures is determined by a variety of factors such as size, type of vegetation, local climate, season and street orientation. For example, local air temperature reduction due to vegetation is most significant in hot, dry cities; woundwort (*Stachys*) and ivy (*Hedera*) have been found to be most successful at lowering air temperatures through green walls. It is worth noting that green roofs are not particularly effective during cold winters, suggesting green roofs may be more valuable in warmer climates. A large number of studies have concluded that, through a combination of primary and secondary data collection and modelling, green infrastructure lowers temperatures in urban environments. Of particular significance is a meta-analysis of 47 different studies on green infrastructure which concluded urban parks can lower temperatures by an average of 0.94°C (Bowler et al., 2010).

9.4.2 Designing vegetation intervention

As part of seeking a natural remedy, pollution deposition to vegetation has been of considerable interest – mainly because of its potential as a large-scale pollution sink. Leaves with complex shapes and large circumference-to-area ratios have been found to collect pollutants more efficiently, suggesting that conifers have greater efficiencies than deciduous species. Nevertheless, pollution removal by tree canopies remains a complex science with variable parameterisation of the sink term as a function of vegetation type, canopy density, terrain and meteorological conditions. In this section, canopy-level deposition is characterised in terms of simplified formulations, as described in Section 9.4.3.

In addition to the future scenarios discussed in Chapter 11, it is interesting to note that any climate change–driven environmental perturbation would also implicate the role of trees in mitigating air pollution in the following ways:

- Higher temperature and higher CO_2 concentrations could result in increased foliage biomass and surface area, thereby enhancing pollution uptake by foliar surfaces.
- Increased foliar biomass and higher daytime temperature would increase biogenic VOC (BVOC) emission rates of certain plant species (discussed later in Section 9.4.4). Although, there is an argument that this could be offset by reduced photosynthetically active radiation resulting from increased cloudiness.
- Changing concentrations of different air pollutants and water stress may accentuate large-scale BVOC emissions, which in turn would feed into the spiralling effect of enhancing tropospheric ozone and particulate pollution.
- Changes in the distribution of plant species would also affect regional BVOC emission and carbon sequestration potentials.

FOR REFERENCE PURPOSES ONLY

9.4.2.1 Canopy design

It has been noted that the vertical penetration of the depositing pollutants, mainly aerosols, through the canopy is influenced by variation in biomass, wind velocity and turbulence within the canopy. In addition, the *edge effect* due to the action of turbulent eddies generated further downwind also plays an important role in enhancing the deposition.

The UK Greater London Authority has developed the All London Green Grid – an interlinked network of new and existing green space along the River Thames. This is designed to improve local air quality, apart from fulfilling several other purposes. A recent study assessed the PM_{10} reduction potentials of a 10 × 10 km region of this site (Figure 9.9, National Grid Reference TQ 401801, 51°30′N, 0°01′E) covering an area of 547 ha (which is 5.5% of the total Green Grid). The integrated approach for estimating the PM_{10} flux potential included the following steps:

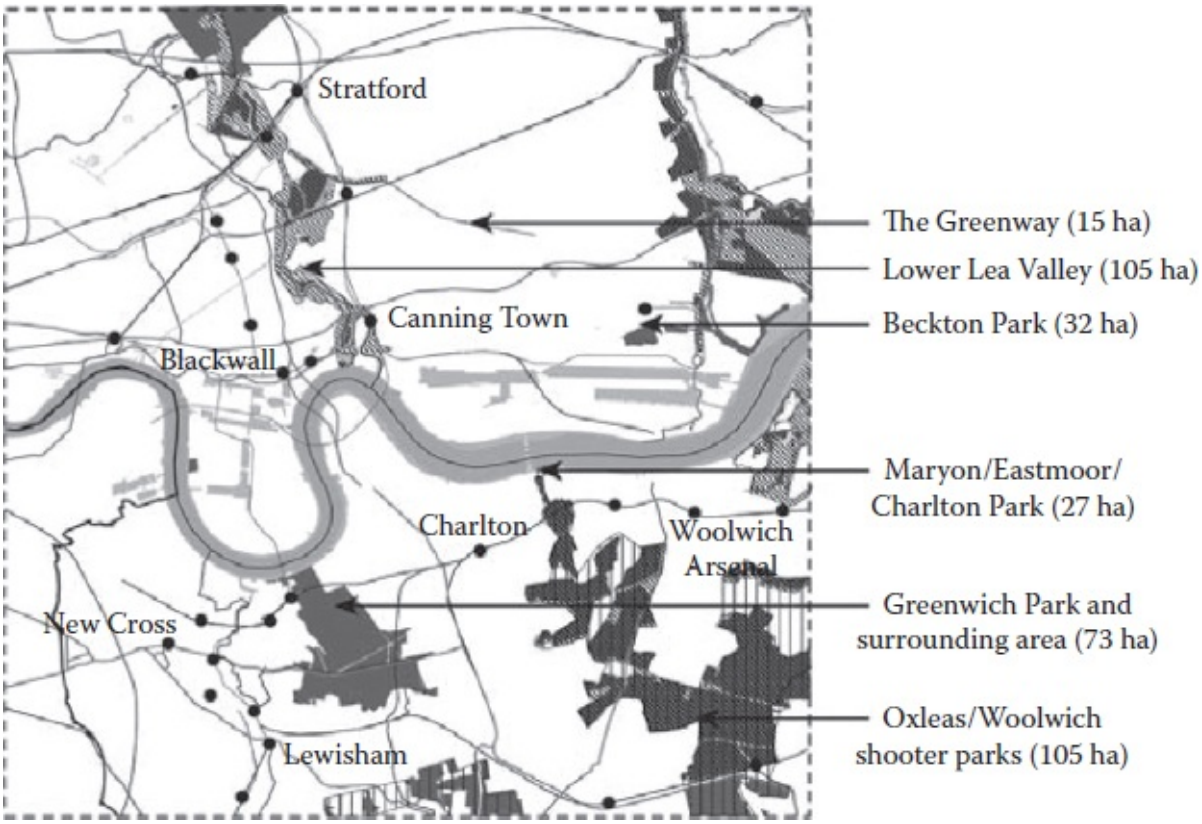

Figure 9.9 Spatial location of green space areas within the East London Green Grid used in the assessment of vegetation intervention to PM_{10} pollution. (From Tiwary, A. et al., *Environ. Pollut.*, 157, 2645–2653, 2009.)

- Set up the *status quo* pollution scenario (PM_{10} concentration) using emission and meteorological data for the site in a dedicated air dispersion modelling package.
- Estimate the PM_{10} interception/uptake for the given concentration and meteorology using a canopy PM_{10}-uptake model based on Urban Forest Effects (UFORE; as

FOR REFERENCE PURPOSES ONLY

described in Section 9.2.2).

- Model the post-intervention PM_{10} flux to vegetation canopy on a spatial scale based on the flux potential and vegetation geometry.

Using a plantation scenario representative of the UK vegetation mix, composed of 75% grassland, 20% *Acer pseudoplatanus* (sycamore) and 5% *Pseudotsuga menziesii* (Douglas fir), Figure 9.10 shows the spatial distribution of the estimated PM_{10} uptake potential (%) over the study area. It can be seen that the PM_{10} removal potential of the canopy is up to 7% in some regions. Based on this information the overall PM_{10} removal rate from the entire Green Grid is estimated to be 0.009 t ha^{-1} yr^{-1}. A separate study for Beijing has reported a much higher PM_{10} removal rate of approximately 0.025 t ha^{-1} yr^{-1} from 16.4% tree cover.

9.4.2.2 Filter strip design

Several studies have reported the influence of natural filter strips, such as windbreaks and shelterbelts, on the local pollutant microclimate – based on either field measurements, wind tunnel studies or purely numerical simulations. A wind tunnel study of a three-row shelterbelt system performed by the windbreak research group at Iowa State University in the United States quantified reductions of 35%–56% in the downwind mass transport of inorganic particles (dust and aerosols). For optimal vegetation density and wind environment this downwind reduction is estimated to reach 70%–90%. In another study, the Optimum Aerosol Technology (OAT), developed by the pesticide drift mitigation research group at the Institute of Chemical Kinetics and Combustion in Novosibirsk, Russia, showed that vegetation species such as birch leaves, pine needles, wheat grass and brome grass are efficient collectors of agricultural pesticide aerosols in the size range 1–40 μm.

FOR REFERENCE PURPOSES ONLY

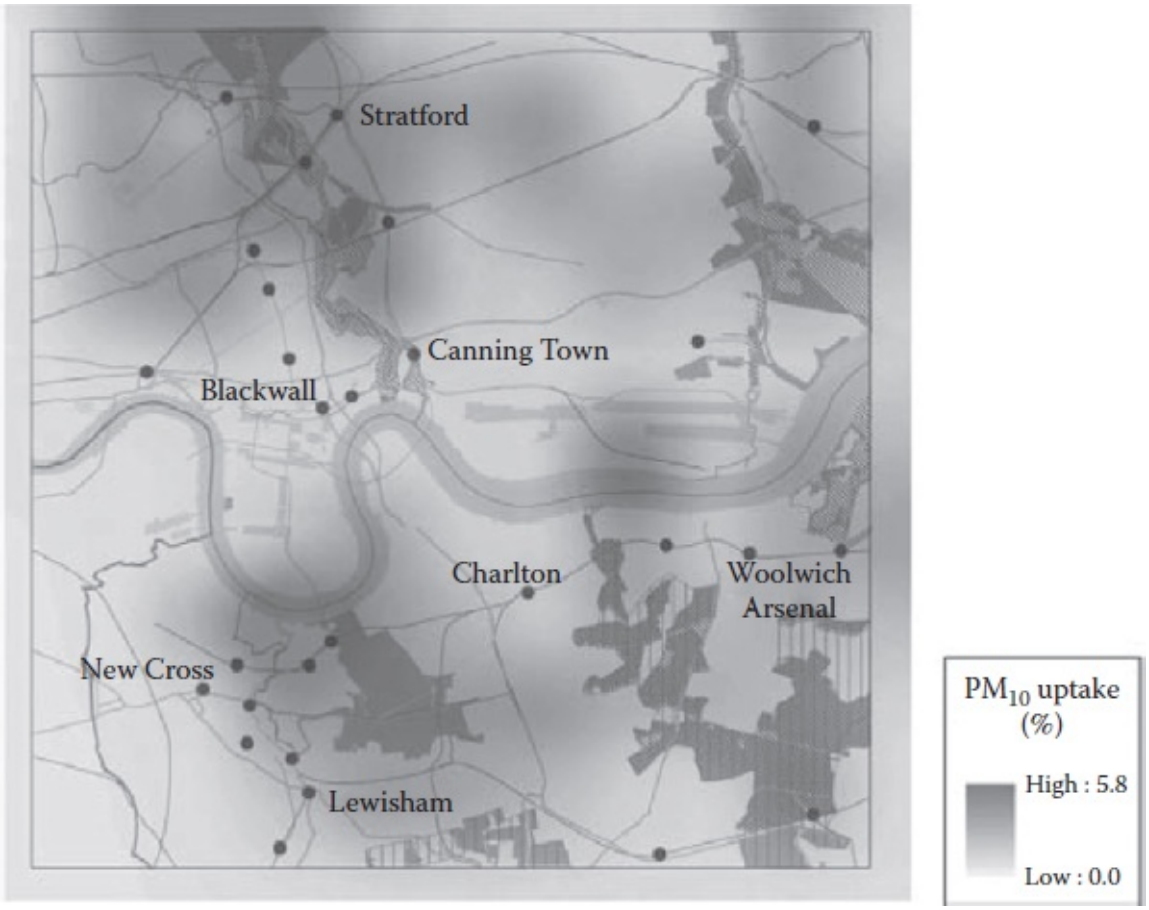

Figure 9.10 Potential reduction in PM_{10} concentrations from a plantation of 75% grassland, 20% *Acer pseudoplatanus* (sycamore) and 5% *Pseudotsuga menziesii* (Douglas fir). (From Tiwary, A. et al., *Environ. Pollut.*, 157, 2645–2653, 2009.)

The capability of porous vegetation strips to act as natural filters suggests their application as a cost-effective mitigation measure to alleviate air pollution on a regional scale. For instance, it has been found that hedgerows can be used to reduce ambient aerosol concentrations in regions of greater vulnerability. As hedgerows form an integral feature of suburban as well as rural landscapes in much of the United Kingdom and elsewhere, their capability to create tortuous airflows, thereby accentuating the likelihood of pollutants depositing on their foliage surfaces, appears to play a vital role in the near-ground flux of air pollutants – mainly dust and other particulate matter in the PM_{10} size range. In its conservation practice report published in 2002, the Natural Resources Conservation Services of the state of Minnesota in the United States has recommended the use of filter strips, such as shelterbelts, to reduce movement of particulate organic sediment, pesticides and other toxic material towards sensitive features.

The report from the Spray Drift Task Force in the UK and evidence from several other studies conducted worldwide suggest that filter strips of appropriate design can contribute to pesticide drift reductions of 45%–90%. Continuous stands of vegetation over 1 m high

have also been shown to be efficient pollen collectors. It is accepted that inertial impaction is the most common method for collection of micro-particles in the size range 1–5 μm. Filter strips therefore appear to be useful for the along-wind (advective) deposition of ambient aerosols near the ground. This means they can be treated as useful sinks to the near-source aerosol concentrations enveloping the region where the majority of life forms, primarily humans, are more susceptible to the harmful impacts of the elevated particle concentration. However, designing a natural filter with optimal efficiency presents a bigger challenge than manufacturing industrial filters, as the foliage and vegetative components have spatially non-uniform aerodynamic profiles that also vary seasonally. This adds to the challenge in making realistic quantification of their filtration efficiency for air pollutants.

9.4.2.3 Factors influencing particle deposition

According to the existing literature, the parameters discussed in the following sections influence particle deposition to vegetation surfaces.

9.4.2.3.1 Surface characteristics

- *Surface geometry*: Expressed in terms of the Reynolds number (*Re*) of the collectors, which is the ratio of the inertial force on the particles to the viscous force of the carrier fluid. Although it has been suggested that the particle collection efficiency is a direct function of the area available for collection, the impaction parameter bears an inverse relation to the length-scale of the collecting elements.
- *Reactivity*: Expressed in terms of the chemical or biological affinity of the collecting surface for the airborne particles.
- *Wetness and roughness*: Particles in the air stream tend to impact more readily onto moist, rough or electrically charged surfaces. Studies have found that in the size range 1–5 μm, the detailed structure of the surface roughness, in particular the presence or absence of hairs on leaves and stems, plays an important role. In this size range the roughness of the adaxial (upper) surfaces or occurrence of prominent venation on the abaxial (lower) surfaces of leaves increases the deposition of particles by up to seven times due to the generation of a more turbulent boundary layer. This strong dependence of particle deposition on the microscale surface roughness complicates the process of making a precise prediction of the deposited particles using a numerical approach.

9.4.2.3.2 Particle characteristics

- *Particle shape and size*: This is a function of the particle Stokes number (*Stk*), which is the ratio of the particle stop distance to the diameter of the collecting element

FOR REFERENCE PURPOSES ONLY

(cylinder, sphere, disc, etc.). These features are discussed in more detail in Section 9.3.2 while describing the stages of modelling the particle removal efficiency of vegetation. The larger the particle, the greater the number of collection mechanisms that may potentially lead to its deposition (Figure 9.11). Experimental studies on pine and oak shoots in a wind tunnel suggest that for low and moderate wind speeds, particle deposition velocity is related to the fourth power of particle diameter.

- *Agglomeration*: The reactive properties and stickiness of some particles, especially those of biological origin, cause their agglomeration into larger particles, and affect their collection properties.
- *Hygroscopity*: Many atmospheric particles, such as natural sea salt nuclei and the salts of ammonium nitrate and ammonium sulphate, are hygroscopic. Studies have found a change in the rate of deposition of these particles after their hygroscopic growth.

9.4.2.3.3 Atmospheric characteristics

- *Wind speed*: Experiments with cylindrical collectors have shown that collection efficiencies for all the vegetation elements increase with the mean wind speed. The local wind field also generates high levels of turbulence (typically encountered in vegetation canopies), which enhances the collection efficiency beyond the levels predicted. However, in the case of stems and twigs, sufficiently high wind speeds tend to reduce the impaction efficiency to almost zero due to increased *bounce off*; collection on laminas or petioles is not affected by such phenomena.

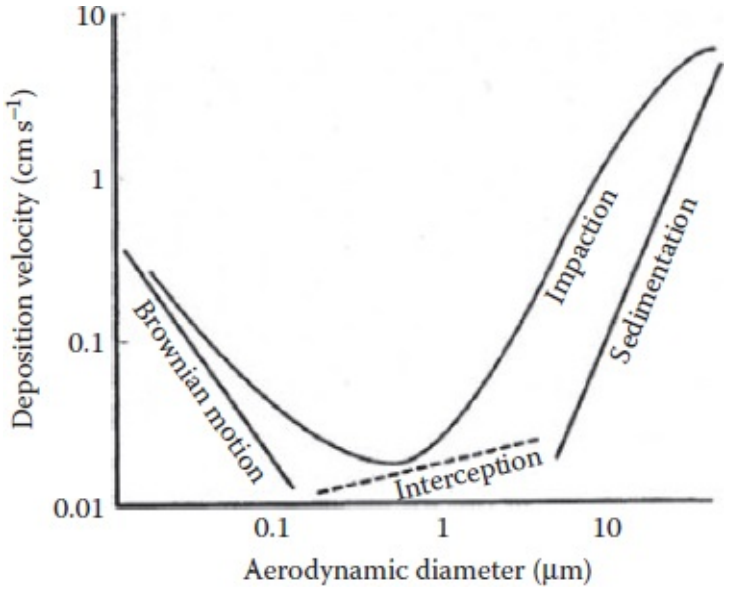

Figure 9.11 Dependence of deposition mechanism on particle aerodynamic diameter.

- *Temperature*: This mainly influences atmospheric stability through the vertical

FOR REFERENCE PURPOSES ONLY

temperature profile and the presence of *inversions*. Under temperature inversions, the particles accumulate in stable air, have longer residence times and hence are more likely to be deposited to collecting surfaces.

- *Humidity*: Particle collection tends to increase on wet collecting elements due to reduced bounce-off and re-entrainment under stronger wind conditions. On the other hand, humidity also affects the ambient concentration and the amount of drift that occurs for volatile particles, especially influencing the deposition of pesticide droplets. Atmospheric humidity also affects the growth of hygroscopic particles.

9.4.3 Modelling vegetation pollution uptake

9.4.3.1 Vegetation canopy model

Models are useful as they provide an indication of the level of contribution that different green infrastructure schemes have in improving air quality, although absolute values from models should be viewed with caution. The UFORE model, originally developed by the US Department of Agriculture, applied meteorological, pollution concentration and tree cover data to provide a comprehensive estimate of air pollution removal of CO, NO_x, O_3, PM_{10} and SO_2. Although this model has been extensively applied to estimate uptake of these air pollutants, especially for urban trees, it provides only a first-order estimate of the magnitude of pollution removal by trees. This is a result of the need for a range of assumptions in the model on variables that are hard to quantify. More sophisticated models and programmes, such as i-Tree, Park Value Calculator and CITYgreen, have been developed to quantify the value of green infrastructure (McPherson, 2010).

As shown in Figure 9.12, the downward pollutant flux (F; in g m^{-2} s^{-1}) can be calculated as the product of the deposition velocity (V_d; m s^{-1}) and the incident pollutant concentration (C_{in}; g m^{-3}):

$$F = V_d . C_{in}$$

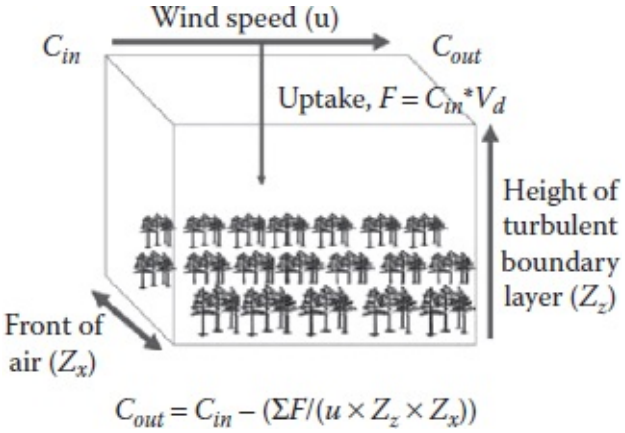

FOR REFERENCE PURPOSES ONLY

Figure 9.12 Schematic diagram of pollution interception and uptake by a vegetation canopy.

We have seen in Chapter 6 that deposition velocity is calculated as the inverse of the sum of the aerodynamic (R_a), quasi-laminar boundary layer (R_b) and canopy (R_c) resistances:

$$V_d = (R_a + R_b + R_c)^{-1}$$

Hourly meteorological data is used to estimate R_a and R_b as follows:

$$R_a = u(z).u_*^{-2}$$

where $u(z)$ is the mean wind speed at height z (m s^{-1}) and is the friction velocity (m s^{-1}).

$$u_* = (k.u(z-d))[\ln((z-d).z_0^{-1}) - \psi_m((z-d).L^{-1}) + \psi_m(z_0.L^{-1})]^{-1}$$

where:

k is the von Karman constant
d is the displacement height (m)
z_0 is the roughness length (m)
ψ_m is the stability function for momentum
L is the Monin–Obukhov stability length

L is estimated by classifying hourly local meteorological data into stability classes using Pasquill's stability classification scheme as described previously in Chapter 8.

When $L < 0$ (unstable):

$$\psi_m = 2\ln[0.5(1+X)] + \ln[0.5(1+X^2)] - 2\tan^{-1}(X) + 0.5\pi$$

where $X = (1–28\ z\ L^{-1})^{0.25}$.

When $L > 0$ (stable conditions):

$$\psi_m = -17(1-\exp(-0.29(z-d)/L)$$

On the other hand:

$$R_b = B^{-1}u_*^{-1}$$

where $B^{-1} = 2.2u_*^{-1/3}$

It has been found that dependence on R_a and R_b is small compared to that on R_c. A modified hybrid of big-leaf and multilayer canopy models is used to calculate the hourly R_c

FOR REFERENCE PURPOSES ONLY

values for O_3, SO_2, and NO_2 as follows:

$$\frac{1}{R_c} = \frac{1}{(r_s + r_m)} + \frac{1}{r_t}$$

where:

r_s is the stomatal resistance
r_m is the mesophyll resistance
r_t is the cuticular resistance

Typically, for SO_2, O_3 and NO_2, mesophyll resistance is set to 0 s m^{-1}, 10 s m^{-1} and 100 s m^{-1}, respectively. Similarly, typical cuticular resistance values for these three pollutants are 8000, 10,000 and 20,000 s m^{-1}, respectively. As the removal of CO and PM_{10} by vegetation is not directly related to photosynthesis/transpiration, R_c for CO is set to a constant value for in-leaf season (typically 50,000 s m^{-1}) and without-leaf season (typically 1,000,000 s m^{-1}).

For PM_{10}, yearly averaged R_a and R_b and species-specific V_g values are used to estimate R_c values, as shown in the following:

$$R_c = \frac{1}{V_g} - (\overline{R}_a + \overline{R}_b)$$

Table 9.2 provides a list of species-specific deposition velocities (V_g) to common trees and grasslands for particles of different diameter in different wind speeds. However, for PM_{10}, based on their 50% resuspension rate, typical median V_d of 6.4 cm s^{-1} is recommended for most urban forest species. In order to limit the deposition estimates to periods of dry deposition only, the deposition velocities are set to 0 over periods of precipitation.

Table 9.2 Capture efficiencies (C_p) and deposition velocities (V_g) to trees and grassland for particles of different diameter (D_p) and in different wind speeds (u)

Vegetation species	D_p (μm)	u (m s^{-1})	C_p (%)	V_g (cm s^{-1})
Picea abies (spruce)	Various	Various	–	0.55
Fraxinus excelsior	0.1–20	2	3	6.8
Quercus petraea	0.1–20	2	1	3.2
Betula pubescens	0.1–20	2	3	6.4
Corylus avellana	0.1–20	2	1	20
Picea glehnii (spruce)	20	1.4	15	20
Picea abies (spruce)	1	0.5	–	0.02
Populus nigra × *Cupressocyparis leylandii Acer campestre Populus deltoides* × *trichocarpa*	0.8	0.7	0.01–0.16	0.02–0.12

FOR REFERENCE PURPOSES ONLY

As above and *Sorbus intermedia*	1.28	1, 3, 8 and 10	0.02–2.8	0.03–28.05
Lolium perenne (perennial rye grass)		2	7–23	
Quercus petraea	0.8	3–9	0.3	0.8–3.1
Alnus glutinosa	0.8		0.04–0.09	0.1–0.8
Fraxinus excelsior	0.8		0.06–0.08	0.2–0.7
Acer pseudo platanus	0.8		0.01–0.04	0.04–0.3
Grassland	0.01–12	–	–	0.02–10
Pseudotsuga menchizii (Douglas fir)	0.01–10	Various	–	0.1–10

Source: Freer-Smith, P.H. et al., *Environ. Pollut.*, 133, 157–167, 2005.

Note: This data could form the basis for estimating the uptake of particles by specific planting schemes.

The height of the atmospheric boundary layer, Z_z (m) is calculated from wind speed and canopy height as:

$$Z_z = \frac{275cu_z}{\left(\sin(\varphi)ln\left(\frac{z-d}{z_0}\right)\right)}$$

Here c is a parameter related to atmospheric stability; c is close to 0.2 under neutral conditions but can be as high as 0.4 under convective conditions (e.g. daytime in summer) or as low as 0.02 under stable conditions (e.g. night-time high pressure). Pasquill stability classes are usually applied to estimate c. For instance, a c value of 0.02 and 0.4 is assigned to Pasquill Class A and E, respectively. The remaining Pasquill classes can be assigned at regular intervals between 0.02 and 0.4; u_z is the wind speed at canopy height, φ is latitude, z is canopy height, d is the zero plane displacement (= 0.7 z) and z_0 is aerodynamic roughness (= 0.1 z).

F for each pollutant can then be extrapolated across the canopy using known values of species-specific leaf area indices (LAIs) multiplied by 2 (to account for deposition to both sides of the leaf). LAI value for trees and large shrubs (i.e. minimum 1-inch stem diameter) is total leaf area (m^2) divided by total canopy cover (m^2), including layering of canopies. Seasonal LAI variation for deciduous species can be accounted for on the basis of regional leaf-on and leaf-off dates. Typically, the total tree canopy cover for a forest is determined by digital aerial photography or advanced very high resolution radiometer data.

On the basis of the hourly pollution concentration (modelled or monitored) the potential flux for each of the pollutants can be estimated. Hourly values of boundary layer heights (Z_z), estimated using the earlier formulation, are used in conjunction with local deposition velocities (V_d) to estimate percentage air quality improvement due to dry deposition to

vegetation. Based on estimated values provided in the literature, typical boundary-layer heights range between 150 and 250 m for night and day, respectively. In order to extrapolate total pollution within the boundary layer from ground-level concentrations, a well-mixed boundary layer is assumed. This is common during the daytime (unstable conditions). Hourly mixing heights (m) can then be used in conjunction with pollution concentrations (μg m^{-3}) to calculate the amount of pollution within the mixing layer. Following this, hourly percentage air quality improvement from pollutant uptake by vegetation can be calculated as:

$$\frac{\text{Grams removed}}{(\text{Grams removed} + \text{Grams in atmosphere})}$$

where

$$\text{Grams in atmosphere} = \text{Measured concentration (g m}^{-3}) \times \text{Boundary layer height (m)} \times \text{City area (m}^2)$$

To estimate pollution removal by all urban trees in a region, the pollution concentration data (monitored or modelled) have to be combined with standardised local or regional pollution removal rates (g m^{-2} of tree cover). As flux rates are directly proportional to pollutant concentrations, standardised removal rates are used to account for concentration differences on a spatial scale. Thus, standardised pollution removal rates, when multiplied by average pollutant concentration and total amount of tree cover, yields total pollution removal for each pollutant in every urban area. It is noteworthy that the UFORE model only considers dry deposition to vegetation, which may lead to underestimation of the total deposition by not accounting for the additional occult or wet deposition occurring at the same time.

9.4.3.2 Modelling collection efficiency of vegetative filter strips

This section provides a quantitative approach to estimate particle deposition to filter strips. It describes a numerical simulation of a porous barrier that can be utilised as a management tool for drift mitigation of micro-particulate pollutants. Conventionally, the collection efficiency (*CE*) of a solid object is the ratio of the number of particles that are deposited on its collecting surface to the number which would have been deposited had they not been deviated by the fluid flow. In aerosol mechanics, this efficiency is expressed either in terms of the particle number collection efficiency (*CE*) or the mass collection efficiency (CE_m) depending upon the manner in which particle concentration has been measured. It has been suggested that generally CE_m is higher than *CE*.

The overall *CE* of a porous barrier can be considered as the net result of two distinct

processes – (1) the deviation of a proportion of the approaching particle-laden flow by the hedge acting as a permeable resistance, (2) filtration of particles from the remaining through-flow by the distribution of collecting elements within. Therefore, *CE* for a porous barrier can be expressed as:

$$CE = CE_{\text{flow}} \times CE_{\text{filtration}}$$

where CE_{flow} is the ratio of the particle flux that actually occurs on the upwind face to the flux which would have occurred if not deviated by the fluid flow. On the other hand, $CE_{\text{filtration}}$ is the ratio of the particle concentration filtered by the vegetation elements to the particle concentration reaching the upwind face of the barrier. These model steps are described in the following sections.

9.4.3.2.1 Collection efficiency from flow deviation

A computational fluid dynamics (CFD) approach to simulate the flow fields in and around a porous barrier is required as a first step. Adequate parameterisation of the model domain and initial and boundary conditions would allow successful representation of the real barrier (Figure 9.13). A *homogenous two-phase flow model*, which considers air as the continuous phase and particles as the dispersed phase, has to be applied. *One-way coupling* is used to model the interaction between particles and the airflow, implying that the fluid affects the particle trajectories, not *vice versa*. This allows calculation of the particle trajectories for idealised spherical particles by accounting for the combined effects of the flow field and gravity using the following simplified equation of particle motion:

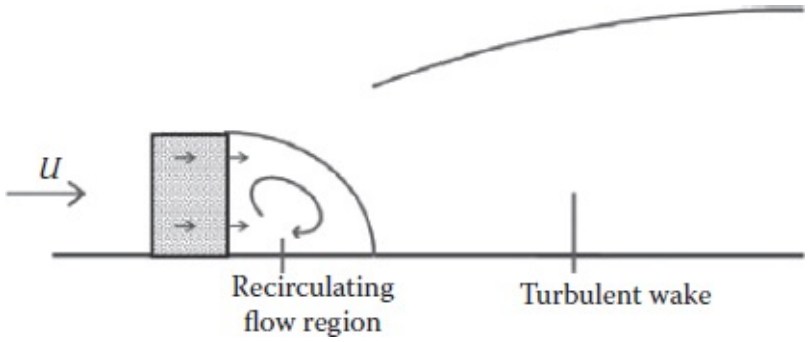

Figure 9.13 Depiction of flow fields around a porous vegetation barrier.

$$\frac{dV_p}{dt} = \frac{3\mu}{4\rho_p d_p^2} C_D \text{Re}_p (V_f - V_p) + \frac{\rho - \rho_p}{\rho_p} g$$

In the previous equation, V_f and V_p are fluid and particle speeds at each time step; ρ_p and Re_p are particle density and Reynolds number, respectively; d_p is the particle diameter; g is

acceleration due to gravity. C_D is the particle drag coefficient, which is a non-dimensional representation of the drag force (including consideration of both skin and form effects) exerted by the air on the particles. In situations with Re_p ranging between 0.1 and 10^3 (this covers the particle size range of ambient aerosols), C_D is considered as a complex function of Re_p reaching a maximum value of 0.44. It is usually estimated by implementing the Schiller Naumann drag model, which provides a correlation between the two parameters for the dilute limit of very small solid-phase volume fractions of particles (small enough to be approximated as spheres). The trajectories of non-spherical particles are then modelled through the application of appropriate shape factors (typically ranging between 0.25 and 1, where the latter represents a perfect sphere). This allows for characterisation of non-uniform drag distribution over atmospheric particles of varying shapes.

The numerical scheme uses forward integration; that is, V_p calculated at the start of each time step is assumed to prevail over the entire time step. At the end of each time step, new V_p is calculated from the analytical solution to the previous equation using a Euler integration in time. The trajectories of the injected particles are tracked from the inlet boundary to the upwind face of the barrier. The threshold particle release heights ($z_{\text{threshold}}$), which produce grazing trajectories on the upwind face of the barrier for the respective particle sizes, are thus used to calculate:

$$CE_{\text{flow}} = \frac{z_{\text{threshold}}}{H}$$

where H is the barrier height.

9.4.3.2.2 Collection efficiency from filtration by vegetation elements

In ambient conditions, particle deposition on vegetation elements occurs due to concurrent contributions from the following mechanisms – Brownian diffusion of finer particles, inertial impaction and interception of larger particles (d_p> 0.5 μm), and sedimentation due to gravity. Processes such as diffusiophoresis, thermophoresis or electrophoresis have been considered less important for natural plant surfaces. Numerically, particle collection on a 3D cellular grid representing a barrier of width W and height H can be parameterised on the basis of two variables – the velocity distribution profile $U(x, z)$ (x and z representing stream-wise and vertical directions, respectively) and the number of particles lost to foliage elements within each cell. The latter is expressed as the difference between the particle concentration entering a cell (C_{in}) and the concentration emerging from that cell (C_{out}). Based on this concept, the collection processes of extended barriers can be modelled as follows:

FOR REFERENCE PURPOSES ONLY

$$\text{Particle flux to a barrier} = \int_{0}^{H}\int_{-W}^{0} U(x,z)(C_{\text{in}} - C_{\text{out}})\,dx\,dz$$

We can also write the previous equation as:

$$\text{Particle flux to a barrier} = \int_{0}^{H}\int_{-W}^{0} U(x,z)\,CE_{\text{cell}}\,C_{\text{in}}\,dx\,dz$$

where CE_{cell} is the filtration collection efficiency for a grid cell:

$$CE_{\text{cell}} = \frac{C_{\text{in}} - C_{\text{out}}}{C_{\text{in}}}$$

Now, the $U(x, z)$ profile for a barrier of given porosity can be modelled with CFD. CE_{cell} values for each grid cell with horizontal grid spacing Δx and parameterisation of vegetation surface area density (SAD_{cell}) can then be modelled as:

$$CE_{\text{cell}} = 1 - \exp(-SAD_{\text{cell}}\,E\,\Delta x)$$

Here E is the collection efficiency of individual vegetation elements (typically approximated by cylinders and discs) which can be calculated cumulatively from all the deposition mechanisms considered – diffusion, interception and inertial impaction.

The Brownian-diffusion collection efficiency ($E_{\text{Diffusion}}$) of individual elements submerged in a lamina boundary layer can be modelled using the following expression:

$$E_{\text{Diffusion}} = \frac{\kappa C_{\text{Pol}} \text{Re}^{1/2} Sc^{1/3}}{DU_{\text{cell}}}$$

where:

- κ is a measure of the Brownian diffusivity of the particles
- Re is the Reynolds number ($Re = \rho DU_{\text{cell}}/\mu$) for flow around a barrier element of cross-section D
- U_{cell} is the flow velocity within each grid cell
- Sc is the Schmidt number ($Sc = \mu/\kappa\rho$)
- C_{Pol} is the Polhausen coefficient

For foliage elements, a typical value of C_{Pol}= 1.32 has been suggested in the literature. Interception is only considered an important deposition mechanism for vegetation with hairy surfaces; therefore, the contribution of interception to deposition is usually combined with inertial impaction and expressed as:

$$E_{\text{interception+impaction}} = \left(\frac{Stk}{Stk+0.8} - \frac{2.56-\log_{10}\text{Re}-3.2R}{10\sqrt{Stk}} \right) \times (1+R)$$

As shown in Chapter 3, *Stk* is the Stokes number of the foliage element:

$$Stk = \frac{{d_p}^2 \rho_p U_{\text{cell}}}{18\mu D}$$

where:

μ is the dynamic viscosity of air

R is an interception parameter expressed as $R = d_p/D$

Once all collection parameters have been accounted for, the resulting $CE_{\text{filtration}}$ for the entire cross-section of a barrier at a given height can be calculated as:

$$CE_{\text{filtration}} = \sum_{-W}^{0} [CE_{\text{cell}}]$$

Re-entrainment of particles already deposited on the vegetation elements remains a major issue to be modelled precisely while assessing their filtration efficiency. However, available research suggests that individual particles smaller than 50 μm diameter are unlikely to be removed by re-entrainment as they remain embedded within the viscous boundary layer of the foliage.

9.4.4 Practical concerns of greening

As shown in the previous sections, for both forest canopy and shelterbelts, use of vegetation in mitigating air pollution can be optimised through appropriate design and species selection. However, despite having the potential to effectively remove widespread air pollution at low maintenance costs, natural vegetation intervention has some practical issues that need to be considered before deciding on the best available option. These can range from eutrophication of water courses from fertiliser use, damage to civic infrastructure from tree roots and spread of invasive species, littering, and so on. There are also economic costs associated with implementation and maintenance of green infrastructure programmes. Under drought conditions, representing extreme climate scenarios, reduced evapotranspiration by grass can raise the air temperature. In this section we first address some of the prominent issues, including resuspension of pollutants (mainly particulates), emission of VOCs and pollen production. Finally, we provide a brief case study covering the net effect of vegetation intervention, combining both air pollution deposition to and emissions from different tree species in order to rank their utilisation in sustainable air pollution mitigation.

FOR REFERENCE PURPOSES ONLY

9.4.4.1 Resuspension of pollutants

Resuspension, which is also known as *re-entrainment*, is mainly relevant to particulate air pollutants. Particles deposited onto vegetation elements may remain there, get resuspended to the atmosphere by wind or be washed off during precipitation events. The tendency of particles to resuspend at a given wind speed is a property of both the particle and the foliage it adheres to. For example, at moderate wind speeds, resuspension of silica particles from an experimental spruce canopy has been found to be extremely low (approximately 1% of the deposited material per day). Another study, using pine and oak shoots in a wind tunnel, showed that individual particles smaller than 50 μm diameter are unlikely to be removed from the surface by re-entrainment because they remain embedded within the viscous boundary layer. Overall, it has been found that resuspension is an issue in arid regions with strong wind environments. In humid regions, or in locations of frequent precipitation, resuspension is minimised through wash-off or strong adhesion of pollutants to the foliage elements.

9.4.4.2 Emission of volatile organic compounds

One can argue that application of natural vegetation to control air pollution may not be effective as plants, particularly tree species, release substantial amounts of non-methane BVOCs including isoprene (C_5H_8), monoterpenes ($C_{10}H_{18}$), sesquiterpenes ($C_{15}H_{28}$) and oxygenated compounds ($C_nH_{2n-2}O$). These compounds can accentuate air pollution through production of secondary organic aerosols (SOAs). Results from recent laboratory studies suggest that acid-catalysed multiphase reactions of isoprene produce oligomeric humic-like material resulting in substantial aerosol formation. Recent research also suggests possible enhancement in the generation of aerosols from isoprene and its oxidation derivatives (e.g. methacrolein and methyl vinyl ketone) via condensed phase reactions with hydrogen peroxide. In addition, some of the BVOCs (e.g. isoprene), because of their alkene chemical structure, play important roles in suppressing concentrations of the hydroxy (OH) radical, enhancing the production of peroxy (HO_2 and RO_2) radicals, enhancing tropospheric CO concentrations, generating organic nitrates that can sequester NO_x and allowing long-range transport of reactive N. The latter plays a vital role in atmospheric chemistry as it leads to photochemical production of tropospheric ozone.

In order to avoid the generation of additional air pollution from vegetation, adequate plant species with lower BVOC emission potential should be selected. The integration of BVOC emissions from single foliage elements to the ecosystem level is normally achieved by the coupling of active biomass distribution, environmental conditions influencing emissions, and basal emission rates. BVOC emission inventories exist at different scales – global, continental and regional – with different levels of reliability. Recently, a highly resolved biogenic isoprene and monoterpene emission inventory for Great Britain has been developed, which uses a very detailed plant-species-specific methodology. Table 9.3

FOR REFERENCE PURPOSES ONLY

provides the emission potentials for selected vegetation species only; a more exhaustive list of values for additional tree species can be found on an in-house database maintained by the Institute of Environmental and Natural Sciences at Lancaster University, UK (http://www.es.lancs.ac.uk/cnhgroup/iso-emissions.pdf). This allows for allocation of emission potentials for these two BVOCs while estimating their emissions from an individual plant species using the following formulation:

$$ER_s = ER_b \times M \times \gamma \times \delta$$

where:

ER_s is the emission from an individual plant species (μg m^{-2} ground.h^{-1})

ER_b is the emission potential (μg.g^{-1} dry mass.h^{-1}, or μg.m^{-2} leaf area.h^{-1}) of the compound from the plant species at standard conditions of 30°C and 1000 μmol.m^{-2}.s^{-1} PAR

M is the biomass (g.m^{-2} ground) or leaf area index (LAI; m^2/m^2), respectively

γ is the short-term temperature and light-scaling factor

δ is a long-term composite environmental scaling factor (depending on age, season, stress etc.)

Table 9.3 Isoprene and monoterpene emission potentials of some common vegetation species (μg gdw^{-1} h^{-1})

Species name	*Common name*	*Isoprene emission potential*	*Monoterpene emission potential*
P. sitchensis	Sitka spruce	3.28	3.36
Calluna vulgaris	Heather	0	2.42
Brassica napus	Oil-seed rape	0	0.12
Dactylis glomerata	Cocksfoot grass	0	0.10
P. sylvestris	Scots pine	0	6.45
Phleum pratense	Timothy	0	0.32
Cirsium arvense	Creeping thistle	0	4.00
Elymus repens	Common couch	0	0.32
P. abies	Norway spruce	1.07	4.00
Zea mays	Corn/maize	0	0.10
Agrostis capillaris	Common bent	0	0.51
Quercus spp.	Oak	38.45	0.94
Solanum tuberosum	Potato	0	0.55
Eriophorum vaginatum	Harestail cotton grass	0	0.10
Poa annua	Annual meadow grass	0	0.32
Pisum sativum	Pea	0.10	4.40
Taraxacum agg.	Dandelion	0	4
Rumex acetosa	Common sorrel	0	0.10
Cirsium vulgare	Spear thistle	0	4.00

FOR REFERENCE PURPOSES ONLY

Erica tetralix	Cross-leaved heath	3.21	0.14
Pseudotsuga menziesii	Douglas fir	0	0.36
Vaccinium myrtillus	Bilberry	0.10	0
Crataegus monogyna[a]	Hawthorn	0.03	0.88
Acer pseudoplatanus[a]	Sycamore	3.90	0.00
Tilia sp.[a]	Limes	5.50	0.00
Cupressus, Chamaecyparis[a]	Cypress types	0.10	0.67
Fraxinus excelsior[a]	Ash	0.00	0.00
Betula pendula[a]	Birch	0.05	2.63
Sorbus spp.[a]	Rowan/whitebeam	0.50	1.50
Populus nigra[a]	Poplars	52.50	2.30
Malus sp.[a]	Apples	0.50	0.60
Prunus sp.[a]	Plums	0.10	0.13
Salix alba, Salix caprea, Salix spp.[a]	Willow	22.70	1.00

Source: Stewart, H.E. et al., *J Geophys. Res.*, 108, 4644–4666, 2003.
Note: gdw is the gram dry weight of biomass.
[a] Owen, S.M. et al., *Ecol. Appl.*, 13, 927–938.

For isoprene, and light- and temperature-dependent monoterpenes:

$$\gamma = C_L C_{T_i}$$

and for monoterpene emissions dependent on temperature, T, alone:

$$\gamma = C_{T_m}$$

where:

$$C_L = \frac{\alpha C_{L1} L}{\sqrt{(1+\alpha^2 L^2)}}$$

$$C_{T_i} = \frac{e^{[C_{T1}(T-T_s)\cdot(RT_sT)^{-1}]}}{1+e^{[C_{T2}(T-T_m)\cdot(RT_sT)^{-1}]}}$$

$$C_{T_m} = e^{[\beta(T-T_s)]}$$

where:

$\alpha = 0.0027$ m^2.s^{-1}.µmol^{-1} (moles of quanta)
C_{L1}=1.066 units
C_{T1}=95,000 J/mol (moles of emitted gas)
C_{T2}=230,000 J/mol
T_m = 314 K

FOR REFERENCE PURPOSES ONLY

β= 0.09 K^{-1} are empirically derived constants

R (gas constant) = 8.314 $J.K^{-1}.mole^{-1}$

L is the flux of PAR ($\mu mol.m^{-2}.s^{-1}$)

T_s is the leaf temperature at standard condition (assumed to be 303 K for temperate locations)

Earlier studies suggest that at standard conditions of 1000$\mu mol.m^{-2}.s^{-1}$ PAR and 303 K, $(C_L \times C_T)_{std}$ = 1. Parameterisation of δ, the long-term scaling factor, depends on several variables – CO_2 concentrations, cuticle hydration, nutrient availability, water stress seasonality, pollutant stress, humidity and shade adaptation being the prominent ones. It has been found that these parameters affect the BVOC synthase enzymes activities and it is a subject of ongoing research. Figures 9.14 and 9.15 show the short-term (diurnal) and the long-term (seasonal) patterns respectively of isoprene emissions from a mixed deciduous temperate forest (Borden, Ontario, Canada; 44°19′N, 80°56′W). As shown in Figure 9.14, the diurnal isoprene flux is closely correlated with increase in both PAR and leaf temperature, especially during the middle of the day. Furthermore, on an annual basis (Figure 9.15), the maximum isoprene flux occurs during the middle of the growing season (between day of year [DOY] 180 and 240), which corresponds to high PAR levels and leaf cover. Seasonal isoprene emissions from commonly occurring deciduous species in tropical countries seem to exhibit a similar pattern, with maximum emission during summer and minimum during the winter or early spring (Table 9.4).

BVOC emissions from different forest canopies have been estimated based on the average tree cover and tree species (Table 9.5). It can be seen that estimated isoprene emission is higher than monoterpene emissions for most canopy types. Deciduous forests make the greater contribution to isoprene whereas conifers, such as Sitka spruce, have high contributions to both isoprene and monoterpenes. In the context of regional ozone formation, peak levels of VOC emissions have been considered more important than annual total emissions. Despite high reactivity of the BVOCs compared to anthropogenic VOCs, they have been found to play a minor role in the photochemistry, mainly due to their lower contributions to the overall regional emissions in most locations. However, this may change in the face of stringent emission controls to reduce anthropogenic VOC emissions – especially if any future vegetation intervention to mitigate air pollution does not allow for their BVOC emissions.

FOR REFERENCE PURPOSES ONLY

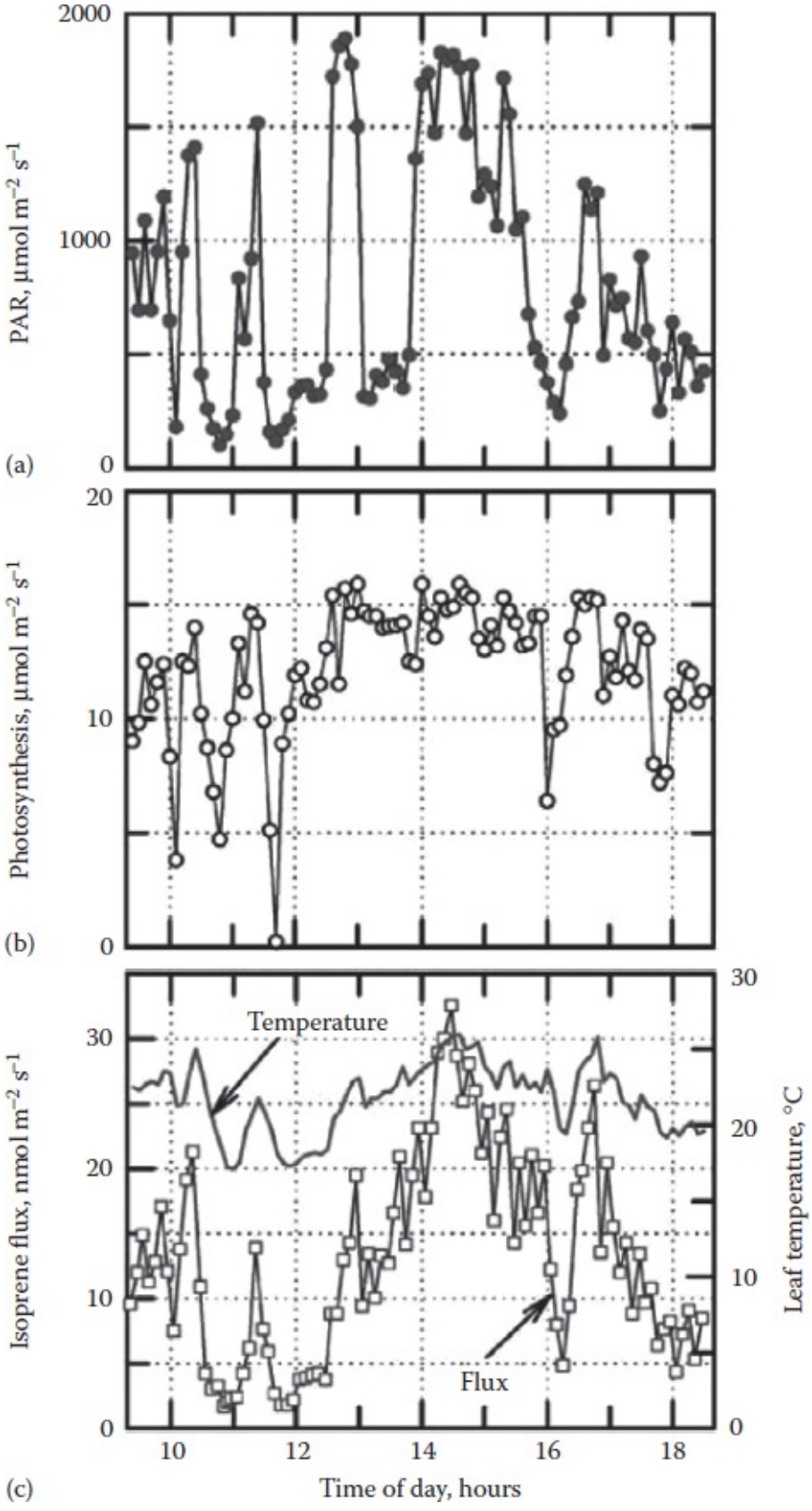

Figure 9.14 Diurnal patterns of PAR: (a), net photosynthesis (b), isoprene emissions and leaf temperature (c) for poplar leaves measured at the top (22 m) of the Borden Forest, Canada. (From Wang, D. and Fuentes, J.D., *Agric. For. Meteorol.*, 116,

FOR REFERENCE PURPOSES ONLY

37–48, 2003.)

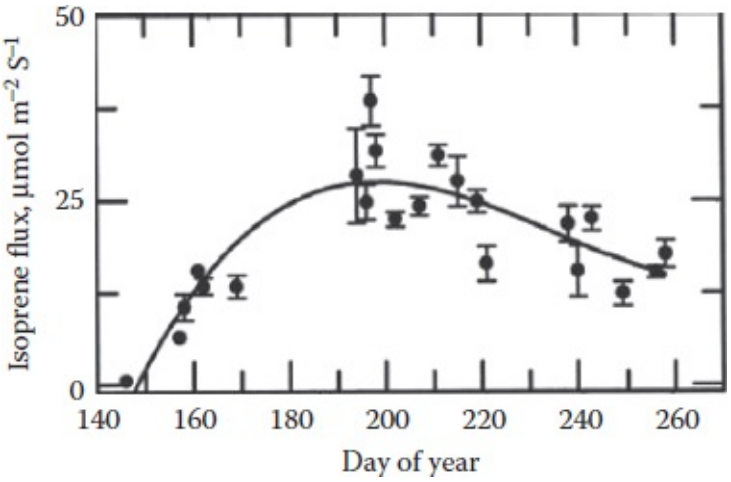

Figure 9.15 Seasonal pattern of canopy isoprene-emission rates (●; means ± 1 standard deviation; the solid line represents the best fit to data points) for the boreal forest, Canada (normalised at canopy temperature of 25°C and PAR of 1000 µmol.m^{-2}.s^{-1}). (From Fuentes, J.D. et al., *J. Appl. Meteorol.*, 38, 855–869, 1999.)

Table 9.4 Seasonal variation in isoprene emission in four tropical deciduous plant species (µg gdw^{-1} h^{-1})

Plant species	*Winter (December–February)*	*Spring (March–April)*	*Summer (May–June)*	*Autumn (September–November)*
Ficus relegiosa	15.9 ± 10	12.5 ± 17	116 ± 48	108 ± 61
Ficus infectoria	2.3 ± 4	58.5 ± 33	155 ± 7	57 ± 37
Pongamia pinnata	6.7 ± 4	NED	53.5 ± 5	42.3 ± 27
Morus alba	0.73 ± 1	17.4 ± 11	57.1 ± 4	19.2 ± 14

Source: Singh, A.P. et al., *Environ. Monit. Assess.*, 131, 231–235, 2007.

Note: NED is no emission detectable.

Table 9.5 Biogenic VOC emission estimated from different vegetation type (for 30°C and 1000 µmol m^{-2} s^{-1} PAR) (g.km^{-2}.h^{-1})

Vegetation type	*Isoprene emission*	*Monoterpene emission*
Deciduous forest (UK area-weighted average)	7164	–
Coniferous forest (UK area-weighted average)	2718	–
Scrubland (UK area-weighted average)	2606	–
Grassland (UK area-weighted average)	2171	–
Sitka spruce (1.7% UK land cover)[a]	658–6760	638–6920
Gorse (0.06% UK land cover)[a]	42.6	4.7
Urban Tucson, Arizona (United States)[b]	2849	355

FOR REFERENCE PURPOSES ONLY

Urban Tucson, Arizona (United States)[c]	0	54

Source: Owen, S.M. et al., *Ecol. Appl.*, 13, 927–938.

[a] The summertime field measurements of emissions.

[b] The highly vegetated residential area.

[c] The highly developed urban area.

9.4.4.3 Pollen production

Pollen grains, or other paucimicronic allergen-carrying airborne particles released from natural vegetation, increase the frequency of respiratory diseases such as hay fever and bronchial asthma. This is only an issue for specific plant species which pollinate through air (anemophilous); therefore, the adverse effects can be mitigated through appropriate species selection. On the other hand, stands of vegetation over 1 m high have been found to be efficient pollen collectors. In addition, unlike their inorganic counterparts, biological particles such as pollens and spores are often aerosolised in agglomerates, such as chains and compacts. Thus, because of their large size they are more likely to be scavenged by vegetation elements downstream. Several aerobiological studies have been carried out for the elaboration of pollen calendars that are indicative of the allergenic potential present in the atmosphere and the seasonality of pollen activities. Based on this information, process-based models have been developed for predicting the start and peak periods of pollen seasons for a number of plant species. The majority of the epidemiological studies have reported exacerbation of respiratory allergy from pollen sensitisation, released mainly from grasses and weeds. Only recently, attention has been drawn to tree pollen allergy. For example, Table 9.6 provides the pollen season and peak pollen concentrations of six tree species studied in Porto, Portugal, for 2007. Although the main pollen season of different trees shows inter-annual variations, the average dates for peak pollen concentrations for most of these trees are in March and April.

Table 9.6 Main pollen season of some tree species studied in Porto, Portugal. The table shows the beginning, the end, duration, day of peak pollen concentration in Julian days and the peak pollen concentration (in Pollen m^{-3})

Tree species	*Beginning*	*End*	*Duration*	*Day of peak concentration*	*Peak concentration*
Acer	72	94	22	83	179
Betula	99	114	15	107	133
Platanus	77	99	22	88	508
Quercus	88	116	28	102	100
Salix	58	90	32	74	16
Populus	70	98	28	84	33

FOR REFERENCE PURPOSES ONLY

Source: Ribeiro, H. et al., *Environ. Res.*, doi:10.1016/j.envres.2008.11.008, 2008.

9.4.4.4 Evaluating pros and cons of urban vegetation intervention

As we have seen earlier, trees can act as both sink and source of air pollutants. It has been widely agreed that all trees can be beneficial for improving air quality through deposition of O_3, NO_2, CO and HNO_3. However, some trees have the potential to enhance the air pollution level, mainly through release of pollens and BVOCs. The latter contributes to photochemical ozone formation through its reaction with NO_x. Therefore, for sustainable air quality mitigation, it is considered useful to evaluate the vegetation intervention potential as a net influence – combining the effects of both pollution deposition and emissions. To this end, recently an atmospheric chemistry model, the Cambridge tropospheric trajectory model of chemistry and transport (CiTTyCAT), was applied to quantify the effects of trees on urban air quality in scenarios of high photochemical pollution in the West Midlands in the UK. CiTTyCAT is an air parcel model which includes dry deposition for O_3, NO, NO_2, NO_3, N_2O_5, HNO_3, HNO_4, H_2O_2, CO, HCHO, CH_3CHO, CH_3OOH, CH_3COO_2H and peroxyacetyl nitrate (PAN). More information on this model and the case study itself can be found in the literature source listed in the References and Further Reading section at the end of the chapter. For the 900 km^2 study area, the biogenic emissions of isoprene and α-pinene were estimated at a spatial resolution of 1 × 1 km.

The trade-off between air pollution deposition to and biogenic emissions from the trees for the model scenarios were ranked using an urban tree air quality score (UTAQS). Of the 30 tree species considered (Figure 9.16), pine, larch, and silver birch showed the greatest potential to improve air quality while oaks, willows and poplars showed potential to worsen downwind air quality if planted in very large numbers. This model appears to be a useful tool for estimating the net effect of vegetation intervention, as it claims to be directly applicable to all areas of the world using the appropriate input data.

FOR REFERENCE PURPOSES ONLY

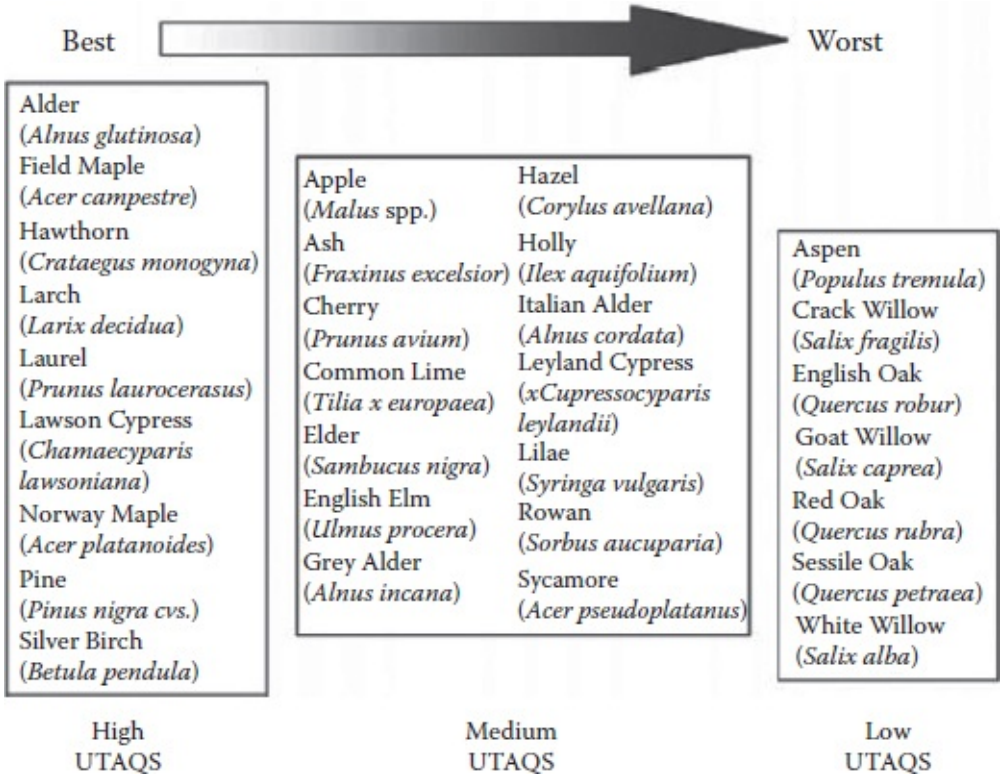

Figure 9.16 UTAQS classification for 30 most common trees in the West Midlands metropolitan area, UK. (From Donovan, R.G. et al., *Environ. Sci. Technol.*, 39, 6730–6738, 2005.)

9.5 CASE STUDY I – SEVESO INDUSTRIAL DISASTER

The so-called *Seveso disaster* was an industrial accident that occurred in July 1976. The event was named after the Milan suburb of Seveso in Northern Italy where the accident occurred, although other nearby communities were also affected. The chemical released was 2,3,7,8-tetrachlorodibenzo-p-dioxin (TCDD), often known simply as *dioxin*. Dioxins are persistent environmental pollutants that are chemically stable and potentially highly toxic to organisms (Figure 9.17). Once they enter an organism's body, they are absorbed by fatty tissue and are stored in the body, with a typical half-life of 7–11 years. Dioxins therefore accumulate in the food chain and can bioaccumulate in higher organisms.

The name *dioxin* actually applies to a family of structurally and chemically related polychlorinated dibenzo-p-dioxins (PCDDs) and polychlorinated dibenzofurans (PCDFs). Other substances with similar toxic properties are also included under the term *dioxin*, including polychlorinated biphenyls (PCBs). A total of 419 types of dioxin-related compounds have been identified; about 30 are considered to have significant toxicity, with TCDD being the most toxic. Dioxins can damage the immune system, interfere with hormones, and cause reproductive and developmental problems.

Dioxins are mainly formed when chlorine or a material containing chlorine is heated at

FOR REFERENCE PURPOSES ONLY

high temperatures. They are mostly released to the environment via the uncontrolled incineration of hospital waste and municipal solid waste containing certain plastics such as polyvinyl chloride (PVC). Dioxins are found throughout the world even though formation of dioxins is local.

The accident in Seveso in 1976 produced 2,4,5-trichlorophenol from an industrial plant owned by Industrie Chimiche Meda Società Azionaria (ICMESA), where a relief valve on a chemical reactor ruptured, releasing a cloud of vapour through a vent leading to the roof. This resulted in the aerial release of approximately 6 tonnes of chemicals, including about 1 kg of TCDD. The chemicals settled over about 18 km^2 of the surrounding area.

More than 3,300 animals, mostly rabbits and poultry, were found dead within days and more than 730 people living near the plant were evacuated. Emergency slaughtering of animals to prevent TCDD entering the food chain resulted in approximately 80,000 animals being killed. No human deaths were attributed to the release of TCDD, but a number of children were hospitalised with skin inflammation and a number of pregnant women chose to have abortions because of fears over birth defects. Bertazzi et al. (1998) reported that chloracne was the only conclusive health effect from the accident, with almost 200 cases clearly showing definite exposure dependence, although other health effects showed increased occurrence.

The incident prompted the European Union (EU) to develop and adopt legislation for the prevention and control of such accidents. This yielded the so-called Seveso Directive (Directive 82/501/EEC), later amended in view of the lessons learned from subsequent accidents (e.g. Bhopal, Enschede), resulting in Seveso-II (Directive 96/82/EC). In 2012 Seveso II was replaced by Seveso-III (Directive 2012/18/EU), which was developed in order to take into account issues such as changes in the EU legislation on the classification of chemicals and increased rights for citizens to access information and justice. The directive currently applies to more than 10,000 industrial establishments in the EU where dangerous substances are used or stored in large quantities. The initial Seveso Directive and its successors have contributed to achieving a low frequency of major accidents in Europe, which has a high rate of industrialisation. The directive is regarded as a benchmark for industrial accident policy and has been a role model for legislation in many countries.

FOR REFERENCE PURPOSES ONLY

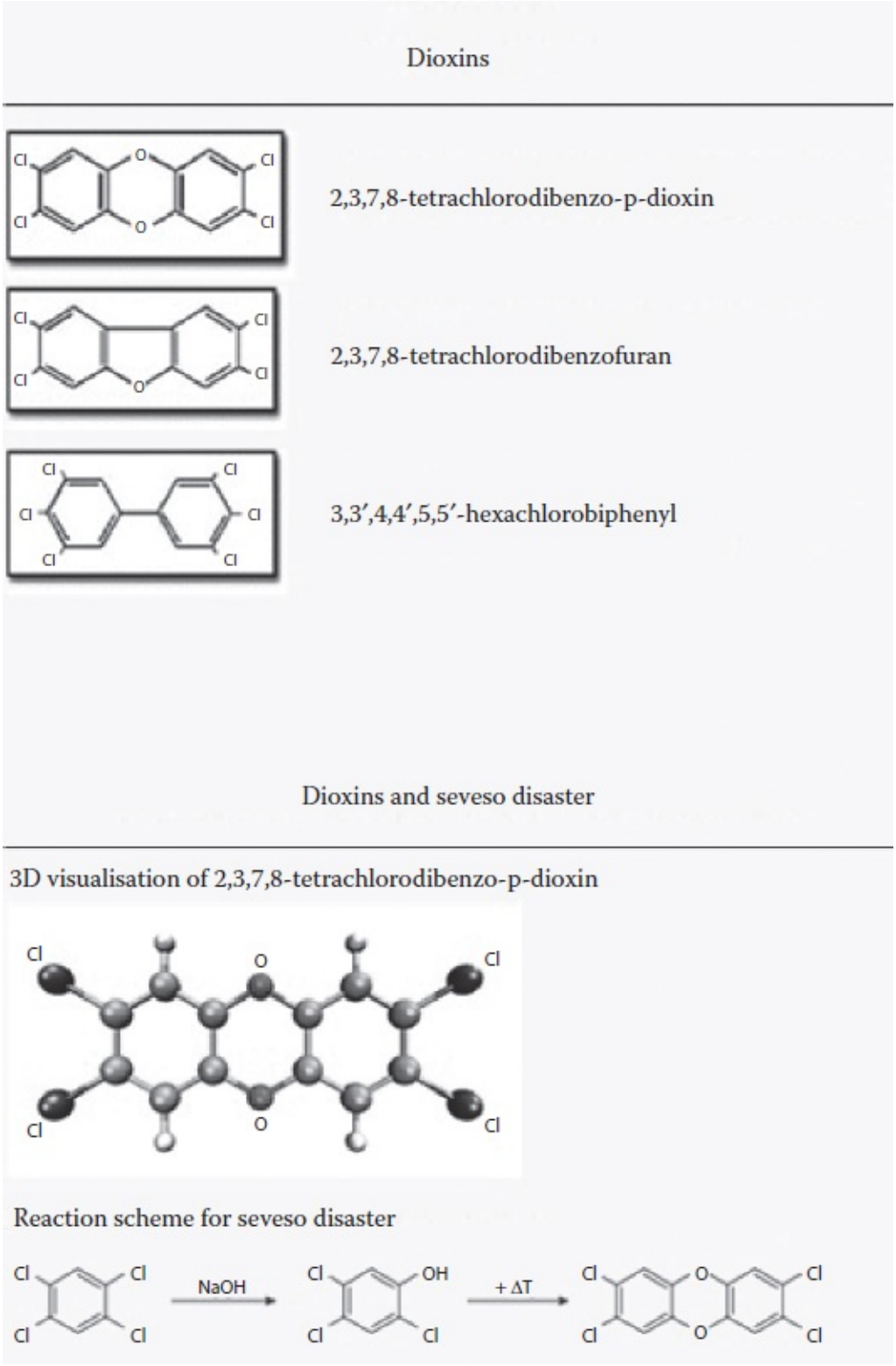

Figure 9.17 Chemical structure of dioxins and their reaction scheme during the Seveso disaster.

9.6 CASE STUDY II – AMBIENT AIR POLLUTION CONTROL

9.6.1 Role of hedgerows in the UK for mitigating ambient aerosols

A comparative investigation of aerosol deposition to three popular UK hedgerow species – hawthorn (*Crataegus monogyna*), holly (*Ilex aquifolium*) and yew (*Taxus baccata*) – was undertaken between July 2002 and October 2004 for several suburban and rural locations in Nottinghamshire, UK. The hedges have been considered as natural filter strips with marked seasonal variations in their foliage development and resulting aerodynamic structures. Table 9.7 provides their detailed 3D structural profiles. All the readings were taken with two identical optical particle counters. Experiments were set up on days when the forecast indicated a favourable wind direction and a wind speed exceeding 5 miles hour^{-1} (2 m s^{-1}). Corresponding values of $CE_{\text{filtration}}$ were also modelled using the approach presented in Section 9.3.2. Comparisons between $CE_{\text{filtration}}$ from the experiments and from model simulations for the three hedges are presented in Figure 9.18a, b, c, respectively.

Table 9.7 Description of the 3D structural profiles for the three studied hedges

	Hawthorn	*Holly*	*Yew*
Height [H] (m)	2.2	1.7	2.4
Width [W] (m)	1.6	2.1	3.2
Height of maximum foliage density (m)	1.9	1.5	1.2
Depth of the layer with maximum foliage density (m)	0.6	0.9	1.1
Stem diameter (m)	0.05	0.08	0.1
Stem number at z~0.1 H in the innermost cell	1	1	2
Stem diameter (m)	0.01	0.01	0.03
Stem number at $z \sim z_{max}$ in the innermost cell	3	4	3
Shape factors (a, b) used in beta function	3, 1.2	2, 1.2	1.2, 1.2
Foliage profile	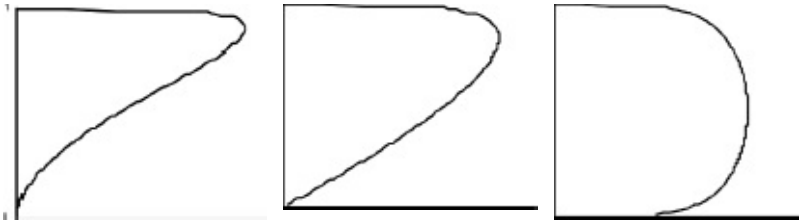		

Source: Tiwary, A. et al., *J. Aerosol Sci.*, 37, 990–1015, 2006.

Generalised scenarios from all three hedges suggest that $CE_{\text{filtration}}$ for particles larger than about 5 μm is driven by impaction and increases with particle diameter. It is a minimum between 1 and 5 μm, and increases again below 1 μm due to Brownian diffusion. For all three species $CE_{\text{filtration}}$ increases with particle size beyond 5 μm. For hawthorn (Figure 9.18a), $CE_{\text{filtration}}$ of up to 35% was predicted for particles with central diameter 15 μm during moderate wind speeds of 2.3 m s^{-1}. Simulated results for holly (Figure 9.18b) gave $CE_{\text{filtration}}$ of up to 23% in the corresponding size class in moderate wind conditions

FOR REFERENCE PURPOSES ONLY

averaging 2.5 m s^{-1}. Using similar parameters, $CE_{\text{filtration}}$ for yew was found to be about 15% (Figure 9.18c). It was concluded that denser hedges, such as yew, tend to lift the approaching airflow more strongly and increase turbulence in their wakes, thereby encouraging recirculation of finer particles on their downwind sides. The positive slopes of the predicted profiles for the largest particle size indicate $CE_{\text{filtration}}$ to be increasing for larger particles in the case of all three hedges.

FOR REFERENCE PURPOSES ONLY

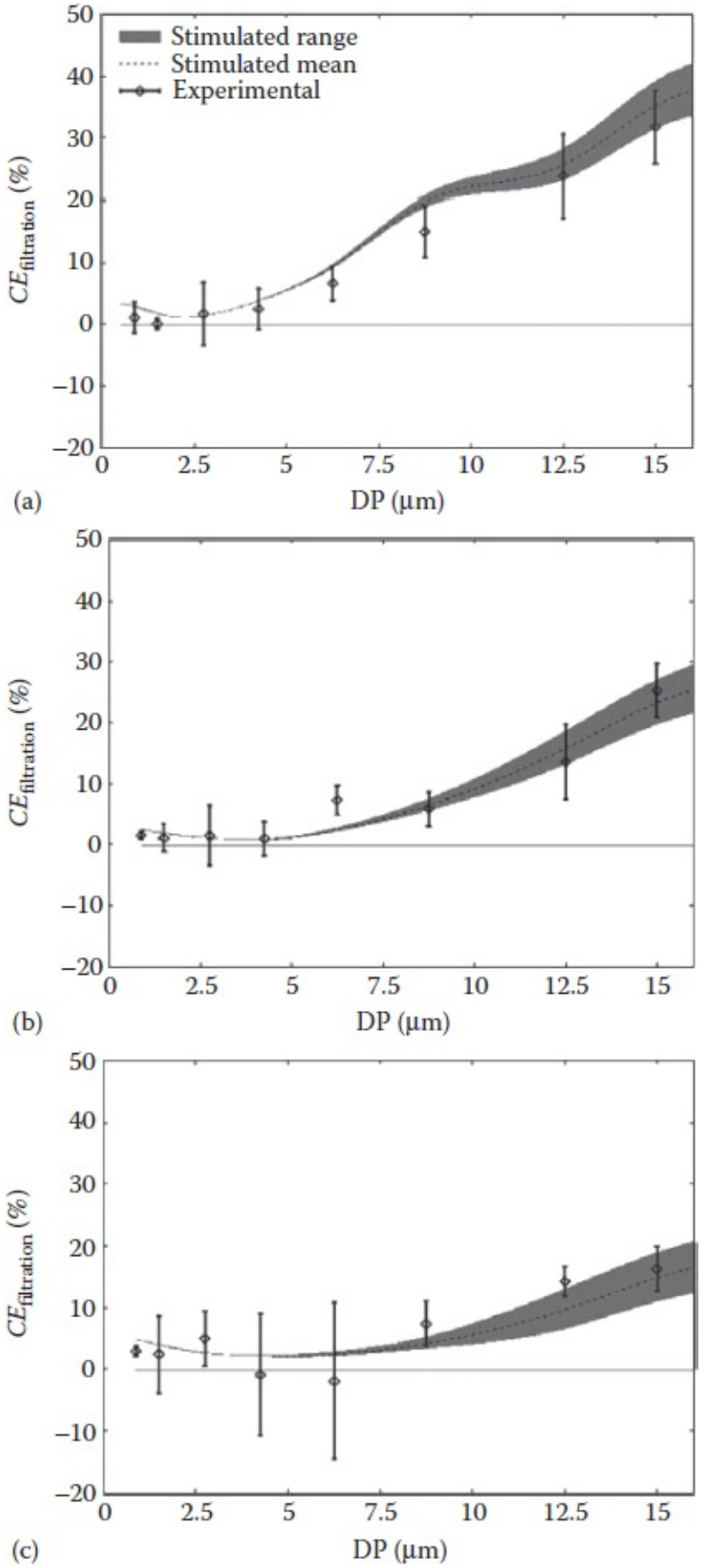

Figure 9.18 $CE_{filtration}$ of hawthorn (*Crataegus monogyna*), holly (*Ilex aquifolium*) and yew (*Taxus baccata*) from numerical simulations (–) and field measurements (◊) a,

FOR REFERENCE PURPOSES ONLY

b and c, respectively. Alongside, one standard deviation of the measured values shows the extent of variation in the measured mean particle concentration on different sampling days for the three-hedge species. The bands plotted over the mean predicted $CE_{filtration}$ in all three cases represent the range of variation in the numerical outputs based on the selection of turbulence closure scheme and empirical constants in the CFD model. (From Tiwary, A. et al., *J. Aerosol Sci.*, 37, 990–1015, 2006.)

9.6.2 Role of greenbelts in air quality management for quarries in India

Implementation of greenbelts has been considered as an effective measure for mitigating air pollution at the source. Greenbelts are mostly used around open cast mines and quarries with large operational areas. A typical greenbelt involves the mass plantation of pollutant-tolerant trees (evergreen and deciduous) for the purpose of reducing the air pollution by filtering, intercepting and absorbing pollutants. A recent study reported for the Ib Valley Coalfield in India has adopted growth of green plants in and around the polluting source as a cost-effective mitigation measure. Greenbelt attenuation models have been developed to optimise important factors in greenbelt development – distance of the stand from the source, as well as the width and height of the belt. The attenuation factor based on these parameters determines the mitigation potential of the belt. The attenuation factor is defined as the ratio of the mass flux reaching a particular distance in the absence of the greenbelt, to the mass flux reaching the same distance in the presence of the greenbelt. However, trees being natural barriers have varying responses towards pollutants – some species are highly sensitive and others are hardy and tolerant. In addition, due to variations in leaf size, composition and leaf-shedding periods, they also have varying aerodynamics. Therefore, the selection of tree species that can be grown around a mining site is very important. The recommended pollution-controlling plant species for greenbelt development in India are listed in Table 9.8. These plant species are dust attenuating and can also lower SO_2 and NO_x concentrations effectively.

Table 9.8 Recommended pollution-retarding plant species for green belt development

Pollutants	*Species name*	*Family*	*Indian name of plant*	*Evergreen (E) or deciduous (D)*
TSP	*Butea monsperma*	Moraceae	Palas	D
	Spathodea companulata	Bignoniaceae	Sapeta	E
	Fiscus infectoria	Moraceae	Pakur	E
	Cassia fistula	Caesalpiniaceae	Amaltas	D
	Anthocephalus cadamba	Rubiaceae	Kadam	D
	Casia siamea	Caesalpiniaceae	Minjari	D
SO_2	*Pterospermum acerifolium*	Sterculiaceae	Muchkun	E
	Bauhinia variegata	Leguminosae	Kanchhar	D
	Bambusa spp.	Gramineae	Bans	D

FOR REFERENCE PURPOSES ONLY

	Delbergia sisoo	Papolionaceae	Sisum	D
	Ecalyptus spp.	Myrtaceae	Eucalyptus	E
	Cassia siamea	Caesalpiniaceae	Minjari	D
	Zizyphus jujuba	Rhamnaceae	Ber	D
NO_x	*Bauhinia variegata*	Leguminosae	Kanchhar	D
	Zizyphys jujuba	Rhamnaceae	Ber	D
	Syzigium cuminii	Myrtaceae	Jamun	D
	Mimusops elengi	Sapotaceae	Bakul	E
	Eucalyptus spp.	Myrtaceae	Eucalyptus	E
	Pterospermum acerifolium	Sterculiaceae	Muchkun	D
	Mangifera indica	Anacardiaceae	Aam	E

Source: Chaulya, S.K., *J. Environ. Manage.*, 70, 1–14, 2004.

However, this case study indicates that greenbelts can only mitigate near-source air pollution from mining activities. Supporting measures that enable more widespread air pollution control from such activities should include use of covered transportation, remote control sprinkling system on haul and transport roads, regular maintenance of all heavy earth-moving machinery, application of a chemical binder in the haul road, enclosure of crushers of coal-handling plants, re-vegetation of reclaimed former overburden dumps using grass and other sturdy plant species and proper dampening of active overburden dumps to avoid wind erosion.

REFERENCES AND FURTHER READING RESOURCES

Baumann, H., and Tillman, A. (2004) *The Hitch Hiker's Guide to LCA*. Studentlitteratur AB, Lund, Sweden.

Bekö, G., Clausen, G., and Weschler, C.J. (2008) Sensory pollution from bag filters, carbon filters and combinations. *Indoor Air*, 18: 27–36.

Benedict, M. A., and McMahon, E. T. (2006) *Green Infrastructure*. Island Press, Washington, DC.

Bertazzi, P. A., Bernucci, I., Brambilla, G., Consonni, D., and Pesatori, A. C. (1998) The Seveso studies on early and long-term effects of dioxin exposure: A review. *Environmental Health Perspectives*, 106 (Suppl 2): 625.

Bowler, D. E., Buyung-Ali, L., Knight, T. M., and Pullin, A. S. (2010) Urban greening to cool towns and cities: A systematic review of the empirical evidence. *Landscape and Urban Planning*, 97(3): 147–155.

Chaulya, S. K. (2004) Assessment and management of air quality for an opencast coal mining area. *Journal of Environmental Management*, 70: 1–14.

Choi, H. J., Kim, J. U., Kim, S. H., and Lee, M. H. (2014) Preparation of granular ceramic filter and prediction of its collection efficiency. *Aerosol Science and Technology*, 48(10): 1070–1079.

Currie, B. A., and Bass, B. (2008) Estimates of air pollution mitigation with green plants and green roofs using the UFORE model. *Urban Ecosystems*, 11(4): 409–422.

DEFRA. (2016) Paints and surfaces for the removal of nitrogen oxides. Air Quality Expert Group. http://uk-air.defra.gov.uk.

Delhomenie, M., and Heitz, M. (2005) Biofiltration of air: A review. *Critical Reviews in Biotechnology*, 25(1): 53–72.

De Nevers, N. (2000) *Air Pollution Control Engineering* (2nd ed.). McGraw-Hill, New York.

Donovan, R. G., Stewart, H. E., Owen, S. M., MacKenzie, A. R., and Hewitt, C. N. (2005) Development and application of an urban tree air quality score for photochemical pollution episodes using the Birmingham, United Kingdom, area

FOR REFERENCE PURPOSES ONLY

as a case study. *Environmental Science and Technology*, 39(17): 6730–6738.

Escobedo, F. J., and Nowak, D. J. (2009) Spatial heterogeneity and air pollution removal by an urban forest. *Landscape and Urban Planning*, 90(3–4): 102–110.

Escobedo, F., Kroeger, T., and Wagner, J. E. (2010) Urban forests and pollution mitigation: Analyzing ecosystem services and disservices. *Environmental Pollution*, 159 (8–9): 2078–2087.

Finlayson-Pitts, B. J., and Pitts, J. N. (1993) Atmospheric chemistry of tropospheric ozone formation: Scientific and regulatory implications. *Journal of the Air and Waste Management Association*, 43: 1091–1100.

Foster, J., Lowe, A., and Winkelman, S. (2011) The value of green infrastructure for urban climate adaptation.http://dev.cakex.org/sites/default/files/Green_Infrastructure_FINAL.pdf.

Freer-Smith, P. H., Beckett, K. P., and Taylor, G. (2005) Deposition velocities to *Sorbus aria*, *Acer campestre*, *Populus deltoides* × *trichocarpa* 'Beaupre', *Pinus nigra* and × *Cupressocyparis leylandii* for coarse, fine and ultra-fine particles in the urban environment. *Environmental Pollution*, 133(1): 157–167.

Fuentes, J. D., Wang, D., and Gu, L. (1999) Seasonal variations in isoprene emissions from a boreal aspen forest. *Journal of Applied Meteorology*, 38(7): 855–869.

Getter, K. L., and Rowe, D. B. (2006) The role of extensive green roofs in sustainable development. *Horticultural Science*, 41(5): 1276–1285.

Getter, K. L., Rowe, D. B., Robertson, G. P., Cregg, B. M., and Andersen, J. A. (2009) Carbon sequestration potential of extensive green roofs. *Environment, Science and Technology*, 43: 7564–7570.

Hammel, E. C., Ighodaro, O. R., and Okoli, O. I. (2014) Processing and properties of advanced porous ceramics: An application-based review. *Ceramics International*, 40(10): 15351–15370.

Heck, R. M., Farrauto, R. J., and Gulati, S. T. (2009) *Catalytic Air Pollution Control: Commercial Technology*. John Wiley & Sons, Hoboken, NJ.

Hunter, A. M., Williams, N. S. G., Rayner, J. P., Aye, L., Hes, D., and Livesley, S. J. (2014) Quantifying the thermal performance of green façades: A critical review. *Ecological Engineering*, 63: 102–113.

Jim, C. Y., and Chen, W. Y. (2008) Assessing the ecosystem service of air pollutant removal by urban trees in Guangzhou (China). *Journal of Environmental Management*, 88(4): 665–676.

Johnsson, J. E. (1998) Urban sources of air pollution. In: J. Fenger, O. Hertel and F. Palmgren (Eds.), *Urban Air Pollution: European Aspects*. Kluwer Academic Publishers, Dordrecht, the Netherlands.

Kambites, C., and Owen, S. (2006) Renewed prospects for green infrastructure planning in the UK 1. *Planning, Practice and Research*, 21(4): 483–496.

Kuo, Y. M., Huang, S. H., Lin, W. Y., Hsiao, M. F., and Chen, C. C. (2010) Filtration and loading characteristics of granular bed filters. *Journal of Aerosol Science*, 41(2): 223–229.

Matulevicius, J., Kliucininkas, L., Prasauskas, T., Buivydiene, D., and Martuzevicius, D. (2016) The comparative study of aerosol filtration by electrospun polyamide, polyvinyl acetate, polyacrylonitrile and cellulose acetate nanofiber media. *Journal of Aerosol Science*, 92: 27–37.

McPherson, E. G. (2010) Tools for valuing tree and park services. *Western Arborist*, 36: 58–63.

Natural England. (2010) Green infrastructure by design: Adding value to development. http://www.naturalengland.org.uk/.

Naumann, S., Davis, M., Kaphengst, T., Pieterse, M., and Rayment, M. (2011) Design, implementation and cost elements of green infrastructure projects. Final report to the European Commission, DG Environment, Ecologic Institute and GHK Consulting Berlin, Germany.

Niemelä, J., Saarela, S. R., Söderman, T., Kopperoinen, L., Yli-Pelkonen, V., Väre, S., and Kotze, D. J. (2010) Using the ecosystem services approach for better planning and conservation of urban green spaces: A Finland case study. *Biodiversity and Conservation*, 19(11): 3225–3243.

Nowak, D. J., Crane, D. E., and Stevens, J. C. (2006) Air pollution removal by urban trees and shrubs in the United States. *Urban Forestry & Urban Greening*, 4(3): 115–123.

Oliveira, S., Andrade, H., and Vaz, T. (2011) The cooling effect of green spaces as a contribution to the mitigation of urban heat: A case study in Lisbon. *Building and Environment*, 46(11): 2186–2194.

Owen, S. M., Mackenzie, A. R., Stewart, H., Donovan, R., and Hewitt, C. N. (2003) Biogenic volatile organic compound (VOC) emission estimates from an urban tree canopy. *Ecological Applications*, 13(4): 927–938.

Park, J. H., Byeon, J. H., Yoon, K. Y., and Hwang, J. (2008) Lab-scale test of a ventilation system including a dielectric barrier discharger and UV-photocatalyst filters for simultaneous removal of gaseous and particulate contaminants.

FOR REFERENCE PURPOSES ONLY

Indoor Air, 18: 44–50.

Peirce, J. J., Weiner, R. F., and Vesilind, P. A. (1998) *Environmental Pollution and Control*. Butterworth-Heinemann, Boston, MA.

Pugh, T. A., MacKenzie, A. R., Whyatt, J. D., and Hewitt, C. N. (2012) Effectiveness of green infrastructure for improvement of air quality in urban street canyons. *Environmental Science & Technology*, 46(14): 7692–7699.

Qureshi, S., Hasan Kazmi, S. J., and Breuste, J. H. (2010) Ecological disturbances due to high cutback in the green infrastructure of Karachi: Analyses of public perception about associated health problems. *Urban Forestry & Urban Greening*, 9(3): 187–198.

Ribeiro, H., Oliveira, M., Ribeiro, N., Cruz, A., Ferreira, A., Machado, H., Reis, A., and Abreu, I. (2008) Pollen allergenic potential nature of some trees species: A multidisciplinary approach using aerobiological, immunochemical and hospital admissions. *Environmental Research*, doi:10.1016/j.envres.2008.11.008.

Sambaer, W., Zatloukal, M., and Kimmer, D. (2011) 3D modelling of filtration process via polyurethane nanofiber based nonwoven filters prepared by electrospinning process. *Chemical Engineering Science*, 66(4): 613–623.

Setälä, H., Viippola, V., Rantalainen, A. L., Pennanen, A., and Yli-Pelkonen, V. (2013) Does urban vegetation mitigate air pollution in northern conditions? *Environmental Pollution*, 183: 104–112.

Shareefdeen, Z., and Singh, A. (2005) *Biotechnology for Odor and Air Pollution Control*. Springer, Berlin, Germany.

Singh, A. P., Varshney, C. K., and Singh, U. K. (2007) Seasonal variations in isoprene emission from tropical deciduous tree species. *Environmental Monitoring and Assessment*, 131: 231–235.

Stewart, H. E., Hewitt, C. N., Bunce, R. G. H., Steinbrecher, R., Smiatek, G., and Schoenemeyer, T. (2003) A highly spatially and temporally resolved inventory for biogenic isoprene and monoterpene emissions: Model description and application to Great Britain. *Journal of Geophysical Research*, 108(D20): 4644–4666.

Tiwary, A., Williams, I. D., Heidrich, O., Namdeo, A., Bandaru, V., and Calfapietra, C. (2016). Development of multi-functional streetscape green infrastructure using a performance index approach. *Environmental Pollution*, 208: 209–220.

Tiwary, A., Sinnett, D., Peachey, C., Chalabi, Z., Vardoulakis, S., Fletcher, T., and Hutchings, T. R. (2009). An integrated tool to assess the role of new planting in PM 10 capture and the human health benefits: A case study in London. *Environmental Pollution*, 157(10): 2645–2653.

Tiwary, A., Morvan, H. P., and Colls, J. J. (2006) Modelling the size-dependent collection efficiency of hedgerows for ambient aerosols. *Journal of Aerosol Science*, 37(8): 990–1015.

van Loon, G. W., and Duffy, S. J. (2000) *Environmental Chemistry – A Global Perspective*. Oxford University Press, Oxford, UK.

Wang, D., and Fuentes, J. D. (2003) In situ isoprene measurements from foliage using a fast-response hydrocarbon instrument. *Agriculture and Forest Meteorology*, 116: 37–48.

WHO (2011) Urban outdoor air pollution database.http://www.who.int/phe/health_topics/outdoorair/databases/en/.

Yang, J., Yu, Q., and Gong, P. (2008) Quantifying air pollution removal by green roofs in Chicago. *Atmospheric Environment*, 42: 7266–7273.

Yang, D. S., Pennisi, S. V., Son, K., and Kays, S. J. (2009) Screening indoor plants for volatile organic pollutant removal efficiency. *Horticultural Science*, 44 (5): 1377–1381.

Yurika, N., Jonathan, L., and Gregory, N. (2006) Integrating air pollution, climate change and economics in a risk-based life-cycle analysis: A case study of residential insulation. *Human and Ecological Risk Assessment*, 12(3): 552–571.

Zhang, R., Liu, C., Hsu, P. C., Zhang, C., Liu, N., Zhang, J., Lee, H. R. et al. (2016) Nanofiber air filters with high-temperature stability for efficient PM2.5 removal from the pollution sources. *Nano Letters*, 16(6): 3642–3649.

FOR REFERENCE PURPOSES ONLY

Chapter 10

Air pollution impacts

10.1 EFFECTS ON VISUAL RANGE

Visual range has been considered a useful measure of urban air properties. Atmospheric particles reduce visibility by scattering and absorbing light. In Europe, this issue gets lower priority than many other environmental topics because there is no biological toxicity or clearly definable cost associated with it; however, it results in a pervasive and apparent reduction in environmental quality. In the US, impairment of visibility has been a much more significant issue because of the large areas of pristine national park, and legislation has been designed specifically to protect and improve visual range. The original Clean Air Act made it a goal to remedy any existing impairment of visual range due to air pollution, but recognised that understanding of cause and effect was too limited at that time to bring in legislation.

10.1.1 Regional haze in Asian megacities

Regional haze is visibility impairment caused by a multitude of sources and activities, which emit ultrafine particles and their precursors and which are located across broad geographic areas. There is a natural variability of visual range with humidity and background aerosol. The value of atmospheric attenuation coefficient (σ) decreases (i.e. the visual range increases) with wavelength (Table 10.1), with the value at 0.7 μm (red) typically being about half that at 0.4 μm (blue). Winter weather factors – such as high humidity and situations when warmer air aloft holds colder air at the surface – intensify haze formation in Asian megacities such as New Delhi, Beijing and Chongqing. In winter, slower airflow and stable atmospheric outer layers – which inhibit smog diffusion – plus the burning of coal and agricultural residue for heat result in much more hazy days than in other seasons. Primary carbon and secondary sulphate particles have been identified as the main components of the aerosol responsible for light scattering. Sulphate has been associated with 45%–90% of the light extinction coefficient on the 20% most impaired

FOR REFERENCE PURPOSES ONLY

days. These particles or their precursors may be transported 1000 km from their sources.

In 2016–2017 residents of Beijing, Tianjin, and many other northern Chinese cities suffered through one of the longest stretch of stifling air pollution ever recorded in the country. They choked through eight continuous days of thick, light-blocking haze, starting 30 December 2016. This stretch of bad air began only a week after people in 70 northern Chinese cities were enveloped by similar days of haze composed of high concentrations of $PM_{2.5}$. This included black carbon from incomplete combustion as well as sulphates and nitrates from industrial and transport emissions. Geography plays an important role in increasing episodes of regional haze in Chinese megacities. For example, the Beijing-Tianjin-Hebei region is surrounded by mountains which block diffusion of the haze and the resulting air pollution becomes worse during winters.

Table 10.1 Variation of visual range and extinction coefficient

Descriptor	*Visual range/km*	*Attenuation coefficient σ/km^{-1}*
Haze	3	1.1
Light haze	8	0.5
Clear	15	0.28
Very clear	40	0.1
Exceptionally clear	60	0.07

The earliest haze measurements were made as coefficient of haze (COH). The COH is determined by drawing 300 m of air through a filter tape, and comparing the optical absorbance of the stain on the tape with standards. The COH = 100 × absorbance, and the critical value of six has been identified as a level that could cause adverse symptoms in sensitive individuals such as asthma sufferers. The US EPA uses deciviews to specify changes in visual range. The *deciview* is to visual range measurement what the decibel is to sound measurement. The definition is not very tight – 'a one deciview change in haziness is a small but noticeable change under most circumstances when viewing scenes in Class I areas'. The scale is derived by observing a large range of values of visual range for the same scenes and then comparing differences qualitatively to identify the smallest perceptible changes at different visual range values. It indicates the perceived change, and has the advantage that, for example, a three deciview change when the visual range is poor will mean as much to the observer as a three deciview change when the visual range is good. In contrast, an absolute change in visual range expressed in km would represent a huge change at poor visual range or a tiny one at large visual range.

These changes in visual range have also been related to the mass loading of particles in the air. From empirical analysis of extinction values, mass loadings and chemical analyses, a dry extinction coefficient has been developed for each aerosol component corresponding to the amount of light extinction (in units of Mm^{-1}, or inverse megametres) caused by 1 μg m^{-3} of that component. The dry value is then corrected for the effect of relative humidity.

FOR REFERENCE PURPOSES ONLY

We have already seen Chapter 3 the variations in the size distributions of particles in the atmosphere from a multiplicity of natural and human sources. The optical properties are likely to be most strongly influenced by the surface area of the particles rather than by their number or mass distributions. The key radius range for light scattering is around the wavelength of visible light, which covers the band 400–700 nm (0.4–0.7 μm). Although individual dust storms, which may be a result of wind erosion from poor land management practices, can produce very high particle loadings, the particles themselves are comparatively large in diameter, do not scatter light effectively per unit mass, and soon sediment out. In contrast, *urban particles* are formed from gas-to-particle conversions (e.g. condensation of volatiles from combustion smoke, or photochemical formation of ammonium sulphate from ammonia and sulphur dioxide) and are in the size range which not only accumulates in the atmosphere because Brownian diffusion and sedimentation are both ineffective but also scatters light effectively.

10.1.2 Rayleigh scattering

Very small particles (<0.03 μm) scatter according to the Rayleigh mechanism that applies to molecules, so that the scattering coefficient is proportional to λ^{-4}. There are relatively few of these tiny particles in the atmosphere because they coagulate with each other very rapidly, so this strongly wavelength-dependent scattering mode is usually dominated by molecular scattering. Under some circumstances, however, such particles may be significant. The particles formed from the condensation of biogenic volatiles (e.g. pinenes from the conifers in the Smoky Mountains, US or from eucalyptus in the Blue Mountains, Australia) are around 0.1 μm in diameter; small enough to scatter blue light preferentially and create the eponymous blue haze. This wavelength dependence also accounts for the blue colour of cigarette smoke.

10.1.3 Mie scattering

At larger diameters, the scattering is described by Mie theory. The theory derives a scattering cross-section for each particle based on its diameter and refractive index and the wavelength of the light. The theory is very difficult to apply usefully, because we do not usually know the variation of refractive index with particle size distribution, and even if we did the calculations are extremely complex. Mie theory predicts a total scattering ratio, K_s, which is the ratio of the apparent scattering cross-section S to the geometrical cross-section.

$$K_s = \frac{S}{\pi r^2}$$

This factor K_s can then be incorporated into the Beer–Lambert law that describes the reduction of flux density through a uniform medium on a macroscopic scale:

FOR REFERENCE PURPOSES ONLY

$$I = I_0 \exp(-bL)$$

where:

I_0 is the initial flux density

I is the flux density after the beam has passed through distance L of a medium having extinction coefficient b

When scattering (the redirection of radiation without a change of wavelength) and absorption (the removal of energy followed by subsequent emission at a different, usually thermal, wavelength) are both present, b is the sum of a separate absorption coefficient (b_a) and a scattering coefficient (b_s), and we can write

$$b_s = \pi r^2 N K_s$$

where N is the number of scattering particles per unit volume. As natural aerosols are always polydisperse (contain a range of sizes), any practical procedure involves the multiple applications of Beer–Lambert for different combinations of wavelength, particle size distribution and composition.

$$b_s = \pi \int_{r_{min}}^{r_{max}} r^2 n(r) K_s dr$$

Table 10.2 Calculated contributions of gases and particles to the atmospheric extinction coefficient[a]

	Material				
	Air	*Particles*	NO_2	SO_2	O_3
Concentration	1.3 kg m^{-3}	40 μg m^{-3}	50 μg m^{-3}	50 μg m^{-3}	200 μg m^{-3}
Extinction coefficient at 550 nm/Mm^{-1}	11.6	160	8.6	10^{-5}	1.0
Contribution to extinction/%	6.4	88.3	4.7	<0.05	0.6

[a] The units for extinction coefficient are per million meteres, or per 1000 km. An extinction coefficient of 10.0 Mm^{-1} means that the flux density will have been reduced by a factor of 10n over a distance of 1 Mm.

Particles are highly effective light scattering materials, as can be seen from Table 10.2. The atmospheric extinction coefficient has been calculated for the *air* molecules that make up most of the gas in the atmosphere, for typical concentrations of the common gaseous pollutants, and similarly for particles. The contributions of the gases depend both on their concentrations and on their scattering effectiveness in the visible wavelength range. Despite

its overwhelming concentration, the air itself only makes a 6% contribution to the overall extinction coefficient. You really can see for ever on a clear day. In comparison, the tiny mass concentration of particles contributes nearly 90%. Note also that O_3 and NO_2 are much more effective than SO_2, which is one of the reasons for the severe effects of photochemical smog on visual range.

It should also be noted that it is the effectiveness of the particulate form of the material, rather than its opacity or refractive index, that is mainly responsible for the reduction in visual range. This can be seen most clearly by considering the effects of a specific concentration of water which is present either as vapour or as droplets. If 18 g m^{-3} water is present as vapour, the visual range would be over 200 km. If the same density of water is present as 10 μm droplets, the visual range drops to less than a metre.

10.1.4 Contrast reduction

An object can only be seen if there is an observable contrast between it and its background (i.e. a different flux density of light coming from the object compared to that coming from the background). The concurrent processes of scattering and absorption *increase* the amount of light travelling from a dark object to the observer, and *reduce* the light coming from the background (or *vice versa*). The contrast between the object and the background is thereby reduced. When this contrast drops to about 0.01 the object is invisible for practical purposes. Hence the visual range, commonly known as the visibility, is conventionally taken to be the distance in km at which the contrast between a white object and its dark background has fallen from 1 to 0.01. Even in a particle-free atmosphere, molecular scattering would limit the visual range to around 300 km.

Contrast reduction follows the Beer–Lambert law:

$$C = C_0 \exp(-bL)$$

where:

C_0 is the initial contrast

C is the contrast as observed at distance L

If the object is black and white, then $C_0 = 1$ by definition. The critical contrast at which the object can no longer be discerned has been the subject of some discussion. The most careful measurements have given values of C/C_0 of less than 0.01. However, this means that the object will only be distinguished on 50% of occasions at that level of contrast. To be on the safe side, the threshold has been internationally accepted as 0.02, which leads to Koschmeider's formula

$$L = \frac{3.91}{b}$$

FOR REFERENCE PURPOSES ONLY

where 3.91 = ln(0.02). Thus for $b = 0.004\ m^{-1}$, which is typical of a photochemical haze, $L = 1$ km. This is a very crude approximation, which varies with the physical properties of the particles, with the initial darkness of the object, and between individual observers. Nevertheless, it has been adopted to define the international visibility code (Table 10.3). The combined extinction coefficient of the atmosphere specified in Table 10.2 is 181 Mm^{-1}, which corresponds to a Koschmeider visual range of 22 km.

10.1.5 Hygroscopic particles

Many atmospheric particles, such as the natural sea-salt nuclei on which cloud droplets form and the man-made salts of ammonium nitrate and ammonium sulphate, are hygroscopic (they absorb water vapour from the air). At a sufficiently high relative humidity they deliquesce (dissolve into their own water content) to form a highly saturated solution droplet. As the relative humidity increases further, each droplet takes up more water vapour, increases in diameter and scatters more light. Figure 10.1 gives examples of calculated and measured changes of extinction coefficient (on the left axis, with the corresponding visual range on the right axis) with humidity for particles of both ammonium sulphate (on the left) and ammonium nitrate (on the right).

Table 10.3 International visibility code

Code no	*Description*	*L/km*	*b/km^{-1}*
0	Dense fog	<0.05	>78.2
1	Thick fog	0.05–0.2	78.2–19.6
2	Moderate fog	0.2–0.5	19.6–7.8
3	Light fog	0.5–1.0	7.8–3.9
4	Thin fog	1–2	3.9–2.0
5	Haze	2–A	2.0–1.0
6	Light haze	4–10	1.0–0.39
7	Clear	10–20	0.39–0.20
8	Very clear	20–50	0.20–0.08
9	Exceptionally clear	>50	<0.08

FOR REFERENCE PURPOSES ONLY

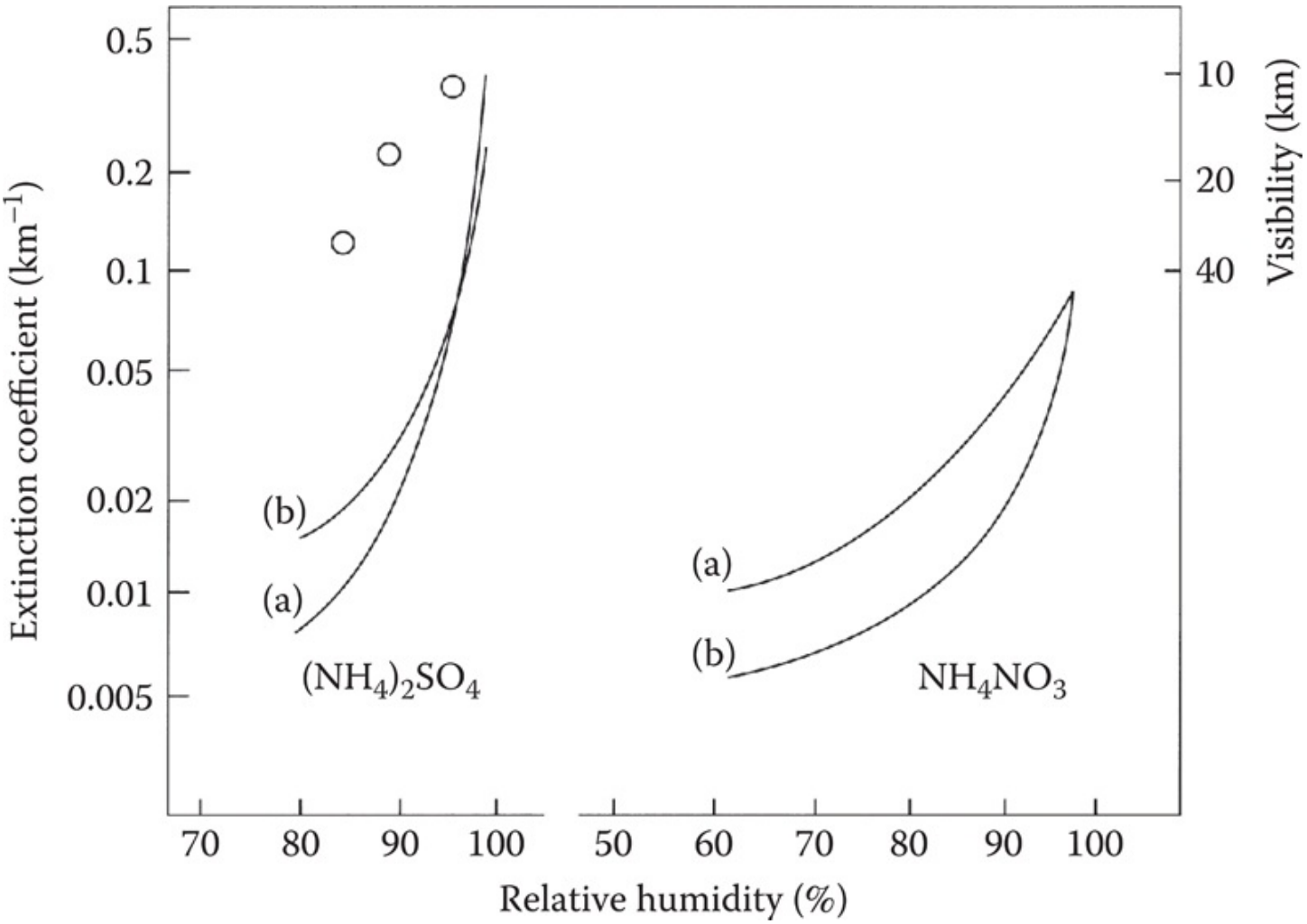

Figure 10.1 The variation of extinction coefficient (km^{-1}) with relative humidity for ammonium sulphate (left) and ammonium nitrate (right) aerosols. The salt concentrations are both 1 μg m^{-3}. The calculated curves (a) are for monodisperse aerosol; those marked (b) for polydisperse aerosol; and the open circles are experimental points for an ammonium sulphate concentration of 20 μg m^{-3}.

At high relative humidity the visibility becomes a sensitive function, so that when such particles accumulate in stable air under a temperature inversion, rising atmospheric humidity can increase the effective size of the scattering centres and reduce the visual range, a characteristic feature of photochemical smogs. The difference between hygroscopic and non-hygroscopic particles is shown more clearly in Figure 10.2. Aerosol collected at the Grand Canyon was exposed to controlled relative humidities in the range 10%–96%, and the scattering coefficient determined.

The change in scattering coefficient is expressed as the growth factor, which is the ratio of the scattering coefficient in the humid air to a reference scattering coefficient in dry air. On Day 216, when the proportion of soluble salts was low, the growth factor was quite insensitive to humidity. On Day 211, when soluble salts comprised 40% of the aerosol, the

FOR REFERENCE PURPOSES ONLY

growth factor started to increase at a relative humidity of 60% and eventually rose by a factor of three.

An overall relationship between particle concentration and visual range, taken from the US National Acid Precipitation Assessment Program (NAPAP), is shown in Figure 10.3. The concentrations of total suspended particulate matter normally measured in the English Midlands (around 30 μg m^{-3}) would result in a visual range of around 20 km. The NAPAP data also showed clearly the relationship between increasing SO_2 emissions and the reduction in visual range due to sulphate aerosol (Figure 10.4), particularly during the summer months (lower graph) when photochemical particle production rates are highest. Visual range contours over the United States (Figure 10.5) confirmed the expected pattern of high range in less populated regions and lowest ranges associated with the urban/industrial areas on the east and west coasts.

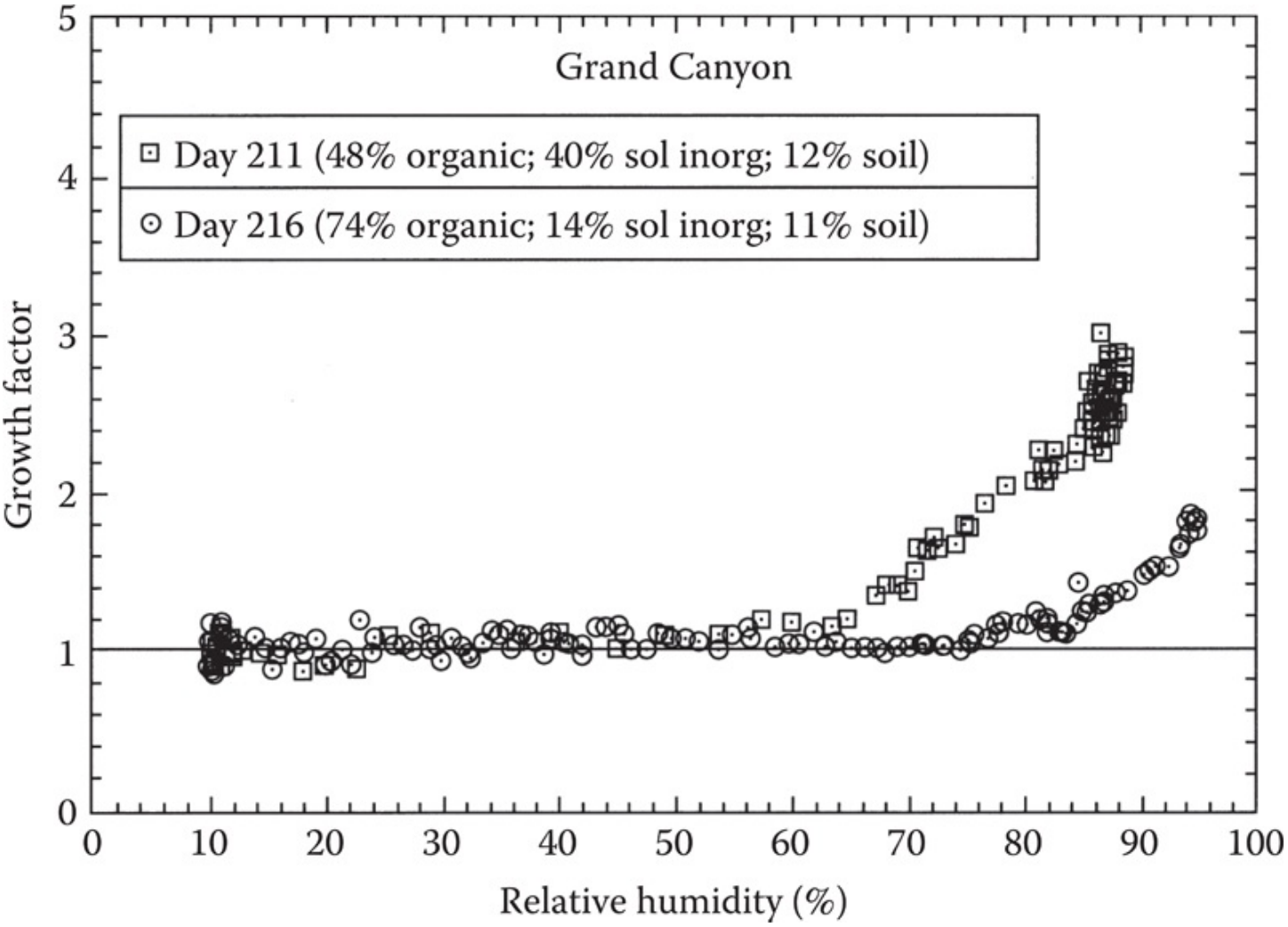

Figure 10.2 Scattering growth factors for aerosol at the Grand Canyon. (From Day, D.E. and Malm, W.C., Atmos. Environ., 35, 5169–5176, 2001.)

FOR REFERENCE PURPOSES ONLY

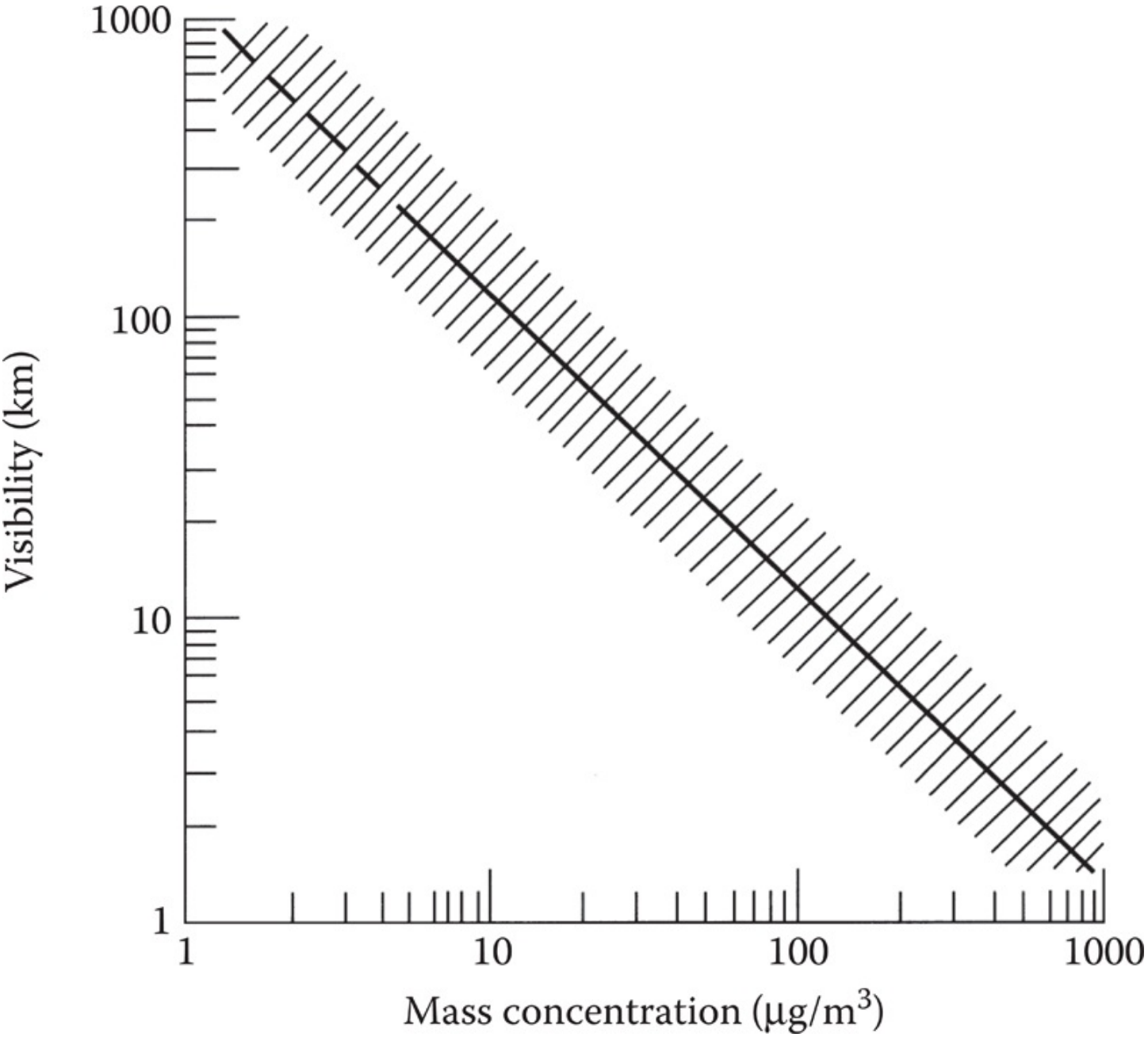

Figure 10.3 A general relationship between atmospheric visual range (km) and particle mass concentration. (From NAPAP, Interim assessment – The causes and effects of acidic deposition, National Acid Precipitation Assessment Program, Washington, DC, 1987.)

FOR REFERENCE PURPOSES ONLY

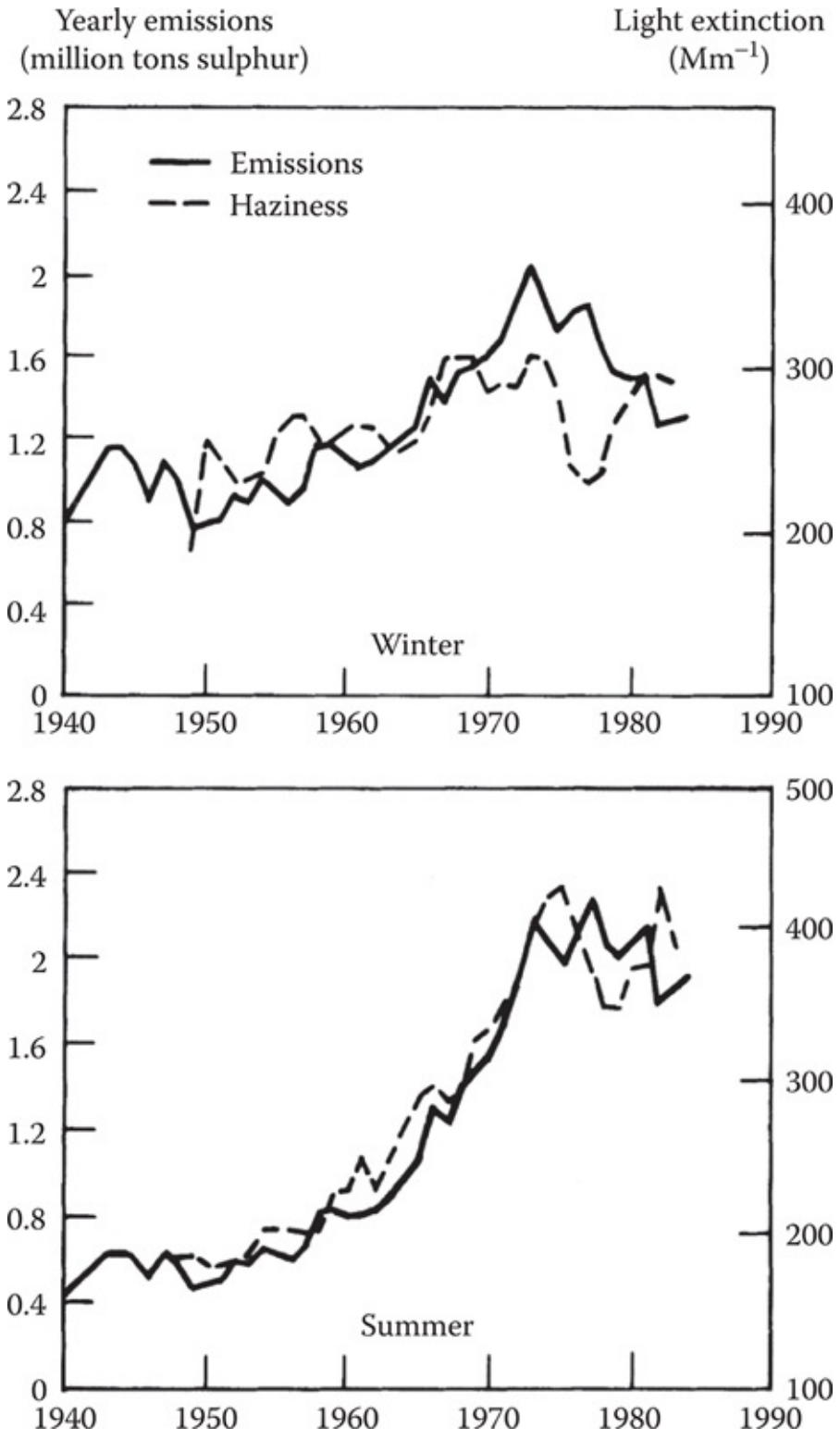

Figure 10.4 The historical relationship between sulphur emissions and atmospheric scattering for the south-eastern US, 1940–1990. Upper graph – winter; lower graph – summer. (From NAPAP, Integrated assessment report, National Acid Precipitation Assessment Program, Washington, DC, 1990.)

FOR REFERENCE PURPOSES ONLY

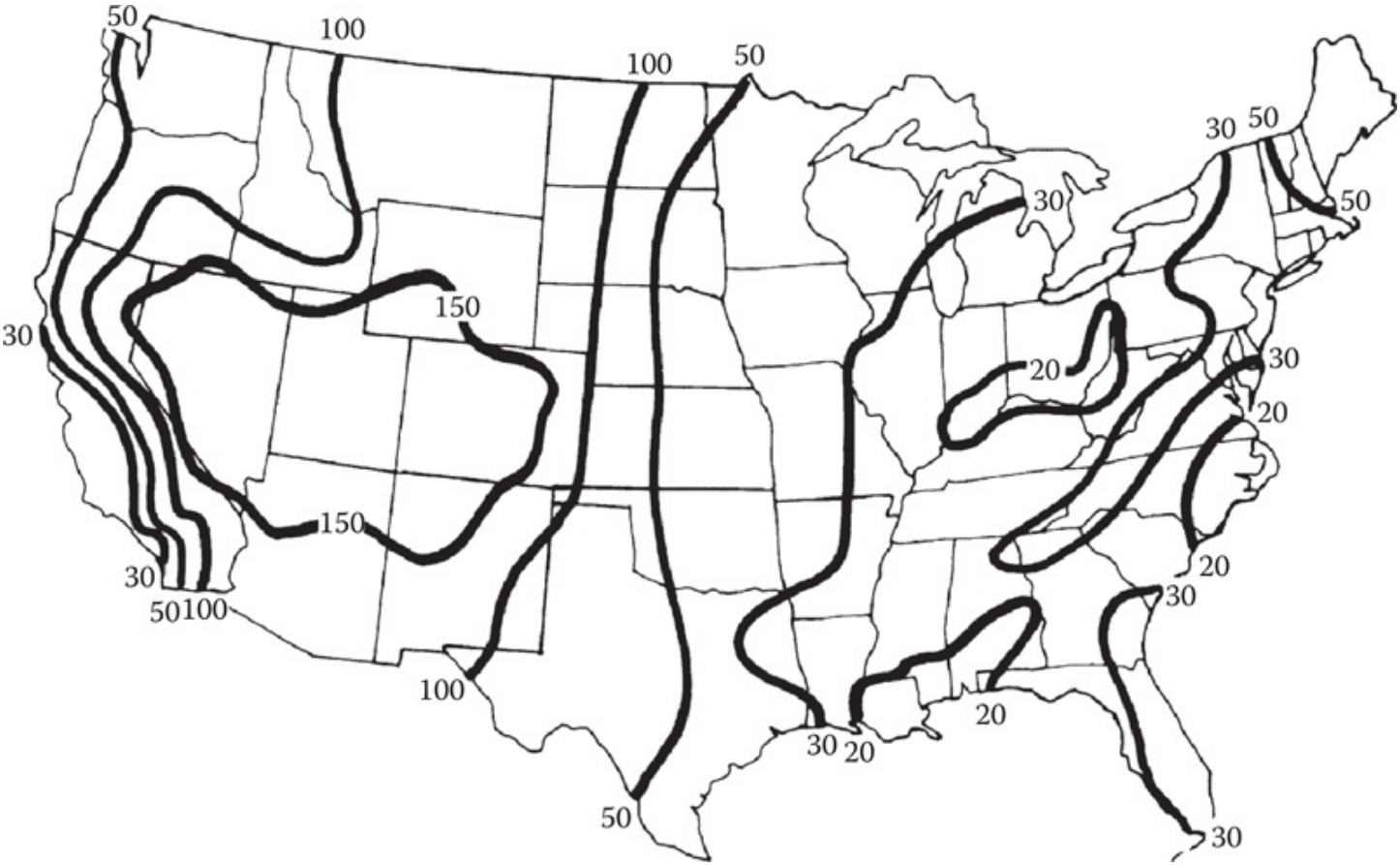

Figure 10.5 Contours of median visual range (km) for rural areas of the US. (From NAPAP, Integrated assessment report, National Acid Precipitation Assessment Program, Washington, DC, 1990.)

10.2 IMPACT ON HUMANS

The World Health Organisation (WHO) defines health as the state of complete physical, mental and social well-being, rather than the absence of disease or infirmity. By this definition, very few people could be classed as completely healthy. Hence identifying the health effects of pollutants (or anything else) becomes a matter of degree. WHO considers air pollution exposure as a significant determinant of human health. According to the evidence generated in the recent epidemiological literature, air pollution disproportionately affects the poorest and the most vulnerable population. The latter mainly includes children and elderly, and air pollution is increasingly becoming a global concern with the rise in the share of the elderly population (i.e. aged 80 years and over), largely due to improved longevity from wellbeing and medical advancements. By 2050, the average proportion of people aged 80 and above is expected to be more than 20%, however, regional increments over 30% are expected in North America, Europe (UN2015, World Population Prospects Report). Also, by 2050 the global population of 60 and above is projected to more than double its size in 2015, reaching nearly 2.1 billion Increased air pollution exposure reduces

FOR REFERENCE PURPOSES ONLY
life expectancy by increasing mortality and morbidity risks from heart disease and strokes, respiratory diseases, lung cancer and other conditions. Occurrence of respiratory diseases in South Asia resulting from air pollution, both indoors and outdoors, is estimated to be quite substantial. In addition to the direct heal risks, air pollution exposure also exacerbates disease risks and burdens from further interaction with other health determinants. There is still inadequate knowledge of the relative effectiveness of submicron particles compared with larger particles, or the specific roles of black carbon and organic carbon. This section covers the responses of humans and other animals to air pollution. Our understanding of human responses to air pollutants has come via a number of different routes. First, air pollution disasters in which the effects have been clear-cut; second, epidemiological studies of affected populations; third, controlled experiments on individuals and animal models. A number of different types of adverse health effect have been attributed to air pollution, although the severity of response depends greatly on the type of pollution, the level of exposure and individual susceptibility. Typical health effects include:

- Reduced lung functioning
- Irritation of the eyes, nose, mouth and throat
- Asthma attacks
- Respiratory symptoms such as coughing and wheezing
- Restricted activity or reduced energy level
- Increased use of medication
- Increased hospital admissions
- Increased respiratory disease such as bronchitis
- Premature death

Children are particularly susceptible to poor air quality, as they show enhanced response to atmospheric contaminants, both in terms of the severity and nature of the impact. This has been attributed to several reasons: children breathe more air per kg of body weight because they have a higher level of activity than adults; their breathing occurs mainly through mouth, which bypasses the process of deposition of pollutants in the upper respiratory tract and accentuates their deposition directly into the lungs. Long-term exposure to outdoor air pollution has been found to suppress the growth and development of children's lungs. Children with chronic illness such as asthma are also likely to be more adversely affected during periods of poor air quality. In a recent survey (2016), conducted by a reputed UK firm, almost 43% of 1015 parents of school age children ranked air pollution as the biggest health threat in London. However, the issue is further complicated by variations in public perception – for example, part of the reason for the steady increase in reported asthma cases is the increased public awareness that asthma exists and might be treatable. Table 10.4 shows the health effects of some of the common air pollutants.

In February 2016, the Royal College of Physicians published a report estimating that the costs of people who suffer from illness and premature deaths in the UK (including cots to the health services and businesses) add up to more than £20 billion every year. Each year in

FOR REFERENCE PURPOSES ONLY

the UK, around 40,000 deaths are attributable to exposure to outdoor air pollution, primarily linked to cancer, asthma, stroke and heart diseases, diabetes, obesity, and changes linked to dementia. The Environmental Audit Committee Action on Air Quality Report (2014) based on results from their own personal air quality monitoring states that, 'drivers and passengers in vehicles on congested roads are more at risk than people walking alongside busy traffic'.

While carbon dioxide is not considered as health impacting pollutant under ambient concentrations in the atmosphere, breathing air with more than 3% CO_2 can quickly lead to headaches, dizziness, increased heart rate and difficulty breathing. Further, at mixing ratios exceeding about 15%, CO_2 can even cause unconsciousness and death.

Table 10.4 Potential health effects and main sources of some common air pollutants

Pollutant	*Main source*	*Potential health effects*
Benzene	Motor vehicles	Causes cancer
	Chemical industry	Affects the central nervous system
Heavy metals (e.g. arsenic, cadmium, lead, mercury and nickel)	Industrial processes	Cause cancer
	Energy production	Give digestive problems
	Motor vehicles	Damages lung tissues
Nitrogen dioxide	Motor vehicles	Causes respiratory problems
	Other fuel combustion processes	Damages lung tissue
Ozone	Transformation of nitrogen oxides and volatile organic compounds produced by traffic in the presence of sunlight	Produces respiratory problems
		Reduces lung function
		Worsens asthma
		Irritates eyes and nose
		Reduces resistance to infections
Particulates	Fuel burning – e.g. diesel and wood	Cause cancer
	Industry	Produce cardiac problems
	Agriculture – e.g. ploughing, burning-off for fields	Give rise to respiratory diseases
	Secondary chemical reactions	Increase the risk of infant mortality
Sulphur dioxide	Fuel combustion	Causes respiratory problems

10.2.1 Episodes and epidemiology

10.2.1.1 Severe combustion smog

FOR REFERENCE PURPOSES ONLY

Ever since coal became the primary urban and industrial energy source, well before the Industrial Revolution got up to speed in the eighteenth century, people had suffered from exposure to high concentrations of toxic gases and particles. It is likely that significant numbers of people died from these exposures, but they were not recorded as such. Matters came to a head in the middle of the twentieth century, when severe pollution incidents in the Meuse Valley, Belgium in 1930; Donora, Pennsylvania in 1948 (see the case study presented at the end of this chapter); and London, England in 1952 and 1962 marked the peak of acute air pollution problems due to emissions from fossil fuel combustion. In all these cases, emissions from industrial and domestic coal combustion were trapped by topography and/or atmospheric temperature inversions. Concentrations of SO_2 and particles increased to levels that seem amazingly high today – in the 1962 London episode, the daily average SO_2 was 3000–4000 μg m^{-3} on three successive days, associated with peak particle loadings of 7000–8000 μg m^{-3}. Both morbidity (the illness rate) and mortality (the death rate) were clearly correlated with pollution, as is shown by the London data for 1962–1963 (Figure 10.6). Not only are the main spikes in early December coincident, but many of the minor features at other times within this period are apparently correlated. There were about 60 deaths that were statistically attributable to air pollution in the Meuse, 20 in Donora, and an extraordinary 4000 and 700 in London in 1952 and 1962, respectively. Mortality was highest among groups with existing respiratory or cardio-vascular disease. Morbidity was characterised by chest pain, coughing, shortness of breath, and eye, nose and throat irritation. Retrospective surveys have shown that similar but more minor incidents had occurred previously but not been recognised.

FOR REFERENCE PURPOSES ONLY

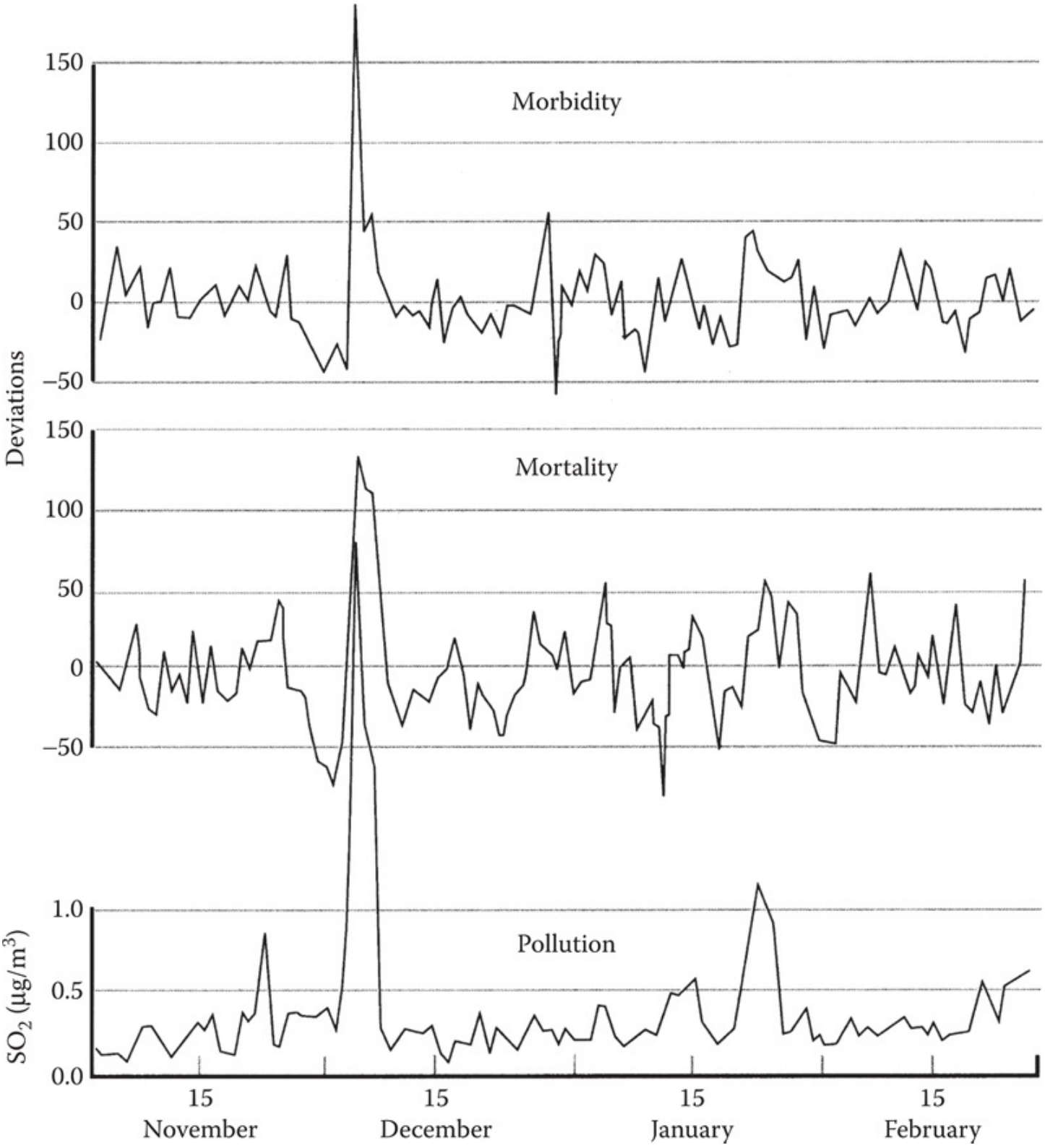

Figure 10.6 The variations of morbidity, mortality and SO_2 concentration during smog episodes in London between November 1962 and February 1963. (From Quality of Urban Air Review Group, Diesel vehicle emissions and urban air quality, Department of the Environment, London, UK, 1993.)

London had been known for its high incidence of fog for centuries. The severe air

FOR REFERENCE PURPOSES ONLY

pollution fog, or smog (smog = smoke + fog) was due to a synergism between SO_2 and soot particles. On its own, SO_2 is not toxic at the concentrations experienced. For example, maximum urban concentrations were around 3–4 ppm. The statutory safe limit for occupational exposure to SO_2, in which one is supposed to be able to work for the whole of one's working life, is 5 ppm, and the concentration has to be around 100 ppm before it is lethal. The respiratory tract reduces exposure to toxic gases. Gaseous SO_2 has a fairly high solubility in the aqueous mucosal fluids, so that about 95% has been absorbed before the inhaled air reaches the lungs, and only 1% penetrates to the gas-exchange surfaces of the alveoli. However, another penetration route is available when soot particles and water vapour are also present. Water vapour and SO_2 are absorbed onto the soot particles while they are all present together in the ambient air, and trace metals such as vanadium in the particles catalyse the formation of sulphuric acid. These particles are then inhaled. This mechanism focussed attention on particle inhalation processes and led to the identification of the aerodynamic size classes such as PM_{10} and $PM_{2.5}$ discussed previously.

FOR REFERENCE PURPOSES ONLY

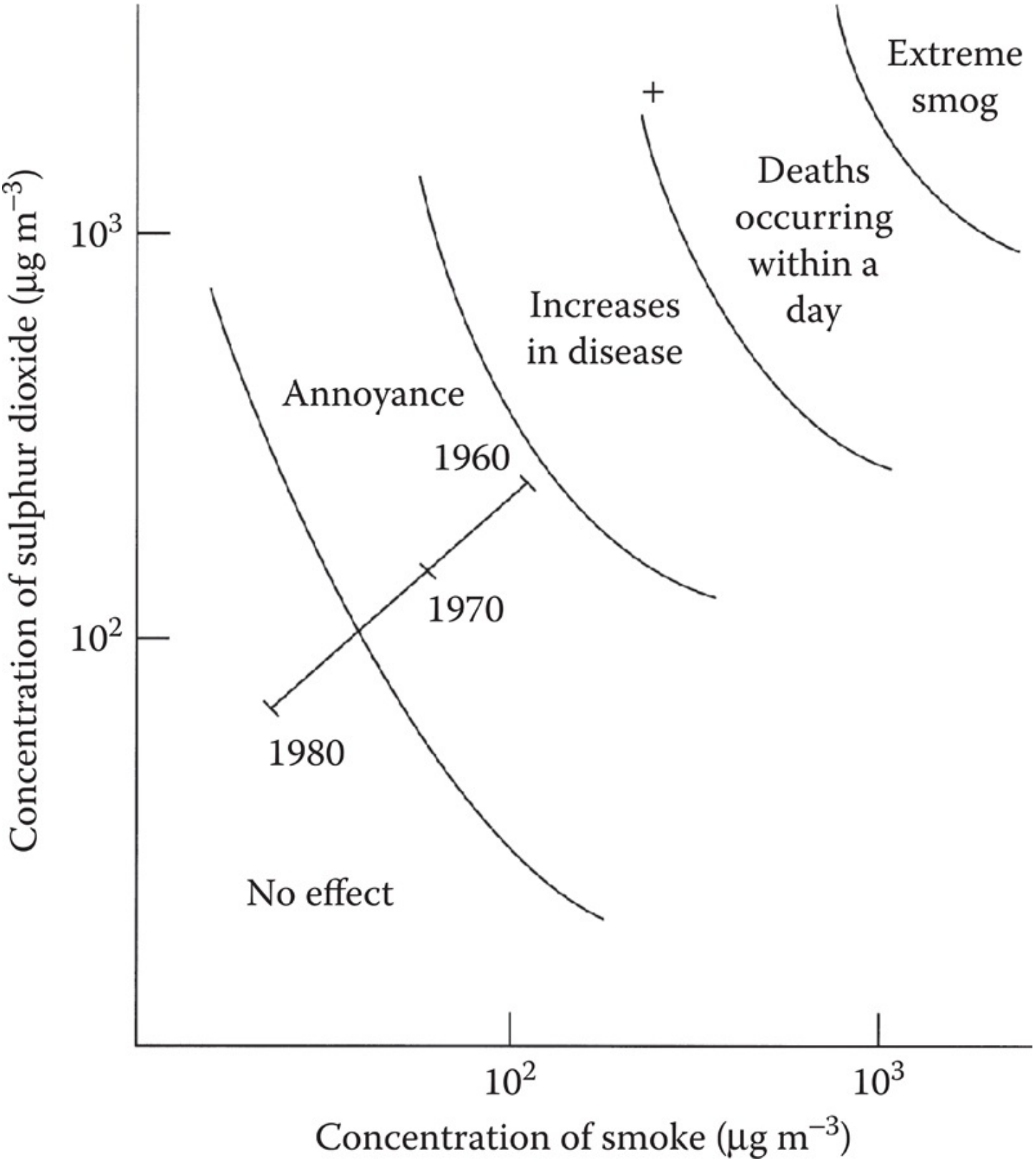

Figure 10.7 The health effects of combined exposure to SO_2 and smoke. The cross marks the worst day of the London smog in December 1952, while the straight line shows the trend in annual mean London concentrations between 1960 and 1980.

FOR REFERENCE PURPOSES ONLY

Compilation of data on morbidity, mortality and pollution concentrations from a range of smog episodes (Figure 10.7) indicates the bands of joint occurrence of particles and sulphur dioxide within which health effects of different severities may be expected. There is a trade-off between the two pollutants, with higher levels of SO_2 being acceptable when the concentration of particles is lower, and *vice versa*. It was concluded from the London smogs of 1952, 1956, 1962 and 1975 that a short-term significant response from chronic bronchitis to an air pollution episode could not be detected when the daily mean concentration of SO_2 was below 500 μg m^{-3} while the smoke concentration was at 250 μg m^{-3}.

This synergism has been incorporated into legislation: the EC, for example, has previously specified an annual mean of 120 μg m^{-3} of SO_2 unless the particle concentration is greater than 40 μg m^{-3}, in which case the upper limit for SO_2 is reduced to 80 μg m^{-3}.

10.2.1.2 Chronic low concentrations

The combustion smogs that were experienced in London in 1952 and 1962 were extreme examples of the responses of a large group of people to an air pollutant. In those and similar cases, the correlation between pollutant concentrations and morbidity or mortality was clearly identifiable. In the developed industrial countries, the reduction in air pollutant concentrations has almost eliminated these severe episodes. At the lower air pollution concentrations currently prevailing, effects are still probable, but relating them to a specific cause becomes much more difficult. The identification of the causes of a disease from a study of its occurrence is known as epidemiology. The results of such studies can be used to determine the effects of a particular pollutant and to predict the benefits of any future reduction. Many different experimental designs have been used.

- In a case-control study, the previous pollutant exposures of diseased individuals are compared with those of non-diseased controls.
- In a cohort study, disease incidence in groups having different exposures is compared over a period.
- In a cross-sectional study, a snapshot is taken of disease incidence and pollution exposure.

The Harvard Six-Cities study, described in Section 10.2.1.3, is a good example of a cohort study. About 20,000 subjects (adults and children) in the six cities were identified between 1974 and 1976. The cities themselves were chosen to represent a gradient of pollutant concentrations. Key pollutants were measured. The subjects were tracked for 17 years, during which periodic measurements were made of lung function and respiratory symptoms. Data were also compiled on their morbidity and mortality. Much effort was put into reducing the effects of so-called confounding factors, which are the non-air pollutant factors that vary between the populations and affect morbidity and mortality. Such factors include income, occupation, diet, exercise level, and smoking.

FOR REFERENCE PURPOSES ONLY

More recently, time-series analysis has been used to derive the relationships between concentrations and responses. Such analyses use sophisticated statistical methods such as Fourier analysis and auto-regression to discriminate the signal (changes in morbidity or mortality due to pollutant concentration changes) from the noise (changes in morbidity or mortality due to other causes). For example, although high and low temperatures both increase morbidity, high and low O_3 have opposite effects. Effects of confounding variables are reduced in time - series analysis, because these characteristics are relatively constant within the population from day to day. Seasonality (the recognised long-term correlation between time of year, pollutant concentrations and population responses) is the main confounding factor that must be taken into account.

There are many exposure metrics for which we need to know the response relationship. For a single pollutant such as ozone, there are acute responses to individual short term peaks (hourly means), or to sequences of such peaks (as would be experienced during a protracted ozone episode under unfavourable meteorological conditions). For such exposures, the recovery time after each peak influences the severity of response to subsequent peaks. There are also chronic responses to living in an area that has high average ozone concentrations. In addition to these types of response for individual pollutants, there are many combinations of co-occurrence with either additive or antagonistic effects.

10.2.1.3 Photochemical smogs

As already described, long-term measurements of urban SO_2 and particle pollution have shown concentrations falling steadily during the second-half of the twentieth century. Acute pollution disasters of the type that occurred in London in 1952 have been averted, and short-term correlations between illness and pollution concentrations cannot now be seen. However, evidence is accumulating that chronic levels of air pollution are responsible for significantly reducing the lifespan of the exposed population. Furthermore, there has been a steady increase in the incidence of respiratory illnesses such as asthma, which is strongly associated in the public's mind with vehicle pollutant emissions and photochemical smog. In fact, there is not yet sufficient evidence to show that specific pollutants, or air pollution in general, either initiates or promotes asthma. Major research programmes are going on around the world to decipher the interrelationships between air quality and health.

In the six-cities study, the results from which were published in 1993, cohorts of young people were selected in the 1970s from six US cities. Their health records and mortality rates were studied throughout the following two decades, and the concentrations of various air pollutants were also measured. The health of the cohorts was expressed in terms of a relative mortality, after allowing for confounding factors such as age, body weight, income and tobacco consumption. Figure 10.8a shows that there was indeed a relationship between relative mortality (here expressed as the ratio of the mortality rate in the target cohort to the rate in the control) and PM_{10} concentration; an even stronger relationship (Figure 10.8b)

FOR REFERENCE PURPOSES ONLY

was obtained when only the concentration of fine particles less than 2.5 μm was included.

As mentioned earlier, this is the fraction that can penetrate right down into the alveolar region of the lungs. This study showed that particle concentrations similar to those measured in European cities increased the relative mortality by 26% and reduced average lifespan by 2–3 years (compared with 15 years for smokers). The present view resulting from this and other work is that an increase of 10 μg m^{-3} in PM_{10} increases hospital visits by 2%–4% and total mortality by 1%, and that this gearing increases to 3.4% in the case of respiratory mortality. It has also been estimated that if the United States had achieved the targets for sulphate concentrations set in the Clean Air Act Amendments of 1997, around 2500 premature deaths would have been saved that year in the Eastern United States, with a monetary value of around $9 billion. The reduction would have had a correspondingly impressive effect on morbidity such as asthma, cardiac and respiratory illness. Attention has also been paid to ultrafine particles (less than 100 nm). These are always present in very large numbers (although their mass loading is usually small). Their small size makes them very reactive (large surface area per unit mass) and they may be able to penetrate through airway walls and into blood vessels.

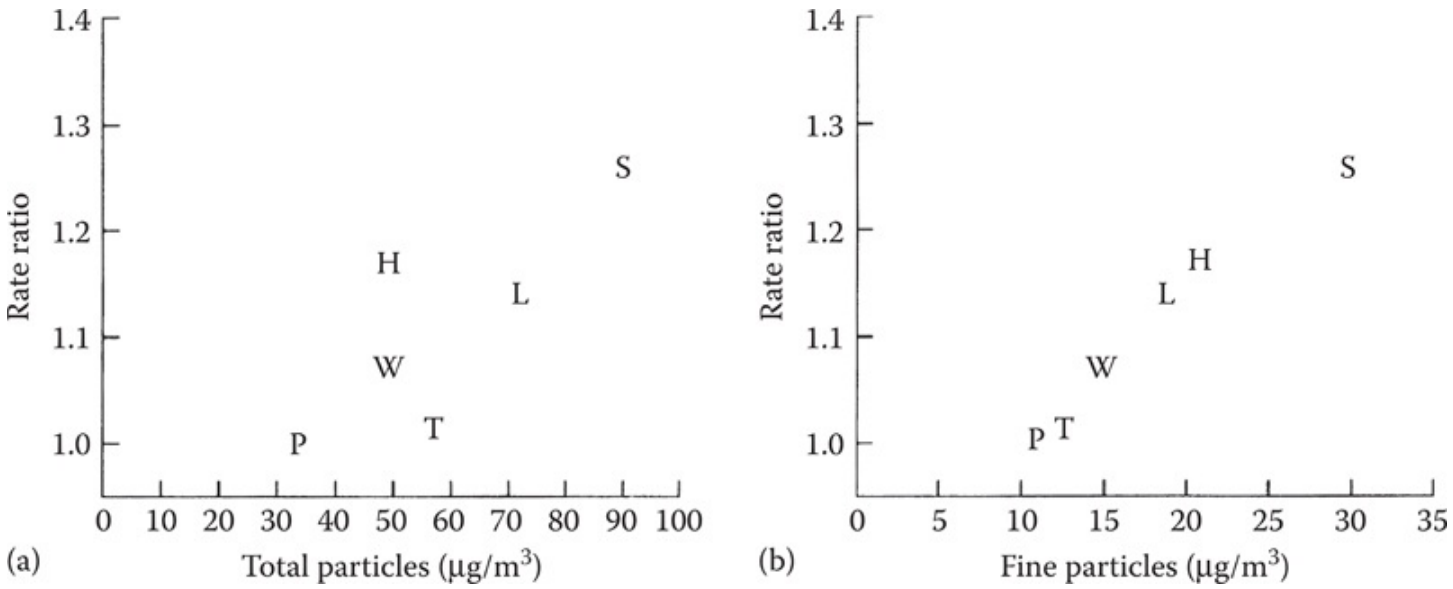

Figure 10.8 (a) The mortality ratio in six US cities as a function of total particle concentration. P is Portage, Wisconsin; T is Topeka, Kansas; W is Watertown, Massachusetts; L is St Louis, Missouri; H is Harriman, Tennessee and S is Steubenville, Ohio; and (b) shows the mortality ratio in six US cities as a function of $PM_{2.5}$ concentration. (From Dockery, D.W. et al., *N. Engl. J. Med.*, 329, 1753–1759, 1993.)

Combustion smogs were identified by the co-occurrence of carbonaceous particles and sulphur dioxide gas. In a similar way, sulphur dioxide interacts with sulphate particles to make it hard to separate the health effects of one from the other. The emitted SO_2 is

converted in the atmosphere to SO_3, which then combines with water vapour to create ultrafine droplets of H_2SO_4. This sulphuric acid aerosol is eventually neutralised by ammonia via the strong acid ammonium bisulphate (NH_4HSO_4) to the nearly neutral salt ammonium sulphate $(NH_4)_2SO_4$. The resulting particles are typically 0.5–1.0 μm in size, putting them in the accumulation mode with long atmospheric residence times and high penetration into the respiratory system. Hence there is always a division of the sulphur between these solid, liquid and gaseous species. The exact partition depends on the history of the emissions in the airmass, critical factors being residence time, photochemical conditions and sources of ammonia (high over agricultural areas, medium over urban areas, low over water bodies). Principal responses to the sulphate aerosol component are bronchospasm in asthmatics and chronic bronchitis. Even though sulphur emissions and concentrations have been decreasing dramatically in the older industrialised nations during the last 30 years, measurable responses to sulphate particulate have been determined at concentrations as low as 0.04–0.8 μg m^{-3}.

10.2.1.4 Animal models

It is not usually possible to study the responses of people to air pollutants under controlled conditions. An animal model, in this sense, is an animal for which the behaviour or results can be applied with some confidence to humans. Such models have been used to understand aspects such as pollutant deposition and clearance, as well as biological action. The experimental animals (which have often been mice, rats, hamsters, guinea pigs, rabbits, dogs or primates) have usually been normally healthy. Certain research areas have favoured certain species. For example, rats have become the species of choice for work on carcinogenicity, whereas particle deposition studies have required animals such as pigs that have lungs more similar to those of humans. In addition to work with healthy animals, animals with pre-existing conditions have been used to model the enhanced susceptibility to air pollutants found in humans with equivalent pre-existing conditions. Such conditions include age, dietary deficiency, asthma, allergy, bronchitis and lung disease. There are many difficulties and caveats in the interpretation of results from animal trials. For example, sensitivity of mice to gaseous pollutants varies widely between strains, and pollutant deposition to small animal respiratory systems is very different to that of humans. Nevertheless, much of our current understanding of air pollutant toxicology is due to work with these animal models.

10.2.1.5 Heat waves

Air quality often gets worse during a heat wave. According to the UK Office of National Statistics, during the 2003 Europe-wide heat wave almost one-third of 2000 additional deaths in the UK were caused by air pollution. Similarly, for the 2006 heat wave in the UK, the Health Protection Agency attributed a part of the 75 extra deaths per week for each

FOR REFERENCE PURPOSES ONLY

degree of increase in temperature to air pollution. It is suggested that an estimate of the increase in deaths brought forward from the increase in pollution during the heat wave periods can be made using established coefficients from time-series studies.

10.2.2 The respiratory system

The respiratory system is by far the most important route for entry of air pollutants into the body. The basic structure is shown in Figure 10.9. When the ribs and/or diaphragm are expanded, the increased volume (and hence reduced pressure) in the chest draws air in through the nose or mouth. The nasopharyngeal region is the complex of larger passages in the nose, sinuses and upper throat through which the air passes before going into the throat (trachea). In the tracheobronchial region, the trachea divides into two bronchi, each of which leads to one of the two lungs. The bronchi then branch repeatedly into bronchioles before ending, in the pulmonary region, in clusters of tiny sacs called alveoles (Figure 10.10). There are around 300 million alveoles in the lungs, each having an inflated diameter of about 0.25 mm. The total area of these alveoles is 50–100 m^2. The alveoles, where oxygen, water vapour and CO_2 are exchanged, effectively present a very thin membrane of large surface area to the blood supply.

All the internal surfaces of the respiratory tract are lined with various secretions. In many parts, the secretions are cleared continuously by cilia (motile hairs which wave in phase) to remove trapped material. There are about 200 cilia on the surface of each epithelial cell, they beat at about 10 Hz, and can move the surface fluid at speeds of up to 10 mm min^{-1}. This process is effective at removing dissolved gases and particles and undissolved particles. However, the very fine structure of the ciliated surface, with its large surface area, also makes it susceptible to the same gases. There are no cilia in the alveoles. The respiratory system is a beautiful example of a highly specialised multi-tasking design that has evolved to meet parallel requirements. The main task is the gas exchange in the alveolar region – 10–20 m^3 of air are drawn in per day by a healthy resting adult, substantially more during exercise. The air drawn in for this exchange is conditioned to constant temperature and humidity during its passage into the lungs.

FOR REFERENCE PURPOSES ONLY

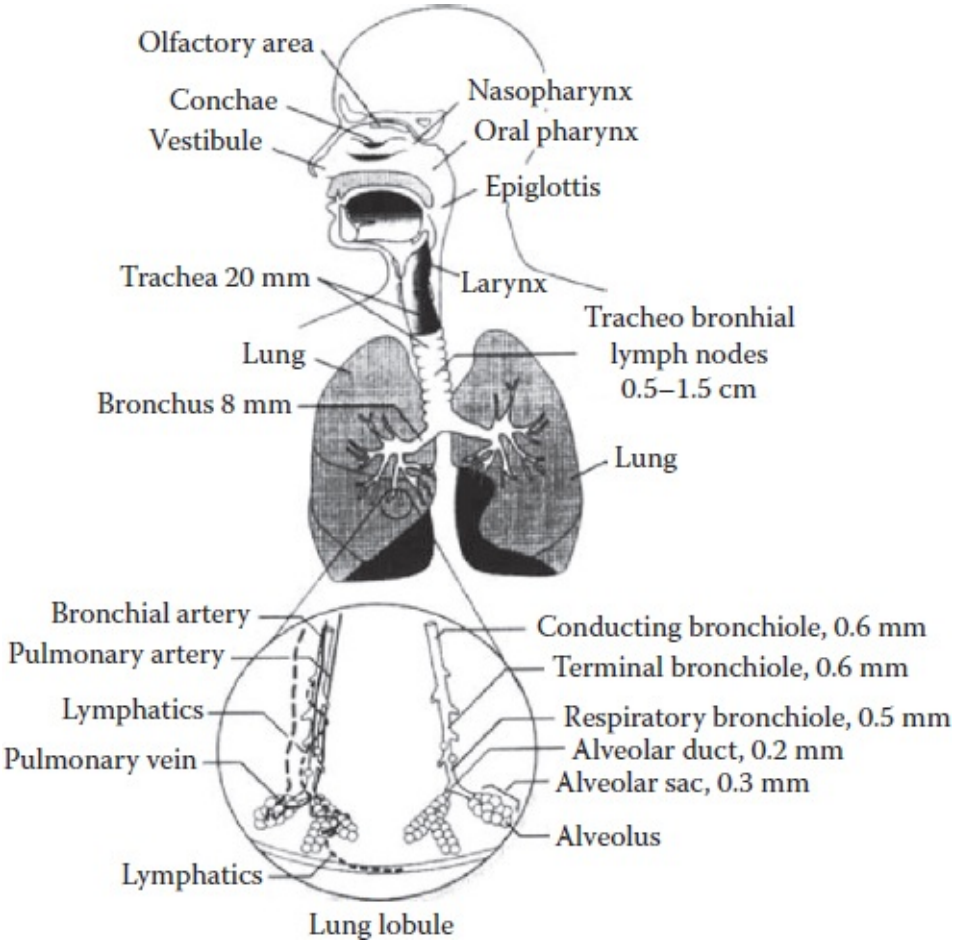

Figure 10.9 Structure of the respiratory tract.

FOR REFERENCE PURPOSES ONLY

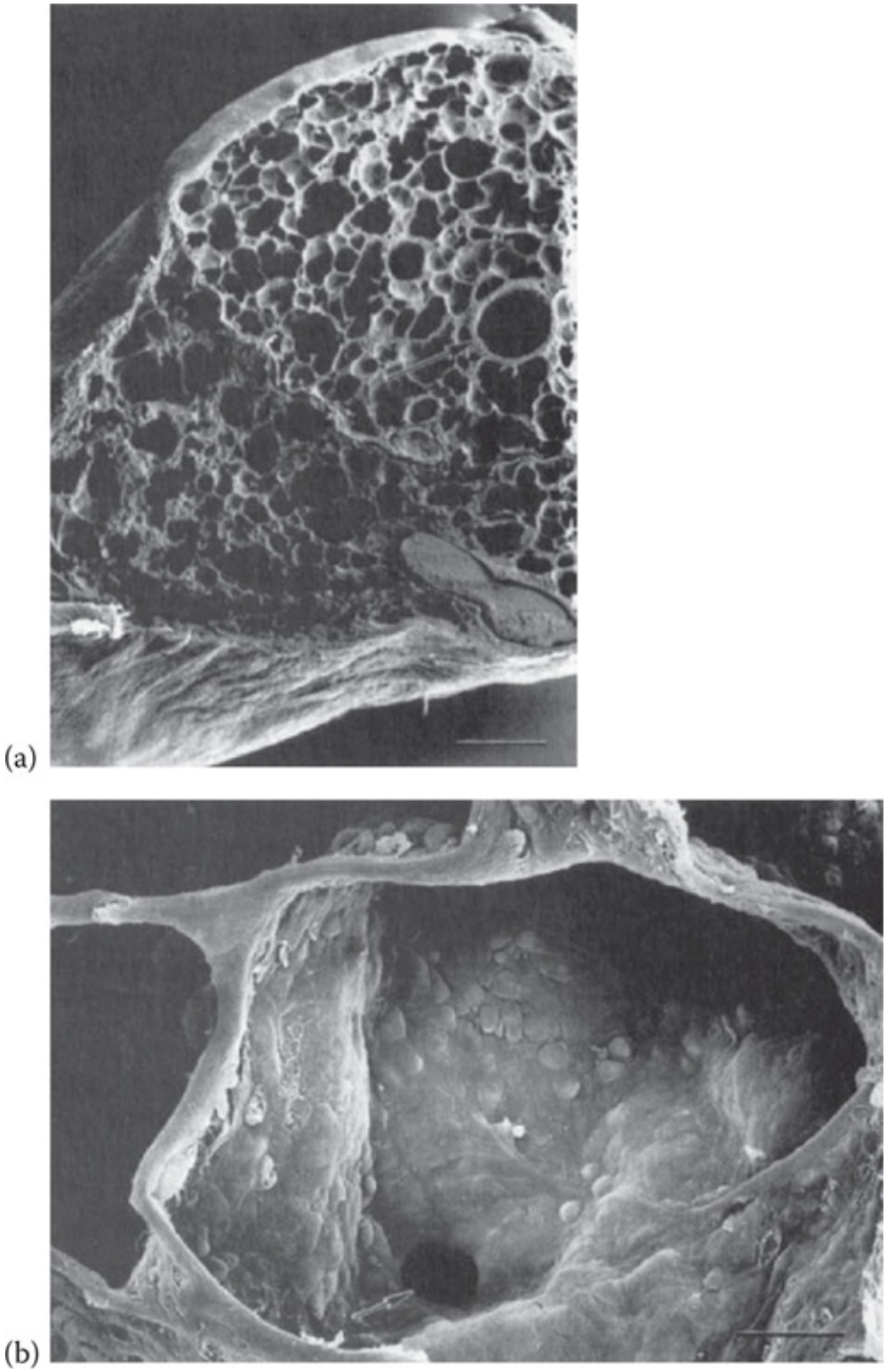

Figure 10.10 (a) Terminal bronchiole and associated alveole scale bar 200 μm and (b) an individual alveole scale bar 50 μm. (From Jeffery, P.K., Effects of cigarette smoke and air pollutants on the lower respiratory tract, in Holgate, S.T., Samet, J.M., Koren, H.S., and Maynard, R.L. (Eds.), *Air Pollution and Health*, Academic Press, London, UK, 1999.)

The sensitive alveolar surfaces are protected from particles by tortuous passages, hairs

FOR REFERENCE PURPOSES ONLY

and moist mucus linings. The moist linings also absorb some gases and are rich in antioxidants such as ascorbic acid, uric acid and glutathione. Absorbed gases and trapped particles are removed by mucus flow. Hence, broadly speaking, penetration of gases depends on solubility in aqueous solution, and penetration of particles depends on aerodynamic diameter (Table 10.5). The actual air exchange rate is itself variable. At rest, the tidal volume (the volume that flows in and out of the lung at each breath) might be only 0.5 l, exchanged every 5 s at 12 breaths min^{-1} to give a ventilation rate of 6 l min^{-1}. During heavy exercise these values could rise to 3 l every 2 s with a ventilation rate of 90 l min^{-1}. A value of 17.5 l min^{-1} is often used for gas and particle sampling.

Table 10.5 Dimensions and flows in the lungs

Region	*Number*	*Diameter* cm	*Total cross section* cm^2	*Cumulative volume* cm^3	*Typical velocity* cm s^{-1}	*Reynolds no.* Re
Nasal passages	2	0.65	0.6		550	2500
Trachea	1	1.7	2.3	70	145	1670
Main bronchi	2	1.3	2.7	80	125	1100
Divided bronchi	18	0.5	3.6	100	90	310
Bronchioles	500	0.2	16	150	20	28
Terminal bronchioles	1.2×10^4	0.07	47	200	7	3.4
Respiratory bronchioles	1.7×10^5	0.05	340	270	1	0.33
Alveolar ducts	8×10^5	0.08	4200	800	0.08	0.04
Alveoles	$3–5 \times 10^8$	0.015		3000		

Table 10.6 Air exchange rates during breathing

Activity level	*Pulse rate/min^{-1}*	*Air flow rate/min^{-1}*
Resting	70	6
Light exercise	80	10
Walking	110	20
Hard work	130–150	30–60

Flow in pipes tends to be turbulent above a Reynolds number of around 2000, so flow in the bronchi and below is laminar. The flow in the alveolar region is very slow and gentle

FOR REFERENCE PURPOSES ONLY

(air speeds less than 1 mm s^{-1}), even during heavy breathing (Table 10.6).

10.2.3 Responses to particles

The World Health Organisation estimates that about 2.4 million people die prematurely every year due to inhaling fine particles. The annual mortality attributable to outdoor air pollution for different world regions is shown in Figure 10.11, which indicates the highest mortality levels in the developing countries of Asia and the Pacific.

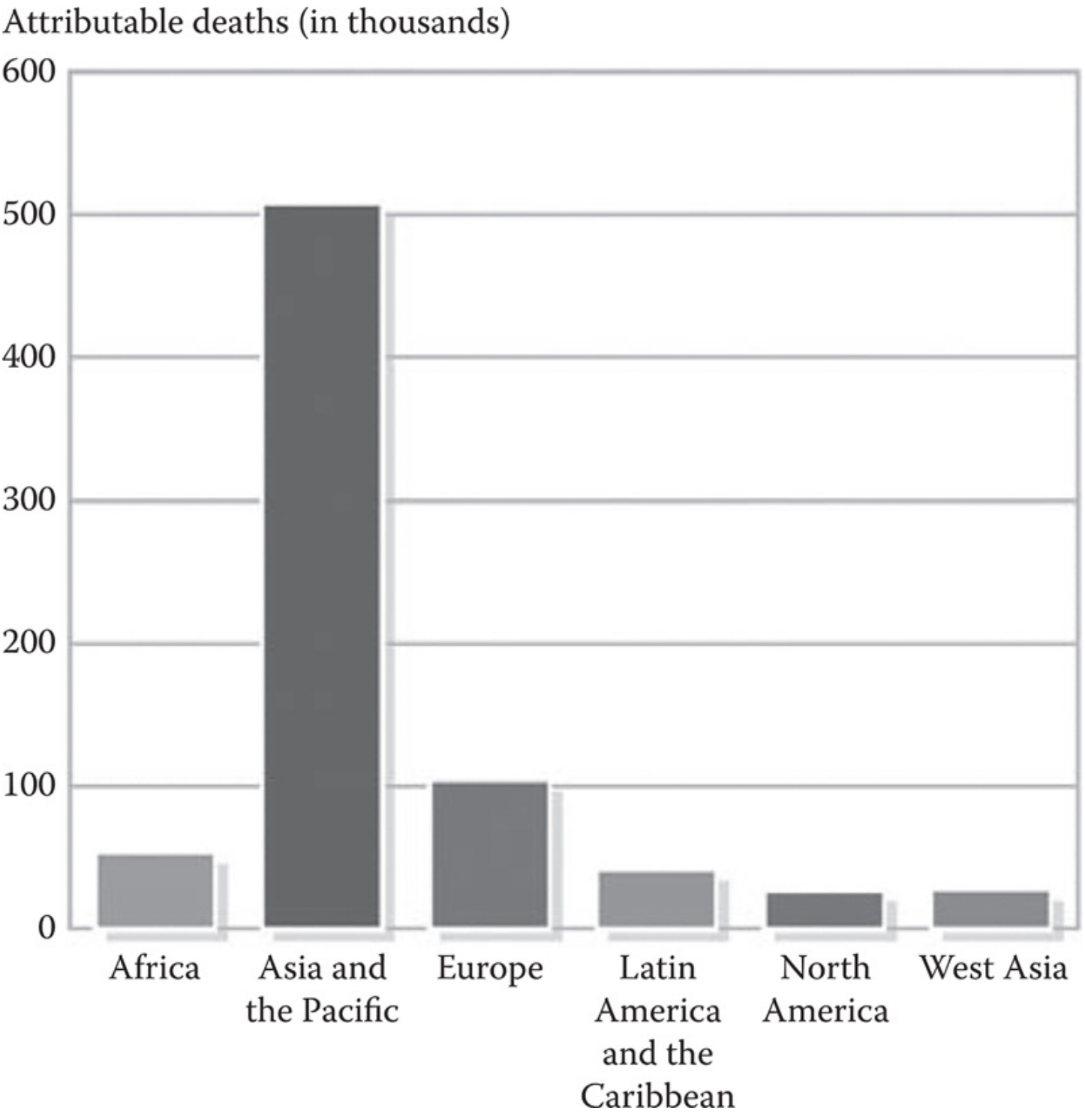

FOR REFERENCE PURPOSES ONLY

Figure 10.11 Premature deaths due to outdoor urban PM_{10} exposure by region in 2000. (From UNEP, Global environmental outlook – GEO4: Environment for Development, United Nations Environment Programme, Nairobi, KE, 2007.)

10.2.3.1 Particle deposition in the lung

In Chapter 3 we looked at particle deposition processes in general. One of the most important aspects of particle deposition is the way in which the construction of the human respiratory system interacts with the deposition processes to influence which particles are deposited in which regions. Research into this topic has been stimulated by problems in occupational health, cigarette smoking, and long-term exposures to low ambient aerosol concentrations. Studies have confirmed that particles are deposited in a fairly characteristic manner depending on the relationships between aerodynamic diameter, local airspeed and residence time. The initially inhaled particles are typically less than 100 μm. Particles larger than 50 μm are unlikely to be drawn in through the nose and mouth, because their terminal speeds are greater than the air speed into the nostrils. If they are drawn in, their stopping distance is greater than the passage dimension and they will be deposited immediately, before entering the trachea. For example, a 30 μm particle with a stopping distance of 1.6 cm will probably be deposited in the nasal passages (passage diameters less than 1 cm).

Those particles greater than 10 μm aerodynamic diameter are deposited efficiently by inertial impaction and interception on hairs in the nasal passages and the walls of the nose, sinuses and throat. The larger inhaled particles are known to become trapped in the mucus that lines the airways and are transported by cilia away from the lungs (the so-called mucociliary escalator) and subsequently expectorated or swallowed (gastrointestinal pathway). The respirable fraction (less than about 10 μm aerodynamic diameter) penetrate to the bronchi and may penetrate into the lower respiratory tract to reach the tracheobronchial region. Larger particles have high inertial impaction efficiencies where the airspeeds are high and the passages tortuous. The smallest particles have high Brownian diffusion velocities to the walls where the airspeeds are low, the passages small and the residence time long. Sedimentation also acts, although efficiency is low because the small particles have low terminal velocities. The combined effect of these processes is the deposition curve of Figure 10.12; there is a diameter range centred on 0.5 μm where total deposition is a minimum. This is the diameter region where atmospheric mass loadings are a maximum, for just the same reasons. This sub-range of particles, around 0.1–1.0 μm in diameter, is too small to either impact or diffuse to the walls efficiently and may penetrate deep into the lung. For the same reasons, the particles might be breathed out again before they can be deposited.

FOR REFERENCE PURPOSES ONLY

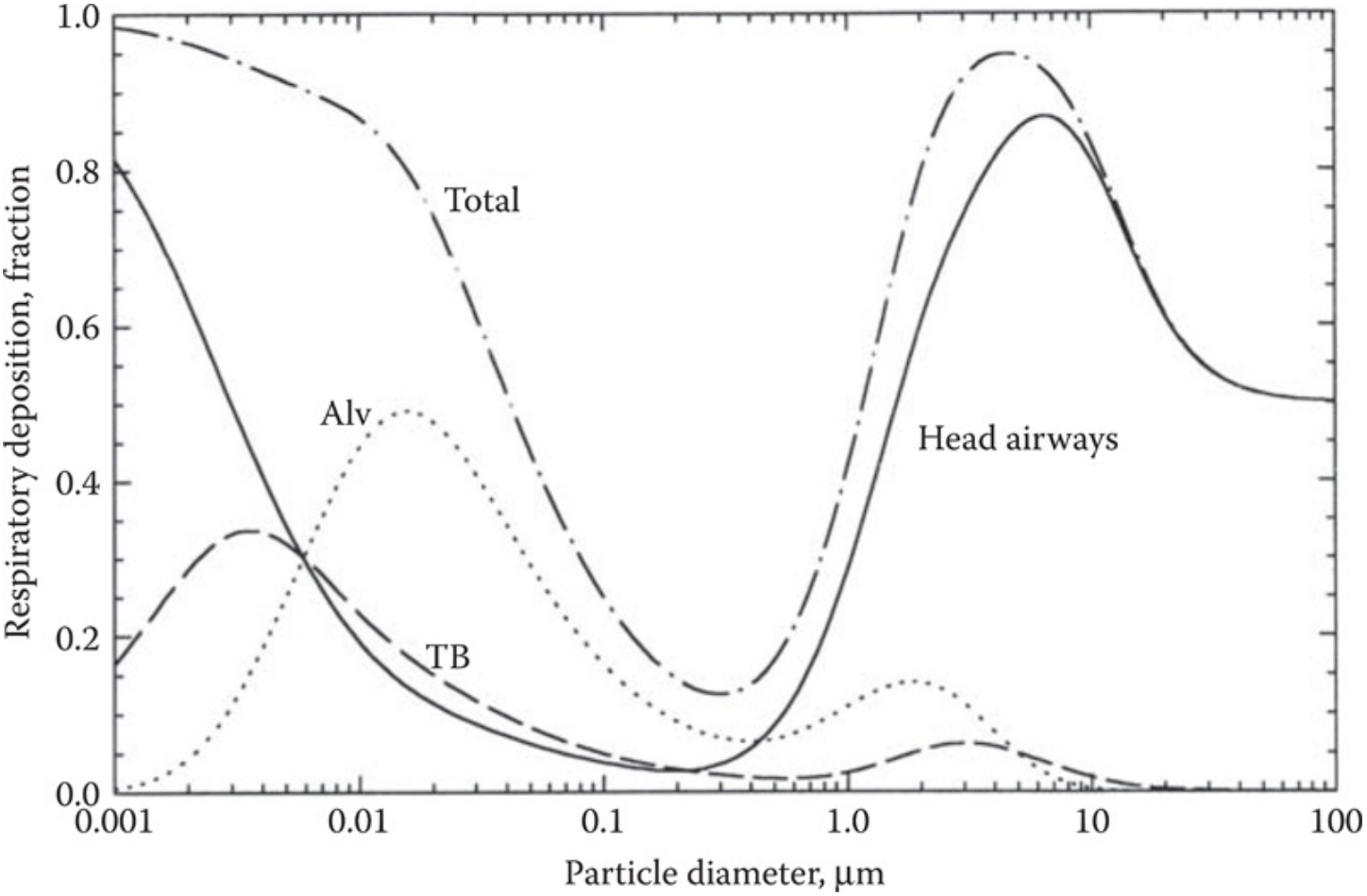

Figure 10.12 Deposition of particles in different regions of the respiratory tract. (From Hinds, W.C., *Aerosol Technology: Properties, Behaviour and Measurement of Airborne Particles*, Wiley, New York, 1999.)

Clearly, the breathing pattern influences the balance between deposition modes. During periods of rest, with shallow breathing, there are low airspeeds during inhalation and exhalation, and a significant intervening period when the air is stationary. We would expect impaction losses to be reduced, and settling and diffusion losses to be increased. During heavy exercise, not only would the reverse hold but the total volume of *processed* air would be increased.

An additional effect of increased tidal volume will be mouth-breathing, which will bypass the particle cleaning properties of the nose and increase the penetration of coarse particles. The change from nose to mouth-breathing normally happens at a volume flow rate of 30–40 l min^{-1}. If the inhaled particles are hygroscopic, as is the case with the most common photochemical ammonium sulphate and ammonium nitrate particles, the particles will absorb water vapour at the 100% humidity that prevails throughout the respiratory system. This will tend to increase their diameters and hence their deposition velocities, although the significance of this effect in humans is not known.

FOR REFERENCE PURPOSES ONLY

10.2.3.2 Standards for particle deposition

As the different parts of the respiratory system sample particles of different aerodynamic diameters with different efficiencies, any measurement system that is used to evaluate, for example, the mass loading of particles that can penetrate down to the alveolar regions of the lung must reproduce this efficiency variation. Several international groups have produced conventions that define the variation of sampling efficiency with diameter. The International Standards Organisation (ISO 7708) has defined four main fractions, which all have exact mathematical descriptions:

- *Inhalable*: The mass fraction E_I of total airborne particles which is inhaled through the nose and/or mouth. This is an empirical relationship which has been determined from wind-tunnel measurements on full-scale mannequins. It describes the efficiency with which the nose and mouth extract particles from the airstream blowing past the face, and is given by

  $$E_I = 0.5(1 + \exp[-0.06D]) + 10^{-5}\, U^{2.75} \exp(0.05D)$$

  where:
  D is the aerodynamic diameter of the particle in μm
  U is the wind speed in ms^{-1} (valid for $U < 10$)

  This fraction is potentially significant for understanding deposition and assimilation of coarse soluble particles in the nose and mouth.

  The remaining three fractions all use cumulative lognormal curves to define the proportion of total airborne particles that penetrate to specific regions of the respiratory tract. In each case the curve is defined by the median aerodynamic diameter and geometric standard deviation given in Table 10.7.

- *Thoracic*: The mass fraction of inhaled particles that penetrates the respiratory system beyond the larynx. Potentially of significance for diseases such as bronchitis, asthma and other upper-airway illness.
- *Respirable*: The mass fraction of inhaled particles that penetrates to the unciliated regions of the lung. Potentially of significance for deep-lung diseases such as pneumoconioses.
- *High-risk respirable*: This is applicable to vulnerable groups such as the sick or infirm, or to children.

The conventions are also shown in Figure 10.13. It can be seen that the ISO thoracic convention corresponds closely to the PM_{10} sampling definition. The 50% cut diameter of the high risk respirable convention corresponds to that for $PM_{2.5}$, although the variation about that diameter is not as sharp. These are efficiencies, not size distributions. To find the

FOR REFERENCE PURPOSES ONLY

size distribution of particles that penetrate to the thoracic region, the total airborne size distribution would be multiplied by the corresponding efficiency at each diameter across the distribution.

Table 10.7 ISO sampling conventions

Convention	*Median diameter/μm*	*Geometric standard deviation*
Thoracic	10	1.5
Respirable	4	1.5
High-risk respirable	2.5	1.5

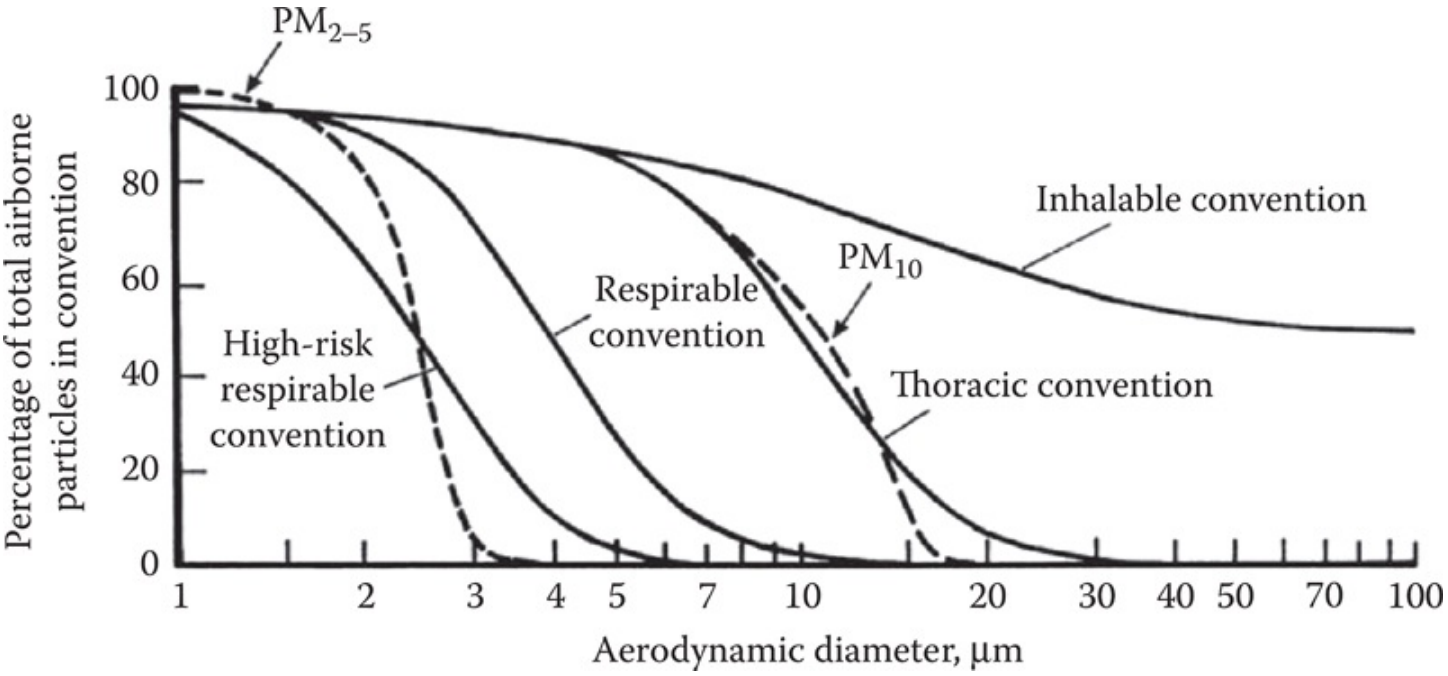

Figure 10.13 ISO particle deposition conventions. (From Harrison, R.M., Measurements of concentrations of air pollutants, in Holgate, S.T., Samet, J.M., Koren, H.S., and Mayhard, R.L. (Eds.), *Air Pollution and Health*, Academic Press, London, UK, 1999.)

The only device that can accurately reproduce deposition in the lung is the lung itself. We can approximate the lung deposition by measuring the fraction of particles below certain aerodynamic diameters. PM_{10} is used as a surrogate for the thoracic convention, and $PM_{2.5}$ for the high-risk respirable convention. Penetration through to different parts of the respiratory tract can hence be measured by appropriate samplers. These are usually impactor or cyclone-based, with suitably designed cut-offs. Porous polyurethane foam has also been used as a particle separator to allow the thoracic fraction to pass through to a collection filter. Some devices are able to measure either thoracic or respirable fractions by adjusting the flowrate (and hence cut diameter). The penetration through such a device can

often be reasonably described by a logistic model such as

$$\text{Penetration} = \frac{1}{1+(D_{\text{aer}}/k)^2}$$

where:

D_{aer} is the particle aerodynamic diameter

k is a constant

For example, if k = 10 μm, there will be 50% penetration for 10 μm particles.

10.2.3.3 Particle clearance

Clearance of deposited particles is another essential function of the respiratory system. If it did not occur the system would rapidly clog up. Clearance is brought about in the following main ways

- Dissolution and transfer into the blood
- Macrophage consumption
- Mucociliary transport to the larynx, then ingestion

FOR REFERENCE PURPOSES ONLY

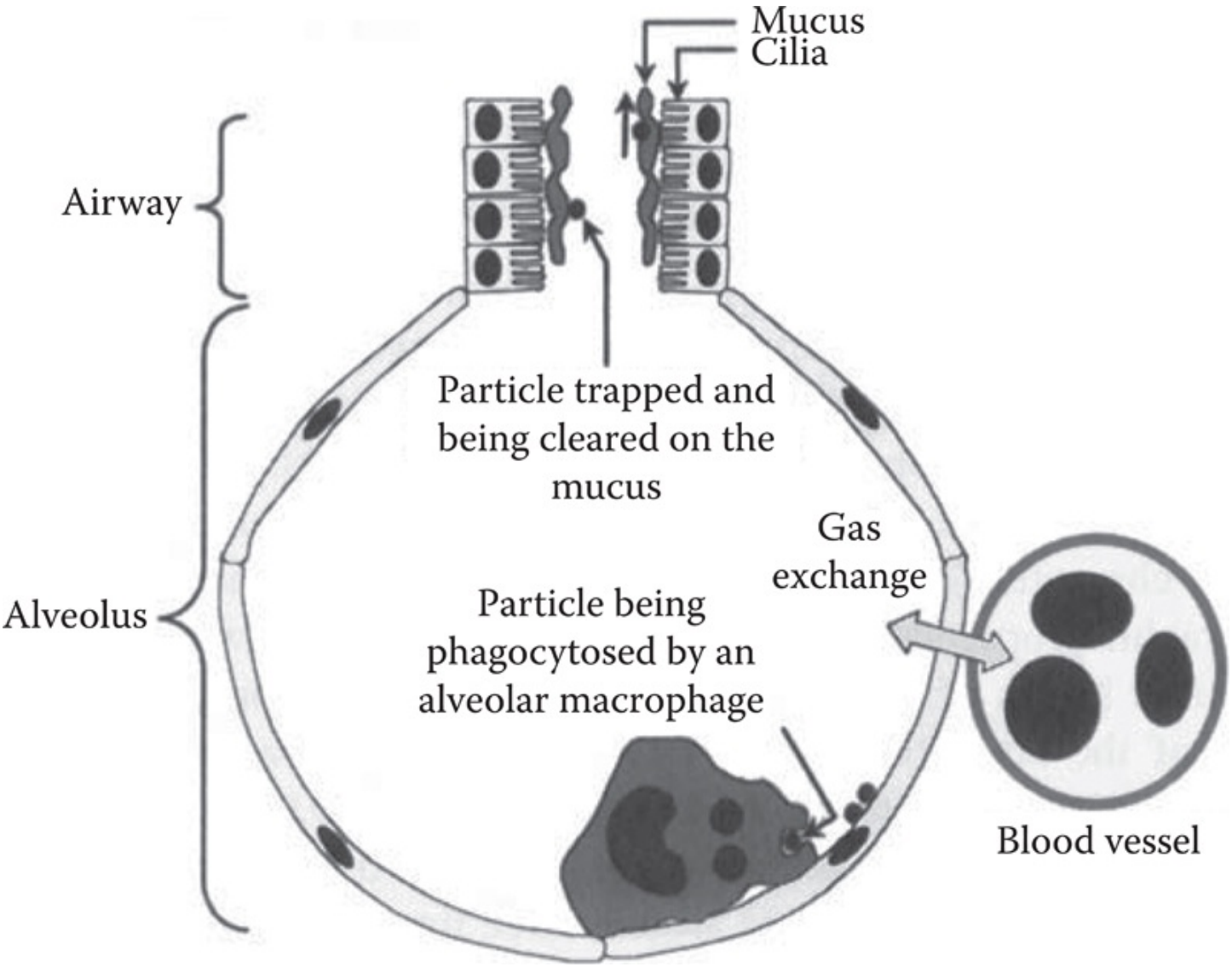

Figure 10.14 Particle removal mechanisms from the alveole. (From Stone, V. and Donaldson, K., *Aerosol Soc. Newsletter*, 33, 12–15, 1998.)

The layer of mucus which lines the breathing passages is moved towards the throat by the cilia and then ingested. Insoluble particles which have been deposited onto the epithelial surfaces of the lower respiratory tract are cleared by mucociliary action in a time scale of between a few hours and one day. The mucus speed is a few mm min^{-1} at the trachea, decreasing with each branching of the airways down to a few μm min^{-1}. Hence particles that penetrate deep into the lung have to be cleared greater distances, at lower speeds, than those deposited closer to the trachea. After one day the clearance rate drops sharply. Particles which have penetrated into the alveolar region, which is not protected by the mucous lining, are cleared more slowly (on a time scale of months) by dissolution and by macrophages. The latter are mobile cells that move around the surface of the alveole and engulf any particles encountered – a process known as phagocytosis (Figure 10.14).

The macrophage then migrates to the terminal bronchiole and is removed from the lung

FOR REFERENCE PURPOSES ONLY

by the mucociliary escalator. All these processes can be overloaded or bypassed under some conditions. The presence of particles stimulates mucus secretion by the goblet cells, although hypersecretion is characteristic of bronchitis. Chronic obstructive pulmonary disease (COPD) and smoking not only lead to hypersecretion of mucus by the goblet cells but also damage the mucociliary escalator. It is currently being suggested that the toxic effects of nanoparticles are a combination of overwhelming the macrophage defences by sheer numbers and the stimulation of oxidant species secretion with their large surface area. Perhaps surprisingly, there is also evidence that inhaled particles can affect organs other than the lungs. For example, there is increased incidence of thrombosis (clots) being formed in either the heart or brain. The mechanism is uncertain, but is believed to involve the production of coagulating chemicals in the blood due to inflammation by particles. Particles may also carry transition metals into the alveolar region, where they catalyse the formation of free radicals and increase oxidative stress.

Most of the chemicals present in particles (such as ammonium salts and carbon) are not toxic in other ways – by ingestion, for example. Hence there is something of a mystery as to how the high toxicity of very low concentrations of PM_{10} is achieved. There are differing opinions as to whether it is the presence themselves of tiny particles in large numbers (regardless of their composition), or the ability of these nanoparticles to deliver specific chemicals directly to the highly effective exchange region of the lung, or a combination of these. There is also debate about whether it is the number or surface area of the particles that controls their effects. Certainly at very high concentrations found in occupational environments, defence mechanisms such as macrophage removal may be overloaded, but this is not relevant at low ambient concentrations.

Fate of the inhaled pollutant particle is the key determinant of its impact on the human health, which largely depends on its chemical interaction with the lung component. A particle inhaled into the lung can reside in one of at least two *compartments*: the extracellular environment typified by lung fluid of neutral pH and the more acidic environment within macrophages. More recent studies have simulated particle deposition into lung by mimicking the composition and concentrations of *in vitro* lung bioaccessibility fluids, which represent the extracellular environment of the lung. The pioneer *synthetic lung fluid* (SLF), commonly referred to as Gamble's solution, has been widely used for the exposure assessment of humans to inhalable pollutants. Gamble's solution attempts to simulate the extracellular environment of the deep lung. A concentration of 100 mg L^{-1} dipalmitoyl phosphatidyl choline (DPPC) is suitable for mimicking the airway's fluid surfactant properties. A critical review of the published literature indicates that inorganic salts, surfactant lipids, large molecular-mass proteins, low molecular mass antioxidant proteins and organic acids are all native to the epithelial lung fluids of *healthy non-smoking humans* (Boisa et al., 2014).

10.2.3.4 Heavy metals

FOR REFERENCE PURPOSES ONLY

Particles of heavy metals, both from aerial and soil sources, have been linked to deterioration of the immune system, the metabolic system and the nervous system. Some heavy metals (e.g. arsenic and mercury) have been proven to be carcinogenic while many others have been found to cause distortion of human behaviour. Aerial depositions of heavy metals influence the quality of surface and ground water. In many developing countries, extensive use of water from open sources such as lakes and ponds has been the prime route of exposure to heavy metals for both humans and livestock. Heavy metal entry through food chain, associated with both plant uptake of the respective metals and accumulation of heavy metals in fish and birds (e.g. mercury in Scandinavia), have been considered to be the other major exposure pathway.

10.2.4 Responses to gases

10.2.4.1 Sulphur dioxide

At low concentrations of gaseous SO_2 alone, the first symptom to develop is bronchoconstriction, which leads to wheezing and is apparent after 1 min. Measurable increases in airway resistance of normally healthy people are found after 1 h of exposure to 1,000 ppb (Table 10.8). Although such concentrations were found in towns in the 1950s and 1960s, they would today only be associated with close proximity to a point source. Relief from exposure leads to recovery in about 30 min. As with other gaseous pollutants, responses increase in severity with the level of exercise, and tolerance develops during continuous exposure. People with respiratory complaints such as asthma or bronchitis are more at risk, responses having been measured at a minimum of around 100 ppb – this is lower than the peak UK concentrations of SO_2. Specific responses include changes to the tracheobronchial mucociliary clearance rate, alveolar macrophages and production of reactive oxygen species.

Table 10.8 Health effects of sulphur dioxide

Concentration/ppm	*Period*	*Effect*
0.03–0.5	Continuous	Bronchitic patients affected
0.5–1.4	1 min	Odour detected
0.3–1.5	15 min	Eye irritation
1–5	30 min	Increased airway resistance sense of smell lost
5–20	>6 h	Reversible lung damage
>20	>6 h	Waterlogging of lung tissues

A research programme in Europe called Air Pollution and Health – a European Approach (APHEA) conducted a meta-analysis of air pollution and health data sets from 15 European cities. The data covered the general period 1976–1991, although the exact period varied between cities. APHEA found that an increase of 50 μg m^{-3} in the 24-h average SO_2

FOR REFERENCE PURPOSES ONLY

concentration would lead to a 3% increase in mortality from all causes. Such an increase would also lead to an increase in hospital admissions due to chronic obstructive pulmonary disorder and a reduction in forced expiratory volume (FEV) of around 7%. There is currently no statistical basis on which these results could be applied to short pollution episodes.

10.2.4.2 Ozone

Fundamental ozone exposure is a direct function of the time sequence of airborne concentration inhaled by the individual, both outdoors and indoors. As it is generated by outdoor photochemistry and stratospheric intrusion, and deposits efficiently to most surfaces, the indoor ozone concentration decays rapidly.

The only likely indoor sources are photocopiers and electrostatic air cleaners. This concentration sequence is compounded by factors such as tidal volume – for example, a heavily exercising, heavily breathing person will extract the ozone (and any other air pollutants) from the air at a higher rate than a resting person. The removal efficiency of the respiratory system for ozone is around 90%. Unlike NO_2, O_3 is virtually insoluble in water but is highly reactive. Hence it is deposited along the whole of the respiratory system. About 40% of inhaled ozone is absorbed in the nasopharyngeal region, leaving 60% that penetrates to the lower respiratory tract. At concentrations above about 200 ppb, the ozone is thought to target the fatty acids and proteins that comprise cell membranes, and hence to damage cells in the bronchiolar and alveolar epithelia, leading in the short term to changes in lung biochemistry and induced localised airway inflammation. The released pro-inflammatory mediators can cause inflammatory cells such as macrophages and leucocytes to adhere to the endothelial cells that line blood vessels close to the site of ozone attack. Chronic ozone exposure seems to be associated with an irreversible thickening or stiffening of the lung tissue structure. Evidence from exposure of laboratory animals to ozone was summarised by the UK Advisory Group on the Medical Aspects of Air Pollution Episodes in 1991. They concluded that it is unlikely that current UK levels of ozone exposure would cause irreversible changes in the lungs or that summer pollution episodes would cause changes in lung biochemistry or localised airway inflammation. Getting at the truth can be difficult in these cases – for example, the highest O_3 concentrations in the UK occurred during the summer of 1976, and mortality and hospital admissions certainly increased. However, the episode was associated with unusually high air temperatures, which also result in increased mortality and hospital admissions. Unless a control is available for comparison, it is hard to determine the relative contributions of the two factors.

Experiments have also been performed on people in ozone exposure chambers, where the usual performance measure is FEV_1 (the volume of air in litres that can be breathed out by an experimental subject in 1 s). It has been shown that lung performance decreases with increasing ozone concentration (Figure 10.15), and that the more heavily the subject is exercising, the more she or he is affected. The results of these and similar experiments are

FOR REFERENCE PURPOSES ONLY

summarised in Table 10.9. Other measurements have shown that exposure on successive days shows acclimation, the response declining with repeated exposures. Because we breath in air pollutants, and asthma is an allergic response of the respiratory system, there is currently a widespread popular belief that ozone and photochemical smogs are affecting the health of the population in general, and of children and asthmatics in particular. The number of in-patient hospital treatments for asthma in England rose from around 40,000 in 1980 to over 100,000 in 1989, and a similar proportional increase in asthma incidence was reported by GPs over the same period.

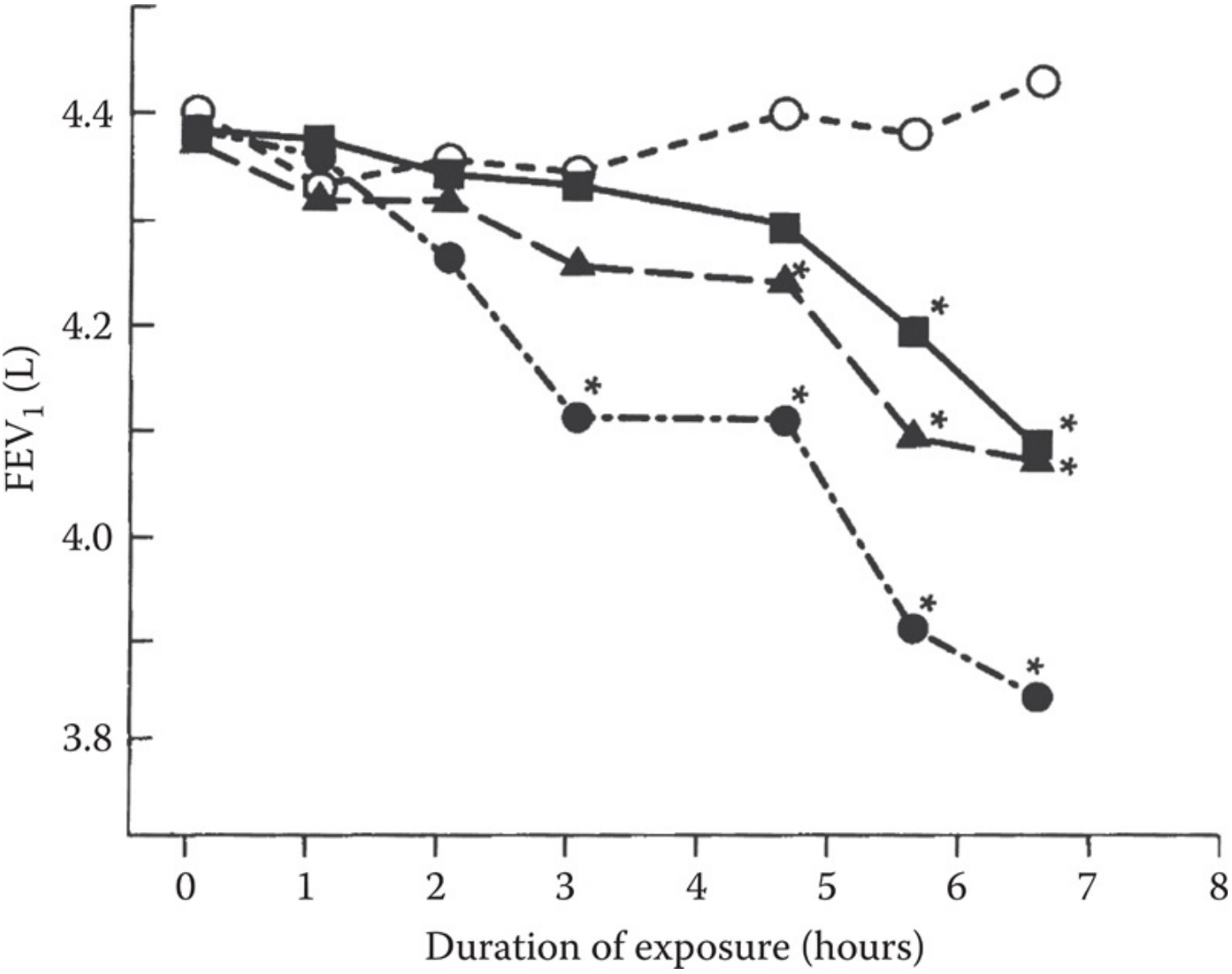

Figure 10.15 The effect of increasing concentrations of ozone on forced expiratory volume after 1 s (FEV_1). (From Lippmann, M., Ozone, in Lippmann, M. (Ed.), Environmental Toxicants, Wiley, New York, 2000.)

Table 10.9 Health effects of ozone

Ozone concentration (ppb) producing a 5% reduction in FEV_1 after various periods and levels of exercise

FOR REFERENCE PURPOSES ONLY

	2 h moderate	*2 h heavy*	*6.6 h moderate*	*2.5 h very heavy*
Normal person	300	250	70	160
Most sensitive	150–100	120–80	–	–

However, there is no proven increased susceptibility to ambient concentrations of air pollutants for those with chronic bronchitis, cardiopulmonary disease or asthma. An association with asthma is certainly suspected, but experimental and epidemiological evidence of chronic health effects is lacking. Many other factors, such as changes in lifestyle, exposure to new allergenic chemicals, and diet could be involved.

10.2.4.3 Nitrogen oxides

We have seen in Section 2.2.3 that NO and NO_2 are present in variable proportions in the outdoor atmosphere. While the initial emissions, principally from motor vehicles and other combustion sources, are usually dominated by NO, the latter is oxidised to NO_2 during photochemical reactions in the atmosphere, and ambient NO_2 concentrations may be higher than those of NO. There are also significant indoor emissions and exposures due to sources such as gas hobs. Of the two gases, NO_2 has much the higher toxicity to people; the occupational exposure limit for NO is 25 ppm, whereas that for NO_2 is 3 ppm. NO_2 has lower solubility than SO_2, so that a much higher proportion penetrates into the deep lung, and the main sites of action are the terminal bronchioles. As with other soluble gases, nasal breathing will protect better against NO_2 than oral breathing. NO_2 is a powerful oxidant, and it is thought that its main damage mechanism is destruction of cell membranes by lipid peroxidation. The body does have natural defences against this process due to antioxidant chemicals in the alveolar epithelium. High NO_2 concentrations can overwhelm the antioxidative defence capacity and allow penetration of the NO_2 through to the cell walls. There are also direct effects on the respiratory system, including increased airway resistance (due to inflammation), increased incidence of respiratory illness and damage to lung tissue.

Many of the studies over the past 30 years have been stimulated by concern over the indoor exposure due to gas cookers and other indoor combustion sources. Usually these have compared responses between houses with and without such sources. The consensus view is that there would be a 20% increase in the incidence of respiratory illness for children under the age of 12 if they live in a house with a gas cooker. Studies on adults have been less conclusive, showing a range of results from no effect to decreased lung function. Short-term exposure trials have shown that asthma sufferers may experience enhanced sensitivity after NO_2 exposure, and that those with normal respiratory function may experience increased airway resistance. For outdoor studies, it has often been difficult to separate NO_2 responses from those due to co-occurring pollutants, especially particulates. Short-duration exposure to NO_2 has also been shown to increase lung reactivity to other

FOR REFERENCE PURPOSES ONLY

pollutants (Table 10.10). Different workers have linked NO_2 exposure to a wide range of disease symptoms, such as intrauterine, infant and cardiovascular death, hospital visits for asthma, and chronic obstructive pulmonary disease. The low solubility of NO in aqueous media means that, when inhaled, it is more likely to penetrate deep into the lung and to diffuse through pulmonary tissue into the blood stream. There it binds to haemoglobin (Hb) to produce nitrosylhaemoglobin (NOHb), which is in turn oxidised to methaemoglobin (MetHb) in the presence of oxygen. However, exposures to NO concentrations as high as 10 ppm have shown no significant impairment of the blood's oxygen transport capacity. In fact, endogenous NO is an important component of the body's natural systems, such as nervous system signalling and regulation of pulmonary resistance.

Table 10.10 Health effects of nitrogen dioxide

NO_2 concentration range/ppm	*Effects (short-term only)*
0–0.2	No effects
0.1–0.2	Odour detected
0.2–1	Metabolic effects detected
1–2	Change of respiratory rate, increased likelihood of lung infection
2–5	Deterioration of lung tissue
>5	Severe damage to lung tissue, emphysema

10.2.4.4 Volatile organic compounds

Volatile organic compounds are important air pollutants for two distinct reasons. First, they are precursors required for the photochemical production of ozone. Second, they include species that are individually carcinogenic and mutagenic in their own right. The situation is complex, as there are several hundred chemical compounds involved and the most toxic (such as benzene) are not necessarily the most effective at ozone formation. It is usual to disregard methane from estimates of concentration, since although that gas is naturally present at ppm concentrations – dominating the other hydrocarbons – it is not toxic at those levels. It is, however, involved in ozone photochemistry. Typical compounds are propane, benzene, ethanol, methanol, ether, carbon tetrachloride and vinyl chloride; materials such as petrol, oil and resins may contain dozens of individual VOCs, and many more are produced during combustion processes.

10.2.4.5 Benzene

Data on urban hydrocarbon concentrations is now flowing from the UK DEFRA hydrocarbon network. Health effects have focused on benzene. Acute effects are only found at concentrations above 10 ppm, higher than is ever experienced in ambient air. Responses to prolonged ambient exposures have been predicted *pro rata* from industrial exposures to

higher concentrations. The main response is acute non-lymphocytic leukaemia. Hence there is a body of knowledge about responses to concentrations that are typically 1000 times those found in the ambient air, making it difficult to generalise or set limits. The WHO does not recommend a safe concentration for benzene because it is a carcinogen. Instead they give the geometric mean of the range of estimates of the excess lifetime risk of contracting leukaemia from a benzene concentration of 1 μg m^{-3}. This value is 6 cases per 100,000 population. Looked at another way, concentrations of 17, 1.7 and 0.17 μg m^{-3} would be expected to lead to 100, 10 and 1 case of cancer, respectively, in a population of one million. It is thought that benzene and 1,3-butadiene exposure may account for around 10% of leukaemia incidence across the UK. The present benzene *policy target* is 5 μg m^{-3}, with an eventual target of 1.5 μg m^{-3}.

The dominant contribution to benzene emissions used to be from petrol, either from combustion or evaporation. However, the benzene content of UK petrol was reduced from around 5% in 1990 to 1% in 2000, so that motor vehicle emissions contributed only 15% of the total 17 kt emission in 2006. Ironically, the benzene that had been added to maintain vehicle performance may have been a worse threat to human health than the lead that it displaced.

10.2.4.6 Toluene

Although toluene occurs naturally in crude oil, natural gas and natural combustion products, there is now a much greater presence from human operations. The main industrial sources are catalytic reforming at petroleum refineries, styrene production, coke ovens and solvent evaporation from paint, rubber, printing, cosmetics and adhesives. It is one of the components of petrol and so is released by combustion and evaporation. Around 25 kt (2006) are emitted in the UK, of which 25% is from petrol exhaust and 50% from solvents.

As with benzene, there is documented evidence of the acute effects of exposure to high toluene concentrations from workplace environments. The main recorded effects are dysfunction of the central nervous system resulting in behavioural problems, memory loss and disturbance of the circadian rhythm. Annual average concentrations outdoors in urban areas have been found to be similar to those of benzene at around 1 ppb, but there is uncertainty about extending these findings to predict responses to prolonged low-level exposures. For non-cancer effects, the US Environment Protection Agency (USEPA) has recommended that the long-term concentration should not be greater than 100 ppb.

10.2.4.7 1,3-Butadiene

Urban ambient levels are similar to those of benzene and toluene at around 1 ppb. 1,3-butadiene is carcinogenic; hence a safe threshold concentration cannot be specified, and the hazard must be estimated in terms of the risk of contracting cancer through lifelong exposure to a reference concentration. There have been no epidemiological findings that

FOR REFERENCE PURPOSES ONLY

have identified the risk due specifically to this chemical. Based on workplace observations at far higher concentrations and on experimental results from animal models, the UK set an air quality standard of 1 ppb.

10.2.4.8 Carbon monoxide

Carbon monoxide combines with blood haemoglobin 200 times more readily than oxygen. The resulting carboxyhaemoglobin (COHb) molecules can no longer transport oxygen from the lungs around the body, and hence the oxygen supply to the brain and other organs is reduced. The reaction is reversible, and exposure to clean air removes most of the gas from the body with a half-life of 3–4 h. The degree of CO absorption depends on its concentration in the air, the period of exposure and the activity of the individual. The WHO has calculated the relationship given in Table 10.11 between CO concentration and blood COHb for a lightly exercising person. The COHb values will be reduced by about a factor of two for a person resting, and increased by a similar factor by heavy exercise. The COHb concentration is around 0.5% when there is no CO in the atmosphere. Note that there is an equilibrium COHb concentration, so that longer exposure does not necessarily result in larger uptake. Also, the time to achieve equilibrium depends on airflow rate, so that equilibration that would take 4 h at rest would only take 1 h during hard exercise. Uptake rate depends on the difference between the applied concentration and the blood concentration. Hence the rate is maximum at the start and falls away as the blood concentration increases. Do not jog in the city on bad air-pollution days.

Table 10.11 Health effects of carbon monoxide

Ambient CO		*Carboxyhaemoglobin/%*		
ppm	mg m^{-3}	*After 1 h*	*After 8 h*	*At equilibrium*
100	117	3.6	12.9	15
60	70	2.5	8.7	10
30	35	1.3	4.5	5
20	23	0.8	2.8	3.3
10	12	0.4	1.4	1.7

Carbon monoxide is generated by combustion processes in which there is inadequate oxygen to produce CO_2. Three types of exposure represent the most severe situations. First, when an appliance such as a gas fire or central heating boiler has a blocked flue due to poor maintenance, or when open stoves are used for cooking. Not only do the combustion gases have a high CO concentration, but they cannot escape through the flue and come out into the building. Furthermore, CO is colourless and odourless which reduces its chances of detection. Around 1000 people in the US, and 50 in the UK die each year by this cause. Clearly, indoor exposure is a hazard for the population at large. Second, cigarette smoke

FOR REFERENCE PURPOSES ONLY
contains around 1% CO (10,000 ppm), so that heavy smokers may have 10% COHb. In addition, COHb crosses the placental barrier and results in a greater proportional change in the foetus than in the mother. Third, elevated outdoor ambient concentrations up to a few 10s of ppb CO may be created in urban centres by the restricted dispersion of motor vehicle exhaust gases. The highest COHb concentrations shown in Table 10.11 would be expected to result in a range of symptoms such as dizziness, nausea, headaches and measurably reduce mental performance. In the UK, CO concentrations in urban areas are monitored by the Automated Network, and show city centre 8-h maximum concentrations of a few ppm. A blood COHb of around 1% might be achieved from an exposure to 30 ppm CO for 1 h or about 9 ppm for 8 h. Such an exposure, which is typical of those expected of someone outdoors in a severely polluted urban environment, will cause minor symptoms such as headache in sensitive members of the population.

There is a lag in uptake of CO from the air and release back to the air, so calculating actual exposure from a time series of contacts with atmospheres at different concentrations is difficult. Thus far as long-term exposures are concerned, no epidemiological studies have shown the influence of chronic CO exposure on health outcomes.

10.2.5 Immunosuppression

It has been shown in many animal experiments that air pollutants such as ozone and nitrogen dioxide reduce the body's capacity to defend itself against harmful microorganisms such as bacteria. This appears to be due to a weakening of the pulmonary clearance mechanism – the bacteria remain in the lung rather than being removed from it. Similar responses have been found for particles.

10.2.6 Passive smoking

Passive smoking is the exposure to tobacco smoke created by others' smoking. Clearly, it leads to inhalation of a similar range of compounds, albeit at lower concentrations, to those inhaled by the smoker. In some circumstances, the total exposure may be significant, as for a bar worker who is in the bar all day. Mortality rates have been calculated from cohort studies, and it has been shown that around 46,000 deaths per year are attributable to passive smoking in the United States, of which 3000 are from lung cancer, 11,000 from other cancers, and 32,000 from heart disease.

10.2.7 Persistent organic pollutants

These pollutants have been found to show chronic toxic effects on human health. Many of them have been shown to be carcinogenic or mutagenic when given at relatively high concentrations to laboratory animals, and many can also be concentrated in terrestrial and aquatic food chains so that they achieve high concentrations in, for example, breast milk.

FOR REFERENCE PURPOSES ONLY

As shown earlier in Section 2.2.8, the principal classes of chemical within the category are polychlorinated biphenyls (PCBs); polycyclic aromatic hydrocarbons (PAHs); polychlorinated dibenzodioxins (PCDDs, or dioxins) and polychlorinated dibenzofurans (PCDFs, or furans). Within each class there are many individual compounds with their own properties. Their atmospheric concentrations are normally extremely low in comparison to the air pollutants discussed earlier; while individual PAHs may be present at ng m^{-3} levels, individual PCDDs may only occur at pg m^{-3} or even fg m^{-3} levels. Nevertheless, there is increasing concern about their chronic long-term effects. In the United States, these compounds are known as *air toxics*. As these compounds are carcinogenic, there is no threshold concentration. It is only possible to specify a risk of contracting cancer if exposed to that concentration for a lifetime.

Polychlorinated dibenzodioxins and dibenzofurans are released mainly from municipal and hospital waste incinerators, metallurgical processes and coal combustion. Their initial form is gaseous, but they are strongly absorbed onto particles (dust and fly ash) before emission. They are subsequently deposited onto soil, vegetation and water surfaces, and incorporated into food chains as well as being inhaled or ingested. With so many different chemicals to consider, it has become common to describe the effective toxicity of a range of these POPs with a single toxic equivalent (TEQ), which is the toxicity equivalent to the same weight or concentration of the most toxic POP, known as 2,3,7,8-TCDD. It has been estimated that only about 3% of daily TEQ intake comes directly from the air, compared with 16% from vegetables, 19% from meat and eggs, 36% from dairy products, and 26% from fish. The total average daily intake in European countries is about 120 pg TEQ day^{-1}. This represents about 2 pg per kg body weight (kgbw) per day for adults, a figure which may rise to ten for babies because of their intake of breast milk and dairy products. Experimental toxicological and epidemiological data indicate a lowest effect level of between 100 and 1000 pg $kgbw^{-1}$ day^{-1}. The airborne dioxin concentration is around 5 pg m^{-3}; this is higher than would be expected from the source strengths and deposition velocity, so it is probably due largely to resuspension of particles from the ground. The World Health Organisation (WHO) published a modification to the TEQ values in 1997 and further revision in 2006 and called them toxic equivalent factors (TEFs). Of the 210 congeners (i.e. different compounds within a family having a similar structure) of PCDD/F there are 17 (7 PCDDs and 10 PCDFs) which are recognised to have toxic effects.

PCBs have been associated with reduced mail fertility and long-term behavioural and learning impairment. There are about 12 of the 209 known PCBs which have recognised toxic effects. They have been considered to be carcinogenic. These compounds are insoluble in water but accumulate in body fat. As a consequence, the major exposure pathway for humans is considered to be accumulation of PCBs present in the environmental reservoirs (soils and sediments) through the food chain.

PAHs are found in the environment both as gases and associated with particulate matter. Studies suggest that after absorption into the body they may be altered into substances that

FOR REFERENCE PURPOSES ONLY

tend to damage the genetic material in cells and initiate the development of cancer. Six to eight of the possible PAHs are thought to be carcinogenic. Most attention has been paid to few particularly carcinogenic PAHs such as benzo(a)anthracene, benzo(a)pyrene and dibenz(ah)anthracene.

10.2.8 Quantification of health effects

10.2.8.1 PM_{10} and SO_2

The UK Committee on the Medical Effects of Air Pollutants (COMEAP) estimated the effects (Table 10.12) due to PM_{10} and SO_2. For comparison, the total deaths and respiratory hospital admissions in the equivalent areas of Britain are around 430,000 and 530,000 per year, respectively.

The DEFRA consultation document on the review of the air quality strategy for England, Scotland, Wales and Northern Ireland (published in April 2006) estimated the cost of man-made particulate air pollution on human health in the UK to be between 9.1 and 21.4 billion pounds.

At present there is general uncertainty about which particle property or properties are mainly responsible for health effects, and hence what to measure and what standards to set in legislation. If it is not $PM_{2.5}$ as a mass concentration, then it might be the sulphate fraction, or the number concentration of ultrafine particles (<0.50 μm), or whether the latter are acid-coated, or the mass concentration of soluble transition metals. The overall epidemiological evidence is that there is a linear relationship between some indicator of particle concentration and excess mortality – that is, as for carcinogenic chemicals, there is no threshold concentration above which effects are found and below which it is safe.

10.2.8.2 Ozone

For acute exposures, the UK Advisory Group concluded that 200 ppb of ozone, which is below the UK record hourly mean but has been commonly achieved in the United States, would cause eye, nose and throat irritation in more than 50% of the population at large; FEV_1 would be decreased by 25% for normal people being active outdoors and by 50% for the most sensitive 10% of the population. Responses as large as these clearly have to be taken seriously. The compilation of many separate epidemiological studies has shown that relative mortality risk is increased by 4%–5% when 1-h peak O_3 concentration increases by 100 ppb. The corresponding figure for morbidity (identified as hospital admissions due to respiratory illness) was 18%. For at-risk groups such as asthmatics, this can rise above 50%. Ironically, some of the most useful data on population responses to O_3 has been obtained from American summer camps, where healthy activities are enjoyed in rural high-altitude, but also high-O_3 locations. Figure 10.16 shows a prediction of the acute adverse health effects that could be avoided in New York by achieving the US EPA's standard of 80

FOR REFERENCE PURPOSES ONLY

ppb as an average daily maximum.

Table 10.12 Effects of PM_{10} and SO_2 on mortality and respiratory illness

Pollutant	*Health outcome*	*No. of cases in urban GB*
PM_{10}	Deaths brought forward	8100
	Hospital admissions (respiratory)	10,500
SO_2	Deaths brought forward	3500
	Hospital admissions (respiratory)	3500

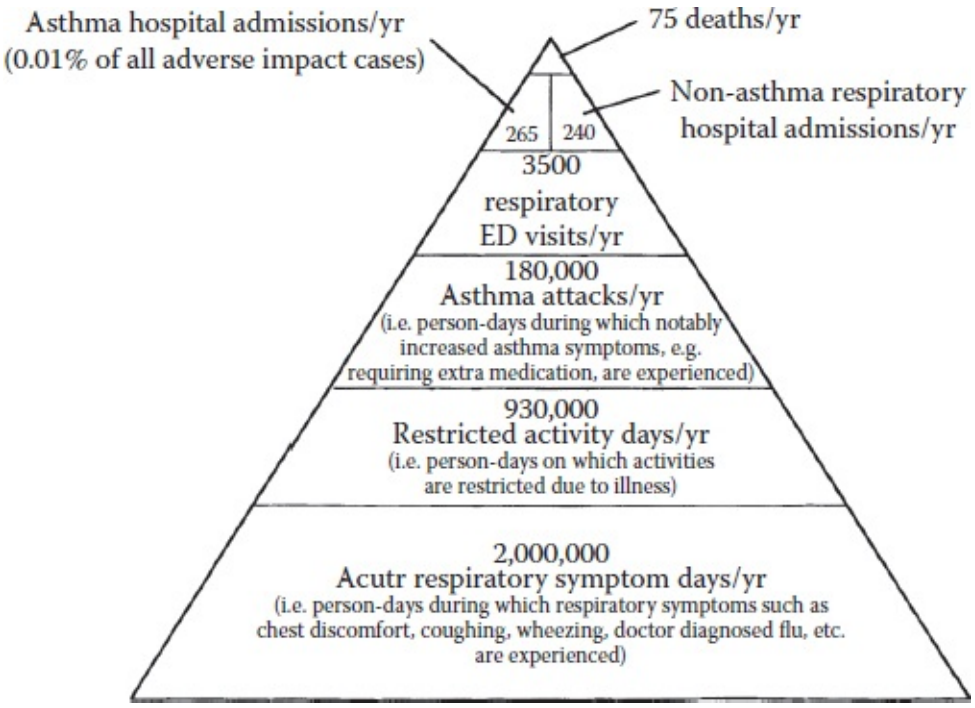

Figure 10.16 Health benefits to New Yorkers of meeting the ozone standard. (From Thurston, G.D. and Ito, K., Epidemiological studies of ozone exposure effects, in Holgate, S.T., Samet, J.M., Koren, H.S., and Maynard, R.L. (Eds.), *Air Pollution and Health*, Academic Press, London, UK, 1999.)

It is likely that there are chronic responses due to long-term exposure to low-O_3 concentrations, although it is even harder to separate this signal from the background noise. The UK government has set the target for ozone concentration; the 97th percentile of the daily maximum 8-h running mean not to exceed 50 ppb (equivalent to exceedances on no more than 11 days per year). This health criterion was exceeded over almost all the UK in 1996, especially along the south coast of England. COMEAP considered the likely effects of O_3 on deaths and respiratory illness to be as given in Table 10.13. The European Environment Agency has calculated that 0.3% of EU hospital admissions are attributable to high ozone concentrations, with up to 0.7% in Belgium, Greece and France. For the UK this

FOR REFERENCE PURPOSES ONLY

figure is probably less than 0.1%.

Table 10.13 Effects of ozone on mortality and respiratory illness

Pollutant	*Health outcome*	*No. of cases at specified threshold, per 10^6 population*
O_3	Deaths brought forward	700, 50 ppb
		12,500, 0 ppb
	Hospital admissions	500, 50 ppb
		9900, 0 ppb

10.2.8.3 Benefits of achieving NAQS targets

Calculating the costs of pollution control is complex enough, but may seem straightforward in comparison to calculating the values of the benefits. Yet such a comparison is useful if the end-point for pollution control is to be judged. For example, we could continue to reduce the concentration of a given pollutant towards the natural background by insisting on tighter and tighter emission controls. The laws of diminishing returns would apply, and the cost per unit concentration (1 ppb, e.g.) by which the concentration was reduced would increase as the concentration was lowered. In order to find out the health benefits (purely in terms of morbidity and mortality) we need good understanding of the exposure–response relationship. Then we also need to convert those morbidity and mortality figures into financial equivalents.

The UK National Air Quality Strategy (NAQS) has determined targets for key air pollutants and a timetable for meeting them (Chapter 14). These target values have been combined with previously established dose–response relationships to predict the net health benefits of achieving the targets. The dose–response coefficients are given in Table 10.14. On the basis given, they are all remarkably similar, with coefficients close to 0.6% per 10 μg m^{-3}. The corresponding predictions of health benefits for an urban population of around 40 million people are given in Table 10.15. The figures imply that the total of deaths brought forward should be reduced by around 18,000 by the measures currently in place.

Table 10.14 Dose–response coefficients

Pollutant	*Health outcome*	*Coefficient*
PM_{10}	Deaths brought forward	+0.75% per 10 μg m^{-3} (24-h mean)
	Respiratory hospital admissions	+0.8% per 10 μg m^{-3} (24-h mean)
SO_2	Deaths brought forward	+0.6% per 10 μg m^{-3} (24-h mean)
	Respiratory hospital admissions	+0.5% per 10 μg m^{-3} (24-h mean)
O_3	Deaths brought forward	+0.6% per 10 μg m^{-3} (8-h mean)
	Respiratory hospital admissions	+0.7% per 10 μg m^{-3} (8-h mean)
NO_2	Respiratory hospital admissions	+0.5% per 10 μg m^{-3} (24-h mean)

FOR REFERENCE PURPOSES ONLY

Table 10.15 Health benefits from achieving NAQS targets[a]

Pollutant	Deaths brought forward			Respiratory hospital admissions		
	In 1996 (1995 for O_3)	In 2005 (2010 for O_3)	Total reduction over period	In 1996 (1995 for O_3)	In 2005 (2010 for O_3)	Total reduction over period
PM_{10}	7390	6480	4860	6090	5345	4015
SO_2	3305	1370	9675	2125	880	6230
O_3	720	235	3890	615	200	3320
NO_2	Not predicted			5160	3505	8255

[a] This table is a highly simplified summary of a complex topic and report, and for any detailed application of this information the reader is encouraged to refer to the original documentation.

Is it worth it? One way of assessing effects in financial terms is by willingness to pay (WTP). The idea is to get people to estimate how much they are willing to pay for a safety improvement which will reduce their individual risk of death during the coming year by, say, 1 in 100,000 (equivalent to one fewer death in a group of 100,000 people). If this figure were £10, then the value of one life would be £10 × 100,000 = £1m. Another technique is to use quality-adjusted life years (QALYs). Quality of life is scored on a scale from one (full health) down to zero (death). Then the product of this score times the period in years for which it is experienced is the QALY. To aggregate different types of damages to human health the WHO and World Bank apply a tool for comparative weighting of disabilities called DALY (Disability Adjusted Life Years). This scale lists many different disabilities on a scale between 0 and 1 (0 meaning being perfectly healthy and 1 meaning death).

In the UK, DEFRA reported on economic aspects of reducing particle concentrations, working from a base case in which total UK emissions of PM_{10} would decrease from 186 kt in 1999 to 98 kt in 2010. They found that the introduction of an illustrative package of additional measures to further control mobile and stationary sources would reduce emissions in 2010 to 65 kt and PM_{10} concentrations in 2010 by 0.751 μg m^{-3} at a cost of around £1,000 m. The health benefits would amount to a gain of around 400,000 life-years over the period 2010–2110. Although this sounds a large figure, it is summed over a lot of people and a long time. Put another way, the gain corresponds to an increase in life expectancy of 2–3 days per person. The costs of such improvements can seem very high – the DEFRA report calculated that some measures, such as fitting particulate traps to diesel cars, would cost up to £1 m per tonne of particulate emission saved.

10.2.8.4 WHO methodology

A detailed methodology for health impacts assessment has been developed by WHO. Suppose a health effect such as respiratory disease can be causally related to exposure to a

pollutant such as PM_{10}. Some cases of respiratory disease may be attributable to the pollutant, but others will not. The attributable proportion is called P_a.

$$P_a = \frac{\sum\{(R_R(c)-1)\times p(c)\}}{\sum\{R_R(c)\times p(c)\}}$$

where:

$R_R(c)$ is the relative risk for the health effect in category c of exposure

$p(c)$ is the proportion of the target population that lies in category c

The underlying (i.e. independent of pollution) frequency of the effect in the population is called I. Then the frequency I_E due to exposure to the pollutant is given by

$$I_E = P_a \times I$$

and the frequency of the effect in the population free from exposure is

$$I_{NE} = I - I_E = I \times (1 - P_a)$$

For a population of N, the number of cases attributed to the exposure will be

$$N_E = N \times I_E$$

This response is often translated into an *excess* number of cases, which is the number over and above the number that would have been anticipated without exposure to the pollutant.

The excess incidence

$$I_{excess}(c) = (R_R(c) - 1) \times p(c) \times I_{NE}$$

and

$$N_{excess}(c) = I_{excess}(c) \times N$$

10.2.8.5 Example case study

Use one year of PM_{10} monitoring data to calculate the number of hospital admissions for respiratory diseases in a city of 400,000 inhabitants. First, form an exposure estimate for each of the 365 days of the year. This gives a frequency distribution of days that have a given category of pollution $p(c)$. The WHO Air Quality Guidelines for Europe give the relative risk for PM_{10} as 1.008 per 10 μg m^{-3} increase in concentration, starting from a background concentration of 20 μg m^{-3} at which the relative risk is one. Hence P_a can be calculated as 0.0276, which means that 2.76% of hospital admissions for respiratory illness

FOR REFERENCE PURPOSES ONLY

can be attributed to PM_{10}. National statistics are then used to show that I = 126 per 10,000 population per year, corresponding to 5040 for our city. Of this number, 139 (which is 2.76% of 5040) can be attributed to PM_{10}. Furthermore, the data in the last column of Table 10.16 show that only a small proportion of the cases is due to short exposures to very high concentrations, and that benefits of reductions will only be felt if the whole pollution distribution is moved downwards.

Table 10.16 Example of hospital admissions due to PM_{10}

PM_{10}/mg m^{-3}	*No of days in category c*	*Proportion of days in category c*	*Relative risk in category c*	*Excess cases due to category c*
	(c)	*p(c)*	*$R_R(c)$*	*Nexcess(c)*
<20	10	0.027	1.000	0
20–29	30	0.082	1.008	3
30–39	71	0.195	1.016	15
40–49	83	0.227	1.024	27
50–59	76	0.208	1.032	33
60–69	50	0.137	1.040	27
70–79	20	0.055	1.048	13
80–89	10	0.027	1.056	8
90–99	8	0.022	1.064	7
100–109	5	0.014	1.072	5
110–119	2	0.005	1.080	2
120–129	0	0.000	1.088	0
Total	365	1.000		139

10.2.9 Odours

Odour can be one of the most intractable and indefinable problems in air pollution. Some specific gases, such as ammonia and hydrogen sulphide (H_2S), have specific and easily defined odours. Yet even for those the odour threshold – the concentration above which they can be detected – can vary by an order of magnitude from one individual to another. Odour thresholds also vary widely from gas to gas, and give little idea of toxicity. Interestingly, the human nose is more sensitive to H_2S than any gas monitoring instrument we have today: air mixtures with as little as 0.000001% H_2S are associated with a rotten egg smell. Unfortunately, however, our sense of smell is not a reliable alarm – at mixing ratios above about 0.01%, H_2S becomes odourless and very toxic, causing irritation of the upper respiratory tract and, during long exposure, *pulmonary edema*. Exposure to 500 ppm can cause a human to fall unconscious in 5 min and die in an hour or less. Table 10.17 gives the odour thresholds of some common gases. There are often complex mixtures of compounds for which there is no simple relationship between the responses. Detection of odour depends on molecules of the substance being received by the nose. Even materials

FOR REFERENCE PURPOSES ONLY

usually thought of as inert, such as stainless steel, emit sufficient molecules to produce an odour. Although sophisticated analytical equipment, such as gas chromatography and mass spectroscopy, can shed light on the exact mix of compounds present in a sample, none of them can measure the smell of it. That is best left to the human nose. The response of the latter can be quantified through dynamic dilution olfactometry. A panel of 8–10 trained observers is exposed to a series of dilutions of an air sample, and record the odour concentration (the number of dilutions after which 50% of the panel can only just detect the odour). Electronic noses, based on rapid gas chromatography analysis of the components, are also increasingly being used.

Table 10.17 Odour thresholds of some gases

Gas	*Threshold/ppb*
Acetic acid	210
Butyric acid	0.5
Carbon disulphide	100
P-cresol	0.5
Dimethyl amine (fishy)	21
Dimethyl sulphide (bad cabbage)	1
Ethyl acrylate	0.1
Ethyl mercaptan	0.5
Formaldehyde	1000
Hydrogen cyanide (bitter almonds)	900
Hydrogen sulphide (bad eggs)	0.2
Methyl mercaptan (bad cabbage)	1
Nitrobenzene	4.7
Ozone (acrid)	100
Phenol	21
Phosgene	470
Pyridene	10
Styrene	47
Sulphur dioxide	470
Trimethylamine	0.2

10.3 IMPACTS ON OTHER ANIMALS

As compared to people, we know very little about the consequences of air pollution for the great majority of animals, whether they be mammals, insects or birds.

10.3.1 Fish and other aquatic species

FOR REFERENCE PURPOSES ONLY

One of the major environmental issues of the late twentieth century has been acid rain, meaning the wet and dry deposition of sulphur, nitrogen and acidity to terrestrial ecosystems. Combinations of observations, theory and experiments have confirmed that acidification of surface water bodies such as lakes is mainly due to acid deposition, exacerbated in some cases by natural processes and changes in catchment land-use and management. These changes certainly started around 150 years ago in industrialised parts of the world, and have been particularly severe where the location of the water body makes it sensitive to deposited acidity. For example, in Scandinavia, two factors combine to amplify the responses. First, much of the region is based on acidic granitic rock which does not buffer acid deposition. Second, the acid precipitation is stored as snow during the winter before being released during the short spring thaw. The combination of these two factors causes a large acid flush of reduced pH, to which salmonids are particularly sensitive, just during the fish breeding season.

With general S deposition, acidification of soils starts as base cations are stripped from the ion-exchange complex and base saturation decreases. The soil's capacity to adsorb SO_4 is eventually exhausted. If the rate of supply of base cations by primary weathering is less than the incoming flux of strong acid anions, the base cation store in the soil becomes depleted and there will be a net flux of hydrogen ions, acid anions and aluminium from the soil into the surface water. The rainfall pH is the general indicator of the severity of acid deposition – this can be seen to relate strongly to the strength of local emissions of acid gases (Figure 10.17).

Populations of freshwater animals such as brown trout have been declining in certain areas of both Europe (Wales, Western Scotland, Norway and Sweden) and northeast North America. These declines are associated with parallel declines in the populations of animals such as mayfly larvae, beetle larvae and molluscs. Aquatic bird species such as the dipper, which feed on these benthic invertebrates, have also declined. For example, surveys on the River Irfon in Wales showed that the population of breeding dippers had declined from around 9–10 pairs per 10 km in the mid 1950s to around 1–2 pairs by 1982. The toxic effects on fish are believed to be due both to low pH by itself (in Canada, anglers use pH meters to find the best fishing) and to the enhanced solubility of aluminium from the stream bed and adjacent soil. The aluminium accumulates on specialised cells on the fish gills that are responsible for maintaining sodium balance. All freshwater animals have a higher salt concentration than the water they live in – if they excrete more salt than they absorb, they will die.

In contrast to S, N is a larger component of the terrestrial ecosystem. Hence most deposited N is immobilised in the soil, and some leaks to surface waters. This leakage will be increased by other factors such as local deforestation. If the N is deposited in the form of NH_4, it will first be assimilated by plants and microbes before being mineralised to NO_3, after which it can act as a strong acid anion. Experimental studies have shown that the process of acidification is reversible, and many countries that experienced severe acidification of their freshwaters during the 1970s and 1980s are now adding lime, in the

FOR REFERENCE PURPOSES ONLY

form of limestone or dolomite, to the lakes or their catchments rather than wait for natural restoration of the pH as acid deposition declines. The lime is either added from a boat as a fine powder mixed directly into the lake water, or dispersed as a powder across the surface by helicopter, or spread as larger lumps across the catchment. This is a really large-scale logistical operation. For example, the liming programme in Sweden involves 7,500 lakes and 11,000 km of watercourses, into which 200,000 tonnes of limestone powder are dispersed each year. The typical dose to lakes is 10–30 g m^{-3}, and results in the pH recovering from 5.5 to 6.5.

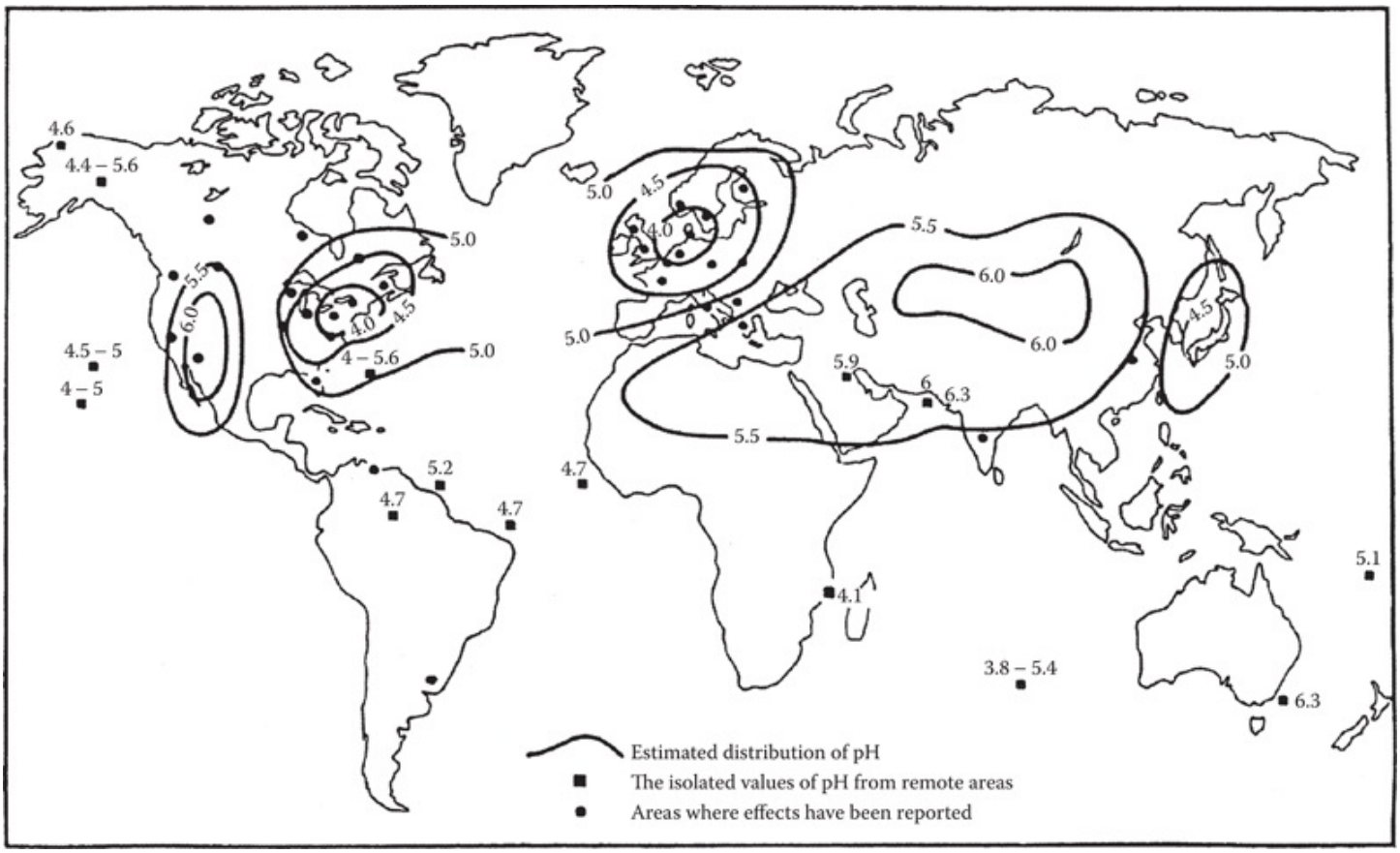

Figure 10.17 Global contours of precipitation acidity. (From Seinfeld, J.H. and Pandis, S.N., Atmospheric Chemistry and Physics, Wiley, New York, 2000.)

The falling trends in emissions of S and N in the industrialised countries that were discussed in Chapter 2 will inevitably reduce S and N deposition to ecosystems, although this will not necessarily happen *pro rata*. Hence there is much interest in the extent and rate of recovery of affected soil and water ecosystems. Long-term measurements have been taken at many affected sites in the UK. These have generally shown a clear improvement in the chemical composition, marked by raised pH, raised acid neutralising capacity and lowered (non-sea salt) sulphate concentrations. However, biological improvements to indicator species such as aquatic invertebrates, fish, macrophytes, river birds and diatoms have not yet been identified. Modelling studies have indicated that it may take a further 50

FOR REFERENCE PURPOSES ONLY

years for this biological recovery to be achieved. Although acid rain and acid deposition have been major air pollution issues in the past, they are now largely understood and under control. This environmental issue has effectively been transferred from the air to the soil and water, and we will not treat it here in any greater detail.

10.3.2 Industrial melanism

The peppered moth (*Biston betularia*) is found all over the UK. The species occurs mainly in two distinctive forms, one of which (the melanic form) is much darker than the other. In the natural environment, the paler form is better camouflaged from predators on bare or lichen-covered tree trunks and therefore predominates. In polluted environments, the trunks are blackened by soot and the pale lichen is killed by SO_2. Evolutionary pressures then favour the melanic form of the moth because it is better camouflaged, and it predominates. Transects between rural and urban environments have shown a smooth progression between the two forms. Recent surveys have shown the pale form to be recovering as soot levels decline. Similar responses have been found in spittel bugs and ladybirds in former Czechoslovakia, and with the peppered moth in Finland, Germany, Scandinavia and Russia.

10.3.3 Aphid stimulation

Aphids feed by drilling through the plant cuticle into the phloem and extracting the fluid. It has been shown that when plants are exposed to sulphur dioxide or nitrogen dioxide, aphids living on them grow and breed at a higher rate. Figure 10.18 shows the results of an experiment in which pea aphids were feeding on pea plants exposed to SO_2. The mean relative growth rate (MRGR, which is simply a measure of aphid vitality) increased steadily with SO_2 concentration until the latter reached 100 ppb. At higher concentrations, the health of the plant itself started to suffer, and consequently that of the aphids as well. It is thought that both S and N act as nutrients, improving (from the aphid's point of view) the quality of certain fractions of the phloem such as amino acids. Interactions such as these, which are only poorly understood as yet, have important implications for world food production.

FOR REFERENCE PURPOSES ONLY

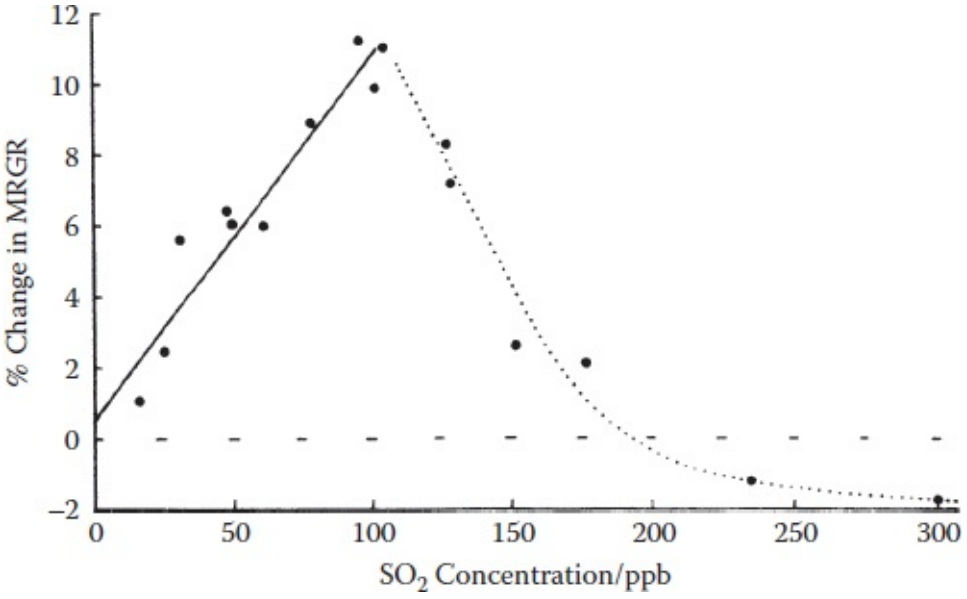

Figure 10.18 Percent change in mean relative growth rate (MRGR) of aphids feeding on plants exposed to sulphur dioxide at various concentrations. (From Warrington, S., *Environ. Pollut.*, 43, 155–162.)

10.4 EFFECTS ON PLANTS

An interesting recent study has shown that floral scents, released as hydrocarbons to the atmosphere, are being either destroyed or altered through chemical interactions with air pollutants such as ozone – potentially offsetting the pollination cycles of plants. This chapter will demonstrate that air pollutants can have both long-term (chronic) and short-term (acute) effects on plants, which are economically significant. They also affect visual range by absorbing and scattering light, and they damage materials by chemical action. Table 10.18 shows the major effects of various pollutants on plants.

Table 10.18 Summary of the major sources, impacts and scale of effects of the major air pollutants on plants

Pollutant	*Major sources*	*Major impacts*	*Major scale of effects*
Sulphur dioxide (SO_2)	Power generation; industry; commercial and domestic heating	Visible folia injury; altered plant growth; elimination of lichens and bryophytes; forest decline	Local
Nitrogen oxides (NO_x)	Power generation; transport	Altered plant growth; enhanced sensitivity to secondary stresses; eutrophication	Local
Ozone (O_3)	Secondary pollutant formed from NO_x and hydrocarbons	Visible folia injury; reduced growth; forest decline	Regional
Suspended particulate matter (SPM)	Power generation; transport; industry; domestic heating	Altered plant growth; enhanced sensitivity to secondary stresses	Local
Fluorides	Manufacturing and smelting industries	Reduced plant growth; fluorosis in grazing animals	Local

FOR REFERENCE PURPOSES ONLY

Source: Emberson, L., Air pollution impacts on crops and forests: An introduction, in: Emberson, L. et al. (Eds.), *Air Pollution Impacts on Crops and Forests: A Global Assessment*, 3–29, Imperial College Press, London, UK, 2003.

10.4.1 Historical evidence

Before World War I, Cohen and Ruston carried out a series of experiments in Leeds (UK) to determine the effects of urban air pollution on a range of plants. At that time Leeds was typical of a thriving urban/industrial complex. There was a profusion of small industrial coal-fired premises releasing smoke and sulphur dioxide from rather inadequate chimneys, set amongst large areas of closely packed terraced housing which was again dependant on coal for energy. Cohen and Ruston set experimental plants out in pots of standard soil in various parts of Leeds, chosen because of their different levels of air pollution. They found severe growth reductions to both roots and shoots of a range of plants, from radish and lettuce to wallflower. There were no sophisticated gas analysers available at the time, and the growth reductions were attributed to a variety of possible causes, from acid rain and sulphurous fumes to the reduction in flux density of solar radiation caused by the pall of smoke particles.

Between World Wars I and II, there was rapid expansion of the smelting industry in parts of Canada. Ore deposits at Copper Cliff, Trail, Sudbury and Wa-Wa were rich in iron, tin, zinc and copper. Sulphur is associated both with the ores and with the coal used for smelting, so that large volumes of sulphur dioxide at high concentration were released, often from undersized stacks. For example, the iron smelter at Wa-Wa in Ontario released its emissions into the south-west prevailing wind, so that ground-level concentrations were confined to the north-east sector. Large tracts of native boreal forest (spruce, cedar, larch and pine) to the north-east were destroyed, in a belt stretching some 30 km from the smelter. Furthermore, the damage pattern clearly reflected the interaction between two competing influences: (1) the decline of average concentration with increasing distance away from the source; (2) the different exposure of different vegetation types. The trees are aerodynamically rough and, being tall, experience the highest wind speeds and lowest boundary layer resistances. They therefore had the highest potential gas deposition fluxes. The understory of bushes was not only lower but was protected to some degree by the trees. Finally, there were lichens, mosses and other low-lying species that survived to within a few km of the source. Investigators described the vegetation as having been peeled off in layers. Other pollutants, such as copper and arsenic, contributed to the effects of these emissions. Although these smelter emissions have now been controlled, there are still parts of the world, such as the *Black Triangle* in Eastern Europe referred to below, where forests are being killed by intense sulphur dioxide concentrations.

The Black Triangle is the area where the borders of Germany, Poland and the Czech Republic meet. It is a region of managed forests which is also the location of substantial brown coal deposits. The latter have been strip-mined and burned for electricity production, resulting in high sulphur emissions and deposition. Sulphur deposition in the Erzgebirge

mountains was up to 125 kg ha^{-1} a^{-1} in 1989, but is now down to around 40 (for comparison, the UK maximum is around 15). Damage to the mainly Norway spruce forest (reddening of the needles followed by defoliation) spread gradually during the 1950s and 1960s, and worsened suddenly in 1979 after an unusually sudden fall in air temperature. Many square kilometres of forest have now been devastated, particularly above an altitude of 750 m.

10.4.2 Experimental methods

It is not hard to demonstrate experimentally the sensitivity of plants to high concentrations of air pollutants. In the early days of such research, plants would be exposed, for example, to a few ppm of SO_2, a concentration within the range found during the worst episodes in urban areas: acute damage was caused to the plant within hours or days. Nowadays, the situation is rather different. Although acute damage does still occur, it is usually localised and the source is identifiable. Control is then a matter of policy and economics rather than science. In addition to these short-range problems, large areas of the world are experiencing low concentrations of various gaseous and particulate air pollutants that may or may not be causing chronic *invisible* plant damage. How do plants respond to these low pollutant levels? Is there damage that is economically or ecologically significant? A range of different experimental techniques has been developed to address these questions. They all have their own advantages and limitations. The great majority of experiments has been undertaken on single agricultural species such as grasses, cereals and legumes; although this gives important economic information, it tells us very little about the responses of complex communities of mixed natural species.

10.4.2.1 Laboratory chambers

This is the most straightforward experimental approach. Plants are grown in *growth cabinets*, and exposed to the pollutant(s) of interest. There are many factors that have to be considered in assessing the results of such an exposure: was the plant grown for the whole of its life cycle (e.g. all the way to final yield for a cereal); what are the changes in response brought about by environmental differences in lighting (quality and quantity), temperature, humidity, wind speed, soil conditions or plant density? For example, many early experiments were undertaken with rather stagnant air in the cabinets. It is now recognised that the leaf boundary layer resistances were artificially high, pollutant transport to the leaf surface reduced, and responses to a particular concentration of that pollutant suppressed. The cure in this case was simple – to stir the air in the chamber with fans – but many other aspects of plant growth need to be optimised if useful results are to be obtained. In general, it is now accepted that laboratory chambers cannot be used to obtain *quantitative* data on responses to pollutants that can be applied to plants grown outdoors. However, such

chambers are much more useful than field facilities for short-term qualitative experiments – to elucidate biochemical mechanisms.

10.4.2.2 Field release systems

Field release systems lie at the logical extreme from laboratory chambers. The principle is to expose an area of forest, ecosystem or commercial crop to an elevated pollutant concentration without changing any other environmental parameter. In one system, developed at a UK university to investigate the responses of winter cereals to sulphur dioxide (Figure 10.19), a square of gas release pipes, 20 m on each side, was supported about 10 cm above the growing crop. Each pipe was pierced with small holes along its length and acted as a line source. Gas release was controlled by computer in the following sequence:

- Check the wind direction, and operate solenoid valves to release gas only from the upwind pipe (or from two adjacent pipes if the wind direction was blowing close to a diagonal)
- Measure the gas concentration upwind of the square (ambient value)
- Measure the gas concentration within the square
- Adjust mass flow controllers to increase the gas release rate if the concentration is below target, and *vice versa*
- Repeat the loop

FOR REFERENCE PURPOSES ONLY

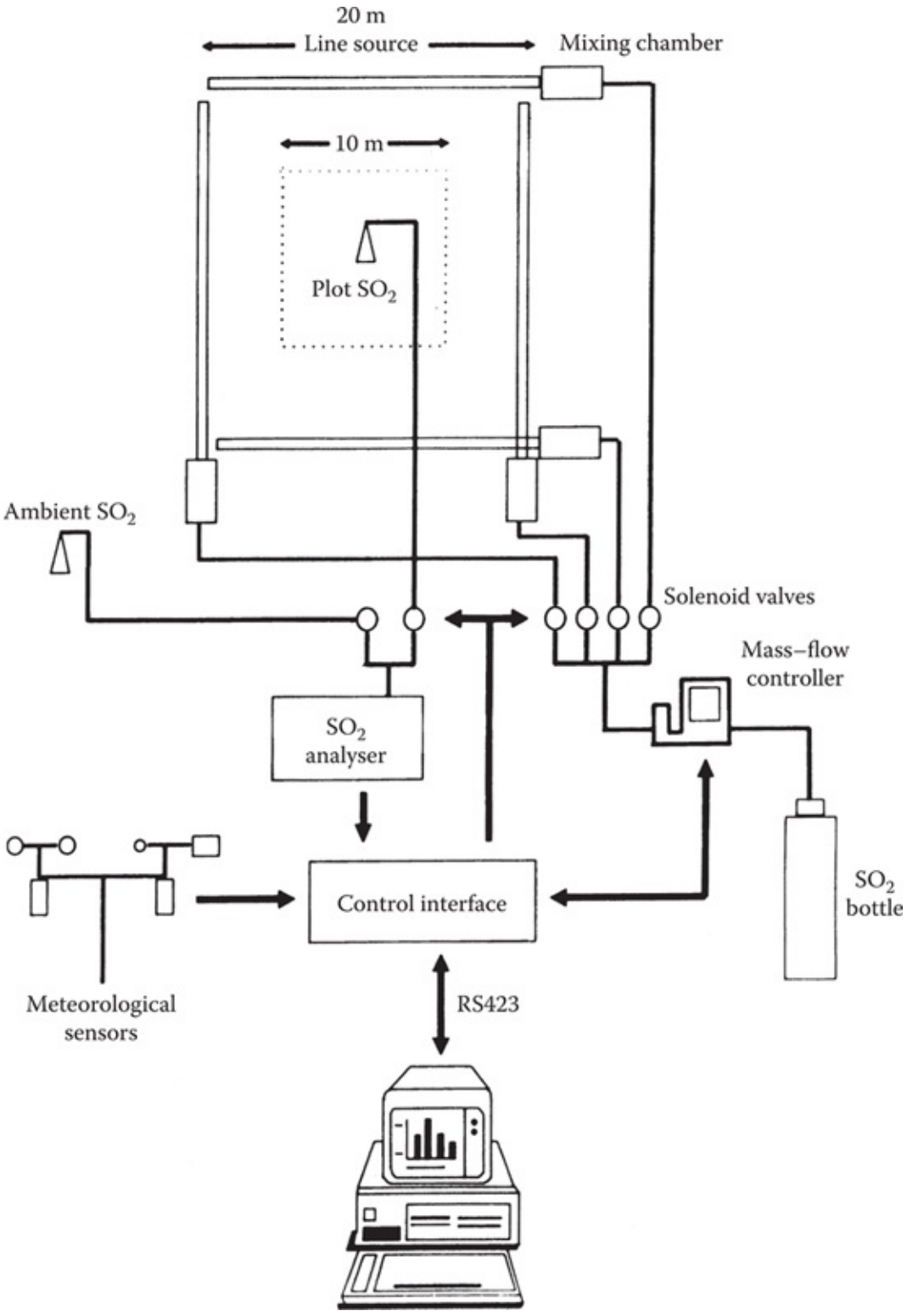

Figure 10.19 A field release system for sulphur dioxide. (From Colls, J.J. et al., *Atmos. Environ.*, 25A, 2895–2901.)

In a typical experiment, the equipment was set up on a commercial field of winter wheat or winter barley soon after crop emergence in the autumn and operated continuously until harvest in July or August. The plants were thereby exposed to elevated SO_2 concentrations

FOR REFERENCE PURPOSES ONLY

for almost their whole lives, growing under completely natural conditions with no modification of temperature, wind speed or other environmental variables.

This principle has also been adapted for studying responses to carbon dioxide. In the Free Air Carbon Dioxide Enrichment (FACE) system developed by the Brookhaven National Laboratory, a circle of release pipes, around 25 m in diameter, is used; the circular pattern increases the uniformity of exposure above that possible with the square design. The main practical difference is that CO_2 enrichment involves raising the concentration by several hundred ppm instead of the tens or hundreds of ppb typical of ozone or SO_2, so that very high rates of gas supply are needed. If possible, an experiment involving CO_2 release is sited close to a brewery, fertiliser factory, natural CO_2 well or other low-cost source to reduce the operating cost.

There have been other designs of field release system. In one, an array of vertical pipes hanging down between rows of vines has been used to study responses to low concentrations of fluoride. In another, ozone release pipes have been distributed within a canopy of mature trees, with the release rate automatically adjusted to keep the local concentration approximately constant. The limitations of field release systems include:

- There is no possibility of reducing pollutant concentrations below ambient – they cannot answer the question 'what is the prevailing level of air pollution doing to plants?' Of course, one solution might be to grow the plants in an area that has very low background concentrations of the pollutant of interest (such as the south of England for SO_2). Then additions can be used to raise the concentration and simulate the pollution environment at the original location. This procedure raises other issues – the soil, climate and background levels of other pollutants will be different at the new site, and these changes may themselves affect the growth of the plants. This problem has been tackled with field filtration systems (Section 10.2.3).
- In addition, whatever burden of other pollutants that exists in the ambient air has to be accepted, and may interact in an unknown way with the experimental gas. There are mixed views on this. We certainly need to understand the responses of plants to individual pollutants. On the other hand, many locations such as the English Midlands only experience mixtures of pollutants. Changing the concentration of one gas against a steady background of the others is then a realistic experiment.
- It is difficult in practice to achieve a uniform exposure over the experimental area. The gas must be released at a rather high concentration from a distributed array of point sources (small holes in the pipe). It diffuses rapidly within the first few meters, so that a guard area of plants has to be sacrificed where it is known that the concentration field is unacceptable. With the square geometry described earlier, there were also significant variations of exposure with wind direction.
- A large ground area is required, within which the plant cover has to be reasonably uniform. Associated with this aspect of size is the large gas release rate that an open air system requires. This is especially true with forests because of the depth of

atmosphere over which the gas concentration has to be increased.

10.4.2.3 Field filtration

Field filtration systems have been used to retain the natural environmental qualities of field release, while enabling the reduction of concentrations below ambient. Pipes are laid between rows of plants, and charcoal-filtered air blown out amongst the plants, so that pollutant concentrations are greatly reduced. Experience has shown that the pipes have to be quite large in diameter and quite close together in order to blow clean air out at a sufficiently high rate: this means that a normal field planting density cannot be used and one of the attractions of a field-based system is therefore reduced.

10.4.2.4 Open-top chambers

Open-top chambers (OTCs) were designed in America in the early 1970s as a way of controlling the air quality (both adding and subtracting pollutants) to which field grown plants were exposed without creating unacceptable environmental changes. Typically, an OTC consists of an upright cylindrical aluminium framework covered in transparent plastic film. In one design, the lower half of the film is double-skinned, and there are several hundred holes on the inside wall (Figure 10.20).

Alongside the OTC is a fan unit, which draws in ambient air and blows it into the double skin and out through the holes to the inside of the chamber. The air can be passed through a charcoal filter to reduce concentrations of O_3, SO_2 and NO_2, or it can have controlled concentrations of these gases added to it. Hence the plants growing inside the chamber are exposed to the controlled air supply. The ventilation rate is kept high (3–4 air changes per minute). This both stirs the air inside the OTC to keep the boundary layer resistance down and keeps the temperature close to ambient. Other designs of gas distribution have been used – from holes in a toroidal plenum suspended above the canopy or from grilles in the chamber floor. Chamber sizes have ranged from portable units 1.25 m in diameter to designs 5 m in diameter, 8 m tall for use on trees. Open-top chambers also have their limitations:

- Although the environmental conditions are significantly closer to ambient than they are in laboratory chambers, they are by no means perfect. Temperatures may be 4°C higher than ambient in the middle of a sunny afternoon, and average 0.5°C–1°C higher over the year. Apart from the short-term impact of these excursions on photosynthesis and transpiration, for example, thermal time will accumulate faster in OTCs than outside so that experimental plants go through their growth stages faster. Rainfall inside OTCs is significantly reduced, as most rain falls at an angle to the vertical and the shelter effect is substantial. The wind environment is quite unnatural, with rather high wind speed at the edges of the circular area, decreasing towards the centre.

FOR REFERENCE PURPOSES ONLY

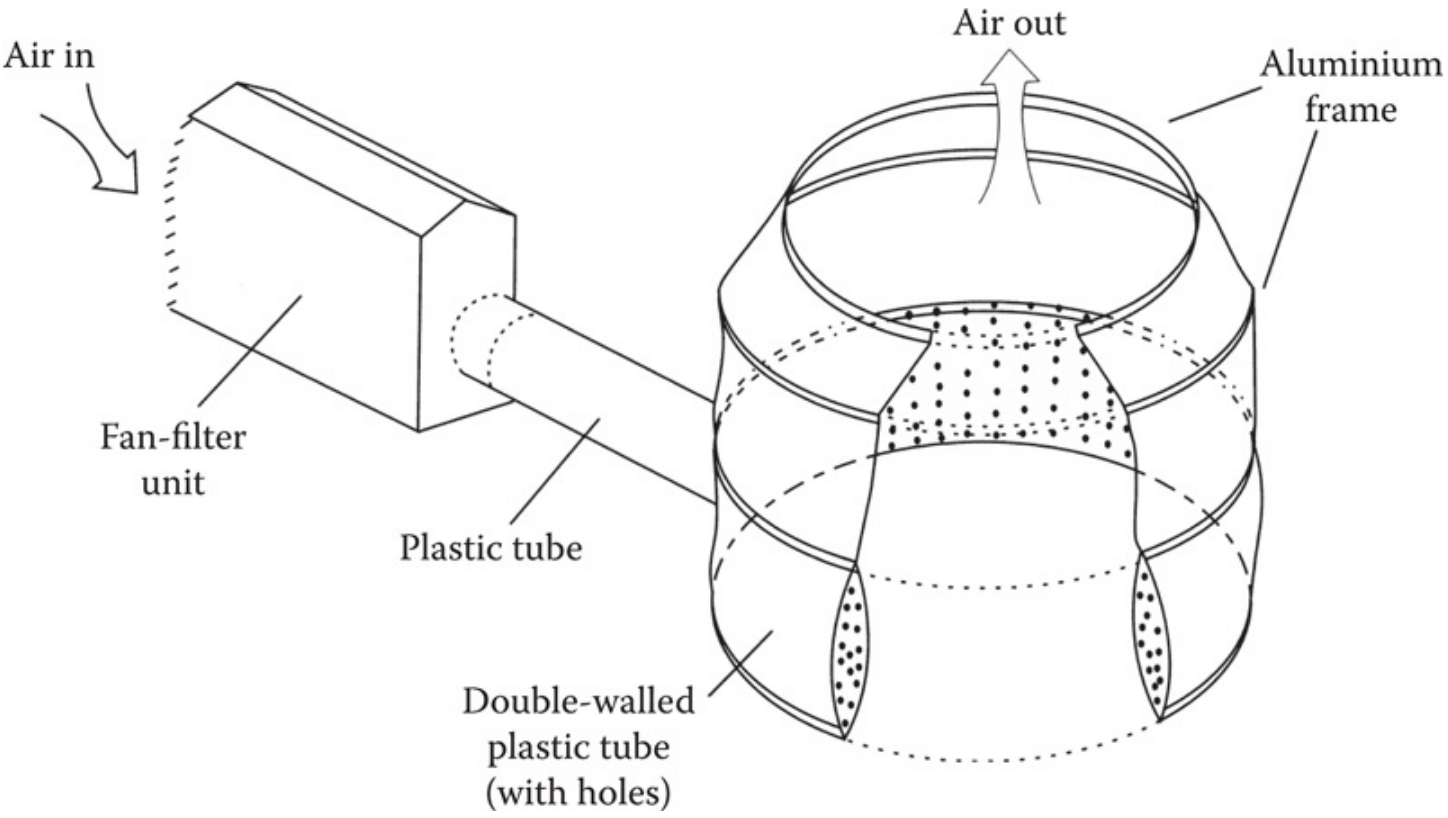

Figure 10.20 An open-top chamber.

- The small environmental changes may be tolerated for the annual plants typical of most agricultural crops. The situation is quite different for trees, however. Very small proportional changes in growth, maintained over tens or hundreds of years, can have large cumulative effects. A new design of chamber at Nottingham has been used to minimise these differences. The chambers have been constructed with roll-down side panels for use in experiments involving intermittent ozone exposures. For most of the year, the panels are rolled up and the trees inside are effectively in the open air. For about 30 days spread over the spring and summer, the panels are rolled down to form a complete chamber while ozone exposures are carried out. In this way, the environmental changes due to the chambers themselves are minimised.
- Scientists like to find out what is happening to plants during the course of a growing season rather than waiting until the end, and will want to take destructive plant harvests for measurements in the laboratory. Similar to any chamber, OTCs only offer small areas of plant material for measurements. Furthermore, destructive harvests disrupt the vegetation canopy and may cause the remaining plants to grow differently and to have different exposures to the pollutant.

10.4.2.5 Ventilated glasshouses

A wide variety of controlled-environment buildings has been used for pollution control studies. In an early example, rye-grass was studied in glasshouses near Manchester. The

ventilation air was scrubbed with water sprays to reduce the sulphur dioxide concentration before it entered the glasshouse. In the UK, small hemispherical forced-ventilation glasshouses known as *solardomes* have been popular. Such systems are cheaper and more permanent than OTCs, and usually located closer to a research laboratory for more intensive supervision of experiments. Their main disadvantage is that they are one stage further removed from the outdoor environment, particularly as plants are grown in pots rather than in the ground.

10.4.2.6 Branch bags

The size and longevity of mature trees has usually made it unrealistic to enclose them with chambers of any sort for a significant proportion of their lives. Instead, parts of the tree have been enclosed. A mini-chamber is constructed around a single branch, with the appropriate ventilation to prevent the temperature and humidity increasing unacceptably. A gas such as ozone can then be added to the air supply. The technique has the advantage that it can be applied to mature trees growing in their natural environment. However, as only part of the tree is exposed to the stress, it begs the question of whether the tree is able to mitigate the effects by importing resources from, or exporting toxic products to, other parts of the tree.

10.4.2.7 Ethylene diurea

One specific experimental method is available for ozone that is quite different to the methods discussed previously. It has been found that ethylene diurea (EDU), when applied to plants as either a soil drench or to the foliage, can protect the plant against elevated ozone concentrations. Hence the responses of EDU-treated and untreated plants can be compared to derive dose–response functions. This relationship has been used as the basis of a European programme on ozone effects research coordinated by the United Nations Economic Commission for Europe (UNECE).

10.4.2.8 Bioindicators

Some species of plant have fairly high specificity towards individual pollutants. For example, gladioli are sensitive to fluoride, tobacco plants to ozone and lichen to sulphur dioxide. Such species (or, more usually, a particularly sensitive variety of the species) can be used to show variations in pollutant concentration, either with time at one place, or from place to place. An unambiguous response is needed (e.g. formation of brown upper-surface speckle by ozone) which can be at least approximately linked to pollutant concentration. The Netherlands has had a long-term bio-indicator programme to monitor HF and O_3. In 1999, EuroBionet, the ‘European Network for the Assessment of Air Quality by the Use of Bioindicator Plants’, was established as a network of research institutes and municipal

FOR REFERENCE PURPOSES ONLY

environmental authorities from twelve urban agglomerations in eight EU member states. The extremely ozone-sensitive tobacco cultivar (*Nicotiana tabacum* L.) Bel-W3 has been used in numerous biomonitoring studies worldwide for more than four decades, including an extensive biomonitoring study comprising of 100 sites conducted in twelve European cities between 2000 and 2002. Figure 10.21 shows a linear relationship between ozone pollution and the corresponding leaf injury for a European city.

In another version of this idea, mosses have been used extensively to measure the deposition of heavy metals from the atmosphere. Mosses have no root system to take up minerals from the substrate on which they grow, and accumulate materials such as heavy metals from wet and dry deposition. Either indigenous mosses are harvested or a network of mossbags is set up, with the moss being collected and analysed after a period. Figure 10.22 shows the results of lead analyses of mosses in Poland, with the highest concentrations associated with the most heavily industrialised part of the country.

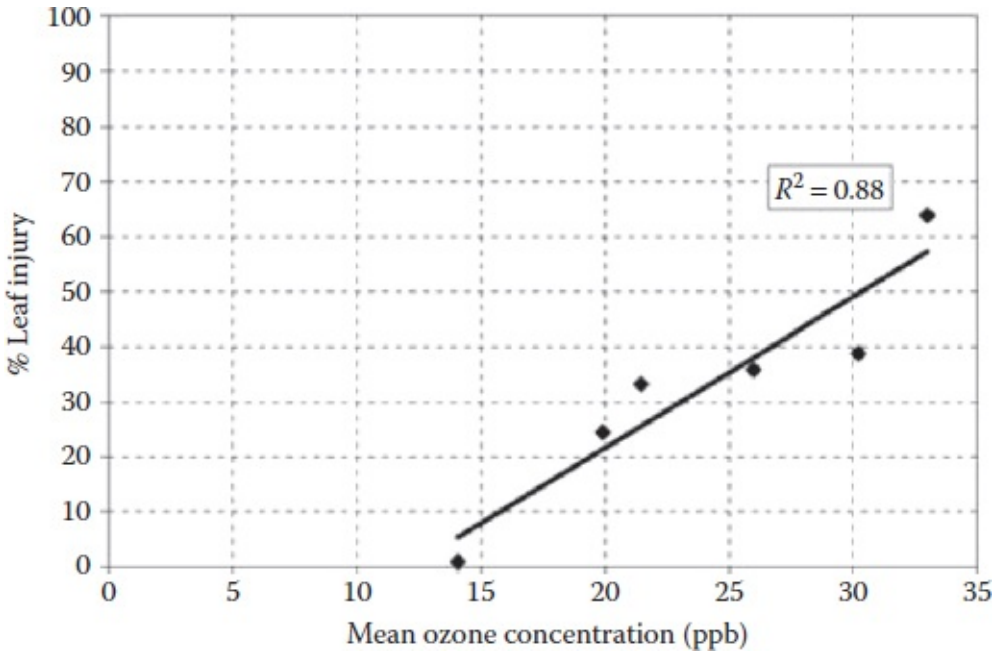

Figure 10.21 Scatter plot (with regression line and coefficient of determination R^2) of the relationship between ozone induced leaf injury and the mean ozone concentration at the *Lörick* site in Düsseldorf (Germany) during 2001. (From Klumpp, A. et al., *Atmos. Environ.*, 40, 7437–7448, 2006.)

FOR REFERENCE PURPOSES ONLY

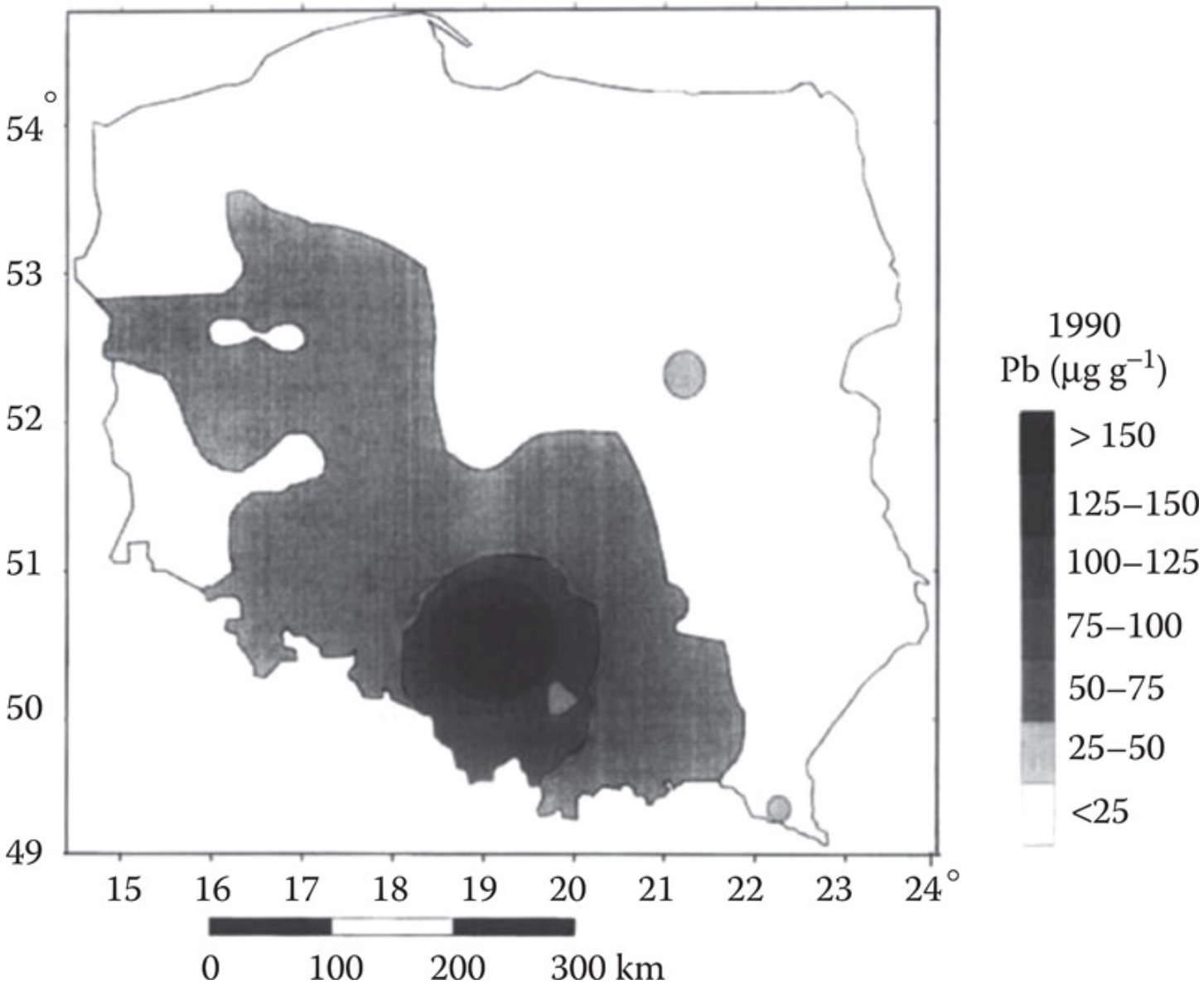

Figure 10.22 Contours of moss lead content in Poland. (From Grodzinska, K. and Szarek-Lukaszewska, G., *Environ. Pollut.*, 114, 443–451, 2001.)

10.4.2.9 Lichens

Lichens are widespread symbiotic associations of fungi and algae that grow slowly on rocks, roofs and other mineral surfaces. Surveys of lichen abundance and species diversity across the UK have shown a strong correlation with the distribution of SO_2 sources and therefore with ground-level SO_2 concentrations. Parts of the UK have become *lichen-deserts*, although the reduction of SO_2 concentrations is expected to foreshadow a recovery. Certain areas from which a particular species was found to be absent during the 1970s have been recolonised during the 1980s and 1990s, and resurveys of specific sites where air pollutant concentrations are known to have decreased have shown a general reduction in the proportion of grid squares from which species are absent. Of course, long term acidification

of the growth substrate may mean that the recovery takes much longer than the initial response. For example, oak trees do not shed their bark, so once the bark has been given a reduced pH, it tends to stay that way.

10.4.2.10 Diatoms

Diatoms are microscopic (a few tens of μm), single celled algae which occur in great abundance in all aquatic habitats. Individual species of diatom have been found to have quite different sensitivities to the pH of the water that they inhabit. When they die, each species leaves behind a characteristic silica *skeleton* which is preserved in lake sediments. Hence, changes in the relative abundance of the various species can be used to track changes in pH. The sediments accumulate at about 1 mm per year, and if a true chronology can be assigned to the sediment record, then the change of pH with time will also be known. Over the last two decades, intensive sampling of Scottish fresh-water lochs and lakes in Europe and North America has shown the impact of fossil-fuel emissions on the acidity of rainfall and its consequences for life in fresh waters.

10.4.3 Plant responses to specific air pollutants

Summary data on plant responses to air pollutants, particularly at low levels, show complex and often inconsistent results. We shall describe them from two directions: the observed responses regardless of mechanism and the mechanisms themselves.

10.4.3.1 Visible injury

Visible injury to leaves is the most obvious indicator of air pollution damage when the concentrations have been high enough. Different gases produce different symptoms:

- *Ozone*: A speckle of brown spots, which appear on the flat areas of leaf between the veins (hence, also called interveinal necrosis)
- *Sulphur dioxide*: Larger bleached-looking areas
- *Nitrogen dioxide*: Irregular brown or white collapsed lesions on intercostal tissue and near the leaf edge
- *Hydrogen fluoride*: Brown necrosis at the tip or edge, working its way inward across the otherwise healthy tissue, with which there is a sharp division at a brown/red band
- *Ammonia*: Unnatural green appearance with tissue drying out

10.4.3.2 Long-term response of agricultural yields to single gases

The economic importance of agricultural crops, together with the simplicity of working with single plant species compared to mixed natural systems, has made them the most

FOR REFERENCE PURPOSES ONLY

heavily investigated plants. Research can be conveniently divided into NF/CF and additions experiments.

NF/CF experiments. Open-top chambers have been used in America and Europe to expose plants to air from which ambient pollutants have been removed by charcoal. Typically, plants from three treatments are compared – AA (an unchambered plot in ambient air), NF (chamber with non-filtered ambient air) and CF (chamber with charcoal-filtered air). Two factors are currently affecting the interpretation of such experiments. First, if the plants grow differently in the NF chambers compared to AA treatments, how should differences between CF and NF be interpreted? Second, with the small differences expected from low concentrations, how can we ever get enough statistical confidence from a practical number of replicates? In the US, only 7 of the 73 results from the National Crop Loss Assessment (NCLAN) programme showed a statistically significant yield reduction in NF compared to CF. It was concluded that the cumulative frequency of occurrence of intermediate ozone concentrations (50–87 ppb) was the best damage predictor, and this argument was supported with the observation that the highest concentrations tended to occur in the late afternoon when stomata were already closing.

Additions experiments. Experiments with laboratory chambers, open-top chambers (NCLAN and European OTC programme) and field release systems have shown changes in crop yield with increasing gas concentration for many species and varieties. Ideally, such an experiment involves the precise application of many different concentrations to different treatments so that response curves, called dose–response functions, can be fitted. One dangerous temptation with additions experiments is to apply unrealistically high concentrations in order to get a statistically significant response. This does not necessarily result in higher statistical confidence at low concentrations. The dose–response function may take several forms: flat (e.g. barley and oats to ozone, Figure 10.23; a steady decline (e.g. wheat to ozone, Figure 10.24, or barley to SO_2, Figure 10.25); or a stimulation at low concentration followed by a decrease at higher concentrations (beans to ozone, Figure 10.26). The common protocol of both the NCLAN and European OTC programmes involved varying the parameters of one family of curves to fit different experiments. The family chosen was the Weibull distribution, which gives the yield Y_i as a function of ozone concentration X_i:

FOR REFERENCE PURPOSES ONLY

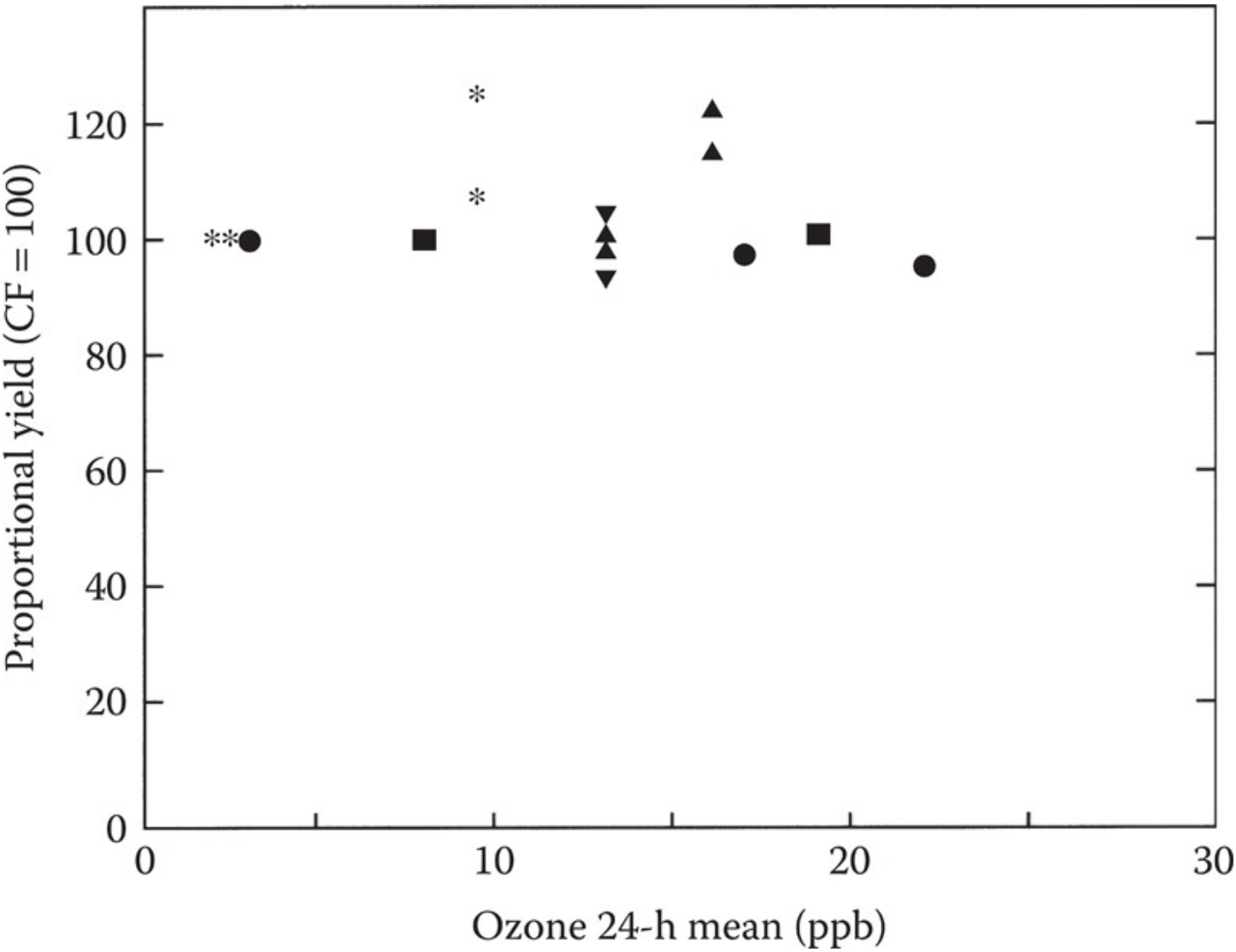

Figure 10.23 The responses of barley and oats yields to ozone in open-top chambers. ▪, = oats; , , * = barley. Yields are expressed as a percentage of the yield in charcoal-filtered air. (From Skarby, L. et al., Responses of cereals exposed to air pollutants in open-top chambers, in Jager, H.J., Unsworth, M.H., de Temmerman, L., and Mathy, P. (Eds.), *Effects of Air Pollution on Agricultural Crops in Europe*, Air Pollution Research Report 46, CEC, Brussels, Belgium, 1993.)

$$Y_i = \alpha \exp\left[-\frac{X_i}{\omega}\right]^{\lambda}$$

where:

α is the theoretical yield at zero ozone concentration

ω is the ozone concentration giving a yield of e^{-1} α (= 0.37α)

λ is the parameter controlling the shape of the curve – usually in the range 1–5

FOR REFERENCE PURPOSES ONLY

The parameter λ can be adjusted to give curves that involve exponential decay, linear decrease, or a plateau followed by a sigmoidal decrease. Figure 10.27 shows the Weibull curves that were fitted by the NCLAN team to proportional yields from dicotyledenous agricultural crops. The simple Weibull distribution cannot give the stimulation and decline that has been observed in some experiments, but it can be modified to do so (by compounding it with a linear model).

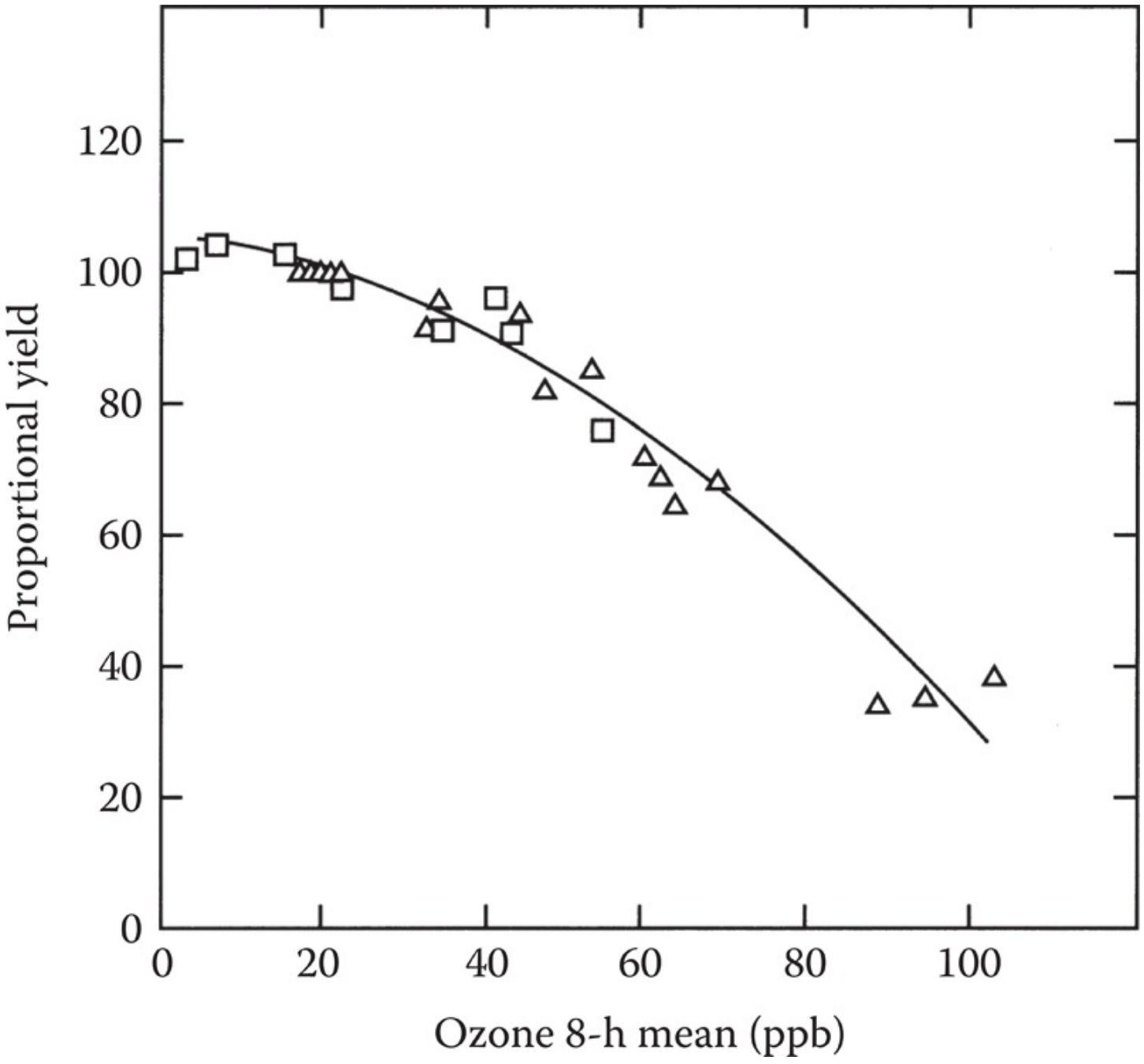

Figure 10.24 The response of spring wheat yield to ozone in open-top chambers. Yields are expressed as a percentage of the yield in charcoal-filtered air. (From Skarby, L. et al., Responses of cereals exposed to air pollutants in open-top chambers, in Jager, H.J., Unsworth, M.H., de Temmerman, L., and Mathy, P. (Eds.),

FOR REFERENCE PURPOSES ONLY

Effects of Air Pollution on Agricultural Crops in Europe, Air Pollution Research Report 46, CEC, Brussels, Beligium, 1993.)

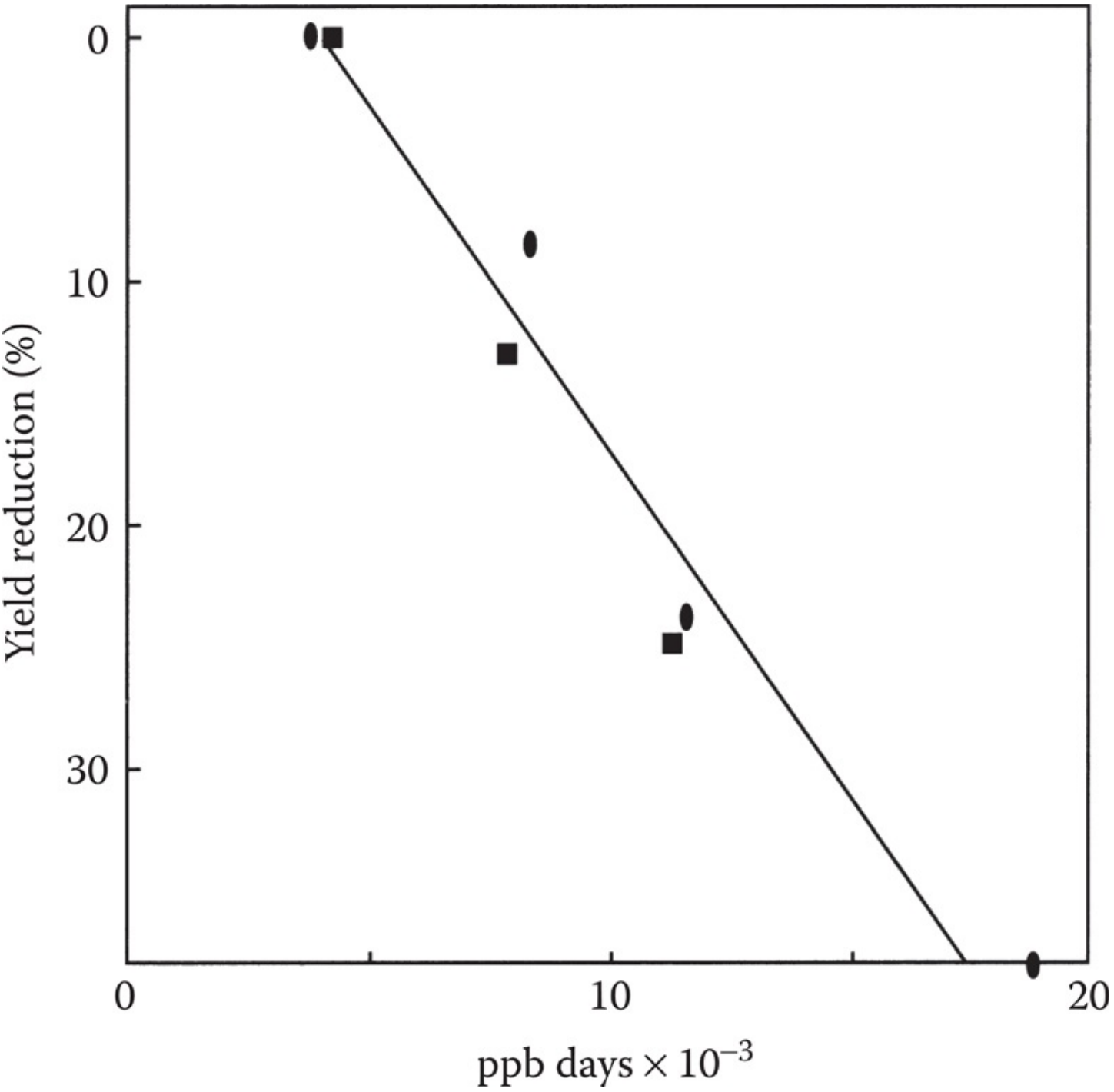

Figure 10.25 The response of winter barley yield to SO_2 in a field release experiment. Yield is expressed as a percentage reduction from that of unexposed control plants. (From Baker, C.K. et al., *New Phytol.*, 104, 233–241, 1986.)

FOR REFERENCE PURPOSES ONLY

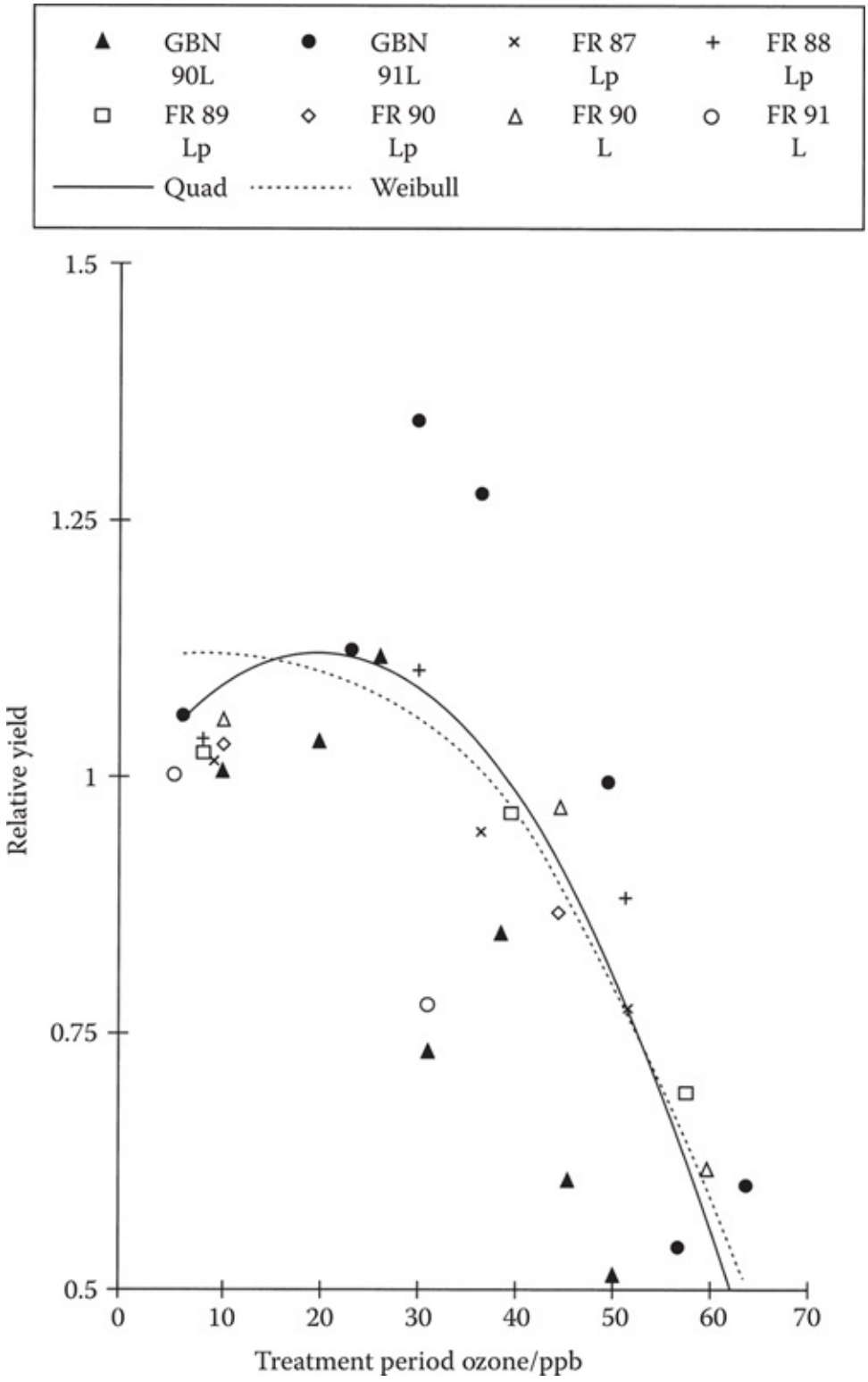

Figure 10.26 The response of green bean (*Phaseolus vulgaris* cv. Lit) yield to ozone. The yield is expressed as a proportion of the yield at an ozone concentration of 5 ppb. (From Colls, J.J. et al., The responses of beans exposed to air pollution in open-top chambers, in Jager, H.J., Unsworth, M.H., de Temmerman, L., and Mathy, P. (Eds.), *Effects of Air Pollution on Agricultural Crops in Europe*, Air Pollution Research Report 46, CEC, Brussels, Belgium, 1993.)

FOR REFERENCE PURPOSES ONLY

A different approach has been used by a group in Germany to evaluate the combinations of ozone concentration (specified to be at the top of the plant canopy) and exposure period that might result in plant damage. They pooled results from published experiments and derived the relationships shown in Figure 10.28 for agricultural crops and wild plant species, and in Figure 10.29 for European coniferous and deciduous trees. In each case, the three shaded bands represent exposure–response regions in which direct ozone effects are unlikely, possible or likely, at the probability indicated.

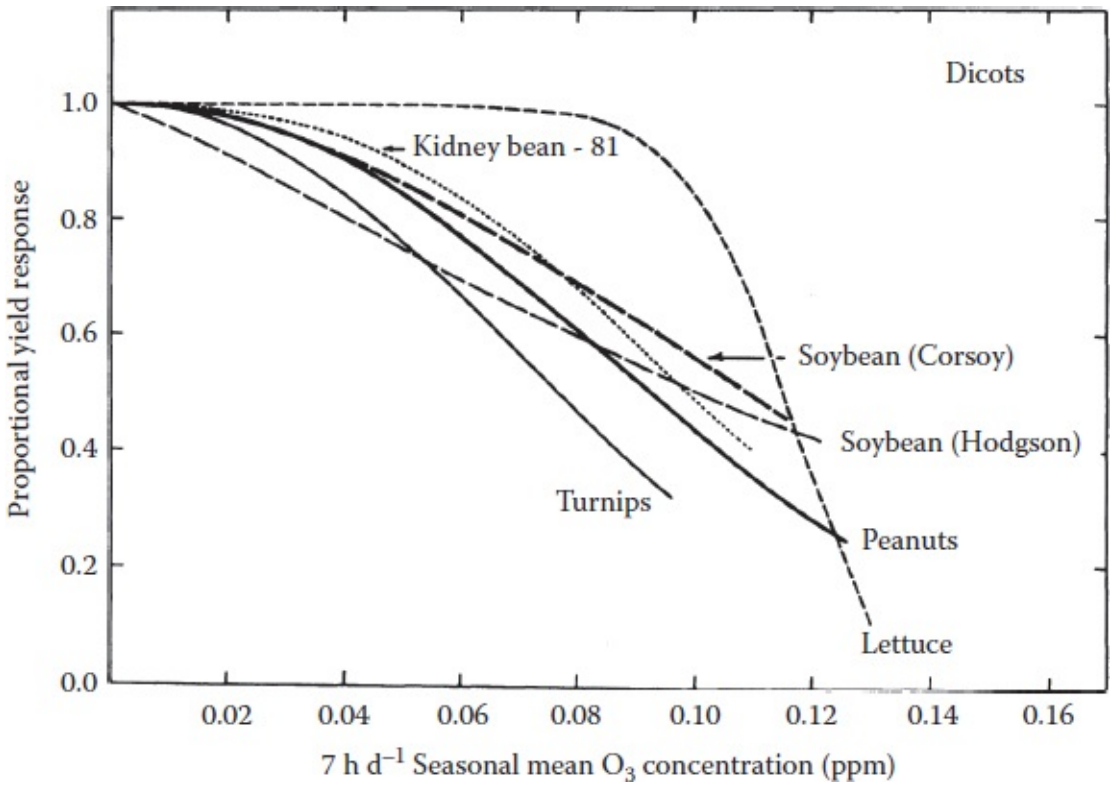

Figure 10.27 The range of Weibull curves fitted to experimental results for different dicotyledenous species during the NCLAN programme. (From Heagle, A.S. et al., Factors influencing ozone dose–yield response relationships in open-top field chamber studies, in Heck, W.W., Taylor, O.C., and Tingey, D.T. (Eds.), *Assessment of Crop Loss from Air Pollutants*, Elsevier, Barking, UK, 1987.)

FOR REFERENCE PURPOSES ONLY

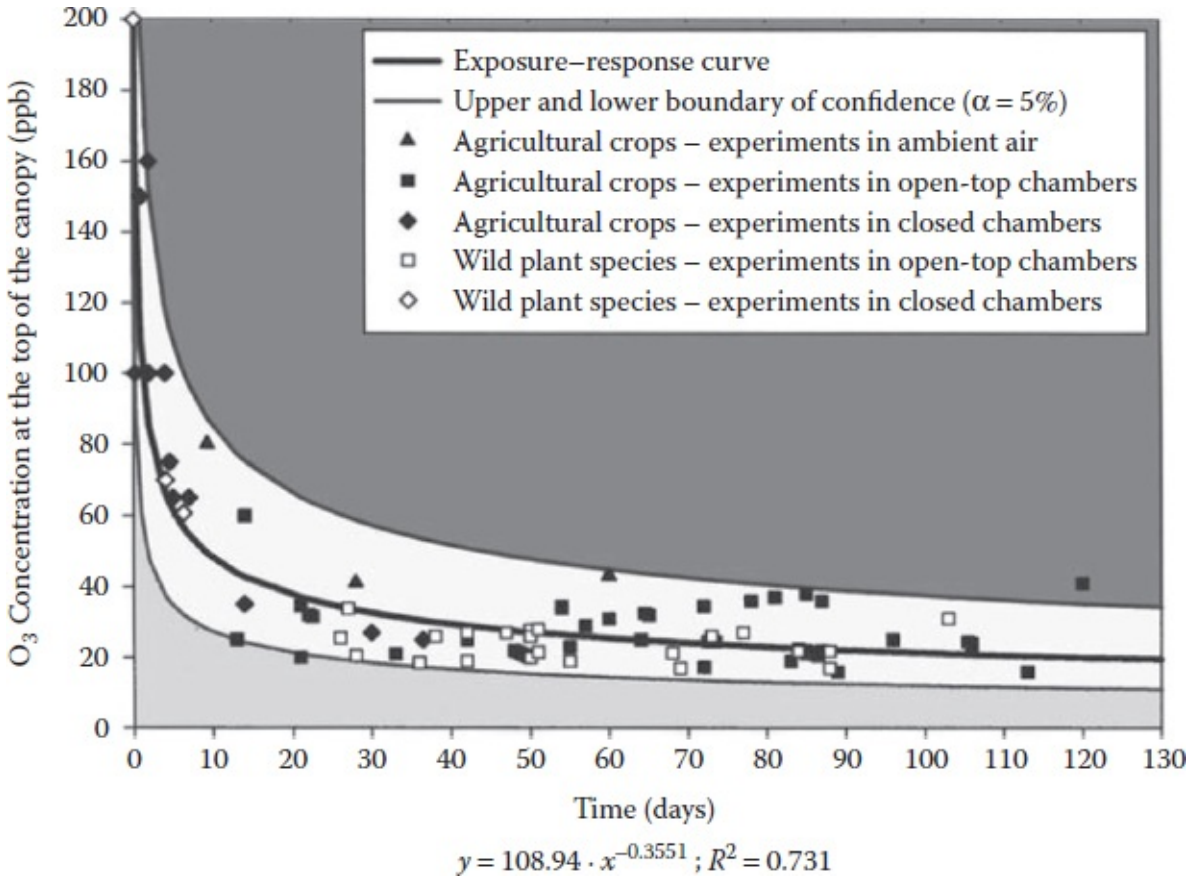

Figure 10.28 Ozone exposure–response for European crops and wild plant species. (From Grünhage, L. et al., *Environ. Pollut.*, 111, 355–362, 2001.)

FOR REFERENCE PURPOSES ONLY

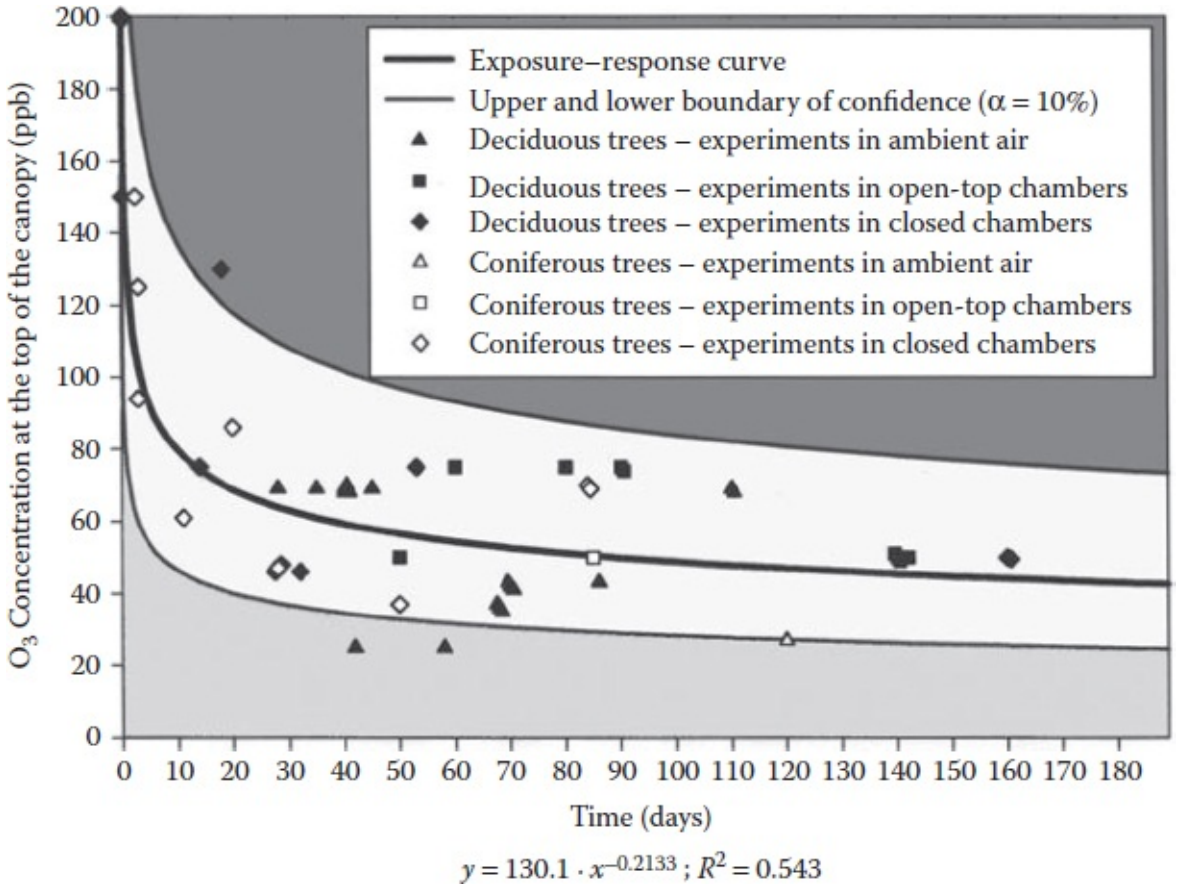

Figure 10.29 Ozone exposure–response for European trees. (From Grünhage, L. et al., *Environ. Pollut.*, 111, 355–362.)

10.4.3.3 Nutrient inputs

When atmospheric concentrations of SO_2 are high, plants can receive a significant proportion of their S input by deposition. There is evidence that in areas of the UK where there is limited sulphur available in the soil, some agricultural crops have benefitted from this atmospheric deposition. Conversely, as concentrations have declined, farmers in these areas have had to apply more S in fertiliser to compensate. Plants in the UK are not thought to be significantly affected by the prevailing concentrations of NO or NO_2 *per se*. Nitrogen deposition, however, is another matter. Nitrogen is the key plant nutrient, and several hundred kg ha^{-1} may be added to agricultural crops to improve yield. Atmospheric inputs may be significant even on this scale. This is not likely to be important in areas where nitrogen availability is high. In many N-deficient areas these nitrogen inputs may affect the species composition, usually promoting grasses at the expense of shrubs, mosses and other understorey species that thrive in nitrogen-poor soils. This process has been most noticeable in parts of the Netherlands where high ammonia concentrations from intensive livestock production have led to atmospheric N deposition fluxes that are comparable to fertiliser inputs. High N deposition may also increase sensitivity to frost and droughts, and

FOR REFERENCE PURPOSES ONLY

the severity of insect damage.

10.4.4 Pollutant entry into the plant

The simplest model of external leaf structure involves a waxy, relatively impermeable sheet of cuticle, punctuated at frequent intervals by stomata through which gas exchange occurs. The stomata, which are typically 10–20 μm long, are not simply open holes. They are protected by guard cells – pairs of sausage shaped cells that open in response to turgor pressure. For most plants, the guard cells open during the daytime to allow gas exchange for photosynthesis while the sun is up, and close at night to conserve water. Gaseous pollutants are just as able to diffuse through the stomata as are CO_2 and water vapour. The single most important impact of air pollutants on plants is to impair the functioning of the stomatal guard cells. Conversely, it is unlikely that air pollutants damage plants easily when the stomata are closed – at night or under drought stress, for instance. Although the area of the cuticle is far larger than the combined area of stomata, the rate of diffusion of pollutant gases through the cuticle is typically lower by a factor of 10,000.

The first site of action for ozone, as for other oxidative gaseous pollutants, is believed to be the cell plasma membrane. The integrity and full functioning of this membrane is particularly important for guard cells, because it controls water flow into and out of the cells, cell turgor and hence shape and stomatal aperture. If the guard cells do not function efficiently, there are several possible consequences: for well-watered plants, stomata will not open to their full capacity so that photosynthesis is reduced; for drought-stressed plants, they will not close as tightly so that water loss is increased; neither will they close as tightly when the plant is ozone-stressed, so that the ozone flux through the stomata is increased. Hence the ozone-exposed plant is in a lose-lose situation – it cannot photosynthesise as strongly when water is in good supply, and it cannot restrict water loss as effectively when water is scarce. Looked at from the opposite perspective, there are many experimental observations that stomata close in response to ozone exposure, potentially reducing gas exchange, photosynthesis and growth. There is a much smaller number of observations that suggest the opposite – that at low concentrations, ozone can stimulate stomatal opening.

Sulphur dioxide is converted to sulphite and bisulphite within the plant. These ions interfere with the fluxes into the guard cells of other materials such as potassium and calcium. When the relative humidity is high, these changes cause guard cells to become more turgid, so that they open wider and improve pollutant access. As with ozone, this opening may increase the transpirational water loss and lead to long-term water stress. At low humidities, stomatal apertures are reduced and the plant is protected from the pollutant.

10.4.5 Pollutants inside plants

Once pollutant gases have entered the stomata, they are in the highly aqueous environments

FOR REFERENCE PURPOSES ONLY

of the substomatal cavity and the mesophyll. Their influence is strongly affected by their solubility in, and speed of reactions with, the water that makes up 90% of active plant tissue. For SO_2, the sulphite and bisulphite from these initial processes are eventually oxidised to sulphate; during this sequence, reactive free radicals are formed that in turn promote disruptive effects such as oxidation of fatty acid double bonds. The reactions generate H^+ fluxes that disturb the pH – this change is buffered by proteins and amino acids. The rate constants of all these processes are not yet available, so quantitative response analysis is not possible. The overall effects of sulphur on plants depend on the exposure and other factors in the plants' sulphur environment. As sulphur is a nutrient essential for growth, low concentrations of SO_2 may stimulate the growth of plants growing in sulphur-poor soils. On the other hand, high atmospheric concentrations offer no benefit if soil sulphur supplies are already adequate and may only result in adverse effects due to the free radical formation.

As with sulphur, nitrogen is an element that is essential for plant growth, is usually accessed as nitrate via the roots from the soil, and is also taken up through the leaves when significant atmospheric concentrations of nitrogen oxides are present. Root nitrate is either reduced by nitrate reductase in the roots or is transported in the xylem flow to the leaves. Plants that are nitrogen-deficient are more likely to be at risk from atmospheric N deposition. Nitrogen oxides taken up through the stomata are thought to interfere with nitrate and nitrite reductase activity, although the exact damage mechanisms are not yet clear. It is thought that the main response is disruption of N metabolism by excess nitrite. Nitric oxide behaves quite differently to nitrogen dioxide, and these two gases should not be lumped together as NO_x for plant effects purposes. For example, NO is only sparingly soluble in aqueous fluids, while NO_2 reacts with water to increase its apparent solubility.

Plants respond to ozone by defensive or compensatory mechanisms such as stomatal closure, detoxification by chemical reaction, re-attainment of equilibrium by biochemical adjustment, repair of injured tissue. Many different responses have been observed, including:

- Decreased photosynthesis
- Decreased leaf area and leaf conductance
- Decreased water use efficiency
- Decreased flower and fruit number, and fruit yield
- Decreased dry matter production and yield
- Increased sensitivity to drought or nutrient stress
- Increased or decreased disease susceptibility

The type and degree of response depends on the intensity and timing of the ozone exposure, and on prevailing environmental factors, as well as on the species and cultivar. For example, a given ozone exposure will generally have a larger effect at high humidities than at low, because the stomata will be more open and gas conductance into the plant will be

FOR REFERENCE PURPOSES ONLY

higher. Or a relatively low ozone flux into the plant may be more damaging late in the day when the defensive mechanisms have been weakened by previous exposure. Passive responses to ozone exposure involve the scavenging of ozone molecules by available plant antioxidants such as ascorbate and glutathione. Active defences involve the alteration of biochemical pathways or the production of additional antioxidants. There is only poor understanding of these processes in general. Ozone is highly reactive and is thought not to travel far from the stomata before interacting with other molecules and being transformed or decomposed. Hydrogen peroxide, some radicals and superoxide are known to be produced, but the proportions and the specific consequences for cell homeostasis are not yet understood. Neither do we yet understand rather simple damage phenomena, such as why visible ozone injury appears as spots of necrotic tissue, and the exact mechanism thereof. A popular hypothesis has been that ethylene, emitted from within the plant as a response to the ozone stress, reacts with the ozone within the plant to generate free radicals or hydroperoxides and disrupt cell biochemistry. Both ozone and sulphur dioxide generally decrease net photosynthesis and shoot:root ratio. Stomatal conductance may be either increased or decreased depending on other environmental conditions such as nutrient and water stress.

Plants also have long-term structural responses to pollutant stress, although these have not been investigated very intensively. For example, ozone exposure has been found to increase stomatal density on birch leaves – the birch responded to the reduced diffusive conductance of each stomata by increasing the number of stomata to maintain the overall rates of CO_2 diffusion and photosynthesis.

10.4.6 Exposure dynamics

There is a growing evidence that we not only need to consider the average concentration to which a plant is exposed, but also the concentration frequency distribution. This concept has only reluctantly been grasped by the effects community, because the extra level of variability makes it more difficult to compare one exposure with another, and to perform meaningful experiments, and to decide on practical guidelines for effects thresholds. It makes physiological sense, because the frequency distribution effectively defines the relative importance of the periods at low concentrations during which the plant has an opportunity to repair the damage done by episodes at high concentrations.

Exposure concentrations for ozone are normally described in terms of the treatment-period mean – the concentration averaged over the period of application – rather than the 24-h mean. This is a consequence of several factors: ozone concentrations at ground level follow a strong diurnal cycle as seen in Chapter 2, increasing after about 10 am to a maximum value at 2–3 pm before decreasing to the background value by about 5 pm; plant stomatal conductance follows a similar pattern; experimental ozone additions have frequently been made during the working day. Treatment means are therefore usually specified as 7-h or 8-h means. There is an increasing, and logical, trend to specify the mean

FOR REFERENCE PURPOSES ONLY

as an average over daylight hours as that is the period over which the stomata will normally be open.

10.4.7 Premature senescence

It is now well established that one characteristic response to ozone stress is premature loss of leaves towards the end of the growing season. The higher the concentration, the lower the maximum number of leaves and the earlier in the season they die. This loss reduces the average green leaf area available for photosynthesis and may therefore reduce the amount of plant growth.

10.4.8 Resistance

When a species grows in a region with high levels of a particular pollutant, natural selection may operate to promote plant genes that confer resistance to that pollutant and hence give a higher chance of long-term survival. We give two examples of experiments in which the tolerance of grasses to sulphur dioxide was investigated in contrasting ways. First, samples of grasses, including red fescue, were taken at different distances downwind of a smokeless fuel plant in Yorkshire. It was found that red fescue grown from seeds collected near the source was less sensitive to subsequent laboratory SO_2 exposure than that grown from seeds collected from further downwind (Figure 10.30). Second, grasses were sampled from lawns of different ages growing in the Temple district of central London. The red fescue from the oldest lawns (planted in about 1780, when pollution concentrations in central London were very high) was more tolerant to laboratory SO_2 exposure than that from the newer lawns (the most recent one had been planted in 1977) (Figure 10.31).

Work at Newcastle University, UK has shown a corresponding response to ozone. Seeds of the common plantain (*Plantago major*) were gathered from 28 sites around the UK. As we have seen in Chapter 5, there is a strong gradient of ozone concentration in the UK, increasing from north to south. The seeds were germinated, exposed to ozone in laboratory chambers, and their relative growth rates (a measure of plant vigour) compared. The results, which are plotted as contours of ozone resistance in Figure 10.32, show that not only did ozone resistance also increase from north to south, but even reproduced the dip in ozone concentration found in the London urban region.

FOR REFERENCE PURPOSES ONLY

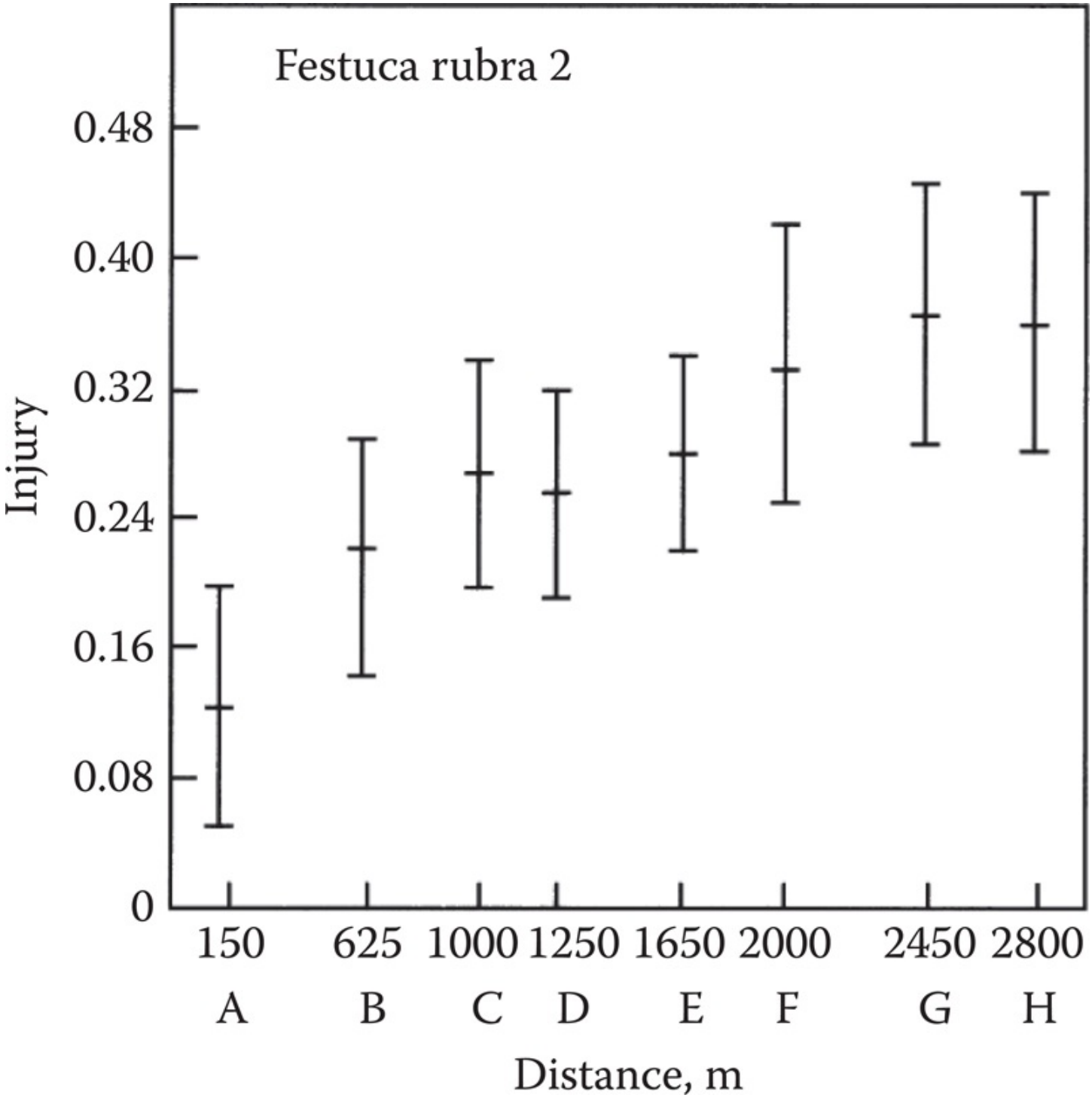

Figure 10.30 The injury to red fescue by SO_2 exposure in the laboratory, as a function of the distance from a point SO_2 source from which its seed was harvested. (From Wilson, G.B. and Bell, J.N.B., *New Phytol.*, 102, 563–574, 1986.)

FOR REFERENCE PURPOSES ONLY

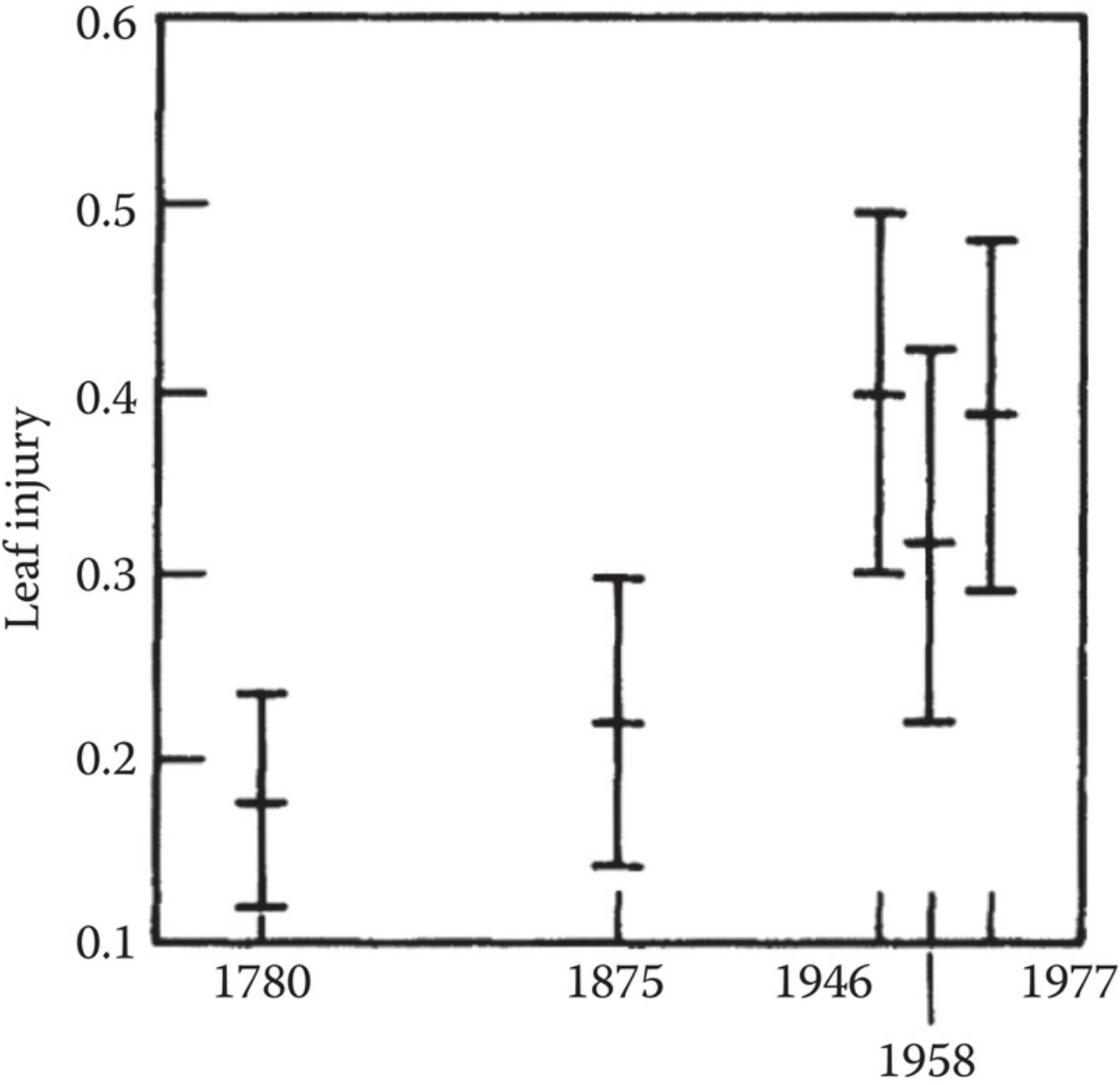

Figure 10.31 The injury to red fescue by SO_2 exposure in the laboratory, as a function of the age of the plant population from which its seed was harvested. (From Wilson, G.B. and Bell, J.N.B., *New Phytol.*, 100, 63–77, 1985.)

10.4.9 Trees

Attention has already been drawn to the special challenges posed by trees, because their long lives and large size make them difficult experimental subjects. Small effects are potentially much more serious than they are for annual plants such as most agricultural crops. For example, consider a tree that grows from being a 0.5 m seedling to its full height

FOR REFERENCE PURPOSES ONLY

of 30 m in 100 years – equivalent to an average compound growth rate of 4.18% per year. Now suppose that air pollution stress reduces this growth rate by 1%, 2%, 5% or 10% per year. Table 10.19 shows that these reductions all have appreciable effects on the final height, with the 10% reduction causing a significant 33% loss.

Figure 10.32 Contours of ozone resistance of plantain grown from seed. The resistance is

FOR REFERENCE PURPOSES ONLY

the mean relative growth rate of ozone-treated plants as a percentage of the mean relative growth rate in clean air. The triangles mark the sites at which seed was collected. (From Reiling, K. and Davison, A.W., *New Phytol.*, 122, 699–708, 1992.)

However, now consider the changes that would be measured in the course of the usual 3-year funded research programme, for a sapling that has an initial height of 3 m (Table 10.20). Even the most severe growth reduction results in only a 41 mm difference in height over the 3 years, which would normally be extremely hard to detect because of the natural variability from tree to tree. The problem of detecting such tiny rates of change, in growth or any other parameter, remains unsolved.

Table 10.19 Effects of growth rate reductions on tree height

Reduction/%	*Actual rate/% a^{-1}*	*Final height/m*
0	4.18	60.0
1	4.14	57.8
2	4.10	55.5
5	3.97	49.1
10	3.76	40.1

Table 10.20 Reductions in tree height increment over a 3-year period

Reduction/%	*Initial height/m*	*Ht after 1 year*	*Ht after 2 years*	*Ht after 3 years*
0	3.000	3.125	3.256	3.392
1	3.000	3.124	3.254	3.388
2	3.000	3.123	3.251	3.384
5	3.000	3.119	3.242	3.371
10	3.000	3.113	3.230	3.351

Much of the work on tree responses has centred on the issue of acid rain, which is a popular term embracing the combination of dry and wet deposition of sulphur and nitrogen to vegetation. Although, there is now no doubt that acid deposition to fresh waters can destroy aquatic ecosystems, the cause and effect relationship for forests is far less clear-cut. The forest die-back that has been experienced in Germany and Scandinavia appears to be the result of many complex interacting factors, including drought, severe cold, disease and management practice as well as air pollution. The roles of air pollutants are probably manifold:

- Direct effects of ozone and sulphur dioxide.
- Interactive effects of ozone and sulphur dioxide on stomatal control, reducing photosynthesis and control over transpiration loss.

FOR REFERENCE PURPOSES ONLY

- Nitrogen deposition stimulates new growth, which is then more susceptible to damage from severe frosts.
- Ozone damages the leaf cuticle, so that acid rain can leach out cations such as calcium and magnesium.
- Soil aluminium concentration is elevated by the lowered pH, which reduces the growth of the fine rootlets that are important for extracting nutrients from the soil.

For practical reasons, most experiments have been carried out for short periods on small juvenile trees and it has not been possible to reproduce the characteristic symptoms of forest dieback, such as storks' nests (adventitious shoots) and crown thinning (chronic defoliation of the upper parts of the tree). Although field surveys and recording of tree condition has been extensive in Europe and North America, much of the data has inevitably been semi-quantitative, using measures such as crown transparency which is obtained by visual assessment from the ground by a trained observer. Predictions of the demise of forests in Scandinavia and Germany have not been borne out, with continuing damage limited to relatively small areas such the black triangle in central Europe.

The Forestry Commission has operated a continuing survey of British tree health since 1986. Sitka and Norway spruce, Scots pine, oak and beech trees are surveyed at 80 sites, with a total 9600 trees. Results thus far have not shown a clear dependence on air pollution. Other biotic (e.g. spruce aphid and winter moth attack) and abiotic (e.g. drought) stresses tend to obscure the geographical patterns that one might expect. Secondary effects may also be important. For example, air pollution might reduce the needle density in a coniferous tree, leading to a change in the insect or spider populations and hence in the populations of the birds that feed on them. Currently, there is not thought to be any hard evidence that either acid deposition or air pollution is resulting in chronic damage to UK forests. It remains possible that these anthropogenic stresses, especially that of increased nitrogen deposition, are enhancing the trees' sensitivity to the natural stresses, but that is an even more difficult case to prove.

Different kinds of damage have been reported for southern European forests. The ozone critical level for trees of 10 ppm.h is exceeded over most of southern Europe, and visible damage is commonplace. There have been many reports on damage to coastal forests by polluted sea spray. Strong onshore winds, without rain, blowing overseas that have been polluted with surfactants and/or oil, are the most damaging. As with the British forests, other damage symptoms may be confused with the effects of non-pollutant environmental stress and disease.

Effects of pollutant gases, especially ozone, have been studied in open-top chambers and field exposures. Again, the work has largely been carried out on seedlings or juvenile trees because the time taken and size needed make the use of mature trees impracticable. Unfortunately, it is not good practice to apply ozone exposures to already-mature trees, as they would have grown differently, and possibly adapted, had they been exposed to ozone throughout their lives. Many of the short-term responses reported earlier for crops have also

been reported for trees, but it is uncertain to what extent these will become incorporated into the long-term response over periods of 50 or 100 years. Indeed, forests consist of communities of trees, and this aspect adds yet another layer of complexity and uncertainty. As it is unlikely that really long-term experiments of sufficient quality will be carried out, predictions of long-term tree and forest responses will probably have to rely on scaling up and process modelling.

10.4.10 Critical loads and levels

In the 1985 Helsinki Protocol, many European countries agreed to try and achieve, by 1993, a 30% reduction from the 1980 sulphur emissions responsible for acid rain (the 30% club). This was a purely arbitrary target chosen for its political acceptability, without scientific basis. During the intervening period, it was recognised that a more rational basis for emission reduction would be needed for the future. The approach adopted has been that of critical loads and critical levels. According to this philosophy, which was first developed in Canada in the 1970s during investigations of lake acidification, the sensitivity of an ecosystem in any part of Europe to acid deposition or to gaseous pollutants will first be determined, and a critical load of wet deposition, or a critical level of gases, will be specified below which the ecosystem will not be significantly damaged. The critical loads are expressed in terms of acidity, sulphur or nitrogen fluxes (kg ha^{-1} a^{-1} of H^+, S or N) and the critical levels in terms of gaseous concentrations or doses (ppb, or ppb.h). Then modelling will be used to calculate the contribution to those loads and levels from different source regions of Europe. In cases for which the critical load or level is exceeded, emission reductions will be imposed to bring the region below the threshold of damage.

10.4.10.1 Critical loads

The definition of critical loads adopted by UNECE is ‘a quantitative estimate of exposure to one or more pollutants below which significant harmful effects on – sensitive elements of the environment do not occur according to present knowledge’. The sensitivity of any particular ecosystem to pollutant inputs depends on physical, chemical, ecological, geological and hydrological factors. These can be mapped. Once a map of the spatial distribution of critical loads is available for a particular receptor–pollutant combination, comparison with current deposition loads (e.g. S and N from wet and dry deposition) generates a corresponding map of the areas of exceedance. A value of deposition above the critical load for a particular ecosystem is not, by definition, sustainable in the long term. The primary inputs to a calculation of critical loads are wet deposition, dry deposition of gases and particles and cloud droplet deposition. Reduced nitrogen species, such as gaseous ammonia and the ammonium in rain cloud and aerosols also contribute to acidification. The critical load of acidity for an ecosystem is determined by the net input of acidity, so that the atmospheric inputs of base cations – in particular, calcium and magnesium – must also be

FOR REFERENCE PURPOSES ONLY

estimated. The dominant acidifying anion in precipitation is sulphate; areas of highest deposition are the high-rainfall areas of north-west England, west-central Scotland and north Wales. There is a clear gradient of decreasing wet deposition from north-west to south-east, with the low rainfall areas of East Anglia receiving 30%–40% of their annual acidic inputs this way, compared to 80% for high-rainfall areas. The concentration of ions in cloud droplet water can be much higher than in rain water, and some areas of upland forest receive up to 30% of their acidic input by this route. In central and southern England, where rainfall amounts are lower and gaseous concentrations higher, dry deposition dominates.

The earliest critical loads were set to prevent soil chemical change (an increase in soil acidity or a decline in base saturation). It was then recognised that deposition of acidity, by whatever route, occurs to complex soil–plant–animal systems which may have many responses. The aim when setting critical loads for a given system was refined to determine the maximum load of a given pollutant which would not produce significant changes in the structure or function of the system. According to the formal procedure, a biological indicator is identified, the health of which is indicative of the whole soil–plant–animal system. A critical chemical value is then established for a given parameter above which the indicator will show an adverse response (e.g. a reduction in growth). The currently favoured indicator is the health of the fine roots of trees, as these are believed to be sensitive to factors such as aluminium mobilisation that are associated with acidification. The favoured chemical value is the ratio of (calcium + magnesium) to aluminium in the soil solution. There are fundamental problems in defining critical loads – for example, should the critical load be set at the level that just causes a response in *current* (already damaged) ecosystems, or should it be set to a lower value that will allow the ecosystem to return to some previous condition? If so, what previous condition is the goal, and what acidity inputs are required to achieve it?

Once both total deposition and critical load maps of an area have been prepared, a critical load exceedance map can be made of the difference between the two values at each grid square. This map is the input to the emission/dispersion/deposition modelling process which is needed to identify which emission reductions will most efficiently reduce deposition to the exceedance grid squares and bring them below critical load. A high value of exceedance can be due either to a high value of deposition or to a low critical load for that area. There are large possible variations – for example, the critical load for sulphur deposition can vary from 50 to 5000 mg S m^{-2} a^{-1}.

The principle of electroneutrality is that any change in the concentration of a negative ion (anion) contributed by acid deposition must be matched by corresponding changes in the concentrations of other anions or of positive ions (cations) so that overall charge neutrality is maintained in the surface water. Hence if sulphate and/or nitrate concentrations increase, some or all of the following changes will occur:

- Decrease in bicarbonate anions, reducing the acid neutralising capacity.

FOR REFERENCE PURPOSES ONLY

- Increase in base cations (calcium, magnesium, sodium potassium). This reduces acidification *per se*, but may deplete soil reserves and affect vegetation growth.
- Increase in hydrogen cation (decreased pH). Adverse effects on aquatic life.
- Increased aluminium cation. Adverse effects on aquatic life. This is the principal way in which fish are affected by acidification.

An increase in the concentration of base cations in drainage waters due to acid deposition can work both ways. Removal of base cations from soils to balance sulphate or nitrate from acid deposition minimises the extent of surface water acidification. However, base cation reserves may be depleted from the soil over time if they are lost faster than they are replaced by deposition and weathering. The store of nutrients in the foliage, such as calcium, can be seriously depleted by acid deposition. This may alter the photosynthesis to respiration ratios and cause reductions in carbon fixation rates and growth rates.

The UNECE Second Sulphur Protocol, based on these critical load concepts, was signed in Oslo in July 1994, and further protocols cover other key pollutants. Modelling of the consequences of the second protocol indicated that there would only be a small recovery in the acid status of UK surface waters, and provided some of the arguments needed to develop the Gothenburg Protocol (Chapter 14).

10.4.10.2 Critical levels

The corresponding definition of critical levels is 'the concentrations in the atmosphere above which direct adverse effects on receptors such as plants, ecosystems or materials may occur according to our present knowledge'. International workshops were held in 1988, 1992 and 1993 to pool data on responses to ozone, sulphur dioxide and nitrogen oxides and decide on critical levels. Separate critical levels for crops and trees have been specified for ozone; they are based on the accumulated dose (expressed in ppb.h) over a threshold concentration of 40 ppb. Thus 1 h at a concentration of 55 ppb would add 15 ppb.h to the AOT40. AOT40s up to 20,000 ppb.h may be recorded in the areas of Europe with the highest ozone concentrations.

- For crops, 6000 ppb.h AOT40 for a 10% yield loss; 3000 ppb.h AOT40 for a 5% yield loss, accumulated during daylight hours (i.e. with solar radiation levels > 50 W m^{-2}) during the 3-month period May to July.
- For semi-natural vegetation, the same AOT40 is used as for crops.
- For trees, 10,000 ppb.h AOT40, accumulated during daylight hours over a 6-month growing season.
- Serious plant damage can result from short episodes that do not cause the general critical level to be breached. The short-term critical level for ozone foliar injury involves an ozone exposure of more than 500 ppb.h during daylight hours within five consecutive days.

FOR REFERENCE PURPOSES ONLY

No critical level has been set for natural vegetation due to lack of sufficient decisive data.

It is important to note that, as damage for some species increases continuously with concentration rather than starting at some threshold, setting critical levels must involve some value judgement as to the level of acceptable damage. The 6000 ppb.h critical level, for example, is expected to lead to a 10% reduction of crop yield below that of a control crop grown at background ozone concentrations. The critical level values are based on experiments with a small number of varieties of a small number of agricultural species – mainly wheat, barley and green beans. Although they are the best that can be done at present, they should only be regarded as crude and temporary indicators of plant responses to air pollutants.

There is a continuing debate about the best metric for predicting ozone impacts. The front runners at the moment are the AOT40 in Europe and the SUM60 in the United States. SUM60 is the sum of all hourly mean concentrations ≥60 ppb. Unlike AOT40, the concentrations are added without subtracting the threshold, which makes it much less sensitive to threshold variability than the AOT40. The conclusion from the NCLAN programme mentioned earlier was that a 3-month, growing-season SUM60 of 26.4 ppm.h would protect 50% of the studied crops from yield losses of more than 10%. It is possible that more sophisticated metrics, weighted differently in different concentration ranges, will eventually be used. Future work may also lead to a redefinition of critical levels in terms of fluxes rather than concentrations. Peak monthly average fluxes to wheat in Europe have been shown to be around 2 nmol m^{-2} s^{-1}, with cumulative fluxes over the growing season of around 7 mmol m^{-2}.

Ozone concentrations will eventually be reduced by the ongoing reductions in emissions of the ozone precursors (hydrocarbons and NO_x). It is now possible to predict the resulting changes in some detail, as shown in Figure 10.33. Although the sharp reductions in emissions of ozone precursors are expected to reduce AOT40 doses substantially, there will still be room for improvement, with significant areas of southern Europe exceeding the critical level in 2010. The main precursor sources for these exceedances are expected to be heavy goods vehicles (HGVs) and evaporative emissions. In some areas, notably in parts of England, ozone concentrations were predicted to increase because there would not be so much NO around to react with the O_3.

FOR REFERENCE PURPOSES ONLY

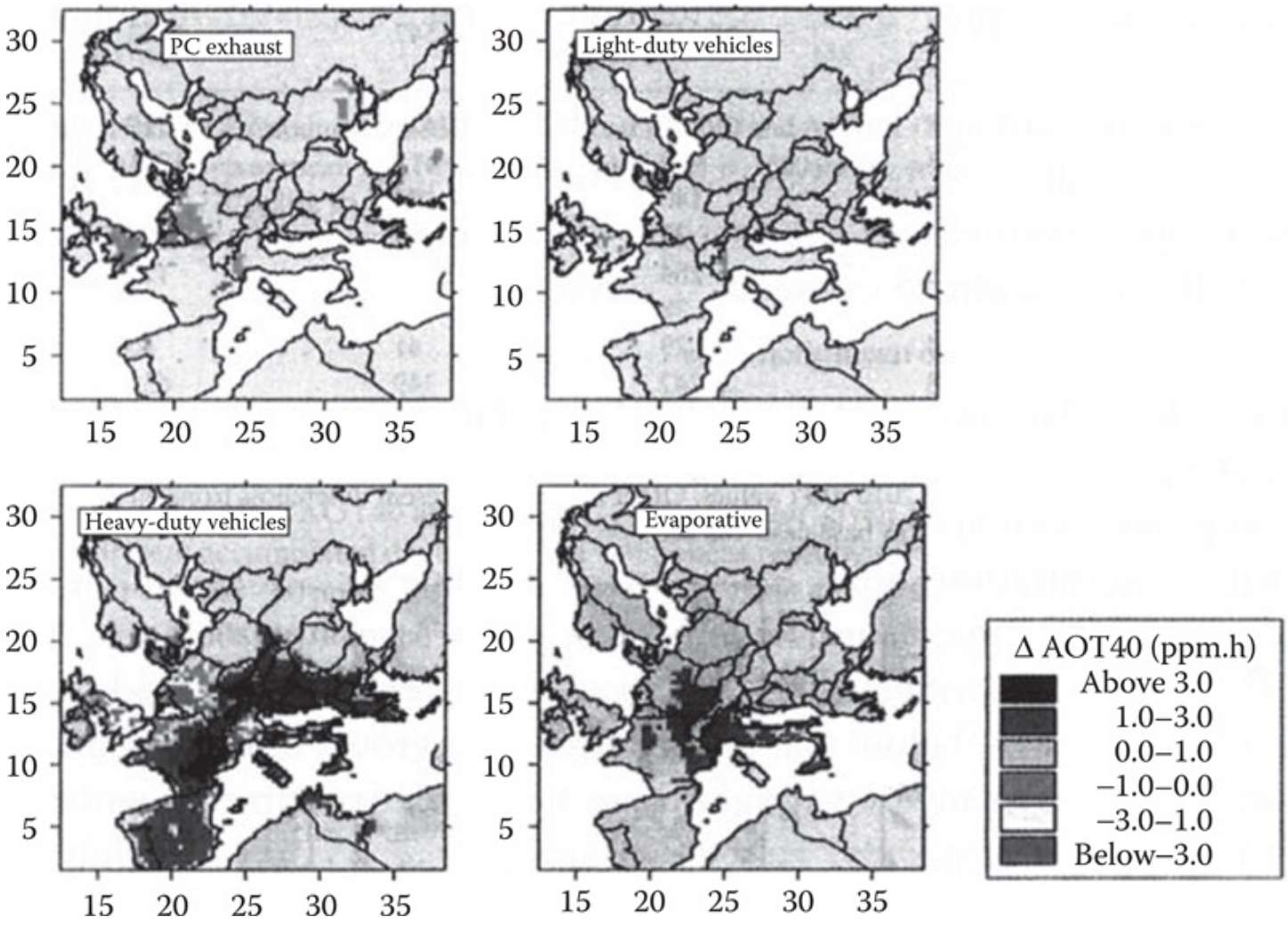

Figure 10.33 Modelled changes in ozone AOT40 in Europe, 1990–2010. (From Reis, S. et al., *Atmos. Environ.*, 34, 4701–4710, 2000.)

For sulphur dioxide, the long-term critical level has been set at 30 μg m^{-3} (11 ppb) for agricultural crops and 20 μg m^{-3} (8 ppb) for forests and natural ecosystems. It has also been proposed that in low-temperature regions (defined as being those for which the accumulated temperature does not exceed 1000 degree days above 5°C), the critical level should be set at 15 μg m^{-3} (6 ppb). This change recognises the field and laboratory evidence that SO_2 has a greater impact on plants in general, and trees in particular, at low temperatures. An additional critical level of 10 μg m^{-3} (as an annual mean) has been proposed for cyanobacterial lichens, which are especially sensitive to SO_2. This is a good example of the requirement that critical levels should be set low enough to encourage the recovery of damaged systems rather than simply to maintain the *status quo*. Lichens have been eradicated from large areas of Europe, including central and north-west England, by centuries of SO_2 fumigation. Although we do not yet know whether they will recolonise, it is a reasonable assumption that the lower the SO_2 concentration, the faster the process will be. It should be noted that in practice, the only critical level that matters is the lowest one

FOR REFERENCE PURPOSES ONLY

that applies to a grid square. Thus, although the critical level for forests might be 30 μg m^{-3}, all trees might be expected to support lichen, so that 10 μg m^{-3} will actually apply. Unless we decide that certain areas are forever to be lichenfree, 10 μg m^{-3} will have to be met everywhere.

For nitrogen oxides, the critical level for all plants has been set at an annual mean NO_x concentration of 30 μg m^{-3} (16 ppb). The lack of discrimination between crops, trees and natural vegetation simply reflects the lack of experimental data on different plant communities. It is thought that natural mixed vegetation is likely to be more sensitive than managed monocultures, particularly for nitrogen deposition, because adequate nitrogen is usually applied to crops as fertiliser to increase yield. Having defined critical levels, we are then in a position to compare them with measurements and hence to generate exceedance maps in just the same way as for critical loads. Figures 10.34 and 10.35 show that, in the UK in 1994–1998, the ozone critical level for forests (10,000 ppb.h above 40 ppb over 6 months) was exceeded in the south of England only, whereas that for crops and semi-natural vegetation (3000 ppb.h above 40 ppb over 3 months) was exceeded over most of the country.

Average ozone concentrations are thought to be rising, and this will probably increase the area in exceedance, although this depends to some extent on the concentration variability. In Europe, data on ozone trends is much more sparse than for the UK. The highest ozone concentrations are found in the southern European and Adriatic countries. Peak AOT40s are currently up to 14,000 ppb.h for annual plants (April–June) and 28,000 ppb.h for trees (April–September). Both of these values are about three times the respective UNECE critical levels. Even these values are probably underestimates at high altitude sites, because the ozone concentrations reported are for low altitude sites where the diurnal variation reduces the concentration in the evening, at night and in the early morning. The critical level of sulphur dioxide for crops and trees is not now exceeded in the UK. However, the lowest lichen critical level is exceeded over a significant area of central England. Average SO_2 concentrations have fallen drastically in the past decade, mainly as a result of the role of flue gas desulphurisation plants and displacement of coal by natural gas. The database for rural NO_x is sparser than for SO_2.

FOR REFERENCE PURPOSES ONLY

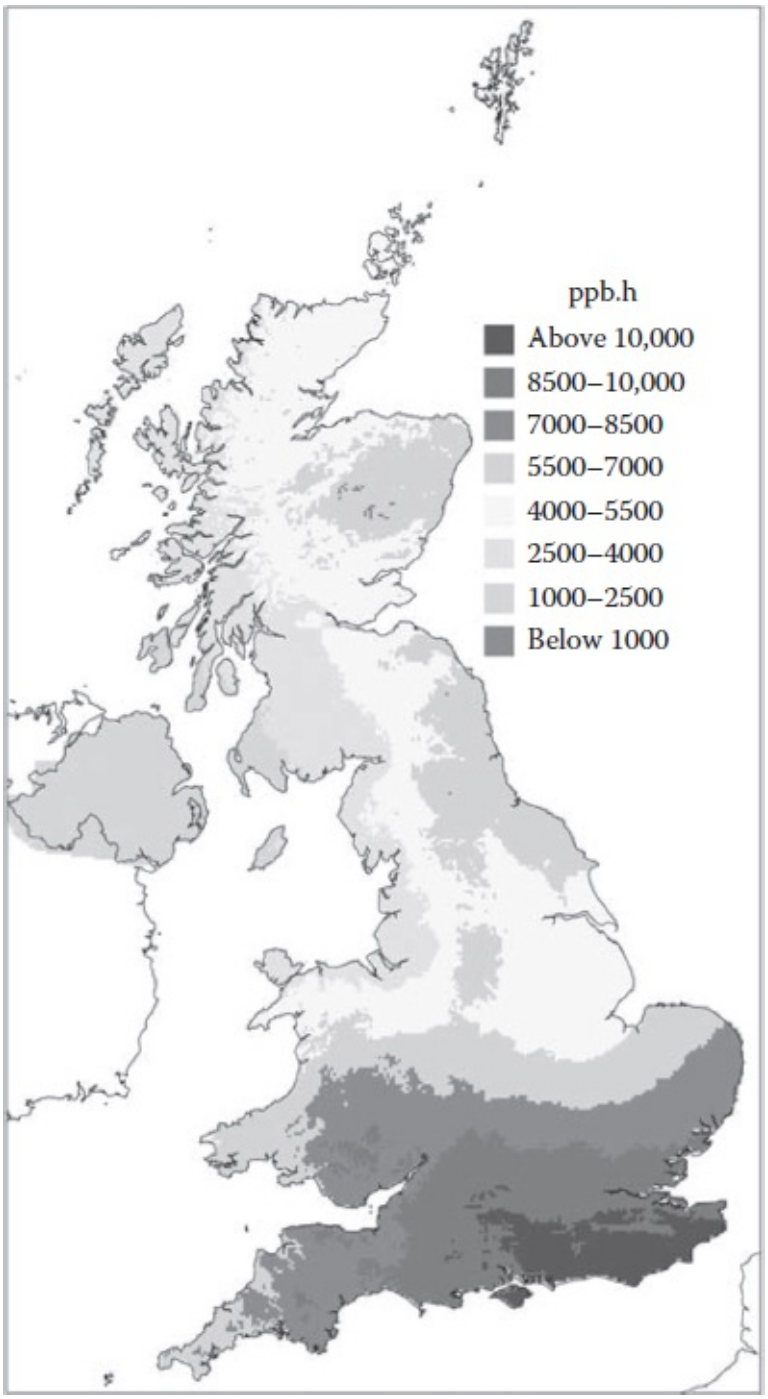

Figure 10.34 UK ozone AOT40 for forests, 1994–1998. (From National Expert Group on Transboundary Air Pollution, Transboundary air pollution: Acidification, eutrophication and ground-level ozone in the UK, Centre for Ecology and Hydrology, Edinburgh, Scotland, 2001.)

10.4.11 Interactions

The majority of air pollutant effects experiments are carried out on plants that are experiencing no other stress – this is necessary in order to meet the usual scientific principle of only changing one variable at a time. In the real world, however, this condition

FOR REFERENCE PURPOSES ONLY
is rarely met. Even crop plants, which represent the simplest plant monocultures and have their pests and diseases controlled for economic reasons, may experience drought stress. At the other extreme, a forest involves many plant and animal species, each of which, from the worms in the soil and fungi on the floor to the topmost leaf, may be affected directly or indirectly by air pollutants. There may be competition for resources between just two species (e.g. a grass/clover sward) in which one species is more affected by a pollutant than the other. Alternatively, one stressor such as drought may affect the ability of a plant to respond to another stressor such as ozone.

FOR REFERENCE PURPOSES ONLY

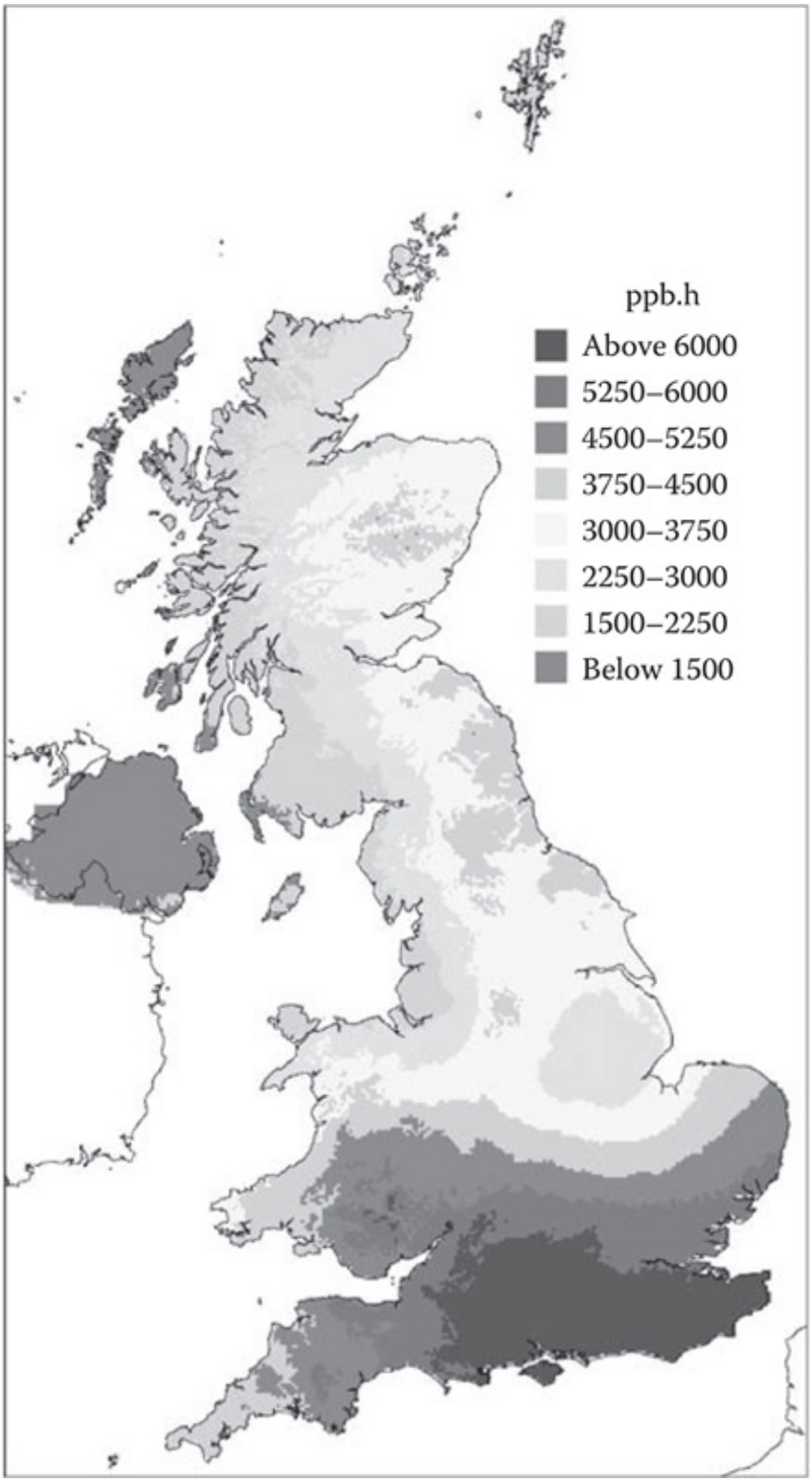

Figure 10.35 UK ozone AOT40 for crops and semi-natural vegetation 1994–1998. (From National Expert Group on Transboundary Air Pollution, Transboundary air pollution: Acidification, eutrophication and ground-level ozone in the UK, Centre for Ecology and Hydrology, Edinburgh, Scotland, 2001.)

10.5 DAMAGE TO MATERIALS

Atmospheric corrosion is the consequence of the interaction between any material such as metal, stone, glass, plastic or paint, and the gases and particles in the air. The key mediating factor is water, which is present in thin films on most surfaces. Even at 20% relative humidity there will be one or two equivalent monolayers present, increasing to eight or ten at 80%. The physical distribution of these water molecules depends strongly on the surface characteristics – whether it is hydrophilic or hydrophobic, for example. Particles in the atmosphere cause complications – hydrophilic or even hygroscopic particles may be deposited onto a hydrophobic surface. Water molecules may bond in either molecular or dissociated form, with the latter resulting in the formation of surface hydroxyl groups. Atmospheric gases such as CO_2, NO_2, SO_2, HCl, H_2S can all dissolve into the water film. Aerosol particles supply sulphates, chlorides and nitrates. Electrochemical reactions then occur at the interface between the solid substrate and the water layer. Local micro-variability means that some surface sites will support anode (e.g. metal dissolution, electron-generating) reactions, and others cathode (electron-consuming, reduction of oxygen to OH^-) reactions. For the cathodic sites, the required electrons are supplied by the easy diffusion of atmospheric oxygen through the thin water films. The composition of the aqueous layer changes dramatically and rapidly with the weather conditions, with orders of magnitude changes in ionic concentration, and hence several pH units, depending on the relative humidity. Eventually corrosion products, often hydroxides or oxyhydroxides, are precipitated from the ionic solution and cover the material surface. Corrosion rates are then affected by the transport of ions inward and outward across the layer, or by the transport of electrons from anodic to cathodic sites. We can expect corrosion to depend both on gaseous deposition velocity (supply of new gas to the water film) and on solubility (storage of material in the film). It may be very difficult to separate out the current effects from the historical ones. For example, even after a damaged stone surface has been cleaned, the effects of past pollution may make the stone more susceptible to current pollution.

10.5.1 Building materials

Recent projections indicated accentuations in the theoretical building dose-response functions (DRFs; the metrics commonly used to assess integrated exposure of building materials due to air pollutants and meteorological parameters) under air pollution and changing environment, mainly due to the altered micro-meteorological profile and chemical withering of building materials (including concrete, steel, stone, wood) under changing weather patterns (Brimblecombe and Grossi, 2008; Kumar and Imam, 2013). The DRFs serve as a tool for assessing the material recession rate as a consequence integrated exposure of building materials to air pollutants (mainly NO_2, SO_2, PM_{10}, O_3 and CO_2) and meteorological parameters (primarily ambient temperature, relative humidity, wind field, pH) (Table 10.21). Attention in the UK has been mainly directed at historic monuments

FOR REFERENCE PURPOSES ONLY

such as St Paul's (London), Lincoln and York cathedrals, which stand either in areas of high urban pollution or downwind from coal-fired power stations. On any stone building, we normally find a mixture of *clean* surfaces that are stone-coloured, and blackened surfaces. The latter soiling may in itself be a serious environmental problem.

The clean surfaces are exposed to falling rain and running rain water; damage is mainly due to rapid deposition of gaseous SO_2 to wet stone surfaces rather than to the acid rain itself. The blackened surfaces are regions protected from the direct effects of the acid rain. Particles that are deposited to these surfaces are not washed off. Eventually the particles, together with dry-deposited gases such as SO_2, produce a crystalline gypsum lattice within the stonework interstices. The volume occupied by hydrated calcium sulphate is 1.7 times that of the carbonate that it replaces, so that pressure from the crystal growth breaks off small areas of stone, also exposing a more vulnerable surface. Furthermore, the loss of the sulphur results in the remaining solution becoming increasingly acidic and dissolving the original carbonate stone more rapidly. All building stone is porous to a degree, and some is very porous. While the porosity of marble may be only 1%, that of limestone may be as high as 40%. Hence water, and any chemical species dissolved in it, has access to the interior of the stone as well as to the outside surface. The primary role of water in stone corrosion, compared with metal corrosion, is to provide the medium into which the calcium carbonate can dissolve. The products are carbonates such as dolomite, sulphites, sulphates, nitrates and oxalates.

Table 10.21 List of dose–response functions for estimating the impact of air pollutants and meteorological parameters on common building materials

Material	*Dose–response function*
Carbon steel	$R = 1.58[SO_2]^{0.52}\, e^{[0.02Rh + fCs(T)]} + 0.166Rn[H^+] + 0.0761\, PM_{10} + 0.102D_{Cl}^{0.33} e^{[0.033Rh + 0.040T]}$
	$f_{Cs}(T) = 0.150(T–10)$ when $T \leq 10°C$
	$f_{Cs}(T) = –0.054(T–10)$ when $T > 10°C$
	$R = 1.77[SO2]^{0.52}\, e^{[0.20Rh + fws(T)]} + g(Cl^–, Rh, T)$
	$ML = 29.1 + t^{0.6}\, (21.7 + 1.39[SO_2]^{0.6}\, Rh_{60}\, e^{fWs(T)} + 1.29\, Rn[H^+] + 0.593PM_{10})$
	$f_{ws}(T) = 0.150(T–10)$ when $T \leq 10°C$
	$f_{ws}(T) = –0.054(T–10)$ when $T > 10°C$
Portland limestone	$R = 2.7\, [SO_2]^{0.48}\, e^{–0.018T} t^{0.96} + 0.019\, Rn[H^+]\, t^{0.96}$
	$R = 3.1 + t(0.85 + 0.0059\, Rh_{60}\, [SO_2] + 0.078\, Rh_{60}\, [HNO_3] + 0.054\, Rn[H^+] + 0.0258\, PM_{10})$
	$[HNO_3] = 516\, e^{–3400/(T+273)}\, ([NO_2][O_3]\, Rh)^{0.5}$
	$R = 18.8\, Rn + 0.016\, [H^+]\, Rn + 0.18\, (V_{dS}\, [SO2] + V_{dN}\, [HNO_3])$
	[a]$R = 3.1 + t\, (0.85 + 0.0059[SO_2]\, Rh_{60} + 0.054\, Rn[H^+] + 0.078\, (516\, e^{–3400/(T+273)}\, ([NO_2]\, [O_3]\, Rh)^{0.5}\, Rh_{60}) + 0.0258\, PM_{10})$

Source: Kumar, P. and Imam, B., *Sci. Total Environ.*, 444, 85–101, 2013.

Nomenclature:
ML is the mass loss (g m^{-2})

FOR REFERENCE PURPOSES ONLY

R is the surface recession (μm yr^{-1})

SO_2 is sulphur dioxide (μg m^{-3})

NO_2 is nitrogen dioxide (μg m^{-3})

O_3 is ozone (μg m^{-3})

PM_{10} is the particulate matter ≤10 μm in diameter (μg m^{-3})

T is the ambient temperature (°C)

t is the time (years)

$f_{Cs}(T)$ is the correction factor depending on temperature (–)

$f_{ws}(T)$ is the correction factor depending on temperature (–)

Rh is the relative humidity (%)

V_{dS} is the deposition velocity of sulphur dioxide, SO_2 (cm s^{-1})

V_{dN} is the deposition velocity of nitric acid, HNO_3 (cm s^{-1})

D_{cl} is the chloride deposition (mg m^{-2} day^{-1})

Rn is the precipitation (m yr^{-1})

[a] ML and R stand for mass loss by corrosion attack in g m^{-2} and surface recession or thickness loss in μm (>1–year exposure) or μm yr^{-1} (1–year exposure), respectively. Gaseous and ion concentrations are annual mean in μg m^{-3} and mg L^{-1}. D_{cl} is chloride deposition (mg m^{-2} day^{-1}) and Rh_{60} = (Rh–60) when Rh >60; otherwise 0. Rn is precipitation in m yr^{-1}; V_{dS} and V_{dN} are deposition velocities (cm s^{-1}) for SO_2 and HNO_3, respectively.

At St Paul's, lead dowels used in the original construction have been used to measure the long-term erosion rates of stonework. The dowels were originally flush with the stone surface, but have been left standing proud as the stonework has decayed. The average erosion rate over the period 1727–1982 was found to be 80 μm a^{-1} (=8 mm $century^{-1}$). In short-term measurements, the erosion rate was found to be higher (up to 220 μm a^{-1}) but this was an interpretation of a mass-loss measurement, and some of the mass could have been coming from below the surface. Of course, even clean rain is already weak carbonic acid (pH 5.6) that dissolves limestone, and building damage must be seen in this context. Portland stone, for example, has long been favoured as a building material because of its known resistance to pollution. In the National Materials Exposure Programme, test specimens of stone (Portland limestone, dolomitic sandstone and Monks Park limestone) and coated and bare metals (mild and galvanised steel, painted steel, aluminium and copper) were put out at 29 sites across the UK in the period 1987–1995 to map the effects, and to relate them to local SO_2 concentrations and acid deposition rates. The metal samples (75 × 50 × 3 mm) were mounted on sloping racks and exposed to direct rainfall. The stone samples (50 × 50 × 8 mm tablets) were either exposed to, or sheltered from, direct rainfall. Provisional results from these experimental programmes show that linear damage functions can account for up to 70% of the observed variation of surface erosion with environmental factors. Damage to stone is measured by weight change, because dissolution is not only a surface effect. At remote (unpolluted) sites with high rainfall, damage to exposed stone is dominated by dissolution losses, whereas sheltered stone at high SO_2 may show a weight gain due to gypsum formation. In direct comparisons, the erosion rates of stone samples in London were found to be three times those of identical samples in rural Hertfordshire.

FOR REFERENCE PURPOSES ONLY

10.5.2 Other materials

Sulphur dioxide reacts with many other materials, such as the zinc on galvanised steel (corrugated iron, electricity pylons). The former UK Central Electricity Generating Board was responsible for maintaining 20,000 galvanised steel pylons and was therefore interested in the effects of pollution in shortening pylon life. Test squares of galvanised steel were put out all over the country; results showed a strong correlation between corrosion rate and known sources of SO_2, as well as with proximity to the sea. Another important effect is the expansion of metal as it corrodes. This process exerts huge pressures on the surrounding structure, which it can eventually split. Additional results from NAPAP have shown that corrosion rates in industrial US cities have declined in step with SO_2 concentrations, and that corrosion rates have been low in areas of low sulphur dioxide concentration. Paint consists of a substrate (natural or synthetic oil or resin) and a pigment (e.g. titanium dioxide, white lead, zinc oxide). Both the substrate and the pigment are subject to attack by SO_2, H_2S and O_3. SO_2 also attacks the paper in books and the leather on the binding of hardbacks, because metallic impurities in the paper and leather catalyse the conversion of SO_2 to sulphuric acid. Ozone is a powerful oxidising agent, responsible for the decay of elastic materials by attacking the double bonds of compounds such as butadiene-styrene.

One of the factors responsible for the loss of elasticity of rubber bands is ozone in the air; in fact, the depth of cracks in rubber was used as an early O_3 measurement technique in California. Other effects are insidious and hard to control. For example, ozone bleaches the colours on paintings. As paintings are expected to last for hundreds of years, even very low O_3 concentrations of around 1 ppb can supply a significant dose (= concentration × time) and threaten the appearance (and hence value) of works of art. Museums and galleries have to consider how to reduce the air concentration of ozone down to 1 ppb (compared to the ambient background of around 20 ppb and peak levels in Los Angeles of around 600 ppb). This can be achieved by charcoal filtration, but only if very tight controls are imposed on door opening and other routes for infiltration of ambient air. NO_2 has also had serious effects on colours of materials – in particular, the NO_2 generated by indoor gas fires discoloured nylon fabrics until various additives in the fabrics were changed by the manufacturers.

10.6 CASE STUDY: DONORA ACID RAIN

In 1948, the town of Donora in Pennsylvania was hit by a smog that was responsible for the deaths of 20 people. The smog was caused by a mixture of fog, chimney smoke and effluents from the three factories in the town. This mixture caused people with existing respiratory conditions to suffer immensely and in some cases they died. The toxic smog also probably effected the surrounding environment however the deaths were so shocking this was no focused on the report. This incident raised awareness of air pollution and may

FOR REFERENCE PURPOSES ONLY

have been a contributing factor to the Clean Air Act 1963. Unfortunately, this incident caused the industry in Donora to close and the town has less than half the population it had in 1948. In Donora in 1948, the smog was not only made up from pure smoke; there were also compounds produced from the three factories in town. The substances emitted into the atmosphere included: nitrogen oxides, hydrogen sulphide, fluoride, chloride and cadmium oxide (Townsend, 1950).

Donora is situated in the valley of the Monongahela River with the bottom of the valley 400 feet below the top, south of Pittsburgh (Figure 10.36). Originally the town was set up to produce oil but by 1948 the town produced galvanised wire from three factories: a steel plant, a wire mill and a zinc plant. The loss of this industry caused the town to go into economic decline and in 2010 the average income was $27,939 compared to the US national average of $41,994 (ePodunk, 2007; Vesilind et al., 2010). In October 1948, a series of events occurred that resulted in 20 people dying in just 5 days; their deaths were caused by severe air pollution (smog) (Vesilind et al., 2010). As well as covering the chronology of the event, this case study will outline the health, environmental and socio-economic effects of the incident.

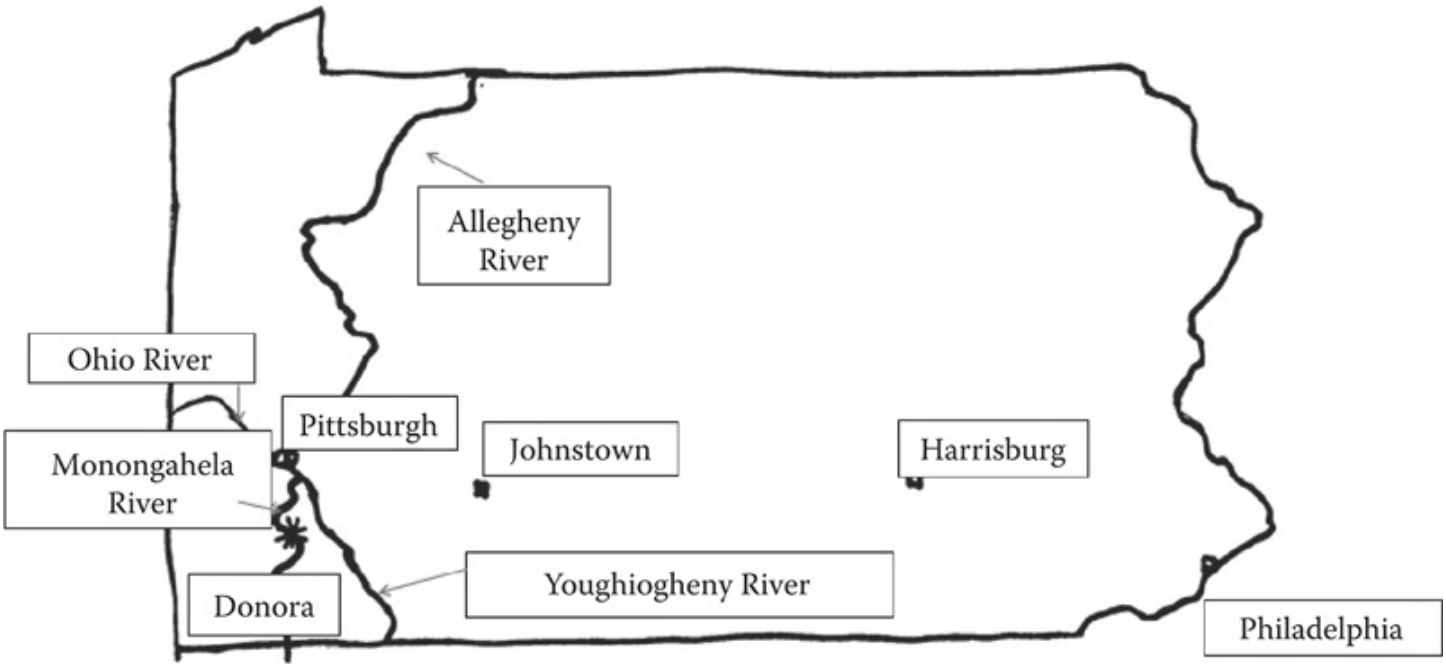

Figure 10.36 A sketch of Pennsylvania showing the location of Donora.

FOR REFERENCE PURPOSES ONLY

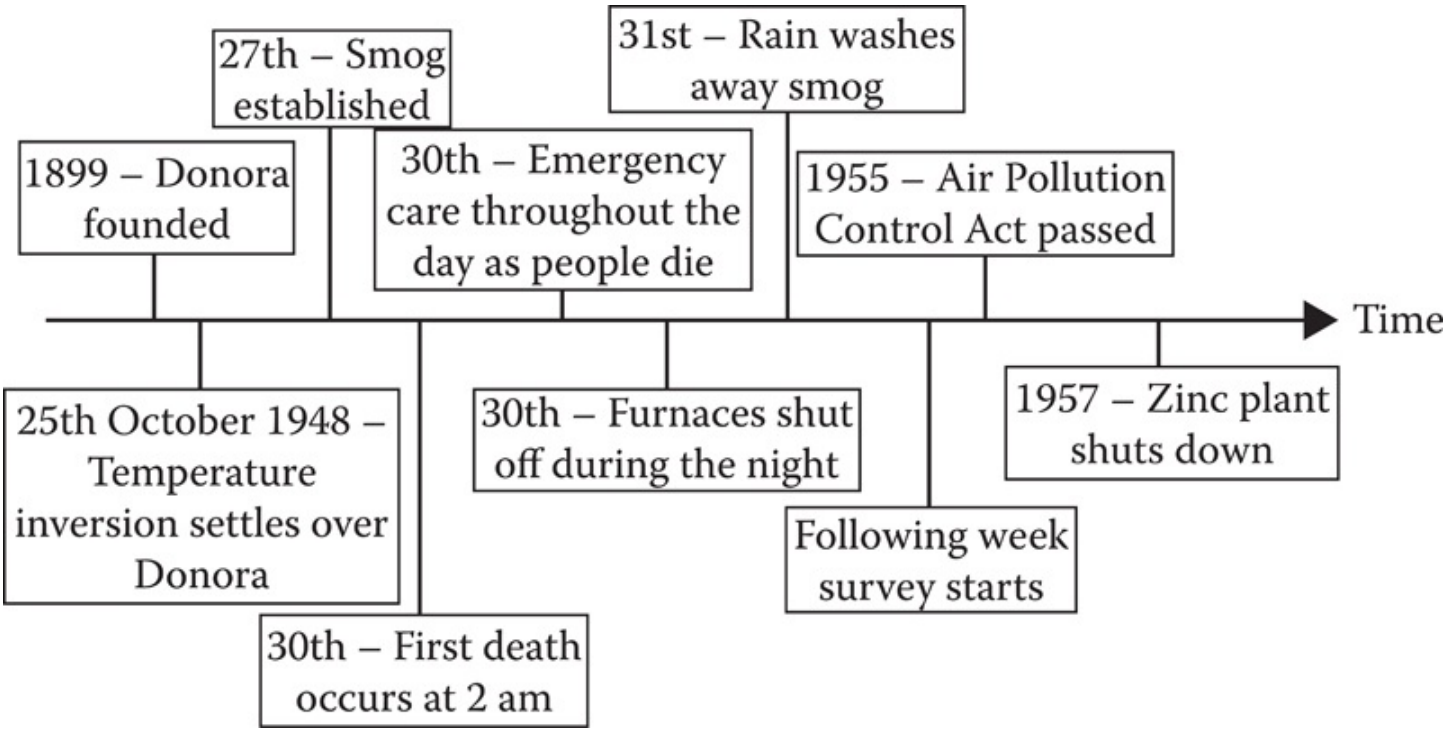

Figure 10.37 Timeline showing the order of events prior to and after the 1948 smog in Donora.

10.6.1 Chronology of event

The town of Donora was founded in 1899 by William H. *Don*ner and he named is after himself and *Nora* McMullen Mellon. At the start of the year 1900, there were only 12 residents, but the area's industrial potential meant that by 1901 there were 4000 residents. Originally, oil was produced, but steel eventually became the dominant industry (Stacey et al., 2010) and by 1948, the population totalled 13 thousand. All of the houses and shops burnt coal for energy and so did the three factories. Coal smoke contains particulates and sulphur dioxide as well as other contaminants of measurable quantities (Townsend, 1950) and this meant that smog was a familiar occurrence in Donora before 1948 (Townsend, 1950).

Usually the pollutants dispersed, but on Monday 25th October 1948, a temperature inversion settled over Donora; see Figure 10.37. The town is surrounded by hills that rise 400 feet above the valley bottom and so by Wednesday the smog was well established (Townsend, 1950). At 2 am on the Saturday morning, the first death occurred (Townsend, 1950). Throughout the day emergency care became a problem and firemen were sent around the town with oxygen tanks to give the sick a breath of oxygen before moving on (Vesilind et al., 2010). By the end of Saturday, 17 deaths had occurred and that night the furnaces in the plants were shut off to help reduce pollution (Townsend, 1950; Vesilind et al., 2010). On Sunday, rain came and ended the smog. However, by this time 20 deaths had been caused and 6000 residents had been affected (Helfand et al., 2001; Townsend, 1950).

FOR REFERENCE PURPOSES ONLY

The following week, a survey was started at the instigation of the Town Council. No report was ever published as a consequence of this survey but some results were later published in the *American Journal of Public Health* (Townsend, 1950).

The zinc plant shut down in 1957 and shortly afterwards the steel plant and wire mill also closed. These events may have lead to the economic demise of Donora (Vesilind et al., 2010).

10.6.2 Health effects

The original survey in 1948 used nurses to systematically survey the residents in one-third of the houses in Donora (Ciocco and Thompson, 1961; Townsend, 1950). Ciocco and Thompson (1961) also undertook a survey of the same households and managed to track 99% of the original families to 1957 when their survey took place. The original survey also recorded the constituents of the gas being released from the three plants and the outcomes of three autopsies (Townsend, 1950).

The initial survey (Townsend, 1950) found that about 6000 residents had been adversely affected by the air pollution to some degree. Unfortunately, many downplayed their symptoms as they many were workers at the three plants. The survey found that 15.5% of the population were mildly affected, 16.8% of the population were moderately affected and 10.4% of the population were severely affected. Usually the older the person, the more severely affected they were. Pre-existing conditions, especially cardiopulmonary ones, also caused people to be more severely affected. The three autopsies confirmed that the causes of death were cardiopulmonary failure associated with pre-existing cardiopulmonary diseases (Townsend, 1950).

The longer term effects were recorded by Ciocco and Thompson's study, published in 1961. They found that the residents of Donora who reported adverse health effects in the original survey had higher long term mortality than those persons who did not report symptoms. There was also a correlation between the severity of their symptoms and a higher mortality rate.

A survey by engineers of the gaseous and aerosol outputs of the three plants found measurable concentrations of: nitrogen oxides, hydrogen sulphide, fluoride, chloride and cadmium oxide, and of course, sulphur dioxide. None of the concentrations were high enough to cause an effect by themselves; the combined effect may however have been significant (Townsend, 1950).

Sulphur dioxide is produced from the combustion of the coal for fuel and it is also produced from the smelting of both iron and zinc ores. Chen et al. (2007) found that sulphur dioxide can cause as well as aggravate existing respiratory symptoms. In particular, sulphur dioxide can cause asthma (Koenig, 1999; Chen et al., 2007). Acute respiratory infections can occur at concentrations greater than 1.5 ppmv (parts per million by volume) (Jacobson, 2002). Heyder and Takenaka (1996) found that acidic particulates (such as the soot particles with sulphuric acid) at concentrations found in ambient air conditions caused bronchitis and

FOR REFERENCE PURPOSES ONLY

emphysema in dogs. Zinc oxide particles can react with sulphur dioxide and the subsequently products can produce an irritating effect in lungs (Dyson and Quon, 1976).

Carbon monoxide is created when oxygen is limited during combustion. It is tasteless, colourless and odourless and can cause a wide range of adverse cardiopulmonary effects (Chen et al., 2007). It bonds to haemoglobin in place of oxygen to form a compound called carboxyhaemoglobin (COHb) and stops the haemoglobin adsorbing enough oxygen. This can cause suffocation, although at low COHb values, the effect is reversible (Jacobson, 2002).

Nitrogen oxides refer to molecules containing nitrogen and oxygen, for example: nitrogen dioxide (NO_2) and dinitrogen tetroxide (N_2O_4). They are generated in flames as fuels are burned in air rather than pure oxygen (O_2). Over the long term, in mammals, they can destroy lung tissue leading to emphysema and lung infections and they can lower the lungs' defences to pneumonia and influenza. At a concentration of 3 ppmv, lung function is measurably decreased and at concentrations less than this, the lungs can become irritated and lung function is measurably decreased in asthmatics (WDNR, 2007).

Carbon monoxide reacts in the presence of nitrogen oxides to produce ground-level ozone (O_3) (Jacobson, 2002):

$$CO_{(g)} + 2O_{2\,(g)} \rightarrow CO_{2(g)} + O_{3(g)}$$

High concentrations of ground-level ozone can lead to respiratory tract inflammation. This in turn leads to a reduction in lung function and an aggravation of long term diseases (Townsend et al., 2003). Children who exercise in the course of an air pollution episode, such as during a football match in Donora in the 1948 event, have an increased chance of developing asthma (Townsend, 1950; Townsend et al., 2003).

A pioneering study by Jäppinen et al. (1990) found that a concentration of hydrogen sulphide that was ten times higher than ambient conditions had no effect on non-asthmatic people. The study also found a minimal effect on asthmatics, although two of them were severely affected, with a bronchial constriction of 30%. The test group was small and thus the study is not conclusive; but the severe reactions of the two asthmatics test subjects could have occurred in the Donora smog.

Inhalation of airborne fluoride is linked with respiratory failure. It also can become included in food stuffs and it then causes fluorosis of the bones and teeth (Ando et al., 2001). Townsend (1950 p. 186) found: 'there was no evidence of excessive inhalation or ingestion of fluoride in the community' however this has not stopped many people using Donora as a case against fluoridation of water (Bryson, 1998; Hattersley, 1999).

Chlorinated organics, such as methylene chloride, occur naturally when chlorine is combusted with fuel. Chlorinated organics can have negative health effects by being a central nervous system depressant or carcinogenic (Naeher et al., 2007).

Cadmium oxide is a product of zinc refining because sphalerite, a common zinc ore, contains high levels of cadmium impurities (Shiel et al., 2010). It is highly absorbable and

has been found to be carcinogenic on rats (Satarug et al., 2003; Waalkes, 2003). The No-Observable-Adverse-Effects-Level was found by Dunnick (1995) to be 0.025 mg/m^3. This was, however, on rats rather than humans and the rats had minimal lung lesions that were not life threatening.

10.6.3 Environmental effects

In the 1948 Donora survey, environmental effects were not covered (Townsend, 1950). From the constituents of the smoke, however, we can infer they were numerable.

One of the largest constituents of smoke is sulphur dioxide and, as previously seen, it can react to produce sulphuric acid. Sulphuric acid can cause acid deposition (the deposition of acid gases/aerosols/fog droplets/raindrops). Sulphuric acid (and other acids that may be caused by smoke such as nitric acid or hydrogen chloride) damage the surface of buildings. It predominantly affects limestone, although some sandstones, mortar and roof slate may also be damaged (Committee on Air Pollution, 1953).

$$H_2SO_{4(aq)} + CaCO_{3(s)} + H_2O_{(I)} \rightarrow CO_{2(g)} + CaSO_{4(s)}.2H_2O_{(I)}$$

The result of acid deposition to buildings is blistering, scaling and pocking, which mars the appearance of buildings and causes money to be spent to repair structural damage (Committee on Air Pollution, 1953).

Acid deposition can destroy far more material culture than just buildings. Iron and steel rust faster in acid conditions; leather, wool and cotton may be destroyed or damaged. Finer articles such as furnishing materials and works of art can be damaged by acid deposition. Acid deposition to the soil usually decreases plant growth. This occurs via two mechanisms:

1. The concentration of nutrients in the soil is reduced because the acid dissolves the some nutrients faster than water alone can. This increases leaching. In this case the lack of nutrients limits the growth.
2. Acid dissolves metal more easily than water and so Al^{3+} and Fe^{3+} become available for uptake by the plant. Al^{3+} and Fe^{3+} are toxic and so the plants start to die (Jacobson, 2002).

The second effect also kills fish in acid lakes. In this situation, the acid dissolves the Al^{3+} which irritates the fish's gills. The fish then produce more mucus on their gills; this extra mucus stops them absorbing oxygen and so the fish suffocate (Williams, 2003).

Nitrogen oxides can seriously effect vegetation by reducing the growth rate, bleaching plant tissue and causing the leaves to fall off. Nitrogen oxides can deteriorate fabrics, fade dyes and corrode metals (WDNR, 2007). They also contribute to global warming and acid deposition:

FOR REFERENCE PURPOSES ONLY

$$HNO_{3(g)} \rightleftarrows HNO_{3(aq)} \rightleftarrows H^+ + NO_3^-$$

Carbon monoxide and nitrogen oxides can react to produce ground-level ozone. Ozone damages rubber and so tyres and insulation will get damaged; it also damages many types of fabric. Ozone also severely damages plants by causing necrotic patterns on the leaves, growth alterations and reduced yields. This damage then makes the plants susceptible to disease which cumulates the damaged caused.

Hydrogen sulphide is the gas that smells like rotten eggs. It has high acute toxicity to aquatic life, birds, and animal and effects humans by upsetting their respiratory system and their central nervous system (Elsom, 1992; National Pollution Inventory, 2010).

Fluoride can be taken in through the stomata of plants or from the soil and causes leaf cell damage, which slows growth or even cell death (Domingos et al., 2003). In animals, large amounts of fluoride can accumulate in their bodies from eating fluorine high plants. Fluoride mainly accumulates in bones causing bones to suffer, tooth decay and loss of weight.

Cadmium can be absorbed by plants through their roots and, by some plants, directly from the air. The plants that adsorb straight from the air are used as indicator species of pollution. Cadmium effects plants by reducing their growth, causing wilting, leaf discolouration and necrosis (Hiatt and Huff, 1975). Cadmium can then be passed up through the food chain and this is where the effects can be most easily recorded as plants are more tolerant to cadmium than animals. The cadmium accumulates in the livers and kidneys of animals (Satarug et al., 2003). The major effect from inhalation in animals is the same as we have seen above for humans.

Deposition of soot can destroy the appearance of building materials within a few years. Soot can smother the leaves of plants, which reduces their ability to photosynthesise and grow.

10.6.4 Socio-economic effects

After the Donora incident, many states started to pass legislation on air pollution. In 1955 the first piece of national legislation was written. This was the Air Pollution Control Act 1955. This act identified air pollution as a national concern. This was followed in 1963 by the first version of the Clean Air Act was passed and this set emission limits. As then the Clean Air Act has been amended many times (Mallette, 1956; Seinfeld, 2004). Donora was not the only incident that helped to raise the awareness of air pollution. The development of the legislation was also helped in the United States by the identification of a so-called smog type, photochemical *smog* in Los Angelis. During the winter of 1952 there was also a large smog in London (Chapter 1), with a death toll 4000 in one week. These events helped to catalyse the reaction to make air quality legislation (Seinfeld, 2004).

The people in Donora did not want to blame the industry as they worked there unfortunately soon after the industry closed and the little town of Donora went in to

FOR REFERENCE PURPOSES ONLY

economic decline (Townsend, 1950; Vesilind et al., 2010). These days there is a small museum, which opened in 2008 (http://www.donorasmog.com/).

Scientific research into air pollution increased after the Donora event. The Air Pollution Control Act 1955 was enacted to research into air pollution. The product of this act was another, the Clean Air Act 1963, which funded more research and the cleanup of air pollution (Eubanks, 2009).

We can infer that the smog caused some economic loss due to the shutting down of the plants during the incident and running the plant at less than full capacity afterwards (Townsend, 1950). Many of the environmental effects above cause lower crop growth and this may have also affected the area economically. The loss of man-hours and a reduction in the population's healthy life years are other way in which the smog could have caused economic loss (Cifuentes and Lave, 1993).

REFERENCES AND FURTHER READING RESOURCES

Absalom, H. W. L. (1954) Meteorological aspects of smog. *Quarterly Journal of Royal Meteorological Society*, 80: 261–266.

Agrawal, S. B. and Agrawal, M. (Eds.). (2000) *Environmental Pollution and Plant Responses*. CRC Press, Boca Raton, FL.

Ahrens, C. D. (2007) *Meteorology Today: An Introduction to Weather Climate, and the Environment*, 8th ed. Thompson Higher Education, Belmont, CA.

Ando, M., Tadano, M., Yamamoto, S., Tamura, K., Asanuma, S., Watanabe, T., Kondo, T. et al. (2001) Health effects of fluoride pollution caused by coal burning. *The Science of the Total Environment*, 271: 107–116.

Andrews, J. E., Brimblecombe, P., Jickells, T. D., Liss, P. S., and Reid, B. J. (2004) *An Introduction to Environmental Chemistry*, 2nd ed. Blackwell Science, Oxford, UK.

Ashmore, M. R. (2005) Assessing the future global impacts of ozone on vegetation. *Plant, Cell & Environment*, 28(8): 949–964.

Ayres, J., Maynard, R., and Richards, R. (2006) *Air Pollution and Health*. Imperial College Press, London, UK.

Baker, C. K., Colls, J. J., Fullwood, A. E., and Seaton, G. G. R. (1986) Depression of growth and yield in winter barley exposed to sulphur dioxide in the field. *New Phytologist*, 104: 233–241.

Binkova, B., Bobak, M., Chatterjee, A., Chauhan, A., Dejmek, J., Dockery, D., Everard, M. et al. (2004) *The Effects of Air Pollution on Children's Health and Development: A Review of the Evidence*. World Health Organization, Geneva, Switzerland.

Boisa, N., Elom, N., Dean, J. R., Deary, M. E., Bird, G., and Entwistle, J. A. (2014) Development and application of an inhalation bioaccessibility method (IBM) for lead in the PM10 size fraction of soil. *Environment International*, 70: 132–142.

Brimblecombe, P. and Grossi, C. (2008) Millennium-long recession of limestone facades in London. *Environmental Geology*, 56: 463–471.

Bryson, C. (1998) The Donora Fluoride Fog: A secret history of America's worst air pollution disaster. *Earth Island Journal*, 13: 36–37.

Chen, T. M., Gokhale, J., Shafer, S., and Kuschner, W. G. (2007) Outdoor air pollution: Nitrogen dioxide, sulphur dioxide, and carbon monoxide health effects. *The American Journal of the Medical Sciences*, 333: 249–256.

Cifuentes, L. A. and Lave, L. B. (1993) Economic valuation of pollution abatement: Benefits from health effects. *Annual Review of Energy and the Environment*, 18: 319–342.

Ciocco, A. and Thompson, D. J. (1961) A follow-up of Donora ten years after: Methodology and findings. *American Journal of Public Health*, 51: 155–164.

Colls, J. J., Sanders, G. E., Geissler, P. A., Boute, J., Galaup, S., Weigel, H. J., Brown, V. C., and Jones, M. (1993) The

FOR REFERENCE PURPOSES ONLY

responses of beans exposed to air pollution in open-top chambers. In: H. J. Jager, M. H. Unsworth, L. de Temmerman and P. Mathy (Eds.), *Effects of Air Pollution on Agricultural Crops in Europe*, Air Pollution Research Report 46, CEC, Brussels, Belgium.

Colls, J. J., Geissler, P. A., and Baker, C. K. (1991) Long term performance of a field release system for the intermittent exposure of agricultural crops to sulphur dioxide. *Atmospheric Environment*, 25A: 2895–2901.

Committee on Air Pollution (1953) *Interim Report*. HMSO, London, UK.

Day, D. E. and Malm, W. C. (2001) Aerosol light scattering measurements as a function of relative humidity: A comparison between measurements made at three different sites. *Atmospheric Environment*, 35: 5169–5176.

De Kok, L. J. and Stulen, I. (1998) *Responses of Plant Metabolism to Air Pollution and Global Change*. Backhuys Publishers, Amsterdam, the Netherlands.

Dockery, D. W., Pope, C. A., Xu, X., Spengler, J. D., Ware, J. H., Fay, M. E., Ferris Jr, B. G. and Speizer, F. E. (1993) An association between air pollution and mortality in six US cities. *New England Journal of Medicine*, 329: 1753–1759.

Domingos, M., Klumpp, A., Rinaldi, M. C. S., Modesto, I. F., Klumpp, G., and Delitti, W. B. C. (2003) Combined effects of air and soil pollution by fluoride emissions on *Tibouchina pulchra* Cogn., at Cubatão, SE Brazil, and their relations with aluminium. *Plant and Soil*, 249: 297–308.

Dominici, F., Sheppard, L., and Clyde, M. (2008) Health effects of air pollution: A statistical review. *International Statistical Review*, 71(2): 243–276.

Dunnick, J. K. (1995) *NTP technical report on toxicity studies of cadmium oxide*. National Toxicology Program, Toxicity Report Series, Number 39. United States Department of Health and Human Services, Washington, DC.

Dyson, W. L. and Quon, J. E. (1976) Reactivity of zinc oxide fume with sulfur dioxide in air. *Environmental Science and Technology*, 10(5): 476–481.

Elsom, D. M. (1992) *Atmospheric Pollution: A Global Problem*, 2nd ed. Basil Blackwell, Cambridge, MA.

Emberson, L. (2003) Air pollution impacts on crops and forests: An introduction. In: L. Emberson; M. R. Ashmore and F. Murray (Eds.), *Air Pollution Impacts on Crops and Forests: A Global Assessment* (pp. 3–29), Imperial College Press, London.

ePodunk (2007) The power of place – Donora population overview [Online]. http://www.epodunk.com/cgi-bin/popInfo.php?locIndex=13843 (Accessed: 18th September 2010).

Eubanks, W. S. (2009) The clean air act's new source review programs: Beneficial to public health or merely a smoke- and mirrors scheme? *Journal of Land, Resources and Environmental Law*, 29: 361–375.

Finlay, W. H. (2001) *The Mechanics of Inhaled Pharmaceutical Aerosols: An Introduction*. Academic Press, San Diego, CA.

Goodman, A., Wilkinson, P., Stafford, M., and Tonne, C. (2011) Characterising socioeconomic inequalities in exposure to air pollution: A comparison of socio-economic markers and scales of measurement. *Health & Place*, 17: 767–774.

Green, H. L. and Lane, W. R. (1964) *Particulate Clouds, Dusts, Smokes and Mists*, 2nd ed. SPON, London, UK.

Grodzinska, K., and Szarek-Lukaszewska, G. (2001) Response of mosses to the heavy metal pollution in Poland. *Environmental Pollution*, 114: 443–451.

Grünhage, L., Krause, G. H. M., Köllner, B., Bender, J., Weigel, H.-J., Jäger, H.-J., and Guderian, R. (2001) A new flux-oriented concept to derive critical levels for ozone to protect vegetation. *Environmental Pollution*, 111: 355–362.

Harrad, S. (Ed.). (2000) *Persistent Organic Pollutants: Environmental Behavior and Pathways of Human Exposure*. Springer, New York.

Harrison, R. M. (1999) Measurements of concentrations of air pollutants. In: S. T. Holgate, J. M. Samet, H. S. Koren and R. L. Mayhard (Eds.), *Air Pollution and Health*, Academic Press, London, UK.

Hattersley, J. G. (1999) The case against fluoridation. *Journal of Orthomolecular Medicine*, 14: 185–187.

Heagle, A. S., Kress, L. W., Temple, P. J., Kohut, R. J., Miller, J. E., and Heggestad, H. E. (1987) Factors influencing ozone dose–yield response relationships in open-top field chamber studies. In: W. W. Heck, O. C. Taylor and D. T. Tingey (Eds.), *Assessment of Crop Loss from Air Pollutants*, Elsevier, Barking, UK.

Helfand, W. H., Lazarus, J., and Theerman, P. (2001) Images of health: Donora, Pennsylvania: An environmental disaster of the 20th century. *American Journal of Public Health*, 91(4): 553.

Hester, R. E. and Harrison, R. M. (Eds.) (2007) *Nanotechnology: Consequences for Human Health and the Environment* (Vol. 24). Royal Society of Chemistry, Cambridge, UK.

FOR REFERENCE PURPOSES ONLY

Heyder, J. and Takenaka, S. (1996) Long-term canine exposure studies with ambient air pollutants. *European Respiratory Journal*, 9(3): 571–584.

Hiatt, V. and Huff, J. E. (1975) The environmental impact of cadmium: An overview. *International Journal of Environmental Studies*, 7(4): 277–285.

Hinds, W. C. (1999) *Aerosol Technology: Properties, Behaviour and Measurement of Airborne Particles*. Wiley, New York.

Ho, M. S. (2007) *Clearing the Air: The Health and Economic Damages of Air Pollution in China*. MIT Press, Cambridge, MA.

Jacobson, M. Z. (2002) *Atmospheric Pollution: History, Science, and Regulation*. Cambridge University Press, Cambridge, UK.

Jäppinen, P., Vilkka, V., Marttila, O., and Haahtela, T. (1990) Exposure to hydrogen sulphide and respiratory function. *British Journal of Industrial Medicine*, 47: 824–828.

Jeffery, P. K. (1999) Effects of cigarette smoke and air pollutants on the lower respiratory tract. In: S. T. Holgate, J. M. Samet, H. S. Koren and R. L. Maynard (Eds.), *Air Pollution and Health*, Academic Press, London.

Klumpp, A., Ansel, W., Klumpp, G., Vergne, P., Sifakis, N., Sanz, M. J., Rasmussen, S. et al. (2006) Ozone pollution and ozone biomonitoring in European cities. Part II. Ozone-induced plant injury and its relationship with descriptors of ozone pollution. *Atmospheric Environment*, 40: 7437–7448.

Koenig, J. Q. (1999) Air pollution and asthma. *Journal of Allergy and Clinical Immunology*, 104: 717–722.

Krzyzanowski, M., Kuna-Dibbert, B., and Schneider, J. (2005) *Health Effects of Transport-Related Air Pollution*. World Health Organization, Geneva, Switzerland.

Kumar, P. and Imam, B. (2013) Footprints of air pollution and changing environment on the sustainability of built infrastructure. *Science of the Total Environment*, 444: 85–101.

Lippmann, M. 2000. Ozone. In: Lippmann, M. (Ed.), *Environmental Toxicants*. Wiley, New York.

Mallette, F. S. (1956) Legislation on air pollution. *Public Health Reports*, 71(11): 1069–1074.

Mukhopadhyay, K. (2009) *Air Pollution in India and Its Impact on the Health of Different Income Groups*. Nova Science Publishers, New York.

Naeher, L. P., Brauer, M., Lipsett, M., Zelikoff, J. T., Simpson, C. D., Koenig, J. Q., and Smith, K. R. (2007) Woodsmoke health effects: A review. *Inhalation Toxicology*, 19: 67–106.

NAPAP (1987) *Interim assessment—The causes and effects of acidic deposition*. National Acid Precipitation Assessment Program, Washington, DC.

NAPAP (1990) *Integrated assessment report*. National Acid Precipitation Assessment Program, Washington, DC.

National Expert Group on Transboundary Air Pollution (2001) Transboundary air pollution: Acidification, eutrophication and ground-level ozone in the UK, Centre for Ecology and Hydrology, Edinburgh, Scotland.

National Pollution Inventory (2010) Hydrogen sulfide: Environmental effects [Online] http://www.npi.gov.au/substances/hydrogen-sulfide/environmental.html (Accessed: 1st September 2010).

Omasa, K., Nouchi, I., and De Kok, L. J. (2006) *Plant Responses to Air Pollution and Global Change*. Springer, Japan.

Pope, C. A. and Dockery, D. W. (2006) Critical review–Health effects of fine particulate air pollution: Lines that connect. *Journal of the Air and Waste Management Association*, 56(6): 709–742.

Porter, F. C. (1991) *Zinc Handbook: Properties, Processing, Use in Design*. Marcel Dekker, New York.

Reiling, K. and Davison, A. W. (1992) Spatial variations in ozone resistance of British populations of *Plantago major L. New Phytologist*, 122: 699–708.

Reis, S., Simpson, D., Friedrich, R., Jonson, J. E., Unger, S., and Obermeier, A. (2000) Road traffic emissions – predictions of future contributions to regional ozone levels in Europe. *Atmospheric Environment*, 34: 4701–4710.

Royal College of Physicians (2016) *Every breath we take: The lifelong impact of air pollution*. Report of a working party. London, UK.

Ruzer, L. S. and Harley, N. H. (Eds.) (2004) *Aerosol Handbook: Measurement, Dosimetry and Health Effects*. CRC Press, Boca Raton, FL.

Satarug, S., Baker, J. R., Urbenjapol, S., Haswell-Elkins, M., Reilly, P. E. B., Williams, D. J., Moore, M. R. (2003) A global perspective on cadmium pollution and toxicity in non-occupationally exposed population. *Toxicology Letters*, 137: 65–83.

Seinfeld, J. (2004) Air pollution: A half century of progress. *Environmental and Energy Engineering*, 50(6): 1096–1108.

FOR REFERENCE PURPOSES ONLY

Seinfeld, J. H. and Pandis, S. N. (2000) *Atmospheric Chemistry and Physics*. Wiley, New York.

Sheppard, L. J. and Cape, J. N. (Eds) *Forest Growth Responses to the Pollution Climate of the 21st Century*. Springer, Dordrecht, the Netherlands.

Shiel, A. S., Weis, D., and Orians, K. J. (2010) Evaluation of zinc, cadmium and lead isotope fractionation during smelting and refining. *Science of the Total Environment*, 408(11): 2357–2368.

Singh, S. N. (Ed.) (2000) *Trace Gas Emissions and Plants*. Kluwer Academic, Dordrecht, the Netherlands.

Skarby, L. et al. (1993) Responses of cereals exposed to air pollutants in open-top chambers. In: H. J. Jager, M. H. Unsworth, L. de Temmerman and P. Mathy (Eds.), *Effects of Air Pollution on Agricultural Crops in Europe*, Air Pollution Research Report 46, CEC, Brussels.

Stacey, C. E., Charlton, B., and Lonich, D. (2010) *Donora*. Arcadia Publishing, Charlston, SC.

Stone, V. and Donaldson, K. (1998) Small particles–Big problem. *Aerosol Society Newsletter*, 33: 12–15.

Thurston, G. D. and Ito, K. (1999) Epidemiological studies of ozone exposure effects. In: S. T. Holgate, J. M. Samet, H. S. Koren and R. L. Maynard (Eds.), *Air Pollution and Health*, Academic Press, London.

Townsend, A. R., Howarth, R. W., Bazzaz, F. A., Booth, M. S., Cleveland, C. C., Collinge, S. K., Dobson, A. P. et al. (2003) Human health effects of a changing global nitrogen cycle. *Frontiers in Ecology and the Environment*, 1(5): 240–246.

Townsend, J. G. (1950) Investigation of the smog incident in Donora, Pa., and Vicinity. *American Journal of Public Health*, 40: 183–189.

UNEP, Global environmental outlook – GEO4: Environment for Development, United Nations Environment Programme, Nairobi, 2007.

USEPA (2011) School Siting Guidelines. EPA-100-K-11-004/October. www.epa.gov/schools/siting.

Vesilind, P. A., Morgan, S. M., and Heine, L. G. (2010) *Introduction to Environmental Engineering*, 3rd ed. Cengage Learning, Stanford, CA.

Waalkes, M. P. (2003) Cadmium carcinogenesis. *Mutation Research*, 533: 107–120.

Warrington, S. (1987) Relationship between SO2 dose and growth of the Pea Aphid, *Acyrthosiphon pisum*, on peas. *Environmental Pollution*, 43: 155–162.

WHO (2013) Review of evidence on health aspects of air pollution–REVIHAAP Project Report.

WHO (2015) Economic cost of the health impact of air pollution in Europe: Clean Air, Health and Wealth.

Williams, I. (2003) *Environmental Chemistry*. John Wiley & Sons, Chichester, UK.

Wilson, G. B. and Bell, J. N. B. (1985) Studies on the tolerance to sulphur dioxide of grass populations in polluted areas. III. Investigations of the rate of development of tolerance. *New Phytologist*, 100: 63–77.

Wilson, G. B. and Bell, J. N. B. (1986) Studies on the tolerance to sulphur dioxide of grass populations in polluted areas. IV. The spatial relationship between tolerance and a point source of pollution. *New Phytologist*, 102: 563–574.

Wisconsin Department of Natural Resources (WDNR) (2007) Nitrogen oxides sources and health effects (Online) http://dnr.wi.gov/air/aq/pollutant/oxides.htm

Chapter 11

Air pollution and climate change

11.1 STATE OF CLIMATE SCIENCE

Although we have coped with air quality problems such as combustion emissions, photochemical smog and depletion of the ozone layer by putting preventative measures in place when the symptoms got bad enough, climate change is more complex and intense. If you are young enough while you are reading this book to expect to live well into the second half of the twenty-first century, then you will probably experience the greatest level of environmental change, and the greatest efforts by humans to deal with it, that we have ever experienced. Words such as *climate change*, *global warming* and *greenhouse gases* have become integral to conversation on topics such as environmental protection and sustaining human existence on Earth. In this chapter we will look at the physical causes, and at some of the possible consequences of these changes, specifically in the context of atmospheric emissions of carbon dioxide (CO_2), methane (CH_4) and nitrous oxide (N_2O) – collectively known as the key *greenhouse gases* (GHGs, described in more detail in Section 11.1.3.1). Nearing the end of the twentieth century, it became evident that the mankind have now entered an era where our releases to the atmosphere have the potential to change the whole of Earth's environment more than ever before.

11.1.1 Intergovernmental Panel on Climate Change

In 2014 the Intergovernmental Panel on Climate Change (IPCC), the UN watchdog on climate change matters, issued a stark warning that the growing human influence on the climate system on all the continents will increase the likelihood of severe, pervasive and irreversible impacts for people and ecosystems. The IPCC has produced a series of reports generating the evidence base on the causes and consequences of climate change by collating existing data and coordinating new studies on the topic for two decades. Five Assessment Reports, each of which represents the efforts of hundreds of scientists around the world over periods of several years, and in which the whole topic of climate change is discussed

FOR REFERENCE PURPOSES ONLY

in exhaustive detail, have been published since 1990. In addition, IPCC has published subsidiary reports on specialist topics such as aircraft emissions and safeguarding the ozone layer. Parts of this chapter make extensive use of material from the first (FAR, 1990), second (Second Assessment Report [SAR], 1995), third (Third Assessment Report [TAR], 2001), fourth (AR4, 2007) and fifth (AR5, 2014) assessment reports. In particular, AR5 expressed the projections of the future changes with a qualitative level of confidence (from very low to very high) and, when possible, probabilistically with a quantified likelihood (from exceptionally unlikely to virtually certain). For this report, the future projections are made using the new Representative Concentration Pathways (RCPs) for greenhouse gases, to allow us to explore the choice we face, ranging between extremes of *do nothing* about climate change (RCP8.5) and *moderate-to-aggressive* interventions (RCP2.6 and RCP4.5).

Our understanding of the *human influence* on the Earth's climate has been progressively improving, largely through IPPC's collective efforts on summarising global climate research. AR4 indicated that warming of the climate system is *unequivocal* (i.e. undeniable), with the eleven of the twelve years between 1995 and 2006 ranking among the twelve warmest years in the instrumental record of global surface temperature (since 1850). AR5 concluded the period 1983–2012 was very likely the warmest 30-year period of the last 800 years (high confidence) and likely the warmest 30-year period of the last 1400 years (medium confidence). The central piece of information that has focussed attention on climate change has been the global average temperature. We have a reasonably well calibrated global data set going back to 1861, so that is the main starting date which has been used for these assessments of change. In fact, the SAR estimated that the temperature had increased by about 0.55°C during the last 140 years, the TAR raised this rate of increase to 0.6°C during the twentieth century, AR4 raised it further to 0.74°C. AR5 has projected the global surface temperature change for the end of the twenty-first century (2081–2100) relative to 1850–1900 to range between 1.5°C and 2°C (respectively representing high and medium confidence in predictions) (Figure 11.1). Predictions beyond 2100 are more sketchy at present, with plausible 2300 scenarios subjected to the level of interventions adopted, ranging from an increase of up to 8°C for RCP8.5 (i.e. do nothing) to stabilisation (or even cooling) for RCP2.6 and RCP4.5 scenarios. However, the warming has been erratic, and there is so much noise on the air temperature signal that it is hard to show that the trend is not just due to natural variability. The average temperature appears to have been fairly steady from 1860 to 1910, to have increased between 1910 and 1940, to have declined slightly between 1940 and 1975, and to have resumed its increase since then.

FOR REFERENCE PURPOSES ONLY

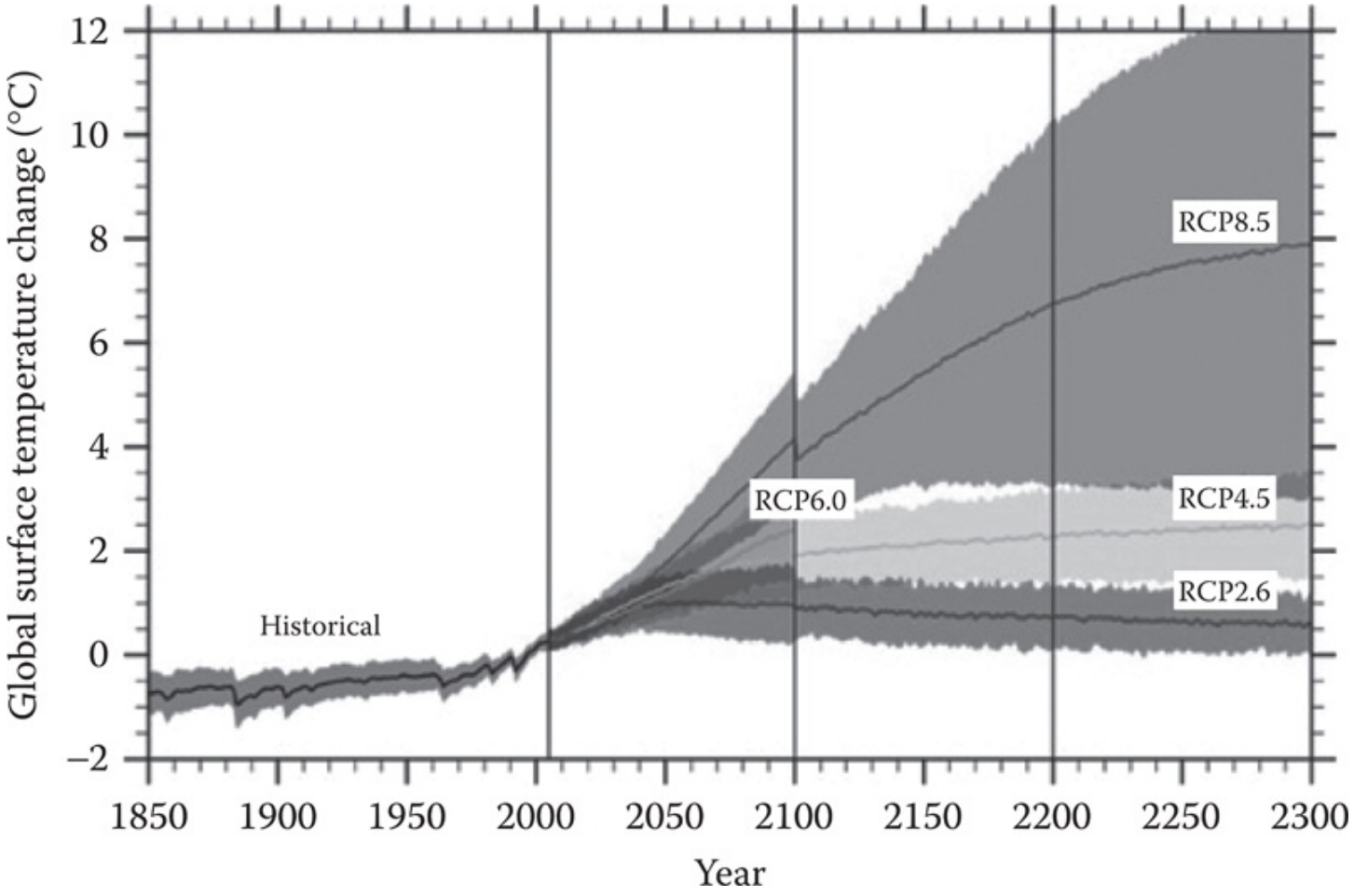

Figure 11.1 Time series of global annual mean surface air temperature anomalies, historical (1860–2000) and projected (2000–2300), relative to the average temperature for the period 1986–2005. (From IPCC, *Climate Change 2013: The Physical Science Basis, Contribution of Working Group I to the Fifth Assessment Report of the Intergovernmental Panel on Climate Change*, Cambridge University Press, Cambridge, UK, 2013.)

11.1.2 Trends in co-managing air pollution and climate change

Strategic interventions for reducing emissions from specific anthropogenic activity sector, such as transportation or energy, offer co-benefits to mitigating both climate change and air quality. However, co-emitted species within the targeted sector lead to a complex mix of chemistry and climate perturbations. The global impact of stringent climate policy on air pollutant emissions has been estimated for 2050 over 2005 levels (Figure 11.2). This incorporates mainly black carbon (BC) and sulphur dioxide (SO_2). The plot shows a comparative evaluation of the scenarios with stringent mitigation policies (achieving 430–530 ppm CO_2eq concentrations by 2100) against baselines scenarios (without additional efforts to reduce GHG emissions beyond those in place today). In both cases, the reduced air pollution loadings (>50% for BC and around 75% for SO_2) will particularly benefit

FOR REFERENCE PURPOSES ONLY

countries with weaker air pollution controls. Such initiatives with reduced costs for achieving air quality will accrue significant co-benefits for human health, ecosystem impacts.

On the other hand, improving air quality can influence climate warming (see emerging concept of *Co-management*, described in Section 14.11). Specifically, initiatives for reducing tropospheric ozone and particulate matter can affect the complex interactions between emissions, resulting in mixed cooling and warming effects (Figure 11.3). However, air pollutants affect climate differently according to their physical and chemical characteristics. For example, reduced SO_2 emission (primary precursor to scattering sulphate aerosols) can accelerate warming whereas reduced NO_x emission can induce cooling (through reducing tropospheric O_3) as we all warming (through influence on methane and aerosol concentrations). Controls on anthropogenic emissions of CH_4 to lower surface ozone have been identified as *win–win situations*. Overall, VOCs, NO_x and Black carbon seem to have both cooling and warming effects, depending on the nature of their interactions.

However, while well-mixed GHGs can have longer atmospheric presence (typically 100s of years), air pollutants typically may only last for few days to weeks. Also, air pollutants mainly impact locally by forcing local or regional perturbations to climate, whereas their global impact on the climate will be negligible. Pollution-generated GHGs will impact climate primarily through shortwave and longwave radiation, while aerosols can in addition affect climate through cloud–aerosol interactions. Some couplings between the targeted emissions and climate are still poorly understood or identified, including the effects of air pollutants on precipitation patterns, making it difficult to fully quantify these consequences. Further, at mixing ratios exceeding about 15%, even CO_2 can cause unconsciousness and death, therefore, treated as a potent air pollutant under exceptionally high concentrations (discussed in Chapter 10).

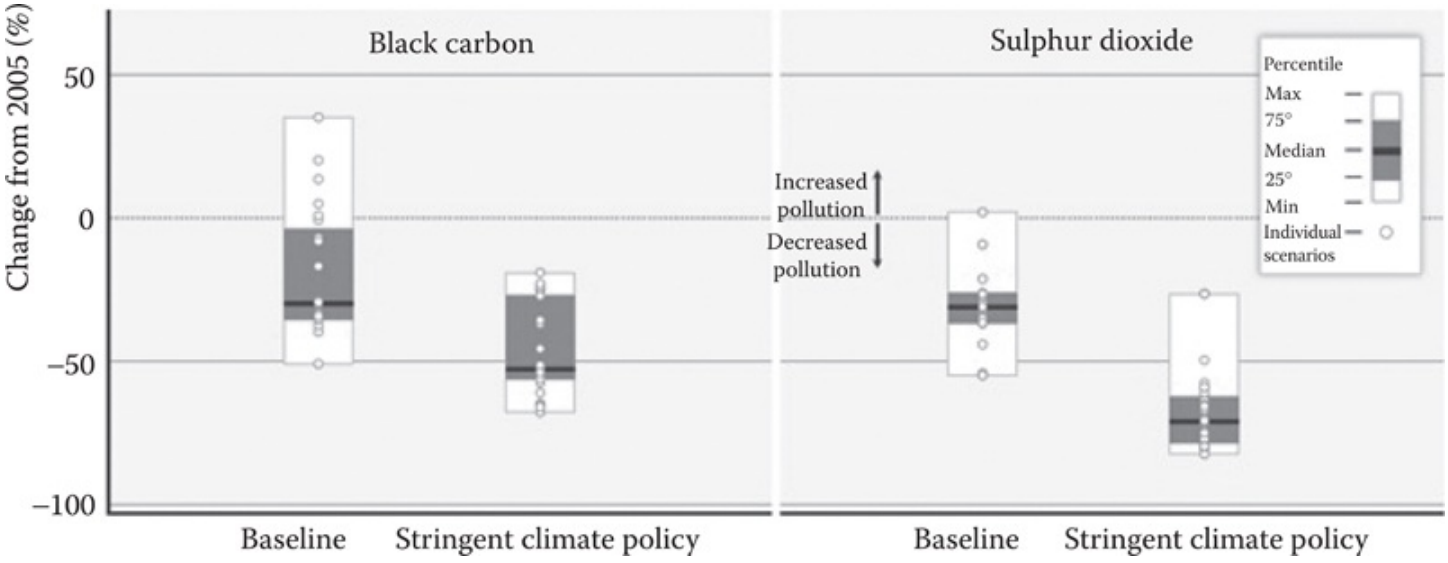

FOR REFERENCE PURPOSES ONLY

Figure 11.2 Implications for reduction in air pollution emission levels for black carbon (BC) and sulphur dioxide (SO_2) in 2050 relative to 2005 attributed to stringent climate change mitigation policies. (From IPCC, Summary for policymakers, in: *Climate Change 2014: Mitigation of Climate Change, Contribution of Working Group III to the Fifth Assessment Report of the Intergovernmental Panel on Climate Change*, Cambridge University Press, Cambridge, UK, 2014.)

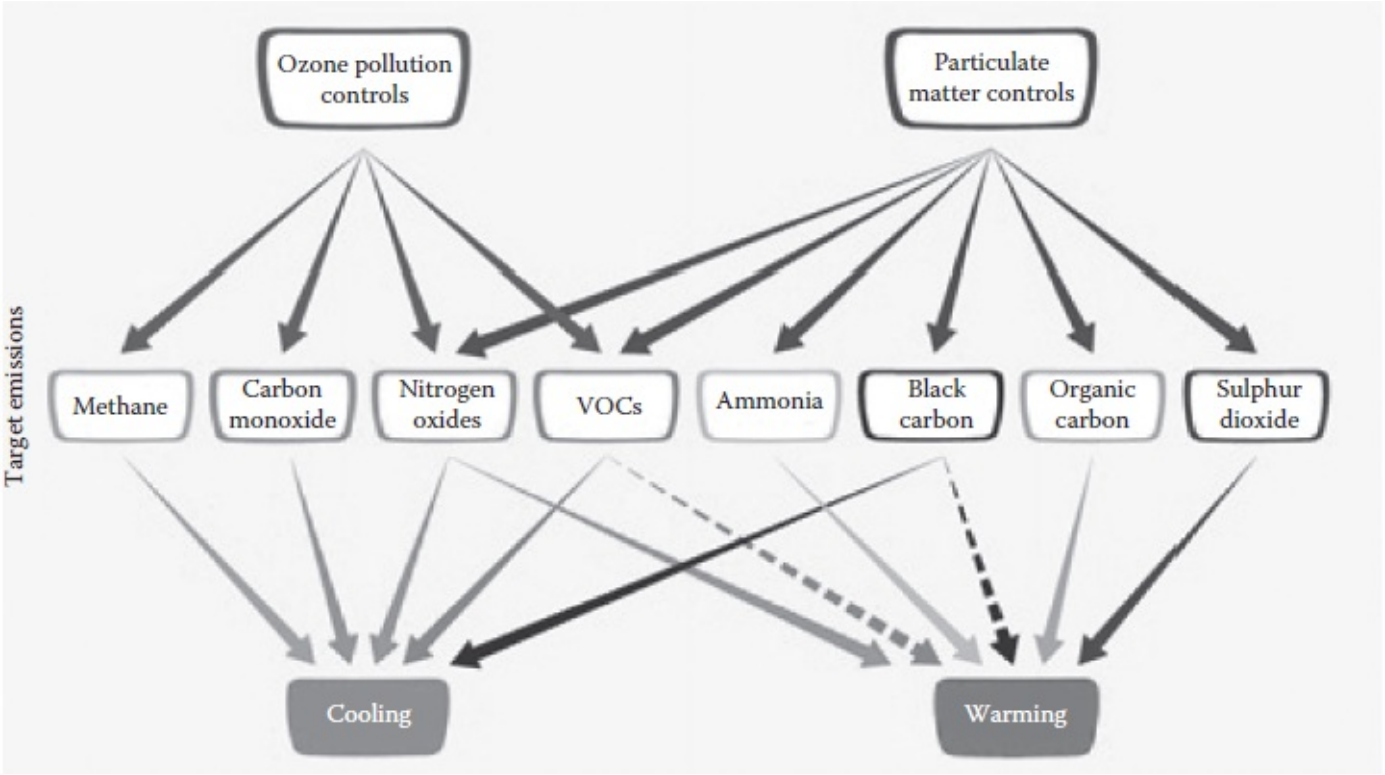

Figure 11.3 Schematic diagram of the impact of pollution controls on specific emissions and climate impact. Solid black line indicates known impact; dashed line indicates uncertain impact. (From IPCC, *Climate Change 2013: The Physical Science Basis, Contribution of Working Group I to the Fifth Assessment Report of the Intergovernmental Panel on Climate Change*, Cambridge University Press, Cambridge, UK, 2013.)

11.1.3 Earth's radiation environment

All objects that have temperatures above absolute zero (0 K, or –273°C) radiate electromagnetic energy. As the temperature increases, not only does the amount of radiated energy increase but the typical wavelength of emission falls. In everyday life, we experience radiation from objects having two quite distinct temperature ranges; first, incoming radiation from the sun, which has an effective surface temperature of 5800 K and

FOR REFERENCE PURPOSES ONLY

a peak wavelength of 0.5 μm; second, radiation emitted by the surface of the Earth and all objects on it, which have temperatures of around 300 K and peak wavelengths of around 10 μm. The corresponding spectral bands are shown in Figure 11.4. The vertical scales have been adjusted to make them the same – it is only the relative positions along the wavelength scale that are relevant here. The solar radiation spectrum is almost completely confined to 0–3 μm, while the terrestrial spectrum occupies 3–30+ μm, so there is almost no overlap between them.

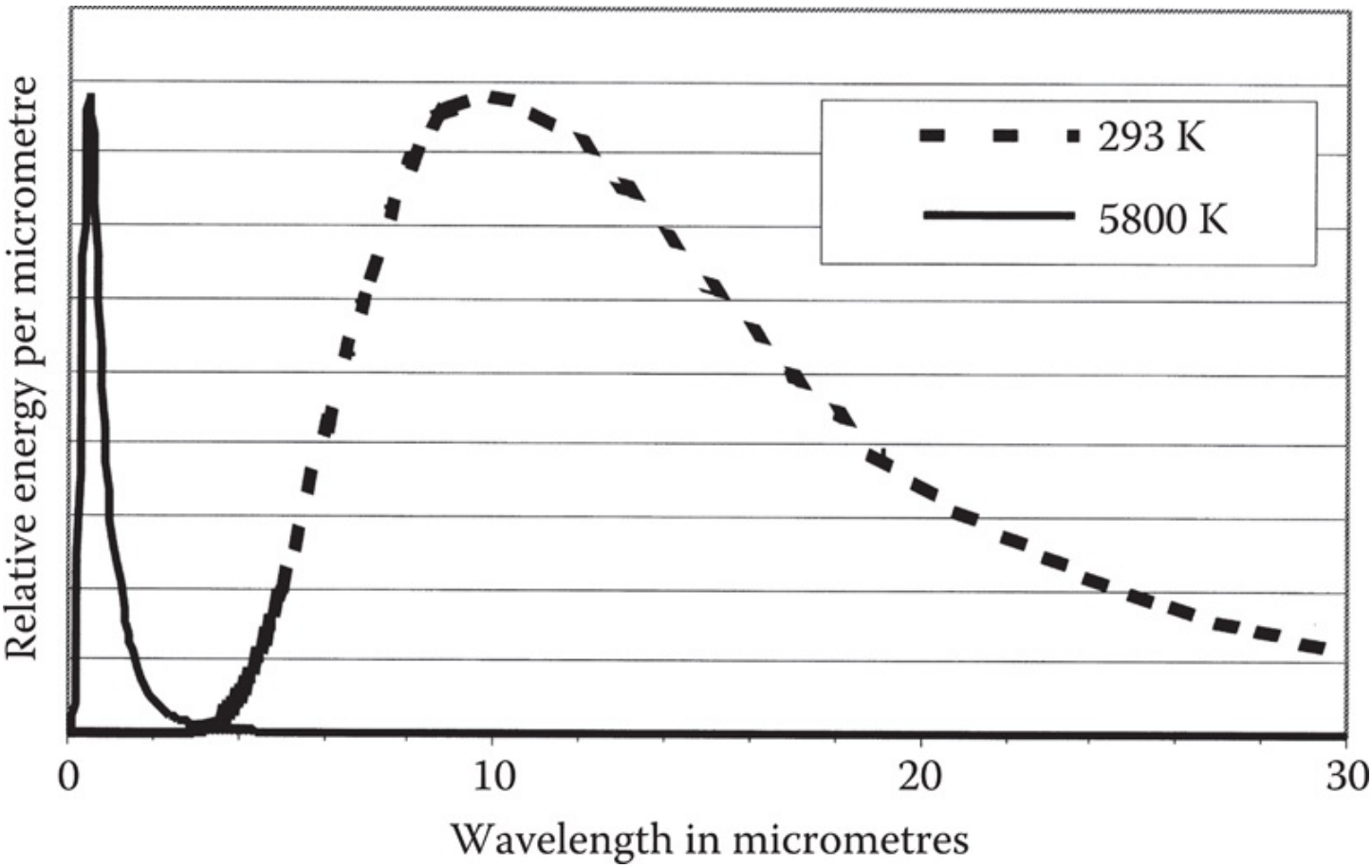

Figure 11.4 The solar and terrestrial spectral bands.

11.1.3.1 Variations in solar input

The Solar Constant is the name given to the global long-term average solar radiation flux density incident on the Earth from the Sun. It has a value of 1367 W m^{-2}; in fact it is not quite constant, having short-term variations over periods of months to years of plus or minus a few percent due mainly to sunspots and the eccentricity of the Earth's orbit. Sunspots are magnetic storms which create relatively cool areas of the Sun's surface, but which are surrounded by hotter rings called faculae. The number of sunspots varies on an 11-year cycle for reasons that are not understood, but have been observed by astronomers since telescopes were invented (Figure 11.5). The overall effect is to vary the solar constant

FOR REFERENCE PURPOSES ONLY

by about 0.1% (the larger the number of sunspots, the higher the output), which in turn is thought to vary the Earth's temperature by 0.2% over the 11 years of the sunspot cycle.

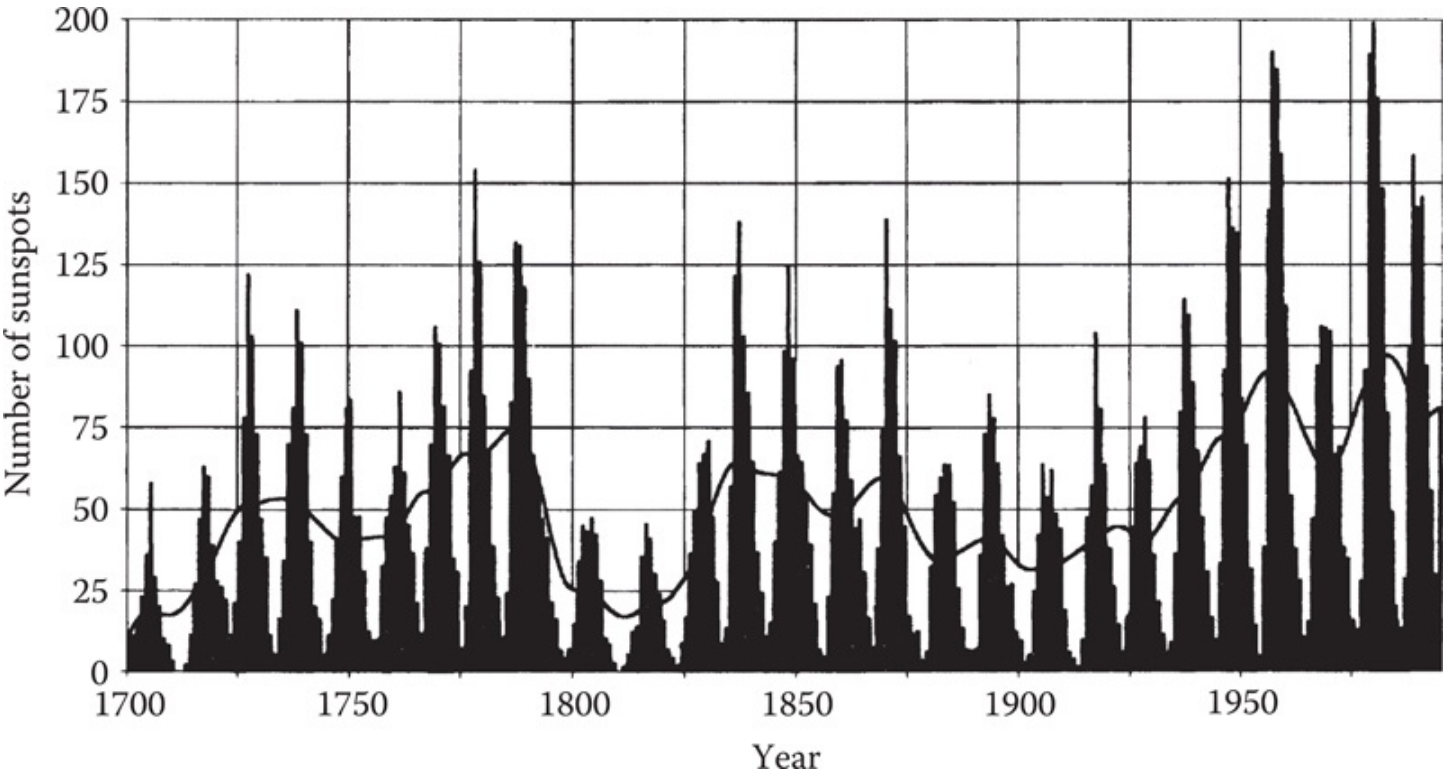

Figure 11.5 Variation in sunspot number, 1700–1990. (From Burroughs, W.J., *Climate Change: A Multidisciplinary Approach*, Cambridge University Press, Cambridge, UK, 2001.)

Three quite regular variations occur in the orbit of the Earth about the Sun. First, the orbit is not exactly circular, but elliptical, and the eccentricity of the ellipse varies with a period of about 100,000 years. Although the total radiation incident on the Earth would remain constant, the maximum received at perihelion (when it is closest) and the minimum received at aphelion (when it is furthest away) would vary by ±10%. Second, the angle that the Earth's spin axis makes with the plane of the orbit (also known as the obliquity), which is currently 23.5°, varies between 21.6° and 24.5° over a period of 41,000 years. This again affects the seasonal variation in the distribution of radiation over the Earth's surface. Third, the time in the year when the Earth is at perihelion moves through the months of the year with a period of 23,000 years. These variations can all be summed independently to form a complicated time series. Celestial mechanics is quite well-established science, and hence we can calculate the effects of these variations on the solar energy received at the Earth going back hundreds of thousands of years (Figure 11.6). The variations amount to about 0.2 MJ m^{-2} at the poles, about 10% of the summer sunshine received, and have been responsible for the quasi-regular ice ages. The regular cycles are called Milankovitch cycles, after the Serbian scientist who first recognised them.

FOR REFERENCE PURPOSES ONLY

Sections 11.2.1 and 11.5.2 describe how the Milankovitch cycles show up in historical evidence about the Earth's climate, and can be used to explain the broad periodicity of the climate changes on the Earth solely in terms of the variation in received solar energy. However, the climate appears to respond in a more vigorous way than predicted by the magnitude of the solar energy change alone, and climate models indicate that some sort of positive feedback involving vegetation and greenhouse gases is also needed. It does get difficult to distinguish chickens from eggs in this analysis. Furthermore, it should be noted that the Milankovitch changes are mainly connected with the orientation of the Earth with respect to the Sun, not with the distance of the Earth from the Sun. Hence, while they affect the distribution of solar energy receipts over the surface of the Earth, they have much less effect on the overall total.

FOR REFERENCE PURPOSES ONLY

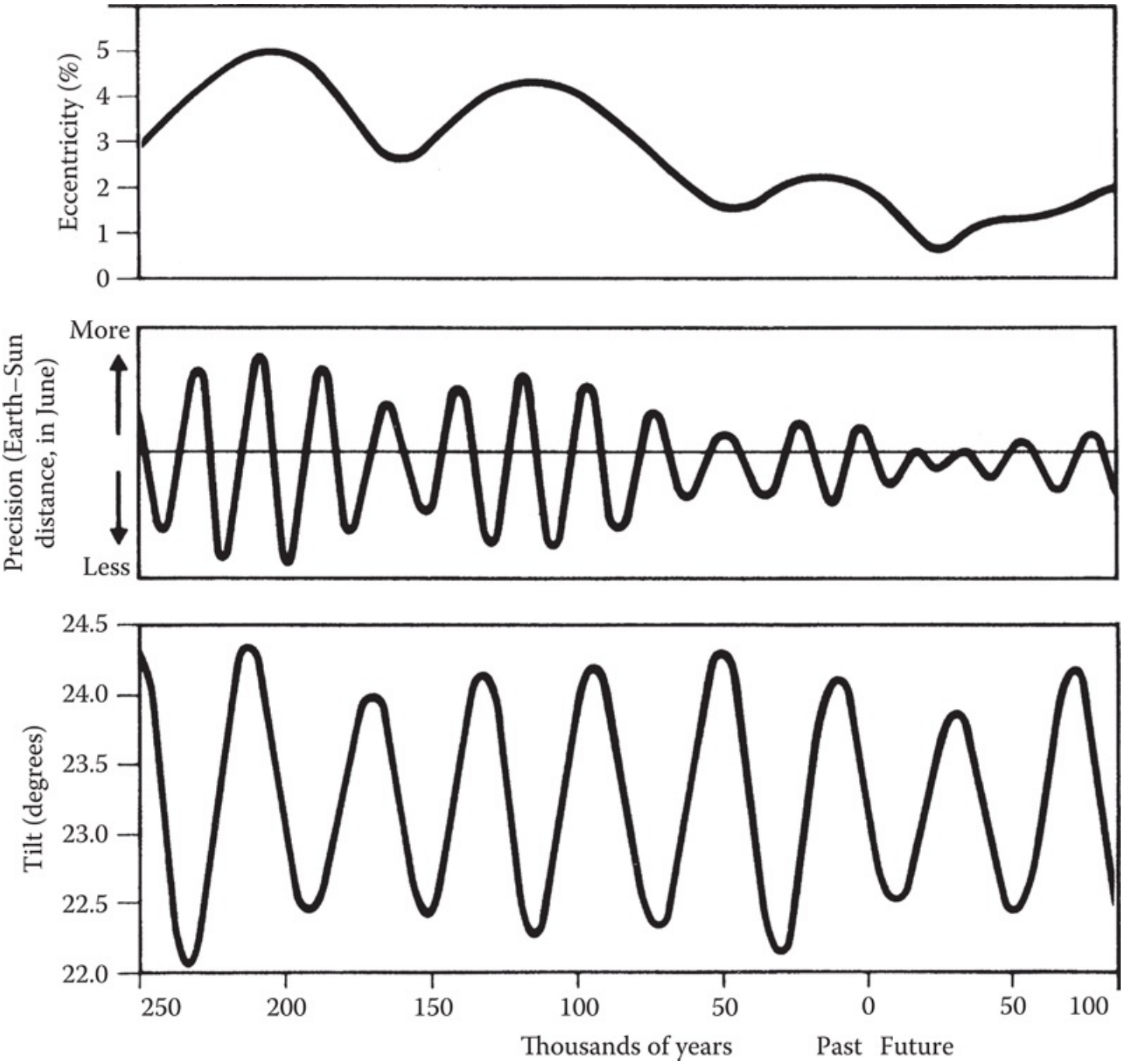

Figure 11.6 Changes in the Earth's orbital parameters. (From Burroughs, W.J., *Climate Change: A Multidisciplinary Approach*, Cambridge University Press, Cambridge, 2001.)

Apart from small amounts released internally by radioactive decay, the Earth receives all its initial energy supply as shortwave radiation from the Sun. The Earth reflects some of this energy, absorbs the rest, and then reradiates it into space in the longwave form. As the Earth moves through the almost perfect vacuum of space, there can be no energy transfer by conduction or convection, and the sum of shortwave and longwave energy leaving the planet must balance the shortwave input in order to maintain thermal equilibrium.

FOR REFERENCE PURPOSES ONLY

Figure 11.7 gives a stylised view of the way in which this input energy is partitioned during its flow through the system. In this figure, the Solar Constant of 1367 W m^{-2} is represented by 100 units. Of these, for example, 8 are backscattered by the air, 17 reflected by clouds and 6 reflected from the Earth's surface. Of the remainder, 46 units are ultimately absorbed at the surface.

For the planet as a whole, the equilibrium radiative temperature (i.e. the temperature required to reradiate all the energy received from the sun) at the outside of the atmosphere is 255 K (–18°C). If the atmosphere was perfectly transparent to all wavelengths of radiation, then it could neither absorb nor emit radiation, and the average temperature at the surface would also be close to 255 K. However, certain gases in the atmosphere, known as radiatively active gases (RAGs), or greenhouse gases (GHGs), absorb some of the upward-going longwave radiation after it has left the Earth's surface. The gases then emit longwave radiation in all directions. The downward-going portion adds to the shortwave radiation arriving at the surface of the Earth and raises the equilibrium temperature.

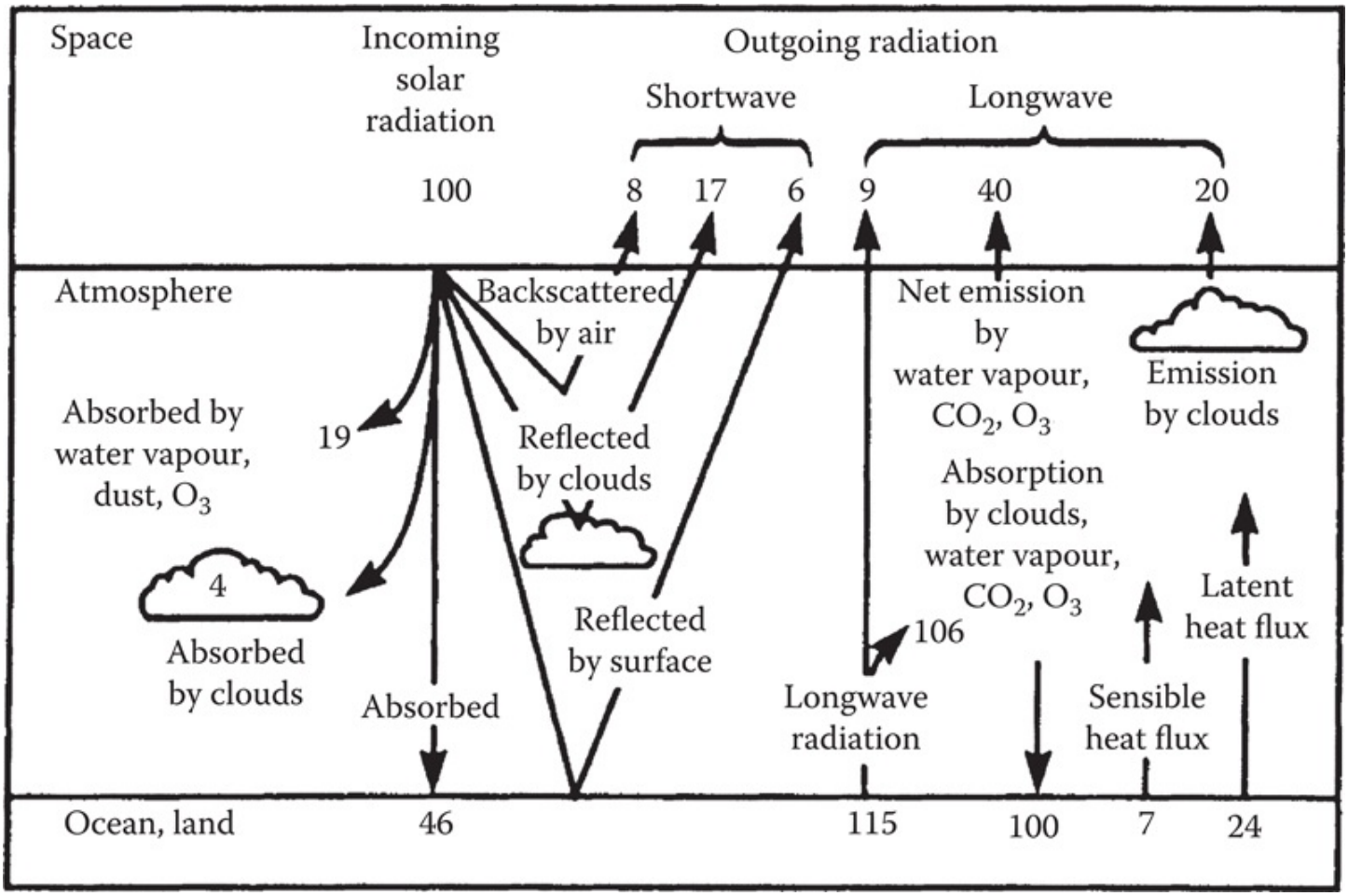

Figure 11.7 Main components of the global average energy balance. The initial input of shortwave solar energy is taken to be 100 units. (From Wuebbles, D.J., Global climate change due to radiatively active gases, in: Hewitt, C.N. and Sturges, W.T. (Eds.), *Global Atmospheric Chemical Change*, Chapman and Hall,

FOR REFERENCE PURPOSES ONLY

London, UK, 1993.)

Referring again to Figure 11.7, of the 115 units of longwave energy emitted from the Earth's surface, 106 units are absorbed by clouds and GHGs in the atmosphere and 100 units eventually returned to the Earth. Thus, the atmosphere acts as an extremely effective longwave insulator. The overall process is known as radiative forcing, or colloquially as the Greenhouse Effect. The most important GHGs are water, carbon dioxide, methane, ozone and nitrous oxide.

For thousands of millions of years there has been a large radiative forcing of the surface energy balance due to GHGs in the atmosphere. In the early history of the Earth, the forcing was due partly to water vapour and mostly to a CO_2 concentration far higher than today's. It is thought that when the Earth was formed the power output from the Sun was only about 75% of its current value. In the absence of any greenhouse effect, the equilibrium radiative temperature would have been only 237 K (–36°C), the seas if any would have been frozen, and life could not have developed. The greenhouse effect was provided by CO_2, NH_3 and CH_4 concentrations that were far higher than any experienced today, equivalent in their radiative forcing to several hundred times the current CO_2 concentration. The power output from the Sun has increased during the 4 billion years of the Earth's lifetime, and during this period the CO_2 concentration has decreased, due largely to its sequestration in organic and later inorganic (e.g. calcium carbonate) forms by biological organisms as they developed. Hence, the surface temperature has remained within a relatively narrow band. The Gaia hypothesis is that this process is a consequence of the drive by living systems to optimise their survival environment. Today, water vapour is a completely natural, and by far the most important, GHG; its presence at concentrations of up to a few percent elevates the average temperature at the bottom of the atmosphere by 33°C, from –18°C to +15°C, thereby making life on Earth possible. On Venus (90% of whose atmosphere consists of CO_2 at a much higher pressure than the Earth's) and Mars (80% CO_2), carbon dioxide is the dominant natural GHG, and elevates the surface temperatures by 523 and 10°C, respectively. On Earth, anthropogenic CO_2 and other GHGs such as methane, nitrous oxide, ozone and chlorofluorocarbons are now increasing in concentration to the point at which they may be appreciably raising the global average temperature and thereby also influencing rainfall patterns and sea level.

Each of the GHGs absorbs longwave radiation in characteristic regions of the spectrum shown on the top five graphs of Figure 11.8. These individual spectra are combined on the sixth graph. For example, water absorbs in the ranges 2.5–3.5 μm, 5–7 μm, as well as a broad range above 13 μm. In the bottom graph of Figure 11.8, these absorption spectra have been combined within the solar and terrestrial spectra that we referred to in Figure 11.4.

Note that the wavelength scale of the solar radiation spectrum has been expanded relative to that for terrestrial radiation. High absorption can have no influence if there is no radiation there to absorb, and although GHGs are effective absorbers in the 1–5 μm region, there is little longwave energy there due to the separation of the black-body distributions.

FOR REFERENCE PURPOSES ONLY

Between 5 and 20 μm all the GHGs have important absorption bands, and above 20 μm the atmosphere is opaque due to absorption by water vapour. The region between 8 and 13 μm (the narrow spike centred on 10 μm in Figure 11.8) is known as the atmospheric window because its relative transparency allows the passage of radiation to the ground from space and *vice versa*. Water vapour absorption is confined to bands – for example, the high absorption between 5 and 8 μm is due to one such band. Water is not active in the window between 8 and 13 μm, although there is a narrow absorption band at 9.7 μm due to ozone. Beyond 14 μm, transmission is suppressed again by both water vapour and carbon dioxide.

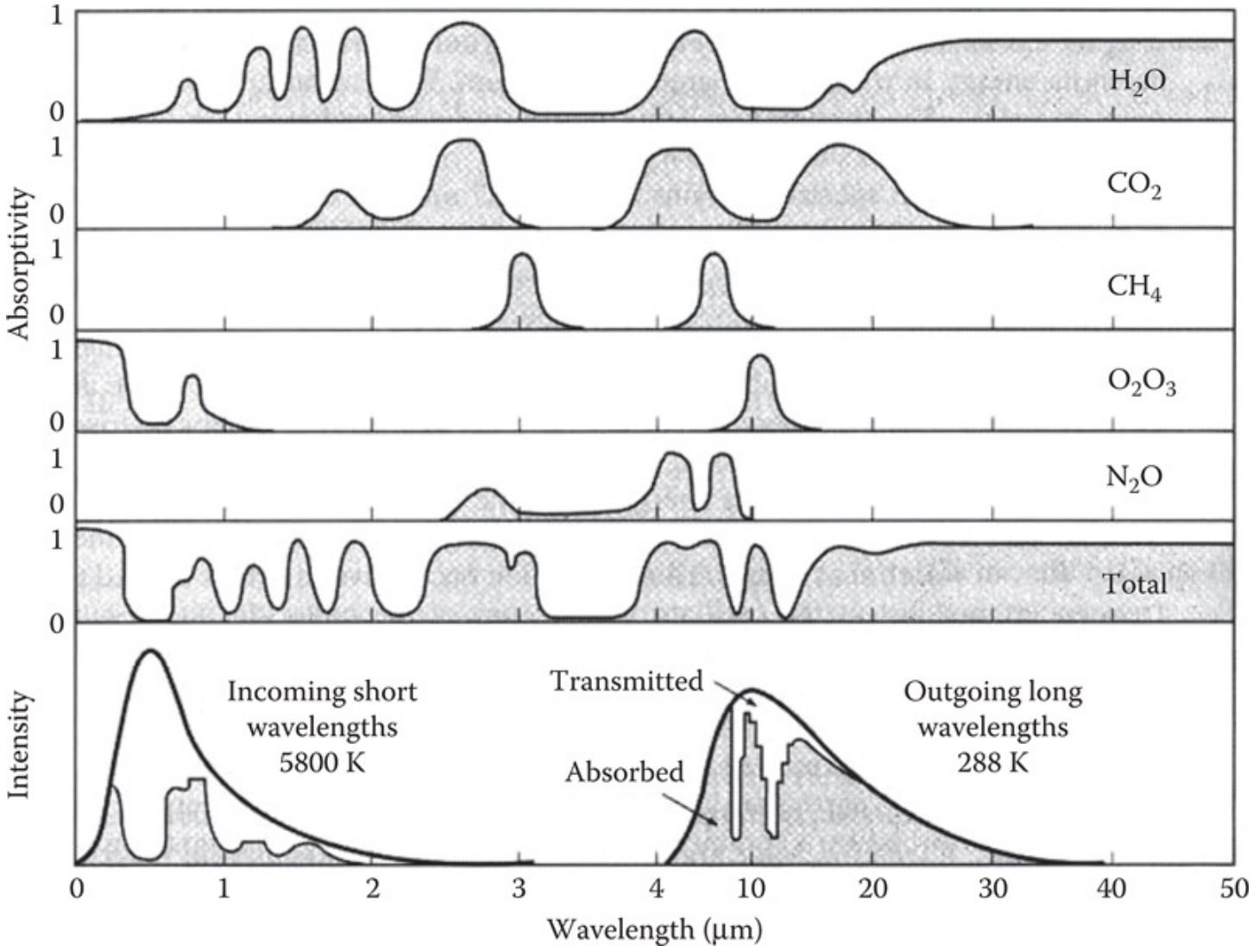

Figure 11.8 Absorption bands of the important GHGs. (From Masters, G.M., *Environmental Engineering and Science*, Prentice Hall, Upper Saddle River, NJ, 1998.)

11.2 GREENHOUSE GASES

FOR REFERENCE PURPOSES ONLY

Fossil fuel combustion has been the key *human influence*, responsible for emissions of greenhouse gases (GHGs) alongside air pollution. Which fossil fuel is burned also makes a difference. The chemical reactions by which carbon (in coal), methane (in natural gas) and hydrocarbons (in oil) are oxidised all have different enthalpies and emit different masses of CO_2 for each unit of energy released. These amount to about 112, 50 and 70 kg kJ^{-1}, respectively. The low CO_2 emission from natural gas has been another reason for it displacing coal in large scale energy operations such as electricity generation. In addition, agriculture and natural emissions are responsible for a significant share of the total GHG emissions and their interactions with other air pollutants, in particular during conversion of methane into carbon dioxide through radical chemistry.

Globally, economic and population growth continue to be the most important drivers of increases in CO_2 emissions from fossil fuel combustion. The contribution of population growth between 2000 and 2010 remained roughly identical to the previous three decades, while the contribution of economic growth has risen sharply. Correspondingly, the GHG emissions have increased over this period by 10 $GtCO_2eq\ yr^{-1}$, with the majority attributed to energy supply (47%), industry (30%), transport (11%) and buildings (3%) sectors (Figure 11.9).

FOR REFERENCE PURPOSES ONLY

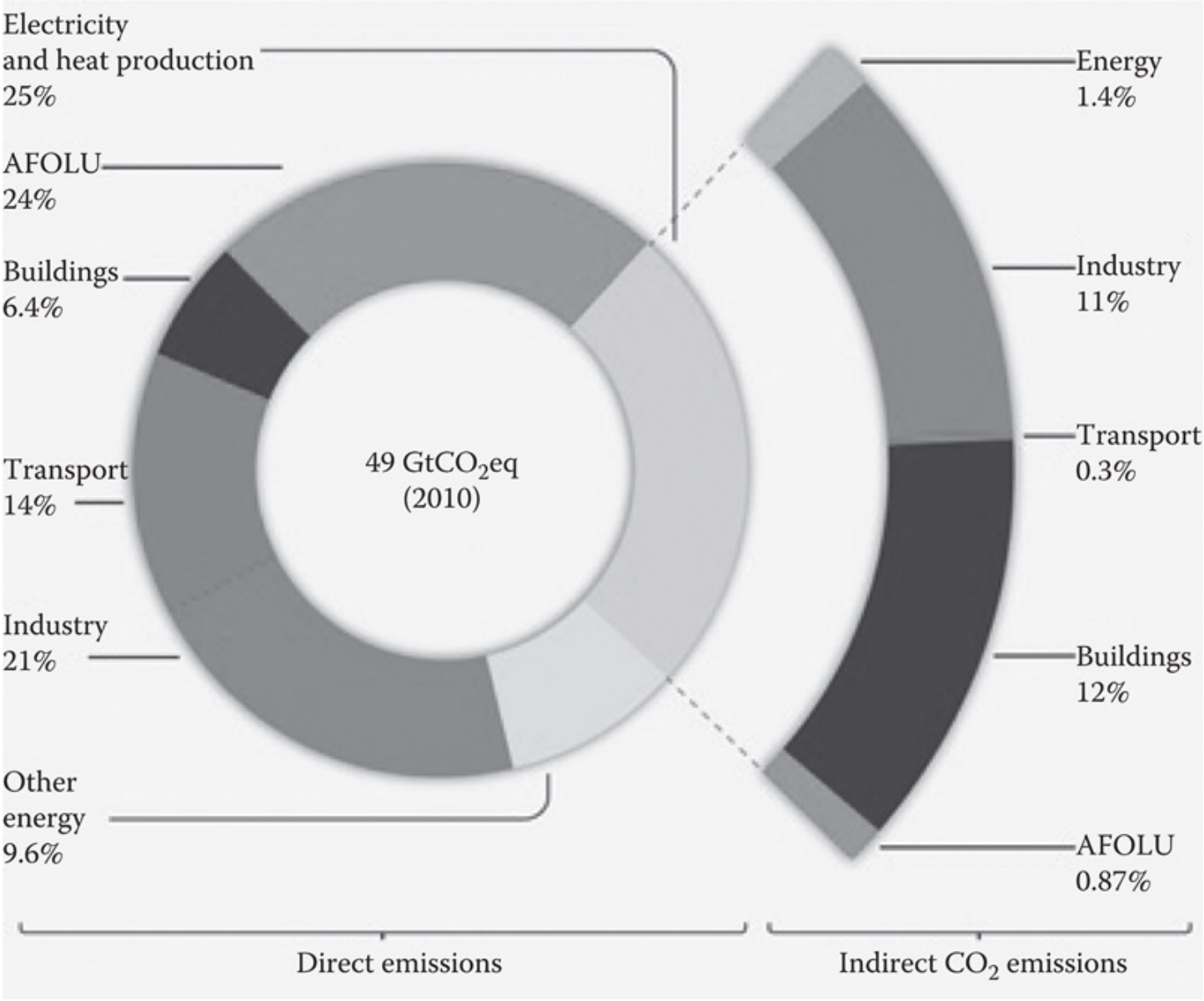

Figure 11.9 Breakdown of total anthropogenic GHG emissions ($GtCO_2eq\ yr^{-1}$) for 2010 into direct and indirect emissions (in % of total anthropogenic GHG emissions) by economic sectors. (From IPCC, Summary for policymakers, in: *Climate Change 2014: Mitigation of Climate Change, Contribution of Working Group III to the Fifth Assessment Report of the Intergovernmental Panel on Climate Change*, Cambridge University Press, Cambridge, UK, 2014.)

11.2.1 Carbon dioxide

Carbon is at the heart not only of life but also of energy production and climate change. The carbon content of past organisms has been stored in the form of oil, gas and coal. A rather small proportion of this carbon is accumulating in the atmosphere where it is helping the Earth to warm up faster than it has ever done previously. Although we have no direct evidence of CO_2 concentrations from millions of years ago, we have been able to derive

FOR REFERENCE PURPOSES ONLY

them over a surprisingly long period. This history of the global atmospheric carbon dioxide concentration has been taken from ice core measurements. When snow falls, air is trapped amongst the ice crystals. Subsequent snowfalls build up in layers, each of which is a record of the air and water quality prevailing at the time. Eventually, the snow layers become compressed into ice, and the air is trapped in bubbles within the ice. By drilling down up to 5 km in Antarctica and Greenland, it has been possible to reconstruct the history of fluctuations in CO_2, CH_4 and temperature (which is derived from $^{18}O/^{16}O$ isotopic ratios) going back over 400,000 years. Figure 11.10 shows such a record, taken from the 4000 m Vostok ice core in east Antarctica.

At the start of this record, carbon dioxide was close to its preindustrial concentration of 280 ppm. Over the next 400,000 years, the concentration fell four times to around 200 ppm before recovering rapidly (on a geological timescale) to its original value. There is a remarkable correlation between the CO_2, methane and temperature records, both for the long-term cycles and the more rapid fluctuations within them. Frequency analysis shows dominant periods of 100,000, 41,000, 23,000 and 19,000 years, which correlate with the Milankovitch cyclical changes in the Earth's orbital parameters, such as eccentricity, precession and tilt (Figure 11.6). These changes affect the radiation budget directly, and hence temperature, plant life and CO_2 concentration. The simple explanation is that when the Earth is cooling, the surface waters of the oceans are cooler and therefore able to absorb more CO_2, so that the atmospheric concentration decreases, and *vice versa*.

FOR REFERENCE PURPOSES ONLY

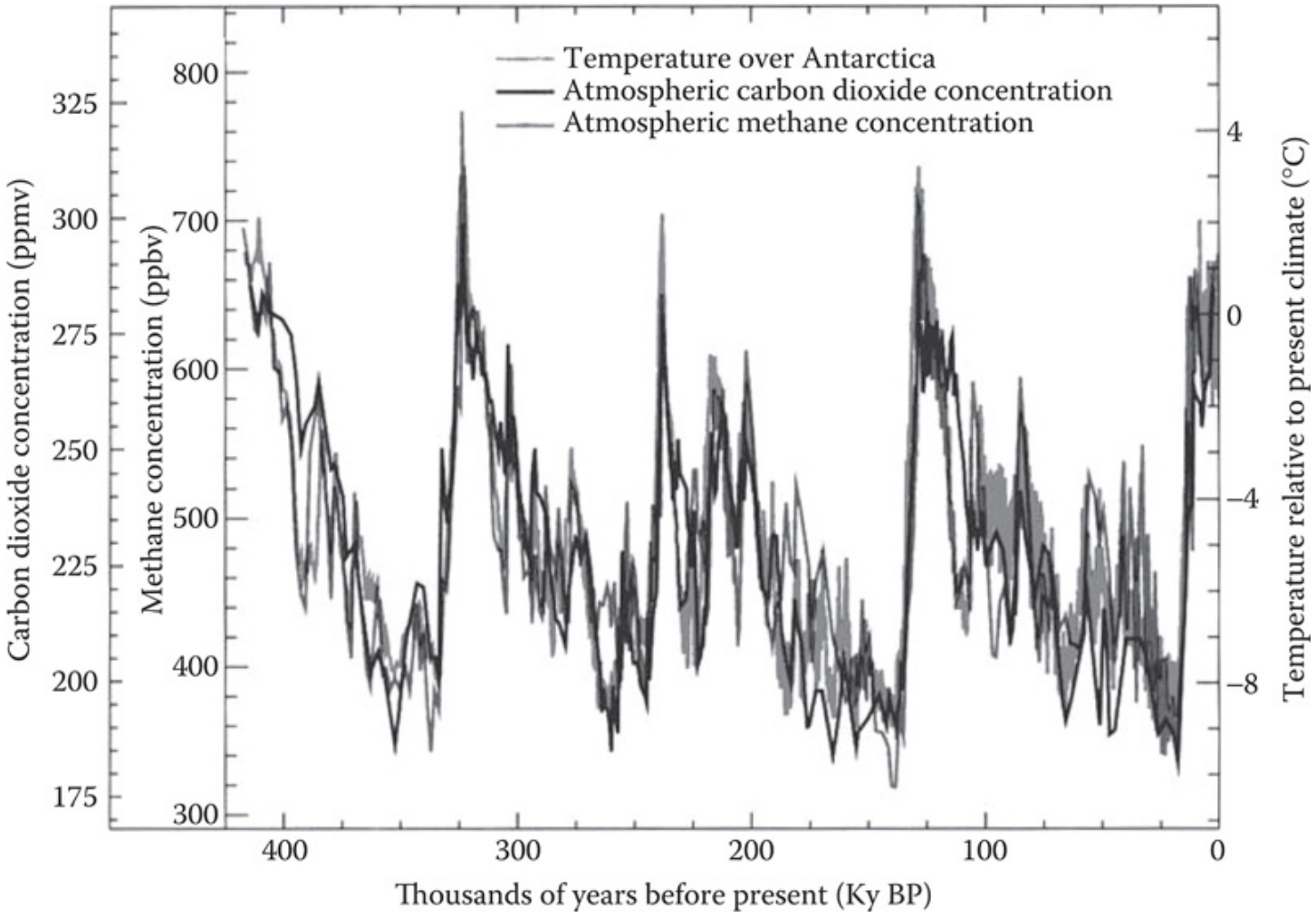

Figure 11.10 An example of the ice-core record of CO_2, methane and temperature changes over the last 400,000 years. (From IPCC, *Climate Change: Third Assessment Report*, Cambridge University Press, Cambridge, UK, 2001.)

However, modelling shows that the orbital changes alone are not sufficient to cause the observed changes in climate, and hence some feedback or amplification mechanism must exist. There is no way of telling from this record alone whether it is CO_2 changes that are driving temperature changes, or *vice versa*, or indeed whether they are both being driven by an unmeasured third variable. Although there were major variations in CO_2 throughout the period, the concentration was never greater than 320 ppm. During the past 1000 years, the concentration has shot up at an unprecedented rate, from the previous typical peak level of 280 ppm to the current value of 385 ppm (Figure 11.11). This recent sharp rise in CO_2 concentration is due to the anthropogenic addition of CO_2 to the Earth's atmosphere by biomass burning and combustion of fossil fuels, strongly associated with population growth and industrialisation. This figure also shows that the more recent ice-core values tie in well with the atmospheric measurements, which gives confidence to the whole ice-core record.

FOR REFERENCE PURPOSES ONLY

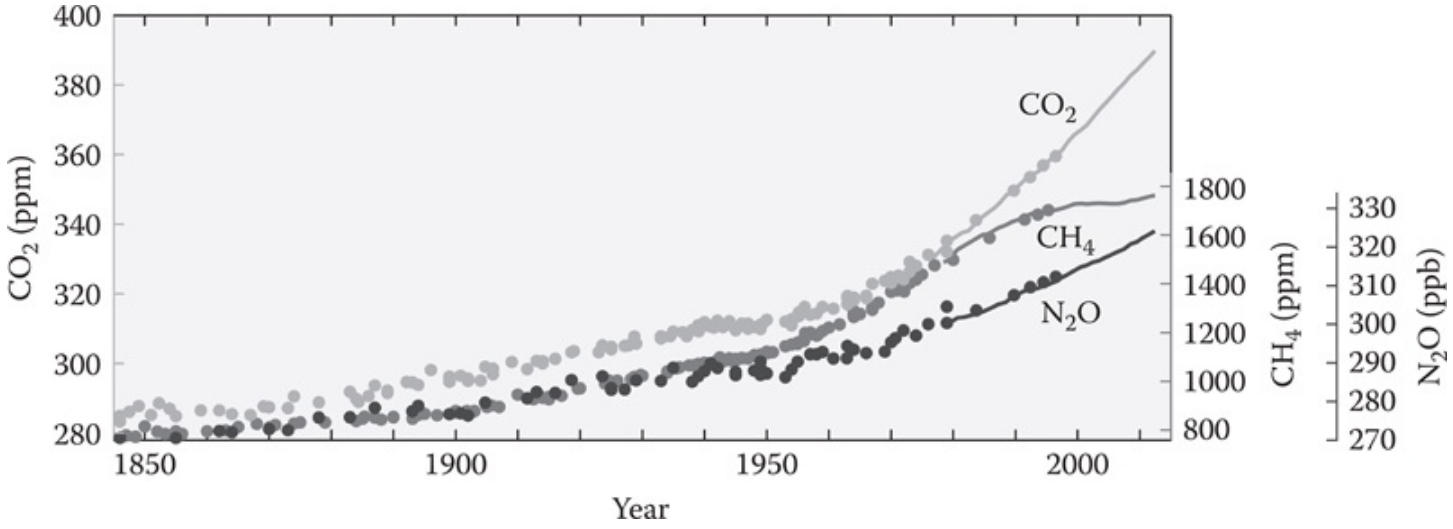

Figure 11.11 Atmospheric concentrations of the greenhouse gases (carbon dioxide, methane and nitrous oxide determined from ice core data [dots] and from direct atmospheric measurements [lines]. (From IPCC, Summary for policymakers, in: *Climate Change 2014: Mitigation of Climate Change, Contribution of Working Group III to the Fifth Assessment Report of the Intergovernmental Panel on Climate Change*, Cambridge University Press, Cambridge, UK, 2014.)

FOR REFERENCE PURPOSES ONLY

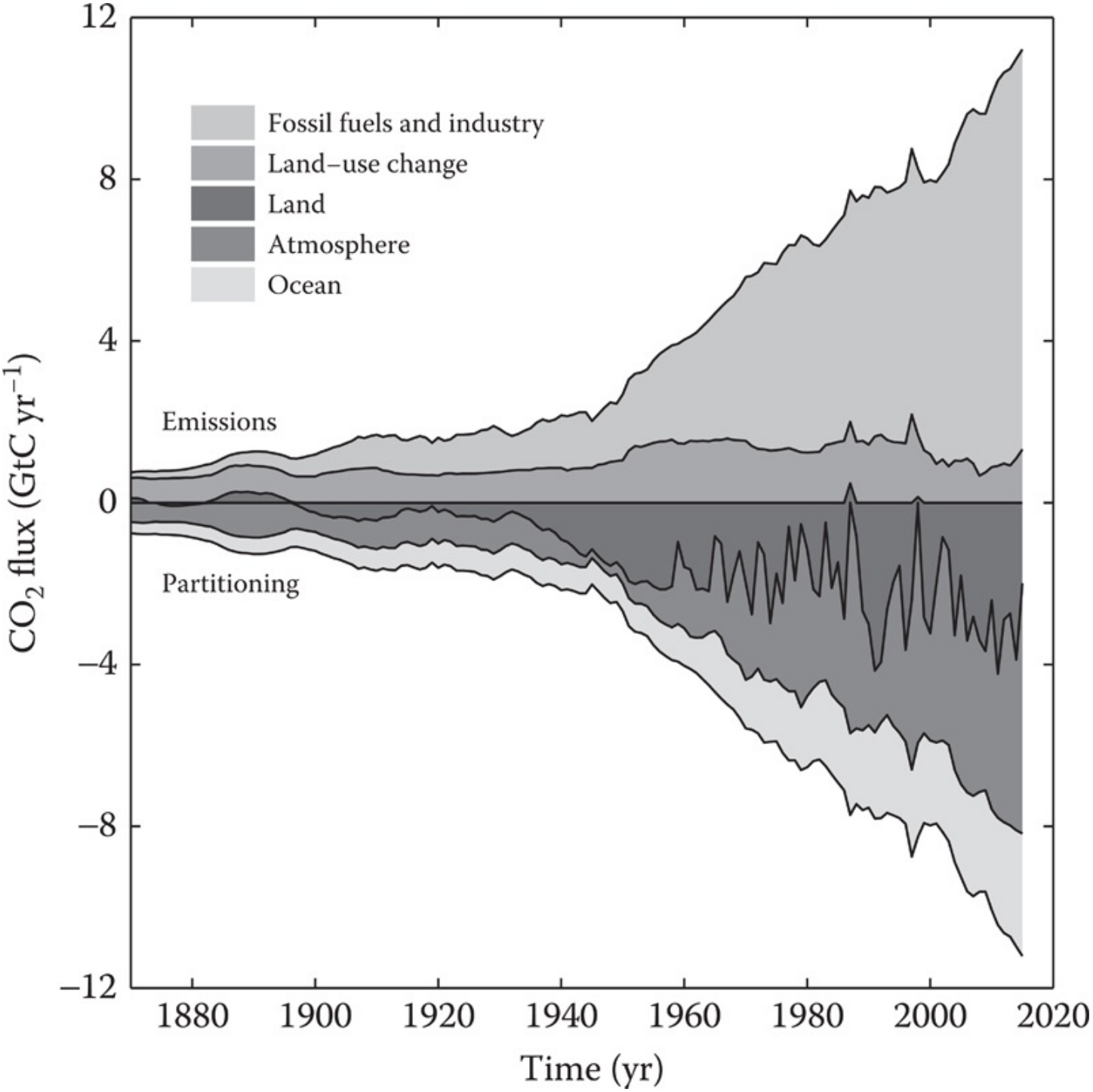

Figure 11.12 Annual global budget of carbon dioxide. (From Le Quéré, C. et al., *Earth Syst. Sci. Data*, 8, 605–649, 2016.)

The time series of annual global CO_2 fluxes (emissions and sinks) in GtC yr^{-1} are presented in Figure 11.12. Between 2006 and 2015 about 91% of the total emissions were caused by fossil fuels and industry, and 9% by land-use change. The total emissions were partitioned among the atmosphere (44%), ocean (26%), and land (30%) sinks. All components except land use-change emissions have grown since 1959, with important inter-

FOR REFERENCE PURPOSES ONLY

annual variability in the growth rate in atmospheric CO_2 concentration and in the land CO_2 sink and some decadal variability in all terms. The residual terrestrial CO_2 sink increased from 1.7 ± 0.7 GtC yr^{-1} in the 1960s to 3.1 ± 0.9 GtC yr^{-1} during 2006–2015, with important inter-annual variations of up to 2 GtC yr^{-1}. The average annual growth rate in atmospheric CO_2 for 2006–2015 is 4.5 ± 0.1 GtC yr^{-1}. About three-quarters of the increase in atmospheric CO_2 concentration is due to fossil fuel burning, with the remainder being due mainly to land-use change, especially deforestation. Superimposed on the general increase measured at Mauna Loa is a strong annual variation due to seasonal changes in uptake by vegetation and oceanic phytoplankton. A net increase of 2.12 GtC corresponds to an increase of 1 ppm in the global average CO_2 concentration, so that the atmospheric concentration is increasing at about 2.12 ppm per year.

A more detailed breakdown of CO_2 emissions (ktonnes C yr^{-1}) by source type (mainly transport, domestic and industrial sectors) on a national basis between 1990 and 2015 for the UK is shown in Figure 11.13. While the emissions from the majority of source categories have remained uniform, there has been significant reduction in the contribution from the combustion of fossil fuels in power stations post 2013. This has resulted in an overall reduction of 37% in CO_2 emissions over this period from energy industry.

Apart from the anthropogenic emissions, carbon is heavily involved in two natural cycles of very different timescales. The long-term cycle starts with the emission of CO_2 in volcanic gases, both as steady releases and violent explosions. Some of this CO_2 is dissolved into cloud droplets and eventually rained out. Clean rain is weak carbonic acid with a pH of 5.6 due to this effect. When the rainwater washes on igneous rocks, the resulting stream and river water contains bicarbonate ions. Eventually, this bicarbonate is precipitated as sedimentary rocks on the ocean floor, which are then in turn subducted at tectonic plate boundaries, where volcanic activity releases the CO_2. This cycle takes 100 million years, but without it the atmospheric CO_2 would eventually be depleted.

The second cycle is a short term one which involves living organisms. On the plant side, the Earth's terrestrial and aquatic plants take up CO_2 from the atmosphere by photosynthesis and lock up the carbon as plant parts. The carbon is eventually returned to the atmosphere – slowly by respiration and rotting, or rapidly by forest fires. Animals burn food and release CO_2 as a by-product. There is a large continuing exchange between the atmosphere and the oceans, in which the surface layers are saturated with CO_2 and alternately take up new CO_2 from the atmosphere and release it back again.

FOR REFERENCE PURPOSES ONLY

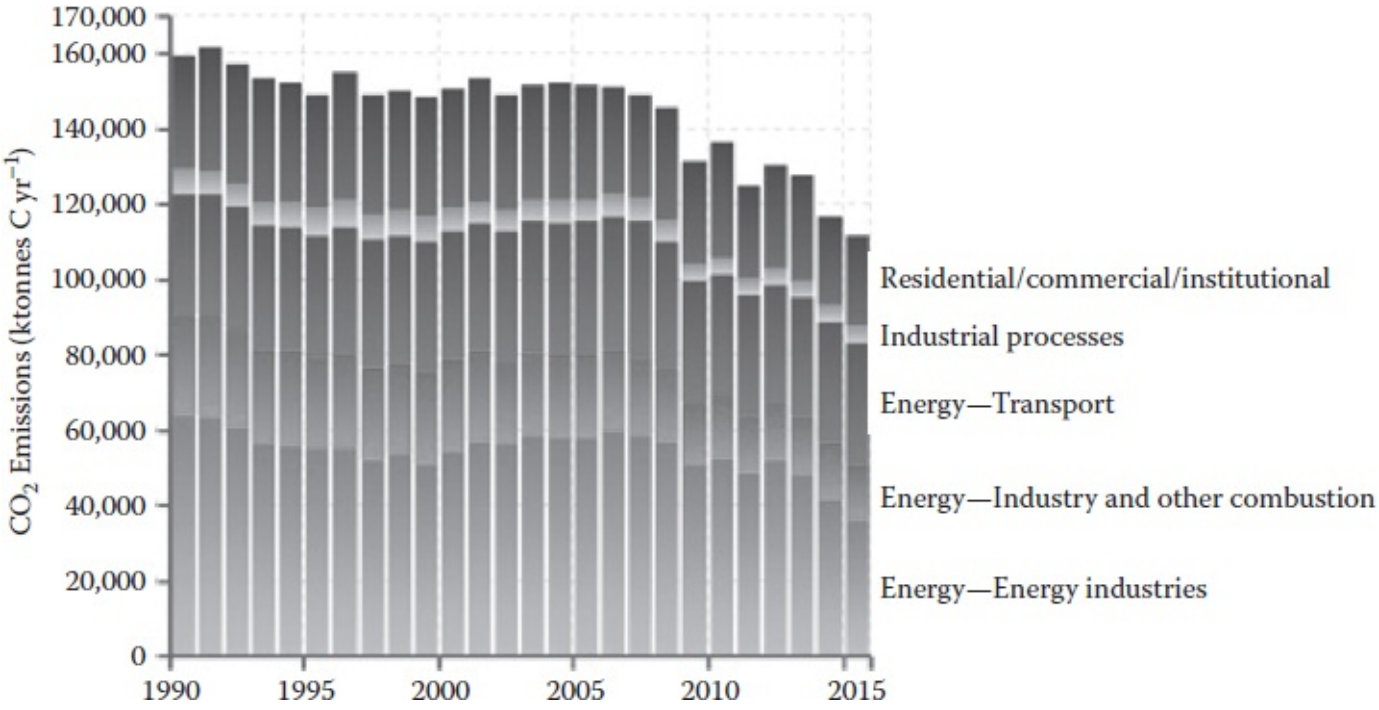

Figure 11.13 UK CO_2 emissions by source between 1990 and 2015 (ktonnes C yr^{-1}). (From Brown, P. et al., *UK Greenhouse Gas Inventory, 1990–2015: Annual Report for Submission under the Framework Convention on Climate Change*, National Atmospheric Emissions Inventory, London, UK.)

In addition to a global rise, CO_2 undergoes diurnal variations locally and annual variations globally due to assimilation and respiration by plants and the release from decaying biomass.

11.2.2 Methane

Methane is produced by a wide variety of anaerobic processes. The main natural source is bacterial decay in wetlands, while anthropogenic sources are paddy fields, the digestive tracts of ruminant animals such as cattle, and natural gas emissions from fossil fuel supplies. Methane is eventually oxidised to CO_2 (another GHG) in the atmosphere; as this is achieved via reaction with the OH radical, CH_4 is also involved in ozone photochemistry. If the oxidation occurs in the presence of high NO_x concentrations, then O_3 is produced; if NO_x is low, then O_3 is consumed (Table 11.1).

The atmospheric sink (due to reaction with OH in the troposphere, $CH_4 + OH \rightarrow CH_3 + H_2O$) is around 500 Mt a^{-1}, with a net atmospheric increase of 15 Mt a^{-1}. The long-term ice core record shows a very similar pattern of fluctuations to that of CO_2, ending up with a pre-industrial concentration of 700–800 ppb. Since then the concentration has more than doubled to 1750 ppb (Figure 11.11).

However, the most recent data suggest that the rate of increase in CH_4 has decreased

FOR REFERENCE PURPOSES ONLY

rather rapidly, from 20 ppb a^{-1} in 1975 to only a few ppb a^{-1} currently. This decrease is not understood at present and may only be a temporary response to a short-term disturbance such as the eruption of Mt Pinatubo.

In general, farm animals produce a lot of methane. Cattle and sheep are adapted to eat grass and other forage materials which have a high content of plant cell walls made up from structural carbohydrates. The rumen, which is the first stomach, acts as a fermentation chamber in which a microbial population of bacteria, fungi and protozoa break down the ingested carbohydrate into soluble digestible materials. The rumen bacteria generate methane as a waste product, which is lost by eructation (belching). One cow emits about 70 kg methane per year, one sheep about 8 kg, and one pig about 1.5 kg. Cattle and sheep emit about 70% and 20% respectively of the total animal emission. Each cow or sheep also creates around 15 or 1.2 t yr^{-1} respectively of excreta, which eventually returns on to the land as dung, manure or slurry.

Table 11.1 Global methane emissions (Mt yr^{-1})

Natural		*Human (biosphere)*		*Human (fossil fuels)*	
Wetlands	100–200	Enteric fermentation (mainly cattle)	100	Natural gas	40
Termites	20	Rice paddies	60	Coal mining	20
Oceans	10	Biomass burning	40	Coal burning	25
Other	15	Wastes, landfill and sewage	90	Petroleum processing	15
Total	145–245	Total	290	Total	100

FOR REFERENCE PURPOSES ONLY

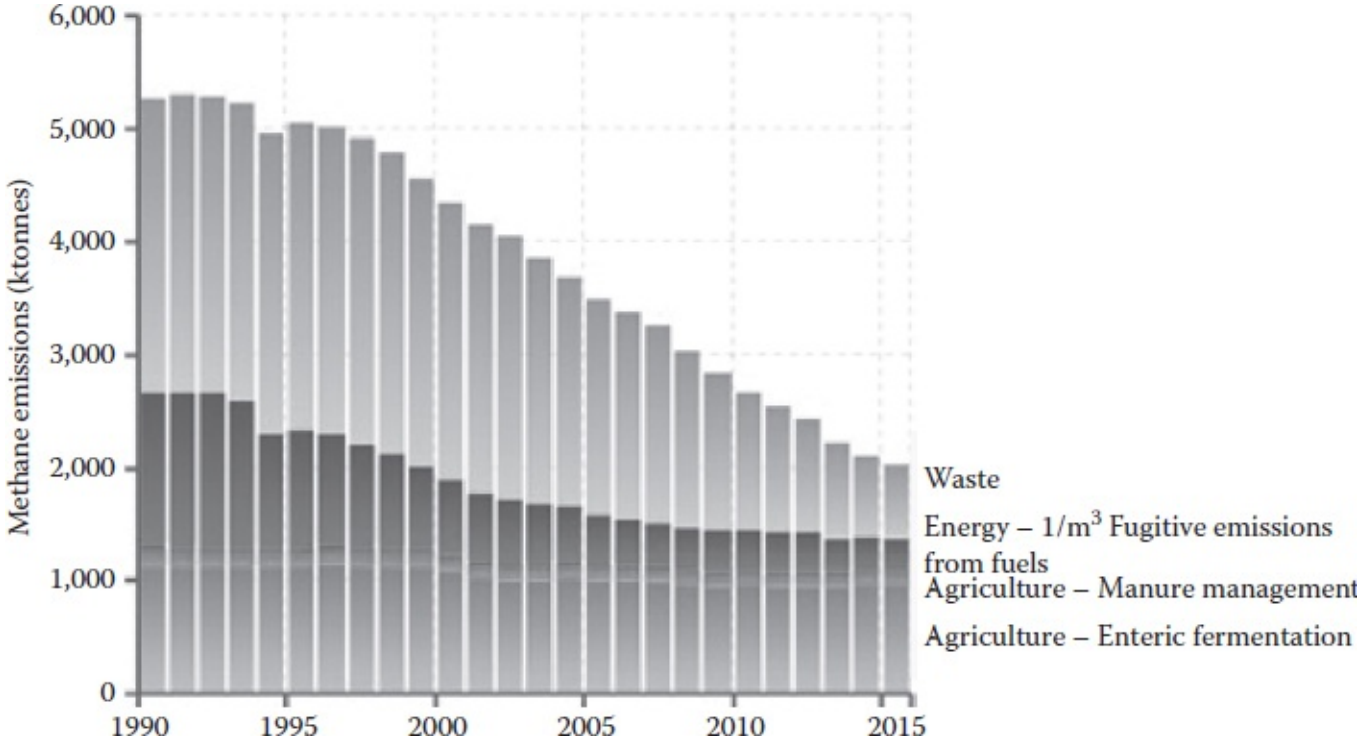

Figure 11.14 UK methane emissions by source between 1990 and 2015 (ktonnes yr^{-1}). (From Brown, P. et al., *UK Greenhouse Gas Inventory, 1990–2015: Annual Report for Submission under the Framework Convention on Climate Change*, National Atmospheric Emissions Inventory, London, UK.)

Coal and methane are always associated, and coal seams contain up to 20 m^3 methane t^{-1} from the firedamp (which is 80%–95% methane) absorbed in the coal. Hence, methane is released during mining and ventilated to atmosphere. It is also released from open-cast coal faces and from coal stocks. In the UK, the methane from coal mining used to dominate the total, but has declined with the coal industry.

A more detailed breakdown of methane emissions by source between 1990 and 2015 from the UK is given in Figure 11.14. In recent years, waste (landfill sites), livestock (enteric fermentation) and agriculture (manure management) have been the most dominant sources. Against the 1990 base scenarios the corresponding emissions from landfill and energy related fugitive emissions have fallen by over 70%, while the aggregated emissions from agriculture sector have remained largely unchanged. In the case of landfills this is associated with two factors – (1) reduction in the level of landfill wastes through enhanced waste management practices adopted by the Local Authorities; (2) introduction of well-capped landfills where the methane is recovered as an energy resource.

11.2.3 Nitrous oxide

Nitrous oxide (N_2O) is produced by a variety of biological nitrification and denitrification processes in water and in soil. Although not toxic at normal atmospheric concentrations, it

FOR REFERENCE PURPOSES ONLY

is a radiatively active gas that contributes to the greenhouse effect and climate change. The soil component of the emission results from anaerobic microbial denitrification and nitrification. This is more intensive in agricultural areas where N is added to the soil, but wet and dry N deposition to other areas could be increasing N_2O emissions. Land-use changes such as forest clearance, drainage and cultivation stimulate emission. There are large spatial variations that make it difficult to quantify regional emissions; approximate global totals are given in Table 11.2.

Table 11.2 Global sources of nitrous oxide

Source	*Production/Mt N a^{-1}*
Tropical forest soils	4.2
Temperate forest soils	4.0
Fertiliser application	1.5
Biomass burning	0.1
Fossil fuel combustion	0.6
Industrial sources	0.7
Oceans	2.0

The major removal mechanism is photolysis in the stratosphere, which accounts for 10 Mt a^{-1} (and for its long lifetime of 150 years), with the quantity in the atmosphere increasing by 3 Mt a^{-1}. Pre-industrial concentrations of N_2O were about 285 ppb, have since increased to about 310 ppb, and are currently rising at 0.8 ppb yr^{-1} (Figure 11.11). Natural emissions make up about 80% of the total. The component from cultivated soils is potentially the largest of the man-made sectors, although there is a lot of uncertainty attached to it. Corresponding values for the UK emissions by different sources are shown in Figure 11.15. Agricultural activities form the most dominant source (both soil and manure management), whereas industrial processes and combustion processes in power generation and road transport contribute to additional N_2O.

FOR REFERENCE PURPOSES ONLY

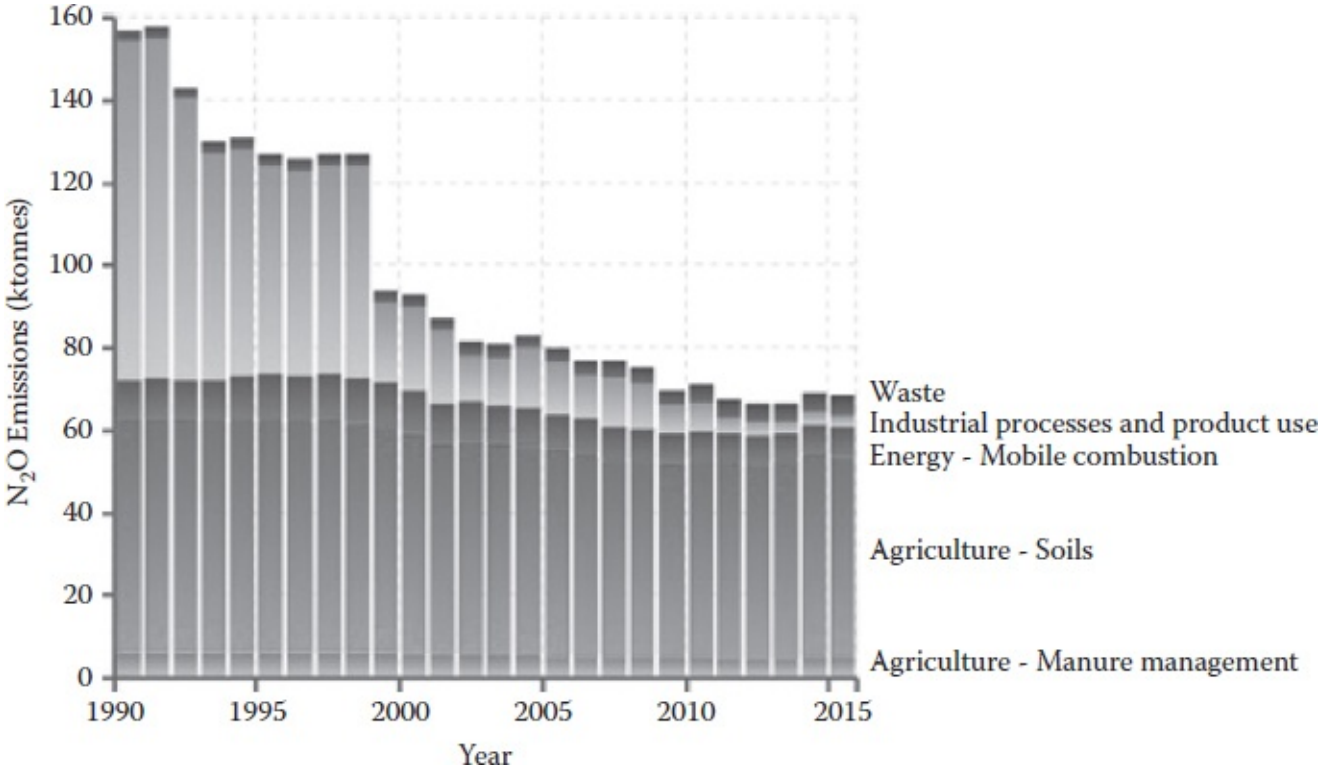

Figure 11.15 UK N_2O emissions by source between 1990 and 2015 (ktonnes yr^{-1}). (From Brown, P. et al., *UK Greenhouse Gas Inventory, 1990–2015: Annual Report for Submission under the Framework Convention on Climate Change*, National Atmospheric Emissions Inventory, London, UK.)

11.2.4 Halocarbons

Unlike carbon dioxide, methane and nitrous oxide, halocarbons have no natural source or background. There are at least 12 principal halocarbons that are a cause of concern for the Earth's radiation balance. In the past, they have been used for three main purposes: as the heat transfer medium in refrigerators and air conditioning systems; as the propellant in aerosol spray cans; and as the foaming agent in expanded polystyrene packaging and insulation. Two of the desirable properties that make them so suitable for these purposes are their chemical inertness and thermal stability, the very properties that also result in their having very long lifetimes in the atmosphere.

The main consequent problem that has received attention is the chemical effect on stratospheric ozone (Chapter 12), but there is also a physical effect. The halocarbon molecules absorb infrared radiation effectively in the waveband of the atmospheric window. They are hence strongly radiatively active on a per-molecule basis and contribute a significant radiative forcing despite their low concentrations. One chlorofluorocarbon (CFC) molecule in the atmosphere is 5–10,000 times more effective at trapping longwave radiation than one molecule of CO_2. As a result, the tiny CFC concentrations account for about 20% of the radiative forcing in the tropics. The net effect is reduced at high latitudes

FOR REFERENCE PURPOSES ONLY

because the CFCs have reduced the O_3, which is also a greenhouse gas. The two most important halocarbons are the chlorofluorocarbons CFC-11 and CFC-12, which have average concentrations of a few hundred ppt.

Detailed information on the different halocarbons and their production rates is given in Chapter 12. Although their destructive effect on the ozone layer led to an international agreement (the Montreal Protocol) to phase out production, their long lifetimes mean that their effects will persist for a considerable portion of the twenty-first century. The atmospheric concentration of CFCs increased significantly after World War II (Figure 11.16).

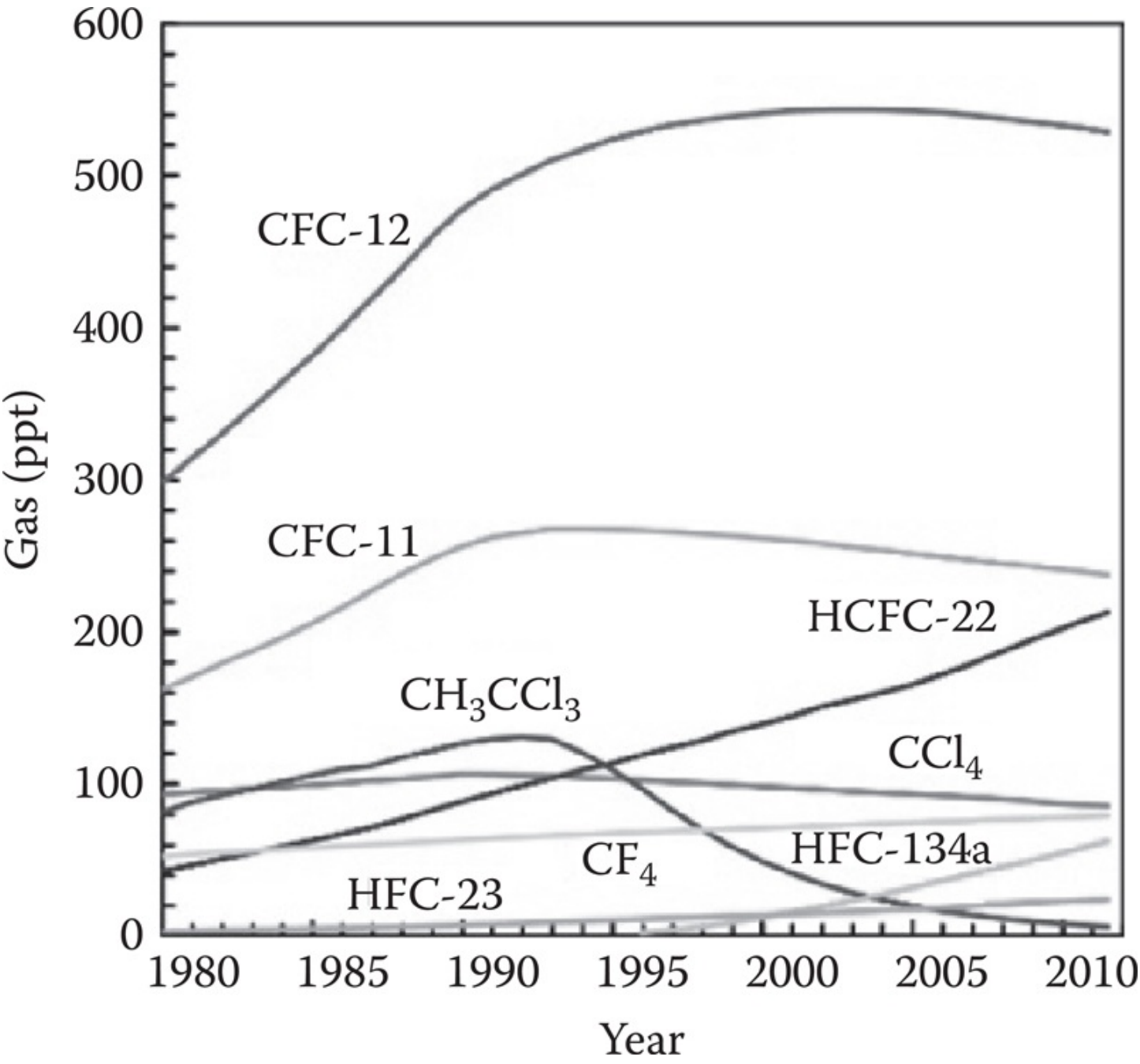

Figure 11.16 Time series of atmospheric concentration of halocarbons. (From IPCC,

Climate Change 2013: The Physical Science Basis, Contribution of Working Group I to the Fifth Assessment Report of the Intergovernmental Panel on Climate Change, Cambridge University Press, Cambridge, UK, 2013.)

11.3 RADIATIVE FORCING

Radiative forcing (W m^{-2}) is the change in energy flux caused by a driver (i.e. natural or anthropogenic substances and processes that alter the Earth's energy budget, such as gas or aerosols) and is calculated at the tropopause or at the top of the atmosphere. It is a major task to calculate the effect due to each GHG over the next century because it depends on the current and future release rates, on the lifetime of the gas in the atmosphere (assuming well-mixed conditions) and on the spectral absorptivity for radiation of the particular gas.

11.3.1 Contributions to radiative forcing

On average, radiative processes warm the surface and cool the atmosphere, which is balanced by the hydrological cycle and sensible heating. However, these properties and parameters vary widely from gas to gas, as shown by Table 11.3. The global warming potential (GWP) is a measure of the relative, globally averaged warming effect due to the emission of unit mass of the gas. The GWP was first presented in the FAR (1990) as a concept; in AR5 (2014) GWP is defined as the time-integrated radiative forcing due to a pulse emission of a given component, relative to a pulse emission of an equal mass of CO_2. The AR5 GWP values for typical time horizon of impact over 100 years are: CO_2 = 1; CH_4 = 28; N_2O = 265; HFC-23 = 12,400; HFC-134 = 1,300; CF_4 (PFC) = 6,630; SF_6 = 23,500; NF_3 = 16,100. There is still uncertainty attached to this value, since although the direct warming by the gas can be calculated, indirect warming after its conversion to other gases is a far more complex process. The table shows that on a per-mass basis, the CFCs are thousands of times more effective than carbon dioxide as GHGs. However, they are emitted in far smaller quantities, so that their overall impact on radiation balance remains low. In Table 11.3, the relative importance of the different gases is shown in terms of the calculated increase in the radiative flux at the surface of the Earth between 1765 and 2000. Sixty percent of the overall increase of 2.45 W m^{-2} has been due to carbon dioxide.

Note that despite the dominance of CO_2, methane also makes a significant contribution due to its higher GWP per kg. Although the contribution from CFCs is significant, it will decline over the next 50 years due to controls on CFC production designed to reduce damage to the ozone layer (see Chapter 12). In fact, the reduction in stratospheric ozone has caused a *negative* radiative forcing of –0.15 W m^{-2}, so the decrease in one will tend to offset the increase in the other in the medium-term future.

On the other hand, *tropospheric* ozone has increased by about 36% since 1750, as we

FOR REFERENCE PURPOSES ONLY

have seen previously in this book, increasing radiative forcing by about 0.35 W m^{-2}. The latter is an average figure, as tropospheric ozone is a local-scale short-lived gas which, unlike carbon dioxide, is not well mixed throughout the lower atmosphere. Looked at another way, if the CO_2 in the atmosphere were to be halved from its current value, the average radiative forcing would be reduced by around 4 W m^{-2}, and the global surface temperature would fall by 1°C–2°C. If the CO_2 were to be removed altogether, outgoing radiation would increase by 25 W m^{-2} and temperature would fall by over 10°C.

Table 11.3 Effects of GHGs on global energy flux

Date	*CO_2/ppm*	*CH_4/ppb*	*N_2O/ppb*	*CFC-11/ppt*	*CFC-12/ppt*	*HCFC/ppt*
2011	390	1803	324	220	520	240
1750	234	901	259	0	0	0
Heat flux increase (W m^{-2})	1.47	0.48	0.16	0.07	0.17	0.1
% contribution	60	20	6		14	

Perfluorocarbons (CF_4, C_2F_6) and sulphur hexafluoride (SF_6), which are also radiatively active, are used in some industrial processes and released to atmosphere in quite small quantities but have long lifetimes. The radiative forcing due to such gases is not significant at present.

There are considerable geographical variations in the global distribution of this forcing. The calculated increase in forcing has been about 1 W m^{-2} at the poles, increasing to 2.5 W m^{-2} in the tropics. Note also that because the GHGs have fairly long lifetimes and are well-mixed into the atmosphere, the patterns of forcing reflect global differences in surface temperature and solar radiation rather than the source distributions of the GHGs themselves. This is a truly international problem, and emission reductions by one country will make little difference to that country's climate change. Figure 11.17 shows the trends in radiative forcing with increasing atmospheric concentrations of CO_2, CH_4 and N_2O over the last 10,000 years which clearly indicates a steep rise in radiative forcing in the decades preceding 2005.

11.3.2 The role of aerosols

In addition to the gases described earlier, there is a second important factor that has also been modifying global energy fluxes – absorption and reflection of solar radiation by atmospheric aerosol. There are large natural sources of particles – volcanoes and forest fires, for example, which we would not have expected to increase or decrease on average during the last century. However, the increases in population and fossil fuel combustion that were responsible for the GHG emissions also produced particles – directly, or

FOR REFERENCE PURPOSES ONLY
indirectly via gas-to-particle conversions. If these particles remain in the troposphere, their lifetimes are only days or weeks. If they are injected into the stratosphere by a sufficiently violent process such as a volcanic eruption or a nuclear weapon test, they may remain there for years. Much of the aerosol mass consists of particles that are about the same size as the wavelength of visible light, so they interact strongly with it.

The exact effect of an aerosol layer depends on its optical depth and height in the atmosphere. In general, the aerosol will absorb both down-going solar radiation and up-going terrestrial radiation. Naturally, the greater the optical depth the greater the radiation exchange. If that radiation exchange occurs high in the atmosphere, there will tend to be warming at that height and cooling at the ground. Conversely, aerosol in the troposphere will tend to warm the troposphere. Aerosol radiative properties also depend on the size distribution of the particles – if the effective radius is greater than about 2 μm, then they act like a GHG and there will be net warming due to the absorption of longwave terrestrial radiation. If the effective radius is less than 2 μm, then reflection of shortwave solar radiation is more important, and there is net cooling. At the top of the aerosol cloud, warming by absorption of solar radiation in the near infrared dominates over the enhanced IR cooling from the aerosol particles. In the lower stratosphere, the atmosphere is warmed by absorption of upward longwave radiation from the troposphere and surface. In the troposphere, there are only small net radiative effects, because although the reduced supply of near IR means there is less warming due to absorption by water vapour, this is compensated for by the increased flux of longwave from the aerosol particles.

FOR REFERENCE PURPOSES ONLY

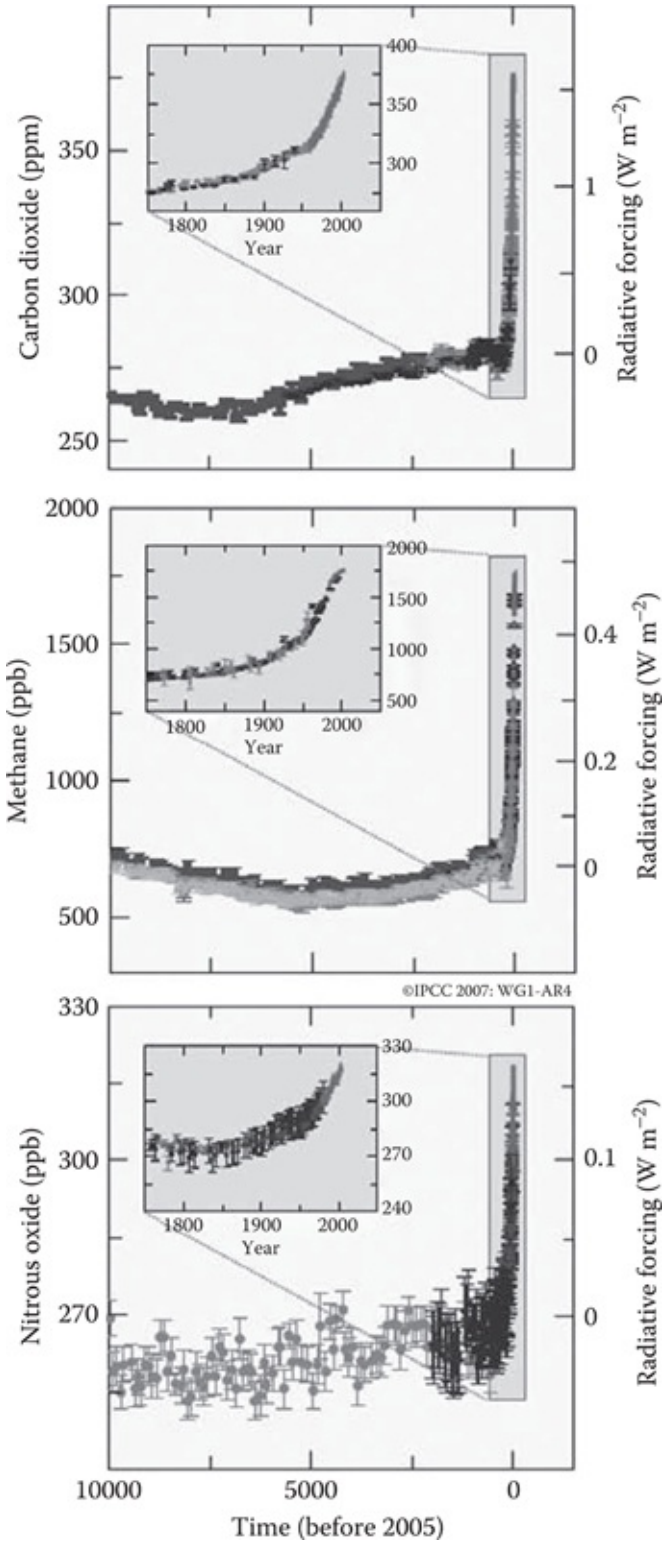

Figure 11.17 Atmospheric concentrations of CO_2, CH_4 and N_2O over the last 10,000 years (large panels) and since 1750 (inset panels) and their corresponding radiative forcings (shown on the right hand axes of the lower panels). Measurements are based on ice core data. (From IPCC, *Climate Change: Fourth Assessment Report*, Cambridge University Press, Cambridge, UK, 2007.)

FOR REFERENCE PURPOSES ONLY

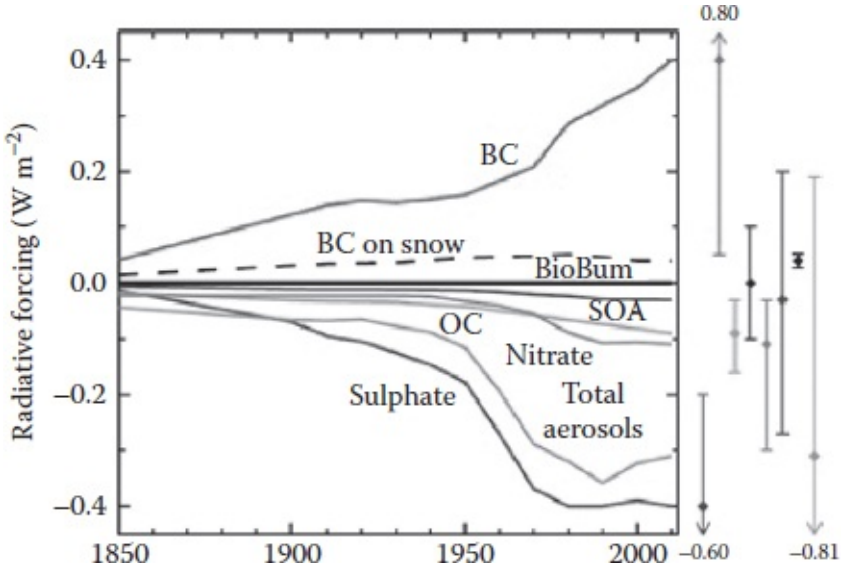

Figure 11.18 Time evolution of radiative forcing due to aerosol–radiation interaction and BC on snow and ice. (From IPCC, *Climate Change 2013: The Physical Science Basis, Contribution of Working Group I to the Fifth Assessment Report of the Intergovernmental Panel on Climate Change*, Cambridge University Press, Cambridge, UK, 2013.)

Figure 11.18 gives a summary of the positive and negative radiative forcings due to aerosol–radiation interaction for the six main aerosol source categories between 1850–2000, with the largest effect being a negative forcing due to sulphate from the sulphur released by fossil fuel combustion between 1950 and 1990. After 1990, the change has been small with even a weakening of the radiative forcing due to aerosol–radiation interaction, mainly attributed to a stronger black carbon radiative forcing as a result of increased emissions in East and Southeast Asia. Aerosol cooling occurs through aerosol–radiation and aerosol–cloud interactions and is estimated at –0.9 W m^{-2} (all aerosols combined). Black carbon or soot, on the other hand, absorbs heat in the atmosphere (leading to a 0.4 W m^{-2} radiative forcing from anthropogenic fossil and biofuel emissions) and, when deposited on snow, reduces its albedo, or ability to reflect sunlight. Reductions of black carbon emissions can therefore have a cooling effect, but the additional interaction of black carbon with clouds is uncertain and could lead to some counteracting warming.

11.3.3 Volcanoes and aerosol formation

Scientists have used large volcanic eruptions to test their models of climate change scenarios and to separate human from natural effects. An eruption is a perturbation to a system that is in quasi-equilibrium, and creates detectable oscillations in various measured climate change parameters. It also perturbs the ozone layer, as described in Chapter 12. There are two distinct families of volcano from this perspective. Effusive volcanoes, of

FOR REFERENCE PURPOSES ONLY

which Mt Etna in Sicily is a good example, emit continuously with low thermal energy and momentum. The emissions from effusive volcanoes do not have sufficient energy to penetrate the temperature inversion at the tropopause, so they remain in the troposphere. As a consequence, the emissions are involved in local small-scale deposition processes on timescales of hours or days. Explosive volcanoes, on the other hand, have sufficient energy to inject large amounts of material into the stratosphere, where the inherent atmospheric stability gives long lifetimes of weeks to years and potentially global coverage. Ironically, the volcanic plume is not usually buoyant at source because of the high solid density but becomes buoyant by entraining large volumes of ambient air which is heated by the hot solids. Hence, an injection into the stratosphere brings with it not only the volcanic material but tropospheric air with its own pollutant concentration profile.

On 14 June 1991, Mount Pinatubo in the Philippines erupted violently after 635 years of inactivity. The heaviest phase of the eruption lasted for 36 h, and ash falls were observed in Thailand and Singapore. More than 19 Mt of SO_2 (2–3 months worth of total global SO_2 emissions, or about 20 years of UK emissions) were injected up to an altitude of 20–30 km in the stratosphere and eventually converted into 40–50 Mt of sulphuric acid aerosol. These aerosols are effective at scattering shortwave radiation (and at depleting stratospheric ozone – see Chapter 13). Data from the NASA earth radiation budget satellite (ERBS) stratospheric aerosol and gas experiment (SAGE) have shown that the optical depth of stratospheric aerosol increased by over two orders of magnitude between 40°N and 40°S during the first 5 months after the eruption, and that the total aerosol optical depth over the tropical Pacific increased by a factor of five. Based on estimates this increase in aerosol forcing accentuated reflected radiation by up to 4.5 W m^{-2} in early 1992, decaying exponentially to a negligible amount by 1995, which in turn resulted in a short-term decrease in mean global surface temperature of up to 0.5°C. Hence, natural events can certainly produce radiative and temperature changes of comparable magnitude to the human ones, but they are transient rather than incremental. Eruptions themselves may be transient or continuous in nature. If a volcanic plume rises 20 km into the atmosphere at a speed of 150 m s^{-1}, then it will take 2–3 min to become established. Measurements on many different eruptions have shown that plume height α (total heat content)$^{1/4}$ for a transient plume or (heat release rate)$^{1/4}$ for a continuous plume. Mt Pinatubo achieved a maximum height of 40 km. On a far larger scale, flood basalt eruptions have involved the ejection of over 1000 km^3 of solids within a few months, with an estimated plume height of 30 km. A caldera eruption such as Tambora or Krakatoa would eject *several thousand* km^3 in a day or so.

Two main measures of volcanic impact have been used. The volcanic explosivity index (VEI) ranks volcanoes according to the rate of energy release, giving a range for recent volcanoes of up to 7 for Tambora, Indonesia in 1815, and 6 for Krakatoa and Pinatubo. The dust veil index (DVI) is compounded from various observations of the severity of an eruption, and of the extent and effects of the resulting dust cloud. These might include

FOR REFERENCE PURPOSES ONLY

historical reports of the eruption itself, optical phenomena such as obscuration of the sun or moon, radiation measurements, temperature measurements, or estimates of the volume of ejected material. The DVI takes on values of 3000, 1000 and 1000 for the same three volcanoes, respectively. The two measures are well correlated in general, although individual eruptions may not fit. For example, Mt St Helen's in 1980 was a powerful eruption with VEI = 5, but because it mainly came out sideways the stratospheric injection was low. Large eruptions (greater than 5 on the VEI) overcome the temperature inversion at the stratopause and project material into the stratosphere, where it has a long residence time. Smaller volcanic emissions are much more common, but material remains in the troposphere and has shorter lifetime.

It is not only the size of the eruption that matters but its location on the Earth. A tropical volcano will generate larger tropospheric heating at the equator than at the poles, enhancing the pole-to-equator temperature gradient, especially in winter. In the northern hemisphere winter advective forces dominate over convective, so the driving force on the Polar vortex (the jet stream) is increased and the Arctic Oscillation is perturbed. The actual effect on ground-level conditions depends on season and the state of El Niño (i.e. sea surface temperature). These interactions can lead to winter warming for temperate latitudes in the northern hemisphere, even due to a tropical volcanic eruption.

Volcanoes are responsible for around 10% of global atmospheric sulphate, but passive degassing from effusive volcanoes can raise this to 30% away from industrial sources. Etna, for example, is the largest continuous global source of SO_2 and releases around 5000 t day^{-1} at a concentration of about 1 ppm, equivalent to the emission from 10–20 2000 MW coal-fired power stations. During a more active phase, the flux rises to 25,000 t day^{-1}. As the physical release height is 3300 m, and the effective release height due to buoyancy higher still, the emissions have a long residence time in the atmosphere in which to undergo gas-to-particle conversion. A contrast is seen with the Laki, Iceland eruption of 1783. This was a low altitude event, which was effusive rather than eruptive. Estimates put the total sulphur emission at 122 Mt, equivalent to the total current annual human sulphur emission. Unusual climate events such as dry fogs and high temperatures were recorded across Europe, notably by Benjamin Franklin who was US ambassador to France at the time. Secondary effects of such eruptions include increased sulphur deposition to wetlands and a consequent increase in methane emissions. For volcanic emissions, the initial dust and ash falls out in the troposphere, while the SO_2 rises in the plume. While the SO_2 is rising, it reacts with water vapour from both the plume and from entrained air to form sulphuric acid aerosols, which are small and very effective at scattering radiation. The processes are summarised in Figure 11.19.

FOR REFERENCE PURPOSES ONLY

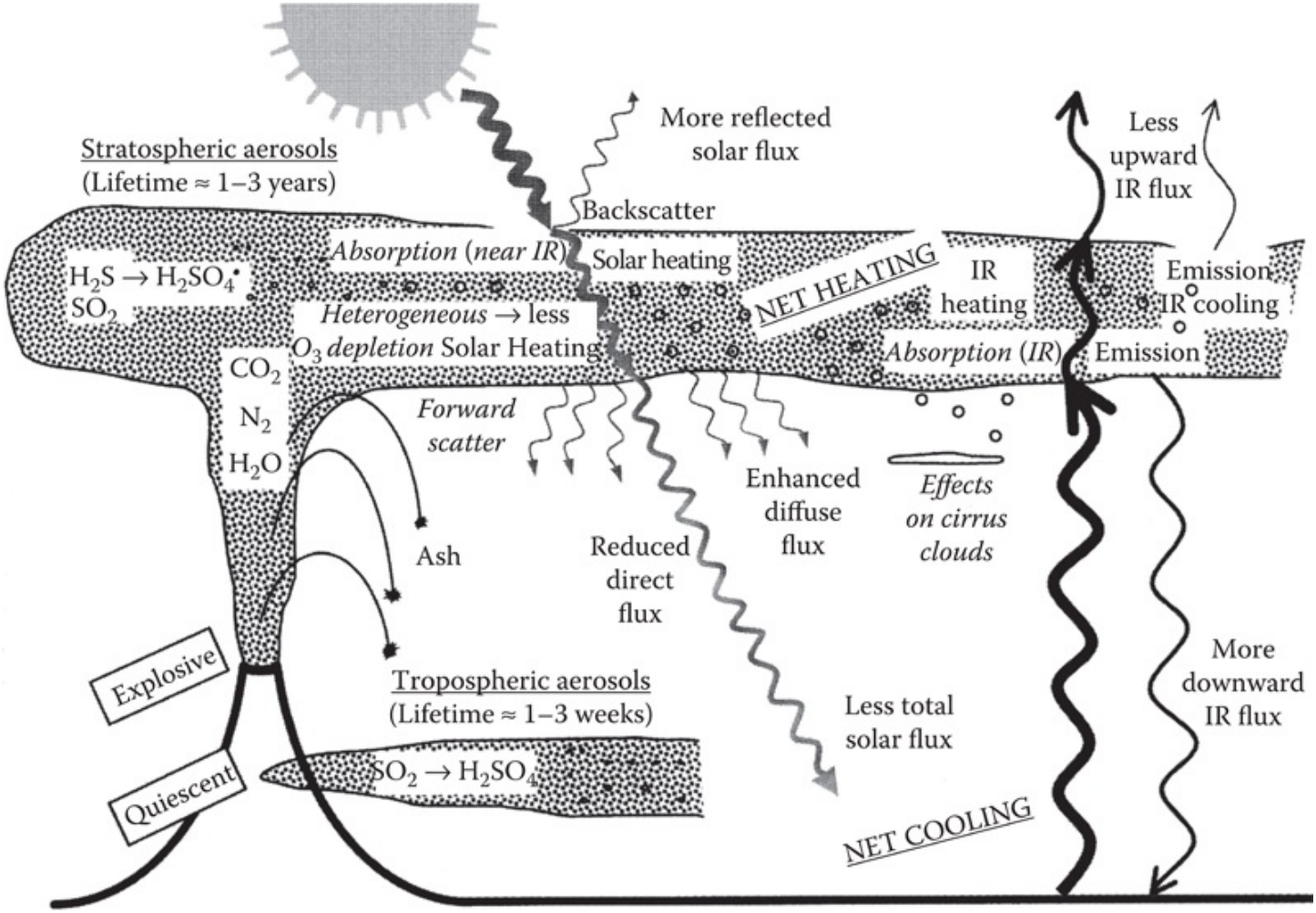

Figure 11.19 Volcanic inputs to the atmosphere and their effects on the radiation budget. (From Robock, A., *Rev. Geophys.*, 38, 191–219, 2000.)

FOR REFERENCE PURPOSES ONLY

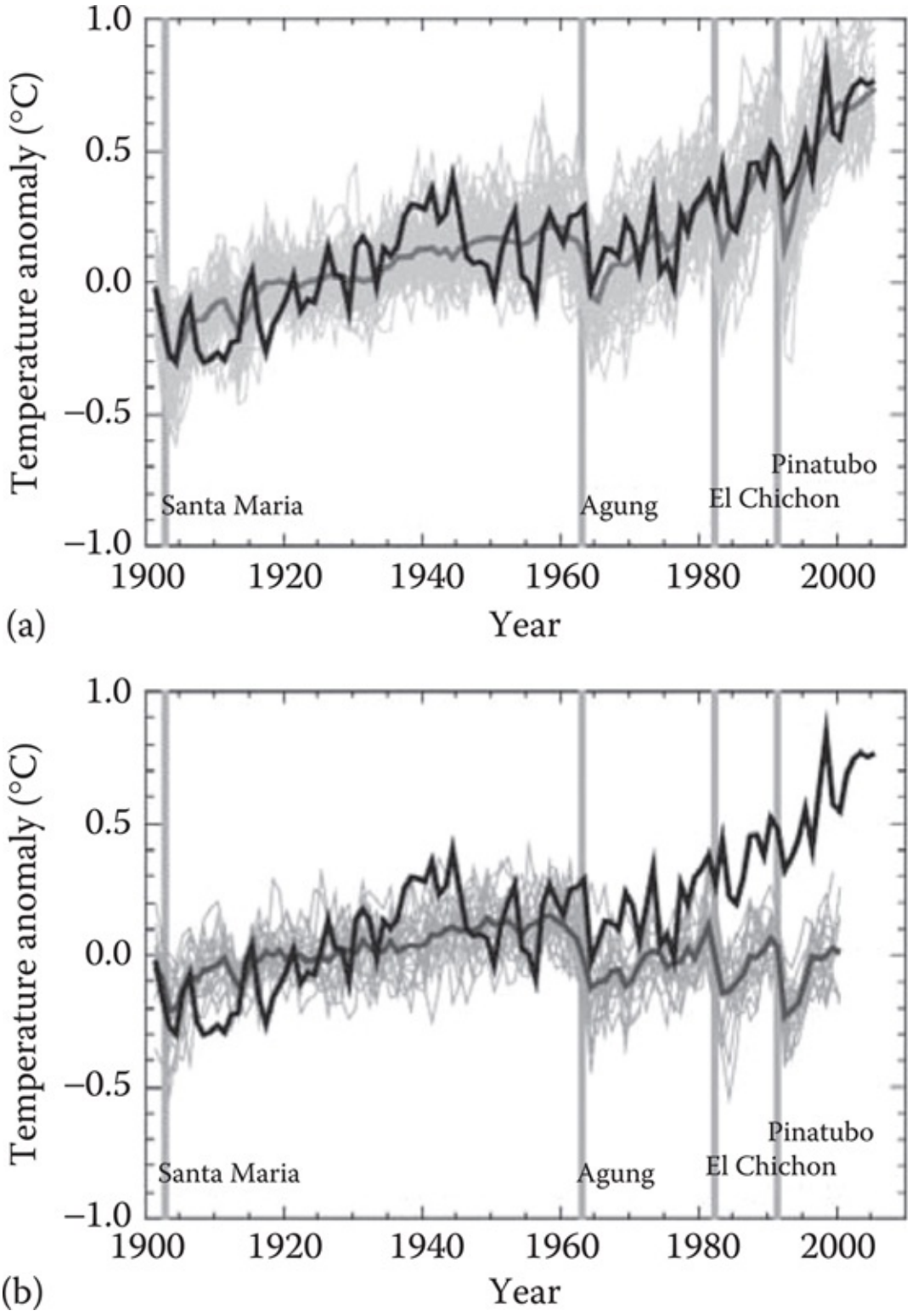

Figure 11.20 Comparison between global mean surface temperature anomalies (°C) from observations (dark line) and AOGCM simulations forced with (a) both anthropogenic and natural forcings and (b) natural forcings only. Note the global impact of major volcanic eruptions. (From IPCC, *Climate Change: Fourth Assessment Report*, Cambridge University Press, Cambridge, 2007.)

FOR REFERENCE PURPOSES ONLY

Aerosol area densities of up to 40 $\mu m^2\ cm^{-3}$ were measured in the Pinatubo plume, compared to 1 $\mu m^2\ cm^{-3}$ present as background. These resulting changes in irradiance naturally change the temperature of the atmosphere as well. In Figure 11.20, the occurrences of major eruptions from Santa Maria until Pinatubo are marked while comparing the global mean surface temperature anomalies (°C) from observations (dark lines) with general circulation model (GCM) simulations for two cases – one, combining anthropogenic and natural forcings and two, natural forcings only. As well as scattering solar radiation directly, these aerosol particles have indirect effects on the planetary albedo via cloud droplet formation. As seen previously, water droplets are unlikely to form spontaneously at realistic supersaturations because of the excess vapour pressure associated with the very small radius of curvature of the nascent droplet. Sulphate particles, which are hygroscopic and deliquesce to form *starter* droplets at low supersaturations, are ideal nuclei for the formation of cloud drops. Any increase of such nuclei due to natural or man-made emissions will therefore have consequences for the number density and diameter of cloud drops, and indirect effects on albedo. If a fixed amount of water vapour is available for cloud formation, then a larger number of smaller drops will give a higher reflectivity, changing the radiation balance in the same sense as did the aerosol particles themselves.

11.3.4 Modelling the radiative impact of aerosol

Radiation attenuation by aerosol particles is described by the Bouguer–Lambert Law

$$V_m(\lambda) = V_0(\lambda)\exp(-\tau_{\text{atm}} m)$$

where:

$V_0(\lambda)$ is the solar flux at zero airmass at wavelength λ

$V_m(\lambda)$ is the measured solar flux

τ_{atm} is the total optical depth of the atmosphere

m is the airmass factor, expressed as 1/cos (zenith angle)

Typically, the measured optical depth is the sum of several components, including those due to Rayleigh scattering and gaseous absorption; these are measured or calculated and the aerosol component obtained by difference. Measurements at many wavelengths enable the spectrum to be inverted and the particle size distribution to be calculated.

The size distributions of aerosol from volcanoes such as Pinatubo have been modelled by formulas such as:

$$n(r) = \frac{1}{r}\,\frac{N}{\sqrt{2\pi}\ln\sigma}\exp\left[-\frac{(\ln r-\ln r_0)^2}{2(\ln\sigma)^2}\right]\left[\frac{\text{number}}{\text{cm}^3\,\mu\text{m}}\right]$$

where:

$n(r)$ is the number of aerosol particles per unit volume and radius

r is the aerosol radius

σ is the geometric standard deviation which characterises the width of the distribution

r_0 is the median radius

N is the total particle density, which varies in space and time

This is a unimodal log-normal size distribution, which in this case was sulphuric acid droplets. In this work, an experimental value r_{eff} was retrieved from SAGE data or from Upper Atmosphere Research Satellite (UARS) data. Then

$$r_0 = r_{\text{eff}} \exp\left[-2.5(\ln\sigma)^2\right]$$

The values used for Pinatubo aerosol were r_{eff} around 0.4–0.8 μm, σ around 1.2, peak aerosol extinction coefficients of around 0.015 km^{-1}. The latter value E (m^{-1}) is found from

$$E(\lambda) = \int Q_{\text{ext}}\left\{\frac{2\pi r}{\lambda}, m(\lambda)\right\}\pi r^2 n(r)dr \times 10^{-6}$$

where Q_{ext} is a dimensionless Mie refraction efficiency factor, which is a function of complex refractive index $m(\lambda)$, wavelength λ (μm) and particle radius r (μm).

The overall optical depth is found by integrating these expressions down the atmospheric column. Typical peak values from Pinatubo were 0.3–0.45 at a wavelength of 0.55 μm. The Pinatubo scenario is that initially SO_2 gas (having low scattering) was injected into the stratosphere, and aerosol formation started. Aerosol extinction then increased for nearly six months. The largest particles, with r_{eff} ~ 0.5 μm, settle faster, which affects the radiation exchange differently at different altitudes. The highest, smallest particles (up at 10–20 mb) with r_{eff} ~ 0.2–0.3 μm are more effective in scattering visible wavelengths than near IR. This in turn affects the radiative forcing. Total maximum radiative forcing was found to be ~–6 W m^{-2} (cooling) over large areas. An important additional feature is stratospheric warming due to absorption of near-IR by small particles near the top of the cloud.

11.3.5 Gases and aerosols combined

Figure 11.21 summarises the total radiative forcing (gas + particle components) between 1980 and 2011. The plot clearly suggests that the majority of the forcing components are anthropogenic, with magnitude of RF values (in W m^{-2}) on the right of the vertical line showing positive forcing, increasing the tropospheric temperature, and *vice versa*. An important assumption is that different forcing mechanisms can be treated additively to

calculate the total forcing. Overall, the net anthropogenic radiative forcing is considered to be positive. Although CO_2 has the largest effect, the other gases and factors may have equal significance and act to either increase or decrease atmospheric temperature. The forcing due to aerosols is rather weak and contributing to the major uncertainties in the time evolution of the anthropogenic forcing.

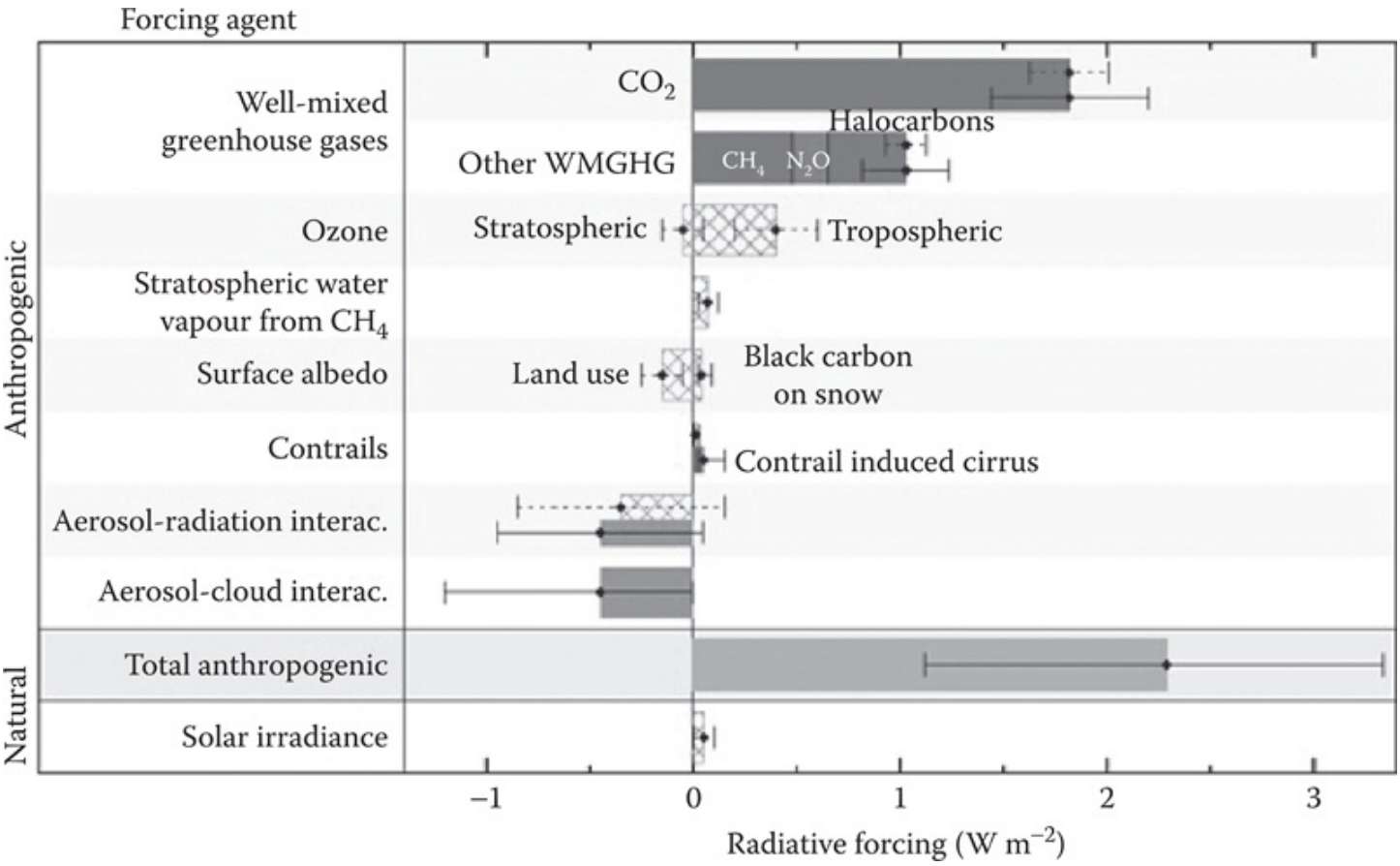

Figure 11.21 Radiative forcing of climate between 1750 and 2011. Uncertainties (5%–95% confidence range) are given for RF (dotted lines) and ERF (solid lines). (From IPCC, *Climate Change 2013: The Physical Science Basis, Contribution of Working Group I to the Fifth Assessment Report of the Intergovernmental Panel on Climate Change*, Cambridge University Press, Cambridge, UK, 2013.)

11.4 THE MAIN IMPACTS

Based on the available scientific literature since the IPCC AR4 report, there are substantially more impacts in recent decades now attributed to climate change. Recent climate changes have had widespread impacts on human and natural systems. Figure 11.22 summarises the global impacts across the geophysical, biological and human (and managed) systems, identified as directly associated with climate change in the AR5 report.

FOR REFERENCE PURPOSES ONLY

These are established on the basis of available studies in different regions (numbers in the ovals represent the climate change publications from 2001 to 2010, based on the Scopus bibliographic database for publications in English with individual countries mentioned in title, abstract or key words (as of July 2011)). The most comprehensive available literature evidence is suggestive of climate change impacts to the natural systems (mostly represented by alteration in hydrological systems by changing precipitation patterns/melting snow and ice; shift in abundance and seasonal activities of terrestrial, freshwater and marine species). Impacts on human systems are found to be relatively smaller and the negative impacts of climate change on crop yields have been more common than positive impacts. Although some impacts of ocean acidification on marine organisms have been attributed to human influence.

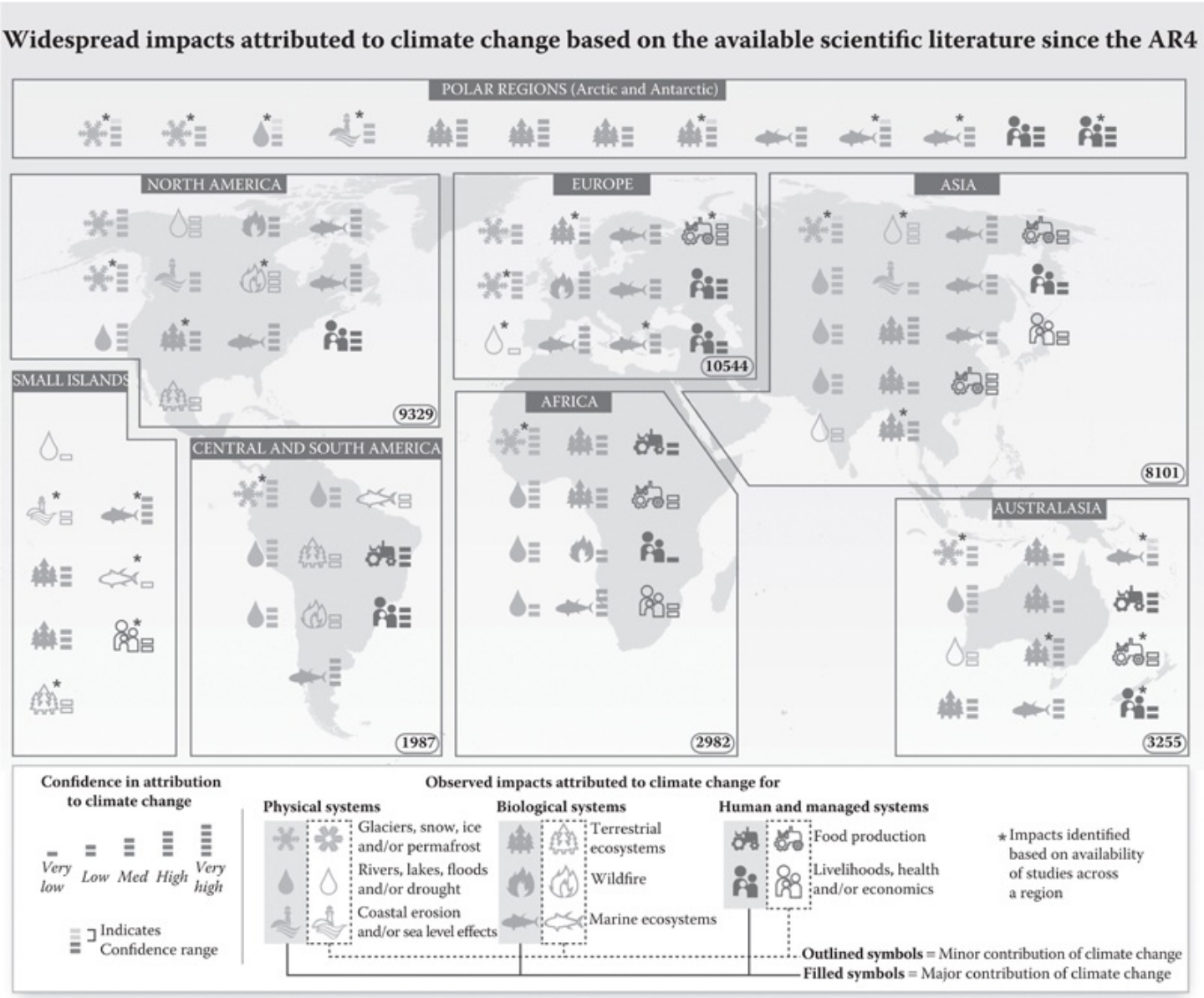

Figure 11.22 Regional variations in climate change impacts derived from literature evidence. The symbols indicate categories of attributed impacts, the relative

contribution of climate change (major or minor) to the observed impact and confidence in attribution. (From IPCC, Summary for policymakers, in: *Climate Change 2014: Mitigation of Climate Change, Contribution of Working Group III to the Fifth Assessment Report of the Intergovernmental Panel on Climate Change*, Cambridge University Press, Cambridge, UK, 2014.)

11.5 FUTURE SCENARIOS AND PREDICTIONS

The Inter-Governmental Panel on Climate Change has outlined a range of scenarios for the future pattern of GHG emissions up to 2100. The forecasts are based on evaluations of underlying scientific understanding and expressed using either a qualitative level of confidence (ranging from very low to very high) or probabilistically with a quantified likelihood (from exceptionally unlikely to virtually certain) or as statements of fact without using uncertainty qualifiers. In 2000, IPCC published a Special Report on Emission Scenarios (SRES), grouping them into four scenario families (A1, A2, B1 and B2) that explore alternative development pathways. Without any preference to any one scenario over another, these scenarios assume different levels of economic growth, global population and introduction of new and more efficient technologies. In recent years some amendments to these underlying assumptions have led to development of post-SRES scenarios. For example, the cooling effect of aerosols and aerosol precursor emissions, including sulphur dioxide, has been accounted for more accurately in recent predictions. AR5 used the following four Representative Concentration Pathways (RCPs), describing different twenty-first century pathways of GHG emissions and atmospheric concentrations, air pollutant emissions and land use – a stringent mitigation scenario (RCP2.6), two intermediate scenarios (RCP4.5 and RCP6.0) and one baseline scenario with very high GHG emissions (RCP8.5). RCP2.6 is representative of a scenario that aims to keep global warming likely below 2°C above pre-industrial temperatures.

Figure 11.23 presents global CO_2 emissions, combining the historical emissions between 1950 and 2010 with the projected IPCC AR5 future RCP emission scenarios up to 2100. Emission pathways likely to limit warming below 2°C (above pre-industrial) by 2100 show emissions of about 31–46 Pg(CO_2-eq) yr^{-1} and 17–23 Pg(CO2-eq) yr^{-1} by 2020 and 2050, respectively. However, as many scenarios still have positive emissions in 2100, they imply that the warming may exceed the target after 2100.

11.5.1 Atmospheric temperature

Effects on air temperature and other aspects of climate have been predicted by general circulation models (GCMs) – very complicated computer models of the physics of atmospheric and ocean movement and heat budgets. The models are first used to convert

FOR REFERENCE PURPOSES ONLY

the GHG emission scenarios into concentration scenarios. The models predict that as atmospheric CO_2 concentration increases, the uptake by marine and terrestrial surfaces will decrease, so that a higher proportion remains in the atmosphere as a greenhouse gas. AR5 predicts a strong, consistent, almost linear relationship between cumulative CO_2 emissions and projected global temperature change to the year 2100. The resulting atmospheric CO_2 concentration in 2100 will be between 500 and 970 ppm, corresponding to a global average air temperature increase of between 1.4°C and 6.0°C, with a most probable value of about 3°C. By 2100, the net forcing will have increased from its current value of 1.4 W m^{-2} to lie within a band from 4 to 9 W m^{-2}. The warming in nearly all land areas, especially in northern high-latitude winters, will be greater than the global average. Northern high latitudes will warm by 6°C–8°C. Figure 11.24 presents the combined influence of GHG emissions and radiative forcing (representing emissions of other atmospheric pollutants) on the global average surface warming projected up to 2150. Clearly, scenarios with reduced GHG and pollutant emissions will reduce future warming potentials but much of the warming is expected to persist for centuries after GHG emissions have stopped. On contrary, *runaway climate change* or *runaway global warming* is a hypothesised future scenario with constant emissions (or even further aggravation), marking a tipping point in the climate system. This is expected to trigger Earth's climate to change rapidly, deviating catastrophically and permanently from the original state, until it reaches a new stable condition.

FOR REFERENCE PURPOSES ONLY

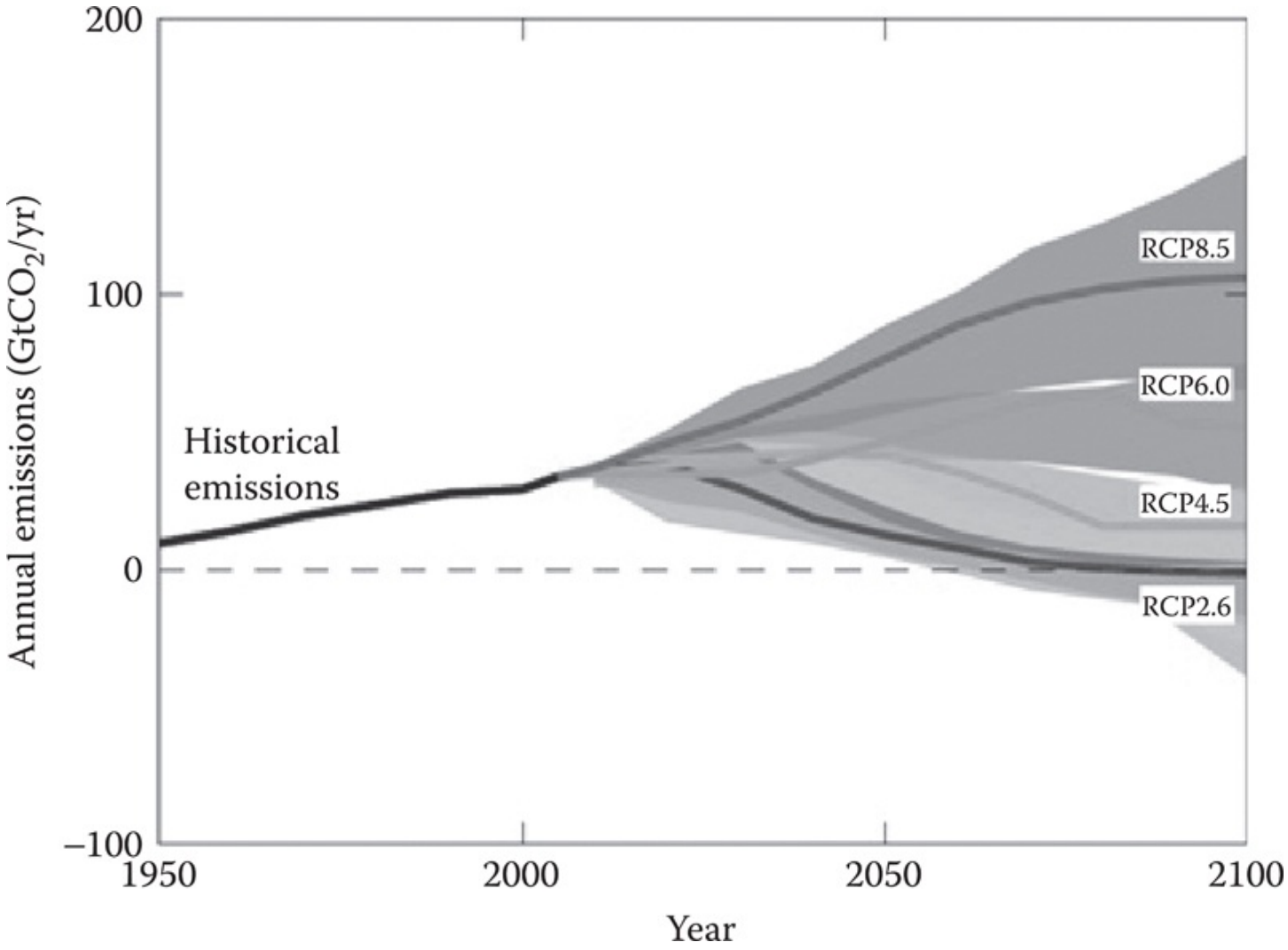

Figure 11.23 Annual emissions of CO_2 up to 2100 for AR5 representative concentration pathway (RCPs) scenarios. (From IPCC, Summary for policymakers, in: *Climate Change 2014: Mitigation of Climate Change, Contribution of Working Group III to the Fifth Assessment Report of the Intergovernmental Panel on Climate Change*, Cambridge University Press, Cambridge, UK, 2014.)

11.5.2 Sea level

Two main factors control sea level. First, there is only so much water to share between sea and ice. Hence in cold periods of the Milankovitch cycle (ice ages), water will be locked up in the polar ice sheets and in glaciers and sea level will fall. Sea level 18,000 years ago was about 100 m lower than today, while 120,000 years ago it was 5 or 6 m higher. This factor predominates in long-term changes. Second, in the shorter term, the volume of a fixed mass of sea water varies with its temperature according to its coefficient of expansion, α. The value of α is not constant, as water has its maximum density at a temperature of 4°C. At 5°C, α is one part in 10,000°C, while at 25°C it is three parts in 10,000. Hence, as the sea

FOR REFERENCE PURPOSES ONLY

warms, its expansion accelerates.

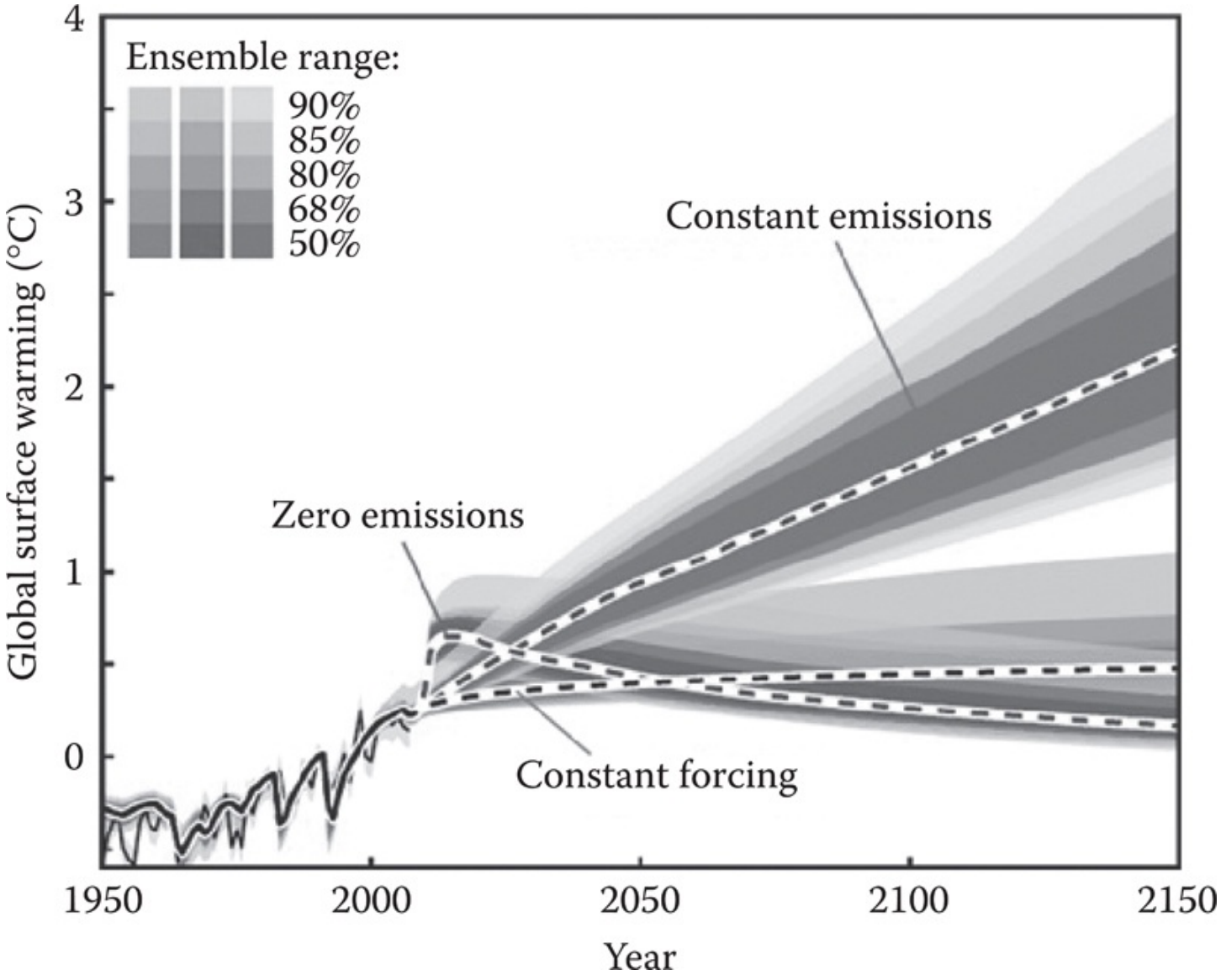

Figure 11.24 Projections of global surface warming from carbon cycle model for constant atmospheric composition (constant radiative forcing), constant and zero future GHG emissions. (From IPCC, *Climate Change 2013: The Physical Science Basis, Contribution of Working Group I to the Fifth Assessment Report of the Intergovernmental Panel on Climate Change*, Cambridge University Press, Cambridge, UK, 2013.)

In a warming world, sea level is predicted to rise due to glacier melt, ice sheet melt and thermal expansion of sea water. One of the initial reactions to predictions of increasing global temperatures over the next century was that the Antarctic and Greenland ice sheets might melt; they hold amounts of ice equivalent to global sea level increases of 65 and 7 m, respectively. However, as saturated vapour pressure increases with temperature, the air will actually hold *more* water vapour at higher temperatures, more snow will fall, and more

water will be locked up as snow and ice. Hence, temperature increases of a few degrees will *lower* sea level (from this cause), not raise it. This will remain true provided that the increasing temperature does not take the ground temperature above 0°C, when all the snow would melt anyway.

Over the period of the global temperature record shown earlier, sea level is estimated to have risen at an average rate of 1–2 mm a^{-1}. Of more concern is the probable rise in the future. If the equivalent CO_2 concentration rises to 850 ppm by 2100, with a 3.3°C temperature increase, sea level would rise by 0.65 m. Increases of this magnitude would probably be contained in some low-lying areas such as the Netherlands, but threaten others such as Bangladesh, the Nile delta and the Maldives in the Indian Ocean, where the land is only 1–2 m above sea level. In many areas, the rise in sea level is already being compounded by subsidence of the land due to water extraction. The predicted range of sea level rise given in AR5 for 2100 is 0.4–0.7 m.

11.5.3 Rainfall

In a warmer world, there will be net increases in rainfall, surface evaporation and plant transpiration. However, there will be substantial differences in the changes between geographical locations. AR5 predicts that by the end of the twenty-first century, the average amount of water vapour in the atmosphere could increase by 5% to 25%, depending on the amount of human emissions of greenhouse gases and radiatively active particles, such as smoke; heavy precipitation events will become more frequent. However, there is even less certainty about the rainfall changes than there is about temperature changes. For example, in the UK a predicted annual average temperature increase of 1.5°C–2.1°C could be associated with rainfall changes of ±15%. If precipitation is higher, then there would probably be an overall benefit from warmer temperatures and higher CO_2, whereas if it is lower the reverse would hold. By the end of the twenty-first century, under the most extreme emissions scenario, parts of the deep tropics and polar latitudes show an increase in precipitation (exceeding 50%). On contrary, large areas of the subtropics could have reduced precipitation by as much as 30% or more. Because of these uncertainties, examination of the consequences of climate change can only be made via *what if* scenarios, without any very clear idea as to which scenario will eventually turn out to be correct. A planner's nightmare!

11.5.4 Effects in the UK

Temperature changes of around 1°C may sound small, but they can have profound consequences for both natural and managed ecosystems. For comparison, a *little ice age* occurred in the sixteenth century with temperatures about 1°C cooler than now; when the Romans occupied Britain in the first centuries of the first millennium the temperature was

FOR REFERENCE PURPOSES ONLY

about 1°C warmer and grapes were grown all over England. Following are some of the consequences that are currently thought to be most likely for the UK.

- Summers will be warmer, and summer precipitation about the same. As evaporation will be higher, the soil will be drier. Winter temperatures and precipitation will both be higher.
- The summer/winter cycle of soil drying and wetting will become more pronounced, resulting in reduced soil organic matter content, changes in drainage pathways and an increase in swell/shrink factors (which affect building foundations on clay).
- The steady increase in atmospheric CO_2 concentration, which is not in dispute, combined with higher temperatures and an increase in the length of the growing season (for grasses and trees, about 15 days per °C temperature rise), will increase biomass production in both natural and managed ecosystems if water does not become a limiting factor. However, one of the responses to elevated CO_2 of many plant species is to partially close their stomata, thereby restricting the flux into the leaf. This results in increased plant dry matter without increasing the total water used, so that water use efficiency is increased. If woody species experience reduced stomatal conductance and evapotranspiration at elevated CO_2, then more water will be retained in the soil and woodland ecosystems will be affected. Many agricultural plant species yield about 10% more biomass when grown at the CO_2 concentrations anticipated in 2050. The response of economic yield may not be so clear cut – for example, higher temperatures reduce the grain-filling period for cereal crops, offsetting the benefit of higher CO_2.
- Some species (both animals and plants) will spread northwards and/or to higher altitude sites (the potential rate of northward movement is 200–300 km/°C, or around 100 km/decade). For plants, changes in viable latitude that become available due to temperature change may be restricted by photoperiod limitations.
- Many indigenous species will be lost from montane, coastal, wetland and peatland habitats. There will be increased pest and disease outbreaks – for example, milder winters with fewer frosts enable aphids to use the *green bridge*.
- A number of low-lying areas such as East Anglia and the Thames estuary would be particularly vulnerable to sea level rise. A possible increase in storm events would also increase wind damage and flooding.
- Both natural and man-made systems respond to extremes as well as to averages. A single frost or drought that is barely noticeable on the annual average temperature or rainfall total may cause damage from which ecosystems take years to recover. Small changes in mean temperature due to climate change will have disproportionate effects on the extremes. For example, an increase in mean winter temperature in the UK of 2.4°C would increase the probability of a winter temperature exceeding 6.6°C from 0.023 to 0.44, a factor of nearly 20. Of course, this calculation assumes that the variability will not itself change. Corresponding results for the distribution of summer temperatures show that summers similar to the one that occurred in 1976 (a drought

year, when mean summer temperature was 2.4°C above the average) may occur every third year by 2050. UK experienced its warmest June in 40 years (2017), the wettest winter recorded in 100 years (2014) and the warmest winter (2015/16), in around three centuries of records being kept – this may be coincidence, or it may be a harbinger of future change.

11.5.5 Effects in developing countries

Developing countries will be more adversely affected by climate change than industrialised economies. IPCC AR5 projects (with very high confidence) that coastal systems and low-lying areas will increasingly experience submergence, flooding and erosion throughout the twenty-first century and beyond, due to sea level rise. In these countries the human pressures on coastal ecosystems will increase significantly in the coming decades due to population growth, economic development and urbanisation (high confidence). Some low-lying developing countries and small island states are expected to face very high impacts that could have associated damage and adaptation costs of several percentage points of gross domestic product (GDP). The IPCC projects a reduction in these countries' gross domestic products of 2%–9% per year. This compounds the crisis from decreasing availability of suitable agricultural land, increased terrestrial biofuel cultivation, increased soil fertility depletion, increasing reliance on marginal lands. Less rainfall is predicted for much of Africa, which is already the one region in which increased food production has failed to match the population increase. This would exacerbate poverty in most developing countries and create new poverty pockets in countries with increasing inequality.

The global N cycle is also being altered, with industrial N fixation (140 Mt $year^{-1}$) now exceeding biological (100 Mt $year^{-1}$). Seventy percent of anthropogenic N_2O emissions are from agriculture, and 8%–16% of applied fertiliser N is emitted to atmosphere as N_2O. Demand for fertilisers in developing countries increase from 62 Mt in 1990 to 122 Mt in 2020. Again there are strong links between cultivation practices and pollution. If fertiliser N is applied at a time when there is a lot of runoff and plant growth is slow, then a high proportion will be lost to the water. If it is applied as urea or ammonia, then it will be lost to atmosphere. Plants are capable of recovering up to 60% of the applied N, but the proportion may be only 20% if the conditions are unfavourable. The increased population will occupy more land, and hence the pressure will be on to gain the additional food production by intensification (more production per area). The main GHGs produced are then CH_4 and N_2O. However, there is also social pressure to increase production by extensification (more area). The main GHG is then CO_2. Extensification usually involves slash and burn forest clearances – these activities in Sumatra in 1997 were the cause of long-lasting regional haze, poor air quality and loss of life. There are great uncertainties about the interactions between CO_2 increase itself and the other related changes in climate factors such as soil water and temperature. Theoretical, growth-chamber and ecosystem

studies have shown a greater proportional response to elevated CO_2 in dry years. If growth is water-limited, elevated CO_2 can result in greater water availability for longer in the growing season. Warmer temperatures will probably increase the response to CO_2 in warm-season grassland systems such as short grass steppe and tall-grass prairie. In other systems, however, responses may be more complex, possibly involving increased productivity at some times of the year and decreases at other times. The overall effect also depends on which component of the plant is economically important – cereal yields, for example, decrease at higher temperatures because of the reduced length of the fruiting season. There will also be changes in species composition. For rangelands, elevated CO_2 will increase woodland thickening, woody scrub invasion and grass suppression, tending to reduce nutritive value. If there are effects on the growth of pastures and forage plants, then there will inevitably be effects on the animals that consume them, although even less is understood about this at present. Overall, as the annual variability of agricultural output is high due to other factors, the additional perturbations due to climate change may not make much difference in this particular respect.

Throughout the twenty-first century, there is expected to be increase in ill-health in many regions and especially in developing countries with low income, as compared to a baseline without climate change (high confidence). Include greater likelihood of injury and death due to more intense heat waves and fires, increased risks from foodborne and waterborne diseases and loss of work capacity and reduced labour productivity in vulnerable populations (high confidence). Risks of undernutrition in poor regions will increase (high confidence). Risks from vector-borne diseases are projected to generally increase with warming, due to the extension of the infection area and season, despite reductions in some areas that become too hot for disease vectors (medium confidence). Globally, the magnitude and severity of negative impacts will increasingly outweigh positive impacts (high confidence). By 2100 for RCP8.5, the combination of high temperature and humidity in some areas for parts of the year is expected to compromise common human activities, including growing food and working outdoors (high confidence).

11.5.6 Biodiversity changes

Humans are having a huge impact on biodiversity as well as on the physical and chemical properties of the atmosphere. We are responsible for a large fraction of recent extinctions. The rate of species extinctions is running at 100–1000 times the ongoing background rate, and 20% of mammal species and 10% of bird species are currently threatened. The global change and terrestrial ecosystems (GCTE) project identified five main drivers that influence biodiversity – land use, climate, nitrogen deposition, biotic exchange and atmospheric CO_2 concentration. Of these five, three are primarily air pollution mediated. The balance between the five is very different depending on the situation – for example, GCTE predicted that climate change would predominate in the Arctic, because warming will be greatest in high latitudes whereas little land use change is expected. In tropical and

southern temperate forests, on the other hand, land use change will dominate the other drivers. Overall, land use change was identified as the most important factor, with climate, N deposition and CO_2 concentration being about 65%, 50% and 35% of that, respectively. However, understanding about interactions between the drivers is very limited, and the results are really more of an exploration of possibilities than a definite prediction. IPCC AR5 predicts that by the mid twenty-first century marine biodiversity reduction in sensitive regions will challenge the sustained provision of fisheries productivity and other ecosystem services, especially at low latitudes (high confidence).

11.6 FEEDBACKS

The processes that control the Earth's climate and generate the global average temperature of +15°C that we take for granted are extremely complicated, and it is very hard to predict the consequences of change. The climate system contains many feedbacks, by which a change in one parameter changes a second parameter in such a way as to amplify the effect of the first change (positive feedback) or reduce it (negative feedback). As the overall climate is determined by small differences between much larger terms, it is very sensitive to the sign and strength of these feedbacks. Consider a few examples:

Water vapour: An increase in global average temperature is predicted to increase the amount of evaporation from the oceans, and also the amount of water vapour in the atmosphere (because saturated vapour pressure increases with temperature). Water vapour is the most powerful GHG, so the additional water vapour will increase the longwave optical depth, trap more longwave radiation and increase the temperature further.

Clouds: About 30% of the solar radiation incident on the Earth is reflected back into space, more than half (17%) by clouds. This 17% amounts to about 228 W m^{-2}. Hence, if the increased water vapour in the atmosphere were to increase the cloud cover by 1% (i.e. increasing the albedo from 30% to 30.3%), that would decrease the radiant flux reaching the Earth's surface by 2 W m^{-2} and cancel out the radiative forcing due to GHGs. However, clouds also act as better absorbers of infrared radiation than the clear atmosphere and hence can increase the positive forcing by around 100 W m^{-2}. The net effect of clouds on the radiation budget depends not only on the cloudiness but on the detailed structure of the clouds and their distribution with height in the atmosphere. There is a great range of different cloud types, densities and altitudes. Some of them are made of water droplets, some of ice crystals of different shapes, and they all have different albedos (Table 11.4). In order to model such factors, we need a very sophisticated understanding of how aspects of cloud cover (amount, density, position in the atmosphere, droplet diameter distribution, ice crystal type) relate to other environmental factors such as water vapour density and air temperature. It turns out

FOR REFERENCE PURPOSES ONLY

that low-level clouds tend to produce net cooling, whereas high-level clouds tend to produce net warming. Climate change models have only recently become sufficiently advanced that predictions of cloud cover are generated as output rather than being specified as input.

Table 11.4 Albedos of natural surfaces

Surface	*Albedo/%*
Ocean (calm)	2–4
Ocean (rough)	5–10
Forest (tall coniferous trees)	5–10
Forest (short broadleaved trees)	10–15
Grass (tall savannah-type)	10
Grass (short mown)	25
Soil	10–20
Desert sand	35–45
Ice (old and rough-new and smooth)	70–20
Fresh snow	80–95
Clouds – low	60–70
Clouds – middle	40–60
Clouds – high (cirrus)	18–24
Clouds – cumulus	65–75

Methane: Rising temperatures at high latitudes in the northern hemisphere are expected to melt regions that are currently permafrost. Very large quantities of methane are locked up in these permafrost regions as clathrate hydrates such as $CH_4.6H_2O$, which are methane compounds trapped in the gaps between ice crystals. If the ice melts, the methane will be released. As methane is a GHG, there would be a positive feedback, although the deposits are so deep down that release would take place over centuries rather than decades. In a more subtle example of a positive feedback, some of the methane diffuses up into the stratosphere and forms water molecules. The water molecules are not only radiatively active but can form additional polar stratospheric cloud particles, enhance ozone depletion and raise tropospheric temperatures. Incidentally, there is also much interest in accessing the methane hydrates as the next supply of fossil fuels when the oil and gas wells have run dry.

Albedo: As well as the cloud albedo mentioned earlier, there are already strong seasonal and latitudinal variations caused by snow cover, which increases the mean albedo at 60°N from 40% in July up to 65% in February. Although the albedo in north and south polar regions is higher still at 80%, the latter constitute <10% of the total surface area. The reflectivity of fresh ice and snow can be as high as 90%, compared to around 20% for bare soil and 25% for vegetation. If temperatures rise and significant areas of the Earth that are currently snow-covered become soil, the energy absorbed at the surface

FOR REFERENCE PURPOSES ONLY

will increase, warming the atmosphere and melting more snow – another positive feedback. At a greater level of detail, any changes in vegetation will also have small effects on radiation balance, due to the range of albedos shown in Table 11.4.

Cloud nuclei: Cloud condensation nuclei (CCN) are a significant factor in the Earth's albedo, and an increase of 30% in CCN would reduce radiative forcing by about 1 W m^{-2}. Some CCN are produced by the conversion of gaseous dimethyl sulphide (DMS) to sulphate particles. Dimethyl sulphide in turn is produced by oceanic phytoplankton that will breed faster in warmer water. Hence, higher temperatures could produce more DMS and more cloud cover and less radiation penetrating to the ground and lower temperatures – a negative feedback. Other CCN are produced from sulphate particles formed in the atmosphere from gaseous SO_2 produced by the burning of fossil fuel. The more CO_2 that is generated to give a warming, the more sulphate aerosol is generated to give a cooling.

Ocean circulation: The atmosphere is coupled to the oceans by processes such as evaporation and heat transfer, and anything that affects the atmosphere must affect the oceans in due course. The changes tend to be slower, because the mass and heat capacity of the oceans is so huge compared to that of the atmosphere. For example, the top 3 m of the oceans hold as much heat as the whole atmosphere. As with cloud cover, small percentage changes in ocean heat transfer may have large effects on heat balance. Changes in rainfall and evaporation will affect salinity, which will affect the global scale currents that continually redistribute heat energy in the oceans.

There may be interactions that are much more powerful, and much harder to predict, than any of those mentioned earlier. The Earth has many complex systems that we take for granted on a day-to-day basis; climate change may disturb these systems in profound ways. For example, the global thermohaline conveyor belt moves huge quantities of energy around the planet in the form of slow-moving currents of water having different salinities and temperatures. It is estimated that 10^{12} kW is transported from the southern to the northern hemisphere by the Atlantic Ocean. Part of that flow, the Gulf Stream, brings an amount of energy equivalent to about 30,000 times the entire UK electricity generating capacity, and warms the UK by several degrees Celsius. There is a possibility that the flow is unstable and that perturbations in the climate system could switch the flow quite quickly (within decades) into another pattern.

11.7 GLOBAL RESPONSES

Initial responses to the threat of climate change were made on a rather piecemeal basis – for example, the EU decided in 1990 on the objective to stabilise EU CO_2 emissions at 1990 levels by the year 2000. These efforts were coordinated on a global basis by the United Nations Framework Convention on Climate Change (UNFCCC), which was agreed in Rio

FOR REFERENCE PURPOSES ONLY

de Janeiro in 1992. At the 3rd Conference of Parties (COP3), held in Kyoto in 1997, different binding GHG emission targets were set for different countries. The Kyoto Protocol, for the first time, set ambitious targets to reduce aggregated emissions of six GHGs (CO_2, CH_4, N_2O, HFCs, PFCs, SF_6) by at least 5% below 1990 levels before a *commitment* period 2008–2012. Within this protocol, the EU accepted a target reduction of 8%, distributed among the member states according to a burden-sharing agreement which allowed the less developed nations to increase their emissions (by up to a maximum of 27% for Portugal), while the more developed ones cut theirs (by a maximum of 21% for Germany).

At the 21st Conference of Parties (COP21), held in Paris in December 2015, 196 parties to the UNFCCC adopted a new legally binding framework to 'strengthen the global response to the threat of climate change' (Art. 2) through an internationally coordinated effort. The Paris Agreement establishes a global warming goal of well below 2°C on pre-industrial averages. It requires countries to formulate progressively more ambitious climate targets which are consistent with this goal. The Paris Agreement puts emphasis on processes rather than on defined mitigation goals. Unlike the Kyoto Protocol, the Paris Agreement does not formulate country specific emissions targets. Instead, the Paris Agreement depends on voluntary mitigation contributions and a series of processes that seek to ensure collective and individual progress in meeting the initial and progressively more ambitious mitigation contributions. It aims for an ambitious collective goal to limit warming to 1.5°C; greenhouse gas emissions to peak as soon as possible, and to achieve net-zero emissions in the second half of this century. However, substantially greater reductions, of around 60%–70%, will be needed if the CO_2 concentration is to be stabilised even at 550 ppm.

If global energy consumption was not reduced, this would involve generating 35–40% of their energy requirements from non-fossil fuel sources. Nuclear power is not really seen as an option and is predicted to decrease from the current 6.6% to 4.4% by 2020. As shown previously in Figure 11.17, total global emissions of CO_2 due to fuel combustion increased steadily since the 1970s and show no signs of abating.

11.7.1 European responses

EU countries have agreed on a new 2030 Framework for climate and energy, including EU-wide targets and policy objectives for the period between 2020 and 2030. These targets aim to help the EU achieve a more competitive, secure and sustainable energy system and to meet its long-term 2050 greenhouse gas reductions target. The key targets for 2030 include:

- A 40% cut in greenhouse gas emissions compared to 1990 levels
- At least a 27% share of renewable energy consumption
- At least 27% energy savings compared with the business-as-usual scenario

FOR REFERENCE PURPOSES ONLY

However, to date there are wide differences in the approach of different countries to reducing emissions and in their overall success. For example, although the EU as a whole reduced GHG emissions by 2.5% from 4.15 to 4.05 Gg between 1990 and 1998, emissions from Spain increased by 19% while those from Germany decreased by 16%. Nevertheless, CO_2 emissions, which make up around 80% of the GHG total, are almost stable.

The EU needs to achieve its 8% cut overall, so it does not matter if some countries do not manage it provided that others compensate. The EU is now operating a reformed *Emissions Trading Scheme* (EU ETS), which serves as a *cap and trade scheme*. This means that any installation within the scheme is given an allocation of emissions allowance each year. If the installation's actual emissions are above this initial allocation for the year in question, then the installation must either purchase allowance through the scheme or bring forward some allowance from the following year's allocation, so as to cover the deficit. Conversely, installations with a surplus of emissions compared with their cap are allowed to either sell allowances or carry them over into the following year's allocation, thus providing a financial incentive to reduce emissions. As there is a finite limit of allowances in the scheme (i.e. the cap), any allowances purchased should come from installations which have reduced emissions.

11.7.2 UK responses

The UK government has set five-yearly carbon budgets which currently run until 2032. They restrict the amount of greenhouse gas the UK can legally emit in a five year period. In its fifth carbon budget it aims to reduce the GHG emissions by 57% below 1990 levels by 2030. The UK GHG emissions are broken down into the Kyoto *basket* of seven gases (Table 11.5). The last four gases are collectively referred to as fluorinated gases or F gases. The values for each individual gas exclude emissions from UK overseas territories but the Kyoto basket total includes their emissions. Kyoto base year consists of emissions of CO_2, CH_4 and N_2O in 1990, and of HFCs, PFCs and SF_6 in 1995.

Table 11.5 UK GHG emissions between 1990 and 2015

FOR REFERENCE PURPOSES ONLY

	Emission weighted by global warming potential (million tonnes CO_2 equivalent)				
Greenhouse gas	*1990*	*1995*	*2000*	*2010*	*2015*
Net CO_2 emissions (i.e. emissions minus removal)	595.7	557.5	555.7	496.7	403.8
Methane (CH_4)	134.8	128.3	110.5	67.8	52.2
Nitrous oxide (N_2O)	51.2	41.7	31.3	24.0	23.1
Hydrofluorocarbons (HFC)	14.4	19.1	9.8	13.1	15.8
Perfluorocarbons (PFC)	1.7	0.6	0.6	0.4	0.3
Sulphur hexafluoride (SF_6)	1.3	1.3	1.8	0.7	0.5
Nitrogen trifluoride (NF_3)	0.0	0.0	0.0	0.0	0.0
Total greenhouse gases	799.0	748.5	709.7	685.8	495.7

Further, through the Climate Change Act 2008, the government has committed to: reduce emissions by at least 80% of 1990 levels by 2050; and, contribute to global emission reductions, to limit global temperature rise to as little as possible above 2°C. The Non Fossil Fuel Obligation (NFFO) requires electricity suppliers to generate specific amounts of electricity from non-fossil fuel sources. In the UK these are mainly biofuels, waste incineration, landfill gas, wind and hydro. A Fossil Fuel Levy (FFL) is paid by suppliers of electricity from non-renewable energy sources, mainly towards funding the development of new renewable schemes.

Emission reduction strategy on such a scale would have great implications for our way of life. The UK government in 2017 announced changes to the rules on electricity usage and storage, allowing individual households to generate and sell renewable energy. However, renewable energy sources are very diffuse compared to fossil fuels. A typical 1 MW wind turbine, for example, might generate an actual 0.4 MW on average, compared to 2000 MW by a major power station. Hence, it would take 5000 such turbines to replace the electricity output from a single fossil-fuel power station. There are schemes for concentrating the CO_2 in the waste gases from coal-fired power stations and pumping it either into permeable rock strata or into the deep ocean, but neither of these options has been tested on a large scale and the environmental and ecological consequences are uncertain.

Such methods should be seen as short-term technical fixes which simply transfer the problem without solving it. The better option is to reduce energy usage by many different measures, which would have the added spin-off of reducing pollutant emissions. UK energy consumption has been rising at an average of 0.5% per year since 1965; this sounds small, but if it continues at this rate it will increase by a further 30% by 2050. The fastest rate of expansion has been in the transport sector, while domestic use has remained about constant and industrial use has declined. The latter decline is partly due to substitution of gas for coal, a process which has largely been completed. Energy costs have declined in real terms over the same period, so there has been no incentive to reduce consumption. Domestic energy efficiency, especially in the housing stock built in the nineteenth and early twentieth

centuries, is very poor. Combined heat and power (CHP) schemes, in which the waste heat from electricity generation is used to provide hot water for industrial and domestic space heating, increases thermal efficiency from below 40% to around 80%.

11.8 CASE STUDY – CARBON FOOTPRINTING

The need to tackle anthropogenic greenhouse gas (GHG) emissions has become imperative as understanding of the risks of climate change has developed. Mechanisms to bring about a reduction in the quantities of anthropogenic GHG emissions have been devised so that responsibility for anthropogenic climate forcing may be equitably assigned and specific emissions reduction objectives can be set and progress measured.

The concept of *ecological footprinting* was introduced in the mid-1990s. It rapidly became recognised as an important tool for quantifying anthropogenic environmental impact. Ecological footprinting is a methodology for estimating the area of the Earth's surface needed to provide all necessary resources to, and process waste and pollution from, a given population, organisation or activity (Wackernagel and Rees, 1996). The term *footprint* has become popular and applied largely to measurement of CO_2 and other GHG emissions, fresh water and nutrient demand.

Carbon footprints provide a tool for the calculation of emissions linked to a process, activity or behaviour. The potential merits of the carbon footprint are based on its simplicity, making the metric economically viable, (potentially) internationally comparable and readily understandable. However, numerous definitions of a carbon footprint have been put forward in both the academic press and grey literature. These definitions have been reviewed by Wright et al. (2011) who proposed a practical definition (below) that required only relatively easily obtainable data whilst still capturing the bulk of anthropogenic climate forcing:

> A measure of the total amount of CO_2 and CH_4 [methane] emissions of a defined population, system or activity, considering all relevant sources, sinks and storage within the spatial and temporal boundary of the population, system or activity of interest. Calculated as CO_2e [carbon *dioxide equivalent*] using the relevant 100-year global warming potential (GWP100).

This definition was used as the basis for the British Standards Institution's (2014) Publicaly Available Specification (PAS) 2070: *Specification for the Assessment of Greenhouse Gas Emissions of a City*. In addition to the definition of a carbon footprint, Wright et al. (2011) also suggested a definition for a *climate footprint*, which is a wider measure of all GHGs controlled under the Kyoto Protocol caused by a defined population, system or activity. The definition of a climate footprint recognises that in some situations a more comprehensive metric for the assessment of further GHGs may be required; the name reflects the inclusion

FOR REFERENCE PURPOSES ONLY

of further Kyoto Basket non-carbon gases, encompassing the full range of gases in the global communities' response to climate change.

A number of standards exist that concern the calculation of various types for carbon and/or climate footprints, including: guidance from the Intergovernmental Panel on Climate Change (IPCC) on compiling national GHG inventories (IPCC, 2006); the Local Government GHG Emissions Analysis Protocol (ICLEI, 2009); the GHG Protocol Standard for Corporate Carbon Footprinting (Ranganathan et al., 2004); the PAS (Publicly Available Standard) 2050 for the Assessment of Life Cycle GHG Emissions of Goods and Services (BSI, 2008); and BSI PAS 2070. These standards do not use a common definition of a carbon footprint. Nevertheless, these standards provide useful information and outline various techniques that can be used in the compilation of carbon footprints as defined by Wright et al. (2011).

Calculating a *carbon footprint* is a relatively simple process encompassing five steps:

1. All conceivable emissions sources for the subject of interest should be identified and categorised. The World Resource Institute differentiates emissions sources in terms of *scopes* (1–3) that relate to the spatial boundary of the activity or process (Greenhalgh, 2006). Scope 1 encompasses direct emissions. Scope 2 is defined as emissions associated with electricity consumption. Scope 3 encompasses all *physical* out of boundary, process linked emissions. Emissions sources can be further differentiated by life-cycle perspective, single process or production chain emissions. Production chain emissions occur upstream (e.g. service provision, energy production) and downstream (e.g. waste).
2. A decision making process must then determine which emissions sources are relevant to the subject of the carbon footprint, and which should therefore be included in carbon footprint calculation. Carbon footprinting involves gathering and processing data and thus involves a cost in terms of time and resources. It is often not practical for all plausible emissions sources to be considered when calculating a carbon footprint. Therefore, boundaries must be set that determine which processes are included in the footprint. The issue of boundary selection is largely addressed through the consideration of emissions responsibility. Broadly, there are two perspectives, production (at source) and consumption (end-user) accounting. Production accounting assigns emissions responsibility to the producer of emissions, whereas consumption accounting locates emissions associated with production to the final consumption of goods and services. Production accounting methodologies are currently widely used but may lead to *burden-shifting*, whereby energy intensive process are exported to less-developed countries and imports of products then increase in consumer countries.
3. An appropriate method for translating the measurable activities of each emissions source to a weight of CO_2e emissions must be selected from a range of methods that can be applied to calculating carbon footprints. For example, the unit of activity could be litres of liquid fuel consumed, which is then multiplied by emissions factors

(mass/l), giving quantities of CO_2 and CH_4 emitted. Emissions factors can either apply directly to the use of fuels, energy products (e.g. electricity) or to other activities, such as travelling a distance using a certain mode of transport, consuming a quantity of fresh water or generating a quantity of waste. The IPCC categorise methods for calculating emission into three tiers. Tier One methods are the least accurate and specific but tend to be the easiest to apply. Tier three methods are the most accurate but also more time consuming and costly to apply.

4. The necessary data should be gathered and the method applied to calculate a total weight of CO_2 and CH_4 emissions, expressed as CO_2e.
5. The method must be thoroughly documented in order that future iterations of the carbon footprint can be undertaken with the same methods and, therefore, be comparable.

For more detailed reading, Williams et al. (2012) have provided an introductory guide to the methods, approaches, terminology and applications of carbon foot printing for the interested lay person or researcher.

REFERENCES AND FURTHER READING RESOURCES

British Standards Institution (BSI) (2008) *BSI PAS 2050:2008: Specification for the Assessment of the Life Cycle Greenhouse Gas Emissions of Goods and Services*. BSI, London, UK.

British Standards Institution (BSI) (2014) *BSI PAS 2070:2014: Specification for the Assessment of Greenhouse Gas Emissions of a City*. BSI, London, UK.

Brown, P., Broomfield, M., Cardenas, L., Choudrie, S., Kilroy, E., Jones, L., Passant, N., Thomson, A., and Wakeling, D. (2017) *UK Greenhouse Gas Inventory, 1990–2015: Annual Report for Submission under the Framework Convention on Climate Change*. National Atmospheric Emissions Inventory, London, UK.

Burroughs, W. J. (2001) *Climate Change: A Multidisciplinary Approach*. Cambridge University Press, Cambridge, UK.

Chapman, L. (2007) Transport and climate change: A review. *Journal of Transport Geography*, 15(5): 354–367.

European Commission (2013) The EU strategy on adaptation to climate change. climate-adapt.eea.europa.eu/eu-adaptation-policy/strategy.

Gössling, S., and Upham, P. (2009) *Climate Change and Aviation: Issues, Challenges and Solutions*. Earthscan, London, UK.

Greenhalgh, S., Daviet, F., and Weninger, E. (2006) *The Land Use, Land-Use Change, and Forestry Guidance for GHG Project Accounting*. World Resources Institute, Washington, DC.

Hedegaard, G. B., Brandt, J., Christensen, J. H., Frohn, L. M., Geels, C., Hansen, K. M., and Stendel, M. (2008) Impacts of climate change on air pollution levels in the Northern Hemisphere with special focus on Europe and the Arctic. *Atmospheric Chemistry and Physics*, 8(12): 3337–3367.

Heintzenberg, J. (2009) *Clouds in the Perturbed Climate System: Their Relationship to Energy Balance, Atmospheric Dynamics and Precipitation*. MIT Press, Cambridge, MA.

Houghton, J. (2004) *Global Warming: The Complete Briefing*. Cambridge University Press, Cambridge, UK.

ICLEI (2009) *Local Government GHG Emissions Analysis Protocol (IEAP)*. International Council for Local Environmental Initiatives, Bonn, Germany.

IPCC (2001) *Climate Change: Third Assessment Report*. Cambridge University Press, Cambridge, UK.

IPCC (2006) *IPCC Guidelines for National Greenhouse Gas Inventories*. Prepared by the National Greenhouse Gas Inventories Programme, Eggleston, H. S., Buendia, L., Miwa, K., Ngara, T., and Tanabe, K. (Eds.), Institute for Global Environmental Strategies, Hayama, Japan.

FOR REFERENCE PURPOSES ONLY

IPCC (2007) *Climate Change: Fourth Assessment Report*. Cambridge University Press, Cambridge, UK.

IPCC (2013) *Climate Change 2013: The Physical Science Basis. Contribution of Working Group I to the Fifth Assessment Report of the Intergovernmental Panel on Climate Change*. Cambridge University Press, Cambridge, UK.

IPCC (2014) Summary for policymakers. In: *Climate Change 2014: Mitigation of Climate Change. Contribution of Working Group III to the Fifth Assessment Report of the Intergovernmental Panel on Climate Change*. Cambridge University Press, Cambridge, UK.

IPCC (2015) *Climate Change 2014: Mitigation of Climate Change*, Vol. 3. Intergovernmental Panel on Climate Change, Cambridge University Press, Cambridge, UK.

Le Quéré, C. et al. (2016) Global carbon budget 2016. *Earth System Science Data*, 8: 605–649.

Mall, R., Singh, R., Gupta, A., Srinivasan, G., and Rathore, L. S. (2006) Impact of climate change on Indian agriculture: A review. *Climatic Change*, 78(2–4): 445–478.

Masters, G. M. (1998) *Environmental Engineering and Science*. Prentice Hall, Upper Saddle River, NJ.

Metcalfe, S., and Derwent, D. (2005) *Atmospheric Pollution and Environmental Change*. Hodder Arnold, London, UK.

Mingxing, W., Qiang, L., and Xin, Y. (2004) A review of research on human activity induced climate change – I. Greenhouse gases and aerosols. *Advances in Atmospheric Sciences*, 21(3): 314–321.

Omasa, K., Nouchi, I., and De Kok, L. J. (2006) *Plant Responses to Air Pollution and Global Change*. Springer, Japan.

Pittock, B. (2009) *Climate Change: Science, Impacts and Solutions*. Earthscan, London, UK.

Ranganathan, J., Corbier, L., Bhatia, P., Schmitz, S., Gage, P., and Oren, K. (2004) *The Greenhouse Gas Protocol: A Corporate Accounting and Reporting Standard*, revised ed. World Business Council for Sustainable Development and World Resources Institute, Geneva, Switzerland.

Robock, A. (2000) Volcanic eruptions and climate. *Reviews of Geophysics*, 38: 191–219.

Song, L., and Woo, W. T. (Eds.) (2008) *China's Dilemma: Economic Growth, the Environment and Climate Change*. Brookings Institution, Washington, DC.

Stern, N. (2007) *The Economics of Climate Change: The Stern Review*. Cambridge University Press, Cambridge, UK.

Stocker, T. (Ed.) (2014) *Climate Change 2013: The Physical Science Basis: Working Group I Contribution to the Fifth Assessment Report of the Intergovernmental Panel on Climate Change*. Cambridge University Press, New York.

Thomas, J., and Thistlethwaite, G. (2006) *Greenhouse Gas Emissions Data for International Aviation and Shipping, 1990–2006*. AEAT, Oxfordshire, UK.

Tiwary, A., Chatterton, T., and Namdeo, A. (2014) Co-managing carbon and air quality: Pros and cons of local sustainability initiatives. *Journal of Environmental Planning and Management*, 57(8): 1266–1283.

Toulmin, C. (2009) *Climate Change in Africa*. Zed Books, London, UK.

Wilby, R. L. (2006) Climate change, biodiversity and the urban environment: A critical review based on London, UK. *Progress in Physical Geography*, 30(1): 73–98.

Wilby, R. L. (2007) A review of climate change impacts on the built environment. *Built Environment*, 33: 31–45.

Wuebbles, D. J. (1993) Global climate change due to radiatively active gases. In: C. N., Hewitt and W. T., Sturges (Eds.), *Global Atmospheric Chemical Change*. Chapman and Hall, London, UK.

UKCCRA (2017) UK climate change risk assessment synthesis report, UK Committee on Climate Change.

Wackernagel, M., and Rees, W. (1996) *Our Ecological Footprint: Reducing Human Impact on the Earth*. New Society Publishers, Gabriola, Canada.

Williams, I., Kemp, S., Coello, J., Turner, D. A., and Wright, L. A. (2012) A beginner's guide to carbon footprinting. *Carbon Management*, 3(1): 55–67.

Wright, L. A., Coello, J., Kemp, S., and Williams, I. (2011) Carbon footprinting for climate change management in cities. *Carbon Management*, 2(1): 49–60.

FOR REFERENCE PURPOSES ONLY

Chapter 12

Air pollution impacts on ozone

Ozone is basically a secondary pollutant in the troposphere (as introduced in Chapter 2) while it is a natural constituent in the stratosphere (between heights of 15 and 50 km). This chapter mainly develops an understanding of the distinct impact the changing air pollution levels have on the resulting ozone profiles in these two atmospheric layers. In the troposphere this is associated with the alterations in the nitrogen oxide and biogenic volatile organic compounds, whereas in the stratosphere this is linked to the alterations in the chlorofluorocarbons. The later part also covers some harmful impacts of stratospheric ozone depletion on UV radiation and the state of art of the protective measures to reduce exposure.

12.1 TROPOSPHERIC OZONE

While Chapter 2 covers the introductory material on tropospheric ozone, this chapter provides additional insight into the underlying mechanisms impacting the changing tropospheric ozone concentration profile, mainly the role of precursors NO_x and biogenic volatile organic compounds (BVOCs). Detailed modelling of these photochemical reactions, combined with single-site measurements of both precursors and products, is now enabling predictions to be made of the proportionate contribution of individual hydrocarbons to overall ozone generation. In one case study covering reactions of 34 different hydrocarbons, it was calculated that methane, butene, carbon monoxide, ethylene and isoprene together accounted for over 50% of the ozone production and that 19 of the 34 modelled species had to be included to account for 90%. The potential for ozone production by the different hydrocarbons can be ranked in comparison to ethylene (taken as 100). For example, propene is 103, propane is 42, octane is 53, benzene is 19 and methanol is 12. We are also able to model the ozone production rate due to specific VOCs. In one example, a total rate of ozone formation of 1.323 ppb h^{-1} was calculated, with contributions of 0.249 from isobutene, 0.147 from ethylene and 0.116 from isoprene.

12.1.1 Chemical reactions in the troposphere

We need to introduce some important concepts before we discuss tropospheric chemistry in more detail.

12.1.1.1 Allotropy

Allotropy is the property of some chemical elements to exist in two or more different forms. These different forms of an element are known as allotropes. Allotropes are different structural modifications of an element; essentially the atoms of the element are bonded together in a different manner, for example, carbon, where allotropes include diamond, graphite, graphene and the fullerenes. For some elements, allotropes have different molecular formulae which can even persist in different phases; the two best-known allotropes of oxygen (dioxygen, O_2, and ozone, O_3), can exist in the solid, liquid and gaseous states. Other known allotropes of oxygen include:

- Atomic oxygen (O); more accurately denoted O(^{3}P), O(3P) or O((3)P). This allotrope is very reactive, as the single atoms of oxygen tend to quickly bond with nearby molecules. This allotrope does not exist naturally for very long on Earth's surface.
- Singlet oxygen (dioxygen), which is the common name used for an electronically excited state of molecular oxygen (O_2). The ground state – in which the total energy of the electrons cannot be lowered by transferring one or more electrons to different orbitals – is known as triplet oxygen but there are also two metastable states – states that spend an extended time in a configuration other than the ground state – called singlet oxygen [O(^{1}D)].
- Tetraoxygen (O_4), discovered in 2001. It is possible that O_4 consists of two dumbbell-shaped O_2 molecules held together by dispersion forces.
- Solid oxygen, which has six known distinct phases.

12.1.1.2 Free radical chain reaction

The chemical pathways for the formation and removal of gaseous pollutants in the troposphere are controlled largely by atoms and *free radicals*, despite the fact that they are present at low concentrations. The term *free radical* refers to any atom or group of atoms that has an odd number of electrons (i.e. an unpaired electron in the outer (valence) shell) and is capable of independent existence. Because of this unpaired electron, radicals have high free energies[1] and are much more reactive than non-radical species whose electrons are all paired up. Some free radicals can carry an electrical charge that will influence their properties. The high reactivity of free radicals is responsible for their low concentrations in the troposphere and also for their importance as intermediates in tropospheric reactions.

Free radicals are denoted by a dot next to the appropriate chemical symbol – the dot

indicating the presence of an unpaired electron in an outer orbit around the nucleus. Examples of atmospheric free radicals include:

$O^{\bullet}$	Oxygen radical
$^{\bullet}OH$	Hydroxyl radical
$HO_2^{\bullet}$	Hydroperoxyl radical
$^{\bullet}O_2^-$	Superoxide radical
$^{\bullet}F_2^-$	Fluoride radical

As we have already seen, atmospheric gases are present at low concentrations – considerably lower than the concentrations typically used in industrial processes or laboratory experiments. As a consequence, collisions between gas molecules are relatively infrequent. With few exceptions, the only reactions between atmospheric gas molecules that proceed at significant rates are those involving at least one radical species. Of these, the most important free radical in the troposphere is the hydroxyl radical and this is what we shall examine as the first of the key chemical reactions in this particular region of the atmosphere.

One way of working out if a chemical species is a radical or not is by counting its electrons. As a general rule, an odd number of electrons typically distinguishes a radical and an even number a non-radical. For example, nitric oxide (NO) has an odd number of electrons (7 + 8 = 15 electrons) and hence is a free radical. Nitric acid (HNO_3) has an even number of electrons (1 + 7 + (3 × 8) = 32 electrons) and is a non-radical.

An important exception to this rule is atomic oxygen (O), which has eight electrons but two unpaired valence shell electrons in its *triplet* O(^{3}P) ground state (2s 22px 22py 12pz1) and is therefore a radical (or more exactly a bi-radical). Atomic oxygen with all electrons paired (2s 22px 22py2) is in a higher-energy *singlet* O(^{1}D) state and is even more reactive than O(^{3}P).

Because radicals have high free energies, their formation (from non-radical species) requires an external source of energy (i.e. endothermic). In the atmosphere, this source of energy is supplied by solar radiation:

$$\text{Non-radical} \xrightarrow{h\nu} \text{radical}\,(\mathrm{X}^{\bullet}) + \text{radical}\,(\mathrm{Y}^{\bullet})$$

Generation of radicals by this type of reaction provide an initiation step for reaction chains that are propagated by subsequent reactions of radicals with non-radical species, as illustrated in the following:

$$\text{Non-radical} + \text{radical} \rightarrow \text{radical} + \text{non-radical}$$

The reaction of a radical with a non-radical must always produce a radical in order to

FOR REFERENCE PURPOSES ONLY

conserve the total odd number of electrons. The radical produced then goes on to react with another non-radical, promulgating the chain. For the chain to be terminated, reactions between radicals must occur:

$$\text{Radical} + \text{radical} \rightarrow \text{non-radical} + \text{non-radical, or}$$

$$\text{Non-radical} + \text{radical} + \text{M} \rightarrow \text{M} + \text{non-radical}$$

Termination reactions are generally slower than propagation reactions because radicals are present at low concentrations and collisions between radicals are therefore relatively infrequent.

12.1.1.3 Removal of methane

The reaction paths leading to the removal of methane from the atmosphere are shown in Figure 12.1. As you can see, the process involves a complex series of reactions.

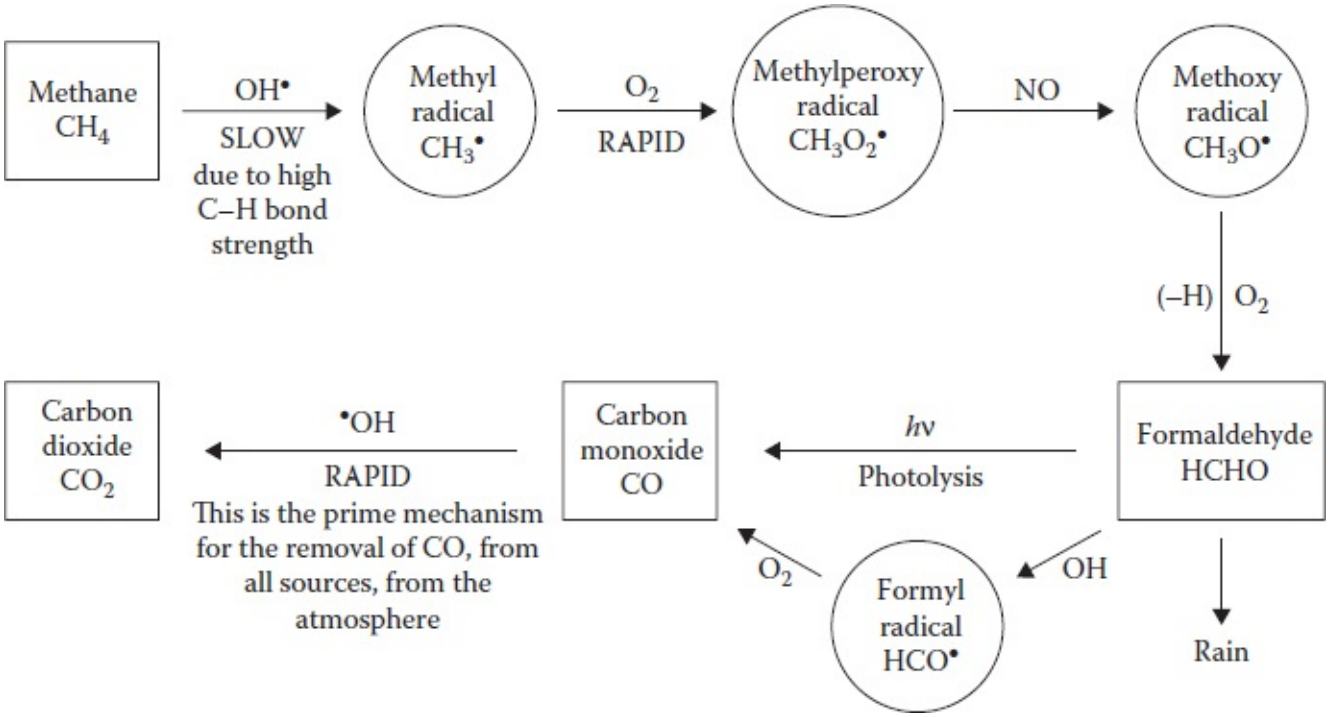

Figure 12.1 Reaction paths for conversion of methane into CO_2 in the atmosphere.

12.1.1.4 Removal of carbon monoxide

The hydroxyl radical reacts with carbon monoxide to form carbon dioxide (in a similar way to that seen earlier as part of the reaction path involved in the removal of methane).

$$CO + {}^\bullet OH \rightarrow CO_2 + H^\bullet$$

The $H^{\bullet}$ atom immediately attacks O_2 molecules, producing hydroperoxyl radicals, which produce more hydroxyl radicals:

$$H^{\bullet} + O_2 \rightarrow HO_2^{\bullet}$$

12.1.2 Tropospheric ozone formation

The tropospheric ozone production sequence described in Chapter 2 is dominant in the highly polluted, strongly irradiated atmospheres. This section describes additional routes to tropospheric ozone formation from more complex cycles.

12.1.2.1 Reactions involving methane and/or carbon monoxide

Ozone can be formed from oxidation of methane and/or carbon monoxide, in the presence of nitrogen oxide catalysts. For example

$$CH_4 + 8O_2 \xrightarrow{h\nu} CO + 4O_3 + 2OH + H_2O$$

The OH goes on to attack methane

$$CH_4 + OH \rightarrow CH_3 + H_2O$$

which starts the cycle again. The CO may go on to produce O_3 if NO_x concentrations are high, or to *deplete* O_3 if they are low. For example:

$$HO_2 + O_3 \rightarrow OH + 2O_2$$

$$OH + CO \rightarrow H + CO_2$$

$$H + O_2 + M \rightarrow HO_2 + M$$

$$\text{Net } CO + O_3 \rightarrow CO_2 + O_2$$

An example of a cyclical catalytic process for ozone production is

$$NO_2 + h\nu(\lambda < 400\text{nm}) \rightarrow NO + O$$
$$O + O_2 + M \rightarrow O_3 + M$$
$$OH + CO \rightarrow H + CO_2$$
$$H + O_2 + M \rightarrow HO_2 + M$$
$$HO_2 + NO \rightarrow OH + NO_2$$
$$\text{Net } CO + 2O_2 + h\nu \rightarrow CO_2 + O_3$$

Methane, which is present at average global background concentrations of 1700 ppb as against 20 ppb for O_3, is involved in many complex oxidation reactions which affect the overall balance of OH radicals and O_3 molecules.

The first reaction step for methane is with the hydroxyl radical:

$$OH + CH_4 \rightarrow CH_3 + H_2O$$

The resulting methyl radicals are then involved in further oxidation reactions. One of the major advances in atmospheric chemistry in the last decade has been realisation of the importance of the OH hydroxyl radical in many atmospheric reactions that remove pollutants, despite its low concentration of a few ppt. Hydroxyl radicals oxidise many of the trace constituents in a low-temperature burning of atmospheric rubbish which dominates the daytime chemistry of the troposphere. Production of OH is by reaction of water vapour with $O(^1D)$, which is the oxygen atom in the excited singlet state in which it is most reactive.

$$O_3 \xrightarrow{h\nu} O_2 + O(^1D)$$
$$O(^1D) + M \rightarrow O + M$$
$$O(^1D) + H_2O \rightarrow 2OH$$

As shown in the next section, OH production strongly depends on solar UV photons. It was originally thought that OH reactions would only be significant in the stratosphere where the UV flux is strong. The creation of $O(^1D)$ needs a photon of less than 320 nm wavelength, but the flux of photons of less than 300 nm at the bottom of the atmosphere is very small, so the window is tiny. In fact, it turned out that there is sufficient OH generated in the troposphere (partly due to the larger mixing ratio of water found there than in the stratosphere) for it to play a significant role in oxidation of species such as CO and CH_4. The lifetime of OH in the presence of gases such as CO is only a few seconds, so the atmospheric concentration is highly variable and dependent on local sources and sinks.

12.1.2.2 Reactions involving the hydroxyl radical

The hydroxyl radical ($^{\bullet}OH$) is the most important oxidant found in the troposphere and is formed continuously by a series of photochemical reactions. The global mean OH concentration has been estimated, from its reaction with the industrial solvent methyl chloroform (CH_3CCl_3), as ~1 × 10^6 molecules cm^{-3}. The solvent is one of the gases responsible for attrition of the ozone layer by delivering chlorine into the stratosphere, and its main oxidation route is via OH. OH production rate was perceived as a problem in the 1970s, because it was realised that insufficient O_3 was diffusing from the stratosphere into the troposphere to supply OH production, and that hence all OH would be immediately

reacted with an excess of CO and CH_4 molecules, leaving these and other molecules such as hydrochloro fluorocarbons (HCFCs) to accumulate. In fact this is prevented by NO_x, which not only allows the regeneration of OH but also produces new O_3 from which additional OH can be produced.

There are two main pathways for such reactions, which are discussed below.

12.1.2.2.1 Photolysis of ozone

Ozone (O_3) is a high-energy form of oxygen which, as we have seen, mainly exists in the stratosphere. A small fraction of stratospheric O_3 passes down to the troposphere where some of it is lost via photochemistry (and other reactions) as it is deposited to the Earth's surface (Stockwell et al., 2012). The rate of photolysis of O_3 is the product of its concentration and the reaction's photolysis frequency. There are very few O_3 molecules in the troposphere and they rarely encounter UV photons (from UV light which has passed through the stratosphere). However, when they do, ozone is photolysed:

$$O_3 \xrightarrow{h\nu} O^{\bullet} + O_2 \ \text{(given that } \lambda < 320 \text{ nm)}$$

The $O^{\bullet}$ is rapidly quenched by O_2 and N_2 in the atmosphere. With O_2, it reforms O_3 which is then photolysed and the cycle is repeated.

$$O^{\bullet} + O_2 \rightarrow O_3$$

The $O^{\bullet}$ atoms have sufficient energy to react with water, producing hydroxyl radicals:

$$O^{\bullet} + H_2O \leftrightarrow 2^{\bullet}OH$$

↑

This is the electronically excited O atom formed by photolysis of ozone.

Another way of showing the same reactions (Stockwell et al., 2012) is to highlight that O atoms in an excited singlet state [$O(^1D)$] are formed which are then rapidly stabilised to $O(^3P)$ by collision with, for example, N_2 or O_2:

$$O_3 \xrightarrow{h\nu} O(^1D) + O_2 \ \text{(given that } \lambda < 320 \text{ nm)}$$

$$O(^1D) + N_2 \rightarrow O(^3P) + N_2$$

$$O(^1D) + O_2 \rightarrow O(^3P) + O_2$$

The $O(^3P)$ reacts very fast with tropospheric O_2 because of high pressures and high oxygen

concentrations:

$$O(^3P) + O_2 + M \rightarrow O_3 + M$$

Although this is the dominant reaction, a faction of the $O(^1D)$ react with water vapour to form the hydroxyl radical:

$$O(^1D) + H_2O \rightarrow 2HO^\bullet$$

12.1.2.2.2 Photolysis of carbonyl compounds

The hydroxyl radical is also formed by the photolysis of carbonyl compounds (aldehydes and ketones). The carbonyl group (C=O) is a strong chromophore[2] for UV radiation and its absorption causes photodissociation; for example, the tropospheric photodissociation of formaldehyde produces both molecular and radical products (Stockwell et al., 2012):

Molecular products

$$HCHO \xrightarrow{h\nu} CO + H_2$$

Radical products

$$HCHO \xrightarrow{h\nu} CHO^\bullet + H^\bullet$$

$$H^\bullet + O_2 \rightarrow HO_2^\bullet \qquad \leftarrow \text{this is the hydroperoxyl radical}$$

$$\text{then } HO_2^\bullet + NO \; + \; NO_2 + \; {}^\bullet OH$$

At some point in the chain reaction mechanisms, the process must terminate. Examples of two of the most important radical termination reactions include the formation of nitric acid and hydrogen peroxide:

$$HO^\bullet + NO_2 \rightarrow HNO_3$$

$$HO_2^\bullet + HO_2^\bullet (+H_2O, M) \rightarrow \; H_2O_2 + O_2$$

H_2O_2 is an important product of the recombination of hydroperoxyl radicals in the atmosphere: Hence, although hydroxyl radicals in the troposphere are relatively fewer than in the stratosphere, they are so reactive that they constitute the main pathways for the removal of most oxidisable molecules in this region of the atmosphere.

12.1.2.3 Formation of peroxyacetyl nitrates

FOR REFERENCE PURPOSES ONLY

Peroxyacetyl nitrate (PAN) is the first compound in a series of compounds known as the peroxyacetyl nitrates. The general formula for PAN is $RC(O)OONO_2$ and the first two compounds in the series are peroxyacetyl nitrate [$CH_3C(O)OONO_2$] and peroxypropionyl nitrate [$CH_3CH_2C(O)OONO_2$].

PAN is formed by reactions of aldehydes with OH^* followed by reaction with NO_2 – for example:

$$CH_3HC{=}O + {}^{\bullet}OH \rightarrow CH_3C^{\bullet} = O + H_2O$$

$$\text{then } CH_3C^{\bullet}{=}O + \rightarrow CH_3(C = O)O_2^{\bullet}$$

$$CH_3(C{=}O)O_2^{\bullet} + NO_2 \rightarrow CH_3(C = O)O_2NO_2$$

PAN can decompose thermally back to its reactants:

$$CH_3(C{=}O)O_2NO_2 \rightarrow CH_3(C = O)O_2^{\bullet} + NO_2$$

PAN's importance stems from the fact that it is more stable at lower temperatures and hence its lifetime becomes longer. In the upper troposphere where temperatures are colder, PAN can be transported long distances. PAN can hence act as a reservoir species for both $CH_3(CO)O_2$ radicals and NO_x, releasing NO_2 as it moves from cooler to warmer regions.

12.2 STRATOSPHERIC OZONE

In this book thus far, we have been largely concerned with the troposphere because that is mainly where the emissions, transformations, deposition and effects occur. The stratosphere, though, is not some remote, disconnected and inert structure where nothing happens that has any influence. The stratosphere is an important reaction chamber for a number of processes that depend on either very cold conditions, very high solar UV fluxes, or both.

The stratospheric *ozone layer* (often referred to as *good ozone*) accounts for about 90% of all atmospheric ozone. Its importance, though, is due to the fact that it absorbs all radiation between 240 and 290 nm (radiation which would otherwise reach the earth and be harmful to plants and animals). Thus, it plays a vital biological role in absorbing high energy photons of ultraviolet radiation from the sun. The absorbed radiation also warms the stratosphere and provides energy for circulation. In Chapter 1, Figure 1.3 showed the average vertical temperature structure of the atmosphere. In the troposphere, which extends from ground level up to around 10 km, the temperature decreases with height, reaching just over 200 K at the tropopause. From there up to the stratopause at 50 km, the temperature increases again, although at a gentler rate, to around 270 K. This increase in temperature is partly due to the absorption, within a layer of the atmosphere containing a higher proportion

FOR REFERENCE PURPOSES ONLY

of ozone (O_3) molecules, of solar UV radiation with wavelengths between 200 and 300 nm.

12.2.1 Origins of the ozone layer

In Chapter 1 we looked at two types of photochemical processes – *photosynthesis* and *photosensitisation* (Section 1.5.5). *Photodissociation* (also known as photolysis and photodecomposition), is another photochemical process occurring in both the troposphere and stratosphere whereby a single molecule or compound splits into two or more smaller products (which may be capable of recombining to form the reactants). It forms the basis of the theory for the origin of the ozone layer, originally proposed by the British scientist Sidney Chapman in 1930 (hence known as the *Chapman mechanism*). It laid the foundation for our understanding of modern stratospheric chemistry. Chapman proposed that the ozone layer originated from the photodissociation of atmospheric O_2. He highlighted that the bond energy of the O_2 molecule (498 kJ mol^{-1}) is equivalent to the energy of a 240 nm UV photon; hence only photons of wavelengths <240 nm can photolyse the O_2 molecule. These high energy photons are present at high altitude above the Earth's surface.

We can represent this in the following equation:

$$O_2 \xrightarrow{h\nu} O^\bullet + O^\bullet (\lambda < 240\,\text{nm})$$

where the O atoms are in the ground-level triplet state $O(^3P)$ and are highly reactive due to their two unpaired electrons. These then combine rapidly with other oxygen molecules, in the presence of a third impartial molecule M such as nitrogen to form ozone

$$O_2 + O^\bullet + M \rightarrow M + O_3$$

The O_3 molecules produced in the earlier reaction go on to photolyse. Note that because the bonds in the O_3 molecule are weaker than those in the O_2 molecule, photolysis is achieved with lower-energy photons:

$$O_3 \xrightarrow{h\nu} O_2 + O^\bullet (^1D)\ (\lambda < 320\,\text{nm})$$

$$O^\bullet\ (^1D) + M \rightarrow M + O$$

where $O(^1D)$ is the O atom in an excited singlet state which is rapidly stabilised to $O(^3P)$ by collision with, for example N_2 or O_2.

Note that this reaction is not a terminal sink (the final chemical reaction in a progression of chemical reactions) for O_3 as the O atom product may recombine with O_2 to regenerate O_3. For O_3 to be actually lost, the O atom must undergo another reaction, which in the Chapman mechanism is:

$$O_3 + O^{\bullet} \rightarrow 2O_2$$

Another example of a photodissociation process is the photolysis of hydrogen peroxide (H_2O_2) at 157.8 nm yielding electronically excited OH radicals:

$$H_2O_2 \xrightarrow{h\nu} 2HO^{\bullet}$$

Where dissociation is incomplete, a chemical equilibrium exists between the compound and its dissociation products – as, for example, in:

$$NO_2 \overset{h\nu}{\leftrightarrow} NO^{\bullet} + O^{\bullet}$$

$$\text{or } HCl \overset{h\nu}{\leftrightarrow} H^{\bullet} + Cl^{\bullet}$$

At very high altitudes, there is plenty of UV radiation but little oxygen for it to act on, whereas at low altitudes there is plenty of oxygen but little UV radiation. The interaction of these two competing processes results in an optimum height for O_3 formation at about 30 km.

12.2.1.1 Stratospheric ozone concentrations

Local ozone concentrations are usually expressed as partial pressures (Pa), volume mixing ratios (ppb or ppm) or more rarely as number densities (molecules cm^{-3}). The global average atmospheric concentration is around 0.5 ppm at 15 km, rising to 8 ppm at 35 km and falling back to 3 ppm at 45 km. Even though it is found only in very small quantities, ozone is the most important compound in the stratosphere.

An alternative measure of ozone amount is the column depth, which integrates the ozone density over the height of the atmosphere. This value, which is the physical depth that all the ozone would occupy if it were a pure gas at standard temperature and pressure (STP, which is 0°C and 1 atmosphere) is measured in Dobson units (DU) after the scientist who devised the method. One Dobson unit is 0.01 mm of ozone (sometimes expressed as milli-atmosphere-centimetres), and typical column depths are in the range 300–400 DU.

If all stratospheric ozone could be brought down to sea level and spread evenly around the globe, the pressure of the atmosphere above it would squeeze it into a layer of 3 mm thickness. It is remarkable that a layer of the pure gas that is effectively only a few mm deep turns out to have played such an important role in the development of life on the Earth. The most common ground-based method of measuring total column ozone is the Dobson spectrophotometer, which determines the differences in atmospheric attenuation of solar UV radiation across spectral lines centred on 320 nm. Satellite measurements are also being made of both total column ozone and vertical variation, using ultraviolet radiation backscattered from the atmosphere.

FOR REFERENCE PURPOSES ONLY

Ozone production is at a maximum in the tropical stratosphere. The Earth's meridional circulation pattern then transports the ozone towards the Poles, with a preference for the winter pole. Hence, the latitudinal ozone distribution (Figure 12.2) shows that total column amounts are higher towards the poles than in equatorial regions, and that the peak values are reached in March/April in the northern hemisphere and September/October in the southern hemisphere.

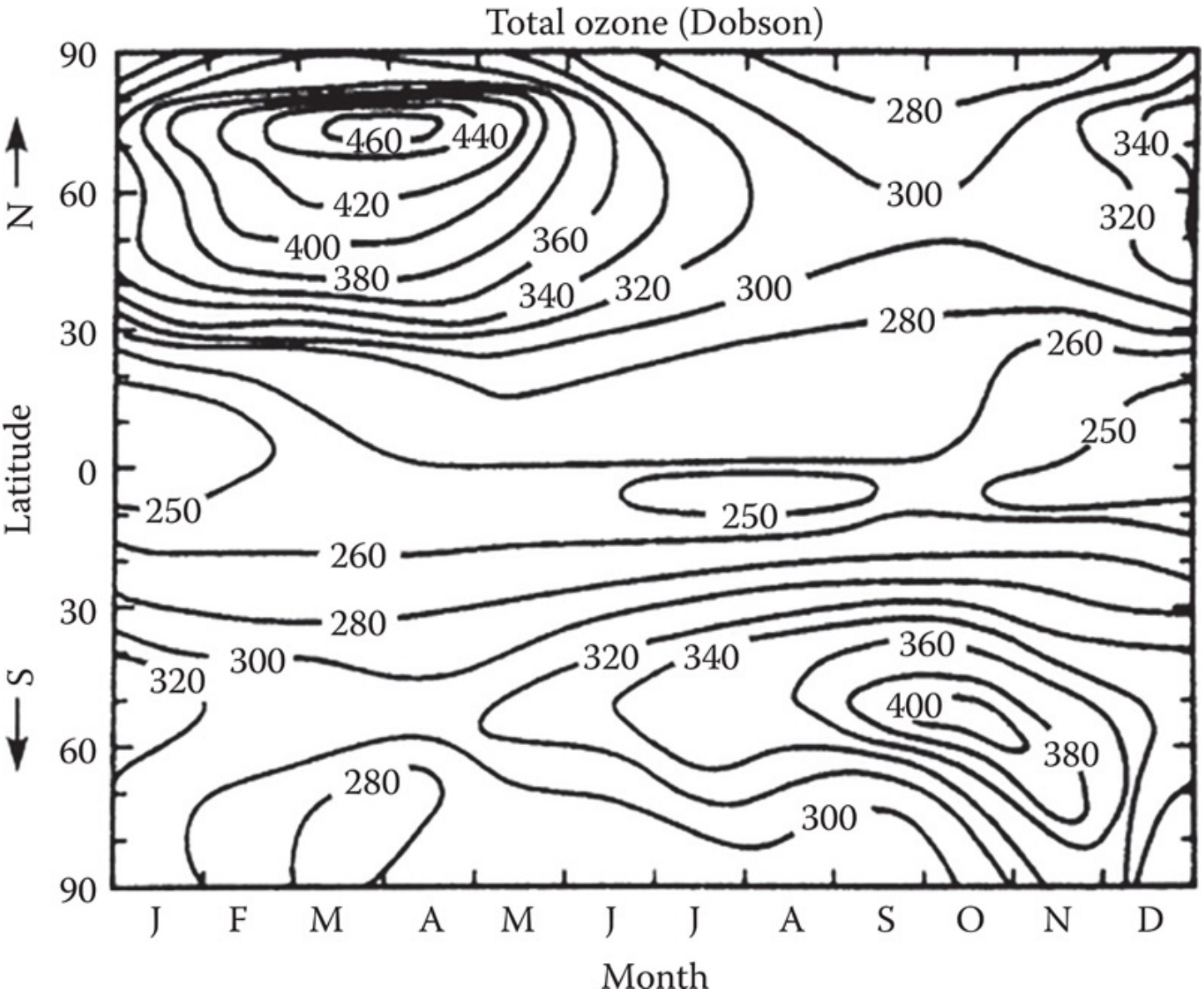

Figure 12.2 Contours to show the average variation of total column ozone with latitude and season over the globe. (From Peter, T., *Environ. Pollut.*, 83, 69–79, 1994.)

The characteristic vertical profile shown in Figure 12.3 is established. The left-hand graph is the number of O_3 molecules per cm^3, which will naturally tend to decrease with height because the total pressure and density both decrease. In the right-hand graph of this figure, the concentration has been expressed as a volume mixing ratio, which improves the

FOR REFERENCE PURPOSES ONLY

definition of the peak concentration at around 30 km. Until the mid-1970s, the ozone concentration over Antarctica had a similar vertical profile (the right-hand curve in Figure 12.4), with the partial pressure typically increasing from a few mPa at 8 km to 15 mPa at 18 km, and decreasing again to a few mPa at 30 km.

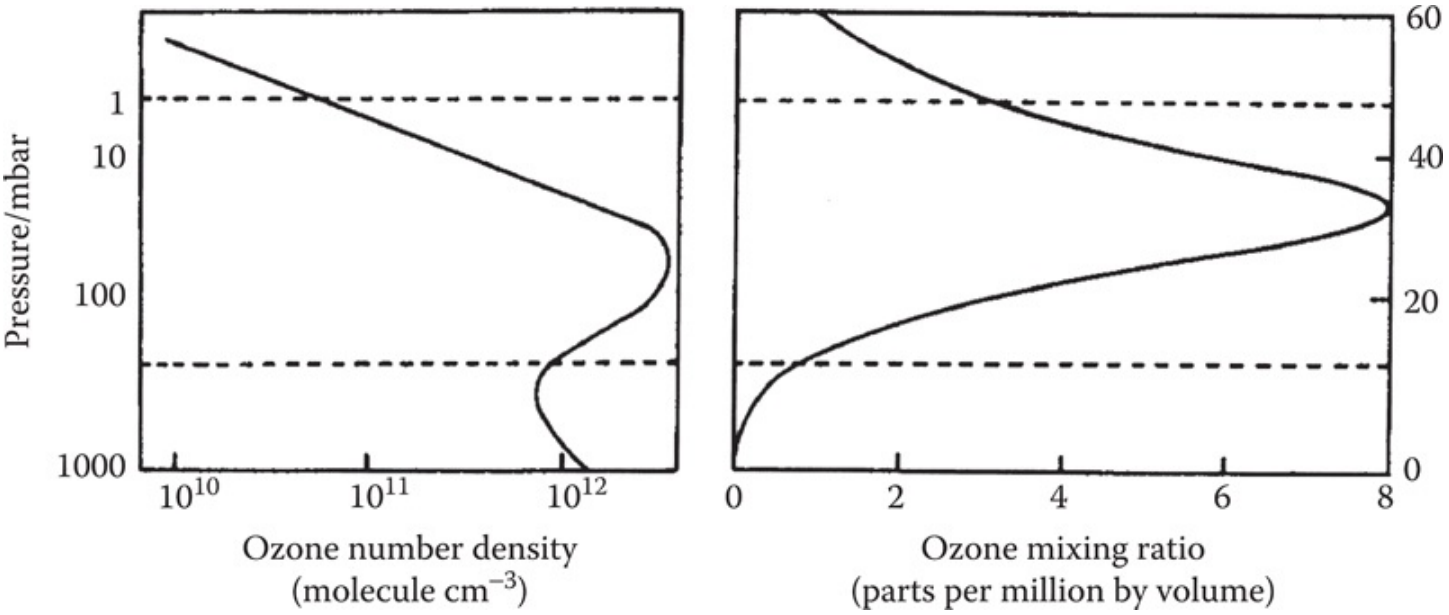

Figure 12.3 Vertical ozone profiles. (From Stratospheric Ozone Review Group, *Stratospheric Ozone 1988*, HMSO, London, UK, 1988.)

FOR REFERENCE PURPOSES ONLY

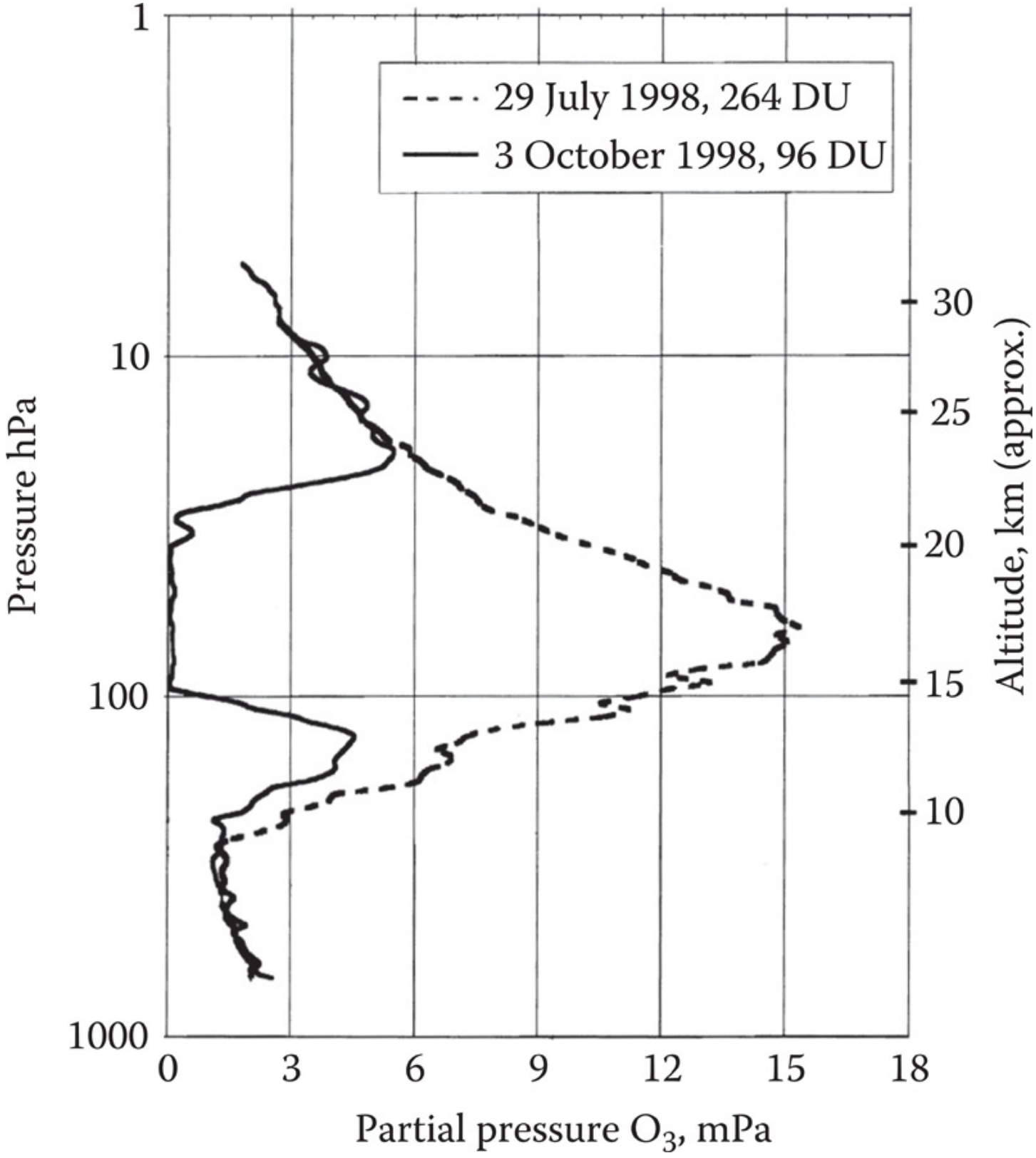

Figure 12.4 Vertical profiles of ozone partial pressure over the South Pole. The normal profile (dashed line) is replaced during the Austral Spring by the severely depleted profile shown by the full line. (From World Meteorological Organisation, WMO Global Ozone Research and Monitoring Report No 44, Scientific Assessment of Ozone Depletion 1998, WMO, Geneva, Switzerland,

FOR REFERENCE PURPOSES ONLY

1999.)

Figure 12.4 also shows the startling change in this profile that now occurs in the Austral Spring (in October, when the sun first rises above the horizon after the Austral winter). The ozone concentration declines throughout the whole profile, decreasing close to zero where it used to be at its maximum. Although this abrupt seasonal change was only noticed in the mid-1980s, it soon became clear that the trend had existed for some time.

The thickness of the ozone layer above Europe has decreased significantly since the beginning of the 1980s and is declining at the rate of up to 8% per decade. It has been shown that a polar vortex system similar to, but weaker than, that in the Antarctic exists in the northern hemisphere. In the winter of 1999–2000, over 60% of the O_3 at an altitude of 18 km was destroyed. After this springtime ozone destruction, ozone-depleted air moves out into lower latitude regions and reduces the column ozone. Figure 12.5 gives the total column ozone at Arosa, Switzerland, between 1930 and 1997; there is a clear downward trend after 1960. Average measurements from networks of Dobson spectrophotometers in Europe and North America show reductions of around 20 DU between 1960 and 1988 (Figure 12.6). It is not known to what extent the latter reductions are due to the movement of ozone-depleted air from the Poles, rather than to ozone destruction *in situ*. Overall, column ozone between latitudes 66N and 66S has been declining by 3% per decade.

12.2.2 Ozone destructive chemistry

Concern about impact of air pollution in the stratosphere centres on destruction of the ozone layer, that is ozone depletion. There are several routes by which ozone is naturally depleted.

FOR REFERENCE PURPOSES ONLY

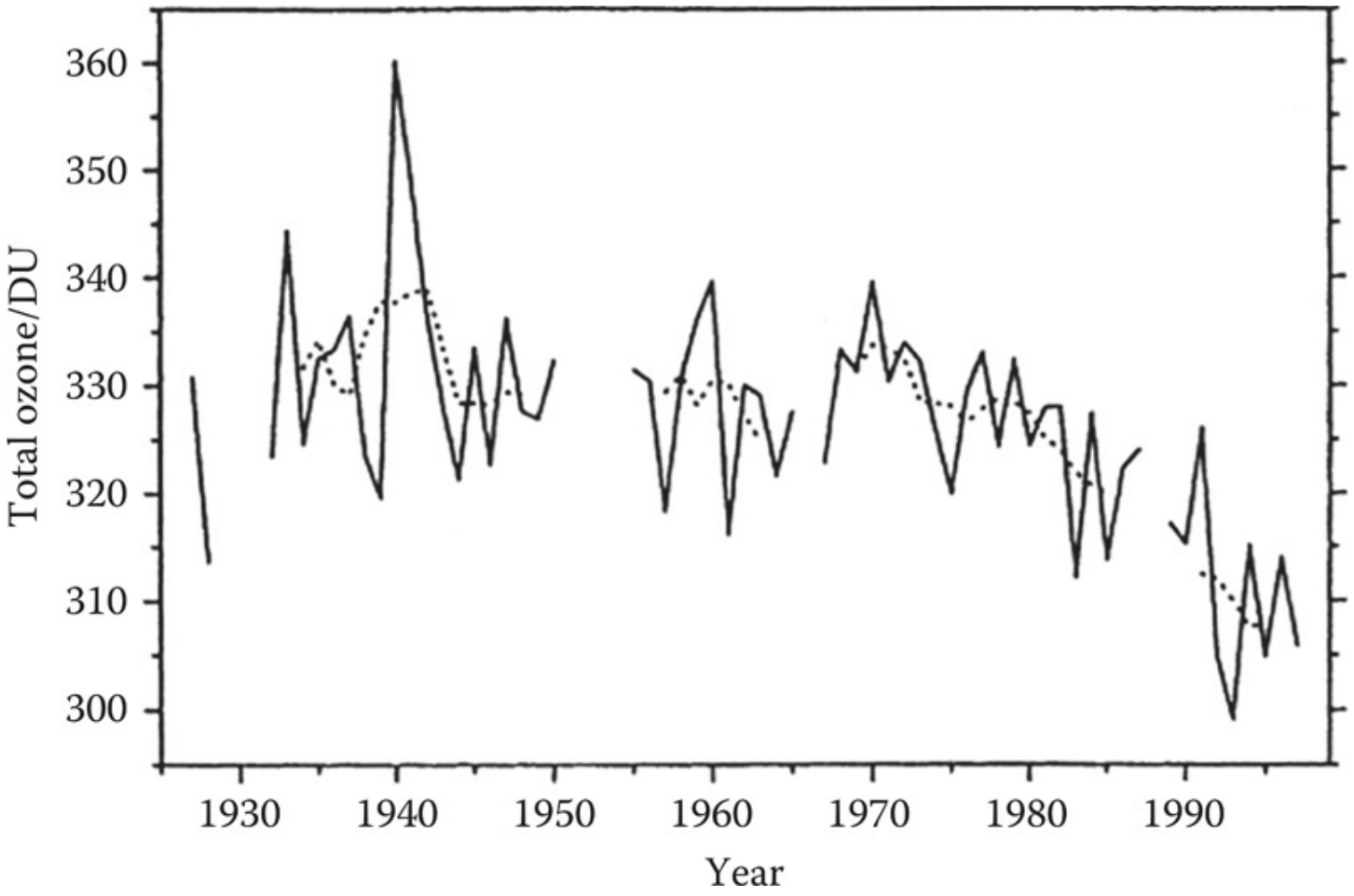

Figure 12.5 The time course of average column ozone over Arosa, Switzerland between 1930 and 1997. (From Staehelin, J. et al., *Journal of Geophysical Research: Atmospheres*, 103, 5827–5841, 1998.)

FOR REFERENCE PURPOSES ONLY

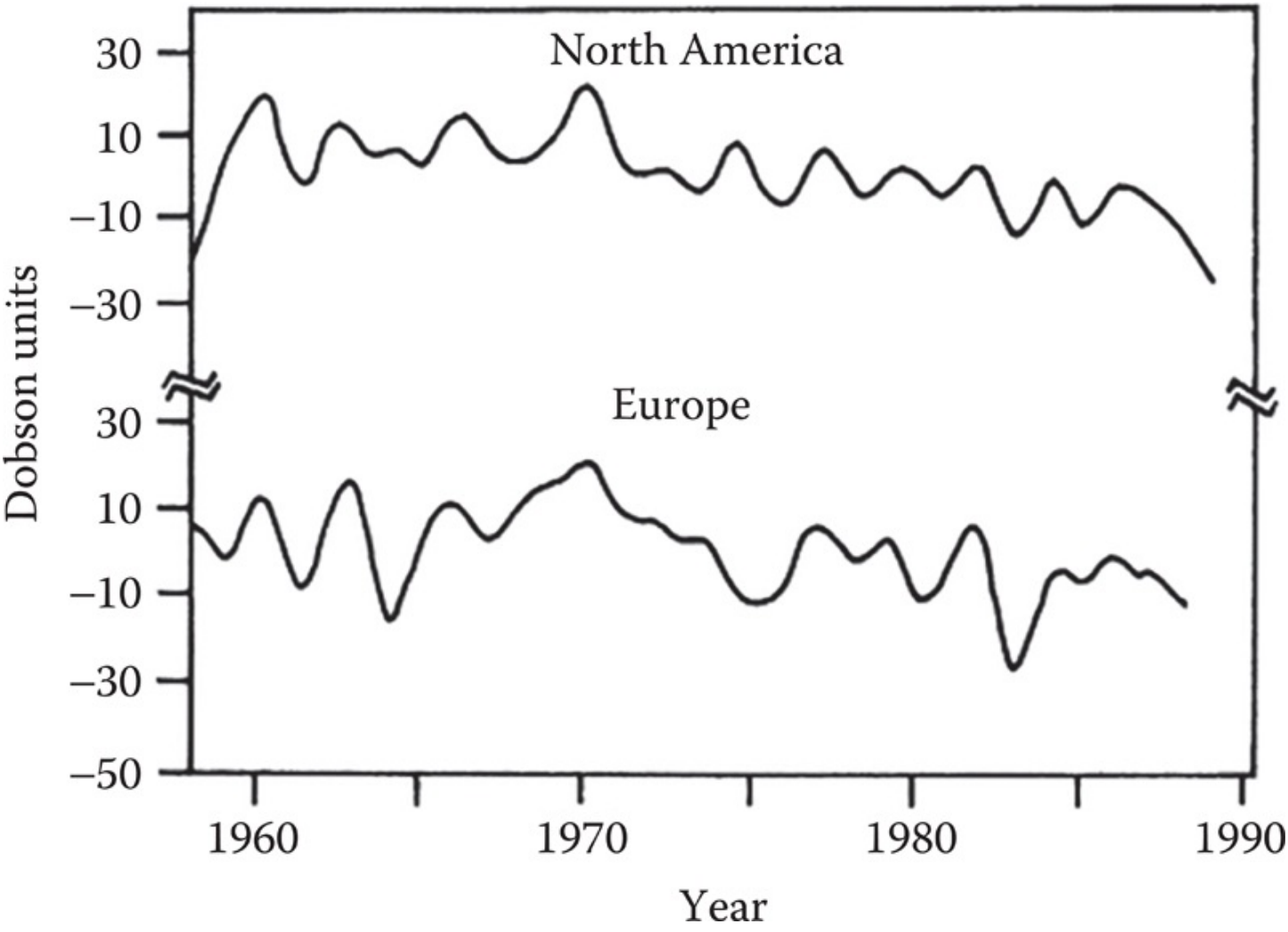

Figure 12.6 The time courses of change in average column ozone above North America and Europe between 1958 and 1988. (From Stratospheric Ozone Review Group, *Stratospheric Ozone 1990*, HMSO, London, UK, 1990.)

First, by photo dissociation and recombination with atomic oxygen:

$$O_3 \xrightarrow{h\nu} O + O_2 \ (\lambda < 1140\,\text{nm})$$

$$O + O_3 \rightarrow 2O_2$$

If the O_3 absorbs a higher-energy photon with a wavelength of less than 310 nm, then it can dissociate into O_2 and an excited oxygen atom such as $O(^1D)$. The latter energetic atom will then participate in reactions with other atmospheric species. The formation of $O(^1D)$ is doubly dependent on wavelength, because the quantum yield increases sharply in just the same spectral range as the solar radiation flux is decreasing sharply (Figure 12.7).

FOR REFERENCE PURPOSES ONLY

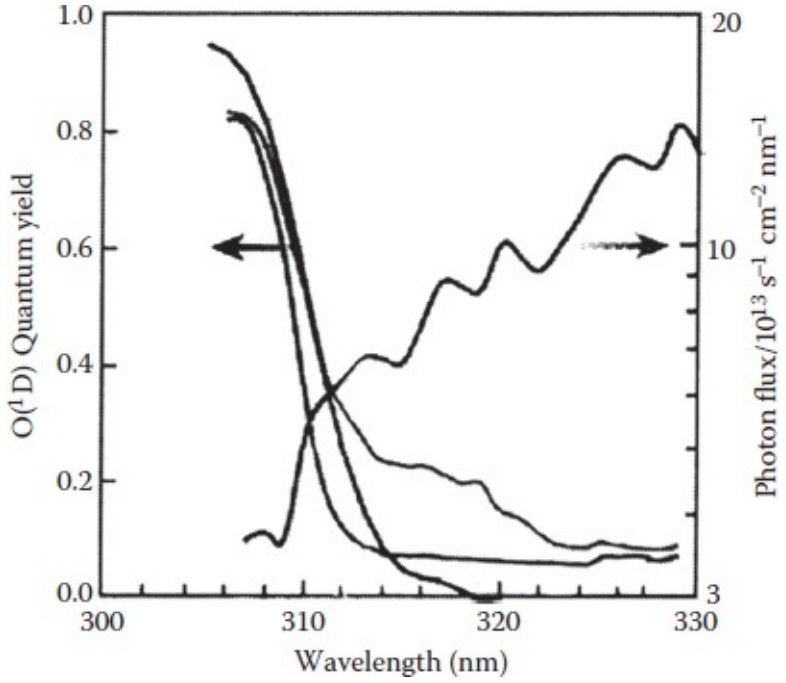

Figure 12.7 Quantum yield for $O(^1D)$ formation. (From Ravishankara, A.R. et al., *Science*, 280, 60–61, 1998.)

Second, by more complex chains of catalytic reactions with a variety of other substances (X), the most important groups being free radical species in the nitrogen, hydrogen, bromine and chlorine families such as OH and NO. These are pairs of reactions of the form:

$$\begin{aligned} O_3 + X &\rightarrow O_2 + OX \\ OX + O &\rightarrow O_2 + X \\ \text{----------} & \\ \text{net: } O + O_3 &\rightarrow 2O_2 \end{aligned}$$

where X is the catalytic compound, which destroys two odd oxygens – both an O (which could later have formed an O_3) and an O_3.

$$\begin{aligned} \text{specifically: } Cl + O_3 &\rightarrow ClO + O_2 \\ Cl + O_3 &\rightarrow ClO + O_2 \\ ClO + ClO + M &\rightarrow Cl_2O_2 + M \\ Cl_2O_2 &\xrightarrow{h\nu} 2Cl + O_2 \\ \text{----------} & \\ \text{net: } 2O_3 &\xrightarrow{h\nu} 3O_2 \end{aligned}$$

Although these ozone consumers are present at extremely low concentrations, they are conserved through the reaction. Hence, one chlorine molecule can be involved in the

FOR REFERENCE PURPOSES ONLY

catalytic destruction of tens of thousands of ozone molecules. When ozone depletion first became a matter of international concern, the reactions given earlier were hypothetical. Figure 12.8 shows the concentrations of both O_3 and ClO measured from an aeroplane as it flew towards Antarctica in the spring of 1987, as the ozone hole was developing. As O_3 concentration declined, there was a symmetrical increase in ClO concentration, powerful though circumstantial evidence for the mechanism given earlier. This destruction cycle is thought to be responsible for 70% of the ozone loss in Antarctica.

Third, more complicated and much faster heterogeneous reactions take place on the surfaces of polar stratospheric cloud particles (PSCs) – frozen mixtures of nitric acid and water that form at temperatures below 195 K (–78°C) and make up the nacreous or mother-of-pearl clouds frequently observed above Antarctica. In particular, chlorine nitrate and hydrogen chloride attach to the particle surfaces, whence

$$ClONO_2 + HCl \rightarrow Cl_2 + HNO_3$$

The chlorine released by this and other related reactions are volatilised to take part in ozone destruction. The nitric acid remains bound to the particle surface and hence depletes NO_2 (denoxification) which is then not available to neutralise ClO. Hence, the level of active chlorine atoms is maintained.

The most effective type of PSC particle is formed at the very low Antarctic temperatures, but not at Arctic temperatures which are some 10°C–15°C warmer. It appears that stratospheric sulphuric acid aerosol particles may offer surface conditions which can accelerate the destruction of ozone in much the same way as the polar clouds. This has been particularly apparent after major injections of sulphate particles and SO_2 (which eventually forms particles) into the stratosphere by volcanoes such as Mt Pinatubo in 1991. A second ozone destruction cycle is believed to be important under these slightly warmer conditions:

FOR REFERENCE PURPOSES ONLY

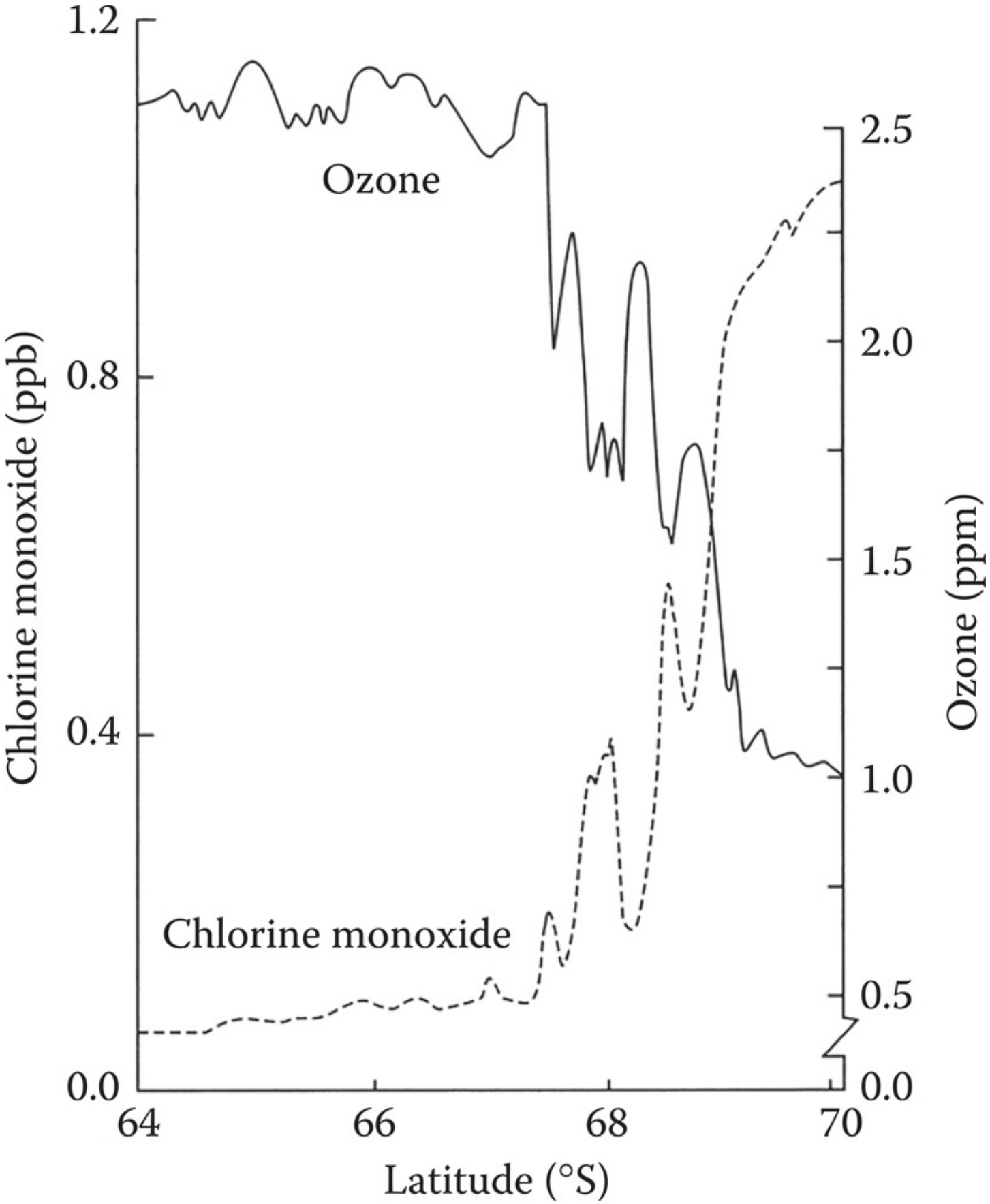

Figure 12.8 Variation of ozone and chlorine monoxide concentrations with latitude, between 64 and 70°S.

$$\begin{aligned} ClO + BrO &\rightarrow Br + Cl + O_2 \\ Cl + O_3 &\rightarrow ClO + O_2 \\ Br + O_3 &\rightarrow BrO + O_2 \\ &\text{----------} \\ \text{net: } 2O_3 &\rightarrow 3O_2 \end{aligned}$$

Modelling suggests that one result of the ozone loss will be a cooling of the lower stratosphere, and this has been supported by temperature soundings that show a decline in the 15 km temperature in November. There is a possible positive feedback mechanism involved – ozone loss cools the air, more PSC particles are formed, more ozone is destroyed. It is also becoming apparent that PSC formation is not restricted to the polar vortices but can occur at temperate latitudes in the core of the stratospheric jet stream. It has become clear from the Antarctic aerosol investigations that heterogeneous processes involving particles of ice, soot, sulphuric acid and sulphates are an important component of stratospheric chemistry everywhere.

If we could envisage an *oxygen-only* atmosphere, ozone generation and consumption would have to be due only to the following reactions, as proposed by Chapman in 1930:

1. *Ozone formation*

$$O_2 \xrightarrow{h\nu} 2O^{\bullet} \quad (\text{given } \lambda = 242 \text{ nm})$$

$$O_2 + O^{\bullet} + {}^{1}M \rightarrow O_3 + M$$

2. *Ozone destruction*

$$O_3 \xrightarrow{h\nu} O_2 + O^{\bullet}$$

$$O_3 + O^{\bullet} \rightarrow 2O_2$$

The free oxygen atoms produced in reaction (a) are very reactive, and some will react with other oxygen molecules to make ozone. This can only happen if some other molecule is present to take up the kinetic energy produced in the reaction – usually the other molecule will be nitrogen, but it could be almost anything. As well as producing ozone, this pair of reactions provides energy to molecule M, making it move faster. When molecules of gas move faster, the gas becomes hotter. Therefore, UV radiation is absorbed, converting oxygen into ozone and warming the atmosphere.

Under the conditions of reactions (a) and (b), there would be a dynamic balance between formation and consumption – a steady-state. However, there are many other substances present in the atmosphere that will react with ozone and hence they play an important role in the abundance and distribution of stratospheric ozone. For example, ozone can be destroyed in catalytic chain reactions in which it is converted to dioxygen by a chain

carrier, $X^{\bullet}$, as follows:

$$\text{General reactions}: \quad O_3 + X^{\bullet} \rightarrow XO + O_2$$
$$XO + O^{\bullet} \rightarrow X^{\bullet} + O_2$$
$$\text{Overall reaction:} \quad O_3 + O^{\bullet} \rightarrow 2O_2$$

Research has shown that the main substances that can act as the chain carrier X in the stratosphere are nitrogen oxides, halogen compounds and the hydroxyl radical. We shall, then examine the processes involved in reactions involving these elements. Research by Wennberg et al. (1994) has suggested that $^{\bullet}OH$ may play an important part in the destruction of O_3 in the lower stratosphere, perhaps accounting for half of the total O_3 destruction in the region. When many such species are participating in ozone destruction, there will be interactions between species that may increase or decrease the overall rate. In the *clean* environment, the ozone concentration takes on a stable value at any particular altitude, depending on the local balance between production and destruction.

12.2.2.1 The role of chlorofluorocarbons

Chlorofluorocarbons (CFCs) were first made in 1930 by T. C. Midgeley Jr., a chemist with General Motors. They proved amazingly useful – being chemically stable, odourless, non-flammable, non-toxic and non-corrosive, they found uses as aerosol spray propellants, refrigerants, solvents and plastic foaming agents. Examples of CFCs include $CFCl_3$ (CFC-11), CF_2Cl_2 (CFC-12), CF_3Cl (CFC-13), CF_4, C_2F_6, CCl_4, $C_2Cl_3F_3$, $CBrF_3$ and C_2BrClF_4. The ClO chemistry described earlier depends on the arrival in the stratosphere of a supply of Cl atoms. There has always been a natural supply, in the form of methyl chloride (CH_3Cl) from marine biological emissions, forest fires and volcanoes. The main post-war disturbance to the stability of the ozone layer came about through the release at ground level of chlorofluorocarbons (CFCs), artificial chemicals which have been used specifically as heat transfer fluids in refrigerators, as propellants in aerosol sprays, as blowing agents in expanded polystyrene packaging and insulation, and as cleansing fluids for electronic circuits.

The molecules are very stable and unreactive (that was why they were developed in the first place), and so have very long lifetimes in the atmosphere. A proportion of the released molecules has been diffusing upwards into the stratosphere, a process with a time constant of tens of years because of the stable lapse rate. When sufficiently high in the stratosphere, they are broken down by the UV and release chlorine atoms to take part in the aforementioned reaction sequence. Other molecules, carrying halons such as bromine instead of chlorine, are also effective ozone scavengers.

The most prevalent chlorofluorocarbons are listed in Table 12.1. CFC nomenclature specifies the first digit as the number of carbon atoms minus one (omitted if zero), the

FOR REFERENCE PURPOSES ONLY

second digit as the number of hydrogen atoms plus one, and the final digit as the number of fluorine atoms. Thus, the CFC-114 molecule has two carbon atoms, no hydrogen atoms and four fluorine atoms (as well as two chlorine atoms). Although there are substantial natural sources of chlorine, the combined effect of these synthetic molecules has been to increase the global average concentration of chlorine atoms from the natural background of 0.6 ppb to a current value of 3.8 ppb. The Antarctic ozone hole is believed to have become noticeable when global average chlorine concentration rose above 2 ppb. Table 12.2 gives a chronological profile of different halocarbons between 1990 and 2004. The release rates are for the 1990 scenario, which have been used to estimate the steady state concentrations in the column on the right. It is clear that, if left uncontrolled, the equilibrium total chlorine concentration resulting from 1990 release rates would have risen to around 13 ppb – more than three times the prevailing concentration – with severe consequences for stratospheric ozone.

The discovery of ozone depletion in the Antarctic in 1985, and the recognition of the potentially severe consequences for the UV climate, resulted in a fast piece of international pollution control legislation. The Vienna Convention for the Protection of the Ozone Layer was established in 1985, and the Montreal protocol was signed in 1987 and strengthened in London (1990), Copenhagen (1992), Vienna (1995), Montreal (1997) and Beijing (1999). A timetable was set out for production of the major CFCs, and other ozone-depleting substances, to be severely reduced, with a different timetable for developed and developing countries. Although the Montreal Protocol originally identified five CFCs and three halons for reduction, by 1999 no fewer than 95 individual substances were controlled. The agreed control measures resulted in a rapid reduction of halocarbon production, as summarised in Figure 12.9.

Table 12.1 CFCs involved in ozone destruction

Name	*Chemical formula*
CFC-11	Trichlorofluoromethane, $CFCl_3$
CFC-12	Dichlorodifluoromethane, CF_2Cl_2
CFC-113	Trichlorotrifluoromethane, $C_2F_3Cl_3$
CFC-114	Dichlorotetrafluoroethane, $C_2Cl_2F_4$
CFC-115	Chloropentafluoroethane, C_2ClF_5
Halon-1211	Bromochlorodifluoromethane, CF_2ClBr
Halon-1301	Bromotrifluoromethane, CF_3Br

Table 12.2 Historical concentrations and release rates of halocarbons

FOR REFERENCE PURPOSES ONLY

Halocarbon	Annual mean mole fraction (ppt Cl)			Release rate (ppt Cl yr^{-1})	Steady state concentration (ppt)
	1990	2000	2004		
CFC-11	858	262	255	56	3346
CFC-12	962	534	535	53	6349
CFC-113	170	82	80	19	1683
CCl_4	428	100	96	15	728
HCFC-22	103	142	162	12	175
CH_3CCl_3	479	46	22	96	623
CH_3Cl	600	532	527		
Total	3624			250	12904

On the other hand, Figure 12.10 demonstrates very clearly what would have happened to the equivalent effective stratospheric chlorine (EESC) concentration if the Montreal Protocol had not been agreed, and why the follow-up agreements were needed as well. WMO estimated that if the Montreal Protocol had not been put into effect, the concentration of ozone-depleting substances in 2050 would have reached 17 ppb (five times the current value), there would have been 50%–70% ozone depletion at mid latitudes, and surface ultraviolet B (UVB) radiation would have been doubled in northern mid-latitudes and quadrupled in southern mid-latitudes. With the emission reductions specified in the protocol, the chlorine loading of the stratosphere would peak in the late 1990s, and by 2050 will have fallen back to the 2 ppb concentration at which ozone destruction was first observed in the 1970s. Furthermore, some of the global stock of CFCs that is presently contained in refrigerators and air conditioners will continue to be released, despite improved efforts to recover and destroy it. In order to reduce the global average chlorine concentration below 2 ppb by 2050, an 85% reduction (from 1990 values) in the release of all long-lived halocarbons had to be achieved by the mid-1990s and zero release by 2000; all release of short-lived halocarbons would have to end by 2030.

FOR REFERENCE PURPOSES ONLY

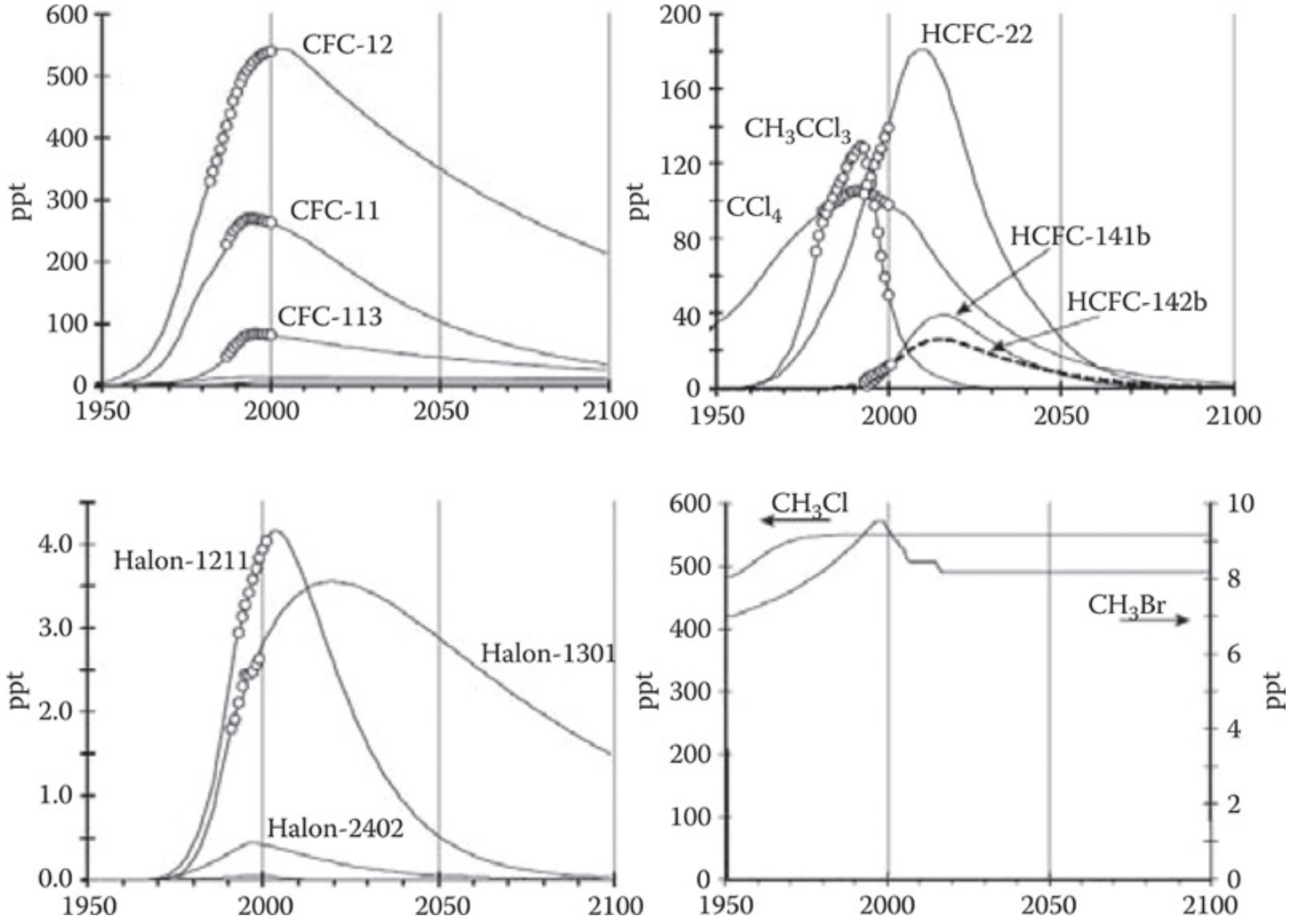

Figure 12.9 Global atmospheric surface mixing ratios (ppt) for halocarbons from model predictions (lines) and the mean observed values (circles). (From WMO, Global Ozone Research and Monitoring Report No 47, Scientific Assessment of Ozone Depletion: 2002, World Meteorological Organisation, Geneva, Switzerland, 2002.)

FOR REFERENCE PURPOSES ONLY

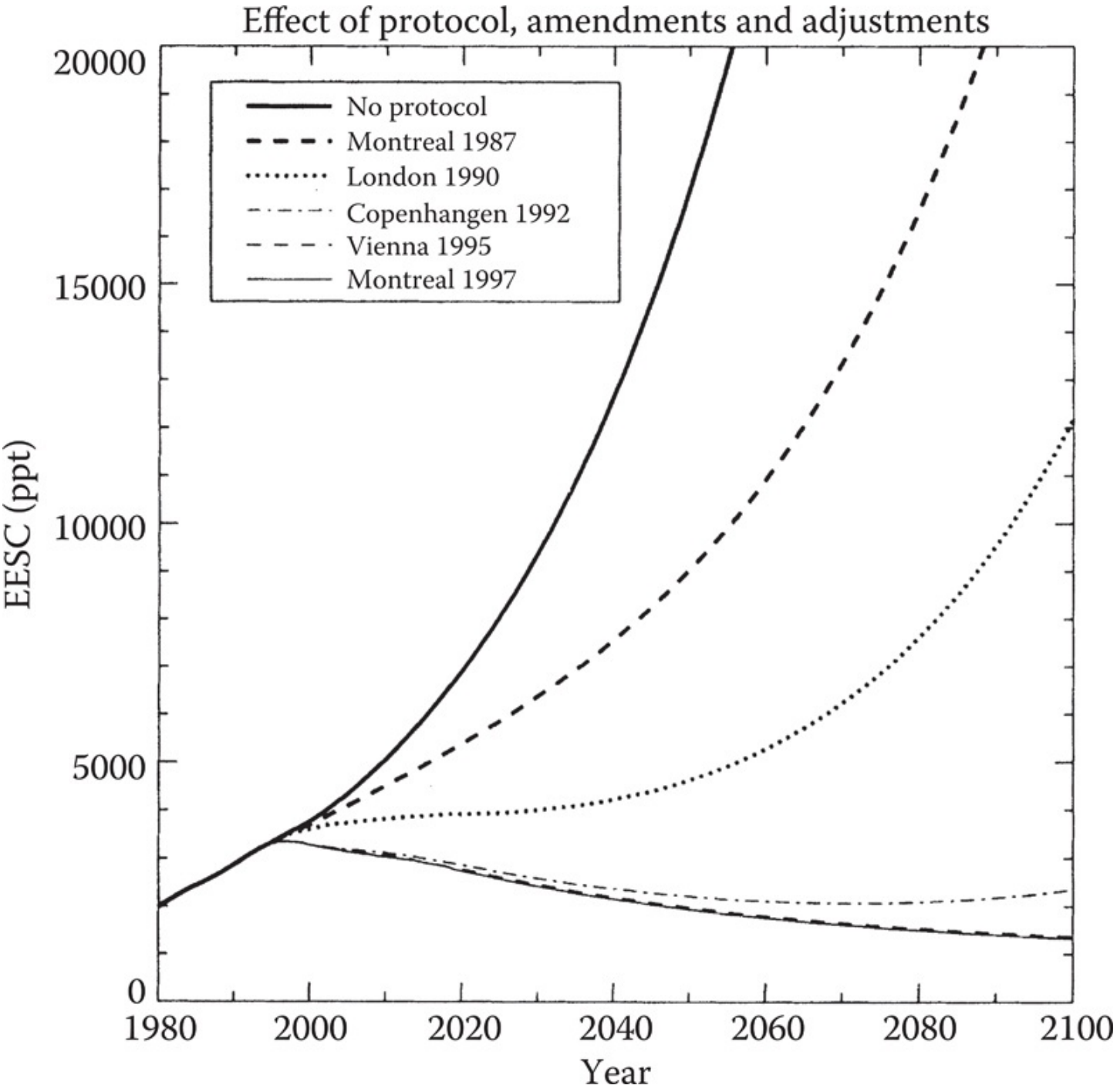

Figure 12.10 The impact of the Montreal Protocol on stratospheric concentrations of chlorine-equivalent gases. (From WMO, Global Ozone Research and Monitoring Report No 44, Scientific Assessment of Ozone Depletion: 1998, World Meteorological Organisation, Geneva, Switzerland, 1999.)

12.2.2.2 Methyl bromide

Atom for atom, stratospheric bromine is about 50 times more effective than chlorine at destroying ozone in the stratosphere; it is thought that bromine reactions have been responsible for 20% of the loss in the Antarctic ozone hole, and for an even higher

proportion in the Arctic and at lower latitudes. The principal bromine carrier is methyl bromide (CH_3Br), but much less is known about sources and cycles for this gas than for CFCs. The sources are both natural (oceanic emissions, biomass burning) and human (soil fumigation, leaded petrol combustion) amounting to some 100 kt a^{-1}. These emissions, and a lifetime of less than one year, give an average global methyl bromide concentration of 10 ppt.

12.2.3 Ozone depletion potentials

Ozone depletion potential (ODP) is considered one of the key indicators in environmental impact assessment. Other substances have been developed to replace CFCs as refrigerants and aerosol propellants, and naturally there is continued concern as to their environmental impact. Hydrochlorofluorocarbons (HCFCs) and hydrofluorocarbons (HFCs) contain at least one hydrogen atom in each molecule, and are oxidised in the troposphere during reactions with OH radicals:

$$OH + CHCl_xF_y \rightarrow H_2O + CCl_xF_y \rightarrow \text{products}$$

This is thought to result in a shorter overall lifetime, although the chain of atmospheric chemistry and the reaction rates remain uncertain. In order to compare the harmful effects of different CFCs and their proposed substitutes, the concept of ozone depletion potential (ODP) has been established. The ODP for a given halocarbon is defined by

$$ODP = \frac{\text{Ozone depletion due to compound}}{\text{Ozone depletion due to CFC-11}}$$

where the ozone depletion is the equilibrium change in the globally averaged total column ozone per unit mass emission rate. Calculation of ODPs relies on models of atmospheric transport and chemistry, and values therefore vary according to the sophistication of the model used. Relative values should nevertheless give a useful guide to the threat from different compounds (Table 12.3). These steady-state ODPs assume that equilibrium concentrations have been achieved in the atmosphere – a process which itself has a timescale of a hundred years. As emissions at the Earth's surface are changing with a timescale of tens of years, the ODPs will seriously underestimate the potential impact of many halocarbons. An alternative approach has been to calculate the total chlorine loading, defined as the instantaneous tropospheric mixing ratio of the chlorine atoms in all the halocarbons. When combined with atmospheric transport models, the time and altitude dependencies of chlorine atom concentration can be derived. Such calculations have shown a time lag of 5–10 years between the onset of maximum chlorine loading in the troposphere and of maximum inorganic chlorine release in the upper stratosphere, implying that ozone depletion will get worse before it gets better.

FOR REFERENCE PURPOSES ONLY

Table 12.3 Ozone depletion potentials of different halocarbons

Halocarbon	*ODP*	*Lifetime/years*
CFC-11	1.00 (by definition)	60
12	0.90	120
113	0.85	90
114	0.60	200
115	0.37	400
HCFC-22	0.05	15.3
123	0.017	1.6
124	0.020	6.6
HFC-125	0	28.1
134a	0	15.5
HCFC-141b	0.095	7.8
142b	0.05	19.1
HFC-143a	0	41.0
152a	0	1.7
Carbon tetrachloride (CCl_4)	1.1	50
Methyl chloroform (CH_3CCl_3)	0.14	6.3

12.2.3.1 Reactions leading to O_3 depletion in the stratosphere

N_2O has no sink in the troposphere and therefore undergoes slow transportation upwards into the stratosphere where two processes may occur:

$$\textbf{Main cycle:}\ \mathbf{N_2O} \xrightarrow{h\nu(\mathrm{UV})} \mathbf{N_2 + O^{\bullet}}$$

$$\textbf{and}\ \mathbf{N_2O} \xrightarrow{\mathbf{O^{\bullet}}} \mathbf{2NO}\ \ \textbf{(which then enters the } \mathbf{NO_x} \textbf{ cycle)}$$

The NO_x cycle is illustrated in Figure 12.11. It is a highly efficient catalytic cycle that has a strong control on ambient O_3 concentrations.

The overall effect of the NO ↔ NO_2 cycle is the consumption of O atoms and O_3, forming molecular O_2. This process can occur independently but is very slow (as it has a high activation energy – the energy required for colliding molecules to react). The role of NO_x is to act as a catalyst for the reaction and this accounts for 60% of ozone removal. The following two main sources have been suggested for the increase in NO_x in the atmosphere and the subsequent rising rate of O_3 depletion:

Aircraft emissions: In the 1960s and 1970s there was speculation by atmospheric scientists that supersonic transports (SSTs) would affect stratospheric chemistry. The effect of supersonic aircraft (and subsonic aircraft on polar flights) would be to inject

FOR REFERENCE PURPOSES ONLY

NO and NO_2 directly into the lower stratosphere and, hence, enhance the natural cycle. It was expected that eventually several hundred SSTs would be flying at altitudes of 17–20 km – well into the stratosphere – and that their emissions, especially of the catalytically active NO, might have serious consequences. Original predictions of the impact were very large – up to 10% reduction in global average ozone column. However, well-tested computer models have shown that the effect of such direct injections is negligible.

Fertilisers: It is more difficult to interpret the effect of increased use of fertilisers on the natural N_2O cycle. This uncertainty in linking their usage to environmental damage gives rise to ethical, political, moral and economic dilemmas – for example, should their use be limited or even prevented (not popular with fertiliser manufacturers and their employees, or in developing countries) if there is no hard evidence of harmful consequences, or can we risk continued usage at current rates if there is a chance of producing significant changes in the ozone cover? We need more evidence to help us make such difficult decisions.

FOR REFERENCE PURPOSES ONLY

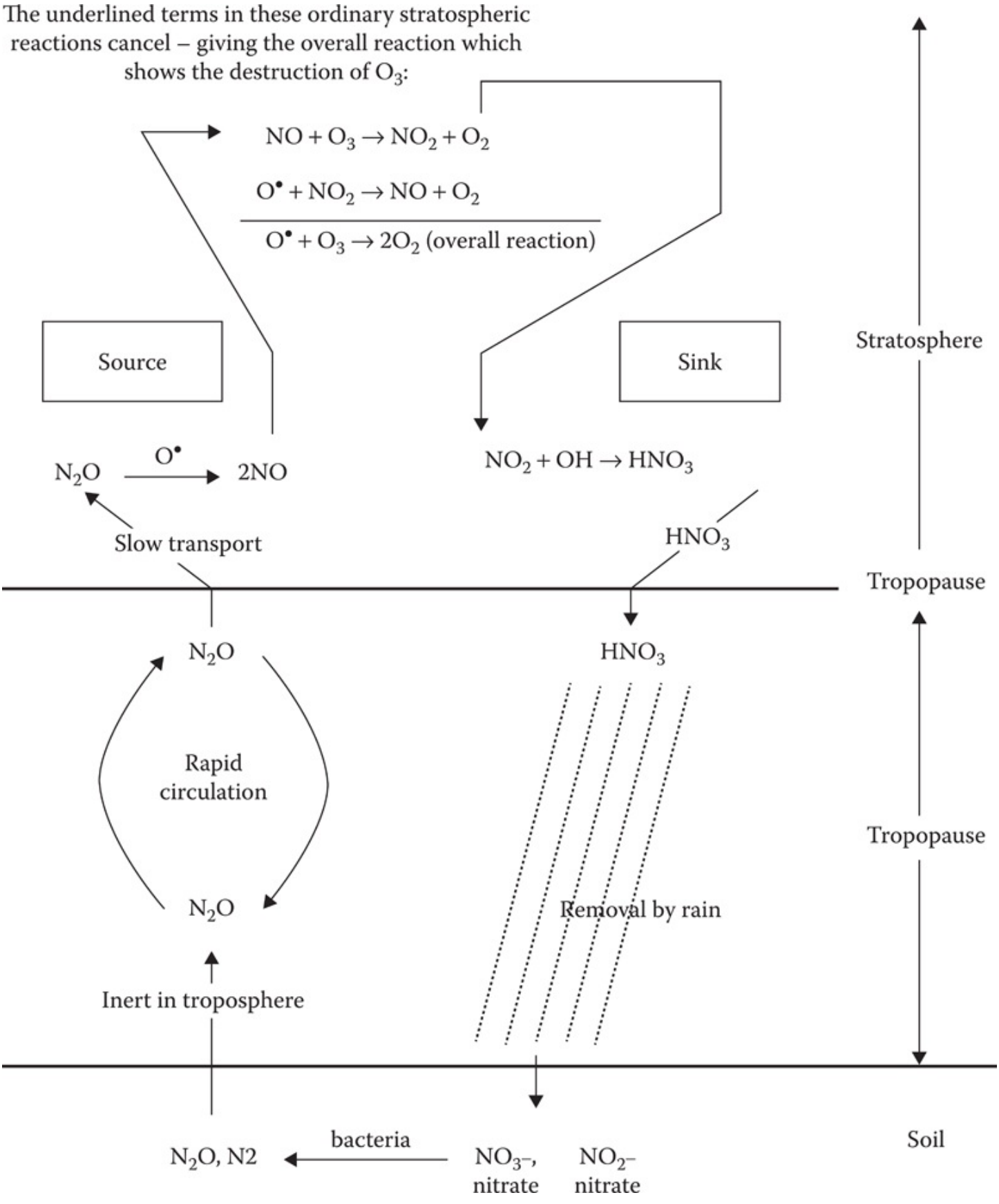

Figure 12.11 Main features of the NO_x cycle with sources and sinks.

12.2.4 Current situation

Continued declines in ozone depleting substance (ODS) emissions are expected to result in a near complete recovery of the ozone layer near the middle of the twenty-first century. The long time scale for this recovery is due to the slow rate at which these substances are removed from the atmosphere by natural processes. In 2014 the World Meteorological Organisation (WMO) and the United Nations Environmental Programme (UNEP) conducted a scientific assessment of ozone depletion. According to this report, the sum of the measured tropospheric abundances of substances controlled under the Montreal Protocol continues to decrease. Most of the major controlled ODSs are decreasing largely as projected, and hydrochlorofluorocarbons (HCFCs) and halon-1301 are still increasing. Unknown or unreported sources of carbon tetrachloride are needed to explain its abundance.

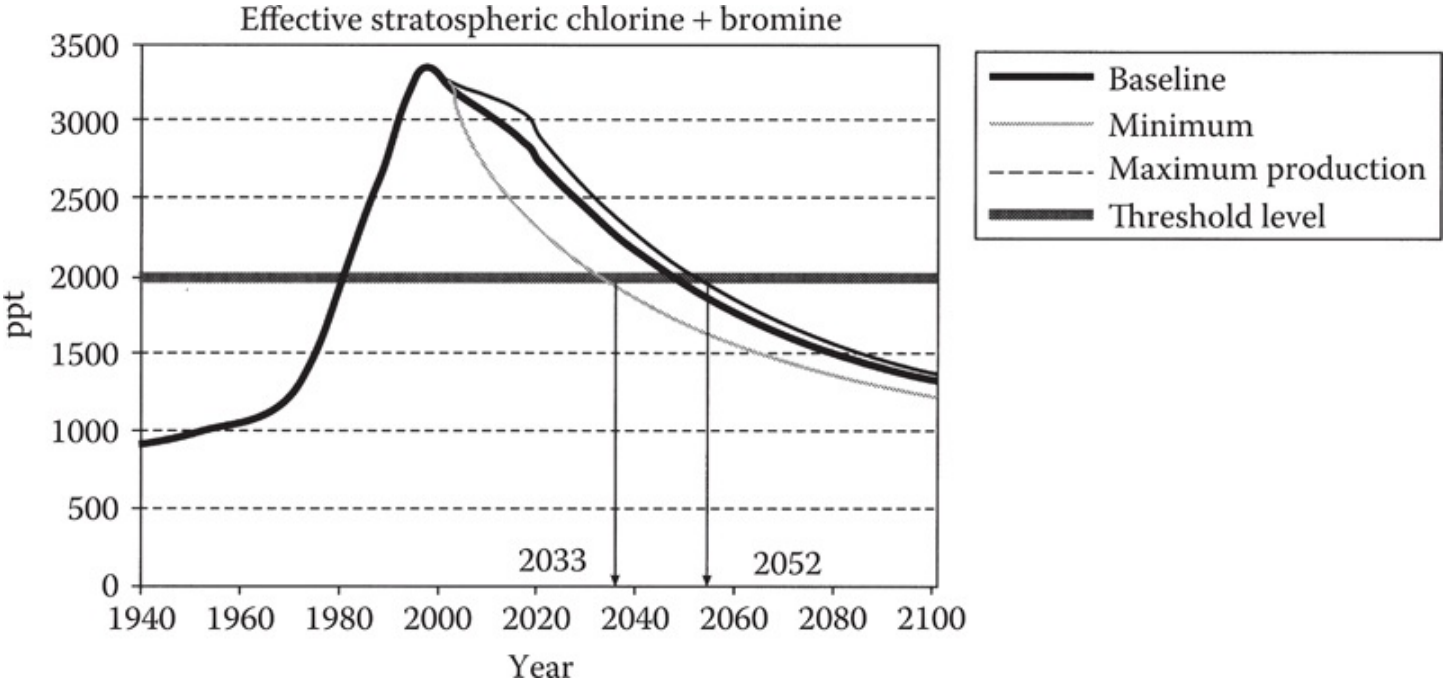

Figure 12.12 Historical and predicted concentrations of chlorine and bromine. (From EEA, *Annual Topic Update on Air Quality*, European Environment Agency, Copenhagen, Denmark, 1999.)

According to the WMO, methyl bromide abundance has decreased by 14% between 1997 and 2004 – corresponding to a reduction in the global tropospheric mixing ratio of approximately 1.3 ppt. Figure 12.12 shows the dramatic impact of the international controls on the stratospheric concentration of chlorine + bromine. After the peak in 2000, the concentration has been declining less quickly than it rose, and is predicted to fall below 2000 ppt between 2033 and 2052 (depending on which scenario for stopping the emission of ozone-depleting substances actually occurs). However, a substantial decrease in stratospheric bromine is yet to be identified and at present bromine continues to play a major role in stratospheric ozone depletion. The role of chemical reactions of chlorine and

FOR REFERENCE PURPOSES ONLY

bromine in the polar stratosphere has been better quantified. Recent studies suggest chlorine catalysed ozone loss over Antarctica and the Arctic to be much slower than earlier expected, primarily due to much slower photolysis of the chlorine dimer molecules (ClOOCl) at longer wavelengths.

The tropospheric concentration of ODSs had indeed peaked in around 1994, when the chlorine concentration was 3.7 ppb, and the stratospheric concentration had peaked in around 2000 (due to the lag time of gaseous diffusion up through the troposphere). Nonetheless, the peak was so flat and the random variability so great that it would take a further 20 years to identify whether the ozone layer has started to recover. However, by 2005, the total combined abundance of anthropogenic ODS (gaseous) in the troposphere had decreased by 8%–9% from the peak value observed in the 1992–1994 time period. Figure 12.13 shows the variation in northern hemisphere mid-latitude (35°N–60°N) total column ozone from six runs of a 2D model. The simulations are based on three different GHG scenarios. Note also that the model outputs are supported by the measurements from the Total Ozone Mapping Spectrometer (TOMS) satellite. In 1993, there was a large perturbation caused by the eruption of Mt Pinatubo. From 1996, the column ozone has been slightly increasing and the predicted values for different scenarios beyond 2020 seem to have high divergence. This has been associated with stratospheric cooling due to the rise in CO_2 emissions.

At present the ozone hole shows large year-to-year variations, mainly attributed to meteorological conditions. The expected ozone level is considered to be highly affected by climate change. Total column ozone declined over most of the globe during the 1980s and early 1990s (by about 2.5% averaged over 60°S to 60°N). It has remained relatively unchanged since 2000, with indications of a small increase in total column ozone in recent years, as expected. Total column ozone will recover toward the 1980 benchmark levels over most of the globe under full compliance with the Montreal Protocol. This recovery is expected to occur before midcentury in midlatitudes and the Arctic, and somewhat later for the Antarctic ozone hole. Model simulations indicate that total column ozone outside of the tropics will recover to 1980s values by 2020 to 2050 and to 1960s values by 2025 to 2060, later in the Antarctic (Table 12.4). The recovery rates and the evolution of stratospheric ozone (and the corresponding years) depend on future GHG emissions (especially CO_2, N_2O, CH_4, and water vapour, i.e. H_2O), but are expected to remain in this range for different plausible IPCC emission scenarios (as discussed in Chapter 11). In the second half of the twenty-first century, ozone columns may even exceed historical levels. Figure 12.14 shows the expected range of near global (60°S to 60°N) annual mean total column ozone anomalies.

FOR REFERENCE PURPOSES ONLY

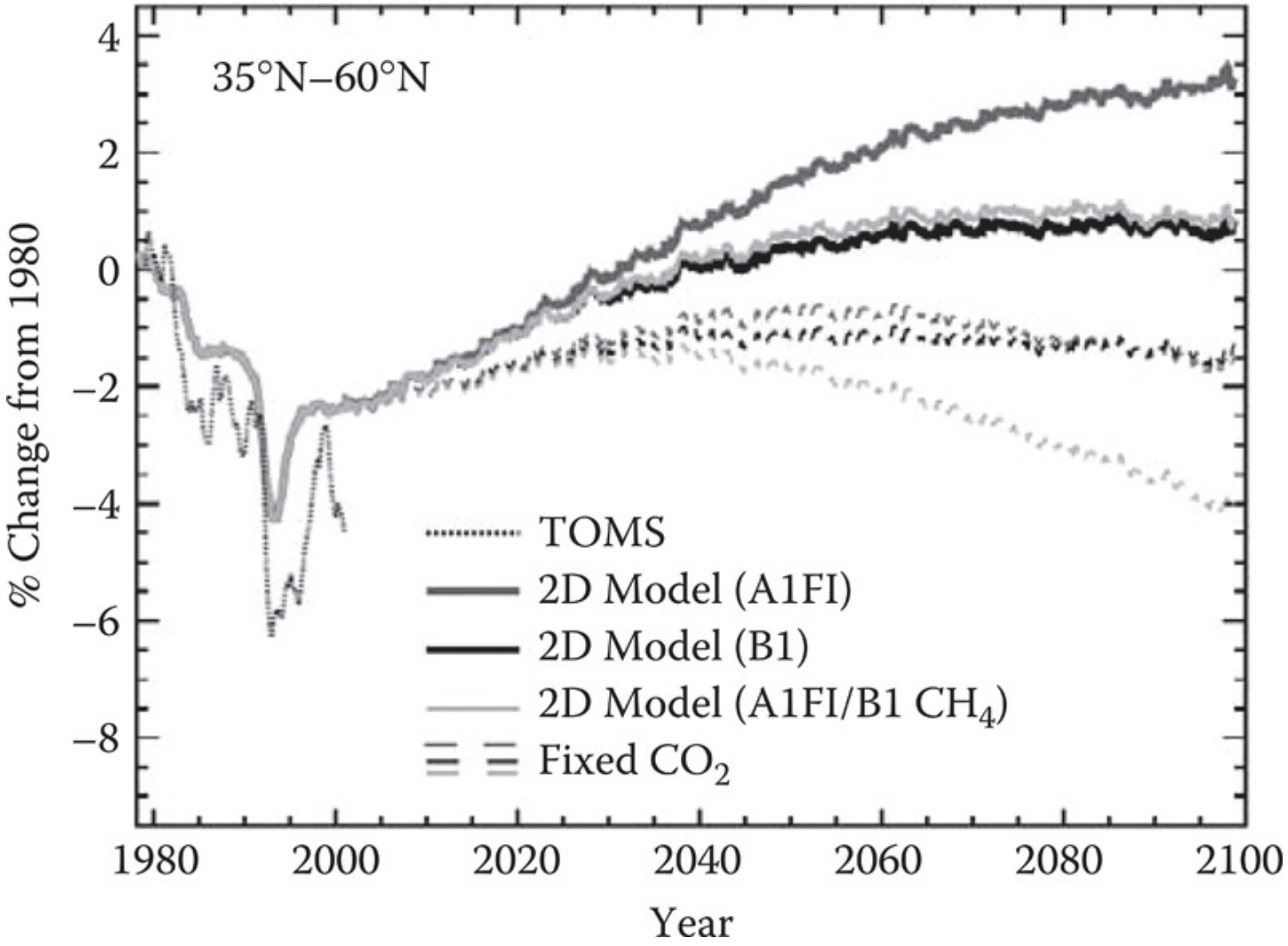

Figure 12.13 Variation in total column ozone (% change since 1980). The simulations used three different GHG scenarios (A1FI, B1 and A1FI with B1 CH_4 emissions), with results shown with (solid lines) and without (dashed lines) stratospheric cooling due to CO_2 increases. (From Chipperfield, M.P. and Feng, W., *Geophys. Res. Lett.*, 30, 1389, 2003.)

Table 12.4 Expected return years when ozone columns will return to 1960 or 1980 values

		Estimated year of recovery to the baseline		
Region	*Baseline year*	*2053*	*2046*	*2064*
Global annual mean	1960	2053	2046	2064
	1980	2032	2027	2038
Tropics annual mean	1960	–	–	–
	1980	2042	2028	–
Northern midlatitude annual mean	1960	2029	2024	2036
	1980	2021	2017	2026
Southern midlatitude annual mean	1960	2055	2049	2064
	1980	2035	2030	2040

FOR REFERENCE PURPOSES ONLY

Source: World Meteorological Organisation, *Update on Global Ozone: Past, Present, and Future*, WMO Global Ozone Research and Monitoring Project Report No 55, WMO, Geneva, Switzerland, 2014.

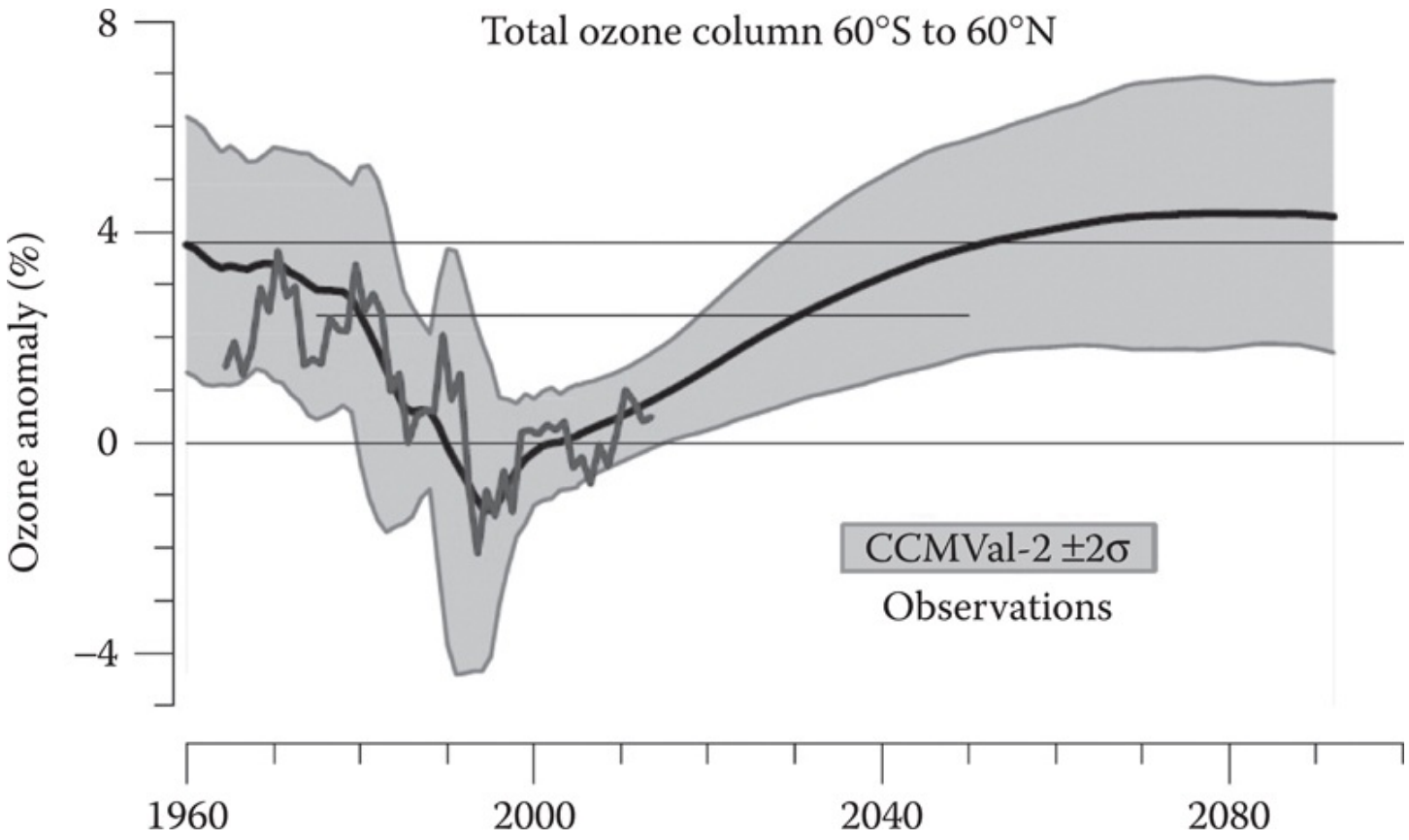

Figure 12.14 Simulated and observed evolution of the near global total ozone column. Observations are annual mean anomalies averaged over all available ground- and satellite-based measurements. (From WMO, *Update on Global Ozone: Past, Present, and Future*, WMO Global Ozone Research and Monitoring Project Report No 55, World Meteorological Organisation, Geneva, Switzerland, 2014.)

12.2.5 Stratospheric ozone and ultraviolet radiation

Ozone and ultraviolet radiation are inseparable. It takes UV photons to form ozone from oxygen and UV photons to release the chlorine from CFCs to destroy ozone. The ozone layer absorbs UV, and it is the potential increase of ground-level UV that is seen as the main environmental hazard of ozone depletion. Known effects of this increased UV in humans are sunburn, melanoma and cataracts; there may be corresponding effects that are not yet understood in plants and in other animals. The waveband of the electromagnetic spectrum that is visible to the human eye and photosynthetically active for plants lies between 400 nm (the short wavelength blue end) and 700 nm (the long wavelength red end). Wavelengths below 400 nm in the ultraviolet are invisible to the unaided human eye. The UV region is conventionally subdivided into UVA (320–400 nm), UVB (280–320 nm) and

FOR REFERENCE PURPOSES ONLY

UVC (200–280 nm). Some workers divide UVA at 315 nm rather than 320, or at 290 nm rather than 280. Natural UV is supplied exclusively by the sun, which radiates energy as a black body with an effective surface temperature of about 6000 K. Outside the Earth's atmosphere, the total solar radiation flux density of 1367 W m^{-2} is shown in Table 12.5.

12.2.5.1 Penetration of UV through the atmosphere

The solar spectrum is modified as it passes through the atmosphere by two main processes. First, Rayleigh scattering by molecules of oxygen and nitrogen is more effective the shorter the wavelength (by a factor of 16 at 200 nm compared to 400 nm). Second, the stratospheric ozone layer absorbs very effectively over a band centred on 255 nm. Figure 12.15 shows the absorption cross-sections for both ozone and oxygen in the UV and visible wavelength range. The oxygen peak is centred on 150 nm where there is almost no radiation, whereas the ozone peak occurs well over the shortwave edge of the solar spectrum. This strong absorption and scattering in the UV has a profound effect on that end of the spectrum, as seen in Figure 12.16.

Table 12.5 Flux densities in different wavebands of the solar spectrum

Waveband	*Flux density/ W m^{-2} (%)*
Visible and infrared	1254 (91.7)
UVA	85.7 (6.3)
UVB	21.1 (1.5)
UVC	6.4 (0.5)
Total	1367 (100)

Close to the top of the Earth's atmosphere (50 km), the spectrum is essentially extra-terrestrial. By 40 km O_3 absorption has already made a significant difference, reducing the flux most around 250 nm because that corresponds to the centre of the O_3 absorption band. At 20 km above the surface, the photon flux is almost the same as the surface value, except for a residual peak at 200 nm. Note, however, that although the ground-level and 20-km spectra look very similar around 300 nm, at any *individual* wavelength the logarithmic scale gives an order of magnitude difference in the fluxes. UVC (wavelengths below 280 nm), which is small to start with, is effectively eliminated. Although UVB is attenuated, the UV source flux increases towards the blue and the ozone absorption band weakens towards 300 nm – both these influences combine to give a significant UVB flux which is very sensitive to small shifts in ozone absorption. The general relationship is shown in Figure 12.17, where measurements from six stations around the world confirm that the percentage increase in surface UVB is around twice the reduction in ozone column depth (OCD).

FOR REFERENCE PURPOSES ONLY

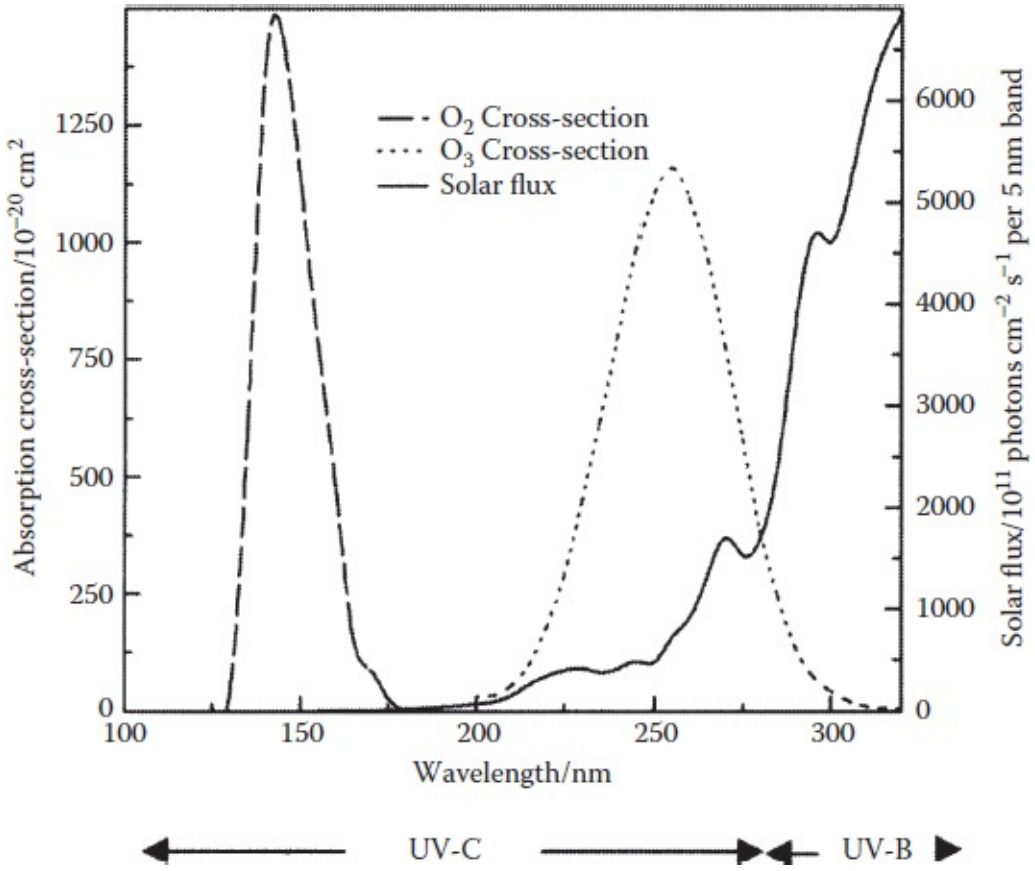

Figure 12.15 Absorption cross-sections of ozone and oxygen. (From van Loon, G.W. and Duffy, S.J., *Environmental Chemistry – A Global Perspective*, Oxford University Press, Oxford, UK, 2000.)

FOR REFERENCE PURPOSES ONLY

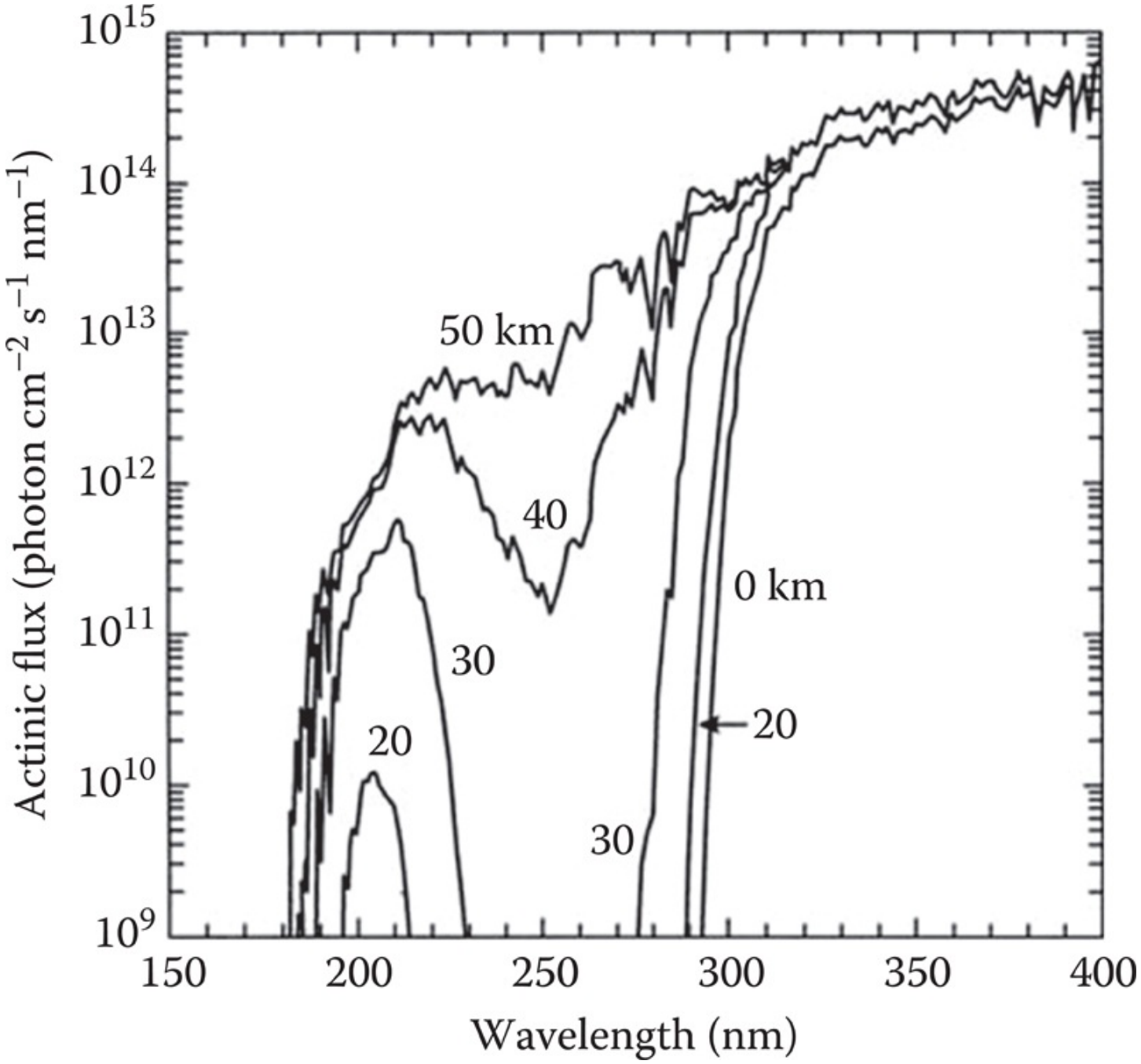

Figure 12.16 Variation of UV radiation with altitude. (From Jacob, D.J., *Introduction to Atmospheric Chemistry*, Princeton University Press, Princeton, NJ, 1999.)

FOR REFERENCE PURPOSES ONLY

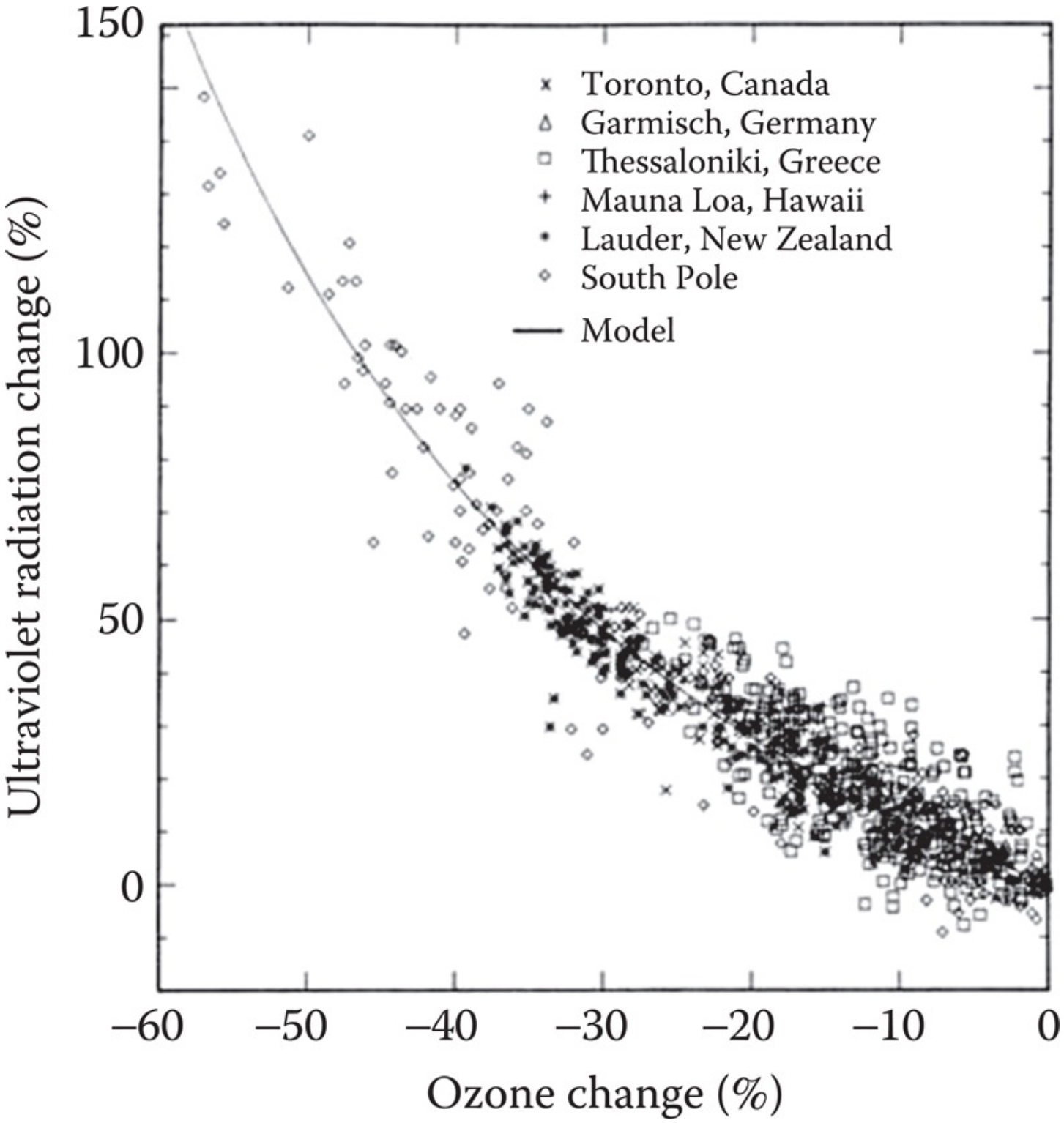

Figure 12.17 Measured and modelled relationship between OCD and UVB. (From WMO, Global Ozone Research and Monitoring Report No 44, Scientific Assessment of Ozone Depletion: 1998, World Meteorological Organisation, Geneva, Switzerland, 1999.)

FOR REFERENCE PURPOSES ONLY

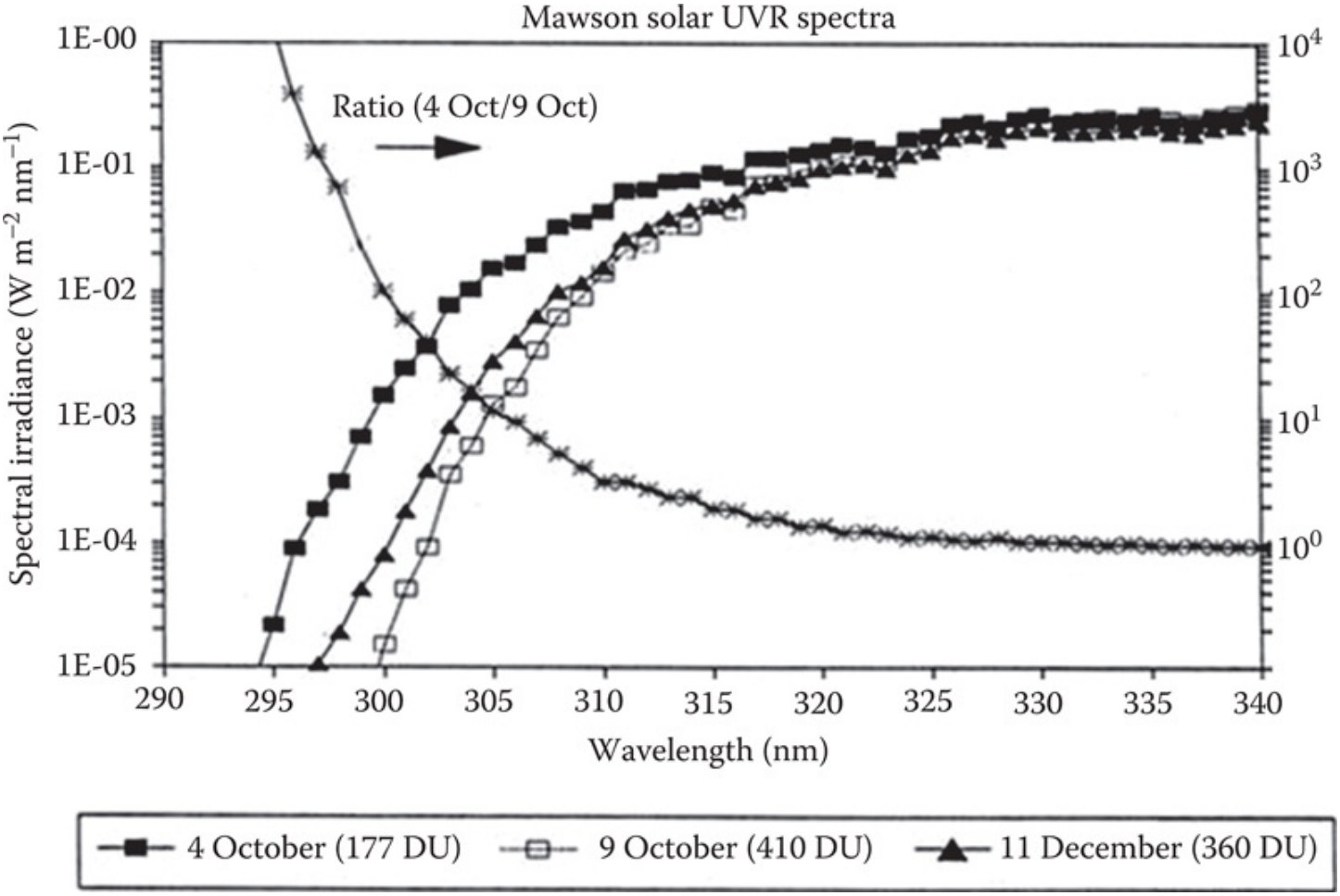

Figure 12.18 Effect of ozone column depth on spectral composition. (From Roy, C.R. et al., Effects of ozone depletion on the ultraviolet radiation environment at the Australian stations in Antarctica, in: *Ultraviolet Radiation in Antarctica: Measurements and Biological Effects*, Antarctic Research Series 62, 1–15, 1994.)

The increase in UV becomes more marked at shorter wavelengths, as seen in Figure 12.18. The UV irradiance was measured on 2 days having OCDs of 177 and 410 DU, and is presented both as the measured spectral distributions and as the ratio of the values on the two days.

The decline in ozone caused what looks at first sight to be a rather moderate increase in the UV penetration below wavelengths of 320 nm. However, when this change is plotted as the ratio of the flux density at that wavelength to the flux density at 340 nm (chosen because it would not be affected by ozone changes), a dramatic increase is seen, by up to a factor of 10,000 at 295 nm. Put another way, any change in OCD is amplified, with the amplification factor increasing as wavelength falls. Figure 12.19 shows the variation of this radiation amplification factor with wavelength for a 1% reduction in OCD at a range of solar zenith angles (at a zenith angle of zero the sun is overhead). At the shortest wavelengths, the irradiance is increased by a factor of three or four. Recent measurements

FOR REFERENCE PURPOSES ONLY

from some stations in unpolluted locations indicate that UV irradiance has been decreasing since the late 1990s, in accordance with observed ozone increases. However, at some northern hemisphere stations UV irradiance is still increasing, as a consequence of long-term changes in other factors, such as solar activity, that also affect UV radiation., In the Polar Regions, high UV irradiance lasting for a few days has been observed in association with episodes of low total ozone.

The optical amplification factor (OAF) is the percentage increase in carcinogenically effective irradiance caused by a 1% decrease in column ozone. The factor is different for different effects, but is usually in the range 1.6–2.0. Some molecules in biological organisms, notably DNA, are sensitive to these short wavelengths. In addition, the total or global flux involves a direct component (that travels straight to the receptor) and a diffuse component (that comes to the receptor after scattering in the atmosphere). When the angle of the sun above the horizontal is low, the path length through the atmosphere is long and the ratio of scattered diffuse radiation to direct radiation is high.

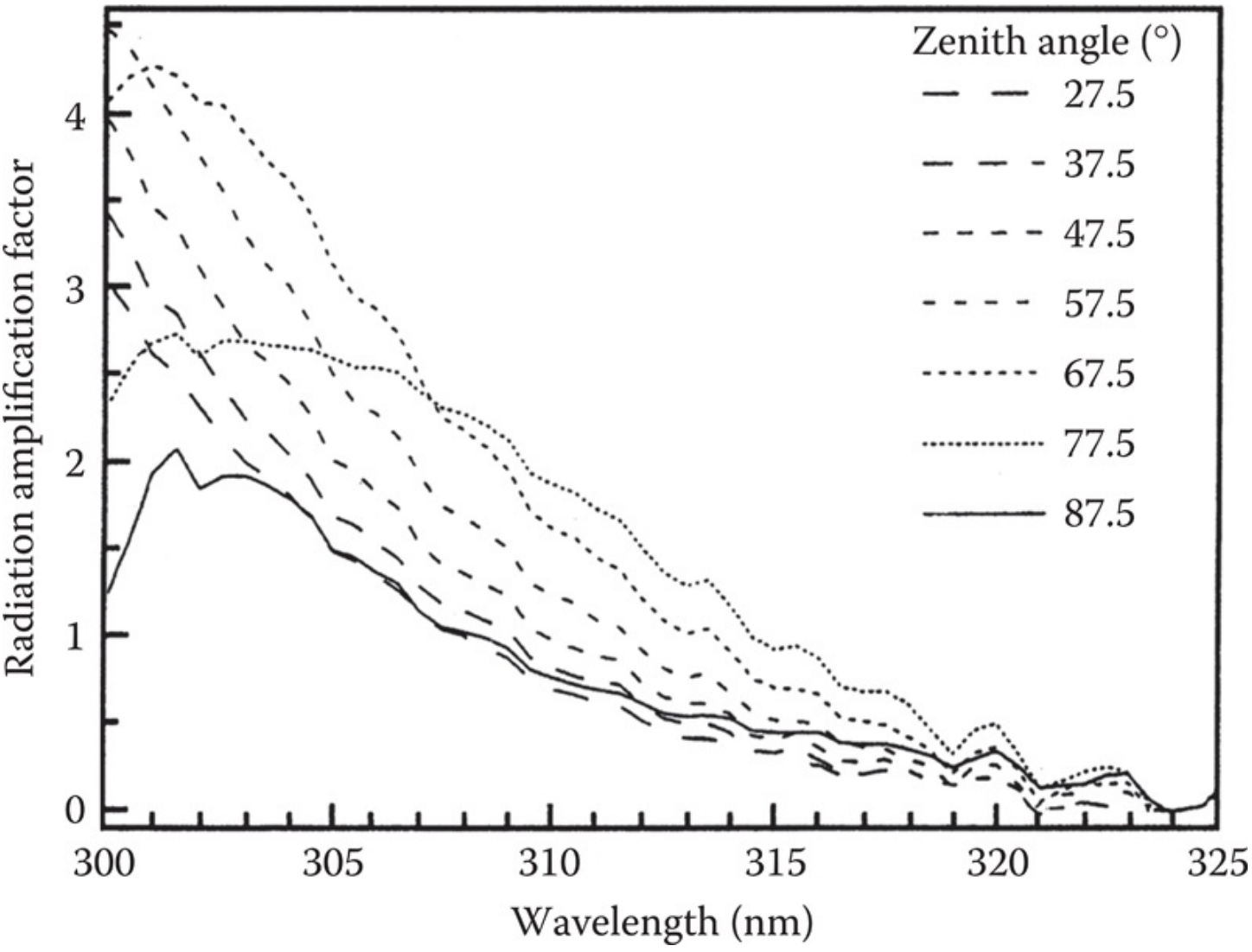

Figure 12.19 Variation of radiation amplification factor with wavelength for a 1% decrease

FOR REFERENCE PURPOSES ONLY

in OCD. (From Wayne, R.P., *Chemistry of Atmospheres*, Oxford University Press, Oxford, UK, 2000.)

The significance of diffuse/direct ratios depends on the geometry of the receptor, but typically UVB in the lower troposphere is 50% diffuse. The proportion of total UV to total solar radiation, which is around 8% outside the atmosphere, is decreased to 5%, 3% and 1% at zenith angles of 0°, 60° and 80°, respectively. This effect protects the Arctic and Antarctic regions from high UV fluxes because of the high zenith angles of the solar radiation. Even with ozone depletion, UV fluxes in the Antarctic are less than those at the equator. Cloud transmissivity is often higher in the UV than in the visible, and surface reflectivities are different (Table 12.6).

12.2.5.2 Penetration of UV into water

Aquatic and marine ecologies depend on solar radiation just as do terrestrial ones, and UV changes will impact on them too. The first attenuation takes place when the light strikes the water surface. If the water surface is calm, then direct reflectance increases from a few percent when the sun is overhead to more than 60% at grazing incidence. When diffuse radiation from a clear sky is included, the maximum percentage reflected drops to 40. When diffuse only is considered (as under a cloudy sky), about 6% is reflected. When the sea is rough, which is usually linked to increased wind speed, the effect is small for high solar elevations but tends to reduce the percentage reflected at low solar elevations.

Table 12.6 UV albedos

Surface	*UV albedo %*
Grass	2
Concrete	10
Sand	20
Snow	60–90

As the transmitted light penetrates the water column, it is both scattered and absorbed by the water itself, by suspended particles and by dissolved organic material. The overall effect of these processes is to attenuate the flux density according to the Beer–Lambert law with an attenuation coefficient K_d (m^{-1}). If the variation of flux with depth is measured, then 10% of the initial flux will remain at a depth of $2.3/K_d$. K_d varies with wavelength, so that usually UV will be much more rapidly attenuated than photosynthetically active radiation (PAR) or IR, especially in coastal waters that are high in dissolved organic carbon. The 90% attenuation depth of 305 nm UV, for example, might range from 1 m in the rather murky Baltic to 5 m in the North Sea and 15–20 m in the clean ocean. The value of K_d for pure water is about 0.01 m^{-1}. An interesting interaction here is that one of the

FOR REFERENCE PURPOSES ONLY

effects of acidification is to increase water clarity, thereby reducing the attenuation of UV in the water column.

12.2.5.3 Absorption of UVB

The energy E associated with individual photons of radiation varies inversely with their wavelength λ according to Planck's formula $E = hc/\lambda$, where h is Planck's constant and c is the speed of light. The shorter the wavelength, therefore, the more the energy per photon and the more damage can potentially be caused. The effects of UV, however, can be much more sensitive to wavelength than indicated by that relationship. The variation of effectiveness of the radiation with wavelength can be described by an action spectrum, usually obtained from laboratory experiments. Any tissue molecules capable of absorbing electromagnetic energy are called chromophores. Absorption of the photon puts the molecule into a high-energy unstable state, initiating a series of biochemical and cellular changes. Important UV chromophores include DNA, proteins, urocyanic acid and melanins. Ideally, the action spectrum will correspond to the absorption spectrum of the chromophores; this is modified for different parts of the body by site-specific factors such as the thickness of overlying tissue. Figure 12.20 shows the action spectra for erythema (see Section 12.2.5.5) and for damage to the DNA molecule. The effectiveness increases by a factor of over 10,000 as the wavelength is reduced from 320 to 280 nm – the upper and lower limits of the UVB range.

Also shown in Figure 12.20 is the solar spectrum in the UVA and UVB (the thick solid line). The combination of the sharp changes in both these spectra makes the biological effectiveness extremely sensitive to small changes in UV radiation, and therefore in ozone amount. Thus, it is very important when predicting health effects to have sound knowledge of the spectral distribution as well as the bandwidth flux density. This is shown in another way by Figure 12.21. Here, the dashed curve represents the percent change in spectral irradiance when the OCD is reduced by 1%, from 300 to 297 DU. The corresponding absolute change is shown by the dotted curve (which is read from the right scale). When the irradiance is weighted by the erythemal action spectrum, the solid curve, which shows a peak in erythemal effectiveness at 305 nm, results. The biological amplification factor (BAF) is the power to which the UV dose D is raised to predict the incidence of cancer. That is, incidence = Constant D^{BAF}.

Values of BAF are different for different types of skin cancer, lying in the range 1.4–2.5 for fair-skinned people. The overall biological response to a change in the ozone column density is thus the product of both the optical and biological amplification factors.

FOR REFERENCE PURPOSES ONLY

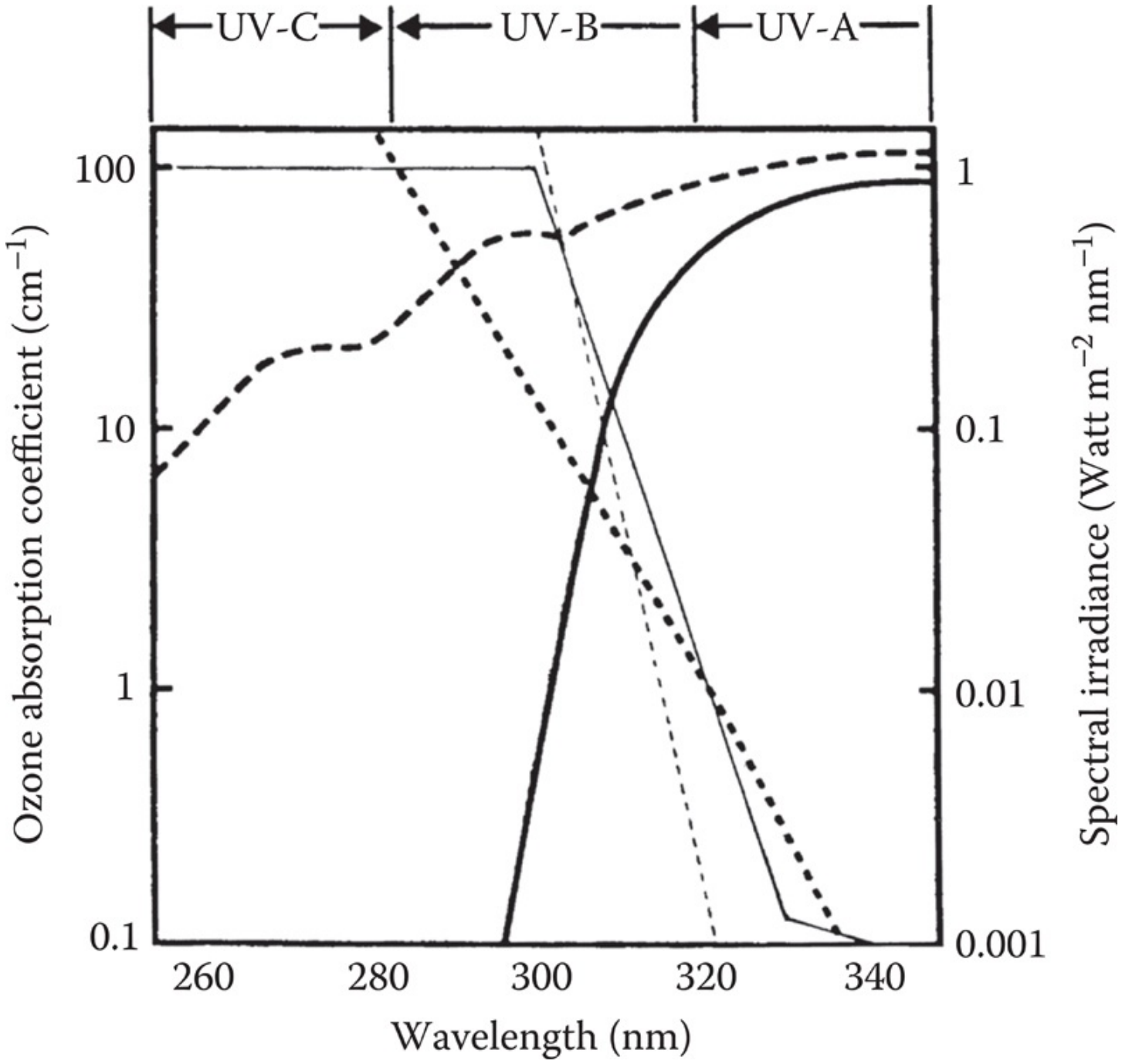

Figure 12.20 The action spectrum of DNA sensitivity to UV radiation, together with the UV spectrum of solar radiation. Note that both vertical scales are logarithmic. (From Webb, A.R., Ozone depletion and changes in environmental UV-B radiation, in: R. E. Hester and R. M. Harrison (Eds.), *Causes and Environmental Implications of Increased UV-B Radiation*, Royal Society of Chemistry, Cambridge, UK, 2000.)

FOR REFERENCE PURPOSES ONLY

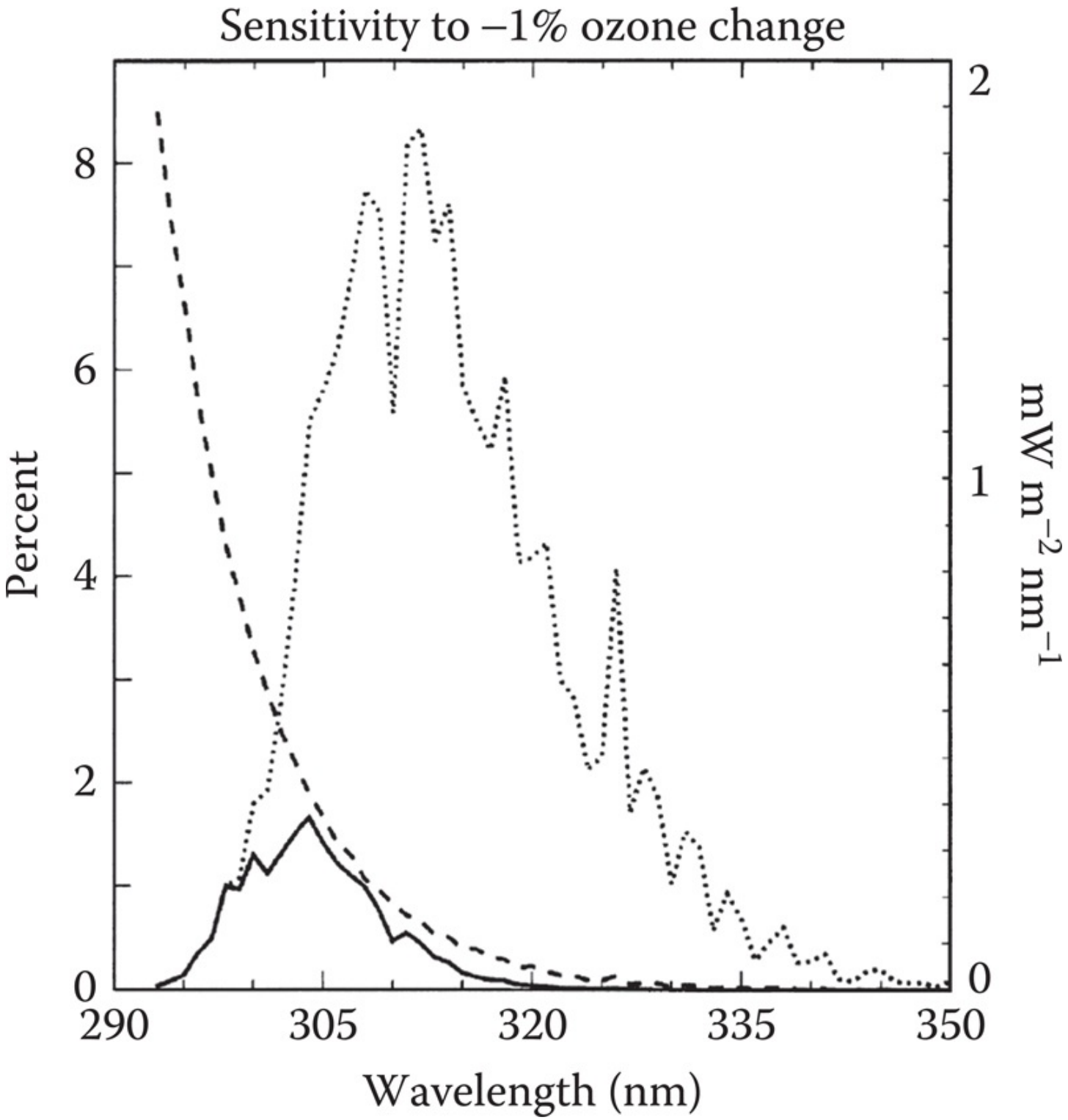

Figure 12.21 Changes in spectral irradiance and erythemal effect for a 1% reduction in OCD. The dashed curve shows the percent increase in the spectral irradiance (left scale); the dotted curve shows the absolute change in spectral irradiance (right scale); and the solid curve shows the absolute change in spectral irradiance weighted by the erythemal action spectrum (right scale). (From WMO, Global Ozone Research and Monitoring Report No 44, Scientific Assessment of Ozone Depletion: 1998, World Meteorological Organisation,

FOR REFERENCE PURPOSES ONLY

Geneva, Switzerland, 1999.)

12.2.5.4 Effects of UV on people

The main responses that have received attention for humans are those involving damage to the skin (sunburn, non-melanoma skin cancer and melanoma), eyes (cataracts) and the immune system.

12.2.5.5 Skin responses

Tanning is the induced production of melanin by epidermal melanocytes, as a consequence of UV-induced damage to DNA. Being tanned confers a photoprotection equivalent to a Sun Protection Factor of 2 or 3. Ironically, sunscreen users are more likely to burn than shade seekers; they probably feel that any application of sunscreen will give them protection for any length of time, despite the fact that the average application is only one quarter of the recommended 2 mg cm^{-2}. There are some medical benefits: vitamin D is produced, but this only needs about 10 min exposure per day; a feeling of well-being is created; psoriasis and eczema are reduced.

12.2.5.5.1 Acute responses

The most well-known acute responses are sunburn and pigmentation. Both UVA (320–400 nm) and UVB (280–320 nm) develop similar visual responses in human skin, although UVA typically requires a flux density that is several orders of magnitude higher. UVB activity is confined to the outer 0.03 mm of epidermis, while UVA penetrates three times as far – through the epidermis and into the dermis. About 1% of UVA penetrates into the subcutaneous tissue. UVB stimulates melanin (brown pigment) synthesis; the tanning effect becomes visible 3 days after exposure, continues for some days after, and provides some protection against subsequent UVB exposure. The longer wavelength UVA is more immediate in action but previous exposure provides little subsequent protection. Over-exposure induces erythema (the characteristic red inflammation due to dilation of small blood vessels just below the epidermis), weeping and blistering, followed by shedding of skin layers and pigmentation. Interestingly, some drugs, for example those used for heart complaints, photosensitise the skin so that it becomes sunburned very quickly. Contact with giant hogweed has the same effect.

The melanin pigment molecules that characterise naturally dark skin absorb UV and prevent its penetration into the skin (Figure 12.22). Fair skin, on the other hand, transmits effectively in the visible and UVA regions, and retains a higher transmissivity well into the UVB region, before cutting off sharply below 290 nm. The total sunburning potential of a given radiation environment can be summarised by the erythemally effective radiation (EER, with units of mW m^{-2}), which is the integral of the energy in the solar spectrum at

FOR REFERENCE PURPOSES ONLY

each wavelength weighted by the erythemal action spectrum. When skin is exposed to EER, a dose accumulates which eventually causes just-perceptible reddening of the skin. This standard erythemal dose (SED) has been set at 200 J m^{-2} for the most sensitive skins, based on exposure to monochromatic radiation at the maximum spectral efficiency for erythema (around 300 nm). Maximum daily UV doses under clear summer skies are about 70 SED in the tropics, 60 SED at mid-latitudes and 45 SED at temperate (UK) latitudes.

Table 12.7 shows the maximum values for erythemally effective clear-sky UVB irradiance for the northern hemisphere. The effects of clouds are highly variable, depending on their type and coverage. For radiation in general, a formula has been used that cloud cover of C tenths reduces the solar flux density to a fraction $F = 1 - 0.06C$. However, greater reductions in UVB than are suggested by this formula have been observed in practice.

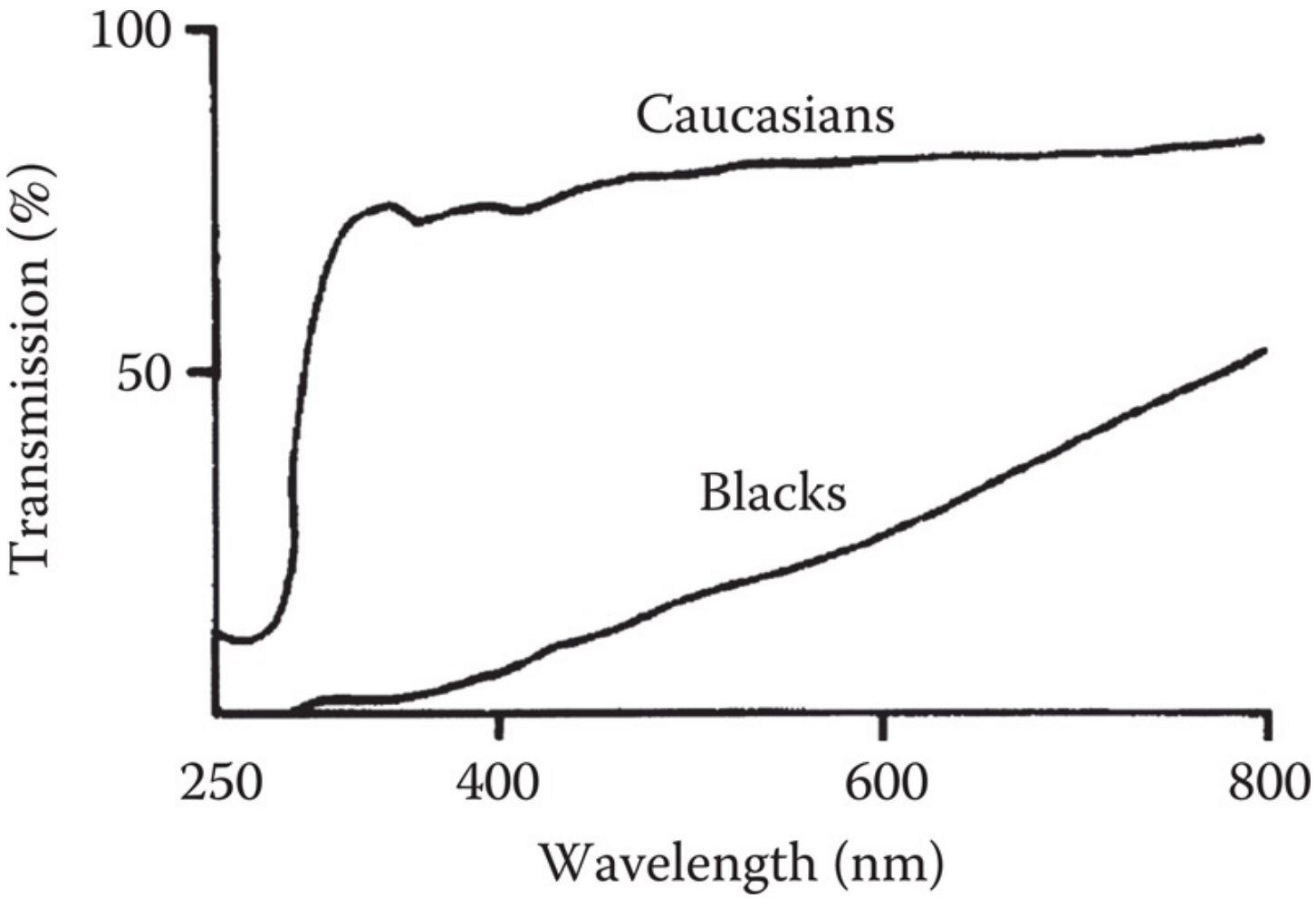

Figure 12.22 Spectral transmissivity of skin tissue from Caucasian and Black subjects. (From Jones, R.R., Consequences for human health of stratospheric ozone depletion, in: R.R. Jones and T. Wigley (Eds.), *Ozone Depletion: Health and Environmental Consequences*, John Wiley & Sons, Chichester, UK, 1989.)

FOR REFERENCE PURPOSES ONLY

Table 12.7 Maximum erythemally effective radiation (EER) values in the northern hemisphere (mW m^{-2})

Latitude, degrees	*January*	*March*	*June*	*December*
0	229	260	207	221
30	79	157	215	56
60	4	21	105	2
90	0	0	16	0

12.2.5.5.2 Chronic responses

Chronic responses to UV include skin photoageing and skin cancer. First, long term exposure to high UV fluxes leaves skin dry, wrinkled and leathery. This is mainly a cosmetic problem, but the change in skin texture can lead to chronic cracking and infection. Another chronic response is dilated blood vessels, giving the skin an inflamed appearance. Solar keratoses are small scaly lesions, which are considered to be premalignant and which may progress into squamous cell carcinoma, although this is rare. More importantly, DNA is one of the strongest UVA chromophores and genotoxic responses are to be expected. The carcinomas are divided into melanomas and non-melanomas. For our purposes, a melanoma is a malignant tumour that arises from melanocytes – the cells of the skin that produce melanin. It is the least treatable, and hence the most important, type of skin cancer. Non-melanoma cancers are divided into basal cell carcinomas (BCCs, which account for about 75% of cases) and squamous cell carcinomas (SCCs). Basal cell carcinomas are raised translucent nodules, which develop slowly on the face, neck and head. Squamous cell carcinomas appear as persistent red crusted lesions on sun-exposed skin. Chronic over-exposure increases the incidence of both melanoma and non-melanoma skin cancers. Skin carcinomas are already the most common human malignancies. Multifactorial analysis has shown that age and UV exposure are the two most important factors in the epidemiology of the carcinomas, with the risk being expressed as a power law of the form:

$$\text{Risk} = (\text{annual UV dose})^{a}(\text{age})^{b}$$

a and *b* are typically 1.7 and 3.2 for basal cell carcinoma, and 2.3 and 5.1 for squamous cell carcinoma.

12.2.5.6 Eye responses

Potential UV damage to any area of the body is initially a question of exposure. It has been calculated that because the front of the eye is mainly vertical, eyelid exposure (i.e. the flux density actually available at the eye, as compared to the irradiance on a horizontal surface) is about 20% of the corresponding irradiance falling on the top of the head. Under strong

FOR REFERENCE PURPOSES ONLY

sun conditions, radiation reaching the eye itself is normally further reduced to 5% by the squint reflex. The cornea absorbs UV strongly, with over 90% of UV <300 nm being absorbed. The young lens transmits UVA well (75%), although this falls away to <20% for adults. On the retina, the focussing action of the lens produces an enhancement of flux density by many orders of magnitude. UV can cause two main types of damage to the eye – at the cornea, and at the lens. There is a smaller prevalence of a condition called pterigium – small benign growths on the white of the eye. Although the cornea has high transmissivity to radiation in the visible band, it does absorb UV. In principle, the cornea can develop photokeratitis in just the same manner as skin develops erythema, but rarely does so because of natural exposure avoidance. The most common example is snow-blindness, when total UV exposure is elevated by a combination of high direct values from cloud-free skies and high diffuse values by reflection from the snow. Sensitivity is very high, being typically 30–40 J m^{-2} compared to the 200 J m^{-2} for skin erythema. There is an issue here for pilots and mountaineers, because UV flux at 10,000 m is 100 times that at the ground. A cataract is a progressive opacity of the eye lens, which occurs at an increasing frequency with age. Production of cataracts is accelerated by UV radiation (Figure 12.23), and there is an observable dependency on latitude, as shown in Table 12.8.

The US Environment Protection Agency (USEPA) has quantified the relationship between UVB flux and cataracts, estimating that a 30% increase in UVB (which would result from a 15% decrease in total column ozone) would increase cataract prevalence by around 14%, depending on age. Calculations using similar action spectrum ideas to those that we used above for skin lesions have predicted that a 10% reduction in column ozone over the US would increase the number of cataract cases by about 600,000 in the current population, and by about 4 million in the cohort born between 1986 and 2029. In their worst-case scenario for growth in the use of ozone-depleting substances, the same cohort would experience an additional 10 million cataracts.

12.2.5.7 Immune responses

The skin is a major site of entry for foreign antigens into the body and plays an active role in immunological defence. UV affects the immune system by interaction with the skin. Many skin cells, such as the keratinocytes, secrete cytokines which mediate the control of immune and inflammatory responses. A number of studies has shown that exposure to UV suppresses responses of the immune system and resistance to viral and bacterial infections. For example, activation of the herpes virus, leading to cold sores, commonly occurs at the start of a summer holiday due to the immunosuppressive effect of UV on the skin. Furthermore, especially in developing countries, high UV radiation levels may reduce the effectiveness of vaccines. This can have major impact on public health.

FOR REFERENCE PURPOSES ONLY

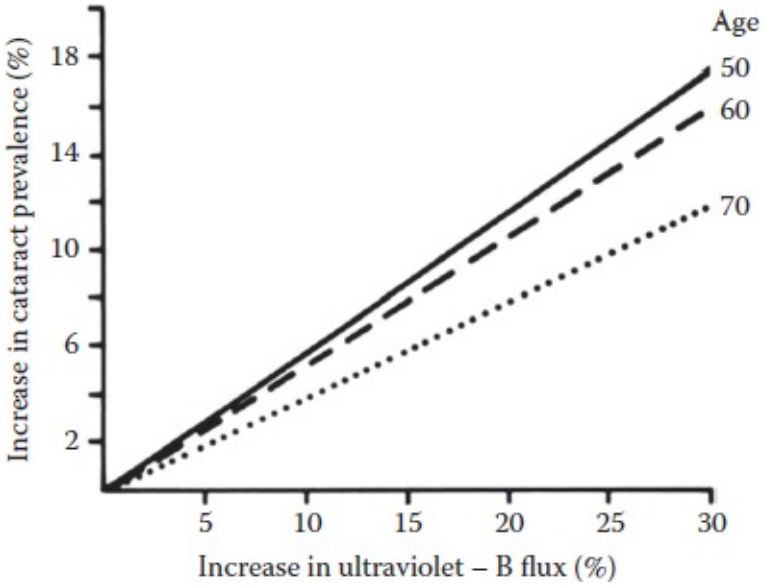

Figure 12.23 Sensitivity of cataract prevalence in different age groups to proportionate increase in UVB flux. (From Jones, R.R., Consequences for human health of stratospheric ozone depletion, in: R. R. Jones and T. Wigley (Eds.), *Ozone Depletion: Health and Environmental Consequences*, John Wiley & Sons, Chichester, UK, 1989.)

Table 12.8 Variation of cataract occurrence with latitude

Location	*Cataract occurrence/%*
Rochester, New York (42°N)	9
Tampa, Florida (28°N)	20
Manila (15°N)	43

12.2.5.8 Effects of UV radiation on terrestrial biota

It is thought that early in the Earth's existence the Sun produced much higher UV than today even though its total output was lower. As there was no oxygen, and hence no ozone layer, the UV levels at the Earth's surface were too great for life to develop. One of the reasons why early life developed underwater was that the water shielded the UV. As oxygen and ozone increased in step, UV levels were reduced to tolerable amounts by about 500 million years ago when the first terrestrial plants appeared. Even so, UV levels were almost certainly higher at that time than they are now, which raises the possibility that some ancient and more primitive plant species such as algae and lichen may show greater UV tolerance than more recent evolutionary developments. Some developments in plants involved the manufacture of phenolic compounds such as tannins, flavonoids and lignin, which in addition to their other plant functions were UV-screening. In addition, plants have defence mechanisms such as DNA repair, radical scavenging and polyamine stabilisation of

FOR REFERENCE PURPOSES ONLY

injured membranes.

Many experimental studies of plant responses to elevated UVB have now been published. Contrary to expectations, these have not generally shown a reduction in primary productivity. However, we must stress again here that the results of such an experiment are only as good as the experiment itself. It is always a major, and in many ways insuperable, problem to change only the UVB radiation that is the variable of interest. If the plants are grown under controlled conditions (e.g. in a laboratory growth chamber) then the temperature, humidity, soil structure, wind speed and other key variables will all be different to those outdoors. In particular, the spectral composition of the lighting will be different, even after strenuous and expensive efforts, using contributions from a range of sources, have been made in order to simulate solar daylight. For example, Figure 12.24 shows that a QTH (Quartz envelope, Tungsten element, Halogen gas fill) or Xenon bulb, which both cross the natural UV spectrum at 305 nm, under-represent the PAR and exceed the shorter wavelength UV by an increasing proportion. When this is translated into an action spectrum (Figure 12.25) it is clear that if we simply go outdoors and shine lights on vegetation we cannot be certain of getting valid responses. In this case, the weighted irradiance from the artificial sources is 10,000 times higher than that from natural light at 290 nm.

Instead of supplementing the UV with artificial sources, filtering can be used to deplete it. Figure 12.26 shows the transmission spectra of four *transparent* materials, characterised by the wavelength at which the transmittance is 50% – 220 nm for quartz, 305 nm for Pyrex, 320 nm for mylar and 350 nm for Plexiglas. Cellulose diacetate (300 nm) and polycarbonate (390 nm) filters are also used. Even within the UVB band, a supplementary source will have a different distribution of flux with wavelength to that in sunlight, and a weighting function will be used to correct for this. Some studies, particularly of secondary responses such as plant pathogens, have used sources with such high UVC components that they are not representative of conditions at the surface. If the experiments are done outdoors, the naturalness of many factors can be improved, although the spectral problem will remain whether it is increased by supplementation or reduced by filtering. In addition, the variability of the conditions and the growth will increase, so that responses have to be correspondingly larger for statistical confidence to be maintained. For trees, the detailed optical properties of individual leaves (needles for conifers) and communities is important. Only 10%–20% of the incident radiation penetrates down to the lowest foliage in typical forests, so the exposure of the youngest and oldest leaves may vary by a factor of ten. As with air pollution studies, there have been few controlled experiments on mature trees – for example, most of our knowledge on conifer responses has been acquired from experiments on 1-year-old seedlings.

FOR REFERENCE PURPOSES ONLY

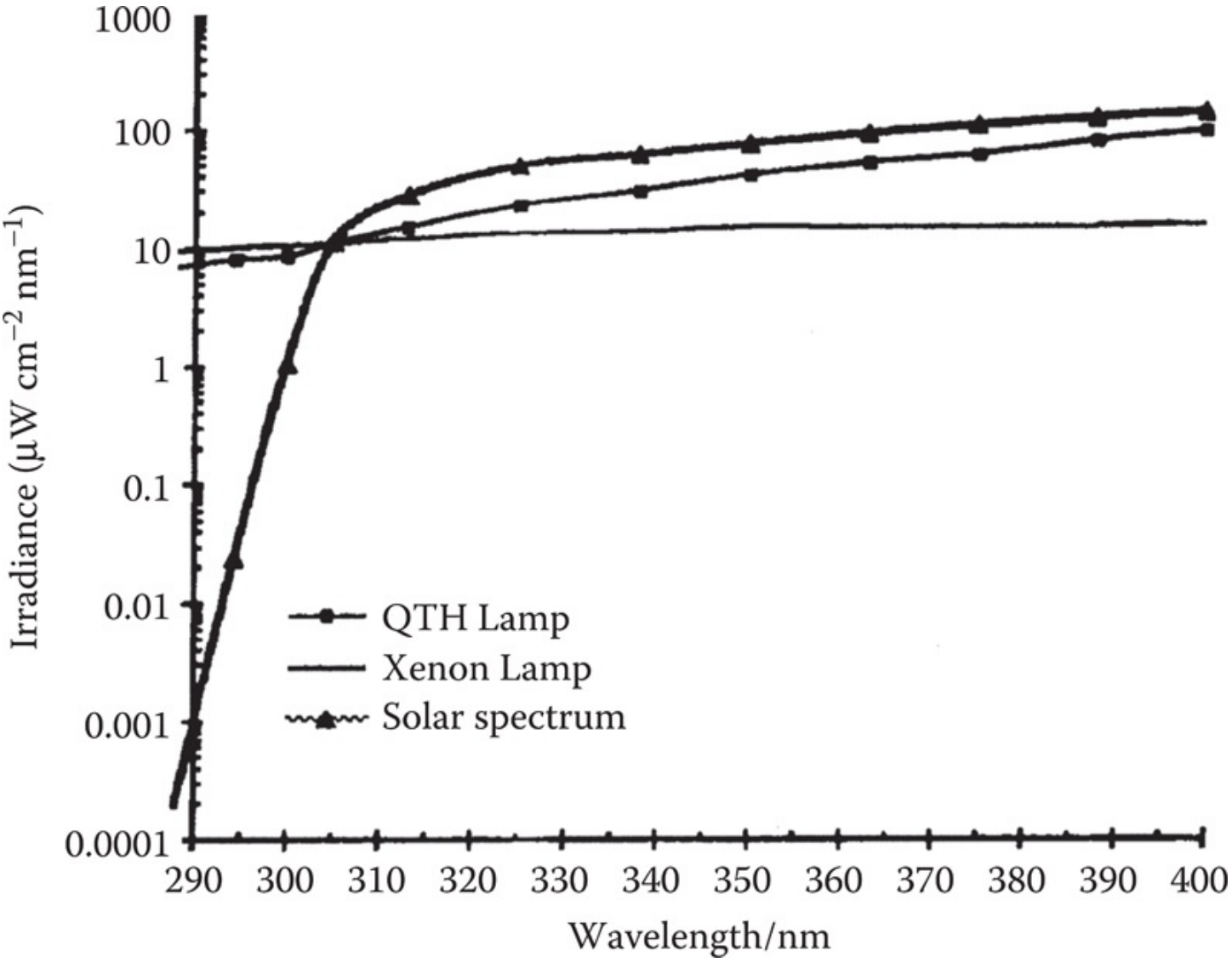

Figure 12.24 Spectra of UV sources and solar radiation. (From Diaz, S.B. et al., UV physics and optics, in: de Mora, S., Demers, S., and Vernet, M. (Eds.), The Effects of UV Radiation in the Marine Environment, Cambridge University Press, Cambridge, UK, 2000.)

FOR REFERENCE PURPOSES ONLY

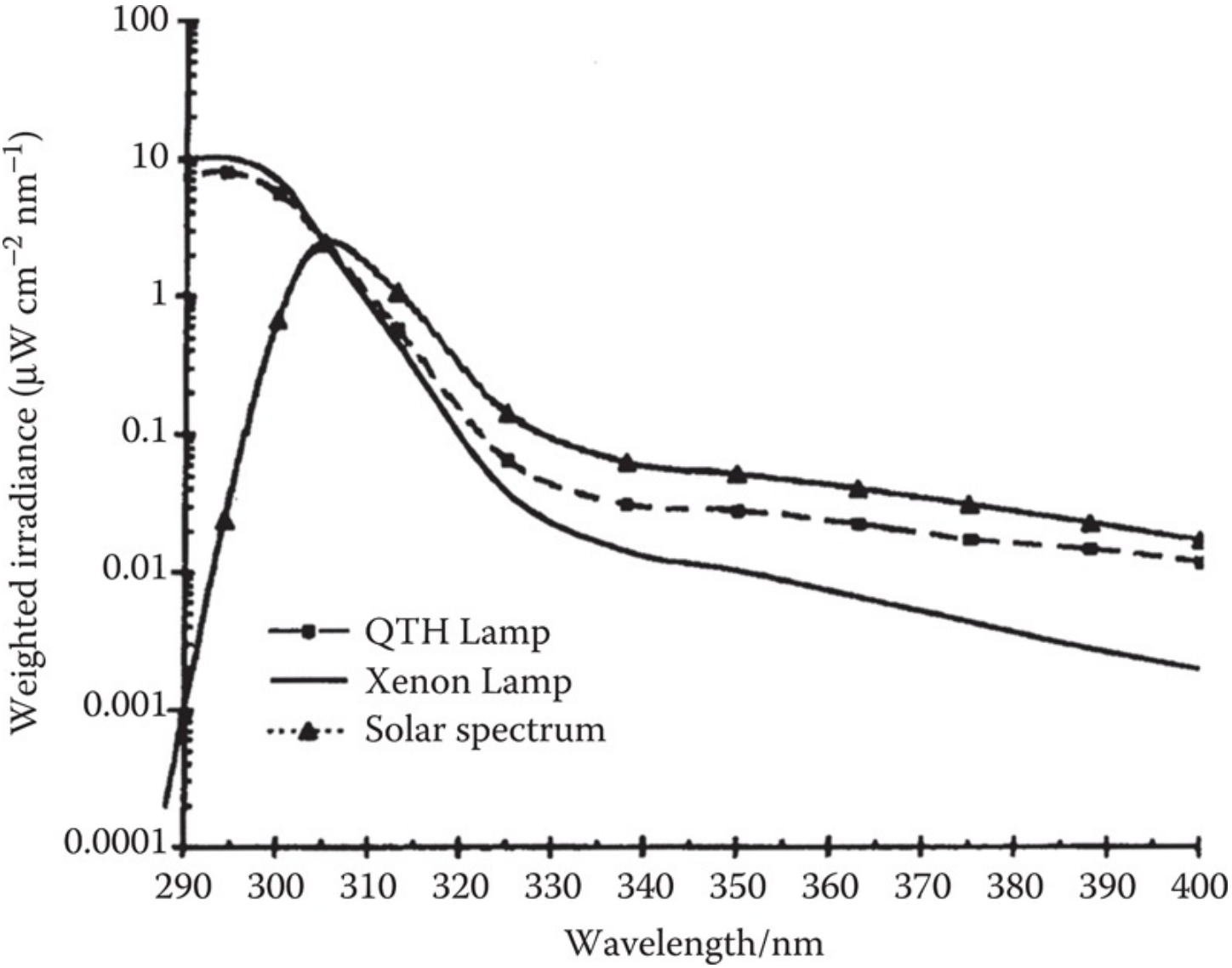

Figure 12.25 Action spectra due to UV sources and solar radiation. (From Diaz, S.B. et al., UV physics and optics, in: de Mora, S., Demers, S., and Vernet, M. (Eds.), *The Effects of UV Radiation in the Marine Environment*, Cambridge University Press, Cambridge, UK, 2000.)

FOR REFERENCE PURPOSES ONLY

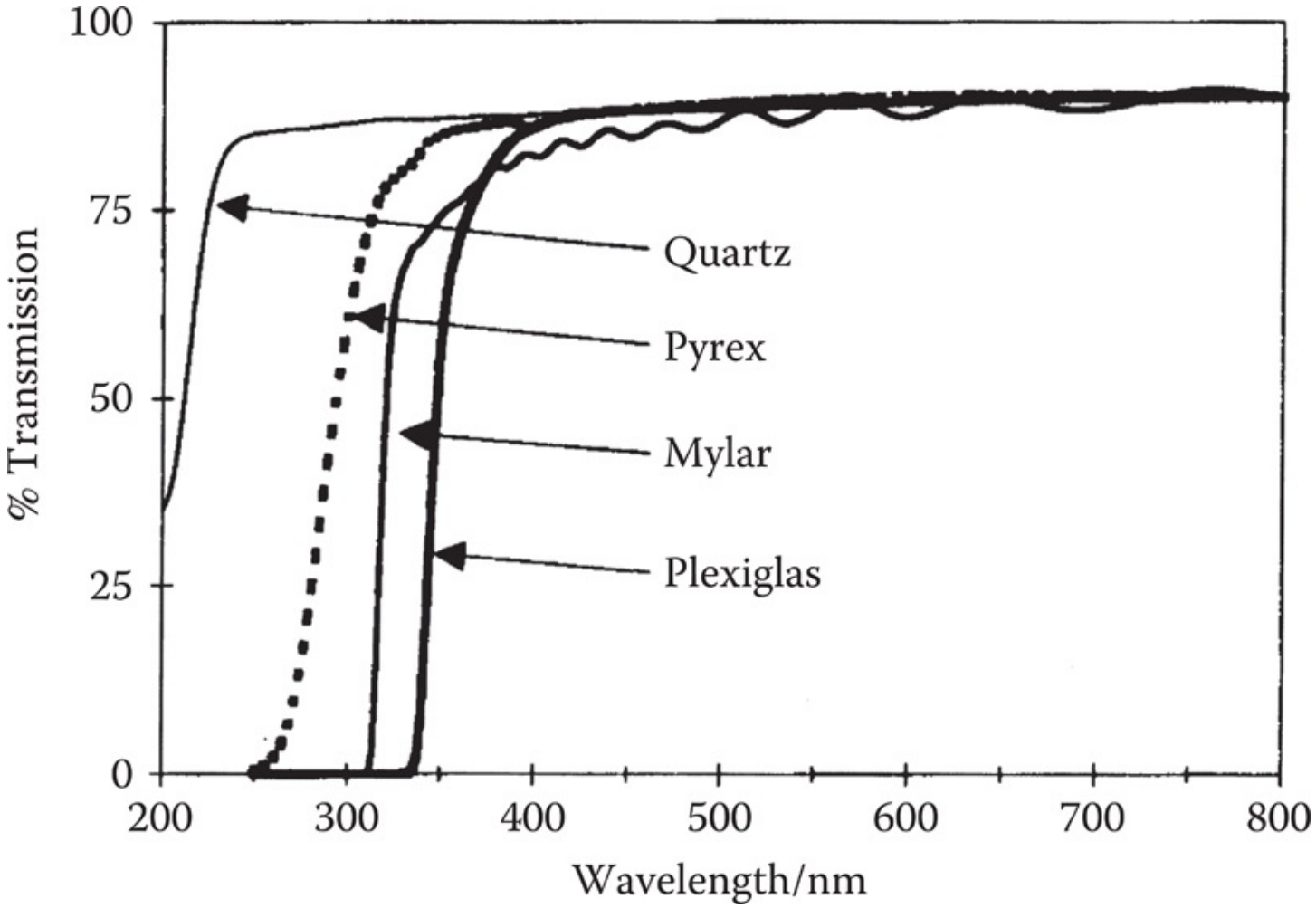

Figure 12.26 Transmission curves of four materials used to deplete UV radiation. (From Vernet, M. et al., The response of Antarctic phytoplankton to ultraviolet radiation: Absorption, photosynthesis and taxonomic composition, in: *Ultraviolet Radiation in Antarctica: Measurements and Biological Effects*, Antarctic Research Series 62, 1–15, 1994.)

The greatest reductions of column ozone and associated increases in UV have occurred in Antarctica, where plant densities are low. Over the globe as a whole, we would not expect the total column ozone changes that have occurred thus far (a few percent over 20 years) to be reflected in observable changes in plant communities. Hence, we have to rely on the results of relatively short experiments conducted in middle latitudes on a small number of mainly agricultural species to predict the future consequences of ozone depletion. A few hundred species have been screened for UV tolerance. Of these, about two-thirds have proved sensitive to some degree, and there is a wide variation of sensitivity between cultivars of the same species. There are large differences in the quantitative sensitivity of field-grown plants, although the qualitative responses are typically: reduced photosynthetic activity, reduced leaf and stem growth, and reduced dry weight. For some crops, there are also important quality changes – for example, the protein and oil content of soybean is

reduced. As with tropospheric air pollution, it is impractical to investigate the responses of mature trees because of their size and longevity. Plant diseases such as fungi have been amplified by enhanced UVB, because sporulation is enhanced. On the other hand, diseases such as *Septoria* (leaf blotch) have been reduced because the UVB damages spores and reduces infection. In much of the experimental work, the validity of the results is governed by the degree to which the imposed UV spectrum matches the natural spectrum, because of the extreme sensitivity of the action spectrum to small changes in wavelength. We know very little about the responses of non-human animals to elevated UV exposures. Clearly, there are possible carcinoma and eye implications. Observations were reported of increased eye defects in rabbits living in the southern parts of South America (i.e. close to the Antarctic ozone hole), but these have not been substantiated.

12.2.5.9 Effects on marine organisms

Although the UVB waveband represents only 0.8% of the total energy reaching the surface of the Earth, it is responsible for almost half the photochemical effects on marine organisms. UVB penetrates the water column to significant depths – 20–40 m – and may have a serious impact on aquatic life. This issue has been particularly identified with the seas around Antarctica, where the increase in UVB is greatest below the ozone hole. Furthermore, the protection afforded by low solar elevations in reducing UV flux densities has led to the evolution of UV-intolerant ecologies which are especially liable to disturbance by enhanced UV. Increased UV may have consequences for food web dynamics, starting with bacteria and algae. The UV will increase the rate at which substrates are made available photochemically, promoting growth rates in areas where carbon is in short supply. Photosynthetic organisms such as phytoplankton naturally populate the upper water layers where the flux of solar radiation, and hence of UV, is strongest. UV cannot only damage photosynthesis, but also carbon allocation, photosynthetic pigmentation, nutrient uptake and cell motility. Some organisms can limit the damage by UV avoidance – for example, by moving to a greater depth below the surface where the UV is weaker. The overall response to enhanced UV is to reduce primary productivity. The base of the food chain is then weakened, so that krill and whales are in turn affected. There are also direct effects on animals – zooplankton DNA is affected, fish eggs are vulnerable and fish can get sunburned. Results are now being published for the biological weighting functions for damage to individual species. These generally show the critical influence of wavelengths in the 280–320 nm region.

Depletion of the ozone layer has spurred interest in marine photochemistry, which is largely driven by UVB. The key factor here is the relationship of the photon energies (which decrease as wavelength increases) to the bond energies of the relevant molecules in natural systems. Bonds in the energy ranges 300–370 kJ mol^{-1} (H-C=C, for example), 370–425 kJ mol^{-1} (S-S, for example) and 425–600 kJ mol^{-1} (O=O or H-OH, for example) can be photolysed by UVA, UVB and UVC, respectively. It has been recently suggested that UVB

could be impacting the aqueous Hg cycle, including effects on Hg volatilisation (photo-reduction), solubilisation (photo-oxidation), methyl-Hg demethylation and Hg methylation. Such Hg cycling has adverse impacts on marine ecosystem functions and life.

Pure water and the inorganic salts that seawater contains absorb only weakly in the UV. The absorption is mainly due to dissolved organic matter (DOM), which is present in the range 1–4 mg C L^{-1} in surface seawater. This represents a major pool of reduced carbon at the surface of the Earth. Typically less than half of the DOM is common biomolecules such as amino acids and polysaccharides, the remainder being complex humic substances, which are not well characterised but are responsible for absorbing UVB photons and triggering the resulting photochemical responses. Among the immediate photoproducts, hydrogen peroxide, hydroxyl radical, carbonyl sulphide and formaldehyde have been determined. These react rapidly to generate a wide range of stable low molecular weight organic end products, which have important consequences for carbon cycling in the oceans. Some of the species, for example CO, CO_2, CS_2 and methyl iodide, can diffuse into the atmosphere and affect atmospheric chemistry. We do not know yet how these relationships are being impacted by the increase in UVB. Experimental investigations of these processes are hampered not only by the variability of the chromophoric DOM but also by the strong wavelength dependence of the photochemistry which makes accurate replication of the natural spectrum very difficult.

12.2.6 Clothing protection from ultraviolet radiation

Clothing provides a complex and variable level of protection from UV radiation. The level of protection depends on fabric structure (fibre content and thickness, and the knit or weave) and colour. Individual fabrics can be tested and given a Clothing Protection Factor (CPF) analogous to the Sun Protection Factor (SPF) given to sunscreens. The test firstly involves spectral measurement of the transmissivity (the fraction of the incident radiation that is transmitted through the fabric) over the wavelength range 290–400 nm. The solar irradiance at each wavelength is then multiplied first by the transmissivity and second by the erythemal activity, and the results integrated across the wavelength range to find the erythemally effective UV radiation that penetrates the fabric. The CPF is then the ratio of the erythemally effective UV incident on the fabric to that transmitted through the fabric. Hence, a high value of CPF indicates a high level of protection. Clothing Protection Factor is not constant for any one fabric, as it may change with stretch or wetness. Clothing with a CPF of 30 or more confers a high degree of protection. If the CPF is less than 10, then a hazardous level of UV exposure will be experienced if the wearer is outdoors all day in strong sunlight. In some countries, CPF is indicated on clothing for sale if the garment is likely to be worn under UV-hazardous conditions – T-shirts, for example. The CPFs of some clothing are surprisingly low. For example, measurements on a white football shirt gave a CPF of 5–10 (equivalent to using a sunscreen with a protection factor of 5–10).

FOR REFERENCE PURPOSES ONLY

12.3 CASE STUDY – DISCOVERY OF THE OZONE HOLE

Around 1985, it was discovered that the ozone concentration above the continent of Antarctica was decreasing (initially termed as the *ozone hole*); this was found to be due to chemical reactions with chlorine derived from stable chemicals known as chlorofluorocarbons (CFCs). Retrospective analysis of data from all sources showed that gradual decreases had started in the 1960s and accelerated dramatically in the last decade (Figure 12.27). To some extent, these decreases had been concealed by other effects such as instrument calibration changes, the annual cycle of the seasons, the quasi-biennial oscillation of the stratospheric winds, and the 11-year cycle of sunspots. However, in 1993 Antarctic column ozone fell from its winter value of 350 DU to just 90 DU, the lowest-ever recorded value.

The ozone *hole* appeared in the Antarctic, rather than elsewhere, because of distinctive atmospheric circulations in that region; these are shown in Figure 12.28. There is a specific meteorology during the winter and spring that sets up a cold isolated airmass (the polar vortex) within which O_3 cannot be replenished by flows from lower-latitude regions. The vortex develops a core of very cold air, within which polar stratospheric cloud particles form, on the surfaces of which many of the important ozone-destroying reactions occur. However, the problem is not confined to the Antarctic, and less severe reductions have since been measured over the Arctic and elsewhere. In 1989, a patch of the ozone hole drifted up over Melbourne in December (Australian summer), and the column ozone was reduced by 50%. The reduction in ozone concentration has now been observed globally, and has potentially severe implications for life on the surface. The WMO issues bulletins containing information of the state of the Antarctic ozone layer at roughly two week intervals from August to November every year.

Since the first identification of the problem of ozone depletion, there have been various international agreements trying to deal with this question. The first international agreement was the 1987 Montreal Protocol. This committed signatories to cut production of CFCs to 50% of the 1986 levels by the year 1999, a level which the UK achieved in 1989. The London amendment of 1990 strengthened the Montreal Protocol and committed governments to phasing out CFCs completely by 2000. They were to be replaced by less damaging substitutes – the hydrochlorofluorocarbons (HCFCs). However, the speed of stratospheric O_3 destruction caused an acceleration of the London timetable. The 1992 Copenhagen agreements brought forward the phase-out of CFCs to 1 January 1996, with a 75% reduction (based on 1986 levels) by 1994. Carbon tetrachloride, methyl chloroform and halons were phased out by January 1996. Consumption of HCFCs was capped in January 1996, and a phase-down schedule was agreed which includes a complete ban by 2030. The long-term aim is to find HCFC substitutes that do not contain chlorine or fluorine.

FOR REFERENCE PURPOSES ONLY

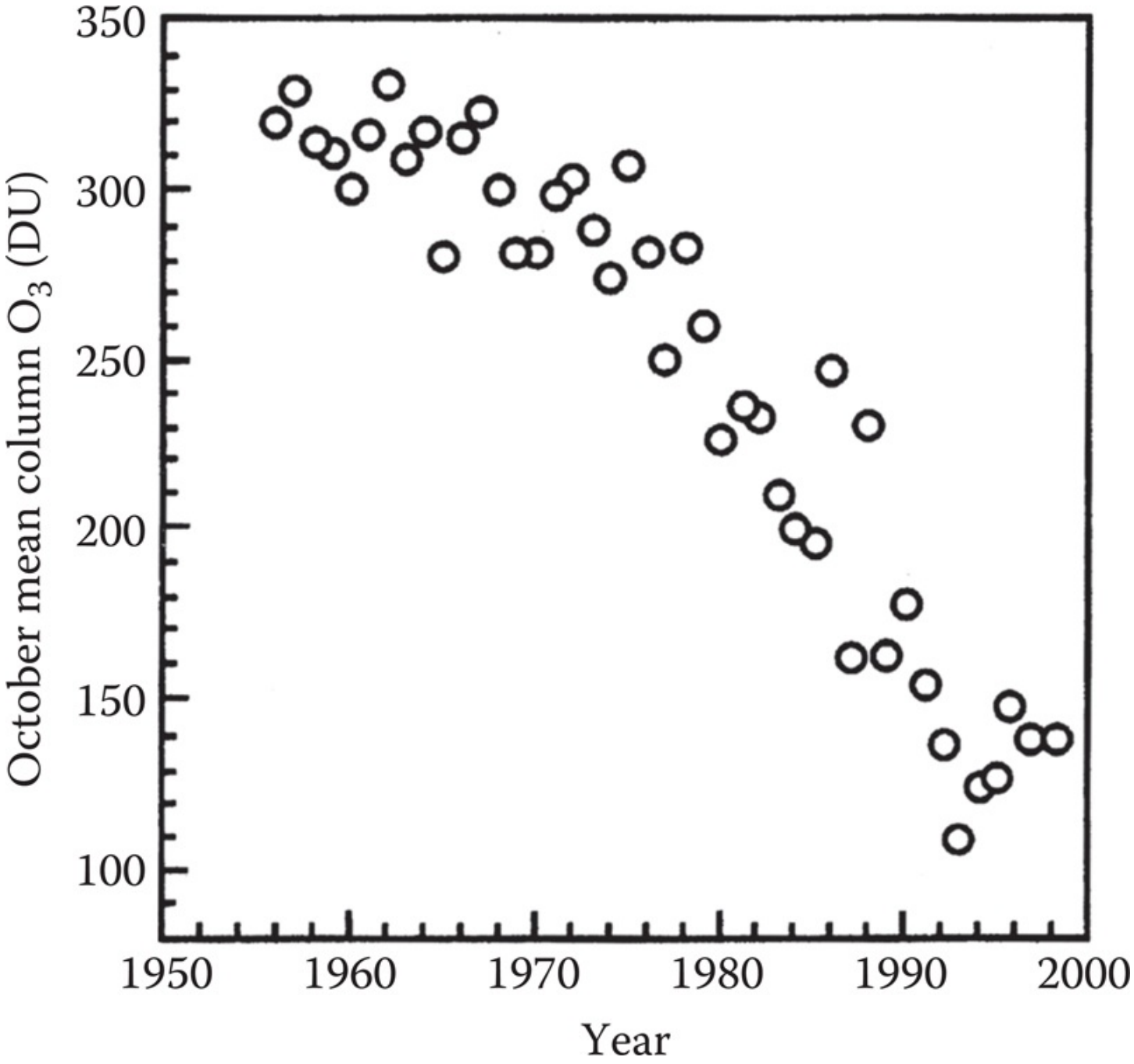

Figure 12.27 The time course of October column ozone over Halley, Antarctica between 1957 and 1998. (From Stratospheric Ozone Review Group, *Stratospheric Ozone 1996*, Department of the Environment, London, UK, 1996.)

FOR REFERENCE PURPOSES ONLY

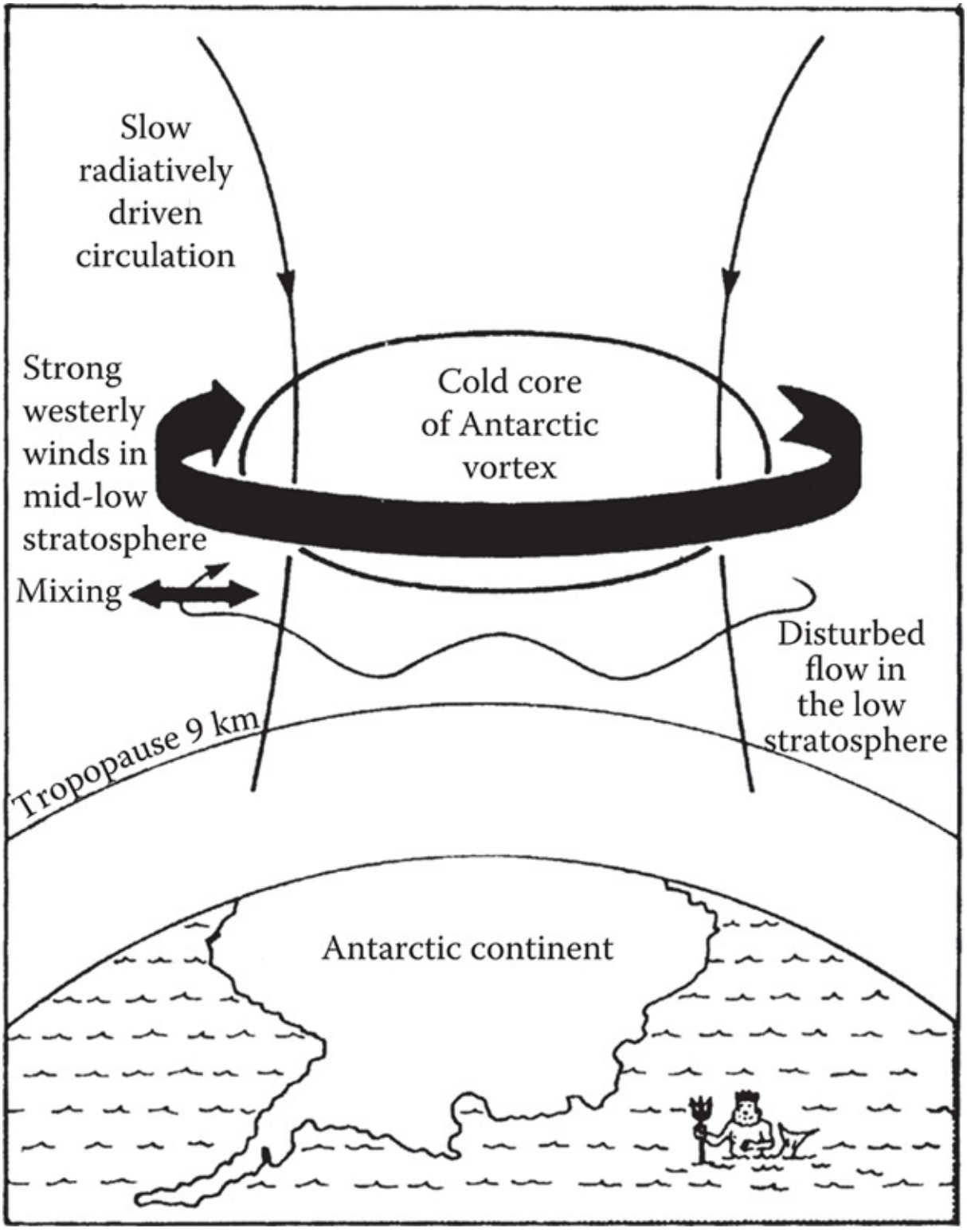

Figure 12.28 The Antarctic Winter Vortex. (From Wayne, R.P., *Chemistry of Atmospheres*, Oxford University Press, Oxford, UK, 2000.)

In 1974, the first research was published which indicated that CFCs were lowering the average concentration of O_3 in the stratosphere and creating a global time bomb. However, this information was largely ignored until Farman's discovery of the first hole in the ozone layer in 1982. Since then, a great deal of attention has been given to the processes involved.

FOR REFERENCE PURPOSES ONLY

Major European and American experimental programmes, called THESEO and SOLVE respectively, have investigated ozone destruction in the northern hemisphere. Between them, these programmes in 1999/2000 involved contributions from over 500 scientists, 30 instrumented research balloons, 600 ozone sondes, 6 aircraft and 30 ground stations, as well as various satellites.

CFCs accumulate in the atmosphere – mainly $CFCl_3$ and CF_2Cl_2, which are inert in the troposphere but not in the stratosphere where reactions occur. By a complicated series of reactions, CFCs are broken down by light or by reaction with monatomic oxygen to produce chlorine or bromine atoms. These react with, and remove, O_3 from the stratosphere:

$$Cl + O_3 \rightarrow ClO + O_2$$
$$ClO + O^{\bullet} \rightarrow Cl + O_2$$

Note that the chlorine atom is regenerated.

Further research has shown that the chlorine and bromine atoms react with nitrogen oxides to produce unusual halogen nitrate compounds:

$$ClO + NO_2 + M \rightarrow ClNO_3 + M$$

$$2ClNO_3 + H_2O \rightarrow 2HNO_3 + 2HCl + O_2$$

The rate of stratospheric ozone depletion has been shown to increase dramatically in the spring of each year over Antarctica. As the temperature rises, the frozen aerosol breaks up, releasing *extra* chlorine and bromine atoms (as well as hydroxyl radicals) which rapidly increase the rate of reaction and, hence, the removal of ozone. There are important differences between the pollution caused by CFCs and N_2O being released into the atmosphere and that caused by the direct injection of NO/NO_2 into the stratosphere by aircraft. In the latter case, ozone recovery occurs within approximately 3 years. However, in the former situation, recovery takes a great deal longer, mainly due to:

- The buffer effect of the large mass of the troposphere (approximately 10 times that of the stratosphere)
- The slow rate of transport from the troposphere into the stratosphere (across the tropopause)

Consequently, each CFC molecule can last for 65–110 years in the stratosphere – and during that time, each Cl atom in these molecules can convert as many as 100,000 molecules of O_3 to O_2. The picture with respect to the impact of halogen compounds is by no means complete. Other compounds and/or reactions may well be discovered, and the effect of other Cl containing compounds is also unknown – for example, natural sources of CH_3Cl and CCl_4 may have similar effects.

REFERENCES AND FURTHER READING RESOURCES

Bolaji, B. O., and Huan, Z. (2013) Ozone depletion and global warming: Case for the use of natural refrigerant – A review. *Renewable and Sustainable Energy Reviews*, 18: 49–54.

Bornman, J. F., Barnes, P. W., Robinson, S. A., Ballare, C. L., Flint, S. D., and Caldwell, M. M. (2015) Solar ultraviolet radiation and ozone depletion-driven climate change: Effects on terrestrial ecosystems. *Photochemical & Photobiological Sciences*, 14(1): 88–107.

Caldwell, M. M., Bornman, J. F., Ballaré, C. L., Flint, S. D., and Kulandaivelu, G. (2007) Terrestrial ecosystems, increased solar ultraviolet radiation and intersections with other climate change factors. *Photochemical & Photobiological Sciences*, 6: 252–266.

Chipperfield, M. P., and Feng, W. (2003) Comment on: Stratospheric ozone depletion at northern midlatitudes in the 21st century: The importance of future concentrations of greenhouse gases nitrous oxide and methane. *Geophysical Research Letters*, 30(7): 1389.

Collins, W. J., Sanderson, M. G., Manning, A. J., Redington, A. L., and Derwent, R. G. (2007) *Global Modelling of Transboundary Air Pollution*. AEAT, Oxfordshire, UK.

Cook, J., Nuccitelli, D., Green, S. A., Richardson, M., Winkler, B., Painting, R., Way, R., Jacobs, P., and Skuce, A. (2013) Quantifying the consensus on anthropogenic global warming in the scientific literature. *Environmental Research Letters*, 8: 1–7.

de Mora, S., Demers, S., and Vernet, M. (Eds.) (2000) *The Effects of UV Radiation in the Marine Environment*. Cambridge University Press, Cambridge, UK.

Diaz, S. B., Morrow, J. H., and Booth, C. R. (2000) UV physics and optics. In: S. de Mora, S. Demers and M. Vernet (Eds.), *The Effects of UV Radiation in the Marine Environment*. Cambridge University Press, Cambridge, UK.

Diffey, B. (2003) Climate change, ozone depletion and the impact on ultraviolet exposure of human skin. *Physics in Medicine and Biology*, 49(1): R1.

EEA (1999) *Annual Topic Update on Air Quality*. European Environment Agency, Copenhagen, Denmark.

Gallagher, R. P., and Lee, T. K. (2006) Adverse effects of ultraviolet radiation: A brief review. *Progress in Biophysics and Molecular Biology*, 92(1): 119–131.

Häder, D., Kumar, H. D., Smith, R. C., and Worrest, R. C. (2007) Effects of solar UV radiation on aquatic ecosystems and interactions with climate change. *Photochemical & Photobiological Sciences* 6: 267–285.

Hester, R. E., and Harrison, R. M. (Eds.) (2000) *Causes and Environmental Implications of Increased UV-B Radiation*. Royal Society of Chemistry, Cambridge, UK.

Jacob, D. J. (1999) *Introduction to Atmospheric Chemistry*. Princeton University Press, Princeton, NJ.

Jones, R. R. (1989) Consequences for human health of stratospheric ozone depletion. In: R. R. Jones and T. Wigley (Eds.), *Ozone Depletion: Health and Environmental Consequences*. John Wiley & Sons, Chichester, UK.

Krupa, S. (1998) *Elevated Ultraviolet (UV)-B Radiation and Agriculture*. Landes Bioscience & Springer, Austin, TX.

Lumsden, P. (1997) *Plants and UV-B: Responses to Environmental Change*. Cambridge University Press, Cambridge, UK.

Martens, P. (2014) *Health and Climate Change: Modelling the Impacts of Global Warming and Ozone Depletion*. Routledge, Abingdon, UK.

Peter, T. (1994) The stratospheric ozone layer – An overview. *Environmental Pollution*, 83: 69–79.

Ravishankara, A. R., Daniel, J. S., and Portmann, R. W. (2009) Nitrous oxide (N2O): The dominant ozone-depleting substance emitted in the 21st century. *Science*, 326(5949): 123–125.

Ravishankara, A. R., Hancock, G., Kawasaki, M., and Matsumi, Y. (1998) Photochemistry of ozone: Surprises and recent lessons. *Science*, 280: 60–61.

Rowland, F. S. (2006) Stratospheric ozone depletion. *Philosophical Transactions of the Royal Society*, B361(1469): 769–790.

Roy, C. R., Gies, H. P., and Tomlinson, D. W. (1994) Effects of ozone depletion on the ultraviolet radiation environment at the Australian stations in Antarctica. In: *Ultraviolet Radiation in Antarctica: Measurements and Biological Effects*, Antarctic Research Series 62: 1–15.

Rozema, J. (1999) *Stratospheric Ozone Depletion: The Effects of Enhanced UVB Radiation on Terrestrial Ecosystems*. Backhuys, Leiden, the Netherlands.

FOR REFERENCE PURPOSES ONLY

Russell Jones, R., and Wigley, T. (Eds.) (1989) *Ozone Depletion: Health and Environmental Consequences*. John Wiley & Sons, Chichester, UK.

Staehelin, J., Renaud, A., Bader, J., McPeters, R., Viatte, P., Hoegger, B., and Schill, H. (1998) Total ozone series at Arosa (Switzerland): Homogenization and data comparison. *Journal of Geophysical Research: Atmospheres*, 103(D5): 5827–5841.

Stockwell, W. R., Lawson, C. V., Saunders, E., and Goliff, W. S. (2012) A review of tropospheric atmospheric chemistry and gas-phase chemical mechanisms for air quality modeling. *Atmosphere*, 3: 1–32.

Stonehouse, B. (2009) *Arctic Air Pollution*. Cambridge University Press, Cambridge, UK.

Stratospheric Ozone Review Group (1988) *Stratospheric Ozone 1988*. HMSO, London, UK.

Stratospheric Ozone Review Group (1990) *Stratospheric Ozone 1990*. HMSO, London, UK.

Stratospheric Ozone Review Group (1996) *Stratospheric Ozone 1996*. Department of the Environment, London, UK.

Szopa, S., Aumont, B., and Madronich, S. (2005) Assessment of the reduction methods used to develop chemical schemes; Building of a new chemical scheme for VOC oxidation suited to three-dimensional multiscale HOx-NOx-VOC chemistry simulations. *Atmospheric Chemistry and Physics*, 5: 2519–2538.

Tedetti, M., and Sempéré, R. (2008) Penetration of ultraviolet radiation in the marine environment: A review. *Photochemistry and Photobiology*, 82(2): 389–397.

USEPA (2018) Clean Air Act Overview, US Environmental Protection Agency. https://www.epa.gov/clean-air-act-overview/.

van Loon, G. W., and Duffy, S. J. (2000) *Environmental Chemistry – A Global Perspective*. Oxford University Press, Oxford, UK.

Vernet, M., Brody, E. A., Holm-Hansen, O., and Mitchell, B. G. (1994) The response of Antarctic phytoplankton to ultraviolet radiation: absorption, photosynthesis and taxonomic composition. In: *Ultraviolet Radiation in Antarctica: Measurements and Biological Effects*, Antarctic Research Series 62: 1–15.

Ward, P. L. (2016) Ozone depletion explains global warming. *Current Physical Chemistry*, 6(4): 275–296.

Wayne, R. P. (2000) *Chemistry of Atmospheres*. Oxford University Press, Oxford, UK.

Webb, A. R. (2000) Ozone depletion and changes in environmental UV-B radiation, In: R. E. Hester and R. M. Harrison (Eds.), *Causes and Environmental Implications of Increased UV-B Radiation*. Royal Society of Chemistry, Cambridge, UK.

WMO (1999) *WMO global ozone research and monitoring report No 44, Scientific Assessment of Ozone Depletion: 1998*, World Meteorological Organisation, Geneva, Switzerland.

WMO (2002) *WMO global ozone research and monitoring report No 47. Scientific Assessment of Ozone Depletion: 2002* World Meteorological Organisation, Geneva, Switzerland.

WMO (2014) *Update on Global Ozone: Past, Present, and Future*. WMO Global Ozone Research and Monitoring Project Report No 55, World Meteorological Organisation, Geneva, Switzerland.

Zigman, S. (2008) Near UV light and cataracts. *Photochemistry and Photobiology*, 26(4): 437–441.

---

[1] Free Energy is a thermodynamic quantity given by the subtraction between the internal energy of a system and the product of its absolute temperature and entropy.

[2] A chromophore is the part of a molecule (atom or group of atoms) responsible for its colour. The colour arises when a molecule absorbs specific wavelengths of visible light and transmits or reflects others.

FOR REFERENCE PURPOSES ONLY

Chapter 13

Noise and light pollution

While the majority of topics covered in this book are central to air pollution, we thought it was appropriate to introduce briefly two related pollution issues which are synonymous with urban traffic and street environments. The first part of this chapter covers noise pollution, which is followed by a discussion on light pollution.

13.1 NOISE AS A POLLUTANT

Sound surrounds us daily and it would be difficult to live without it. Sound is a vibration that usually propagates as an audible mechanical wave of pressure and displacement through a medium such as air or water. *Noise* is defined as unwanted sound, which can cause irritation and stress. Noise is subjective, and different people react to it in different ways. What can cause annoyance to some people may be barely noticeable by others. It can interfere with normal activities such as sleeping or conversation, or even disrupt or diminish the quality of life. In extreme conditions, noise can cause physical damage to those affected. Noise pollution has received little attention compared to other types of pollution, such as air or water pollution. This is probably because it is not possible to see, taste or smell noise.

Noise can be classified into fairly broad categories:

- *Occupational noise*: Experienced at work
- *Neighbour noise:* Noise from inside and outside people's homes
- *Neighbourhood noise*: Arises within the community such as industrial and entertainment premises, trade and business premises, construction sites and noise in the street
- *Environmental* (*ambient*) *noise*: Noise arising from transport and industry

Noise pollution increases or decreases in accordance with the prevailing rate of pressure it exerts. Unlike air pollution, noise is transient; once the pollution stops, the environment is

FOR REFERENCE PURPOSES ONLY

free of it. This is not the case for chemicals, sewage, and other pollutants introduced into the air, soil or water. Most forms of pollution can be measured in that the amount of material which can be introduced into the environment before harm is done can be estimated. Individual sounds that may damage human hearing can be measured, but it is difficult to monitor cumulative exposure to noise or to determine just how much is too much.

The definition of noise itself is highly subjective. To some people, the roar of an engine is satisfying or thrilling whilst to others it is an annoyance. Loud music may be enjoyable or a torment, depending on the listener and the circumstances. In general, any form of unwelcome sound may be regarded as noise pollution, whether it is the roar of a jet plane overhead or the sound of a barking dog a block away. The actual loudness of a sound is only one component of the effect it has on human beings. Other factors include the time and place, the duration, the source of the sound, and whether the listener has any control over it.

13.2 TYPES OF NOISE POLLUTION

When assessing the impact of noise on human well-being, it is usually classified either as

- Occupational noise (i.e. noise in the workplace)
- Environmental noise (i.e. noise in all other settings, including domestic, residential or community, for example, music, sports, traffic, playgrounds, etc.)

The corresponding means to reduce noise pollution are described in Section 13.5.

13.2.1 Occupational

Noise-related hearing loss is a common occupational health issue. When workers are exposed to loud noise over a short period, this can cause a temporary change in hearing. Such temporary changes may include a ringing in the ears (tinnitus) and a feeling that ears have been blocked or *stuffed up*. Although short-term problems may dissipate within a few minutes or hours after leaving or removing the noise, recurrent exposures to loud noise can lead to permanent tinnitus and/or hearing loss.

Loud noise can interfere with communication and concentration, reduce productivity, generate physical and psychological stress, and be a factor in workplace accidents and injuries by making it difficult to hear warning signals. Other impacts of workplace noise may include hypertension, irritation/distraction, anxiety, reduced self-esteem, disturbance of psychosocial well-being, psychiatric disorders and social isolation. The effects of noise-induced hearing loss can be substantial, curbing one's ability to understand speech and/or hear high-frequency sounds, and seriously damaging an individual's capability to communicate and interact with others.

FOR REFERENCE PURPOSES ONLY

13.2.2 Environmental

As the world's population grows and we are living in increasingly higher-density urban areas, environmental noise has become a growing problem. Environmental noise typically includes:

- Transport (road vehicles, ships, trains, aeroplanes)
- Neighbourhood
  - Outdoor, for example, pumps, gardening equipment (lawnmowers, hedge-cutters, pressure hoses, sprinklers, etc.), do-it-yourself equipment/activities (drills, hammering, sawing, etc.)
  - Indoor (music, parties, appliances such as vacuum cleaners, etc.)
- Public works and services (roadwork, street cleansing, etc.)
- Industrial activities
- Construction work and sites
- Cultural, sporting and leisure activities
  - Fireworks
  - Music from clubs, concerts and festivals
  - Recreational vehicles (children's toys, motorcycles, snowmobiles, etc.)

13.3 MEASURING SOUND

Sound energy travels in waves and is measured in frequency and amplitude. Frequency is the number of sound vibrations in one second. A healthy ear can hear sounds from a very low frequency (20 Hz or 20 cycles per second) to a very high frequency (20,000 Hz); the human sensitivity is highest between 2000 and 5000 Hz (Figure 13.1a). The graph in Figure 13.1a is a frequency-weighting of sound pressure levels that mimics the sensitivity of the auditory system. (To put this in context, the lowest A key on the piano is 27 Hz. The middle C key on a piano creates a 262 Hz tone. The highest key on the piano is 4186 Hz.) Figure 13.1b illustrates the contextual dependence of whether or not a sound is perceived as a noise or not. For example, music at a rock concert is not perceived as a noise by the spectators, whereas residents at home in nearby houses may treat this as noise, even though sound pressure levels are much lower there.

Amplitude measures how forceful the wave is. It is measured in decibels (dBA) of sound pressure; 0 dBA is the softest level that a person can hear. Normal speaking voices are around 65 dBA. A rock concert can be about 120 dBA. The decibel scale is logarithmic, not arithmetic. A doubling of sound intensity is not represented as a doubling of the decibel level. An increase of just 3 dB means twice as much sound, and an increase of 10 dB means ten times as much sound. However, the perception of loudness by the human ear is not directly proportional to the decibel level. For example, a sound 10 dB greater than another is not perceived as being ten times as loud but only about three times as loud.

FOR REFERENCE PURPOSES ONLY

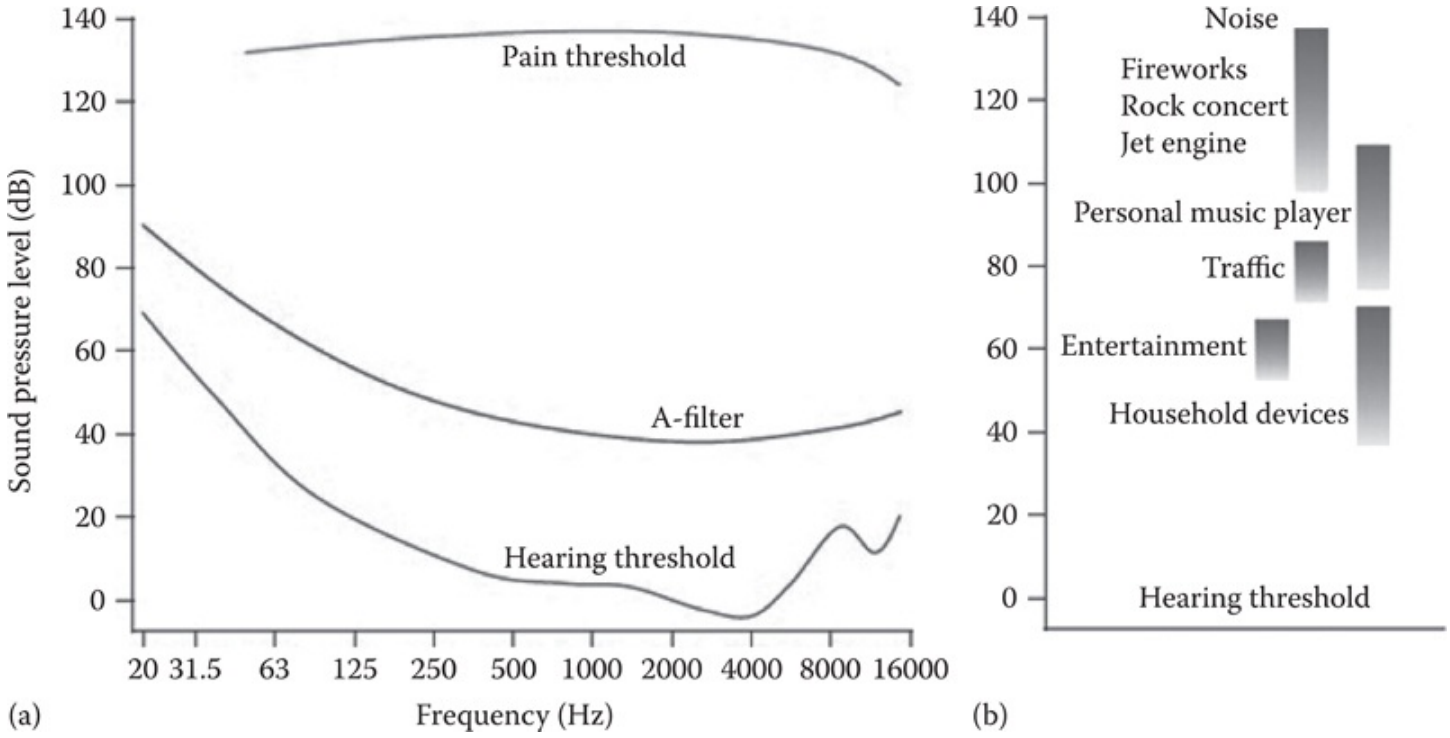

Figure 13.1 Sound pressure levels for – (a) acceptable hearing and pain thresholds; (b) different environmental noises. (From Basner, M. et al., *Lancet*, 383, 1325–1332, 2014.)

Sound meters and noise-recording equipment are used when a recording of noise needs to be made in order to follow a noise complaint or where examples of noise are required, for example, for a court case. Environmental health practitioners use equipment that meets the standards set in the International Standard IEC 61672-1 (IEC, 2002). This standard gives electro-acoustical performance specifications for three kinds of sound measuring instruments:

- A conventional sound-level meter that measures exponential time-weighted sound level
- An integrating-averaging sound-level meter that measures time-average sound level
- An integrating sound-level meter that measures sound exposure level

A single instrument may make any, or all, of the three kinds of measurements. Two performance categories, class 1 and class 2, are specified. In general, specifications for class 1 and class 2 sound-level meters have the same design goals and differ mainly in the tolerance limits and the range of operational temperatures. Tolerance limits for class 2 specifications are greater than, or equal to, those for class 1 specifications.

The standard is applicable to a range of designs for sound level meters. Examples include self-contained handheld instruments with an attached microphone and a built-in display device, or separate components in one or more enclosures. They may be capable of displaying a variety of acoustical signal levels. Sound-level meters may include extensive

FOR REFERENCE PURPOSES ONLY
analogue or digital signal processing, separately or in combination, with multiple analogue and digital outputs. They may also include general-purpose computers, recorders, printers and other devices that form a necessary part of the complete instrument. The UK's Health and Safety Executive (HSE) provides noise exposure calculators that help you work out your daily and weekly noise exposure, and estimate the performance of hearing protection (HSE, 2011).

13.4 NOISE AND HEALTH

Studies have shown that there are direct links between noise and health (Niemann and Maschke, 2004). Noise-induced hearing loss (NIHL) is the most common and often discussed health effect, but other problems related to noise include stress-related illnesses, high blood pressure, speech interference, hearing loss, sleep disruption and lost productivity. Figure 13.2 shows some of the adverse reactions to health caused by noise. Noise can cause sleep disturbances. Acute sleep disturbances effect performance and, in the long run, health. For adults this elevates the risk of disease in the cardiovascular system, the respiratory system and the musculoskeletal system as well as increasing the risk of depression. Many of these diseases increase with age and therefore they only rarely appear in children. Children do have a significantly elevated risk, however, of respiratory system diseases and also migraines. Annoyance is the most prevalent noise impact affecting the well-being and health of large number of people. Severe damage can cause loss of hearing ability, and people may also suffer a permanent sensation of ringing in the ears, known as tinnitus.

The World Health Organisation (WHO) definition of *deafness* refers to the complete loss of hearing ability in one or two ears. The cases included in this category are those having hearing loss more than 90 dB in the better ear (profound impairment) or total loss of hearing in both the ears. The WHO definition of *hearing impairment* refers to both complete and partial loss of ability to hear (WHO, 2010). Instant hearing damage can be caused by very loud or explosive noises. Because permanent hearing loss is usually a long-term process, it is impossible to know at exactly what point noise becomes loud enough to cause damage to the ears. Hearing loss caused by exposure to noise at work is a significant occupational disease. Over 170,000 people in the UK suffer deafness, tinnitus or other ear conditions as a result of exposure to excessive noise at work.

FOR REFERENCE PURPOSES ONLY

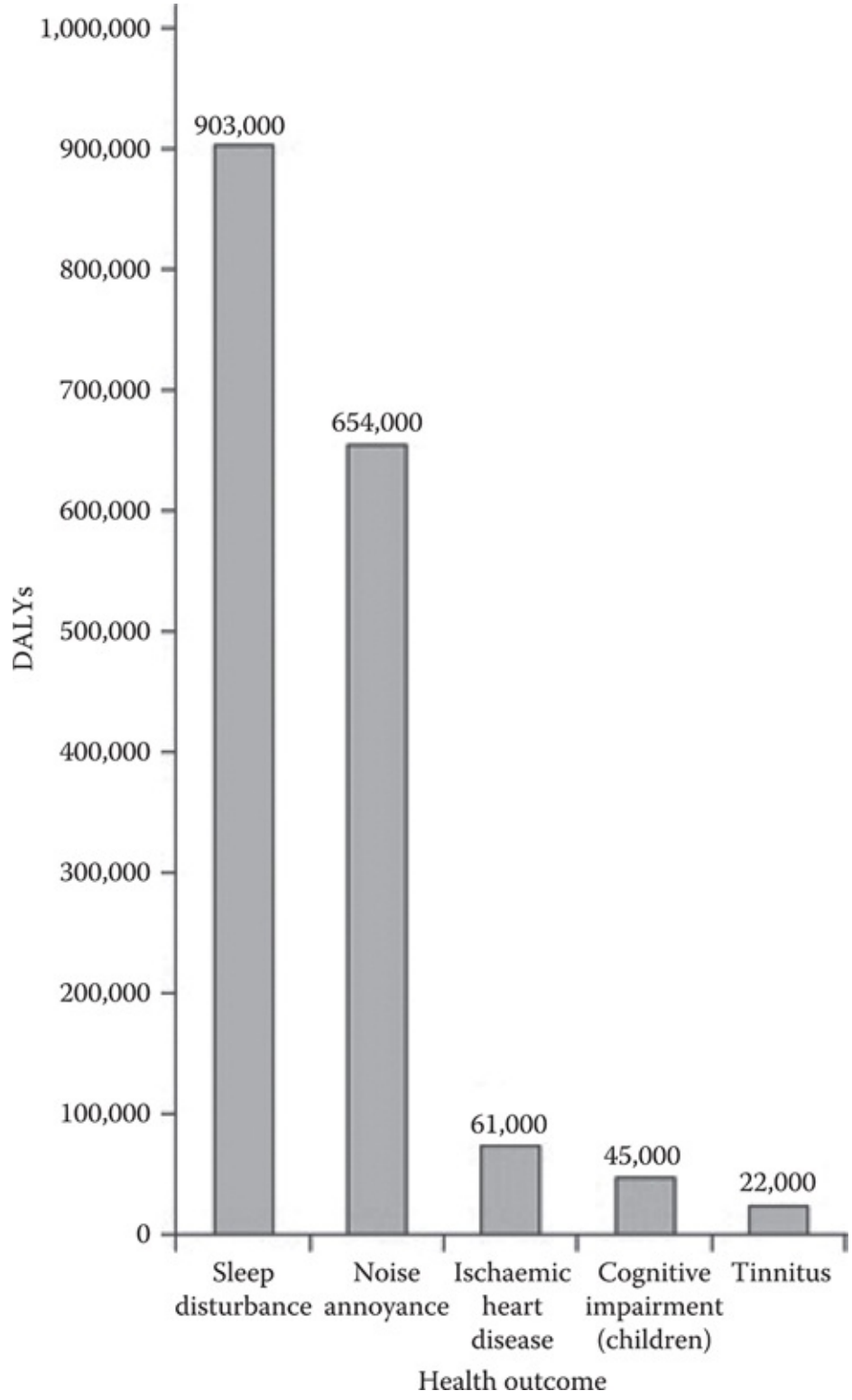

Figure 13.2 Disability-Adjusted Life Years (DALYs) attributed to environmental noise exposure in Europe. (From Basner, M. et al., *Lancet*, 383, 1325–1332, 2014.)

Table 13.1 Summary of effects and threshold levels for effects where sufficient evidence is available

Effect	*Threshold, dB*

FOR REFERENCE PURPOSES ONLY

Biological effects	Change in cardiovascular activity	–[a]
	Electroencephalogram (EEG) awakening	35
	Motility, onset of motility	32
	Changes in duration of various stages of sleep, in-sleep structure and fragmentation of sleep	35
Sleep quality	Waking up in the night and/or too early in the morning	42
	Prolongation of the sleep inception period, difficulty getting to sleep	–[a]
	Sleep fragmentation, reduced sleeping time	–[a]
	Increased average motility when sleeping	42
Well-being	Self-reported sleep disturbance	42
	Use of somnifacient drugs and sedatives	40
Medical conditions	Environmental insomnia[b]	42

Source: WHO, *Night Noise Guidelines for Europe*, World Health Organization Regional Office for Europe, Copenhagen, Denmark, 2009.

[a] Although the effect has been shown to occur or a plausible biological pathway could be constructed, threshold levels could not be determined.

[b] Note that *environmental insomnia* is the result of diagnosis by a medical professional whilst *self-reported sleep disturbance* is essentially the same, but reported in the context of a social survey. Number of questions and exact wording may differ.

Factors that contribute to hearing damage are noise levels and the length of time people are exposed to the noise, daily or over a number of years (Table 13.1).

13.5 REDUCTION OF NOISE POLLUTION

There are many ways of reducing noise and noise exposure – often a combination of methods works best. First, if realistic, the loud noise should be removed altogether. If that is not possible, the noise should be controlled at the source as much as possible, such as by redesigning the workplace and reorganising working patterns. Individuals can take many steps to protect themselves from the harmful effects of noise pollution. If people must be around loud sounds, they can protect their ears with hearing protection, such as earplugs or ear muffs.

13.5.1 Occupational noise

The most efficient and effective way of controlling noise in a work environment is by technical and organisational means that protect workers at the source. These methods can include the following:

- Replace the noise source with something that is less noisy.
- Change the processes – such as avoiding metal-on-metal impacts, for example, line chutes with abrasion-resistant rubber, and reduce drop heights.

- Reduce vibration reduced (damping).
- Fit silencers to air exhausts and blowing nozzles.
- Limit the time workers spend in noisy areas.
- Modify the paths by which the noise travels through the air to the people exposed, for example:
  - Enclosures erected around machines to reduce the amount of noise emitted into the workplace or environment.
  - Barriers and screens used to block the direct path of sound.
  - Noise sources positioned further away from workers.
  - The use of absorptive materials within the building to reduce reflected sound.
  - Noisy machinery and processes kept away from quieter areas.
  - Workflow designed to keep noisy machinery out of areas where people spend most of their time.

13.5.2 Household and neighbourhood noise

Although the amount of noise made by any one person or household may seem negligible, it can make a real difference to the comfort of neighbours and even other members of the household. The following simple measures can easily be taken by individuals to reduce annoyance:

- Position noisy household equipment (e.g. washing machines) away from partition walls.
- When buying a new household appliance, ask how noisy it is. If people opt for quiet appliances, manufacturers will make them!
- Perform noisy do-it-yourself (DIY) jobs during normal waking hours.
- Apologise to neighbours in advance for disturbance caused by DIY.
- Keep the volume of TV, radio and music as low as possible, especially late at night. If you want to turn the volume up, use headphones (but be careful not to deafen yourself!).
- If your dog barks when left alone, arrange to leave it with a friend.
- If you have an old or faulty burglar alarm, replace it with one complying with up-to-date standards, such as the British Standard BS 4737. Notify the local authority that you have an alarm and register a key holder.
- If you have a party, tell your neighbours in advance, and keep the noise to a minimum.
- If using fireworks for a celebration, tell neighbours, especially if they have pets.

13.5.3 Environmental noise

There are three main approaches to reduce environmental noise:

FOR REFERENCE PURPOSES ONLY

The *first* approach entails reducing noise at its source. This usually involves using quieter working methods or technologies. For example, noise from motor vehicles is usually controlled by law and should meet national and/or internationally recognised vehicle noise emission standards. Transport noise can also be reduced at the source by laying noise absorptive materials on road surfaces to reduce road/tyre interaction noise.

The *second* approach entails reducing noise through the transmission path. For example, noise from transport may be reduced by screening roads from residential housing via noise barriers (e.g. fences) and enclosures (e.g. sound blankets), vegetation (e.g. trees, bushes, earth bunds), noise-tolerant building (e.g. car parks), architectural features (e.g. fins and balconies) and podium decking (noise dampening). In addition, careful land-use planning can be used to avoid busy roads slicing across residential developments or coming too close to sensitive uses. Such methods can pre-empt noise problems at the design stage. Other options to avoid or minimise transport noise may include siting roads underground or adopting alternative transport methods such as cycle paths.

The *third* approach involves protecting people at the receiver end. This can involve use of glazed window insulation and noise cladding on walls or positioning noise sensitive areas (e.g. bedrooms) so that they face away from noise sources. This approach may prevent, for example, an *open-window* lifestyle, and thus it is habitually used as last resort.

However, there is no easy solution to some environmental noise issues, including traffic noise. Quieter road surfaces, quieter tyres, noise barriers or traffic management can all help reduce traffic noise but none of these are quick to implement. People living alongside new or improved roads in the UK may be eligible for noise insulation grants if the traffic is causing excessive noise. If a property depreciates in value because of noise arising from a road/aerodrome construction or alteration, the owner may be entitled to compensation.

Many people living near civil and military airports are severely affected by regular *aircraft noise*, mainly during take-off and landing. The impact is greatest near the perimeter of the airport and below flight paths. For example, the UK government only has direct responsibility for aircraft noise management at Heathrow, Gatwick and Stansted airports. Measures introduced to reduce noise include noise preferential routes and restrictions on night flying. Maximum noise limits for departing aircraft are set and monitored, and noise insulation schemes are in operation. Noise from aircraft on the ground is the responsibility of the airport management company. To comply with the EU Environmental Noise Directive, operators of airports with over 50,000 movements a year are responsible for drawing up noise action plans.

Railway noise is the dominant source of noise for most people living near railways. If particular trains are causing a problem, complaints should be addressed to the company operating the train in question. To comply with the EU Environmental Noise Directive, for railways with over 30,000 movements, noise action plans should be drawn up – in the UK,

FOR REFERENCE PURPOSES ONLY

this would be by the Secretary of State.

Fireworks have become an increasing noise problem for people and pets. They are let off for celebrations year-round. In the UK, Fireworks Regulations of 2004 prohibits anyone under 18 from possessing a firework, and anyone except professionals from possessing display fireworks. They also prohibit the use of fireworks between 11:00 pm and 7:00 am except for Chinese New Year, Diwali, New Year's Eve and Bonfire Night. Since January 2005 only licensed traders can supply fireworks year-round. Unlicensed traders can only sell them for short periods around the festivals mentioned earlier. (Chapter 6 provides details on air pollution from fireworks.)

13.6 NOISE LEGISLATION AND REGULATION

Noise in the workplace (i.e. occupational noise) is regulated in many areas of the world. However, environmental, neighbour and neighbourhood noise is not so well regulated. Many guidelines have been issued to help reduce and control the problem. The need for *health-based* guidelines originated in part from the European Union Directive 2002/49/EC (EU Directive, 2002) relating to the assessment and management of environmental noise (commonly known as the Environmental Noise Directive [END]) which compels European Union member states to produce noise maps and data about night exposure.

Noise management is a complex issue and at times requires complex solutions. Unlike air quality, regulation on noise is still not stringent enough, although there can be specific local limits for specific developments. As discussed earlier, sound only becomes noise (often defined as *unwanted sound*) when it exists in the wrong place or at the wrong time such that it causes or contributes to some harmful or otherwise unwanted effect, such as annoyance or sleep disturbance. Unlike many other pollutants, noise pollution depends not just on the physical aspects of the sound itself but also on the human reaction to it. Consequently, the Noise Policy Statement for England (NPSE) (DEFRA, 2010) provides a clear description of desired outcome from the noise management of a particular situation.

13.6.1 Occupational noise

The aim of noise regulations is to ensure that workers' hearing is protected from excessive noise at their workplace, which could cause them to lose their hearing and/or to suffer from tinnitus. The regulations do not apply when the general public is exposed to noise from non-work activities, or when people make an informed choice to go to noisy places. In the UK, the 2005 Noise Regulations (UK Regulation, 2005) replaced the 1989 Noise Regulations (UK Regulation, 1989) and introduced new requirements for action to be taken by employers. Both the 1989 and the 2005 sets of noise regulations are based on European Union directives requiring similar basic laws throughout the EU on protecting workers from the health risks caused by noise.

FOR REFERENCE PURPOSES ONLY

Under these regulations, employers have a duty to assess noise levels. The level at which employers must provide hearing protection and hearing protection zones is 85 dBA (daily or weekly average exposure), and the level at which employers must assess the risk to workers' health and provide them with information and training is 80 dBA. There is also an exposure limit value of 87 dBA, taking account of any reduction in exposure provided by hearing protection, above which workers must not be exposed.

In the US, the Environmental Protection Agency (EPA) has established 70 dBA as a safe average noise level for a 24-hour day (This figure is based only on the risk to hearing and does not take into account other health factors such as loss of sleep.) As sound intensity doubles with every increase of 3 dB, the time of safe exposure would be cut in half with each such increase. Thus a worker should wear ear protection if exposed to a steady 75 dBA for eight hours, 78 dBA for 4 h, and so on. Brief exposure to noises of up to 100 dBA is not considered risky, provided the average remains within the prescribed levels.

13.6.2 Environmental, neighbour and neighbourhood noise

The EU Environmental Noise Directive sets out a programme for EU member states to map noise in densely populated areas and from major roads, airports and railways. Information from the noise maps will be used to introduce plans to manage noise in mapped areas where it is judged necessary and to prevent specified quiet areas from getting noisier. Measures must be taken to reduce, on a prioritised basis, the harmful effects of environmental noise (noise from transport and industrial activity). The UK does not have a consolidated body of legislation on noise pollution. The following list provides some selected pieces of legislation that deal with noise pollution:

- The Environment Protection Act 1990 (EPA).
- The Control of Pollution Act 1974 (COPA). Part III provides legislative controls for construction site noise and certain levels of street noise. See also noise abatement zones in Section 13.6.4.
- The Noise and Statutory Nuisance Act 1993 contains amendments to the EPA and COPA and also deals with noise from vehicles, burglar alarms and street equipment. Part III treats noise as a statutory nuisance and extends to noise nuisance from vehicles (e.g. car alarms but not traffic noise), machinery and other equipment such as loudspeakers, in the street.
- The Noise Act 1996 criminalises certain forms of night-time noise and gives local councils power to confiscate certain kinds of noise-making equipment.
- The Clean Neighbourhoods and Environment Act 2005 (CNEA) amends the Noise Act 1996 and grants Local Authorities with powers to investigate complaints from residents about excessive night noise coming from licensed or residential permits.
- The Housing Act 1996 and the Crime and Disorder Act 1998 both tackle anti-social behaviour including excessive noise.

- The Pollution Prevention and Control Act 1999 provides Local Authorities and the Environment Agency with powers to control emissions from industrial processes including noise emissions.
- The Criminal Justice and Police Act 2001 amends the Licensing Act of 1964 and gives the police summary powers to close a licensed premise that is causing excessive noise.
- Anti-Social Behaviour Act 2003 provides powers to close down noisy premises if they cause a public nuisance.
- Firework Act 2003 and Fireworks Regulations 2004 both provides controls on the use of fireworks, especially in public places. These prohibit the use of fireworks between 11:00 pm and 7:00 am except for Chinese New Year, Diwali, New Year's Eve and Bonfire Night.

13.6.3 Building and planning guidelines

Building development is regulated in the UK by requiring that construction meets certain standards, including sound insulation standards. In England, there is also statutory planning guidance (UK Government [1994]) in relation to noise. The guidance note includes the following:

- Wherever practicable, noise-sensitive developments should be separated from major sources of noise such as road, rail and air transport and certain types of industrial development.
- New development involving noisy activities should, if possible, be sited away from noise-sensitive land uses.
- Where it is not possible to achieve such a separation of land uses, local planning authorities should consider whether it is practicable to control or reduce noise levels, or to mitigate the impact of noise, through the use of conditions or planning obligations.
- In the case of residential developments, the guidance note sets out noise exposure categories, which are designed to help local planning authorities in their consideration of applications for development near transport-related noise sources.

13.6.4 Noise abatement zones

Under the Control of Pollution Act 1974, a local authority may designate all or part of its area as a noise abatement zone (NAZ). When a NAZ is in operation, the local authority records the levels of noise from specified premises – these may be factories or commercial or domestic premises. The register is open to public inspection, and once a noise has been registered, it can only be exceeded with the local authority's consent. Noise reductions can be sought later if it is in the public interest and can be achieved at reasonable cost. This covers inherently noisy operations – building works, roadwork, demolition, dredging, and

so on. Under the Control of Pollution Act 1974, Local Authorities can serve a notice imposing requirements as to how the construction works should be carried out to minimise noise. The environmental health department sets noise limits, taking into account the character of the local area. Anyone intending to carry out construction work may apply in advance for a consent. Compliance with the terms of a notice or consent does not rule out proceedings by an individual on the grounds of noise nuisance under section 82 of the Environmental Protection Act 1990.

13.6.5 Night-time noise

The Anti-Social Behaviour Act 2003 amended and the Noise Act 1996 enable Local Authorities in England and Wales to tackle night-time noise emitted from dwellings and gardens between the hours of 11:00 pm and 7:00 am To enforce these powers, Local Authorities must ensure that an environmental health officer takes reasonable steps to investigate complaints about noise emitted from dwellings. If the officer is satisfied that noise exceeds the permitted level, a warning notice may be served on the person responsible. If the warning is ignored, the officer may issue a fixed penalty notice of £100, enter the dwelling and confiscate the noise-making equipment (obstructing confiscation carries a fine of up to £1000), or prosecute (fine up to £1000). An extension of the Noise Act came into force in February 2008, enabling Local Authorities in England and Wales to tackle night-time noise from licensed premises.

13.6.6 Road traffic

This is one of the most widespread sources of noise and unfortunately the most difficult to control. Research shows that over 40% of the population are bothered by noise from road traffic. The noise made by individual vehicles is limited by the Road Vehicles (Construction and Use Regulations) 1986. Vehicles must be fitted with an efficient exhaust silencer, and there are general regulations requiring road users not to make excessive noise or run the engine unnecessarily when stationary.

Noise from motor horns is regulated by the Road Traffic Act 1972. Horns may not be sounded in a restricted road between 11:30 pm and 7:00 am and not by a stationary vehicle unless there is a danger to another moving vehicle. Private vehicles must not be fitted with a gong, bell, siren or two-tone horn. Offenders should be reported to the police.

The Land Compensation Act 1973 and the Noise Insulation Regulations 1975 and 1996 allow for grants for the cost of sound insulation in premises subjected to noise from new or upgraded roads or railways which result in excessive noise levels beyond stated thresholds.

13.6.7 Loudspeakers and burglar alarms

The use of loudspeakers in the streets is banned in the UK between 9:00 pm and 8:00 am

(the police, ambulance and fire brigade are exempt). Local Authorities can license use of loudspeakers outside these hours, for example for entertainment but not for advertising purposes or electioneering. Vehicles selling perishable foods may use loudspeakers between 12:00 noon and 7:00 pm, and these times can be varied with local authority consent.

Under the Clean Neighbourhoods and Environment Act 2005, Local Authorities in England and Wales can designate all or part of their area as an *alarm notification area*. Anyone responsible for premises in a designated area where an intruder alarm is installed must nominate a key holder and notify the local authority. The key holder should live nearby, be able to gain access and know how to silence the alarm if it goes off accidentally. Failure to register a key holder may result in a fine. If an alarm (whether in a designated area or not) has been sounding continuously for 20 min or intermittently for more than an hour, and is judged to be giving reasonable cause for annoyance (and, in a designated area, reasonable steps have been taken to contact the nominated key holder), an authorised officer of the local authority can enter the premises to silence the alarm. If entry can only be gained by force, a warrant is required.

13.6.8 Handling noise nuisance

A nuisance is often difficult to establish but, generally speaking, if something is unreasonable to the average person, a court might decide it is a statutory nuisance. The law empowers Local Authorities in the UK to deal with noise from fixed premises (including land) if they consider that the noise amounts to a statutory nuisance. Proceedings may be taken against noise from factories, shops, pubs, dwellings and stationary vehicles. People with a complaint about noise pollution are encouraged to approach whoever is responsible for the noise and explain the problem. People causing the noise often do not realise they are causing a disturbance. The majority of noise complaints are resolved informally.

Many areas in the UK have mediation services that can help resolve noise disputes. This often proves quicker than the legislative route and is useful where there is a problem, but a statutory nuisance cannot be proved. The local authority should be able to provide information about local mediation services if they are available in the area. Complaints to the environmental health department of a UK local authority must be investigated. If it is agreed that the noise is a nuisance, the offender is contacted, informally at first, but with an abatement notice if necessary. If the offender fails to comply with the notice, proceedings can be taken in the Magistrates Court (Sheriff Court in Scotland) under section 82 of the Environmental Protection Act 1990 or an injunction sought in the High Court.

13.7 LIGHT AS A POLLUTANT

Artificial light is used for many purposes, such as safely performing tasks, illuminating information and enhancing the aesthetic appearance of buildings. However, artificial light

FOR REFERENCE PURPOSES ONLY

that is allowed to illuminate, or intrude upon, areas not intended to be lit is called *light pollution*. This also includes light that needlessly shines up into the sky. This is mainly an issue in developed countries with a developed infrastructure. The Reading for the Really Inspired Pun (2007) shows a survey of light pollution in Hong Kong. This report also outlines the use of sky quality meters and their use by the amateur astronomy community to help complete the survey of the illumination of the night sky, or sky glow, in Hong Kong. Figure 13.3 shows how a streetlight can cause light pollution. The four components of light pollution are often combined and overlap, as shown in Table 13.2.

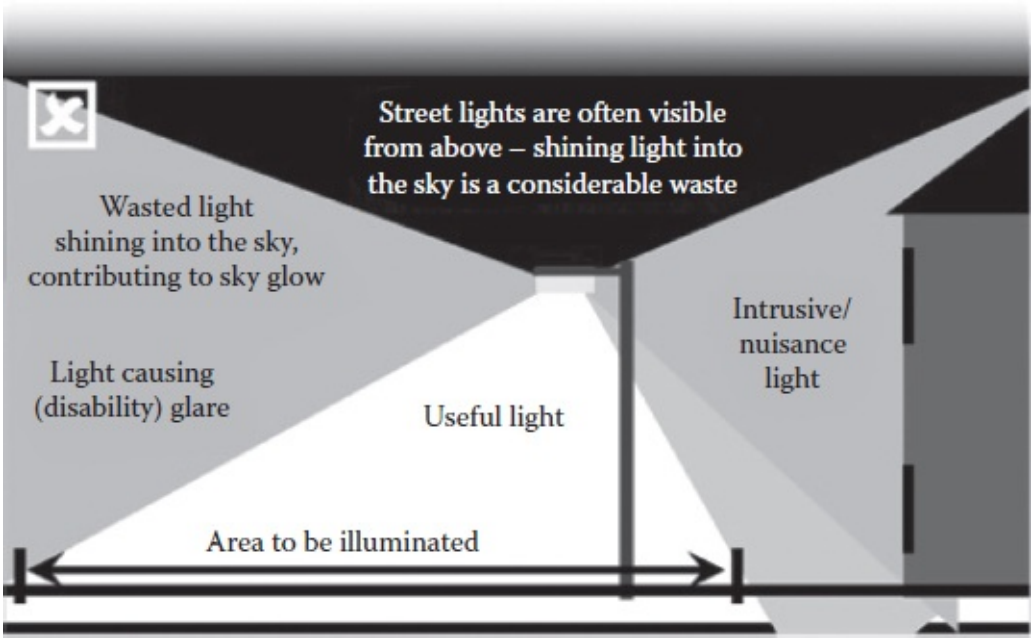

Figure 13.3 Typical inefficient street lighting showing a sag lens non-cut-off lamp. (From Commission for Dark Skies, *Lighting Guidelines*, British Astronomical Association.)

Table 13.2 The four components of light pollution and their effects

Type of light pollution	*Description*	*Example of effect*	*Example*
Intrusive light or light trespass	The intrusion of bright or poorly directed lights onto a neighbouring property.	Reduces neighbours' right to enjoy their own property. Can cause health problems.	Inconsiderately directing a security light so that it shines into a bedroom window.
Sky glow	The brightening of the night sky over inhabited areas.	Wastes energy. Disturbs natural cycles of animals, birds and insects. Reduction in number of stars visible. Disrupted circadian rhythm.	Unshielded outdoor lights, such as floodlights, security lights or streetlights.
Glare	Excessive brightness which causes visual	Lights have blinded drivers,	Security lights shining into roads.

FOR REFERENCE PURPOSES ONLY

	discomfort. High levels of glare can decrease visibility.	pedestrians and aircraft pilots. Produce high-contrast shadows, which can become corridors of darkness – hiding places for potential criminals.	
Clutter	Bright, confusing and excessive groupings of light sources, commonly found in overly lit urban areas. The proliferation of clutter contributes to sky glow, trespass and glare.	Can make driving difficult and cause distraction.	Billboards and outdoor signs are designed to attract our attention. Often these are lit up with bright flashing lights. These light sources add considerably to the overall light pollution.

It is difficult to measure light trespass because the occurrences are so different. Illuminance on a vertical plane, such as through a window, may be appropriate in some cases. Horizontal illuminance might be appropriate in other cases, for example, on a bed. An illuminance level of 1 lux (0.1 footcandle) might be acceptable to some and completely objectionable to others. For reference, 0.3 lux (0.03 footcandle) is typical of the illuminance that results from moonlight (Lighting Research Center, 2011).

Inefficient lighting can cause the following problems:

- *Reduced health*:
  - Light at night can disrupt the body's production of the essential hormone melatonin, which in turn increases the risk of developing breast cancer.
  - Intrusive light at night also leads to restless nights and psychological stresses.
- *Economic losses*:
  - Over £1bn per annum is wasted in the UK through inefficient outdoor lighting.
- *Environmental impacts*:
  - A vast amount of carbon dioxide is needlessly pumped into the atmosphere to generate the electricity that is wasted by inefficient lighting
  - Lights at night have a detrimental effect on nocturnal wildlife that has evolved to take advantage of the night (e.g. bats, moths, etc.), and also keep daytime creatures (such as birds) awake throughout the night, without rest. Most of the world's species are nocturnal.
- *Crime*:
  - Lighting can assist criminals in what would otherwise be unfamiliar territory.
- *Dangers*:
  - Fatal accidents have occurred when lights have blinded drivers, pedestrians and aircraft pilots.
  - People drive faster under lit roads, and accidents often involve impact with street lighting columns.

Growth in artificial lighting is linked closely to economic and urban development, especially in rapidly developing parts of the world. Europe has experienced a marked net

FOR REFERENCE PURPOSES ONLY

increase in night-time light pollution as satellite images first became available in the 1970s (Figure 13.4). However, while several Asian countries have seen rapid increase in bright spots over megacities, the economically developed European countries, including Sweden, Finland, Denmark, Norway, the United Kingdom, Belgium and Northern Germany, are apparently experiencing detectable localised declines in brightness. The latter impact of alleviation in artificial light pollution is considered as a consequence of sustainability initiatives in these countries while delivering cost and energy-saving benefits.

The first UK law tackling light pollution came into force on 6 April 2006. Exterior lighting joined noise and smells on the list of things that can be treated as a statutory nuisance under the Environmental Protection Act 1990. These are things against which, in the UK, the local council's environmental health department can take legal action. The law (Section 102 of the Clean Neighbourhoods and Environment Act 2005) makes 'exterior light emitted from premises so as to be prejudicial to health or a nuisance' a criminal offence. The law does not tackle all forms of light pollution, only incidents of particularly bad lighting from some types of premises which cause people real nuisance. *The Campaign for Dark Skies* (CfDS) is not anti-lighting but anti-bad-lighting! The aim of the CfDS is to preserve and restore the beauty of the night sky by campaigning against excessive, inefficient and irresponsible lighting that shines where it is not wanted nor needed. The CfDS actively encourages the use of efficient, good quality lighting. Outdoor lighting does not need to be turned off to reduce light pollution – it just needs to be directed to where it is needed.

FOR REFERENCE PURPOSES ONLY

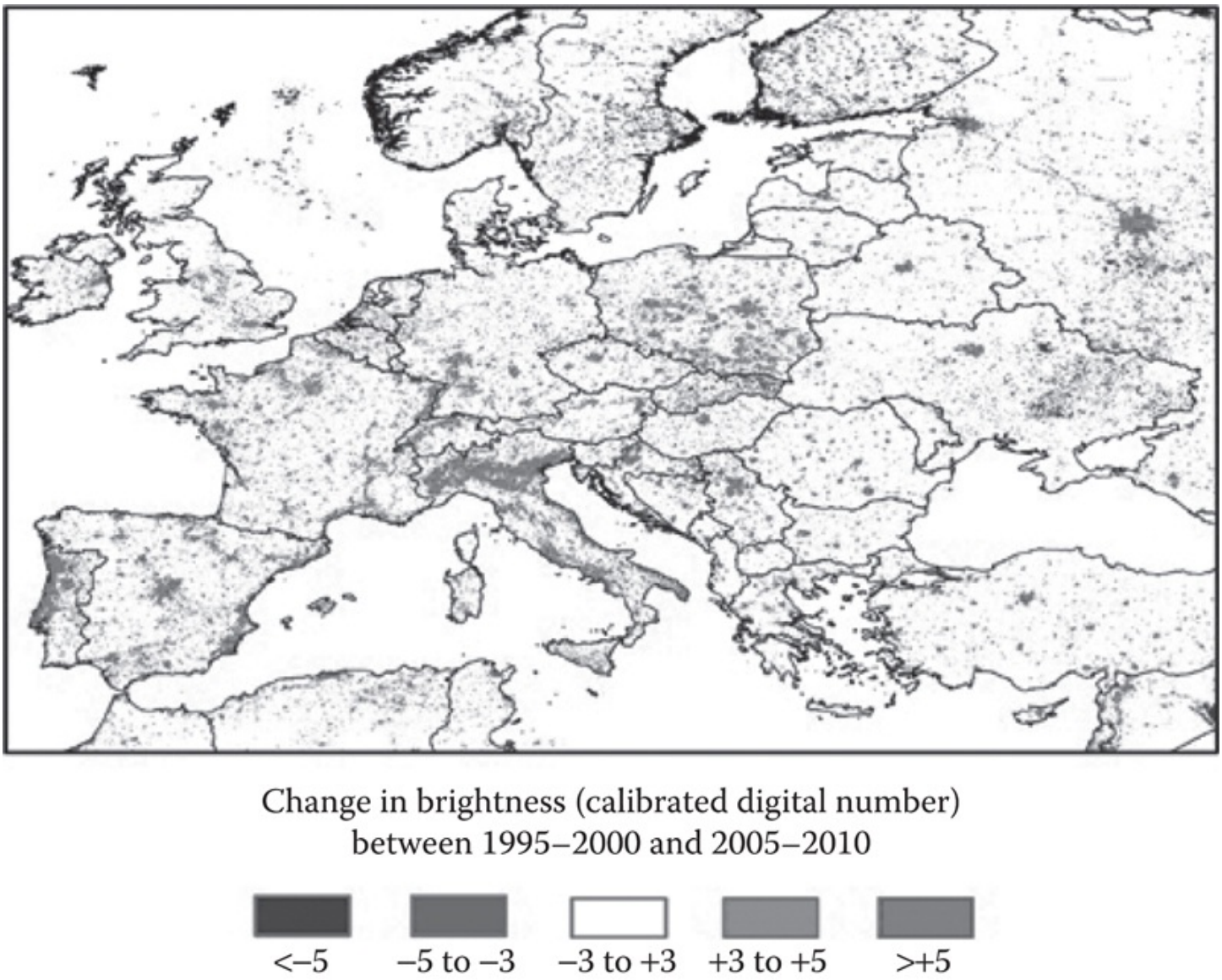

Figure 13.4 Ten-year change in brightness, calculated as the difference in mean values for the periods 2005–2010 and 1995–2000. (Grey areas are saturated throughout the time period, so trends cannot be detected; From Bennie, J. et al., *Sci. Rep.*, 4, 3789, 2014.)

13.8 MEASURING LIGHT POLLUTION

Measuring light pollution is a challenging task because many factors play a role in sky glow. As well as considering the light pollution source, other influences include light reflected from the ground and its angular distribution, the atmospheric effects of humidity and the interaction of light with aerosols, all of which can alter from one second to the next. In recent years, many amateur and professional astronomers have recorded sky brightness measurements to monitor the increase in sky brightness. For example, the International Dark Sky Association (IDSA) initiated the *Globe at Night* programme, an international

FOR REFERENCE PURPOSES ONLY

citizen-science campaign to raise public awareness of the impact of light pollution. The IDSA's programme uses so-called *citizen-scientists* (i.e. civic volunteers that partner with scientists to answer real-world questions) to measure night sky brightness and subsequently submit their observations from a computer or smart phone. These observations are used to create regional and global maps of sky glow as part of a light pollution awareness campaign. From these data, a number of methods have been developed to estimate sky glow. A study analysed satellite images of European night-time lights over 15 years using an innovative technique to show the continental trends in observed brightness between 1995 and 2010, capturing the complex regional patterns from expansion of the European Union and disintegration of the Soviet Union over this period (Bennie et al., 2014).

13.9 LIGHT POLLUTION AND HEALTH

Humans evolved to the diurnal sequence of day and night and exposure to the natural light-dark cycle. This contributes to the *circadian rhythm* – a 24-hour internal clock that runs in a human brain and cycles between alertness and sleepiness at regular intervals (the wake/sleep cycle). However, the spread of artificial lighting means that most humans no longer experience genuinely dark nights because of the prevalence of night-time artificial light. Human bodies produce the hormone melatonin in response to circadian rhythm. Melatonin has antioxidant properties; induces sleep; lowers cholesterol; boosts the immune system; and helps the functioning of the pancreas, thyroid, ovaries, testes and adrenal glands. Research has indicated that night-time exposure to artificial light suppresses melatonin production and that this can adversely affect human health, increasing risks for depression, obesity, sleep disorders, diabetes, and others. There are some indications that exposure to blue light at night is particularly harmful. This is of concern because most light-emitting diodes (LEDs) used for outdoor lighting, televisions, computer screens and other electronic displays produce intense blue light.

Plants and animals also depend on Earth's light-dark cycle to govern life-sustaining behaviours such as reproduction, nourishment, sleep and protection from predators. Evidence suggests that night-time artificial light has negative effects on many creatures including plants, birds, mammals, insects and amphibians. Artificial light can have drastic effects on nocturnal ecology as prey species use darkness as cover, predators use light to hunt, and many insects are drawn to light. Artificial light can cause them to change their behaviour, leading to their early death. A well-known example is that of sea turtle hatchlings that are drawn away from the sea by artificial lights towards urban areas where they rapidly perish. Excessive and wasteful use of artificial lighting can have significant negative economic, environmental and social consequences, including increases in vandalism and graffiti and reduction of safety by making victims and property easier to view.

FOR REFERENCE PURPOSES ONLY

13.10 CASE STUDY – NOISE POLLUTION IN KOLKATA

The prevalence of deafness in South-East Asia ranges from 4.6% to 8.8% of the total population. Kolkata (previously known as Calcutta) is the first city to legislate noise pollution in India. It is one of the oldest metropolitan cities in the Indian subcontinent and was the capital city of India during the British Empire. Due to the rapid population growth and the resulting traffic over the past century, the city transport infrastructure has come under immense pressure from regular traffic congestion and consequent noise pollution. Kolkata has been considered the noisiest city among all metro cities in India. The problem has a historical bearing: in 1970 Narayan Ganguly, a Bengali author, wrote the following phrases on noise pollution in his satirical column for a literary magazine: 'Even today, there was no respite from the demonic duet of loud music and firecrackers'. In the late 1990s for the first time in India, use of microphones was banned during night hours—from 9 pm to 7 am.

13.10.1 The major sources

There are two major sources of noise pollution in Kolkata – traffic noise and festival noise (includes fireworks used). Moving traffic and unnecessary honking (horns) are the major contributors to ambient noise pollution across Kolkata. They shoot up the decibel level of busy traffic. Many auto-rickshaw and motorbike drivers use shrill hooters. Besides heavy movement of lorries, aircraft, railways and increase in construction activities also add to the growing noise pollution in certain parts of the city, especially on the outskirts. An investigation was undertaken to map the spatial change in noise pollution across the city between 2007 and 2012, mainly to understand the split in noise characteristics between north and south Kolkata (Table 13.3). Overall, noise level has increased during the summer months in most places (shown as positive changes) during this period, with more locations lying in south Kolkata. Within the city, the southern part of Kolkata is much noisier in comparison to the central and northern parts of the city. This is mainly attributed to the slow traffic moving zone in this part of the city, where volume of traffic, honking events and chaotic traffic situations are always alarming. The highest and lowest average traffic noise have been found during the years 2011 and 2012. The highest and lowest average noise values were 71.8 and 70.8 dBA, respectively.

Table 13.3 Change in noise level in Kolkata between 2007 and 2012

FOR REFERENCE PURPOSES ONLY

	Winter (January) (%)				Summer (June) (%)			
Locations	Peak		Non-peak		Peak		Non-peak	
A. North Kolkata	Day	Night	Day	Night	Day	Night	Day	Night
Shyambazar	0.3	2.1	−0.9	0.3	−0.6	−0.4	−1.2	0.7
Ultadanga	−2.3	−2.1	−3.8	−3.6	−2.4	−1.5	−0.8	−5.0
Maniktola	1.2	0.0	0.9	1.2	−1.5	3.1	1.2	−3.1
Hatibagan	−0.4	−0.1	−1.2	1	−2.9	−1.6	−2.8	−0.7
Baghbazar	2.4	3.6	0.0	−1.5	−2.0	−0.4	−5.4	−2.2
Rajabazar	4.6	3.2	2.9	3.6	0.1	1.8	6.2	1.5
Chitpur	0.9	2.7	1.2	−0.1	−0.1	5.2	−2.6	−1.7
B. South Kolkata	Day	Night	Day	Night	Day	Night	Day	Night
Kidderpore	−0.8	−4.7	−1.8	1.4	2.4	1.5	0.5	1.5
Behala	4.3	5.0	0.8	0	2.1	1.4	0.5	0.5
Garia	2.1	4.2	−4.1	4.7	9.0	6.7	0.5	1.5
Rashbehari	1.5	−0.6	1.7	2.8	6.0	5.1	−2.8	−0.4
Hazra	3.9	2.8	2.0	−1.6	4.2	4.3	0.6	−1.6
Ballygunge	−4.0	−0.4	−0.3	−1.1	7.3	3.4	−1.1	−4.0

Source: Chakraborty, A., Noise pollution: Its magnitude and control in the city of Kolkata, PhD thesis, University of Calcutta, West Bengal, India, http://hdl.handle.net/10603/164802, 2013.

13.10.2 Health impacts

Noise-induced hearing loss (NIHL) is commonly found in public transport and auto-rickshaw operators, as well as among factory workers with regular contact with moving machine parts and thus constantly exposed to 100 dBA of noise, for example, at a welding factory. Common occurrences include cases of tinnitus (i.e. symptoms of irritating ringing in the ears), sudden deafness (medically known as sensory-neural hearing loss) and more severe impacts such as heart disease and cognitive impairment. Health effects of festival noise (e.g. loudspeakers during Durga Puja) on children, mainly children within the age group of 6–14 years, have been studied. The cases of fatigue among children are the highest in number in almost all study sites of the city. It was followed by cases of low blood pressure. The highest frequency of auditory problem has been reported from the study sites of central Kolkata (Chakraborty, 2013).

Fifty percent of NIHL is preventable. Acute noise-related health impacts can be prevented by improving one's diet. Dietary supplements rich in antioxidants can protect hair cells in the inner ear. Food rich in beta-carotene, vitamins C and E, and magnesium protect from threshold shifts. In the workplace environments, use of ear plugs and muffs is a sound protective measure.

FOR REFERENCE PURPOSES ONLY

13.10.3 Mitigation measures

Lack of awareness about noise pollution and lack of rigorous implementation of noise reduction measures are the key issues which need attention, both to reduce regular sources from traffic and industrial noise and periodic hikes in noise pollution during festival seasons and fireworks displays. To reduce traffic noise pollution, it is necessary to first identify the traffic noise hot spots in the city. On the basis of these hot spots, noise risk zones need to be prepared. Based on these noise hot spots and their requirements, proper legislations and policies need to be framed and implemented. Noise enclosures or barriers can be effective along busy roads. Choice of soundproof building materials in residential units or high-rise buildings is also recommended. Use of green infrastructure can also reduce urban noise level up to a specific standard.

According to the West Bengal Pollution Control Board (WBPCB), the noise level in Kolkata dropped by about 10 dBA from 1994 to 2009. But it is not enough compared to the ambient noise standards. The impact of a rise in noise level is visible countrywide. Indian Standards: 1884–1993 sets 125 dBA as the maximum decibel limit for horns used in commercial vehicles; 105 dB is the maximum limit for horns of two-wheelers. Its violation can lead to seizure of the driver's licence. However, to avoid unnecessary honking, a proper traffic signalling system is needed, and pedestrians should carefully cross the road, preferably through zebra lines. To control the extreme noise level, the Indian Ministry of Environment and Forest (MOEF) has implemented many laws under Article 21 to minimise noise levels in the country. The judiciary's commitment should not to be confined in minimisation of festival noise levels; rather it should give attention towards noise-producing vehicles, air horns and workshops within the city periphery. Under the Motor Vehicles Act, use of loud air-pressure horns in trucks and buses is banned. The government of India has launched the National Programme for Prevention and Control of Deafness (NPPCD), which is being implemented at the primary healthcare level and focuses on reducing deafness and prevention of future hearing loss in India.

REFERENCES AND FURTHER READING RESOURCES

Babisch, W. (2002) The noise/stress concept, risk assessment and research needs. *Noise & Health*, 4(16): 1–11.

Basner, M., Babisch, W., Davis, A., Brink, M., Clark, C., Janssen, S., and Stansfeld, S. (2014) Auditory and non-auditory effects of noise on health. *The Lancet*, 383(9925): 1325–1332.

Bennie, J., Davies, T. W., Duffy, J. P., Inger, R., and Gaston, K. J. (2014) Contrasting trends in light pollution across Europe based on satellite observed night time lights. *Scientific Reports*, 4: 3789.

Bondello, M. C. (1976) The effects of high-intensity motorcycle sounds on the acoustical sensitivity of the desert iguana, Dipsosaurus dorsalis. M.A. thesis, California State University, Fullerton, CA, 37 pp.

Bondello, M. C. and Brattstrom, B. H. (1979) The experimental effects of off-road vehicle sounds on three species of desert invertebrates. Report to the Bureau of Land Management, p. 61.

Chakraborty, A. (2013) Noise pollution: Its magnitude and control in the city of Kolkata. PhD thesis, University of Calcutta, West Bengal, India. http://hdl.handle.net/10603/164802.

Commission for Dark Skies. (2017) *Lighting Guidelines*. British Astronomical Association, London, UK.

DEFRA (2010) *Noise Policy Statement for England* (*NPSE*). Department for Environment, Food and Rural Affairs,

FOR REFERENCE PURPOSES ONLY

London, UK.

Derbyshire, D. (2008) End of the dawn chorus: How noise pollution is driving out birds from towns and cities. *Daily Mail*, Science Tech. article – 546488, 26 March 2008.

European Parliament (2002) Directive relating to the assessment and management of environmental noise, 2002/49/EC, Brussels, European Union.

Fletcher, J. L. (1980) Effects of noise on wildlife: A review of relevant literature 1971–1978. *Third International Congress on Noise as a Public Health Problem*, Rockville, MD.

Fletcher, J. L. (1990) Review of noise and terrestrial species: 1983–1988. In: Berglund, B., and Lindvall, T. (Eds.), *Noise as a Public Health Problem Vol. 5: New Advances in Noise Research Part II*, pp. 181–188. Swedish Council for Building Research, Stockholm, Sweden.

Friis, R. H. (2007) *Essentials of Environmental Health*, 1st ed. Jones & Bartlett, Sudbury, MA.

Frumkin, H. E. (2010) *Environmental Health: From Global to Local*, 2nd ed. Jossey-Bass, San Francisco, CA.

Fure, A. (2006) Bats and lighting. *The London Naturalist*, vol. 85.

Harder, B. (2002) Deprived of darkness: The unnatural ecology of artificial light at night. *Science News*, 161(16): 248. doi:10.2307/4013350.

Harrison, M. E. (2001) *Pollution: Causes, Effects and Control*, 4th ed. Royal Society of Chemistry, Cambridge, UK.

HSE (2005) *Controlling Noise at Work*. Health and Safety Executive. Office of the Scientific Assistant and Office of Noise Abatement and Control (1981) – Fort Walton Beach, Florida, EPA 500-9-82-106.

HSE (2008) *Noise at Work – Guidance for Employers on the Control of Noise at Work Regulations 2005*. Health and Safety Executive. Office of the Scientific Assistant and Office of Noise Abatement and Control (1981) – Fort Walton Beach, Florida, EPA 500-9-82-106.

HSE (2011) Exposure calculators and ready-reckoners. http://www.hse.gov.uk/noise/calculator.htm.

Huseynov, R. (2010) *Noise and Light Pollution*. Committee on the Environment, Agriculture and Local and Regional Affairs, Strasbourg, France.

IEC (2002) *International Standard IEC 61672-1, Electroacoustics – Sound Level Meters*. International Electrotechnical Commission, Geneva, Switzerland.

National Park Service (1994). Report on Effects of Aircraft Overflights on the National Park System. Report to Congress.

Niemann, H. and Maschke, C. (2004). WHO LARES: Final Report – Noise effects and morbidity, WHO Europe, pp. 1–20.

Office of the Deputy Prime Minister (2004). Reducing adverse effects of public development – Mitigation works. Office of the Deputy Prime Minister, London, UK, 04PD02635/5.

Office of the Scientific Assistant and Office of Noise Abatement and Control (1981). *Noise Effects Handbook. A Desk Reference to Health and Welfare Effects of Noise*. U.S. Environmental Protection Agency.

Scottish Executive (2007) *Guidance Note Controlling Light Pollution and Reducing Lighting Energy Consumption*. Scottish Executive, Edinburgh, Scotland.

Suter, A. H. (1991) Noise and its effects. *Administrative Conference of the United States*, Montpelier, US.

UK Regulation (2005) *The Control of Noise at Work Regulations 2005*. UK Government.

UK Regulation (1989) *The Noise at Work Regulations 1989*. UK Government.

UNEP (2008) *Governments and Wildlife Groups Take Soundings on Noise Pollution and Ship Strike Threats to Whales and Dolphins*. United Nations Environmental Program, Nairobi, Kenya.

WHO (2009) *Night Noise Guidelines for Europe*. World Health Organization Regional Office for Europe, Copenhagen, Denmark.

WHO (2010) World Health Organization. Deafness and Hearing Impairment – Fact sheet, April 2010.

Worthington, D. (2003) *Dictionary of Environmental Health*. Spon Press, London, UK.

FOR REFERENCE PURPOSES ONLY

Chapter 14

Air quality standards and legislations

14.1 WHY DO WE NEED AIR QUALITY STANDARDS?

Air quality standards are emission rates or concentrations or deposition rates that are designed to protect people and the environment from harm. The Earth's atmosphere is one of the global commons – those regions, which also include Antarctica, the ocean floor and outer space, over which no one nation has individual control. There is clear distinction between *airspace*, which is the 3D volume extending from the surface of a nation up to the top of the atmosphere, and the air that flows through it. Although each nation has sole responsibility for its own airspace, it has joint responsibility for the air within it.

A variety of different philosophies has been used to control air pollution. They fall into three general categories. Historically, the philosophy has focused on emissions standards, the assumption being that if we set appropriate maximum emission concentrations, then ambient concentration targets can be achieved. In Europe and the United States, legislation has been framed in terms of *air quality standards* (AQS) – potential new emitters have to show that their emissions will not cause AQS to be exceeded. On a larger scale, the critical loads and levels approach (see Chapter 10) is a more recent concept that relates the maximum deposition fluxes of gaseous and liquid pollutants to their effects on local ecosystems. The concept depends on sophisticated dispersion modelling to calculate the maximum emissions that can be accepted if critical loads and levels at a given receptor site are not to be exceeded.

There is a common thread to these ideas. It is assumed that exposure to a pollutant stresses an organism, and that the organism's natural repair processes can make good any damage provided that the exposure does not rise above some threshold value. This threshold value, sometimes divided by some arbitrary *safety* factor such as 2 or 10, can then be set as the standard. Although this idea is convenient for both scientists and legislators, it seems increasingly likely that organisms do not respond in such a straightforward fashion and instead show some response, however small, at all concentrations. Whether such responses are economically and socially significant then becomes a matter of comparing the risk from that pollutant against the other risks to which the population is exposed.

FOR REFERENCE PURPOSES ONLY

Very often receptors that are superficially similar (whether they are people, animals, plants or materials) display a very wide range of responses between sensitive and resistant. Standards are usually set to protect the most sensitive receptor.

If there were precise concentrations at which such harm was observed to occur, then setting the standards would be straightforward. Unfortunately life is never that simple. As a perfect recent example – the UK High Court ordered the government to amend its 2015 Air Quality Plan in 2017 on the basis that it was based on *over-optimistic modelling*. In this chapter, we will review the limits that have been set in different parts of the world.

14.1.1 Estimation of standards

It is often not possible to determine whether short-term experimental responses result in long-term health effects. In addition, the responses depend not only on the concentration but on the period over which it occurs. A statistical indicator, such as the 98th percentile of daily means, then has to be determined and agreed upon. In some cases (e.g. with particles and SO_2), there may be synergism between pollutants so that standards for one cannot be considered without regard to the other. For carcinogenic or genotoxic materials, it is thought that just one molecule can initiate a cancer, so that there is no safe limit. Instead, the standard is expressed in terms of a risk of cancer formation per population per unit time at a given concentration.

Inputs to the standard-setting process come from two main sources:

- Observations of the short-term or long-term impact of environmental pollutants; actual incidents that result in human morbidity or mortality, or quantifiable damage to a receptor; epidemiological studies of populations or other targets.
- Specific experiments under controlled conditions. These might involve experiments on laboratory animals that then have to be interpreted for humans, or studies on a small number of plant species that have to represent the whole gamut of possible plants.

Increasingly, the powerful computer models that have been developed to understand the relationships between the many interacting variables are also being used to determine standards. Emission limits for sulphur and nitrogen are calculated from dispersion, deposition and critical load models; emission limits of ozone precursors are calculated from dispersion and critical level models; and reductions in chlorofluorocarbon (CFC) release rates set from models of ozone destruction in the stratosphere.

Different organisations have independently evaluated the evidence on different pollutants and arrived at somewhat different standards. The World Health Organisation (WHO), the European Union (EU), United Nations Economic Commission for Europe (UNECE) and the United States Environmental Protection Agency (USEPA) have been the most influential groups. Various terms such as standards, guidelines and limit values are used by different organisations. European Union limit values are mandatory and must be met by the member

states, while guide values only give guidance. Standards (or EU directives) can contain both limit and guide values. WHO guideline values have no statutory basis but are widely used by governments to assess the impact of pollutants for which there are no national standards.

14.2 UK AIR QUALITY LEGISLATION

14.2.1 Background

In order to regulate pollution across the media boundaries, the UK Environment Agency (EA) was established in 1995. This was followed by the Pollution Prevention and Control Act (PPCA) legislation in 1999, which brought into force in the UK EU Directive 96/91 on integrated pollution prevention and control (IPPC). The IPPC philosophy is to target all emissions into all environmental media, so that it embraces not only air, soil and water but waste generation and energy efficiency as well.

The large-scale processes come under the central (Environment Agency) control, and smaller ones remain under the control of Local Authorities for planning and operational purposes. Within a local authority, businesses whose premises produce pollution are known as *installations*. These installations are one of the following:

- Part A2, sectors regulated under integrated pollution prevention and control, known as Local Authority Industrial Pollution Prevention and Control (LA-IPPC)
- Part B, known as Local Air Pollution Prevention and Control (LAPPC)

For example, a major iron and steel works using 100-t electric arc furnaces would have to meet EA standards for emissions, whereas small furnaces (<7 t), of which there might be many around a manufacturing centre such as Birmingham, are regulated by the local authority.

New installations have been subject to IPPC regulation since 1999, while existing ones had to be brought within IPPC by 2007. Each process operator must apply to the appropriate regulator (Environment Agency or Local Authority in England and Wales, Scottish Environmental Protection Agency in Scotland) for a permit to operate. If granted, the permit includes a set of emission limit values (ELVs) for the relevant pollutants, identifies best available technologies (BATs) to ensure the necessary level of environmental protection and specifies the monitoring that must be done to confirm compliance. IPPC targets toxic pollutants rather than climate change – for example, carbon dioxide is not on the list of pollutants that should be considered, although it would be affected by controls on energy efficiency.

In the PPCA, *best available techniques not entailing excessive cost* (*BATNEEC*) must be employed. This philosophy (with the T standing for *technology* rather than *techniques*) was first used in EC Directive 84/360/EEC, which limited emissions from large industrial plants. The BAT part covers both the process itself – the technology – and the operating

FOR REFERENCE PURPOSES ONLY

practices. Thus, it includes factors such as staff numbers, working methods and training. The NEEC part in BATNEEC implies a level of judgement as to whether the extra cost of a higher emission standard is warranted, or indeed supportable by the financial strength of the organisation. There are around 80 process guidance notes, which set out not only the BATNEEC for specific processes but also give emission limits, the timetable for bringing old plants up to the control standard required of new plants, and details of any relevant environmental quality standards or EU legislation. These process guidance notes are available for a wide range of processes, from animal carcass incineration to tobacco processing, from bitumen processing to vegetable matter drying. Clearly, the words such as *best* and *excessive* used in BATNEEC are to some degree open to judgement and have to be interpreted with caution. Emission limits are specified as a mass concentration of the pollutant per unit volume of gas. For particles in general, the limits are designed to make the emission invisible – for low-volume emissions of coarse particles, 0.46 g m^{-3} might be adequate, reducing to 0.115 g m^{-3} for large volume flow rates carrying fine material (the arbitrary-looking values are derived from old Imperial units – they were originally specified as whole numbers of grains per cubic foot). In individual cases, for example, when there is an unusually large volume flow rate, a lower limit such as 0.070 g m^{-3} might be set. For toxic materials, whether particles or gases, the limits are based on dispersion calculations designed to reduce the ground-level concentration to some small fraction of the occupational exposure limit for that material, or the prevailing air quality limit value, as appropriate. Emissions to the atmosphere may also be considered within a wider regulatory process involving planning permission from Local Authorities, environmental impact assessment, environmental management systems and environmental auditing.

Although industrial emissions have been controlled by national legislation since 1863, no systematic action was taken against domestic emissions until much later. Following investigation by the Beaver Committee of the pollution smog in London in December 1952, the Clean Air Act was passed in 1956. This was extended in 1968, and both acts were consolidated into the Clean Air Act 1993. The main provisions of the 1993 act are to control the emission of dark and black smoke from chimneys; to control the emission of smoke, grit, dust and fumes from boilers and processes not regulated by the EA; to control the heights of new industrial chimneys; and to require the use of smokeless fuel in domestic grates in urban areas. Emission of dark smoke is generally prohibited. However, it is recognised in the act that such emissions are technically unavoidable when lighting up small boilers from cold, and three standards of emission limit must be met. For example, an aggregate of 10 min in any period of 8 h is permitted from a chimney serving a single furnace, provided that no dark smoke emission involves a continuous period of more than 4 min or an aggregate of more than 2 min of black smoke in any 30-min period. In addition to the earlier emission regulations, certain other forms of air pollution control fall within the Clean Air Act – the lead content of petrol, sulphur content of gas oil and fuel oil, and cable burning.

Increasingly, UK legislation has been influenced by the overarching EC directives. The

FOR REFERENCE PURPOSES ONLY

EEC had historically taken an approach to air pollution based on air quality standards rather than emission limits – EU legislation on air quality, such as 80/779/EEC on SO_2 and suspended particulates, is implemented in the UK through Air Quality Standards Regulations. The regulations are identical in most respects to their EU counterparts, except that local provisions (called derogations) are incorporated. For example, a number of districts in the UK were allowed additional time to meet the required suspended particulate levels, provided that they submitted detailed plans in advance of how this was to be achieved.

A revised National Emission Reduction Plan came into force in September 2007. In England and Wales this followed the introduction of the EU Industrial Emissions Directive (Section 14.6), which transposed into legislation by the Environmental Permitting (England and Wales) (Amendment) Regulations 2013. In Scotland and Northern Ireland, IED was brought into effect by the Pollution Prevention Control (Scotland) Regulations 2012 and the Pollution Prevention and Control (Industrial Emissions) Regulations (Northern Ireland) 2013.

14.2.2 UK National Air Quality Strategy

The first air quality strategy was adopted in the UK in early 1997. This was later replaced by the National Air Quality Strategy (NAQS), which was published in January 2000. This NAQS worked in a timeframe up to 2005, and set out both the *standards* for air pollutants and *objectives* to be achieved within a specified time, after allowing for costs and benefits as well as feasibility and practicality. The strategy identified actions at local, national and international level to improve air quality. NAQS 2000 has now been replaced with the Air Quality Standards Regulations 2010, which contains targets for reductions in the concentrations of nine major pollutants, to be achieved between 2010 and 2020. These are summarised in Table 14.1. The values largely reflect the conclusions of detailed previous reviews by the expert panel on air quality standards (EPAQS).

As a landmark ruling, the UK High Court imposed a legal obligation under the Air Quality Standards Regulation for the government to put in place a legally compliant air quality plan, mainly for meeting the NO_2 standards (in 2019). But the NAQS goes much further than that, because it lays out the ways in which NAQS is influenced by, and interacts with, other legislation and programmes. These include public transport provision, reduction of traffic congestion, bicycle tracks, road user charging and workplace parking levies. Some Local Authorities are implementing Low Emission Zones (LEZs) to limit access by bad emitters. Such a control system might be based on the Euro standards (Stages 1–5) achieved by vehicles. Some minor tax incentives have also been brought in to favour smaller engine sizes. In 2007 the UK government announced that it would consider the case for incentivising the early uptake of Euro 5 (and subsequently Euro 6) technology through Company Car Tax and other instruments.

FOR REFERENCE PURPOSES ONLY

Table 14.1 UK national air quality objectives

National air quality objectives and target values for the protection of human health				
Pollutant	*Applies to*	*Objective*	*Concentration measured as*	*Date to be achieved and maintained thereafter*
Particles (PM_{10})	UK	50 μg m^{-3}, not to be exceeded more than 35 times a year	24 h mean	31 December 2004
	UK	40 μg m^{-3}	Annual mean	31 December 2004
	Scotland	50 μg m^{-3}, not to be exceeded more than 7 times a year	24 h mean	31 December 2010
	Scotland	18 μg m^{-3}	Annual mean	31 December 2010 2020
Particles ($PM_{2.5}$) exposure reduction	UK (except Scotland)	25 μg m^{-3}		
	Scotland	10 μg m^{-3}		31 December 2020
	UK urban areas	Target of 15% reduction in concentrations at urban background	Annual mean	Between 2010 and 2020
Nitrogen dioxide	UK	200 μg m^{-3} not to be exceeded more than 18 times a year	1 h mean	31 December 2005
		40 μg m^{-3}	Annual mean	31 December 2005
Ozone (O_3)	UK	100 μg m^{-3} not to be exceeded more than 10 times a year	8 h mean	31 December 2005
SO_2	UK	266 μg m^{-3} (100 ppb) not to be exceeded more than 35 times a year	15 min mean	31 December 2005
	UK	350 μg m^{-3} (132 ppb) not to be exceeded more than 24 times a year	1 h mean	31 December 2004
	UK	125 μg m^{-3} (47 ppb) not to be exceeded more than 3 times a year	24 h mean	31 December 2004
Polycyclic aromatic hydrocarbons (PAHs)	UK	0.25 ng m^{-3} (expressed as B[a]P, that is, concentration of Benzo(a)pyrene)	As annual average	31 December 2012
Benzene	UK	16.25 μg m^{-3} (5 ppb)	Running annual mean	31 December 2003
	England and Wales	5 μg m^{-3}	Annual average	31 December 2010
	Scotland, Northern Ireland	3.25 μg m^{-3}	Running annual mean	31 December 2010
1,3-butadiene	UK	2.25 μg m^{-3} (1 ppb)	Running annual mean	31 December 2003
Carbon monoxide (CO)	UK	10 mg m^{-3}	Maximum daily running 8 h mean (in Scotland as running 8 h mean)	31 December 2003
Lead	UK	0.5 μg m^{-3}	Annual mean	31 December 2004
		0.25 μg m^{-3}	Annual mean	31 December 2008
National air quality objectives and target values for the protection of vegetation and ecosystems				

NO_x	30 µg m^{-3} (16 ppb)	Annual mean	31 December 2000
SO_2	20 µg m^{-3} (8 ppb)	Annual mean	31 December 2000
	20 µg m^{-3} (8 ppb)	Winter average	31 December 2000
Ozone: protection of vegetation and ecosystems	Target value of 18,000 µg m^{-3} based on AOT40 to be calculated from 1-hour values from May to July, and to be achieved, so far as possible by 2010	Average over 5 years	1 January 2010

14.2.2.1 Additional measures

The NAQS also considers what additional measures might be needed in the longer term to bring the concentration targets below the objectives and meet the standards. The following problem pollutants were identified:

- NO_2, which is unlikely to meet the objectives in dense urban areas or at busy roadsides. The main mechanism for further improvement was thought to be local traffic management.
- O_3 is certainly the most intractable pollutant. The NAQS objectives are currently being exceeded across most of the UK, and computer models of O_3 formation indicate that large reductions in precursor emissions, of the order of 50% or more across the whole of Europe, will be needed to meet the standards.

It is estimated that by around 2050, levels of nitrogen dioxide in London could be reduced by approximately 55% and 70% below 2007 values at background and roadside locations, respectively. Also, over the same period, levels of fine particles ($PM_{2.5}$) in London could potentially be reduced by up to 55% at urban background locations and up to 63% beside the most polluted roads. Both these scenarios assume improvements in emissions of toxic pollutants from energy generation and from the road transport sector.

14.2.3 Local Air Quality Management

The UK Environment Act 1995 and the European Air Quality Directive (1996/62/EC) led to the establishment of the Local Air Quality Management (LAQM) processes in the UK. Local Authorities (LAs) must conduct a review and assessment of air quality in their area, in the light of the objectives set in the NAQS. There is extensive guidance provided by the UK Department for Environment, Food and Rural Affairs (DEFRA) to help LAs carry out their responsibilities. The necessary first stage of such a review is an initial screening of all pollution sources (mainly road transport and industry) that could have a significant impact within each LA's area, and a collation of all relevant existing data. It was expected that some LAs would be able to complete this first stage simply by accessing the national database. For other LAs, additional basic monitoring and/or modelling would be needed. Second and third stages may be required if local air quality is falling short of the objectives.

Second- and third-stage reviews involve increasingly intensive consideration of locations that are at risk of not meeting the NAQS objectives for any of the prescribed pollutants, together with more sophisticated modelling and monitoring.

If the third-stage review shows that prescribed air quality objectives are not likely to be met by the appropriate dates, the authority must designate an Air Quality Management Area (AQMA) and work out an action plan which will achieve the air quality objectives. Such a plan would take into consideration the relevant local circumstances (meteorology, topography, densities of people and vehicles, specialised sources etc.) in a cost-effective manner. There are many elements that the action plan might include, such as low-emission zones in the city centre, roadside testing of vehicle emissions, increased park and ride provision, increased city centre parking charges, workplace parking levies, traffic management improvements, increased bus lanes. By itself, each of these changes would only have a small impact on air pollution, but collectively they would not only reduce concentrations but, perhaps more significantly, change the public attitude towards pollutant emissions.

14.3 EU AIR QUALITY LEGISLATION

The EU requires its member states to divide their territory into specified zones and agglomerations and to undertake assessments of air pollution levels using measurements and modelling and other empirical techniques. Legislation has been framed in terms of two categories: limit values, and target (or guide) values. Under EU law a limit value is legally binding from the date it enters into force, subject to any exceedances permitted by the legislation. A guide value is to be attained as far as possible by the attainment date and so is less strict than a limit value. The central piece of legislation is the Air Quality Framework Directive (96/62/EC) on air quality assessment and management. Twelve air pollutants are identified for which limit values will be required, and provision is made for a sequence of daughter directives which address these specifically. The 12 air pollutants are those that have been examined by EPAQS (except for 1,3-butadiene), plus cadmium, arsenic, nickel and mercury. The first daughter directive, on SO_2, NO_2, particulate matter and lead, was adopted in April 1999 and entered into force in July 1999 (99/30/EC). Member states had to implement the directive within 2 years. The second daughter directive (2000/69/EC) covered CO (to be met by 2005) and benzene (2010). The third daughter directive required ozone standards corresponding to those set by the WHO to be met by 2010. The Ambient Air Quality and Cleaner Air for Europe (CAFE) Directive (2008/50/EC) entered into force on 11 June 2008.

As part of the continuing CAFE programme, the EU has proposed a revision of the National Emissions Ceilings Directive (NECD) setting new ceilings for 2020. The NECD 2016/2284/EU replaces Directive 2001/81/EC; it focuses on the reduction of national emissions of certain atmospheric pollutants and sets binding emissions ceilings to be

achieved for the following five pollutants: SO_2, NO_x, non-methane volatile organic compounds (NMVOCs), NH_3 and fine particulate matter. These are considered key pollutants responsible for acidification, eutrophication and ground-level ozone pollution which lead to significant negative impacts on human health and the environment. The new directive also transposes the reduction commitments for 2020 taken by the EU and its member states under the revised Gothenburg Protocol (discussed in Section 14.4) and sets more ambitious reduction commitments for 2030 to cut the health impacts of air pollution by half compared with 2005.

In 2008 the European Commission introduced Council Directive (2008/50/EC) concerning IPPC. The framework directive envisages two types of air quality objectives. The normal one is the limit value, defined as:

> a level fixed on the basis of scientific knowledge with the aim of avoiding, preventing or reducing harmful effects on human health and/or the environment as a whole, to be attained within a given period and not to be exceeded once attained.

There are also additional $PM_{2.5}$ objectives, targeting the exposure of the population to fine particles. These objectives are set at the national level and are based on the average exposure indicator (AEI) (Table 14.2). AEI is determined as a 3-year running annual mean $PM_{2.5}$ concentration averaged over the selected monitoring stations in agglomerations and larger urban areas, set in urban background locations to best assess the $PM_{2.5}$ exposure to the general population.

For ozone, in recognition of the transboundary regional nature of this gas, target values can be set instead of limit values. Target values must be met by states if possible. If they cannot be met, the EC will evaluate whether additional measures are necessary at EU level (Table 14.2). There are currently no EU limit or target values for ammonia.

14.4 UNITED NATIONS COMMISSION FOR EUROPE

The United Nations Economic Commission for Europe (UNECE) is an organisation of 34 countries that includes the United States, the EU and many non-EU countries in Europe. UNECE has been at the forefront in identifying environmental issues and working out measures to ameliorate them. The measures are formulated in terms of protocols and conventions. Although these are not legally binding, countries that ratify them are under a strong moral obligation to achieve the identified pollution control targets.

Table 14.2 EU Air Quality Directive (2008/50/EC) concentrations

Pollutant	*Concentration*	*Averaging period*	*Legal nature*	*Permitted exceedances each year*
Fine particles	25 μg m^{-3}[c]	1 year	Target value entered into force 1 January 2010	N/A

FOR REFERENCE PURPOSES ONLY

($PM_{2.5}$)			Limit value entered into force 1 January 2015	
$PM_{2.5}$ exposure concentration obligation	20 μg m^{-3}[d] (AEI)	Based on 3-year average	Legally binding in 2015	N/A
$PM_{2.5}$ exposure reduction target	Percentage reduction (0,10,15 or 20%) + all measures to reach 18 μg m^{-3} (AEI)	Based on 3-year average	Reduction to be attained where possible in 2020, determined on the basis of the value of exposure indicator in 2010	N/A
SO_2	350 μg m^{-3}	1 h	Limit value entered into force 1 January 2010	24
	125 μg m^{-3}	24 h	Limit value entered into force 1 January 2005	3
NO_2	200 μg m^{-3}	1 h	Limit value entered into force 1 January 2010	18
	40 μg m^{-3}	1 year	Limit value entered into force 1 January 2010[a]	N/A
PM_{10}	50 μg m^{-3}	24 h	Limit value entered into force 1 January 2005[b]	35
	40 μg m^{-3}	1 year	Limit value entered into force 1 January 2005[b]	N/A
Lead	0.5 μg m^{-3}	1 year	Limit value entered into force 1 January 2005 (or 1 January 2010 in the immediate vicinity of specific, notified industrial sources; and a 1.0 μg m^{-3} limit value applies from 1 January 2005 to 31 December 2009)	N/A
CO	10 mg m^{-3}	Maximum daily 8 h mean	Limit value entered into force 1 January 2005	N/A
Benzene	5 μg m^{-3}	1 year	Limit value entered into force 1 January 2010[b]	N/A
Ozone	120 μg m^{-3}	Maximum daily 8 h mean	Target value entered into force 1 January 2010	25 days averaged over 3 years
Arsenic	6 ng m^{-3}	1 year	Target value entered into force 31 December 2012	N/A
Cadmium	5 ng m^{-3}	1 year	Target value entered into force 31 December 2012	N/A
Nickel	20 ng m^{-3}	1 year	Target value entered into force 31 December 2012	N/A
PAH	1 ng m^{-3} (expressed as concentration of Benzo(a)pyrene)	1 year	Target value entered into force 31 December 2012	N/A

[a] Under the directive, the member state can apply for an extension of up to 5 years (i.e. maximum up to 2015) in a specific zone, subject to assessment of the commission.

[b] Under the new directive, the member state can apply for an extension until 3 years after the date of entry into force of the new directive (i.e. May 2011) in a specific zone, subject to assessment of the commission.

[c] Standard introduced by Directive 2008/50/EC.

[d] Determined as 3-year running mean, targeting the exposure to fine particles.

- The first such agreement was the Convention on Long-Range Transboundary Air Pollution (CLRTAP), agreed at Geneva in 1979, which committed countries to take a BATNEEC approach to curbing the long-range transport and deposition of sulphur and nitrogen.
- The 1984 European Monitoring and Evaluation Protocol set up the machinery and funding for a network of measurement sites across Europe to provide data on all

substances that are the subjects of UNECE agreements.

- The 1985 Helsinki Sulphur Protocol requires ratifying countries to reduce national S emissions or their transboundary fluxes by 30% from a 1980 base by 1993. This set up the *30% club*, which was not joined by either the EU as a whole or by the UK in particular. The UK objected to the choice of 1980 as the base date, as an industrial recession had caused its own sulphur emissions to be particularly low that year. The protocol was redrawn in terms of critical loads in 1994. The second sulphur protocol came into force in August 1998. The UK agreed to target a reduction of at least 80% in its national annual SO_2 emissions, compared to 1980.
- The 1987 Montreal Protocol on substances that deplete the ozone layer has been described elsewhere.
- The 1988 Sofia Nitrogen Oxides Protocol required ratifying countries to restore their NO_x emissions or transboundary fluxes to a 1987 base by 1994. The target was met comfortably by the EU15.
- The 1991 Geneva VOC Protocol required a 30% reduction in volatile organic compound (VOC) emissions from a 1988 base by 1999, and subsequently to adopt a further range of measures to reduce VOC emissions.
- The Aarhus Heavy Metal and Persistent Organic Pollutant (POP) Protocol (1998) required that emissions of heavy metals – lead, cadmium and mercury – be reduced below 1990 levels. The main sources of these materials are leaded petrol, battery production and disposal, and the chlor-alkali industry. It was also required to ban certain POP emissions (mainly pesticides) and to reduce emissions and/or use of others such as dioxins, furans and polycyclic aromatic hydrocarbons (PAHs). This would be achieved mainly by upgrading municipal waste incinerators.
- In 1999 CLRTAP adopted historic measures to reduce EU-level transboundary air pollution and to abate acidification, eutrophication and ground-level ozone (popularly called the *Gothenburg Protocol*). This entered into force in 2005. The protocol sets emission ceilings for pollutants such as sulphur and nitrogen oxides, non-methane VOCs and ammonia. The protocol also sets tight limit values for specific emission sources (e.g. combustion plant, electricity production, and vehicles) and requires best available techniques to be used to keep emissions down.

In 2007, CLRTAP initiated a revision of the Gothenburg Protocol, which got amended in May 2012. Table 14.3 shows the revised emission reductions targets for the EU as a whole and for Britain in particular. This scenario assumes (a) full implementation of all the emission control legislation as is already laid down in the national laws, (b) compliance with the existing National Emission Ceilings Directive and (c) implementation of all recent proposals on further emission control measures. The UK is in the process of implementing air pollution reduction targets for 2020 and 2030 under the amendments proposed to the Gothenburg Protocol and the new EU NECD, in order to tackle transboundary air pollution.

These successive protocols have had a profound effect on EU sulphur emissions since the

FOR REFERENCE PURPOSES ONLY

1980s, as seen in Figure 14.1. Achieving the amended Gothenburg Protocol beyond 2020 will reduce sulphur emission to a value below that which prevailed in 1860.

Table 14.3 National emission reduction commitments for 2020 following amendments to the Gothenburg Protocol, expressed on the basis of the 2005 absolute emissions

Pollutant	*UK 2005 (k tonnes)*	*UK change (%)*	*EU 2005 (k tonnes)*	*EU change (%)*
SO_2	706	59	7828	59
NO_x	1580	55	11355	42
NH_3	307	8	3813	6
VOC	1088	32	8842	28
$PM_{2.5}$	81	30	1504	22

FOR REFERENCE PURPOSES ONLY

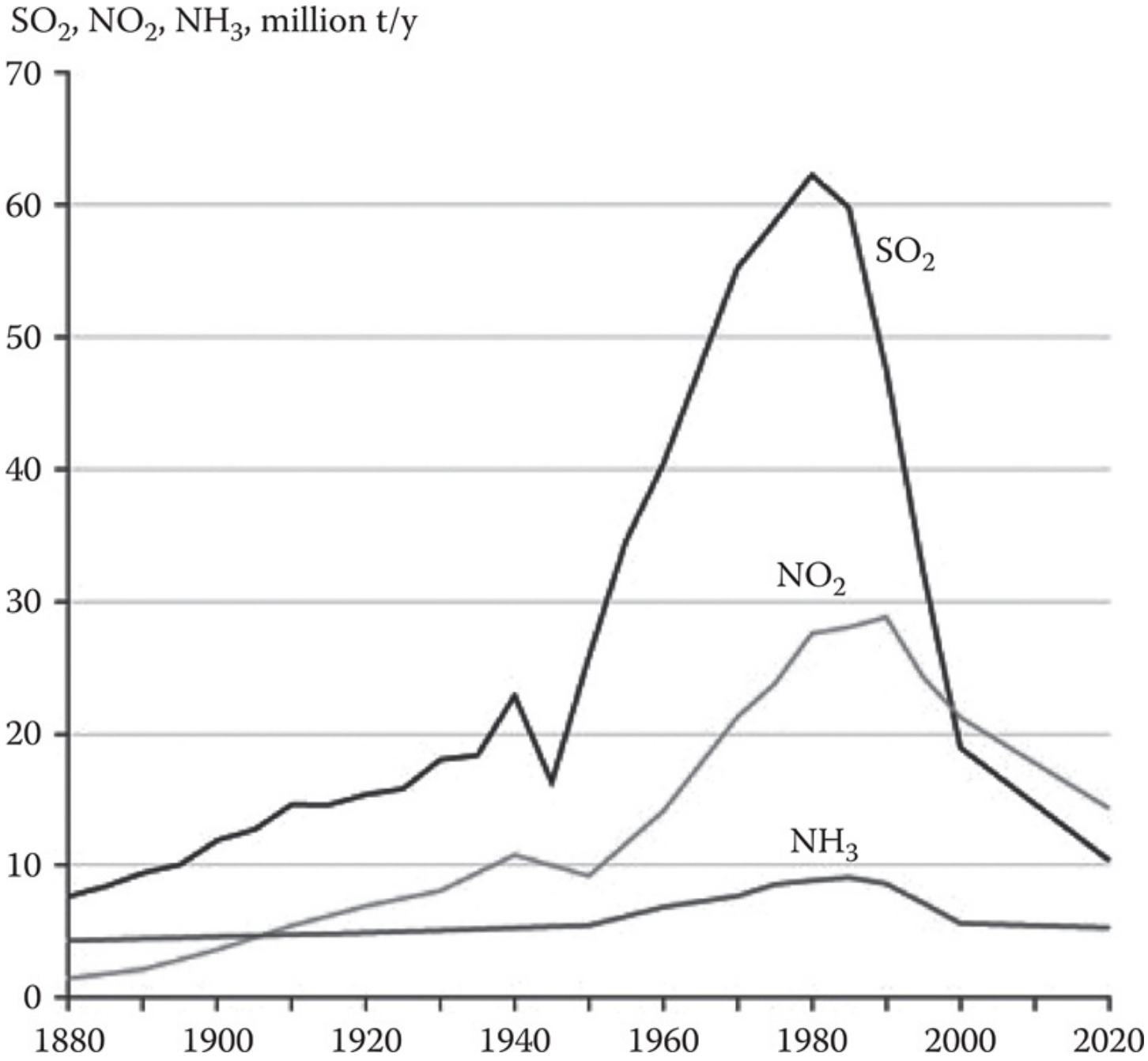

Figure 14.1 The effect of CLRTAP on European emissions of SO_2, NO_2 and NH_3. (From Mass, R., and Grennfelt, P., Towards cleaner air, Scientific assessment report. EMEP Steering Body and Working Group on Effects of the Convention on Long-Range Transboundary Air Pollution, 2016.)

14.5 WORLD HEALTH ORGANISATION

The WHO has played a key role in assessing the responses of people to pollutant concentrations. In 1987, it published a summary of air quality guidelines for 28 substances, based on human health criteria. For 18 toxic chemicals, WHO gave a concentration below

FOR REFERENCE PURPOSES ONLY

which there was believed to be no risk to human health. For 7 of the 9 carcinogenic chemicals, for which there is no safe low concentration, an estimate was given of the risk of cancer for a lifetime exposure to a concentration of 1 μg m^{-3}. These guidelines were revised in 1997 (Tables 14.4 and 14.5). In 2005 a revised global update on air quality guidelines for particulate matter, ozone, nitrogen dioxide and sulphur dioxide was released based on results from more recent studies.

14.5.1 Exceedances

Having established monitoring programmes and legislated concentration guidelines, the natural next step is to work out whether the guidelines are being exceeded and, if so, how badly. For example, the EU ozone threshold for the protection of human health (120 μg m^{-3} as an 8-h mean) is being exceeded for about 330 million people (most of the population of the EU) at least once per year; and the threshold value for the protection of vegetation is being exceeded *widely and frequently*.

Table 14.4 WHO guideline values for carcinogenic chemicals

Substance	*Unit risk*[a] *[μg m^{-3}]$^{-1}$/site of tumour*
Acrylonitrile	2×10^{-5}/lung
Arsenic	1.5×10^{-3}/lung
Benzene	6×10^{-6}/blood (leukaemia)
Benzo[a]pyrene	8.7×10^{-2}/lung
Chromium (VI)	4×10^{-2}/lung
Diesel exhaust	4×10^{-5}/lung
Nickel	3.8×10^{-4}/lung
PAH (expressed as BaP)	8.7×10^{-2}/lung
Trichloroethylene	4.3×10^{-7}
Vinyl chloride	1×10^{-6}/liver and other sites
Asbestos (concentration of 500 fibres m^{-3}, rather than 1 μg m^{-3})	10^{-6} to 10^{-5} (lung cancer)
	10^{-5} to 10^{-4} (mesothelioma)

[a] Unit risk is defined as 'the additional lifetime cancer risk occurring in a hypothetical population in which all individuals are exposed continuously from birth throughout their lifetimes to a concentration of 1 μg m^{-3} of the agent in the air they breathe'.

Table 14.5 WHO guideline values for particulate matter

Health outcome	*Relative risk*[a]
Use of bronchodilator	1.0305
Cough	1.0356
Lower respiratory symptoms	1.0324

FOR REFERENCE PURPOSES ONLY

Change in peak expiratory flow rate	– 0.13%
Respiratory hospital admissions	1.0080
Death	1.0074 (PM_{10})
	1.015 ($PM_{2.5}$)

[a] Relative risk associated with a 10 μg m^{-3} increase in the 24-h average concentration of PM_{10} (or $PM_{2.5}$).

A complication is caused by the fact that health effects are not related to concentration in a black-and-white fashion and that a small part of the population may experience symptoms at concentrations around the guideline value. For example, 8-h exposure to an O_3 concentration of 120 μg m^{-3} is expected to reduce the forced expiratory volume (FEV_1, which is respiratory function as forced expiratory volume in 1 s) of 10% of the population (the most active, healthy and sensitive 10%) by 5%.

Overall, it is evident that air quality legislation is by no means fixed. There is a dynamic, iterative series of international comparisons under way (Table 14.6) in which new studies of pollutant effects are being incorporated year by year. Two phases have been seen. In the first phase, during the 1970s and 1980s, a higher set of limits and guidelines was identified which would reduce acute effects during short-term episodes. Subsequently, epidemiology has been used more effectively to specify a lower set of values which will protect populations from chronic effects due to long-term low-level exposures. One result of this sequence is that emission reductions are always chasing ever-lower ambient targets. The major part of the work has probably now been done, for it is becoming clear that future fine-tuning will yield diminishing returns in reduced morbidity and mortality.

Table 14.6 Selected air quality exceedances for different regulatory guidelines and standards (time-weighted average concentrations, μg m^{-3})

FOR REFERENCE PURPOSES ONLY

Source	SO_2	NO_2	PM_{10}	$PM_{2.5}$	O_3	Averaging time
WHO		40	20	10		1 year
	20		50[a]	25[a]		24 h
					100	8 h
		200				1 h
	500					10 min
EU		40	40	25		1 year
	125		50[b]			24 h
					120	8 h
	350	200				1 h
						10 min
United States	78	100	50	15		1 year
	366		150	65		24 h
					157	8 h
						1 h
						10 min
California			20	12		1 year
	105[c]		50	65		24 h
					137	8 h
	655	470[c]			180[c]	1 h
						10 min
Japan						1 year
	105	113	100			24 h
						8 h
	262				118[c]	1 h
						10 min
Brazil	80	100	50			1 year
	365		150			24 h
						8 h
		320			160	1 h
						10 min
Mexico	78		50	15		1 year
	341		120	65		24 h
					157[c]	8 h
		395			216	1 h
						10 min
South Africa	50	94	60			1 year
	125	188	180			24 h
						8 h
		376			235	1 h
	500					10 min

FOR REFERENCE PURPOSES ONLY

India (residential and industrial/ ecologically sensitive area)	50/20 80/80	40/30 80/80	60/60 100/100	40/40 60/60	100/100 180/180	1 year 24 h 8 h 1 h 10 min
China (Classes I/ II/III)[d]	20/60/100	40/40/80	40/100/150			1 year
	50/150/250	80/80/120	50/150/250			24 h 8 h
	150/500/700	120/120/ 240			120/160/200	1 h 10 min

[a] Not to be exceeded more than 3 days per year.

[b] Not to be exceeded more than 35 days per year.

[c] Photochemical oxidants.

[d] Class I: tourist, historical and conservation areas; Class II: residential urban and rural areas; Class III: Industrial and heavy traffic areas.

14.5.2 Uncertainty

Establishing the relationship between exposure and response is marked with many uncertainties. It is left up to the decision maker to evaluate the evidence and uncertainties involved, through the application of available tools, prior to making appropriate judgements. While evaluating the literature, one may come across contradicting results from different studies, or insufficient information about the impacts of pollutants, the population at risk and the magnitude of the effect. In other cases there may be uncertainty about the mechanism of any cause-effect relationship. Another issue pertains to the process of extrapolating results from the study population to another population, in particular for developing countries where few local studies are available. Uncertainty is also added through environmental factors, because of the difference in the levels, composition, mixes and distribution patterns of pollutants, all of which may be different in the local setting compared to those of the studies used in establishing guidelines or standards. However, the mere presence of uncertainty should not have detrimental implications for applying regulations, as scientific uncertainty is bound to exist in all cases and may never be completely resolved.

14.6 EU INDUSTRIAL EMISSIONS LEGISLATION

Industrial processes account for a considerable share of the overall air pollution in Europe.

Acid deposition has been a major environmental concern in the EU since the 1970s, and legislation has been passed to reduce deposition levels.

The Industrial Emissions Directive (IED) (2010/75/EU) is the main EU instrument regulating pollutant emissions from industrial installations. The IED, adopted on 24 November 2010, is based on a European Commission proposal recasting 7 previously existing directives (including in particular the IPPC directive). Around 50,000 installations undertaking the industrial activities listed in Annex I of the IED are required to operate in accordance with a permit (granted by the authorities in the member states). These fall into the following categories:

- *Energy production and distribution*: Emissions from public heat and electricity generation, oil refining, production of solid fuels, extraction and distribution of solid fossil fuels and geothermal energy.
- *Energy use in industry*: Emissions from combustion processes used in the manufacturing industry including boilers, gas turbines and stationary engines.
- *Industrial processes and product use*: Emissions derived from non-combustion-related processes such as the production of minerals, chemicals and metal production, non-combustion-related emissions mainly in the services and household sectors including from activities such as paint application, dry cleaning and other uses of solvents.

The IED is based on several pillars, in particular (1) an integrated approach, (2) use of best available techniques (BATs), (3) flexibility, (4) inspections and (5) public participation.

In addition, through the European Pollutant Release and Transfer Register (E-PRTR), emission data reported by the member states are made accessible in a public register, which is intended to provide environmental information on major industrial activities. The medium combustion plants (MCPs) directive (2015/2193/EU) regulates emissions of sulphur dioxide (SO_2), nitrogen oxides (NO_x) and dust from the combustion of fuels in plants with a rated thermal input equal to or greater than 1 megawatt (MWth) and less than 50 MWth.

The Large Combustion Plant Directive (LCPD) (88/609/EEC) is designed to reduce emissions of sulphur and nitrogen oxides from industrial plant (>50 MW thermal, mainly power stations) burning fossil fuel. Chapter 3 (with Annex V) of the IED replaced the revised LCP directive (2001/80/EC) since 1 January 2016, with the overall aim of reducing emissions of acidifying pollutants, particles and ozone precursors. The LCPD encourages the combined generation of heat and power and sets specific emission limit values for the use of biomass as fuel.

14.7 EU VEHICLE EMISSIONS

The first European directive on vehicle emissions for petrol cars was adopted in 1970 and

FOR REFERENCE PURPOSES ONLY

for diesel cars in 1983, but the emission limits were voluntary; member states were not required to adopt them into national law. However, the first mandatory emissions standards for petrol and diesel cars were developed through introduction of the Euro 1 standards. This mandated that new petrol cars registered after 1992 to be fitted with three-way catalysts.

An integrated approach to air pollution problems has been followed in the European Commission's Auto-Oil Programmes (1994–2000). Through this initiative the European Commission introduced a new set of vehicle emissions limits based on the environmental capacity, that is, identifying the most effective package of measures to meet air quality targets set for the protection of human health. The directives introduced as a result of Auto-Oil I resulted in reductions in emissions per vehicle of around 70% compared to prevailing standards. Auto-Oil II has shown that measures currently in place will reduce vehicle emissions of toxic pollutants and ozone precursors to below around 15% of their 1995 values by 2020. It was regarded as an exemplar approach which led to the development of the new fuel quality standards: the Euro 3 and 4 standards for light-duty vehicles and the III and IV standards for heavy-duty vehicles.

The latest Euro standard for cars is Euro 6. In 2015, 11% of the total number of kilometres driven in diesel cars were in Euro 6 vehicles; by 2025 this is expected to increase to 88%.

14.7.1 Emissions testing cycles

Tailpipe emissions standards specify the maximum amount of pollutants allowed in exhaust gases discharged from the engine. Regulated emissions include:

- *Diesel particulate matter* (PM), measured by gravimetric methods. Sometimes diesel smoke opacity measured by optical methods is also regulated.
- *Nitrogen oxides* (NO_x), composed of nitric oxide (NO) and nitrogen dioxide (NO_2). Other oxides of nitrogen which may be present in exhaust gases, such as N_2O, are not regulated.
- *Hydrocarbons* (HCs), regulated either as total hydrocarbon emissions (THCs) or as non-methane hydrocarbons (NMHCs). One combined limit for HC + NO_x is sometimes used instead of two separate limits.
- *Carbon monoxide* (CO). The permitted pollutant emissions must be specified in a standard way, and new models must be tested in the same standard way to find out whether they meet the specification. Emissions are therefore measured over an engine or vehicle test cycle which is an important part of every emissions standard. Regulatory test procedures are necessary to verify and ensure compliance with the various standards. These test cycles are intended to create repeatable emissions measurement conditions and, at the same time, simulate a real driving condition of a given application.

FOR REFERENCE PURPOSES ONLY

As it is clearly impractical to instrument all new models and drive the test cycle on real roads, emissions test cycles are used which are a sequence of speed and load conditions performed on an engine or chassis dynamometer. The former is usually more appropriate if the engine is a general-purpose power source that might be used in a wide range of applications (not necessarily vehicles). Emissions measured on vehicle (chassis) dynamometers (instrumented rolling roads) are usually expressed in grams of pollutant per unit of travelled distance, for example, g km^{-1} or g mi^{-1}. Emissions measured according to an engine dynamometer test cycle are expressed in grams of pollutant per unit of mechanical energy delivered by the engine, typically g $(kWh)^{-1}$ or g $(bhph)^{-1}$. Depending on the character of speed and load changes, cycles can be divided into steady-state cycles and transient cycles. Steady-state cycles are sequences of constant engine speed and load modes. Emissions are analysed for each test mode. Then, the overall emissions result is calculated as a (time-weighted) average from all test modes. In a transient cycle, the vehicle (or engine) follows a prescribed driving pattern which includes accelerations, decelerations and changes of speed and load. The final test results can be obtained either by analysis of exhaust gas samples collected over the duration of the cycle or by electronic integration of measurements from fast response, continuous emissions monitors. Regulatory authorities in different countries have not been consistent in adopting emissions test procedures and at least 25 types of cycle are in use. As exhaust emissions depend on the engine speed and load conditions, specific engine emissions which have been measured on different test cycles may not be comparable.

14.7.1.1 The ECE15 + EUDC test cycle

The ECE + EUDC cycle, also known as the New European Driving Cycle (NEDC) or the Motor Vehicle Emissions Group (MVEG-A) cycle, is an urban driving cycle for light-duty vehicles (such as cars and small vans) devised to represent city driving conditions and performed on a chassis dynamometer. Updated in 1990, it is characterised by low vehicle speed, low engine load and low exhaust gas temperature. The vehicle is taken through four cycles of steady acceleration, cruising at constant speed, and steady deceleration (see top graph in Figure 14.2). Emissions are sampled during the cycle according to the *constant volume sampling* technique, analysed, and expressed in g km^{-1} for each of the pollutants.

FOR REFERENCE PURPOSES ONLY

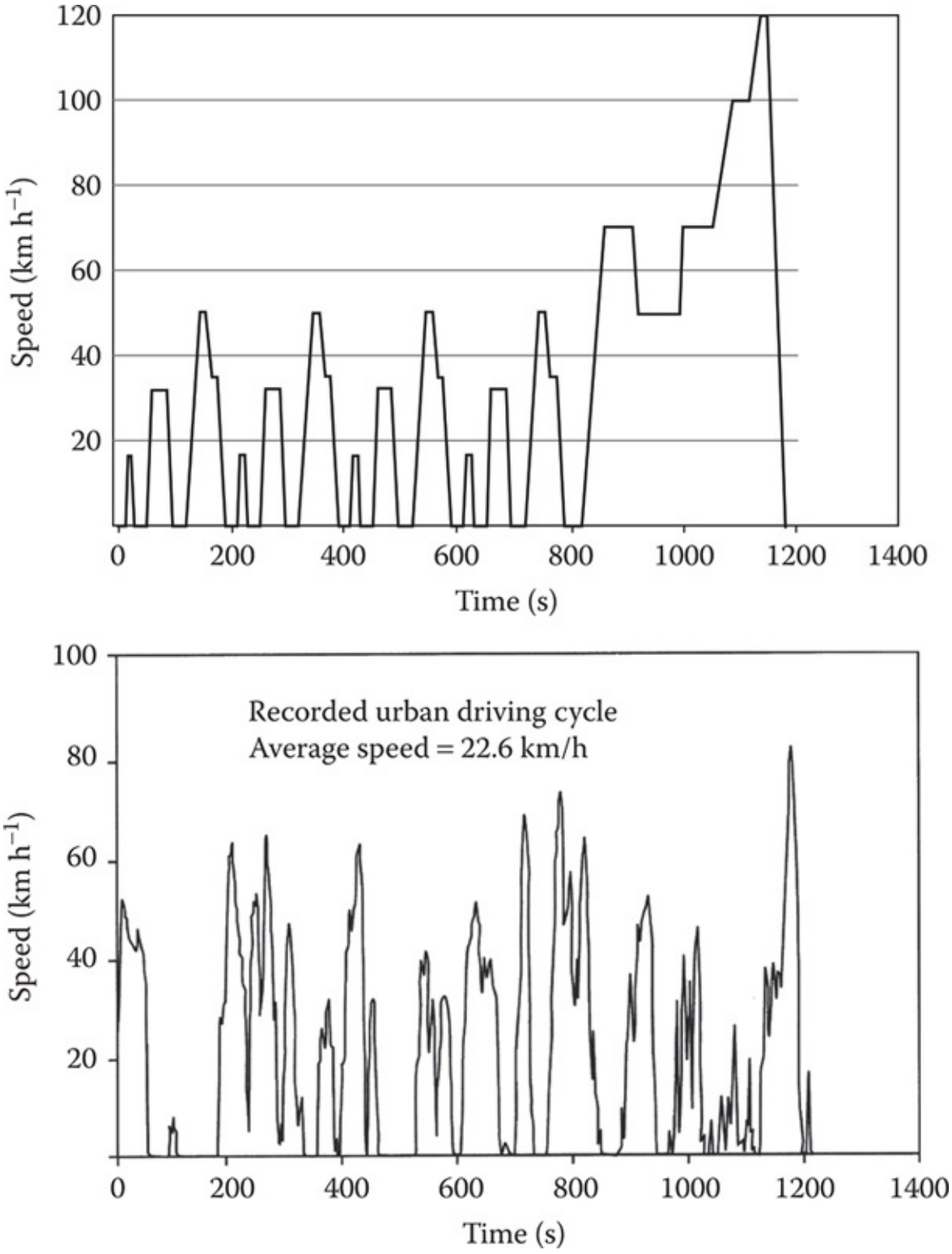

Figure 14.2 The EU test cycle and a real driving pattern for comparison. (From Mock, P. et al., The WLTP: How a new test procedure for cars will affect fuel consumption values in the EU, The International Council on Clean Transportation, Working Paper 2014–2019, 2014.)

This urban driving cycle represents a Type I test, as defined by the original ECE emissions procedure. The test cycle assumes moderate ambient temperatures and no

FOR REFERENCE PURPOSES ONLY

application of heating or cooling systems. While this is a simplification in order to standardise values across the EU, the actual performance of the vehicle might substantially deviate from the measured performance. The Type II test is a warmed-up-idle tailpipe CO test conducted immediately after the fourth cycle of the Type I test. The Type III test is a two-mode (idle and 50 km h^{-1}) chassis dynamometer procedure for crankcase emission determination. The extra urban driving cycle (EUDC) segment has been added after the fourth ECE cycle to account for more aggressive, high-speed driving modes and has a maximum speed of 120 km h^{-1}. There has been a lot of debate about the exact details of the driving cycles, because these affect emissions and therefore the costs for the vehicle manufacturer in meeting the targets. In fact, the legislated driving cycles are quite simplified compared to the real thing, as can be seen in the lower graph in Figure 14.2. This is a problem because the more transient the driving cycle, the worse the engine combustion control and the worse the catalyst efficiency, as we saw in Chapter 9. Regulatory driving cycles remain generally less transient than real ones.

14.7.1.2 Real driving emissions testing

The NEDC regulatory emissions testing framework covering vehicular air pollution from diesel engines came under heavy criticism for the gaps between real-world and laboratory test emissions. In response, the European Commission introduced the Real Driving Emissions (RDE) test procedure, and there is a series of initiatives underway to improve and harmonise the test standards up to mid-2020. The proposed RDE testing using some form of *onboard* portable emissions measurement systems (*PEMS*) is meant to overcome the shortcomings of measurements taken under chassis dynamometer. The RDE testing marks the transition from the existing NEDC regulations to the Worldwide Harmonised Light Vehicle Test Procedure (WLTP). The latter developed was under the UNECE is expected to take over NEDC entirely from 2021 onwards. The RDE conditions have introduced more stringent testing parameters, including ambient temperature, altitude, speed, driver aggression levels and gradient. The NEDC and WLTP driving cycles have similar profiles but differ in terms of speed, duration and profile regularity. The NEDC has a total 780 s urban driving cycle with an average speed of 18.35 km h^{-1}, and four identical cycles of speeding up and slowing down (it also has an EUDC of 400 s with speeds reaching 120 km h^{-1}). On the other hand, the WLTP has four sections representing low, medium, high and extra high speeds. The test cycle used depends on the vehicle power but can last up to a total of 1800 s, reaching speeds of 130 km h^{-1}.

The RDE testing is split into several progression stages: the first package was initiated on 31 March 2016 but limited to NO_x monitoring purpose only; the second package was initiated 1 September 2017, with full rollout to evaluate new car model for NO_x; the third package is expected to start around 2020, for measuring particulates and including effect of vehicle cold start into the RDE testing; the fourth package is RDE testing for in-service

vehicles. A number of organisations have measured NO_x emissions from Euro 6 diesel cars, either on real roads or in a simulation of real-world driving conditions on rolling roads (mimicking RDE). Overall, these tests suggest that:

- On average, Euro 6 diesel cars emit significantly more than the emissions standard.
- There is a great deal of variability between different vehicles, mainly attributed to the variations in the emission-control strategies used.
- A small number of vehicles have very high NO_x emission rates, hence resulting in disproportionate levels of average emissions.
- Emissions vary significantly according to vehicle driving conditions.
- Emissions are significantly increased at low ambient temperatures, mainly due to the reduction/deactivation of the emission controls in order to protect the vehicle.
- Despite emitting more than the emissions standard, on average Euro 6 vehicles seem to produce significantly less NO_x than Euro 5 or Euro 4 diesel vehicles.

14.7.2 EU emissions legislation

This emissions legislation is adopted as part of the EU framework for the type approval of cars, vans, trucks, buses and coaches. It divides vehicles into cars (<2.5 t), light-duty (<3.5 t) vehicles and heavy-duty vehicles. EU standards for petrol-engine vehicles are divided by engine capacity categories into small (less than 1.4 L), medium (1.4–2 L) and large (over 2 L). This mainly ensures a single market for vehicles across the EU. The first directive on vehicles was approved in 1970, being an adaptation of UNECE Regulation No 15. Since then there have been seven major directives. The most significant early directives were 83/351/EEC (maximum values of CO, HC and NO_x), 88/76/EEC (reduced maximum values for the two larger engine capacities) and 89/458/EEC (reduced maximum values for the smallest engine capacity). These directives were soon superseded by the Consolidated Directive 91/441/EEC, which implemented tighter controls for all passenger cars (regardless of engine capacity, but excluding those having direct injection diesel engines) weighing less than 2500 kg. The current standards are: for light-duty vehicles (cars and vans) – Euro 6; for heavy-duty vehicles – Euro VI. There have been the following vehicle emissions laws (listed in Table 14.7):

- Directive 2005/55/EC adopted in 2005 introduced durability and onboard diagnostic (OBD) requirements, as well as re-stated the emission limits for Euro IV and Euro V which were originally published in 1999/96/EC
- Directive 2007/46/EC provides a common legal framework for the type approval of cars, vans, trucks, buses and coaches

Table 14.7 Chronological list of EU vehicle emissions legislation

Standard	*Directive*	*Vehicles affected*	*Date of introduction*

FOR REFERENCE PURPOSES ONLY

Euro 1	91/444/EEC	Passenger cars	31 December 1992
Euro I	93/59/EEC	LGVs	1 October 1994
	91/542/EEC	HGVs	1 October 1993
Euro 2	94/12/EC	Passenger cars	1 January 1997
Euro II	96/69/EC	LGVs	1 October 1997
	91/542/EEC	HGVs	1 October 1996
Euro 3	98/69/EC	Passenger cars and LGVs	1 January 2001
Euro III	common position	HGVs	1 January 2001
Euro 4	98/69/EC (& 2002/80/EC)	Passenger cars and LGVs	1 January 2006
Euro IV	common position	HGVs	1 January 2006
Euro 5	2007/715/EC	Passenger cars and LGVs	1 October 2008
Euro V		HGVs	
Euro 6	2016/427[a]	Passenger cars and LGVs	10 March 2016
Euro VI	595/2009/EC	HGVs	1 January 2013

[a] Amended Regulation (EC) No 692/2008 for Euro 6.

- Euro 5 and Euro 6 Regulation 715/2007/EC sets the emission limits for cars for regulated pollutants, in particular nitrogen oxides (NO_x, i.e. the combined emissions of NO and NO_2) of 80 mg km^{-1}
- Regulation 692/2008/EC implements and amends Regulation (EC) No 715/2007 on type approval of motor vehicles with respect to emissions from light passenger and commercial vehicles (Euro 5 and Euro 6) and on access to vehicle repair and maintenance information
- Regulation (EU) 2016/427 of 10 March 2016 amends Regulation (EC) No 692/2008 as regards emissions from light passenger and commercial vehicles (Euro 6)
- Regulation 595/2009/EC requires new heavy-duty vehicles and engines to comply with new emissions limits and introduces additional requirements on access to information
- Commission Regulation (EU) 582/2011 implements and amends Regulation (EC) No 595/2009 with respect to emissions from heavy-duty vehicles (Euro VI)

Specifically for various pollutants, successive emissions standards have led to significant drops in emissions of exhaust PM and other pollutants such as HC and CO. The Euro 6, VI standards also introduced particle number (PN) emission limits (Tables 14.8 and 14.9), stricter OBD requirements and a number of new testing requirements—including off-cycle and in-use PEMS testing.

Table 14.8 EU emission standards for passenger cars

FOR REFERENCE PURPOSES ONLY

Tier	Date	CO	HC	NO_x	$HC + NO_x$	PM	PN
		g km^{-1}					# km^{-1}
Diesel							
Euro 1	July 1992	2.72	–	–	0.97	0.14	
Euro 2 (IDI)	January 1996	1.0	–	–	0.7	0.08	
Euro 2 (DI)	January 1996[a]	1.0	–	–	0.9	0.10	
Euro 3	January 2000	0.64	–	0.50	0.56	0.05	
Euro 4	January 2005	0.50	–	0.25	0.30	0.025	
Euro 5A	September 2009[b]	0.50	–	0.18	0.23	0.005[f]	
Euro 5B	September 2011[c]	0.50	–	0.18	0.23	0.005[f]	6×10^{11}
Euro 6	September 2014	0.50	–	0.08	0.17	0.005[f]	6×10^{11}
Petrol (Gasoline)							
Euro 1	July 1992	2.72	–	–	0.97	–	
Euro 2	January 1996	2.2	–	–	0.5	–	
Euro 3	January 2000	2.3	0.20	0.15	–	–	
Euro 4	January 2005	1.0	0.10	0.08	–	–	
Euro 5	September 2009[b]	1.0	0.10[d]	0.06	–	0.005[e,f]	
Euro 6	September 2014	1.0	0.10[d]	0.06	–	0.005[e,f]	6×10^{11} [e,g]

Note: IDI is indirect injection; DI is direct injection.

[a] Until 9 September 1999. After that date DI engines must meet the IDI limits.

[b] January 2011 for all models.

[c] January 2013 for all models.

[d] And NMHC = 0.068 g km^{-1}.

[e] Applicable only to vehicles using DI engines.

[f] 0.0045 g km^{-1} using the PMP measurement procedure.

[g] 6.0 × 1012 1/km within first three years from Euro 6 effective dates.

Table 14.9 EU emission standards for heavy-duty diesel engines: Steady-state testing

FOR REFERENCE PURPOSES ONLY

Tier	Date	Test cycle	CO	HC	NO_x	PM	PN	Smoke
			g $(kWh)^{-1}$				$(kWh)^{-1}$	m^{-1}
Euro I	1992, <85 kW	ECE R-49	4.5	1.1	8.0	0.612		
	1992, >85 kW		4.5	1.1	8.0	0.36		
Euro II	October 1996		4.0	1.1	7.0	0.25		
	October 1998		4.0	1.1	7.0	0.15		
Euro III	October 1999 EEVs only	ESC & ELR	1.5	0.25	2.0	0.02		0.15
	October 2000		2.1	0.66	5.0	0.10[a]		0.8
Euro IV	October 2005		1.5	0.46	3.5	0.02		0.5
Euro V	October 2008		1.5	0.46	2.0	0.02		0.5
Euro VI	January 2013	WHSC	1.5	0.13	0.4	0.01	8.0×10^{11}	

Note: Emissions standards applicable to diesel (compression ignition, CI) engines only. Engines with diesel and gas (positive ignition) should meet the transient testing requirements not mentioned here.

[a] PM = 0.13 g kWh^{-1} for engines <0.75 dm^3 swept volume per cylinder and a rated power speed > 3000 min^{-1}.

Directive 2009/28/EC introduced a binding target of 10% share of renewable energy in transport by 2020, including biofuels. Further, Directive 2009/30/EC, regulating the specification of petrol, diesel and gas-oil, allows for the blending of ethanol into petrol up to 10% (v/v) and for a Fatty acid methyl esters (FAME) content of 7% (v/v) in diesel. However, in its revised renewable energy targets beyond 2020, the EU has introduced a cap on the contribution of food-based biofuels, starting at 7% in 2021 and going down progressively to 3.8% in 2030.

From 1 January 1993, all new petrol cars were required to meet emissions standards that imply the use of three-way catalysts. The standards specified that emissions be less than 2.72 g CO, 0.97 g (HC + NO_x) and 0.14 g particles km^{-1} when driven over a 7 km test track that included conditions equivalent to urban and motorway driving. The cars also had to be able to pass the test after having been driven 30,000 km. Table 14.8 provides the EU emissions standards for passenger cars, both diesel and petrol, which clearly shows the tightening of the regulations. Corresponding values for heavy-duty diesel vehicles are shown in Table 14.9, which also shows that the regulatory emission test cycles have been changed several times. Since the Euro III stage (2000), the earlier steady-state engine test ECE R-49 has been replaced by two cycles: the European Stationary Cycle (ESC) and the European Transient Cycle (ETC). Smoke opacity was measured over the European Load Response (ELR) test. The more recent World Harmonized Stationary Cycle (WHSC) test is a steady-state engine dynamometer schedule defined by the global technical regulation of the UNECE.

The sale of leaded petrol has been banned since 1 January 2000. This last change has been accompanied by the provision at filling stations of lead replacement petrol (LRP), in which sodium and other additives are used to maintain the lubricant properties of lead.

FOR REFERENCE PURPOSES ONLY

The long-term consequence for relative emissions of the measures enforced in these various European programmes is shown in Figure 14.3. For CO, HC and NO_x the baseline has been taken as a pre-Euro I petrol car. For PM, it has been taken as a pre-Euro I diesel car. The reductions are most marked for petrol-powered passenger cars and vans, but significant improvements to diesel vehicle emissions have followed as well. Any computer model that is designed to predict vehicle emissions has to take all this complexity into account – for example, there have been seven levels of emission control for petrol cars since 1970, and cars built to meet all those different emissions standards will still be on the road today. Additional EU directives are designed to reduce VOC emissions from the storage and distribution of petrol by 90% over a 10-year period (Com(92) 277), to ensure that catalytic converters meet a CO emissions standard of 0.5% when idling and 0.3% at 2000 rpm (92/55/EEC), to ensure that non-catalysed exhausts meet a CO emissions standard of 3.5% and to restrict the benzene content of petrol to 5% (85/210/EEC).

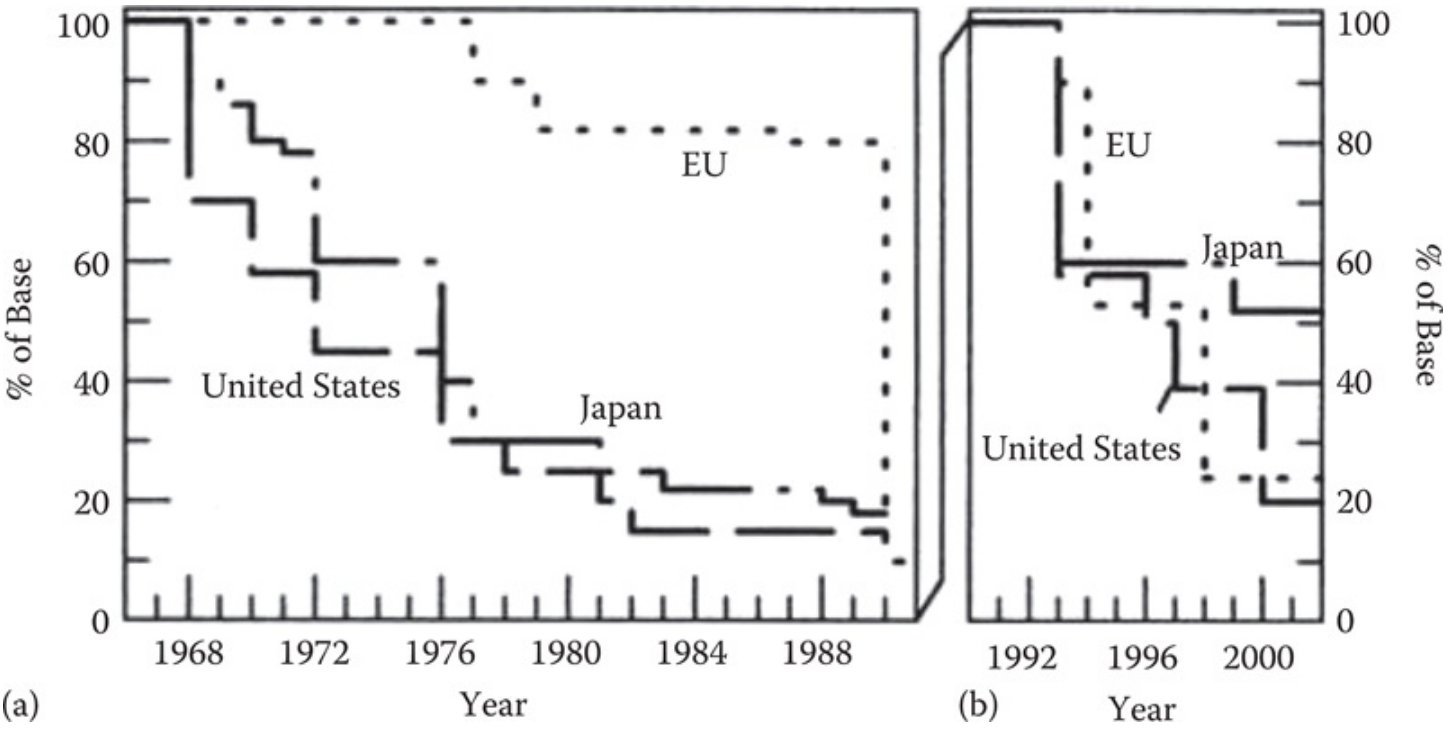

Figure 14.3 (a and b) Historical trends in relative vehicle emission changes due to European legislation. (From Eastwood, P., *Critical Topics in Exhaust Gas Aftertreatment*, Research Studies Press, Baldock, UK, 2000.)

14.8 US LEGISLATION

14.8.1 Background

The organisation responsible for air quality in the United States is the Environmental

FOR REFERENCE PURPOSES ONLY

Protection Agency (EPA). The Clean Air Act (CAA) was passed in the United States in 1963, and was air quality–driven rather than emissions-driven. Procedures were established for setting standards for the main air pollutants. The CAA was first amended in 1970, and the new standards promulgated in 1971. National Ambient Air Quality Standards (NAAQS) were established, plus control measures designed to achieve them. There were two types of NAAQS: (1) primary (designed to protect against adverse health effects in sensitive population groups, with a safety margin) and (2) secondary (the same or lower, designed to protect against welfare effects such as vegetation damage and visibility reduction). The original intention was to meet primary standards everywhere in the United States by 1977, and secondary standards *within a reasonable time*.

The EPA has set NAAQS for six principal pollutants, referred to as criteria pollutants (Table 14.10). The current standards (mostly 2008) are set centrally (by the federal government), but the individual American states are responsible for achieving them. There is a complex process of updating whereby new scientific findings on health effects are used to generate an air quality criteria document (AQCD), which leads to proposed decisions and then final decisions. At all stages there are opportunities for review and comment by non-EPA scientists, interested parties and the public at large, so that the process of revision can take some years. For example, the particles standard was originally defined (in 1971) in terms of total suspended particles (TSPs); when it became clear that health effects were largely due to the PM_{10} fraction, the standard was redefined in 1987 in those terms. Subsequently, $PM_{2.5}$ has come to the fore. A periodic review of the health effects of PM led to an AQCD in 1996. In 1997, new NAAQSs for PM were promulgated which incorporated the standards for $PM_{2.5}$ shown in Table 14.10. In the course of the consultation process on this one standard, over 50,000 written and oral comments had been received on the proposed revisions. The same revision process was applied to O_3 over the same period, resulting in the addition of the maximum 8-h average. It has been estimated that 113 million Americans were living in areas that failed to meet the new O_3 standard. Table 14.10 shows the new O_3 standard which is effective from 28 December 2015; the previous (2008) O_3 standards also remain in effect in some areas. This process of rolling re-evaluation sometimes results in changes but not always; the original NO_2 standards have remained unchanged following detailed re-evaluations, whereas the previous SO_2 standards remain in effect in certain areas but changed to current (2010) standards in others.

Table 14.10 US ambient air quality standards

FOR REFERENCE PURPOSES ONLY

Pollutant		*P/S*[a]	*Level*	*Averaging time*	*Permitted exceedances each year*
CO		P	9 ppm	8 h	Not to be exceeded more than once per year
			35 ppm	1 h	
Lead		P & S	0.15 μg m^{-3}	Rolling 3 month average	Not to be exceeded
NO_2		P	100 ppb	1 h	98th percentile of 1-hour daily maximum concentrations, averaged over 3 years
		P & S	53 ppb[b]	1 year	Annual mean
Ozone		P & S	0.07 ppm	8 h	Annual fourth-highest daily max. 8-h concentration, averaged over 3 years
Particle (PM)	$PM_{2.5}$	P	12 μg m^{-3}	1 year	Annual mean, averaged over 3 years
		S	15 μg m^{-3}	1 year	Annual mean, averaged over 3 years
		P & S	35 μg m^{-3}	24 h	98th percentile, averaged over 3 years
	PM_{10}	P & S	150 μg m^{-3}	24 h	Not to be exceeded more than once per year on average over 3 years
SO_2		P	75 ppb	1 h	99th percentile of 1-h daily max. concentrations, averaged over 3 years
		S	0.5 ppm	3 h	Not to be exceeded more than once per year

[a] P is primary; S is secondary.

[b] The level of the annual NO_2 standard is 0.053 ppm. It is shown here in terms of ppb for the purposes of clearer comparison to the 1-hour standard level.

Each state must develop a state implementation plan (SIP) describing the control strategies (called the menu of control measures [MCMs]) that the state will use to bring non-attainment areas into compliance with NAAQS for the criteria pollutants. The EPA in turn approves these plans. The CAA is adaptable, in the sense that health justifications for all NAAQS had to be re-evaluated every 5 years and modified to reflect new scientific understanding of effects.

Despite the flexibility and continuous updating of this approach, air pollution has proved to be a more intractable problem than expected, and the control measures have failed to achieve the intended air quality standards. A major revision and expansion of the CAA – the Clean Air Act Amendments (CAAA) – was passed in 1990. It was nearly 800 pages long, in place of the original Act's 50 pages. The CAAA includes provision for operating permits for stationary sources, and tradeable emission credits – if an emitter reduces emissions below the target standard or ahead of the target timetable, emissions credits are earned that can be applied to future emissions or sold to another emitter. These market-based initiatives were characteristic of the new legislation. Non-attainment areas are identified that fail to meet NAAQS for CO, O_3 or PM_{10}, in categories called marginal, moderate, serious or severe. Los Angeles merits the special category of extreme. The size of the source regarded as major depends on how badly the NAAQSs in that area are exceeded. Exceeding regions are required to make steady progress towards meeting targets. States must reduce overall

emissions from all sources by 15% per year for the first 6 years. Vapour recovery must be installed at petrol stations in exceedance areas, and vehicle inspection and maintenance programmes operated. If the SIPs are inadequate, then the USEPA can impose federal implementation plans.

Reformulation of petrol can be used to reduce volatility, reduce sulphur (to increase catalyst efficiency and reduce sulphate emissions), or add oxygenated blend stocks (to reduce the proportion of high-octane aromatic HCs such as benzene that might otherwise be required). The most popular additive has been methyl tertiary butyl ether (MTBE), although other ethers and alcohols (especially ethanol) have been used. Oxygenated fuels bring additional oxygen to the combustion reactions, reducing the formation of CO but increasing NO_x; on the other hand, the flame temperature is reduced which lowers NO_x. However, they also raise the Reid vapour pressure (RVP) – the RVP of ethanol is about 7 kPa higher than for standard petrol – which is also the subject of controls in order to reduce evaporation losses. Vehicle evaporative emissions can account for 30%–50% of total HC emissions, and increasing the RVP from 62 to 82 kPa can double the evaporative emissions. If the vehicle has evaporative emission controls but the mass emissions are lower, the proportional increase may be greater – about five times – if the fuel tank carbon canister saturates. Reduced fuel RVP also has an immediate benefit for HC emissions without having to wait for the vehicle stock to be replaced. The CAAA requires RVP to be reduced from 62 to 56 kPa in northern (cooler) US cities and to 50 kPa in southern (warmer) ones. There are complex wider issues here. For example, ethanol is produced from wheat, and the wheat is grown on large areas of high-intensity agricultural land. The emissions from the fossil fuels used in making the fertiliser and other agricultural inputs must be offset against the benefits of reduced vehicle CO emissions.

14.8.2 Hazardous air pollutants

Dozens of air pollutants normally occur at ppb or ppt concentrations in ambient air and are known to be harmful. More than half of these pollutants are known or suspected to be carcinogenic or mutagenic. Others have respiratory, neurological, immune or reproductive effects, especially for more sensitive populations such as children or frail adults. Many are also known to have adverse effects on plants and animals. These are materials such as heavy metals, chloroform and polycyclic organics which are not mainstream criteria pollutants but which can reasonably be expected to cause a health hazard. These compounds, or subsets of them, are variously known as air toxics, hazardous air pollutants (HAPs) or toxic organic micro-pollutants (TOMPs). Diesel exhaust particles, although not listed as HAP, contain many of them and are therefore treated as such. The USEPA currently identifies 188 HAPs, including 17 that represent groups of chemicals (such as PAHs) rather than discrete compounds. Maximum achievable control technology (MACT) must be used on any source emitting more than 10 t annually of any one HAP, or 25 t total. The USEPA is committed to reducing air toxin emissions by 75% below their 1993 level.

FOR REFERENCE PURPOSES ONLY

By the end of a 10-year upgrading period (in 2002), it was predicted that total annual HAP emissions would be reduced by at least 1 million tons. The emission controls are accompanied by a complex procedure for assessing the residual risk from regulated emissions.

Thirty-three of the listed HAPs (Table 14.11) have been identified as posing the greatest threat to public health in the majority of urban areas, and 30 of these are emitted from smaller industrial sources known as *area* sources; such sources are characteristic of urban areas in general rather than particular process plants or similar operations. The potential sources are small and diverse, such as wood-burning stoves, residential space heaters, landfills, filling stations and vehicles. The subset of 33 was chosen by means of a ranking system based on toxicity, risk and concentration (measured and modelled). These area sources will be controlled by an integrated urban air toxins strategy.

Through motor vehicle emissions simulators, the USEPA has projected that the emissions of toxic pollutants in 2030 will be 20% of the levels seen in 1990 (when their emissions regulations were first introduced). It is estimated that levels of VOCs emitted per mile will also be reduced by 96% by 2030, compared to the 1970 levels (Figure 14.4).

Table 14.11 Hazardous air pollutants for primary control

Chemical name	*Chemical name*
Acetaldehyde	Formaldehyde
Acrolein	Hexachlorobenzene
Acrylonitrile	Hydrazine
Arsenic compounds	Lead
Benzene	
Beryllium compounds	Manganese
1,3 Butadiene	
Cadmium compounds	Mercury compounds
Carbon Tetrachloride	Methylene Chloride
Chloroform	Nickel
Chromium	Polychlorinated biphenyls (PCBs)
Coke oven emissions	Polycyclic organic matter (POM)
1,2 dibromoethane	Quinoline
1,2 dichloropropane	Tetrachloroethane
1,3 dichloropropene	Tetrachloroethylene
Dioxins	Trichloroethylene
Ethylene dichloride	Vinyl Chloride
Ethylene oxide	

FOR REFERENCE PURPOSES ONLY

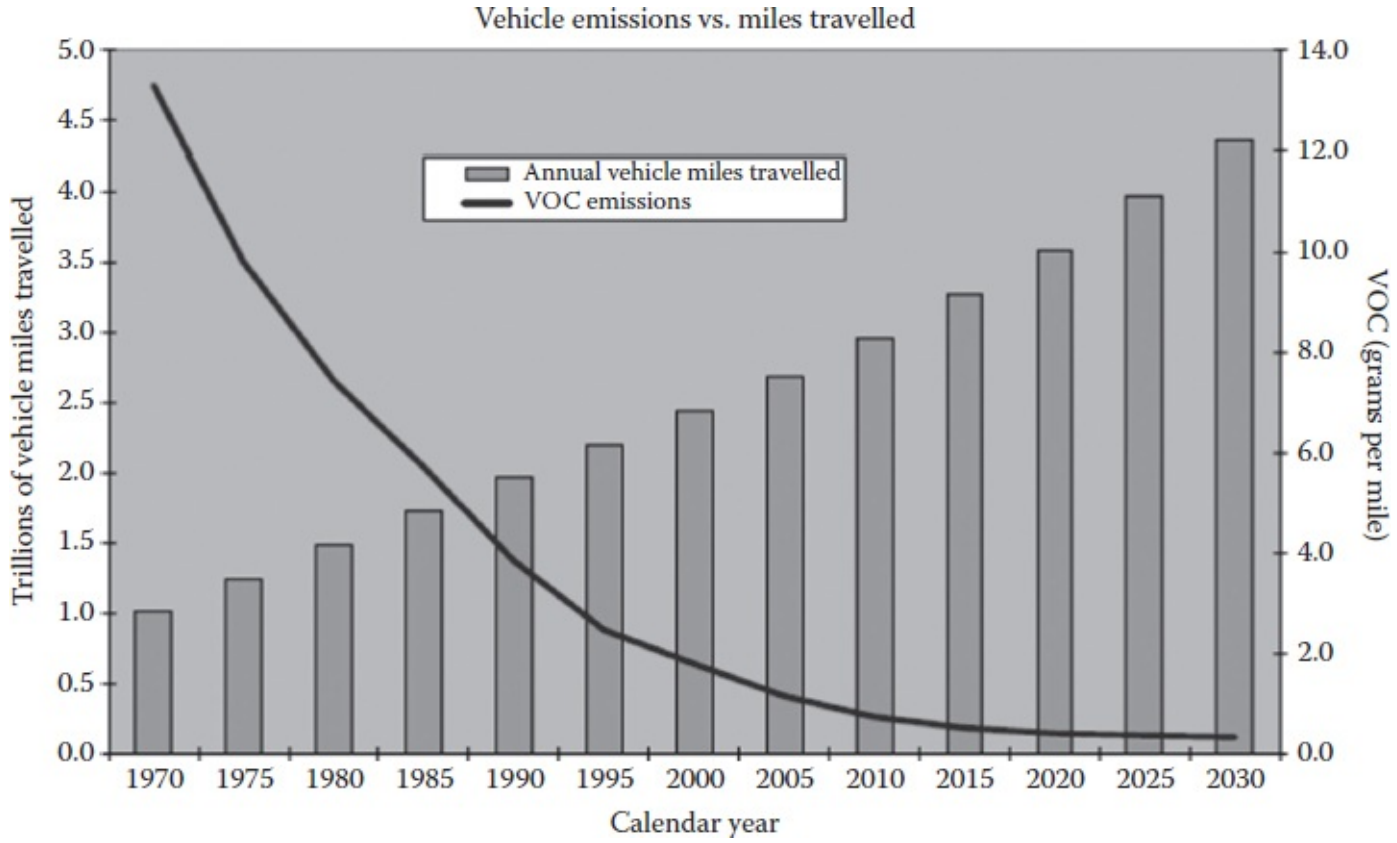

Figure 14.4 Vehicle miles travelled compared to VOC emissions per mile. (From the USEPA Clean Air Act overview.)

14.8.3 US vehicle emissions

14.8.3.1 US drive cycles

The United States has a set of drive cycles for emissions testing, representative of real-world conditions such as cold engine starts, highway driving, and so on, known as federal test procedures (FTPs). In 1975, FTP-75 was the outcome of the progressive development in the United States of a dynamometer drive cycle designed to suit American roads, vehicles and driving habits, which started in the 1950s and was based on a driving cycle through Los Angeles, California. FTP-75 consists of four different phases (cold start, stabilised phase, hot soak, hot start transient phase) with a total duration of around 1877 s, distance of 11.04 mi, average speed of 21.2 mph and a maximum speed of 56.7 mph. In addition to the FTP-75 test, a supplemental federal test procedure (SFTP) was phased in between 2000 and 2004 for use on models produced from 2000 onwards to make up for some shortcomings of the FTP cycle that made it a not completely accurate reflection of real-world driving. The two SFTP tests cycles measure emissions during aggressive highway driving (US06 cycle) and urban driving emissions while the vehicle's air-conditioning system is operating (SC03 cycle), respectively. The three test cycles are compared in Figure 14.5.

The FTP heavy-duty transient cycle consists of four phases: the first is a New York non-

FOR REFERENCE PURPOSES ONLY

freeway (NYNF) phase typical of light urban traffic with frequent stops and start; the second is a Los Angeles non-freeway (LANF) phase typical of crowded urban traffic with few stops, the third is a Los Angeles freeway (LAFY) phase simulating crowded expressway traffic in Los Angeles; and the fourth repeats the first NYNF phase.

Unlike the EU, the United States has a lack of interest in adopting WLTP, which limits the potential contribution of the new test procedure to comparability of standards beyond 2020.

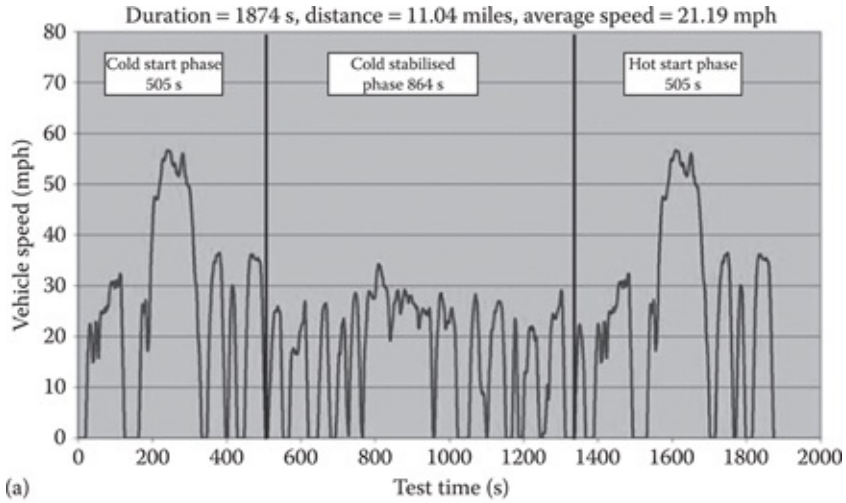

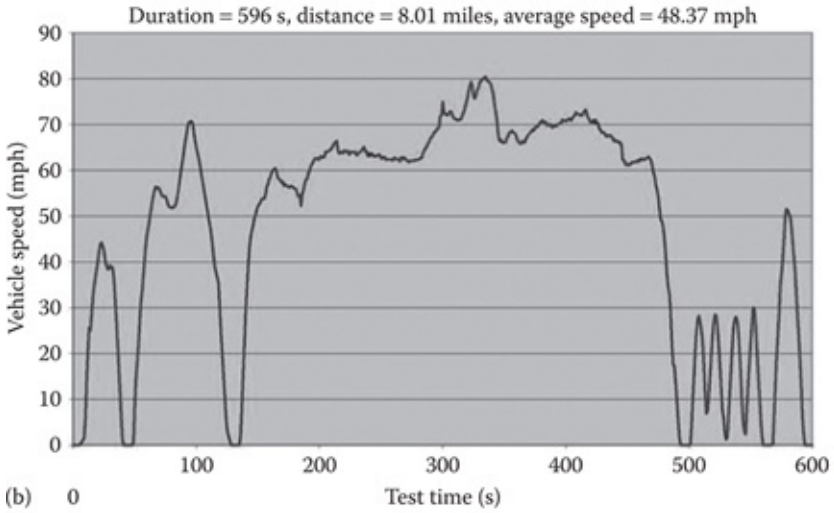

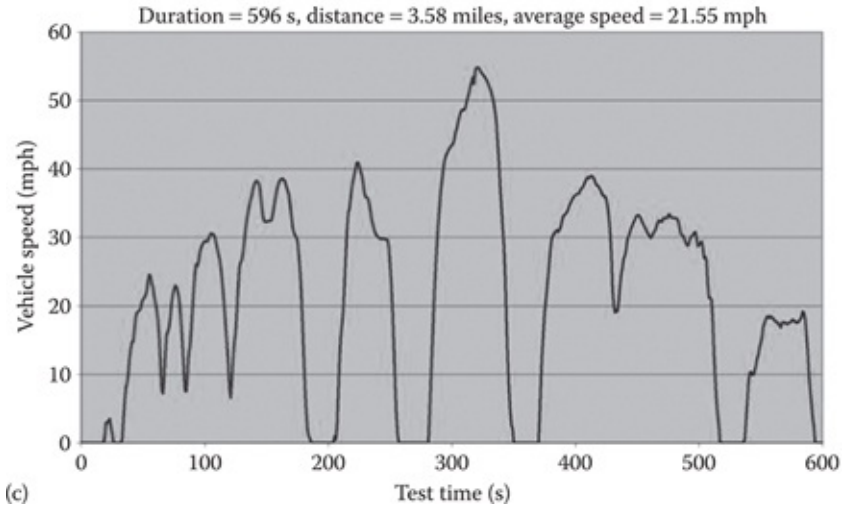

FOR REFERENCE PURPOSES ONLY

Figure 14.5 US driving cycles: (a) FTP, (b) SFTP-US06 and (c) SFTP-SC03.

14.8.3.2 US cars and light-duty vehicles

14.8.3.2.1 Federal standards

Unlike the Euro standards, US legislation on NO_x emissions from petrol and diesel cars is technology neutral. The United States was the first country to mandate the use of catalytic converters, following recognition of the causes of the photochemical smog events in the 1960s. The first oxidation catalysts were fitted in that decade, and emissions standards were steadily tightened, with all new cars required to have a TWC after 1981. Figure 14.6 provides a breakdown of different NO_x abatement technologies exhaust gas recirculation (EGR); lean NO_x trap (LNT); selective catalytic reduction (SCR) in the United States and EU for comparison using Euro 6-equivalent diesel cars in 2014. The plots indicate tighter standards and more advanced stage of implementation in the United States, with SCR fitted to two-thirds of all new diesel vehicles by 2014 (in some cases in combination with LNT). In the EU, LNT seems the dominant technology and SCR is fitted to less than 40% of diesel cars. The doughnut sizes are indicative of the dissimilarities in the two markets for diesel cars, representing approximately 50% and 1% of the new car sales in the EU and the United States, respectively. However, with the introduction of the stringent RDE test in Europe, the De-NO_x technology should progressively match with those in the United States, having steady growth in the application of SCR technology, sometimes in combination with LNT.

Three sets of standards, Tier 1, Tier 2 and Tier 3, have been progressively defined for light-duty vehicles (LDVs) in the CAAA. Introduced in 1991 with a phase-in period running from 1994 until 1997, Tier 1 standards applied to all new passenger cars, Light light-duty trucks (LLDTs) with a gross vehicle weight rating (GVWR) of less than 6000 lbs, and heavy light-duty trucks (HLDTs) with a GVWR of greater than 6000 lb but less than 8500 lbs that were manufactured within the phase-in period (Table 14.12). The *Tier 2* standards were adopted in 1999 and phased in from 2004 to 2009. The difference between diesel and petrol car standards is a more relaxed NO_x limit for diesels, which applies to vehicles through the 2003 model year (Table 14.13). Car and light truck emissions are measured over the FTP-75 test and expressed in g mi^{-1}. Additional testing was introduced from 2000 to 2004 in order to address new standards for non-methane hydrocarbons (NMHCs), NO_x and CO using an SFTP.

The Tier 2 standards bring significant emission reductions relative to Tier 1. These standards specifically restrict emissions of CO, NO_x, PM, formaldehyde (HCHO) and non-methane organic gases (NMOGs). Under the Tier 2 standard, the same emissions standards apply to all vehicle weight categories; that is, cars, minivans, light-duty trucks, and sport-utility vehicles (SUVs) have the same emission limit. As light-duty emissions standards are expressed in grams of pollutants per mile, large engines (such as those used in light trucks or SUVs) have to utilise more advanced emission control technologies than smaller engines

FOR REFERENCE PURPOSES ONLY

in order to meet the standard. The Tier 2 emissions standards are structured into eight permanent and 3 temporary certification levels of different stringency, called *certification bins*, and an average fleet standard for NO_x emissions. Vehicle manufacturers have a choice to certify particular vehicles to any of the available bins, with 1 being the cleanest (zero emissions vehicle) and higher numbers denoting more polluting vehicles. When fully implemented in 2009, the average NO_x emission of the entire light-duty vehicle fleet sold by each manufacturer has to meet the average NO_x standard of 0.07 g mi^{-1}. The temporary certification bins (bin 9, 10, and an medium-duty passenger vehicle [MDPV] bin 11) with more relaxed emissions limits are available in the phase-in period and expire after the 2008 model year.

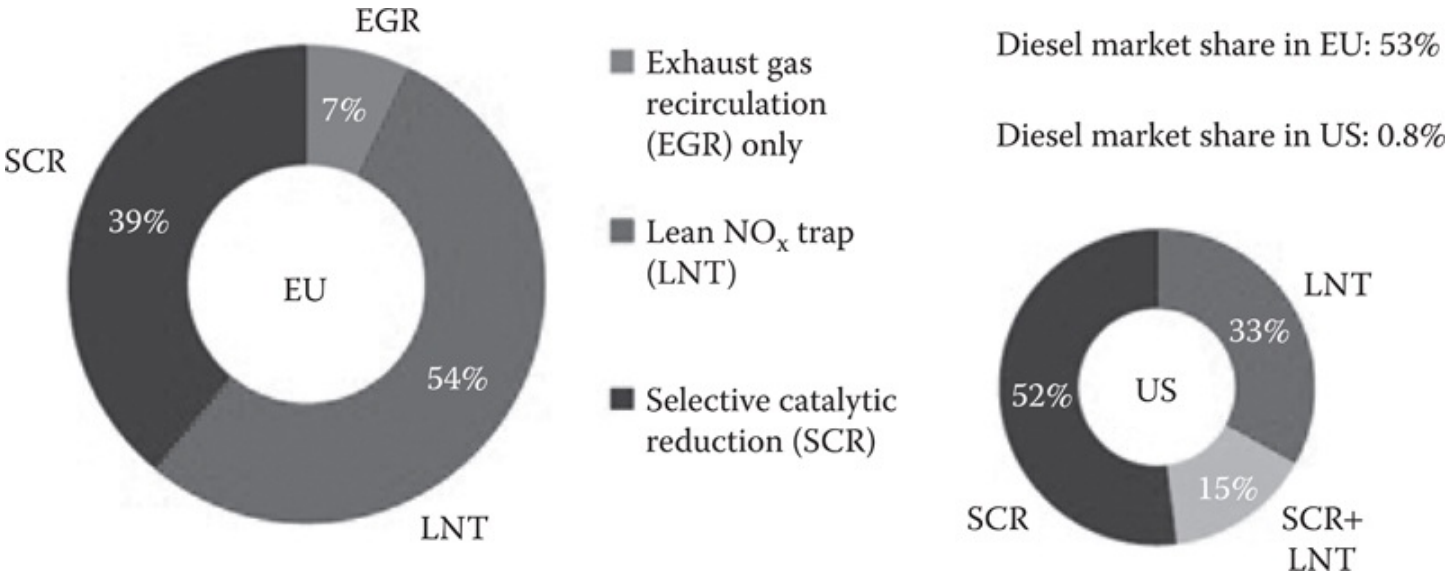

Figure 14.6 Application of diesel De-NO_x technologies in new cars in 2014. (From Mock, P. et al., The WLTP: How a new test procedure for cars will affect fuel consumption values in the EU, The International Council on Clean Transportation, Working Paper 2014–2019, 2014.)

Table 14.12 EPA Tier 1 emissions standards for passenger cars and light-duty trucks, FTP 75 (g mi^{-1})

FOR REFERENCE PURPOSES ONLY

Category	100,000 miles/10 years					
	THC	NMHC	CO	NO_x diesel	NO_x petrol	PM
Passenger cars	—	0.31	4.2	1.25	0.6	0.10
<3 750 lbs	0.80	0.31	4.2	1.25	0.6	0.10
>3 750 lbs	0.80	0.40	5.5	0.97	0.97	0.10
Light-duty truck <5 750 lbs	0.80	0.46	6.4	0.98	0.98	0.10
Light-duty truck >5 750 lbs	0.80	0.56	7.3	1.53	1.53	0.12

Table 14.13 Tier 2 emissions standards, FTP 75 (g mi^{-1})

	120,000 miles				
Bin number	NMOG	CO	NO_x[a]	PM	HCHO
11	0.280	7.3	0.9	0.12	0.032
10	0.156 (0.230)	4.2 (6.4)	0.6	0.08	0.018 (0.027)
9	0.090 (0.180)	4.2	0.3	0.06	0.018
8	0.125 (0.156)	4.2	0.20	0.02	0.018
7	0.090	4.2	0.15	0.02	0.018
6	0.090	4.2	0.10	0.01	0.018
5	0.090	4.2	0.07	0.01	0.018
4	0.070	2.1	0.04	0.01	0.011
3	0.055	2.1	0.03	0.01	0.011
2	0.010	2.1	0.02	0.01	0.004
1	0.000	0.0	0.00	0.00	0.000

[a] Average manufacturer fleet NO_x standard is 0.07 g mi^{-1}.

The Tier 2 emissions standards for all pollutants (certification bins) are shown in Table 14.13. The vehicle's *full useful life* period has been extended to 120,000 mi. The EPA bins cover California's Low-Emission Vehicle (LEV) II emissions categories, to make certification to the federal and California standards easier for vehicle manufacturers. The Tier 2 regulation also brings new requirements for fuel quality.

Table 14.14 Tier 3 emissions standards, FTP 75 (g mi^{-1})

	150,000 miles			
Bin#	$NMOG + NO_x$	PM*	CO	HCHO
160	0.062	0.00116	1.63	0.0015
125	0.049	0.00116	0.81	0.0015
70	0.027	0.00116	0.66	0.0015
50	0.019	0.00116	0.66	0.0015

FOR REFERENCE PURPOSES ONLY

30	0.012	0.00116	0.39	0.0015
20	0.008	0.00116	0.39	0.0015
0	0.00	0.00	0.00	0.00

* PM standards applicable to diesel vehicles only.

Tier 3 standards, which were adopted in 2014 for implementation from 2017, tighten sulphur limits for petrol but follow the structure of Tier 2 standards with the certification bins (although they have been relabelled as the relevant $NMOG + NO_x$ limit, where NMOGs are the diesel fuel equivalent of NMHC) and fleet average standards. Standards are also more stringent (Table 14.14) and emission durability/vehicle lifespan was also increased to 150,000 from 120,000 mi. Tier 3 standards are now in line with the California LEV III standards (see Section 14.8.4) to bring consistency on a national level. Tier 3 standards cover all new vehicles that fall into the categories of Tier 1 and Tier 2 as well as all heavy-duty vehicles with a GVWR of less than 14,000 lbs.

14.8.4 Vehicle emissions in California

California has had the world's worst air quality problems due to motor vehicles for most of the second half of the twentieth century and had therefore taken draconian measures – beyond those required by the CAAA – to try and control them. The California Air Resources Board (CARB) set low-emissions vehicle standards for passenger cars and light-duty trucks in 1994. They are designed to reduce precursor emissions and O_3 formation, and to allow for and encourage the introduction of alternative fuels such as ethanol, methanol, compressed natural gas, or liquefied petroleum gas. Under California's original LEV programme, emissions standards were expressed through the following emissions categories:

- Tier I
- Transitional Low-Emission Vehicles (TLEV)
- Low-Emission Vehicles (LEV)
- Ultra Low-Emission Vehicles (ULEV)
- Super Ultra Low-Emission Vehicles (SULEV)
- Zero Emission Vehicles (ZEV, assumed to be electric)

A second round of California standards, known as Low-Emission Vehicle II, was phased in between 2004 and 2010, timed with the Tier 2 rollout. Under LEV II regulations, the Tier I and TLEV classifications were removed in 2004, and the remaining LEV, ULEV and SULEV categories have been made more stringent, specifically for NO_x and PM standards for all emission categories. These stricter versions are known as LEV II, ULEV II and SULEV II. In addition, the following new categories were created:

- Inherently Low-Emission Vehicle (ILEV)
- Partial Zero Emission Vehicle (PZEV)
- Advanced Technology Partial Zero Emission Vehicle (AT-PZEV)
- National Low-Emission Vehicle (NLEV)

LEV III standards were adopted in 2012 for implementation between 2015 and 2025. These standards continue to progress towards even stricter regulations, in line with the federal Tier 3 standards. They include fleet average emission requirements relating to NMOG + NO_x for compliance by 2025. Car manufacturers are required to produce a percentage of vehicles certified to increasingly more stringent emission categories. The phase-in schedules, which are fairly complex, are generally based on vehicle fleet emissions averages. The exact schedules can be found on the EPA website. The CARB also stipulated that 10% of new cars sold in California in and after 2003 must be ZEVs. The initiative has spawned a host of new developments in ZEV technology, together with advances in hybrid vehicles and alternative fuels. The major car manufacturers are allowed to substitute 6% of the 10% with *almost-ZEVs* which achieve extremely low emissions. As totally ZEVs can only be battery-powered at present, this change has allowed the use of alternative fuels, hybrid vehicles and fuel cells. The main limitation of the battery-powered vehicles produced thus far is their short range – typically 100 mi.

The same standards for gaseous pollutants apply to diesel- and petrol-fuelled vehicles. Particulate matter standards apply to diesel vehicles only. Emissions are measured over the FTP-75 test and are expressed in g mi^{-1}. The additional SFTP has been phased-in in California between 2001 and 2005. The Californian emissions values incorporate the concept of reactivity-weighted VOC mass emissions, together with NO_x reductions. The reactivity adjustment factor (RAF) for any new fuel is defined as the mass of O_3 formed from 1 g of emissions from the new fuel, taken as a proportion of the mass of O_3 formed from 1 g of emissions from standard-grade petrol. Hence, the allowed NMVOC for a particular fuel is found from the aforementioned value divided by the appropriate RAF. For example, the typical fuel for a TLEV would be 85% methanol, 15% petrol, with a RAF of 0.41 and permitted NMVOC emissions of 0.125/0.41 = 0.30 g mi^{-1}. Accurate assessment of the RAF for a particular fuel requires quantitative speciation of at least 50, and probably 170, combustion products. The CARB estimates that 27,000 t of PM are emitted each year in California from around 1.25 million diesel engines and plans to reduce this by 90%. The control programme involves 12 measures, including the use of PM traps on all new and most existing diesel engines (this covers private as well as commercial, although private diesel vehicles are less common in the United States than in Europe), low-sulphur diesel fuel, in-use emissions testing and broader use of alternative fuels in place of diesel.

14.8.5 US locomotives

In the United States, emissions from diesel-powered locomotives are also regulated. On 17

FOR REFERENCE PURPOSES ONLY

December 1997 the USEPA adopted emissions standards for oxides of nitrogen (NO_x), hydrocarbons (HC), carbon monoxide (CO), particulate matter (PM) and smoke for newly manufactured and remanufactured railroad locomotives and locomotive engines. The ruling, which took effect in 2000, applies to locomotives originally manufactured from 1973, any time they are manufactured or remanufactured. Electric locomotives, historic steam-powered locomotives, and locomotives originally manufactured before 1973 are not regulated. Three separate sets of emissions standards have been adopted, with the applicability of the standards depending on the date a locomotive is first manufactured.

The first set of standards (Tier 0) applies to locomotives and locomotive engines originally manufactured from 1973 through 1992, any time they are manufactured or remanufactured. The second set of standards (Tier 1) applies to locomotives and locomotive engines originally manufactured from 1993 through 2004. These locomotives and locomotive engines are required to meet the Tier 1 standards at the time of manufacture and each subsequent remanufacture. The subsequent standards (Tier 2, 3 and 4) apply to locomotives and locomotive engines originally manufactured between 2005–2011, 2012–2014 and 2015 onward, respectively.

Table 14.15 Emission standards for locomotives, g (bhp h)$^{-1}$

Duty cycle	*HC*[a]	*CO*	*NOx*	*PM*
Tier 0 (1973–1992)				
Line-haul	1.0	5.0	9.5	0.22
Switch	2.1	8.0	11.8	0.26
Tier 1 (1993–2004)				
Line-haul	0.55	2.2	7.4	0.22
Switch	1.2	2.5	11.0	0.26
Tier 2 (2005–2011)				
Line-haul	0.3	1.5	5.5	0.10
Switch	0.6	2.4	8.1	0.13
Tier 3 (2012–2014)				
Line-haul	0.3	1.5	5.5	0.10
Switch	0.6	2.4	5.0	0.10
Tier 4 (2015+)				
Line-haul	0.14	1.5	1.3	0.03
Switch	0.14	2.4	1.3	0.03

[a] HC standard is in the form of total hydrocarbons for diesel engines.

The emissions are measured over two steady-state test cycles which represent two different types of service, including the *line-haul* and *switch* locomotives. The duty cycles include different weighting factors for each of the 8 throttle notch modes, which are used to operate locomotive engines at different power levels, as well as for idle and dynamic brake

FOR REFERENCE PURPOSES ONLY

modes. The switch operation involves much time in idle and low power notches, whereas the line-haul operation is characterised by a much higher percentage of time in the high power notches, especially notch 8.

A dual-cycle approach has been adopted in the regulation; that is, all locomotives are required to comply with both the line-haul and switch duty cycle standards, regardless of intended usage. The emissions standards and current locomotive emission levels are listed in Table 14.15. The smoke opacity standards are listed in Table 14.16. The regulations contain several other provisions, including a production line testing (PLT) programme, in-use compliance emissions testing, as well as averaging, banking and trading (ABT) of emissions.

14.8.6 National parks and wilderness areas

There are many forests and national parks in the United States where controlled burning is a routine management requirement. Yet such burning unavoidably creates emissions of many air pollutants. The US Clean Air Act designated 156 national parks, wilderness areas and wildlife protection zones as Class I areas. Many of these areas have names that are very familiar such as Grand Canyon, Great Smokies, Yellowstone, Yosemite and the Everglades. The managers of such areas have an affirmative responsibility to protect the air quality related values (AQRVs) from adverse air pollution impacts. AQRVs are those features or properties of a Class I area which can be changed by air pollution. If the area concerned is adjacent to a non-attainment area for NAAQS, the proposed burn must include prediction of the impact on local air quality. If any process or activity is proposed, then it must be shown that it will not result in significant deterioration of air quality.

Table 14.16 Smoke standards for locomotives, % opacity – Normalised

	Steady-state	*30-s peak*	*3-s peak*
Tier 0	30	40	50
Tier 1	25	40	50
Tier 2	20	40	50

14.9 LEGISLATION IN THE ASIAN REGION

The issue of air quality in Asia is accentuated by increased economic development, resulting from a combination of intense industrial activity, large populations and increased motor vehicle usage. Over the past decade, member states of the Regional Co-operation Agreement (RCA), an intergovernmental agreement for the East Asia and Pacific region, have decided to implement policies and legislation for air pollution abatement. This has prompted the definition of ambient and emissions standards, especially in urban and industrialised areas. environmental impact assessments are now a common requirement.

FOR REFERENCE PURPOSES ONLY

The majority of these activities occur with the assistance of international organisations and financial institutions such as the World Bank and the Asian Development Bank. In South Asia, many institutions involved with environmental governance and protection are being strengthened. Many new public sector institutions have been established, including environmental ministries, while independent environment agencies and departments have been created to assist them.

14.9.1 National standards

Monitoring and enforcement of standards in East Asia have been generally weak. Japan has one of the strictest regulation regimes in the world for emissions of SO_2 and NO_x, the air pollutants causing acid rain. In Japan, legislative initiatives in the late 1960s, including the establishment of an Environment Agency, were compromised by rapid industrial growth and economic development. However, by the end of the 1980s Japan's growing international role and the generally poor state of the national environment forced a re-evaluation of environmental and development goals. New legislation was enacted, for example to reduce vehicle emissions, and by 1993 the government had established a basic environment plan (Environment Agency of Japan 1994) which outlined policies and policy instruments, and defined the roles of each sector of society.

Transboundary pollution has attracted significant regional cooperation. For instance, since 1993 the Environment Agency of Japan has been advocating the establishment of the Acid Deposition Monitoring Network in East Asia to establish uniform monitoring techniques, share data and information, create a common understanding of the state of acid deposition and provide inputs for decision making at all levels. This monitoring network includes nine collaborating countries – China, Indonesia, Japan, the Republic of Korea, Malaysia, Mongolia, the Philippines, Thailand and the Russian Federation. India has adopted the air quality standards which are listed under the NAAQS in Table 14.17. Table 14.6 earlier in the chapter presented air quality standards for major air pollutants for selected Asian countries alongside those of several developing countries around the world.

Table 14.17 National Ambient Air Quality Standards (NAAQS) for India (in μg m^{-3})

	Concentration in ambient air		
Pollutant and time-weighted average	*Industrial, residential, rural and other areas*	*Ecologically sensitive area*	*Methods of measurement*
Sulphur dioxide			
Annual average	50	20	1. Improved West and Gaeke method
24 h	80	80	2. Ultraviolet fluorescence
Nitrogen dioxide			
Annual average	40	30	1. Modified Jacob & Hochheiser
24 h	80	80	2. Gas-phase chemiluminescene
PM_{10}			

FOR REFERENCE PURPOSES ONLY

Annual average	60	60	1. Gravimetric
24 h	100	100	2. TEOM
			3. Beta attenuation
$PM_{2.5}$			
Annual average	40	40	1. Gravimetric
24 h	60	60	2. TEOM
			3. Beta attenuation
O_3			
8 h	100	100	1. UV photometric
1 h	180	180	2. Chemiluminescence
			3. Chemical method
Lead			
Annual average	0.5	0.5	1. AAS/ICP method after sampling using EPM 2000 or an equivalent filter paper
24 h	1.0	1.0	2. ED-XRF using Teflon filter
Ammonia			
Annual average	100	100	1. Chemiluminescence
24 h	400	400	2. Indophenol blue method
Benzene			
Annual	5	5	1. Gas chromatography-based continuous analyser
			2. Adsorption and desorption followed by GC analysis
Carbon monoxide			
8 ha[a]	2	2	Non-dispersive infrared (NDIR) spectroscopy
1 ha[a]	4	4	
Benzo(a)Pyrene (particulate phase only)			
Annual[b]	1	1	Solvent extraction followed by HPLC/GC analysis
Arsenic			
Annual[b]	6	6	AAS/ICP method after sampling on EPM 2000 or equivalent filter paper
Nickel			
Annual[b]	20	20	AAS/ICP method after sampling on EPM 2000 or equivalent filter paper

Source: Central Pollution Control Board (CPCB), Ministry of Environment and Forests, Government of India, 18 November 2009.

[a] Expressed in mg m^{-3}.

[b] ng m^{-3}.

The following points should be taken into account when interpreting the earlier standards:

- Annual average is annual arithmetic mean of minimum 104 measurements in a year taken twice a week at 24-hour intervals.
- Twenty-four-hourly and 8-hourly values should be met 98% of the time within a year.

FOR REFERENCE PURPOSES ONLY

However, it may be exceeded 2% of the time but not on 2 consecutive days.

- NAAQS levels have adequate margins for the safety of public health, vegetation and property.
- Whenever and wherever two consecutive values exceed the limit specified earlier for the respective category, it is considered adequate to initiate regular/continuous monitoring and further investigations.
- The state (provincial) government or a state board shall notify the sensitive and other areas in the respective states within a period of six months from the date of notification on the NAAQS.
- The ammonia standard is specified in a notification dated 14 October 1998. It does not mention either the type of areas for its applicability or the method used for its measurement. This has to be verified with the CPCB.

14.9.2 Vehicle emissions regulations in Asia

China introduced its first emissions controls on automobiles, which were equivalent to Euro I standards, in 2000. In 2004, they were upgraded to Euro II. During July 2007 these were replaced with the more stringent emissions standards of National Standard III (equivalent to Euro III). It was initially planned that Euro IV equivalent standards would go into effect in 2010. However, in the light of the 2008 Olympic Games, Beijing introduced Euro IV standards in advance on 1 January 2008. In the case of Hong Kong, since 1 January 2006 all new passenger cars with spark-ignition engines have had to meet either Euro IV petrol standard, Japanese Heisei 17 standard or US EPA Tier 2 Bin 5 standards. For new passenger cars with compression-ignition engines, the corresponding requirement is USEPA Tier 2 Bin 5.

In Japan, to mitigate NO_x pollution problems from existing vehicle fleets, the *Motor Vehicle NO_x Law* was introduced in 1992. In June 2001, this regulation was amended as the *Automotive NO_x and PM Law* with further tightening of existing NO_x requirements and inclusion of PM control provisions. This law is enforced in conjunction with the Japanese vehicle inspection program. Vehicles have a grace period, between 9 and 12 years from the initial registration, to comply. Non-complying vehicles cannot undergo the inspection in the designated areas. This, in turn, may trigger an injunction on the vehicle's operation under the Road Transport Vehicle Law.

India has developed extensive emission regulations ever as the first one became effective in 1989. These were idle emission limits which were replaced by mass emissions limits for both gasoline (1991) and diesel (1992) vehicles. During October 2003, the National Auto Policy was announced, which introduced Euro 2–4 emissions standards and fuel regulations. In May 2014, the Auto Fuel Vision and Policy 2025 set out a path for implementation of BS IV–VI. Table 14.18 shows the implementation schedule of EU emissions standards in India for 4-wheel vehicles. For 2- and 3-wheelers, Bharat Stage II (Euro 2) has applied from 1 April 2005, Stage III (Euro 3) in April 2010. Bharat Stage IV standards for gasoline fuelled

FOR REFERENCE PURPOSES ONLY

2-wheelers came into force 1 April 2016.

Table 14.18 Implementation schedule for vehicle emissions standards (4-wheel) in India

Standard	*Reference*	*Date*	*Region*
India 2000	Euro 1	2000	Nationwide
Bharat Stage II	Euro 2	2001	NCR[a], Mumbai, Kolkata, Chennai
		2003	NCR[a], 11 cities[b]
		2005	Nationwide
Bharat Stage III	Euro 3	2005	NCR[a], 11 cities[b]
		2010	Nationwide
Bharat Stage IV	Euro 4	2010	NCR[a], 13 cities[b]
		2015	North India (9 states)
		2016	Western India (10 states and Union Territories)
		2017	Nationwide
Bharat Stage V	Euro 5	–[c]	
Bharat Stage VI	Euro 6	2020	Nationwide

[a] NCR is the National Capital Region (i.e. Delhi).

[b] Mumbai, Kolkata, Chennai, Bangalore, Hyderabad, Ahmedabad, Pune, Surat, Kanpur and Agra.

[c] Supreme Court Ruling January 2016 has asked India government to skip BS V.

Emissions standards for new heavy-duty diesel engines (applicable to vehicles of GVWR > 3500 kg) are listed in Table 14.19. As shown, the emissions are progressively tested over the ECE R49 13-mode test (equivalent of Euro II stage), European Stationary Cycle (ESC), European Transient Cycle (ETC), World Harmonized Stationary/Transient Cycle (WHSC/WHTC).

Table 14.19 Emission standards for diesel truck and bus engines in India

FOR REFERENCE PURPOSES ONLY

Stage	Year	Test	CO	HC	CH_4	NO_x	PM	PN	NH_3
			g (kWh)$^{-1}$					kWh^{-1}	ppm
	1992	ECE R49	17.3	2.7					
	1996	ECE R49	11.2	2.4		14.4			
India 2000	2000	ECE R49	4.5	1.1		8.0	0.36[a]		
BS II	2005	ECE R49	4.0	1.1		7.0	0.15		
BS III	2010	ESC	2.1	0.66		5.0	0.10		
		ETC	5.45	0.78		5.0	0.16		
BS IV	2010	ESC	1.5	0.46		3.5	0.02		
		ETC	4.0	0.55		3.5	0.03		
BS V	N/A	ESC	1.5	0.46		2.0	0.02		
		ETC	4.0	0.55	1.1[b]	2.0	0.03		
BS VI	2020	WHSC (CI)	1.5	0.13		0.40	0.01	8×10^{11}	10
		WHTC (CI)	4.0	0.16[d]	0.50	0.46	0.01	6×10^{11}[c]	10

[a] 0.612 for engines below 85 kW.

[b] For CNG engines only.

[c] Applicable from 1 April 2025 for new models and 1 April 2026 for existing models.

[d] NMHC.

14.10 AIR POLLUTION INFORMATION SYSTEMS

While scientists, administrators and legislators may anguish over the relationships between the concentrations of a particular pollutant and their effects, non-expert members of the public need more immediate information to tell them how clean the *air* is, whether it is safe and to warn them if it is not. The general approach is to avoid the complexities of unfamiliar units such as ppb and μg m^{-3} by relating effects to a standard scale such as 1–100, and to describe the air quality in everyday terms such as *good* or *moderate* or *hazardous*, using colour-coded bands. For instance, to present the air quality in European cities in a comparable and easy-to-understand way, all detailed measurements are transformed into a single relative measure: the Common Air Quality Index.

14.10.1 Air quality indices

The air quality index is a tool for effective communication of air quality status to people in terms which are easy to understand. It transforms complex air quality data of various pollutants into a single number (index value), nomenclature and colour.

14.10.1.1 UK Daily Air Quality Index

FOR REFERENCE PURPOSES ONLY

The first approach along these lines in the UK was the Air Pollution Information System, which is designed to inform the public about air quality without using specific concentrations or units. The banding system is approved by the Committee on the Medical Effects of Air Pollutants (COMEAP) on the basis of epidemiological studies on the short-term air pollution impacts. The Daily Air Quality Index (DAQI) is generated using the weather and air pollution forecasts from the UK Met Office and published daily on the UK-AIR (Air Information Resource) website. The main components include three threshold concentrations (standard, information and alert) for each of five pollutants. The system uses a 1–10 index divided into four bands (low = 1–3; moderate = 4–6; high = 7–9; and very high = 10) to provide more detail about air pollution levels in a simple way, similar to the sun index or pollen index. The thresholds were chosen for their significance to health effects, and these bandings have been widely used, for example, during TV weather forecasts, to alert people both to prevailing and predicted conditions (Table 14.20).

Table 14.20 UK Daily Air Quality Index Bandings

		Ozone (Running 8-h mean)	*NO_2 (Hourly mean)*	*SO_2 (15-min mean)*	*$PM_{2.5}$ (24-h mean)*	*PM_{10} (24-h mean)*
Band	*Index*			$\mu g\ m^{-3}$		
Low	1	0–33	0–67	0–88	0–11	0–16
	2	34–66	68–134	89–177	12–23	17–33
	3	67–100	135–200	178–266	24–35	34–50
Moderate	4	101–120	201–267	267–354	36–41	51–58
	5	121–140	268–334	355–443	42–47	59–66
	6	141–160	335–400	444–532	48–53	67–75
High	7	161–187	401–467	533–710	54–58	76–83
	8	188–213	468–534	711–887	59–64	84–91
	9	214–240	535–600	888–1064	65–70	92–100
Very high	10	>240	>600	>1064	>70	>100

Table 14.21 The NAQI categories and their ambient air pollutant thresholds

NAQI category (range)	PM_{10} (24-h)	$PM_{2.5}$ (24-h)	NO_2 (24-h)	O_3 (8-h)	SO_2 (24-h)	NH_3 (24-h)	Pb (24-h)	CO (8-h)
	$\mu g\ m^{-3}$							$mg\ m^{-3}$
Good (0–50)	0–50	0–30	0–40	0–50	0–40	0–200	0–0.5	0–1.0
Satisfactory (51–100)	51–100	31–60	41–80	51–100	41–80	201–400	0.51–1.0	1.12.0
Moderately polluted (101–200)	101–250	61–90	81–180	101–168	81–380	401–800	1.1–2.0	2.1–10
Poor (201–300)	251–350	91–120	181–280	169–208	381–800	801–1200	2.1–3.0	10.1–17
Very poor (301–400)	351–430	121–250	281–400	209–748[a]	801–1600	1201–1800	3.1–3.5	17.1–34
Severe (401–500)	>430	>250	>400	>748[a]	>1600	>1800	>3.5	>34

[a] 1-hour monitoring values.

14.10.1.2 Indian National Air Quality Index

The Indian National Air Quality Index (NAQI), launched in October 2014, has six categories – good, satisfactory, moderately polluted, poor, very poor and severe (Table 14.21). Each of these categories is decided based on ambient concentration values of air pollutants and their likely health impacts (known as health breakpoints). AQ sub-index and health breakpoints are tabulated for eight pollutants (PM_{10}, $PM_{2.5}$, NO_2, SO_2, CO, O_3, NH_3, and Pb) for which short-term (up to 24 hours) National Ambient Air Quality Standards are prescribed (Table 14.17). Based on the measured ambient concentrations of a pollutant, sub-index is calculated, which is a linear function of concentration (e.g. the sub-index for $PM_{2.5}$ would be 51 at concentration 31 $\mu g\ m^{-3}$, 100 at concentration 60 $\mu g\ m^{-3}$ and 75 at concentration of 45 $\mu g\ m^{-3}$). The worst sub-index is used to determine the overall NAQI.

14.10.1.3 Pollutant Standards Index

The Pollutant Standards Index (PSI) is based on a scale devised by the USEPA. In the United States, the PSI equates the scale value 100 to the shortest-term NAAQS concentration, which is called moderate. The index value then rises, approximately *pro rata* with the actual concentration, to values of 200 (alert), 300 (warning), 400 (emergency) and 500 (significant harm). At each level, the general health effects are summarised and appropriate precautions indicated. Of course, one danger of this approach is that equal index values for quite different pollutants will be perceived as equally hazardous to health. Initially, PSI was based on five air pollutants, but since 1 April 2014, it has also included

fine particulate matter ($PM_{2.5}$). The PSI is used by metropolitan areas to report an overall assessment of each day's air quality to the public. Hence, the PSI method does not attempt to evaluate the overall impact of combined pollutants, about which even less is understood than the impacts of the individual pollutants. Trends in potential health impacts of air pollution have been analysed in terms of the number of days on which PSI values of 100 were exceeded. In addition to the PSI derived by averaging data collected for the past 24 h, Singapore also publishes a 3-h-PSI based on $PM_{2.5}$ concentrations for the past 3 h. One-hour $PM_{2.5}$ concentrations are also published every hour.

14.10.2 Headline indicator

Another approach that has been investigated in the UK is that of the Headline Indicator. This has been suggested as useful not only for communicating with the public but also to feed in to assessments of overall environmental quality and sustainability. After considering various options, DEFRA adopted the concept of *days exceeding* as the criterion for a headline indicator. Correct terminology is vital in this subject – for example, days exceeding is a different concept, and generates quite different values, to daily exceedances. Days exceeding is the sum of days with an exceedance of any pollutant, with a maximum of one exceedance per day. It was recommended that the standard threshold be used for counting exceedances, as this corresponds to the standard concentration set in NAQS, and to the concentration below which health effects are unlikely to be found. Thus, if one monitoring site recorded CO concentrations above standard for 5 days, SO_2 concentrations above standard on 6 days and PM_{10} concentrations above standard for 8 days during one year, the days exceeding the figure for that site would be 19. If the days overlap, however, they should only be counted once.

14.11 CASE STUDY – LOCAL AIR QUALITY MANAGEMENT

14.11.1 Background

Air quality has a strong spatial association with residential population (expressed in legislation and guidance as *exceedances of the objectives* at *relevant locations*) and requires a management-at-source approach to avoid adverse impacts. The UK Environment Act 1995 and the European Air Quality Framework Directive (1992/62/EC) led to the establishment of an air quality management process in the UK. Contrary to air pollution control, which focuses on emission reductions, the core focus of this initiative has been to address issues related to ambient air pollution concentrations. Since 1997, the UK statutory LAQM regime has served to support Local Authorities (LAs) on collaborative action to assess and manage air pollution sources within their jurisdiction (Longhurst et al., 2009). According to the

FOR REFERENCE PURPOSES ONLY

Department of Environmental Food and Rural Affairs Air Quality Strategy (2007), the primary intention of the prescribed LAQM approach has been to protect and improve *local* population health and well-being, which is underpinned by the notion that pollution sources (mainly traffic-related) are best managed at the lowest administrative level through proportionate, collaborative initiatives accounting for the local context. LAs in the UK have conducted rigorous assessments and declarations of AQMAs under the LAQM policy framework. To date, over 230 of LAs (approximately 60%) have declared one or more AQMAs for different pollutants (predominantly nitrogen dioxide, NO_2 and particulate matter, PM_{10}). Transportation, being a major urban activity, has been identified as the main source of pollution in the majority of the AQMAs (approximately 92%) (Tiwary et al., 2014).

14.11.2 Recommended methodology

LAQM adopts a two-stage effects-based approach (i.e. air quality assessment in the context of likely public exposure). Undertaken in periodic cycles, LAQM's two stages are (Figure 14.7):

Stage i: Review and assessment: A phased risk-management approach to review air quality in locations where the public is likely to be regularly present constitutes updating and screening assessment. If air quality objective (AQO) breaches are confirmed or likely (determined by monitored or modelled data) and the exposure duration is appropriate to the averaging period of pollutant(s) AQO(s), a detailed assessment and AQMA declaration is required. At a minimum, AQMAs should define the area of technical exceedance.

Stage ii: Action planning: Following AQMA declaration, LAs must develop and implement an air quality action plan (AQAP) of collaborative, proportionate, cost-effective and timebound mitigation and management measures. In these areas, LAs must work towards achieving specified AQOs. Further assessments test the validity of the AQMA declaration and provide further evidence (e.g. source apportionment) and quality assurance to support AQAPs.

However, recent studies have called for effective LAQM processes, mainly to address the epidemiology of air pollution by incorporating a good understanding of the local air pollution problems and solutions in the broadest possible public health context (Brunt et al., 2016).

FOR REFERENCE PURPOSES ONLY

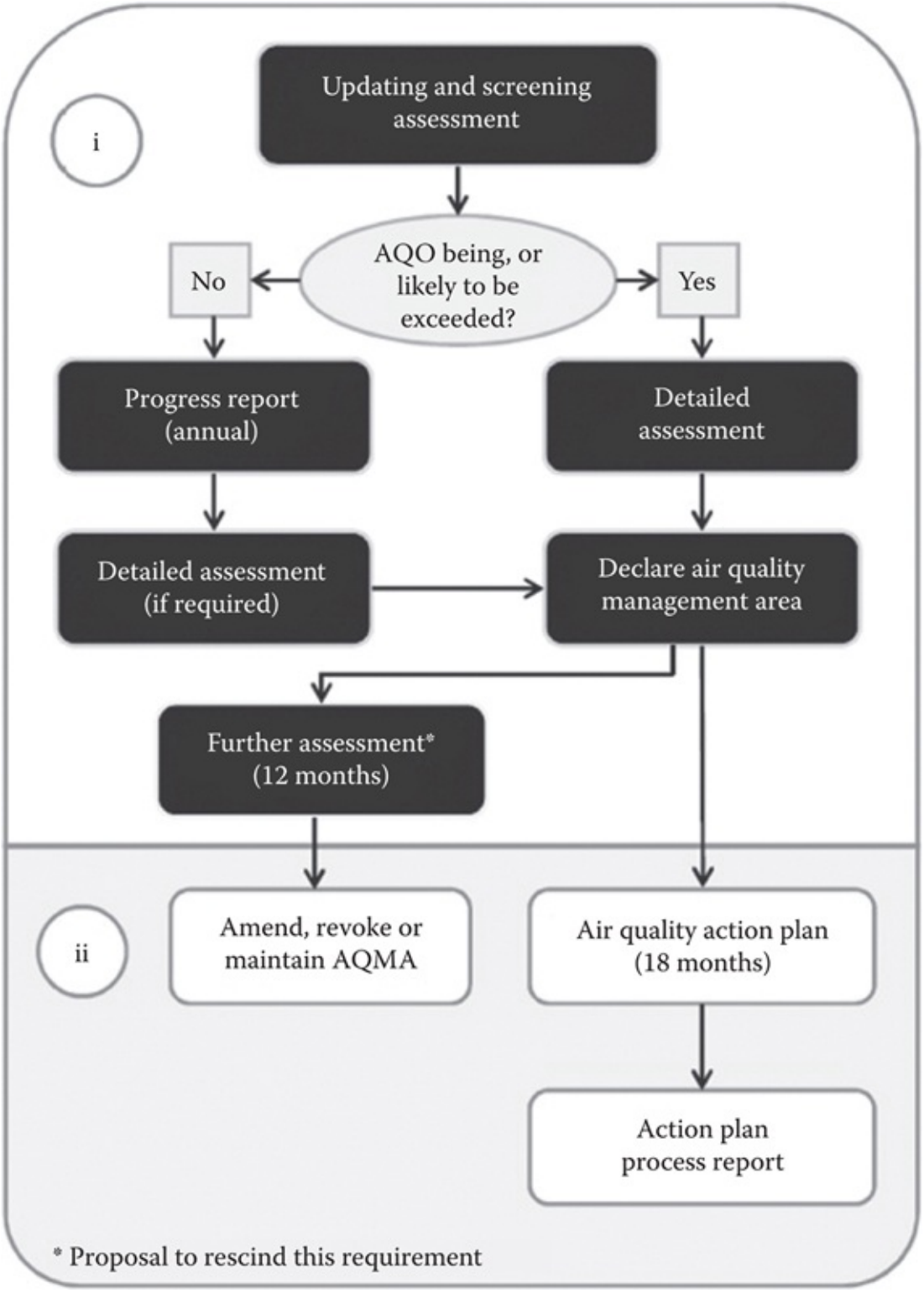

Figure 14.7 Overview of the two-stage LAQM process (as of July 2015). (From DEFRA, *Review of Local Air Quality Management: Consultation on Regulatory and Guidance Change*, Department for Environment, Food and Rural Affairs, London, UK, 2014.)

14.11.3 Limitations of the local air quality management approach

FOR REFERENCE PURPOSES ONLY

The scope of the LAQM approach is mainly to manage the pollution hot spots rather than addressing the issues with more diffused and/or overall background pollution concentrations. In effect, this approach thus far has largely concentrated on controlling the emissions (e.g. improving the traffic flow) rather than addressing the human factors in pollution exacerbations and subsequent exposure. The scope of LAQM is quite narrow, with activities restricted to small areas, the so-called *hot spots* where there are actual or potential breaches of air quality objectives. They are rarely considered in a broad public health context and therefore this framework is devoid of civic engagement. Hence, it currently lacks the attributes of an adequate citizen-based LAQM.

Further, the conventional LAQM framework lacks the rigour to accommodate *co-management*, that is, concerted, inter-sectoral local actions towards achieving cost effective air quality improvements while managing CO_2 reduction targets alongside (Tiwary et al., 2014). This is imperative as the majority of *conventional* air pollution and CO_2 emissions at a local level originate from anthropogenic sources, and measures to reduce one problem are likely to have some impact (either positive or negative) on the other. Embedding co-management into existing LAQM approach has both pros and cons. The immediate benefit is through empowering LAs to take action through localised management solutions given their wide range of responsibilities and greater understanding of the underlying activities simultaneously implicating air quality and greenhouse gas (GHG) emissions. Integrated air quality management and GHG reduction measures have been reported to offer greater benefits than those obtained from the implementation of isolated measures (Chae and Park, 2011). Hence, greater emphasis is placed on *holistic* LAQM plans and strategies, incorporating climate change considerations, or vice versa; for example, see London Borough of Brent (2012). However, despite the high-level calls for joint action on air quality and climate change, the notion of *co-management* has received little in-depth exploration at local scales. This is also marred by recent reports from several European countries, indicating *uneven adoption* of the Local Agenda 21 framework, suggesting weak (or at least very uneven) support for the local sustainable development strategies at local governance levels across Europe (Fidélis and Pires, 2009; Barrutia and Echebarria, 2012). Economically, air quality co-benefits of GHG reduction policies could potentially offset a large proportion of the cost of the mitigation actions, particularly in developing countries (Stern et al., 2007; Nemet et al., 2010). Planned actions to reduce certain air pollutants (so-called *short-lived climate forcers*) have been reported to be advantageous in slowing the rate of warming (Ravishankara et al., 2012). But the greatest hindrance is in terms of the limited skill-base within the LAs (developed and developing countries alike) in delivering this innovative, cross-cutting agenda, augmented by the complexities in integrating local and scientific knowledge (Raymond et al., 2010), which is likely to impede the expected outcome from improved integration of these two issues.

FOR REFERENCE PURPOSES ONLY

REFERENCES AND FURTHER READING RESOURCES

Amann, M., Bertok, I., Borken-Kleefeld, J., Cofala, J., Heyes, C., Hoeglund-Isaksson, L., Klimont, Z. et al. (2011) An updated set of scenarios of cost-effective emission reductions for the revision of the Gothenburg Protocol. CIAM report, 4.

Barrutia, J. M., and Echebarria, C. (2012) Greening regions: The effect of social entrepreneurship, co-decision and co-creation on the embrace of good sustainable development practices. *Journal of Environmental Planning and Management*, 55(10): 1348–1368.

Bell, S. (2000) *Ball & Bell on Environmental Law: The Law and Policy Relating to the Protection of the Environment*, 5th ed. Blackstone Press, London, UK.

Brunta, H., Barnes, J., Longhurst, J. W. S., Scally, G., and Hayes, E. (2016) Local air quality management policy and practice in the UK: The case for greater public health integration and engagement. *Environmental Science & Policy*, 58: 52–60.

CPCB (2006) National ambient air quality monitoring. Central Pollution Control Board, Ministry of Environment and Forests, Government of India, 18 November 2009.

Chae Y., and Park, J. (2011) Quantifying costs and benefits of integrated environmental strategies of air quality management and greenhouse gas reduction in the Seoul metropolitan area. *Energy Policy*, 39(9): 5296–5308.

DEFRA (2014) *Review of Local Air Quality Management: Consultation on Regulatory and Guidance Change*. Department for Environment, Food and Rural Affairs, London, UK.

DEFRA (2016) *Local Air Quality Management Technical Guidance (TG16)*. Department for Environment, Food and Rural Affairs, London, UK.

Eastwood, P. (2000) *Critical Topics in Exhaust Gas Aftertreatment*. Research Studies Press, Baldock, UK.

Fidélis, T., and Pires, S. M. (2009) Surrender or resistance to the implementation of local agenda 21 in Portugal: The challenges of local governance for sustainable development. *Journal of Environmental Planning and Management*, 52(4): 497–518.

IIASA (2008) *Baseline Emission Projections for the Revision of the Gothenburg Protocol Up to 2020*. International Institute for Applied System Analysis, Laxenburg, Austria.

Jans, J. H. (2000) *European Environmental Law*, 2nd revised ed. Europa Law Publishing, Groningen, the Netherlands.

Le Quéré, C., Andrew, R. M., Canadell, J. G., Sitch, S., Korsbakken, J. I., Peters, G. P., Manning, A. C. et al. (2016) Global carbon budget. *Earth System Science Data*, 8(2): 605–649.

London Borough of Brent (2012) *Air Quality Action Plan 2012–15*. Brent Borough Council, London, UK.

Longhurst, J. W. S., Irwin, J. G., Chatterton, T. J., Hayes, E. T., Leksmono, N. S., and Symons, J. K. (2009) The development of effects based air quality management regimes. *Atmospheric Environment*, 43: 64–78.

Mass, R., and Grennfelt, P. (2016) Towards cleaner air. Scientific Assessment report. EMEP Steering Body and Working Group on Effects of the Convention on Long-Range Transboundary Air Pollution.

McEldowney, J. F., and McEldowney, S. (2001) *Environmental Law and Regulation*. Blackstone Press, London, UK.

Mock, P., Kühlwein, J., Tietge, U., Franco, V., Bandivadekar, A., German, J. (2014) The WLTP: How a new test procedure for cars will affect fuel consumption values in the EU. The International Council on Clean Transportation, Working Paper 2014-2019.

Nemet, G. F., Holloway, T., and Meier, P. (2010) Implications of incorporating air-quality co-benefits into climate change policymaking. *Environmental Research Letters*, 5(1): 014007.

Ravishankara, A. R., Dawson, J. P., and Winner, D. A. (2012) New directions: Adapting air quality management to climate change: A must for planning. *Atmospheric Environment*, 50: 387–389.

Raymond, C. M., Fazey, I., Reed, M. S., Stringer, L. C., Robinson, G. M., and Evely, A. C. (2010) Integrating local and scientific knowledge for environmental management. *Journal of Environmental Management*, 91(8): 1766–1777.

Stern, N. (2007) *The Economics of Climate Change: The Stern Review*. HM Treasury and Cambridge University Press, Cambridge, MA.

Tiwary, A., Chatterton, T., and Namdeo, A. (2014) Co-managing carbon and air quality: Pros and cons of local sustainability initiatives. *Journal of Environmental Planning and Management*, 57(8): 1266–1283.

USEPA (2018) Clean Air Act Overview, US Environmental Protection Agency, https://www.epa.gov/clean-air-act-overview/.

FOR REFERENCE PURPOSES ONLY

Chapter 15

Air quality experiments

Experimental hazards disclaimer: To conduct the experiments prescribed in this chapter, students should be aware of the hazards associated with the use of all the chemicals, glassware (cuts) and electrical equipment (shock, burns), and so on, and should be following appropriate health and safety procedures.

15.1 EXPERIMENT I: ATOMIC ABSORPTION SPECTROMETRY

Aim: To determine the concentration of magnesium in rainwater

15.1.1 Introduction to experiment

The concentration of elements in rainwater varies from place to place. As an example, in the UK, elements can be broadly classified according to rainwater concentrations (soluble fraction only) as follows:

- Concentrations >1000 mg L^{-1}: Na
- Concentrations between 100–1000 mg L^{-1}: Ca, K, Mg
- Concentrations between 10–100 mg L^{-1}: Al, Zn
- Concentrations between 1–10 mg L^{-1}: Cu, Fe, Mn, Pb
- Concentrations of <1 mg L^{-1}: As, Cd, Co, Cr, Mo, Se, V, W

In terms of analytical determination, compounds of Group I metals and of the heavier Group II metals give a visible colour to a methane/air flame when aspirated into it. With other metallic elements, the energy required to excite atoms present in a flame is too high and any atoms produced by the flame remain in their ground state. If light is shone through

the flame, however, these atoms may absorb the light and be raised to higher electronic states. The result is an atomic line absorption spectrum. This process is used for analysis in the atomic absorption spectrometry. To achieve the required sensitivity and selectivity for an element, the light to be absorbed is produced in a discharge lamp containing the element as a cathode. This light is then passed through a long acetylene/oxygen flame into which the analyte is aspirated. Acetylene/oxygen is used since at this temperature most compounds are atomised. The light is then detected by a spectrophotometer which can measure the absorbance at a particular wavelength. It is usually found that over a certain range of concentration the absorbance is approximately proportional to concentration.

Time required

Two to three hours

Experimental chemicals

Rainwater (collected using the method outlined in Experiment 15.1)

Magnesium chloride solution (10 mg dm^{-3} solution of magnesium)

Double-distilled, de-ionised water

Apparatus

- Atomic absorption spectrometer and Mg lamp
- A range of beakers, as necessary
- A range of graduated pipettes with fillers, as necessary
- A range of volumetric flasks, as necessary (to include several 100 cm^3 volumetric flasks)

15.1.2 Experimental procedure

1. Prepare a set of seven (0, 0.1, 0.2, 0.4, 0.6, 0.8, 1.0 mg dm^{-3}) calibration standards for magnesium from the 10 mg dm^{-3} solution of magnesium (prepared from magnesium chloride) provided. You will require about 100 cm^3 of each standard.
2. Rainwater typically contains between 100–1000 mg L^{-1} Mg. Accurately dilute rainwater into two 100 cm^3 volumetric flasks to give concentrations of Mg that fall in the upper range of your calibration graph.
3. Obtain assistance from a technician or qualified demonstrator to place the magnesium hollow cathode lamp in the spectrometer, to light the flame and to adjust the sensitivity. The required parameters are as follows: bandpass 0.5 nm; air/acetylene flame; fuel flow rate 1.0 dm^{-3} min^{-1}. Check that you have set the instrument to take 3 replicates of each solution.
4. Tune the instrument with double-distilled, deionised water being aspirated and set the absorbance to zero, via *autozero*.
5. Measure and record the absorbance of each standard when it is aspirated into the flame. Measure the absorbance when the diluted rainwater solutions are aspirated.

Ensure that the absorbance for the samples is not greater than the absorbance for your top standard. No absorbance values should be greater than 0.9 Abs units.

6. Complete the dilution tables (illustrated in Section 15.1.3) and include them in your report.
7. Plot calibration curves of absorbance against concentration for magnesium. Note that these may *not* be straight lines. Draw a smooth curve through the calibration points if this appears appropriate.
8. Determine the concentration of Mg in your diluted rainwater from these graphs.
9. Determine the concentration of Mg in the rainwater provided.

15.1.3 Report generation

15.1.3.1 Issues to consider for your practical report

- What are the potential sources of error in this analytical determination? How could they be overcome?
- What are the alternative methods for determining the concentration of Mg in rainwater? How do they compare with this method?
- What are typical concentrations of Mg in rainwater in your local or national area? How do your data compare with these values?
- What are the main sources of Mg in rainwater?

Dilutions used to prepare standards (please state your units).

Initial concentration	*Volume taken*	*Final volume*	*Final concentration*

Dilution used to prepare rainwater for analysis (please state you units).

Initial concentration	*Volume taken*	*Final volume*	*Final concentration*

15.2 EXPERIMENT II: COLORIMETRIC ANALYSIS FOR NITROGEN DIOXIDE

Aim: To determine the concentration of atmospheric nitrogen dioxide (NO_2)

15.2.1 Introduction to experiment

Natural sources of nitrogen oxides (NO_x) are ubiquitous and include lightning, volcanic eruptions and bacterial action in the soil. Anthropogenic sources of NO_x are dominated by the combustion of fossil fuels, mainly by vehicles and power stations. Globally, annual natural emissions of NO_x far outweigh anthropogenic NO_x emissions. Nitrous oxide (N_2O) is the most abundant NO_x, formed by natural microbiological processes in the soil, although it is not normally considered a pollutant. Other nitrogen oxides present in the atmosphere include nitrogen pentoxide (N_2O_5), nitrogen trioxide (NO_3), dinitrogen trioxide (N_2O_3) and dinitrogen tetroxide (N_2O_4). However, in urban areas, the most important atmospheric nitrogen compounds are nitric oxide (NO) and nitrogen dioxide (NO_2).

Nitric oxide and nitrogen dioxide are formed in combustion processes as nitrogen in the air and the fuel combines with oxygen at temperatures of 1800°C or higher. Nitric oxide is the major contributor to oxidised nitrogen pollution, but at ambient temperatures NO is oxidised to the more toxic secondary pollutant NO_2, a process which is accelerated by the presence of reactive hydrocarbons and ozone. Nitrogen dioxide can be decomposed by ultraviolet (UV) light from the sun to NO, thus producing an equilibrium situation. It has been estimated that motor vehicles emit approximately one-third of the total anthropogenic NO_x emissions in the UK, making them a major source of NO_x in urban areas. Thus, a measurement of NO_x could be an approximate index of air pollution from mobile sources in urban areas.

Many direct or indirect techniques have been developed for measuring NO_2 in the laboratory and/or in the field. Spectroscopic methods, for example, differential optical absorption spectroscopy (DOAS), laser-induced fluorescence (LIF), cavity ring down spectroscopy (CRDS) and resonance-enhanced multi-photon ionisation (REMPI), have been used for selective NO_2 detection. The most widely used technique for the measurement of NO_2 in monitoring networks is the *chemiluminescence* method. This method involves the reduction of NO_2 to NO using heated (300°C–350°C) molybdenum (Mo) surfaces. Another commonly used technique is the *luminol-chemiluminescence* method, which employs the reaction between NO_2 and an alkaline solution of luminol resulting in light emission.

FOR REFERENCE PURPOSES ONLY

Although some of the methods have very low-detection limits (e.g. REMPI, LIF), most techniques require considerable operational expertise, are expensive and have complex system components (Kleffmann et al., 2013).

The colorimetric method described here, commonly known as the *Griess-Saltzman reaction*, is a relatively cheap and pretty robust technique and is sensitive over a range from a few ppb to about 5 ppm (v). Interferences from other trace gases normally found in the atmosphere are negligible. However, for concentrations of NO_2 in excess of 5 ppm (v), as occur in industrial atmospheres, gas burner stacks or automotive exhaust, or for samples with relatively high sulphur dioxide content, other methods should be applied; for example, the phenol-disulphonic acid procedure can be applied for NO_2 analysis from combustion sources. Air is drawn through a fritted glass bubbler containing an absorbing reagent which reacts with NO_2 to yield a pink-coloured azo-compound between sulphanilic acid, nitrite ion and a-naphthylamine in an acid medium (Figure 15.1). The concentration of NO_2 can be determined from the colour intensity of the absorbing reagent, measured by means of a spectrophotometer. If a measurement of NO is also needed, air can be driven through a bubbler containing an oxidising solution (e.g. potassium permanganate), which converts NO to NO_2.

Time required

Three hours – although advance preparation is also required. This method allows the determination of atmospheric nitrogen dioxide in the range from 4 to 10,000 μg/m^3 (0.002–5 ppm-v) when sampling is conducted in fritted-tip bubblers.

FOR REFERENCE PURPOSES ONLY

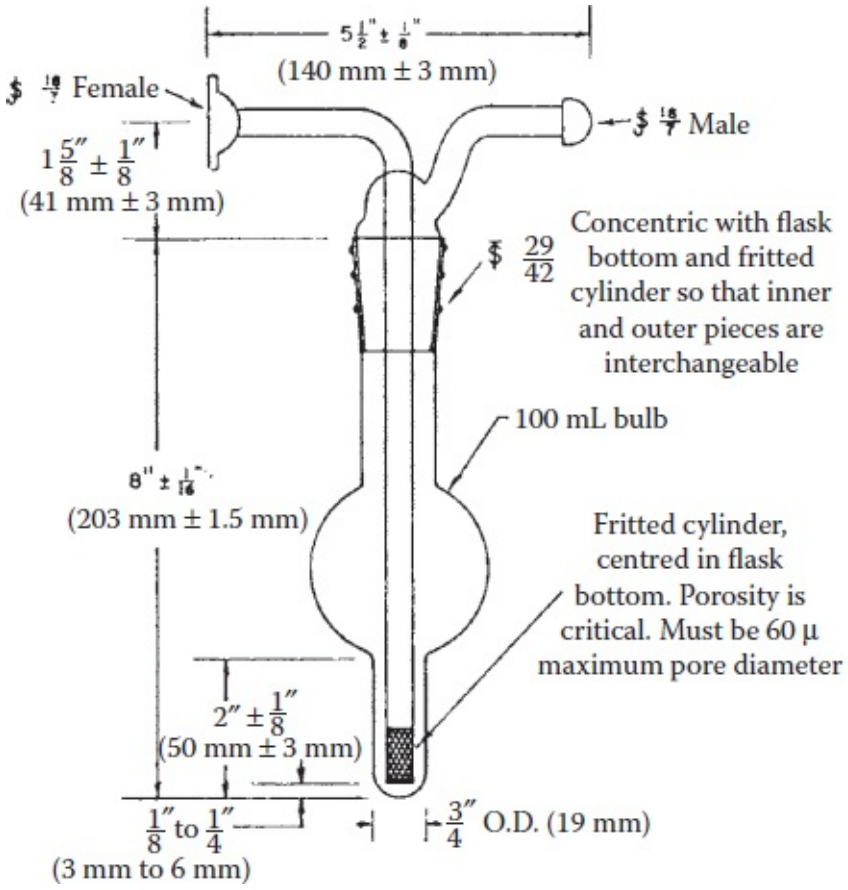

Figure 15.1 Fritted bubbler for sampling combined nitrogen oxides.

Chemicals

N-(1-Naphthyl)-ethylenediamine dihydrochloride; 100 cm^3 of a 0.1% solution
Sulphanilic acid
Glacial acetic acid
Sodium nitrite ($NaNO_2$) solution; 2.03 g L^{-1}

Apparatus

- UV spectrophotometer and spectrophotometer cells
- Bunsen burner, tripod and gauze
- 400 cm^3 beaker
- Watch glass
- Glass rod
- 125 cm^3 fritted glass bubblers
- Graduated pipettes
- Teflon tubing
- Gas meter
- Air pump (with controllable flow)
- Filter holder and filter paper
- Volumetric flask (1 × 100 cm^3, 1 × 250 cm^3 and 5 × 25 cm^3)

15.2.2 Experimental procedure

15.2.2.1 Preparation of absorbing reagent

1. Dissolve 1.25 g of sulphanilic acid in approximately 150 cm^3 of double distilled, de-ionised water in a 400 cm^3 beaker.
2. Add 35 cm^3 of glacial acetic acid.
3. Gently heat the solution using a Bunsen burner in order to effect complete solution.
4. To the cooled solution, add 5 cm^3 of 0.1% N-(1-Naphthyl)-ethylenediamine dihydrochloride.
5. Carefully transfer the solution to a volumetric flask and dilute to 250 cm^3 with double distilled, de-ionised water.

Avoid lengthy contact of the solution with the air during preparation as absorption of NO_2 causes discolouration of the reagent. The absorbing reagent should be at room temperature when used.

15.2.2.2 Sampling procedure

1. Pipette 40 cm^3 of absorbing reagent into a 125 cm^3-fritted glass bubbler.
2. Set up suitable apparatus for drawing air through the absorbing reagent. Use the diagram shown in Figure 15.1 to help you.
3. Set the pump to draw air through the apparatus at a flow rate of 0.4 L/min (or less). Make sure you note the gas meter reading and the time sampling is commenced in your logbook.
4. Aspirate an authentic air sample through the absorber for a maximum of 1 h (you may take a little longer if the local atmospheric NO_2 concentration is low). Note the total air volume sampled and the duration of sampling.
5. After the sample has been collected, allow 15 min for complete colour development. Transfer a portion of the sample to a 4 cm spectrophotometer cell and read off the absorbance at 550 nm using unexposed absorbing reagent as reference. Compare your value to those of the standards you have prepared (see the following). You may need to dilute the sample to ensure it is within the linear range – the measured absorbance is then multiplied by the dilution factor.

15.2.2.3 Calibration procedure

To save time you should prepare the calibration standards while the sample is being collected.

1. Dilute the standard sodium nitrite solution provided by pipetting 1 cm^3 into a 100 cm^3 volumetric flask and diluting to the mark with double distilled, de-ionised water.
2. It has been determined empirically that 0.72 mole of sodium nitrite produces the same colour as 1 mole of nitrogen dioxide; 1 cm^3 of this diluted $NaNO_2$ solution produces a colour equivalent to 10 mL of NO_2 (10 ppm in 1 L of air at 298 K and 1013 mb).
3. Pipette 0.00, 0.25, 0.50, 0.75 and 1.00 cm^3 of the diluted $NaNO_2$ solution into each of five 25 cm^3 volumetric flasks. Dilute to the marks with absorbing reagent, mix well, and allow 15 min for colour development. The standards contain progressively, 0.00, 0.10, 0.20, 0.30 and 0.40 µL NO_2 per cm^3 of absorbing solution.
4. Measure the absorbance of each of these solutions in a spectrophotometer at 550 nm using 1 cm cells. The reference should be unexposed absorbing reagent (why?).
5. Plot the absorbance of the standards against the µL NO_2 per cm^3 of absorbing solutions to generate a calibration graph.

15.2.2.4 Calculation

Calculate the concentration of nitrogen dioxide in the sample as follows:

$$\mathrm{NO_2\ (ppm)} = \mu\mathrm{L\ NO_2\ mL^{-1}} \times \frac{10}{\text{sample volume (L)}}$$

Convert this value to µg/m^3 using:

$$\mu\mathrm{g\ m^{-3}} = \mathrm{ppb} \times \frac{\text{molecular weight}}{\text{molar volume (L)}}$$

15.2.3 Report generation

15.2.3.1 Issues to consider for your practical report

- What are the potential sources of error in this analytical determination? How could they be overcome?
- What are the alternative methods for determining the atmospheric nitrogen dioxide? How do they compare with this method?
- What are typical (hourly averaged) atmospheric NO_2 concentrations in your local or national area? How do your data compare with these values?
- What are the main sources of atmospheric nitrogen dioxide?
- What are the potential human health and environmental effects (if any) of elevated atmospheric concentrations of nitrogen dioxide?

15.3 EXPERIMENT III: COLORIMETRIC ANALYSIS FOR OZONE

Aim: To determine the concentration of atmospheric ozone

15.3.1 Introduction to experiment

Tropospheric (or ground-level) ozone is formed by a complex series of photochemical reactions. Stratospheric ozone is produced naturally, although some may be transported to the troposphere by large-scale air movements. Background concentrations of ozone are on the order of 10–80 μg m^{-3}, with some seasonal variations interspersed with irregular maxima due to specific meteorological events. Ozone concentrations are often lower in urban/industrial areas than in rural areas due to the reaction between O_3 and NO. Generally, however, monthly mean and peak urban O_3 concentrations are higher in spring and summer than in winter months, with daily levels usually highest around midday as O_3 destruction frequently occurs during peak morning and afternoon traffic periods.

Ozone causes increased susceptibility to respiratory infections and is a strong pulmonary irritant. It has also been claimed that ozone causes coughing, eye, nose and throat irritation, and headaches, particularly in people who exercise. As far as environmental effects are concerned, ozone contributes to ground-level haze and photochemical smog. Elevated or long-term exposure may cause vegetation damage, and ozone is also associated with the degradation of rubber and a number of other polymers, the induction of fading in dyes and damage to photographic materials and books.

An approximate method for the determination of atmospheric ozone is based on the liberation of micro-amounts of iodine when ozone (and other oxidants) is absorbed in a 1% solution of potassium iodine buffered at pH 6.8 + 0.2. The iodine is determined spectrophotometrically by measuring the absorption of tri-iodide ion at 352 nm. The stoichiometry is approximated by the following reaction:

$$O_3 + 3KI + H_2O \rightarrow KI_3 + 2KOH + O_2$$

Time required

Three hours – although advance preparation is also required.

Experimental chemicals

Double-distilled, de-ionised water

Absorbing solution (see Section 15.3.2)

Iodine stock solution (see Section 15.3.2)

Apparatus

- UV spectrophotometer and spectrophotometer cells (capable of measuring absorbance at 352 nm)
- Analytical balance

- pH meter
- Fritted glass bubbler
- Graduated beakers
- Watch glass
- Glass rod
- Graduated pipettes
- Teflon tubing
- Gas meter
- Air pump (with controllable flow; must be capable of drawing the required sample flow rate of 1–2 L per min)
- Volumetric flasks
- Glass-stoppered brown bottle (for storage)

15.3.2 Experimental procedure

15.3.2.1 Preparation of absorbing reagent (1% KI in 0.1 m phosphate buffer)

1. Dissolve 13.6 g of potassium dihydrogen phosphate (KH_2PO_4), 14.2 g of disodium hydrogen phosphate (Na_2HPO_4) *or* 35.8 g of the dodecahydrate salt ($Na_2HPO_2 \cdot 12 H_2O$), and 10.0 g of potassium iodide in sequence and dilute the mixture to 1 L in a volumetric flask with double distilled, de-ionised water.
2. Keep at room temperature for at least 1 day before use.
3. Measure pH and adjust to 6.8 + 0.2 with NaOH or KH_2PO_4.
4. This absorbing reagent can be stored for several months in a glass-stoppered brown bottle at room temperature without deterioration. It should not be exposed to direct sunlight.

Avoid lengthy contact of the reagent with the air during preparation as absorption of oxidants can cause discolouration of the reagent. The absorbing reagent should be at room temperature when used.

15.3.2.2 Preparation of iodine stock solution (0.025 M I_2)

1. Dissolve 16 g of potassium iodide and 3.173 g of re-sublimed iodine successively and dilute the mixture to exactly 500 cm^3 in a volumetric flask with double distilled, de-ionised water.
2. Keep at room temperature for at least 1 day before use.
3. Standardise shortly before use, against 0.025 M $Na_2S_2O_3$. The sodium thiosulphate can be standardised against primary standard bi-iodate [$KH(IO_3)_2$] or potassium

dichromate ($K_2Cr_2O_7$).

15.3.2.3 Preparation of M I_2 solution for calibration

1. Pipette exactly 4.00 cm^3 of the 0.025 M stock solution into a 100 cm^3 low actinic volumetric flask and dilute to the mark with absorbing reagent.
2. Protect from strong light. Discard after use.

15.3.2.4 Sampling procedure

1. Pipette 10 cm^3 of absorbing reagent into a 125 cm^3 fritted glass bubbler.
2. Set up suitable apparatus for drawing air through the absorbing reagent.
3. Set the pump to draw air through the apparatus at a flow rate of approximately 1.0 L/min. Make sure you note the gas meter reading and the time sampling is commenced in your logbook.
4. Aspirate an authentic air sample through the absorber for approximately one hour (you may take a little longer if the local atmospheric O_3 concentration is low). Note the total air volume sampled and the duration of sampling.
5. If appreciable evaporation of the absorbing reagent occurs during sampling, add double-distilled, de-ionised water to bring the liquid volume to 10 cm^3.
6. After the sample has been collected, transfer to a sample storage bottle.

Within 30–60 min after sample collection, transfer a portion of the collected sample to a spectrophotometer cell and read off the absorbance at 352 nm using unexposed absorbing reagent as a reference. Compare your value to those of the standards you have prepared (see the following). You may need to dilute the sample to ensure it is within the linear range – the measured absorbance is then multiplied by the dilution factor. Measure the absorbance of the unexposed reagent and subtract the value from the absorbance of the sample.

15.3.2.5 Calibration procedure

To save time you should prepare the calibration standards while the sample is being collected.

1. Dilute the 0.001 M I_2 solution by pipetting 5.1 cm^3 into a 100 cm^3 volumetric flask and diluting to the mark with double distilled, de-ionised water. This gives a final concentration equivalent to 1 μL of O_3/cm^3. This solution preparation accounts for the stoichiometric equation (outlined in Section 15.3.1) at standard conditions of 101.3 kPa and 25°C. Discard this solution after use.

2. Pipette 1.0, 2.0, 4.0, 6.0, 8.0 and 10.0 cm^3 of the calibrating iodine solution into each of six 10 cm^3 volumetric flasks. Dilute to the marks with absorbing reagent, mix well, and allow time for colour development. The standards contain progressively 1–10 µL of ozone equivalent per 10.0 per cm^3 of absorbing reagent.
3. Measure the absorbance of each of these solutions in a spectrophotometer at 352 nm using 1 cm^3 cells. The reference should be unexposed absorbing reagent (why?).
4. Plot the absorbance of the standards against the µL O_3 per cm^3 of absorbing solutions to generate a calibration graph.

15.3.2.6 Calculation

Calculate the concentration of ozone in the collected sample as follows:

$$C(O_3 \mu g/m^3) = (As - Ab) \times CF \times 1.962/Va$$

where:

CO_3 is the concentration of ozone in µg/m^3
As is the absorbance of the sample
Ab is the absorbance of the reagent blank
CF is the calibration factor
Va is the volume of air sampled in m^3
1.962 is the conversion factor, µL to µg

15.3.3 Report generation

15.3.3.1 Issues to consider for your practical report

- What are the potential sources of error in this analytical determination? How could they be overcome?
- What are the alternative methods for determining the atmospheric ozone? How do they compare with this method?
- What are typical (hourly averaged) atmospheric O_3 concentrations in your local or national area? How do your data compare with these values?
- What are the main sources of atmospheric ozone in (1) urban areas and (2) rural areas?
- What are the potential human health and environmental effects (if any) of elevated atmospheric concentrations of ozone?

15.4 EXPERIMENT IV: SPECTROPHOTOMETRIC METHOD FOR SULPHUR DIOXIDE

FOR REFERENCE PURPOSES ONLY

Aim: To determine the concentration of atmospheric sulphur dioxide

15.4.1 Introduction to experiment

Globally, emissions of sulphur compounds into the atmosphere by natural sources approximately equal those derived from anthropogenic sources. Natural sources of SO_x include volcanoes and windblown aerosols from the sea surface. Human-made sources of SO_x are dominated by emissions resulting from the combustion of fossil fuels for heating and energy production, although industries such as petroleum refining, metal smelting and wood pulping also make significant contributions. During combustion, the sulphur is oxidised to sulphur dioxide which is then discharged into the atmosphere via the exhaust system. Small quantities of SO_2 are further oxidised to SO_3, which immediately dissolves in the existing water vapour to form a sulphuric acid aerosol. Sulphuric acid is eventually formed in the atmosphere from the emitted SO_2.

Internationally, emissions of SO_2 are decreasing from a peak in the early 1970s. For example, SO_2 emissions in the United States rose steeply from 1940–1970, largely as a result of increases in coal-fired electricity production without any thought as to the consequent emissions. UK emissions of sulphur dioxide fell 95% from 1970 to 2014. This is a result of reduced emissions from the industrial and public power sectors arising from the decreasing use of coal and increasing use of abatement equipment. As a consequence, atmospheric concentrations of SO_2 are also decreasing, although they remain high in some parts of the world.

The experiment described here is a modified West-Gaeke method, initially suggested by West and Gaeke (1956). This method attempts to address complications in this type of analysis caused by the presence of oxygen and other pollutants (e.g. ozone, oxides of nitrogen) that either react with sulphur dioxide during sampling/storage or interfere with subsequent analytical processes.

SO_2 from air is absorbed in a solution of potassium tetrachloromercurate (TCM). A dichlorosulphitomercurate complex that resists oxidation by the oxygen in the air is subsequently formed. This complex is stable to strong atmospheric oxidants such as ozone, and therefore the absorber solution may be stored for some time prior to analysis. The complex is made to react with pararosaniline hydrochloride and formaldehyde to form the intensely coloured pararosaniline methylsulphonic acid. The absorbance of the solution is measured by means of a suitable spectrophotometer.

The sampling equipment should be located carefully, typically where it can easily be checked; supplied with power; and left safely and without fear of interference, vandalism or theft. Generally, sampling devices of this nature are kept at a height of approximately 3–10 m from ground level and away from direct contact with the pollution source under consideration.

Time required

Depends upon amount of preparation time required and varies by experience of analysts.

Experimental

Note: All chemicals should meet specifications of analytical reagent grade.

Chemicals for sampling

- Double-distilled, deionised water (must be Cl_2 free)
- Mercuric chloride
- Potassium chloride
- Ethylenediaminetetraacetic acid (EDTA) disodium salt ($C_{10}H_{14}N_2Na_2O_8.2H_2O$)
- Absorbing reagent, 0.04 M potassium tetrachloromercurate (TCM). If you cannot purchase this reagent you can make it. Dissolve 10.86 g mercuric chloride (highly poisonous – caution), 0.066 g EDTA and 6.0 g potassium chloride and making up to the mark in a 1 L volumetric flask. The pH of this reagent should be approximately 4.0. The absorbing reagent is normally stable for six months; however, if, a precipitate forms, discard the reagent after recovering the mercury. The EDTA is added to eliminate interferences from trace metals.

  Sulphamic acid (0.6%) (dissolve 0.6 g sulphamic acid in 100 cm^3 double-distilled, deionised water; prepare fresh daily). The sulphamic acid is added to eliminate effect of oxides of nitrogen.

  Formaldehyde (0.2%) (dilute 5 cm^3 formaldehyde solution (36%–38%) to 1 L with double-distilled, deionised water distilled water; prepare fresh daily).

  Purified pararosaniline stock solution (0.2% nominal) (dissolve 0.500 g of specially purified pararosaniline [PRA] in 100 cm^3 of double-distilled, deionised water and keep for 2 days).

  Pararosaniline working solution (10 cm^3 of stock PRA placed into a 250 cm^3 volumetric flask, then add 15 cm^3 conc. HCl and make up to volume with double-distilled, deionised water).

  Stock iodine solution (0.1 N) (place 12.7 g iodine in a 250 cm^3 beaker, add 40 g potassium iodide and 25 cm^3 double-distilled, deionised water; stir until all is dissolved, then dilute to 1 L with double-distilled, deionised water).

Chemicals for laboratory analysis

- Double-distilled, deionised water (must be Cl_2 free)
- Purified pararosaniline stock solution (0.2% nominal) and working solution
- Standard sulphur dioxide solution (dissolve 0.4 g sodium metabisulphite in 250 cm^3 double-distilled, deionised water)

Apparatus

- Standard fritted glass bubblers (at least 2) (also known as midget impingers)
- Airflow rotameter
- Plastic tubing

- Gas pump
- Spectrophotometer (to read at 540 nm)
- A range of beakers, as necessary
- A range of graduated pipettes with fillers, as necessary
- A range of volumetric flasks, as necessary (to include several 100 cm^3 volumetric flasks)

15.4.2 Experimental procedure

15.4.2.1 Sampling

1. Prepare a sampling train of at least 2 fritted glass bubblers, thoroughly washed with double-distilled, deionised water and air dried.
2. Place bubblers in the sampling system. Connect the pump and rotameter in series and connect together securely with plastic tubes. Ensure that all parts of the system are securely fixed (e.g. by using clamps and bosses).
3. Fill the bubblers with an absorbing reagent with an amount sufficient to last at least for 24 h (approximately 15–20 cm^3 for 8 h sampling; then pro-rata).
4. Start the air pump and adjust flow rate to approximately 2 L/min.
5. Note the flow rate at the end of the desired sampling period. Switch off the sampler.
6. Transit the bubblers carefully to the environmental laboratory for analysis with appropriate scientific precautions to preserve the integrity of the sample.

In the laboratory, transfer samples to a 25 cm^3 flask and develop colour as outlined in the calibration procedure (below). Transfer a portion of the collected sample to a spectrophotometer cell and read the absorbance at 540 nm using unexposed absorbing reagent as a reference. Compare your value to those of the standards you have prepared (see Section 15.4.2.2). You may need to dilute the sample to ensure it is within the linear range – the measured absorbance is then multiplied by the dilution factor. Measure the absorbance of the unexposed reagent and subtract the value from the absorbance of the sample. The concentration (µg SO_2) can be obtained corresponding to the measured absorbance from the calibration curve.

15.4.2.2 Calibration procedure

To save time you should prepare the calibration standards while the sample is being collected.

1. Prepare standard solutions of SO_2 concentrations ranging from 0 to 25 µg SO_2 using the standard SO_2 solution (prepared as outlined in Section 15.4.1).
2. Add 14 cm^3 of absorbing reagent and 1 cm^3 of pararosanaline hydrochloride to each

of the flasks, making a total volume of 20 cm^3.

3. Measure the absorbance of each of these solutions in a spectrophotometer at 540 nm using 1 cm cells. The reference should be unexposed absorbing reagent (why?).
4. Plot the absorbance of the standards against the concentrations of the SO^2 solutions to generate a calibration graph.

15.4.2.3 Calculations

1. Average flow rate in L/min = (initial flow rate + final flow rate)/2.
2. Total volume of air sampled (TVA) in m^3 = average flow rate (L/min) * 10^{-3} (m^3/L) * sampling time (h) * 60 (min/h).
3. Concentration = µg SO_2/TVA.

15.4.3 Report generation

15.4.3.1 Issues to consider for your practical report

- What are the potential sources of error in this analytical determination? How could they be overcome?
- What are the alternative methods for determining atmospheric sulphur dioxide? How do they compare with this method?
- What are typical (hourly averaged) atmospheric SO_2 concentrations in your local or national area? How do your data compare with these values?
- What are the main sources of atmospheric sulphur dioxide?
- What are the potential human health and environmental effects (if any) of elevated atmospheric concentrations of sulphur?

15.5 EXPERIMENT V: COLORIMETRIC ANALYSIS FOR CARBONYLS

Aim: To determine the concentration of atmospheric carbonyl compounds

15.5.1 Introduction to experiment

Carbonyl compounds (aldehydes and ketones) play a critical role in atmospheric chemistry. They are photochemically active, generating free radicals, and are precursors of organic aerosols, tropospheric ozone and peroxyacetyl nitrate (PAN; a component of photochemical smog), with deleterious human health effects. Carbonyl compounds arise from anthropogenic and biogenic sources, both as primary products and as secondary

FOR REFERENCE PURPOSES ONLY

photochemical products. Research studies have focussed on urban air quality associated with traffic emissions and rural/remote air quality, particularly within forests to assess the contribution of biogenic carbonyl emissions and their precursors.

Formaldehyde has been found to be the most abundant aldehyde in ambient air, with concentrations typically between 5 and 30 parts per billion (ppb) in highly polluted urban air (Grojean et al., 1996; Williams et al., 1996; Viskari et al., 2000; Possanzini et al., 2002). Many other carbonyl species, including acetaldehyde, proprionaldehyde, butyraldehyde, acetone, benzaldehyde, acrolein, crotonaldehyde and hexanal, may be found in urban and/or rural air samples.

Derivatisation of carbonyls to form stable hydrazones, followed by high-performance liquid chromatography (HPLC) or gas chromatography (GC) analysis, has become an industry standard mechanism for assessing carbonyl concentrations in ambient air, requiring only simple/inexpensive field equipment. Derivatisation is achieved by active carbonyl capture via impingers or low-pressure solid-phase extraction (SPE) cartridges containing the acidified hydrazine reagent. SPE stationary phase sorbents include silica-gel (polar) and octadecyl silica (C_{18}, non-polar). The most common reagent used in derivatisation studies has been dinitrophenylhydrazine (DNPH), although 2,4,6-trichlorophenylhydrazine (TCPH) and dansylhydrazine (DNSH) have also been used.

This experiment can be adapted to determine carbonyl concentrations at different locations, different distances from an identified source, at a single location close to a busy road in order to compare morning and afternoon rush-hour periods, or at different height of an office block and at ground level below to examine vertical concentration variations.

The concentrations of four carbonyl compounds (e.g. formaldehyde, acetaldehyde, acrolein and crotonaldehyde) can be measured using a method based on the US Environmental Protection Agency (EPA) Compendium Method TO-11A (US EPA, 1999). Carbonyls present in ambient air samples react with DNPH to form their stable hydrazone derivatives. The DNPH derivatisation mechanism (Figure 15.2) is initiated by nucleophilic attack by the hydrazine group on the carbonyl carbon followed by acid catalysed dehydration to form the hydrazone.

Time required

This experiment may take place over a number of days. It may be set as an individual or group project for more advanced students.

Experimental chemicals

- Acetonitrile (liquid chromatography–mass spectrometry [LC-MS] grade)
- Calibration standard (e.g. Supelco Aldehyde/Ketone-DNPH Mix)

Apparatus

- SPE cartridges (e.g. Supelco LpDNPH S10 cartridges) consisting of a polypropylene tube containing high-purity silica coated with acidified DNPH

FOR REFERENCE PURPOSES ONLY

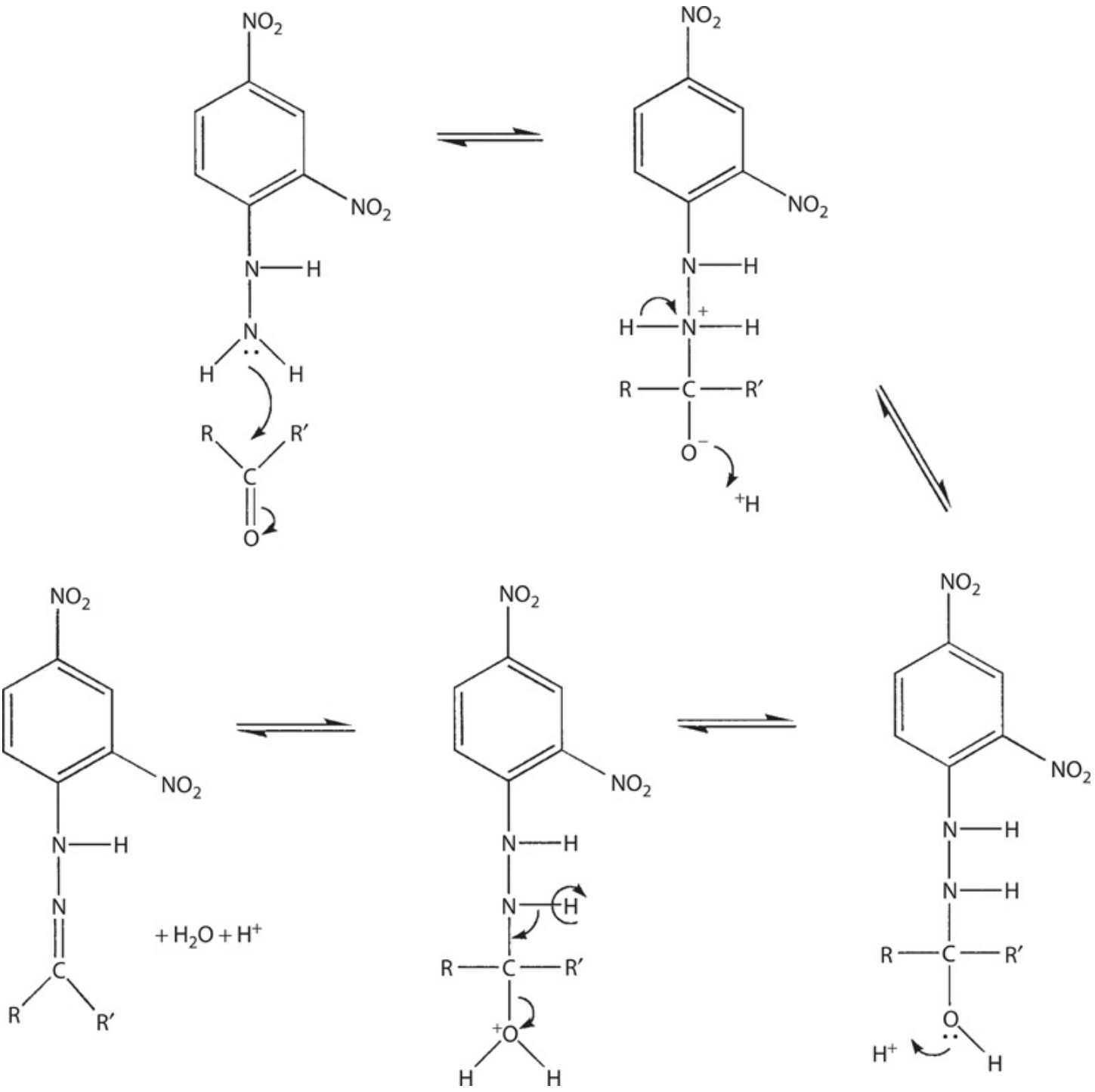

Figure 15.2 Carbonyl derivatisation mechanism with DNPH.

- Ozone scrubber (e.g. Supelco LpDNPH Ozone Scrubber) (optional)
- Luer fittings
- Portable air sampling pumps (e.g. Gilian 5000, SKC Universal 224-PCEX8)
- Rotameter
- Polyvinyl chloride (PVC) tubing (e.g. Nalgene 180 PVC, ¼″ ID)
- Waterproof plastic box with lid (approximately 80–120 L)
- Sealable foil bags (or similar)

- Weather station (to record ambient temperature and pressure)
- Reverse phase HPLC with UV/visible absorption detection
- Insulated bags
- Volumetric flasks (10 cm^3)
- Glass vials (1 and 2 cm^3) with sealable foil-lined polypropylene screw caps

15.5.2 Experimental procedure

15.5.2.1 Sampling of ambient air

1. Find a suitable location (or locations) for your study (see Section 15.5.1).
2. Set up the sampling train as shown in Figure 15.3. A sampling cartridge should be connected to a portable air sampling pump via 1–3 m of PVC tubing. Pumps at each sampling location should be stored in a waterproof plastic box. Tubing can be fed through drilled holes to allow collection of ambient air.
3. Air should be drawn through a bespoke SPE DNPH cartridge (see above) using a portable sampling pump. Air should be drawn through the cartridge at a rate of 2.0 L/min.
4. An ozone scrubber may be used to remove ozone prior to the sample air reaching the cartridge to avoid known negative hydrazone interference. An ozone scrubber typically consists of a polypropylene tube containing high-purity KI, connected in front of the DNPH cartridge by Luer fittings (Figure 15.4).
5. Air sampling pumps should be calibrated regularly using a rotameter.
6. If samples are collected at different heights, the heights above ground level should be recorded. Successive sampling points should be vertically above the first, wherever possible.
7. For sampling during rush hours, recommended sampling periods are between 07:30–10:30 and 15:30–18:30. Sampling periods of 180–240 min per sample are suggested.
8. Control samples should be collected at each height or at each location, with one control cartridge for each sampling period.
9. Ambient temperature and pressure should be recorded at the start and end of each sample using a weather station. The recorded values can assist in the calculation of sample volumes using calibrated pump flow rates.

15.5.2.2 Storage of samples

1. Each SPE DNPH cartridge should be capped, placed into individually sealed foil bags and refrigerated when not in use.
2. Cartridges should be transported in an insulated bag maintained at a temperature below 4°C. Samples may be stored for up to 14 days before being analysed.

FOR REFERENCE PURPOSES ONLY

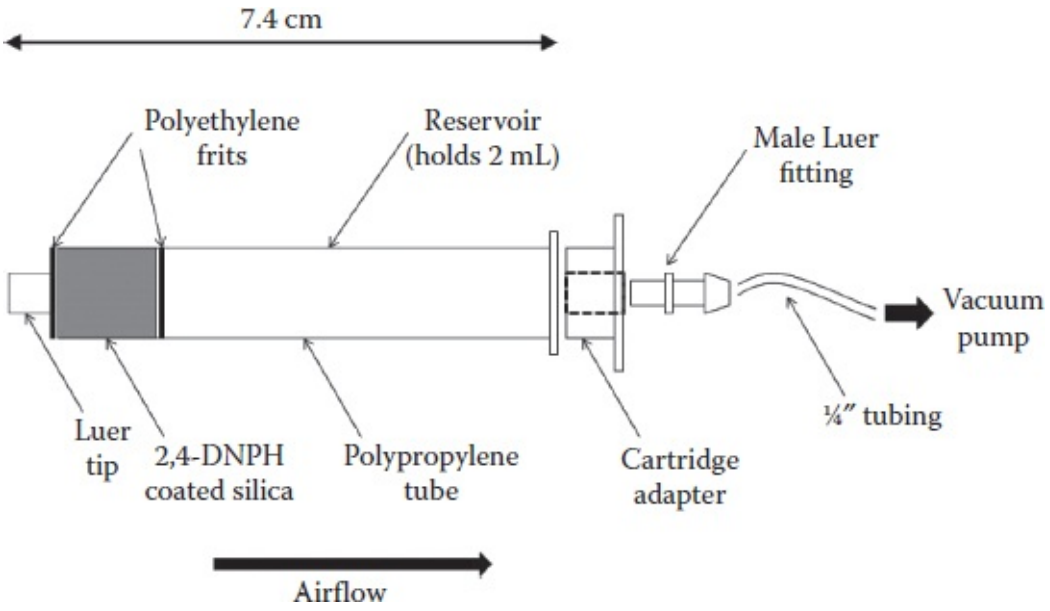

Figure 15.3 Sampling train setup.

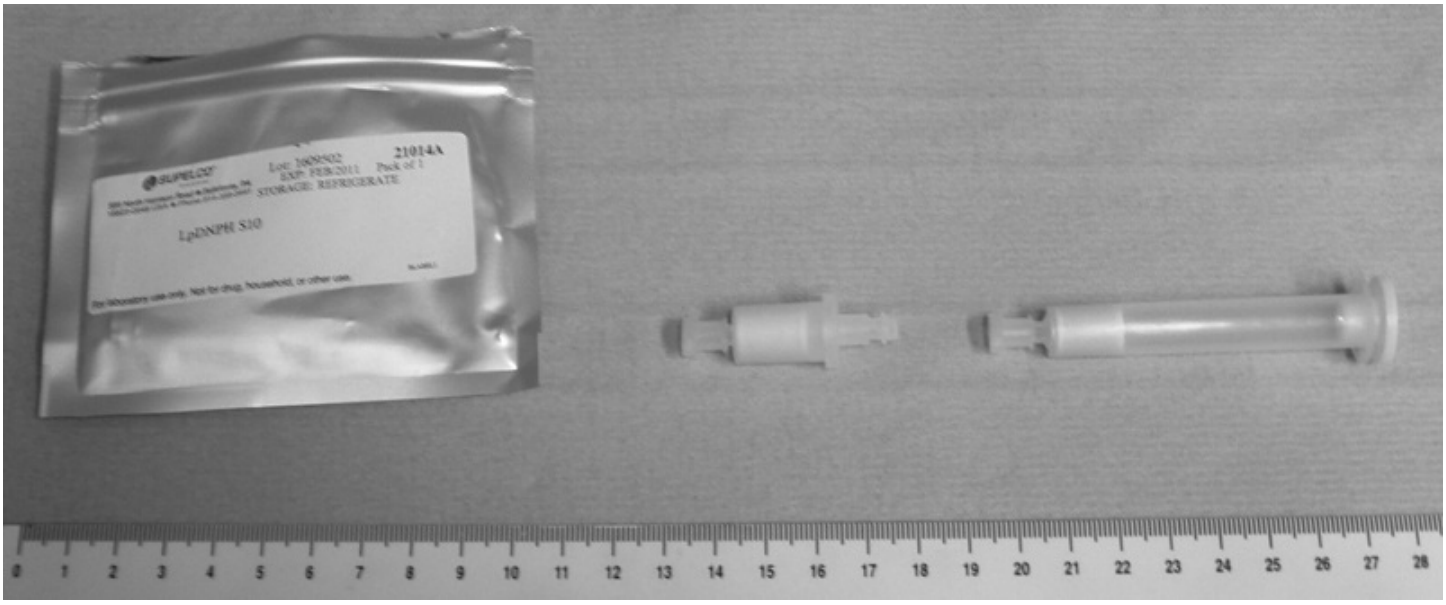

Figure 15.4 Foil bag, cartridge and ozone scrubber (cm scale).

15.5.2.3 Elution of samples

Hydrazone derivatives, along with excess DNPH reagent, should be eluted from the cartridges and analysed by reverse phase HPLC with UV/visible absorption detection to determine the concentration of each carbonyl in the sample.

Cartridges may be eluted with 2 cm^3 aliquots of acetonitrile under gravity feed. Eluate should be collected to the 5 cm^3 mark on a volumetric flask. A portion of the eluate from each cartridge should be immediately transferred to a 1 cm^3 glass vial and sealed with a

polytetrafluoroethylene (PTFE)-lined closure ready for HPLC analysis. The remaining eluate from each cartridge may be transferred to 2 cm^3 glass vials, sealed with foil-lined polypropylene screw caps, and stored in a refrigerator for potential further analysis. Analysis of the eluate should be within 1–2 h of elution.

15.5.2.4 HPLC configuration and sample analysis

Reversed-phase HPLC analysis should be conducted using a C_{18} column (e.g. Waters Xterra MS, 4.6 × 50 mm, 5 µm particle size), maintained at 44.8°C. Gradient elution allows peak separation to be achieved for smaller carbonyls if short columns are used. A mobile phase of 60:40 v/v water:acetonitrile should be used for 4.6 min, with a linear gradient to 100% acetonitrile over 10.4 min, held for 3 min. All solvents should be LC-MS grade. The flow rate should be 1.0 cm^3/min, with detection at 360 nm (absorption maximum of the DNPH chromophore). Ten microlitre HPLC injections of each cartridge extract may be made via an auto-injector. Standard software may be used to process the HPLC data.

15.5.2.5 Calibration procedure

A calibration standard (e.g. Supelco TO11/IP-6A Aldehyde/Ketone-DNPH Mix; this contains 15 carbonyl-hydrazones in acetonitrile) should be used to develop a linear calibration response for the HPLC system. This standard should be diluted to appropriate concentrations covering the carbonyl concentration range identified during the sampling campaign (Figure 15.5).

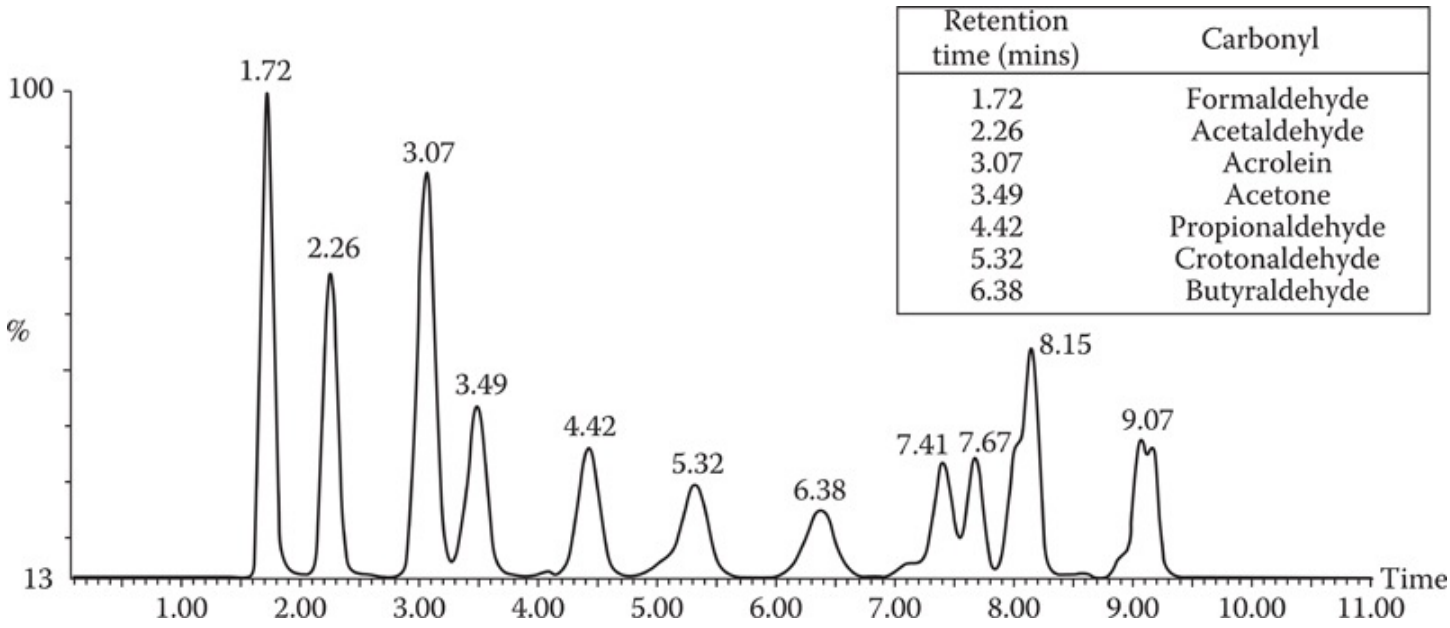

Figure 15.5 An example chromatogram of a standard aldehyde/ketone DNPH mix used for calibration.

15.5.2.6 Efficiency and interference studies

In order to test whether all carbonyls in the sampled air react with DNPH in the cartridge, two cartridges may be placed in series during a sampling period. Any unreacted carbonyls from the cartridge first in-line are assumed to be captured by the second cartridge.

Elution efficiency may be tested by spiking cartridges with a known quantity of each carbonyl-hydrazone (e.g. 1.50 µg of each carbonyl equivalent), and eluting the cartridge as normal. The quantity of carbonyl equivalent selected should represent a slightly greater concentration than found during a sampling campaign. Spiked cartridges should be eluted immediately, and also capped and eluted after 1 h (cartridges stored at room temperature, upright in an elution rack). A quantitative measure of elution efficiency may be calculated using the previously determined calibration responses.

15.5.2.7 Calculations

Assume a calibration standard is 15 µL/cm^3 of each carbonyl equivalent. Injection is 10 µL, Therefore, mass of carbonyl injected = (15 µg/1 × 10^{-3} L) × 10 × 10^{-6} L = 0.15 µg. Formaldehyde (FA) molecular weight = 30.03 g/mol. Therefore, for a 10 µL injection of FA, the number of moles of:

$$\mathrm{FA} = \frac{0.15 \times 10^{-6}\ \mathrm{g}}{30.03\ \mathrm{g\,mol^{-1}}} = 4.995 \times 10^{-9}\ \mathrm{moles}$$

This number of moles is for a 10 µL injection of undiluted hydrazone standard. Dilutions of this standard may then be used to create a calibration response (e.g. 100%, 50%, 10%, 5%, 1%, 0.2%; see Figure 15.6). This calibration graph may then be used to estimate ambient carbonyl compound concentrations alongside temperature and pressure data collected via the weather station.

FOR REFERENCE PURPOSES ONLY

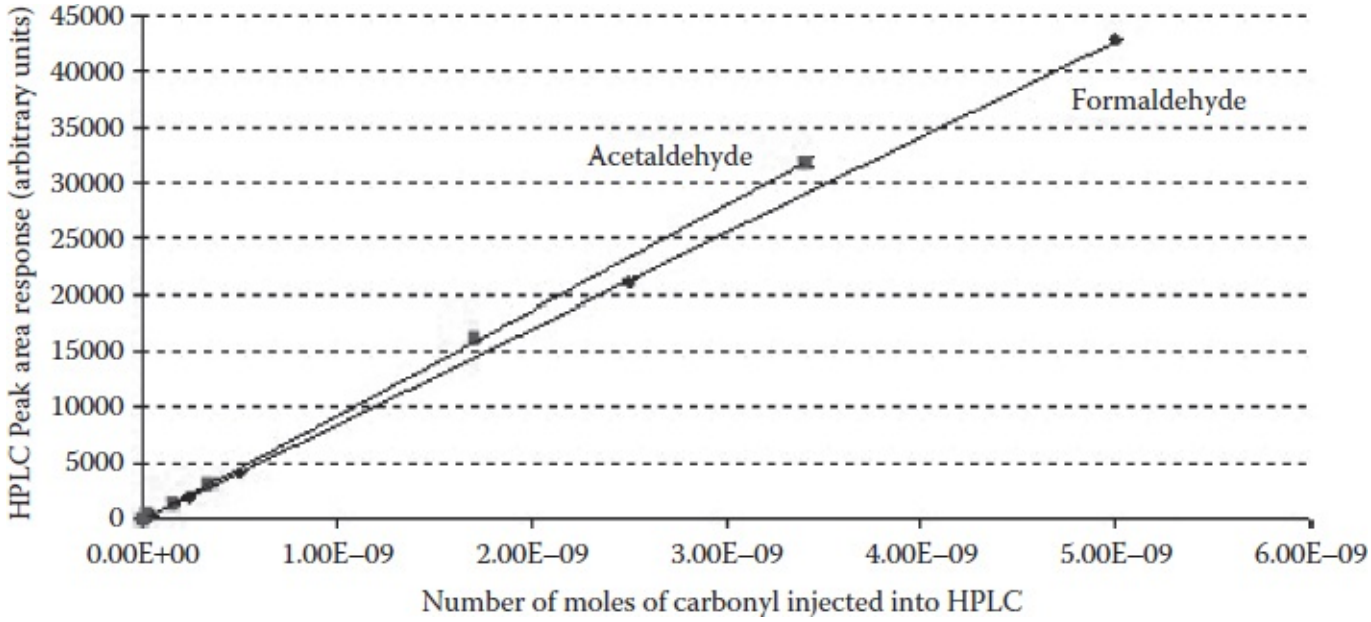

Figure 15.6 Calibration response graphs (peak area) for formaldehyde and acetaldehyde.

15.5.3 Report generation

15.5.3.1 Issues to consider for your practical report

What are the potential sources of error in this analytical determination? How could they be overcome?

15.6 EXPERIMENT VI: AMBIENT PARTICULATE MATTER ANALYSIS

Aim: To analyse suspended particulate matter in a sample

15.6.1 Introduction to experiment

The most accurate way to determine particulate mass concentration is to pass a known volume of air through a filter medium and then to determine the increase in mass of the filter due to the aerosol particles collected. The measurement of airborne (suspended) particulate matter thus involves batch sampling over relatively long collection periods. The collection period, determined to prevent filter clogging, is a function of ambient concentration, pump flow rate, filter area and collection efficiency.

Sampling for suspended particulate matter takes place for various purposes. It is often conducted to allow ambient air concentrations to be compared with national standards, which are often set for 24 h time periods. It can also be conducted to investigate suspended particulate matter concentrations over shorter or longer periods, for example, over a

weekend or during rush-hour traffic periods.

The sampling equipment should be located carefully, typically where it can easily be checked; supplied with power; and left safely and without fear of interference, vandalism or theft. Generally sampling devices of this nature are kept at a height of approximately 3–10 m from ground level and away from direct obstacles from the pollution source under consideration.

Apparatus

- Low- (30 L/min) or high- (100 L/min) volume sampler (e.g. Rotheroe and Mitchell medium- or high-volume sampling pump)
- Electric timer
- Airflow manometer (if not built into the pump, for measuring airflow)
- Glass fibre filter papers (to fit sampler head – Whatman GF/A filters have a collection efficiency of more than 99% for particles of between 0.1 and 1.0 μm)
- Open-faced filter holders
- Gas meter

15.6.2 Experimental procedure

1. The filter papers should be conditioned prior to sampling for at least 48 h at 20°C in a humidity-controlled, conditioning cabinet. After conditioning, each filter paper should be accurately weighed (w_i, mg) and placed in a labelled petri dish. Clean, dry petri dishes, closed with adhesive tape, should be used to transport filters to and from the sample sites.
2. Prepare the sampling assembly onsite. The weighed filter papers should be placed carefully into the appropriate face of the sampling pump or into open-faced filter holders connected by a short length of plastic tubing if the site requires this arrangement. In an external environment, it may be necessary to construct a protective canopy over the filter assembly.
3. Set the electronic timer for the period of sampling. Low- (30 L/min) volume sampling pumps are typically used to allow a sampling period of 24 h, whereas high- (100 L/min) volume sampling pumps may be used for periods of, for example, 4 h to cover rush-hour traffic. Low-volume sampling pumps typically have operational flow rates of approximately 25–30 L/min, and high-volume sampling pumps typically operate at 90–95 L/min.
4. Start sampling as necessary. Note the flow rate (an online gas meter can also be used in some systems).
5. Note the flow rate (and gas meter reading if appropriate) at the end of the desired sampling period. Switch off the sampler.
6. Condition the filter paper again for the same period and in the same way as done prior to sampling. Take the final weight of the exposed filter (w_f, mg).

15.6.2.1 Calculations

1. Average flow rate in L/min = (initial flow rate + final flow rate)/2
2. Total volume of air sampled (TVA) in m^3= average flow rate (L/min) * 10^{-3} (m^3/L) * sampling time (h) * 60 (min/h)
3. Concentration of suspended particulate matter in µg/m^3 = ($w_f - w_i$)/(TVA) (m^3) * 10^6 µg/m^3

15.6.3 Report generation

15.6.3.1 Issues to consider for your practical report

- What are the potential sources of error in this analytical determination? How could they be overcome?
- Identify other methods that could be used for the determination of suspended particulate matter.
- Discuss how you could assess variability of this type of analysis.
- Discuss the relationship (if any) between gravimetric and visual methods of assessing suspended particulate matter.
- What are the main sources of atmospheric particulate matter?
- What are the potential human health and environmental effects (if any) of elevated atmospheric concentrations of suspended particulate matter?

15.7 EXPERIMENT VII: PURGE AND TRAP ANALYSIS FOR VOCs

Aim: To identify volatile organic compounds in solid samples

15.7.1 Introduction to experiment

This experiment involves solid phase membrane extraction (SPME) with head space analysis. Gas chromatography–mass spectrometry (GC-MS) is used as the separation and detection technique.

SPME is a solvent-free sample preparation technique introduced in 1990. The equipment involves a small fused silica fibre which is usually coated with a polymeric phase. The fibre is mounted for protection in a syringe-like device. The analytes are absorbed or adsorbed (depending on the coating) by the fibre phase until an equilibrium is reached.

Time required

Three to four hours

Experimental chemicals

- Nicotine (solid)
- Potassium chloride (3 M)
- Tobacco

Apparatus

- SPME fibre: polydimethylsiloxane
- Head space analysis/extraction time: 10 min
- Desorption of nicotine from fibre: 1 min at 250°C
- Column programme: start at 40°C and raise to 250°C in 1 min
- Splitless injector used at 250°C
- Nicotine standard: 100 mg/100 cm^3

15.7.2 Experimental procedure

1. Weigh approximately 1 g of tobacco and place in a pestle and mortar with some sand.
2. Grind the mixture.
3. Place the ground sample (with sand) into a vial and add 3 cm^3 of 3.0 M KCl.
4. Seal the vial and place in a graphite bath at 95°C.
5. Allow the sample to reach the required temperature (leave approximately 10–15 min) and then do a headspace analysis of the sample for 5 min with the SPME fibre. After a fibre has been used, it can be regenerated by heating at 250°C for 10 min. You must do this cleaning operation between each use of the fibre.
6. Repeat the previous procedure with a standard of nicotine (you do not need to grind the sample), and then repeat the procedure three times, with three different aliquots of the tobacco sample.

You must ensure that, within the experiments you run, you have the following data:

1. The same experiment repeated 2 or 3 times. This will allow you to look at the variability within the experiment.
2. A standard of nicotine which has been exposed to the SPME fibre for the same length of time as the tobacco sample. This will allow you to proceed with the calculations in Step 2 in Section 15.7.2.1.

You may want to investigate the effect of the length of time for which the SPME fibre is left in the sample headspace. (Hint: Maybe keep the needle in place for 1, 5 and 10 min.)

15.7.2.1 Calculation

From the resulting chromatographic data, obtain

1. Chromatograms and identification of peaks.
2. An estimate of the concentration ($g.g^{-1}$) of nicotine in the tobacco sample.

15.7.3 Report generation

15.7.3.1 Issues to consider for your practical report

- What are the potential sources of error in this analytical determination? How could they be overcome?
- Identify other methods that could be used for the determination of volatiles.
- Discuss the variability shown in the experiment when performing replicate analysis.
- Outline briefly how SPME works.

REFERENCES AND FURTHER READING RESOURCES

Ahmad, R., Cartwright, M., and Taylor, F. (Eds.) (2001) *Analytical Methods for Environmental Monitoring*. Pearson Education, Harlow, UK.

Clarke, A. G. (Ed.) (1997) *Industrial Air Pollution Monitoring: Gaseous and Particulate Emissions*. Chapman & Hall, London, UK.

Grosjean, E., Grosjean, D., Fraser, M. P., and Cass, G. (1996) Air quality model evaluation data for organics. 2. C1-C14 carbonyls in Los Angeles air. *Environmental Science and Technology*, 30: 2687–2703.

Grzywacz, C. M. (2006) *Monitoring for Gaseous Pollutants in Museum Environments*. Getty Publishing, Los Angeles, CA.

Harrison, R. M., and Perry, R. (Eds.) (1986) *Handbook of Air Pollution Analysis*. Chapman & Hall, London, UK.

Hewitt, C. N. (Ed.) (1991) *Instrumental Analysis of Air Pollutants*. Elsevier, Barking, UK.

Jahnke, J. A. (2000) *Continuous Emissions Monitoring*. Wiley, New York.

Kettrup, A. (2003) *Analyses of Hazardous Substances in Air: Air Monitoring Methods*. Wiley VCH, Weinheim, UK.

Kleffmann, J., Tapia, G. V., Bejan, I., Kurtenbach, R., and Wiesen, P. (2013) NO2 measurement techniques: Pitfalls and new developments. In *Disposal of Dangerous Chemicals in Urban Areas and Mega Cities*, Barnes, I., & Rudziński, K. J. (Eds.), pp. 15–28. Springer, Dordrecht, the Netherlands.

McDermott, J. (2004) *Air Monitoring for Toxic Exposures: An Integrated Approach*. Wiley-Blackwell, Hoboken, NJ.

Parlar, H., and Greim, H. (Eds.) (2009) *Essential Air Monitoring Methods*. Wiley VCH, Weinheim, UK.

Possanzini, M., Di Palo, V., and Cecinato, A. (2002) Sources and photodecomposition of formaldehyde and acetaldehyde in Rome ambient air. *Atmospheric Environment*, 36: 3195–3201.

Saltzmann, B. E. (1954) Colorimetric microdetermination of nitrogen dioxide in the atmosphere. *Analytical Chemistry*, 26: 1949–1955.

Scaringelli, F. P., Saltzman, B. E., and Frey, S. A. (1967) Spectrophotometric determination of atmospheric sulphur dioxide. *Analytical Chemistry*, 39: 1709–1719.

Sritharathikhun, P., Oshima, M., Wei, Y., Simon, J., and Motomizu, S. (2004) On-line collection/concentration and detection of sulfur dioxide in air by flow-injection spectrophotometry coupled with a chromatomembrane cell. *Analytical Sciences*, 20(1): 113–118.

Theodore, L. (2008) *Air Pollution Control Equipment Calculations*. Wiley-Blackwell, Hoboken, NJ.

US Environmental Protection Agency (EPA) (1999) *Compendium Method TO-11A. Determination of Formaldehyde in Ambient Air Using Adsorbent Cartridge Followed by High Performance Liquid Chromatography (HPLC)*. EPA, Cincinnati, OH.

Viskari, E-L., Vartianinen, M., and Pasanen, P. (2000). Seasonal and diurnal variation in formaldehyde and acetaldehyde concentrations along a highway in Eastern Finland. *Atmospheric Environment*, 32: 917–923.

FOR REFERENCE PURPOSES ONLY

West, P. W., and Gaeke, G. C. (1956) Fixation of sulfur dioxide as disulfitomercurate (II) and subsequent colorimetric estimation. *Analytical Chemistry*, 28: 1816.

Williams, I. D., Revitt, D. M., and Hamilton, R. S. (1996). A comparison of carbonyl compound concentrations at urban roadside and indoor sites. *Science of the Total Environment*, 189/190: 475–483.

Review questions

PART A – REVIEW QUESTIONS (WITH ANSWERS)

Q1. Identify the major regulated air pollutants.

Q2. Identify the four gases that compose more than 99.9% of the volume of the atmosphere.

Q3. What is flue gas?

Q4. What are fugitive emissions?

Q5. What are the units associated with:

a. Gaseous air pollutants

b. Particulate air pollutants

Q6. Convert:

a. 50 ppb of ozone (O_3) at 298 K and 1005 mb to μg m^{-3}

b. 12 ppb of toluene (C_7H_8) at 283 K and 1010 mb to μg m^{-3}

c. 5 ppm of carbon monoxide (CO) at 291 K and 1018 mb to mg m^{-3}

Q7. Convert:

a. 51 μg m^{-3} of sulphur dioxide (SO_2) at 293 K and 1011 mb to ppb

b. 175 μg m^{-3} of nitrogen dioxide (NO_2) at 279 K and 1001 mb to ppb

c. 350 mg m^{-3} of carbon dioxide (CO_2) at 300 K and 1020 mb to ppm

Q8. Define the terms:

a. Secondary pollutant

b. Anthropogenic pollutant

c. Area source

d. Emissions inventory

e. Volume mixing ratio

f. Dry adiabatic lapse rate

Q9. Classify the following pollutant sources:

FOR REFERENCE PURPOSES ONLY

a. A motorway
b. A coal mine
c. A large supermarket complex
d. A steam engine
e. A nuclear power station
f. A hospital incinerator

Q10. Give examples of how air pollution can damage human health. Include chronic and acute health effects.
Q11. Create a list of indoor air pollutants, their sources and potential health effects.
Q12. Use your research skills to find the most up-to-date information on sources of the principal pollutants in (a) the UK, (b) the United States, (c) Australia and (d) Hong Kong by fuel type.
Q13. Give examples of *natural air pollutants*.
Q14. What is the difference between primary and secondary air pollutants?
Q15. What is the difference between *London smog* and *Los Angeles smog*?
Q16. Outline the contrasting air quality issues that can be prominently identified in the urban and the rural areas of the developed and the developing countries during the twenty-first century.
Q17. How accurate do you think emission inventories are? What is your evidence for this?
Q18. Imagine you are a policy maker for the day. Using available data, draw up a 5-point plan to reduce air pollutant emissions in the most cost-effective fashion.
Q19. Discuss the pros and cons of integrated air quality and carbon management, giving examples of how this can be implemented into local sustainability initiatives.
Q20. Who invented the petrol and the diesel engines?
Q21. Why do diesel engines smoke?
Q22. Why are fossil-fuelled motor vehicle combustion systems inefficient?
Q23. What is a catalytic convertor on a motor car?
Q24. What is the difference between a two-way and a three-way catalytic convertor?
Q25. What is a congestion charge scheme?
Q26. Identify the main sources of each of the following gaseous pollutants in the urban atmosphere:
a. Nitrogen oxides
b. Aldehydes
c. Sulphur oxides

Q27. Explain briefly why time-series data are often used to illustrate the emissions of gaseous pollutants.
Q28. Identify, for each of the following pollutants, the typical urban concentration range.
a. Benzene
b. Sulphur dioxide

c. Carbon monoxide
d. Formaldehyde
e. Acetone
f. Nitrogen oxide
g. Polycyclic aromatic hydrocarbons

Q29. Which of the following statements are true and which are false?
a. Petrol engines produce higher levels of aldehydes than diesel engines.
b. NO_2 concentrations are higher in the summer and the spring.
c. O_3 concentrations are higher in urban/industrial areas than in rural areas.
d. SO_x is emitted by natural sources in similar quantities to anthropogenic sources.

Q30. List the six main types of volatile organic compounds (VOCs).
Q31. Suggest potential sources of VOCs in the home.
Q32. What are the possible units for CO emissions from motor vehicles?
Q33. Define the following terms:
a. Particles
b. PM_{10}
c. Accumulation mode
d. Dry deposition
e. In-cloud scavenging

Q34. Distinguish between gravimetric smoke and black smoke.
Q35. Explain how fine particles are formed in the atmosphere.
Q36. Outline the main sources of primary particulate matter.
Q37. Identify the typical urban concentrations of the following components of airborne particulate matter:
a. PM10
b. Lead
c. PCBs
d. Sulphates
e. Nitrates
f. Elemental carbon
g. Dioxins
h. Zinc

Q38. The different chemical structures of VOCs give rise to their different health and environmental effects. Consequently, it is important to understand the differences between the VOC types outlined in the unit. Draw the structural formula for the following VOCs, making sure you understand the structural distinctions between them.

Pentane	Propene
1-Butyne	1,3-Butadiene
Benzene	Toluene
Formaldehyde	1-Hexanal
Acetone	Ethanol
Anthracene	Naphthalene

Q39. It could be argued that spatial and temporal variation in air quality in cities renders mean values inadequate for assessing the risks of air pollution on health during physical activity. What are your views on this debate?

Q40. Define the term *toxicant* (poison).

Q41. Identify the different routes of toxicants into the body.

Q42. Identify factors that influence the way in which organisms are exposed to toxic substances.

Q43. Identify the main routes of the following substances into the human body:

- Ozone
- White phosphorus
- Carbon monoxide
- Methanol
- Asbestos
- Lead

Q44. Explain why children are more vulnerable to the adverse effects of environmental chemicals than adults.

Q45. Define the following terms:

- Critical load
- Critical level

Q46. What are the effects of acid precipitation on lakes and aquatic ecosystems?

Q47. What are the effects of acid precipitation on trees and soils?

Q48. Define the following terms:

a. Photochemistry
b. Quantum yield
c. The troposphere
d. Photo-ionisation
e. Quenching
f. Positive lapse rate

Q49. State the regions of the Earth's atmosphere, indicating the approximate height above sea level of each.

Q50. Write out Planck's equation, defining all the terms.

Q51. Explain, using diagrams as appropriate, the meaning of each of the following terms.

a. Highest Occupied Molecular Orbital (HOMO)
b. Molecular bonding orbital
c. Triplet state

Q52. Explain the following terms:
a. Free radical
b. Photo-stationary state
c. Allotropes

Q53. State the equation that summarises the photolytic destruction of ozone in the troposphere.
Q54. Explain why the hydroxyl radical is such an important component of the troposphere?
Q55. Explain how the hydroxyl radical is formed from carbonyl compounds in the troposphere, using equations to illustrate your answer.
Q56. Describe why the hydroxyl radical plays such an important part in the dry removal of tropospheric sulphur dioxide.
Q57. List the main requirements for the formation of photochemical smog in urban areas.
Q58. Which conditions are associated with high ozone pollution episodes?
Q59. Explain the importance of ozone in the stratosphere to life on earth.
Q60. Outline the evidence supporting the claim that the stratospheric ozone layer is depleting.
Q61. State the Chapman equations that summarise the formation and destruction of ozone in the stratosphere.
Q62. Outline the physico-chemical properties and uses of chlorofluorocarbons (CFCs).
Q63. Explain the phenomena of fluorescence and phosphorescence.
Q64. State the equation that summarises the photolytic destruction of ozone in the troposphere.
Q65. Explain how the hydroxyl radical is formed from carbonyl compounds in the troposphere, using equations to illustrate your answer.

ANSWERS TO REVIEW QUESTIONS

A1. Sulphur dioxide; nitrogen oxides; carbon monoxide; trace metals such as lead (Pb), cadmium (Cd), platinum (Pt); organic compounds such as benzene and polycyclic aromatic hydrocarbons (PAHs); and photochemical oxidants such as ozone (O_3) and peroxyacetyl nitrates (PANs).
A2. Nitrogen, oxygen, argon and carbon dioxide.
A3. It is the gas exiting a combustion process via a flue (i.e. a vent, a pipe or channel for conveying exhaust gases). The composition of the flue gas depends on the fuel burned, but it mainly comprises of nitrogen (nearly 75%), CO_2, water vapours, PM (soot), CO, NO_2, SO_2.

A4. They are unintended emissions of foul gases or vapours from industrial processes due to leaks or unavoidable situations and accidental releases. Example, emissions of volatile organic compounds such as benzene from oil refineries, methane and other evaporative emissions from sources such as wastewater treatment ponds and storage tanks.

A5.

a. There are three measurements for gaseous air pollutants – mass per unit of volume (μg m^{-3}), volume per unit volume of air (μL L^{-1}) and volume mixing ratio (ppm, etc.).
b. There is just the one measure for particulate pollutants – mass per unit of volume (μg m^{-3}).

A6.

a. 97 μg m^{-3}
b. 47 μg m^{-3}
c. 6 mg m^{-3}

A7.

a. 19 ppb
b. 88 ppb
c. 194 ppm

A8.

a. A pollutant formed in the air as a result of chemical reactions with other pollutants and atmospheric gases.
b. A pollutant emitted as a result of human activity (from a man-made source), such as the combustion of fossil fuel for energy.
c. A collection of small geographically dispersed emitters that are not significant individually, but are important collectively.
d. A schedule of the sources of an air pollutant or pollutants within a particular geographical area.
e. The ratio of the pollutant volume and the original air volume – this is equivalent to the ratio of the number of pollutant gas molecules to the total number of air molecules (usually measured in ppm or ppmv, parts per million i.e. per 106; ppb, parts per billion i.e. per 109; ppt, parts per trillion i.e. per 1012).
f. The rate of decrease of temperature with height caused by this type of displacement is called the dry adiabatic lapse rate (DALR). Adiabatic simply means that the air parcel's total energy content is conserved during the displacement, not exchanged with the surrounding air.

A9.

a. A line source
b. A point source
c. An area source
d. A line source
e. An area source
f. A point source

A10. Examples of how air pollution can damage human health.
Major human health impacts of environmental exposures to air pollutant chemicals:

Health impact	*Environmental exposure*
Cancer	• Smoke/environmental tobacco smoke, ETS (<$PM_{2.5}$)
	• Pesticide aerosols
	• Asbestos
	• Natural toxins (aflatoxin)
	• Polycyclic aromatic hydrocarbons (e.g. diesel fumes)
	• Metals (e.g. arsenic, cadmium, chromium)
	• Radiation (UV light)
	• Radon
	• Dioxins
Cardiovascular diseases	• Air pollution (carbon monoxide, ozone, PM)
	• Smoking and ETS
	• Lead
	• Noise
Respiratory diseases (asthma)	• Smoking and ETS
	• Sulphur dioxide
	• Nitrogen dioxide
	• Inhalable particles (PM_{10}, $PM_{2.5}$)
	• Tropospheric ozone
	• Fungal spores
	• Dust mites
	• Pollen
	• Pet hair, skin and excreta
Skin diseases	• UV radiation
	• Heavy metals (e.g. nickel)
	• Pentachlorophenol
	• Dioxins
Reproduction dysfunctionalities	• Polychlorinated biphenyls (PCBs)
	• Dichlorodiphenyltrichloroethane (DDT)
	• Cadmium
	• Phthalates
Developmental (foetal and childhood) disorders	• Lead
	• Mercury
	• Smoking and ETS
	• Cadmium
	• Pesticide aerosols
Nervous system disorders	• Lead
	• PCBs
	• Methyl mercury
	• Manganese
	• Organophosphates
Immune response	• UVB radiation
	• Pesticides
Increased chemical sensitivity	• Multiple chemical exposures at low doses

Source: European Environment Agency, Europe's environment, the third assessment, Environmental assessment report no. 10, 2003.

A11. A list of indoor air pollutants, their sources and potential health effects

Pollutant	*Major indoor sources*	*Potential health effects*[a]
Environmental tobacco smoke	Cigarettes, cigars and pipes	Respiratory irritation, bronchitis and pneumonia in children, emphysema, lung cancer, and heart disease
Carbon monoxide	Unvented or malfunctioning gas appliances, wood stoves, and tobacco smoke	Headache; nausea; angina; impaired vision and mental functioning; fatal at high concentrations
Nitrogen oxides	Unvented or malfunctioning gas appliances	Eye, nose, and throat irritation; increased respiratory infections in children
Organic chemicals	Aerosol sprays, solvents, glues, cleaning agents, pesticides, paints, moth repellents, air fresheners, dry cleaned clothing, and treated water	Eye, nose, and throat irritation; headaches; loss of coordination; damage to liver, kidney and brain; various types of cancer
Formaldehyde	Pressed wood products such as plywood and particleboard; furnishings; wallpaper; durable press fabrics	Eye, nose, and throat irritation; headache; allergic reactions; cancer
Respirable particles	Cigarettes, wood stoves, fireplaces, aerosol sprays, and house dust	Eye, nose and throat irritation; increased susceptibility to respiratory infections and bronchitis; lung cancer
Biological agents (bacteria, viruses, fungi, animal dander, mites)	House dust; pets; bedding; poorly maintained air conditioners, humidifiers and dehumidifiers; wet or moist structures; furnishings	Allergic reactions; asthma; eye, nose, and throat irritation; humidifier fever, influenza, and other infectious diseases
Asbestos	Damaged or deteriorating insulation, fireproofing, and acoustical materials	Asbestosis, lung cancer, mesothelioma, and other cancers
Lead	Sanding or open-flame burning of lead paint; house dust	Nerve and brain damage, particularly in children; anaemia; kidney damage; growth retardation
Radon	Soil under buildings, some earth-derived construction materials and groundwater	Lung cancer

[a] Depends on factors such as the amount of pollutant inhaled, the duration of exposure and susceptibility of the individual exposed.

A12. Lists of country-specific pollutant sources:
A. UK principal pollutants and sources

Pollutant	*Sources*
Ammonia	Livestock manure, slurry management, fertilisers, waste disposal and transport (DEFRA, 2015).
Arsenic	Use of wood treated with arsenic-containing preservatives (NAEI, 2014).
Benzene	Domestic combustion, industrial combustion and road transport (DEFRA, 2015).
Benzo(a)pyrene	Domestic coal and wood burning, fires, and industrial processes (DEFRA, 2015).
Cadmium	Energy production, non-ferrous metal production, iron and steel manufacture, and other industrial combustion (NAEI, 2014).
Carbon monoxide	Road transport, combustion of fuels with insufficient oxygen to convert all carbon to carbon dioxide (DEFRA, 2015).

FOR REFERENCE PURPOSES ONLY

Lead	Metal production and industrial combustion of lead-containing lubricants (NAEI, 2014).
Mercury	Fossil fuel combustion, iron and steel production, waste incineration, manufacture of chlorine in mercury cells, and coal combustion (NAEI, 2014).
Nickel	Oil and coal combustion, metal processes and manufacturing (NAEI, 2014).
Nitrogen oxides	Power generation, industrial combustion and road transport (which accounts for almost one-third of UK emissions) (DEFRA, 2015).
Ozone	Secondary pollutant produced by sunlight interacting with nitrogen oxides and volatile organic compounds from vehicles and industry (DEFRA, 2015).
Particulate matter	(Primary PM) Stationary fuel combustion, quarrying, construction, non-road mobile sources and road transport engine emissions, tyre-wear and non-exhaust emissions (DEFRA, 2015). (Secondary PM) Emissions of ammonia, organic compounds, sulphur dioxides and nitrogen dioxides (DEFRA, 2015).
Sulphur dioxide	Power generation, industry, commercial fuel use and some residential fuel use (DEFRA, 2015).

Source: DEFRA, Annual report 2015 issue 1, DEFRA [Online], Available at: https://uk-air.defra.gov.uk/library/annualreport/viewonline?year=2015_issue_1&jump=3-1, 2015; NAEI, *Pollutant Information*, National Atmospheric Emissions Inventory [Online], Available at: http://naei.defra.gov.uk/overview/pollutants, 2014.

B. US principal pollutants and sources

Pollutant	*Sources*
Carbon monoxide	Vehicles or machinery that burn fossil fuels, unvented kerosene and gas space heaters, leaking chimneys, gas stoves (EPA, 2016a).
Lead	Ore and metals processing, lead-fuelled piston-engine aircraft operation, waste incinerators, utilities, lead-acid battery manufacturing, lead smelting (EPA, 2016b).
Nitrogen dioxide	Vehicle emissions, power plant emissions and off-road equipment emissions (EPA, 2016c).
Ozone	Chemical reactions between pollutants emitted by vehicles, power plants, industrial boilers, refineries, chemical plants, in the presence of sunlight (EPA, 2016d).
Particulate matter	Emissions from construction sites, unpaved roads, fields, smokestacks or fires, or formed in the atmosphere by reactions with pollutants from power plants, industry and cars (EPA, 2016e).
Sulphur dioxide	Burning fossil fuels by power plants and other industrial facilities, extracting metal from ore, volcano emissions, vehicles or heavy equipment that burns fuel with high sulphur content (EPA, 2016f).

Source: EPA, *Basic Information about Carbon Monoxide (CO) Outdoor Air Pollution*, EPA [Online], Available at: https://www.epa.gov/co-pollution/basic-information-about-carbon-monoxide-co-outdoor-air-pollution, 2016a; EPA, *Basic Information about Lead Outdoor Air Pollution*, EPA [Online], Available at: https://www.epa.gov/lead-air-pollution/basic-information-about-lead-air-pollution, 2016b; EPA, *Basic Information about NO_2*, EPA [Online], Available at: https://www.epa.gov/no2-pollution/basic-information-about-no2, 2016c; EPA, *Ozone Basics*, EPA [Online], Available at: https://www.epa.gov/ozone-pollution/ozone-basics, 2016d; EPA, *Particulate Matter (PM) Basics*, EPA [Online], Available at: https://www.epa.gov/pm-pollution/particulate-matter-pm-basics, 2016e; EPA, *Sulfur Dioxide Basics*, EPA [Online], Available at: https://www.epa.gov/so2-pollution/sulfur-dioxide-basics, 2016f.

C. Australia principal pollutants and sources

Pollutant	*Sources*
Carbon monoxide	Motor vehicle exhaust, some industrial activities (e.g. steel manufacture) and bushfires (Department of the Environment and Heritage, 2005a).

Lead	Mining and metal manufacturing are the largest sources, but there is also waste incineration, battery recycling and other manufacturing processes (Department of the Environment and Energy, 2016).
Nitrogen dioxide	Burning of fossil fuels, motor vehicle exhaust (contributing to 80% of NO_2 in cities), petrol and metal refining, other manufacturing industries and food processing (Department of the Environment and Heritage, 2005b).
Ozone	Formed when nitrogen oxide reacts with reactive organic air pollutants in the presence of sunlight, which come from sources such as vehicle exhaust, oil refining, printing, petrochemicals, aviation, bushfires and lawn mowing (Department of the Environment and Heritage, 2005c).
Particles	Bushfires, dust storms, pollen, sea spray, motor vehicle emissions, industrial processes, unpaved roads and wood heaters (Department of the Environment and Heritage, 2005d).
Sulphur dioxide	Industrial processing of sulphur-containing materials, for example, generation of electricity from sulphur-containing fossil fuels, and the processing or sulphur-containing mineral oils (Department of the Environment and Heritage, 2005e).

Source: Department of the Environment and Heritage, *Carbon Monoxide* (*CO*), Australian Government [Online], Available at: http://www.environment.gov.au/protection/publications/factsheet-carbon-monoxide-co, 2005a; Department of the Environment and Energy, *Lead*, Australian Government [Online], Available at: http://www.environment.gov.au/protection/chemicals-management/lead, 2016; Department of the Environment and Heritage, *Nitrogen Dioxide* (*NO2*), Australian Government [Online], Available at: http://www.environment.gov.au/protection/publications/factsheet-nitrogen-dioxide-no2, 2005b; Department of the Environment and Heritage, *Ground-Level Ozone* (*O3*), Australian Government [Online], Available at: http://www.environment.gov.au/protection/publications/factsheet-ground-level-ozone-o3, 2005c; Department of the Environment and Heritage, *Particles*, Australian Government [Online], Available at: http://www.environment.gov.au/resource/particles, 2005d; Department of the Environment and Heritage, *Sulfur Dioxide* (*SO2*), Australian Government [Online], Available at: http://www.environment.gov.au/protection/publications/factsheet-sulfur-dioxide-so2, 2005e.

D. Hong Kong principal pollutants and sources

Pollutant	*Sources*
Carbon monoxide	Incomplete combustion of carbon-based fuel from automobiles and industrial processes (AQHI, 2016a).
Nitrogen dioxide	Vehicle emissions, particularly from diesel vehicles, including emissions from marine vessels (EPD, 2016), and power plant emissions (AQHI, 2016b).
Ozone	Secondary pollutant formed by the action of UV light from the sun on nitrogen oxides arising from vehicle emissions (AQHI, 2016c).
Particulate matter	Vehicle emissions, particularly from diesel vehicles, including emissions from marine vessels (EPD, 2016).
Sulphur dioxide	Fossil fuel burning power plants, industrial processes and vehicular emissions (AQHI, 2016d).
Volatile organic compounds	Road vehicle emissions, manufacturing of products such as paint, printing ink, aerosols and insecticides (EPD, 2016).

Source: AQHI, *Sources of Air Pollutant: Carbon Monoxide*, Environmental Protection Department [Online], Available at: http://www.aqhi.gov.hk/en/health-advice/sources-of-air-pollutants2985.html?showall=&start=3, 2016a; AQHI, *Sources of Air Pollutant: Nitrogen Dioxide*, Environmental Protection Department [Online], Available at: http://www.aqhi.gov.hk/en/health-advice/sources-of-air-pollutantsc666.html?showall=&start=2, 2016b; AQHI, *Sources of Air Pollutant: Ozone*, Environmental Protection Department [Online], Available at: http://www.aqhi.gov.hk/en/health-advice/sources-of-air-pollutants052c.html?showall=&start=4, 2016c; AQHI, *Sources of Air Pollutant: Sulphur Dioxide*, Environmental Protection Department [Online], Available at: http://www.aqhi.gov.hk/en/health-advice/sources-of-air-pollutantse469.html?showall=&start=1, 2016d; EPD, *Air*, Environmental Protection Department [Online], Available at: http://www.epd.gov.hk/epd/english/environmentinhk/air/air_maincontent.html, 2016.

A13. Volcanoes, forest fires, dust storms, sea salt nuclei form wave action, pollen, mould

spores.

A14. Primary pollutants are added directly to air. Secondary pollutants are formed as a result of chemical and physical reactions between the primary pollutants and other atmospheric components such as water vapour or each other.

A15. *London smog* is a mixture of fog and smoke and it occurs in cool foggy areas. *Los Angeles smog* is caused by a photochemical reaction between the pollutants (mostly from auto exhaust and industry) and light and occurs in warm sunny areas.

A16. Typical answer should address the predominantly distinct air pollution emissions characteristics of the source activities in the urban and the rural areas during the twenty-first century. This should be extended to discuss briefly the differences in such emissions profiles for the developed and the developing countries, associated mainly with the differences in the process technologies (mainly combustion related in transport and energy production), emissions abatement technologies and the legislative framework.

A17. The accuracy of emissions factors is a thorny subject – see this link for some idea of the issues involved: https://www.epa.gov/air-emissions-factors-and-quantification/emissions-factor-uncertainty-assessment.

A18. Since it is in urban areas that traffic congestion and hence air quality is worst, the pros and cons of exercise in cities has become a hot topic (BBC News, 4 May 2016 and subsequent coverage). In their forthcoming paper, however, Tainio et al. (2016)* conclude that the benefits of physical activity outweigh 'the harm caused by air pollution in all but the most extreme air pollution concentrations'. While the publicity generated by Tainio et al. is welcome, and I do not disagree that harm would be greatest at the highest air pollution concentrations, I question whether the data used in their analysis are suitable to address the question. The average pollutant concentrations they use conceal large spatial and temporal variations within cities. It is easy to imagine that a cyclist commuting to work daily during peak traffic hours and along busy routes would experience not the average but peak exposure. It could be argued therefore that at present, air pollution monitoring is not at a fine enough resolution either spatially or temporally to provide feedback to citizens on where and when it is safe to exercise, highlighting a serious gap in knowledge and understanding. I also question whether the conversion constants used by Tainio et al. are sufficient to convert background $PM_{2.5}$ concentrations to risk. For cyclists, they assume exposure (inhaled dose) to be twice the background level multiplied by 2.55 to allow for an elevated ventilation rate. It seems likely, however, that ventilation rate is additionally influenced by externalities such as general fitness, effort exerted, incline, external temperature, thermal comfort and complicating factors such as stress induced by near-miss incidents with traffic. These factors are themselves spatially and temporally variable. Real-time studies of physiological responses to environmental conditions are few, especially for non-elite performance such as physical activity during *active travel* (walking or cycling to work). This is another

research gap that hampers our ability to address the issue whether the health benefits of physical activity outweigh the risks in an urban setting.

A19. There is no precise, *correct* answer to this question. Exemplary answers should elaborate on the means to promote more integrated Local Air Quality Management that is Air Quality and Climate Change Strategy Action Plan at local-to-urban scales, specifically regarding policies on emissions sources from transportation and decentralised energy sectors. This should discuss the relevance and timeliness of an integrated approach, highlighting its cost-effectiveness and the merits and the trade-offs of implementing such practices, using a more integrated planning framework than what is currently under offer.

For the second part of this question, use of suitable case study examples from local sustainability initiatives is desired. This would be essentially adopting a co-management approach in addressing the issues on pollution remediation and carbon management locally.

(Supporting information available in: Tiwary, A., Chatterton, T., and Namdeo, A. (2014) Co-managing carbon and air quality: Pros and cons of local sustainability initiatives. *Journal of Environmental Planning and Management*, 57(8): 1266–1283. doi:10.1080/09640568.2013.802677.)

A20. The petrol engine was devised in 1885 by Gottlieb Daimler and Karl Benz. The diesel engine was devised by Herbert Akroyd in 1890 and applied practically by Rudolf Diesel in 1892.

A21. Black smoke from a diesel engine is caused by too much fuel in the air–fuel mixture, also called a *rich* mixture. This is often caused by worn out fuel injectors. Fuel is injected into diesel engines through very small holes under very high pressure in order to get good atomisation. As the fuel flows, the hole erodes, getting larger. Over time, the holes get large enough to let too much fuel through.

A22. Primarily because:

- Are frequently oxygen deficient (whereas most other combustion systems are not).
- Preheat their air–fuel mixtures (which most other combustion systems do not).
- Have unsteady combustion (whilst most other combustion systems do not).
- In auto engines, flames directly contact cooled surfaces (which is not common in most other combustion systems).

A23. To reduce emissions of CO, HC and NO_x from vehicle exhaust, a catalytic converter is required. A catalytic converter looks similar to a cylindrical bulge on a conventional exhaust pipe and consists of a ceramic honeycomb coated with aluminium. The structure is honeycombed to increase its surface area and is coated with rare metals which act as catalysts. Catalytic converters must be positioned within the exhaust stream close to the engine to achieve the high operating temperatures required by the catalyst.

A24. The earliest converters contained only platinum, which chiefly assisted in the

oxidation of CO and HCs. These converters – known as *two-way* or *oxidation converters* – were unpopular since they were expensive, reduced engine performance and required unleaded petrol (since lead de-activated the catalysts). Modern converters are better designed and also use palladium (which enhances the oxidation process) and rhodium (which reduces NO_x) as catalysts. Such converters are known as *oxidation-reduction* or *three-way catalysts* (TWCs).

A25. A congestion charge scheme is a daily levy imposed on vehicle drivers that drive within a specific urban area in specific time periods.

A26.

a. *Nitrogen oxides*: road transport
b. *Aldehydes*: road transport
c. *Sulphur oxides*: combustion of fossil fuels for heating and energy

A27. Times series data enable the identification of daily or seasonal variations, as well as trends.

A28.

a. Benzene: 10–12 mg m^{-3}
b. Sulphur dioxide: 3–20 ppb
c. Carbon monoxide: (3–15) × 10^3 ppb
d. Formaldehyde: 5–40 ppb
e. Acetone: 10–20 ppbv
f. Nitrogen oxide: 10–50 ppb
g. Polycyclic aromatic hydrocarbons: (5–10) × 10^{-2} μg m^{-3}

A29.

a. False – diesel engines produce higher levels of aldehydes than petrol engines
b. True
c. False – O_3 concentrations are higher in rural areas
d. True

A30. Hydrocarbons (HCs)
Aldehydes
Ketones
Alcohols
Heterocycles and other organics
Toxic organic micro-pollutants (TOMPs)

A31. Examples include household chemicals (cleaning and bleaching agents, polishes, air fresheners, deodorants, pesticide sprays, solvents), building materials and furnishings (paints, glues, varnishes), tobacco smoke, and gas and paraffin heaters.

A32. There are a number of possible units for pollution emissions from motor emissions,

including:

- Mass of pollutant emitted per distance travelled per vehicle – for example, g/km/vehicle or g/mile/vehicle.
- Mass of pollutant emitted per volume of fuel consumed per vehicle – for example, g/l/vehicle or g/gallon/vehicle.

A33.

a. Particles – aggregations of matter, either solid or liquid, which are larger than individual molecules.
b. PM_{10} – particles that are able to pass through a size-selective inlet with a 50% efficiency cut-off at 10 μm aerodynamic diameter.
c. Accumulation mode – particles of size 0.05–2 μm AD formed by the coagulation of particles from the nuclei mode and condensation on existing material, and having an atmospheric lifetime of days.
d. Dry deposition – the continuous transfer of particles (and gases) by impaction, sedimentation and Brownian motion.
e. In-cloud scavenging – the main route for wet deposition, whereby particles are included in the developing water droplet in a cloud (also known as rain-in).

A34. Dark smoke is measured by reflectance, whereas gravimetric smoke is measured in terms of mass.

A35.

a. The condensation of hot vapour (from recent combustion) into primary particles.
b. The nucleation of low volatility vapour and condensation on to existing material.
c. Coagulation between existing particles.

A36. Primary particulate matter is emitted directly to the atmosphere from a combustion source (including both mobile and stationary sources).

A37.

a. PM_{10}: 30 μg m^{-3}
b. Lead: 0.1 μg m^{-3}
c. PCBs: approx. 1 ng m^{-3}
d. Sulphates: 5–10 μg m^{-3}
e. Nitrates: 2–10 μg m^{-3}
f. Elemental carbon: 3 μg m^{-3}
g. Dioxins: 400–600 fg m^{-3}
h. Zinc (Poland): 50–60 ng m^{-3}

A38.

Pentane
$CH_3CH_2CH_2CH_2CH_3$

Propene
$H_2C{=}CHCH_3$

1-Butyne
$HC{\equiv}CCH_2CH_3$

1,3-Butadiene
$H_2C{=}CHHC{=}CH_2$

Benzene
C_6H_6

Toluene
C_6H_8 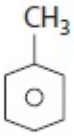

Formaldehyde
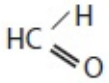

1-Hexanal
$CH_3CH_2CH_2CH_2CH_2C(=O)H$

Acetone
H_3CCCH_3 (C=O)

Ethanol
CH_3CH_2OH

Anthracene
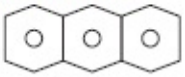

Naphthalene
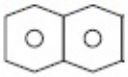

A39. Since it is in urban areas that traffic congestion and hence air quality is worst, the pros and cons of exercise in cities has become a hot topic. Researchers have concluded that the benefits of physical activity outweigh the harm caused by air pollution in all but the most extreme air pollution concentrations. However, it is debateable whether the data used in their analyses are suitable to address the question. The average pollutant concentrations typically used by researchers conceal large spatial and temporal variations within cities. It is easy to imagine that a cyclist commuting to work daily during peak traffic hours and along busy routes would experience not the average but peak exposure. It could be argued therefore that at present, air pollution monitoring is not at a fine enough resolution either spatially or temporally to provide feedback to citizens on where and when it is safe to exercise, highlighting a serious gap in knowledge and understanding. It is also questionable whether the conversion constants used by scientists are sufficient to convert background $PM_{2.5}$ concentrations to risk. For cyclists, they assume exposure (inhaled dose) to be twice the background level multiplied by 2.55 to allow for an elevated ventilation rate. It seems likely, however, that ventilation rate is additionally influenced by externalities such as general fitness, effort exerted, incline, external temperature, thermal comfort and complicating factors such as stress induced by near-miss incidents with traffic. These factors are themselves spatially and temporally variable. Real-time studies of physiological responses to environmental conditions are few, especially for non-elite performance such as physical activity during *active travel* (walking or cycling to work). This is another research gap that hampers our ability to address the issue whether the health benefits of physical

activity outweigh the risks in an urban setting.

A40. A toxicant, or poison, is a substance that is harmful to living organisms because of its detrimental effects on tissues, organs, or biological processes.

A41. The major routes of accidental (or intentional exposure to toxicants by humans and other animals are

- The skin (percutaneous route)
- The lungs (inhalation, respiration, pulmonary route)
- The mouth (oral route)
- Minor routes include rectal, vaginal and parenteral (intravenous or intramuscular)

The way that a toxic substance is introduced into the complex system of an organism is strongly dependent upon the physical and chemical properties of the substance. The pulmonary system is most likely to take in toxic gases or very fine, respirable solid or liquid particles. In other than respirable form, a solid usually enters the body orally. Absorption through the skin is most likely for liquids, solutes in solution, and semi-solids.

A42. Key factors that influence the way in which organisms are exposed to toxic substances include:

- The dose
- The toxicant concentration (100% very dilute solution)
- Duration of exposure per exposure incident
- Frequency of exposure
- Rate of exposure
- Total time period of exposure
- Exposure site
- Exposure route

A43. The main routes of the following substances into the human body:

- *Ozone*: Inhalation
- *White phosphorus*: Inhalation, skin contact or orally
- *Carbon monoxide*: Inhalation
- *Methanol*: Orally; inhalation of methanol fumes is also possible
- *Asbestos*: Inhalation
- *Lead*: Inhalation, oral

A44. Children are more vulnerable to the adverse effects of environmental chemicals than adults for a range of reasons. Children breathe more air per kilo of body weight than adults. The baseline rate of breathing is faster in a child than in an adult, and it speeds up more often because children tend to be more active, especially outdoors and often during peak air pollution times, such as travelling to and from school during the morning and evening rush hours. Children spend more time outside and are more

physically active, which further increases their exposure to air pollution. Because their brains and other organs are still developing, the toxic effects of pollution can cause damage that has the potential to affect them for the rest of their lives. In addition, their internal air passageways are smaller, which means more lung tissue surface is exposed per volume of air. Children inhale air closer to the ground and floor compared to adults. Studies have shown that certain contaminants in air pollution (e.g. dense vapours) and dust particles settle in a vertical gradient, meaning that they are higher in concentration and therefore more available within a child's breathing zone. Playing at ground level also raises dust that may be inhaled or ingested through hand-to-mouth activity. As well, the metabolic need for oxygen is greater in the child because of growth, leading to higher basal (resting) respiratory requirements.

A45.

- Critical load refers to the deposition of pollutants. It is defined by the United Nations Economic Commission for Europe (UNECE) as 'a quantitative estimate of exposure to one or more pollutants below which significant harmful effects on sensitive elements of the environment do not occur, according to present knowledge'.
- Critical levels refer to threshold gaseous concentrations and are defined as 'the concentrations in the atmosphere above which direct adverse effects on receptors such as plants, ecosystems or materials may occur, according to present knowledge'.

A46. Acid rain can have a direct effect on lakes and the ecosystems within them. This effect can be very dramatic – between 1961 and 1971, Lumsden Lake in the Killarney region of Ontario, Canada, went from a pH reading of 6.8 to 4.4 – an increase in acidity of more than 200 times. Most lakes with falling pH values are usually small and are located at high altitudes and on watersheds where the rock and soil have a low neutralising capacity.

There are several routes through which acidic chemicals can enter lakes.

- They may enter the water directly – as dry particles falling through the air or as wet particles falling as precipitation, including rain, snow, sleet, hail, dew or fog.
- Lakes can also be thought of as the *sinks* of the earth, whereby rain falling on to land eventually makes its way into them. Acid rain falling onto the earth washes nutrients out of the soil and carries toxic metals that have been released from the soil into the lakes.

A particularly harmful example of the latter method by which acids can enter lakes is *spring acid shock*. When snow melts rapidly in spring, the acids and chemicals in the snow are released into the soil. The melted snow also runs off into streams and rivers, and gradually makes its way into lakes. The sudden introduction of these acids and chemicals into the lakes can cause a drastic change in their pH value – hence the term

FOR REFERENCE PURPOSES ONLY

spring acid shock.

One effect of spring acid shock is that the aquatic ecosystem does not have sufficient time to adjust to the sudden change. In addition, spring is an especially vulnerable time for many aquatic species since this is when amphibians, fish and insects reproduce. Many of these species lay their eggs in the water to hatch. The sudden pH change is dangerous because the acids can cause serious deformities in the immature creatures, and can even annihilate whole species since the young of many such species spend a significant part of their life cycle in the water.

Acids in water can affect the fish in lakes in two ways:

Direct effects: Sulphuric acid directly interferes with a fish's ability to take in the oxygen, salt and nutrients needed to stay alive. For freshwater fish, maintaining osmoregulation is a key to their survival. Osmoregulation is the process of maintaining the delicate balance of salts and minerals in their tissues. Acid molecules in the water cause mucus to form in a fish's gills and this prevents it from absorbing oxygen efficiently. If the build-up of mucus increases, the fish can suffocate.

In addition, a low pH value will throw off the balance of salts in fish tissue. The levels of, for example, calcium (Ca^{2+}) in some fish cannot be maintained due to pH change. This results in poor reproduction – the eggs produced are damaged by either being too brittle or too weak. Decreased Ca^{2+} levels also result in weak spines and deformities – for example, crayfish need Ca^{2+} to maintain a healthy exoskeleton, and low Ca^{2+} levels would lead to a weak exoskeleton. Ammonium salts (NH_4^+) also influence the wellbeing of fish. As nitrogen-containing fertilisers are washed into lakes, the nitrogen stimulates the growth of algae, which logically would mean an increase in oxygen production, thus benefiting the fish. However, because of increased deaths in the fish population due to acid rain, the decomposition process uses up a lot of the oxygen, which leaves less for the surviving fish to take in.

Indirect effects: Indirectly, sulphuric acid causes heavy metals present in soils to be dissociated and released. For example, aluminium (Al^{3+}) is harmless as part of a compound, but because acid rain causes Al^{3+} to be released into the soil and, through leaching and percolation, to make its way gradually into lakes, it becomes lethal to the health of the fish population. Al^{3+} burns the gills of the fish and accumulates in their organs, causing much damage and eventually death. This effect is further augmented by spring acid shock.

The effect of acid rain is dramatically illustrated in a study done on a lake identified simply as Lake 223. Starting in 1976, scientists monitored its pH levels and aquatic ecosystem. They observed that as the pH of the lake decreased over the years, a number of crustaceans died out, mainly because of problems in

reproduction due to the acidity of the lake caused by acid precipitation. At a pH of 5.6, alga growth in the lake was hindered and some types of small fish died out. Eventually, the larger fish died out with the same problems in reproduction. It was noted that there were more adult fish in the lake than there were young. Finally, in 1983, the lake reached a pH of 5 and the surviving fish in the lake were thin, deformed and unable to reproduce.

A47. One of the most serious impacts of acid precipitation is on forests and soils. When sulphuric acid falls on to the earth as rain, nutrients present in the soils are washed away. Aluminium present in the soil is freed and this toxic element can be absorbed by the roots of trees. Thus, the trees are starved to death as they are deprived of such vital nutrients as calcium and magnesium.

Not all of the sulphur dioxide in the atmosphere is converted to sulphuric acid, and a substantial amount can return to the earth unconverted. As this gas falls onto vegetation, it clogs up the stomata in leaves, hindering photosynthesis.

Research has been carried out on red spruce seedlings by spraying them with different combinations of sulphuric and nitric acid, with pH values ranging from 2.5 to 4.5. The needles of these seedlings were observed to develop brown lesions and, eventually, the needles fell off. It was also found that new needles grew more slowly at higher concentrations of acid. Because the rate at which the needles were falling was greater than the rate at which they were replenished, photosynthesis was greatly affected. The actual way in which the needles were killed is still not yet fully understood. However, studies have shown that calcium and magnesium nutrients are washed away from their binding sites when sulphuric acid enters the system. They are replaced by useless hydrogen atoms and this inhibits photosynthesis.

In addition, severe frosts may also further aggravate this situation. With sulphur dioxide, ammonia and ozone present in the air, the frost-hardiness of trees is reduced. Ammonia oxidises with sulphur dioxide to form ammonium sulphate:

$$H_2SO_{4(aq)} + 2NH_{3(g)} \rightarrow (NH_4)_2SO_{4(aq)}$$

This product forms on the surface of the trees. When ammonium sulphate reaches the soil, it reacts to form both sulphuric and nitric acid. Such conditions also stimulate the growth of fungi and pests like the ambrosia beetle. When trees are under such stress, they release chemicals such as terpenes which attract the ambrosia beetle. Nitrogen oxide and nitric oxide, also components of acid rain, can force trees to grow even though they do not have the necessary nutrients. Such trees are sometimes forced to grow well into late autumn when it is actually time for them to prepare for severe frosts in the winter.

A48.

a. Photochemistry is the branch of science that deals with chemical reactions that occur as a direct or indirect result of the absorption of light.

b. The quantum yield in photochemical reactions is defined as the number of

molecules reacting in relation to the number of photons absorbed.

c. The troposphere is the inner layer of the atmosphere, extending for about 17 km above sea level at the equator (8 km over the poles) and containing about 75% of the mass of the Earth's air.

d. Photo-ionisation is the process whereby radiation knocks electrons from atoms, leaving ions in its path.

e. Quenching is the process by which a molecule in an excited state interacts with a chemically unreactive molecule, transferring its energy and becoming reduced to its electronic ground state.

f. A positive lapse rate is where temperature *decreases* with increasing altitude (as in the troposphere).

A49. There are four regions to the Earth's atmosphere:

- The troposphere – ranging from sea level up to 17 km at its highest
- The stratosphere – from 17 to 48 km above sea level
- The mesosphere – from 48 km up to around 80 km
- The thermosphere – from 80 km up to around 400 km

A50. Planck's equation is as follows:

$$E = h\nu = \frac{hc}{\lambda} = hc\sqrt{}$$

where:

h is the Planck's constant (6.6256×10^{-34} J s photon^{-1})

c is the speed of light (2.9979×10^{8} m s^{-1})

ν is the frequency of radiation (s^{-1})

λ is the wavelength of radiation (m)

$\sqrt{}$ is the wavenumber (m^{-1})

A51.

a. The HOMO is the molecular orbit furthest away from the nucleus that contains an (or some) electron(s).

b. A molecular bonding orbital is formed by the overlap (merging) of atomic orbitals. Bonding orbitals include σ (sigma) and π (pi) bonds. (If you are unfamiliar with bonding theory, you will need to study it from any general chemistry textbook.)

c. A triplet state is an excited electronic state in which the unpaired electrons have a parallel spin, giving the EES an overall non-zero spin.

A52.

a. A free radical is any atom or group of atoms that has an odd number of electrons

and is capable of independent existence. It may also carry an electrical charge. Free radicals are highly reactive, making them important as intermediaries in chemical reactions.

b. A photo-stationary state exists when a light catalysed chemical reaction results in no net formation of products (i.e. the reactants and products are generated in equal amounts).

c. Different structural forms of an element are known as *allotropes*.

A53. The photolytic destruction of ozone is described by the following equation:

$$O_3 \xrightarrow{h\nu} O^{\bullet} + O_2 \qquad \text{(given that } \lambda < 320 \text{ nm)}$$

A54. Hydroxyl radicals, although few in number in the troposphere, are so reactive that they constitute the main pathways for the removal of most oxidisable molecules in this region of the atmosphere.

A55. The formation of the hydroxyl radical from carbonyl compounds starts with the photo dissociation of a carbonyl compound – for example:

$$HCHO \xrightarrow{h\nu} CHO^{\bullet} + H^{\bullet}$$

The resultant hydrogen radical (H•) immediately reacts with oxygen gas:

$$H^{\bullet} + O_2 \rightarrow HO_2^{\bullet}$$

This results in the formation of the hydroperoxyl radical ($HO_2^{\bullet}$) which then reacts with nitric oxide and loses an oxygen atom to form $^{\bullet}OH$:

$$HO_2^{\bullet} + NO \rightarrow NO_2 + {}^{\bullet}OH$$

A56. The dry removal of SO_2 from the troposphere is described by the following process:

$$^{\bullet}OH + SO_2 \rightarrow HOSO_2^{\bullet}$$
$$\text{then } HOSO_2^{\bullet} + O_2 \rightarrow SO_3^{\bullet} + HO_2^{\bullet}$$
$$SO_3^{\bullet} + HO_2^{\bullet} \rightarrow H_2SO_4$$

A57. The main requirements for the formation of photochemical smog are the presence of the following factors:

- Strong sunlight
- Stable meteorological conditions
- The presence of NO_x
- The presence of hydrocarbons, particularly unsaturated ones

A58. High ozone episodes are associated with stagnant high pressure systems, clear days and strong temperature inversions.

A59. Ozone in the stratosphere absorbs ultraviolet radiation from the sun, preventing UV-C and reducing the amount of UV-B radiation reaching the Earth's surface.

A60. The main evidence is the reduction of stratospheric ozone concentrations at the poles during springtime, leading to ozone *holes* over the arctic and Antarctic regions.

A61. Ozone formation is described by the following Chapman equations:

$$O_2 + h\nu \rightarrow 2O^{\bullet} \qquad (\text{given } \lambda = 242 \text{ nm})$$

$$O_2 + O^{\bullet} + {}^{1}M \rightarrow O_3 + M$$

Ozone destruction is described as follows:

$$O_3 + h\nu \rightarrow O_2 + O^{\bullet}$$

$$O_3 + O^{\bullet} \rightarrow 2O_2$$

A62. Chlorofluorocarbons are chemically stable, odourless, non-flammable, non-toxic and non-corrosive. They have been used as aerosol spray propellants, refrigerants, solvents and plastic foaming agents.

A63. *Fluorescence* is the emission of light by a substance that has absorbed light or other electromagnetic radiation. In most cases, the emitted light has a longer wavelength, and therefore lower energy, than the absorbed radiation. The most striking examples of fluorescence occur when the absorbed radiation is in the ultraviolet region of the spectrum, and thus invisible to the human eye, and the emitted light is in the visible region.

Phosphorescence is a specific type of photoluminescence related to fluorescence. Unlike fluorescence, a phosphorescent material does not immediately re-emit the radiation it absorbs. As these transitions occur very slowly in certain materials, absorbed radiation may be re-emitted at a lower intensity for up to several hours after the original excitation.

A64. The photolytic destruction of ozone is described:

$$O_3 \xrightarrow{h\nu} O^{\bullet} + O_2 \quad (\text{given that } \lambda < 320 \text{ nm})$$

A65.

The formation of the hydroxyl radical from carbonyl compounds starts with the photo-dissociation of a carbonyl compound – for example:

$$HCHO \xrightarrow{h\nu} CHO^{\bullet} + H^{\bullet}$$

The resultant hydrogen radical ($H^{\bullet}$) immediately reacts with oxygen gas:

$$H^{\bullet} + O_2 \rightarrow HO_2^{\bullet}$$

This results in the formation of the hydroperoxyl radical ($HO_2^{\bullet}$) which then reacts with nitric oxide and loses an oxygen atom to form $^{\bullet}OH$:

$$\text{then } HO_2^{\bullet} + NO \rightarrow NO_2 + {}^{\bullet}OH$$

PART B – ADDITIONAL PRACTICE QUESTIONS (ANSWERS NOT PROVIDED)

QC.1. Identify the four main sources of VOC emissions in 1970, and state how these have changed over time.

QC.2. A heavy-duty total suspended particulate (TSP) sampler runs for 12 complete weeks on a bench at a height of 1.5 m in a car repair garage at an average of 11.55 L per hour. At the end of this time period, the filter paper is totally coated but not blocked. The tare weight of the filter was 52.3571 g and the gross weight of the filter, dried to the same humidity, was 77.5993 g. Calculate the average TSP content of the air in the garage.

QC.3. Convert 12 ppb of toluene (C_7H_8) at 283 K and 1010 mb to μg m^{-3}. [Given: atmospheric pressure = 1013 mb; triple point of water = 273 K; molar volume = 22.4 l at 1013 mb and 273 K; Molar mass – Carbon = 12.00 g; Molar mass – Hydrogen = 1.00 g.]

QC.4. In a Gaussian plume model, the ground-level concentration of a pollutant of a pollutant at a downwind location (x, y, z) is given by the following equation. Explain the meaning of each of the symbols in the equation.

$$q(x,y,z) = \frac{Q}{2\pi\bar{u}\sigma_y\sigma_z} \exp\frac{-y^2}{2\sigma_y^2} \left\{ \exp\frac{-(z-H)^2}{2\sigma_z^2} \right\}$$

QC.5. It is estimated that 95 g s^{-1} of nitrogen dioxide (NO_2) is being emitted from a refinery from an average height of 80 m. At 08:00 on an overcast winter morning, with a surface wind of 5.5 m s^{-1}, what is the ground-level concentration directly downwind from the refinery at a distance of 1500 m? [Hint: Use information on lateral (σ_y) and vertical diffusion coefficients (σ_z) from Chapter 8.]

QC.6. It is estimated that a pile of burning wood on top of a partially constructed building is emitting 5.5 g s^{-1} of sulphur dioxide at an average height of 130 m. At 11:00 on a sunny spring morning, with a surface wind of 3.5 m s^{-1}, what is the ground-level

FOR REFERENCE PURPOSES ONLY

concentration directly downwind from the burning wood at a distance of 3000 m? [Hint: Use information on lateral (σ_y) and vertical diffusion coefficients (σ_z) from Chapter 8.]

QC.7. Briefly outline the types of photochemical processes that typically occur in the atmosphere.

QC.8. Identify technical and organisational methods that may be used to control noise in a work environment in order to protect workers.

QC.9. Discuss the post-combustion techniques for the removal of SO_2 from the waste gases of coal and high-sulphur oil burning power stations.

QC.10. Mention the considerations involved when planning a sampling campaign for ambient air in the vicinity of a motorway.

QC.11. Explain in detail how the physical and chemical properties of atmospheric particulate matter influences their emission; atmospheric lifetime and removal; distribution; health and environmental impacts.

QC.12. With reference to the *art and science* of fireworks, discuss the impact(s) of the traditional annual celebrations of Bonfire Night and Diwali on air quality in major cities.

QC.13. Discuss the technologies that may be used for the quantitative real-time determination of: (a) hydrocarbons, (b) nitrogen oxides, (c) carbon monoxide and (d) PM_{10}.

QC.14. Briefly outline the key technological and operational measures that may be used to reduce atmospheric emissions from shipping.

QC.15. Describe what is an air quality information system.

QC.16. In a lecture at an international conference on air pollution, a prominent atmospheric scientist said the following:

"The chemical pathways for the formation and removal of gaseous pollutants in the troposphere are controlled largely by atoms and free radicals, despite the fact that they are present at low concentrations."

Critically discuss this statement.

QC.17. Critically discuss the design and planning criteria that are pertinent to the creation of an air quality monitoring programme in a typical metropolitan city.

QC.18. Identify the main sources of nitrogen oxides (NO_x) in a city environment.

QC.19. Discuss in detail the health and environmental effects of atmospheric CO.

QC.20. When does noise become a nuisance?

QC.21. What are the steps to investigate a noise complaint?

QC.22. Given unlimited resources, what interventions would you implement to reduce noise (a) in a residential environment and (b) in a manufacturing workplace?

QC.23. Will reducing light pollution lead to more crime or cause safety problems? Justify your answer.

QC.24. How can light pollution be controlled?

QC.25. How does light pollution affect the environment?

FOR REFERENCE PURPOSES ONLY

QC.26. How does light pollution affect the behaviour of migratory birds?

---

* Tainio, M., de Nazelle, A. J., Götschi, T., Kahlmeier, S., Rojas-Rueda, D., Nieuwenhuijsen, M. J., and Woodcock, J. (2016) Can air pollution negate the health benefits of cycling and walking? *Preventive Medicine*, 87: 233–236.

FOR REFERENCE PURPOSES ONLY

Index

Absorption cross-section, 72, 76, 564
Absorption of gases, 63, 70
Absorption spectra of GHGs, 504
Absorption spectroscopy, 72, 75, 77, 151, 649
Acclimation, 306, 441
Accumulation mode, 88, 93, 180–181, 430
Acid deposition, 32, 213, 364, 453
Acid rain, 11, 477, 487
Acid smuts, 44
Action spectrum, 568–569
Activation of CCN, 253
Adsorption of gases, 63, 66, 179, 362, 375
Aerodynamic diameter, 86, 90, 100
Aerodynamic resistance, 251
Aerosol
  mechanics, 95, 395
  precursors, 216
  spectrometer, 125
Aethalometer, 121
Aflatoxin, 303, 674
Air changes per hour (ACH), 291, 293, 381
Aircraft emissions, 213
Air exchange rate, 295, 351, 432–433
Air–fuel ratio, 177, 185, 187
Air quality
  criteria document, 625
  management area, 242, 643
Air toxics, 446
Albedos
  of surfaces, 530–531
  UV, 567
Allergens, 303
Ammonia, 49
Ammonium chloride, 111
Ammonium nitrate, 111
Ammonium sulphate, 111
Animal models, 430
Antarctic winter vortex, 579
Anthropogenic forcing, 522
AOT40, 479
Aphid stimulation, 455
Asbestos, 4, 28, 90, 135

FOR REFERENCE PURPOSES ONLY

Asthma, 160, 280
Atmosphere, 12–13
Atmospheric attenuation, 415
Atmospheric extinction coefficient, 418
Atmospheric stability, 213, 316, 321
Atmospheric temperature profile, 233
Atomic absorption spectroscopy, 75, 77
Atomic emission spectroscopy, 77
Automatic Urban and Rural Networks (AURN), 124, 242
Auto-Oil programme, 618

Bacteria, 90, 302
Baghouse, 371
Beer–Lambert law, 70, 77, 122, 149, 417, 419
Benzene
  human responses, 443
  pollutant, 175
Benzo-*a*-pyrene, 184, 298
Best available technology (BAT), 29
Beta-attenuation, 122
Bioaerosols, 301
Biodiesel, 171, 209
Bioindicators, 463
Biological amplification factor (BAF), 568
Black smoke, 37, 86
Blue haze, 417
Bouguer–Lambert law, 521
Bouguer's law, 152
Boundary layer height, 324, 345, 394
Briggs variable, 331
British Standard smoke method, 120
Brownian diffusion, 97
Building ventilation, 291
Buoyancy of plumes, 284
Butadiene, human responses, 444

Calibration, 79, 116, 652
California Air Resources Board (CARB), 633
Canopy resistance, 251–252
Canyon Plume Box (CPB) model, 348
Carbon cycle, 346, 526
Carbon dioxide
  concentration, 296
  emissions, 222
Carbon monoxide
  concentration, 383
  emission, 166
Carboxyhaemoglobin (COHb), 32, 444, 489
Cascade impactor, 96, 126
Catalyst
  diesel oxidation, 189
  three-way, 174
Catalytic converter, 45, 52, 185
Cataract, 570
Centrifugation, 370

FOR REFERENCE PURPOSES ONLY

Cetane number, 199
Chemical mass balance, 350
Chemical transport model, 217
Chemiluminescence, 650
Chlorofluorocarbons, 11, 554
Chromophores, 568, 571
Clean Air Act, 31, 237
Clean room, 124, 291, 381
Climate feedbacks, 530
Clothing protection factor (CPF), 577
Cloud condensation nuclei (CCN), 129, 531
Cloud droplet formation, 252
CLRTAP protocols, 347, 612
CO_2 enrichment, 460
Coagulation, 99
Coarse particles, 132
Coefficient of haze (COH), 122, 416
Collection efficiency, 64, 106, 395
Condensation nucleus counter (CNC), 117, 129
Condensation trapping, 66
Continuously regenerating trap (CRT), 189
Contrails, 218
Critical load exceedances, 478
Cunningham slip factor, 101
Cut diameter, 86, 106, 125
Cyclone separator, 373

Daughter directives (EU), 610
Deciview, 416
$DeNO_x$, 189
Denuder tube, 66
Deposition velocity, 105, 248
Deutsch equation, 373
Diatoms, 464
Dichotomous sampler, 126
Diesel
  engine, 170
  oxidation catalyst, 189
  particulate filter, 188, 368
Differential absorption LIDAR, 73
Differential mobility analyser (DMA), 127
Differential optical absorption, 72, 151, 649
Diffusion tube, 65, 78, 243, 306
Dilution
  probe, 149
  system, 149
  vehicle exhaust, 190
Dimensions and units, 101
Dimethyl ether, 209
Dioxins, 53
Directional deposit gauge, 134
Dispersion
  aircraft emissions, 220
  line source, 334
  models, 325

FOR REFERENCE PURPOSES ONLY

parameters, 320
point source, 460
Diurnal pollutant variations, 172, 190, 267
Dobson unit, 548
Drag force, 96, 396
Drift velocity, 128, 205
Dry adiabatic lapse rate (DALR), 314
Dry deposition, 60, 230, 246
Dry reactions, 257
Dust veil index, 518
Dynamic dilution olfactometry, 452
Dynamic shape factor, 100

EC Directive Network, 242
Effusive volcanoes, 517
Ekman spiral, 330
Electrical aerosol analyser, 128
Electrical mobility analyser, 127
Electron capture detector, 74
Electroneutrality, 479
Electronic noses, 452
Electron microscopy of particles, 237
Electrostatic low-pressure impactor, 127
Electrostatic precipitator, 152, 373
Emission factors, 7, 194, 202, 206, 210, 212
Emission inventories, 155, 345
Emission standards, 221, 623
Emission testing cycles, 619–621
Endotoxins, 303
Entrainment, 93, 108, 253, 258
Environmental lapse rate, 316
Environmental noise directive, 590
Epidemiology, 425, 616
Equivalent diameter, 90
Erythemally effective radiation, 570
Ethanol vehicle fuel, 171
Ethylene diurea, 462
EU Air Quality Directives, 609
European Monitoring and Evaluation Programme, 112
Evaporative loss, 176
Exhaust gas recirculation, 185
Exposure dynamics, 472
Extinction coefficient, 415–416

Fabric filter, 152
Federal Test Procedures, 629
Fickian diffusion, 326
Field filtration, 460
Field release systems, 458
Filter, 4, 24
Filtration efficiency, 371
Flame ionisation detector, 300
Flame photometer, 74
Flue gas, 362
denitrification, 367

FOR REFERENCE PURPOSES ONLY

desulphurisation, 481
Fluidised-bed aerosol generator, 118
Forced expiratory volume (FEV), 440
Formaldehyde, 4, 28
Fourier transform infrared spectroscopy, 73
Four-stroke cycle, 170
Framework directive (EU), 609
Frisbee deposit gauge, 133
Fuel cell, 208
Fuel cleaning, 364
Fuel composition, 198
Fuel nitrogen content, 44
Fuel NO, 44
Fuel reformulation, 201
Fuel substitution, 364
Fuel sulphur content, 200, 364
Fugitive emissions, 146, 153
Fungi, 303
Furans, 28, 53

Gas chromatography, 73
Gas exchange, 234, 385, 431
Gasification, 28
Gas sample bubbler, 64–68, 78
Gas sampling, 61–63
Gaussian dispersion theory, 326, 338
Glass fibre filters, 64, 118
Global warming potential, 514, 534
Grab sampling, 67
Greenhouse gases, 11, 505
Gulf Stream, 532

Halocarbons, 50, 513, 556
Hazardous air pollutants, 627
Health impacts, 599
Heavy metals, 439
Helsinki Protocol, 477
High-volume sampler, 120
Hot soak losses, 176
Hydrocarbons, 55, 184
Hydrogen chloride, 52
Hydrogen fluoride, 465
Hydrogen fuel, 207
Hydrogen peroxide, 69, 148, 258
Hydrogen sulphide, 14, 41, 109, 188, 452
Hygroscopic particles, 238, 419

Immunosuppression, 445
Impaction process, 92, 103
Impactor, 105, 125
Impregnated filter, 64
Incineration, 28, 53, 376
Indoor air sampling, 306
Indoor concentration, 293, 352
Inductively coupled plasma–mass spectroscopy (ICP-MS), 75, 130
Industrial melanism, 455

FOR REFERENCE PURPOSES ONLY

Inertial impactor, 125
Infiltration, 291, 486
Infrared analyser, 71
Inhalable fraction, 293, 436
In situ gas measurement, 132
Interception, 95, 103
International Toxic Equivalent (I-TEQ), 54
International visibility code, 419
Inversion, 8, 31, 318, 333
IPCC, 497
Isokinetic sampling, 114, 152
I-TEQ. *See* International Toxic Equivalent

Katharometer, 74
Kelvin relationship, 253
Knocking, 182
Köhler curves, 254
Koschmeider's law, 419
Kyoto Protocol, 532, 535

Lambda window, 187
Laminar flow, 129, 370
Land and take-off cycle, 221
Laser microprobe mass spectrometer, 131
Latex beads, 117
Leaded petrol use, 4, 28, 183
Lead emissions, 182
Leaks in gas sample system, 63, 79
Lean-burn, 185, 209
Lichen and air pollution, 464
Light-off temperature, 195
Liming of water, 455
Liquid chromatography, 74, 659
Local Air Quality Management, 609
Locomotive emissions, 210
Log-normal distribution, 92, 521
Low-emission vehicles, 633
Low-NO_x burners, 367
Low-sulphur fuel, 189, 200, 364

Macrophages, 299, 438
Mass spectrometry, 85, 132, 237
Material damage by pollutants, 483
Maximum achievable control technology, 628
Mean free path, 86, 96
Mean relative growth rate, 455, 475
Measurement blanks, 78
Melanin synthesis, 568–570
Melanomas, 571
Membrane filters, 119
Methane
  concentration, 507
  emissions, 510
  feedback, 531
Methanol vehicle fuel, 51, 74, 175

FOR REFERENCE PURPOSES ONLY

Methyl bromide, 557
Micro-orifice uniform deposit impactor (MOUDI), 127
Mie scattering, 72, 417
Milankovitch cycles, 502
Monin–Obukhov Length, 323
Montreal Protocol, 513
Motor vehicle emissions, 185
Mucociliary escalator, 438
Municipal solid waste, 28, 142
Mycotoxins, 303

Nanoparticles, 86, 179
National Acid Precipitation Assessment Program, 241
National Air Quality Strategy, 606
National Ambient Air Quality Standards, 125, 625
National vehicle fleets, 197
Nephelometer, 121
Neutron activation analysis, 131, 349
Nitrogen budget, 261
Nitrogen dioxide
  concentrations, 60, 172
  formation, 47
Non-melanoma skin cancer, 570
Nuclepore filters, 119

Obliquity variations, 502
Octane number, 182
Odour, 188, 299
Olfactory unit, 306
Open-top chambers, 461
Optical amplification factor, 566
Optical particle counter, 407
Ozone column depth, 565
Ozone (tropospheric) concentration diurnal variation, 539
Ozone (stratospheric) depletion potentials, 558
Ozone generator, 539
Ozone hole, 552
Ozone profile, 235, 539

Packed absorption tower, 363
Particles
  analysis, 132
  chemical composition, 238
  collection efficiency, 368
  sampling, 114
  shape, 136
  sources, 108
Particle size
  distribution, 86
  fractionation, 124
  monodispersed, 89
  polydisperse, 89, 128
Particulate elemental carbon, 239
Pasquill stability classes, 322
Passive sampler, 64, 300
Passive smoking, 445

FOR REFERENCE PURPOSES ONLY

Permeation tubes, 79
Persistent organic pollutants (POPs), 347
Personal exposure, 294
Petrol composition, 170
Petrol engine, 178
Photochemical smogs, 428
Pitot probe, 147
Plant responses, 465
Plume
  reflection, 333
  rise, 330
PM_{10}, $PM_{2.5}$ definitions, 86
Polar stratospheric cloud particles, 531
Pollen index, 640
Pollutant rose, 267, 340
Pollution Prevention and Control Act, 592
Polycyclic aromatic hydrocarbons, 55
POPs. *See* Persistent organic pollutants
Portable emissions measurement systems (PEMS), 621
Potential temperature, 318
Precipitation chemistry, 260
Premature senescence, 473
Pressure drop through filter, 118
Primary emissions, 58, 346
Pulsed fluorescence analyser, 69, 242
Pyrolysis, 298

Quality-adjusted life years (QALY), 450
Quality assurance and control, 78

Radiation amplification factor, 566
Radiation budget of the Earth, 507
Radiative forcing, 218, 504
Radiatively active gases, 503
Rainout, 252
Raman scattering, 73, 76
Rayleigh scattering, 417, 521
Real Driving Emissions (RDE), 191, 621
Receptor models, 349
Recirculating flow, 395
Red rain, 107–108
Regional haze, 146, 415, 529
Reid vapour pressure, 176, 627
Relaxation time, 101
Residence time, 89, 95
Resistance, 250
Resistivity, 153, 373
Resonating microbalance, 122
Respirable fraction, 86, 434
Respiratory system, 431
Review and assessment of air quality, 609
Reynolds number, 96, 101
Richardson number, 323
Road dust emissions, 118
Roughness length, 249, 392

FOR REFERENCE PURPOSES ONLY

Running losses, 176

Saltation, 107
Saturated adiabatic lapse rate, 315
Saturated vapour pressure, 15, 179, 253
Scanning mobility particle sizer (SMPS), 128
Scattering ratio, 417
Sea salt, 108
Secondary gaseous pollutants, 56
Secondary particles, 111
Sedimentation, 370
Seeder–feeder mechanism, 259
Selective non-catalytic reduction (SNCR), 368
Shear stress, 107
Shipping emissions, 212
Sick building syndrome, 305
Silt load, 181
Skin responses to UV, 570
Smelter emissions, 457
Smogs
  photochemical, 8, 428
  winter, 8
Solar Constant, 501
Solid adsorbents, 300
Soluble organic fraction, 180
Source attribution, 349
Specific mass extinction coefficient, 153
Spinning disc generator, 117
Stability classes, 321
Stagnation point, 342
Standard erythemal dose, 570
Statistical models, 350
Stoichiometric ratio, 169, 178
Stokes number, 104–105, 390, 397
Stomatal effects, 50, 471
Stopping distance, 102
Stratospheric temperature anomalies, 498, 520
Sulphate aerosol, 532
Sulphur budget, 261
Sulphur emissions, 612
Sulphur hexafluoride, 338
Sulphuric acid, 8, 32
Sulphur trioxide, 44
SUM60, 480
Supersaturation, 129, 520
Suspended particulate matter, 86

Tapered element oscillating microbalance, 123, 242
Terminal speed, 98, 370
Terrestrial radiation, 504
Tetraalkyl lead, 182
Thermophoresis, 107
Thoracic fraction, 293
Three-way catalyst, 174, 186
Time-weighted average concentration, 616

FOR REFERENCE PURPOSES ONLY

Tobacco emissions, 298
TOF-MS, 132
Toluene, human responses, 444
Topography effects on dispersion, 259
Toxic organic micropollutants, 628
Train emissions, 211
Transmissometer, 151, 190
Tri-modal size distribution, 90
Tropospheric ozone, 56
Turbulent diffusion, 17, 246
Two-stroke engine, 170

Urea, 462
US ambient air quality standards, 626
UV
  absorption analyser, 568
  atmospheric penetration, 563
  health effects, 570
  immune response, 472
  ozone generator, 79
  water penetration, 567

Vehicle emissions
  Asia, 638
  European Union, 618
  United States, 629
Vehicle NO_x emission, 111, 188, 380
Velocity head, 147
Vent controls, 185
Ventilated glasshouses, 462
Venturi scrubber, 374
Vertical profiles
  pressure, 320
  temperature, 316
Vibrating orifice, 117
Virtual impactor, 126
Viruses, 303
Visible injury, 465
Visual range, 415
Volatile organic compounds, 50, 236
Volcanic explosivity index, 518
Volume flow rate measurement, 147
von Karman constant, 392
Vostok ice core record, 506

Washout, 256
Water vapour as GHG, 503
Weibull curves, 466
Wet chemical gas sampling, 69
Wet deposition, 252
Wet-only collectors, 244, 258
Wet reactions, 257
WHO (World Health Organization) health impacts methodology, 450
  air quality guidelines, 297, 451
Wind rose, 267, 340

FOR REFERENCE PURPOSES ONLY

Wind speed, 65, 268

X-ray fluorescence, 130

Zero air, 79
Zero emission vehicles, 206, 632